# Synthesis and Coordination Chemistry of the Arsacyclopentadiene Ligand

Ryan Maxwell Kirk

A thesis submitted for the degree of Doctor of Philosophy

of

The Australian National University

May 2023



Australian National University

© Copyright by R. M. Kirk 2023

All rights reserved

# Declaration

The research described in this thesis is the author's own original work, with the exception of that to which reference is made in the text.

R. M. Kirk



*Do not learn the tricks of the trade, learn the trade.*

**Acknowledgements**

When I began my candidature, I could not have predicted the immense feeling of satisfaction in completing this thesis. After some deliberation, the epigraph given on the preceding page is perhaps the only way I can summarise this journey, which of course I have not made alone. There are many kind people who have taken the time and effort to share their knowledge and experience with me so that I might benefit and grow, and that I might become a practitioner of the same trade in which they have found their passion.

First, I must express my unwavering appreciation to Tony Hill, my supervisor and mentor for whom I have the greatest admiration, who in tandem with Mark Santos have treated me as family from the outset. I cannot begin to describe their level of kindness and generosity of which they – being the good souls they are – have expected nothing in return.

I have made so many friends along the way. They have made this journey so much more enjoyable: the impending doctors Rosie Avery, Emer Foyle, Liam Burt, Lachlan Watson and Steve Walsh who have persisted/suffered through their candidatures alongside me; our post-docs Dr Ben Frogley and Dr Richie Manzano who have imparted so much wisdom and left behind so many useful reagents of superb quality; previous group members Yong-Shen Han, Chee-Sheng Onn and Harry Barnett who have graduated to fulfilling careers and whose legacy in the group still remains; mentors-*cum*-friends Dr Jas Ward, Dr Stephanie Boer, Dr Tristan Reekie, Professor Mark Ellison and Mrs Alannah Macleod for whom I have so much respect; my good friends (and future doctors) Lani Davies, Emily Nahon, Aidan Matthews, Liam Pascoe, Andie Delaney and Caitlin Lindsay who I know will find the same, well-deserved feeling of reward in curating their own theses.

I would be remiss if I did not acknowledge the indelible legacies of François Mathey and Edward Abel, two tradesmen who sadly passed away during this work. They laid the foundations of an enormous body of organometallic and heterocyclic chemistry throughout the latter half of the last century, and their contributions to the field will appear frequently throughout this thesis.

Last, but most definitely not least, Mum and Dad who have supported me throughout this journey and whose love and guidance have made me the person I am today. I dedicate this thesis to them.

**Abstract**

This thesis describes investigations into coordination complexes of 1*H*-arsacyclopentadiene (arsole, R'$AsC_4R_4$) and arsacyclopentadienyl (arsolyl, $[AsC_4R_4]^-$) ligands, the chemistry of which has only been sporadically and non-systematically explored in the interim since their discovery in the late 1950's. An introduction to the general chemistry of arsoles is given in **Chapter 1**.

In **Chapter 2**, an improved synthesis of 1-chloro-2,3,4,5-tetraphenylarsole ($ClAsC_4Ph_4$) is described *via* transmetalation from the corresponding 1*H*-stannacyclopentadiene. The first examples of *As*-ethynyl ($RC{\equiv}CAsC_4Ph_4$) and -butadiynyl arsoles ($RC{\equiv}CC{\equiv}CAsC_4Ph_4$) (R = H or $SiMe_3$) were prepared therefrom, and transform in the presence of labile Ru(0) and Ru(II) centres to products of oxidative addition, hydrometallation, or tautomerisation. Accordingly, the first examples of β-arsolylalkynyl ($[RuH\{(C{\equiv}C)_nAsC_4Ph_4\}(CO)_2(PPh_3)_2]$ and $[Ru(C{\equiv}CAsC_4Ph_4)(PPh_3)_2(\eta^5\text{-}C_5H_5)]$, β-arsolylalkenyl ($[RuCl(E\text{-}CH{=}CHAsC_4Ph_4\}(CO)(PPh_3)_2]$ and $[RuCl\{gem\text{-}C(=CH_2)C{\equiv}CAsC_4Ph_4\}(CO)(PPh_3)_2]$) and β-arsolylvinylidene ($[Ru(=C{=}CHAsC_4Ph_4)(PPh_3)_2(\eta^5\text{-}C_5H_5)]^+$) transition metal complexes were obtained. The reaction between $[Ru(PPh_3)_2(\eta^5\text{-}C_5H_5)]^+$ and $HC{\equiv}CC{\equiv}CAsC_4Ph_4$ gave not a butatrienylidene complex but an arylalkynyl $[Ru(C{\equiv}CC_6HPh_4)(PPh_3)_2(\eta^5\text{-}C_5H_5)]$ *via* formal intramolecular extrusion of the arsenic atom with rearrangement of the hydrocarbon chain. The same alkynyl arsoles also react with $[Co_2(CO)_8]$ to provide μ-π complexes $[Co_{2n}(CO)_{6n}\{\mu\text{-}\eta^2{:}\eta^2\text{-}R(C{\equiv}C)_nAsC_4Ph_4\}]$ ($n$ = 1 or 2), which are thermolabile. Crystal structures for all but two new compounds were determined. Treatment of $H(C{\equiv}C)_nAsC_4Ph_4$ with strong bases – in an attempt to deprotonate the carbon terminus – instead led to nucleophilic substitution at the arsenic atom.

In **Chapter 3**, the first examples of late transition metal *pentahapto* arsolyl complexes $[Co(CO)_2(\eta^5\text{-}AsC_4R_4)]$ are obtained by thermolysis of $[Co_2(CO)_8]$ with an arsole R'$AsC_4R_4$, traversing an unknown mechanism but one involving scission of the arsenic-bound residue and reduction of the ring system. Five such compounds with differing substituent patterns were prepared, of which two ($[Co(CO)_2(\eta^5\text{-}AsC_4Ph_2R_2]$, R = Ph or H) were structurally characterised. A further two were subjected to X-ray diffraction as the trimethylphosphite substituted complexes ($[Co\{P(OMe)_3\}(CO)(\eta^5\text{-}AsC_4R_2Me_2)]$, R = Me or $SiMe_3$). A computational study of the model complex $[Co(CO)_2(\eta^5\text{-}AsC_4H_4)]$ revealed both the Co(I) and As(III)

centres to have LEWIS basic character; this was experimentally verified by the formation of novel μ-σ:π complexes of the $[Co(CO)_2(\eta^5\text{-}AsC_4Me_4)]$ "*metallo*-ligand" with LEWIS acidic Hg(II), Pt(II) and Au(I) centres. Attempts to prepare *pentahapto* arsolyl complexes by direct reaction of $[Co(CO)_4]^-$ and $ClAsC_4Ph_4$ instead yielded the thermolabile $[Co(\sigma\text{-}AsC_4Ph_4)(CO)_4]$ which does not convert to $[Co(CO)_2(\eta^5\text{-}AsC_4Ph_4)]$ upon attempted decarbonylation. Instead, a small range of σ-arsolyl complexes stabilised by neutral two-electron ligands ($[Co(AsC_4Ph_4)L(CO)_n]$, L = $PPh_3$, $AsPh_3$, $\kappa^1$-dppm, $\kappa^2$-dppe) were prepared and structurally characterised. The first definitive example of an $\eta^4$-arsole ligand, namely $[Co_2(\mu\text{-}CO)_2(CO)_2(\eta^4\text{-}PhAsC_4Et_4)_2]$, was also isolated during these studies.

Following this, in **Chapter 4** some $\sigma\text{-}AsC_4Ph_4$ complexes of Mo(II), W(II) and Fe(II) first prepared by ABEL were reinvestigated alongside some new examples possessing the $\sigma\text{-}AsC_4Me_4$ ligand, all of which were characterised by X-ray diffraction. These were prepared *via* an alternate synthetic route involving a transmetalation reaction between $ClAsC_4R_4$ and $[M(SnBu_3)(CO)_n(\eta^5\text{-}C_5H_5)]$ (M = Mo or W, $n$ = 3; M = Fe, $n$ = 2), the latter serving as an equivalent for the corresponding cyclopentadienyl metal carbonyl anion. The As(III) atom in $[Mo(AsC_4Me_4)(CO)_3(\eta^5\text{-}C_5H_5)]$ is appreciably nucleophilic and readily alkylated. The reaction between $[Mo(AsC_4Me_4)(CO)_3(\eta^5\text{-}C_5H_5)]$ and electron-poor alkynes RC≡CR (R = $CO_2Me$ or $CF_3$) gives not [4+2] cycloaddition products but instead the novel arsolylpropenoyl *spiro*-complexes $[Mo\{C(O)CR{=}CRAsC_4Me_4\}(CO)_2(\eta^5\text{-}C_5H_5)]$. All new compounds were structurally characterised.

In **Chapter 5**, the nucleophilic $[Mo(AsC_4Me_4)(CO)_3(\eta^5\text{-}C_5H_5)]$ complex also served as a novel "*metallo*-ligand" toward a selection of labile LEWIS acidic metal reagents, giving bimetallic adducts featuring the $\mu\text{-}AsC_4Me_4$ moiety. In one case utilisation of the butadiene function was observed as a component of the first example of a seven-electron arsolyl ligand, $[MoFe_2(\mu_3\text{-}\eta^1{:}\eta^1{:}\eta^4\text{-}AsC_4Me_4)(CO)_9]$. In several other reactions homolytic cleavage of the Mo-As bond was observed, which in one case yielded the first example of a μ-biarsolyl complex $[Mn_2\{\mu\text{-}(AsC_4Me_4)_2\}(CO)_4(\eta^5\text{-}C_5H_4Me)_2]$. All new compounds were structurally characterised.

In **Chapter 6**, the $\sigma\text{-}AsC_4Ph_4$ complexes $[M(AsC_4Ph_4)(CO)_3(\eta^5\text{-}C_5H_5)]$ were shown to react with $Li[N(i\text{-}Pr)_2]$ to give the first example of base-induced arsenide migration $[M(CO)_3\{\eta^5\text{-}C_5H_4(AsC_4Ph_4)\}]^-$ for which the molybdenum example was isolated and spectroscopically characterised. Treatment of this anion

with a small selection of electrophiles gave isolable *As*-cyclopentadienyl arsole complexes [MoR(CO)$_n${$\eta^5$-$C_5H_4(AsC_4Ph_4)$}] (R = Me or I, $n$ = 3; R = NO, $n$ = 2) the molecular structures of which were determined by X-ray diffractometry. An arsolyl-supported metal-metal bonded complex [WRe(CO)$_7${$\mu$-$\eta^1$:$\eta^5$-$C_5H_4(AsC_4Ph_4)$}] was also isolated and structurally characterised, and in one case capture of the arsolyl ring was observed by an incoming unsaturated Rh(I) centre giving a *pentahapto* complex.

Finally, in **Chapter 7** three air stable 1,1'-bis(arsolyl)ferrocenes were prepared by the action of $ClAsC_4R_4$ upon 1,1'-dilithioferrocene; their bidentate coordination faculty was confirmed by formation of [Mo{$\kappa^2$-Fe($\eta^5$-$C_5H_4(AsC_4R_4)$}$_2$}(CO)$_4$] (R = Me, Et or Ph). The most-nucleophilic of these, [Fe{$\eta^5$-$C_5H_4(AsC_4Me_4)$}$_2$] ("tmaf"), was used to prepare a selection of classic bidentate coordination complexes including an air-stable Ni(0) species and a sterically-unobtrusive Pd(II) complex, both of which have obvious catalytic allure. The first examples of arsole coordination to osmium and iridium were demonstrated, and combination of tmaf with labile Fe(0) reagents affords a series of three open-bridged coordination complexes utilising the diene function of the arsole pendants. Most new compounds were structurally characterised.

In total, nearly 100 new arsole compounds are described, of which no fewer than 70 have had their crystal structures determined. The vast majority have been fully characterised by modern spectroscopic methods augmenting the sparse inventory of arsoles and their transition metal complexes which had been described prior to this work.

# Contents


Chapter 1 Introduction to the Chemistry of Arsacyclopentadienes ..... 1

1.1 Preamble ..... 2

1.1 The Question of Aromaticity ..... 4

1.2 Synthesis of Arsoles ..... 9

1.2.1 *Via* 1,4-Dilithiobutadienides ..... 9

1.2.2 *Via* 1,4-Disubstituted Butadiynes ..... 12

1.2.3 *Via* Transmetalation ..... 13

1.3 Transformations of Arsoles ..... 20

1.3.1 Reduction ..... 20

1.3.2 Halogenation and Oxidation ..... 21

1.3.3 Cycloaddition Reactions ..... 24

1.3.4 Conversion to Biarsolyls ..... 27

1.3.5 Conversion to Arsabenzenes ..... 29

1.4 Transition Metal Complexes of Arsole and Arsolyl Ligands ..... 30

1.4.1 σ-Dative Arsole Complexes ..... 32

1.4.2 σ-Covalent Arsolyl Complexes ..... 34

1.4.3 $\eta^4$-Arsole Complexes ..... 35

1.4.4 $\eta^5$-Arsolyl Complexes ..... 37

1.4.5 μ-Arsolyl Complexes ..... 41

1.4.6 Other Coordination Modes ..... 42

1.5 Foreword to this Thesis ..... 42

1.6 References ..... 43

Chapter 2 Coordination Chemistry of *As*-Alkynyl Arsoles ..... 47

2.1 Preamble ..... 48

2.2 *As*-Ethynyl Arsoles ..... 49

2.2.1 Synthesis of $ClAsC_4Ph_4$ ..... 49

2.2.2 Synthesis of $Me_3SiC{\equiv}CAsC_4Ph_4$ ..... 54

2.2.3 Synthesis of $HC{\equiv}CAsC_4Ph_4$ ..... 55

2.3 *As*-Butadiynyl Arsoles ..... 58

2.3.1 Synthesis of $Me_3SiC{\equiv}CC{\equiv}CAsC_4Ph_4$ ..... 58

2.3.2 Synthesis of $HC{\equiv}CC{\equiv}CAsC_4Ph_4$ ..... 60

2.4 Attempted Functionalisation of *As*-Alkynyl Arsoles ..... 62

2.5 Reactions with *trans*-$[Ru(CO)_2(PPh_3)_3]$ ..... 65

2.5.1 Synthesis of $[RuH(C{\equiv}CAsC_4Ph_4)(CO)_2(PPh_3)_2]$ ..... 66

2.5.2 Synthesis of $[RuH(C{\equiv}CC{\equiv}CAsC_4Ph_4)(CO)_2(PPh_3)_2]$ ..... 72

2.6 Reactions with *mer*-$[RuHCl(CO)(PPh_3)_3]$ ..... 75

2.6.1 Synthesis of $[RuCl(E\text{-}CH{=}CHAsC_4Ph_4)(CO)(PPh_3)_2]$ ..... 76

2.6.2 Synthesis of [RuCl{*gem*-C(=$CH_2$)C≡$CAsC_4Ph_4$}(CO)($PPh_3$)$_2$] ..... 78
2.7 Reactions With [$RuCl_2(PPh_3)_3$] and [Ru(THF)($PPh_3$)$_2$($\eta^5$-$C_5H_5$)]$PF_6$ ..... 81
2.7.1 Synthesis of [$Ru_2(\mu$-Cl)$_3$Cl(=C=$CHAsC_4Ph_4$)($PPh_3$)$_4$] ..... 84
2.7.2 Synthesis of [Ru(=C=$CHAsC_4Ph_4$)($PPh_3$)$_2$($\eta^5$-$C_5H_5$)]$PF_6$ ..... 88
2.7.3 Synthesis of [Ru(C≡$CAsC_4Ph_4$)($PPh_3$)$_2$($\eta^5$-$C_5H_5$)] ..... 95
2.7.4 Attempted synthesis of [Ru(=C=C=C=$CHAsC_4Ph_4$)($PPh_3$)$_2$($\eta^5$-$C_5H_5$)]$PF_6$ ..... 97
2.8 Reactions with [$Co_2(CO)_8$] ..... 105
2.8.1 Synthesis of [$Co_2(\mu$-$\eta^2$:$\eta^2$-$Me_3SiC$≡$CAsC_4Ph_4$)$(CO)_6$] ..... 107
2.8.2 Synthesis of [$Co_2(\mu$-$\eta^2$:$\eta^2$-HC≡$CAsC_4Ph_4$)$(CO)_6$] ..... 110
2.8.3 Synthesis of [$Co_4(\mu$-$\eta^2$:$\eta^2$:$\eta^2$-HC≡CC≡$CAsC_4Ph_4$)$(CO)_{12}$] ..... 112
2.9 Summary ..... 114
2.10 Experimental ..... 116
2.10.1 *As*-Alkynyl Arsoles ..... 116
2.10.2 Reactions with [$Ru(CO)_2(PPh_3)_3$] ..... 121
2.10.3 Reactions with *mer*-[RuHCl(CO)($PPh_3$)$_3$] ..... 123
2.10.4 Reactions with [$RuCl_2(PPh_3)_3$] and [Ru(THF)($PPh_3$)$_2$($\eta^5$-$C_5H_5$)]$PF_6$ ..... 124
2.10.5 Reactions with [$Co_2(CO)_8$] ..... 128
2.11 References ..... 130
Chapter 3 Arsole and Arsolyl Complexes of Cobalt ..... 135
3.1 Preamble ..... 136
3.2 Arsole Complexes of Cobalt(0) ..... 137
3.2.1 Synthesis of [$Co_2(PhAsC_4Ph_4)(CO)_7$] ..... 137
3.2.2 Synthesis of [$Co_2(PhAsC_4Me_4)_2(CO)_6$] ..... 139
3.2.3 Synthesis of [$Co_2(PhAsC_4Et_4)_2(CO)_6$] ..... 146
3.2.4 Synthesis of *anti*-[$Co_2(CO)_4$($\eta^4$-$PhAsC_4Et_4$)$_2$] ..... 148
3.3 *Pentahapto* Arsolyl Complexes of Cobalt(I) ..... 151
3.3.1 Synthesis of [$Co(CO)_2$($\eta^5$-$AsC_4Et_4$)] ..... 151
3.3.2 Synthesis of [$Co(CO)_2$($\eta^5$-$AsC_4Ph_4$)] ..... 154
3.3.3 Synthesis of [$Co(CO)_2$($\eta^5$-$AsC_4Ph_2H_2$)] ..... 156
3.3.4 Synthesis of [CoL(CO)($\eta^5$-$AsC_4Me_4$)] (L = CO *or* P(OMe)$_3$) ..... 157
3.3.5 Synthesis of [CoL(CO){$\eta^5$-$AsC_4(SiMe_3)_2Me_2$}] (L = CO *or* P(OMe)$_3$) ..... 160
3.3.6 General Comments Regarding the Synthesis of [$Co(CO)_2$($\eta^5$-$AsC_4R_4$)] ..... 162
3.4 Coordination Complexes of [$Co(CO)_2$($\eta^5$-$AsC_4Me_4$)] ..... 164
3.4.1 Computational Aspects of [$Co(CO)_2$($\eta^5$-$EC_4H_4$)] (E = CH, N, P, As, Sb) ..... 166
3.4.2 Synthesis of [$Co(CO)_2$($\mu$-$\eta^1$:$\eta^5$-$AsC_4Me_4$)·{$Hg(\mu$-Cl)Cl}]$_2$ ..... 169
3.4.3 Synthesis of [$Co(CO)_2$($\mu$-$\eta^1$:$\eta^5$-$AsC_4Me_4$)·{$Pt(C_6F_5)_2(CO)$}] ..... 174
3.4.4 Synthesis of [{$Co(CO)_2$($\mu$-$\eta^1$:$\eta^5$-$AsC_4Me_4$)}$_2$·Au][$Au(C_6F_5)_2$] ..... 179
3.5 σ-Covalent Arsolyl Complexes of Cobalt(I) ..... 184
3.5.1 Attempted Synthesis of [$Co(CO)_2$($\eta^5$-$AsC_4Ph_4$)] from [$Co(CO)_4$]$^-$ and $ClAsC_4Ph_4$ ..... 184
3.5.2 Synthesis of *trans*-[Co($AsC_4Ph_4$)($PPh_3$)$(CO)_3$] ..... 191

3.5.3 Synthesis of *trans*-[Co(AsC$_4$Ph$_4$)(AsPh$_3$)(CO)$_3$] ..... 193
3.5.4 Synthesis of *trans*-[Co(AsC$_4$Ph$_4$)(κ$^1$-dppm)(CO)$_3$] ..... 195
3.5.5 Synthesis of [Co(AsC$_4$Ph$_4$)(κ$^2$-dppe)(CO)$_2$] ..... 197
3.6 Summary ..... 200
3.7 Experimental ..... 202
3.7.1 Arsole complexes of Co(0) ..... 202
3.7.2 η$^5$-Arsolyl Complexes of Co(I) ..... 204
3.7.3 Bimetallic μ-η$^1$:η$^5$-Arsolyl Complexes ..... 208
3.7.4 η$^1$-Arsolyl Complexes of Co(I) ..... 210
3.8 References ..... 213
Chapter 4 Arsolyl Complexes of Molybdenum, Tungsten, and Iron ..... 216
4.1 Preamble ..... 217
4.2 From *As*-Chloroarsoles and Metal-Centred Anions ..... 218
4.3 From *As*-Chloroarsoles and Metal Stannyl Reagents ..... 220
4.1.1 Synthesis of [M(SnBu$_3$)(CO)$_n$(η$^5$-C$_5$H$_5$)] ..... 222
4.1.2 Complexes of the Tetraphenylarsolyl Ligand ..... 222
4.1.3 Complexes of the Tetramethylarsolyl Ligand ..... 231
4.1.4 Complexes of Bulky Arsolyl Ligands ..... 238
4.4 Mechanistic Aspects of Sn→As Transmetalation ..... 244
4.5 Computational Aspects of Metal Arsenido Complexes ..... 247
4.6 Reactions of Arsolyl Complexes with Electrophiles ..... 251
4.1.5 Electrophilic Methylating Agents ..... 252
4.1.6 Activated Alkynes ..... 265
4.7 Summary ..... 273
4.8 Experimental ..... 274
4.1.7 [NaC$_5$H$_5$·DME] ..... 274
4.1.8 [LiC$_5$H$_5$] ..... 274
4.1.9 Synthesis of [M(SnBu$_3$)(CO)$_n$(η$^5$-C$_5$H$_5$)] ..... 274
4.1.10 Synthesis of [M(AsC$_4$Ph$_4$)(CO)$_n$(η$^5$-C$_5$H$_5$)] ..... 277
4.1.11 Synthesis of [M(AsC$_4$Me$_4$)(CO)$_n$(η$^5$-C$_5$H$_5$)] ..... 279
4.1.12 [Mo{AsC$_4$(H)(SiMe$_3$)Me$_2$}(CO)$_3$(η$^5$-C$_5$H$_5$)] ..... 281
4.1.13 Reaction between [Mo(SnBu$_3$)(CO)$_3$(η$^5$-C$_5$H$_5$)] and ClAsC$_4$(*t*-Bu)$_2$Me$_2$ ..... 282
4.1.14 Alkylation of Molybdenum Arsolyl Complexes ..... 282
4.1.15 [Mo{C(O)C(CO$_2$Me)=C(CO$_2$Me)AsC$_4$Me$_4$}(CO)$_2$(η$^5$-C$_5$H$_5$)] ..... 286
4.1.16 [Mo{C(O)C(CF$_3$)=C(CF$_3$)AsC$_4$Me$_4$}(CO)$_2$(η$^5$-C$_5$H$_5$)] ..... 287
4.9 References ..... 288
Chapter 5 Bridging Complexes of the Arsolyl Ligand ..... 291
5.1 Preamble ..... 292
5.2 Coordination Complexes of the [Mo(AsC$_4$Me$_4$)(CO)$_3$(η$^5$-C$_5$H$_5$)] *Metallo*-Ligand ..... 293
5.2.1 Synthesis of [MoAu(μ-AsC$_4$Me$_4$)(CO)$_3$(C$_6$F$_5$)(η$^5$-C$_5$H$_5$)] ..... 293

5.2.2 Synthesis of [CrMo(μ-$AsC_4Me_4$)$(CO)_8$($\eta^5$-$C_5H_5$)] ..... 295
5.2.3 Synthesis of [$MoCo_3$(μ-$AsC_4Me_4$)($\mu_3$-CH)$(CO)_{11}$($\eta^5$-$C_5H_5$)] ..... 297
5.2.4 Synthesis of [MoFe(μ-$AsC_4Me_4$)$(CO)_5$($\eta^5$-$C_5H_5$)$_2$]$PF_6$ ..... 301
5.2.5 Synthesis of [MoMn(μ-$AsC_4Me_4$)$(CO)_5$($\eta^5$-$C_5H_5$)($\eta^5$-$C_5H_4$Me)] ..... 303
5.2.6 General Comments Regarding Features of Bridging-Arsolyl Complexes ..... 305
5.2.7 Synthesis of ($AsC_4Me_4$)$_2$ and [$Mn_2${μ-($AsC_4Me_4$)$_2$}$(CO)_4$($\eta^5$-$C_5H_4$Me)$_2$] ..... 307
5.2.8 Synthesis of [$MoFe_2$($\mu_3$-$\eta^1$:$\eta^1$:$\eta^4$-$AsC_4Me_4$)$(CO)_9$($\eta^5$-$C_5H_5$)] ..... 310
5.3 Summary ..... 319
5.4 Experimental ..... 321
5.4.1 [MoAu(μ-$AsC_4Me_4$)($C_6F_5$)($\eta^5$-$C_5H_5$)] ..... 321
5.4.2 [CrMo(μ-$AsC_4Me_4$)$(CO)_8$($\eta^5$-$C_5H_5$)] ..... 321
5.4.3 [$MoCo_3$(μ-$AsC_4Me_4$)($\mu_3$-CH)$(CO)_{11}$($\eta^5$-$C_5H_5$)] ..... 322
5.4.4 [MoFe(μ-$AsC_4Me_4$)$(CO)_5$($\eta^5$-$C_5H_5$)$_2$]$PF_6$ ..... 323
5.4.5 [MoMn(μ-$AsC_4Me_4$)$(CO)_5$($\eta^5$-$C_5H_5$)($\eta^5$-$C_5H_4$Me)] ..... 324
5.4.6 ($AsC_4Me_4$)$_2$ ..... 325
5.4.7 [$Mn_2$($AsC_4Me_4$)$_2$$(CO)_4$($\eta^5$-$C_5H_5$)$_2$] ..... 326
5.4.8 [$MoFe_2$($\mu_3$-$\eta^1$:$\eta^1$:$\eta^4$-$AsC_4Me_4$)$(CO)_9$($\eta^5$-$C_5H_5$)] ..... 326
5.5 References ..... 327
Chapter 6 Arsolyl-Cyclopentadienyl Complexes of Molybdenum and Tungsten ..... 330
6.1 Preamble ..... 331
6.2 Base-Induced Ligand Migration ..... 333
6.3 Base-Induced Migration of the Arsolyl Ligand ..... 335
6.3.1 Synthesis of [$MoMe(CO)_3${$\eta^5$-$C_5H_4$($AsC_4Ph_4$)}] ..... 336
6.3.2 Synthesis of [$WMe(CO)_3${$\eta^5$-$C_5H_4$($AsC_4Ph_4$)}] ..... 340
6.3.3 Comments Regarding the Base-Induced Migration of Arsolyl Ligands ..... 340
6.3.4 Isolation of [PPN][$Mo(CO)_3${$\eta^5$-$C_5H_4$($AsC_4Ph_4$)}] ..... 342
6.3.5 Synthesis of [Mo(NO)$(CO)_2${$\eta^5$-$C_5H_4$($AsC_4Ph_4$)}] ..... 349
6.3.6 Synthesis of [$MoI(CO)_3${$\eta^5$-$C_5H_4$($AsC_4Ph_4$)}] ..... 351
6.3.7 Attempted Synthesis of [$MoRh(CO)_3$(NBD){μ-$\eta^1$:$\eta^5$-$C_5H_4$($AsC_4Ph_4$)}] ..... 354
6.3.8 Synthesis of [$WRe(CO)_7${μ-$\eta^1$:$\eta^5$-$C_5H_4$($AsC_4Ph_4$)}] ..... 357
6.4 Attempted Syntheses of Free *As*-cyclopentadienyl Arsoles ..... 362
6.5 Summary ..... 365
6.6 Experimental ..... 367
6.6.1 [$MoMe(CO)_3${$\eta^5$-$C_5H_4$($AsC_4Ph_4$)}] ..... 367
6.6.2 [$WMe(CO)_3${$\eta^5$-$C_5H_4$($AsC_4Ph_4$)}] ..... 368
6.6.3 [PPN][$Mo(CO)_3${$\eta^5$-$C_5H_4$($AsC_4Ph_4$)}] ..... 368
6.6.4 [Mo(NO)$(CO)_2${$\eta^5$-$C_5H_4$($AsC_4Ph_4$)}] ..... 369
6.6.5 [$MoI(CO)_3${$\eta^5$-$C_5H_4$($AsC_4Ph_4$)}] ..... 370
6.6.6 [Rh(NBD)($\eta^5$-$AsC_4Ph_4$)] ..... 371
6.6.7 [$WRe(CO)_7${μ-$\eta^1$:$\eta^5$-$C_5H_4$($AsC_4Ph_4$)}] ..... 371

6.7 References ..... 372
Chapter 7 Coordination Complexes of 1,1'-Bis(Arsolyl)Ferrocenes ..... 375
7.1 Preamble ..... 376
7.2 Synthesis of 1,1'-Bis(Arsolyl)Ferrocenes ..... 379
7.2.1 1,1'-Bis(Tetraphenylarsolyl)Ferrocene (tpaf) ..... 379
7.2.2 1,1'-Bis(Tetramethylarsolyl)Ferrocene (tmaf) ..... 380
7.2.3 1,1'-Bis(Tetraethylarsolyl)Ferrocene (teaf) ..... 384
7.3 Classical Bidentate Coordination Complexes ..... 385
7.3.1 Synthesis of *cis*-[Mo($\kappa^2$-tpaf)$(CO)_4$] ..... 385
7.3.2 Synthesis of *cis*-[Mo($\kappa^2$-tmaf)$(CO)_4$] ..... 387
7.3.3 Synthesis of *cis*-[Mo($\kappa^2$-teaf)$(CO)_4$] ..... 388
7.3.4 Synthesis of [Ni($\kappa^2$-tmaf)$(CO)_2$] ..... 391
7.3.5 Synthesis of [Au($\kappa^2$-tmaf)$_2$][Au$(C_6F_5)_2$] ..... 394
7.3.6 Synthesis of *cis*-[Pd($\kappa^2$-tmaf)$Cl_2$] ..... 396
7.4 Monodentate Open-Bridge Coordination Complexes ..... 403
7.4.1 Synthesis of [$Ir_2$($\mu$-$\kappa^1$:$\kappa^1$-tmaf)$Cl_4$($\eta^5$-$C_5Me_5)_2$] ..... 403
7.4.2 Synthesis of [$Os_2$($\mu$-$\kappa^1$:$\kappa^1$-tmaf)$Cl_4${$\eta^6$-$MeC_6H_4$(*i*-Pr)-4}$_2$] ..... 405
7.4.3 Synthesis of [$Fe_2$($\mu$-$\eta^4$:$\eta^4$-tmaf)$(CO)_6$] ..... 406
7.4.4 Synthesis of [$Fe_4$($\mu$-$\kappa^1$:$\kappa^1$-$\eta^4$:$\eta^4$-tmaf)$(CO)_{14}$] ..... 409
7.4.5 Synthesis of [$Fe_2$($\mu$-$\kappa^1$:$\kappa^1$-tmaf)$(CO)_8$] ..... 412
7.5 Summary ..... 413
7.6 Afterword to this Thesis ..... 414
7.7 Experimental ..... 415
7.7.1 Synthesis of 1,1'-Bis(Arsolyl)Ferrocenes ..... 415
7.7.2 Synthesis of Bidentate Coordination Complexes ..... 419
7.7.3 Synthesis of Monodentate Open-Bridge Complexes ..... 424
7.8 References ..... 428
Appendix ..... 430
8.1 Preamble ..... 431
8.2 The Crystal Structure of [Fe($PhAsC_4Ph_4$)$(CO)_4$] ..... 431
8.3 The Crystal Structure of [W($PhAsC_4Me_4$)$(CO)_5$] ..... 432
8.4 The Crystal Structure of [Mn($PhAsC_4Me_4$)(NO)(CO)($\eta^5$-$C_5H_4Me$)]$PF_6$ ..... 434
8.5 The Crystal Structure of (HO)(O)$AsC_4Ph_4$ ..... 436
8.6 The Crystal Structures of $Ph(Cl)_2AsC_4Ph_4$, $Ph(Cl)_2AsC_4Ph_2H_2$ and $(HO)(Cl)_2AsC_4Ph_4$ ..... 437
8.7 The Crystal Structure of ($C_5Me_5$)$AsC_4Ph_4$ ..... 439
8.8 The Crystal Structure of $(AsC_4Me_4)_2$ ..... 441
8.9 The Crystal Structure of $ClAsC_4$(*t*-Bu)$_2Me_2$ ..... 443
8.10 References ..... 445

# Chapter 1

# Introduction to the Chemistry of Arsacyclopentadienes

## 1.1 Preamble

The first arsole* to be described – 1*H*-1,2,3,4,5-pentaphenylarsole – arose as one of many fruits from burgeoning studies into the newly-discovered organolithium reagent 1,4-dilithio-1,2,3,4-tetraphenylbutadienide.[1] Preceding this were the annulated derivatives 9*H*-9-phenylarsafluorene[2, 3] and 1*H*-1-phenylarsaindole,[4] also obtained from their respective organometallics. The short 1959 communication from LEAVITT *et al.* to the editor of the *Journal of the American Chemical Society* mentioned other laboratory curiosities including pentaphenylphosphole and -stibole, hexaphenylgermole and -stannole, and bicyclic octaphenylspiro compounds of the heavier Group 14 elements, with the usual brevity in experimental details typical of the era. Recognition of the conceivable aromatic character of these rings was not lost on LEAVITT, their report concluding with the foretelling statement: "…*Concurrent with the synthetic studies, we are attempting to determine the chemical nature of these new ring systems with regard to the possible aromaticity of the five-membered ring, ability to form π-electron complexes with metals, and the normal diene reactions.*" The same authors would release a full paper in the following year wherein the distinct absence of chemical aromaticity (insofar as it was defined at the time) in several of these compounds was mooted,[5] which was further corroborated in 1961 by BRAYE *et al.* whom independently obtained an even larger array of new tetraphenyl-decorated heterocyclopentadienes *via* the same organolithium route.[6]

The above works were significant since, at the time when the so-called "double bond rule" somewhat prematurely circumscribed chemist's imagination, heterocyclopentadienes for the lighter elements (*e.g.*, N, O, S) were predominant and those of the remaining *p*-block elements (B, Al, Ga, In, Tl; Si, Ge, Sn, Pb; P, As, Sb, Bi; Se, Te; also Zn, Cd, Hg, and transition metals) were perceived as somewhat exotic and could not be prepared by the same "organic" routes.† Some five-membered ring systems or their substituted derivatives (*e.g.*, pyrroles, furans and thiophenes) were naturally occurring synthons and could be isolated from plant, animal, or bituminous matter yet stannole, phosphole, arsole *etc.* had no apparent place within the "Vital Force" (*sic.*) doctrine. The chemical properties of these heavier ring systems were

* Throughout this work, the term "arsole" is reserved exclusively for non-annulated ring systems (the same applies to other heterocyclopentadienes a.k.a. "heteroles"); fused derivatives *e.g.*, 9*H*-arsafluorene or 1*H*-arsaindole – whilst containing an unsaturated five-membered ring with an arsenic atom – will be called as-such and are never referred to as "arsoles".

† For instance, the PAAL-KNORR synthesis of pyrroles/furans/thiophenes from a 1,4-dicarbonyl and a primary amine/BRØNSTED acid/$P_4S_{10}$ fails for many other *p*-block elements including primary phosphines and arsines.

unknown and could not have been accurately envisioned with the knowledge of the time nor interrogated with the available instrumental techniques; in this regard, even the syntheses of these "heteroles" alone was considered an achievement.

During the interregnum between the first reports (late 1950's) and the present day, the chemistry of heterocyclopentadienes has expanded considerably although some platforms have matured at a greater pace than others: silole (1*H*-silylacyclopentadiene) and phosphole (1*H*-phosphacyclopentadiene) are probably the best-studied in the field whilst others are severely underrepresented. One may even find a casual inverse correlation between atomic number *Z* and gross results from database search queries (**Figure 1.1**), perhaps speaking to the preference toward certain elements on behalf of the Synthetic Chemist, not least due to the availability of $^{29}$Si and $^{31}$P NMR spectroscopy. This discussion would be remiss if it were not mentioned that silicon and phosphorus are relatively non-toxic *per se*, a sentiment which cannot be shared by their counterparts tin, lead, arsenic, antimony and so on (bismuth is a notable outlier). The malevolent reputation of these elements must be noted at the outset and is undoubtedly a contributing factor in their underdevelopment.

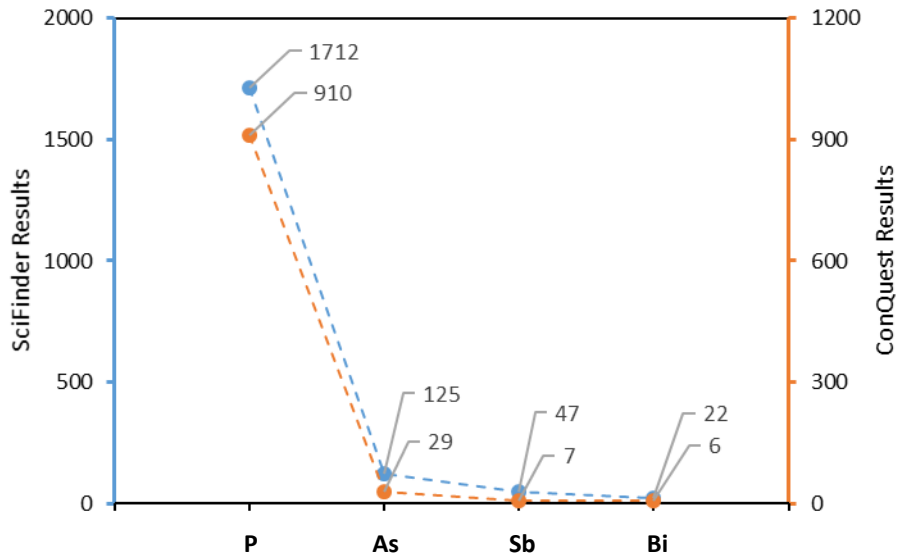



**Figure 1.1**: Net returned results of search queries entered into SciFinder$^{n}$ (CAS) (any mention of "phosphole", "arsole" *etc.* including theoretical studies and reviews but excluding patents and conference proceedings; blue trace) and ConQuest (CSD) (any crystal structure containing a non-annulated 1*H*-heterocyclopentadiene/dienide of P, As *etc.*; orange trace). Numbers are correct as of April 2023. **Note**: the ordinate axes are of differing scales.

The following will be an as-comprehensive-as-possible summary of arsole chemistry, though it is necessarily selective towards non-annulated ring systems only. Heterocycles such as 9-arsafluorenes, 1-arsaindoles, arsabenzenes and the like are excluded from this purview except where comparisons are instructive. To the best of this author's knowledge there are no reviews dedicated purely to arsole chemistry.

## 1.1 The Question of Aromaticity

As mentioned in passing above, the question of aromaticity within any new heterocyclic system is intimately tied with the desire to synthesise the ring itself. LEAVITT *et al.* state as much in their initial reports and posit the potential involvement of the trivalent Group 15 element (P, As, Sb) within ring delocalisation. However, BRAYE and co-workers should be credited with the first experimental insight into the aromatic tendencies of pentaphenylphosphole, -arsole *etc.* to whom it was readily obvious that such compounds were *not* aromatic in the way pyrrole was known to be. In particular, the readiness with which the rings reportedly bound iron(0) tricarbonyl – known for its fondness of conjugated *S-cis* dienes – spoke to a certain availability of the four π-electrons inhabiting the backbone (**Section 1.4.3**). Other reactivity patterns indicated typical diene behaviour, such as DIELS-ALDER adduct formation with dienophiles (**Section 1.3.3**). More relevant to phosphorus (for its increased basicity), *P*-oxide, -sulfide and -selenide adducts also form under mild conditions, especially with regards to aerobic oxidation; neither of these reactions – [4+2] cycloaddition nor oxidation of the heteroatom – are commonplace to (aromatic) pyrroles.

Early studies[1, 5, 6] (all chemical in nature) surmised that the reduced availability of the lone pair was inherently due to the poor basicity of tertiary arsines and not due to involvement in delocalisation. One piece of joint experimental evidence from MÄRKL and MATHEY in the form of photoelectron spectroscopic data concluded that arsoles (also phospholes) were not aromatic compounds as the ionisation potentials of the lone pair *n*-electrons were virtually identical between a series of substituted arsoles (and phospholes) and their fully saturated analogues.[7] Thus, participation of the lone pair in cyclic delocalisation (that is, an *n*-π interaction) was deemed minimal or non-existent since no aromatic stabilisation was measured on going from an arsolane to an arsole (phospholane to phosphole) ring system.

This was subsequently challenged by EPIOTIS and CHERRY who argued that the same photoelectron spectroscopic data were in fact supportive evidence for delocalisation, their own calculations predicting

*some* overlap between the heteroatom hybrid atomic orbital housing the lone pair electrons and α-carbon($p_z$) atomic orbitals.[8] The computed magnitude of this overlap coefficient was modest and notably far from optimum, though the authors offered alternative interpretations of other observations made by MÄRKL and MATHEY including an explanation for why the ionisation potential of the heteroatom was virtually identical between saturated and unsaturated ring systems (tedium beyond the scope of this short overview) which maintain the non-zero aromatic perspective of phosphole and arsole.* More-recent photoelectron spectroscopic interrogation of a wider range of heterocycles estimated 1-methylarsole to have an aromatic stabilisation energy *ca* 36% that of 1-methylpyrrole.[9]

Numerous computational studies[10-18] have since attempted to quantify the "aromatic character" of arsoles using a variety of energetic, magnetic and/or structural criteria with the relative "aromaticity" of arsoles estimated to be ~10—40% that of pyrrole, depending on the specific indicator of aromaticity employed. Whilst some contradictory or inconsistent conclusions do arise between these works, in many regards this is due to the inherent dependence of computational outcomes upon the choice of modelling method, basis set, aromaticity index *and* human interpretation which (like computational resources) naturally become more sophisticated over time and therefore more closely approach reality. However, the greatest caveat undermining the question "*How aromatic is molecule X*?" paradoxically arises from the fact that despite connoting a widely accepted idea of a certain characteristic, *the concept of aromaticity lacks both a universal, indisputable definition and an absolute metric*.[10] This point is important since the apparent means by which "aromaticity" as a phenomenon may be encoded into a molecule are multi-faceted *e.g.*, energetic, magnetic, structural or chemical manifestations which are not necessarily evenly weighted. Furthermore, the criteria used to define these aspects are invariably given with respect to aromatic, non-aromatic and antiaromatic reference molecules. Therein, arbitrary finite boundaries where "aromatic character" may or may not reside must be set, and in this regard it is not surprising that internal contradictions arise. Reviews from BALABAN, ONICIU and KATRITZKY,[19] STANGER,[20] and OTA and KINJO[21] covers aspects of these different definitions of aromaticity within various heterocycles in exquisite detail.

* It should be noted that the authors do not claim phospholes and arsoles to be fully delocalised HÜCKEL aromatic compounds, rather they contest the premise that they are totally non-aromatic. Though it is not explicitly stated as such in the text, nowadays their argument would be considered affirmative of "non-zero aromatic character".

In short, the general consensus is that λ³-arsoles (alongside phospholes, stiboles and bismoles) are not to be explicitly treated as aromatic compounds, or at least not in the same way as pyrrole. That is, they are not HÜCKEL aromatic. There are two insurgent factors – one geometric and one electronic – that dictate this outcome without retreating to computational or quantum mechanical intricacies:

1) *Geometric*: λ³-phosphole, -arsole, -stibole and -bismole ring systems are not planar species, a feature directly tied to the formidable inversion barrier* of the heavier *sp*³-hybridised pnictogens.[17, 22] For this reason, the heteroatom is invariably extruded from the mean plane of the butadiene carbons by up to *ca* 15° in some cases; this folding of the ring (likened to that of an envelope) is also observed in clearly non-aromatic cyclopentadiene(s). Furthermore, whereas the valence geometry of the nitrogen atom in pyrroles is trigonal, the heteroatoms in its heavier cousins are markedly pyramidal such that the P/As/Sb/Bi substituent is projected outboard of the mean plane of the ring by roughly 80—100°; the effect therein is a displacement of the heteroatom lone pair from orthogonality with the butadiene plane, reducing the effective orbital overlap. It should be noted that whilst a planar ring conformation *is* predicted to be a strongly delocalised species,[12, 18] the inversion energy barrier of the heteroatom *which must traverse a planar transition state* is often calculated to exceed the aromatic stabilisation afforded.[17]

2) *Electronic*: the *p* orbital housing the nitrogen lone pair enjoys superb topological and energetic compatibility with carbon *p* orbitals such that π-bonding is proliferous between these elements, that due to small covalent radii naturally form short bonds. In contrast, the aptitude of (*p*-*p*)π mixing decreases sharply for main group elements below the first row wherein orbitals become increasingly diffuse and energetically mismatched,[23] since the relative sizes of the valence n*s* and n*p* atomic orbitals are greater in the case of the heavier pnictogens any hybridization becomes less amenable, resulting in inefficacious and weak π-bonding.[21] In this case, kinetic stabilisation or metallic complexation is the primary means by which, say, a free As=C or As≡C bond might be supported without diverting to lower-energy pathways.[24-28] Arsoles are no

* Descending Group 15 sees the n*s* orbital contribute less-effectively to bonding, resulting in a contraction of inter-substituent angles, so-called *p*³ hybridisation (*i.e.*, non-hybridisation).

different and the propensity for delocalisation suffers extensive diminution compared to pyrroles. The reduced species (an arsolyl anion $[AsC_4R_4]^-$) is, however, a *bona fide* 6π-HÜCKEL aromatic compound.[29-31]

X-ray crystallographic data collected until present have appeared sporadically, and while some 70 unique crystal structures of arsoles and their transition metal complexes have been determined throughout the course of this thesis, it can be said that physical structural evidence for aromatic character is largely absent: the mean endocyclic As-C($sp^2$) bond (*ca* 1.93 Å) is virtually identical to that of a typical acyclic As-C($sp^2$) bond (*ca* 1.95 Å). Internal C=C and C-C bonds within the rings (*ca* 1.35 and 1.45 Å, respectively) are typical and – notably – statistically distinct. Solution $^{13}C\{^1H\}$ NMR data convey a similar conclusion with resonances for the carbon nuclei in the 2,5- and 3,4-ring positions appearing at ~160—140 ppm (depending on substituent pattern) with those closest to the arsenic atom shifted to higher field. Indeed, one may find a monotonous trend to higher chemical shifts for ring carbon atoms upon descending the Group 15 elements, charted for the $PhEC_4H_4$ series (E = N, P, As, Sb) in **Figure 1.2**.

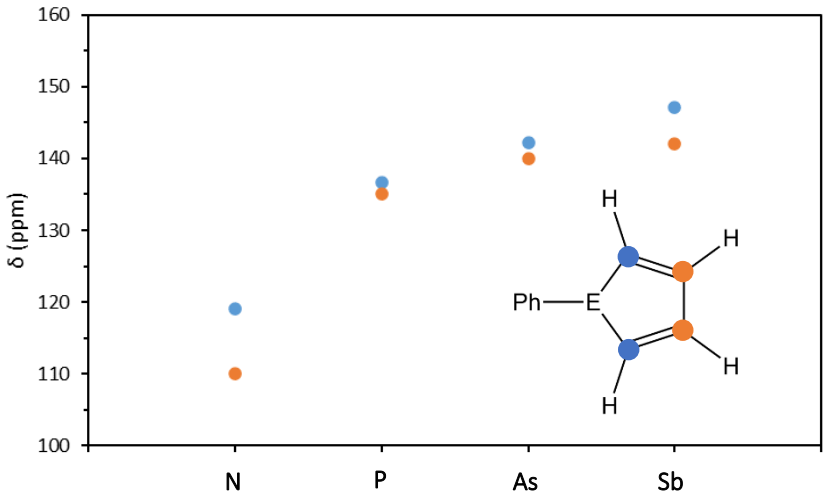



**Figure 1.2**: $^{13}C\{^1H\}$ NMR shifts for ring-carbon nuclei among the series 1-phenylpyrrole, -phosphole, -arsole and -stibole in $CDCl_3$. Data retrieved from *Ref.* 37.

The chemical shifts of the ring-carbon atoms clearly fall beyond the general region of aromatic five-membered rings, the increasing $^{13}C$ displacement to higher frequencies almost certainly an artifact of paramagnetic contributions influencing nucleus deshielding rather than from any appreciable ring current. In cases where directly comparable data exist for a $\lambda^3$-arsole and its anion,[29] the presence of a formal 6π-

electron ring-current causes the $^{13}C$ signals to shift *up*field by only a few ppm, and tens of ppm in the case of *pentahapto* metal complexation (**Chapter 3**, **Section 3.3**). Evidence for paramagnetic deshielding in $\lambda^3$-heteroles is found in calculating the HOMO-LUMO divide ($\Delta E$) for the series $HEC_4H_4$ (E = N, P, As, Sb) using DFT (gas phase: ωB97X-D/6-31G*/LAN2DζΦ) which decreases with ascending atomic number. It is noteworthy that the trend in $^{13}C$ shifts is a near mirror-image of the trend in HOMO-LUMO gap, as would be expected based on the proposals of KARPLUS and PEOPLE that the paramagnetic deshielding component ($\sigma_{para}$) of the total magnetic shielding is inversely proportional to the energy gap $\Delta E$.[32, 33]

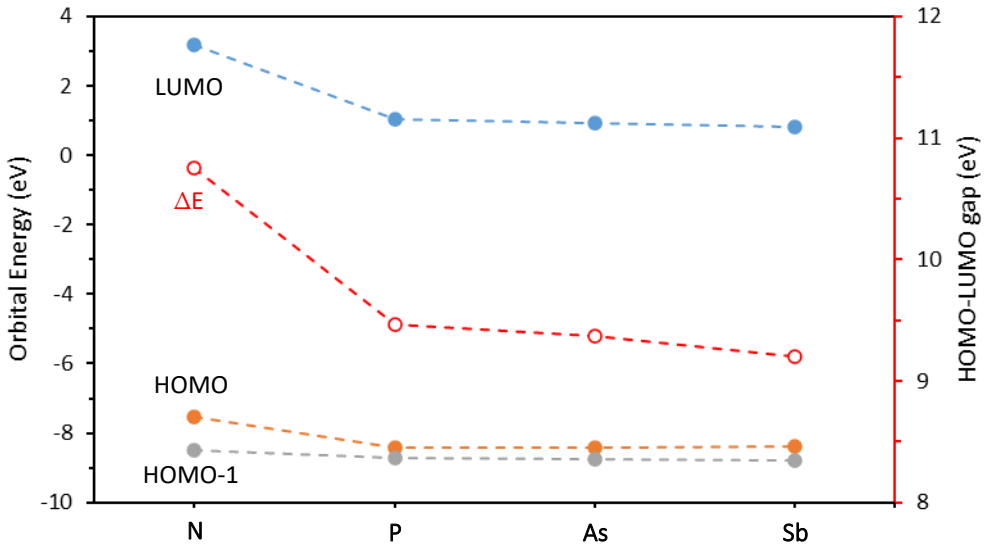



**Figure 1.3**: Calculated frontier orbital energies for $HEC_4H_4$ (E = N, P, As, Sb) and HOMO-LUMO gaps (○) using DFT in the gas phase at the ωB97X-D/6-31G*/LAN2Dζ level of theory (this work). **Note**: the ordinate axes are of differing scales.

The molecular orbitals of the parent arsole and some substituted derivatives are well-known and may be found elsewhere,[34, 35] though some will appear at various stages throughout this work where appropriate, recalculated using Density Functional Theory (DFT) at the ωB97X-D/6-31G* level of theory. Suffice it to say, no molecular orbital of π-symmetry which is delocalised over the entirety of the ring is to be found, as is the case with pyrrole. Perhaps speaking to the poor basicity of the As(III) centre, the HOMO is invariably constructed from the localised butadiene(π) orbitals and the heteroatom lone pair typically found in the HOMO-1.

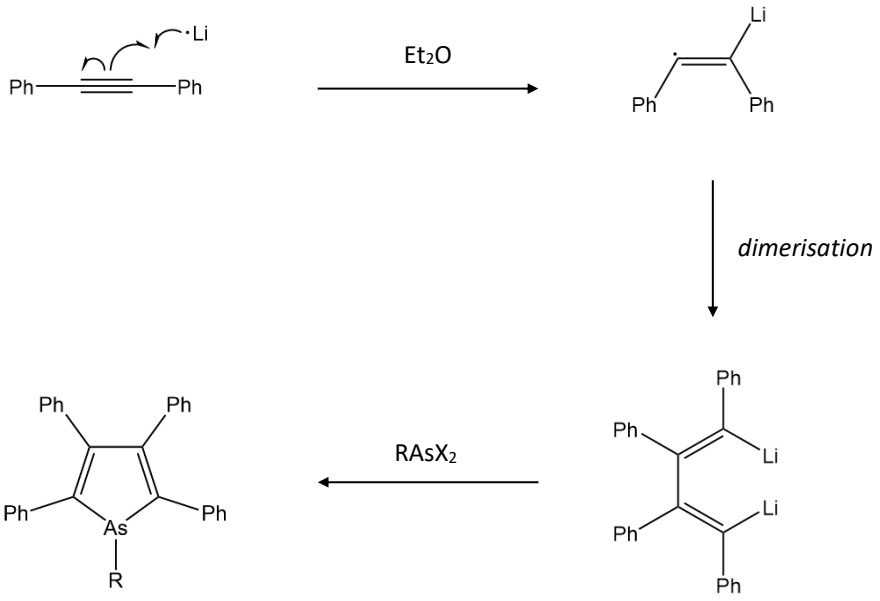
Φ The range-separated ωB97X-D functional is used extensively and consistently in this thesis specifically because – in search of possible conjugation effects – it includes damped atom-atom dispersion corrections capable of capturing not only short but also long-range effects.

## 1.2 Synthesis of Arsoles

At present, there are three prescribed strategies for synthesising arsoles – all involve some means of a direct union between the trivalent arsenic atom and the preassembled four-carbon group. Two of the methods utilise an electrophilic arsenic source and nucleophilic butadiene-diyl fragment, and the other inverts this polarity to reconcile the same outcome. They will be introduced in chronological order and an overview of their scope provided. In all cases the method is generalisable to some extent in one or more ways which will be indicated as appropriate; however, an arsenocentric perspective will predominate throughout.

### 1.2.1 *Via* 1,4-Dilithiobutadienides

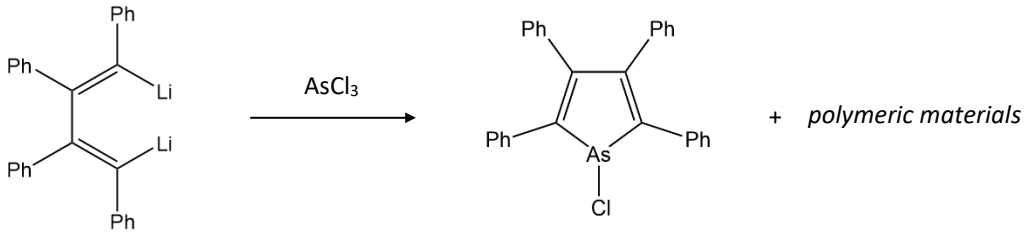
The first method has already been mentioned in the preamble to this section; that is, the addition of an organoarsine dihalide ($R'AsX_2$) to a 1,4-dilithiobutadienide ($Li_2C_4R_4$) in $Et_2O$ medium (**Scheme 1.1**).[1, 5, 6] The necessary organolithium species is obtained *in situ*, though not quantitatively, by reductive dimerisation of diphenylacetylene (PhC≡CPh) with elemental lithium.




**Scheme 1.1**: The original synthesis of 1-R-2,3,4,5-tetraphenylarsole as described separately by LEAVITT and BRAYE.

The method is limited in its scope: only diarylalkynes of inert functionality undergo this reductive coupling and the reaction is beset by *ortho*-phenyl metalation – under certain conditions – producing

triarylnaphthalenes with depletion in the concentration of the dilithiobutadienyl.[5, 36] Practically, this side-reaction is usually of little consequence to the Synthetic Chemist since a great deal of 1-(organyl)-2,3,4,5-tetraphenylarsoles are air stable crystalline compounds amenable to column chromatography or aerobic re-crystallisation. The method is satisfactory when the incoming main group electrophile possesses only two exchangeable halide substituents ($R'_2SnX_2$, $R'AsX_2$, $SX_2$ *etc.*) whereupon ring formation is the prevailing outcome; for main group polyhalides (*e.g.*, $AsCl_3$) stochastic processes such as formation of oligo- or polymeric materials become non-negligible, and this (in addition to the occurrence of naphthalene side-products) can lead to some operational challenges in purification of the target 1-halo-heterole.



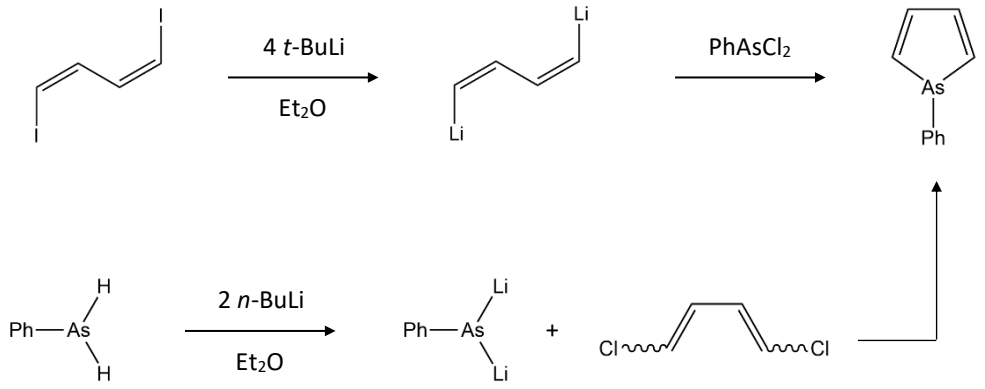

**Scheme 1.2**: BRAYE'S original synthesis of 1-chloro-2,3,4,5-tetraphenylarsole.

Whilst BRAYE only isolated 1-chloro-2,3,4,5-tetraphenylarsole ($ClAsC_4Ph_4$) from the reaction between $Li_2C_4Ph_4$ and $AsCl_3$ in an impure state,* it could be converted to the already encountered $PhAsC_4Ph_4$ by addition of PhLi to the *in situ* formed product. It is fortunate that the authors described this course of events since it serves an illustrative example of why $ClAsC_4Ph_4$ is best *not* synthesised *via* this approach: the reported isolated yield of $PhAsC_4Ph_4$ by direct addition of $PhAsCl_2$ to $Li_2C_4Ph_4$ was *ca* 90% (highly respectable) whereas the sequential addition of $AsCl_3$ followed by PhLi to the same nucleophile gave $PhAsC_4Ph_4$ in only *ca* 30% isolated yield. Given that this particular route is 1) suitable for obtaining *only* symmetrical 2,3,4,5-tetra-arylheteroles, and 2) unsuitable for obtaining heteroles with reactive groups at the heteroatom, the use of 1,4-dilithiobutadienides was gradually superseded by the following two methods (with one exception; *vide infra*) and is practically obsolete in the present day.

* With regards to $ClAsC_4Ph_4$: "… *the combination of difficulties met in purifying the sample and the problems inherent in an analysis of organometallic halides did not allow for unequivocal analysis for this product.*"

The first caveat above can be circumvented (with more resource-intensive efforts on behalf of the Synthetic Chemist) since it is possible to obtain 1,4-dilithiobutadienides without aryl substituents, or indeed any substituents whatsoever. ASHE has described the synthesis of 1-phenylheteroles ($PhEC_4H_4$; E = P, As, Sb) by metal-halogen exchange of *Z*,*Z*-1,4-diiodobutadiene ($C_4H_4I_2$) with *t*-BuLi in ethereal solution, giving the parent 1,4-dilithiobutadienide ($Li_2C_4H_4$) which undergoes ring-closure upon treatment with $PhECl_2$;[37] it should be mentioned that the preparation of the necessary 1,4-diiodobutadiene precursor as-outlined by ASHE is by no means trivial.* The synthesis of undecorated heteroles was impressive at the time and – in line with previous sentiments – linked with the desire to interrogate the potential subtle aromatic character of such rings which might otherwise be disguised by the presence of organic groups on the diene system. It eventuated that no such obscuration was taking place (**Figure 1.2**).

As an aside and to conclude this section, ASHE has also described the reciprocal arrangement whereby a nucleophilic arsenic fragment may be married to the four-carbon chain: dual deprotonation of $PhAsH_2$ with *n*-BuLi generates dilithiophenylarsenide ($PhAsLi_2$) which undergoes ring-closure when introduced to 1,4-dichloro-1,3-butadiene (mixture of isomers) in $Et_2O$ solution, giving 1-phenylarsole in 25% isolated yield.[38]

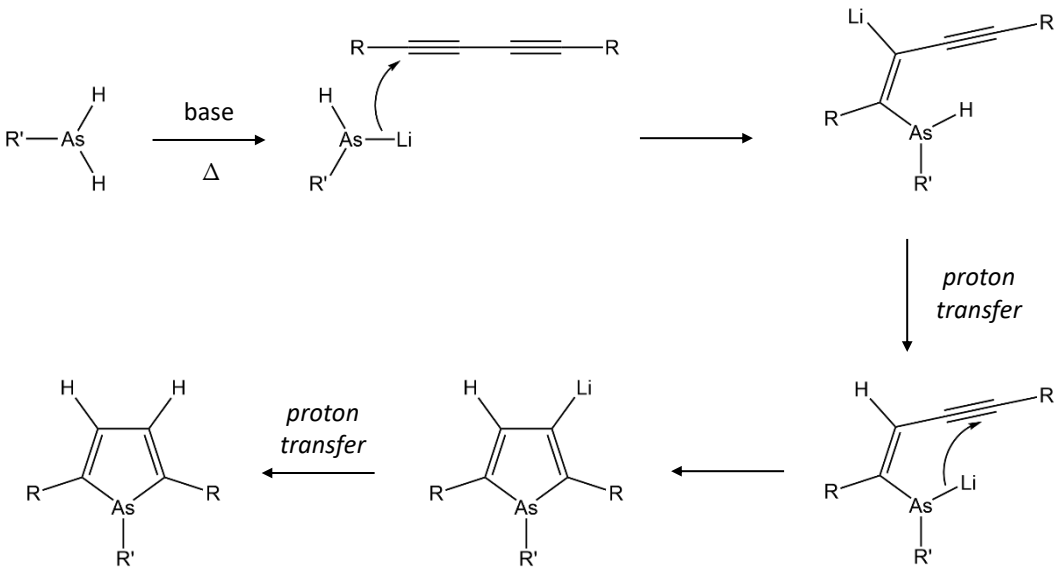



**Scheme 1.3**: ASHE'S convergent syntheses of 1-phenylarsole.

* Dehydrohalogenation of 1,4-dichloro-2-butyne ($ClH_2CC{\equiv}CCH_2Cl$) with excess sodium amide ($NaNH_2$) in liquid ammonia gives disodiumdiacetylide ($NaC{\equiv}CC{\equiv}CNa$) which affords 1,4-diiodobutadiyne upon treatment with $I_2$ (55% over two steps). This undergoes diimide hydrogenation with potassium azobiscarboxylate in alcoholic pyridine which yields the *Z*,*Z* isomer of 1,4-diiodo-1,3-butadiene (55%) upon acidic workup. *Note*: the main text states *n*-BuLi as the lithium-halogen exchange reagent; however, accompanying reaction schemes and subsequent citing papers explicitly list *t*-BuLi for this purpose. The latter appears to be the correct organolithium since *n*-BuLi often requires TMEDA (*N*,*N*,*N*,*N*-tetramethylethylenediamine) or similar to affect double-metalations of unsaturated organic molecules.

### 1.2.2 *Via* 1,4-Disubstituted Butadiynes

The second approach involves the base-catalysed addition of a primary organoarsine ($R'AsH_2$) across a 1,4-disubstituted butadiyne ($RC{\equiv}CC{\equiv}CR$) under moderately forcing thermal conditions,[39, 40] which incidentally provided access to the first examples of 2,5-disubstituted arsoles otherwise unattainable by the original route (*vide supra*). MÄRKL proposes the reaction to begin with a monolithioarsinide (R'AsHLi, formed by action of the catalytic base such as PhLi or *n*-BuLi) which engages in nucleophilic attack upon a terminal carbon atom of the butadiyne (where the LUMO coefficient is greatest), forming a β-carbanion which subsequently undergoes proton-transfer to generate a (*Z*-β-ethynylvinyl)lithioarsenide. The process repeats a second time in an intramolecular manner to generate the five-membered ring and may also be affected by radical initiators.[41]



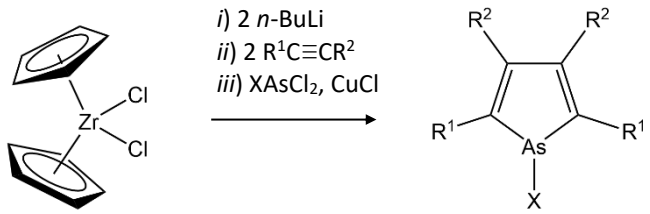

**Scheme 1.4**: MÄRKL'S synthesis of 2,5-disubstituted arsoles.

Isolated yields of the $R'AsC_4R_2H_2$ arsoles from this route follow the electronic nature of the groups garnishing the butadiyne, where yields of *ca* 80% were obtained for R = Ph, *p*-$C_5H_4Cl$ and 2-naphthyl, but 50% for R = *p*-$C_6H_4Me$ and 30% for R = Me. This trend follows the inductive effect that electron-withdrawing substituents have on the molecular orbital framework of the butadiyne, consolidating the LUMO at the 1,4-carbon atoms and increasing their FUKUI coefficient (**Chapter 2**, **Section 2.7.4**) toward nucleophilic attack by the arsenide. It is also worth mentioning that the same inductive effect will

undoubtedly stabilise the carbanion thus formed. The formal addition of As-H bonds across an alkyne (diyne) is superficially reminiscent of other unsymmetrical hydrogenations (*e.g.*, hydrostannylation, hydrozirconation) which can proceed under free-radical or base-catalysed conditions, and has naturally been extended to the synthesis of 2,5-disubstitued phospholes,[42] and other novel ring systems[43, 44] Despite its generalisable utility, the method has in only one apparent case (by BRAYE[41]) been used outside the laboratories of MARKL and ASHE probably due to the inconvenience of first preparing and handling maliferous volatile and toxic primary organoarsines.

### 1.2.3 *Via* Transmetalation

A contemporary synthesis of any heterocyclopentadiene will invariably involve the use of a Group 4 metal (usually zirconium, though titanium or hafnium may also suffice) to assemble the ring before transmetalation to a main-group dihalide. The basis of the FAGAN-NUGENT method[45-47] (as it has come to be known) is the high electropositivity of the early transition metals* in comparison to the *p*-block elements, providing a strong enthalpic incentive for transfer of a nucleophilic carbocyclic fragment. The ability of divalent Zr (also Ti, Hf) to oxidatively-couple a pair of internal alkynes was previously described by ALT and RAUSCH (photolysis of $[ZrMe_2(\eta^5\text{-}C_5H_5)_2]$ in the presence of PhC≡CPh[48, 49]) and by THANEDAR and FARONA (amalgamated magnesium reduction of $[ZrCl_2(\eta^5\text{-}C_5H_5)_2]$ in the presence of PhC≡CPh[50]); however, the approach of NEGISHI reported in 1986 exploiting the di-*n*-butyl zirconocene intermediate is considerably more convenient.[51] Notably, though somewhat passed over, is that 1,1-bis(cyclopentadienyl)-2,3,4,5-tetraphenylzirconacyclopentadiene ($[ZrC_4Ph_4(\eta^5\text{-}C_5H_5)_2]$) was among the heterocycles initially synthesised – incidentally – by BRAYE in the same report which lists pentaphenylarsole.[6]




**Scheme 1.5**: The FAGAN-NUGENT synthesis of heterocyclopentadienes, with an arsole given as a specific example.

* PAULING electronegativities: χ(Ti) = 1.54, χ(Zr) = 1.33, χ(Hf) = 1.30.

To illustrate the pace at which zirconacycle chemistry accelerated, FAGAN and NUGENT would outline their eponymous protocol less than one year after NEGISHI'S description of the organometallic reagent (*vide infra*) that would be the cornerstone of this and other synthetic targets. Organozirconium chemistry is now exceedingly mature and the [2+2+1] cyclisation of unsaturated molecules has been expanded to a gamut of substrates, affording an efficient means to assemble otherwise complicated macrocyclic systems on large scales in a highly predictable manner. Given its central role in preparing the arsoles used throughout this work and profound influence on the course of heterocyclic chemistry in general (and this author's personal fondness for Group 4 chemistry), some discussion will be devoted to aspects of the FAGAN-NUGENT heterocyclopentadiene synthesis.

Three principal steps are inherent to the protocol:

1) Genesis of a synthetic equivalent for low-valent [$Zr(\eta^5\text{-}C_5H_5)_2$] "zirconocene" (**Scheme 1.6**),

2) Oxidative coupling of two alkynes to generate a five-membered zirconacycle (**Scheme 1.7**),

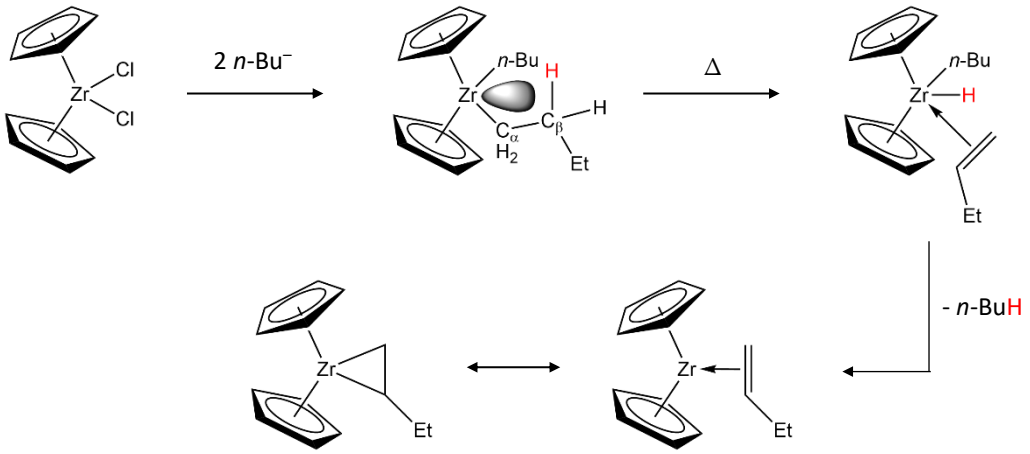
3) Transmetalation of the nucleophilic ring portion to a *p*-block electrophile (**Scheme 1.9**).

Accessing the requisite low-valent zirconium species exploits the ability of their dialkyl metallocenes [$ZrR_2(\eta^5\text{-}C_5H_5)_2$] to engage in thermal β-hydrogen elimination (where possible). The most popular alkyls for this purpose (the ethyl and *n*-butyl residues*) are easily installed onto the metal centre by addition of GRIGNARD or organolithium reagents to the metallocene dihalide [$ZrX_2(\eta^5\text{-}C_5H_5)_2$] at low temperature. The ephemeral diethyl or di-*n*-butyl metallocene – by virtue of coordinative (*pseudo*-tetrahedral) and electronic (16-electron) unsaturation – possesses a vacant metal *d*-orbital which spatially projects between the alkyl ligand-pair and is suitably disposed to interact with a nearby $C_\beta$-H bond. Capture of the hydride followed by reductive elimination of an alkane molecule (*i.e.*, ethane or *n*-butane) ensues upon warming to near-ambient temperatures,[51] generating a metastable Zr(II) species of the form [$Zr(\eta^2\text{-alkene})(\eta^5\text{-}C_5H_5)_2$]† with partial Zr(IV)-metallocyclopropane character. This π-alkene complex is typically *so exceedingly labile* that it is casually viewed as synthetic short-hand for the non-isolable carbenoid

* Diethyl zirconocene [$ZrEt_2(\eta^5\text{-}C_5H_5)_2$]: "TAKAHASHI Reagent". Di-*n*-butyl zirconocene [$ZrBu_2(\eta^5\text{-}C_5H_5)_2$]: "NEGISHI Reagent".

† Since syntheses are typically carried out in THF medium, this 16-electron complex is potentially solvated.

"zirconocene" [Zr($\eta^5$-$C_5H_5$)$_2$].* A handful of such π-alkene complexes have been intercepted and characterised as the 18-electron $PMe_3$-coordinated compounds.[52-55] Elegant experiments carried out by TAKAHASHI have revealed a profound kinetic dependence on the identity of the alkyl group where thermal decomposition of [$ZrR_2$($\eta^5$-$C_5H_5$)$_2$] is encouraged by residues with *least*-substituted β-carbon centres,[56] and a second mechanism involving σ-bond metathesis is hypothesised for aryl groups.[57, 58]

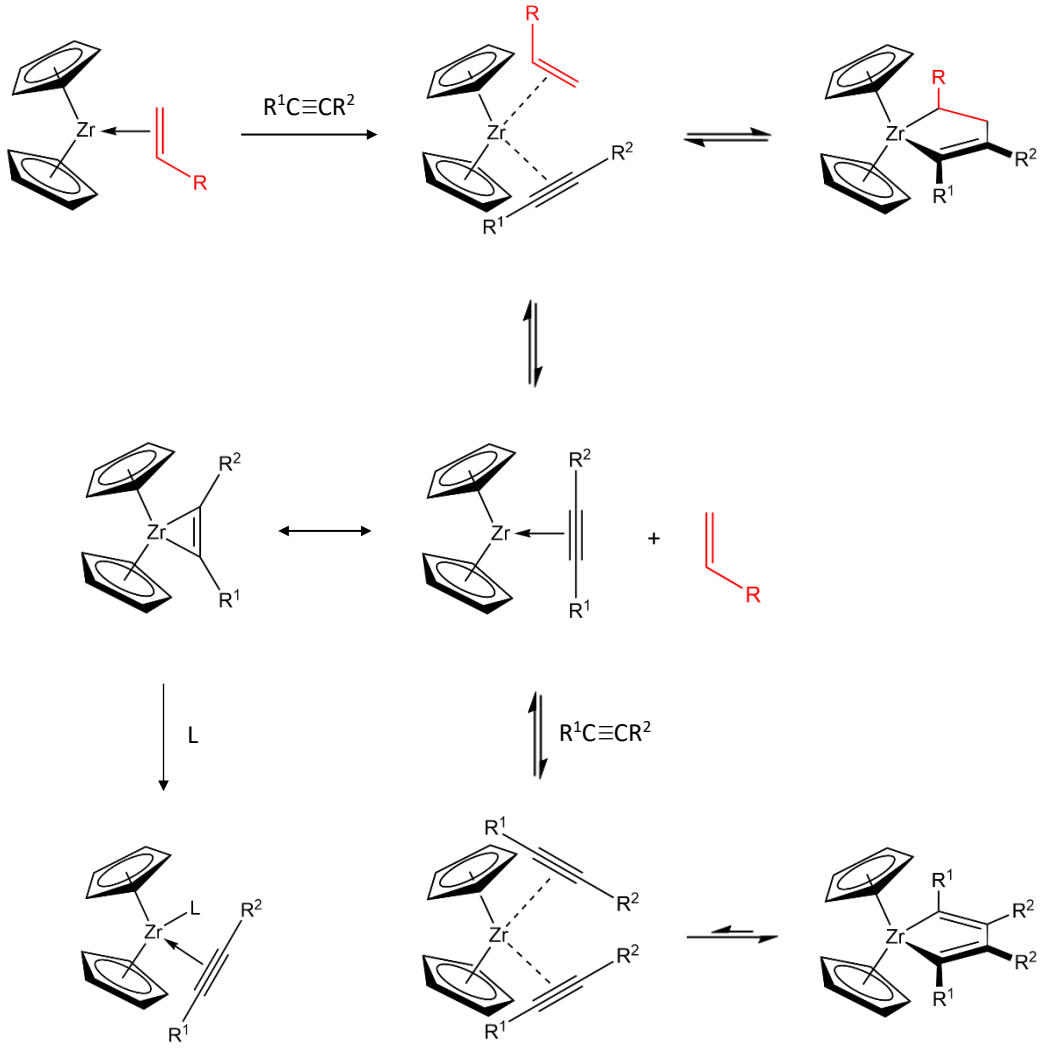



**Scheme 1.6**: Thermal decomposition of [$ZrBu_2$($\eta^5$-$C_5H_5$)$_2$] to [Zr($\eta^2$-1-butene)($\eta^5$-$C_5H_5$)$_2$], a labile Zr(II) equivalent. **Note**: only one lobe of the vacant Zr(IV) *d*-orbital is shown (in the second panel) for visual simplicity and ease of illustration.

Metallacycle formation proceeds through a sequence of microscopically reversible dissociation/association steps (**Scheme 1.7**), a point which is necessary to account for certain regiochemical preferences when unsymmetric substrates are offered to "zirconocene" (*vide infra*). For the specific case of zirconacyclopentadienes, the product initially formed upon addition of an alkyne to [Zr($\eta^2$-alkene)($\eta^5$-$C_5H_5$)$_2$] is an asymmetric ring system derived from coupling of the stabilising olefin; a handful of these have been isolated and characterised where the longevity of the metallacyclopentene so-permits.[59-62] In others, complexes of the form [Zr($\eta^2$-alkyne)L($\eta^5$-$C_5H_5$)$_2$] with partial metallacyclopropene character may be intercepted by addition of a suitable LEWIS base, typically $PMe_3$ or pyridine.[63-66] In most cases, however, the reversible nature of adduct formation means that a second equivalent of incoming alkyne is assiduously

* Early papers claimed to have isolated [Zr($\eta^5$-$C_5H_5$)$_2$] "zirconocene" by reduction of the corresponding dihalide; these are grossly erroneous and "zirconocene" has since been shown to be the dimeric Zr(III) complex [(μ-$\eta^5$:$\eta^5$-$C_{10}H_8$)$Zr_2$(μ-H)$_2$($\eta^5$-$C_5H_5$)$_2$]. "Titanocene" [Ti($\eta^5$-$C_5H_5$)$_2$] has also been shown to be an analogous fulvalene-hydride Ti(III) dimer. See P.J. CHIRIK *Organometallics*, **2010**, *29*, 1500—1517 for an interesting account of the historical significance of these discoveries.

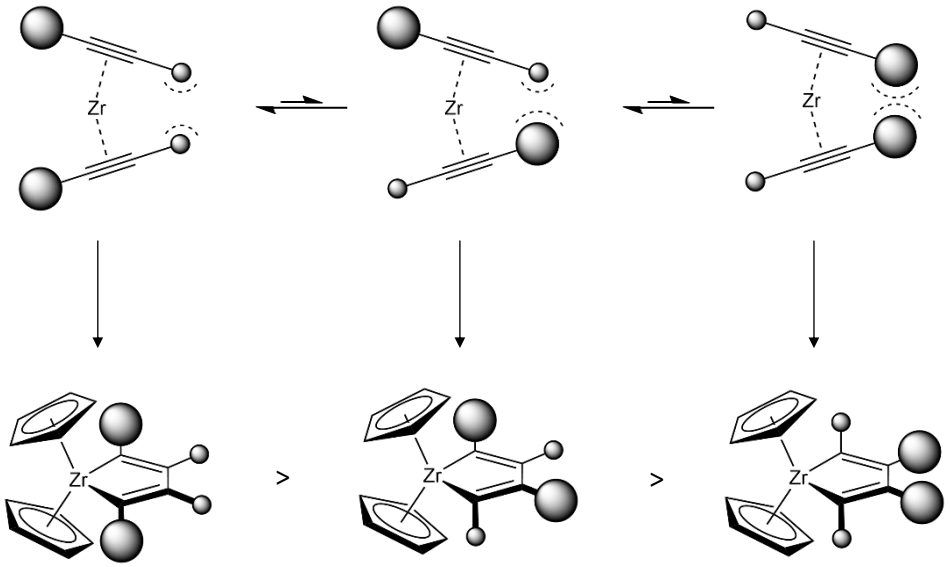
captured with commensurate displacement of the stabilising olefin/base. The olefin is invariably gaseous under the reaction conditions (*viz.*, ethylene or 1-butene) thereby rendering this step of the process effectively irreversible. The process culminates with a bis-π-alkyne adduct [Zr($\eta^2$-alkyne)$_2$($\eta^5$-$C_5H_5$)$_2$] prior to the ultimate C-C and Zr-C bond forming events, which see an accompanying increase in the formal oxidation state of the metal from Zr(II) to Zr(VI) as [Zr$C_4R_4$($\eta^5$-$C_5H_5$)$_2$] assembles.




**Scheme 1.7**: Oxidative alkyne coupling at Zr(II) leading to metallacycle formation.

When the alkyne substrate is unsymmetric the resultant metallacyclopentadiene may assume any one of three regioisomeric configurations (**Scheme 1.8**). In practise, sterically demanding substituents generally adopt the 2,5-ring positions (α to the metal) and electron-withdrawing groups are directed to the 3,4-positions (β to the metal), both in proportions much greater than statistical chance (or in some cases,

exclusively). These preferences are rationalised on the existence of a $[Zr^{IV}C_4R_4(\eta^5\text{-}C_5H_5)_2] \leftrightarrow [Zr^{II}(\eta^2\text{-alkyne})_2(\eta^5\text{-}C_5H_5)_2]$ equilibrium for which free rotation of the π-alkyne(s) is permissible before metallacycle re-formation occurs, thereby allowing for accumulation of the lowest-energy regioisomer in a process of thermodynamic selection. The same equilibrium is invoked to explain the ability of metallacycle substituents to scramble upon addition of extraneous substrate molecules.[67-70]

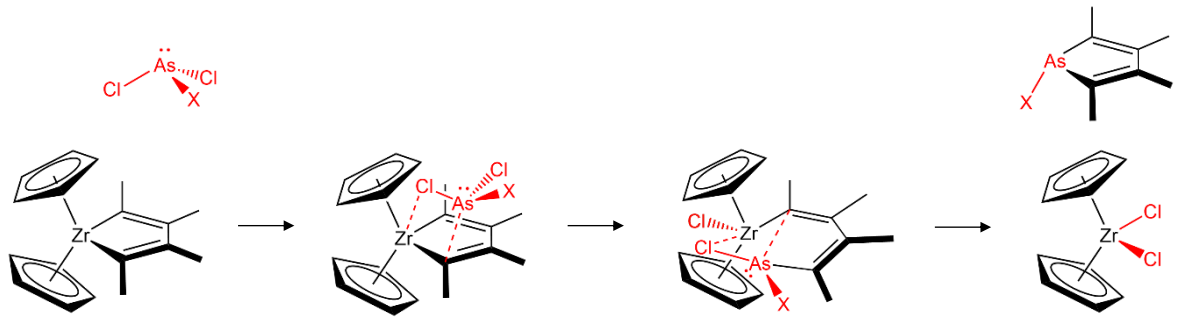



**Scheme 1.8**: Regiochemical outcomes during unsymmetric alkyne coupling at zirconocene, highlighting steric frustrations.

The metal-carbon covalent bonds within metallacyclopentadienes (of the early transition elements) are appreciably polarised in the direction of the carbon atoms, to the extent that the complex serves as a synthetically useful source of a nucleophilic butadiene-diyl fragment and are liable to disengage from the metal centre upon addition of electrophiles or electron-poor substrates. For example, the addition of carbon monoxide to zirconacyclopentadienes leads, depending on reaction conditions, to cyclopentenones or cyclopentadienones (where isolable).[71-73] The addition of a third alkyne equivalent produces benzene derivatives,[74-76] or in the case of the corresponding ethyne-derived titanacyclopentadiene, to polyacetylene.[77] Protonolysis or halogenolysis of the metal-carbon bond proceeds with stereospecific production of the corresponding *Z*,*Z*-1,3-butadiene or -dihalobutadiene in a reaction that is synthetically *very* useful.[78, 79]

As outlined by FAGAN and NUGENT,[45, 46] the addition of main group dihalides to zirconacyclopentadienes results in the formation of a heterocyclopentadiene with simultaneous

regeneration of the zirconocene dihalide – the driving force is entirely enthalpic in origin. The mechanism of metallacycle transfer is believed to proceed *via* a pair of halide-bridged transition states which the heteroatom exchanges for each $sp^2$-carbon sequentially, rather than a symmetric "open-faced" transition state where the heteroatom might form two developing bonds simultaneously.




**Scheme 1.9**: Mechanism of metallacycle transfer from zirconium to arsenic.

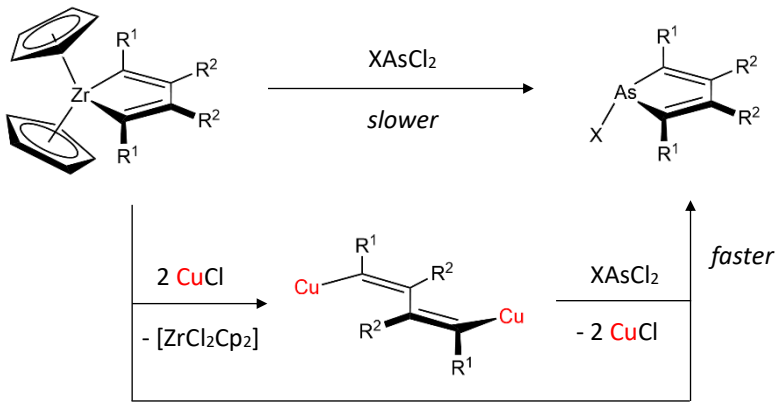
The apparent efficacy of transmetalation varies depending on the group (and to a lesser extent the period) to which the incoming element belongs: the general trend, which is purely empirical in formulation, follows Group 16 ≥ Group 15 > Group 13 > Group 14. Thus, transmetalation facility abides by the ease with which the heteroatom centre can become hypervalent, and for those electrophiles which are sterically unencumbered and/or electronically unsaturated (*vide infra*), which mostly explains the slower reactivity of Group 14 elements if nothing else. Additionally, the lone pair possessed by Group 16 and 15 electrophiles may serve a purpose to initially align the reactants before entering the transition state since the zirconium centre is electronically unsaturated. Practically speaking, the only problematic elements are aluminium and silicon which undergo transmetalation to zirconacyclopentadienes with *great reluctancy* – this can be traced to the appreciably affinity of both for halides (*especially* chloride) and their high electropositivity which renders the synthesis of aluminoles and siloles *via* an unmodified FAGAN-NUGENT protocol essentially non-viable.[47]

Arsenic di- and trichlorides ($XAsCl_2$ and $AsCl_3$) irreversibly react with zirconacyclopentadienes to furnish arsoles of the form $XAsC_4R_4$ or $ClAsC_4R_4$.* For certain combinations of R and X, the velocity of

* An arsenic monohalide *i.e.*, $R_2AsX$ should in principle also react to form a *Z*,*Z*-1,4-diarsinobuta-1,3-diene which could be an interesting bidentate ligand in itself (or a precursor to 1,2-diarsanine – a homologue of pyridazine), though this opportunity does not appear to have been pursued in the chemical literature.

transmetalation from mixing to completion can range from several seconds to several days. Slower reactions are encountered for even moderately encumbering furniture (*e.g.*, phenyl) such that a synthesis of the prototypical 1,2,3,4,5-pentaphenylarsole from $PhAsCl_2$ and $[ZrC_4Ph_4(\eta^5\text{-}C_5H_5)_2]$, for example, requires the use of a Cu(I) catalyst to expedite ring-transfer in a timely manner (*vide infra*). In contrast, $PhAsCl_2$ reacts with 2,3,4,5-tetramethyl and -ethylzirconacyclopentadienes ($[ZrC_4Me_4(\eta^5\text{-}C_5H_5)_2]$ and $[ZrC_4Et_4(\eta^5\text{-}C_5H_5)_2]$) and others of the like without the need for a Cu(I) additive (as observed during this work); $AsCl_3$ reacts with all the zirconacycles above instantaneously. It is seen that steric effects play a substantial role in the efficacy of transmetalation, especially given the congested nature of the transition state during halide/$sp^2$-carbon exchange and the need for the reactants to orient themselves appropriately ($\Delta S^{\ddagger} < 0$; **Scheme 1.9**). Hence, the widespread use of copper(I) salts as a transmetalation aide.

This segues into another useful application of zirconacyclopentadienes – an advantageous route to 1,4-dicupro-1,3-butadienes[80] which serve the same purpose as the zirconium reagent with the benefit that steric interactions are greatly diminished due to the open-chain nature of the organocuprate. The accelerating effect of Cu(I) on the reactivity of Group 4 metallacyclopentadienes was first documented by TAKAHASHI *et al.*[81, 82] who surmounted the difficult Zr → Si/Sn transmetalation by addition of a catalytic quantity of CuCl and the additive has since become staple in the preparation of many heterocyclopentadienes. Indeed, a 1,4-dicuprobutadiene is but a homologue of 1,4-dilithiobutadiene, and it is in some ways satisfying that the syntheses of so many heterocycles nowadays should come full-circle from the pioneering efforts of and LEAVITT and BRAYE.

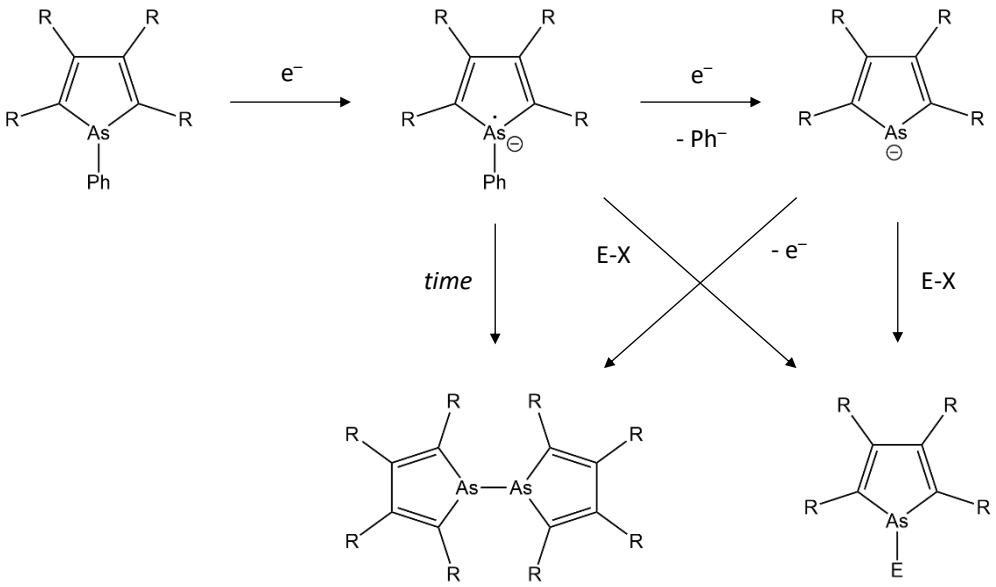



**Scheme 1.10**: Catalytic metallacycle transfer to arsenic *via* a sterically unassuming dicuprobutadiene intermediary. The Cu(I) centres are potentially solvated *e.g.*, by THF molecules, though this is ignored in the scheme for simplicity; Cp = $\eta^5$-$C_5H_5$.

## 1.3 Transformations of Arsoles

### 1.3.1 Reduction

A notable reaction of which arsoles (also phospholes, stiboles, bismoles) participate is reduction of the heteroatom by alkali and alkali earth metals with scission of the exocyclic heteroatom substituent, commonly a phenyl residue due to the moderate leaving group ability of the $[C_6H_5]^-$ anion.[38, 40, 83] A similar reaction is known for $PPh_3$, $AsPh_3$ and $SbPh_3$ which are also reduced to the diphenylpnictide $[EPh_2]^-$ and $Ph^-$.[84-88] Electron-transfer between the reductant and 1-phenylarsoles appears to proceed in a stepwise manner by way of a spectroscopically observable radical anion $[PhAsC_4R_4]^{\cdot-}$, before capturing a second electron and disintegrating into a pair of phenyl and arsolyl $[AsC_4R_4]^-$ anions (**Scheme 1.10**).[83] Since the LUMO in most (if not all) arsoles is chiefly composed of the exocyclic As-C(σ*) orbital it is readily understood why the heteroatom substituent and not an endocyclic As-C bond is ruptured. Although one paper[41] does indeed claim the latter to take place under certain conditions, this outcome has yet to be corroborated. The reduction of *As*-chloro arsoles to the arsolyl anion by alkali (earth) metals is also viable[89] though does not appear in the literature with the same frequency, probably due to the ease of handling of *As*-phenyl compared to *As*-chloro arsoles and the lack of general synthetic routes to the latter when such chemistry was broadly in development (*ca* 1970's—80's).




**Scheme 1.11**: Reduction of 1-phenylarsoles.

The synthetic utility of an arsolyl anion $[AsC_4R_4]^-$ is obvious for treatment thereto with electrophiles affords *As*-functionalised derivatives[29, 40, 83, 90] without requiring the corresponding pool of various $XAsCl_2$ reagents on hand in the laboratory. The reduction of *As*-phenyl arsoles necessarily generates one equivalent of a phenyl anion that may act as a competing nucleophile during subsequent steps; in such an event, selective destruction of $Ph^-$ is possible by treating the reaction mixture with $AlCl_3$, anhydrous $NH_3$ or *t*-BuCl.* In other cases, the presence of $Ph^-$ may be inconsequential and the incoming electrophile simply used in excess; if potassium is used as the reductant specifically, the resultant PhK is often destroyed in any event under the experimental conditions (usually with heating).[91] Of course, the addition of transition metal halides to the arsolyl anion is an expedient route to installation of the ligand in either the $\eta^1$ or $\eta^5$ modes,[91-93] though again the presence of $Ph^-$ may act as a competing nucleophile if not pre-emptively destroyed.

The radical anion may also undergo reactions with organic electrophiles in much the same way as the arsolyl anion; provided the electrophilic radical is of poorer kinetic stability than the phenyl radical this also offers a means to replace the *As*-phenyl substituent with another (benzyl halides are therefore a poor choice of electrophile). The arsole radical anion invariably has non-indefinite lifetime and permitting to stand, or similarly treating the arsolyl anion with suitable 1-electron oxidising agents, leads to *As*-*As* coupling and formation of a biarsolyl $(AsC_4R_4)_2$.[83, 90]

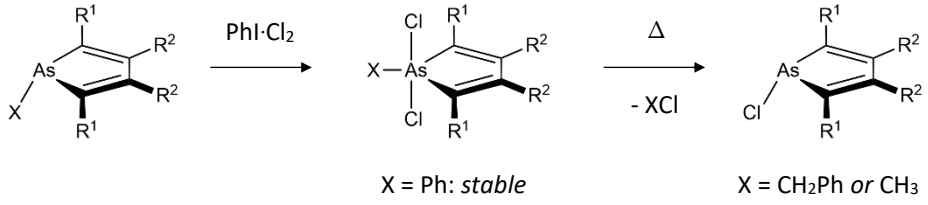
### 1.3.2 Halogenation and Oxidation

Halogenation of the As(III) atom is possible: in common with $AsPh_3$, treatment of $\lambda^3$-arsoles with iodobenzene dichloride ($PhI{\cdot}Cl_2$, a crystalline reagent that is mildly and synthetically equivalent to $Cl_2$) in benzene solution at ambient temperature affords the $\lambda^5$-arsole in high yields (**Scheme 1.11**).[90] Much unlike $Cl_2AsPh_3$ – which dissociates to $[ClAsPh_3]Cl$ and $[ClAsPh_3][Cl_3AsPh_3]$[94] – these oxidised arsoles are non-electrolytes in solution suggesting an appreciable degree of covalency within the As-Cl bonds. A trigonal bipyramidal As(V) centre with the chlorides occupying the axial positions was suggested, and this was indeed shown to be the case when $Ph(Cl)_2AsC_4Ph_4$ and $Ph(Cl)_2AsC_4Ph_2H_2$ were structurally characterised

* The benign products formed are thus: $AlPh_3$ and LiCl; unknown means of destruction, but probably aniline and other amines; benzene, *iso*-butene and LiCl.

during this work (**Appendix**, **Section 8.6**);* the analogous 1,1-dibromo- and 1,1-diiodo-λ⁵-arsoles are presently unknown. The 1,1-dichloro-λ⁵-arsoles are reduced to the normal λ³-arsoles by the agency of $Na_2S$ and revert to the 1-phenyl-λ³-arsole upon treatment with phenyllithium, the mechanism of which is proposed to be metal-halogen exchange by attack of the phenyl nucleophile at an *As*-chloride, followed by elimination of LiCl.[90]

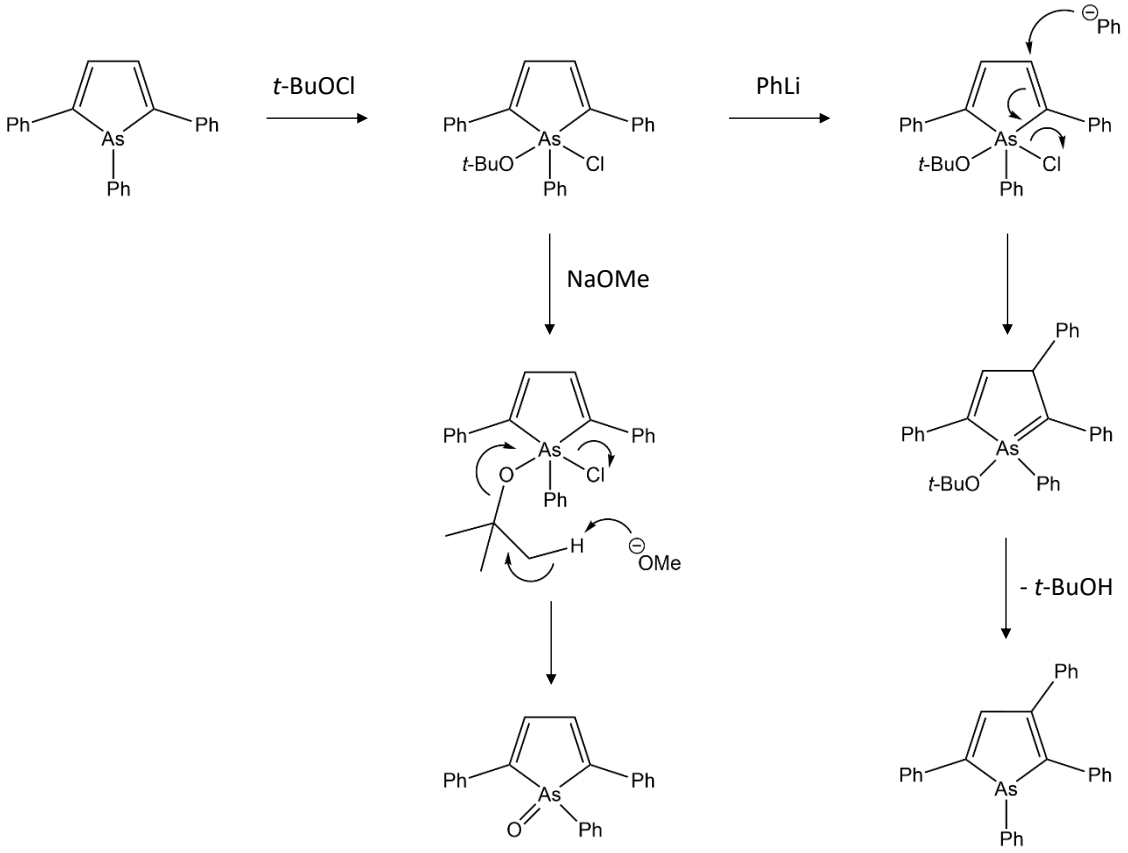
The thermal stability of these 1,1-dichloro-λ⁵-arsoles depends on the nature of the equatorial substituent X. The preferred thermodynamic condition of arsenic is the trivalent oxidation state, and as such arsoles possessing a benzyl ($PhCH_2$) group expel benzyl chloride at or slightly above ambient temperature in a process which superficially resembles reductive elimination,[90] though is probably closer to σ-bond metathesis (or potentially a radical pathway for which benzyl groups are well-known). The 1-chloroarsole remaining (**Scheme 1.12**) was the first practical and high yielding route to such. Similarly, methyl chloride is liberated from $Me(Cl)_2AsC_4R_4$ upon mild warming (*ca* 50 °C) however the *As*-phenyl derivatives are extraordinarily stable: in fact, MÄRKL reports that under forcing thermolysis (> 250 °C) ring-opening of the arsole takes place to give *Z*,*Z*-1-(phenylchloroarsino)-1,4-diphenyl-4-chloro-1,3-butadiene Ph(Cl)AsCPh=CHCH=C(Cl)Ph in low yield amongst a great deal of detritus.[90] The halogenation-elimination method has recently been exploited by NAKA and co-workers to obtain 9-chloroarsafluorenes,[95] though the thermal elimination of alkyl halides by halogenation of tertiary arsines as a means to obtain $R_2AsX$ has been customary for some time.[96]




**Scheme 1.12**: Chlorination of λ³-arsoles with subsequent alkyl chloride elimination.

* A 1,1,1-trichloro-λ⁵-arsole, namely $(Cl)_3AsC_4Ph_4$, was also pursued by treatment of $ClAsC_4Ph_4$ with $PhI{\cdot}Cl_2$ however the product isolated proved to be 1,1-dichloro-1-hydroxy-2,3,4,5-tetraphenylarsole $(HO)(Cl)_2AsC_4Ph_4$. The iodobenzene dichloride prepared in-house is inevitably contaminated with adventitious moisture, which is the presumed origin of the *As*-hydroxy group. The crystal structure of this λ⁵-arsole is also shown **Section 8.6** of the **Appendix**.

The ease with which 1-phenyl-1,1-dichloro-λ$^5$-arsoles are obtained and their appreciable stability renders the compounds most-useful for further study, with all the extant knowledge coming from the laboratory of MÄRKL:[97] treatment of $Ph(Cl)_2AsC_4Ph_2H_2$ with one equivalent of NaOMe ultimately gives 1,2,5-triphenylarsole oxide $Ph(O)AsC_4Ph_2H_2$, presumably *via* elimination of MeCl from $Ph(MeO)(Cl)AsC_4Ph_2H_2$ in an ARBUZOV type of elimination. This outcome is particularly noteworthy in the regard that direct oxidation of many perarylated arsoles with $H_2O_2$ or similar is rather difficult in comparison to the corresponding phospholes which spontaneously convert to the *P*-oxide in air. The *As*-oxides are easily reverted to the *As*-chloro species upon treatment with oxophilic chlorinating agents such as thionyl chloride or chlorosilanes.




**Scheme 1.13**: Reactions of (*t*-BuO)(Cl)$PhAsC_4Ph_2H_2$ with strong bases/nucleophiles.

Isolation of a stable 1-alkoxy-1-chloro-1-phenyl-λ$^5$-arsole is possible by treating $PhAsC_4Ph_2H_2$ with *tert*-butylhypochlorite (*t*-BuOCl) giving the expected As(V) adduct in high yield without ejection of *t*-BuCl (**Scheme 1.13**). Subsequent combination of Ph(*t*-BuO)(Cl)$AsC_4Ph_2H_2$ with one equivalent of NaOMe also leads to quantitative production of the same $Ph(O)AsC_4Ph_4$ observed above; in this case it is thought that

methanol and *iso*-butene are eliminated *via* an $E_2$ pathway.* The $\lambda^5$-arsole Ph(*t*-BuO)(Cl)$AsC_4Ph_2H_2$ reacts with organolithium reagents however counterintuitively the incoming nucleophile is installed at the 3-position of the ring with concurrent reduction to As(III):[97] the mechanism is believed to proceed through a nucleophilic conjugate substitution pathway ($S_N2'$) in much the same way as allylic halides might undergo when treated with nucleophiles.[98]

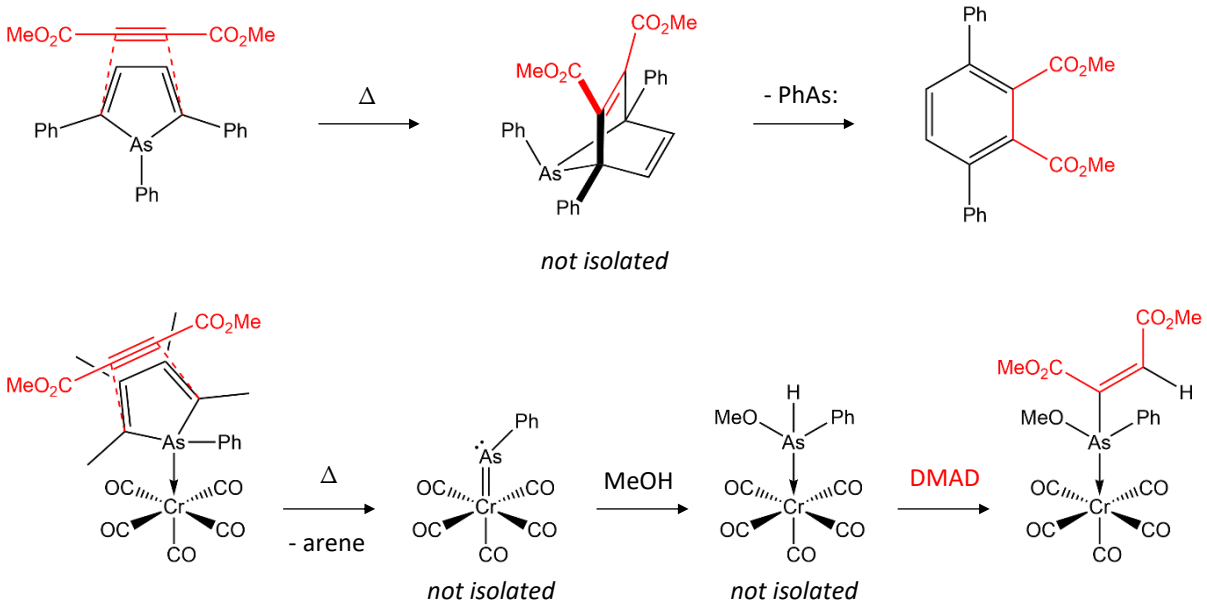
### 1.3.3 Cycloaddition Reactions

Whereas BRAYE and co-workers mooted the low HÜCKEL aromaticity of the heavier Group 15 heterocyclopentadienes – and thus a prominent resemblance to *S-cis* dienes – by $\eta^4$ complexation of iron(0) tricarbonyl (*vide infra*),[6] only a short while later would MÄRKL *et al.* reach a similar conclusion by showing that 1-phenyl-2,5-disubstituted arsoles would enter into [4+2] cycloadditions with dienophiles:[39] the reaction between $PhAsC_4R_2H_2$ (R = Me or Ph) and dimethylacetylene dicarboxylate (DMAD) proceeds with mild warming to the isolation of the corresponding *ortho*-phthalate ester by elimination of phenylarsinidene ("PhAs:") from a 7-arsanorbornadiene transient (**Scheme 1.14**). With tetracyanoethylene (TCNE), MÄRKL reported that the DIELS-ALDER adduct (a 7-arsanorbornene) is isolable and of appreciable thermal stability (M.P. 150 °C), presumably because a *retro*-[4+2] disintegration offers no aromatisation incentive in contrast to DMAD. SCHENK would also later perform [4+2] cycloaddition on $R'AsC_4Me_4$ (R' = Ph or Me) within the coordination sphere of $Cr(CO)_5$ or $W(CO)_5$,[99] almost certainly in attempted emulation of MATHEY'S protocol for generating metal-stabilised phosphinidenes *en route* to the first example of a three-membered phosphirene ($R'PC_2R_2$) ring.[100, 101] In SCHENK'S case, heating $[M(R'AsC_4Me_4)(CO)_5]$† with DMAD in benzene led to formation of the tetramethyl-*ortho*-phthalate dimethylester but the arsinidine was not trapped with another unsaturated substrate; performing the reaction in methanol did however afford the *E*-vinylarsine complex $[Cr\{AsPh(OMe)C(CO_2Me)=CH(CO_2Me)\}(CO)_5]$ (**Scheme 1.14**) by

* An alternative mechanism whereby a 1,1,1-bis(alkoxy)(phenyl)arsole forms by chloride substitution, followed by elimination of *iso*-butene and methanol is less-likely since the *t*-BuO and OMe groups would be expected to reside *trans* to one another about the As(V) centre; geometrically, a concerted intramolecular elimination from this arrangement would be impossible.

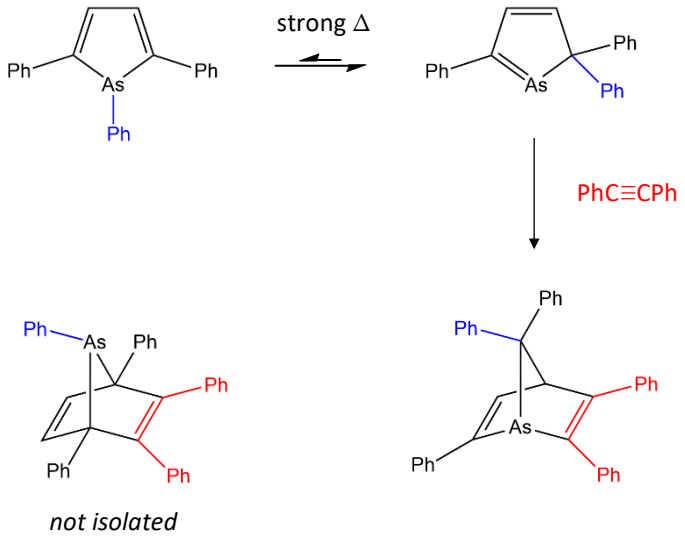
† The complex $[W(PhAsC_4Me_4)(CO)_5]$ was characterised by X-ray diffraction during this work and the structure is shown in **Section 8.3** of the **Appendix**.

insertion of excess DMAD into [Cr{AsPhH(OMe)}(CO)$_5$], itself presumably arising from the unobservable *retro*-[4+2] arsinidene product [Cr(=AsMe)(CO)$_5$] reacting with the solvent.



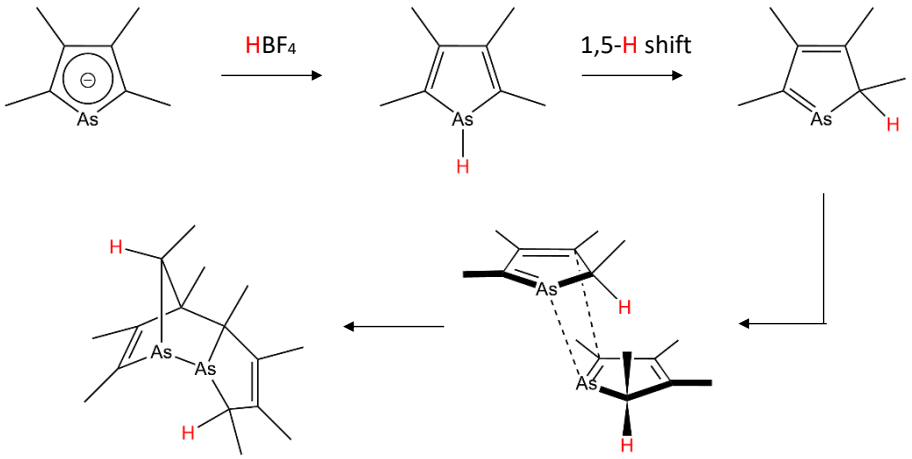

**Scheme 1.14**: Cycloaddition reactions of free and metal-coordinated arsoles with dimethylacetylene dicarboxylate (DMAD) reported by MÄRKL (**top**) and SCHENK (**bottom**).

MATHEY[102] provided a more-detailed study concerning cycloadditions of arsoles (after a similar study on 1*H*-phospholes) at both ambient and elevated temperatures, repeating and expanding upon the above work by MÄRKL and colleagues. A surprising observation was the reversibility of [4+2] adduct formation: the tetracyanoethylene adduct of 1-phenyl-2,5-dimethylarsole (a 7-arsanorbornene) further reacts with 2,3-dimethylbutadiene at 120 °C to regenerate the free arsole instead of arsinidene extrusion; this compares to the *N*-phenylmaleimide [4+2] adduct of the same arsole which proceeds at ambient temperature directly to the isoindole derivative. At higher temperatures (typically > 160 °C), the cycloaddition product(s) obtained point to the existence of a 2*H*-arsole within the reaction mixture; thus, heating 1,2,5-triphenylarsole with diphenylacetylene (forcibly) results in isolation of a pentaphenyl-1-arsanorbornadiene in which the arsenic atom occupies a bridgehead position (**Scheme 1.15**). Similarly, strong heating of 1,2,5-triphenylarsole with 2,3-dimethylbutadiene (160 °C) results in formation of an arsaindolizine, the position of the heteroatom within the compound being attributable to the presence of a 2*H*-arsole arising from a 1,5-phenyl sigmatropic shift.




**Scheme 1.15**: MATHEY'S interception of a 2*H*-arsole generated at high temperature with diphenylacetylene.

THEOPOLD has isolated and structurally characterised the lithium salt of the tetramethylarsolyl anion Li[$AsC_4Me_4$]·TMEDA (TMEDA = *N*,*N*,*N*,*N*-tetramethylethylenediamine) (*vide infra*).[29] Attempts to protonate this species with $HBF_4·Et_2O$ resulted in immediate formation of the DIELS-ALDER dimer *endo*-[octamethyl-1,2-diarsanorbornadiene] arising from [4+2] cycloaddition between a pair of 2*H*-2,3,4,5-tetramethylarsoles (**Scheme 1.16**). Whilst the *As*-protonation of arsoles and their proclivity for 1,5-H shifts has not been the subject of systematic study, instructive information is available for phospholes for which *P*-protonation of a phospholyl anion invites rapid sigmatropic hydride shifts – with rearrangement of the internal π bonds – at temperatures well below 0 °C. In one case the *P*-unsubstituted phosphole could be intercepted by metal complexation *i.e.*, [$W(HPC_4Ph_4)(CO)_5$],[103] though only due to the comparatively long lifetime of the free $HPC_4Ph_4$ at low temperatures compared to ring systems with lesser steric volume. *As*-unsubstituted arsoles are therefore expected to be no different, perhaps even more prone to 1,5-H shift (and dimerisation) given the decreasing basicity of the elements on descending Group 15 (bond dissociation energies: P-H 343 $kJmol^{-1}$; As-H 272 $kJmol^{-1}$). Protonation of a metal-complexed arsolyl anion (*e.g.*, $[W(AsC_4R_4)(CO)_5]^-$) may circumvent such an issue long enough for the species to be characterised,[104] though this does not appear to have been pursued in the literature.

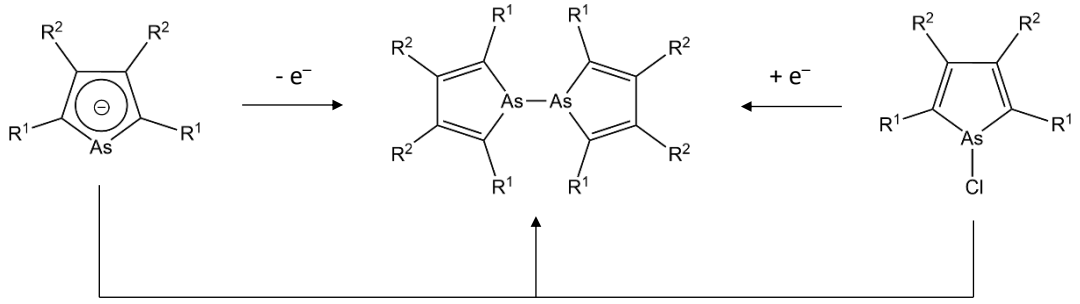



**Scheme 1.16**: Protonation of an arsolyl anion resulting in a 1,2-diarsabornadiene *via* sequential 1,5-H shift followed by *endo*-[4+2] cycloaddition.

### 1.3.4 Conversion to Biarsolyls

As mentioned in passing above, it is possible to synthesise an *As*-*As* bonded biarsolyl $(AsC_4R_4)_2$ by addition of one-electron oxidising agents to the $[AsC_4R_4]^-$ anion; oxidants such as Pb(II) salts,[105] $[CPh_3]^+$,[83] $[Br_3]^-$,[106] and $I_2$[107] have been previously employed by MÄRKL, MATHEY and ASHE to affect union of the two arsenic centres. The addition of hydrated $[Fe(NO_3)_3]$ to the *As*-ethereal arsole* $H_3COCH_2AsC_4Ph_2H_2$ also reportedly gives $(AsC_4Ph_2H_2)_2$.[83] Oxidising agents and certain alkyl halides will also coupling a pair of arsolyl radical anions, as will simply allowing solutions of $[PhAsC_4R_4]^{\cdot-}$ to stand over time.[83, 90] Stoichiometric one-electron reduction of *As*-chloro and -phenyl arsoles is possible by the agency of alkali[29, 40, 83] and alkali earth metals[108, 109] (or their amalgams[92]) though over-reduction to $[AsC_4R_4]^-$ is also facile. In a less strategic fashion, THEOPOLD and co-workers have obtained octamethylbiarsolyl $(AsC_4Me_4)_2$ by attempted chromatography of $ClAsC_4Me_4$ on neutral alumina.[29] The simplest method for biarsolyl synthesis, however, is combination of one equivalent each $[AsC_4R_4]^-$ and $ClAsC_4R_4$ which is the route used in **Section 5.2.7** of **Chapter 5**. Though not explored during this work, this approach in principle has the potential to access unsymmetrical biarsolyls.

* MÄRKL does not state why this reaction was carried out, though given $O_2$ is listed as a reagent it seems plausible the authors were attempting to oxidise the methylether function.




**Scheme 1.17**: Generalised syntheses of biarsolyls.

As will be discussed in **Chapter 4**, the addition of $[Cr(SnBu_3)(CO)_3(\eta^5\text{-}C_5H_5)]$, $[Mo(CO)_3(\eta^5\text{-}C_5H_5)]^-$ or $[Fe(CO)_2(\eta^5\text{-}C_5H_5)]^-$ to *As*-chloro arsoles also leads to one-electron reduction and formation of the biarsolyl (though not cleanly) in a process which initially frustrated synthetic efforts to install the arsolyl residue onto the metal centre. Moreover, **Chapter 5** will encounter several situations where indiscriminate homolysis of a Mo-As covalent bond can be affected by labile 3*d* transition metal reagents leading to the first example (surprisingly) of a complex featuring a $\mu\text{-}\eta^1\text{:}\eta^1\text{-}(AsC_4R_4)_2$ ligand. Indeed, the tendency toward biarsolyl formation would appear rather high. The crystal structure of 2,2',5,5'-tetramethylbiarsolyl $(AsC_4Me_2H_2)_2$ has been determined by ASHE[107] and until this work stood as the only example of such. Two biarsolyls were structurally characterised during this work and it is noteworthy that in all three examples the pair of arsolyl rings are in a mutually *gauche* arrangement about the diarsine bond regardless of steric volume, suggesting stereo-electronic factors may dictate the ground state conformation.[110]

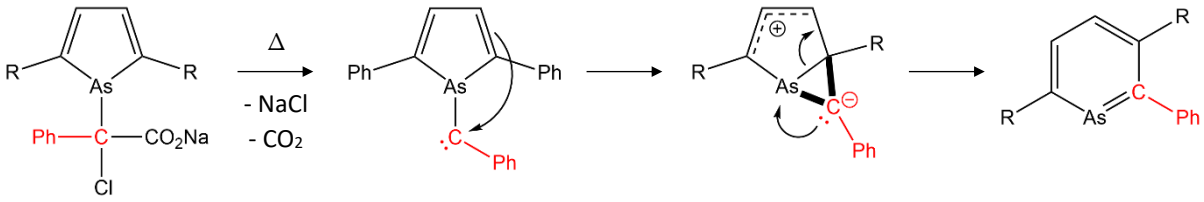
Only a handful of reactions of biarsolyls have been described, all of which involve scission of the diarsine bond. As will be returned to in **Section 1.4.4**, MATHEY has reacted biarsolyls with the actinides Sm, Tm and Yb in their elemental forms to afford, *via* redox transmetalation, *pentahapto* complexes of the same.[105, 106, 111] These reactions are a generalisation of the ability of dipnictogen bonds to undergo reductive cleavage with electropositive metals to the free pnictogenide. Despite this, there are no reported examples of low-valent transition metals *e.g.*, Pd(0), inserting into the *As*-*As* bond in an oxidative manner.

ASHE has demonstrated that Group 15 biheterolyls $(EC_4Me_2H_2)_2$ (E = P, As, Sb, Bi) may undergo scrambling in solution at ambient temperature.[112] In all cases dynamic equilibria containing statistical mixtures are established with formation constants of mixed biheterolyls $(H_2Me_2C_4E\text{-}E'C_4Me_2H_2)$ lying

further toward the products as the heteroatoms E and E' become closer in atomic number. Thus, ($H_2Me_2C_4P$-$AsC_4Me_2H_2$) and ($H_2Me_2C_4As$-$SbC_4Me_2H_2$) form readily upon mixing the appropriate symmetric biheterolyls whereas ($H_2Me_2C_4P$-$SbC_4Me_2H_2$) and ($H_2Me_2C_4As$-$BiC_4Me_2H_2$) only form in small quantities. The extreme case, ($H_2Me_2C_4P$-$BiC_4Me_2H_2$), is apparently undetectable in solution. The kinetic liability of the interpnictogen bond almost certainly varies as the interaction becomes more polarised,[113] and in this regard the position of the symmetric ↔ unsymmetric biheterolyl equilibrium is purely driven by the enthalpic considerations.

### 1.3.5 Conversion to Arsabenzenes

Prior to ASHE'S synthesis of the parent arsabenzene *via* dehydrohalogenation of 1-chloro-1-arsa-2,5-cyclohexadiene (**Chapter 2**, **Scheme 2.2**),[114] MÄRKL discovered that arsoles (and phospholes) may undergo intramolecular ring-expansion by incorporation of an *in situ* generated carbenoid fragment.[115, 116] Thus, 1-(phenylsodiochloroacetato)-arsoles ($PhCl\{NaO_2C\}CAsC_4R_4$) lead with strong heating (*ca* 140°, melt) *via* elimination of NaCl and $CO_2$ to 2,3,6-trisubstituted arsabenzenes. The mechanism is proposed to traverse an ephemeral singlet carbene Ph-C̈-$AsC_4R_4$ which undergoes nucleophilic attack from a carbon atom in the 2,5-ring position, giving a bicyclic betaine of arsacyclopropane which then undergoes ring expansion to generate the aromatic system.




**Scheme 1.18**: MÄRKL'S synthesis of 1,2,6-trisubstituted arsabenzenes by thermal decomposition of 1-sodiochloroacetatoarsoles.

The addition of dihalocarbenes ($:CX_2$) or phenylmercuric bromodichloromethane ($PhHgCCl_2Br$) to 1,2,5-trisubstituted arsoles does not produce isolable arsabenzenes *via* an analogous insertion process, instead opting for nucleophilic attack at the arsenic atom (when the arsenic substituent is a relatively good leaving group *e.g.*, benzyl) or at a butadiene C=C bond giving bicyclic arsolene adducts of limited stability.[117] This is in contrast to the same reagents upon pyrroles which does lead to 2-halopyridines.[118]

## 1.4 Transition Metal Complexes of Arsole and Arsolyl Ligands

The compendium of transition metal arsole complexes prepared prior to this work could best be described as eclectic. In contrast to phospholes – which as alluded have been studied in far greater depth – the loose assortment of arsole/arsolyl compounds reported by previous workers appear in a sporadic and often haphazard fashion throughout the literature. Systematic studies are common for phospholes from which a "natural" progression in knowledge is readily discernible between works, but not for arsoles nor stiboles and bismoles. The variety in potential coordination modes for the heavier Group 15 heterocyclopentadienes is impressive – in many ways this can be tied to the fact that these materials are tantamount to a tertiary pnictogen which so happens to be attached to a diene function (*cf.*, low aromaticity) thereby exhibiting the separate functionalities of both.

Aside from the normal 2-electron mode through the heteroatom (σ-dative coordination, the most common), a neutral arsole ring can in principle serve as a 4-electron donor *via* the butadiene moity ($\eta^4$-coordination); $\eta^2$-coordination through a solitary C=C bond has never been observed since the heteroatom lone pair would invariably be a superior source of two electrons, though one example exists for a phosphole ring.[119] In the anionic arsolyl form of the ring, a 1-electron ligand is of course expected (σ-covalent), as is the 5-electron *pentahapto* mode ($\eta^5$-coordination) binding a single metal centre to all ring atoms. Combinations of these modes are possible *i.e.*, a bridging $\mu$-$\eta^1$:$\eta^1$-arsolyl ligand serves as a 3-electron donor to two separate metals *via* mixing of σ-dative and σ-covalent coordination modes, and the 6-electron $\mu_2$-$\eta^1$:$\eta^4$-arsole ligand *via* the agency of the heteroatom lone pair and the butadiene system. A 7-electron $\mu_3$-$\eta^1$:$\eta^1$:$\eta^4$- (σ-dative + σ-covalent + $\eta^4$) arsolyl ligand has heretofore never been reported (though $\mu_2$-$\eta^1$:$\eta^5$- (σ-dative + $\eta^5$) has two examples), nor has an $\eta^3$-bonding mode akin to an allyl ($[C_3H_5]^-$) group (perhaps the most obdurate of all modes). Some of these coordination modes are illustrated for a generalised case in **Chart 1.1**. One or more examples of *each* model shown, some for the first time, will be found throughout various sections of this work, a sentiment which this author finds highly gratifying.

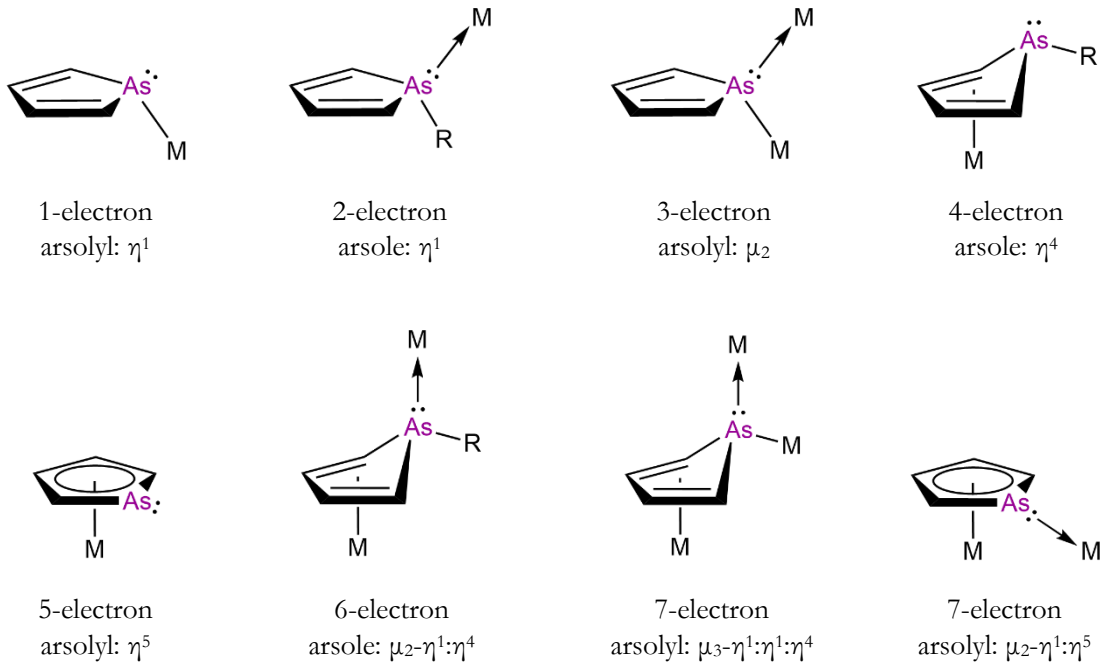



**Chart 1.1**: Eight potential coordination modes of a neutral arsole or anionic arsolyl ligand to one or more transition metal centres.

The entire library of known transition metal complexes featuring a neutral arsole or anionic arsolyl ligand is sufficiently small that a short discussion of their synthesis and any noteworthy features is in order; they will be sub-divided in the forthcoming sections by ascending coordination mode rather than global chronological discovery. **Figure 1.5** collates the total reported number of transition metal arsole and arsolyl complexes by coordination mode (light blue), with proportions that appear in the CSD (dark blue).

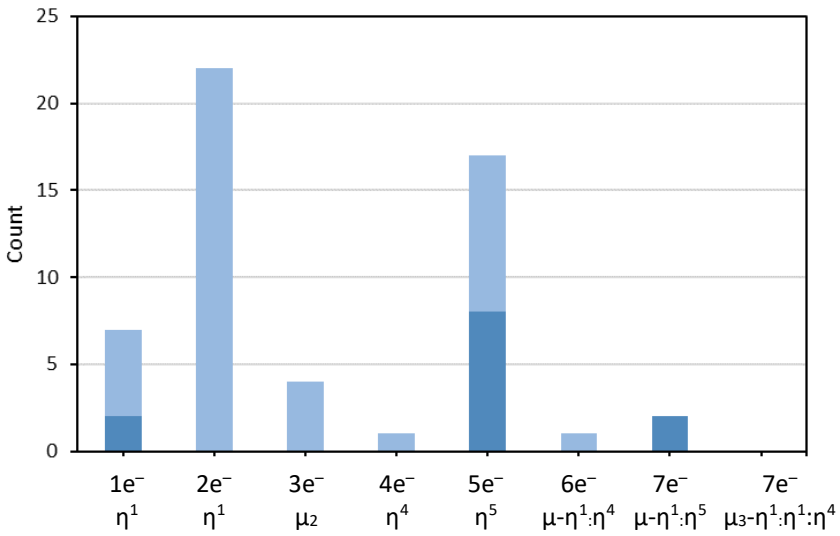



**Figure 1.4**: Number of transition metal arsole (neutral) and arsolyl (anionic) complexes by coordination mode. Numbers are correct as of April 2023. Dark blue areas correspond to proportions which have had crystal structures determined.

### 1.4.1 σ-Dative Arsole Complexes

In 1979, MATHEY provided the first examples of arsole coordination utilising the heteroatom lone pair *via* interactions between 1-phenyl-2,5-dimethylarsole ($PhAsC_4Me_2H_2$) and the trio of iron(0) carbonyls.[120] Thermolysis with $[Fe(CO)_5]$ or $[Fe_2(CO)_9]$ in benzene (80 °C) gives the expected tetracarbonyl complex $[Fe(PhAsC_4Me_2H_2)(CO)_4]$ in high yields. Thermolysis of the same arsole ligand with $[Fe_3(CO)_{12}]$ (toluene, 110 °C) also gives the tetracarbonyl iron(0) complex above as the major product alongside a small quantity of the red $[Fe_2(\mu\text{-}\eta^1\text{:}\eta^4\text{-}PhAsC_4Me_2H_2)(CO)_7]$, featuring a 6-electron arsole ligand binding an $Fe(CO)_4$ group *via* the arsenic lone pair and an $Fe(CO)_3$ group *via* the butadiene system (the second proposed example of such; **Figure 1.5**). Despite MATHEY'S usual rigor with respect to characterisation, only $^1H$, IR and mass spectral data were given as proof of identity of the novel diiron complex – in principle, the pair of iron centres may be mutually *syn* or *anti* about the mean plane of the arsole ring though this was not determined. Carrying out the same reaction at elevated temperatures (xylenes, 140 °C) provided in modest yield the 1*H*-ferracyclopentadiene ("ferrole") $[Fe(\mu\text{-}CO)(\eta^4\text{-}FeC_4Me_2H_2)(CO)_5]$ arising from displacement of the Ph-As: arsinidene fragment (*cf.* desulfurisation of thiophene by $[Fe_3(CO)_{12}]$[121]). Note the dichotomy displayed between $[Fe_3(CO)_{12}]$ which cleaves the *endo*cyclic As-C bond(s), and $[Mn_2(CO)_{10}]$ which cleaves the *exo*cyclic As-C bond (*vide infra*) under the same conditions.

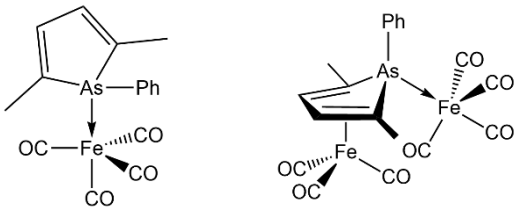



**Figure 1.5**: Two σ-dative arsole complexes of Fe(0) carbonyl prepared by MATHEY.

Shortly after FAGAN and NUGENT reported the synthesis of 1-phenyl-2,3,4,5-tetramethylarsole *via* transmetalation from zirconium, SCHENK described several new coordination complexes of the same arsole pattern.[99] These included a series of $[M(RAsC_4Me_4)(CO)_5]$ (M = Cr, W; R = Me, *t*-Bu, Ph) by displacement of the labile solvent molecule from $[M(NCMe)(CO)_5]$, and a small range of disubstituted tungsten species *cis*-$[W(RAsC_4Me_4)L(CO)_4]$, where L = $C_5H_{11}N$, NCMe or P(*i*-Pr)$_3$ though notably not a second arsole

equivalent. In the presence of $NEt_3$, $[Mn(NO)(CO)_2(\eta^5\text{-}C_5H_4Me)]PF_6$ undergoes thermal decarbonylation with the same arsoles to give the chiral $[Mn(NO)(RAsC_4Me_4)(CO)(\eta^5\text{-}C_5H_4Me)]PF_6$ (R = Me, Ph*) complexes in good yield. Similarly, $[RuClL_2(\eta^5\text{-}C_5H_5)]$ and $[RuClL_2(\eta^5\text{-}C_5Me_5)]$ give in the presence of $[NH_4]PF_6$ the cationic ruthenium-arsole complexes $[Ru(RAsC_4Me_4)L_2(\eta^5\text{-}C_5H_5)]PF_6$ (L = $PPh_3$ or ½·diphosphine) and $[Ru(RAsC_4Me_4)L_2(\eta^5\text{-}C_5Me_5)]PF_6$ (L = $PMe_3$ or ½·diolefin).

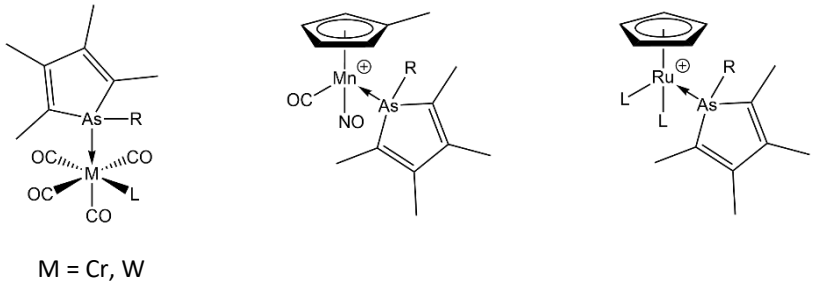



**Figure 1.6**: Tetramethylarsole complexes prepared by SCHENK.

The addition of DMAD to $[Ru(MeAsC_4Me_4)(PMe_3)_2(\eta^5\text{-}C_5Me_5)]PF_6$ gives not a cycloaddition product but instead simple displacement of the arsole ligand and formation of the π-alkyne complex $[Ru(\eta^2\text{-}MeO_2CC{\equiv}CCO_2Me)(PMe_3)_2(\eta^5\text{-}C_5Me_5)]PF_6$ in quantitative yield. Presumably, the electron-richness of the metal centre afforded by the accompanying ligand set labilises the arsole ligand toward dissociative substitution by the alkyne, which due to its superlative π-acidity enjoys a relatively π-basic Ru(II) centre. The chromium complex $[Cr(PhAsC_4Me_4)(CO)_5]$ does undergo a [4+2] cycloaddition reaction with DMAD in methanol in a process which has been outlined in **Scheme 1.15**.

More recently, NAKA and colleagues have revisited the prototypical 1,2,3,4,5-pentaphenyl and 1,2,5-triphenylarsoles with an improved synthesis *via* the FAGAN-NUGENT protocol.[34, 122] The particular interest of the authors lies within the attractive optical properties exhibited by perarylated arsoles (*e.g.*, fluorescing a very pleasant green-blue colour under broad-band UV irradiation) for which coordination to a AuCl centre affects a bathochromic emission shift, perhaps circumstantial evidence for a *very weak* involvement of the arsenic lone pair in ring delocalisation. Crystal structures were determined by NAKA.

* A crystal structure of this species was collected during this work and is shown in **Section 8.4** of the **Appendix**.




**Figure 1.7**: Gold(I) chloride complexes of arsole prepared by NAKA.

### 1.4.2 σ-Covalent Arsolyl Complexes

The first example of a σ-covalent arsolyl ligand was given by MATHEY in 1979 by addition of $K[AsC_4Me_2H_2]$ to $[FeI(CO)_2(\eta^5\text{-}C_5H_5)]$ affording $[Fe(AsC_4Me_2H_2)(CO)_2(\eta^5\text{-}C_5H_5)]$; the arsolyl anion was generated by potassium reduction of the corresponding *As*-phenyl arsole in refluent 1,2-dimethoxyethane.[91] Spectral characterisation was atypically limited compared to other works by the same author, who instead opted to proceed directly to thermal decarbonylation (*vide infra*).

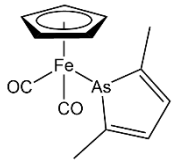



**Figure 1.8**: MATHEY'S σ-covalent Fe(II) complex of the 2,5-dimethylarsolyl ligand.

In the same year, ABEL reported four σ-covalent 2,3,4,5-tetraphenylarsolyl complexes of Mo, W and Fe: all were of the composition $[M(AsC_4Ph_4)(CO)_n(\eta^5\text{-}C_5H_5)]$ (M = Mo or W, $n$ = 3; M = Fe, $n$ = 2) except for one specific molybdenum complex, namely $[Mo(AsC_4Ph_4)(CO)_2(\eta^7\text{-}C_7H_7)]$. In addition, a pair of octahedral Group 7 complexes $[M(AsC_4Ph_4)(CO)_5]$ (M = Mn, Re) were described which would yield the first examples of an $\eta^5$-arsolyl ligand upon thermal decarbonylation (*vide infra*).[92] Two complimentary synthetic routes were used to prepare these complexes, which differed in the use of a nucleophilic metallate anion $[M(CO)_nL]^-$ upon an electrophilic arsenic centre ($ClAsC_4Ph_4$) or the reciprocal arrangement of an arsolyl anion $[AsC_4Ph_4]^-$ upon the metal halide $[MX(CO)_nL]$.

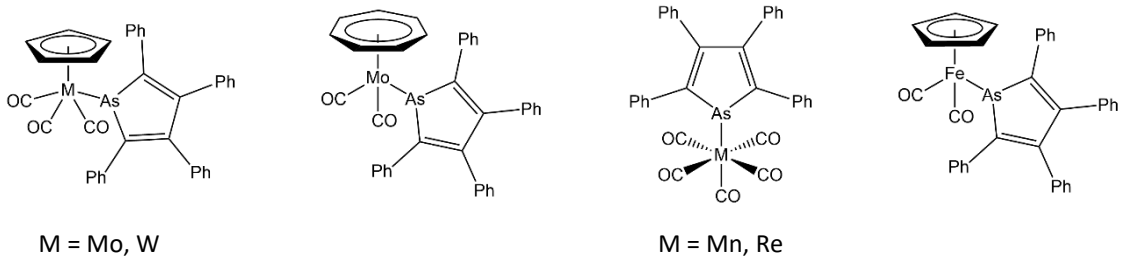



**Figure 1.9**: ABEL'S σ-covalent complexes of the 2,3,4,5-tetraphenylarsolyl ligand.

**Chapters 4**, **5** and **6** of this work involves a greater exploration of the chemistry of $[M(AsC_4Ph_4)(CO)_3(\eta^5\text{-}C_5H_5)]$ (M = Mo, W) and related complexes since the only reactions carried out by ABEL were halogenation and hydrohalogenation of the M-As bond. No other transition metal complexes featuring discrete σ-covalent arsolyl ligands have been described apart from those above, of which none appear to have been structurally characterised.

### 1.4.3 $\eta^4$-Arsole Complexes

The first arsole complex of any kind to be described was surprisingly of the diolefinic kind, and until this work stood as one of only two examples of an $\eta^4$-arsole ligand for > 60 years: BRAYE *et al.* in their 1961 report[6] purportedly obtained $[Fe(\eta^4\text{-}PhAsC_4Ph_4)(CO)_3]$ by thermolysis of pentaphenylarsole with $[Fe(CO)_5]$ (sealed tube, *iso*-octane, 150 °C), the product being encountered as "slightly yellow crystals" which melted with decomposition at 155—170 °C and displayed three terminal $\nu_{CO}$ bands (KBr) at 2053, 1996 and 1980 $cm^{-1}$.*

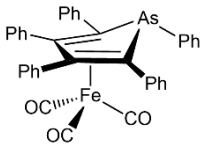



**Figure 1.10**: An $\eta^4$-pentaphenylarsole complex claimed by BRAYE.

* Data provided by the authors were in the wavelength dimension and have been converted to wavenumbers here for easier comparison: 4.87, 5.01 and 5.05 μ in KBr pellet. Relative intensities were not stated.

These IR data compare favourably against some well-known diene complexes of iron(0) tricarbonyl (*e.g.,* [Fe(COT)(CO)$_3$]* $\nu_{CO}$ (*n*-hexane) 2054(vs), 1996(vs), 1979(vs) cm$^{-1}$; [Fe(BDA)(CO)$_3$]* $\nu_{CO}$ (*n*-hexane) 2067(vs), 2007(vs), 1988(vs) cm$^{-1}$) though are somewhat removed from an authentic iron(0) tricabonyl complex of an $\eta^4$-arsole ligand prepared during this work (*cf.*, [Fe$_2${$\mu$-$\eta^4$:$\eta^4$-Fe($\eta^5$-C$_5$H$_4${AsC$_4$Me$_4$})$_2$}(CO)$_6$] $\nu_{CO}$ (*n*-hexane) 2037(vs), 1976(vs), 1965(vs) cm$^{-1}$; **Chapter 7**, **Section 7.4.3**). BRAYE'S elemental microanalysis data were quite satisfactory, though NMR and mass spectral data were absent (still at the time niche techniques) and the complex has not been definitively formulated since.

As an aside, this author has attempted to isolate and more-thoroughly characterise the [Fe($\eta^4$-PhAsC$_4$Ph$_4$)(CO)$_3$] complex claimed by BRAYE *et al.* by bringing both PhAsC$_4$Ph$_4$ and an excess of [Fe(CO)$_5$] to prolonged reflux in xylenes (140 °C; this solvent was chosen in lieu of *iso*-octane for the insolubility of PhAsC$_4$Ph$_4$ in aliphatic hydrocarbons) however the only species obtained was the light yellow [Fe(PhAsC$_4$Ph$_4$)(CO)$_4$] in moderate yield – the crystal structure featuring an ordinary $\sigma$-dative arsole ligand is shown in **Appendix**, **Section 8.2**, and the same compound is obtained quantitatively by combination of the arsole with an excess of [Fe$_2$(CO)$_9$] in THF at ambient temperature or with excess [Fe(COE)$_2$(CO)$_3$] in *n*-hexane. No reaction was observed between PhAsC$_4$Ph$_4$ and [Fe(BDA)(CO)$_3$] (a common source of "Fe(CO)$_3$") in THF at reflux. A melting point of 145—150 °C (with decomposition, unsealed capillary) was obtained for [Fe(PhAsC$_4$Ph$_4$)(CO)$_4$] and the solution IR spectrum (*n*-hexane) displays† four $\nu_{CO}$ bands at 2052(s), 1978(s), 1954(vs) and 1945(vs) cm$^{-1}$ (*viz.*, [Fe(PhAsC$_4$Me$_2$H$_2$)(CO)$_4$][120] $\nu_{CO}$ (decalin) 2054, 1975, 1947, 1941 cm$^{-1}$). On the basis of these IR data, BRAYE'S compound seems unlikely to have been [Fe(PhAsC$_4$Ph$_4$)(CO)$_4$]; benefit of the doubt is given on behalf of this author and it is not implausible that those workers did indeed prepare an authentic sample of [Fe($\eta^4$-PhAsC$_4$Ph$_4$)(CO)$_3$], despite the difficulties encountered in attempting to reproduce this result and coax the arsole toward $\eta^4$-binding.

The only other example of diolefinic coordination of an arsole was the aforementioned diiron species [Fe$_2$($\mu$-$\eta^1$:$\eta^4$-PhAsC$_4$Me$_2$H$_2$)(CO)$_7$] reported by MATHEY (**Figure 1.8**), which was characterised to a

* COT = $\eta^4$-1,3,5,7-cyclooctatetraene; BDA = $\eta^4$-benzylideneacetone.
† The solid-state ATR-IR spectrum was virtually identical to that recorded in *n*-hexane solution.

more convincing standard and does appear authentic. Four examples of $\eta^4$-arsole ligands will be encountered at various stages of this work, all of which were unambiguously confirmed by X-ray diffraction.

### 1.4.4 $\eta^5$-Arsolyl Complexes

The first transition metal arsole complex of any coordination mode to be structurally authenticated by X-ray diffractometry (in 1974) was in fact the *pentahapto* species $[Mn(CO)_3(\eta^5\text{-}AsC_4Ph_4)]$[123] ("tetraphenylarsacymantrene"*), obtained by ABEL after thermal decarbonylation of $[Mn(AsC_4Ph_4)(CO)_5]$ in *n*-decane at reflux (170 °C). The corresponding rhenium analogue $[Re(CO)_3(\eta^5\text{-}AsC_4Ph_4)]$ was also claimed by ABEL and both complexes were well-characterised for the standards of the era.[93] For the manganese complex, ABEL mentions in passing two alternate synthetic routes, those being 1) thermal redistribution of octaphenylbiarsolyl $(AsC_4Ph_4)_2$ with dimanganese decacarbonyl $[Mn_2(CO)_{10}]$ in modest isolated yield, or 2) thermal elimination of $SiMe_3Cl$ from a mixture of $Me_3SiAsC_4Ph_4$ and $[MnCl(CO)_5]$ (in what amounts to a transmetalation metathesis reaction) though experimental details were rather succinct. Carbonyl replacement of $[Mn(CO)_3(\eta^5\text{-}AsC_4Ph_4)]$ was possible upon UV-irradiation in the presence of PhC≡CPh or $PPh_3$, and treatment with $[NO][PF_6]$ gave the corresponding cationic nitrosyl complex.

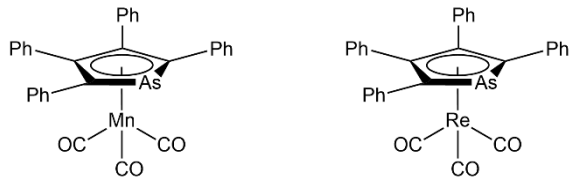



**Figure 1.11**: A pair of $\eta^5$-tetraphenylarsolyl complexes prepared by ABEL.

MATHEY *et al.* also obtained the "arsacymantrene" $[Mn(CO)_3(\eta^5\text{-}AsC_4Me_2H_2)]$ by thermolysis of equal proportions 1-phenyl-2,5-dimethylarsole and $[Mn_2(CO)_{10}]$ (xylenes, 140 °C);[124] an isolated yield of *ca* 50% was obtained though no mention was made regarding the fate of the severed *As*-phenyl substituent during the reaction.† The compound was thoroughly characterised, undoubtedly due to its inherent novelty. The brief 1978 communication also served as the first experimental proof of the HÜCKEL aromaticity of

* Cymantrene is the trivial name for $[Mn(CO)_3(\eta^5\text{-}C_5H_5)]$, a portmanteau of **cy**clopentadienyl **man**ganese **tr**icarbonyl; the "ene" suffix is added presumably as convention with ferrocene, *viz.*, "cyrhetrene" $[Re(CO)_3(\eta^5\text{-}C_5H_5)]$.
† The reaction stoichiometry would imply that $[MnPh(CO)_5]$ is formed which would also account for the remaining equivalent of manganese consumed, though this is only speculative.

the anionic arsolyl ring, a statement so trivially obvious nowadays but one which had no precedent at the time. Electrophilic substitution at the β ring-carbon under ordinary FRIEDEL-CRAFTS acylation conditions afforded the functionalised derivative [$Mn(CO)_3\{\eta^5$-$AsC_4Me_2(C(O)Me)(H)\}$] in acceptable isolated yield. MATHEY notes in passing that β-acylation of the arsolyl ring is in contrast to analogous dimethylphosphacymantrenes which could *only* undergo electrophilic substitution if the ring-carbon atom α to the phosphorus was unoccupied,[125] though a reason for this difference in reactivity was not elaborated.

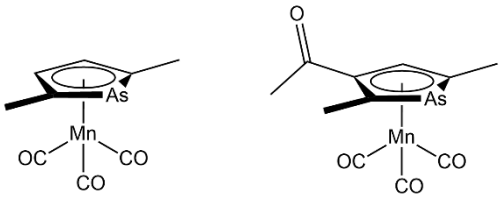



**Figure 1.12**: An $\eta^5$-2,5-dimethylarsolyl complex prepared by MATHEY and its acylated derivative.

Similar to the manganese and rhenium complexes of the $\eta^5$-$AsC_4Ph_4$ ligand prepared by ABEL (*vide supra*), MATHEY has reported thermal decarbonylation of the 2,5-dimethylarsolyl complex [$Fe(AsC_4Me_2H_2)(CO)_2(\eta^5$-$C_5H_5)$] (xylenes, 140 °C) to affect formation of the "arsaferrocene" [$Fe(\eta^5$-$AsC_4Me_2H_2)(\eta^5$-$C_5H_5)$] in modest isolated yield.[91] Obtained alongside this compound was the bridging-arsolyl complex [$Fe_2(\mu$-$AsC_4Me_2H_2)_2(CO)_2(\eta^5$-$C_5H_5)_2$] in low yield (*vide infra*), which is presumably an intermediate *en route* from the σ-covalent precursor to the mixed sandwich complex. The modest combined isolated yield of both complexes probably suggests extensive decomposition in the reaction medium, though no comment was made by the authors regarding such an occurrence. In the same communication,[91] the arsolyl [$AsC_4Me_2H_2$]$^-$ was combined with one-half an equivalent of [$FeCl_2$] (1,2-dimethoxyethane, 80 °C) to provide the first example of a "diarsaferrocene" [$Fe(\eta^5$-$AsC_4Me_2H_2)_2$]; the analogous "diphosphaferrocene" had been prepared by the same authors earlier that year.[126]

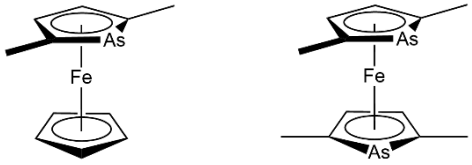



**Figure 1.13**: A pair of mono- and diarsaferrocenes prepared by MATHEY.

Likewise, ASHE has prepared a series of "heteroferrocenes" including [Fe($\eta^5$-$AsC_4Me_4$)$_2$][127] (the crystal structure of which was determined) and the parent [Fe($\eta^5$-$AsC_4H_4$)$_2$][38] by combination of the appropriate arsolyl anion with an Fe(II) source. Spectroelectrochemical characterisation reveals the ferrocene analogues to undergo *quasi*-reversible one-electron oxidations to the radical cation, and irreversible one-electron reductions to the radical anion; the effect of replacing a CH unit with an As(III) atom is a cathodic shift (to more-positive potentials) of both the oxidation and reduction events, a trend which continues monotonously as the Group 15 elements are descended.[128] That is, the "heteroferrocenes" are more difficult to oxidise and easier to reduce compared to ferrocene itself, a feature attributed to the decreased effective π-basicity of the heterocyclopentadienyl *vs.* cyclopentadienyl rings (a feature also noted for Co(I) centres in **Chapter 3** of this work), where the Fe-centred HOMO is destabilised and the LUMO stabilised by the presence of the Group 15 element.[129, 130]

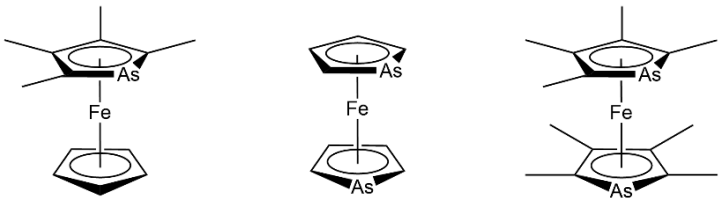



**Figure 1.14**: Mono- and diarsaferrocenes prepared by ASHE, including the parent unsubstituted species.

MATHEY has prepared a small selection of $\eta^5$-arsolyl samarium, thulium and ytterbium complexes by reaction of the corresponding anion with [$MI_2(THF)_2$] salts, or in the cases of Sm and Yb by redox transmetalation of a biarsolyl with the metal in elemental form.[105, 106, 111] The expected [M(THF)($\eta^5$-$AsC_4R_4$)$_2$] adducts readily converted to polymeric materials upon removal of the solvate molecule, linkages which probably feature bridging μ-$\eta^1$:$\eta^5$ arsolyl ligands (or similar) since combination of [Sm($Et_2O$)($\eta^5$-$C_5Me_5$)$_2$] with a biarsolyl (or biphospholyl) gives the dinuclear [$Sm_2$(μ-$\eta^1$:$\eta^5$-$AsC_4R_4$)($\eta^1$-$AsC_4R_4$)($\eta^5$-$C_5Me_5$)$_4$]. The complex was structurally characterised and the pair of arsolyl ligands exchange positions by mutual $\eta^1 \leftrightarrow \eta^5$ slippage in solution.[105] NIEF has continued this work by recently preparing a series of novel uranium(III) complexes of the form [U(THF)($\eta^5$-$EC_4Me_4$)($\eta^8$-$C_8H_8$)] (E = N, P, As) of which all were crystallographically characterised.[131] Electrochemical interrogation finds – in agreement with ASHE'S

observations above – that the heterocyclopentadienyl ligands render the metal centre a slightly less-potent reductant (more difficult to oxidise) than the carbocyclic analogue.

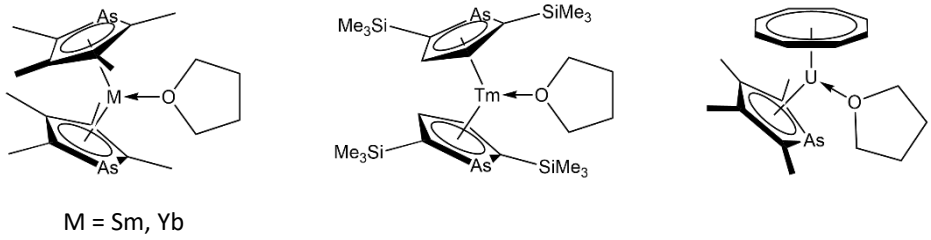



**Figure 1.15**: Lanthanide (**left and centre**) and actinide (**right**) $\eta^5$-arsolyl complexes prepared by MATHEY and NIEF.

Finally, a small library of alkali and alkali earth salts of arsolyl anions have been isolated and characterised. Though not *strictly* transition metal complexes of the $\eta^5$-arsolyl ligand, they are nonetheless included here as an addendum since they are themselves worthy of some mention. THEOPOLD and co-workers have prepared the tetramethylarsolyl anion by reduction of $PhAsC_4Me_4$ or $ClAsC_4Me_4$ with elemental lithium; the diamine-stabilised salt [Li($\eta^5$-$AsC_4Me_4$)·TMEDA] was isolated and structurally characterised.[29] As mentioned previously, protonation of the anion yields a cycloaddition product of a pair of 2*H*-arsoles arising from thermal 1,5-H shift, and the addition of $AlEt_2Cl$ or $GaCl_3$ to the same affords polymeric $[Et_2AlAsC_4Me_4]_x$ or $[Ga(AsC_4Me_4)_4]^-$, respectively. WESTERHAUSEN has investigated the products of $ClAsC_4Et_4$ reduction with the Group 1 metals in donor solvents, their crystal structures revealing ladder-like polymers of $\eta^5$-$AsC_4Et_4$ anions binding the $M^+$ cations *via* both faces of the ring, except in the case of $Na^+$ which forms discrete dimers with $\mu$-$\eta^1$:$\eta^5$-$AsC_4Et_4$ modes.[132]

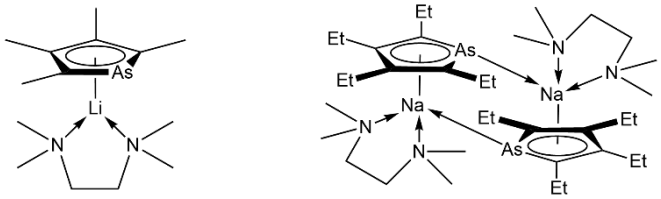



**Figure 1.16**: Diamine-stabilised alkali metal salts of arsolyl anions isolated by THEOPOLD (**left**) and WESTERHAUSEN (**right**).

Calcium reduction of the bulky $ClAsC_4(SiMe_3)Me_2$ in THF provides the dimeric halide bridged complex $[Ca_2(\mu\text{-}Cl)_2(THF)_4\{\eta^5\text{-}AsC_4(SiMe_3)_2Me_2\}_2]$ which was subjected to X-ray diffractometry.[109] The

reaction probably proceeds through initial one-electron reduction of the *As*-chloro arsole to the corresponding biarsolyl $(AsC_4R_4)_2$ which then reacts with another equivalent of calcium in the presence the $CaCl_2$ thus-formed to yield the halo-bridged dimer. This process is invoked since WESTERHAUSEN and co-workers subsequently demonstrated that no reaction whatsoever takes place between $(AsC_4Et_4)_2$ and magnesium or calcium when $MCl_2$ is not present in the reaction mixture[108] however the heavier elements strontium and barium do react *in absentia* of any salts to give the diarsametallocenes $[Sr(\eta^5\text{-}AsC_4Et_4)_2]$ and $[Ba(\eta^5\text{-}AsC_4Et_4)_2]$ by virtue of their enlarged ionic radii and greater ease of oxidation.

### 1.4.5 μ-Arsolyl Complexes

Only three examples of a 3-electron bridging arsolyl ligand have previously been reported. As mentioned earlier, two cases originated from ABEL'S laboratory alongside the normal σ-covalent complexes:[92] $[M_2(\mu\text{-}AsC_4Ph_4)_2(CO)_8]$ (M = Mn, Re) were obtained by relatively mild heating of $[M(AsC_4Ph_4)(CO)_5]$ (*n*-hexane, 65 °C) although no yields were reported and the products were only characterised by IR spectroscopy. These species were isolated *en route* to the corresponding pentahapto arsolyl complexes.

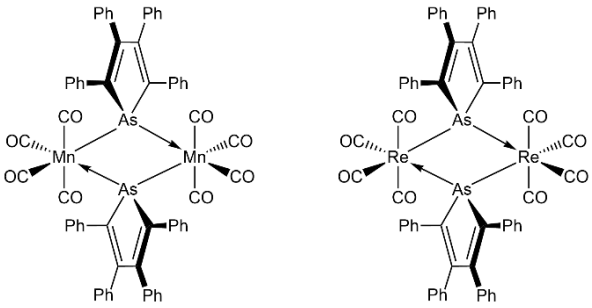



**Figure 1.17**: A pair of binuclear μ-tetraphenylarsolyl complexes prepared by ABEL.

MATHEY has obtained the binuclear complex $[Fe_2(\mu\text{-}AsC_4Me_2H_2)_2(CO)_2(\eta^5\text{-}C_5H_5)_2]$ in low yield as a by-product of "arsaferrocene" $[Fe(\eta^5\text{-}AsC_4Me_2H_2)(\eta^5\text{-}C_5H_5)]$ synthesis.[91] The green dimer occurs as a chromatographically-inseparable mixture of *cis* and *trans* isomers with an estimated 90:10 distribution at ambient temperature, respectively. No mention was made regarding the ability (or lack thereof) of these isomers to interconvert thermally or photochemically as the *cis*/*trans* forms of $[Fe_2(\mu\text{-}EMe_2)_2(CO)_2(\eta^5\text{-}$

$C_5H_5)_2$] (E = P, As) may,[133] which is regrettable since any fluxionality in operation is evidently slower than the NMR timescale and variable temperature spectroscopy may have illuminated such a process.

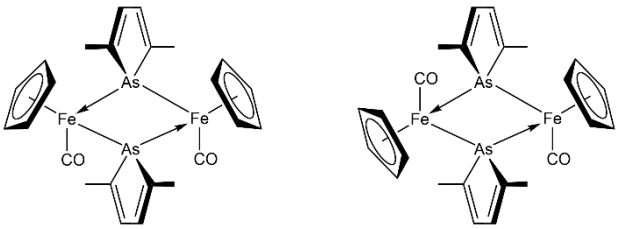



**Figure 1.18**: *Syn*- and *anti*-isomers of a μ-arsolyl complex prepared by MATHEY.

### 1.4.6 Other Coordination Modes

To the best of this author's knowledge, no other transition metal complexes featuring arsole or arsolyl ligand in coordination modes separate from those described above have been reported.

## 1.5 Foreword to this Thesis

The overarching theme of this thesis is the synthesis of new transition metal arsole and arsolyl complexes displaying a range of coordination modes. The contrast in field development *re.* phospholes *vs.* arsoles (also, stiboles and bismoles) is stark, and this work aims to narrow that divide as much as possible, or in some cases surpass the divide by establishing precedents where no phosphorus analogue may yet be known. Given the paucity of previously described compounds which have had their molecular structures determined by X-ray diffractometry (**Figure 1.5**), a secondary focus is the collection of crystallographic data – not necessarily to compare with any known trend(s) – but to establish the trend itself. This thesis has been curated in such a way as to serve as a centralised repository of-sorts for transition metal arsole and arsolyl chemistry, mindful of the fact that this field has never been the subject of a dedicated review or commentary. Where possible, as much helpful information is included for the benefit of future researchers.

It is this author's sincere hope that it will be as much a pleasure to for the reader to survey as it was for him to write. An afterword to this thesis may be found in **Chapter 7**, **Section 7.6**.

## 1.6 References


1. F. C. Leavitt, T. A. Manuel and F. Johnson, *J. Am. Chem. Soc.,* **1959**, *81*, 3163-3164.
2. H. Heaney, D. M. Heinekey, F. G. Mann and I. T. Millar, *J. Chem. Soc.,* **1958**, 3838-3844.
3. D. M. Heinekey and I. T. Millar, *J. Chem. Soc.*, **1959**, 3101-3102.
4. E. R. H. Jones and F. G. Mann, *J. Chem. Soc.,* **1958**, 1719-1721.
5. F. C. Leavitt, T. A. Manuel, F. Johnson, L. U. Matternas and D. S. Lehman, *J. Am. Chem. Soc.,* **1960**, *82*, 5099-5102.
6. E. H. Braye, W. Hübel and I. Caplier, *J. Am. Chem. Soc.,* **1961**, *83*, 4406-4413.
7. W. Schäfer, A. Schweig, G. Märkl, H. Hauptmann and F. Mathey, *Angew. Chem. Int. Ed. Eng.*, **1973**, *12*, 145-146.
8. N. D. Epiotis and W. Cherry, *J. Am. Chem. Soc.*, **1976**, *98*, 4365-4370.
9. L. Nyulászi and T. Veszprémi, *J. Mol. Struct.*, **1995**, *347*, 57-71.
10. M. K. Cyrański, T. M. Krygowski, A. R. Katritzky and P. R. Schleyer, *J. Org. Chem.*, **2002**, *67*, 1333-1338.
11. A. Mazurek and J. C. Dobrowolski, *J. Org. Chem.*, **2012**, *77*, 2608-2618.
12. S. Pelloni and P. Lazzeretti, *Theor. Chem. Acc.*, **2007**, *118*, 89-97.
13. M. K. Cyrański, P. v. R. Schleyer, T. M. Krygowski, H. Jiao and G. Hohlneicher, *Tetrahedron*, **2003**, *59*, 1657-1665.
14. M. P. Johansson and J. Juselius, *Lett. Org. Chem.*, **2005**, *2*, 469-474.
15. H. Fallah-Bagher-Shaidaei, C. S. Wannere, C. Corminboeuf, R. Puchta and P. R. Schleyer, *Org. Lett.*, **2006**, *8*, 863-866.
16. D. B. Chesnut and L. J. Bartolotti, *Chem. Phys.*, **2000**, *253*, 1-11.
17. S. Pelzer, K. Wichmann, R. Wesendrup and P. Schwerdtfeger, *J. Phys. Chem. A*, **2002**, *106*, 6387-6394.
18. I. V. Omelchenko, O. V. Shishkin, L. Gorb and J. Leszczynski, *Struct. Chem.*, **2016**, *27*, 101-109.
19. A. T. Balaban, D. C. Oniciu and A. R. Katritzky, *Chem. Rev.*, **2004**, *104*, 2777-2812.
20. A. Stanger, *Chem. Comm.*, **2009**, 1939-1947.
21. K. Ota and R. Kinjo, *Chem. Soc. Rev.*, **2021**, *50*, 10594-10673.
22. J. D. Andose, A. Rauk and K. Mislow, *J. Am. Chem. Soc.,* **1974**, *96*, 6904-6907.
23. P. Jutzi, *Angew. Chem. Int. Ed. Eng.*, **1975**, *14*, 232-245.
24. D. Seyferth, J. S. Merola and R. S. Henderson, *Organometallics*, **1982**, *1*, 859-866.
25. P. B. Hitchcock, C. Jones and J. F. Nixon, *J. Chem. Soc. Chem. Comm.*, **1994**, 2061-2062.
26. L. Weber, *Eur. J. Inorg. Chem.*, **2007**, 4095-4117.
27. A. Decken, C. J. Carmalt, J. A. C. Clyburne and A. H. Cowley, *Inorg. Chem.*, **1997**, *36*, 3741-3744.
28. M. Bouslikhane, H. Gornitzka, H. Ranaivonjatovo and J. Escudié, *Organometallics*, **2002**, *21*, 1531-1533.
29. S. C. Sendlinger, B. S. Haggerty, A. L. Rbeingold and K. H. Theopold, *Chem. Ber.*, **1991**, *124*, 2453-2456.
30. L. S. Sunderlin, D. Panu, D. B. Puranik, A. J. Ashe and R. R. Squires, *Organometallics*, **1994**, *13*, 4732-4740.
31. R. Ghiasi, *Main Group Chem.*, **2006**, *5*, 153-161.
32. M. Karplus and J. A. Pople, *J. Chem. Phys.*, **1963**, *38*, 2803-2807.
33. J. A. Pople, *Mol. Phys.*, **1964**, *7*, 301-306.
34. H. Imoto, A. Urushizaki, I. Kawashima and K. Naka, *Chem. Eur. J.*, **2018**, *24*, 8797-8803.
35. M. Ishidoshiro, H. Imoto, S. Tanaka and K. Naka, *Dalton Trans.*, **2016**, *45*, 8717-8723.
36. L. I. Smith and H. H. Hoehn, *J. Am. Chem. Soc.*, **1941**, *63*, 1184-1187.
37. A. J. Ashe and F. J. Drone, *Organometallics*, **1985**, *4*, 1478-1480.
38. A. J. Ashe, S. Mahmoud, C. Elschenbroich and M. Wünsch, *Angew. Chem. Int. Ed. Eng.*, **1987**, *26*, 229-230.
39. G. Märkl and H. Hauptmann, *Tet. Lett.*, **1968**, *9*, 3257-3260.
40. G. Märkl, H. Hauptmann and A. Merz, *J. Organomet. Chem.*, **1983**, *249*, 335-363.
41. E. H. Braye, I. Caplier and R. Saussez, *Tetrahedron*, **1971**, *27*, 5523-5537.
42. G. Märkl and R. Potthast, *Angew. Chem.*, **1967**, *79*, 58-59.

43. G. Märkl, D. Matthes, A. Donaubauer and H. Baier, *Tet. Lett.*, **1975**, *16*, 3171-3174.
44. G. Märkl and H. Hauptmann, *Tetrahedron*, **1976**, *32*, 2131-2136.
45. P. J. Fagan and W. A. Nugent, *J. Am. Chem. Soc.*, **1988**, *110*, 2310-2312.
46. P. J. Fagan, W. A. Nugent and J. C. Calabrese, *J. Am. Chem. Soc.*, **1994**, *116*, 1880-1889.
47. X. Yan and C. Xi, *Acc. Chem. Res.,* **2015**, *48*, 935-946.
48. H. Alt and M. D. Rausch, *J. Am. Chem. Soc.*, **1974**, *96*, 5936-5937.
49. J. L. Atwood, W. E. Hunter, H. Alt and M. D. Rausch, *J. Am. Chem. Soc.*, **1976**, *98*, 2454-2459.
50. S. Thanedar and M. F. Farona, *J. Organomet. Chem.*, **1982**, *235*, 65-68.
51. E. I. Negishi, F. E. Cederbaum and T. Takahashi, *Tet. Lett.*, **1986**, *27*, 2829-2832.
52. R. A. Fisher and S. L. Buchwald, *Organometallics*, **1990**, *9*, 871-873.
53. T. V. V. Ramakrishna, S. Lushnikova and P. R. Sharp, *Organometallics*, **2002**, *21*, 5685-5687.
54. E. I. Negishi, S. J. Holmes, J. M. Tour, J. A. Miller, F. E. Cederbaum, D. R. Swanson and T. Takahashi, *J. Am. Chem. Soc.*, **1989**, *111*, 3336-3346.
55. H. G. Alt, C. E. Denner, U. Thewalt and M. D. Rausch, *J. Organomet. Chem.*, **1988**, *356*, C83-C85.
56. E. I. Negishi, T. Nguyen, J. P. Maye, D. Choueiri, N. Suzuki and T. Takahashi, *Chem. Lett.*, **1992**, *21*, 2367-2370.
57. G. Erker and K. Kropp, *J. Am. Chem. Soc.*, **1979**, *101*, 3659-3660.
58. G. Erker, *J. Organomet. Chem.*, **1977**, *134*, 189-202.
59. H. G. Alt and C. E. Denner, *J. Organomet. Chem.*, **1989**, *368*, C15-C17.
60. T. Tamotsu, X. Zhenfeng and S. Noriyuki, *Chem. Lett.*, **1993**, *22*, 1001-1004.
61. T. Takahashi, M. Kageyama, V. Denisov, R. Hara and E. I. Negishi, *Tet. Lett.*, **1993**, *34*, 687-690.
62. K. Kasai, M. Kotora, N. Suzuki and T. Takahashi, *J. Chem. Soc. Chem. Communications*, 1995, 109-110.
63. S. L. Buchwald, B. T. Watson and J. C. Huffman, *J. Am. Chem. Soc.*, **1986**, *108*, 7411-7413.
64. S. L. Buchwald, R. T. Lum and J. C. Dewan, *J. Am. Chem. Soc.,* **1986**, *108*, 7441-7442.
65. S. L. Buchwald, B. T. Watson and J. C. Huffman, *J. Am. Chem. Soc.*, **1987**, *109*, 2544-2546.
66. U. Rosenthal, A. Ohff, W. Baumann, A. Tillack, H. Görls, V. V. Burlakov and V. B. Shur, *Z. Anorg. Allg. Chem.*, **1995**, *621*, 77-83.
67. C. McDade and J. E. Bercaw, *J. Organomet. Chem.*, **1985**, *279*, 281-315.
68. H. Ryuichiro, X. Zhenfeng, K. Martin, X. Chanjuan and T. Tamotsu, *Chem. Lett.*, **1996**, *25*, 1003-1004.
69. A. D. Miller, J. L. McBee and T. D. Tilley, *J. Am. Chem. Soc.*, **2008**, *130*, 4992-4999.
70. A. D. Miller, J. F. Tannaci, S. A. Johnson, H. Lee, J. L. McBee and T. D. Tilley, *J. Am. Chem. Soc.*, **2009**, *131*, 4917-4927.
71. T. Takahashi, S. Huo, R. Hara, Y. Noguchi, K. Nakajima and W. H. Sun, *J. Am. Chem. Soc.*, **1999**, *121*, 1094-1095.
72. T. Takahashi, F. Y. Tsai, Y. Li and K. Nakajima, *Organometallics*, **2001**, *20*, 4122-4125.
73. Z. Xi, H. T. Fan, S. Mito and T. Takahashi, *J. Organomet. Chem.*, **2003**, *682*, 108-112.
74. T. Takahashi, M. Kotora and Z. Xi, *J. Chem. Soc. Chem. Comm.*, **1995**, 361-362.
75. T. Takahashi, Z. Xi, A. Yamazaki, Y. Liu, K. Nakajima and M. Kotora, *J. Am. Chem. Soc.*, **1998**, *120*, 1672-1680.
76. T. Takahashi, F. Y. Tsai, Y. Li, K. Nakajima and M. Kotora, *J. Am. Chem. Soc.*, **1999**, *121*, 11093-11100.
77. H. G. Alt, H. E. Engelhardt, M. D. Rausch and L. B. Kool, *J. Organomet. Chem.*, **1980**, *329*, 61-67.
78. S. L. Buchwald and R. B. Nielsen, *J. Am. Chem. Soc.*, **1989**, *111*, 2870-2874.
79. V. P. Ananikov, O. V. Hazipov and I. P. Beletskaya, *Chem. Asian. J.*, **2011**, *6*, 306-323.
80. L. Liu, W. Geng, Q. Yang, W. X. Zhang and Z. Xi, *Organometallics*, **2015**, *34*, 4198-4201.
81. C. Xi, S. Huo, T. H. Afifi, R. Hara and T. Takahashi, *Tet. Lett.*, **1997**, *38*, 4099-4102.
82. Y. Ura, Y. Li, Z. Xi and T. Takahashi, *Tet. Lett.*, **1998**, *39*, 2787-2790.
83. G. Märkl and H. Hauptmann, *Angew. Chem. Int. Ed. Eng.*, **1972**, *11*, 439-440.
84. K. Issleib and A. Tzschach, *Chem. Ber.*, **1959**, *92*, 1118-1126.
85. A. M. Aguiar, J. Beisler and A. Mills, *J. Org. Chem.*, **1962**, *27*, 1001-1005.
86. D. Wittenberg and H. Gilman, *J. Org. Chem.*, **1958**, *23*, 1063-1065.

87. A. Tzschach and W. Lange, *Z. Anorg. Allg. Chem.*, **1964**, *330*, 317-323.
88. S. I. Sato, Y. Matsumura and R. Okawara, *Inorg. Nucl. Chem. Lett.*, **1972**, *8*, 837-840.
89. M. Westerhausen, C. Gückel, H. Piotrowski, P. Mayer, M. Warchwold and H. Nöth, *Z. Anorg. Allg. Chem.,* **2001**, *627*, 1741-1750.
90. G. Märkl and H. Hauptmann, *J. Organomet. Chem.*, **1983**, *248*, 269-285.
91. G. Thiollet, F. Mathey and R. Poilblanc, *Inorg. Chim. Acta*, **1979**, *32*, L67-L68.
92. E. W. Abel and C. Towers, *J. Chem. Soc. Dalton Trans.,* **1979**, 814-819.
93. E. W. Abel, N. Clark and C. Towers, *J. Chem. Soc., Dalton Trans.*, **1979**, 1552-1556.
94. A. D. Beveridge and G. S. Harris, *J. Chem. Soc.*, **1964**, 6076-6084.
95. S. Tanaka, H. Imoto, T. Yumura and K. Naka, *Organometallics*, **2017**, *36*, 1684-1687.
96. M. D. Smith, *Sci. Synth.*, **2002**, *4*.
97. G. Märkl and H. Hauptmann, *Angew. Chem. Int. Ed. Eng.*, **1972**, *11*, 441-441.
98. R. H. DeWolfe and W. G. Young, *Chem. Rev.*, **1956**, *56*, 753-901.
99. W. A. Schenk and E. Voß, *J. Organomet. Chem.*, **1994**, *467*, 67-73.
100. A. Marinetti, F. Mathey, J. Fischer and A. Mitschler, *J. Am. Chem. Soc.*, **1982**, *104*, 4484-4485.
101. A. Marinetti, F. Mathey, J. Fischer and A. Mitschler, *J. Chem. Soc. Chem. Comm.*, **1984**, 45-46.
102. G. Sennyey and F. Mathey, *Tet. Lett.*, **1981**, *22*, 4713-4716.
103. C. Charrier, H. Bonnard, G. De Lauzon and F. Mathey, *J. Am. Chem. Soc.*, **1983**, *105*, 6871-6877.
104. S. Holand, F. Mathey and J. Fischer, *Polyhedron*, **1986**, *5*, 1413-1421.
105. F. Nief and L. Ricard, *Organometallics*, **2001**, *20*, 3884-3890.
106. F. Nief, L. Ricard and F. Mathey, *Polyhedron*, **1993**, *12*, 19-26.
107. A. J. Ashe, W. M. Butler and T. R. Diephouse, *Organometallics*, **1983**, *2*, 1005-1008.
108. M. Westerhausen, C. Gückel, H. Piotrowski, P. Mayer, M. Warchhold and H. Nöth, *Z. Anorg. Allg. Chem.*, **2001**, *627*, 1741-1750.
109. M. Westerhausen, M. H. Digeser, C. Gückel, H. Nöth, J. Knizek and W. Ponikwar, *Organometallics*, **1999**, *18*, 2491-2496.
110. S. Wolfe, *Acc. Chem. Res.*, **1972**, *5*, 102-111.
111. F. Nief, D. Turcitu and L. Ricard, *Chem. Comm.*, **2002**, 1646-1647.
112. A. J. Ashe and E. G. Ludwig, *J. Organomet. Chem.*, **1986**, *303*, 197-204.
113. S. Burck, M. Nieger and D. Gudat, *Z. Anorg. Allg. Chem.*, **2010**, *636*, 1263-1267.
114. A. J. Ashe, *J. Am. Chem. Soc.*, **1971**, *93*, 3293-3295.
115. G. Märkl, H. Hauptmann and J. Advena, *Angew. Chem. Int. Ed. Eng.*, **1972**, *11*, 441-443.
116. G. Märkl, J. Advena and H. Hauptmann, *Tet. Lett.*, **1974**, *15*, 303-304.
117. V. G. Märkl, J. Advena and H. Hauptmann, *Tet. Lett.*, **1974**, *15*, 203-206.
118. R. L. Jones and C. W. Rees, *J. Chem. Soc. C*, **1969**, 2249-2251.
119. G. Mora, B. Deschamps, S. van Zutphen, X. F. Le Goff, L. Ricard and P. Le Floch, *Organometallics*, **2007**, *26*, 1846-1855.
120. G. Thiollet and F. Mathey, *Inorg. Chim. Acta*, **1979**, *35*, L331-L332.
121. H. D. Kaesz, R. B. King, T. A. Manuel, L. D. Nichols and F. G. A. Stone, *J. Am. Chem. Soc.*, **1960**, *82*, 4749-4750.
122. M. Ishidoshiro, Y. Matsumura, H. Imoto, Y. Irie, T. Kato, S. Watase, K. Matsukawa, S. Inagi, I. Tomita and K. Naka, *Org. Lett.*, **2015**, *17*, 4854-4857.
123. E. W. Abel, I. W. Nowell, A. G. J. Modinos and C. Towers, *J. Chem. Soc. Chem. Comm.*, **1973**, 258-259.
124. G. Thiollet, R. Poilblanc, D. Voigt and F. Mathey, *Inorg. Chim. Acta*, **1978**, *30*, L294.
125. F. Mathey, *Tet. Lett.*, **1976**, *17*, 4155-4158.
126. G. De Lauzon, F. Mathey and M. Simalty, *J. Organomet. Chem.*, **1978**, *156*, C33-C36.
127. A. J. Ashe, J. W. Kampf, S. Pilotek and R. Rousseau, *Organometallics*, **1994**, *13*, 4067-4071.
128. A. J. Ashe and S. Al-Ahmad, *Adv. Organomet. Chem.*, **1996**, *39*, 325-353.
129. A. J. Ashe, S. Al-Ahmad, S. Pilotek, D. B. Puranik, C. Elschenbroich and A. Behrendt, *Organometallics*, **1995**, *14*, 2689-2698.
130. N. M. Kostic and R. F. Fenske, *Organometallics*, **1983**, *2*, 1008-1013.
131. R. J. Kahan, F. G. N. Cloke, S. M. Roe and F. Nief, *New J. Chem.*, **2015**, *39*, 7602-7607.
132. M. Westerhausen, M. W. Ossberger, P. Mayer, H. Piotrowski and H. Nöth, *Organometallics*, **2004**, *23*, 3417-3424.

133. R. G. HAYTER, *J. Am. Chem. Soc.*, **1963**, *85*, 3120-3124.

# Chapter 2

# Coordination Chemistry of *As*-Alkynyl Arsoles

## 2.1 Preamble

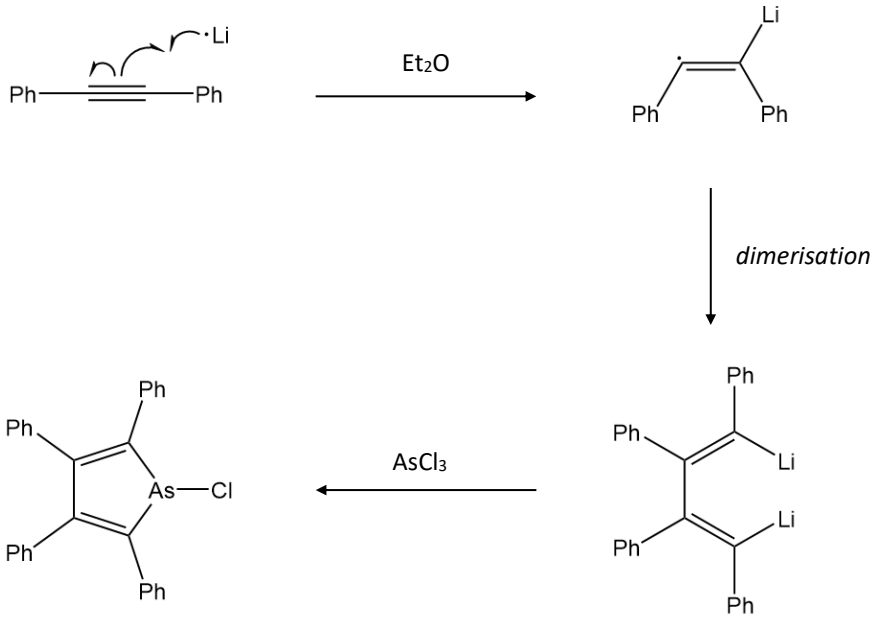
At the outset of this work, one visible caveat to all preceding arsole chemistry was the preponderance of chemically inert *As*-substituents (*metallo*-groups and halides notwithstanding). The majority of previously reported arsoles contain phenyl, methyl, or *tert*-butyl residues (in that order) which is not necessarily attributed to any preference or bias, rather, the availability of the necessary arsenic precursor(s). This somewhat limits any scope to the small range of those reagents which would be easiest to obtain *e.g.*, $PhAsCl_2$ is readily synthesised by an electrophilic aromatic substitution of benzene with $AsCl_3$. The alternative route involving hydroarsination of 1,3-diynes (**Chapter 1**, **Section 1.2.2**) implicitly excludes primary arsines that themselves include unsaturated carbon-carbon bonds in the substituent. The desire to bestow arsoles (and heterocycles in general) with additional chemical functionality was further hindered by difficulties in synthesising rings where the heteroatom possesses a halide substituent, whereby one sole precursor might be utilised as a "late common intermediate" to prepare an innumerable library of derivatives. As outlined in the introduction to this thesis, such challenges were eventually surmounted by MÄRKL and later FAGAN and NUGENT who would provide a reliable means to prepare *As*-chloro arsoles, which have obvious synthetic potential.

Those methods are enormously successful for 2,5-disubstituted and 2,3,4,5-tetralkyl substituted *As*-chloroarsoles however for certain practical reasons (outlined hereto) are not appropriate for the 1-chloro-2,3,4,5-tetra-aryl analogues. Therefore, an initial target of this work was to devise an improved synthetic route to 1-chloro-2,3,4,5-tetraphenylarsole ($ClAsC_4Ph_4$) – so chosen for reasons of crystallinity and economy – which could be used to prepare a library of ring systems with bespoke (*i.e.*, non-alkyl or -aryl) heteroatom functions. One of these would be alkynyl residues as synthons for unsaturated all-carbon chains bearing an arsole pendant at one or both ends. Though some *P*-ethynyl phospholes are previously known, no such arsoles have been described to date. Accordingly, this chapter describes an improved synthesis of $ClAsC_4Ph_4$ and the first examples of *As*-ethynyl and -butadiynyl derivatives, which enter into a variety of transformations within the coordination environments of labile ruthenium and cobalt centres.

## 2.2 *As*-Ethynyl Arsoles

### 2.2.1 Synthesis of $ClAsC_4Ph_4$

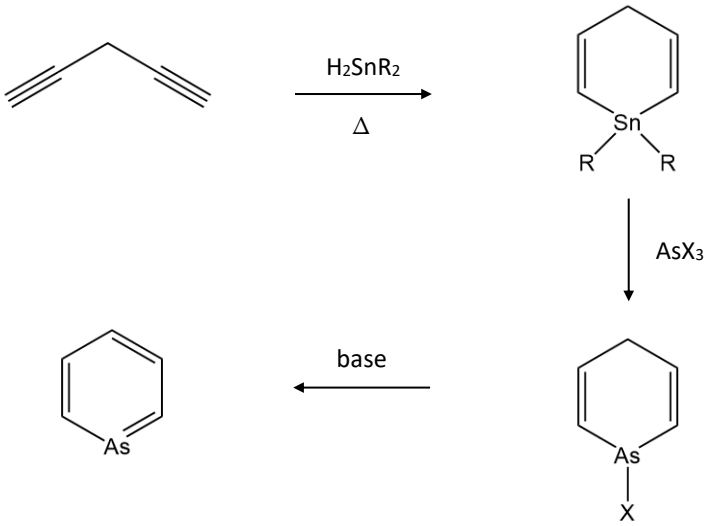
The original synthesis of 1-chloro-2,3,4,5-tetraphenylarsole ($ClAsC_4Ph_4$) as described by LEAVITT and BRAYE (separately) involved the addition of $AsCl_3$ to an ethereal solution of then newly discovered 1,4-dilithio-tetraphenylbutadiene,[1-3] the latter being prepared *in situ* by lithium reduction of diphenylacetylene (**Scheme 2.1**). At a very early stage in this work the same procedure was replicated (although the organolithium was instead generated more reliably by treatment of 1,4-diiodo-tetraphenylbutadiene with *n*-BuLi); however, it became apparent that isolation of the product would not be a straightforward task since the *As*-chloro arsole was not amenable to chromatography. BRAYE and co-workers arrive at a similar conclusion in their 1961 report, noting "*the difficulties encountered in purifying the sample* [$ClAsC_4Ph_4$] *did not allow for an unequivocal analysis of the product*". The intrinsic disadvantages of this synthetic method have been briefly outlined in **Chapter 1**, **Section 1.2.1**.




**Scheme 2.1**: The original synthesis of 1-chloro-2,3,4,5-tetraphenylarsole as described separately by LEAVITT and BRAYE.

An alternative synthesis of $ClAsC_4Ph_4$ was sought, mooting MÄRKL'S preparation of 1-chloro-2,5-diphenylarsole ($ClAsC_4Ph_2H_2$) by treatment of the corresponding 1-benzyl arsole ($PhCH_2AsC_4Ph_2H_2$) with iodobenzene dichloride ($PhI{\cdot}Cl_2$; a crystalline form of $Cl_2$).[4] As mentioned in **Chapter 1**, **Section 1.3.2**,

halogenation of the arsenic atom from the III+ to V+ oxidation state is accompanied quickly thereafter by thermal elimination of benzyl chloride and a return to As(III), the driving force primarily being enthalpic in origin.* The weakness of benzyl-element bonds, attributed to the stability of the benzyl radical, underpins its frequent use as a protecting group in organic synthesis where it is easily removed in reductive, oxidative or LEWIS acid mediated processes. This would necessitate first preparing a sample of benzyldichloroarsine ($PhCH_2AsCl_2$) for which – at the time – there was little desire to do so. Instead, inspiration was taken from ASHE'S synthesis of arsabenzene and arsanaphthalene (also JUTZI'S synthesis of arsaanthracene) for which installation of the arsenic atom within the ring system is accomplished by transmetalation from tin.[5-7]



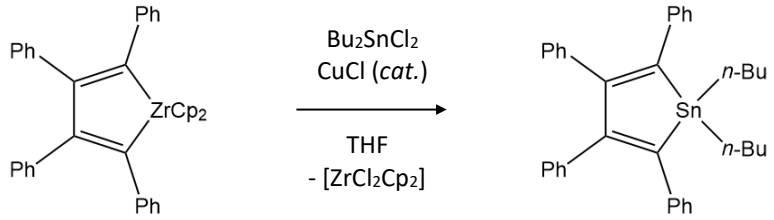

**Scheme 2.2**: ASHE'S synthesis of arsabenzene *via* transmetalation from tin.

A similar approach for syntheses of 1-chloro arsoles has not appeared in the relevant literature,† though the possibility of synthesising $ClAsC_4Ph_4$ by simple treatment of $R_2SnC_4Ph_4$ with $AsCl_3$ was an alluring prospect considered worthy of investigation. The requisite 1*H*-stannacyclopentadiene (henceforth stannole), namely 1,1-di-*n*-butyl-2,3,4,5-tetraphenylstannole $Bu_2SnC_4Ph_4$, was prepared by a copper-catalysed transmetalation between $[ZrC_4Ph_4(\eta^5\text{-}C_5H_5)_2]$ and $Bu_2SnCl_2$ in THF solution (**Scheme 2.3**).[8] The reaction is impractically slow in the absence of the Cu(I) additive (in this case CuCl[9]), probably for kinetic

* This approach has also been utilised to prepare 9-halo-9-arsafluorene by halogenation of 9-methyl-9-arsafluorene with $I_2$ or ICl. See S. TANAKA, H. IMOTO, T. YUMARA and K. NAKA *Organometallics*, **2017**, *36*, 1684—1687.

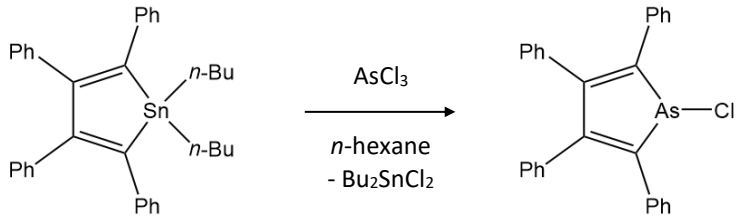
† It is noted however that dithiadiaza-arsoles $RAsN_2S_2$ have been prepared by a transmetalation reaction between $RAsX_2$ and $(Bu_2SnN_2S_2)_2$. See V. MATUSKA, M. Z. SLAWIN, D. J. WOOLLINS *Inorg. Chem.*, **2010**, *49*, 3064—3069.

reasons since both the nucleophilic butadiene carbon and electrophilic tin and zirconium centres are themselves shielded behind phenyl, *n*-butyl and cyclopentadienyl residues, respectively.* The role of the copper additive has been shown[10, 11] to generate a 1,4-dicuprobutadiene *in situ* which – being open-chained and of tempered steric profile – more readily transfers the nucleophile to $Bu_2SnCl_2$, regenerating the CuCl catalyst in the process (**Chapter 1**, **Scheme 1.10**).†




**Scheme 2.3** Synthesis of $Bu_2SnC_4Ph_4$. Cp = $\eta^5$-$C_5H_5$.

The tetraphenylstannole was reproducibly isolated from the reaction mixture in exceptionally high yields (typically ~90%) as a resinous, moderately air- and moisture-stable yellow liquid (the colour and consistency resembling honey, incidentally). Silica gel is to be avoided for risk of protonolysis to *Z*,*Z*-1,2,3,4-tetraphenylbutadiene, however chromatography on neutral alumina is possible without visible decomposition or reduction in yield. Treatment of an *n*-hexane solution of $Bu_2SnC_4Ph_4$ with one equivalent of $AsCl_3$ (**Scheme 2.4**) proceeds at ambient temperature overnight with precipitation of $ClAsC_4Ph_4$ as a bright yellow-orange microcrystalline solid in good yields (typically ≥ 70%).‡




**Scheme 2.4**: Synthesis of $ClAsC_4Ph_4$ *via* transmetalation.

* $PhAsCl_2$ also reacts slowly with $[ZrC_4Ph_4(\eta^5\text{-}C_5H_5)_2]$ in the absence of CuCl, whereas the same reagent reacts instantly with $[ZrC_4Me_4(\eta^5\text{-}C_5H_5)_2]$ with no need for CuCl additive. The ability of the main group electrophile and the carbocyclic fragment to approach one another in solution in the correct orientation to form the cyclic transition state is intuitively understood by kinetic considerations, rather than electronegativity differences, being the governing factor.

† The use of Cu(I) as a catalyst in zirconacycle transformations was most-recently reviewed in the late 1990's, and despite this being somewhat out-of-date remains an informative source. See M. Kotora, Z. Xi and T. Takahashi *J. Syn. Org. Chem. Japan*, **1997**, *55*, 958—969. The review is published in English. Other reviews broadly dedicated to zirconacycle chemistry usually cover copper-catalysed transformations to some extent. See X. Yan and C. Xi *Acc. Chem. Res.*, **2015**, *48*, 935—946 and *Id. Coord. Chem. Rev.*, **2017**, *350*, 275—284.

‡ Extreme caution should be exercised when dispensing $AsCl_3$ for it is a rather potent poison and vesicant (blistering agent). Additionally, contact with moisture produces HCl and various water-soluble arsenates, which are themselves exceedingly toxic. It is worth mentioning that the vast majority of arsenic compounds produced in this work have no physiological or toxicological data, and they should therefore be treated with respect as any arsenic source should *i.e.*, they are assumed to be of **high chronic toxicity**.

The expendable $Bu_2SnCl_2$ is removed by copious washing with *n*-pentane and disposed of appropriately,* and in contrast to other *As*-chloro arsoles prepared throughout this work the tetraphenyl derivative is somewhat air-stable: the product may be isolated and briefly handled under the ambient atmosphere without diminution in quality, though samples do slowly acquire a brown cast over several days exposed to air. It should be noted that $[ZrC_4Ph_4(\eta^5\text{-}C_5H_5)_2]$ could be treated directly with $AsCl_3$ in THF solution (which react *rapidly* and exothermically) however it proved all but impossible to separate the $[ZrCl_2(\eta^5\text{-}C_5H_5)_2]$ by-product from $ClAsC_4Ph_4$ since both share almost identical solubility properties, and chromatography is an unavailable option.†

Composition follows principally from high-resolution mass spectrometry which yields the molecular ion ($m/z \approx 466.0469$) in addition to ionisation of the As-Cl bond (though the former ion signal is dominant). The $^1H$ NMR spectrum contains only aromatic hydrogen signals which are of little diagnostic value however the $^{13}C\{^1H\}$ NMR spectrum ($CDCl_3$) finds the arsole ring-carbon nuclei at 152.0 (2,5-positions) and 145.5 (3,4-positions) ppm, which may be compared to that of the prototypical 1,2,3,4,5-pentaphenylarsole ($CDCl_3$: 152.1 and 150.0 ppm[12]). Single crystals were obtained by cooling a hot benzene/*n*-hexane mixture to -20 °C overnight and the molecular structure is shown in **Figure 2.1**.

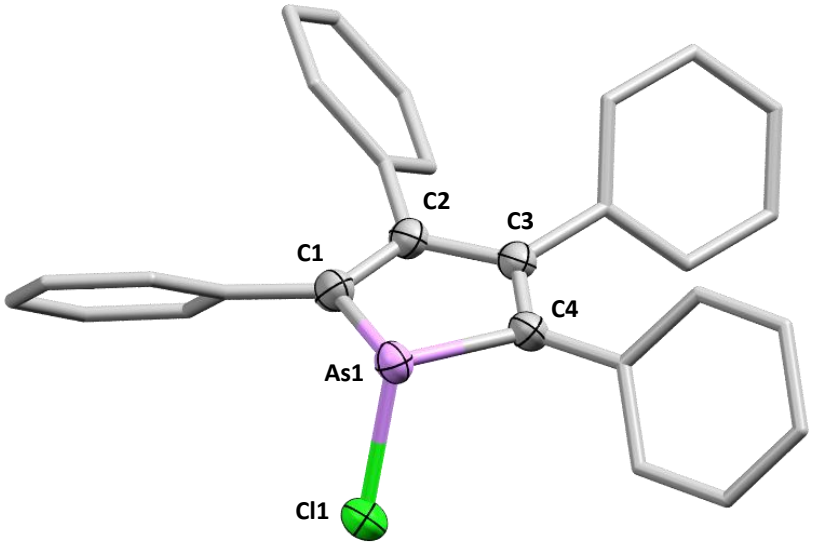



**Figure 2.1**: The molecular structure of $ClAsC_4Ph_4$ in a crystal. Phenyl groups simplified and hydrogen atoms omitted for clarity. The arsenic and chlorine atoms are disordered over two positions by inflection about the mean ring plane (occupancy ratio *ca* 80:20) and the major contributor is shown. Ellipsoids shown at 50% displacement.

* Di-*n*-butyltin dichloride is acutely toxic, mutagenic and an aquatic hazard being not readily biodegradable. Given the quantities employed here, local and national statutes should be consulted for safe and responsible disposal. Wastes/residues containing tin should be segregated from "ordinary" organic/halogenated wastes as part of this procedure.

† The crystal structure of a hydrolysis/oxidation product, $(HO)(O)AsC_4Ph_4$, is shown in **Appendix**, **Section 8.5**.

Noteworthy is that this is the first X-ray structure determination to be carried out on an *As*-halo arsole. Indeed, other than aryls, structural data for arsoles bearing mesomeric *As*-substituents are limited to those for which tetramethylbiarsolyl,[13] a phosphino derivative $(NMesCH)_2P\text{-}AsC_4Et_4$,[14] and a rather exotic germylene,[15] leaving the impact of π-donor/acceptor substituents upon the arsole π-system uncharted. Perhaps undercutting this novelty, interatomic dimensions of interest are largely typical of the individual bonding partners with mean As-$C_\alpha$, mean $C_\alpha$=$C_\beta$ and $C_\beta$-$C_\beta$ distances of 1.972(5), 1.355(4) and 1.496(4) Å,* respectively, which compare unremarkably to those in $PhAsC_4Ph_4$ and $PhAsC_4Ph_2H_2$.[12, 16] The As-Cl bond is crystallographically identical in both disordered components (2.196(2) Å) and the As(III) atom is markedly pyramidal with mean exocyclic ($C_\alpha$-As-Cl) angles of *ca* 98° and an endocyclic ($C_\alpha$-As-$C_\alpha$) angle of *ca* 86°. Furthermore, the arsole ring is measurably non-planar with the arsenic atom extruded by *ca* 13° from the mean plane formed by the butadiene carbon atoms (*cf. ca* 11° in $PhAsC_4Ph_4$[12]). This will prove to be a recurring feature of almost all $\lambda^3$-arsoles structurally characterised throughout this work.

A computational assessment of the electronic structure of $ClAsC_4Ph_4$ was carried out using DFT in the gas phase at the ωB97X-D/6-31G* level of theory and frontier orbitals are shown in **Figure 2.2**.

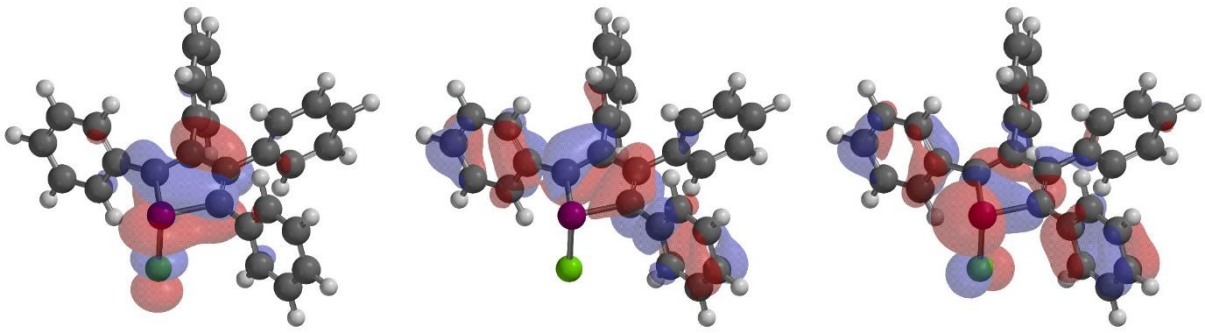



**Figure 2.2**: Calculated frontier orbitals of $ClAsC_4Ph_4$ (DFT, gas phase: ωB97X-D/6-31G*).

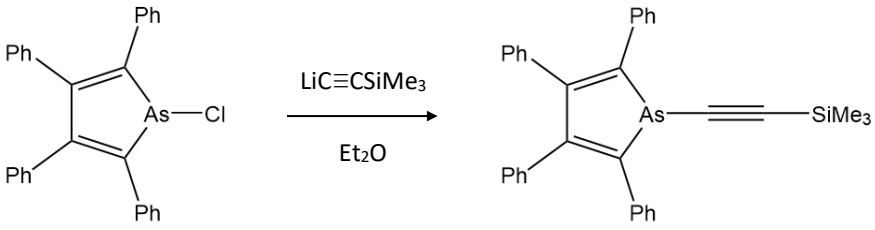
The computational model returns a core geometry in excellent agreement with the crystal structure, the only salient deviation being the nearly orthogonal orientations of the four exocyclic phenyl residues

* Throughout this work, the labels α and β are interchangeably used as shorthand to refer to the carbon atoms in the 2,5- and 3,4-ring positions, respectively.

with respect to the mean arsole plane, unperturbed as these are by crystal-packing effects that operate in the experimentally determined solid state structure. The HOMO, of relevance to [4+2] cycloadditions, is localised primarily on the butadiene π-system with a nodal plane bisecting the orbital through the arsenic atom and the $C_\beta$-$C_\beta$ bond perpendicular to the ring; no contributions from the arsenic atom are observed. The HOMO does, however, comprise a contribution from the phenyl groups in the 2,5-ring positions, a common feature of the heavy Group 15 heteroles and often invoked to explain the effect of ring-substituents on optical properties.[12] The LUMO expands onto the arsenic atom from the carbon atoms in the 2,5-ring positions and receives a significant contribution from the As-Cl(σ*) antibond rendering it – as expected – the foremost site for nucleophilic attack, not least because the arsenic also carries a Natural Charge of +1.018. The arsenic lone pair is found in the HOMO-1 alongside secondary contributions from a non-bonding electron pair on the chloride atom – noteworthy is the mutually antibonding interactions between the orbital housing the arsenic lone pair (appreciably diffuse, accounting for its sizeable *s* character) and the butadiene moiety. A cursory inspection of the 30 highest-energy occupied orbitals finds no convincing evidence for HÜCKEL-type delocalisation throughout the unsaturated five-membered ring.

### 2.2.2 Synthesis of $Me_3SiC{\equiv}CAsC_4Ph_4$

Attempts to prepare the parent *As*-ethynyl arsole $HC{\equiv}CAsC_4Ph_4$ by directly combining $ClAsC_4Ph_4$ with commercially available $HC{\equiv}CMgBr$ solution gave an intractable brown residue from which the target compound was neither detected nor isolated; this contrasts with behaviours of the same GRIGNARD reagent toward $BrPC_4Ph_4$ and $ClPC_4Et_4$ which does afford the corresponding *P*-ethynyl phospholes.[17, 18] The reason(s) for the failure to produce an isolable arsole from this approach is not presently known. Instead, the chloroarsole was treated with a slight excess of the organolithium $LiC{\equiv}CSiMe_3$ (prepared *in situ* from $HC{\equiv}CSiMe_3$ and *n*-BuLi) in $Et_2O$ medium from which the moisture-sensitive $Me_3SiC{\equiv}CAsC_4Ph_4$ is isolated in good yield as a light-yellow solid.

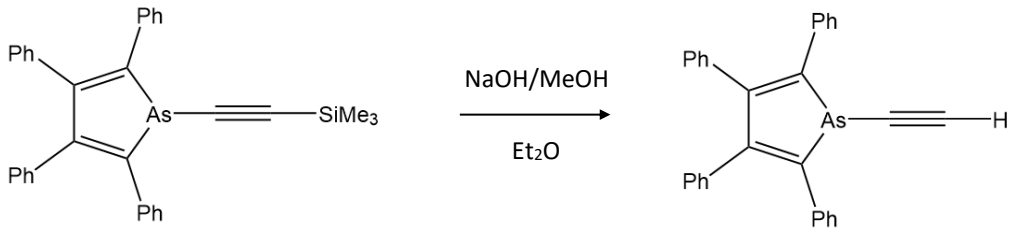



**Scheme 2.5**: Synthesis of $Me_3SiC{\equiv}CAsC_4Ph_4$.

The use of $Et_2O$ as the reaction solvent proved imperative as THF gave consistently low yields (< 10%) of impure product. This compound is promptly desilylated upon contact with adventitious or atmospheric moisture* (or other mild reagents; **Section 2.2.3**) and its identity readily follows from NMR spectroscopy, finding the trimethylsilyl group as a sharp signal at 0.01 ppm in the $^1H$ NMR spectrum and -0.2 ppm in the $^{13}C\{^1H\}$ spectrum. The arsole ring-carbon nuclei are observed in their usual positions (151.3 and 147.8 ppm) with a pair of ethynyl carbon resonances at 115.7 (*As*-bound) and 101.6 (*Si*-bound) ppm. At the time of writing, single crystals suitable for X-ray diffraction have not been forthcoming (despite the high solubility of the compound in non-polar media) however a structural determination carried out on the $Co_2(CO)_6$ adduct (**Section 2.8.1**) was sufficient to unequivocally confirm identity.

### 2.2.3 Synthesis of $HC{\equiv}CAsC_4Ph_4$

As alluded to above, $Me_3SiC{\equiv}CAsC_4Ph_4$ underwent desilylation upon exposure to atmospheric moisture – either in solution or the solid state – to the parent ethynyl arsole $HC{\equiv}CAsC_4Ph_4$. This process could be deliberately induced by chemical desilylation with $KF{\cdot}2H_2O$ or $[Bu_4N]F$ in THF. However, $Me_3SiC{\equiv}CAsC_4Ph_4$ need not be isolated, and the simplest route was to directly treat the $Et_2O$ reaction mixture with an excess of methanolic NaOH from which $HC{\equiv}CAsC_4Ph_4$ precipitates in high yield as an off-white solid. Incidentally, the parent ethynyl arsole may also be obtained from a mixture of $ClAsC_4Ph_4$ and $Bu_3SnC{\equiv}CH$ in refluent THF (65 °C) though complete removal of oily tin-containing residues required treatment with fluoride followed by column chromatography. The compound is indefinitely air- and moisture-stable and whilst quantitative optical measurements were unfortunately not carried out during this work, this arsole fluoresces a very pleasant blue colour under broad-band UV light in both the solid-state and $CH_2Cl_2$ solution.




**Scheme 2.6**: Synthesis of $HC{\equiv}CAsC_4Ph_4$.

* The formation of a $Co_2(CO)_6$ adduct, however, greatly improves resistance to opportunistic desilylation. See **Section 2.8.1**.

The formulation follows from the usual spectroscopic methods and the ethynyl hydrogen is observed at 2.87 ppm in the $^{1}H$ NMR spectrum (of diminished area integration due to partial H/D exchange in $CDCl_3$) and the carbon nuclei of interest are observed in the $^{13}C\{^{1}H\}$ NMR spectrum at 151.3 and 146.9 ppm (arsole ring atoms), and 94.1 and 80.0 ppm for the *As*-bound and terminal ethynyl carbon atoms, respectively. The connectivity and assignment of the ethynyl nuclei was identified by means of an HSQC NMR experiment. High-resolution mass spectrometry reveals the molecular ion ($m/z \approx 456.0859$) and single crystals suitable for X-ray diffraction were obtained from $CH_2Cl_2$/methanol at -20 °C. The molecular structure is shown in **Figure 2.3**.

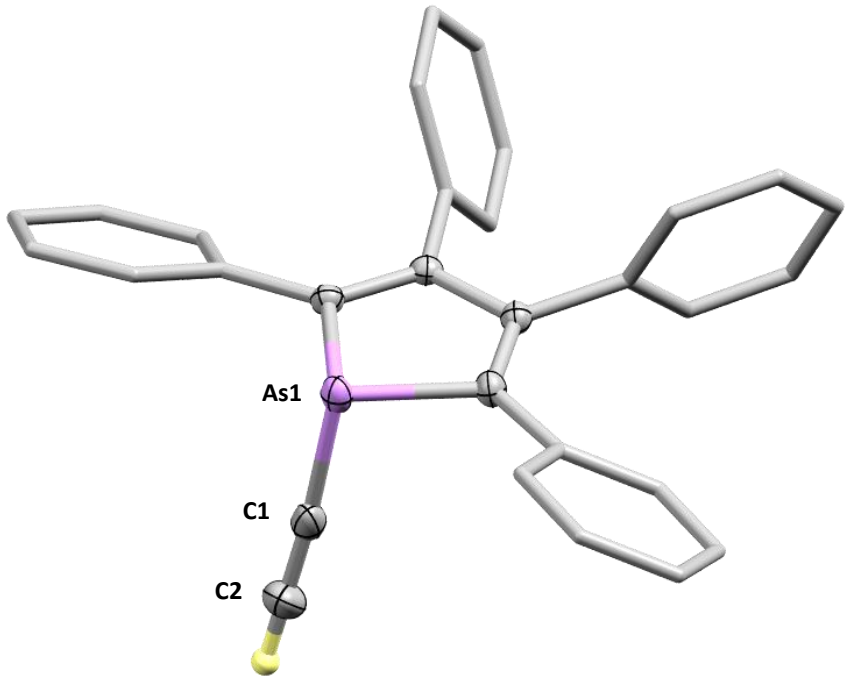



**Figure 2.3**: The molecular structure of $HC{\equiv}CAsC_4Ph_4$ in a crystal. Phenyl groups simplified and most hydrogen atoms omitted for clarity, except for the ethynyl proton which is shown in yellow for emphasis. Ellipsoids shown at 50% displacement.

The expected parent ethynyl arsole is found. Gross molecular features are largely identical to those of other structurally characterised tetraphenylarsoles (*e.g.*, $ClAsC_4Ph_4$ **Figure 2.1**, $PhAsC_4Ph_4$[12]) and the configuration of $HC{\equiv}CAsC_4Ph_4$ will only be briefly discussed. Due to the decreasing covalent radii of carbon with decreasing coordination number ($sp^3 \approx 0.76$, $sp^2 \approx 0.73$, $sp \approx 0.69$ Å), the exocyclic As-C($sp$) bond of 1.898(2) Å is notably shorter than typical As-C($sp^2$) (*ca* 1.95 Å) and As-C($sp^3$) bonds (*ca* 2.0 Å) measured throughout this work, but comparable to that found[19] in $As(C{\equiv}CPh)_3$.* The ethynyl triple bond

* There are no previous CCDC structural data available for unsubstituted ethynyl arsines.

measures 1.180(3) Å and is unremarkable, as are the internal ring-atom bonding distances of *ca* 1.95 (mean As-$C_\alpha$), *ca* 1.35 (mean $C_\alpha$-$C_\beta$) and *ca* 1.49 ($C_\beta$-$C_\beta$) Å. The ethynyl linkage is slightly curved in the solid state (As1-C1-C2 *ca* 174°) and projects from the mean plane of the arsole ring by *ca* 98° (precluding any conventional π-conjugation); the envelope fold of the arsole ring (*ca* 5°) is narrower than that measured in $ClAsC_4Ph_4$ and $PhAsC_4Ph_4$.

A computational assessment of the electronic structure of $HC{\equiv}CAsC_4Ph_4$ was carried out using DFT (gas phase: ωB97X-D/6-31G* level of theory) and frontier orbitals are shown in **Figure 2.4**.

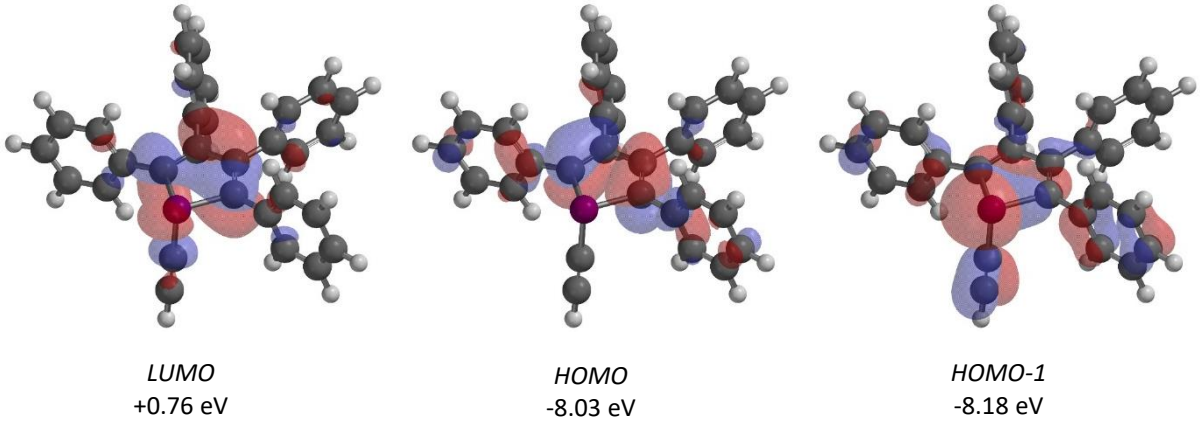



**Figure 2.4**: Calculated frontier orbitals of $HC{\equiv}CAsC_4Ph_4$ (DFT, gas phase: ωB97X-D/6-31G*).

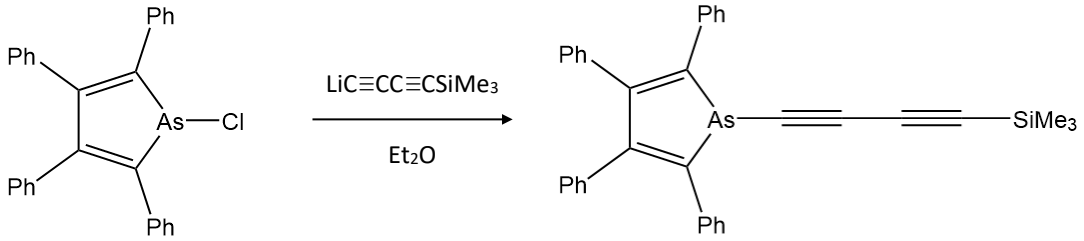
The geometry of $HC{\equiv}CAsC_4Ph_4$ returned is in excellent agreement with the crystal structure, *bar* the orientations of the exocyclic phenyl rings. Like $ClAsC_4Ph_4$ (**Figure 2.2**), the HOMO is strongly centred on the butadiene π-system with a vertical nodal plane bifurcating the ring and minor contributions made from the phenyl residues in the 2,5-ring positions. As expected by replacement of the chloride for a less-electron withdrawing ethynyl substituent, the LUMO is calculated some 0.9 eV higher in energy than the same orbital in $ClAsC_4Ph_4$, comprising almost equally of the mutually antibonding As-C(σ*) and butadiene(π*) orbitals. The fact that the LUMO is centred on the *kinetically accessible* arsenic atom should manifest in a seemingly unavoidable site for nucleophilic attack (**Section 2.4**). Likewise, the HOMO-1 containing the arsenic lone pair electrons is *ca* 0.25 eV higher in energy than the *As*-chloro analogue, protruding substantially from the heteroatom whilst complimented by an ethynyl(π) orbital and residual bonding networks within the butadiene moiety. Notably, however, no orbitals were found which displayed

convincing evidence for communication between the two π-systems and in this regard the arsenic atom appears to serve as an electronic blockade within the molecule.

## 2.3 *As*-Butadiynyl Arsoles

### 2.3.1 Synthesis of $Me_3SiC{\equiv}CC{\equiv}CAsC_4Ph_4$

The four-carbon butadiynyl chain was installed onto the tetraphenylarsole unit by an analogous approach to that of $Me_3SiC{\equiv}CAsC_4Ph_4$: a $Et_2O$ solution of $LiC{\equiv}CC{\equiv}CSiMe_3$ was prepared by treatment of $Me_3SiC{\equiv}CC{\equiv}CSiMe_3$ with one equivalent of MeLi·LiBr complex[20] and combined with $ClAsC_4Ph_4$ to provide the light-yellow $Me_3SiC{\equiv}CC{\equiv}CAsC_4Ph_4$ in good yield, albeit contaminated with a small quantity of $HC{\equiv}CC{\equiv}CSiMe_3$ which was difficult to remove due to the similar solubilities of both compounds.*




**Scheme 2.7**: Synthesis of $Me_3SiC{\equiv}CC{\equiv}CAsC_4Ph_4$.

It was actually advantageous to employ a slight excess of $Me_3SiC{\equiv}CC{\equiv}CSiMe_3$ to guarantee that no unreacted MeLi was present in solution when introduced to $ClAsC_4Ph_4$, since the formation of $MeAsC_4Ph_4$ (**Section 2.4**) was observed in initial experiments and proved to be a more persistent contaminant than $HC{\equiv}CC{\equiv}CSiMe_3$ during downstream reactions. Nonetheless, the identity of the butadiynyl arsole could be unambiguously confirmed by the usual spectroscopic methods and a single crystal structure determination (**Figure 2.5**). Noteworthy is that in contrast to $HC{\equiv}CAsC_4Ph_4$ and $HC{\equiv}CC{\equiv}CAsC_4Ph_4$ (*vide infra*), $Me_3SiC{\equiv}CC{\equiv}CAsC_4Ph_4$ did not fluoresce under broad-band UV light (both solid state and $CH_2Cl_2$ solution); free rotation of the $SiMe_3$ group perhaps allows for non-radiative relaxation of the excited-state molecule.

* NMR: $^1H$ ($C_6D_6$, 400 MHz, 25 °C) δ 1.37, -0.08 ppm.

Resonances for the butadienyl carbon chain are observed in the $^{13}C\{^{1}H\}$ NMR spectrum ($C_6D_6$) at 100.3 (*As*-bound), 90.9 and 89.5 (internal) and 86.2 (*Si*-bound) ppm. Interestingly, the arsole ring-carbons appear to be diastereotopic since *four* signals are observed in the expected region at 154.6, 154.1, 149.6, and 146.8 ppm – this would prove to be a recurring feature of *As*-butadiynyl arsoles prepared during this work. Furthermore, sixteen aromatic carbon resonances corresponding to four inequivalent phenyl substituents are also measured. A means by which the internal plane of molecular symmetry is extinguished by the presence of a butadiynyl residue is not presently obvious, since the $^{1}H$ NMR spectrum and other analytical data confirm the presence of a singular compound. One may envision a "bowstring" type bending of the four-carbon chain, or diastereotopism of the four phenyl substituents, which would indeed lower the overall symmetry of the molecule in solution however these would seem to be low energy inversion processes undoubtedly averaged on the NMR timescale. In the absence of other analytical data, it is not possible to provide a conclusive explanation for the apparent chirality of $Me_3SiC{\equiv}CC{\equiv}CAsC_4Ph_4$ in solution.

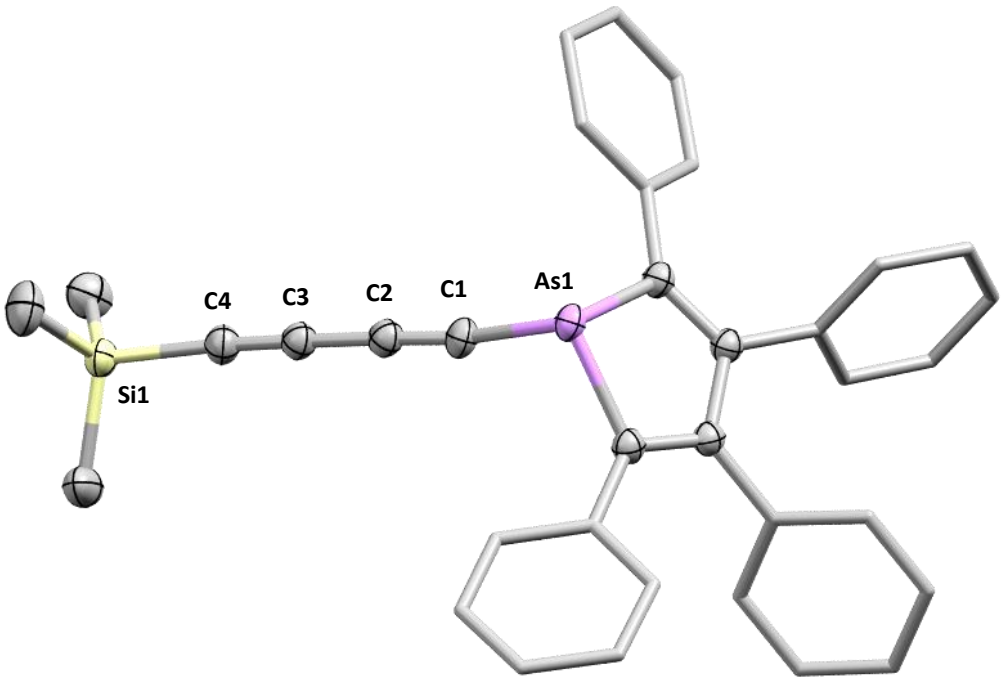



**Figure 2.5**: The molecular structure of $Me_3SiC{\equiv}CC{\equiv}CAsC_4Ph_4$ in a crystal. Phenyl groups simplified and hydrogen atoms omitted for clarity. Ellipsoids shown at 50% displacement.

The first example of an *As*-butadiynyl arsole was found.* The $Me_3SiC{\equiv}CC{\equiv}C$ linkage projects below the arsenic atom by *ca* 100° with an As-C(*sp*) distance of 1.893(2) Å, and the pair of C≡C bonds are crystallographically indistinguishable at 1.201(2) and 1.206(2) Å and in accord with other butadiynyl chains (*cf.* 1.197(9) Å in $PhC{\equiv}CC{\equiv}CPh$[21]). The C1-C2-C3-C4 chain is subtly distorted from linearity at every atom along the linkage although the point angle at C1 displays the greatest deviation (*ca* 12°) whereas the others are no greater than *ca* 4°. Like $HC{\equiv}CAsC_4Ph_4$, the disposition of the unsaturated carbon chain with respect to the arsole ring system probably precludes any appreciable intersystem π-delocalisation, especially since the envelope fold of the arsole ring is the largest of the *As*-alkynyl arsoles in this work, *ca* 13°. Whereas the arsole moiety appears to be diastereotopic in solution at ambient temperature, the geometric disposition of the (trimethylsilyl)butadiynyl residue in the solid state is largely aligned with the internal (non-crystallographic) symmetry plane of the molecule (minor distortions notwithstanding), and no "bowstring" type lateral bend of the four-carbon linkage is found.

### 2.3.2 Synthesis of $HC{\equiv}CC{\equiv}CAsC_4Ph_4$

Desilylation of $Me_3SiC{\equiv}CC{\equiv}CAsC_4Ph_4$ with methanolic NaOH in $Et_2O$ precipitates the parent $HC{\equiv}CC{\equiv}CAsC_4Ph_4$ in high yield as an air-stable off-white solid, which fluoresces blue under broad-band UV light. The terminal butadiynyl hydrogen is observed at 2.22 ppm in the $^1H$ NMR spectrum ($CDCl_3$) and – like the trimethylsilyl substituted compound above – the arsole ring carbon nuclei are all inequivalent in the $^{13}C\{^1H\}$ NMR spectrum finding four signals of equal intensity at 151.8, 151.6, 146.0 and 145.9 ppm. The terminal butadiynyl carbon resonance is located at 68.5 ppm (*via* an HSQC NMR experiment) with the internal *sp*-carbon resonances at 74.8 and 89.2 ppm, and the resonance for the arsenic-bound carbon atom at 90.6 ppm. High-resolution mass spectrometry yields the protonated adduct ($m/z \approx 481.0926$) and single crystals were obtained from $CH_2Cl_2$/methanol at -20 °C and the structure is shown in **Figure 2.6**.

* No previous structural data are available (CCDC) for arsenic-functionalised 1,3-butadiynes. Indeed, for pnictogens other than nitrogen, the only structurally characterised butadiynes are $(Me_3SiC{\equiv}CC{\equiv}C)_2PC_6H_2tBu_3$-2,4,6 and $Mes_2PC{\equiv}CC{\equiv}CPMes_2$. See K. Toyota, M. Shibata, M. Yoshifuji, *Bull. Chem. Soc. Japan*. **1995**, *68*, 2633, and P. Feldhaus, G. Kehr, R. Frohlich, C.G. Daniliuc, G. Erker, *Z. Naturforsch. B*, **2013**, *68*, 666.

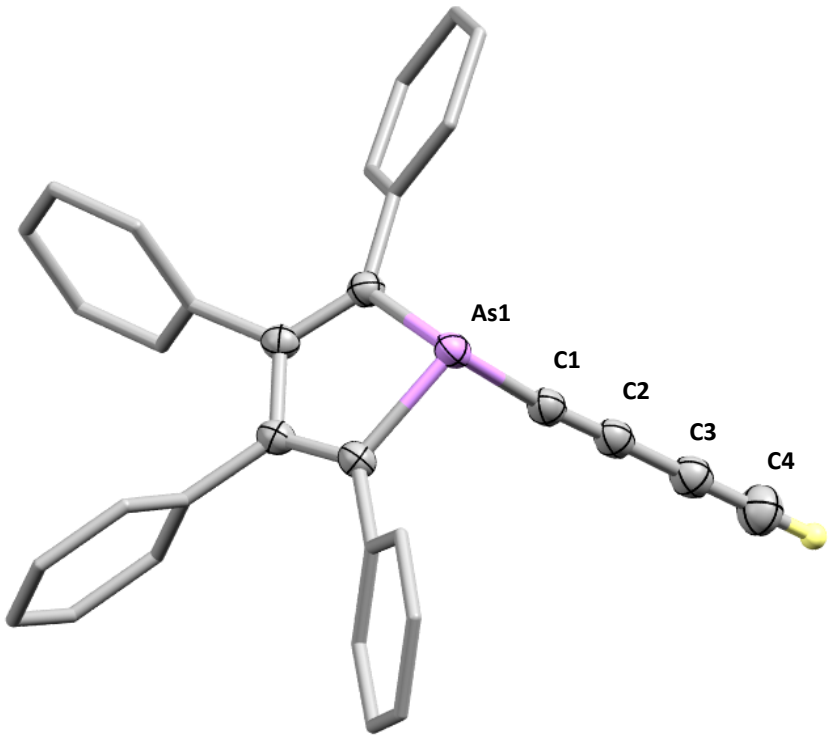



**Figure 2.6**: The molecular structure of HC≡CC≡CAsC$_4$Ph$_4$ in a crystal. Phenyl groups simplified and most hydrogen atoms omitted for clarity, except the butadiynyl proton which is shown in yellow for emphasis. Ellipsoids shown at 50% displacement.

The second example of an *As*-butadiynyl arsole is found within the crystal, the structural features of which not too dissimilar from those of Me$_3$SiC≡CC≡CAsC$_4$Ph$_4$ except for the terminal C-C triple bond (1.191(3) Å), which is crystallographically distinct from the internal C-C triple bond (1.206(2) Å). The butadiynyl linkage itself bows slightly at C1 (*ca* 173°) though the point angles at C2 and C3 stray only 2—3° from linearity. Dimensions within the arsole ring are unremarkable though the extrusion angle of the heteroatom from the mean butadiene plane (*ca* 7°) is closer to that of HC≡CAsC$_4$Ph$_4$ (5°) than Me$_3$SiC≡CC≡CAsC$_4$Ph$_4$ (13°) perhaps suggesting that the decreased steric profile of the parent hydrocarbyl linkage allows the As(III) atom to relax slightly into the ring system, though not to any extent which would suggest formal HÜCKEL delocalisation. Calculations were carried out on HC≡CC≡CAsC$_4$Ph$_4$ in the gas phase using DFT at the ωB97X-D/6-31G* level of theory and frontier orbitals are shown in **Figure 2.7**.

Computational interrogation of HC≡CC≡CAsC$_4$Ph$_4$ finds the LUMO, HOMO and HOMO-1 to be almost identical to those of the parent ethynyl arsole, both in terms of orbital energies and gross topologies (**Figure 2.4**). The LUMO suggests an electrophilic arsenic atom with nucleophilic attack directed toward the As-C(σ*) antibond (**Section 2.4**), and the HOMO primarily composed of the butadiene π-system with a very minor contribution from an internal C≡C(π) bond, and an even smaller provision from the phenyl rings in the 2,5-positions. The HOMO-1 finds the As(*p*) orbital housing the lone pair electrons in addition to two butadiynyl C≡C $\pi_z$-bonds (all mutually antibonding with respect to the other), along with residual σ-bonding networks within the butadiene. Again, no convincing evidence for π-communication between the arsole and butadiynyl systems is found.

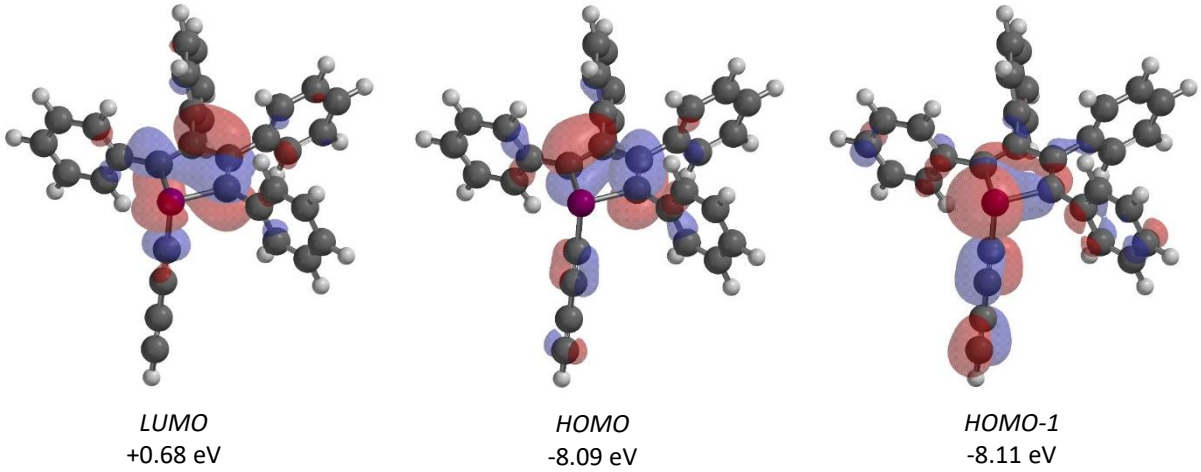
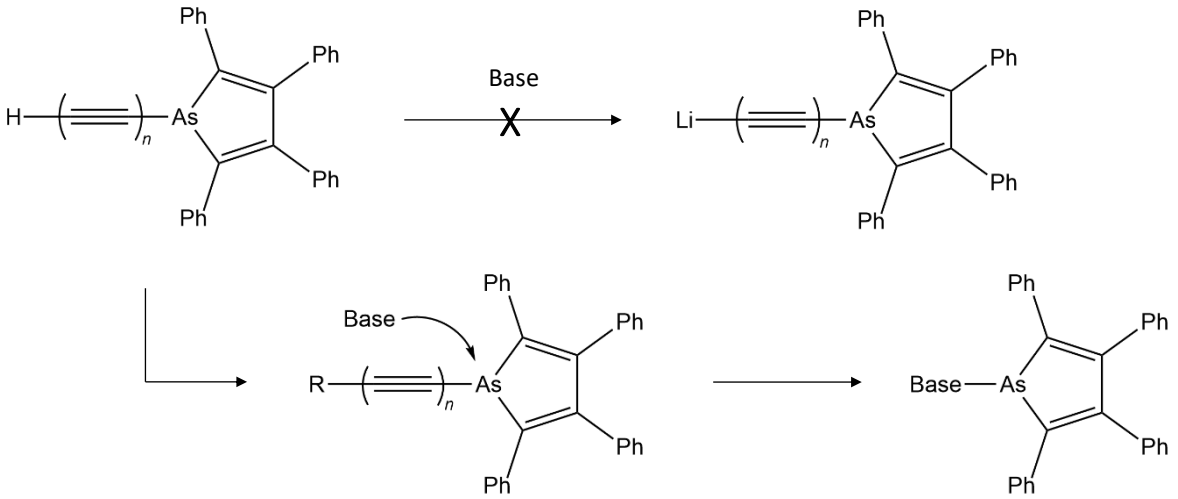



**Figure 2.7**: Calculated frontier orbitals of HC≡CC≡CAsC$_4$Ph$_4$ (DFT, gas phase: ωB97X-D/6-31G*).

## 2.4 Attempted Functionalisation of *As*-Alkynyl Arsoles

Given that alkynyl residues are relatively acidic (as far as hydrocarbons are concerned, p$K_a$ ≈ 26) it was desirable to attempt deprotonation of the H(C≡C)$_n$AsC$_4$Ph$_4$ termini ($n$ = 1 or 2) as a post-synthetic means to functionalise these alkynyl arsoles. One can envision a wide variety of interesting organic and inorganic electrophiles that might be installed onto the ethynyl and/or butadiynyl linkage. Unfortunately, initial experiments revealed a significant predisposition against deprotonation and instead nucleophilic substitution of the alkynyl residue was the inevitable outcome upon treatment with organolithium, GRIGNARD, or lithium amide bases (**Scheme 2.8**). In light of the computational predictions discussed above

this not entirely surprising, though it was nevertheless quite frustrating that the thermodynamic, if not kinetic, acidity of $H(C{\equiv}C)_nAsC_4Ph_4$ was in principle likely sufficient for deprotonation, however the inherent electrophilicity of the arsenic centre invariably diverted the base toward itself.* For example, treatment of $HC{\equiv}CAsC_4Ph_4$ with *t*-BuLi in $Et_2O$ at -78 °C, followed by quenching with an excess of $CH_3I$ gives not $MeC{\equiv}CAsC_4Ph_4$ but instead the heretofore unknown *t*-$BuAsC_4Ph_4$ in high yield, the crystal structure of which is shown in **Figure 2.8**. The same compound is also obtained in **Chapter 6** where *t*-BuLi is deployed with a transition metal σ-arsolyl complex.




**Scheme 2.8**: Addition of strong bases to $H(C{\equiv}C)_nAsC_4Ph_4$ resulting not in nucleophilic substitution. Base = organolithium or lithium amide.

The crystal structure of *t*-$BuAsC_4Ph_4$, albeit a new compound, is not particularly remarkable and no extended discussion will be committed to molecular features; the As-C($sp^3$) bond measures 2.019(7) Å and no intermolecular contacts are found to the benzene solvate molecules which are innocent in the void spaces between discrete arsole entities. Likewise, attempts to prepare $LiC{\equiv}CAsC_4Ph_4$ by treatment of $Me_3SiC{\equiv}CAsC_4Ph_4$ with MeLi·LiBr (*viz.* the synthesis of $LiC{\equiv}CC{\equiv}CSiMe_3$) in $Et_2O$ solution resulted in the isolation of previously unknown $MeAsC_4Ph_4$ in good yield. The crystal structure is shown in **Figure 2.9**. In retrospect, complications encountered when attempting to directly install the ethynyl group by

* This reactivity pattern is not exclusive to these arsoles and is reminiscent of, for example, the synthesis of vinyllithium from $Sn(CH{=}CH_2)_4$ and 4·RLi: See E.C. Juenge and D. Seyferth *J. Org. Chem.*, **1961**, *26*, 563—565. The same outcome is encountered upon treatment of $Bu_3Sn(C{\equiv}CH)$ with *n*-BuLi which displaces ethynyllithium and $SnBu_4$.

employing HC≡CMgBr may well have their origins in the target ethynylarsole product being prone to reaction with further ethynyl nucleophile.

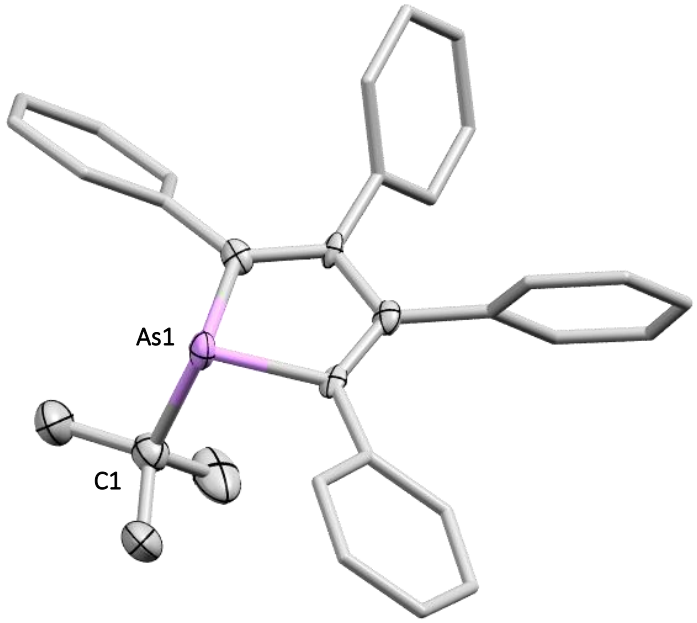



**Figure 2.8**: The molecular structure of *t*-$BuAsC_4Ph_4 \cdot C_6H_6$ in a crystal. Phenyl groups simplified and benzene solvate molecular and hydrogen atoms omitted for clarity. Ellipsoids shown at 50% displacement.

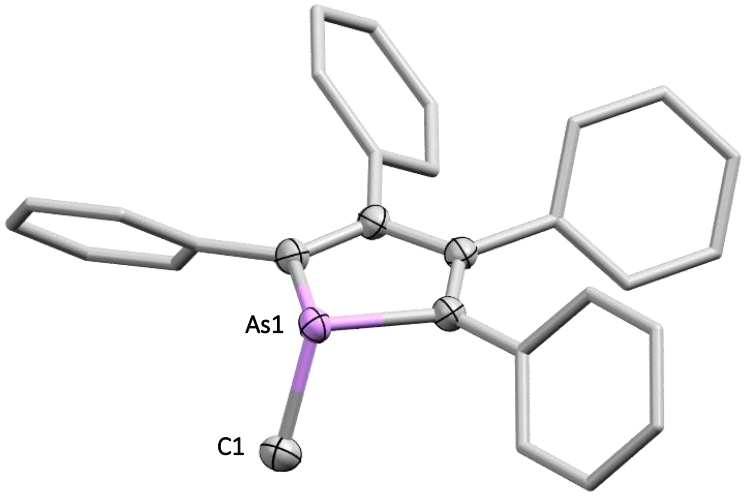



**Figure 2.9**: The molecular structure of $MeAsC_4Ph_4$ in a crystal. Phenyl groups simplified and hydrogen atoms omitted for clarity. The As-Me moiety is disordered over two positions and the major contributor is shown. Ellipsoids shown at 50% displacement.

Attempts to homocouple $H(C\equiv C)_nAsC_4Ph_4$ under routine EGLINTON[22] ($[Cu(OAc)_2]$, pyridine, THF) or HAY[23] (CuCl, TMEDA, acetone, $O_2$) protocols failed to provide evidence for formation of $Ph_4C_4As(C\equiv C)_nAsC_4Ph_4$ ($n$ = 2 or 4) and the majority of the *As*-alkynyl arsole starting material could be

recovered unchanged.* Similarly, incorporation of $HC{\equiv}CAsC_4Ph_4$ into a simple SONOGASHIRA coupling stream ($[Pd(PPh_3)_4]$, *para*-bromotoluene, CuI, $NEt_3$, toluene) failed to produce any isolable quantity of $4\text{-}MeC_6H_4C{\equiv}CAsC_4Ph_4$ (although it *was* detected in the reaction mixture by low resolution mass spectrometry: $m/z \approx 546.13$), and the majority of the ethynyl arsole could be isolated unchanged.

The unifying feature of these failed reactions would seem to be a reluctance of the ethynyl terminus to undergo deprotonation, which is the requisite step for admission into all three coupling cycles. Although alkynyl arsines have been shown to coordinate palladium through the arsenic donor,[24] the presence of the As(III) atom itself as a catalyst poison is unlikely given that NAKA and co-workers have recently demonstrated that arsoles with 4-bromophenyl substituents in the 2,5-ring positions are capable of undergoing Pd-catalysed SUZUKI-MIYAURA couplings.[25-27] The presence of the trivalent arsenic atom β to the acetylenic CH function may very well have a deactivating effect on the acidity of the same, since the "less-nucleophilic" amide base $K[N(SiMe_3)_2]$ (free amine $pK_a \approx 26$) totally failed to react in scrupulously anhydrous $C_6D_6$ solution (by NMR). Furthermore, desilylation of $Me_3SiC{\equiv}CAsC_4Ph_4$ in the presence of an electrophilic metal halide (*e.g.*, *trans*-$[RhCl(CO)(PPh_3)_2]$ or $[AuCl(PCy_3)]$) as a means to install the metal on the alkyne terminus was probably successful (as judged by NMR) however the major product observed in these reaction mixtures was $HC{\equiv}CAsC_4Ph_4$, which proved difficult to separate from any metal complex(es) present. The preference for formation of $HC{\equiv}CAsC_4Ph_4$ must be reasonably strong to account for the difficulties encountered in deprotonation and the alacrity with which any nascent $[C{\equiv}CAsC_4Ph_4]^-$ scavenges a proton from its surroundings.

## 2.5 Reactions with *trans*-$[Ru(CO)_2(PPh_3)_3]$

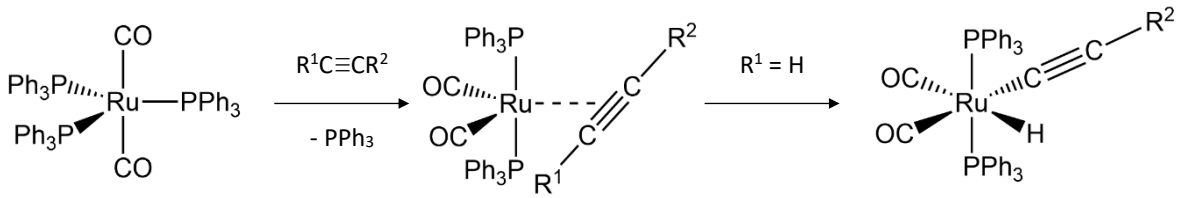
Several classic coordination complexes of ruthenium interact – though not always in a convergent manner – with both terminal and internal alkynes. A universal feature of these reactions is the prior necessity for an unsaturated Ru centre; fortunately, several of the most common ruthenium precursors are either labile in solution or easily activated with a suitable reagent(s) producing the requisite four- or five-coordinate reactive species. With acetylenic substrates, this step precedes formation of a second intermediary species

* The same HAY conditions were successful in synthesising the $Me_3SiC{\equiv}CC{\equiv}CSiMe_3$ precursor used in **Section 2.3.1** which lends evidence toward the alkynyl arsole being a rather stubborn coupling partner, rather than the procedure itself being faulty.

containing a side-bound π-complex of the type [Ru($\eta^2$-RC≡CR)$L_n$]; it is from this point onward that the course of the reaction is generally dictated by the formal oxidation state of the metal centre, the basicity of the adorning ligands, and the substituents furnishing the alkyne. The multitude of ways in which alkynes are activated by $d^6$-Ru(II) or $d^8$-Ru(0) centres (oxidative addition, vinylidene formation, insertion, ligand coupling, polymerisation *etc.*) may in part be traced to the high *d*-occupancy of the metal centre and is the topic of the following sections.

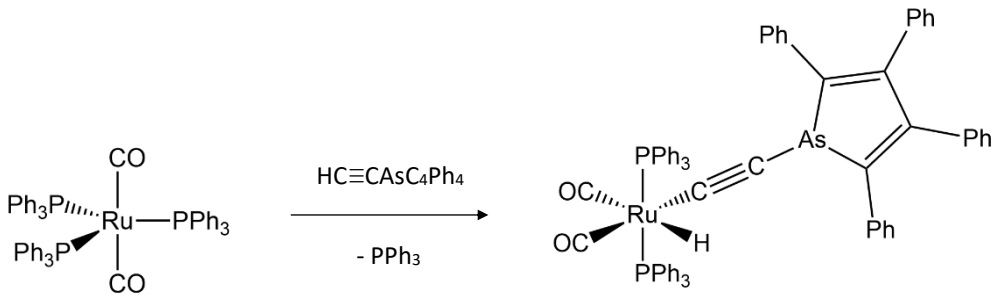
### 2.5.1 Synthesis of [RuH(C≡CAs$C_4Ph_4$)(CO)$_2$($PPh_3$)$_2$]

A particularly illustrative example of the sequence outlined above, the zero-valent complex [Ru(CO)$_2$($PPh_3$)$_3$] possesses a sterically-labilised phosphine ligand which dissociates in solution to the 16-electron species "[Ru(CO)$_2$($PPh_3$)$_2$]". If offered an internal alkyne, a simple alkyne complex [Ru($\eta^2$-RC≡CR)(CO)$_2$($PPh_3$)$_2$] may occasionally be isolated, though such complexes are presently few in number.[28, 29] If a terminal alkyne is instead deployed, the reaction can ultimately yield a ruthenium(II) hydrido-alkynyl complex *via* the same process concluding with insertion of the electron rich Ru(0) centre into the C-H bond of the $\eta^2$-alkyne. The reaction is evidently rather general and a reliable route to σ-alkynyl complexes of the type [RuH(C≡CR)(CO)$_2$($PPh_3$)$_2$]: a variety of substituents decorating the alkynyl linkage tolerate the process making the reaction useful for installing unsaturated carbon chains onto the ruthenium centre whilst simultaneously preserving the functionality of the alkyne and/or the substituent it carries. The effectiveness of this reaction has proven useful in intercepting highly reactive terminal alkynes (*e.g.*, HC≡CC≡CH or [HC≡C$PPh_3$]$^+$) that may be generated *via in situ* desilylation of the corresponding silyl alkyne.[30, 31]




**Scheme 2.9**: Oxidative addition of terminal alkynes by [Ru(CO)$_2$($PPh_3$)$_3$].

Now, despite the reluctance of $HC{\equiv}CAsC_4Ph_4$ to enter into reactions which heterolytically cleave the terminal C-H bond (*vide supra*) the alkynyl arsole reacts smoothy with $[Ru(CO)_2(PPh_3)_3]$ in THF solution at ambient temperature to provide the oxidative addition product *cis,cis,trans*-$[RuH(C{\equiv}CAsC_4Ph_4)(CO)_2(PPh_3)_2]$ as an air-sensitive* cream-coloured solid in high yield.




**Scheme 2.10**: Synthesis of $[RuH(C{\equiv}CAsC_4Ph_4)(CO)_2(PPh_3)_2]$.

The single equivalent of triphenylphosphine liberated is easily removed by washing the crude reaction product with *n*-hexane and spectroscopic features are diagnostic of this class of complex. Of particular interest is the metal-bound hydride which is evident in the $^1H$ NMR spectrum ($C_6D_6$) giving rise to a clearly resolved triplet at -5.22 ppm ($^2J_{PH}$ = 20.1 Hz). The arrangement of the ligand set about the Ru(II) centre is readily deduced from complimentary spectroscopic data: a lone $^{31}P\{^1H\}$ signal is found at 42.9 ppm for the two equivalent *trans* disposed $PPh_3$ ligands, and in the solution IR spectrum (THF) the pair of $\nu_{CO}$ bands at 2035 and 1990 $cm^{-1}$ are of equal intensity, suggesting the intercarbonyl angle is ~90°.† The $^{13}C\{^1H\}$ NMR spectrum reveals two inequivalent carbonyl carbon nuclei at 199.3 and 197.3 ppm ($^2J_{PC}$ = 10.9 and 7.8 Hz, respectively; the latter attributed to the carbonyl *trans* to the hydride), and the arsolyl ring carbon atoms are only narrowly separated at 149.5 and 149.1 ppm. The ethynyl carbon bonded to the Ru(II) centre manifests as a triplet resonance at 136.4 ppm ($^2J_{PC}$ = 22.6 Hz) while the β-ethynyl carbon is found at 100.5 ppm ($^3J_{PC}$ = 3.9 Hz). Single crystals were grown from benzene/*n*-hexane and the molecular structure is shown in **Figure 2.10**.

* This air-sensitivity is not an intrinsic feature of the product *per se*, but rather of the rapid reaction of $[Ru(CO)_2(PPh_3)_3]$ with oxygen to irreversibly afford the dioxygen complex $[Ru(\eta^2\text{-}O_2)(CO)_2(PPh_3)_2]$ thereby providing circumstantial evidence for the reversibility of the alkyne C-H activation process.

† The $\nu_{RuH}$ vibration could not be unambiguously identified in the solution IR spectrum.

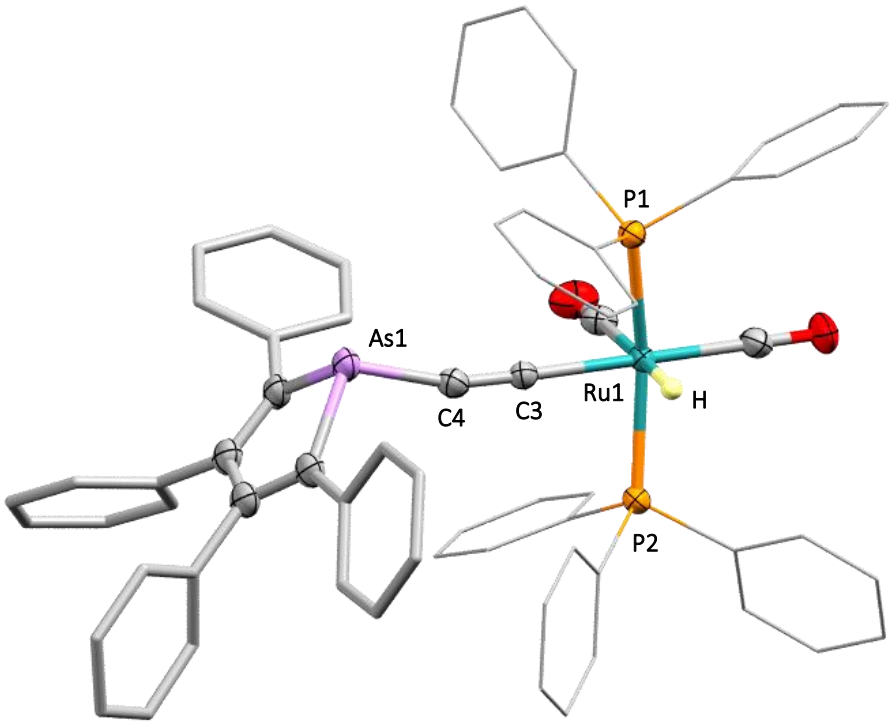



**Figure 2.10**: The molecular structure of [RuH(C≡CAsC$_4$Ph$_4$)(CO)$_2$(PPh$_3$)$_2$]. Phenyl groups simplified and hydrogen atoms omitted for clarity, except for the metal-hydride which is shown in yellow for emphasis. Ellipsoids shown at 50% displacement.

The anticipated Ru(II) complex is found, and the configuration of the ligands is in agreement with that inferred from the spectroscopic features discussed above. A distorted octahedral environment is found with the transphosphine axis bent by *ca* 18° from linearity toward the sterically unimposing hydrido ligand, with an intercarbonyl angle of *ca* 93°, in excellent agreement with the value estimated from solution IR data. Bonding distances around the ruthenium centre reflect the disparate *trans* influences of the hydride (strong) and alkynyl (moderate) ligands: the carbonyl opposite to the hydride displays a Ru-C bond length of 1.948(2) Å, *vs*. 1.916(2) Å for the carbonyl opposite the alkynyl. The pair of C≡O bond lengths (1.132(3) and 1.137(3) Å) are however crystallographically equivalent, which supports the general assertion that metal(*d*)→alkynyl(π*) retrodonation is negligible or non-existent (σ-alkynyl ligands are weakly π-basic if not entirely π-neutral).[32-34] Given the immediate proximity of the hydride to the ruthenium centre, the position of the former could not be located with certainty from a residual electron density map.* Therefore, a Ru-H distance of 1.77 Å (the sum of covalent radii) was initially provided and the model allowed to refine (with

* Initial treatment of the hydride *via* the "riding model" fixed the Ru-H distance to *ca* 0.84 Å which was implausibly short, hence the use of the restraint here.

suitable restraints), eventually converging to a bond length of 1.53(1) Å (*cf.* 1.57(4) Å in [RuH(C≡CC≡CH)(CO)$_2$(PPh$_3$)$_2$];[30] 1.56(6) Å in [RuH{C≡CB(O$_2$CCH$_2$)$_2$NMe}(CO)$_2$(PPh$_3$)$_2$][35]) though the appreciable uncertainly associated with the measurement necessarily demands caution if subjected to interpretation.

The alkynyl linkage finds interatomic Ru-C3, C3-C4 and C4-As1 distances of 2.064(2), 1.210(3) and 1.868(2) Å, respectively; the former is typical,[30, 35, 36] and the latter two compare with bond lengths of 1.180(3) (C≡C) and 1.898(2) Å (C-As) for the same pairs of atoms in the parent ethynyl arsole molecule (**Figure 2.3**). Local angles about the trivalent arsenic atom also vary upon installation of the Ru(II) moiety to the ethynyl terminus which, compared to the free molecule, see a widening of the exocyclic *As*-ring carbon angles from *ca* 94° to *ca* 103° and a noticeable deflection of the C3-C4-As1 linkage from linearity (*ca* 165°). These distortions *are* statistically significant (within the precision limits of the crystallographic data) though are ascribed to packing effects within the crystal lattice* rather than any attempt by the molecule to bring the arsenic lone pair into alignment with the alkynyl π system: a cumulenic-type contribution (*i.e.*, Ru=C=C=As) *can* be envisioned; however, the propensity for *p*(π)-*p*(π) interactions decreases sharply for the heavier Group 15 elements such that multiple bonding with carbon is often energetically and topologically unlikely in the absence of extenuating molecular features (*e.g.*, kinetic stability provided by steric protection). Indeed, a computational assessment of the "pruned" model complex [RuH(C≡CAsC$_4$H$_4$)(CO)$_2$(PH$_3$)$_3$] (DFT, gas phase: ωB97X-D/6-31G*/LAN2Dζ; **Figure 2.11**) finds no convincing evidence for involvement of the arsenic lone pair in multiple bonding with the alkynyl bridge. The HOMO comprises the non-interacting arsole butadiene(π) and ethynyl(π) systems, and the filled As(*p*) orbital is found in the HOMO-1 alongside the remaining ethynyl(π) orbital and although both are co-planar they are strictly antibonding with respect to the other. This model, computed in isolation of solid-state effects, also returns a geometry with a nearly linear Ru-C≡C-As linkage which further supports the physical rather than electronic explanation for the disposition of the arsole group in the crystal structure of [RuH(C≡CAsC$_4$Ph$_4$)(CO)$_2$(PPh$_3$)$_2$].

* A nearby molecule related by means of an inversion centre (space group *P*-1) appears to impinge upon the AsC$_4$Ph$_4$ group which likely results in the deflection observed.

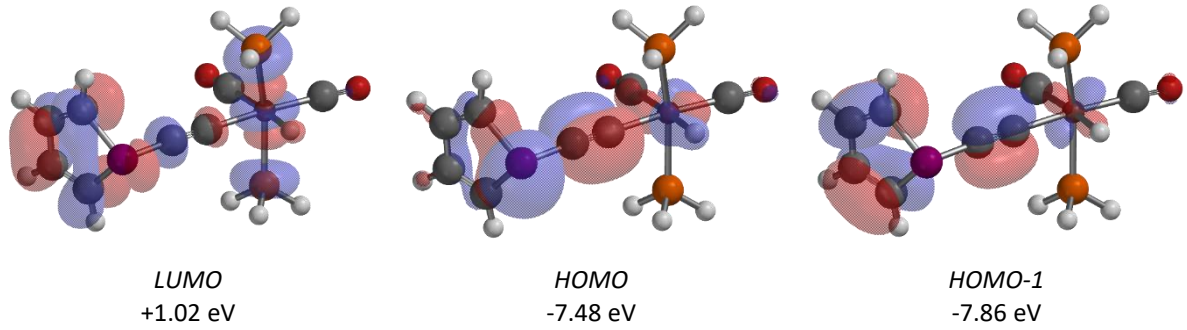
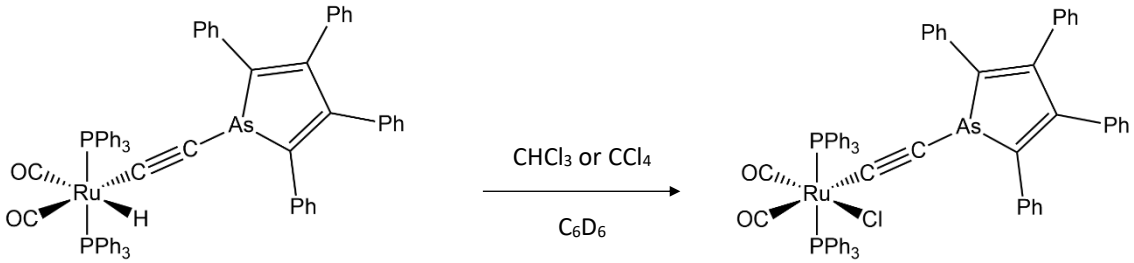



**Figure 2.11**: Calculated frontier orbitals of the model β-arsolylalkynyl [RuH(C≡CAsC$_4$H$_4$)(CO)$_2$(PH$_3$)$_2$] (DFT, gas phase: ωB97X-D/6-31G*/LAN2DZ).

The addition of one drop of $CHCl_3$ or $CCl_4$ to a $C_6D_6$ solution of [RuH(C≡CAsC$_4$Ph$_4$)(CO)$_2$(PPh$_3$)$_2$] produces yellow mixtures containing [RuCl(C≡CAsC$_4$Ph$_4$)(CO)$_2$(PPh$_3$)$_2$] arising from chlorination of the Ru-H bond – acquisition of the $^1$H NMR spectrum in a timely manner finds a complete absence of any hydride resonance, and in this regard halogenation appears rather rapid (< 5 min). The $^{31}$P resonance shifts noticeably (δ = 21.8 ppm) upon introduction of the π-donor chloride ligand, an electronic feature of which the hydride has no amenity.




**Scheme 2.11**: Chlorination of [RuH(C≡CAsC$_4$Ph$_4$)(CO)$_2$(PPh$_3$)$_2$].

The formation of [RuCl(C≡CAsC$_4$Ph$_4$)(CO)$_2$(PPh$_3$)$_2$] in the above mixtures was accompanied by other species as indicated by secondary signals in the $^{31}$P{$^1$H} NMR spectrum, the most notable belonging to the 18-electron vinyl complex [RuCl(*E*-CH=CHAsC$_4$Ph$_4$)(CO)$_2$(PPh$_3$)$_2$] ($^{31}$P{$^1$H} δ = 23.4 ppm; **Figure 2.12**) which finds a corresponding pair of characteristic resonances in the $^1$H NMR spectrum (δ = 8.83 and 6.00 ppm, both a doublet of triplets), and [RuCl$_2$(CO)$_2$(PPh$_3$)$_2$] ($^{31}$P{$^1$H} δ = 28.1 and 16.3 ppm for both *cis* and *trans* isomers) in trace quantities alongside the heretofore unknown *As*-vinyl arsole

$H_2C{=}CHAsC_4Ph_4$.* These three species arise from the action of adventitious HCl often present in halogenated solvents and will be detailed in the following paragraph. The same outcome was obtained with *N*-chlorosuccinimide or $PhI{\cdot}Cl_2$ which were employed to circumvent this occurrence. It was rather difficult to isolate $[RuCl(C{\equiv}CAsC_4Ph_4)(CO)_2(PPh_3)_2]$ in an analytically pure form and single crystals have proven elusive.

The addition of protic acids to ruthenium hydrido-alkynyl complexes $[RuH(C{\equiv}CR)(CO)_2(PPh_3)_2]$ affords a cationic hydrido-vinylidene intermediate $[RuH(=C{=}CHR)(CO)_2(PPh_3)_2]^+$ that rearranges *via* migratory insertion of the hydrido ligand to an alkenyl species of the form $[Ru(CH{=}CHR)(CO)_2(PPh_3)_2]^+$. If a hydrohaloacid is deployed, the conjugate base is readily captured by the LEWIS acidic Ru(II) centre and the coordination octahedron is satisfied. Thus, the addition of anhydrous ethereal HCl to a $C_6D_6$ solution of $[RuH(C{\equiv}CAsC_4Ph_4)(CO)_2(PPh_3)_2]$ gives the *E*-isomer of $[RuCl(CH{=}CHAsC_4Ph_4)(CO)_2(PPh_3)_2]$ almost exclusively,† confirming presence of the same during the previous chlorination experiments. The mutual *trans*-disposition of the vinyl hydrogen nuclei is readily established by the large $^3J_{HH}$ coupling of 17.9 Hz which is typical of such an arrangement, and identity is confirmed by a low precision X-ray diffraction study performed on crystals isolated from the NMR solution (**Figure 2.12**). The use of a large excess of ethereal HCl led to increased quantities of $[RuCl_2(CO)_2(PPh_3)_2]$ and $H_2C{=}CHAsC_4Ph_4$ in the NMR solution which arise from electrophilic cleavage of the Ru-C bond.

* NMR: $^1H$ ($C_6D_6$, 400 MHz, 25 C°) 7.14—7.03 (m, 16H), 6.89—6.84 (m, 4H), 6.60 (dd, $J_{HH}$ = 18.3 & 10.7 Hz, 1H), 6.04 (d, $J_{HH}$ = 10.7 Hz, 1H), 5.90 (d, $J_{HH}$ = 18.3 Hz, 1H) ppm. Geminal H-H coupling was not resolved. Identity confirmed by comparison with an authentic sample.

† A small quantity (~5%) of $[RuCl_2(CO)_2(PPh_3)_2]$ was observed in the $^{31}P\{^1H\}$ NMR spectrum alongside $H_2C{=}CHAsC_4Ph_4$; neither $[RuCl(C{\equiv}CAsC_4Ph_4)(CO)_2(PPh_3)_2]$ nor the *Z*-isomer of $[RuCl(CH{=}CHAsC_4Ph_4)(CO)_2(PPh_3)_2]$ were observed.

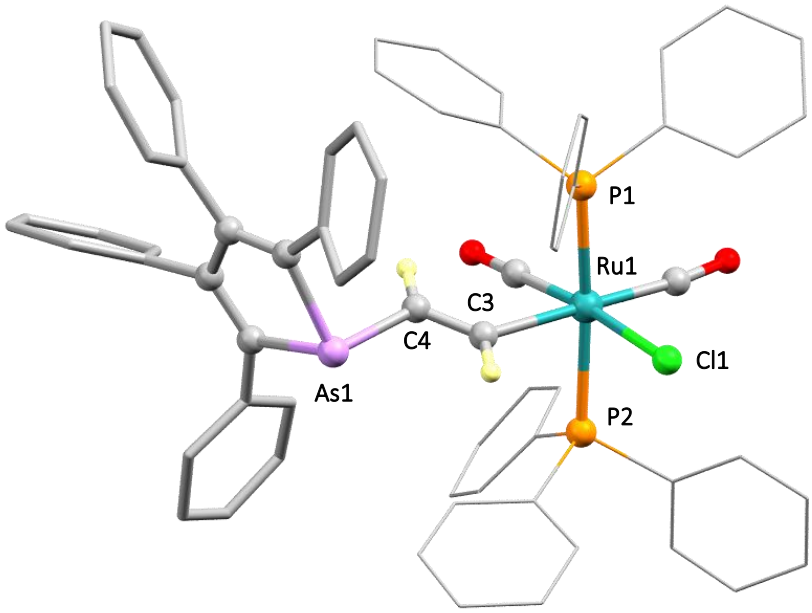
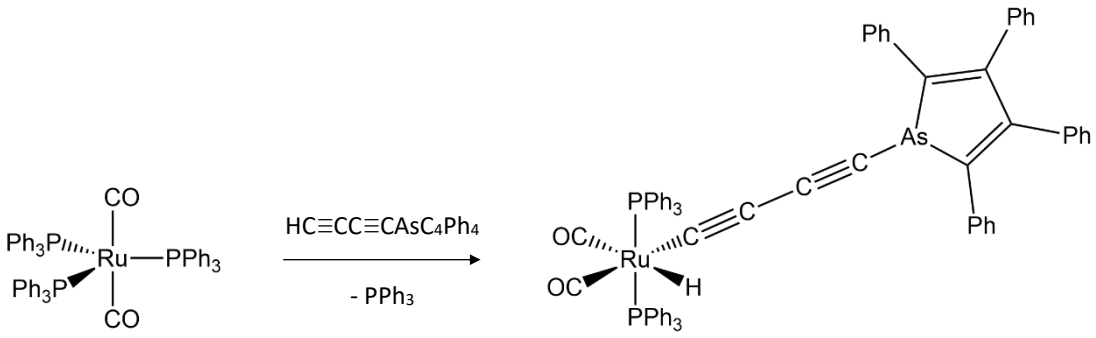



**Figure 2.12**: The molecular structure of [RuCl(*E*-CH=CHAsC$_4$Ph$_4$)(CO)$_2$(PPh$_3$)$_2$]·4C$_6$D$_6$ in a crystal. Phenyl groups simplified and benzene solvate molecules and hydrogen atoms omitted for clarity, except the alkenyl hydrogens which are shown in yellow for emphasis. Non-hydrogen atoms are depicted as rigid spheres without thermal anisotropy due to very poor data quality.

The molecular structure of [RuCl(*E*-CH=CHAsC$_4$Ph$_4$)(CO)$_2$(PPh$_3$)$_2$] in the solid state reveals the anticipated octahedral complex and confirms gross composition and atom connectivity. Unfortunately, extensive twinning (and partial desolvation of the four benzene solvate molecules, which could not be modelled satisfactorily) was encountered in this particular specimen and poor data quality regrettably precludes any meaningful geometric analysis. This is perhaps a moot point since molecular features are largely identical to the five-coordinate monocarbonyl species to be introduced in **Section 2.6.1** (**Figure 2.15**) and – data quality notwithstanding – would otherwise call for little comment.

### 2.5.2 Synthesis of [RuH(C≡CC≡CAsC$_4$Ph$_4$)(CO)$_2$(PPh$_3$)$_2$]

An similar C-H activation reaction was carried out with the butadiynyl arsole HC≡CC≡CAsC$_4$Ph$_4$, which upon stirring at ambient temperature with one equivalent of [Ru(CO)$_2$(PPh$_3$)$_3$] in THF solution overnight provides the expected [RuH(C≡CC≡CAsC$_4$Ph$_4$)(CO)$_2$(PPh$_3$)$_2$] as an air-sensitive, beige-coloured solid in high yield after removal of PPh$_3$ by *n*-hexane washing.




**Scheme 2.12**: Synthesis of [RuH(C≡CC≡CAsC$_4$Ph$_4$)(CO)$_2$(PPh$_3$)$_2$].

Spectroscopic features of the butadiynyl complex are largely identical to the ethynyl analogue discussed above: a pair of triplets are measured at 199.0 ($^2J_{PC}$ = 11.3 Hz) and 196.6 ($^2J_{PC}$ = 6.6 Hz) ppm for the carbonyl ligands *trans* to the butadiynyl and hydride, respectively, and the four butadiynyl carbons appear at 113.9 ($^2J_{PC}$ = 21.5 Hz), 98.6, 96.8 and 91.0 ppm for the respective atoms α, β, γ and ω to the ruthenium centre. The hydride appears at -5.34 ppm ($^2J_{PH}$ = 19.1 Hz) in the $^1$H NMR spectrum and a sharp singlet at 43.0 ppm is measured for the pair of $^{31}$P nuclei in the $^{31}$P{$^1$H} NMR spectrum. The solution IR spectrum in THF finds a pair of equally intense $\nu_{CO}$ absorptions at 2034 and 1989 cm$^{-1}$ which are essentially identical to those of [RuH(C≡CAsC$_4$Ph$_4$)(CO)$_2$(PPh$_3$)$_3$]. Single crystals were grown from benzene/*n*-hexane and the molecular structure (as a benzene solvate) is shown in **Figure 2.13**.

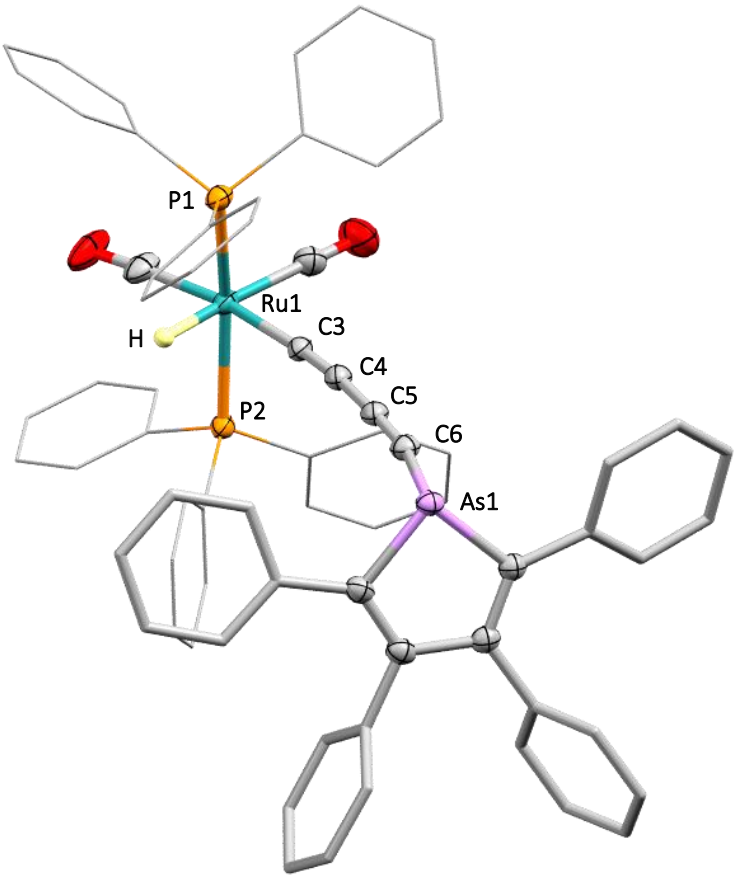


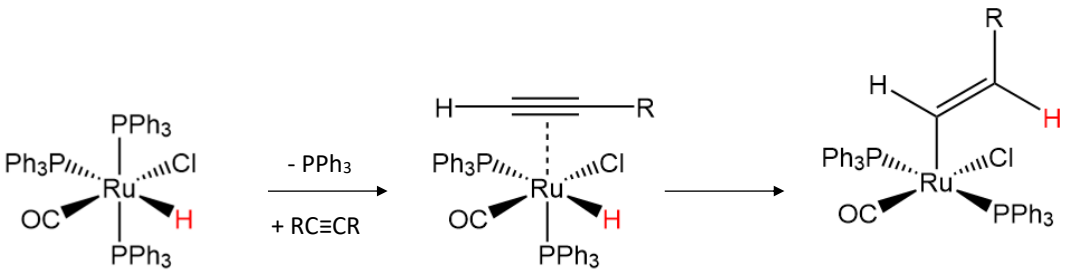

**Figure 2.13**: The molecular structure of $[RuH(C{\equiv}CC{\equiv}CAsC_4Ph_4)(CO)_2(PPh_3)_2]{\cdot}C_6H_6$. Phenyl groups simplified and benzene solvate molecule and hydrogen atoms omitted for clarity, except for the metal-hydride which is shown in yellow for emphasis. Ellipsoids shown at 50% displacement.

X-ray diffraction reveals the expected octahedral ruthenium complex which superficially resembles the ethynylarsole complex in **Figure 2.10**. The unit cell of this specimen (triclinic *P*-1) contains a pair of molecules related by means of the inversion centre and the hydride atom received an analogous treatment as previously discussed, the Ru-H distance converging to 1.53(5) Å. The butadiynyl linkage lies in the equatorial plane containing the hydride and pair of *cis* carbonyl ligands (97°) and the arsolyl group is approximately aligned with the *trans*-bis(phosphine) axis, which is itself bent by 16° from linearity in the direction of the hydride. The local angles about most *sp*-carbon atoms are only within a few degrees of linearity (from C1 through C4: *ca* 174, 174, 177, 167°) the cumulative effect is an appreciable and visible curvature to the four-carbon chain in the direction of the coordination site occupied by the hydride. The effect of this is a least-squares displacement of the arsenic atom by *ca* 1.9 Å from the mean plane containing Ru1, P1, P2 and C3. The differing *trans* influences of the hydride and butadienyl ligands are reflected in the

metal-carbonyl distances (Ru1-C1 1.954(3), Ru1-C2 1.915(2) Å) and the C≡O bond lengths are crystallographically equivalent (mean 1.132(4) Å). Interatomic distances along the butadiynyl chain reflect alternating single and triple bonds (Ru1-C3 2.060(2), C3-C4 1.209(3), C4-C5 1.370(3), C5-C6 1.208(3) and C6-As1 1.881(2) Å). A computational study of the model complex [RuH(C≡CC≡CAsC$_4$H$_4$)(CO)$_2$(PH$_3$)$_2$] using DFT (gas phase: ωB97X-D/6-31G*/LAN2Dζ) revealed no conspicuous communication between the arsolyl and butadienyl π-systems.

## 2.6 Reactions with *mer*-[RuHCl(CO)(PPh$_3$)$_3$]

Another classic ruthenium complex is VASKA'S hydrido-chloride species *mer*-[RuHCl(CO)(PPh$_3$)$_3$] containing a sterically-labilised phosphine *trans* to the hydrido ligand. As is common for transition metal hydrides, the reaction of *mer*-[RuHCl(CO)(PPh$_3$)$_3$] with terminal alkynes is a general one in which a transient $\eta^2$-alkyne complex undergoes regioselective insertion into the Ru-H bond giving *trans*-β-substituted σ-vinyl ligands (**Scheme 2.13**). The alkenyl products formed by this process are almost universally* of *E*-stereochemistry which is mechanistically understood by considering *syn* hydrometallation of the C≡C bond in a concerted process that affords *anti*-MARKOVNIKOV-type regioselectivity.




**Scheme 2.13**: *Syn*-hydrometallation of terminal alkynes with [RuHCl(CO)(PPh$_3$)$_3$].

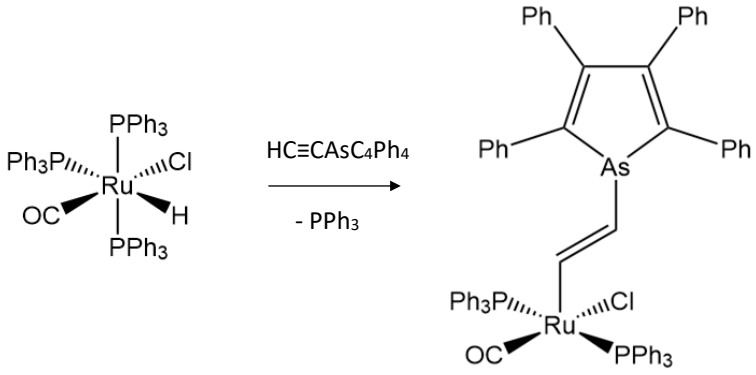
Internal alkynes are also capable of undergoing this sequence giving the corresponding α,β-disubstituted σ-vinyl ligand,[37] though if the substrate is unsymmetrical a mixture of regioisomers may be expected provided the steric properties of the substituents are not wildly disparate.[38, 39] Another consideration is that hydrometallation is in principle reversible (*viz.* β-hydride elimination). While this feature only tends to accentuate itself with *internal* alkynes *in*capable of engaging in secondary interactions

* Notable exceptions include alkynes bearing a pendant ester substituent at C$_\alpha$ for which the carbonyl oxygen is suitably placed to interact with the metal centre, or acetylene itself which is prone to polymerisation.

(*e.g.*, chelation) or with the use of related osmium hydrido-chloride complexes,[40] these exceptions confirm the reversibility of the insertion that allows thermodynamically favoured alternatives to be accessed. Further anecdotal evidence for the reversibility follows from the occasional observation of hydrido-complexes being obtained in certain instances where some co-ligand substitutions of such vinyl complexes are attempted.[41]

### 2.6.1 Synthesis of [RuCl(*E*-CH=CHAsC$_4$Ph$_4$)(CO)(PPh$_3$)$_2$]

The addition of HC≡CAsC$_4$Ph$_4$ to a THF solution of *mer*-[RuHCl(CO)(PPh$_3$)$_3$] at ambient temperature results in the isolation of the bright orange coordinatively unsaturated complex [RuCl(*E*-CH=CHAsC$_4$Ph$_4$)(CO)(PPh$_3$)$_2$] in good yield.




**Scheme 2.14**: Synthesis of [RuCl(*E*-CH=CHAsC$_4$Ph$_4$)(CO)(PPh$_3$)$_2$].

The stereochemistry of the alkenyl linkage follows from $^1$H NMR ($CD_2Cl_2$) finding the α and β vinyl hydrogen atoms as a doublet of triplets (each) at 8.87 and 5.70 ppm, respectively, with $^3J_{HH}$ = 12.9 Hz and $J_{PH}$ = 1.4 (α) and 1.9 (β) Hz. The alkenyl carbon atoms α and β to the Ru(II) centre manifest in the $^{13}$C{$^1$H} NMR spectrum as triplets at 164.3 ($^2J_{PC}$ = 19.2 Hz) and 125.3 ($^3J_{PC}$ = 7.0 Hz) ppm, respectively, with the carbonyl nucleus resonating at 201.3 ppm (also a triplet, $^2J_{PC}$ = 26.8 Hz). The arsole ring-carbon signals are found in their usual region (150.9 and 149.2 ppm) with the $^{31}$P{$^1$H} NMR spectrum displaying a sharp singlet at 29.2 ppm and a lone $\nu_{CO}$ absorption in the solution IR spectrum ($CH_2Cl_2$) at 1929 cm$^{-1}$ ($\nu_{C\equiv C}$ could not be unambiguously identified). Large single crystals were obtained from $CH_2Cl_2$/methanol at -20 °C and the molecular structure is shown in **Figure 2.14**.

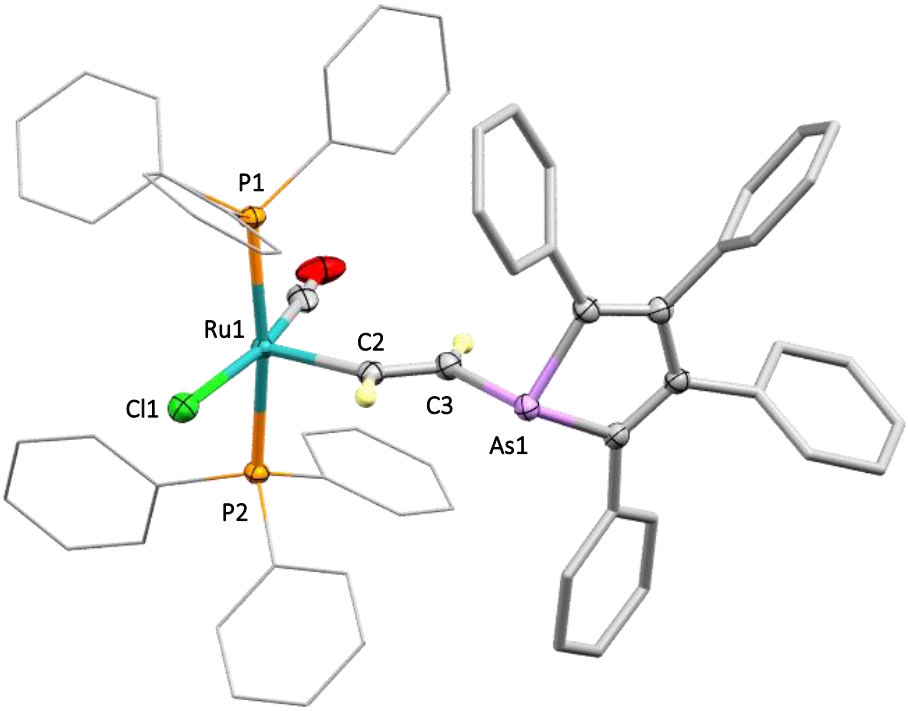



**Figure 2.14**: The molecular structure of [RuCl(*E*-CH=CHAsC$_4$Ph$_4$)(CO)(PPh$_3$)$_2$] in a crystal. Phenyl groups simplified and hydrogen atoms omitted for clarity, except the alkenyl hydrogens which are shown in yellow for emphasis. Ellipsoids shown at 50% displacement.

The expected five-coordinate Ru(II) complex is found. The coordination polyhedron of the metal centre is, as expected for a 5-coordinate 16-electron $d^6$ complex, essentially square pyramidal ($\tau_5 = 0.066$*) with the basal plane composed of the *trans* disposed phosphine ligands and the π-basic chloride ligand *trans* to the π-acidic carbonyl. The *E*-β-arsolylalkenyl group thus occupies the apical coordination site. Of the two retrodative orbitals presented to the vinyl ligand by the $d^6$-Ru(II) centre, that lying orthogonal to the Ru-C-CO-Cl plane is highest in energy due to lack of any interaction with CO. Accordingly, any π-acceptance by the vinyl ligand would be maximised by the vinyl ligand lying in this plane, as observed, though steric factors will also favour this more "open" orientation. Distances along the *E*-Ru-CH=CH-As linkage are typical of the individual bonding partners with Ru1-C2, C2-C3 and C3-As1 bonds of 2.000(3), 1.319(4) and 1.951(3) Å, respectively, and local bonding angles about the *E*-vinyl deviate slightly from

* The $\tau_5$ parameter is a geometry index for classifying five coordinate molecular geometries as either purely trigonal bipyramidal ($\tau_5 = 1$), purely square pyramidal ($\tau_5 = 0$) or some intermediate structure ($0 < \tau_5 < 1$). It is given by the expression $\tau_5 = \frac{\beta-\alpha}{60}$ where α and β are the two greatest valance angles about the coordination centre ($\beta \geq \alpha$, in degrees). It follows that for pure square pyramidal geometry $\alpha = \beta = 180°$, and for pure trigonal bipyramidal geometry $\alpha = 120°$ and $\beta = 180°$. See A.D. Addison *et al. J. Chem. Soc. Dalton Trans.*, **1984**, 1349—1356.

idealised $sp^2$-C geometry with a modest widening at C2 (*ca* 138°) and narrowing at C3 (*ca* 116°) though all four atoms are essentially coplanar. The tetraphenylarsolyl group is approximately symmetrically disposed either side of the plane of the alkenyl group with the phenyl residues in the 2,5-positions aligned with the transphosphine axis. This places the arsenic lone pair electrons orthogonal to the alkenyl(π) system though it is unlikely any conjugation would otherwise be significant for the reasons already outlined previously. This was supported by a computational interrogation of the model complex [RuCl(*E*-CH=CHAs$C_4H_4$)(CO)($PH_3$)$_2$] using DFT (gas phase: ωB97X-D/6-31G*/LAN2DZ)* which find the HOMO to be composed of the vinyl(π) bond and the arsolyl butadiene(π) system, with the non-bonding As(*p*) orbital contributing to the HOMO-1 with no topological proclivity for communication between the three – the heteroatom once again serves as an electronic node between the two unsaturated fragments. The LUMO essentially relates to the vacant coordination site of the complex trans to the vinyl ligand, the implication of which becomes apparent upon treatment with neutral ligands (*vide infra*).

Placing a $C_6D_6$ solution of [RuCl(*E*-CH=CHAs$C_4Ph_4$)(CO)($PPh_3$)$_2$] under an atmosphere of carbon monoxide results in a rapid colour change from orange to a pale yellow and the formation of 18-electron *cis,cis,trans*-[RuCl(*E*-CH=CHAs$C_4Ph_4$)(CO)$_2$($PPh_3$)$_2$], the crystal structure of which was shown in **Figure 2.12** since the same complex arises from hydrochlorination of [RuH(C≡CAs$C_4Ph_4$)(CO)$_2$($PPh_3$)$_2$]. At the time, single crystals of the dicarbonyl species were elusive and unequivocal synthesis *via* carbonylation of [RuCl(*E*-CH=CHAs$C_4Ph_4$)(CO)($PPh_3$)$_2$] provided further confirmation of identity.

### 2.6.2 Synthesis of [RuCl{*gem*-C(=$CH_2$)C≡CAs$C_4Ph_4$}(CO)($PPh_3$)$_2$]

*Mer*-[RuHCl(CO)($PPh_3$)$_3$] also reacts swiftly with one equivalent of HC≡CC≡CAs$C_4Ph_4$ in THF solution to initially provide a bright orange mixture containing the expected [RuCl(*E*-CH=CHC≡CAs$C_4Ph_4$}(CO)($PPh_3$)$_2$] from *syn*-hydroruthenation of the "most-accessible" terminal C≡C bond (*vide infra*). Workup of the reaction mixture, however, affords an unassuming beige solid (yellow in solution) in good yield for which high-resolution mass spectrometry confirms formation of a β-ethynylalkenyl ruthenium complex ($m/z \approx$ 1135.1774 for the $[M - Cl]^+$ ion). However, the isolated product does *not* display spectroscopic features consistent with the presence of an *E*-vinyl ligand. Specifically, the

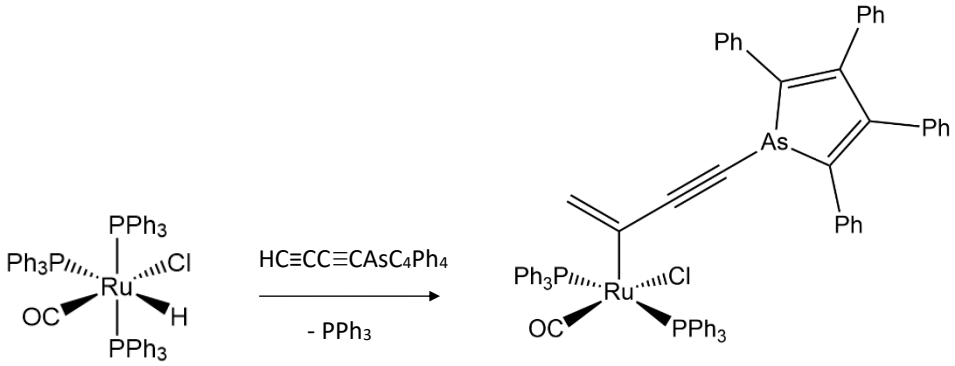
* Replacement of $PPh_3$ by $PH_3$ for reasons of computational parsimony does nevertheless allow for elimination of steric arguments for the orientation of the vinyl ligand orthogonal to the P-P vector.

$^{1}$H NMR spectrum ($CD_2Cl_2$) is absent of the expected signals at ~8 and ~6 ppm (doublets of triplets) for a pair of *trans*-vinylic hydrogen nuclei, instead finding two broad singlets at 5.02 and 4.30 ppm of equal area integration which partially resolve into doublets ($J_{HH} \leq 2$ Hz) in a stronger-field instrument. The $^{13}C\{^{1}H\}$ spectrum finds the ruthenium-bound carbon atom at 152.3 ppm and the methylene carbon atom at 146.6 ppm (by means of HSQC and HMBC NMR experiments; $J_{PC}$ both unresolved) which flank the arsole ring-carbon signals at 150.7 and 148.4 ppm, and are somewhat aberrant from [RuCl(*E*-CH=CHAs$C_4Ph_4$)(CO)($PPh_3$)$_2$] (*cf.* 163.4 and 125.3 ppm). A pair of ethynyl resonances are found at 90.2 and 78.2 ppm devoid of $J_{PC}$ coupling. The $^{31}P\{^{1}H\}$ signal manifests at 33.9 ppm (*cf.* 29.2 ppm in [RuCl(*E*-CH=CHAs$C_4Ph_4$)(CO)($PPh_3$)$_2$]) and the $\nu_{CO}$ absorption (1929 cm$^{-1}$) and $^{13}C\{^{1}H\}$ CO shift (206.7 ppm; $J_{PC}$ = 31.8 Hz) are also comparable to the same.

The product is clearly a Ru(II) complex of the hydrometallated HC≡CC≡CAs$C_4Ph_4$ ligand with alkenyl characteristics (*viz*, mass spectrometry, $\delta_P$, $\delta_{CO}$, and $\nu_{CO}$), though cannot be the expected [RuCl(*E*-CH=CHC≡CAs$C_4Ph_4$)(CO)($PPh_3$)$_2$] (**Scheme 2.16**) on the basis of other $^{1}$H and $^{13}C\{^{1}H\}$ NMR spectral data. An arrangement whereby *syn*-hydroruthenation has taken place at the internal C≡C bond is chemically plausible, although HSQC and HMBC NMR experiments showed *no* correlation between the $^{1}$H signals at 5.02 and 4.30 ppm and the ethynyl $^{13}$C signals at 90.2 and 78.2 ppm and this possibility is therefore ruled out. However, the same 2-D NMR spectra showed both $^{1}$H signals of interest to have one-bond correlation to the $^{13}$C signal at 146.6 ppm *only*, and two-bond correlation to the $^{13}$C signal at 152.3 ppm, itself a quaternary carbon nucleus. On the basis of these observations the isolated compound is formulated as [RuCl{*gem*-C(=$CH_2$)C≡CAs$C_4Ph_4$}(CO)($PPh_3$)$_2$] arising from MARKOVNIKOV-type hydrometallation of the terminal C≡C bond (**Scheme 2.15**). An X-ray diffraction study would unambiguously confirm this conclusion, however at the time of writing the complex has resisted all attempts to grow single crystals. Nevertheless, this proposed connectivity is in accord with the NMR data listed. It should be noted that in one instance hydrometallation of a terminal alkyne (ethynylbenzene) by the same reagent resulted, depending on conditions, in either the deep red trans-β-styryl complex [RuCl(CH=CHPh)(CO)($PPh_3$)$_2$] from $CH_2Cl_2$/$Et_2O$ or the alternative yellow [RuCl{C(=$CH_2$)Ph(CO)($PPh_3$)$_3$]* ($\delta_H$ 5.40 ppm) from

* In the absence of structural characterisation, the formulation of this tris(phosphine) complex is plausible but somewhat equivocal.

$CH_2Cl_2$/methanol. Furthermore, ethyne itself by necessity affords a complex with a vinylic geminal methylene group [RuCl(CH=$CH_2$)(CO)($PPh_3$)$_2$] with $\delta_H$ = 5.11 and 4.51 ppm ($^2J_{HH}$ = 2.0 Hz).

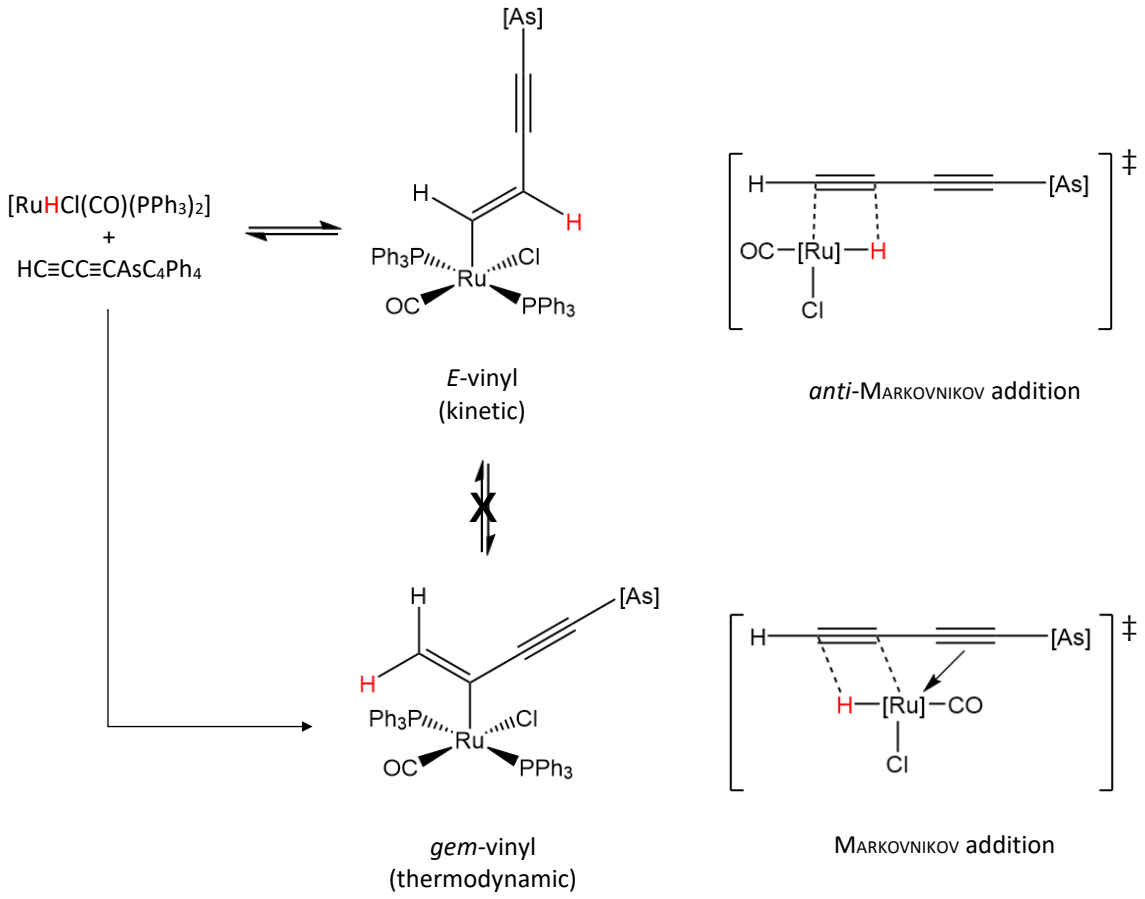



**Scheme 2.15**: Synthesis of [RuCl{*gem*-C(C≡C$AsC_4Ph_4$)=$CH_2$}(CO)$_2$($PPh_3$)$_2$].

This outcome proved reproducible however the reaction between *mer*-[RuHCl(CO)($PPh_3$)$_3$] and HC≡CC≡C$AsC_4Ph_4$ was always observed to proceed *via* a brightly orange-coloured intermediate *en route* to the weakly yellow-coloured *gem*-alkenyl complex. This initial species was presumed to be [RuCl(*E*-CH=CHC≡C$AsC_4Ph_4$)(CO)($PPh_3$)$_2$] which is indeed the case and could be intercepted spectroscopically. Mixing equimolar quantities of the reagents in $CD_2Cl_2$ and following the reaction *via* $^1$H, $^{13}$C{$^1$H} and $^{31}$P{$^1$H} NMR spectroscopies allows partial but nonetheless unambiguous identification of the initial product as an *E*-vinyl complex arising from hydroruthenation of the terminal C≡C bond. The kinetic product [RuCl(*E*-CH=CHC≡C$AsC_4Ph_4$)(CO)($PPh_3$)$_2$] displays the characteristic pair of doublets of triplets at 8.71 and 4.98 ppm for the *E*-alkenyl hydrogens α and β to the Ru(II) centre, respectively, and triplets at 205.9, 172.0 and 124.5 in the $^{13}$C{$^1$H} spectrum correspond to the carbonyl and alkenyl $C_\alpha$ and $C_\beta$ nuclei, respectively.* Conversion to the thermodynamic product [RuCl(*gem*-C(=$CH_2$)C≡C$AsC_4Ph_4$)(CO)$_2$($PPh_3$)$_2$] is suspected to proceed *via* reversible β-hydride elimination to re-establish the alkyne that may either rotate or dissociate/re-coordinate to arrive at the geometry appropriate for concerted (re)insertion allowing the thermodynamic cross-conjugated α-alkynylvinyl product to accumulate. Given this ligand is sterically more

* In unpublished work from this group, the reaction of [RuH(dcpe)(Bp)] with HC≡CC≡C$SiMe_3$ exclusively affords the *trans*-β regiochemistry in [Ru(CH=CHC≡C$SiMe_3$)(dcpe)(Bp): $\delta_H$ = 6.48 (d, $^3J_{HH}$ = 16 Hz, Ru–CH=C*H*), 9.23 (dt, $^3J_{HP}$ = 8 Hz, $^3J_{HH}$ = 16 Hz, Ru–C*H*); $\delta_C$ = 192.8 (t, $^2J_{CP}$ = 12 Hz, Ru–*C*H), 110.9 (C≡C), 110.5 (Ru–CH=*C*H), 81.98 (C≡C). R. J. Abernethy, PhD Thesis, Australian National University, **2008**.

intrusive than the β-alkynylvinyl isomer, it might be concluded that electronic factors play a determinant role. In the regrettable absence of structural data, but noting the pale colour of the final product which is uncharacteristic of five-coordinate unsaturated Ru(II) complexes, the possibility might be considered that weak, hemilabile coordination of the α-alkynyl substituent contributed to this electronic impetus *cf.* [Ru{$\eta^3$-C(=CHPh)(CO)$_2$(PPh$_3$)$_2$]$^+$ and [RuCl{$\eta^3$-C(=CHR)C≡CR}(CO)(PPh$_3$)$_2$] (R = SiMe$_3$, *n*-Bu).[36, 42, 43] The half-life for this (presumably unimolecular) process was estimated *via* NMR to be *ca* 2—3 hours at ambient temperature in $CD_2Cl_2$.

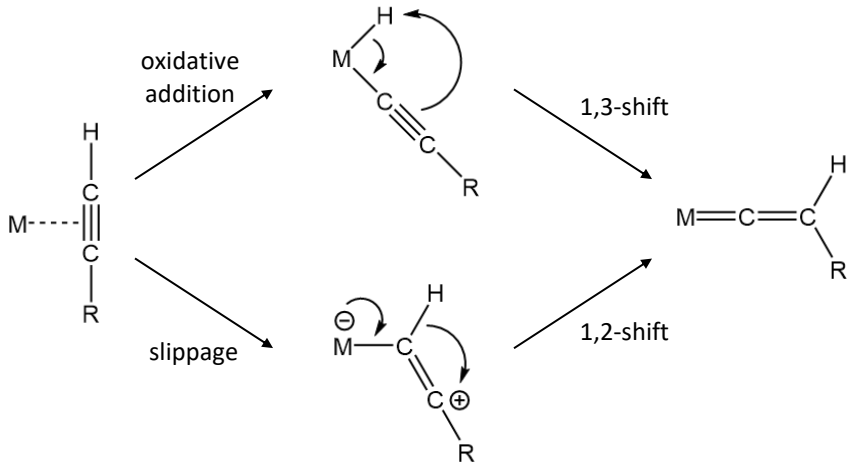



**Scheme 2.16**: Proposed sequence leading to formation of [RuCl{*gem*-C(C≡CAsC$_4$Ph$_4$)=CH$_2$}(CO)(PPh$_3$)$_2$] by gradual decomposition of [RuCl(*E*-CH=CHC≡CAsC$_4$Ph$_4$)(CO)(PPh$_3$)$_2$]; [As] = AsC$_4$Ph$_4$.

## 2.7 Reactions With [RuCl$_2$(PPh$_3$)$_3$] and [Ru(THF)(PPh$_3$)$_2$($\eta^5$-C$_5$H$_5$)]PF$_6$

Another classical alkyne transformation mediated by divalent ruthenium is the tautomerisation of terminal alkynes within the coordination environment of the metal to a vinylidene linkage (M=C=CHR, the bonding of which might be considered, with caveats to which will be returned, to be analogous to that

of an allene $H_2C=C=CH_2$). This process may be observed when the metal coordination sphere comprises innocent co-ligands that unlike hydrido and σ-organyls are unable to participate in subsequent migratory insertion processes.* The heavier Group 8 elements enjoy a central role in this process for reasons which will be outlined in the following paragraph. Two mechanisms have been suggested to account for the alkyne → vinylidene rearrangement which necessarily proceed from a common $\eta^2$-alkyne predecessor. The first involves oxidative addition of the C(*sp*)-H bond followed by a (rather difficult) 1,3-migration of the metal hydride to the β-carbon atom of the resulting σ-alkynyl ligand; the second involves $\eta^2 \rightarrow \eta^1$ slippage of the metal centre to the α-carbon of the alkyne with asynchronous deformation of the terminal hydrogen toward the β-carbon in a 1,2-shift.[44, 45]




**Scheme 2.17**: Two proposed mechanisms for the formation of vinylidene complexes from a terminal alkyne.

Both routes are potentially operative and the choice of one over the other is largely determined by the basicity of the metal centre and therefore the accompanying ligand set: stronger σ- and/or π-donors tend to favour oxidative addition for their ability to accommodate an increased oxidation state during the intermediary step, whereas less-basic ligands are more amenable to the accumulation of electron density on the metal centre during $\eta^2 \rightarrow \eta^1$ alkyne slippage.[45] An illustrative example is found in comparing vinylidene formation at $[Ru(\kappa^2\text{-dippe})(\eta^5\text{-}C_5H_5)]^+$ *vs.* $[Ru(\kappa^2\text{-dippe})(\eta^5\text{-}C_5Me_5)]^+$ (dippe = 1,2-bis(di-

* The special case of an alkynyl co-ligand coupling with a vinylidene underpins the dimerisation of terminal alkynes to ene-ynes catalysed by numerous complexes of ruthenium. See A. Dobson, D. S. Moore, S. D. Robinson, M. D. Hursthouse, L. New, *Polyhedron*, **1985**, *4*, 1119, *ibid. J. Organomet. Chem.*, **1979**, *177*, C8. More recently, M. Ballico, D. Zuccaccia, R. Figliolia, W. Baratta, *Organometallics* **2020**, *39*, 3180 and references therein.

isopropylphosphino)ethane, ($i$-Pr)$_2$PC$_2$H$_4$P($i$-Pr)$_2$) whereby the expedient of replacing a cyclopentadienyl ligand with its permethylated derivative is sufficient to divert the mechanism toward oxidative addition.[46]

The transformation from terminal alkyne to vinylidene is useful for its synthetic utility inasmuch as it is for fundamental understanding of the nature of the alkyne-metal interaction: whereas the electron rich Ru(0) engages in stable $\eta^2$-alkyne complexation (where possible, *vide supra*), complexes of Ru(II) follow an alternative pattern as dictated by the differing electronic configurations of the metal centres. It is informative to consider the DEWAR-CHATT-DUNCANSON model for alkyne complexation and that the frontier orbitals of interest include the filled alkyne($\pi$) and metal($d$) lobes residing in the MC$_2$ plane. The second orthogonal alkyne($\pi$) orbital is typically disregarded in this (simplified) perspective, however for metal centres with lower $d$-occupancies (< 6 electrons) this may serve as a supplementary electron donor toward vacant metal $d$ orbitals of $t_{2g}$ symmetry.[47] It is for this reason the so-called 4-electron alkyne ligand is usually invoked for $d^4$-octahedral metal complexes (*e.g.*, Mo(II), W(II)) to fulfilment of an 18-electron count,[47, 48] while in the case of metals with higher $d$-occupancies, coordination numbers arise that appear in contravention of the 18-electron requirements of the metal centre *e.g.*, [Fe($\eta^2$-EtC≡CEt)(PMe)(dppe)] and [Os($\eta^2$-PhC≡CPh)(CS)(PPh$_3$)$_2$].[49, 50]

In contrast, low-spin $d^6$-octahedral metal complexes (*e.g.*, Ru(II) or Os(II),[44] but also Mo(0),[51, 52] W(0),[53, 54] Mn(I)[55] and Re(I)[56, 57]) possess a fully populated set of $t_{2g}$ orbitals; the consequence of $\eta^2$-alkyne coordination to these centres is therefore a destabilising one given the appreciable repulsion between the filled in-plane alkyne($\pi$) and filled metal($d$) orbitals. Accordingly, interactions between Ru(II) complexes (and the other $d^6$-metals listed above) and alkynes often proceed in such a way as to avoid any persistent $\eta^2$-alkyne coordination: one remedy is the tautomerisation of the terminal acetylene to the vinylidene linkage, a ligand which has no $\pi$-donor capacity but *superb* bifacial $\pi$-acidity. Vinylidene formation is further promoted – thermodynamically – by the expedient that the dominant $\pi$-acceptor C$_\alpha$ finds occupied metal($d$) retrodative orbitals of suitable energy and topology in two orthogonal orientations.* It is finally worth noting

* It is stressed that the $sp$-hybridised vinylidene C$_a$ presents two orbitals of $\pi^*$ symmetry, however these are of subtly different energies due to one of these conjugating with the $\pi$-orbital of the terminal =CR$_2$ group. This feature does in principle lead to orientational preferences and rotational barriers that have on occasion been measured, though for a symmetrical $d^6$-metal coordination sphere, the (near) degeneracy of the pair of metal retrodative orbitals may allow constructive overlap to operate throughout the rotation. Thus, the availability of two metal orbitals of $\pi$-symmetry makes the analogy with allenes (the termini of which each have one atomic $p$ orbital of $\pi$-symmetry) an over-simplification. Notably, secondary factors such as steric interactions or the competing orbital considerations of other ligands may prefer one alignment over the other.

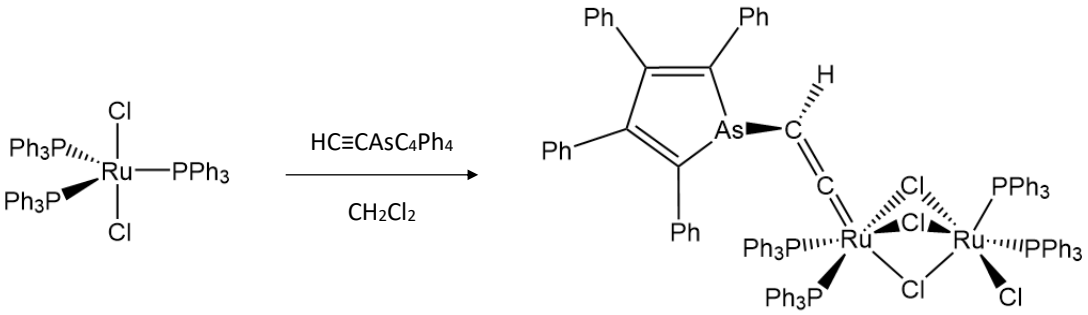
that *some* internal alkynes which possess a *p*-block substituent (*e.g.*, $BR_2$,[58] $SiR_3$,[59] $SnR_3$,[60] SR,[61] SeR[62]), or C($sp^2$) group (*e.g.*, aryl,[63] ester[64]) can also generate vinylidenes in much the same way as terminal alkynes, albeit with less facility and typically under more forcing conditions, showing the same decreased migratory aptitude for 1,2-shifts relative to hydrogen seen in conventional organic transformations. A variety of Ru(II) complexes mediate the direct transformation of a terminal alkyne to vinylidene: three of the most commonly explored platforms *inter alia* are $[RuCl_2(PPh_3)_3]$, *cis*-$[RuCl_2(\kappa^2\text{-dppe})_2]$ (dppe = 1,2-bis(diphenylphosphino)ethane, $Ph_2PC_2H_4PPh_2$), and $[RuCl(PPh_3)_2(\eta^5\text{-}C_5H_5)]$ although for the latter pair an unsaturated cationic 16-electron species is typically prepared in advance by addition of a suitable halide abstractor.

### 2.7.1 Synthesis of $[Ru_2(\mu\text{-}Cl)_3Cl(=C=CHAsC_4Ph_4)(PPh_3)_4]$

Whereas neither *cis*-$[RuCl_2(\kappa^2\text{-dppe})_2]$ was reactive* toward $HC{\equiv}CAsC_4Ph_4$ in the presence of $NaPF_6$, nor pre-formed $[RuCl(\kappa^2\text{-dppe})_2]OTf$,[65] the combination of one equivalent each $[RuCl_2(PPh_3)_3]$ and $HC{\equiv}CAsC_4Ph_4$ in $CH_2Cl_2$ medium provided a deep red solution after *ca* two hours stirring at ambient temperature. An aliquot taken for $^{31}P\{^1H\}$ NMR spectroscopy ($CD_2Cl_2$) revealed four doublets of equal intensity at 49.8 and 46.9 ppm ($^2J_{PP}$ = 37.8 Hz), and 39.7 and 35.8 ppm ($^2J_{PP}$ = 25.5 Hz) in addition to two equivalents of free $PPh_3$ (-5.1 ppm). These coupling constants are indicative of a pair of mutually *cis* $PPh_3$ ligands and the $^{31}P\{^1H\}$ spectrum is otherwise remarkably clean; notably, none of the above resonances may be convincingly attributed to a species of the type $[RuCl_2(=C=CHAsC_4Ph_4)(PPh_3)_2]$ (*cf.* $[RuCl_2(=C=CH\text{-}t\text{-}Bu)(PPh_3)_2]$ $^{31}P\{^1H\}$ δ = 27.2 ppm[66]). By comparison with other literature reports,[67-69] the product is formulated as the binuclear species $[Ru_2(\mu\text{-}Cl)_3Cl(=C=CHAsC_4Ph_4)(PPh_3)_4]$ arising from aggregation of the anticipated monomeric vinylidene $[RuCl_2(=C=CHAsC_4Ph_4)(PPh_3)_2]$ with a "$RuCl_2(PPh_3)_2$" equivalent (**Scheme 2.18**), which was confirmed by high-resolution mass spectrometry and a single crystal structure determination (**Figure 2.15**). Indeed, one equivalent of free $HC{\equiv}CAsC_4Ph_4$ was observed in the $^1H$ spectrum of the crude reaction mixture alongside a poorly resolved triplet at 3.4 ppm ($^4J_{PH} \approx 2$ Hz) for the lone vinylidene hydrogen atom. Workup of the reaction mixture affords $[Ru_2(\mu\text{-}Cl)_3Cl(=C=CHAsC_4Ph_4)(PPh_3)_4]$ as a reasonably air-stable, red-brown solid in modest yield, the vinylidene

* $[W(THF)(CO)_3(\kappa^2\text{-dppe})]$ also failed to give a vinylidene of the form $[W(=C=CHAsC_4Ph_4)(CO)_3(\kappa^2\text{-dppe})]$ upon treatment with $HC{\equiv}CAsC_4Ph_4$. See K.R. Birdwhistle, S.J.N. Burgmayer and J.L. Templeton *J. Am. Chem. Soc.*, **1983**, *105*, 7789—7790.

carbon resonance of which appears at 336.3 ($^{2}J_{PC}$ unresolved) and 94.8 ppm in the $^{13}C\{^{1}H\}$ NMR spectrum, the latter identified by an HSQC NMR experiment.




**Scheme 2.18**: Synthesis of $[Ru_2(\mu\text{-}Cl)_3Cl\{=C=C(H)AsC_4Ph_4\}(PPh_3)_4]$.

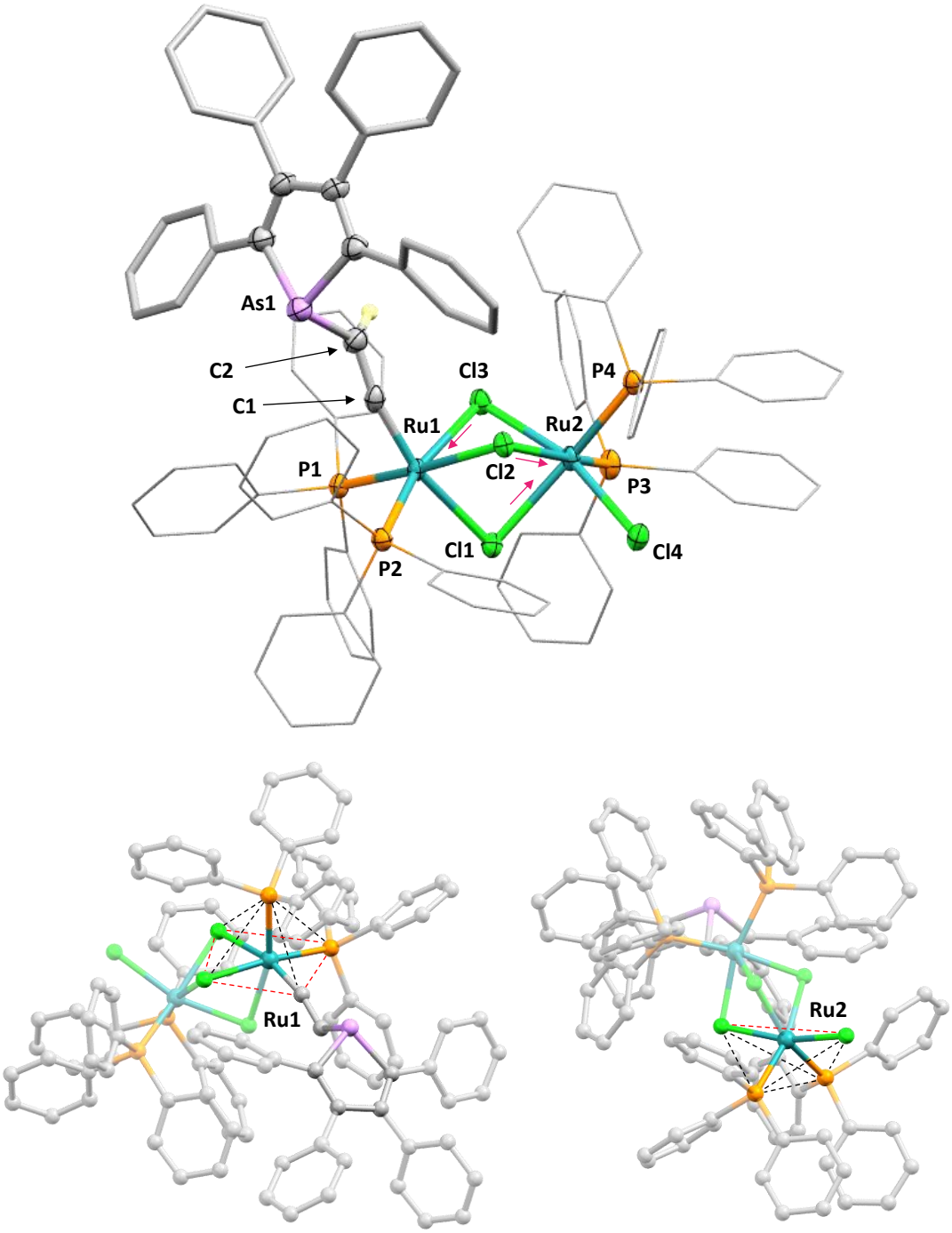



**Figure 2.15**: The molecular structure of $[Ru_2(\mu\text{-}Cl)_3Cl(=C=CHAsC_4Ph_4)(PPh_3)_4]\cdot 4CH_2Cl_2$ in a crystal. Phenyl groups simplified and dichloromethane solvate molecules and hydrogen atoms omitted for clarity. Ellipsoids shown at 50% displacement. Pink arrows denote Cl→Ru dative bonds. **Inset left**: Abbreviated perspective of the complex highlighting the square-based pyramidal geometry of the Ru1 centre. The basal plane is shown in red. **Inset right**: Abbreviated perspective of the complex highlighting the disphenoidal geometry of the Ru2 centre. The principal edge is shown in red.

The complex appears to be the first example of a vinylidene ligand bearing an arsenic substituent. Indeed, structural data for pnictogen-functionalised vinylidenes more generally are limited to a small

number of phenylazo,[70] amino,[71] *N*-heterocyclivinylidenes,[72] phosphonio,[73] phosphonato[74] and a single phosphino derivative, $[Fe(=C=CHPPh_2)(dppe)(\eta^5\text{-}C_5Me_5)]PF_6$ described by PAUL.[75]

Only one Ru(II) centre bears the expected β-arsolylvinylidene ligand; three chlorides adjoin two face-sharing octahedra and to each metal atom is bestowed a pair of *cis*-disposed diastereotopic $PPh_3$ ligands, in agreement with the $^{31}P\{^1H\}$ NMR spectrum. The other Ru(II) centre also possesses a fourth and final terminal chloride ligand and thus each metal atom attains geometric and electronic saturation upon aggregation. If the Cl3-Ru1 interaction is ignored, the local coordination geometry about the Ru1 unit would be that of a slightly distorted square-based pyramid (Ru1 $\tau_5 = 0.14$) with the vinylidene ligand lying in the *quasi*-basal plane of Ru1 (**Figure 2.15**, **Inset left**). Likewise, if the Cl1-Ru2 and Cl2-Ru2 interactions are ignored, the local coordination geometry about the Ru2 unit is a deformed disphenoid ($\tau_4 = 0.65$, $\tau'_4 = 0.46$)* with the pair of chloride ligands lying along the major edge (**Figure 2.15**, **Inset right**). The Ru-C1 and C1-C2 double bonds measure 1.827(6) and 1.322(8) Å, respectively, which are both slightly elongated compared to monomeric five-coordinate Ru(II) vinylidenes[76] being more comparable to octahedral systems.[77-79] The vinylidene linkage bows slightly in the direction of the β-hydrogen by *ca* 16° from linearity though local angles about C2 reflect the $sp^2$-hybridised nature of the hydrocarbon chain terminus (C1-C2-As1, *ca* 124°). Interatomic distances for the bridging chloride ligands reflect alternating covalent (mean Ru-Cl *ca.* 2.44 Å) and dative (mean Cl→Ru *ca.* 2.55 Å) bonds rendering visual dissection of the complex into its mononuclear constituents a straightforward exercise (**Figure 2.15**).

This outcome proved to be quite reproducible despite subsequent attempts to prepare a mononuclear vinylidene species (varying reaction conditions, or order of reagent addition, or the use of excess $HC{\equiv}CAsC_4Ph_4$ had no effect), though once the preferred stoichiometry of the reaction was appreciated, the combination of $[RuCl_2(PPh_3)_3]$ with one-half an equivalent of $HC{\equiv}CAsC_4Ph_4$ in $CH_2Cl_2$ afforded the binuclear vinylidene complex in good yield. Heating $[Ru(\mu\text{-}Cl)_3Cl\{=C=C(H)AsC_4Ph_4\}(PPh_3)_4]$ ($CD_2Cl_2$ 40 °C, $C_6D_6$ 80 °C or toluene-$d_8$ 110 °C) with an additional equivalent of $HC{\equiv}CAsC_4Ph_4$ led in all

* The $\tau_4$ and $\tau'_4$ parameters are geometry indices for classifying four coordinate geometries as either tetrahedral ($\tau_4 = \tau'_4 = 1$), disphenoidal ("seesaw"; $\tau_4 = 0.43$, $\tau'_4 = 0.24$) or square-planar ($\tau_4 = \tau'_4 = 0$). The parameters are given by the formulae $\tau_4 = \frac{360-(\alpha+\beta)}{360-2\theta}$ and $\tau'_4 = \frac{\beta-\alpha}{360-\theta} + \frac{180-\beta}{180-\theta}$ where $\beta \geq \alpha$ and are the greatest valence angles about the metal centre (in degrees), and $\theta = 109.5°$. It follows that for pure tetrahedral geometry $\alpha = \beta = 109.5°$, for pure square-planar geometry $\alpha = \beta = 180°$, and for pure disphenoidal geometry $\alpha = 120°$ and $\beta = 180°$.

three cases to no further reaction, though partial decomposition of the ruthenium species to free phosphine and other species including free $HC{\equiv}CAsC_4Ph_4$ at higher temperature was noted.

The addition of xylyl isocyanide (xylyl = 3,5-dimethylphenyl) to $[Ru(\mu\text{-}Cl)_3Cl(=C=CHAsC_4Ph_4)(PPh_3)_4]$ in an attempt to fragment the dimer into a monomeric vinylidene, instead produced free $HC{\equiv}CAsC_4Ph_4$ and *trans*-$[RuCl_2(CNXyl)_2(PPh_3)_2]$* as the only identifiable products by $^1H$ and $^{31}P\{^1H\}$ NMR spectroscopy, respectively. No characteristic vinylidene hydrogen signal (a triplet at *ca* 3 ppm) was observed in this reaction mixture and it has been previously noted that the introduction of π-acidic ligands affects the reversion of vinylidenes to the free alkyne.[62] Other reported methods for binuclear $[Ru_2(\mu\text{-}Cl)_3Cl(=C=CHR)(PR_3)_4]$ fragmentation including metathesis with $TlOC_6F_5$,[80] or chelating biphosphine[62] or tris(pyrazolyl)borate ligands[81] gave complex mixtures of products which were difficult to purify. Indeed, a cursory survey of the relevant literature suggests $[RuX_2L_3]$ to have a *penchant* toward formation of doubly- or triply-halide bridged diruthenium complexes in unsaturated hydrocarbon tautomerisation,[67, 82-85] with one of the earliest examples being WILKINSON'S thiocarbonyl $[Ru_2(\mu\text{-}Cl)_3Cl(CS)(PPh_3)_4]$ for which an analogy with the vinylidene complex is apparent, ($C{=}CH_2$ being approximately isolobal with CS).[86, 87]

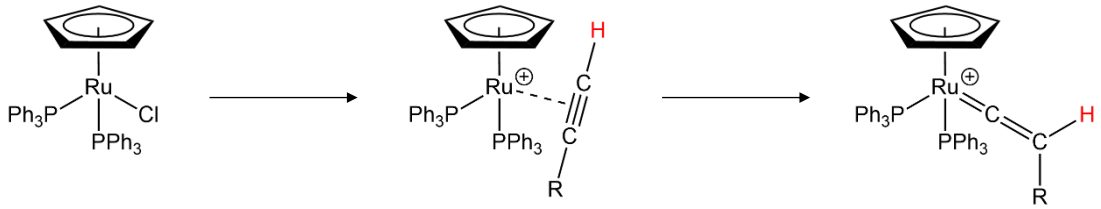
### 2.7.2 Synthesis of $[Ru(=C=CHAsC_4Ph_4)(PPh_3)_2(\eta^5\text{-}C_5H_5)]PF_6$

Another platform – one of the earliest[88] – with proclivity for mediating the tautomerisation of terminal alkynes is the $d^6$ Ru(II) centre within a labile $[Ru(S)(PPh_3)_2(\eta^5\text{-}C_5H_5)]^+$ cation (S = solvent *e.g.*, THF, MeOH, acetone, MeCN). Such complexes are often isolable and may be prepared from $[RuX(PPh_3)_2(\eta^5\text{-}C_5H_5)]$ and a suitable halide abstractor (usually non-coordinating salts of $Na^+$, $K^+$ or $Ag^+$) in a donor solvent,[89, 90] and serve as a synthetic equivalent for the active 16-electron "$Ru(PPh_3)_2(\eta^5\text{-}C_5H_5)^+$" centre. The original method for $[Ru(=C=CHR)(PPh_3)_2(\eta^5\text{-}C_5H_5)]^+$ synthesis (from a terminal alkyne) outlined by BRUCE[91, 92] employed $[NH_4]PF_6$ in methanol and relied on the spontaneous formation of $[Ru(S)(PPh_3)_2(\eta^5\text{-}C_5H_5)]^+$ *in situ*, as $[RuCl(PPh_3)_2(\eta^5\text{-}C_5H_5)]$ had previously been shown by HAINES to autoionise in alcoholic†

* NMR: $^{31}P\{^1H\}$ ($CDCl_3$, 161 MHz, 25 °C) δ 31.8 ppm. Data in agreement with those reported by HILL *et al. Organometallics*, **2000**, *19*, 371—373.

† The use of alcoholic media for vinylidene synthesis is potentially complicated by nucleophilic attack of the solvent upon the electrophilic α-carbon over extended reaction times, producing a FISCHER-type alkoxycarbene. See M.I. BRUCE and A.G. SWINCER *Aus. J. Chem.*, **1980**, *33*, 1471—1483. This side reaction is also prevalent among π-alkyne complexes since in both tautomers the $C_2$-fragment is activated toward nucleophiles by the transition metal centre and was noted prior to the discovery of vinylidenes. See M.H. CHISHOLM and H.C. CLARK *J. Am. Chem. Soc.*, **1972**, *94*, 1532—1539.

solutions.[90] The use of the ammonium cation is a deliberate choice to maintain a weakly acidic environment since $[Ru(=C=CHR)(PPh_3)_2(\eta^5\text{-}C_5H_5)]^+$ complexes are vulnerable to opportunistic deprotonation to their conjugate base, a neutral σ-alkynyl $[Ru(C\equiv CR)(PPh_3)_2(\eta^5\text{-}C_5H_5)]$ (**Section 2.7.3**). With this in mind, it is also possible that the $[NH_4]^+$ cation is not wholly innocent and may participate in the alkyne → vinylidene tautomerisation by providing a means to transfer the terminal hydrogen atom across the hydrocarbon spine. A simplified pathway ignoring the action of any other species is shown in **Scheme 2.19** and, like many $d^6$-metal centres, begins with formation of a π-alkyne complex with truculent C≡C(π) and M($t_{2g}$) interactions. It should be noted that three distinct mechanisms have been proposed, however the sequence involving a concerted 1,2-H shift is favoured for the $[Ru(PPh_3)_2(\eta^5\text{-}C_5H_5)]^+$ system specifically.[93, 94]




**Scheme 2.19**: Tautomerisation of terminal alkynes to vinylidenes within the coordination sphere of $[Ru(PPh_3)_2(\eta^5\text{-}C_5H_5)]^+$ cation

The method outlined BRUCE remains *de rigueur* for the synthesis of cationic ruthenium (and osmium) vinylidene complexes and has been extended by DIXNEUF to the related $[RuCl(\kappa^2\text{-dppe})_2]^+$ platform.[65, 95] In the interim, a library of $[M(=C=CER)L_2(\eta^5\text{-}C_5H_5)]^+$ (M = Ru, Os; L = phosphine, phosphite or ½·diphosphine) vinylidenes have been prepared,[44] and a variety of non-hydrogen entities have been observed to undergo the necessary migration including aryl,[96] silyl,[97] thiolate[61] and selenoate groups,[62] albeit with comparatively diminished faculty. This short discussion would be remiss if the related (and more reactive) allenylidenes $[Ru(=C=C=CER)L_2(\eta^5\text{-}C_5H_5)]^+$ and butatrienylidenes $[Ru(=C=C=C=CER)L_2(\eta^5\text{-}C_5H_5)]^+$ were not mentioned, since their preparative routes from terminal alkynols[98, 99] and diynes,[100, 101] respectively, have afforded a chemistry as potentially rich as their vinylidene counterparts albeit yet to reach the same degree of maturity.

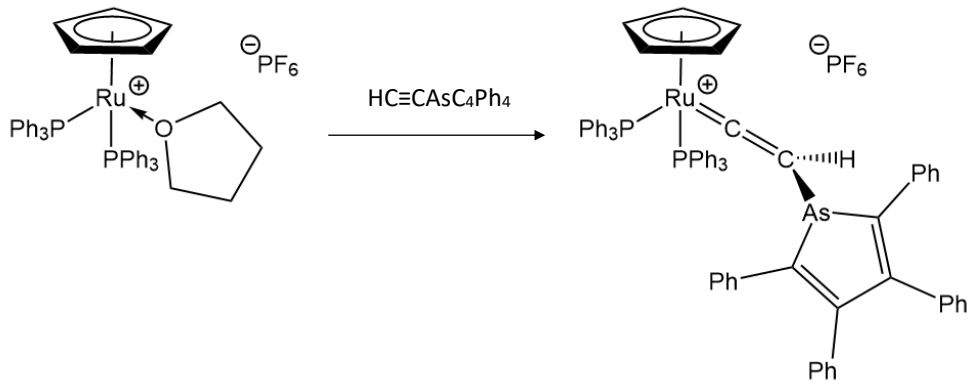
An alternative synthetic method (also first described by BRUCE) involves the addition of electrophiles to the nucleophilic β-carbon of a ruthenium alkynyl *e.g.*, whereas alkyl groups have generally low migratory aptitude and a complex of the form $[Ru(=C=CMe_2)L_2(\eta^5\text{-}C_5R_5)]^+$ cannot be directly

synthesised from 2-butyne, alkylation of $[Ru(C{\equiv}CMe)L_2(\eta^5\text{-}C_5R_5)]$ with $[Me_3O]^+$, $MeOSO_2CF_3$ or even MeI provides the desired vinylidene in high yield.[92, 102, 103] Naturally, $[Ru(C{\equiv}CR)L_2(\eta^5\text{-}C_5R_5)]$ may be protonated at $C_\beta$ though a range of bespoke (*i.e.*, non-hydrogen or -alkyl) electrophiles with additional functionality have been installed onto the alkynyl including *inter alia* diazonium and halonium reagents and chiral ancillaries.[104-110] The entire scope of this chemistry cannot be fully captured here however the comprehensive account published by BRUCE[44] in a 1991 issue of *Chemical Reviews*, and the chapter on $\eta^1$-hydrocarbon ligands curated by HILL[40] in Volume 6 of *Comprehensive Organometallic Chemistry II* remain the authoritative sources for fundamental Group 8 vinylidene chemistry. A broad summary of the general chemistry of the $RuL_2(\eta^5\text{-}C_5R_5)$ fragment has been provided by DAVIES,[111] and a catalysis-centred perspective is given by VERPOORT.[112]

Emulating long-standing recipes, one equivalent each $[RuCl(PPh_3)_2(\eta^5\text{-}C_5H_5)]$, $[NH_4]PF_6$ and $HC{\equiv}CAsC_4Ph_4$ were combined in THF solution, which over the course of one week at ambient temperature afforded a dark red solution containing the β-arsolylvinylidene $[Ru(=C=CHAsC_4Ph_4)(PPh_3)_2(\eta^5\text{-}C_5H_5)]PF_6$. As an aside, it was mentioned above that methanol is the usual medium for this reaction since it encourages ionisation of the chloride ligand, however $HC{\equiv}CAsC_4Ph_4$ is *so poorly soluble* in this solvent that – contrary to expectation – no vinylidene formation was observed. The reaction in THF was intermittently monitored by NMR spectroscopy ($CD_2Cl_2$) and the new complex exhibits a sharp singlet in the $^{31}P\{^1H\}$ NMR spectrum* at 43.0 ppm which is appreciably downfield of the starting material (31.0 ppm), in accord with the cationic charge of the complex and the presence of a potent π-acceptor vinylidene. The $^1H$ spectrum reveals a characteristic triplet at 4.98 ppm with $^4J_{PH}$ = 2.7 Hz alongside a sharp singlet at 4.75 ppm for the cyclopentadienyl ligand, which may be compared resonances for the corresponding nuclei in similar $[Ru(=C=CHR)(PPh_3)_2(\eta^5\text{-}C_5H_5)]^+$ complexes: R = Me, $\delta_H$ 4.70 and $\delta_{Cp}$ 5.15 ppm; R = Ph, $\delta_H$ 5.43 ($J_{PH}$ = 2.4 Hz) and $\delta_{Cp}$ 5.28 ppm; R = $CO_2Me$, $\delta_H$ 5.04 and $\delta_{Cp}$ 5.34 ppm.[92]

* A characteristic septet at -144.4 ppm for the $[PF_6]^-$ anion was also observed.

An aliquot taken for high-resolution mass spectrometry also yields the molecular ion ($m/z \approx$ 1147.2129); unfortunately, analytically pure samples were difficult to obtain from this reaction mixture and the product was contaminated with traces of unknown materials, which were neither [RuCl($PPh_3$)$_2$($\eta^5$-$C_5H_5$)] nor [Ru(THF)($PPh_3$)$_2$($\eta^5$-$C_5H_5$)]$^+$ nor HC≡C$AsC_4Ph_4$. The same outcome was obtained when pre-formed, re-crystallised samples* of [Ru(THF)($PPh_3$)$_2$($\eta^5$-$C_5H_5$)]$^+$ were deployed in a slight molar deficit upon HC≡C$AsC_4Ph_4$ in $CH_2Cl_2$ solution, although in this case tautomerisation was noticeably faster with a visible colour change after several minutes and the reaction was complete within a few hours (*cf.* ~one week for [RuCl($PPh_3$)$_2$($\eta^5$-$C_5H_5$)]/[$NH_4$]$PF_6$).




**Scheme 2.20**: Synthesis of [Ru(=C=CHA$sC_4Ph_4$)($PPh_3$)$_2$($\eta^5$-$C_5H_5$)]$PF_6$.

Even if slightly impure, the novel [Ru(=C=CHA$sC_4Ph_4$)($PPh_3$)$_2$($\eta^5$-$C_5H_5$)]$^+$ vinylidene could nevertheless be fully characterised. The $^{13}C\{^1H\}$ NMR spectrum reveals the strongly deshielded vinylidene α-carbon manifest as a triplet at 331.2 ppm ($^2J_{PC}$ = 15.6 Hz) and the adjutant β-carbon resonance at 115.7 ppm (*via* an HSQC NMR experiment; $^3J_{PC}$ unresolved). The arsole ring-carbon nuclei resonances appear in the usual region (152.7 and 150.9 ppm) with that for the cyclopentadienyl ligand at 94.7 ppm. The chemical shift of the α-carbon falls at the lower end of the greater continuum for [Ru(=C=CER)$L_2$($\eta^5$-$C_5H_5$)]$^+$ complexes (*ca* 320—380 ppm; L = phosphine or ½·diphosphine) as does the β-carbon (*ca* 110—140 ppm). The $\nu_{C=C}$ stretch, which has been reported for other [Ru(=C=CER)$L_2$($\eta^5$-$C_5H_5$)]$^+$ to appear at *ca* 1600—

* NMR: $^1H$ ($CD_2Cl_2$, 400 MHz, 25 °C) δ 4.84 ($\eta^5$-$C_5H_5$) ppm. $^{31}P\{^1H\}$ δ 43.5 ppm.

1650 $cm^{-1}$, could not be unambiguously assigned in the solution IR spectrum since several weak absorptions were present.

In general, the chemical shift of the $C_\alpha$ nucleus is more impacted by the identity of E and R than is $C_\beta$, and whilst a loose trend of electron-releasing substituents correlating to higher frequencies for $C_\alpha$ and *vice-versa* emerges upon inspection of those complexes for which $^{13}C$ NMR data are recorded, this is not ascribed to simple inductive effects. The phenomenon is not exclusive to ruthenium vinylidenes,[44] and is generally attributed to the magnitude of the paramagnetic contribution to nuclear deshielding since the LUMO coefficient is – not coincidentally – greatest at $C_\alpha$.[113] The observation that electron-withdrawing residues result in greater shielding (lower chemical shift) of the $C_\alpha$ nucleus is perhaps counter-intuitive, since these groups will invariably decrease the energy of the LUMO and afford the vinylidene ligand a greater appetite for $Ru(d)\rightarrow C_\alpha{=}C_\beta(\pi^*)$ retrodonation (a *deshielding* influence). However, it is important to consider that an electron-withdrawing group(s) will have the concurrent effect of disseminating the LUMO *away* from $C_\alpha$ toward $C_\beta$ and itself;[114] accordingly, both the π-acidity of the vinylidene α-carbon and the magnitude of the paramagnetic contribution to chemical shift decrease, resulting in an *upfield* shift of $C_\alpha$. This is equivalent to stating that electron-releasing substituents consolidate the LUMO coefficient at $C_\alpha$ and thereby increase the importance of paramagnetic deshielding to that atom. In this regard – and based purely on $^{13}C$ shifts – the $AsC_4Ph_4$ group can be viewed as moderately electron-withdrawing (or only weakly electron-releasing) when installed on the vinylidene ligand.* This is an intuitive outcome in the present context given that the heteroatom has previously been shown to be the centre of nucleophilic attack in **Section 2.4** (see also **Figure 2.4** and **Figure 2.7** for the arsenocentric LUMO's of $H(C{\equiv}C)_nAsC_4Ph_4$). A computational analysis of the model complex $[Ru(=C{=}CHAsC_4H_4)(PH_3)_2(\eta^5\text{-}C_5H_5)]^+$ using DFT (gas phase: ωB97X-D/6-31G*/LAN2Dζ) indeed finds a significant contribution from the arsolyl residue to the LUMO.

* *Cf.* $[Ru(C{=}CHC_6H_4OMe)(PPh_3)_2(\eta^5\text{-}C_5H_5)]^+$ $\delta_C$ 364.5 & 113.7 ppm; $[Ru(C{=}CHPh)(PPh_3)_2(\eta^5\text{-}C_5H_5)]^+$ $\delta_C$ 358.9 & 119.5 ppm; $[Ru(C{=}CHMe)(PPh_3)_2(\eta^5\text{-}C_5H_5)]^+$ $\delta_C$ 349.4 & 119.0 ppm; $[Ru(C{=}CHC_6F_5)(PPh_3)_2(\eta^5\text{-}C_5H_5)]^+$ $\delta_C$ 327.3 & 119.3 ppm. Compiling a more comprehensive set of data for comparison is difficult since the $^{13}C\{^1H\}$ NMR spectra of a great many $[Ru(C{=}CHR)(PPh_3)_2(\eta^5\text{-}C_5H_5)]^+$ complexes have not been reported. These four examples were selected from M.I. Bruce, *Chem. Rev.*, **1991**, *91*, 197—257 and the reader is directed to references therein for the original texts.

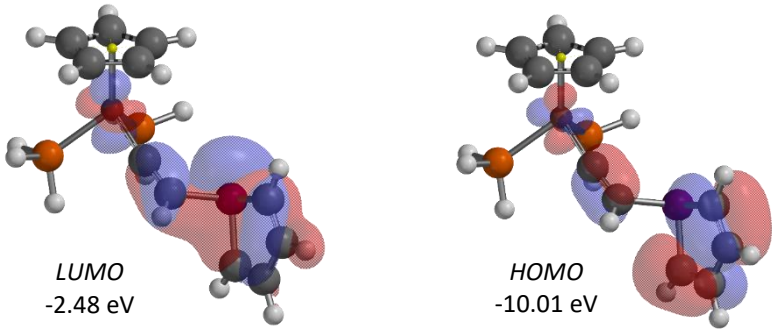



**Figure 2.16**: Calculated frontier orbitals of the model β-arsolylvinylidne cation $[Ru(=C=CHAsC_4H_4)(PH_3)_2(\eta^5\text{-}C_5H_5)]^+$ (DFT, gas phase: ωB97X-D/6-31G*/LAN2DZ).

Single crystals of $[Ru(=C=CHAsC_4Ph_4)(PPh_3)_2(\eta^5\text{-}C_5H_5)]PF_6$ were grown by the vapour diffusion of $Et_2O$ into a $CH_2Cl_2$ solution of the crude product at -30 °C; the molecular structure (as the dichloromethane trisolvate) was determined by X-ray diffraction and is shown in **Figure 2.17**.

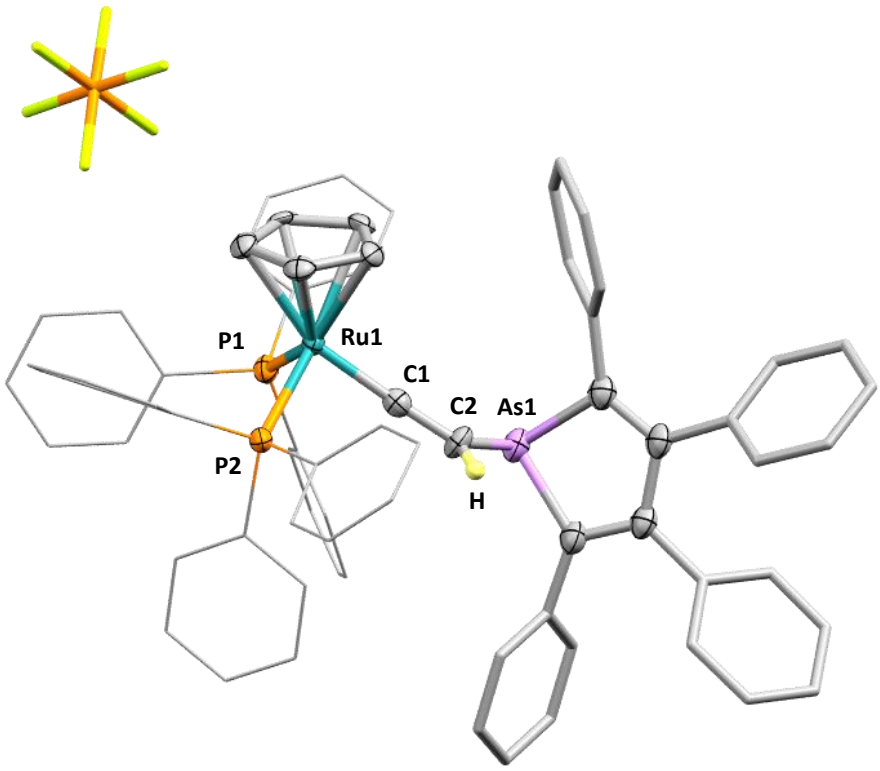



**Figure 2.17**: The molecular structure of $[Ru(=C=CHAsC_4Ph_4)(PPh_3)_2(\eta^5\text{-}C_5H_5)]PF_6{\cdot}3CH_2Cl_2$ in a crystal. Phenyl groups simplified and dichloromethane solvate molecules and hydrogen atoms omitted for clarity, except the vinylidene hydrogen which is shown in light yellow for emphasis. Ellipsoids shown at 50% displacement.

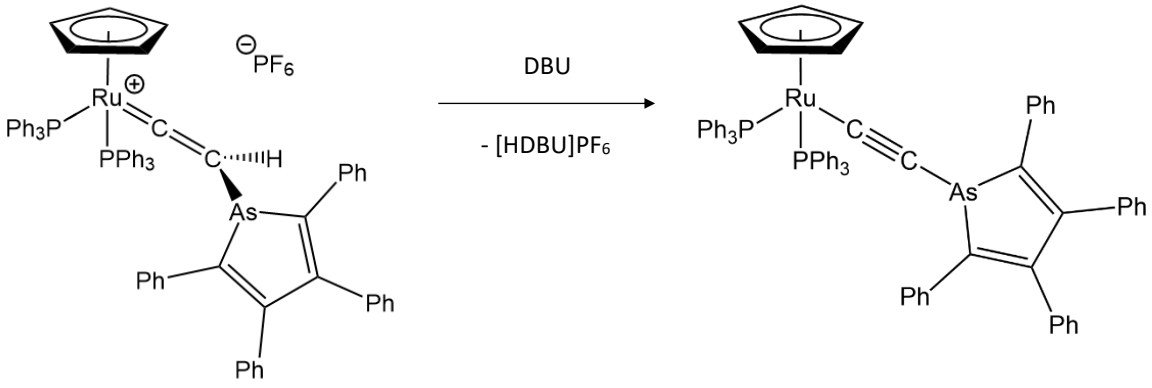
The formulation as the second example of a β-arsolylvinylidene was confirmed; the complex crystallises in triclinic *P*-1 and a pair of enantiomeric molecules, which differ in the lateral disposition of the vinylidene substituents, are found in the unit cell related by means of the crystallographic inversion centre. The local geometry about the *pseudo*-octahedral* Ru(II) atom is that of a three-legged piano stool with nearly right-angles formed between the vinylidene and flanking $PPh_3$ ligands. The body of the $AsC_4Ph_4$ group is positioned about the $C_\beta$-As bond to lie approximately parallel with the (non-crystallographic) symmetry plane bisecting the $Ru(PPh_3)_2(\eta^5\text{-}C_5H_5)$ moiety through the vinylidene spine, which avoids the pendant phenyl rings from infringing upon those borne by the nearby phosphine ligand. This also places the arsenic lone pair of electrons orthogonal to the vinylidene π-system. The vinylidene chain is essentially linear (Ru1-C1-C2 *ca* 175°) with interatomic distances of 1.846(4), 1.294(5) and 1.967(3) Å for the Ru=C, C=C and C-As bonds, respectively. The former and latter are slightly longer (on the order of 0.01—0.02 Å) than the same bonds within $[Ru_2(\mu\text{-}Cl)_3Cl\{=C=C(H)AsC_4Ph_4\}(PPh_3)_4]$ (**Figure 2.15**) whilst the C=C bonds are essentially crystallographically identical. Despite the inclusion of ten phenyl rings, the geometric features and conformational preference for the core of interest are not dissimilar to those calculated in the gas phase above for $[Ru(=C=CHAsC_4H_4)(PH_3)_2(\eta^5\text{-}C_5H_5)]^+$, devoid of inter-ligand and intermolecular interactions.

The addition of $Li[Et_3BH]$ (a potential hydridic nucleophile) to a THF solution of $[Ru(=C=CHAsC_4Ph_4)(PPh_3)_2(\eta^5\text{-}C_5H_5)]PF_6$ afforded $[Ru(C{\equiv}CAsC_4Ph_4)(PPh_3)_2(\eta^5\text{-}C_5H_5)]$ (*vide infra*) and not a neutral vinyl complex of the form $[Ru(CH=CHAsC_4Ph_4)(PPh_3)_2(\eta^5\text{-}C_5H_5)]$, the borohydride acting in this context as a base and not a nucleophile upon $C_\alpha$ as anticipated. An experiment to prepare a FISCHER-type carbene[115] with a β-arsolyl substituent by heating a mixed THF/methanol solution of $[Ru(=C=CHAsC_4Ph_4)(PPh_3)_2(\eta^5\text{-}C_5H_5)]PF_6$ produced an oily yellow-brown residue for which low-resolution mass spectrometry found a molecular ion corresponding to $[Ru\{=C(OMe)CH_2AsC_4Ph_4\}(PPh_3)_2(\eta^5\text{-}C_5H_5)]^+$ ($m/z \approx 1180.23$, for the protonated adduct), however attempts to extricate the compound from the mixture were unsuccessful and it was not characterised further.

* In three-legged piano-stool geometries, the *pentahapto* cyclopentadienyl ligand is nominally considered to assume three *facial* coordination sites of an octahedron.

### 2.7.3 Synthesis of [Ru(C≡CAsC$_4$Ph$_4$)(PPh$_3$)$_2$($\eta^5$-C$_5$H$_5$)]

Vinylidene complexes are so typically acidic at the β-carbon that weak bases are often sufficient for conversion to a neutral σ-alkynyl;[91] thus, to a $CD_2Cl_2$ solution of [Ru(=C=CHAsC$_4$Ph$_4$)(PPh$_3$)$_2$($\eta^5$-C$_5$H$_5$)]$^+$ was added an excess of NEt$_3$ resulting in a gradual colour change over the course of *ca* 30 minutes from red to yellow. The $^{31}P\{^1H\}$ NMR signal of the cationic vinylidene at 43.0 ppm was replaced by a predominant resonance positioned slightly downfield at 49.7 ppm; accordingly, the characteristic triplet for the vinylidene hydrogen at C$_\beta$ is absent from the $^1$H NMR spectrum and the cyclopentadienyl signal shifts slightly upfield to 4.17 ppm. This deprotonation was not particularly clean and secondary signals were observed in both spectra, possibly the result of side-reactions which involve either the amine or adventitious moisture (or both) acting upon the hydrocarbon linkage. A cleaner outcome was instead obtained with the less-nucleophilic DBU (1,8-diazabicyclo[5.4.0]undec-7-ene) in THF solution giving the neutral σ-alkynyl complex [Ru(C≡CAsC$_4$Ph$_4$)(PPh$_3$)$_2$($\eta^5$-C$_5$H$_5$)] in acceptable yield after chromatography as an air-stable yellow solid (**Scheme 2.21**). When the alkynyl is the desired product, the vinylidene intermediate needed not to be isolated and was instead generated and deprotonated *in situ*, noting that since the p$K_a$ of the conjugate acid [HDBU]$^+$ is ~24 (in MeCN), deprotonation of the free alkynyl arsole (p$K_a$ ≈ 26) is unlikely to proceed without the intervention of the ruthenium centre.




**Scheme 2.21**: Synthesis of [Ru(C≡CAsC$_4$Ph$_4$)(PPh$_3$)$_2$($\eta^5$-C$_5$H$_5$)].

Possibly reflecting the nucleophilicity of the β-carbon within the alkynyl complex,[113] the high-resolution mass spectrum yields the protonated adduct of the molecular ion ($m/z$ ≈ 1147.2123, *i.e.*, the

vinylidene) although it is equally plausible that the proton is carried by the arsenic atom,* which was occasionally implicit throughout this work. The $^{13}C\{^1H\}$ NMR ($CD_2Cl_2$) spectrum reveals the ruthenium-bound α-carbon as a triplet at 146.2 ppm ($^2J_{PC}$ = 23.8 Hz), an impressive shift† of some 180 ppm upfield from the same atom in $[Ru(=C=CHAsC_4Ph_4)(PPh_3)_2(\eta^5\text{-}C_5H_5)]^+$. The arsolyl ring-carbon nuclei and the alkynyl β-carbon appear at 152.0, 147.8 and 93.7 ppm, respectively (*cf.* 152.7, 150.9 and 115.7 ppm in the vinylidene) – the modest displacement of these chemical shifts from that in the vinylidene concur with the assertion that $C_\alpha$ is the atom under the greatest electronic duress within these systems. Single crystals of $[Ru(C{\equiv}CAsC_4Ph_4)(PPh_3)_2(\eta^5\text{-}C_5H_5)]$ were grown from $CH_2Cl_2$/*n*-hexane at -20 °C and the crystal structure is shown in **Figure 2.18**.

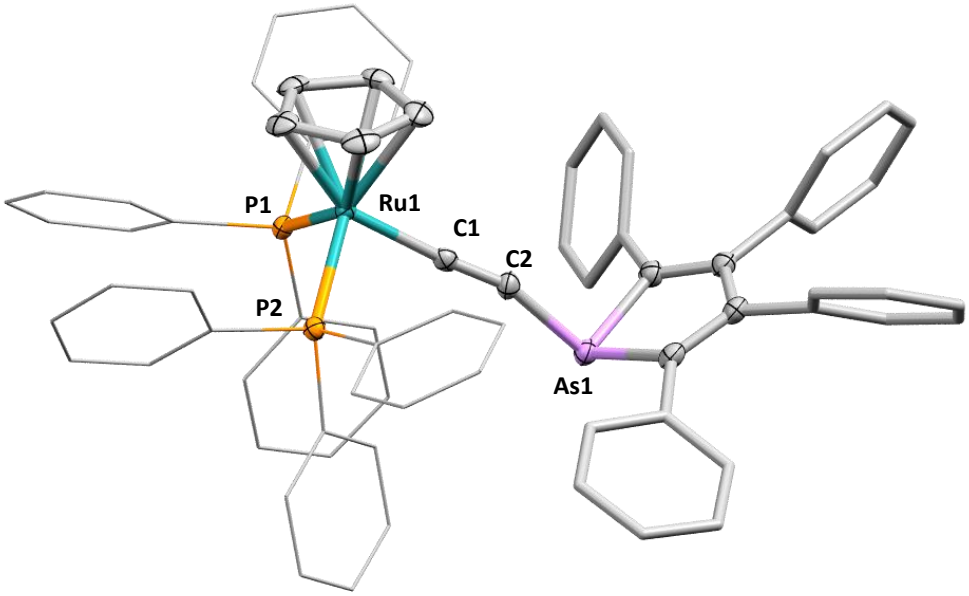



**Figure 2.18**: The molecular structure of $[Ru(C{\equiv}CAsC_4Ph_4)(PPh_3)_2(\eta^5\text{-}C_5H_5)]$ in a crystal. Phenyl groups simplified and hydrogen atoms omitted for clarity. Ellipsoids shown at 50% displacement.

The expected β-arsolylalkynyl is found, and the three-legged piano stool configuration of the Ru(II) centre is retained from that of the vinylidene in **Figure 2.15**.‡ Some considerable structural changes take

* Proton transfer to and from carbon (and transition metals) is accompanied by a geometrical change (here $C_\beta$ from $sp \rightarrow sp^2$) and is typically slower than to heteroatoms bearing 'lone' pairs of electrons (here arsenic $sp^3 \rightarrow sp^3$) that may be protonated rapidly without the need for geometrical rearrangement. Thus, while the ultimate *thermodynamic* site of protonation will reflect the C–H ($sp^2$ *ca* 460 kJmol$^{-1}$) *vs* As–H (*ca* 270 kJmol$^{-1}$) bond enthalpies, this may mask alternative sites of rapid but reversible *kinetic* protonation.

† As a potent π-acceptor, mixing of excited (MLCT) states will contribute to the paramagnetic shielding tensor leading to dramatic shifts to high frequency. The σ-alkynyl ligand is however a rather modest π-acceptor and accordingly the chemical shifts of the alkynyl carbon nuclei are not far removed from those of conventional alkynes.

‡ The CSD includes 131 reports of alkynyls of the form $(\eta^5\text{-}C_5R_5)(PPh_3)_2RuC{\equiv}CX$ (R = H, Me) though none involve hetero-atomic substituents, other than silyl, bound to the alkyne terminus. The heteroatom-functionalised alkynyls $[Ru(C{\equiv}CF)(dppe)(\eta^5\text{-}C_5Me_5)]^+$,

place upon formation of the alkynyl ligand, however, with an elongation of the Ru1-C1 bond to 2.014(2) Å and a compression of the C1-C2 and C2-As1 distances to 1.215(3) and 1.880(2) Å, all of which are consistent with the expected Ru-C, C≡C and C(*sp*)-As linkage. The alkynyl bends at C1 by *ca* 5° and at C2 by *ca* 18° permitting the arsole pendant (horizontally disposed in the solid state) to bow away from the cyclopentadienyl ligand, although the unit cell (triclinic *P*-1) contains a pair of molecules which are mutually-oriented such that the $AsC_4Ph_4$ residues are facing one another, and this slight flexing of the hydrocarbon spine is therefore likely intermolecular and steric in origin. The conversion from a π-acidic vinylidene to π-neutral alkynyl relieves the Ru(II) centre of the associated electronic tariff such that both the Ru-centroid and mean Ru-P distances contract from 1.93 and 2.35 Å in the vinylidene, respectively, to 1.88 and 2.28 Å in the alkynyl as the basicity of the metal centre is augmented. Distances within the arsole ring are crystallographically indistinct between the two complexes, however, and are unremarkable among $AsC_4Ph_4$ residues throughout this work: As-$C_\alpha$ (mean 1.948(3) Å), $C_\alpha$=$C_\beta$ (mean 1.355(3) Å) and $C_\beta$-$C_\beta$ (1.492(3) Å).

[Ru(C≡CAs$C_4Ph_4$)$(PPh_3)_2(\eta^5$-$C_5H_5)$] could be protonated at $C_\beta$ *via* the agency of $HOSO_2CF_3$ or $HBF_4$·$Et_2O$ in $Et_2O$ solution to regenerate the vinylidene encountered previously, though the materials afforded could be not be obtained in an analytically pure forms, especially the triflate salt which appeared to have limited shelf-life and slowly degraded to oily brown residues in both solution and solid state.

### 2.7.4 Attempted synthesis of [Ru(=C=C=C=CHAs$C_4Ph_4$)$(PPh_3)_2(\eta^5$-$C_5H_5)$]$PF_6$

Following the successful preparation(s) of a vinylidene complex *via* tautomerisation of HC≡CAs$C_4Ph_4$ by Ru(II), it was of interest to investigate whether an ambitious (ultimate albeit not concerted) 1,4-H shift could occur with HC≡CC≡CAs$C_4Ph_4$ to afford a cationic ω-arsolylbutatrienylidene* [Ru(=C=C=C=CHAs$C_4Ph_4$)$(PPh_3)_2(\eta^5$-$C_5H_5)$]$^+$, or alternatively a β-alkynylvinylidene. Butatrienylidene complexes have a visible paucity amongst the metallacumulene family for reasons which will become apparent in forthcoming discussions, although some have nevertheless proven amenable to isolation.[116-118]

[Ru(C≡Cl)(dppe)$(\eta^5$-$C_5Me_5)$]$^+$, and [Ru(C≡CS-*n*-hex)$_2$(dppe)$_2$] have however been described and provide the only structural data for ruthenium alkynyls bearing positively mesomeric heteroatom alkynyl substituents. See L. M. Hall, D. P. Tew, N. E. Pridmore, A. C. Whitwood, J. M. Lynam, J. M. Slattery *Angew. Chem. Int. Ed.*, **2017**, *56*, 7551, M. I. Bruce, M. Jervic, C. R. Parker, W. Patalinghug, B. W. Skelton, A. H. White, N. N. Zaitseva *J. Organomet. Chem.* **2008**, *693*, 2915 and A. Yashiro, Y. Tanaka, T. Tada, S. Fujii, T. Nishino, M. Akita *Chem. Eur. J.* **2021**, *27*, 9666.

* ω is deliberately used here to denote the fourth carbon atom in the chain instead of δ (the fourth letter of the Greek alphabet) to avoid any potential confusion, since the latter is also used in this section to express chemical shifts.

The combination of one equivalent each $[Ru(THF)(PPh_3)_2(\eta^5\text{-}C_5H_5)]PF_6$ and $HC{\equiv}CC{\equiv}CAsC_4Ph_4$ in $CH_2Cl_2$ solution afforded a dark yellow-brown suspension after stirring overnight at ambient temperature. A filtered aliquot taken for $^{31}P\{^1H\}$ NMR analysis ($CD_2Cl_2$) finds a plethora of phosphorus signals and the $^1H$ spectrum was devoid of any conspicuous resonances which could be ascribed to a cumulenic hydrogen, and although both reagents were consumed no fewer than six cyclopentadienyl environments were present. Proceeding under the presumption that perhaps the target butatrienylidene $[Ru(=C=C=C=CHAsC_4Ph_4)(PPh_3)_2(\eta^5\text{-}C_5H_5)]^+$ *had* formed but was of limited kinetic stability, the butadiynyl arsole was added to a stirred mixture of $[Ru(THF)(PPh_3)_2(\eta^5\text{-}C_5H_5)]PF_6$ and DBU in $CH_2Cl_2$. The intention was to immediately deprotonate the butatrienylidene upon formation to the corresponding neutral butadiynyl $[Ru(C{\equiv}CC{\equiv}CAsC_4Ph_4)(PPh_3)_2(\eta^5\text{-}C_5H_5)]$, which was hoped to constitute a condition of attenuated lability. Instead, the same yellow-brown suspension was obtained, exhibiting congested $^1H$ and $^{31}P\{^1H\}$ NMR spectra.

Column chromatography of both reaction mixtures (separately) afforded bright yellow bands as the only mobile and isolable compounds which proved to be identical materials. The $^{31}P\{^1H\}$ spectrum reveals a singlet at 51.3 ppm and a lone cyclopentadienyl resonance is found at 4.00 ppm in the $^1H$ spectrum (the same signals were also observed in the crude reaction mixtures though were not predominant amongst the slew of other products). The $^{13}C\{^1H\}$ NMR spectrum was initially confounding since no characteristic arsole ring-carbon signals near *ca* 150 ppm, and no signals near or below *ca* 100 ppm for a $C{\equiv}CC{\equiv}C$ linkage were identified, although a conspicuous triplet at 143.6 ppm ($J_{PC}$ = 24.9 Hz) and singlets at 114.2 and 86.0 ppm (the latter for the cyclopentadienyl ring) were observed. High-resolution mass spectrometry confirmed the presence of ruthenium within the isolated specimen,* though was not initially enlightening with regards to the identity of the compound. Single crystals were obtained from $CH_2Cl_2$/*n*-hexane at 20 °C and X-ray diffraction revealed the molecule to be the tetraphenylarylalkynyl $[Ru(C{\equiv}CC_6HPh_4)(PPh_3)_2(\eta^5\text{-}C_5H_5)]$ *sans* arsenic. The crystal structure is shown in **Figure 2.19**.

* Ruthenium contains seven naturally occurring isotopes which renders visual identification of the relevant molecular ions a straightforward task: $^{96}Ru$ (5.54% abundant), $^{98}Ru$ (1.87%), $^{99}Ru$ (12.8%), $^{100}Ru$ (17.1%), $^{102}Ru$ (31.6%), $^{104}Ru$ (18.6%). The presence or absence of arsenic is less obvious since, while possessing 33 known isotopes, only $^{75}As$ is stable and accordingly naturally occurring arsenic is considered monoisotopic.

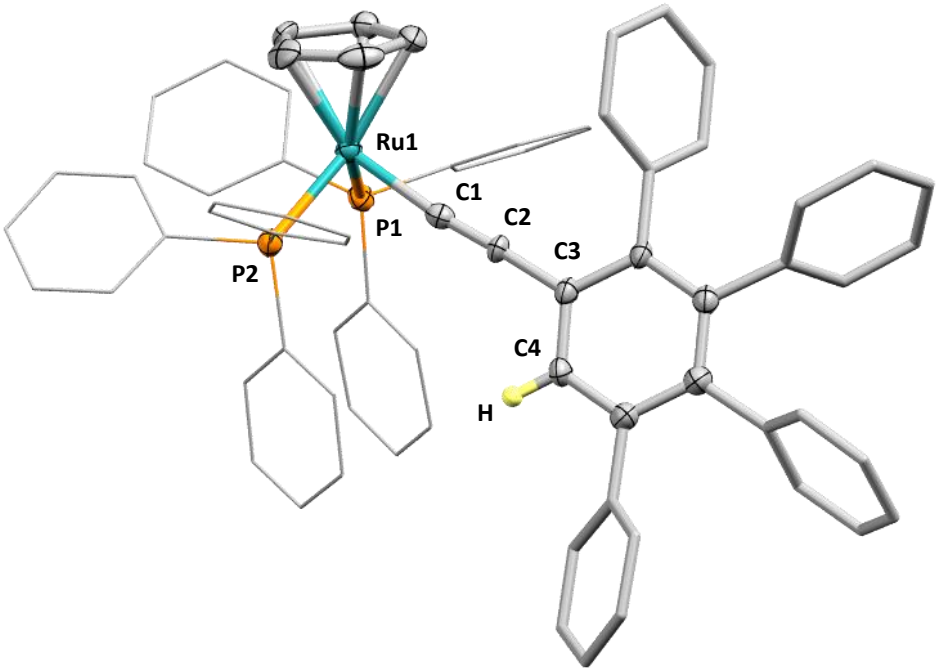



**Figure 2.19**: The molecular structure of $[Ru(C{\equiv}CC_6HPh_4)(PPh_3)_2(\eta^5\text{-}C_5H_5)]2{\cdot}CH_2Cl_2$ in a crystal. Phenyl groups simplified and dichloromethane solvate molecules and hydrogen atoms omitted for clarity, except the arylalkynyl hydrogen which is shown in light yellow for distinction. Ellipsoids shown at 50% displacement.

The complex has evidently undergone elimination of the arsenic atom with coincident insertion of the butadiynyl γ- and ω-carbon atoms into the (former) arsole affording a six-membered aromatic ring; mechanistic conjecture for this unusual transformation are discussed below. The overall molecular configuration is analogous to that of the other alkynyl complex previously discussed (**Figure 2.18**) with Ru-C and C≡C bond lengths of 2.000(6) and 1.193(8) Å, respectively, while the C2-C3 single bond of 1.446(8) Å is unremarkable. Distances within the principal aromatic ring are crystallographically indistinguishable from one another despite the irregular substitution pattern, falling in the range 1.39—1.40 Å. The alkynyl spine is closer to ideal linearity than the β-arsolylalkynyl, bending by *ca* 6° at C1 and *ca* 3° at C2.

The isolation of $[Ru(C{\equiv}CC_6HPh_4)(PPh_3)_2(\eta^5\text{-}C_5H_5)]$ from reaction mixtures of $HC{\equiv}CC{\equiv}CAsC_4Ph_4$ and $[Ru(THF)(PPh_3)_2(\eta^5\text{-}C_5H_5)]PF_6$ was reproducible though isolated yields were variable. The fate of the arsenic atom undoubtedly rests amongst the numerous chromatographically-immobile materials formed in the reaction – the deposition of insoluble dark grey solids might be suggestive of elemental arsenic, though the residue was not analysed. A plausible mechanism for generation of the β-arylalkynyl ligand can be entertained and is shown in **Scheme 2.22**, which begins from the intended cationic

butatrienylidene **A** and is emblematic of the striating electrophilicity and nucleophilicity of odd- and even-numbered carbon atoms (respectively) within metallacumulenic chains.[33, 113] To this end, atom-condensed FUKUI indices for the Ru=C=C=C=C-As chain constituents within the model complex $[Ru(=C=C=C=CHAsC_4H_4)(PH_3)_2(\eta^5\text{-}C_5H_5)]^+$ were calculated. A brief overview of the concept is first in order, since it is less frequently applied to organo-transition metal complexes than simple unsaturated organic systems. The FUKUI function* formally describes the tendency of atoms to either gain or lose an electron, though in a simplified context serves as a regioselective prediction as to which atoms within a molecule nucleophilic or electrophilic attack is more likely to occur.[119, 120] For the case of nucleophilic attack, the function may be given by the expression:

$$f_k^+ = q_k(N) - q_k(N+1)$$

Where $f_k^+$ is the atom-condensed FUKUI index for an atom $k$, $q_k$ is its electronic charge and $N$ is the number of electrons. In essence, the appetite for nucleophilic attack is evaluated by the difference in electrostatic potentials between atoms in their primal ($q_k(N)$) and reduced forms ($q_k(N+1)$) *i.e.*, $[Ru(=C=C=C=CHAsC_4H_4)(PH_3)_2(\eta^5\text{-}C_5H_5)]^+$ and $[Ru(=C=C=C=CHAsC_4H_4)(PH_3)_2(\eta^5\text{-}C_5H_5)]^0$, respectively. The indices provide an indication of whether the regioselectivity of reaction is dictated primarily by charge *i.e.*, a "hard" reaction (minimal value of $f_k^+$) or frontier orbital control i.e., a "soft" reaction (maximal value of $f_k^+$).[121] In general, the greater (more positive) the value of $f_k^+$ the more reactive the atom of interest $k$ is toward attack by nucleophiles. The concept has been successfully deployed in a variety of organic[122-126] and inorganic[127, 128] settings and the *qualitative* utility appears robust. The equilibrium geometry of $[Ru(=C=C=C=CHAsC_4H_4)(PH_3)_2(\eta^5\text{-}C_5H_5)]^+$ was determined using DFT in the gas phase at the ωB97X-D/6-31G*/LAN2Dζ level of theory, shown in **Figure 2.20**. Fixed atom coordinates were then used to calculate the Natural Population charges of the cation and its singly reduced counterpart. Aside from being basis-set dependant,[129] it is important that the molecular configuration remains static when deducting/adding an electron since re-optimising the geometry allows the model to "relax" and therefore alter the electron density polarisation. Other nuances to the FUKUI function, including the contentious

* The concept is named after KENICHI FUKUI who shared the 1981 NOBEL prize in chemistry for theoretical works regarding frontier molecular orbital theory and the conservation of orbital symmetry during chemical reactions.

significance of negative values, are beyond the scope of this brief introduction and are discussed elsewhere.[127, 130-132] Condensed-to-atom FUKUI indices for those of interest are collated in **Table 2.1**, and a corroborating electrostatic potential contour map is in **Figure 2.20**.

**Table 2.1**: Atom-condensed FUKUI indices ($f_k^+$) for selected atoms within [Ru(=C=C=C=CHAsC$_4$H$_4$)(PH$_3$)$_2$($\eta^5$-C$_5$H$_5$)]$^+$. More-positive numbers indicate a greater susceptibility toward nucleophilic attack. $q_k$ denotes the Natural Population charge.

| | **Ru** | **$C_\alpha$** | **$C_\beta$** | **$C_\gamma$** | **$C_\omega$** | **As** |
|---|---|---|---|---|---|---|
| $q_k(N)$ | 0.234 | -0.027 | -0.315 | 0.214 | -0.584 | 1.001 |
| $q_k(N+1)$ | 0.204 | -0.234 | -0.285 | 0.019 | -0.615 | 0.890 |
| $f_k^+$ | 0.030 | 0.207 | -0.030* | 0.195 | 0.031 | 0.111 |

The $f_k^+$ values (and the electrostatic potential map in **Figure 2.20**) highlight the alternating electrophilic/nucleophilic character of the four-carbon chain. The greatest FUKUI indices are found at $C_\alpha$ and $C_\gamma$, though since the former is probably sheltered within the cone of influence of the PPh$_3$ ligands, the latter is expected to be the epicentre of nucleophilic attack since it is comparatively exposed. Conversely, $C_\beta$ and $C_\omega$ are predicted to be indifferent toward nucleophiles; one may expect their $f_k^-$ values to be the greatest within the chain *i.e.*, the regions for *electro*philic attack.† Interestingly, the arsenic atom – despite being shown in **Figure 2.20** as a site of appreciable electron density – also possesses a sizable $f_k^+$ parameter. This potential reactivity towards nucleophilic attack is by no means obvious from simple valence-bond depictions of the arsolyl but appears in some regards appropriate given the ambiphilic nature of this heteroatom observed experimentally. That is to say, the As(III) atom is both nucleophilic *and* prone to nucleophilic attack, two reciprocal behaviours which emerge at varying stages throughout this and forthcoming chapters.

* Though negative, this value is negligibly small and effectively zero.

† While these values might be of limited interest in the current context due to the overall positive charge of the complex deterring reactions with electrophiles, they would perhaps gain in utility for neutral examples of butatrienylidenes, for which a small number exist *e.g.*, [Mn{=C=C=C=C(SnR$_3$)$_2$}(dmpe)($\eta^5$-C$_5$H$_4$Me)] (R = Me, Ph), [W{=C=C=C=C(SnMe$_3$)$_2$}(CO)(dppe)$_2$], and [Ir(=C=C=C=CPh$_2$)Cl(P$^i$Pr$_3$)$_2$]. See K. VENKATESAN, O. BLACQUE, T. FOX, M. ALFONSO, H. W. SCHMALLE, H. BERKE *Organometallics,* **2004**, *23*, 4661, K. VENKATESAN, F. J. FERNANDEZ, O. BLACQUE, T. FOX, M. ALFONSO, H. W. SCHMALLE, H. BERKE *Chem. Comm.,* **2003**, *2006*, S. N. SEMENOV, O. BLACQUE, T. FOX, K. VENKATESAN, H. BERKE *Organometallics* **2010**, *29*, 6321, S. N. SEMENOV, O. BLACQUE, T. FOX, K. VENKATESAN, H. BERKE *Angew. Chem. Int. Ed.,* **2009**, *48*, 5203, and K. ILG, H. WERNER *Chem. Eur. J.*, **2002**, *8*, 2812.

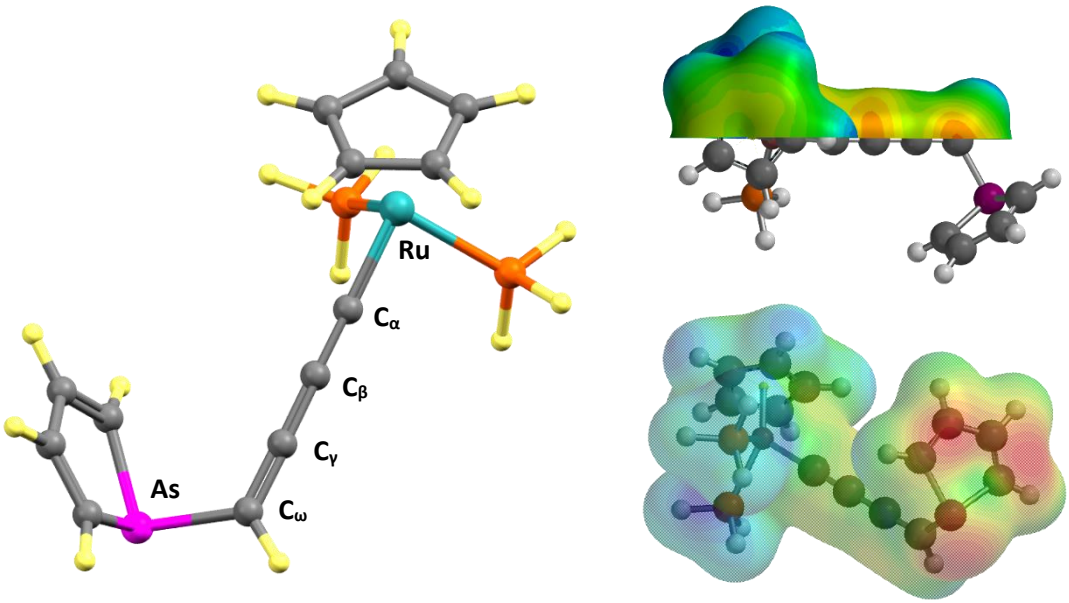



**Figure 2.20**: The DFT optimised geometry of the model butatrienylidene cation $[Ru(=C=C=C=CHAsC_4H_4)(PH_3)_2(\eta^5\text{-}C_5H_5)]^+$ (gas phase, ωB97X-D/6-31G*/LAN2DZ). **Inset**: Calculated electrostatic potential maps for the same model. Red contours correspond to areas of greater negative charge and *vice-versa* for blue contours.

The sequence outlined in **Scheme 2.22** is informed by the FUKUI indices above and previous observations made by BRUCE *et al.*[100, 101, 133] during their attempts to isolate $[Ru(=C=C=C=CHR)L_2(\eta^5\text{-}C_5H_5)]^+$ complexes, which also revert to σ-alkynyls (*inter alia*) in the presence of extraneous nucleophiles *e.g.*, reaction mixtures of $[Ru(THF)L_2(\eta^5\text{-}C_5H_5)]^+$ and HC≡CC≡CH in methanol ultimately yield $[Ru\{C\equiv CC(=O)Me\}L_2(\eta^5\text{-}C_5H_5)]$ *via* nucleophilic attack at $C_\gamma$ of the putative $[Ru(=C=C=C=CH_2)L_2(\eta^5\text{-}C_5H_5)]^+$ by the solvent (or, more likely, adventitious moisture). Other researchers' efforts have been frustrated (or exploited) by similar reactivity patterns.[134-138]

A 1,4-H shift of the terminal butadiynyl hydrogen (or successive 1,2 shifts *via* a β-ethynylvinylidene intermediate) mediated by the *d*⁶-Ru(II) centre provides the $[Ru(=C=C=C=CHAsC_4Ph_4)(PPh_3)_2(\eta^5\text{-}C_5H_5)]^+$ cation (**A**). The crystal structure of $[Ru(C\equiv CC_6HPh_4)(PPh_3)_2(\eta^5\text{-}C_5H_5)]$ shows that $C_\gamma$ (C3 in **Figure 2.19**) has undergone a bond-forming event with a carbon atom in the 2,5-position of the arsole ring – nucleophilic attack of the latter upon the former is invoked to account for this, mindful of the fact that such an action has *no documented precedent* within arsole chemistry aside from the sparse examples of [4+2] cycloadditions.[139, 140] Indeed, the HOMO of the model complex $[Ru(=C=C=C=CHAsC_4H_4)(PH_3)_2(\eta^5\text{-}C_5H_5)]^+$ (**Figure 2.21**) is calculated to have appreciable contributions from the arsole diene system, and

both the LUMO and the electrostatic potential map (and also, the FUKUI indices in **Table 2.1**) show $C_\alpha$ and $C_\gamma$ to be preferred sites for nucleophilic attack .

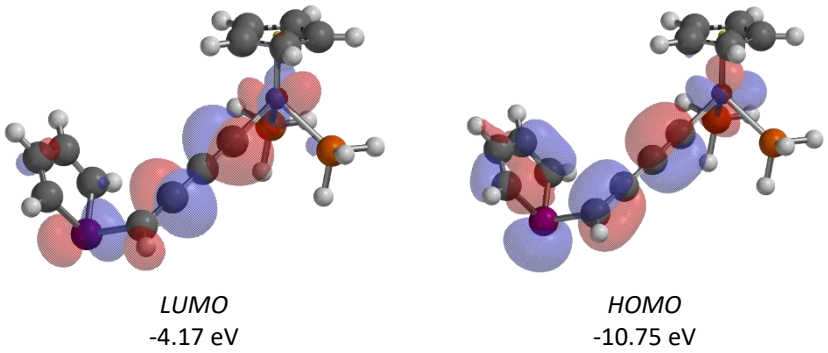
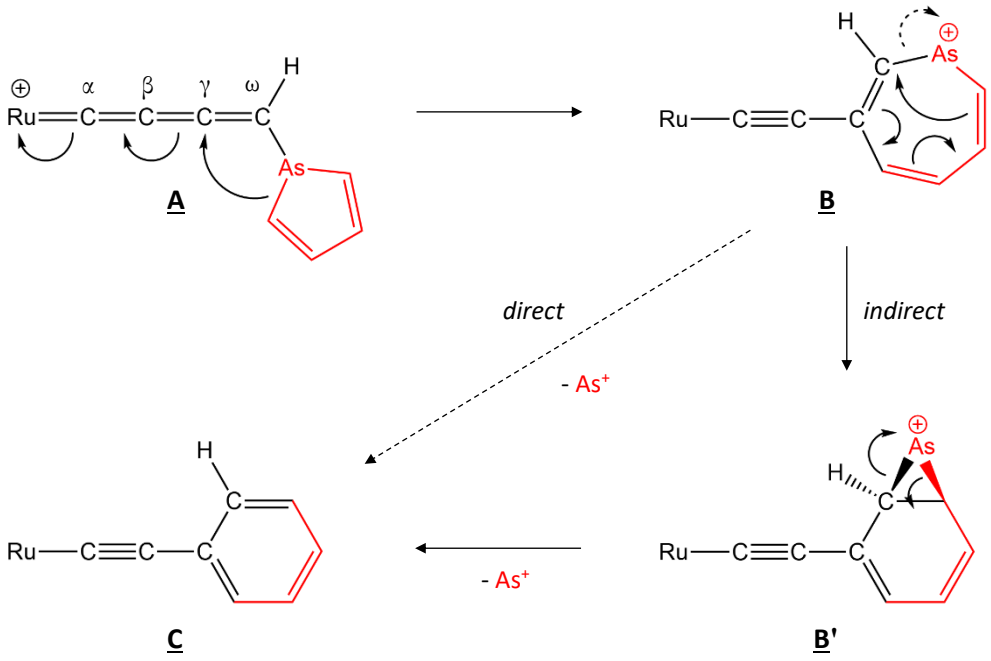



**Figure 2.21**: Calculated frontier orbitals of the model ω-arsolylbutatrienylidene $[Ru(=C=C=C=CHAsC_4H_4)(PH_3)_2(\eta^5\text{-}C_5H_5)]^+$ (DFT, gas phase; ωB97X-D/6-31G*/LAN2DZ).

Note in the DFT-optimised geometry of $[Ru(=C=C=C=CHAsC_4H_4)(PH_3)_2(\eta^5\text{-}C_5H_5)]^+$ (**Figure 2.20**) the posture of the arsole is poised for nucleophilic attack upon $C_\gamma$. It is recalled that the butadiynyl chain in $[RuH(C{\equiv}CC{\equiv}CAsC_4Ph_4)(CO)_2(PPh_3)_2]$ possessed appreciable curvature in the solid state (**Figure 2.13**). Whilst the flexibility of the Ru-C≡C-C≡C-As and Ru=C=C=C=CH-As linkages are by no means expected to be identical, the crystal structure of the above-mentioned hydrido-butadiynyl complex if nothing else demonstrates the pliability of extended unsaturated hydrocarbon chains; even a modest bending of the butatrienylidene spine could offer the nucleophilic arsole carbon sufficient opportunity to approach the electrophilic $C_\gamma$.




**Scheme 2.22**: Proposed mechanism for $[Ru(C{\equiv}CCHPh_4)(PPh_3)_2(\eta^5\text{-}C_5H_5)]$ formation from reaction mixtures containing $[Ru(THF)(PPh_3)_2(\eta^5\text{-}C_5H_5)]^+$ and $HC{\equiv}CC{\equiv}CAsC_4Ph_4$. Ancillary metal ligands and arsole substituents omitted for clarity.

A seven-membered cationic arsacycloheptatriene ring ("arsatropylium") **B** seems plausible and although neither the free molecule nor the corresponding neutral "arsapin" have been isolated to date, some annulated derivatives are known.[141-143] Their thermal stabilities are, however, very modest (*e.g.*, 3-phenyl-3-benzarsapin at 50 °C $t_{½}$ ≈ 240 s) and have been shown to decompose *via* extrusion of an arsenidene fragment* therein lending support to the mechanism proposed in **Scheme 2.22** for which formation of the aromatic system **C** is unquestionably the thermodynamic driving force. Whether ring contraction occurs by a concerted [1+2]-retroaddition directly from **B** or takes place *via* a cheleotropic rearrangement from the bicyclic valence isomer **B'** (an "arsanorcaradiene"†) cannot said with certainty. However, the latter is regularly computed to be a slightly more stable configuration for both neutral and cationic non-annulated arsepins[144, 145] and phosphapins,[146-148] with its formation most likely expedited by incipient homoaromatic bonding between the methyne units bound to arsenic. It is therefore plausible that **B'** is a transient *en route* to the arylalkynyl complex isolated, though the outcome is otherwise the same. Equilibrium geometries for **A**, **B**, **B'** and **C** (simplified versions) were calculated using DFT (gas phase:

* Benzarsapins, for example, afford naphthalene derivatives upon decomposition.
† Whist no isolable examples have been reported to date, a phosphanorcaradiene has been intercepted and characterised. See L.L. LIU, J. ZHOU, R. ANDREWS and D.W. STEPHAN *J. Am. Chem. Soc.*, **2018**, *140*, 7466—7470.

ωB97X-D/6-31G*/LAN2DζΖ), and their relative GIBBS free energies (with **A** taken as the "baseline") are shown alongside in **Figure 2.22**. The reaction is exergonic overall.*

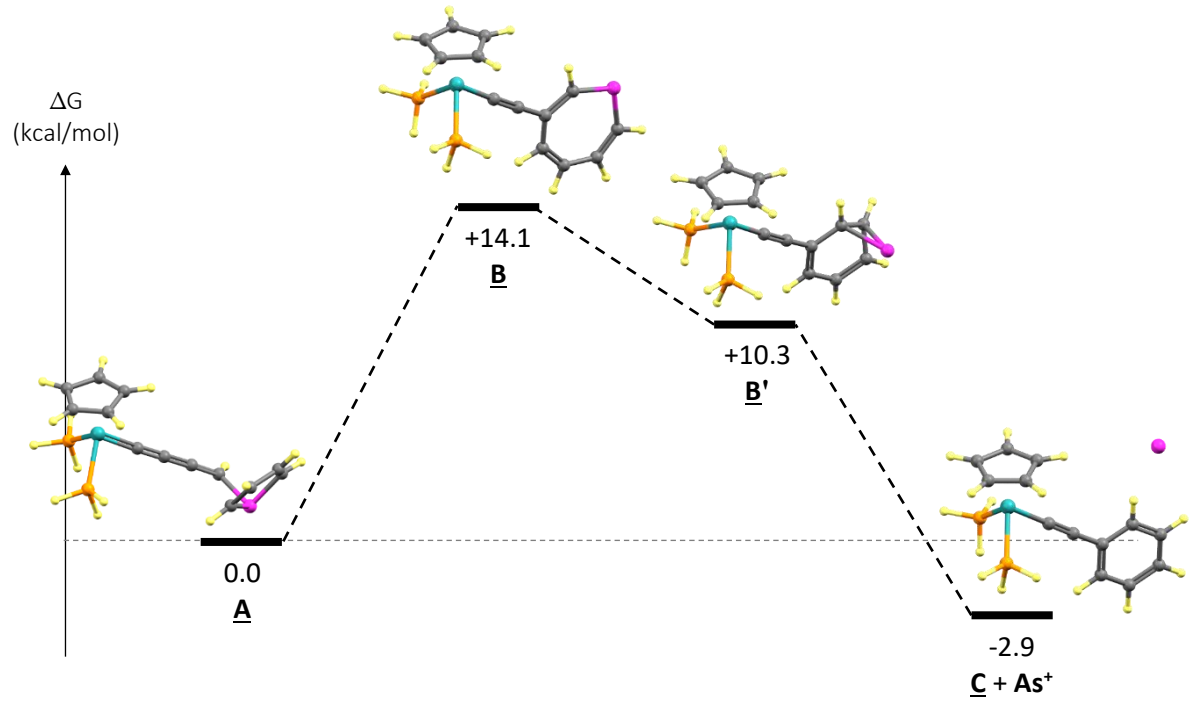



**Figure 2.22**: Optimised geometries and relative GIBBS free energies (in kcal/mol, at 298.15 K) for the simplified reaction intermediates during the ω-arsolylbutatrienylidene → arylacetylide ligand transformation, using DFT in the gas phase at the ωB97X-D/6-31G*/LAN2DζΖ level of theory. The ordinate axis is approximately to scale. Transition states were not modelled.

## 2.8 Reactions with $[Co_2(CO)_8]$

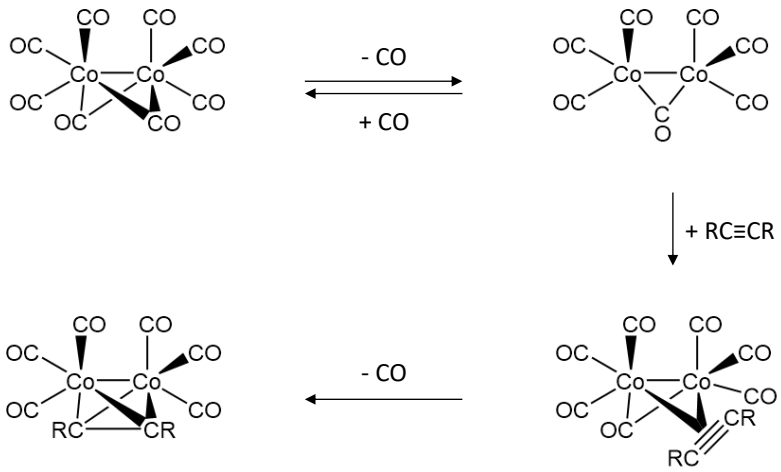
The homoleptic binuclear reagent $[Co_2(CO)_8]$ readily and reliably adds, with liberation of two equivalents of carbon monoxide, across a variety of acetylenic groups to provide dicobalt-tetrahedrane complexes of the general formula $[Co_2(\mu\text{-}\eta^2\text{:}\eta^2\text{-}RC{\equiv}CR)(CO)_6]$ wherein the alkyne bridges both cobalt(0) centres simultaneously.[149] Whereas the unsubstituted $[Co_2(CO)_8]$ is rather active in solution, such alkyne complexes are appreciably more stable and – particularly so in organic settings – the $Co_2(CO)_6$ motif often serves as a convenient protecting group for the alkyne during transformations of any peripheral groups,† which may however also take direct part in C-C bond forming processes *e.g.*, the celebrated PAUSON-KHAND

* Whilst elimination of an $As^+$ cation might seem implausible, there now exist many examples of 1,3,2-diphospharsolane-1,3-diimu-2-ide salts of the form $[R_3PAsPR_3]^+$ such that the ultimate fate of the missing arsenic atom may well be $[Ph_3P{=}As{=}PPh_3]PF_6$, formation of which would contribute favourably to the overall thermodynamics of the process. See J. F. BINDER, S. C. KOSNIK, P. BLAKE J. ST ONGE, C. L. B. MACDONALD *Chem. Eur. J.* **2018**, *24*, 14644, J. ZHOU, L. L. LIU, L. L. CAO, D. W. STEPHAN, *Angew. Chem. Int. Ed.*, **2019**, *58*, 5407.

† See K.M. NICHOLAS *Acc. Chem. Res.*, **1987**, *20*, 207—214 for an illustrative example.

reaction.[150, 151] The affinity for which the $[Co_2(CO)_8]$ molecule displays toward alkynes is enunciated in the observation that donor functions decorating the alkyne are usually disregarded in favour of the $\mu$-$\eta^2$:$\eta^2$-coordination mode: treatment of the bis(phosphino)acetylene $Ph_2PC{\equiv}CPPh_2$ with $[Co_2(CO)_8]$ results purely and preferentially in alkyne complexation,[152] and it is only possible to incorporate the pendant phosphine functions with further equivalents of this or other metal reagents.[153]

The mechanism of adduct formation has been studied and is generally believed to follow a stepwise course involving (reversible) dissociation of $[Co_2(CO)_8]$ to $[Co_2(CO)_7]$ and CO in solution,[154] ensuing alkyne attachment giving the intermediary $[Co_2(\mu\text{-}RC{\equiv}CR)(\mu\text{-}CO)(CO)_6]$[155] and finally additional CO release (**Scheme 2.23**); there is evidently little overall rate-dependence on the concentration or properties of the incoming alkyne with regards to formation of $[Co_2(\mu\text{-}RC{\equiv}CR)(\mu\text{-}CO)(CO)_6]$, however the reaction is unequivocally first-order with respect to $[Co_2(CO)_8]$ and inversely first order for [CO] which support a dissociative (*i.e.*, $S_N1$-like) process.[156] This contrasts with the reaction between $[Co_2(CO)_8]$ and tertiary phosphines which generally follow associative ($S_N2$-like) processes at the cobalt centre(s).[157] The electronic and steric characteristics of the incoming alkyne do appear to play a subtle role in expulsion of the *second* CO molecule, with faster hexacarbonyl adduct formation being measured for substrates with generally superior $\pi$-acidity and/or increased steric encumbrance.[158, 159]

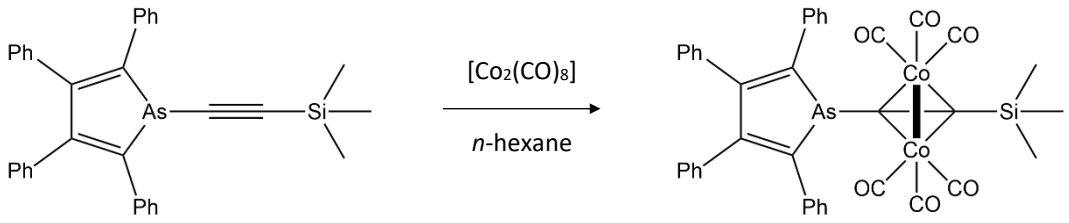



**Scheme 2.23**: Accepted dissociative pathway for the formation of adducts between $[Co_2(CO)_8]$ and alkynes.

### 2.8.1 Synthesis of $[Co_2(\mu\text{-}\eta^2\text{:}\eta^2\text{-}Me_3SiC{\equiv}CAsC_4Ph_4)(CO)_6]$

It was noted in **Section 2.2.2** that single crystals of $Me_3SiC{\equiv}CAsC_4Ph_4$ have remained elusive while the desire for unequivocal identification *via* X-ray diffractometry persisted. Accordingly, the ethynyl arsole was converted to its dicobalt hexacarbonyl adduct which it was hoped would be more amenable to crystal growth. The only structural data available for arsenic-substituted dicobalt-tetrahedranes are the hexanuclear $As\{C{\equiv}CH{\cdot}Co_2(CO)_6\}_3$ and tetrametallic $PhC{\equiv}CAs\{C{\equiv}CPh{\cdot}Co_2(CO)_6\}_2$ assemblies.[160, 161]

Thus, $Me_3SiC{\equiv}CAsC_4Ph_4$ and an excess of $[Co_2(CO)_8]$ were combined in *n*-hexane solution which resulted in rapid gas evolution and the formation of an orange-red mixture. Column chromatography provides the expected $[Co_2(\mu\text{-}\eta^2\text{:}\eta^2\text{-}Me_3SiC{\equiv}CAsC_4Ph_4)(CO)_6]$ as a reasonably air stable red-brown solid in good yield. Notably, whereas the parent alkyne is prone to desilylation upon contact with moisture, the dicobalt adduct exhibited no such vulnerability and the silyl group was seemingly indelible: high-resolution mass spectrometry yielded the molecular ion in contrast to the free alkyne from which it was cleaved.




**Scheme 2.24**: Synthesis of $[Co_2(\mu\text{-}\eta^2\text{:}\eta^2\text{-}Me_3SiC{\equiv}CAsC_4Ph_4)(CO)_6]$.

The solution IR spectrum (*n*-hexane) of the product displays four $\nu_{CO}$ vibrations at 2085(s), 2049(vs), 2026(vs) and 2017(s) $cm^{-1}$ which compare favourably to other unsymmetrical alkyne complexes (*cf.* $[Co_2(\mu\text{-}\eta^2\text{:}\eta^2\text{-}HC{\equiv}CPh)(CO)_6]$[162] $\nu_{CO}$ 2094(s), 2057(vs), 2032(vs), 2027(vs) $cm^{-1}$; $[Co_2(\mu\text{-}\eta^2\text{:}\eta^2\text{-}HC{\equiv}CC_6F_5)(CO)_6]$[163] $\nu_{CO}$ 2098(s), 2061(vs), 2040(vs), 2031(vs) $cm^{-1}$), and in the $^1H$ NMR spectrum ($C_6D_6$) the $SiMe_3$ group is found at 0.04 ppm, only marginally displaced from the free alkyne (0.01 ppm). In the $^{13}C\{^1H\}$ spectrum, a single broad peak is found at 200.3 ppm for the collective of carbonyl ligands which are likely undergoing positional exchange (in addition to the quadrupolar nature of $^{59}Co$ nuclei; $I = 7/2$), and the coordinated ethynyl carbon signals appear at 99.6 (*As*-bound) and 91.9 (*Si*-bound) ppm, being *ca*

10—15 ppm upfield of the same in the free alkyne (**Section 2.2.2**). Single crystals were obtained from *n*-pentane solution at -20 °C and the crystal structure is shown in **Figure 2.23**.

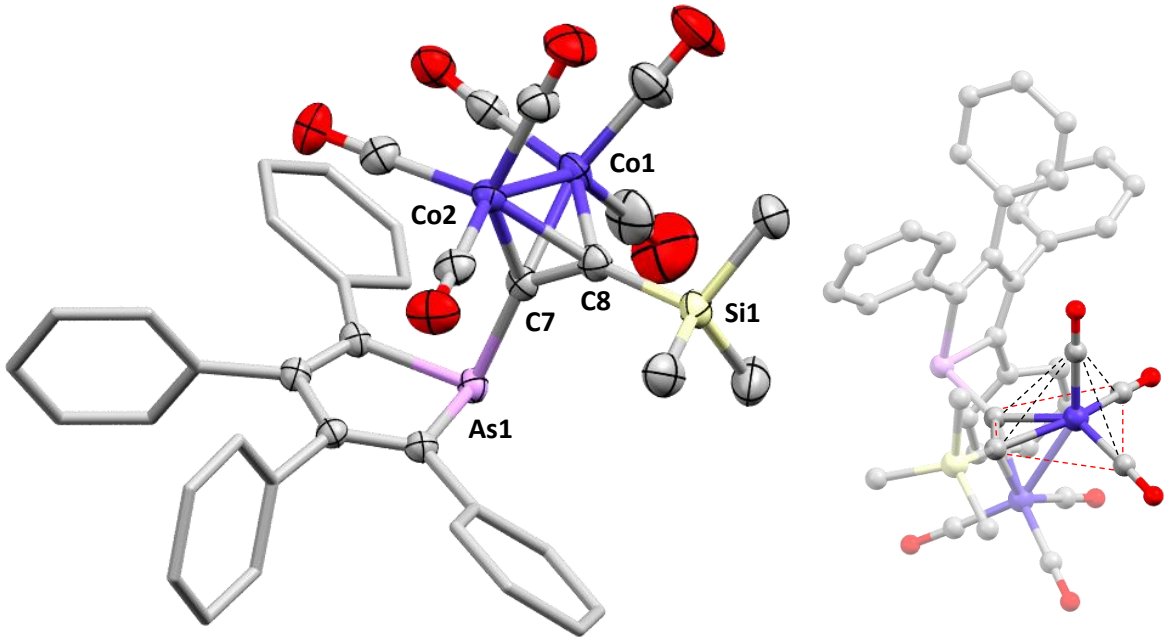



**Figure 2.23**: The molecular structure of $[Co_2(\mu\text{-}\eta^2\text{:}\eta^2\text{-}Me_3SiC{\equiv}CAsC_4Ph_4)(CO)_6]$ in a crystal. Phenyl groups simplified and hydrogen atoms omitted for clarity. Ellipsoids shown at 50% displacement. **Inset**: Abbreviated perspective of the molecule highlighting the square-based pyramidal geometry of the Co(0) centre(s). The *quasi*-basal plane is shown in red.

The expected dicobalt adduct was found, which also served to confirm identity of the free alkynyl arsole ligand. Incidentally, this specimen crystallised in the rhombohedral trigonal space group *R*-3*c* which is noteworthy for no other reason than it is generally uncommon for organometallic/inorganic complexes to crystallise in lattices of three-fold symmetry.* The structural topology of the $Co_2(CO)_6$ unit reflects the bridged $C_{2v}$ isomer of $[Co_2(CO)_8]$ (**Chapter 3**, **Section 3.2**) comprising a pair of deformed, edge-sharing square-based pyramids (Co1 $\tau_5$ = 0.16; Co2 $\tau_5$ = 0.15) with a formal Co-Co "bond" of 2.4717(8) Å that falls in the 2.45—2.49 Å range measured for other structurally characterised dicobalt hexacarbonyl alkyne complexes,[164-166] which are themselves somewhat shorter than the same metric of 2.5293(8) Å in the parent $[Co_2(CO)_8]$.[167] The pair of ethynyl carbon atoms and pair of cobalt atoms comprise an irregular tetrahedron

* A statistical analysis of the >1.2 million structures indexed in the CSD, provided by the Cambridge Crystallographic Database Centre up to the 1st of January 2023, finds *R*-3*c* to be the 24th most-common space group accounting for *ca* 2200 data sets, or 0.18% of all structures. Considering that there are 230 space groups, this places *R*-3*c* in the 90th percentile which outwardly seems impressive until it is seen that monoclinic $P2_1/c$ alone accounts for >34% of all deposited structures, and the ten most-frequent space groups comprise >87% of the entire database.

with the $Me_3SiC{\equiv}CAsC_4Ph_4$ bond lying 1.39 Å above and perpendicular to the intermetallic vector, and a mean Co-C(*sp*) bond of 1.982(4) Å. This latter measurement is somewhat asinine since individual distances from the Co(0) centres to the ethynyl carbon atoms are, on average, longer for those to the silyl terminus: the Co-C7 bonds (mean 1.966(4) Å) are crystallographically distinct from the Co-C8 bonds (mean 1.997(3) Å) and the difference (~6 e.s.d.) is statistically significant within the precision limits of the data. This is attributed to the $AsC_4Ph_4$ group which sterically encumbering in only two dimensions being relatively flat cf. the more conical protuberance of the $SiMe_3$ group, permitting slightly closer approach of the $Co_2(CO)_6$ moiety to the former. As predicted by the DEWAR-CHATT-DUNCANSON model for side-bound olefinic ligands,[168] the C7-C8 bond of 1.341(5) Å in $[Co_2(\mu\text{-}\eta^2{:}\eta^2\text{-}Me_3SiC{\equiv}CAsC_4Ph_4)(CO)_6]$ is far longer than the triple bond in the reference compound $HC{\equiv}CAsC_4Ph_4$ (1.180(3) Å, accompanied by a deflection of the peripheral angles from linearity by *ca* 40°) falling comfortably within the domain expected for a bond order of 2 (*cf.* 1.36 Å for the diene C=C bonds within the arsole ring which serve as a convenient "internal standard").

Crystallographically, the assertion in these $[Co_2(\mu\text{-}\eta^2{:}\eta^2\text{-}RC{\equiv}CR)(CO)_6]$ complexes is that the acetylenic motif retains some multiple bond character during coordination. The bonding situation as drawn in **Scheme 2.24** – although capturing the salient geometric features of the cobalt centre(s) – is not wholly representative of reality and an alternative depiction has been proposed which accounts for the apparent double bond character observed crystallographically; these are illustrated in **Figure 2.24**.

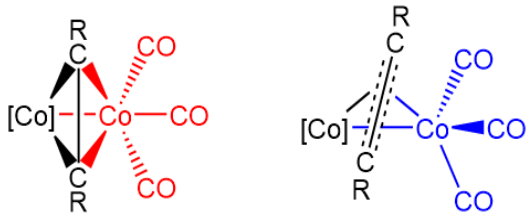



**Figure 2.24**: Complimentary bonding descriptions of π-alkyne adducts of $Co_2(CO)_6$; [Co] = $Co(CO)_3$.

In model **A**, as is typically drawn for such complexes, the metal centre(s) can be viewed in a distorted octahedral $sp^3d^2$ environment (red highlight). If the alkyne is considered a bidentate ligand, the

two orthogonal π orbitals attended by the C≡C bond separately donate a pair of electrons to each cobalt atom affecting a $sp \rightarrow sp^3$ re-hybridisation of the acetylenic carbon atoms – a bonding description which necessarily demands a carbon-carbon single bond and tetrahedral angles thereabout. This valence-bond perspective cannot account for the observed double bond character and trigonal geometry of the coordinated alkyne; a molecular orbital treatment, which has previously been applied to other [$Co_2(\mu\text{-}\eta^2\text{:}\eta^2\text{-}RC{\equiv}CR)(CO)_6$] complexes,[169] is required for more sophisticated explanation. In the meantime, it is noted that at the ωB97X-D/6-31G* level of DFT, LÖWDIN bond orders of 0.55 and 1.67 are derived for the Co-Co, C-C and mean Co-C bonds of the parent [$Co_2(\mu\text{-}\eta^2\text{:}\eta^2\text{-}HC{\equiv}CH)(CO)_6$].

In model **B**, the geometry about each cobalt centre is a distorted tetragonal pyramid (blue highlight). The hybridisation state of each metal remains $sp^3d^2$ and one of the hybrid orbitals (each) is directed toward the midpoint of the C≡C bond forming a trigonal plane (rather than a tetrahedron) containing the $Co_2$ pedestal; this provides a pair of mutually orthogonal three-centre two-electron bonds between the coordinated alkyne and each cobalt atom, as shown by HOFFMANN.[170] Accordingly, this description satisfies that the ethynyl group acts only as a *two*-electron ligand and will therefore possess the approximate double bond character observed crystallographically.

### 2.8.2 Synthesis of [$Co_2(\mu\text{-}\eta^2\text{:}\eta^2\text{-}HC{\equiv}CAsC_4Ph_4)(CO)_6$]

The analogous dicobalt adduct of $HC{\equiv}CAsC_4Ph_4$ was prepared similarly by treatment with one equivalent of [$Co_2(CO)_8$] in $Et_2O$ solution. The dark red [$Co_2(\mu\text{-}\eta^2\text{:}\eta^2\text{-}HC{\equiv}CAsC_4Ph_4)(CO)_6$] was isolated after column chromatography in high yield and large single crystals were obtained from *n*-pentane solution at -20 °C; the molecular structure is shown in **Figure 2.25**. The terminal ethynyl hydrogen nucleus provides a resonance at 5.73 ppm in the $^1H$ NMR spectrum ($C_6D_6$) which manifests some 3 ppm downfield from the corresponding resonance in the free ligand (2.78 ppm). The $^{13}C\{^1H\}$ NMR spectrum finds the ethynyl carbon resonances at 85.4 and 84.3 ppm, the latter identified as the terminal atom by way of an HSQC NMR experiment. The arsole ring carbon signals are rather close together at 150.5 and 150.2 ppm with a broad peak at 199.7 ppm for the six carbonyl ligands that are chemically equivalent on the $^{13}C$ NMR timescale. Four $\nu_{CO}$ absorptions are measured in the solution IR spectrum (*n*-hexane) at 2092(s), 2055(vs), 2032(vs) and 2024(vs) $cm^{-1}$.

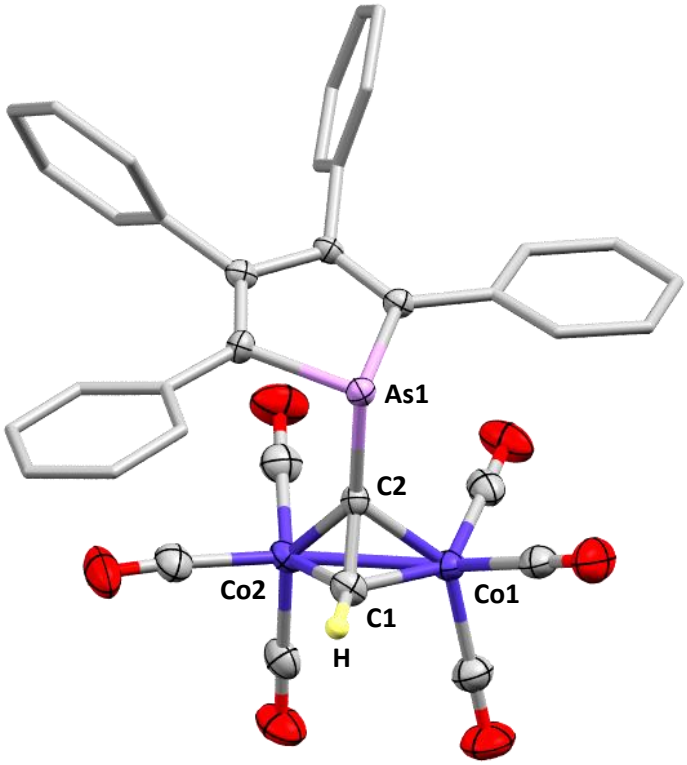
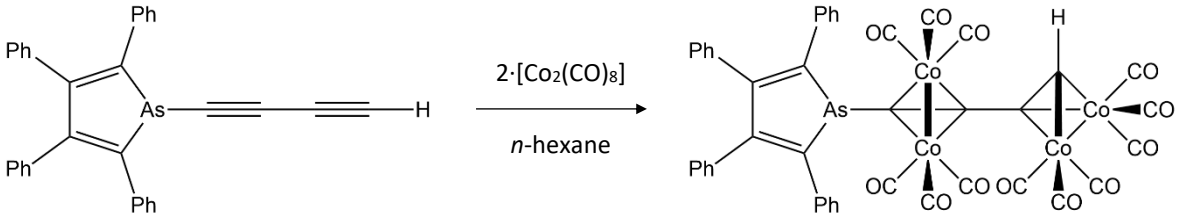



**Figure 2.25**: The molecular structure of $[Co_2(\mu\text{-}\eta^2\text{:}\eta^2\text{-}HC{\equiv}CAsC_4Ph_4)(CO)_6]\cdot 0.5C_5H_{12}$ in a crystal. Phenyl groups simplified and *n*-pentane solvate molecule and hydrogen atoms omitted for clarity, except for the ethynyl hydrogen which is shown in light yellow for emphasis. Ellipsoids shown at 50% displacement. Only one of the crystallographically unique molecules contained within the asymmetric unit (space group *P*-1) is shown.

The asymmetric unit of the crystal contains two crystallographically independent molecules which have virtually identical solid-state configurations though some important interatomic dimensions differ slightly; the values quoted here are averages of both molecules. One molecule of *n*-pentane was also found in the asymmetric unit which was fortunately not disordered. The structure of $[Co_2(\mu\text{-}\eta^2\text{:}\eta^2\text{-}HC{\equiv}CAsC_4Ph_4)(CO)_6]$ is similar to that of $[Co_2(\mu\text{-}\eta^2\text{:}\eta^2\text{-}Me_3SiC{\equiv}CAsC_4Ph_4)(CO)_6]$ preceding it (**Figure 2.23**) with the parent ethynyl function complexing a locally *pseudo*-$C_{2v}$ $Co_2(CO)_6$ unit. The geometry of each Co(0) centre is that of a deformed square-based pyramid (mean $\tau_5$ = 0.12) with a straight-line distance between the midpoints of the C≡C and Co-Co bonds of 1.37 Å. The C1-C2 triple bond is elongated to 1.328 Å from 1.180(3) Å in the free arsole, and the dicobalt covalent bond measures 2.472 Å. Valence angles about the acetylenic carbons are *ca* 135—140° which agree with an atom hybridisation somewhere intermediate between *sp* and $sp^2$.

### 2.8.3 Synthesis of $[Co_4(\mu\text{-}\eta^2\text{:}\eta^2\text{:}\eta^2\text{:}\eta^2\text{-}HC{\equiv}CC{\equiv}CAsC_4Ph_4)(CO)_{12}]$

The coordination of a pair of $Co_2(CO)_6$ units across both alkynyl groups of the butadiynyl arsole could be demonstrated by combining an excess $[Co_2(CO)_8]$ with $HC{\equiv}CC{\equiv}CAsC_4Ph_4$ in ethereal medium giving the tetranuclear $[Co_4(\mu\text{-}\eta^2\text{:}\eta^2\text{:}\eta^2\text{:}\eta^2\text{-}HC{\equiv}CC{\equiv}CAsC_4Ph_4)(CO)_{12}]$ as a dark orange solid in good yield. The presence of four cobalt centres is established by high-resolution mass spectrometry which yields the molecular ion ($m/z \approx 1040.7657$), and the well-populated solution IR spectrum (*n*-hexane) with $\nu_{CO}$ absorptions at 2100(s), 2081(s), 2060(vs), 2054(sh), 2040(m), 2028(vs) and 2014(m) $cm^{-1}$. A similar complex containing the $Me_3SiC{\equiv}CC{\equiv}CAsC_4Ph_4$ ligand was not pursued since this arsole could not be obtained in a pure state, neither was a binuclear complex of the form $[Co_2(\mu\text{-}\eta^2\text{:}\eta^2\text{-}HC{\equiv}CC{\equiv}CAsC_4Ph_4)(CO)_6]$ where one of the butadiynyl C≡C bonds remains free since it was envisioned that any regioisomers, though plausible, may be difficult to separate.




**Scheme 2.25**: Synthesis of $[Co_4(\mu\text{-}\eta^2\text{:}\eta^2\text{:}\eta^2\text{:}\eta^2\text{-}HC{\equiv}CC{\equiv}CAsC_4Ph_4)(CO)_{12}]$.

The $^1H$ NMR spectrum ($C_6D_6$) finds the butadiynyl hydrogen at 5.19 ppm (*cf.* 2.22 ppm in free $HC{\equiv}CC{\equiv}CAsC_4Ph_4$) and the four relevant carbon nuclei are observed in the $^{13}C\{^1H\}$ NMR spectrum at 104.2, 92.5, 92.4 and 81.0 ppm of which the former is *As*-bound and the latter holds the terminus position (by way of an HSQC NMR experiment). Each $Co_2(CO)_6$ moiety is chemically inequivalent and although the carbonyl ligands undergo local positional exchange, the occurrence of two broad resonances at 199.4 and 199.0 ppm suggests no exchange occurs between the pair of tetrahedranes on the NMR timescale. Single crystals were obtained from *n*-pentane at -20 °C and the molecular structure is shown in **Figure 2.26**.

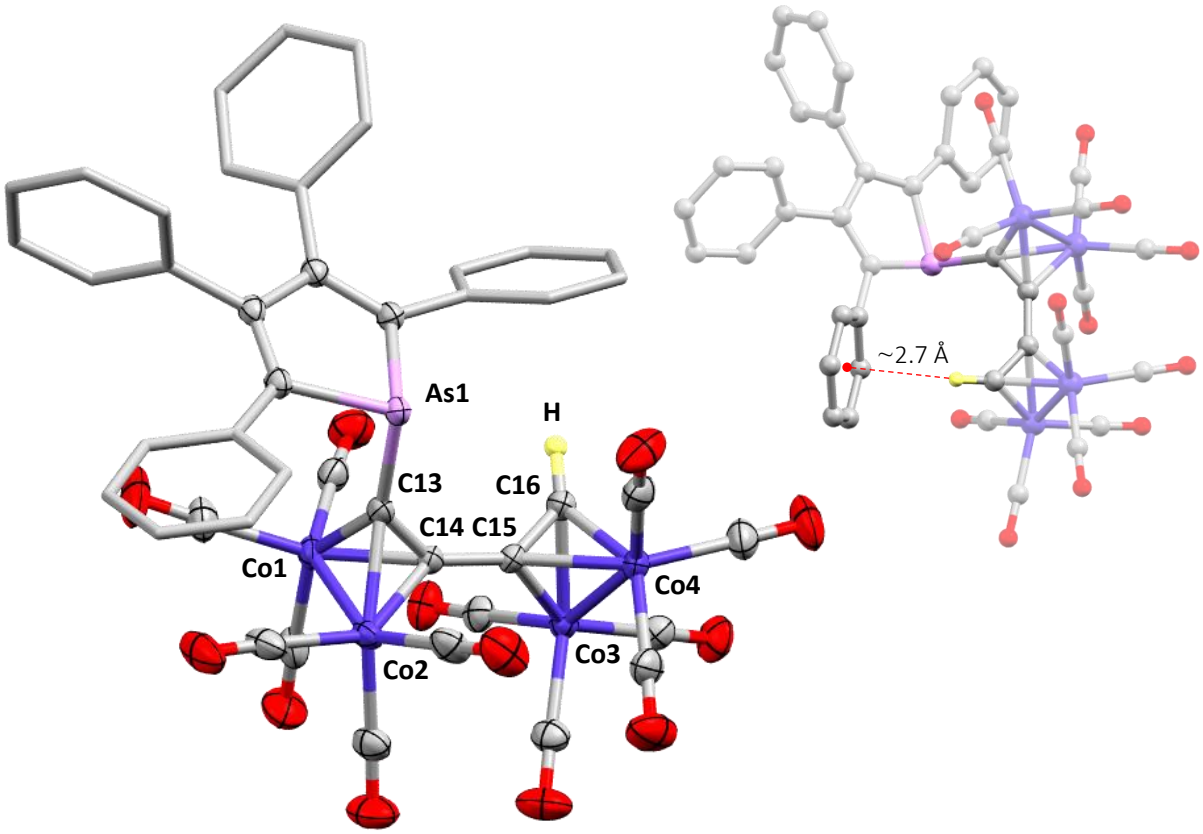



**Figure 2.26**: The molecular structure of $[Co_4(\mu\text{-}\eta^2\text{:}\eta^2\text{:}\eta^2\text{-}HC{\equiv}CC{\equiv}CAsC_4Ph_4)(CO)_{12}]$ in a crystal. Phenyl groups simplified and hydrogen atoms omitted for clarity, except for the butadiynyl hydrogen which is shown in light yellow for emphasis. Ellipsoids shown at 50% displacement. **Inset**: Abbreviated perspective of the molecule to highlight an intramolecular π···H-C contact.

The solid state structure of $[Co_4(\mu\text{-}\eta^2\text{:}\eta^2\text{:}\eta^2\text{-}HC{\equiv}CC{\equiv}CAsC_4Ph_4)(CO)_{12}]$ finds the expected bis(dicobalt hexacarbonyl) adduct of $HC{\equiv}CC{\equiv}CAsC_4Ph_4$. Each $Co_2(CO)_6$ units binds a separate C≡C function and the terminal $Co_2(CO)_6$ moiety is staggered by *ca* 55° with respect to the internal $Co_2(CO)_6$ moity, affording the butadiynyl linkage an appreciable degree of curvature. Given the four-carbon chain approximates contiguous $sp^2$-character along the entire spine, local angles (*ca* 136—141°; idealised octagon: 135°) approach those of the twist-boat chair conformation observed for free 1,3-cyclooctadiene,[171] bearing a close resemblance to the bis(dicobalt hexacarbonyl) adducts of 1,3-cyclooctadiyne derivatives prepared by SOLAN and co-workers[172] and the analogue of ZEISE'S salt $[Pt_2(\mu\text{-}\eta^2\text{:}\eta^2\text{-}C_8H_{12})Cl_6]^{2-}$ described by STEINBORN.[173] The arsole "centre of mass" lies partially above the internal $Co_2(CO)_6$ unit, and the butadiynyl chain contorts in such a way that a phenyl ring in the α ring-position forms a short C-H···π contact with the

butadiynyl hydrogen (H···centroid 2.71 Å, C16···centroid 3.60 Å; **Figure 2.26**, **Inset**).* Distances along the tetra-coordinated butadiynyl residue also resemble alternating C=C and C-C bonds in agreement with the analogous $Co_2(CO)_6$-complexed *As*-ethynyl arsole, with C13-C14, C14-C15 and C15-C16 bond lengths of 1.358(3), 1.429(3) and 1.353(3) Å, respectively. The intermetallic bonds between Co(0) atoms of length 2.46 Å (mean), the As-C13 bond length of 1.931(2) Å are typical, calling for no further comment.

## 2.9 Summary

In this chapter, the first examples of *As*-ethynyl and -butadiynyl arsoles $R(C{\equiv}C)_nAsC_4Ph_4$ (R = H or $SiMe_3$; $n$ = 1 or 2; **Figure 2.3, Figure 2.5** and **Figure 2.6**) were prepared from the corresponding 1-chloro-tetraphenylarsole (**Figure 2.1**), for which an improved synthetic route was described. Attempts to deprotonate $H(C{\equiv}C)_nAsC_4Ph_4$ ($n$ = 1 or 2) with common amide, organolithium or GRIGNARD bases led instead to nucleophilic substitution of the alkynyl residue in what would prove to be a recurring feature of arsole chemistry during the remainder of this work. Computational analyses rationalised this based on an arsenocentric LUMO. The alkynyl arsoles defied admission into conventional Cu-catalysed homocoupling and Pd-catalysed heterocoupling protocols which was tentatively attributed to an atypically poor kinetic acidity of the CH terminus.

Despite this, the ethynyl arsole $HC{\equiv}CAsC_4Ph_4$ reacts as expected with $[Ru(CO)_2(PPh_3)_3]$ and *mer*-$[RuHCl(CO)(PPh_3)_3]$ to give the products of C-H activation $[RuH(C{\equiv}CAsC_4Ph_4)(CO)_2(PPh_3)_2]$ (**Figure 2.10**) and hydrometallation $[RuCl(E\text{-}CH{=}CHAsC_4Ph_4)(CO)(PPh_3)_2]$ (**Figure 2.14**), respectively. Tautomerisation is affected upon treatment with $[Ru(THF)(PPh_3)_2(\eta^5\text{-}C_5H_5)]PF_6$ giving the expected vinylidene $[Ru(=C{=}CHAsC_4Ph_4)(PPh_3)_2(\eta^5\text{-}C_5H_5)]PF_6$ (**Figure 2.17**) which is easily deprotonated to the corresponding alkynyl $[Ru(C{\equiv}CAsC_4Ph_4)(PPh_3)_2(\eta^5\text{-}C_5H_5)]$ (**Figure 2.18**). The deployment of $[RuCl_2(PPh_3)_3]$, another ruthenium complex with proclivity for producing vinylidene linkages, gave the unsymmetrical binuclear vinylidene complex $[Ru_2(\mu\text{-}Cl)_3Cl(=C{=}CHAsC_4Ph_4)(PPh_3)_4]$ (**Figure 2.15**).

* C-H···$\pi_{aryl}$ interactions have been noted in the crystal structures of numerous organic and organometallic compounds with a range of H-bond distances; the distance measured here – although towards the longer end of the wider continuum – falls comfortably amongst other acetylenic hydrogen-aryl interactions. See M. NISHIO *Cryst. Eng. Comm.*, **2004**, *6*, 130—158 for an excellent overview of this phenomenon containing a statistical treatment of Cambridge Crystallographic Structural Database, and K. TANABE *et al. J. Am. Chem. Soc.*, **2000**, *122*, 15, 3746—3757 for a theoretical evaluation of various hydrocarbon-aryl interactions.

The butadiynyl arsole $HC{\equiv}CC{\equiv}CAsC_4Ph_4$ also reacts with $[Ru(CO)_2(PPh_3)_3]$ to give the insertion product $[RuH(C{\equiv}CC{\equiv}CAsC_4Ph_4)(CO)_2(PPh_3)_2]$ (**Figure 2.13**); however, the ultimate product upon combination with *mer*-$[RuHCl(CO)(PPh_3)_3]$ was the MARKOVNIKOV-hydrometallated $[RuCl\{gem\text{-}C(=CH_2)C{\equiv}CAsC_4Ph_4\}(CO)(PPh_3)_2]$ *via* irreversible isomerisation of $[RuCl(E\text{-}CH{=}CHC{\equiv}CAsC_4Ph_4)(CO)(PPh_3)_2]$. Attempts to synthesis a butatrienylidene complex from $[Ru(THF)(PPh_3)_2(\eta^5\text{-}C_5H_5)]PF_6$ instead afforded an arylalkynyl ligand (**Figure 2.19**) from which the arsenic atom had been extruded, traversing a mechanism proposed to involve nucleophilic attack of an arsole carbon upon the electrophilic γ-carbon of the nascent four-carbon chain.

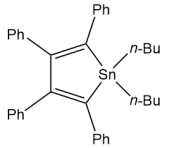
The ethynyl arsoles $RC{\equiv}CAsC_4Ph_4$ (R = H or $SiMe_3$) and the butadiynyl arsole $HC{\equiv}CC{\equiv}CAsC_4Ph_4$ react readily with $[Co_2(CO)_8]$ to give classic π-alkyne complexes $[\{Co_2(CO)_6\}_n\{\mu\text{-}\eta^2{:}\eta^2\text{-}R(C{\equiv}C)_nAsC_4Ph_4\}]$ featuring $Co_2C_2$ tetrahedra (**Figure 2.23**, **Figure 2.25** and **Figure 2.26**). These compounds proved to be thermally sensitive, and their decomposition products directly led to a portion of the work described in **Section 3.3** of the following chapter.

These results taken together provide the first arsolyl functionalised examples of a library of classical transition metal organometallic ligands *viz.* alkynyl, butadiynyl, alkenyl, vinylidene, butatrienylidene (implicit), σ-enynyl, π-alkyne and π-diyne. With the exception of the arsinoalkyne derivatives $As\{C{\equiv}CHCo_2(CO)_6\}_3$ and $PhC{\equiv}CAs\{C{\equiv}CPhCo_2(CO)_6\}_3$ none of these ligand classes have been described even for simple arsenic substituents "$AsR_2$". In passing, though it falls outside the current narrative, during these studies in collaboration with Dr B. J. FROGLEY the first examples of an arsolylcarbyne $[W(\equiv CAsC_4Ph_4)(CO)_2(Tp^*)]$ was also prepared *via* a tandem Sn→Au→As transmetalation relay, further broadening the range of arsolyl-functionalised $C_1$ ligands.[174]

## 2.10 Experimental

### 2.10.1 *As*-Alkynyl Arsoles

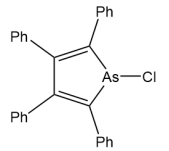
#### 2.10.1.1 $Bu_2SnC_4Ph_4$




To a solution of 10.0 g [$Cp_2ZrCl_2$] (34.2 mmol) dissolved in 150 mL THF and cooled to -78 °C was added 27.5 mL *n*-BuLi solution (68.5 mmol; 2.5 M in hexanes) dropwise over the course of 5—10 minutes. The yellow solution is stirred for one hour at low temperature before 12.2 g solid PhC≡CPh (68 mmol) was added, and the entire mixture allowed to warm to ambient temperature. Evolution of gas is observed and the colour changes to a deep red whilst stirring overnight. After this time, 10.3 g $Bu_2SnCl_2$ (33.8 mmol) and *ca* 170 mg CuCl (~5 mol%) were added and the mixture stirred at ambient temperature for a further 48—72 hours, during which time the red colour converts to a yellow-brown suspension. From this point forward, operations may be carried out in air if desired. Volatiles are removed by rotary evaporation and the product repeatedly extracted with portions of petroleum ether and filtered through a short column of neutral alumina (10 x 5 cm, activity III) with the same solvent until washings ran clear. Evaporation of the yellow filtrate provides the title compound as a viscous yellow liquid (the colour and appearance of which is best described as resembling honey) which is readily soluble in common organic solvents and is reasonably air and moisture stable, though slowly degrades to insoluble white residues over several days. Isolated yield: 18.4 g (31.2 mmol, 91%).

NMR: $^1$H ($CDCl_3$, 400 MHz, 25 °C) δ 7.09—6.79 (m, 20H, $C_6H_5$), 1.65 (p, $J_{HH}$ = 7.6 & 7.3 Hz, 4H, β-$CH_3$), 1.44 (t, $J_{HH}$ = 7.6 Hz, 4H, α-$CH_3$), 1.34 (dq, $J_{HH}$ = 14.5 & 7.3 Hz, 4H, γ-$CH_2$), 0.83 (t, $J_{HH}$ = 7.3 Hz, 6H, ω-$CH_3$) ppm. HR-MS (EI, MeCN, +ve ion) found $m/z$ 590.1996 (calc. for $C_{36}H_{38}{}^{120}Sn_1$ $[M]^+$: 590.1996).

#### 2.10.1.2 $ClAsC_4Ph_4$



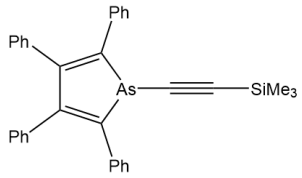

To a solution of 18.2 g $Bu_2SnC_4Ph_4$ (30.8 mmol) in *ca* 100 mL *n*-hexane is added 2.50 mL neat $AsCl_3$ (29.8 mmol) by syringe and the mixture stirred overnight at ambient temperature. The product precipitates from solution as a yellow microcrystalline solid which is collected on a glass frit under nitrogen and washed with 5 x 20 mL portions of *n*-pentane and dried *in vacuo*. The product is readily soluble in polar organic and aromatic solvents, is slightly soluble in $Et_2O$ and less-so in aliphatic hydrocarbons. It is slowly hydrolysed by adventitious moisture to oily brown residues and is decomposed upon contact with silica gel or neutral alumina. The product as-isolated is sufficiently pure for synthetic purposes however an analytically pure sample may be obtained by re-crystallisation from the minimum amount of $CH_2Cl_2$/*n*-hexane or benzene/*n*-hexane at -20 °C. Isolated yield: 10.9 g (23.3 mmol, 75%).

NMR: $^1$H ($CDCl_3$, 400 MHz, 25 °C) δ 7.19—7.15 (m, 10H, $C_6H_5$), 7.10—7.04 (m, 6H, $C_6H_5$), 6.88—6.86 (m, 4H, $C_6H_5$) ppm. $^{13}$C{$^1$H} ($CDCl_3$, 176 MHz, 25 °C) δ 152.0 (arsole {2,5}-*C*), 149.5 (arsole {3,4}-*C*), 137.1 ($C_6H_5$), 136.2

($C_6H_5$), 129.9 ($C_6H_5$), 129.4 ($C_6H_5$), 128.4 ($C_6H_5$), 128.0 ($C_6H_5$), 127.5 ($C_6H_5$), 127.4 ($C_6H_5$) ppm; HR-MS (EI, MeCN, +ve ion) found $m/z$ 466.0469 (calc. for $C_{28}H_{20}{}^{35}Cl_1{}^{75}As_1$ $[M]^+$: 466.0462). Analysis found 72.09% C, 4.45% H (calc. for $C_{28}H_{20}As_1Cl_1$: 72.04% C, 4.32% H).

Single crystals were grown from benzene/*n*-hexane at -20 °C. The As-Cl moity was found to be disordered over two positions by inflection about the mean arsole plane (occupancy ratio 79:21) and was modelled accordingly. $C_{28}H_{20}As_1Cl_1$ ($M$ = 466.81 g mol$^{-1}$): yellow prism 0.067 × 0.154 × 0.181 mm, tetragonal, space group $I4_1/a$ (no. 88), $a$ = $b$ = 26.5125(3) Å, $c$ = 12.1406(2) Å, $V$ = 8533.8(2) Å$^3$, $Z$ = 16, Gaussian correction $T_{min}/T_{max}$ = 0.607/1.000, $\mu$(Cu-K$_\alpha$) = 3.386 mm$^{-1}$, $\varrho_{calc}$ = 1.453 g cm$^{-3}$, 12324 reflections measured (8.01° ≤ 2Θ ≤ 147.282°), 4251 unique ($R_{int}$ = 0.0186, $R_{sigma}$ = 0.0210) which were used in all calculations, $GOF$ = 1.048, $D_{min}/D_{max}$ = -0.37/0.36 e/Å$^{-3}$. The final $R_1$ was 0.0502 (I > 2σ(I)) and $wR_2$ was 0.1159 (all data).

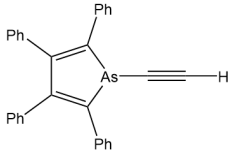
### 2.10.1.3 $Me_3SiC{\equiv}CAsC_4Ph_4$




A dilute solution of $LiC{\equiv}CSiMe_3$ was prepared from 0.75 mL $HC{\equiv}CSiMe_3$ (5.30 mmol) and 3.30 mL *n*-BuLi (5.25 mmol, 1.6 M in hexanes) in 50 mL $Et_2O$ at 0 °C. To this was added 2.0 g $ClAsC_4Ph_4$ (4.30 mmol) and the suspension rapidly stirred, and over the course of *ca* 30 minutes the *As*-chloro arsole gradually dissolves to give a light-yellow mixture. After stirring overnight volatiles are removed under reduced pressure and the residue extracted with *n*-hexane and filtered through a short plug of oven-dried celite (5 x 2.5 cm) under nitrogen, rinsing with portions of *n*-hexane until washings ran clear. The solvent is again removed under reduced pressure leaving the product as a light-yellow solid which is readily soluble in common organic solvents. The product is rather moisture sensitive and hydrolyses when exposed to air, either as a solution or solid, to the parent *As*-ethynyl arsole. The product obtained is sufficiently pure for synthetic purposes. Isolated yield: 1.6 g (3.5 mmol, 81%). The use of THF as the reaction medium leads to very low isolated yields (< 10%).

NMR: $^1$H ($C_6D_6$, 400 MHz, 25 °C) δ 7.50—7.48 (m, 4H, $C_6H_5$), 7.03—7.00 (m, 4H, $C_6H_5$), 6.93—6.81 (m, 12H, $C_6H_5$), 0.01 (s, 9H, Si($CH_3$)$_3$) ppm. $^{13}$C{$^1$H} ($C_6D_6$, 176 MHz, 25 °C) δ 151.3 (arsole {2,5}-*C*), 147.8 (arsole {3,4}-*C*), 130.5 ($C_6H_5$), 129.9 ($C_6H_5$), 128.5 ($C_6H_5$), 128.4 ($C_6H_5$), 128.1 ($C_6H_5$), 128.0 ($C_6H_5$), 127.3 ($C_6H_5$), 127.0 ($C_6H_5$), 115.7 (As*C*≡C), 101.6 (C≡*C*Si), -0.2 (Si($CH_3$)$_3$) ppm. HR-MS (EI, MeCN, +ve ion) found $m/z$ 528.1254 (calc. for $C_{33}H_{29}{}^{75}As_1{}^{29}Si_1$ $[M]^+$: 528.1249). Satisfactory elemental microanalysis could not be obtained.

### 2.10.1.4 $HC{\equiv}CAsC_4Ph_4$

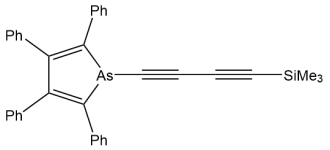


To a stirred solution of crude $Me_3SiC{\equiv}CAsC_4Ph_4$ (prepared *in situ* as above with the same quantities of reagents, followed by evaporation of volatiles) in 30 mL THF was added an excess of either: 1) solid $Na_2CO_3$ and *ca* 50 mL wet methanol, 2) $[Bu_4N]F$ solution (1 M in THF, containing *ca* 5 % water) or 3) NaOH dissolved in *ca* 50 mL wet methanol, and stirred overnight. If routes 1) or 2) are used, the mixture is dried by rotary evaporation and the residue purified by chromatography (silica gel, 9:1 petroleum ether/$CH_2Cl_2$). If route 3) is used, the product precipitates from the reaction medium and is collected by filtration, washed with 1:1 methanol/water followed by methanol and dried under air. Re-crystallisation of the crude material from the minimum amount of $CH_2Cl_2$/methanol at -20 °C provides the title compound as an air-stable off-white solid. The product is readily soluble in polar organic and aromatic solvents, moderately soluble in $Et_2O$ and less-so in aliphatic hydrocarbons and light alcohols. Isolated yield (route 3): 1.25 g (2.7 mmol, 62%).

NMR: $^1H$ ($CDCl_3$, 400 MHz, 25 °C) δ 7.20—7.13 (m, 12H, $C_6H_5$), 7.08—7.03 (m, 8H, $C_6H_5$), 2.78 (s, 1H, C≡C*H*) ppm. $^{13}C\{^1H\}$ ($CDCl_3$, 176 MHz, 25 °C) δ 151.3 (arsole {2,5}-*C*), 146.9 (arsole {3,4}-*C*), 138.1 ($C_6H_5$), 137.3 ($C_6H_5$), 130.2 ($C_6H_5$), 129.5 ($C_6H_5$), 128.2 ($C_6H_5$), 127.9 ($C_6H_5$), 127.0 ($C_6H_5$), 127.0 ($C_6H_5$), 94.1 (As*C*≡C), 80.0 (C≡*C*H) ppm. HR-MS (EI, MeCN, +ve ion) found *m/z* 456.0859 (calc. for $C_{30}H_{21}{}^{75}As_1$ $[M]^+$: 456.0854). Analysis found 79.04% C, 4.77% H (calc. for $C_{30}H_{21}As_1$: 78.95% C, 4.64% H).

Single crystals were obtained from $CH_2Cl_2$/methanol at -20 °C. $C_{30}H_{21}As_1$ ($M$ = 456.39 g/mol), colourless needle, 0.071 x 0.108 x 0.353 mm, monoclinic, space group $P2_1/c$ (no. 14), $a$ = 19.0571(2) Å, $b$ = 6.08720(10) Å, $c$ = 20.2253(2) Å, $\beta$ = 110.4510(10)°, $V$ = 2198.34(5) Å$^3$, $Z$ = 4, multi-scan correction $T_{min}/T_{max}$ = 0.674/1.000, $\mu$(Cu-Kα) = 2.184 mm$^{-1}$, $\varrho_{calc}$ = 1.379 g/cm$^3$, 13330 reflections measured (8.906° ≤ 2Θ ≤ 147.476°), 4440 unique ($R_{int}$ = 0.0254, $R_{sigma}$ = 0.0268) which were used in all calculations, $GOF$ = 1.024, $D_{min}/D_{max}$ = -0.5/1.3 e/Å$^3$. The final $R_1$ was 0.0338 ($I > 2\sigma(I)$) and $wR_2$ was 0.0895 (all data).

### 2.10.1.5 $Me_3SiC{\equiv}CC{\equiv}CAsC_4Ph_4$



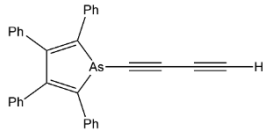

A dilute solution of $LiC{\equiv}CC{\equiv}CSiMe_3$ was prepared from 1.0 g $Me_3SiC{\equiv}CC{\equiv}CSiMe_3$ (6.00 mmol) and 3.90 mL MeLi·LiBr (5.90 mmol; 1.5 M in $Et_2O$) in 50 mL $Et_2O$ at 0 °C. To this was added 2.4 g $ClAsC_4Ph_4$ (5.15 mmol) and stirred overnight, during which time the *As*-chloro arsole dissolves giving a light-yellow mixture. Workup and solubility properties are identical to $Me_3SiC{\equiv}CAsC_4Ph_4$ above. The product is encountered as a light-yellow solid which is appreciably sensitive to moisture and is used without further purification – the product is contaminated with variable but minor quantities of $HC{\equiv}CC{\equiv}CSiMe_3$ however is of no consequence during the following desilylation step. Isolated yield: *ca* 1.85 g (*ca* 3.3 mmol, ~71 %). It is recommended to avoid an excess of MeLi·LiBr since the competitive formation of MeAsC4Ph4 is observed, which proved exceedingly difficult to separate from the target compound.

NMR: $^1H$ ($C_6D_6$, 400 MHz, 25 °C) δ 7.39—7.37 (m, 2H, $C_6H_5$), 7.29—7.27 (m, 2H, $C_6H_5$), 7.03—6.81 (m, 16H, $C_6H_5$), 0.03 (s, 9H, Si($CH_3$)$_3$) ppm (residual $HC{\equiv}CC{\equiv}CSiMe_3$ was observed at 1.37 and -0.08 ppm). $^{13}C\{^1H\}$ δ ($C_6D_6$, 176 MHz, 25 °C) 154.6 (arsole {2,5}-*C*), 152.1 (arsole {2,5}-*C*), 149.6 (arsole {3,4}-*C*), 146.8 (arsole {3,4}-*C*), 139.3 ($C_6H_5$), 139.0 ($C_6H_5$), 138.4 ($C_6H_5$), 137.4 ($C_6H_5$), 130.7 ($C_6H_5$), 130.4 ($C_6H_5$), 129.9 ($C_6H_5$), 129.5 ($C_6H_5$), 128.6 ($C_6H_5$),

128.5 ($C_6H_5$), 127.4 ($C_6H_5$), 127.1 ($C_6H_5$), 126.8 ($C_6H_5$), 100.3 (As*C*≡CC≡CSi), 90.9 (C≡*C*C≡CSi), 89.5 (C≡C*C*≡CSi), 86.2 (C≡CC≡*C*Si) ppm. HR-MS (EI, MeCN, +ve ion) found *m*/*z* 479.0782 (calc. for $C_{32}H_{20}{}^{75}As_1$ [*M* – $SiMe_3$]$^+$: 479.0781). Elemental microanalysis was not pursued given the compound could not be obtained in a pure form.

Single crystals were grown by slow evaporation of *n*-hexane solution at -30 °C. $C_{35}H_{29}As_1Si_1$ (*M* = 552.59 g mol$^{-1}$): yellow prism 0.108 × 0.137 × 0.176 mm, monoclinic, space group $P2_1/c$ (no. 14), *a* = 11.25270(10) Å, *b* = 11.54200(10) Å, *c* = 22.5461(2) Å, *β* = 94.1600(10)°, *V* = 2920.54(4) Å$^3$, *Z* = 4, spherical correction $T_{min}/T_{max}$ = 0.82021/0.82546, *μ*(Cu-K$_α$) = 2.113 mm$^{-1}$, $ϱ_{calc}$ = 1.257 g cm$^{-3}$, 20279 reflections measured (7.864° ≤ 2Θ ≤ 147.604°), 5894 unique ($R_{int}$ = 0.0240, $R_{sigma}$ = 0.0250) which were used in all calculations, *GOF* = 1.042, $D_{min}/D_{max}$ = -0.31/0.45 e/Å$^{-3}$. The final $R_1$ was 0.0275 (I > 2σ(I)) and *w*$R_2$ was 0.0707 (all data).

### 2.10.1.6 HC≡CC≡CAs$C_4Ph_4$

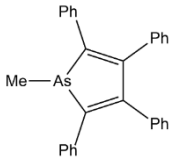



This can be prepared by desilylation of $Me_3SiC≡CC≡CAsC_4Ph_4$ with $Na_2CO_3$/methanol or [$Bu_4N$]F as described for HC≡C$AsC_4Ph_4$, however the simplest method was to treat the $Et_2O$ solution of $Me_3SiC≡CC≡CAsC_4Ph_4$ obtained above (same quantities) with a solution of excess NaOH dissolved in wet methanol from which the title compound rapidly precipitates. This is collected by filtration, washed copiously with 1:1 methanol/water followed by methanol and dried under air. Re-crystallisation of the crude material from the minimum amount of $CH_2Cl_2$/methanol at -20 °C provides the title compound as an air-stable off-white solid. Properties are identical to that of HC≡C$AsC_4Ph_4$ above. Isolated yield: 1.8 g (3.8 mmol, 76%).

NMR: $^1$H ($CDCl_3$, 400 MHz, 25 °C) δ 7.17—7.14 (m, 10H, $C_6H_5$), 7.09—7.04 (m, 6H, $C_6H_5$), 6.88—6.85 (m, 4H, $C_6H_5$), 2.22 (s, 1H, C≡CC≡C*H*) ppm. $^{13}$C{$^1$H} ($CDCl_3$, 176 MHz, 25 °C) δ 151.8 (arsole {2,5}-*C*), 151.6 (arsole {2,5}-*C*), 146.0 (arsole {3,4}-*C*), 145.9 (arsole {3,4}-*C*), 138.0 ($C_6H_5$), 137.9 ($C_6H_5$), 137.0 ($C_6H_5$), 136.9 ($C_6H_5$), 130.1 ($C_6H_5$), 129.6 ($C_6H_5$), 129.5 ($C_6H_5$), 128.2 ($C_6H_5$), 128.4 ($C_6H_5$), 127.9 ($C_6H_5$), 127.8 ($C_6H_5$), 127.1 ($C_6H_5$), 127.1 ($C_6H_5$), 127.0 ($C_6H_5$), 129.6 ($C_6H_5$), 90.6 (As*C*≡CC≡CH), 89.2 (C≡*C*C≡CH), 74.8 (C≡C*C*≡CH), 68.5 (C≡CC≡*C*H) ppm. HR-MS (EI, MeCN, +ve ion) found *m*/*z* 481.0926 (calc. for $C_{32}H_{22}{}^{75}As_1$ [*M* + H]$^+$: 481.0938). Analysis found 80.05% C, 4.60% H (calc. for $C_{32}H_{21}As_1$: 80.00 C%, 4.41% H).

Single crystals were obtained from $CH_2Cl_2$/methanol at -20 °C. $C_{32}H_{21}As_1$ (*M* = 480.41 g mol$^{-1}$): colourless needle, 0.055 × 0.079 × 0.642 mm, monoclinic, space group $P2_1/n$ (no. 14), *a* = 13.5972(2) Å, *b* = 11.80350(10) Å, *c* = 14.68430(10) Å, *β* = 100.3860(10)°, *V* = 2318.14(4) Å3, *Z* = 4, Gaussian correction $T_{min}/T_{max}$ = 0.433/1.000, *μ*(Cu-Kα) = 2.102 mm-1, $ϱ_{calc}$ = 1.377 g/cm$^3$, 14071 reflections measured (8.16° ≤ 2Θ ≤ 147.574°), 4681 unique ($R_{int}$ = 0.0216, $R_{sigma}$ = 0.0250) which were used in all calculations, *GOF* = 1.048, $D_{min}/D_{max}$ = -0.30/0.36 e/Å$^3$. The final $R_1$ was 0.0270 (I > 2σ(I)) and *w*$R_2$ was 0.0758 (all data).

### 2.10.1.7 Reaction between $Me_3SiC{\equiv}CAsC_4Ph_4$ and MeLi·LiBr

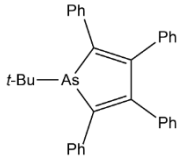



To a stirred solution of 0.25 g $Me_3SiC{\equiv}CAsC_4Ph_4$ (0.47 mmol) in 25 mL $Et_2O$ cooled to -78 °C was added 0.35 mL MeLi·LiBr solution (0.52 mmol; 1.5 M in $Et_2O$). Upon warming to ambient temperature the colour changes to a golden yellow and after 30 minutes three-to-four drops neat methyl iodide (excess) was added; no colour change was observed. The mixture was dried by rotary evaporation and extracted with small portions of petroleum ether and transferred to a column of silica gel (20 x 2.5 cm) made up in the same solvent. Eluting with 4:1 petroleum ether/$Et_2O$ provides a yellow band which is collected and dried. Isolated yield: 0.18 g (0.38 mmol, 81%). The product is readily soluble in common organic solvents and is air stable.

NMR: $^1$H ($CDCl_3$, 400 MHz, 25 °C) δ 7.17—7.04 (m, 16H, $C_6H_5$), 6.92—6.89 (m, 4H, $C_6H_5$), 1.48 (s, 3H, As-$CH_3$) ppm. $^{13}C\{^1H\}$ ($CDCl_3$, 176 MHz, 25 °C) δ 153.8 (arsole {2,5}-*C*), 147.1 (arsole {3,4}-*C*), 138.9 ($C_6H_5$), 138.5 ($C_6H_5$), 130.4 ($C_6H_5$), 129.2 ($C_6H_5$), 128.1 ($C_6H_5$), 127.6 ($C_6H_5$), 126.5 ($C_6H_5$), 126.4 ($C_6H_5$), 10.0 (As-*C*H$_3$) ppm. HR-MS (EI, MeCN, 25 °C) found $m/z$ 446.1006 (calc. for $C_{29}H_{23}{}^{75}As_1$ $[M]^+$: 446.1010). Analysis found: 78.11% C, 5.22% H (calc. for $C_{29}H_{23}As_1$: 78.02% C, 5.19% H).

Single crystals were grown by evaporation of *n*-hexane solution at -20 °C. The As-Me moity was found to be disordered over two positions by inflection about the mean arsole plane (occupancy ratio *ca.* 89:11) and was modelled accordingly. Within experimental error, the unit cell is isomorphous with $ClAsC_4Ph_4$ above. $C_{29}H_{23}As_1$ ($M$ = 446.39 g mol$^{-1}$): yellow prism 0.083 × 0.143 × 0.204 mm, tetragonal, space group $I4_1/a$ (no. 88), $a = b$ = 26.5014(2) Å, $c$ = 12.16700(10) Å, $V$ = 8545.18(15) Å$^3$, $Z$ = 16, empirical correction $T_{min}/T_{max}$ = 0.96719/1.00000, $\mu$(Cu-Kα) = 2.230 mm$^{-1}$, $\varrho_{calc}$ = 1.388 g cm$^{-3}$, 11604 reflections measured (7.996° ≤ 2Θ ≤ 147.138°), 4256 unique ($R_{int}$ = 0.0137, $R_{sigma}$ = 0.0168) which were used in all calculations, $GOF$ = 1.173, $D_{min}/D_{max}$ = -0.30/0.69 e/Å$^{-3}$. The final $R_1$ was 0.0399 (I > 2σ(I)) and $wR_2$ was 0.1001 (all data).

### 2.10.1.8 Reaction between $HC{\equiv}CAsC_4Ph_4$ and *t*-BuLi



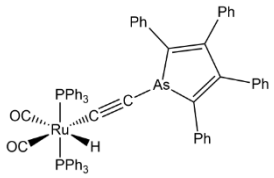

To a stirred suspension of 0.25 g $HC{\equiv}CAsC_4Ph_4$ (0.55 mmol) in 25 mL $Et_2O$ cooled to -78 °C was added 0.4 mL *t*-BuLi solution (0.6 mmol; 1.5 M in *n*-pentane). Upon warming to ambient temperature the arsole dissolves and forms a yellow solution. After 30 minutes three-to-four drops methyl iodide (excess) is added and no colour change is observed. The mixture is dried by rotary evaporation, extracted with portions of petroleum ether and transferred to a column of silica gel (20 x 2.5 cm) made up in the same solvent. Eluting with 9:1 petroleum ether/$Et_2O$ provides a yellow band which is collected and dried. Isolated yield: 0.18 g (0.37 mmol, 67%). The product is readily soluble in common organic solvents and is air stable.

NMR: $^{1}$H ($CDCl_3$, 400 MHz, 25 °C) δ 7.21—7.20 (m, 4H, $C_6H_5$), 7.14—7.12 (m, 4H, $C_6H_5$), 7.07—6.99 (m, 10H, $C_6H_5$), 0.98 (s, 9H, $C(CH_3)_3$) ppm. $^{13}$C{$^{1}$H} ($CDCl_3$, 176 MHz, 25 °C) δ 151.0 (arsole {2,5}-*C*), 150.4 (arsole {3,4}-*C*), 139.9 ($C_6H_5$), 139.0 ($C_6H_5$), 130.6 ($C_6H_5$), 129.8 ($C_6H_5$), 127.9 ($C_6H_5$), 127.4 ($C_6H_5$), 126.3 ($C_6H_5$), 126.0 ($C_6H_5$), 39.3 ($C(CH_3)_3$), 28.9 ($C(CH_3)_3$) ppm. HR-MS (EI, MeCN, +ve ion) found *m/z* 489.1554 (calc. for $C_{32}H_{30}{}^{75}As_1$ [*M* + H]$^{+}$: 489.1563). Satisfactory elemental microanalysis could not be obtained.

Single crystals were obtained by slow evaporation of benzene solution at 10 °C. One-half molecule of benzene was found within the asymmetric unit. $C_{32}H_{29}As_1{\cdot}0.5C_6H_6$ (*M* = 527.52 g/mol): yellow plate 0.055 × 0.104 × 0.365 mm, triclinic, space group *P*-1 (no. 2), $a$ = 6.3050(4) Å, $b$ = 11.7954(10) Å, $c$ = 19.3635(19) Å, α = 78.938(8)°, $\beta$ = 83.072(7)°, $\gamma$ = 77.646(6)°, $V$ = 1375.8(2) Å$^3$, $Z$ = 2, multi-scan correction $T_{min}/T_{max}$ = 0.850/1.000, $\mu$(Mo-Kα) = 1.256 mm$^{-1}$, $\varrho_{calc}$ = 1.273 g/cm$^3$, 9385 reflections measured (6.9° ≤ 2Θ ≤ 52.74°), 5406 unique ($R_{int}$ = 0.0675, $R_{sigma}$ = 0.1454) which were used in all calculations, *GOF* = 1.071, $D_{min}/D_{max}$ = -0.78/0.78 e/Å$^3$. The final $R_1$ was 0.0765 (I > 2σ(I)) and $wR_2$ was 0.1470 (all data).

### 2.10.2 Reactions with $[Ru(CO)_2(PPh_3)_3]$

#### 2.10.2.1 $[RuH(C{\equiv}CAsC_4Ph_4)(CO)_2(PPh_3)_2]$



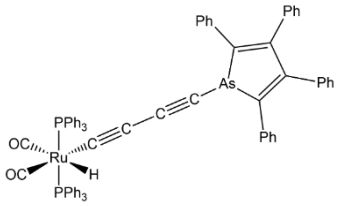

A 25 mL Schlenk tube was charged with 0.35 g $[Ru(CO)_2(PPh_3)_3]$ (0.37 mmol) and 0.17 g $HC{\equiv}CAsC_4Ph_4$ (0.37 mmol) under argon, and 10 mL THF was admitted. The mixture was stirred overnight during which time the yellow colour slowly discharges. The mixture is dried under reduced pressure and the off-white solids washed with 5 x 5 mL *n*-hexane (with trituration) to remove free $PPh_3$. Isolated yield: 0.3 g (0.26 mmol, 71%). The product is readily soluble in $CH_2Cl_2$, acetonitrile, THF, benzene and toluene, slightly soluble in $Et_2O$ and less-so in aliphatic hydrocarbons.

NMR: $^{1}$H ($C_6D_6$, 400 MHz, 25 °C) δ 7.89—7.84 (m, 10H $C_6H_5$), 7.3—7.27 (m, 6H, $C_6H_5$), 7.04—6.70 (m, 20H, $C_6H_5$), 6.97—6.95 (m, 12H, $C_6H_5$), 6.84—6.80 (m, 2H, $C_6H_5$), -5.35 (t, $^{2}J_{PH}$ = 19.7 Hz, Ru-*H*) ppm. $^{13}$C{$^{1}$H} ($C_6D_6$, 176 MHz MHz, 25 °C) δ 199.0 (t, $^{2}J_{PC}$ = 10.3 Hz, *C*O), 196.6 (t, $^{2}J_{PC}$ = 9.6 Hz, *C*O), 152.0 (arsole {2,5}-*C*), 150.4 (arsole {2,5}-*C*), 148.8 (arsole {3,4}-*C*), 146.8 (arsole {3,4}-*C*), 139.0 ($C_6H_5$), 138.4 ($C_6H_5$), 138.4 ($C_6H_5$), 135.6 ($C_6H_5$), 134.3 ($C_6H_5$), 130.6 ($C_6H_5$), 130.4 ($C_6H_5$), 130.1 ($C_6H_5$), 130.0 ($C_6H_5$), 128.5 ($C_6H_5$), 128.4 ($C_6H_5$), 127.3 ($C_6H_5$), 127.1 ($C_6H_5$), 126.8 ($C_6H_5$), 113.9 (t, $^{2}J_{PC}$ = 21.5 Hz, Ru-*C*≡CC≡C), 98.6 (Ru-C≡*C*C≡C), 96.8 (Ru-C≡C*C*≡C), 91.0 (Ru-C≡CC≡*C*) ppm. $^{31}$P{$^{1}$H} ($C_6D_6$, 161 MHz, 25 °C) δ 43.0 ppm. IR (THF, 25 °C) $\nu_{CO}$ 2034(vs), 1989(vs) cm$^{-1}$. HR-MS (ESI, MeCN, +ve ion) found many fragments corresponding to the presence of ruthenium but no chemically sensible formulae could be devised. Satisfactory elemental microanalysis could not be obtained.

Single crystals were obtained by layering a benzene solution with *n*-hexane. One molecule of benzene and one-half a molecule of *n*-hexane were found in the asymmetric unit, of which the latter was severely disordered (and appeared to be of < 1 occupancy) and could not be modelled satisfactorily. A solvent mask was calculated which found 24 electrons in a volume of 120 Å$^3$ per asymmetric unit; this is consistent with the presence of one-half a molecule of $C_6H_{14}$ which account for 24 electrons per asymmetric unit. A Ru-H distance of 1.77 Å was initially provided to the

model and allowed to refine freely. $C_{70}H_{51}O_2As_1P_2Ru_1 \cdot C_6H_6$ ($M$ = 1240.14 g/mol): colourless prism 0.09 × 0.197 × 0.22 mm, triclinic, space group $P$-1 (no. 2), $a$ = 13.6039(2) Å, $b$ = 16.6933(3) Å, $c$ = 17.4284(3) Å, α = 99.387(2)°, $\beta$ = 112.321(2)°, $\gamma$ = 112.832(2)°, $V$ = 3142.75(11) Å$^3$, $Z$ = 2, spherical correction $T_{min}/T_{max}$ = 0.66162/0.68323, $\mu$(Cu-Kα) = 3.438 mm$^{-1}$, $\varrho_{calc}$ = 1.311 g/cm$^3$, 43958 reflections measured (6.802° ≤ 2Θ ≤ 147.776°), 12667 unique ($R_{int}$ = 0.0248, $R_{sigma}$ = 0.0251) which were used in all calculations, $GOF$ = 1.029, $D_{min}/D_{max}$ = -1.34/2.67 e/Å$^3$. The final $R_1$ was 0.0347 (I > 2σ(I)) and $wR_2$ was 0.0862 (all data).

### 2.10.2.2 [RuH(C≡CC≡CAsC$_4$Ph$_4$)(CO)$_2$(PPh$_3$)$_2$]



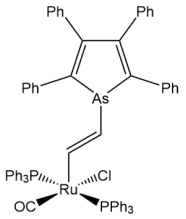

Prepared in an identical manner to the compound above, obtained as an air sensitive beige solid. Quantities: 0.2 g [Ru(CO)$_2$(PPh$_3$)$_3$] (0.22 mmol) and 0.12 g HC≡CC≡CAsC$_4$Ph$_4$ (0.25 mmol). Isolated yield: 0.15 mg (0.13 mmol, 59 %).

NMR: $^1$H (C$_6$D$_6$, 400 MHz, 25 °C) δ 7.89—7.84 (m, 10H C$_6H_5$), 7.3—7.27 (m, 6H, C$_6H_5$), 7.04—6.70 (m, 20H, C$_6H_5$), 6.97—6.95 (m, 12H, C$_6H_5$), 6.84—6.80 (m, 2H, C$_6H_5$), -5.35 (t, $^2J_{PH}$ = 19.7 Hz, Ru-*H*) ppm. $^{13}$C{$^1$H} (C$_6$D$_6$, 176 MHz MHz, 25 °C) δ 199.0 (t, $^2J_{PC}$ = 10.3 Hz, *C*O), 196.6 (t, $^2J_{PC}$ = 9.6 Hz, *C*O), 152.0 (arsole {2,5}-*C*), 150.4 (arsole {2,5}-*C*), 148.8 (arsole {3,4}-*C*), 146.8 (arsole {3,4}-*C*), 139.0 (*C*$_6$H$_5$), 138.4 (*C*$_6$H$_5$), 138.4 (*C*$_6$H$_5$), 135.6 (*C*$_6$H$_5$), 134.3 (*C*$_6$H$_5$), 130.6 (*C*$_6$H$_5$), 130.4 (*C*$_6$H$_5$), 130.1 (*C*$_6$H$_5$), 130.0 (*C*$_6$H$_5$), 128.5 (*C*$_6$H$_5$), 128.4 (*C*$_6$H$_5$), 127.3 (*C*$_6$H$_5$), 127.1 (*C*$_6$H$_5$), 126.8 (*C*$_6$H$_5$), 113.9 (t, $^2J_{PC}$ = 21.5 Hz, Ru-*C*≡CC≡C), 98.6 (Ru-C≡*C*C≡C), 96.8 (Ru-C≡C*C*≡C), 91.0 (Ru-C≡CC≡*C*) ppm. $^{31}$P{$^1$H} (C$_6$D$_6$, 161 MHz, 25 °C) δ 43.0 ppm. IR (THF, 25 °C) $\nu_{CO}$ 2034(vs), 1989(vs) cm$^{-1}$. HR-MS (ESI, MeCN, +ve ion) found many fragments corresponding to the presence of ruthenium but no chemically sensible formulae could be devised. Satisfactory elemental microanalysis could not be obtained.

Single crystals were obtained by layering a benzene solution with *n*-hexane. One molecule of benzene and one-half a molecule of *n*-hexane were found in the asymmetric unit, of which the latter was severely disordered (and appeared to be of < 1 occupancy) and could not be modelled satisfactorily. A solvent mask was calculated which found 24 electrons in a volume of 120 Å$^3$ per asymmetric unit; this is consistent with the presence of one-half a molecule of C$_6$H$_{14}$ which account for 24 electrons per asymmetric unit. A Ru-H distance of 1.77 Å was initially provided to the model and allowed to refine freely. $C_{70}H_{51}O_2As_1P_2Ru_1 \cdot C_6H_6$ ($M$ = 1240.14 g/mol): colourless prism 0.09 × 0.197 × 0.22 mm, triclinic, space group $P$-1 (no. 2), $a$ = 13.6039(2) Å, $b$ = 16.6933(3) Å, $c$ = 17.4284(3) Å, α = 99.387(2)°, $\beta$ = 112.321(2)°, $\gamma$ = 112.832(2)°, $V$ = 3142.75(11) Å$^3$, $Z$ = 2, spherical correction $T_{min}/T_{max}$ = 0.66162/0.68323, $\mu$(Cu-Kα) = 3.438 mm$^{-1}$, $\varrho_{calc}$ = 1.311 g/cm$^3$, 43958 reflections measured (6.802° ≤ 2Θ ≤ 147.776°), 12667 unique ($R_{int}$ = 0.0248, $R_{sigma}$ = 0.0251) which were used in all calculations, $GOF$ = 1.029, $D_{min}/D_{max}$ = -1.34/2.67 e/Å$^3$. The final $R_1$ was 0.0347 (I > 2σ(I)) and $wR_2$ was 0.0862 (all data).

### 2.10.3 Reactions with *mer*-[RuHCl(CO)($PPh_3$)$_3$]

#### 2.10.3.1 [RuCl{*E*-C(H)=C(H)As$C_4Ph_4$}(CO)($PPh_3$)$_2$]

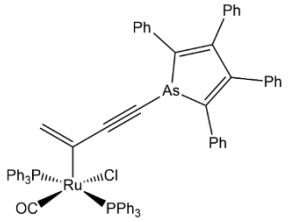



To a solution of 0.3 g *mer*-[RuHCl(CO)($PPh_3$)$_3$] (0.31 mmol) in 10 mL THF is added 0.16 mg HC≡C$AsC_4Ph_4$ (0.35 mmol) and the mixture swirled briefly – as the Ru complex dissolves the colour changes to a bright orange, and the reaction is left to stand at ambient temperature for 60 minutes. After this time 50 mL ethanol is added and the solution slowly concentrated by rotary evaporation to precipitate the product as an orange microcrystalline solid. This is collected by filtration and washed further with ethanol (3 x 20 mL) and $Et_2O$ (2 x 10 mL) and dried under vacuum. An analytically pure sample was obtained by re-crystallisation from $CH_2Cl_2$/methanol at -20 °C under nitrogen. Isolated yield: 0.25 g (0.22 mmol, 70%). The product is reasonably air-stable as a solid and solution, however the latter were observed to decompose over *ca* one week with reformation of HC≡C$AsC_4Ph_4$, and reacts with $CDCl_3$ to give the same. The product is readily soluble in polar organic and aromatic solvents, and poorly soluble in $Et_2O$, light alcohols and aliphatic hydrocarbons.

NMR: $^1$H ($CD_2Cl_2$, 400 MHz, 25 °C) δ 8.87 (dt, 1H, $^3J_{HH}$ = 12.9, $^3J_{PH}$ = 1.5 Hz, Ru-C*H*=CH), 7.43—7.40 (m, 6H, $C_6H_5$), 7.37—7.34 (m, 12H, $C_6H_5$), 7.30—7.27 (m, 14H, $C_6H_5$), 7.08 (m, 6H, $C_6H_5$), 6.97—6.96 (m, 6H, $C_6H_5$), 6.76—6.74 (m, 2H, $C_6H_5$), 6.69—6.67 (m, 4H, $C_6H_5$), 5.70 (dt, 1H, $^3J_{HH}$ = 12.9, $^4J_{PH}$ = 1.5 Hz, CH=C*H*-As) ppm. $^{13}$C{$^1$H} ($CD_2Cl_2$, 176 MHz, 25 °C) δ 201.3 (t, $^2J_{PC}$ = 26.8 Hz, *C*O), 164.3 (t, $^2J_{PC}$ = 19.2 Hz, Ru-*C*H=CH,), 150.9 (arsole {2,5}-*C*), 149.2 (arsole {3,4}-*C*), 140.2 ($C_6H_5$), 138.9 ($C_6H_5$), 134.6 ($^3J_{PC}$ = 12.1 Hz, $C_6H_5$), 132.1 ($^1J_{PC}$ = 43.1 Hz, $C_6H_5$), 130.7 ($C_6H_5$), 129.6 ($C_6H_5$), 128.9 ($^2J_{PC}$ = 9.5 Hz, $C_6H_5$), 128.3 ($C_6H_5$), 128.0 ($C_6H_5$), 126.7 ($C_6H_5$), 126.9 ($C_6H_5$), 125.3 (t, $^3J_{PC}$ = 7 Hz, CH=*C*H-As) ppm. $^{31}$P{$^1$H} ($CD_2Cl_2$, 161 MHz, 25 °C) 29.2 ppm. IR ($CH_2Cl_2$, 25 °C) $\nu_{CO}$ 1929(vs) cm$^{-1}$. HR-MS (ESI, MeCN, +ve ion) found *m*/*z* 1111.1776 (calc. for $C_{67}H_{52}O_1{}^{75}As_1{}^{31}P_2{}^{102}Ru_1$ [*M* - Cl]$^+$: 1111.1771). Analysis found 70.17% C, 4.50% H (calc. for $C_{67}H_{52}O_1As_1Cl_1P_2Ru_1$: 70.19% C, 4.57% H).

Single crystals were obtained from $CH_2Cl_2$/methanol at -20 °C. $C_{67}H_{52}O_1As_1Cl_1P_2Ru_1$ (*M* = 1146.46 g/mol): orange needle 0.066 × 0.094 × 0.161 mm, triclinic, space group *P*-1 (no. 2), *a* = 9.7307(3) Å, *b* = 12.4866(3) Å, *c* = 23.9393(6) Å, α = 77.771(2)°, *β* = 79.780(2)°, *γ* = 71.195(2)°, *V* = 2672.17(13) Å$^3$, *Z* = 2, spherical correction $T_{min}/T_{max}$ = 0.704/0.722, *μ*(Cu-Kα) = 4.427 mm$^{-1}$, $\varrho_{calc}$ = 1.425 g/cm$^3$, 26225 reflections measured (7.584° ≤ 2Θ ≤ 147.592°), 10283 unique ($R_{int}$ = 0.0305, $R_{sigma}$ = 0.0352) which were used in all calculations, *GOF* = 1.024, $D_{min}/D_{max}$ = -0.64/1.13 e/Å$^3$. The final $R_1$ was 0.0371 (I > 2σ(I)) and *w*$R_2$ was 0.0959 (all data).

### 2.10.3.2 [RuCl{*gem*-C(C≡CAsC$_4$Ph$_4$)=CH$_2$}(CO)(PPh$_3$)$_2$]

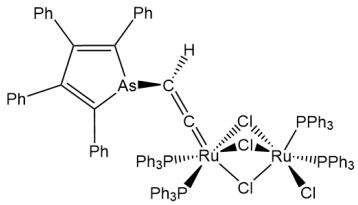



Prepared similarly to that above. Quantities: 0.3 g *mer*-[RuHCl(CO)(PPh$_3$)$_3$] (0.31 mmol) and 0.15 g HC≡CC≡CAsC$_4$Ph$_4$ (0.31 mmol). Initial mixing of the reagents gives a bright orange solution which converts to a dark yellow after stirring overnight. Isolated yield: 0.15 g (0.12 mmol, 40%). Properties are identical to that above.

NMR: $^1$H (CD$_2$Cl$_2$, 400 MHz, 25 °C) δ 7.64—7.62 (m, 10H, C$_6$*H*$_5$), 7.39—7.37 (m 6H, C$_6$*H*$_5$), 7.30—7.28 (m, 10H, C$_6$*H*$_5$), 7.17 (br s, 2H, C$_6$*H*$_5$), 7.11—7.08 (m, 16H, C$_6$*H*$_5$), 6.93—6.92 (m, 4H, C$_6$*H*$_5$), 5.02 (br s, 1H, C=C*H*$_2$), 4.30 (br s, 1H, C=C*H*$_2$) ppm. $^{13}$C{$^1$H} (CD$_2$Cl$_2$, 176 MHz, 25 °C) δ 206.7 (*C*O, $^2J_{PC}$ = 31.8 Hz), 152.3 (arsole {2,5}-*C*), 150.7 (arsole {2,5}-*C*), 148.4 (arsole {3,4}-*C*), 146.6 (arsole {3,4}-*C*), 138.5 (*C*$_6$H$_5$), 137.8 (*C*$_6$H$_5$), 137.4 (*C*$_6$H$_5$), 135.1 (*C*$_6$H$_5$), 132.5 (*C*$_6$H$_5$), 132.4 (*C*$_6$H$_5$), 132.2 (*C*$_6$H$_5$), 130.5 (*C*$_6$H$_5$), 130.0 (*C*$_6$H$_5$), 129.9 (*C*$_6$H$_5$), 128.7 (*C*$_6$H$_5$), 128.6 (*C*$_6$H$_5$), 128.5 (*C*$_6$H$_5$), 128.6 (*C*$_6$H$_5$), 128.2 (*C*$_6$H$_5$), 127.6 (*C*$_6$H$_5$), 127.4 (*C*$_6$H$_5$), 127.3 (*C*$_6$H$_5$), 90.2 (C≡*C*As), 78.2 (*C*≡CAs) ppm. $^{31}$P{$^1$H} (CD$_2$Cl$_2$, 161 MHz, 25 °C) δ 33.9 ppm. IR (CH$_2$Cl$_2$, 25 °C) $\nu_{CO}$ = 1929 cm$^{-1}$. HR-MS (ESI, MeCN, +ve ion) found *m*/*z* 1135.1774 (calc. for C$_{69}$H$_{52}$$^{75}$As$_1$O$_1$$^{31}$P$_2$$^{102}$Ru$_1$ [*M* – Cl]$^+$: 1135.1772). Analysis found 71.15% C, 4.69% H (calc. for C$_{69}$H$_{52}$O$_1$As$_1$Cl$_1$P$_2$Ru$_1$: 70.80% C, 4.48% H).

## 2.10.4 Reactions with [RuCl$_2$(PPh$_3$)$_3$] and [Ru(THF)(PPh$_3$)$_2$($\eta^5$-C$_5$H$_5$)]PF$_6$

### 2.10.4.1 [Ru$_2$(μ-Cl)$_3$Cl{=C=C(H)AsC$_4$Ph$_4$}(PPh$_3$)$_4$]



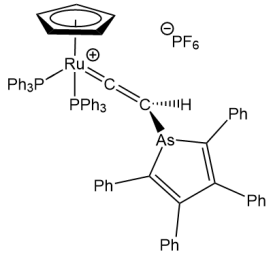

A 50 mL Schlenk tube was charged with 0.2 g [RuCl$_2$(PPh$_3$)$_3$] (0.21 mmol) and 0.1 g HC≡CAsC$_4$Ph$_4$ (0.22 mmol) and 20 mL CH$_2$Cl$_2$ admitted. A green-brown suspension results which gradually converts to a deep red over the course of two hours. Volatiles are removed under reduced pressure and the residue suspended in 50 mL ethanol with trituration and the red-brown solids collected by filtration, which were further washed with 3 x 20 mL ethanol and 3 x 10 mL Et$_2$O and dried under suction. The crude product was re-crystallised from the minimum amount of CH$_2$Cl$_2$/methanol at -20 °C, giving large dark red needles. Isolated yield: 0.31 g (0.16 mmol, 61%). The product is readily soluble in polar organic and aromatic solvents, and poorly soluble in Et$_2$O, aliphatic hydrocarbons and light alcohols. The product is reasonably air-stable in both the solid state and solution.

NMR: $^1$H (CDCl$_3$, 400 MHz, 25 °C) δ 7.39—7.35 (m, 12H, C$_6$*H*$_5$), 7.25—7.24 (m, 4H, C$_6$*H*$_5$), 7.14—7.02 (m, 30H, C$_6$*H*$_5$), 6.98—6.85 (m, 30H, C$_6$*H*$_5$), 6.83—6.72 (m, 4H, C$_6$*H*$_5$), 3.53 (t, $^4J_{PH}$ = 4.1 Hz, 1H, C*H*). $^{13}$C{$^1$H} (176 MHz, CDCl$_3$, 25 °C) δ 336.3 (br, Ru=*C*=C), 151.9 (arsole {2,5}-*C*), 146.9 (arsole {3,4}-*C*), 138.6 (*C*$_6$H$_5$), 136.9 (*C*$_6$H$_5$), 136.6 (*C*$_6$H$_5$), 136.4 (*C*$_6$H$_5$), 136.0 (*C*$_6$H$_5$), 135.5 (*C*$_6$H$_5$), 135.3 (*C*$_6$H$_5$), 135.1 (*C*$_6$H$_5$), 132.8 (*C*$_6$H$_5$), 132.5 (*C*$_6$H$_5$), 132.2 (*C*$_6$H$_5$),

131.8 ($C_6H_5$), 130.3 ($C_6H_5$), 129.5 ($C_6H_5$), 128.4 ($C_6H_5$), 128.1 ($C_6H_5$), 127.8 ($C_6H_5$), 127.3 ($C_6H_5$), 126.8 ($C_6H_5$), 126.4 ($C_6H_5$), 94.7 (br, Ru=C=*C*) ppm. $^{31}P\{^1H\}$ ($CDCl_3$, 161 MHz, 25 °C) 49.8 (d, $^2J_{PP}$ = 37.8 Hz, 1P), 46.9 ppm (d, $^2J_{PP}$ = 37.8 Hz, 1P), 39.7 (d, $^2J_{PP}$ = 25.5 Hz, 1P), 35.8 ppm (d, $^2J_{PP}$ = 25.5 Hz, 1P) ppm. HR-MS (ESI, MeCN, +ve ion) found *m*/*z* 1816.1702 (calc. for $C_{102}H_{81}{}^{75}As_1{}^{35}Cl_3{}^{31}P_4{}^{102}Ru_2$ $[M - Cl]^+$: 1816.1701). Analysis found 66.45% C, 4.60% H (calc. for $C_{102}H_{81}As_1Cl_4P_4Ru_1$: 66.24% C, 4.41% H).

Single crystals were obtained from $CH_2Cl_2$/methanol at -20 °C. Four molecules of dichloromethane were found within the asymmetric unit of which one could be modelled satisfactorily, however the remaining three were severely disordered. A solvent mask was calculated which found 128 electrons in a volume of 715 Å$^3$ per asymmetric unit; this is consistent with the presence of three $CH_2Cl_2$ molecules which account for 126 electrons per asymmetric unit. $C_{102}H_{81}As_1Cl_4P_4Ru_2{\cdot}CH_2Cl_2$ (*M* = 1934.33 g/mol): red needle 0.053 × 0.083 × 0.122 mm, monoclinic, space group $P2_1/n$ (no. 14), *a* = 14.7145(2) Å, *b* = 32.2732(5) Å, *c* = 22.4200(3) Å, $\beta$ = 97.4560(10)°, *V* = 10556.9(3) Å$^3$, *Z* = 4, spherical correction $T_{min}/T_{max}$ = 0.729/0.743, $\mu$(Cu-K$\alpha$) = 4.947 mm$^{-1}$, $\varrho_{calc}$ = 1.217 g/cm$^3$, 34100 reflections measured (7.334° ≤ 2Θ ≤ 142.312°), 19634 unique ($R_{int}$ = 0.0273, $R_{sigma}$ = 0.0513) which were used in all calculations, *GOF* = 1.086, $D_{min}/D_{max}$ = -1.32/1.66 e/Å$^3$. The final $R_1$ was 0.0627 (I > 2$\sigma$(I)) and $wR_2$ was 0.1387 (all data).

### 2.10.4.2 $[Ru\{=C=C(H)AsC_4Ph_4\}(PPh_3)_2(\eta^5\text{-}C_5H_5)]PF_6$



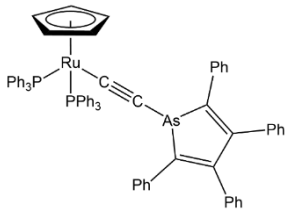

To a stirred solution of 0.3 g $[Ru(THF)(PPh_3)_2(\eta^5\text{-}C_5H_5)]PF_6$ (0.33 mmol) in 20 mL $CH_2Cl_2$ is added 0.16 g $HC{\equiv}CAsC_4Ph_4$ (0.35 mmol). The orange colour gradually changes to a deep red over the course of *ca* 10 minutes and after stirring overnight is filtered through a short plug of oven-dried celite (2.5 x 2.5 cm), and the filtrate dried under reduced pressure. The residue was washed with three 10 mL portions of a 4:1 $Et_2O$/toluene mixture (with trituration) and finally with 3 x 10 mL $Et_2O$ and dried under vacuum. The material was re-dissolved in the minimum amount of $CH_2Cl_2$ and $Et_2O$ added until the solution began to turn cloudy. The mixture stored at -20 °C overnight precipitating the product as a red-brown microcrystalline solid which was decanted from the supernatant, washed with $Et_2O$, and dried under reduced pressure. The product could not be obtained in an analytically pure state. Isolated yield (impure): 0.37 g (~0.28 mmol, ~85%). The product is readily soluble in polar organic solvents and is air- and moisture-sensitive.

NMR: $^1H$ ($CD_2Cl_2$, 400 MHz, 25 °C) δ 7.44—7.40 (m, 12H, $C_6H_5$), 7.29—7.27 (m, 16H, $C_6H_5$), 7.22—7.17 (m, 18H, $C_6H_5$), 7.10—7.04 (m, 4H, $C_6H_5$), 4.98 (t, $^4J_{PH}$ = 2.7 Hz, 1H, Ru=C=C*H*), 4.75 (s, 5H, $\eta^5$-$C_5H_5$) ppm. $^{13}C\{^1H\}$ ($CD_2Cl_2$, 176 MHz, 25 °C) δ 331.2 (t, $^2J_{PC}$ = 15.6 Hz, Ru=*C*=CH), l52.7 (arsole {2,5}-*C*), 150.9 (arsole {3,4}-*C*), 138.7 ($C_6H_5$), 138.1 ($C_6H_5$), 133.7 ($C_6H_5$), 131.5 ($C_6H_5$), 130.5 ($C_6H_5$), 129.7 ($C_6H_5$), 129.1 ($C_6H_5$), 128.8 ($C_6H_5$), 128.6 ($C_6H_5$), 128.1 ($C_6H_5$), 127.6 ($C_6H_5$), 127.4 ($C_6H_5$), 105.7 (Ru=C=*C*H), 94.7 ($\eta^5$-$C_5H_5$) ppm. $^{31}P\{^1H\}$ NMR ($CD_2Cl_2$, 161 MHz) δ 43.0 (2P, $PPh_3$), -144.4 (1P, $[PF_6]^-$) ppm. HR-MS (ESI, MeCN, +ve ion) found *m*/*z* 1147.2129 (calc. for

$C_{71}H_{56}{}^{75}As_1{}^{31}P_2{}^{102}Ru_1$ [*M* ]$^+$: 1147.2136). Elemental microanalysis was not pursued since the product could not be obtained in a sufficiently pure form.

Single crystals were obtained by vapour diffusion of $Et_2O$ into $CH_2Cl_2$ solution at -20 °C. Four molecules of $CH_2Cl_2$ were found in the asymmetric unit of which one was disordered and could not be modelled satisfactorily. A solvent mask was calculated which found 42 electrons in a volume of 183 Å$^3$ per asymmetric unit; this is consistent with the presence of one $CH_2Cl_2$ molecules which account for 42 electrons per asymmetric unit. $C_{71}H_{56}As_1F_6P_3Ru_1{\cdot}3CH_2Cl_2$ (*M* = 1546.83 g/mol): red plate 0.052 × 0.184 × 0.246 mm, triclinic, space group *P*-1 (no. 2), *a* = 14.7378(6) Å, *b* = 14.9118(7) Å, *c* = 19.9976(7) Å, α = 70.137(4)°, *β* = 82.153(3)°, *γ* = 62.039(4)°, *V* = 3649.5(3) Å$^3$, *Z* = 2, Gaussian correction $T_{min}/T_{max}$ = 0.323/1.000, $\mu$(Cu-Kα) = 5.346 mm$^{-1}$, $\varrho_{calc}$ = 1.408 g/cm$^3$, 23633 reflections measured (7.45° ≤ 2Θ ≤ 146.422°), 14085 unique ($R_{int}$ = 0.0284, $R_{sigma}$ = 0.0502) which were used in all calculations, *GOF* = 1.044, $D_{min}/D_{max}$ = -1.23/0.96 e/Å$^3$. The final $R_1$ was 0.0513 (I > 2σ(I)) and $wR_2$ was 0.1442 (all data).

### 2.10.4.3 [Ru(C≡CAsC$_4$Ph$_4$)(PPh$_3$)$_2$(η$^5$-C$_5$H$_5$)]

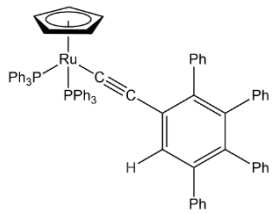



A solution of [Ru{=C=C(H)AsC$_4$Ph$_4$}(PPh$_3$)$_2$(η$^5$-C$_5$H$_5$)]PF$_6$ in $CH_2Cl_2$ was prepared as described above using the same quantities of reagents. After stirring overnight, a solution of 0.075 g DBU (0.50 mmol) in 2 mL $CH_2Cl_2$ was added and the red colour of the vinylidene changes to a yellow-brown over the course of *ca* 10 minutes. After stirring for 3 hours at ambient temperature, the mixture is filtered through a short plug of celite (2.5 x 2.5 cm) and absorbed onto a small quantity of basic alumina by rotary evaporation of the solvent. This was transferred to a column of basic alumina (25 x 2.5 cm) made up in petroleum ether. Eluting with the same solvent, followed by 9:1 petroleum ether/$Et_2O$ gives a pale-yellow band of unreacted HC≡CAsC4Ph4 (isolated *ca* 15 mg, ~10%). Eluting with 4:1 petroleum ether/$CH_2Cl_2$ gives a bright yellow band containing the product which is collected and dried by rotary evaporation. The material was re-crystallised from the minimum amount of $Et_2O$/*n*-hexane at -20 °C under nitrogen giving the product as a yellow microcrystalline solid which was collected by filtration and washed with small portions of *n*-pentane and dried under suction. Isolated yield: 0.2 g (0.17 mmol, 55%). The product is readily soluble in polar organic and aromatic solvents, somewhat soluble in $Et_2O$ and less-so in aliphatic hydrocarbons. The product is reasonably air-stable as a solid or in solution.

NMR: $^1$H ($CD_2Cl_2$, 400 MHz, 25 °C) δ 7.37—7.32 (m, 12H, $C_6H_5$), 7.22—7.17 (m, 12H, $C_6H_5$), 7.09—7.07 (m, 6H, $C_6H_5$), 7.04—7.00 (m, 14H, $C_6H_5$), 6.89—6.74 (m, 6H, $C_6H_5$), 4.17 (s, 5H, η$^5$-$C_5H_5$) ppm. $^{13}$C{$^1$H} NMR ($CD_2Cl_2$, 176 MHz, 25 °C) δ 152.0 (arsole {2,5}-*C*), 147.8 (arsole {3,4}-*C*), 146.2 (t, $^2J_{PC}$ = 23 Hz, Ru-*C*≡C), 140.0 ($C_6H_5$), 139.5 ($C_6H_5$), 139.3 ($C_6H_5$), 139.1 ($C_6H_5$), 134.3 (t, $J_{PC}$ = 5 Hz, $C_6H_5$), 131.0 ($C_6H_5$), 130.1 ($C_6H_5$), 128.9 ($C_6H_5$), 128.1 ($C_6H_5$), 128.0 ($C_6H_5$), 127.8 (t, $J_{PC}$ = 5 Hz, $C_6H_5$), 126.4 ($C_6H_5$), 93.7 (Ru-C≡*C*), 86.2 (η$^5$-$C_5H_5$) ppm. $^{31}$P{$^1$H} NMR ($CD_2Cl_2$, 161 MHz, 25 °C) δ 49.7 ppm. HR-MS (ESI, MeCN, +ve ion) found *m*/*z* 1147.2123 (calc. for $C_{71}H_{56}{}^{75}As_1{}^{31}P_2{}^{102}Ru_1$ [*M* + H]$^+$: 1147.2136). Analysis found 74.49% C, 4.90% H (calc. for $C_{71}H_{55}As_1P_2Ru_1$: 74.40% C, 4.84% H).

Single crystals were obtained by layering a $CH_2Cl_2$ solution with *n*-hexane at -30 °C. $C_{71}H_{55}As_1P_2Ru_1$ ($M$ = 1146.08 g/mol): yellow prism 0.079 × 0.112 × 0.247 mm, triclinic, space group *P*-1 (no. 2), $a$ = 11.1016(2) Å, $b$ = 11.8422(2) Å, $c$ = 21.2040(4) Å, α = 78.044(2)°, $\beta$ = 85.3690(10)°, $\gamma$ = 84.587(2)°, $V$ = 2709.64(9) Å$^3$, $Z$ = 2, multi-scan correction $T_{min}/T_{max}$ = 0.797/1.000, $\mu$(Cu-Kα) = 3.910 mm$^{-1}$, $\varrho_{calc}$ = 1.405 g/cm$^3$, 37747 reflections measured (7.656° ≤ 2Θ ≤ 147.616°), 10921 unique ($R_{int}$ = 0.0201, $R_{sigma}$ = 0.0202) which were used in all calculations, *GOF* = 1.034, $D_{min}/D_{max}$ = -0.50/0.95 e/Å$^3$. The final $R_1$ was 0.0264 (I > 2σ(I)) and $wR_2$ was 0.0683 (all data).

### 2.10.4.4 [Ru{C≡CC$_6$HPh$_4$}(PPh$_3$)$_2$($\eta^5$-C$_5$H$_5$)]




To a solution of 0.3 g [Ru(THF)(PPh$_3$)$_2$($\eta^5$-C$_5$H$_5$)]PF$_6$ (0.33 mmol) in 20 mL $CH_2Cl_2$ is added 0.175 g HC≡CC≡CAsC$_4$Ph$_4$ (0.36 mmol). The orange colour slowly changes to a yellow-brown suspension of the course of *ca* 60 minutes with the formation of dark grey solids. The addition of a slight excess of DBU gave no colour change. After stirring overnight, the solution is filtered through a short plug of celite (2.5 x 2.5 cm) and the filtrate absorbed onto a small quantity of basic alumina by rotary evaporation of the solvent. This was transferred to a column of basic alumina (25 x 2.5 cm) made up in petroleum ether. Eluting with the same solvent, followed by 4:1 petroleum ether/$CH_2Cl_2$ provides a bright yellow band which was collected and dried by rotary evaporation. The residue was re-crystallised from the minimum amount of $Et_2O$/*n*-hexane at -20 °C overnight under nitrogen giving the product as a yellow microcrystalline solid which was collected by filtration, washed with *n*-pentane and dried under suction. Isolated yield: 0.12 g (0.11 mmol, 33%). The product is readily soluble in polar organic and aromatic solvents, somewhat soluble in $Et_2O$ and less-so in aliphatic hydrocarbons. The product is reasonably air-stable as a solid or in solution.

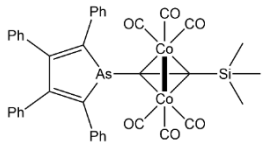
NMR: $^1$H ($CD_2Cl_2$, 400 MHz, 25 °C) δ 7.45—7.41 (m, 13H, C$_6H_5$), 7.41—7.40 (m, 2H, C$_6H_5$), 7.22—7.16 (m, 14H, C$_6H_5$), 7.09—7.05 (m, 14H, C$_6H_5$), 6.91—6.88 (m, 8H, C$_6H_5$), 4.00 (s, 5H, $\eta^5$-C$_5H_5$) ppm (the unique aromatic hydrogen could not be unambiguously identified in the spectrum, though would appear to manifest in the region 7.45—7.41 ppm). $^{13}$C{$^1$H} ($CD_2Cl_2$, 176 MHz, 25 °C) δ 143.62 (t, $^2J_{PC}$ = 24.4 Hz, Ru-*C*≡C), 142.9 (*C*$_6$H$_5$), 142.0 (*C*$_6$H$_5$), 141.8 (*C*$_6$H$_5$), 141.3 (*C*$_6$H$_5$), 140.8 (*C*$_6$H$_5$), 139.3 (*C*$_6$H$_5$), 138.5 (*C*$_6$H$_5$), 137.4 (*C*$_6$H$_5$), 135.2 (*C*$_6$H$_5$), 134.3 (*C*$_6$H$_5$), 132.4 (*C*$_6$H$_5$), 132.0 (*C*$_6$H$_5$), 131.9 (*C*$_6$H$_5$), 130.4 (*C*$_6$H$_5$), 129.9 (*C*$_6$H$_5$), 128.9 (*C*$_6$H$_5$), 128.7 (*C*$_6$H$_5$), 128.2 (*C*$_6$H$_5$), 127.7 (*C*$_6$H$_5$), 127.4 (*C*$_6$H$_5$), 127.1 (*C*$_6$H$_5$), 126.9 (*C*$_6$H$_5$), 126.3 (*C*$_6$H$_5$), 126.0 (*C*$_6$H$_5$), 125.6 (*C*$_6$H$_5$), 123.0 (*C*$_6$H$_5$), 114.2 (Ru-C≡*C*), 85.9 ($\eta^5$-*C*$_5$H$_5$) ppm (the unique aromatic carbon could not be unambiguously identified in the spectrum). $^{31}$P{$^1$H} ($CD_2Cl_2$, 161 MHz, 25 °C) δ 51.3 ppm. HR-MS (ESI, MeCN, +ve ion) found $m/z$ 1097.2990 (calc. for C$_{73}$H$_{56}$$^{31}$P$_2$$^{102}$Ru$_1$ [*M*]$^+$: 1097.2999). Analysis found 80.10% C, 5.21% H (calc. for C$_{73}$H$_{56}$P$_2$Ru$_1$: 79.98% C, 5.15% H).

Crystals were obtained by layering a $CH_2Cl_2$ solution with *n*-hexane at -30 °C. The selected crystal proved to be twinned, and a suitable twin-law was applied. Three molecules of dichloromethane were found within the unit cell, though one was severely disordered and could not be modelled satisfactorily. A solvent mask was calculated which found 42 electrons in a volume of 183 Å$^3$ per asymmetric unit; this is consistent with the presence of one $CH_2Cl_2$ molecules which account for 42 electrons per asymmetric unit. C$_{73}$H$_{56}$P$_2$Ru·2$CH_2Cl_2$ ($M$ = 1266.04 g/mol): yellow

needle 0.041 × 0.125 × 0.587 mm, monoclinic, space group $P2_1/c$ (no. 14), $a$ = 10.26030(10) Å, $b$ = 14.6953(2) Å, $c$ = 44.4064(4) Å, $\beta$ = 93.9510(10)°, $V$ = 6679.60(13) Å$^3$, $Z$ = 4, multi-scan correction $T_{min}/T_{max}$ = 0.573/1.000, $\mu$(Cu-Kα) = 4.132 mm$^{-1}$, $\varrho_{calc}$ = 1.259 g/cm$^3$, 27073 reflections measured (7.218° ≤ 2Θ ≤ 155.588°), 27073 unique ($R_{int}$ = 0.0211, $R_{sigma}$ = 0.0218) which were used in all calculations, $GOF$ = 1.210, $D_{min}/D_{max}$ = -1.17/1.48 e/Å$^3$. The final $R_1$ was 0.0871 (I > 2σ(I)) and $wR_2$ was 0.2053 (all data).

### 2.10.5 Reactions with $[Co_2(CO)_8]$

#### 2.10.5.1 $[Co_2(\mu\text{-}\eta^2\text{:}\eta^2\text{-}Me_3SiC{\equiv}CAsC_4Ph_4)(CO)_6]$

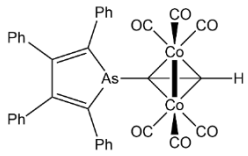



A 25 mL Schlenk tube was charged with 0.25 g $Me_3SiC{\equiv}CAsC_4Ph_4$ (0.47 mmol) and 0.18 g $[Co_2(CO)_8]$ (0.52 mmol), and 10 mL *n*-hexane admitted resulting in immediate gas evolution and the formation a deep red solution. Gas evolution ceases within a few minutes and the mixture is stirred for one hour before being transferred to a column of neutral alumina (20 x 2.5 cm) made up in petroleum ether. Eluting with the same solvent provides a thin grey-brown band (likely $[Co_4(CO)_{12}]$, though it was not analysed and discarded) followed by an orange-red band containing the product, which is collected and dried by rotary evaporation. Re-crystallisation from the minimum amount of *n*-pentane under nitrogen at -20 °C provides large black crystals which are collected by filtration and dried under air. A second crop of crystals was obtained from the supernatant by the same process. Isolated yield: 0.23 g (0.28 mmol, 59%). The product is reasonably air-stable and can be handled without precaution for a short while, however solutions decompose to $HC{\equiv}CAsC_4Ph_4$ and soluble paramagnetic species over several days. The product is readily soluble in common organic solvents however was observed to react with $CDCl_3$.

NMR: $^1$H ($C_6D_6$, 400 MHz, 25 °C) δ 7.53—7.51 (m, 4H, $C_6H_5$), 7.00—6.98 (m, 6H, $C_6H_5$), 6.91—6.89 (m, 6H, $C_6H_5$), 6.84—6.82 (m, 4H, $C_6H_5$) 0.04 (s, 9H, Si($CH_3$)$_3$) ppm. $^{13}$C{$^1$H} ($C_6D_6$, 176 MHz, 25 °C) δ 200.3 (br, *C*O), 151.4 (arsole {2,5}-*C*), 150.4 (arsole {3,4}-*C*), 139.1 ($C_6H_6$), 137.7 ($C_6H_6$), 131.0 ($C_6H_6$), 128.6 ($C_6H_6$), 128.3 ($C_6H_6$),127.4 ($C_6H_6$), 127.1 ($C_6H_6$), 126.9 ($C_6H_5$) 99.6 (As-*C*≡C), 91.9 (C≡*C*-Si), 0.5 (Si(*C*H$_3$)$_3$) ppm. IR (*n*-hexane, 25 °C) $\nu_{CO}$ = 2085(s), 2049(vs), 2026(vs), 2017(s) cm$^{-1}$. HR-MS (ESI, MeCN, +ve ion) found $m/z$ 802.9692 (calc. for $C_{38}H_{30}O_6{}^{75}As_1{}^{59}Co_2{}^{29}Si_1$ [$M$ – CO + O + H]$^+$: 802.9697). Analysis found: 57.52% C, 3.63% H (calc. for $C_{39}H_{29}O_6As_1Co_2Si_2$: 57.51% C, 3.59% H).

Single crystals were obtained from *n*-pentane solution at -20 °C. $C_{39}H_{29}O_6As_1Co_2Si_1$ ($M$ = 814.49 g/mol): black prism 0.098 × 0.118 × 0.155 mm, trigonal, space group $R\text{-}3c$ (no. 167), $a = b = c$ 29.7894(2) Å, $V$ = 11346.6(2) Å$^3$, $Z$ = 12, $\mu$(Mo-Kα) = 1.820 mm$^{-1}$, $\varrho_{calc}$ = 1.430 g/cm$^3$, 134255 reflections measured (6.398° ≤ 2Θ ≤ 64.958°), 12907 unique ($R_{int}$ = 0.0536, $R_{sigma}$ = 0.0546) which were used in all calculations, $GOF$ = 1.099, $D_{min}/D_{max}$ = -0.59/1.43 e/Å$^3$. The final $R_1$ was 0.0410 (I > 2σ(I)) and $wR_2$ was 0.1348 (all data).

### 2.10.5.2 $[Co_2(\mu\text{-}\eta^2\text{:}\eta^2\text{-}HC{\equiv}CAsC_4Ph_4)(CO)_6]$

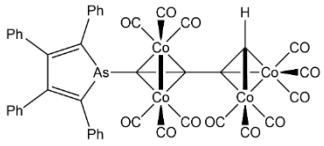


Prepared similarly to that above, except $Et_2O$ was used as the reaction solvent. Quantities: 0.25 g $HC{\equiv}CAsC_4Ph_4$ (0.54 mmol) and 0.2 g $[Co_2(CO)_8]$ (0.58 mmol). Chromatography on neutral alumina (20 x 2.5 cm) with petroleum ether followed by 9:1 petroleum ether/$Et_2O$ provides an orange band which is collected and dried, and the residue re-crystallised from the minimum amount of *n*-pentane under nitrogen at -20 °C giving dark orange crystals. Properties are identical to that above. Isolated yield: 0.26 g (0.35 mmol, 64%).

NMR: $^1H$ ($C_6D_6$, 400 MHz, 25 °C) δ 7.43—7.41 (m, 4H, $C_6H_5$), 7.05—7.01 (m, 8H, $C_6H_5$), 6.94—6.85 (m, 8H, $C_6H_5$), 5.73 (s, 1H, C*H*) ppm. 13C{1H} ($C_6D_6$, 176 MHz, 25 °C) δ 199.7 (br, *C*O), 150.5 (arsole {2,5}-*C*), 150.2 (arsole {3,4}-*C*), 139.1 ($C_6H_5$), 137.7 ($C_6H_5$), 130.4 ($C_6H_5$), 130.3 ($C_6H_5$), 128.6 ($C_6H_5$), 128.4 ($C_6H_5$), 128.3 ($C_6H_5$), 127.4 ($C_6H_5$), 85.4 (As*C*≡CH), 84.3 (AsC≡*C*H) ppm. IR (*n*-hexane, 25 °C) $\nu_{CO}$ = 2092(s), 2055(vs), 2032(vs), 2024(vs) $cm^{-1}$. HR-MS (ESI, MeCN, +ve ion) found $m/z$ 573.9525 (calc. for $C_{30}H_{21}{}^{75}As_1{}^{59}Co_2$ $[M-6CO]^+$: 573.9523). Analysis found 58.25% C, 2.88% H (calc. for $C_{36}H_{21}O_6{}^{75}As_1{}^{59}Co_2$: 58.25% C, 2.80% H).

Single crystals were obtained from *n*-pentane solution at -20 °C. One molecule of *n*-pentane was found in the asymmetric unit. $C_{36}H_{21}O_6As_1Co_2{\cdot}0.5C_5H_{12}$ ($M$ = 778.38 g/mol): black prism 0.115 × 0.258 × 0.472 mm, triclinic, space group *P*-1 (no. 2), $a$ = 12.1430(4) Å, $b$ = 15.7968(5) Å, $c$ = 18.8560(5) Å, $\alpha$ = 74.697(2)°, $\beta$ = 76.195(3)°, $\gamma$ = 87.482(3)°, $V$ = 3387.25(19) Å$^3$, $Z$ = 4, multi-scan correction $T_{min}/T_{max}$ = 0.843/1.000, $\mu$(Mo-Kα) = 1.995 $mm^{-1}$, $\varrho_{calc}$ = 1.526 g/cm$^3$, 32695 reflections measured (6.752° ≤ 2Θ ≤ 60.096°), 16114 unique ($R_{int}$ = 0.0268, $R_{sigma}$ = 0.0487) which were used in all calculations, $GOF$ = 1.027, $D_{min}/D_{max}$ = -1.06/1.11 e/Å$^3$. The final $R_1$ was 0.0393 (I > 2σ(I)) and $wR_2$ was 0.0904 (all data).

### 2.10.5.3 $[Co_2(\mu\text{-}\eta^2\text{:}\eta^2\text{:}\eta^2\text{-}HC{\equiv}CC{\equiv}CAsC_4Ph_4)(CO)_6]$



Prepared similarly to that above, except $Et_2O$ was used as the reaction solvent. Quantities: 0.2 g $HC{\equiv}CC{\equiv}CAsC_4Ph_4$ (0.41 mmol) and 0.3 g $[Co_2(CO)_8]$ (0.88 mmol). Chromatography on neutral alumina (20 x 2.5 cm) with petroleum ether followed by 9:1 petroleum ether/$Et_2O$ provides an orange band which is collected and dried, and the residue re-crystallised from the minimum amount of *n*-pentane under nitrogen at -20 °C. Properties are identical to that above. Isolated yield: 0.27 g (0.25 mmol, 60%).

NMR: $^1H$ ($C_6D_6$, 400 MHz, 25 °C) δ 7.53—7.50 (m, 6H, $C_6H_5$), 7.03—6.99 (m, 6H, $C_6H_5$), 6.92—6.81 (m, 8H, $C_6H_5$), 5.19 (s, 1H, C*H*) ppm. $^{13}C\{^1H\}$ ($C_6D_6$, 176 MHz, 25 °C) δ 199.4 (br, *C*O), 199.0 (br, *C*O), 151.5 (arsole {2,5}-*C*), 150.8 (arsole {3,4}-*C*), 138.9 ($C_6H_5$), 137.9 ($C_6H_5$), 131.0 ($C_6H_5$), 128.6 ($C_6H_5$), 128.3 ($C_6H_5$), 128.3 ($C_6H_5$), 127.5 ($C_6H_5$), 127.1 ($C_6H_5$), 104.2 (As-*C*≡CC≡CH), 92.5 (As-C≡*C*C≡CH), 92.4 (As-C≡C*C*≡CH), 81.0 (As-C≡CC≡*C*H)

ppm. IR (*n*-hexane, 25 °C) 2100(s), 2081(s), 2060(vs), 2054(sh), 2040(m), 2028(vs), 2014(m) $cm^{-1}$. HR-MS (ESI, MeCN, +ve ion) found $m/z$ 1040.7657 (calc. for $C_{43}H_{21}O_{12}{}^{75}As_1{}^{59}Co_4$ $[M]^+$: 1040.7655). Analysis found 50.20% C, 2.09% H (calc. for $C_{44}H_{21}O_{12}As_1Co_2$: 50.22% C, 2.01% H).

Single crystals were obtained from *n*-pentane at -20 °C. $C_{44}H_{21}AsCo_4O_{12}$ ($M$ = 1052.25 g/mol): red block 0.03 × 0.225 × 0.418 mm, monoclinic, space group $P2_1/c$ (no. 14), $a$ = 14.6320(3) Å, $b$ = 11.2023(2) Å, $c$ = 25.8606(4) Å, $\beta$ = 100.747(2)°, $V$ = 4164.51(13) Å$^3$, $Z$ = 4, Gaussian correction $T_{min}/T_{max}$ = 0.116/1.000, $\mu$(Cu-Kα) = 13.688 $mm^{-1}$, $\varrho_{calc}$ = 1.678 g/cm$^3$, 31190 reflections measured (8.386° ≤ 2Θ ≤ 147.418°), 8323 unique ($R_{int}$ = 0.0414, $R_{sigma}$ = 0.0400) which were used in all calculations, $GOF$ = 1.021, $D_{min}/D_{max}$ = -0.41/0.48 e/Å$^3$. The final $R_1$ was 0.0310 (I > 2σ(I)) and $wR_2$ was 0.0784 (all data).

## 2.11 References


1. F. C. Leavitt, T. A. Manuel and F. Johnson, *J. Am. Chem. Soc.,* **1959**, *81*, 3163-3164.
2. F. C. Leavitt, T. A. Manuel, F. Johnson, L. U. Matternas and D. S. Lehman, *J. Am. Chem. Soc.,* **1960**, *82*, 5099-5102.
3. E. H. Braye, W. Hübel and I. Caplier, *J. Am. Chem. Soc.,* **1961**, *83*, 4406-4413.
4. G. Märkl and H. Hauptmann, *J. Organomet. Chem.*, **1983**, *248*, 269-285.
5. A. J. Ashe, *J. Am. Chem. Soc.,* **1971**, *93*, 3293-3295.
6. A. J. Ashe, X. Fang and J. W. Kampf, *Organometallics*, **2001**, *20*, 2109-2113.
7. P. Jutzi and K. Deuchert, *Angew. Chem. Int. Ed. Eng.*, **1969**, *8*, 991-992.
8. Y. Ura, Y. Li, Z. Xi and T. Takahashi, *Tet. Lett.*, **1998**, *39*, 2787-2790.
9. C. Xi, S. Huo, T. H. Afifi, R. Hara and T. Takahashi, *Tet. Lett.*, **1997**, *38*, 4099-4102.
10. L. Liu, W. Geng, Q. Yang, W. X. Zhang and Z. Xi, *Organometallics*, **2015**, *34*, 4198-4201.
11. W. Geng, J. Wei, W. X. Zhang and Z. Xi, *J. Am. Chem. Soc.,* **2014**, *136*, 610-613.
12. H. Imoto, A. Urushizaki, I. Kawashima and K. Naka, *Chem. Eur. J.*, **2018**, *24*, 8797-8803.
13. A. J. Ashe, W. M. Butler and T. R. Diephouse, *Organometallics*, **1983**, *2*, 1005-1008.
14. S. Burck, M. Nieger and D. Gudat, *Z. Anorg. Allg. Chem.*, **2010**, *636*, 1263-1267.
15. Y. He, C. Dai, D. Wang, J. Zhu and G. Tan, *J. Am. Chem. Soc.*, **2022**, *144*, 5126-5135.
16. M. Ishidoshiro, Y. Matsumura, H. Imoto, Y. Irie, T. Kato, S. Watase, K. Matsukawa, S. Inagi, I. Tomita and K. Naka, *Org. Lett.*, **2015**, *17*, 4854-4857.
17. S. Sasaki, T. Mori and M. Yoshifuji, *Heteroatom Chem.*, **2006**, *17*, 344-349.
18. C. Qin, X. Xie, G. Wang, X. Jia and Y. Liu, *Tet. Lett.*, **2020**, *61*, 151388.
19. M. A. Paver, J. S. Joy, S. J. Coles, M. B. Hursthouse and J. E. Davies, *Polyhedron*, **2003**, *22*, 211-216.
20. A. B. Holmes, C. L. D. Jennings-White, A. H. Schulthess, B. Akinde and D. R. M. Walton, *J. Chem. Soc. Chem. Comm.*, **1979**, 840-842.
21. J. K. D. Surette, M. A. MacDonald, M. J. Zaworotko and R. D. Singer, *J. Chem. Cryst.*, **1994**, *24*, 715-717.
22. G. Eglinton and A. R. Galbraith, *J. Chem Soc.,* **1959**, 889-896.
23. A. S. Hay, *J. Org. Chem.*, **1962**, *27*, 3320-3321.
24. S. Chen, S. A. Pullarkat, Y. Li and P. H. Leung, *Eur. J. Inorg. Chem.*, **2011**, 3111-3121.
25. M. Ishidoshiro, H. Imoto, S. Tanaka and K. Naka, *Dalton Trans.,* **2016**, *45*, 8717-8723.
26. S. Iwasaki, Y. Miyake, H. Imoto and K. Naka, *Chem. Eur. J.*, **2022**, *28*, e202202084.
27. H. Imoto, I. Kawashima, C. Yamazawa, S. Tanaka and K. Naka, *J. Mat. Chem. C*, **2017**, *5*, 6697-6703.
28. B. E. Cavit, K. R. Grundy and W. R. Roper, *J. Chem. Soc. Chem. Comm.*, **1972**, 60-61.
29. A. F. Hill, M. Schultz and A. C. Willis, *Organometallics*, **2004**, *23*, 5729-5736.
30. M. J. Bartlett, A. F. Hill and M. K. Smith, *Organometallics*, **2005**, *24*, 5795-5798.
31. R. L. Cordiner, A. F. Hill and J. Wagler, *Organometallics*, **2009**, *28*, 4880-4885.
32. D. L. Lichtenberger, S. K. Renshaw and R. M. Bullock, *J. Am. Chem. Soc.,* **1993**, *115*, 3276-3285.
33. B. E. R. Schilling, R. Hoffmann and D. L. Lichtenberger, *J. Am. Chem. Soc.*, **1979**, *101*, 585-591.

34. J. E. McGrady, T. Lovell, R. Stranger and M. G. Humphrey, *Organometallics*, **1997**, *16*, 4004-4011.
35. A. F. Hill, C. D. Stewart and J. S. Ward, *Dalton Trans.*, **2015**, *44*, 5713-5726.
36. M. J. Bartlett, B. J. Frogley, A. F. Hill, M. Sharma, M. K. Smith and J. S. Ward, *Dalton Trans.*, **2019**, *48*, 16534-16554.
37. M. R. Torres, A. Vegas, A. Santos and J. Ros, *J. Organomet. Chem.*, **1986**, *309*, 169-177.
38. M. R. Torres, A. Vegas, A. Santos and J. Ros, *J. Organomet. Chem.*, **1987**, *326*, 413-421.
39. J. M. Bray and R. J. Mawby, *J. Chem. Soc., Dalton Trans.*, **1989**, 589-594.
40. A. F. Hill, *Comp. Organomet. Chem. II*, **1995**, 299-440.
41. I. D. Burns, A. F. Hill, A. J. P. White, D. J. Williams and J. D. Wilton-Ely, *Organometallics*, **1998**, *17*, 1552-1557.
42. N. W. Alcock, A. F. Hill, R. P. Melling and A. R. Thompsett, *Organometallics*, **1993**, *12*, 641-648.
43. J. Maurer, M. Linseis, B. Sarkar, B. Schwederski, M. Niemeyer, W. Kaim, S. Záliš, C. Anson, M. Zabel and R. F. Winter, *J. Am. Chem. Soc.*, **2008**, *130*, 259-268.
44. M. I. Bruce, *Chem. Rev.*, **1991**, *91*, 197-257.
45. J. Silvestre and R. Hoffmann, *Helv. Chim. Acta*, **1985**, *68*, 1461-1506.
46. I. de los Ríos, M. J. Tenorio, M. C. Puerta and P. Valerga, *J. Am. Chem. Soc.*, **1997**, *119*, 6529-6538.
47. K. Tatsumi, R. Hoffmann and J. L. Templeton, *Inorg. Chem.*, **1982**, *21*, 466-468.
48. J. L. Templeton, *Adv. Organomet. Chem.*, **1989**, *29*, 1-100.
49. B. Burcher, K. J. Sanders, L. Benda, G. Pintacuda, E. Jeanneau, A. A. Danopoulos, P. Braunstein, H. Olivier-Bourbigou and P. A. R. Breuil, *Organometallics*, **2017**, *36*, 605-613.
50. A. K. Burrell, G. P. Elliott, C. E. F. Rickard and W. R. Roper, *Appl. Organomet. Chem.*, **1990**, *4*, 535-542.
51. R. L. Beddoes, C. Bitcon, R. W. Grime, A. Ricalton and M. W. Whiteley, *J. Chem. Soc., Dalton Trans.*, **1995**, 2873-2883.
52. T. Kuwabara, K. Sakajiri, Y. Oyama, S. Kodama and Y. Ishii, *Organometallics*, **2019**, *38*, 1560-1566.
53. K. R. Birdwhistell, S. J. N. Burgmayer and J. L. Templeton, *J. Am. Chem. Soc.*, **1983**, *105*, 7789-7790.
54. K. R. Birdwhistell, T. L. Tonker, J. L. Templeton and W. R. Kenan, *J. Am. Chem. Soc.*, **1985**, *107*, 4474-4483.
55. A. B. Antonova, N. E. Kolobova, P. V. Petrovsky, B. V. Lokshin and N. S. Obezyuk, *J. Organomet. Chem.*, **1977**, *137*, 55-67.
56. A. Wong and J. A. Gladysz, *J. Am. Chem. Soc.*, **1982**, *104*, 4948-4950.
57. A. J. L. Pombeiro, S. S. P. R. Almeida, M. F. Silva, J. C. Jeffrey and R. L. Richards, *J. Chem. Soc. Dalton Trans.*, **1989**, 2381-2387.
58. H. Braunschweig, C. K. L. Brown, R. D. Dewhurst, J. O. C. Jimenez-Halla , T. Kramer, I. Krummenacher and B. Pfaffinger, *Chem. Eur. J.*, **2014**, *20*, 1427-1433.
59. S. Hideki, F. Takeaki and S. Kenkichi, *Chem. Lett.*, **1992**, *21*, 339-342.
60. K. Venkatesan, O. Blacque, T. Fox, M. Alfonso, H. W. Schmalle, S. Kheradmandan and H. Berke, *Organometallics*, **2005**, *24*, 920-932.
61. D. C. Miller and R. J. Angelici, *Organometallics*, **1991**, *10*, 79-89.
62. A. F. Hill, A. G. Hulkes, A. J. P. White and D. J. Williams, *Organometallics*, **2000**, *19*, 371-373.
63. M. Yuichiro, I. Yousuke, K. Yusuke and I. Youichi, *Chem. Lett.*, **2009**, *38*, 534-535.
64. P. J. King, S. A. R. Knox, M. S. Legge, A. G. Orpen, J. N. Wilkinson and E. A. Hill, *J. Chem. Soc., Dalton Trans.*, **2000**, 1547-1548.
65. D. Touchard, P. Haquette, S. Guesmi, L. Le Pichon, A. Daridor, L. Toupet and P. H. Dixneuf, *Organometallics*, **1997**, *16*, 3640-3648.
66. Y. Wakatsuki, H. Yamazaki, N. Kumegawa, T. Satoh and J. Y. Satoh, *J. Am. Chem. Soc.*, **1991**, *113*, 9604-9610.
67. D. Amoroso, G. P. A. Yap and D. E. Fogg, *Organometallics*, **2002**, *21*, 3335-3343.
68. E. A. Shaffer, C. L. Chen, A. M. Beatty, E. J. Valente and H. J. Schanz, *J. Organomet. Chem.*, **2007**, *692*, 5221-5233.
69. F. Strinitz, A. Waterloo, J. Tucher, E. Hübner, R. R. Tykwinski and N. Burzlaff, *Eur. J. Inorg. Chem.*, **2013**, 5181-5186.

70. M. I. Bruce, M. G. Humphrey, G. A. Koutsantonis and B. K. Nicholson, *J. Organomet. Chem.*, **1985**, *296*, C47-C50.
71. K. Helmdach, J. Rüger, A. Villinger and W. W. Seidel, *Chem. Comm.*, **2016**, *52*, 2616-2619.
72. B. J. Frogley and A. F. Hill, *Chem. Comm.*, **2019**, *55*, 15077-15080.
73. B. Liu, H. Wang, H. Xie, B. Zeng, J. Chen, J. Tao, T. B. Wen, Z. Cao and H. Xia, *Angew. Chem. Int. Ed.*, **2009**, *48*, 5430-5434.
74. T. Kuwabara, Y. Aoki, K. Sakajiri, K. Deguchi, S. Takamori, A. Hamano, K. Takano, H. Houjou and Y. Ishii, *Organometallics*, **2020**, *39*, 711-718.
75. A. Tohmé, G. Grelaud, G. Argouarch, T. Roisnel, S. Labouille, D. Carmichael and F. Paul, *Angew. Chem. Int. Ed.*, **2013**, *52*, 4445-4448.
76. Y. Wakatsuki, N. Koga, H. Yamazaki and K. Morokuma, *J. Am. Chem. Soc.*, **1994**, *116*, 8105-8111.
77. C. Slugovc, K. Mereiter, R. Schmid and K. Kirchner, *Organometallics*, **1998**, *17*, 827-831.
78. E. Rüba, C. Gemel, C. Slugovc, K. Mereiter, R. Schmid and K. Kirchner, *Organometallics*, **1999**, *18*, 2275-2280.
79. C. W. Liu, Y. C. Lin, S. L. Huang, Y. H. Liu and Y. Wang, *Organometallics*, **2007**, *26*, 3431-3439.
80. S. D. Drouin, H. M. Foucault, G. P. A. Yap and D. E. Fogg, *Organometallics*, **2004**, *23*, 2583-2590.
81. K. J. Harlow, A. F. Hill and J. D. E. T. Wilton-Ely, *J. Chem. Soc. Dalton Trans.*, **1999**, 285-292.
82. D. Touchard, S. Guesmi, M. Bouchaib, P. Haquette, A. Daridor and P. H. Dixneuf, *Organometallics*, **1996**, *15*, 2579-2581.
83. S. D. Drouin, S. Monfette, D. Amoroso, G. P. A. Yap and D. E. Fogg, *Organometallics*, **2005**, *24*, 4721-4728.
84. L. Quebatte, R. Scopelliti and K. Severin, *Eur. J. Inorg. Chem.*, **2006**, 231-236.
85. T. Biberger, N. Nöthling, M. Leutzsch, C. P. Gordon, C. Copéret and A. Fürstner, *Angew. Chem. Int. Ed.*, **2022**.
86. J. D. Gilbert, M. C. Baird and G. Wilkinson, *J. Chem. Soc. A*, **1968**, 2198-2201.
87. T. A. Stephenson, E. S. Switkes and P. W. Armit, *J. Chem. Soc., Dalton Trans.*, **1974**, 1134-1139.
88. M. I. Bruce and A. G. Swincer, *Adv. Organomet. Chem.*, **1983**, *22*, 59-128.
89. T. Blackmore, M. I. Bruce and F. G. A. Stone, *J. Chem. Soc. A*, **1971**, 2376-2382.
90. R. J. Haines and A. L. Du Preez, *J. Organomet. Chem.*, **1975**, *84*, 357-367.
91. M. I. Bruce and R. C. Wallis, *J. Organomet. Chem.*, **1978**, *161*, C1-C4.
92. M. Bruce and R. Wallis, *Aust. J. Chem.*, **1979**, *32*, 1471-1485.
93. Y. Wakatsuki, *J. Organomet. Chem.*, **2004**, *689*, 4092-4109.
94. M. Otsuka, N. Tsuchida, Y. Ikeda, N. Lambert, R. Nakamura, Y. Mutoh, Y. Ishii and K. Takano, *Organometallics*, **2015**, *34*, 3934-3943.
95. D. Touchard, C. Morice, V. Cadierno, P. Haquette, L. Toupet and P. H. Dixneuf, *J. Chem. Soc. Chem. Comm.*, **1994**, 859-860.
96. Y. Mutoh, K. Imai, Y. Kimura, Y. Ikeda and Y. Ishii, *Organometallics*, **2011**, *30*, 204-207.
97. H. Katayama, C. Wada, K. Taniguchi and F. Ozawa, *Organometallics*, **2002**, *21*, 3285-3291.
98. V. Cadierno, S. Conejero, M. P. Gamasa and J. Gimeno, *J. Chem. Soc. Dalton Trans.*, **2000**, 451-457.
99. V. Cadierno, M. P. Gamasa, J. Gimeno, M. González-Cueva, E. Lastra, J. Borge, S. García-Granda and E. Pérez-Carreño, *Organometallics*, **1996**, *15*, 2137-2147.
100. M. I. Bruce, P. Hinterding, P. J. Low, B. W. Skelton and A. H. White, *J. Chem. Soc. Dalton Trans.*, **1998**, 467-474.
101. M. I. Bruce, B. G. Ellis, B. W. Skelton and A. H. White, *J. Organomet. Chem.*, **2005**, *690*, 1772-1783.
102. M. P. Gamasa, J. Gimeno, B. M. Martin-Vaca, J. Borge, S. Garcia-Granda and E. Perez-Carreno, *Organometallics*, **1994**, *13*, 4045-4057.
103. S. Abbott, S. G. Davies and P. Warner, *J. Organomet. Chem.*, **1983**, *246*, C65-C68.
104. M. I. Bruce, M. G. Humphrey and M. J. Liddell, *J. Organomet. Chem.*, **1987**, *321*, 91-102.
105. M. I. Bruce, G. A. Koutsantonis, M. J. Liddell and B. K. Nicholson, *J. Organomet. Chem.*, **1987**, *320*, 217-227.
106. N. J. Brown, M. A. Fox, M. E. Smith, D. S. Yufit, J. A. K. Howard and P. J. Low, *J. Organomet. Chem.*, **2009**, *694*, 4042-4048.

107. M. I. Bruce, M. P. Cifuentes, M. R. Snow and E. R. T. Tiekink, *J. Organomet. Chem.*, **1989**, *359*, 379-399.
108. Y. Ajioka, Y. Matsushima, K. Onitsuka, H. Yamazaki and S. Takahashi, *J. Organomet. Chem.*, **2001**, *618*, 601-615.
109. V. Cadierno, M. Pilar Gamasa, J. Gimeno, E. Pérez-Carreño and S. García-Granda, *J. Organomet. Chem.*, **2003**, *670*, 75-83.
110. M. J. Cowley, J. M. Lynam, R. S. Moneypenny, A. C. Whitwood and A. J. Wilson, *Dalton Trans.*, **2009**, 9529-9542.
111. S. G. Davies, J. P. McNally and A. J. Smallridge, *Adv. Organomet. Chem.*, **1990**, *30*, 1-76.
112. A. M. Lozano-Vila, S. Monsaert, A. Bajek and F. Verpoort, *Chem. Rev.,* **2010**, *110*, 4865-4909.
113. N. M. Kostic and R. F. Fenske, *Organometallics*, **1982**, *1*, 974-982.
114. P. T. Czech, X. Q. Ye and R. F. Fenske, *Organometallics*, **1990**, *9*, 2016-2022.
115. M. I. Bruce, A. G. Swincer and R. C. Wallis, *J. Organomet. Chem.*, **1979**, *171*, C5-C8.
116. R. F. Winter and F. M. Hornung, *Organometallics*, **1997**, *16*, 4248-4250.
117. F. Coat, M. Guillemot, F. Paul and C. Lapinte, *J. Organomet. Chem.*, **1999**, *578*, 76-84.
118. K. Ilg and H. Werner, *Angew. Chem. Int. Ed.*, **2000**, *39*, 1632-1634.
119. R. G. Parr and W. Yang, *J. Am. Chem. Soc.*, **1984**, *106*, 4049-4050.
120. W. Yang and W. J. Mortier, *J. Am. Chem. Soc.*, **1986**, *108*, 5708-5711.
121. Y. Li and J. N. S. Evans, *J. Am. Chem. Soc.*, **1995**, *117*, 7756-7759.
122. P. Zhou, P. W. Ayers, S. Liu and T. Li, *Phy. Chem. Chem. Phys.*, **2012**, *14*, 9890-9896.
123. M. Zhang, D. Wei, Y. Wang, S. Li, J. Liu, Y. Zhu and M. Tang, *Org. Biomol. Chem.*, **2014**, *12*, 6374-6383.
124. P. P. Zamora, K. Bieger, A. Cuchillo, A. Tello and J. P. Muena, *J. Mol. Struct.*, **2021**, *1227*, 129-139.
125. P. P. Zhou and D. G. Zhou, *J. Phys. Org. Chem.*, **2021**, *34*, 4254-4259.
126. F. Mendez and J. L. Gazquez, *J. Am. Chem. Soc.*, **1994**, *116*, 9298-9301.
127. F. Gilardoni, J. Weber, H. Chermette and T. R. Ward, *J. Phys. Chem. A*, **1998**, *102*, 3607-3613.
128. R. M. Kirk and A. F. Hill, *Chem. Sci.*, **2022**, *13*, 6830-6835.
129. F. A. Bulat, E. Chamorro, P. Fuentealba and A. Toro-Labbé, *J. Phys. Chem. A*, **2004**, *108*, 342-349.
130. P. Bultinck, R. Carbó-Dorca and W. Langenaeker, *J. Chem. Phys.*, **2003**, *118*, 4349-4356.
131. P. Fuentealba, P. Pérez and R. Contreras, *J. Chem. Phys.*, **2000**, *113*, 2544-2551.
132. P. W. Ayers, R. C. Morrison and R. K. Roy, *J. Chem. Phys.*, **2002**, *116*, 8731-8744.
133. M. I. Bruce, P. Hinterding, P. J. Low, B. W. Skelton and A. H. White, *Chem. Comm.*, **1996**, 1009-1010.
134. V. Cadierno, M. P. Gamasa, J. Gimeno, M. C. López-González, J. Borge and S. García-Granda, *Organometallics*, **1997**, *16*, 4453-4463.
135. R. F. Winter, *Eur. J. Inorg. Chem.*, **1999**, 2121-2126.
136. V. Cadierno, S. Conejero, M. P. Gamasa, J. Gimeno, E. Pérez-Carreño and S. García-Granda, *Organometallics*, **2001**, *20*, 3175-3189.
137. M. Baya, M. L. Buil, M. A. Esteruelas, A. M. López, E. Oñate and J. R. Rodríguez, *Organometallics*, **2002**, *21*, 1841-1848.
138. S. H. Tsai, Y. C. Lin and Y. H. Liu, *Chem. Asian J.*, **2016**, *11*, 3072-3083.
139. G. Sennyey and F. Mathey, *Tet. Lett.*, **1981**, *22*, 4713-4716.
140. W. A. Schenk and E. Voß, *J. Organomet. Chem.*, **1994**, *467*, 67-73.
141. S. Yasuike, H. Ohta, S. Shiratori, J. Kurita and T. Tsuchiya, *J. Chem. Soc. Chem. Comm.*, **1993**, 1817-1819.
142. S. Yasuike, T. Kiharada, J. Kurita and T. Tsuchiya, *Chem. Comm.*, **1996**, 2183-2184.
143. I. Kawashima, H. Imoto, M. Ishida, H. Furuta, S. Yamamoto, M. Mitsuishi, S. Tanaka, T. Fujii and K. Naka, *Angew. Chem. Int. Ed.*, **2019**, *58*, 11686-11690.
144. M. Letzel, H. F. Grützmacher, D. Stein and H. Grützmacher, *Dalton Trans.*, **2008**, 3282-3291.
145. S. Y. Kim and J. C. Choe, *Bull. Korean Chem. Soc.*, **2010**, *31*, 2588-2592.
146. M. Z. Kassaee, A. Cheshmehkani, S. M. Musavi, M. Majdi and E. Motamedi, *J. Mol. Struct.* **2008**, *865*, 73-78.
147. H. Jansen, J. C. Slootweg, A. W. Ehlers and K. Lammertsma, *Organometallics*, **2010**, *29*, 6653-6659.

148. S. Y. KIM and J. C. CHOE, *Int. J. Mass Spect.*, **2010**, *294*, 40-46.
149. R. D. W. KEMMITT and D. R. RUSSELL, *Comp. Organomet. Chem.*, **1982**, 1-276.
150. P. L. PAUSON and I. U. KHAND, *Ann. New York Acad. Sci.*, **1977**, *295*, 2-14.
151. J. BLANCO-URGOITI, L. AÑORBE, L. PÉREZ-SERRANO, G. DOMÍNGUEZ and J. PÉREZ-CASTELLS, *Chem. Soc. Rev.,* **2004**, *33*, 32-42.
152. F. E. HONG, Y. C. CHANG, R. E. CHANG, S. C. CHEN and B. T. KO, *Organometallics*, **2002**, *21*, 961-967.
153. A. K. POWELL and M. J. WENT, *J. Chem. Soc. Dalton Trans.*, **1992**, 439-445.
154. F. BASOLO and A. WOJCICKI, *J. Am. Chem. Soc.*, **1961**, *83*, 520-525.
155. F. UNGVÁRY and L. MARKÓ, *Chem. Ber.*, **1972**, *105*, 2457-2461.
156. P. C. ELLGEN, *Inorg. Chem.*, **1972**, *11*, 691-695.
157. R. F. HECK, *J. Am. Chem. Soc.*, **1963**, *85*, 657-661.
158. G. CETINI, O. GAMBINO, R. ROSSETTI and E. SAPPA, *J. Organomet. Chem.*, **1967**, *8*, 149-154.
159. M. R. TIRPAK, C. A. HOLLINGSWORTH and J. H. WOTIZ, *J. Org. Chem.*, **1960**, *25*, 687-690.
160. P. H. BIRD and A. R. FRASER, *J. Chem. Soc. Chem. Comm.*, **1970**, 681-682.
161. H. LANG and L. ZSOLNAI, *Z. Naturfor. B*, **1990**, *45*, 1529-1536.
162. G. BOR, *Chem. Ber.*, **1963**, *96*, 2644-2648.
163. R. DICKSON and D. YAWNEY, *Aust. J. Chem.*, **1968**, *21*, 97-102.
164. W. G. SLY, *J. Am. Chem. Soc.*, **1959**, *81*, 18-20.
165. N. A. BAILEY and R. MASON, *J. Chem. Soc. A*, **1968**, 1293-1299.
166. F. A. COTTON, J. D. JAMERSON and B. R. STULTS, *J. Am. Chem. Soc.*, **1976**, *98*, 1774-1779.
167. P. C. LEUNG and P. COPPENS, *Acta Cryst. B*, **1983**, *39*, 535-542.
168. J. H. NELSON and H. B. JONASSEN, *Coord. Chem. Rev.*, **1971**, *6*, 27-63.
169. R. S. DICKSON and P. J. FRASER, *Adv. Organomet. Chem.*, **1974**, *12*, 323-377.
170. D. M. HOFFMAN, R. HOFFMANN and C. R. FISEL, *J. Am. Chem. Soc.*, **1982**, *104*, 3858-3875.
171. F. A. L. ANET and I. YAVARI, *J. Am. Chem. Soc.*, **1978**, *100*, 7814-7819.
172. R. C. J. ATKINSON, L. J. HOPE-WEEKS, M. J. MAYS and G. A. SOLAN, *J. Organomet. Chem.*, **2007**, *692*, 2076-2085.
173. A. KÖNIG, C. WAGNER, M. BETTE and D. STEINBORN, *Dalton Trans.*, **2012**, *41*, 7156-7162.
174. B. J. FROGLEY, A. F. HILL and R. M. KIRK, *Chem. Comm.*, **2021**, *57*, 8770-8773.

# Chapter 3

# Arsole and Arsolyl Complexes of Cobalt

## 3.1 Preamble

Among the homoleptic transition metal carbonyls, $[Co_2(CO)_8]$ ranks proudly in kinetic lability. Its reactions often require little-to-no additional chemical, thermal or photochemical encouragement (*cf.* $[Cr(CO)_6]$ or $[Fe(CO)_5]$), readily undergoing replacement of one or more carbonyl ligands upon treatment with LEWIS bases. Its reactions with nucleophiles and electrophiles may either preserve or cleave the (relatively fragile) dicobalt interaction, the latter almost universally accompanied by a formal dismutative reduction-oxidation of the metal centres. Indeed, a great deal of organometallic cobalt chemistry is dominated by the 1-, 0 and 1+ oxidation states: the ability of the metal to undergo both one- and two-electron processes is as much a valuable aspect of its synthetic and catalytic utility as it is an opportunistic pathway toward novel (and oftentimes, mechanistically inexplicable) mono- and polynuclear assemblies.

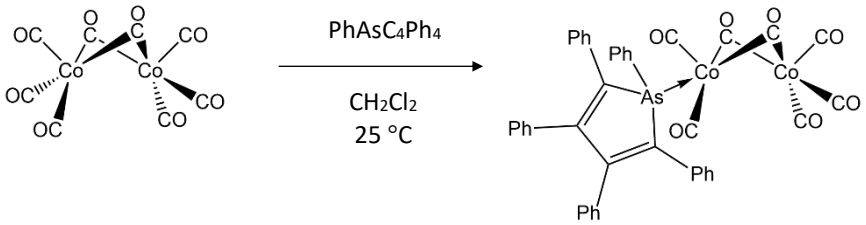
Prior to this work, no cobalt complexes featuring a neutral arsole ($R'AsC_4R_4$) or anionic arsolyl ($[AsC_4R_4]^-$) ligand had been described, and moreover surprisingly few phosphole/phospholyl complexes were known either. Cobalt – despite playing a leading role in establishing and developing many fundamental concepts in coordination and organometallic chemistry – appears to have been largely neglected by practitioners of heterocyclic chemistry in favour of its neighbours, particularly iron and manganese. The conclusion of the previous chapter observed π-alkyne complexes of Co(0) derived from ethynyl/butadiynyl arsoles, and it seemed appropriate to follow this with the first examples of simple $\lambda^3$-arsole coordination to $[Co_2(CO)_8]$. The length of this chapter is testament to how unexpectedly fruitful the outcomes of these endeavours were, beginning with humble σ-arsole complexes of Co(0) and traversing a variety of reaction patterns, culminating in the isolation of novel σ-, π-, and μ-σ:π-arsolyl complexes of Co(I).

A small portion of the following work (**Sections 3.3** and **3.4**) has already been published.[1]

## 3.2 Arsole Complexes of Cobalt(0)

### 3.2.1 Synthesis of $[Co_2(PhAsC_4Ph_4)(CO)_7]$

The combination of equimolar quantities of 1,2,3,4,5-pentaphenylarsole ($PhAsC_4Ph_4$) and $[Co_2(CO)_8]$ in $CH_2Cl_2$ solution at ambient temperature results in gas evolution and the isolation of $[Co_2(PhAsC_4Ph_4)(CO)_7]$ as a dark red solid in good yield (**Scheme 3.1**).* Single crystals were grown from $CH_2Cl_2$/*n*-hexane at -20 °C and the crystal structure (as the $CH_2Cl_2$ solvate) is shown in **Figure 3.1**.




**Scheme 3.1**: Synthesis of $[Co_2(PhAsC_4Ph_4)(CO)_7]$.

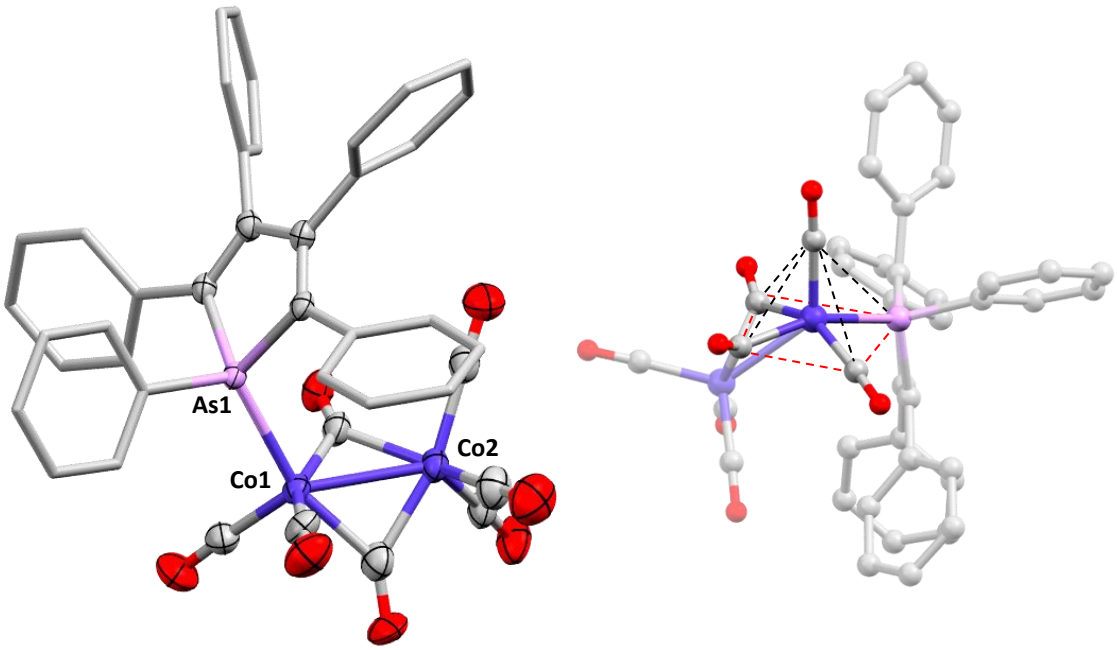



**Figure 3.1**: The molecular structure of $[Co_2(PhAsC_4Ph_4)(CO)_7]\cdot CH_2Cl_2$ in a crystal. Phenyl groups simplified, and dichloromethane solvate molecule and hydrogen atoms omitted for clarity. Ellipsoids shown at 50% displacement. **Inset**: Abbreviated perspective of the molecule highlighting the square-based pyramidal geometry of the Co(0) centre(s).

* Throughout this chapter the depictions of $[Co_2(CO)_8]$ and derivatives may on occasion omit a formal Co-Co bond. Although representation of such a bond is prevalent in the literature and textbooks, recent theoretical analysis of the bonding argues against this, however reassuring it might be for electron-counting purposes. See J. C. Green, M. L. H. Green, G. Parkin *Chem. Comm.*, **2012**, *48*, 11481—111503.

The molecular structure reveals mono-substitution of the $[Co_2(CO)_8]$ molecule with retention of the locally *pseudo*-$C_{2v}$ $Co_2(\mu\text{-}CO)_2$ carbonyl-bridged, bent framework. The geometries of both Co(0) atoms are that of distorted square-based pyramids (Co1 $\tau_5 = 0.12$; Co2 $\tau_5 = 0.23$) with the pentaphenylarsole ligand occupying a basal coordination site (**Figure 3.1**, **Inset**) *trans* to one of the bridging carbonyls. The angle of intersection of these mean basal planes is *ca* 88° with the local fold angle of the bridging carbonyl ligands being *ca* 55°. The As→Co dative bond measures 2.3623(9) Å, and the Co-Co covalent bond of 2.4994(1) Å is slightly shorter than the same bond in the parent $[Co_2(CO)_8]$ (2.5293(8) Å;[2] sum of covalent radii 2.52 Å*). Replacement of one or more carbonyl ligands appears to fortify the dicobalt interaction by raising the energy of the metal-centred LUMO and rendering homolysis an energetically less-accessible process (either by thermal or photochemical means). Circumstantial evidence for an increased HOMO-LUMO gap upon substitution is found in the bathochromic shift of observed complexes colours *cf.* $[Co_2(CO)_8]$ is orange whereas $[Co_2L_2(CO)_6]$ are invariably shades of red.[3] The increased basicity of the substituted cobalt centre is also reflected in distances to the carbonyl ligands: the mean Co-$C_{bridging}$ distances are shorter to Co1 (1.912(6) Å) than to Co2 (1.969(6) Å), as are the mean Co-$C_{terminal}$ distances *viz.* Co1-$C_{basal}$ 1.807(4) and Co1-$C_{axial}$ 1.784(5) Å *vs.* Co2-$C_{basal}$ 1.829(5) and Co2-$C_{axial}$ 1.806(5) Å, though these differences admittedly lie at the boundary of statistical certainty (6 e.s.d).

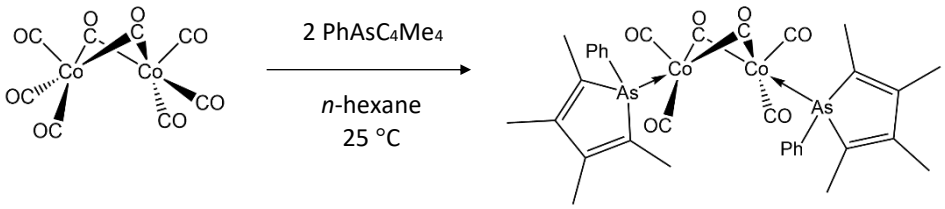
Attempts to prepare a disubstituted complex of the form $[Co_2(PhAsC_4Ph_4)_2(CO)_6]$ were unsuccessful, either due to the poor nucleophilicity of pentaphenylarsole or the steric encumbrance of the ligand, or both. Combination of $[Co_2(CO)_8]$ with two equivalents of $PhAsC_4Ph_4$ in $CH_2Cl_2$ led to the isolation of $[Co_2(PhAsC_4Ph_4)(CO)_7]$ only and most of the unreacted arsole ligand could be recovered by chromatography. This contrasts with the increased basicity of $PhAsC_4Me_4$ and $PhAsC_4Et_4$ which always lead to the formation of disubstituted products regardless of reagent stoichiometry (**Sections 3.2.2** and **3.2.3**). Characterisation of $[Co_2(PhAsC_4Ph_4)(CO)_7]$ was most easily achieved *via* high-resolution mass spectrometry which yielded the molecular ion (and fragments of decarbonylation) since attempts to collect

* The crystal structure of $[Co_2(CO)_8]$ at 298 K was originally reported by SUMNER, KLUG, and ALEXANDER in 1964 who measured a Co-Co bond of 2.524(2) Å. See *Acta Cryst.*, **1964**, *17*, 732—742. The value given in the text here was reported by LEUNG and COPPENS in 1983 who collected a higher-precision dataset at 100 K.

satisfactory NMR spectra (in both $C_6D_6$ and $CD_2Cl_2$) were complicated by the presence of severely broadened signals, seemingly from trace quantities of soluble paramagnetic species which could not be removed by chromatography: $[Co_2(CO)_8]$ and derivatives are known to undergo homolysis in solution to a pair of metal-centred radicals.[4, 5]

### 3.2.2 Synthesis of $[Co_2(PhAsC_4Me_4)_2(CO)_6]$

As mentioned above, the combination of the stronger σ-base 1-phenyl-2,3,4,5-tetramethylarsole ($PhAsC_4Me_4$) with $[Co_2(CO)_8]$ in *n*-hexane solution led to the formation of disubstituted $[Co_2(PhAsC_4Me_4)_2(CO)_6]$, irrespective of reagent stoichiometry (**Scheme 3.2**). The bis(arsole) complex was isolated in good yield as a dark red solid and single crystals confirming its formulation were obtained by slow evaporation of *n*-hexane solution at -30 °C; the molecular structure as determined by X-ray diffraction is shown in **Figure 3.2**. Satisfactory NMR spectra could not be acquired, unfortunately.




**Scheme 3.2**: Synthesis of $[Co_2(PhAsC_4Me_4)(CO)_6]$.

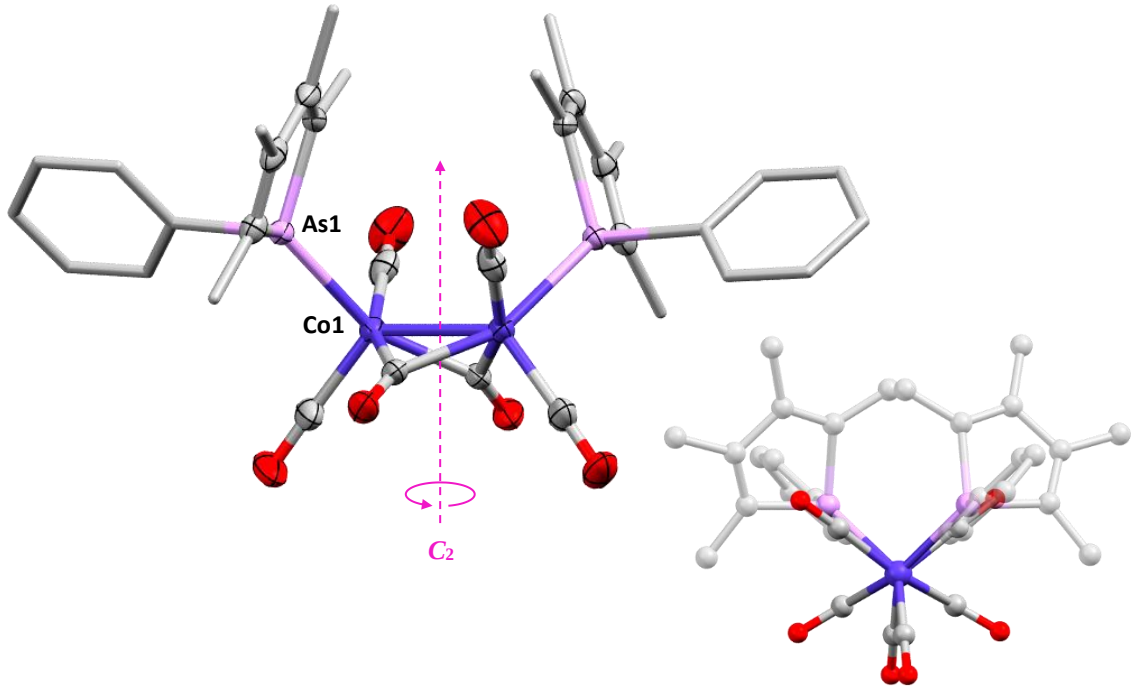



**Figure 3.2**: The molecular structure of $[Co_2(PhAsC_4Me_4)_2(CO)_6]$ in a crystal. Phenyl and methyl groups simplified and hydrogen atoms omitted for clarity. Ellipsoids shown at 50% displacement. **Inset**: Abbreviated perspective of the molecule highlighting the eclipsing ligand field, viewed along the Co-Co vector. $C_2$ = crystallographic two-fold axis of rotation.

Like the pentaphenylarsole complex (**Figure 3.1**), the $C_{2v}$-symmetric carbonyl-bridged core of the parent $[Co_2(CO)_8]$ platform is preserved upon substitution by $PhAsC_4Me_4$. The complex crystallises in monoclinic *I*2/*a* and a crystallographic two-fold rotation axis lies perpendicular to the Co-Co vector such that one half of the molecule is unique. The Co-Co separation (2.4966(5) Å) is crystallographically identical to that in $[Co_2(PhAsC_4Ph_4)(CO)_7]$ (2.4994(1) Å) as is the As→Co dative bond (2.3592(6) Å). The coordination environment of the Co(0) centre(s) is also firmly that of a square-based pyramid ($\tau_5$ = 0.06) with the pair of mean basal planes intersecting at *ca* 87° and a local fold angle at the bridging carbonyl ligands of *ca* 60°. The ligands decorating each Co(0) centre are approximately eclipsed when viewed along the dicobalt vector (As-Co-Co-As torsion angle *ca* 92°; **Figure 3.2, Inset**), and both arsole ligands occupy basal coordination sites with the *As*-phenyl residues projected toward the exterior of the molecule approximately parallel to the Co-Co vector.

The complex $[Co_2(PhAsC_4Me_4)_2(CO)_6]$ displays a different solution IR spectrum depending on the polarity of the medium in which it is dissolved and serves as an illustrative example of the non-rigidity of many complexes derived from the $[Co_2(CO)_8]$ platform, including $[Co_2(CO)_8]$ itself. The presence of three

distinct structural isomers (in dynamic equilibrium) had been deduced by meticulous examination of numerous IR data[6-16] throughout the 1950's—70's, conclusions which were eventually proven correct by low-temperature matrix isolation[17] and X-ray diffraction studies,[2, 18-20] and recently re-investigated by ultra-fast IR spectroscopy[21] and DFT-computational modelling.[22] These three isomers are illustrated in **Figure 3.3** and comprise a $C_{2v}$-symmetric carbonyl-bridged species with a pair of square-pyramidal Co(0) centres (the ground state structure), and two non-bridged species which differ in the arrangement of the trigonal bipyramidal Co(0) moieties, either axially ($D_{3d}$-symmetry) or radially ($D_{2d}$-symmetry) bonded to the second metal.* In principle, each isomer may be further sub-divided by the relative positions of the two non-carbonyl ligands which lends an additional degree of complexity to the system, though this point will be elaborated at a later stage in this section (*viz.* **Figure 3.5**).

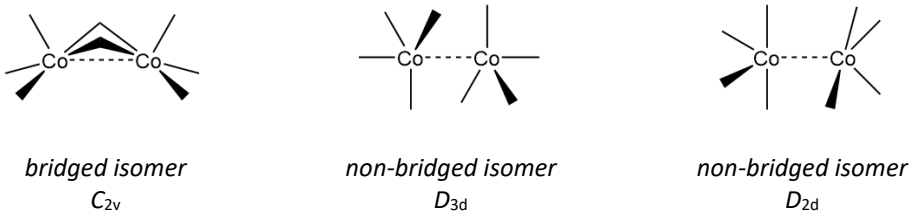



**Figure 3.3**: Illustrations of three isomeric cores of $[Co_2(CO)_8]$ (and substituted derivatives) generated by structural redistribution of the eight ligands, which have been omitted for simplicity. The cobalt-cobalt vector is hashed for distinction.

The specific isomer(s) of $[Co_2L_2(CO)_6]$ observed in solution depends on several factors:

1) *The electronic properties of the ligands L*: stronger σ-donors tend to favour non-bridged configurations since the increased basicity of the Co(0) centre(s) is more efficiently disseminated *via* π-retrodonation to terminal rather than bridging carbonyl ligands *viz.*, $[Co_2(AsEt_3)_2(CO)_6]$ exists as a *ca* 2:1 ratio of bridged and non-bridged isomers in cyclohexane, whereas $[Co_2(PEt_3)_2(CO)_6]$ is almost exclusively the latter in the same solvent.[12] $[Co_2(SbEt_3)_2(CO)_6]$ is especially reticent with the equilibrium lying almost wholly toward

* These $D_{3d}$ and $D_{2d}$ non-bridged isomers will be henceforth referred to in collective terms since they may readily interconvert by BERRY *pseudo*-rotation in a process which has a much lower energy barrier than the $D_{3d}/D_{2d} \rightarrow C_{2v}$ rearrangement. With this in mind, the staggered conformation of a $D_{3d}$ configuration has obvious geometric advantages over the $D_{2d}$ form with respect to mutual steric/electrostatic interactions the radial ligands may experience. See D. KARAKAŞ and S.E. KARIPER *J. Mol. Struc.*, **2014**, *1062*, 77—81. In practice, distinguishing between the two non-bridged forms from IR spectroscopy alone can be difficult due to the extensive overlap of $\nu_{CO}$ vibrations.

carbonyl-bridged isomers in cyclohexane. Further increasing the nucleophilicity of the ligand promotes heterolytic Co-Co bond rupture and the formation of ionic compounds *cf.* $[Co\{P(n\text{-}Bu)_3\}_2(CO)_3][Co(CO)_4]$,[14] also observed for isocyanides and *N*-heterocyclic carbenes. This is rationalised on L imparting a strong *trans* influence on the Co-Co bond and the $[Co(CO)_4]^-$ anion being a reasonably good nucleofuge.*

2) *The steric properties of the ligands L*: ligands of greater steric cone angle tend to favour non-bridged isomers since the spatial arrangement of the eight substituents is less congested within the coordination spheres of two trigonal bipyramids ($D_{3d}$ especially), compared to a pair of edge-sharing square-based pyramids ($C_{2v}$). Completely segregating electronic from steric effects is a not a simple task since ligands with larger geometric volume are, on average, expected to contain a greater number of electron-releasing atoms.[23] With this caveat in mind, the trend may be observed with judicious selection of ligand composition *viz.* $[Co_2\{As(n\text{-}Pr)_3\}_2(CO)_6]$ and $[Co_2\{As(n\text{-}Bu)_3\}_2(CO)_6]$ both exists as an equilibrium mixture of bridged (major) and non-bridged (minor) isomers whereas $[Co_2\{As(i\text{-}Pr)_3\}_2(CO)_6]$ and $[Co_2\{As(i\text{-}Bu)_3\}_2(CO)_6]$ are almost solely non-bridged (in *n*-heptane).[14]

3) *The solvent*: higher polarity media favour non-bridged isomers since terminal carbonyl ligands have a greater local dipole moment than bridging carbonyls *viz.* $[Co_2(AsEt_3)_2(CO)_6]$ is exclusively non-bridged in tetrahydrofuran whereas in cyclohexane the proportion of bridged isomers dominates.[12] Subtle dipole-dipole interactions between the electrophilic carbonyl carbon atom and solvents bearing lone pair electrons are also a contribution which should not be excluded from consideration. It is expected that bridged ↔ non-bridged equilibria of $[Co_2L_2(CO)_6]$ bearing ligands with poorer σ-donor faculty will be more sensitive to changes in solvent polarity since the Co(0) centres are, on average, less π-basic and the carbonyl carbon centres therefore more nucleophilic. The carbonyl ligands in this context are thus more receptive to extraneous interactions with solvents of greater dipole moment.

* Amongst the common carbonyl metallates $[Co(CO)_4]^-$ is the least nucleophilic, with the continuum spanning some six orders of magnitude. See C. K. Lai, W. G. Feighery, Y. Zhen, J. Atwood, *Inorg. Chem.*, **1989**, *28*, 3929-3930.

4) *Temperature*: higher ambient temperatures* tend to shift the bridged ↔ non-bridged equilibrium toward a greater proportion of the latter.[6, 14] The explanation probably lies in a thermodynamic (BOLTZMANN) argument since the experimental order of free energies for $[Co_2(CO)_8]$ follows the trend $C_{2v} < D_{3d} < D_{2d}$.[17] The ultra-fast IR spectroscopy measurements performed on $[Co_2(CO)_8]$ (*n*-hexane solution) by ANNA *et al.*[21] have determined that at 25 °C the algebraic signs of $\Delta H°$, $\Delta S°$ and $\Delta G°$ are all *negative* for a $D_{3d} \rightarrow C_{2v}$ interconversion *i.e.*, the process is enthalpically favourable but entropically unfavourable, though the former is *overwhelming dominant* (this attests to the conclusion that the $C_{2v}$ isomer of $[Co_2(CO)_8]$ is the lowest-energy and most compact, geometrically constrained conformation[24, 25]). However, the activation energy barrier for $D_{3d} \rightarrow C_{2v}$ isomerisation at 25 °C is only slightly less than the reverse process (*cf.* 5.4 *vs.* 5.8 kcal $mol^{-1}$, respectively – these values are upper-bound estimates[21]) and one may surmise that even a mild temperature increase will be sufficient to elevate the importance of the entropy term, and allow for greater proportions of the non-bridged isomers.† It is stressed that although these experiments were carried out on $[Co_2(CO)_8]$ the general qualitative trend should nevertheless apply to $[Co_2L_2(CO)_6]$ from which it is derived and shares a great deal of underlying similarities.

* In this context, "higher temperature" refers to ~25 °C since $[Co_2(CO)_8]$ decarbonylates to $[Co_4(CO)_{12}]$ at or near 50 °C.
† A crude interpretation of the temperature dependence of the bridged ↔ non-bridged equilibrium considers the latter to have a greater degree of roto-vibrational freedom, which is desirable from an entropic perspective.

The ambient temperature IR spectrum of $[Co_2(PhAsC_4Me_4)_2(CO)_6]$ measured in *n*-hexane, dichloromethane, and acetonitrile (equal concentrations) are shown in **Figure 3.4**, and exhibit markedly different profiles in the carbonyl stretching region due to the presence of bridged and non-bridged isomers.

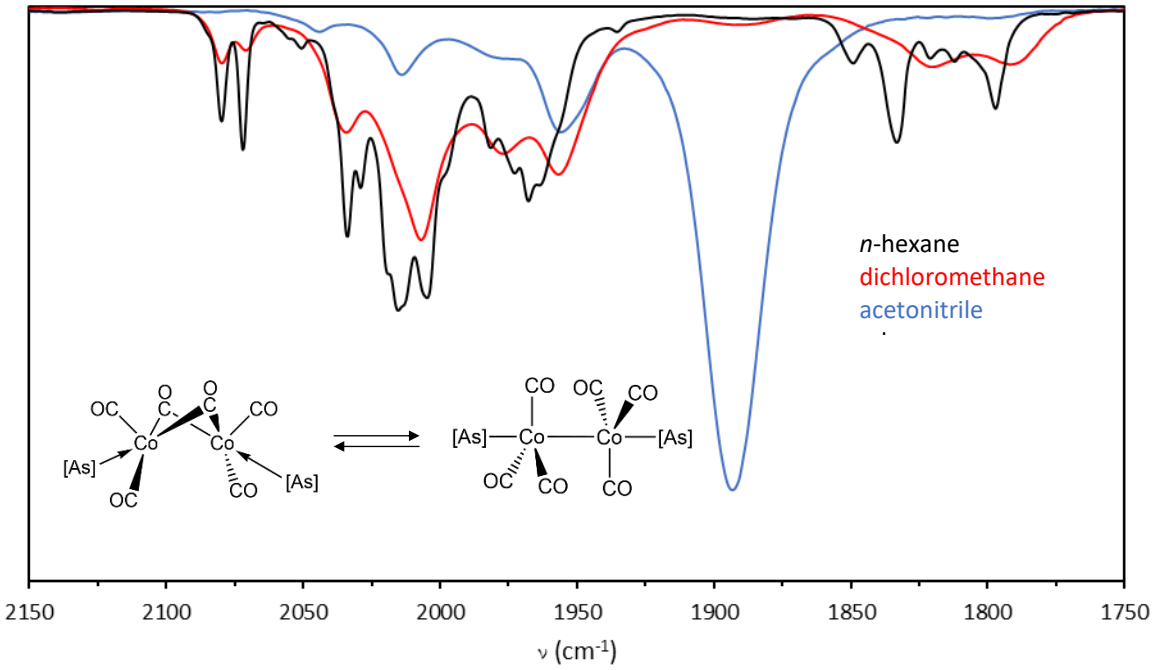



**Figure 3.4**: Solvent-dependant IR spectra of $[Co_2(PhAsC_4Me_4)_2(CO)_6]$ measured in *n*-hexane (black trace, ε = 1.37), dichloromethane (red trace, ε = 9.08) and acetonitrile (blue trace, ε = 36.64). [As] = $PhAsC_4Me_4$.

The complete absence of $\nu_{CO}$ absorptions attributable to bridging carbonyl ligands in MeCN solution (ε = 36.64; blue trace) are consistent with point 3) made above. That is, $[Co_2(PhAsC_4Me_4)_2(CO)_6]$ exists almost purely as a non-bridged isomer with a prominent (degenerate) $\nu_{CO}$ stretch at 1894 $cm^{-1}$ and weaker absorptions at 1956, 2013 and 2043 $cm^{-1}$, all of which are indicative of terminal carbonyl ligands. It should be noted that a $[Co_2L_2(CO)_6]$ complex of idealised $D_{3d}$ symmetry (which the present example is assumed to be; **Figure 3.3**) is predicted to possess only two IR-active fundamental $\nu_{CO}$ modes ($A_{1u}$ + $E_u$); this is indeed observed in situations where L is considered a point ligand of three-fold symmetry *e.g.*, $PPh_3$,[26] though as the crystal structure of $[Co_2(PhAsC_4Me_4)_2(CO)_6]$ makes apparent (**Figure 3.2**) the 1-phenyl-2,3,4,5-tetramethylarsole ligand does not radiate a uniformly conical or axially symmetric field of influence.

The subtle dipolar distortions induced by the arsole ligand(s) may allow some symmetric $\nu_{CO}$ modes of $D_{3d}$-$[Co_2(PhAsC_4Me_4)_2(CO)_6]$ (namely $A_{1g}$ and $E_g$) to become weakly IR active.*

The IR spectra of $[Co_2(PhAsC_4Me_4)_2(CO)_6]$ in less-polar $CH_2Cl_2$ ($\varepsilon$ = 9.08) and practically non-polar *n*-hexane ($\varepsilon$ = 1.37) solutions indicate the presence of carbonyl-bridged isomers – in the former only two broad $\nu_{CO}$ bands at 1820 and 1793 $cm^{-1}$ are found which resolve into no fewer than five (1848, 1832, 1821, 1812, 1797 $cm^{-1}$) in the latter. This, alongside the congested terminal CO region consisting of at least twelve $\nu_{CO}$ vibrational modes, clearly indicate that *more than one* bridged configuration of the dicobalt complex is present in *n*-hexane solution; there are in fact four possible arrangements of $[Co_2L_2(CO)_6]$, as illustrated in **Figure 3.5**.

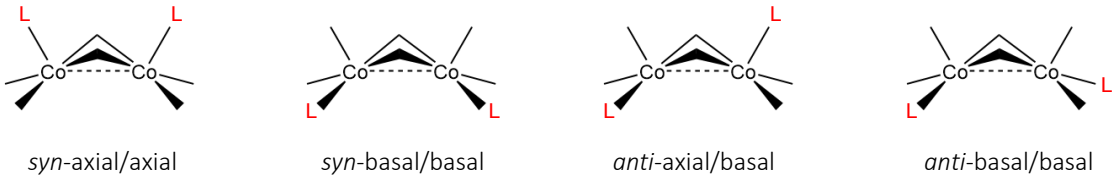



**Figure 3.5**: The four regioisomers of the carbonyl-bridged conformation of $[Co_2L_2(CO)_6]$. Carbonyl ligands omitted for simplicity.

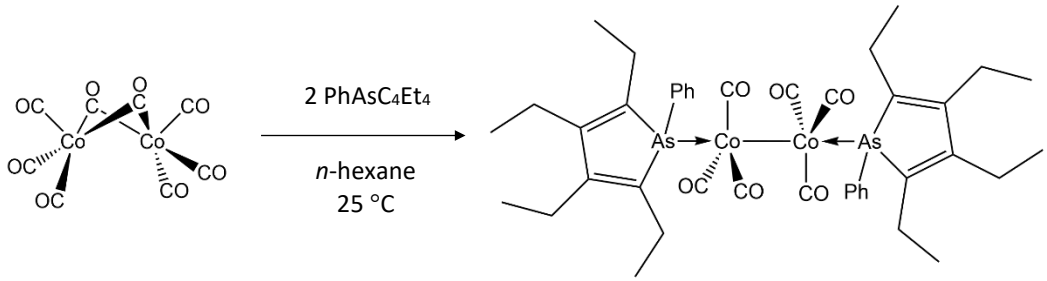
Attempting to deconvolute the *n*-hexane spectrum and unambiguously assign each $\nu_{CO}$ absorption to a specific carbonyl-bridged isomer would be a formidable task and was not conducted here. MANNING has heroically pursued such an activity[16] though even he notes that some assignments cannot be made with total confidence given the complexity of the system(s) under study. Rather, the intent here is to qualitatively illustrate the inherent dynamic nature of the dicobalt skeleton and the ability of this and related complexes to adopt unique structures in response to both internal and external influences. That the crystal structures of $[Co_2(PhAsC_4Me_4)_2(CO)_6]$ and $[Co_2(PhAsC_4Et_4)_2(CO)_6]$ (**Figure 3.6**) – *both obtained from n-hexane solution* – can adopt strikingly different forms in the solid state perhaps speaks to the relatively modest energy barrier governing the equilibrium process.†

* Strictly speaking, a non-bridged $[Co_2(PhAsC_4Me_4)_2(CO)_6]$ with the pair of arsole ligands lying in axial coordination sites would display formal $C_s$ symmetry (see **Figure 3.6**): one may therefore predict six fundamental $\nu_{CO}$ modes ($4A' + 2A''$). It is plausible that six carbonyl vibrations are indeed present in the spectrum shown, though they are evidently poorly resolved which is not an uncommon occurrence in solvents of especially high polarity.

† It is acknowledged that crystals that form from a particular solvent do not necessarily represent the predominant species dissolved in that solvent.

### 3.2.3 Synthesis of $[Co_2(PhAsC_4Et_4)_2(CO)_6]$

The 1-phenyl-2,3,4,5-tetraethylarsole complex $[Co_2(PhAsC_4Et_4)_2(CO)_6]$ was prepared similarly and obtained from *n*-hexane solution in modest yield as a red-brown solid (**Scheme 3.3**); the solution IR spectrum is also solvent dependant and the results of this are presented in **Figure 3.7**. Single crystals of $[Co_2(PhAsC_4Et_4)_2(CO)_6]$ were obtained by evaporation of *n*-hexane solution at -30 °C and the molecular structure is shown in **Figure 3.6**.




**Scheme 3.3**: Synthesis of $[Co_2(PhAsC_4Et_4)_2(CO)_6]$.

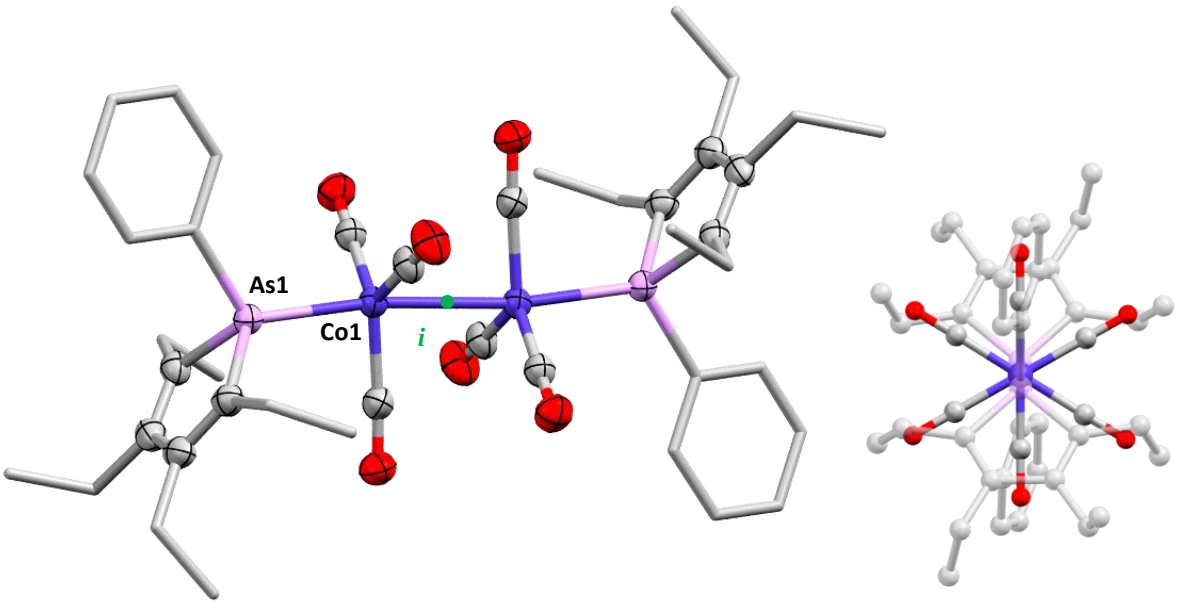



**Figure 3.6**: The molecular structure of centrosymmetric $[Co_2(PhAsC_4Et_4)_2(CO)_6]$ in a crystal. Phenyl and ethyl groups simplified and hydrogen atoms omitted for clarity. Ellipsoids are shown at 50% displacement. **Inset**: Abbreviated perspective of the molecule highlighting the staggered nature of the ligands, viewed along the Co-Co vector. • = crystallographic inversion centre.

The most conspicuous feature of the expected bis(arsole) complex is the *pseudo*-$D_{3d}$ symmetric molecular core geometry with an unsupported Co-Co bond, whereas the analogous

$[Co_2(PhAsC_4Me_4)_2(CO)_6]$ was encountered (**Figure 3.2**) with a bent $Co_2(\mu\text{-}CO)_2$ unit of approximate $C_{2v}$ symmetry. Here, $[Co_2(PhAsC_4Et_4)_2(CO)_6]$ has a roughly cylindrical profile in the solid state with each cobalt centre existing in a slightly distorted trigonal bipyramidal environment ($\tau_5$ = 0.85) and the arsole ligands *trans* to the dicobalt interaction, both lying on the principal axis with the six carbonyl ligands in a staggered conformation (**Figure 3.6**, **Inset**; dihedral angle *ca* 58—61°). A crystallographic inversion centre is imposed upon the midpoint of the Co-Co bond and only one half of the molecule is crystallographically unique. The As→Co and Co-Co bonds measure 2.2878(5) and 2.6394(6) Å, respectively; the former is somewhat shorter, and the latter appreciably longer, than the same in $[Co_2(PhAsC_4Ph_4)(CO)_7]$ (2.3623(9) and 2.4994(1) Å) and $[Co_2(PhAsC_4Me_4)_2(CO)_6]$ (2.3592(6) and 2.4966(5) Å). The elongation of the intermetallic covalent bond here probably reflects the non-negligible *trans* influence of the arsole donor in addition to the absence of any bridging carbonyl ligands which might otherwise constrain the metal atoms to closer proximity. The contraction of the As→Co dative bond is likely a consequence of a less congested trigonal bipyramidal geometry compared to a more crowded tetragonal pyramid, allowing slightly closer approach of the donor function despite an enlarged steric profile afforded by four peripheral ethyl groups.

The occurrence of the non-bridged isomer of $[Co_2(PhAsC_4Et_4)_2(CO)_6]$ in the solid state is noteworthy and may very well be a consequence of the subtly augmented LEWIS basicity of the arsole ligand, rendered more electron-releasing by the increased degree of substitution of the four peripheral alkyl groups. As mentioned in the previous section, such complexes are highly fluxional in solution with modest energy barriers to isomerisation; however, stronger σ-donors do confer thermodynamic preference on non-bridged configurations since the increased basicity of the metal centre(s) is available to all-terminal carbonyl ligands. Like the preceding case of $[Co_2(PhAsC_4Me_4)_2(CO)_6]$, the IR spectrum of $[Co_2(PhAsC_4Et_4)_2(CO)_6]$ varies between *n*-hexane, dichloromethane and acetonitrile media (**Figure 3.7**) with the non-bridged $D_{3d}$ conformation (**Figure 3.3**) totally dominant in the latter, and the structure shifting to *pseudo*-$C_{2v}$ carbonyl-bridged in the former. The observation of no fewer than twelve $\nu_{CO}$ vibrations in *n*-hexane solution once again indicates than more than one carbonyl-bridged complex is present, though any attempt to assign the specific absorptions to a particular molecule would be made in very low confidence.

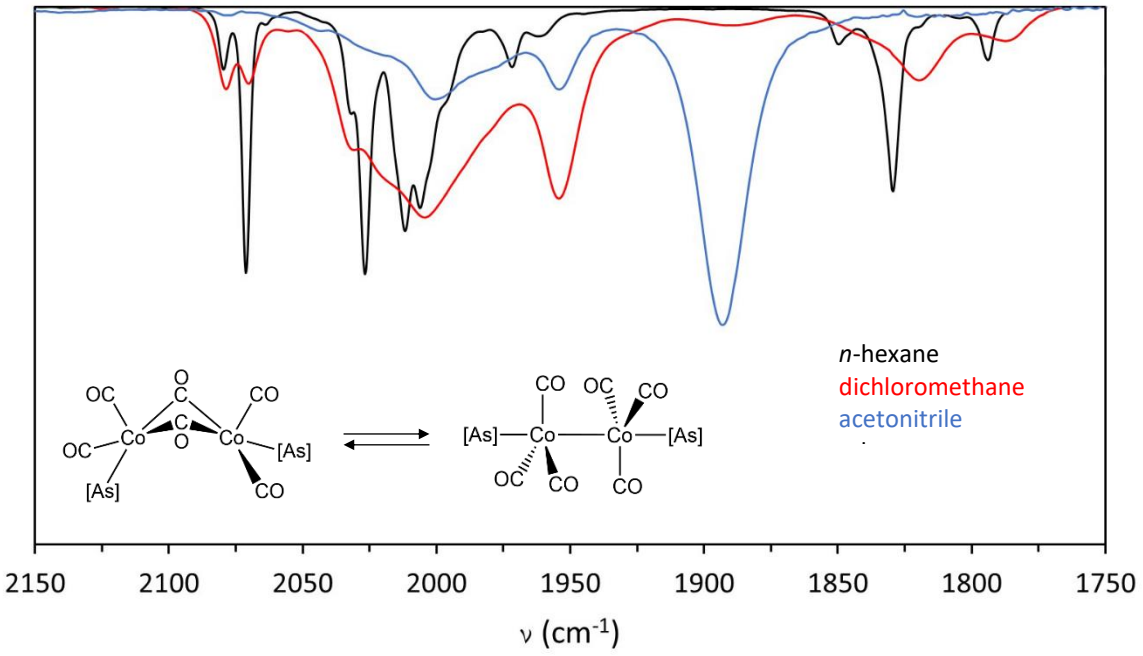



**Figure 3.7**: Solvent-dependant IR spectra of $[Co_2(PhAsC_4Et_4)_2(CO)_6]$ measured in *n*-hexane (black trace, ε = 1.37), dichloromethane (red trace, ε = 9.08) and acetonitrile (blue trace, ε = 36.64). [As] = $PhAsC_4Et_4$.

### 3.2.4 Synthesis of *anti*-$[Co_2(CO)_4(\eta^4\text{-}PhAsC_4Et_4)_2]$

During one preparation of $[Co_2(PhAsC_4Et_4)_2(CO)_6]$ attempts were made to recrystallise the crude reaction product from boiling $Et_2O$ (*ca* 35 °C); the purpose of this activity was to see if the complex might crystallise in an alternative molecular conformation due to a different dielectric solvent environment.* Instead, several *yellow* crystals were observed amongst the residues of decomposition (it became apparent that $[Co_2(PhAsC_4Et_4)_2(CO)_6]$ was thermally sensitive; **Section 3.3.1**) after cooling the flask to -20 °C. X-ray diffraction unexpectedly revealed the compound to be a product of decarbonylation, namely the dimeric species and first definitive example† of a diene-bound arsole ligand, $[Co_2(\mu\text{-}CO)_2(CO)_2(\eta^4\text{-}PhAsC_4Et_4)_2]$. The molecular structure is shown in **Figure 3.8** and serves as the first of many demonstrations (in this work) of the generally low aromatic character of arsoles, notwithstanding the prominent structural similarities to the range of π-diolefin complexes of Co(0) first prepared by WILKINSON[27] and the $\eta^4$-silole dimer $[Co_2(\mu\text{-}CO)_2(CO)_2(\eta^4\text{-}Me_2SiC_4Ph_2H_2)_2]$ described by CORRIU.[28]

* This was not the case, in fact $[Co_2(PhAsC_4Et_4)_2(CO)_6]$ repeatedly resisted crystallisation from $Et_2O$.

† BRAYE has previously described a diene complex of pentaphenylarsole, namely $[Fe(CO)_3(\eta^4\text{-}PhAsC_4Ph_4)]$, though characterisation was limited to elemental microanalysis and low resolution IR spectra. The material obtained by the authors seems likely to be correctly formulated, though has yet to be confirmed by contemporary techniques. See **Chapter 1**, **Section 1.4.3**.

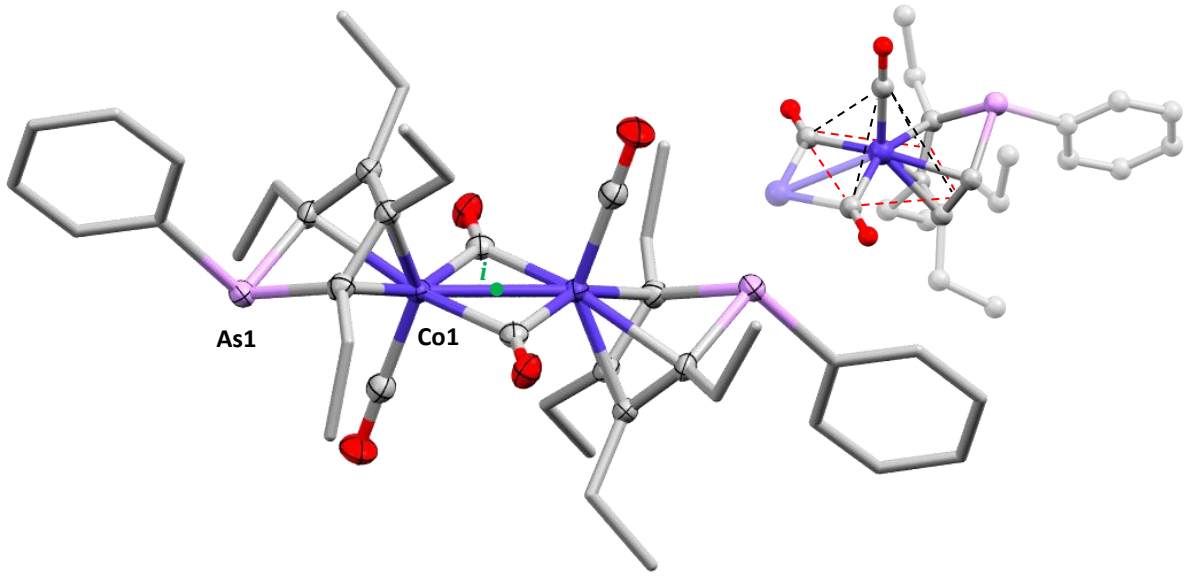



**Figure 3.8**: The molecular structure of centrosymmetric $[Co_2(\mu\text{-}CO)_2(CO)_2(\eta^4\text{-}PhAsC_4Et_4)_2]$ in a crystal. Phenyl and ethyl groups simplified and hydrogen atoms omitted for clarity. Ellipsoids shown at 50% displacement. **Inset**: Abbreviated perspective of the molecule highlighting the geometry of the Co(0) centre(s). • = crystallographic centre of inversion.

The molecular structure of $[Co_2(\mu\text{-}CO)_2(CO)_2(\eta^4\text{-}PhAsC_4Et_4)_2]$ finds a dimetallic arrangement with a planar $Co_2(\mu\text{-}CO)_2$ unit decorated by a pair of mutually *anti* $PhAsC_4Et_4$ ligands which bind the Co(0) centre(s) *via* the butadiene function(s) in a *tetrahapto* manner. The compound crystallises in the triclinic *P*-1 space group and the crystallographic centre of inversion lies at the midpoint of the dicobalt bond – only one half of the complex is therefore unique. The pair of cobalt atoms and bridging carbonyl carbon atoms form a rhomboid with Co-C side lengths of 1.928(3) and 1.917(3) Å, bisected by a Co-Co covalent bond length of 2.5706(6) Å (*cf.* 2.5293(8) Å in $[Co_2(CO)_8]$). The Co(0) atoms exist in slightly deformed square-based pyramidal environments ($\tau_5$ = 0.15) with the arsole diene and bridging carbonyl groups populating the basal plane (**Figure 3.8**, **Inset**) and a lone terminal carbonyl ligand completing the axial coordination site. *Tetrahapto* coordination brings about an appreciable envelope folding of the heterocycle with the arsenic atom extruded by *ca* 24° from the mean place of the butadiene carbon atoms.* Moreover, the face of the butadiene function is asymmetrically disposed against the cobalt centre, with the carbon atoms in the 3,4-ring positions (β to arsenic) being measurably closer (mean 2.098 Å) than those in the 2,5-positions (mean

* The free arsole is a liquid at ambient temperature and no crystal structure of this heterocycle is available. However, the DFT-optimised geometry (gas phase: ωB97X-D/6-31G*) of $PhAsC_4Et_4$ returned an envelope angle of *ca* 10° which is in accord with other structurally characterised $\lambda^3$-arsoles and may be considered a reliable estimate of the ground state conformation for the purposes of comparison.

2.176 Å; α to arsenic). Consistent with a depletion in the $sp^2$-character of the diene carbon atoms upon π-complexation, an elongation of the mean $C_\alpha$-$C_\beta$ distances (1.418(6) Å) and a compression of the $C_\beta$-$C_\beta$ distance (1.449(4) Å) is measured, compared to the same bonding partners in $[Co_2(PhAsC_4Et_4)_2(CO)_6]$ which features the same ligand albeit σ-bound (**Figure 3.6**) *cf.* 1.343(6) and 1.494(5) Å, respectively.

The superficial bonding arrangement here recalls that of well-known monomeric $[Fe(CO)_3(\eta^4\text{-diene})]$ complexes ("piano stool" Fe(0)). The elongated Co-centroid distance in $[Co_2(\mu\text{-}CO)_2(CO)_2(\eta^4\text{-}PhAsC_4Et_4)_2]$ (1.769 Å) compared to the Fe-centroid distances in the three $[Fe(CO)_3(\eta^4\text{-arsole})]$ complexes (1.700, 1.704 and 1.715 Å) prepared in forthcoming stages of this work is noted. Since the covalent radius of iron is larger than cobalt (1.32 *vs.* 1.26 Å, respectively) this increased separation most likely reflects difference in the coordination numbers of the two elements. Thus whilst Co-C bonds to bridging carbonyls are typically longer than those to terminal carbonyls, a Co-Co bond must also be accommodated, resulting in a higher coordination number *cf.* the locally $C_{3v}$ $Fe(CO)_3$ unit.

The compound could be deliberately prepared by *briefly* heating $[Co_2(CO)_8]$ with two equivalents of $PhAsC_4Et_4$ to reflux in *n*-pentane (*ca* 35 °C), and isolated by anaerobic chromatography in very low yields (milligram quantities) as a yellow residue. Acquiring complete spectroscopic data for $[Co_2(\mu\text{-}CO)_2(CO)_2(\eta^4\text{-}PhAsC_4Et_4)_2]$ proved difficult since – like $[Co_2(PhAsC_4Et_4)_2(CO)_6]$ – the complex was labile in solution and was observed to gradually decompose over the course of one day at ambient temperature. An IR spectrum in *n*-hexane confirmed that the *anti*-configuration (**Figure 3.9**) is maintained in solution* finding two $\nu_{CO}$ vibrations at 2001(vs) and 1817(s) $cm^{-1}$ .These data may be compared to $[Co_2(\mu\text{-}CO)_2(CO)_2(NBD)_2]$ for which the norbornadiene ligands are mutually *syn* ($\nu_{CO}$ 2019(vs), 1995(m), 1816(sh), 1804(s) $cm^{-1}$ in *n*-heptane), and $[Co_2(\mu\text{-}CO)_2(CO)_2(DMB)_2]$ for which the 2,3-dimethylbutadiene ligands are mutually *anti* ($\nu_{CO}$ 1997(vs), 1811(s) $cm^{-1}$ in *n*-heptane[29]). Attempts to collect satisfactory NMR spectra were hampered by the presence of soluble paramagnetic impurities, presumed to arise from gradual and irreversible decomposition in $C_6D_6$.

* For a $C_{2h}$-symmetric *anti*-$[Co_2(\mu\text{-}CO)_2(CO)_2(\eta^4\text{-diene})_2]$, two IR-active $\nu_{CO}$ vibrations are expected ($A_u + B_u$), whereas the $C_{2v}$ *syn*-isomer predicts four such modes ($2A_1 + B_1 + B_2$).




*anti* ($C_{2h}$) *syn* ($C_{2v}$)

**Figure 3.9**: Stereoisomers of $[Co_2(\mu\text{-}CO)_2(CO)_2(\eta^4\text{-diene})_2]$. **Note**: the *syn* isomer is depicted with a planar $Co_2(\mu\text{-}CO)_2$ unit for ease of illustration however in reality is bent like that observed in the crystal structure of $[Co_2(PhAsC_4Me_4)_2(CO)_6]$ (**Figure 3.2**).

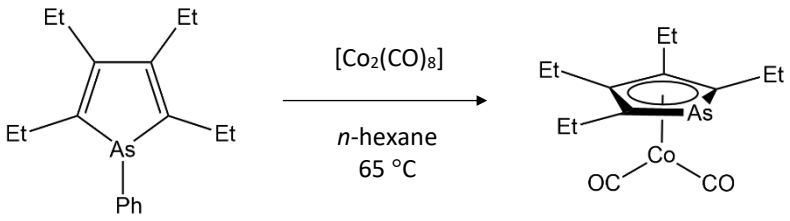
The $\eta^4$-arsole complex was pursed on numerous attempts with limited success, and for reasons which remain presently inexplicable $PhAsC_4Et_4$ was the *only* arsole on hand (at the time) observed to participate in this bonding mode: no analogous $\eta^4$-$PhAsC_4Me_4$ species *i.e.*, $[Co_2(\mu\text{-}CO)_2(CO)_2(\eta^4\text{-}PhAsC_4Me_4)_2]$, was ever observed under similar preparative conditions (despite the prominence of $[M - 2CO]^+$ peaks in the high-resolution mass spectra of $[Co_2(PhAsC_4R_4)_2(CO)_6]$, R = Me or Et). The major complication arose from the formation of another type of cobalt complex, which is the subject of the two forthcoming sections. It is regrettable that the *especially novel* $[Co_2(\mu\text{-}CO)_2(CO)_2(\eta^4\text{-}PhAsC_4Et_4)_2]$ could not be characterised to the same standard as most other compounds throughout this work.

## 3.3 *Pentahapto* Arsolyl Complexes of Cobalt(I)

### 3.3.1 Synthesis of $[Co(CO)_2(\eta^5\text{-}AsC_4Et_4)]$

During attempts to isolate $[Co_2(CO)_4(\eta^4\text{-}PhAsC_4Et_4)_2]$ in greater quantities (for more thorough characterisation, and downstream chemistry), WILKINSON'S method[27] for preparing diolefin complexes of dicobalt tetracarbonyl was followed: this broadly involved heating $[Co_2(CO)_8]$ with an excess of the diolefin to moderate temperatures (*n*-hexane, 65 °C), which afforded $[Co_2(CO)_4(\eta^4\text{-diene})_2]$ in generally good yields.

Thus, an excess of $PhAsC_4Et_4$ was combined with $[Co_2(CO)_8]$ in *n*-hexane at reflux; anaerobic column chromatography of the reaction material afforded *not* the yellow $[Co_2(CO)_4(\eta^4\text{-}PhAsC_4Et_4)_2]$ but instead an air-sensitive, dark orange liquid in low yield. The product displayed only two $\nu_{CO}$ absorptions in *n*-hexane solution of equal intensity at 2017(vs) and 1965(vs) $cm^{-1}$ (suggesting an intercarbonyl angle of *ca* 90°; see the footnote on **page 197**) and the $^1H$ NMR spectrum – whilst clearly containing a tetraethylarsole ring – was unexpectedly devoid of any aromatic hydrogen signals. The product was formulated on the basis of these data as the novel *pentahapto* arsolyl complex $[Co(CO)_2(\eta^5\text{-}AsC_4Et_4)]$ arising from scission of the *As*-phenyl group (**Scheme 3.4**), the compositions of which was subsequently verified by a high-resolution mass spectrum (molecular ion $m/z \approx 354.0011$).



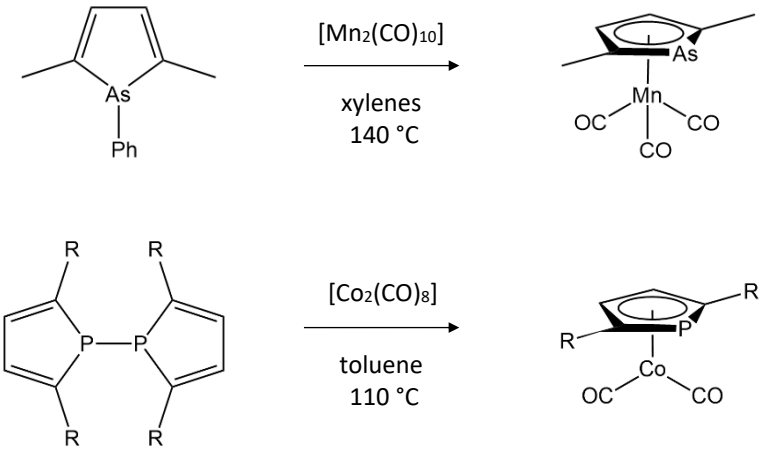

**Scheme 3.4**: Synthesis of $[Co(CO)_2(\eta^5\text{-}AsC_4Et_4)]$ *via* thermolysis of $PhAsC_4Et_4$ with $[Co_2(CO)_8]$.

The complex is the first example of a late transition metal arsolyl complex and the preparation outlined above was both reproducible and generalisable (as following sections will detail). The $^{13}C\{^1H\}$ NMR spectrum ($C_6D_6$) finds a single, broadened resonance at 205.3 ppm for the pair of chemically equivalent carbonyl ligands bound to the quadrupolar $^{59}Co$ nucleus ($I$ = 7/2, 100% abundant), alongside a pair of sharp signals at 128.3 and 117.8 ppm corresponding to the arsolyl ring-carbon atoms in the 2,5- and 3,4-positions (α and β to the arsenic atom, respectively). Notably, these nuclei are to appreciably lower frequency of the starting material ($PhAsC_4Et_4$: $\delta_C$ 151.1 and 149.5 ppm) primarily due to the magnetic shielding imparted by π-retrodonation from the electron-rich Co(I) centre.* The methylene protons of the four ethyl residues are diastereotopic and in solution experience restricted motion about the periphery of the arsolyl ring, as evidenced by four distinct methylene ($CH_2$) resonances in the $^1H$ and $^{13}C\{^1H\}$ NMR

* The effect of π-delocalisation within the formally aromatic arsolyl ring is of secondary importance, since $[Li(AsC_4Me_4)\cdot TMEDA]$ in THF-$d_8$ finds the ring-carbon signals at 145.4 and 126.2 ppm which may be compared to the same in $ClAsC_4Me_4$: 147.7 and 141.9 ppm (THF-$d_8$). See K.H. Theopold *et al. Chem. Ber.*, **1991**, *124*, 2453—2456.

spectra. The phenomenon has been well-documented in other ring systems displaying multiple ethyl groups *e.g.*, hexaethylbenzene and its π-complexes.[30, 31]

All previous examples of $\eta^5$-arsolyl complexes (**Chapter 1**, **Section 1.4.4**) were invariably obtained at some point from an arsolide anion $[AsC_4R_4]^-$. The present complex $[Co(CO)_2(\eta^5\text{-}AsC_4Et_4)]$ deviates from this pattern and is only the second known example of situational *As*-phenyl scission leading directly to the *pentahapto* ligand (alkali metal reductions[32-34] notwithstanding): MATHEY has reported[35] the "arsacymantrene" $[Mn(CO)_3(\eta^5\text{-}AsC_4Me_2H_2)]$ which may be obtained by thermolysis of $[Mn_2(CO)_{10}]$ with $PhAsC_4Me_2H_2$ (1-phenyl-2,5-dimethylarsole), though more-forcing temperatures were required (xylenes, 140 °C) and no mention was made regarding the fate of the *As*-phenyl ring.* MATHEY has also described analogous *pentahapto* phospholyl complexes $[Co(CO)_2(\eta^5\text{-}PC_4R_2H_2)]$ (R = Ph or *t*-Bu) obtained by thermolysis of $[Co_2(CO)_8]$ with the corresponding *P-P* bonded biphospholyl $(PC_4R_2H_2)_2$ in toluene (110 °C).[36, 37]

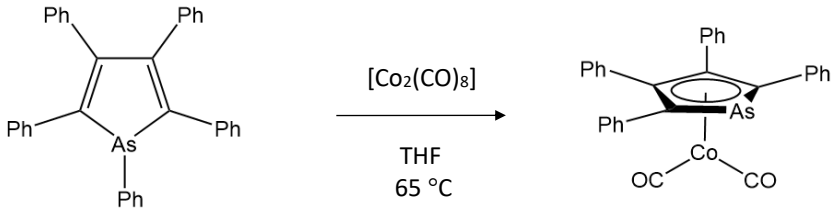



**Scheme 3.5**: Synthesis of $\eta^5$-arsolyl and -phospholyl complexes *via* thermolysis previously reported by MATHEY.

* MATHEY employed a 1:1 ratio of $[Mn_2(CO)_{10}]$ to $PhAsC_4Me_2H_2$ and obtained an isolated yield of *ca* 50%. In an idealised interpretation, this amounts to quantitative partition of the manganese atoms giving $[MnPh(CO)_5]$ as the co-product, though the authors do not state to which reagent the isolated yield is with respect to.

### 3.3.2 Synthesis of $[Co(CO)_2(\eta^5\text{-}AsC_4Ph_4)]$

Following the identification of $[Co(CO)_2(\eta^5\text{-}AsC_4Et_4)]$ as a thermolysis product, it was recalled that the $\eta^2$-alkyne complexes $[Co_2(\mu\text{-}\eta^2\text{:}\eta^2\text{-}RC{\equiv}CAsC_4Ph_4)(CO)_6]$ (R = H or $SiMe_3$) prepared in the previous chapter would decompose during hot solvent re-crystallisations. At the time, the decomposition materials were presumed to contain an insipid mixture of cobalt species (which was not entirely untrue); however, following the serendipitous isolation of $[Co(CO)_2(\eta^5\text{-}AsC_4Et_4)]$ it was suspected that an analagous $[Co(CO)_2(\eta^5\text{-}AsC_4Ph_4)]$ complex may have been among the thermal degradation products (and it indeed was). Thus, heating a sample of $[Co_2(\mu\text{-}\eta^2\text{:}\eta^2\text{-}HC{\equiv}CAsC_4Ph_4)(CO)_6]$ or $[Co_2(PhAsC_4Ph_4)(CO)_7]$ to reflux in THF followed by anaerobic column chromatography afforded in both cases a very small quantity of a dark orange, moderately air-sensitive crystalline solid; spectroscopic analysis was in agreement with the formation of a *pentahapto* arsolyl complex of cobalt dicarbonyl. A higher (but still modest) yielding synthesis of $[Co(CO)_2(\eta^5\text{-}AsC_4Ph_4)]$ entailed heating an $RAsC_4Ph_4$ arsole (R = Cl or Ph) with $[Co_2(CO)_8]$ to reflux in THF (**Scheme 3.6**).




**Scheme 3.6**: Synthesis of $[Co(CO)_2(\eta^5\text{-}AsC_4Ph_4)]$.

$[Co(CO)_2(\eta^5\text{-}AsC_4Ph_4)]$ is a counterpart to the $[M(CO)_3(\eta^5\text{-}AsC_4Ph_4)]$ complexes (M = Mn, Re) previously described by ABEL,[38, 39] and displays two $\nu_{CO}$ vibrations in *n*-hexane solution at 2022(vs) and 1963(vs) $cm^{-1}$ of approximately equal intensity. The $^{13}C\{^1H\}$ NMR spectrum ($C_6D_6$) finds a single, broad peak for the carbonyl carbon nuclei at 203.8 ppm, and the arsolyl ring-carbon nuclei are found as sharp resonances at 137.2 (2,5-positions) and 135.1 (3,4) ppm which are shifted to lower frequency of the same nuclei found in $ClAsC_4Ph_4$ (*cf.* 152.0 and 149.5 ppm). High-resolution mass spectrometry yields the molecular ion ($m/z \approx 546.0014$) alongside fragments of consecutive decarbonylation, and single crystals suitable for X-ray diffraction were grown from benzene/*n*-hexane at -20 °C. The molecular structure is shown in **Figure 3.10**.

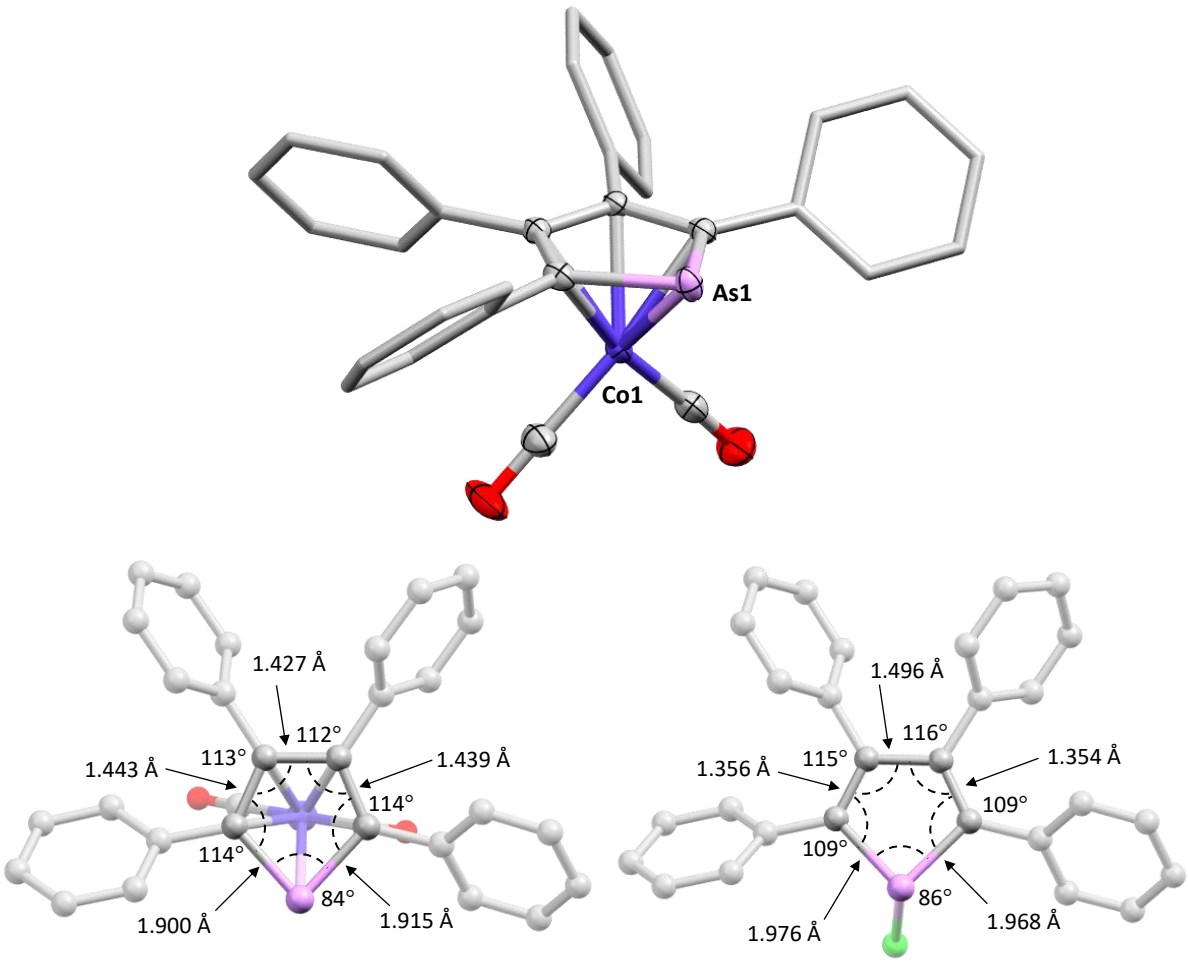



**Figure 3.10**: The molecular structure of $[Co(CO)_2(\eta^5\text{-}AsC_4Ph_4)]$ in a crystal. Phenyl groups simplified and hydrogen atoms omitted for clarity. Ellipsoids shown at 50% displacement. Inset, top right: view of the abbreviated molecular parallel to the arsolyl ring highlighting the slight envelope fold. **Inset, bottom**: view of the complex perpendicular to the arsolyl ring with interatomic distances and angles noted, beside $ClAsC_4Ph_4$ for comparison.

The compound crystallises in the triclinic space group *P*-1, and two enantiomeric molecules related by the inversion centre are found within the unit cell. The origin of chirality (in the solid state) is a slight rotation of the $Co(CO)_2$ group by *ca* 10° from the imaginary vertical plane which bisects the arsolyl ring. The molecular structure is that of a two-legged piano stool with an intercarbonyl angle of *ca* 91° with the cobalt centre lying 1.721 Å below the centroid of the aromatic arsolyl system, which is itself nearly planar (envelope *ca* 4°; *cf.* $ClAsC_4Ph_4$ *ca* 13°). Given the differing covalent radii of $sp^2$-carbon and arsenic (0.73 Å and 1.19 Å, respectively) the cobalt centre is asymmetrically disposed about the ring atoms with a mean Co-C distance of *ca* 2.11 Å and a Co-As distance of 2.4277(4) Å – the latter is only slightly smaller than the sum of the respective element covalent radii (2.45 Å) and compares favourably to the Mn-As distance found in $[Mn(CO)_3(\eta^5\text{-}AsC_4Ph_4)]$[38] (2.492(2) Å). Interatomic distances and angles within the arsolyl ring are compared to that of the non-aromatic $ClAsC_4Ph_4$ in the insets of **Figure 3.10**; *pentahapto* coordination of the ligand brings with it formal 6π-aromaticity and an elongation of the $C_\alpha$-$C_\beta$ distance by *ca* 0.09 Å (decreased multiple bonding character), and a compression of both the As-$C_\alpha$ and $C_\beta$-$C_\beta$ bonds by *ca* 0.05—0.06 Å (increased multiple bonding character). The arsolyl ring remains a distorted pentagon with the only appreciable change to the internal ring angles being a uniformity of the vertices defined by the C($sp^2$) atoms.

### 3.3.3 Synthesis of $[Co(CO)_2(\eta^5\text{-}AsC_4Ph_2H_2)]$

The 2,5-diphenylarsolyl complex was prepared similarly: heating a mixture of $PhAsC_4Ph_2H_2$ with $[Co_2(CO)_8]$ to reflux in THF followed by anaerobic chromatography provides $[Co(CO)_2(\eta^5\text{-}AsC_4Ph_2H_2)]$ in modest yield as an air-sensitive dark orange solid. Spectroscopic features are comparable with the tetraphenyl species above, revealing a pair of $\nu_{CO}$ absorptions at 2032(vs), 1980(vs) $cm^{-1}$ (*n*-hexane; *cf.* $[Co(CO)_2(\eta^5\text{-}PC_4Ph_2H_2)]$[36] $\nu_{CO}$ 2030(vs), 1980(vs) $cm^{-1}$) and the carbonyl carbon nuclei as a broad resonance at 203.0 ppm ($C_6D_6$). Ring carbon atoms are observed at 138.1 and 95.4 ppm for those in the 2,5- and 3,4-ring positions, respectively, with the corresponding 3,4-hydrogens found at 5.93 ppm in the $^1H$ spectrum (*cf.* $PhAsC_4Ph_2H_2$ $\delta_H$ = 7.38 ppm). These latter data may be compared to that of prototypical $[Co(CO)_2(\eta^5\text{-}C_5H_5)]$ ($\delta_C$ = 84.5 ppm, $\delta_H$ = 5.04 ppm in $CDCl_3$).[40] Single crystals were grown from benzene/*n*-hexane and the molecular structure is shown in **Figure 3.11** which confirms the expected two-legged "piano stool" geometry. In contrast to the tetraphenylarsolyl complex, the pair of carbonyl ligands are rotated about the Co-centroid axis to a position slightly offset from the imaginary vertical plane of the arsolyl ring (*ca* 16°

between mean planes). The cobalt-centroid and cobalt-arsenic distances of 1.732 and 2.392(1) Å are regular amongst the complexes in this work and interatomic arsolyl distances reflect the delocalisation within the ring, with mean As-$C_\alpha$, $C_\alpha$-$C_\beta$ and $C_\beta$-$C_\beta$ bonds of 1.913(5), 1.387(6) and 1.377(6) Å, respectively, which may be compared to the same in non-aromatic $PhAsC_4Ph_2H_2$ (1.949(3), 1.343(4) and 1.448(3) Å).[41]

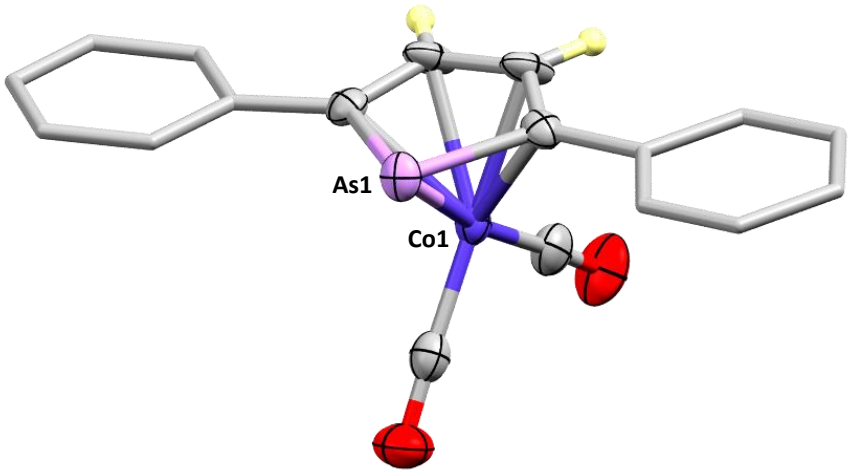
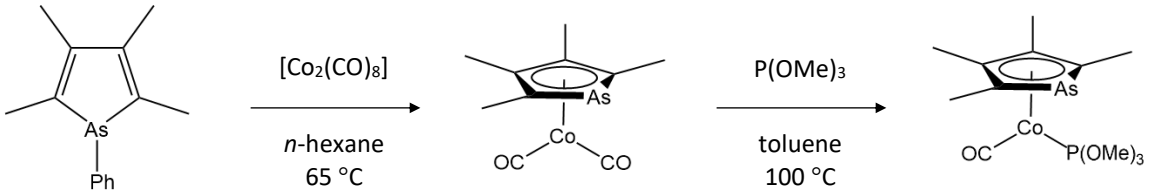



**Figure 3.11**: The molecular structure of $[Co(CO)_2(\eta^5\text{-}AsC_4Ph_2H_2)]$ in a crystal. Phenyl rings simplified and most hydrogen atoms omitted for clarity, except for those in the 3,4-ring positions which are in light yellow for emphasis. Ellipsoids shown at 50% displacement.

### 3.3.4 Synthesis of $[CoL(CO)(\eta^5\text{-}AsC_4Me_4)]$ (L = CO *or* $P(OMe)_3$)

The tetramethyl analogue $[Co(CO)_2(\eta^5\text{-}AsC_4Me_4)]$ was prepared by heating a mixture of $ClAsC_4Me_4$ and $[Co_2(CO)_8]$ to reflux in *n*-hexane medium (**Scheme 3.7**); anaerobic chromatography provides the target compound in modest yield as an air-sensitive orange-red liquid which did crystallise (in neat form) at -30 °C, though the low melting point frustrated attempts at X-ray diffraction studies. The identity was instead confirmed by the usual spectroscopic methods: the $^1H$ NMR spectrum ($C_6D_6$) is predictably simple finding only a pair of methyl signals at 2.12 and 1.85 ppm (which are not remarkably displaced from other $AsC_4Me_4$ ligands throughout this work), and the $^{13}C\{^1H\}$ NMR spectrum reveals the arsolyl ring-carbon nuclei at 118.9 and 113.1 ppm. The carbonyl resonance is observed as a broad peak at 205.1 ppm, slightly downfield of the perarylarsolyl complexes above as expected from the electron-releasing effect of alkyl *vs.* aryl substituents. The IR spectrum mirrors the increased Co(I) basicity with a pair of $\nu_{CO}$

at 2019(vs) and 1967(vs) $cm^{-1}$ (*n*-hexane), and high-resolution mass spectrometry yields the molecular ion ($m/z \approx 297.9389$) in addition to fragments of consecutive decarbonylation.




**Scheme 3.7**: Syntheses of $[Co(CO)_2(\eta^5\text{-}AsC_4Me_4)]$ and $[Co\{P(OMe)_3\}(CO)(\eta^5\text{-}AsC_4Me_4)]$.

The dicarbonyl complex could be converted in quantitative yield to a crystalline derivative by heating $[Co(CO)_2(\eta^5\text{-}AsC_4Me_4)]$ to 100 °C with an excess of $P(OMe)_3$ in toluene, followed by anaerobic chromatography. The complex $[Co\{P(OMe)_3\}(CO)(\eta^5\text{-}AsC_4Me_4)]$ was isolated as a bright orange solid in high yield and the composition readily follows from spectroscopic interrogation: only a single carbonyl ligand is displayed ($\nu_{CO}$ 1947(vs) $cm^{-1}$ in *n*-hexane) and coordination of the phosphite affects a shift of the arsolyl methyl hydrogens (at 1.95, 1.84 ppm) to higher frequency of the dicarbonyl precursor. The $P(OMe)_3$ group is observed in the $^1H$ NMR spectrum as a doublet at 3.37 ppm ($^3J_{PH}$ = 12.1 Hz), and in the $^{31}P\{^1H\}$ NMR spectrum as a broad singlet at 3.20 ppm due to one-bond proximity with the $^{59}Co$ nucleus. The lone carbonyl ligand is found at 206.9 ppm in the $^{13}C\{^1H\}$ NMR spectrum – slightly downfield of the corresponding dicarbonyl complex – and the arsolyl ring-carbon nuclei shift upfield to 114.4 and 110.0 ppm. A high-resolution mass spectrum finds the molecular ion ($m/z \approx 393.9725$) in addition to a decarbonylated fragment, but no loss of the phosphite ligand was observed. Single crystals were obtained by slow evaporation of *n*-pentane solution at -30 °C and the molecular structure is shown in **Figure 3.12**.

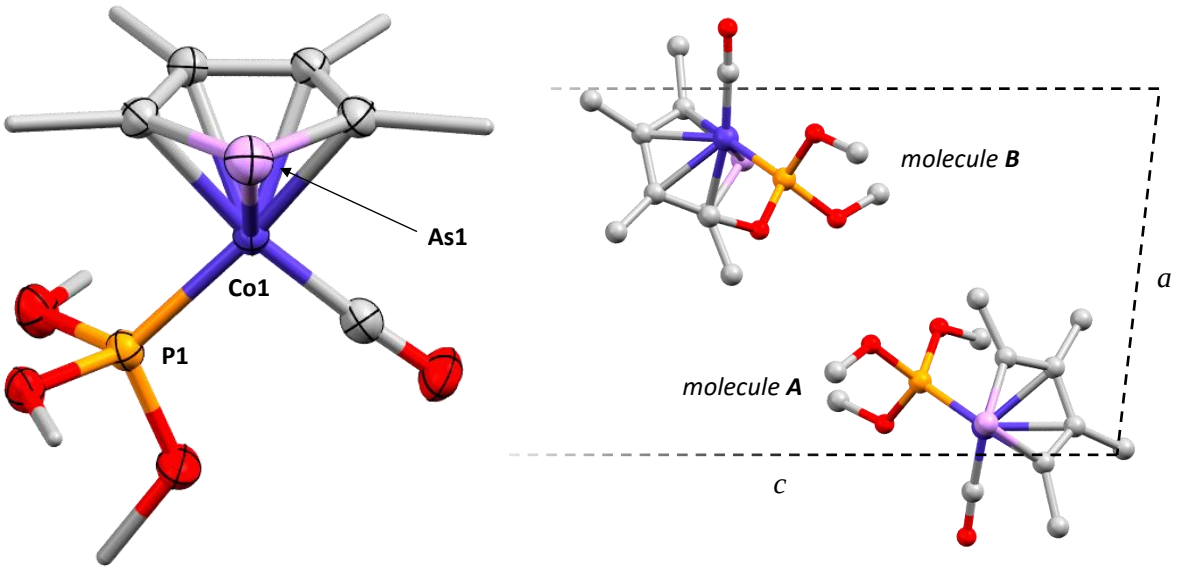
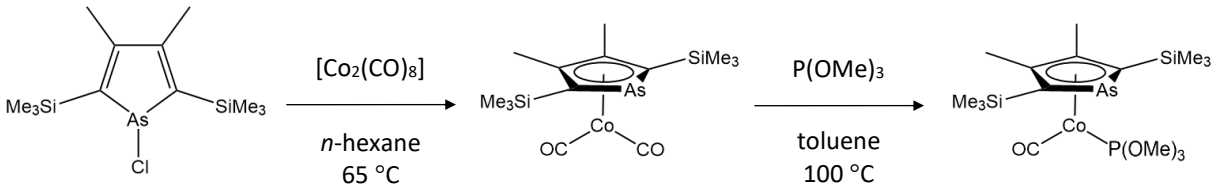



**Figure 3.12**: The molecular structure of [Co{P(OMe)$_3$}(CO)($\eta^5$-AsC$_4$Me$_4$)] in a crystal. Methyl groups simplified and hydrogen atoms omitted for clarity. Only one of two crystallographically unique molecules contained within the asymmetric unit is shown. Ellipsoids shown at 50% displacement. **Inset**: A portion of the unit cell ($P2_1/n$) comprising the asymmetric unit, viewed along the crystallographic *b* axis.

The asymmetric unit comprises two crystallographically distinct molecules with the remainder of the unit cell contents ($Z$ = 8, monoclinic $P2_1/n$) generated by symmetry operations, though interatomic dimensions between the unique molecules are statistically identical. The only salient difference is the placement of the P(OMe)$_3$ group with respect to the orientation of the arsolyl ring (either to the "left" (molecule **A**) or "right" (molecule **B**) of the arsenic atom) though free rotation about the cobalt-centroid axis in solution obliviates this chirality. The non-cylindrical ligand field has little measurable effect on the gross disposition of the arsolyl system and ring dimensions either side of the phosphite ligand are crystallographically indistinguishable. The mean P→Co dative bond of 2.0975(5) Å is unremarkable and the mean Co-As and Co-centroid distances of 2.4081(5) and 1.676 Å are slightly shorter than those measured in other $\eta^5$-arsolyl complexes contained within this section, the increased basicity of the metal centre drawing the *pentahapto* ring slightly closer through more-efficient π-retrodonation. This is also seen in the marginally shorter mean Co-C and marginally longer mean C≡O bond distances of 1.719(3) and 1.158(3) Å, respectively (*cf.* 1.747(3) and 1.144(3) in [Co(CO)$_2$($\eta^5$-AsC$_4$Ph$_4$)]). The arsolyl ring is also reasonably planar with a fold angle of only *ca* 3°.

### 3.3.5 Synthesis of [CoL(CO){$\eta^5$-$AsC_4(SiMe_3)_2Me_2$}] (L = CO *or* $P(OMe)_3$)

The bulky 2,5-di(trimethylsilyl)-3,4-dimethylarsolyl group was installed onto the $Co(CO)_2$ centre by the protocol established so far: heating $ClAsC_4(SiMe_3)_2Me_2$ to reflux in *n*-hexane with $[Co_2(CO)_8]$ followed by anaerobic column chromatography provides [$Co(CO)_2${$\eta^5$-$AsC_4(SiMe_3)_2Me_2$}] as an orange-red liquid in modest yield (**Scheme 3.8**). The identity follows from the usual spectroscopic features: the IR spectrum finds a pair of equally intense $\nu_{CO}$ absorptions at 2015(vs) and 1962(vs) $cm^{-1}$ (*n*-hexane solution) and a single broadened carbonyl resonance at 204.5 ppm is revealed in the $^{13}C\{^1H\}$ NMR spectrum ($C_6D_6$). The arsolyl ring-carbon nuclei manifest at 122.4 and 119.8 ppm, and high-resolution mass spectrometry yields the molecular ion. Like [$Co(CO)_2(\eta^5$-$AsC_4Me_4)$], the product does crystallise (neat) at -30 °C though the low melting point precluded crystallographic interrogation.




**Scheme 3.8**: Syntheses of [$Co(CO)_2${$\eta^5$-$AsC_4(SiMe_3)_2Me_2$}] and [$Co\{P(OMe)_3\}(CO)\{\eta^5$-$AsC_4(SiMe_3)_2Me_2$}].

Also like [$Co(CO)_2(\eta^5$-$AsC_4Me_4$)], the complex could be converted to a crystalline derivative by substitution with trimethyl phosphite in toluene at 100 °C: [$Co\{P(OMe)_3\}(CO)\{\eta^5$-$AsC_4(SiMe_3)_2Me_2$}] is isolated after anaerobic chromatography as a bright orange solid and a crystal structure was determined (**Figure 3.13**). Spectroscopic features need only be mentioned in brief: a single $\nu_{CO}$ vibration is found at 1941(vs) $cm^{-1}$ (*n*-hexane) and the $^{31}P\{^1H\}$ NMR spectrum exhibits only a broad singlet at 4.41 ppm. The lone carbonyl carbon nucleus manifests at 205.6 ppm alongside the arsolyl ring-carbon signals at 118.7 (2,5-positions) and 116.1 (3,4) ppm, and high-resolution mass spectrometry yields the molecular ion ($m/z \approx$ 510.0199).

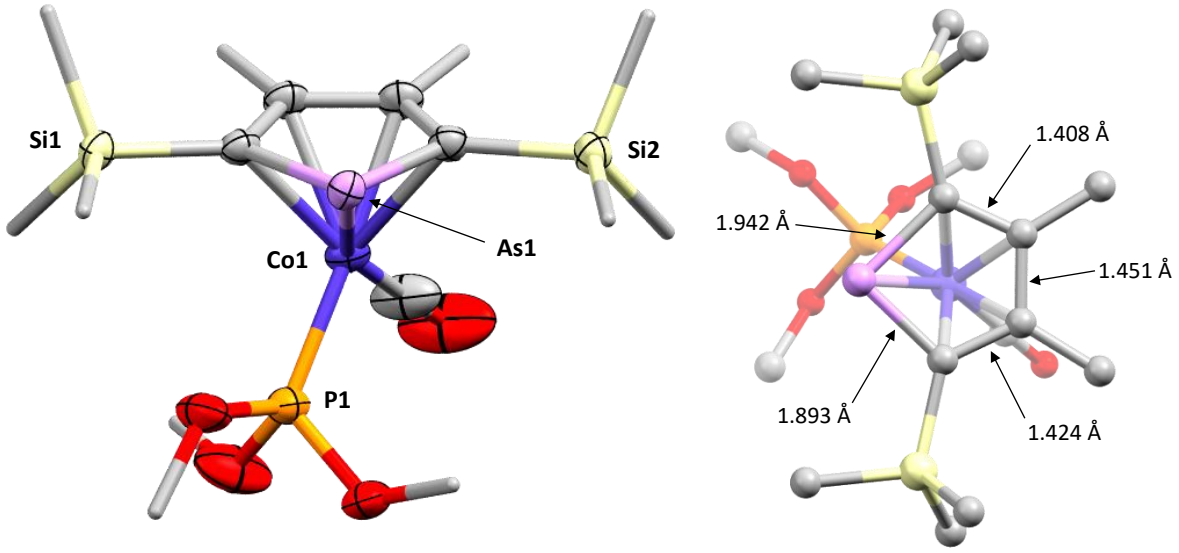



**Figure 3.13**: The molecular structure of [Co{P(OMe)$_3$}(CO){$\eta^5$-AsC$_4$(SiMe$_3$)$_2$Me$_2$}] in a crystal. Methyl groups simplified and hydrogen atoms omitted for clarity. Ellipsoids shown at 50% displacement. **Inset**: An abbreviated perspective of the molecule highlighting the subtle asymmetry within the arsolyl ring.

X-ray diffraction reveals the expected *pentahapto* arsolyl complex. The phosphite and carbonyl ligands are offset from the vertical (non-crystallographic) symmetry plane of the AsC$_4$(SiMe$_3$)$_2$Me$_2$ ring such that the conical P(OMe)$_3$ group may avoid the steric influence imparted by the SiMe$_3$ residues in the 2,5-ring positions. The complex is therefore chiral in the solid state though the unit cell (monoclinic *Cc*) contains molecules of opposing configurations generated by means of the *c* glide plane. The cobalt-centroid and cobalt-arsenic distances of 1.695 and 2.3957(6) Å, respectively, compare favourably with [Co{P(OMe)$_3$}(CO)($\eta^5$-AsC$_4$Me$_4$)] (**Figure 3.12**) and are shorter – despite the bulky silyl groups – than the same in [Co(CO)$_2$($\eta^5$-AsC$_4$Ph$_4$)] and [Co(CO)$_2$($\eta^5$-AsC$_4$Ph$_2$H$_2$)], which lends support to the assertion that improved Co(I) basicity is responsible for the closer approach of the two moieties. Unlike [Co{P(OMe)$_3$}(CO)($\eta^5$-AsC$_4$Me$_4$)], however, the non-cylindrical ligand field imposed by the Co{P(OMe)$_3$}(CO) unit does impart asymmetry to the $\eta^5$-arsolyl ring: the As-C bond lying above the phosphite group (1.942(3) Å) is distinctly longer than its counterpart (1.893(3) Å), and similarly the C$_\alpha$-C$_\beta$ bond situated above the carbonyl ligand (1.424(4) Å) is marginally longer than its equivalent on the opposite side of the ring (1.408(4) Å). This is perhaps a stereo-electronic effect since – if the Co(I) centre is conveniently viewed as a distorted square-based pyramid – both above-mentioned elongated bonds are situated *trans* to a ligand of privileged (CO) or moderate (P(OMe)$_3$) $\pi$-acceptor capacity (**Figure 3.13**, **Inset**).

A similar antagonistic feature has been noted in other contexts *e.g.*, crystal structures of cyclopentadienyl complexes possessing non-disordered nitrosyl ligands.[42] This phenomenon is conversely *not* observed in $[Co\{P(OMe)_3\}(CO)(\eta^5\text{-}AsC_4Me_4)]$ since the geometric disposition of the carbonyl and phosphite ligands with respect to the arsolyl system ensures that no bond within the ring is truly *trans* to a π-acceptor entity.*

As a final comment, MATHEY has determined the crystal structure of $[Co\{P(OMe)_3\}(CO)\{\eta^5\text{-}PC_4(t\text{-}Bu)_2H_2\}]$[37] and noted similar lateral distortions within the phospholyl ring, which were attributed (in passing, with little elaboration) to an allyl-ene-type bonding contribution within the five-membered ring. This phenomenon has also been proposed to account for the breaking of $C_{5v}$ symmetry within the solid-state structures of cyclopentadienyl rings in other $[Co(CO)_2(\eta^5\text{-}C_5R_5)]$ complexes (R = Me, Ph, $CH_2Ph$)[43-45] although no convincing crystallographic evidence was found in any of the cobalt arsolyl complexes here, nor upon re-examination of the few known crystal structures of other transition metal arsolyls, for the presence of such a canonical form.

### 3.3.6 General Comments Regarding the Synthesis of $[Co(CO)_2(\eta^5\text{-}AsC_4R_4)]$

The preparation of the above arsolyl complexes was carried out on numerous occasions during efforts to optimise the reaction conditions; some observations are summarised below:

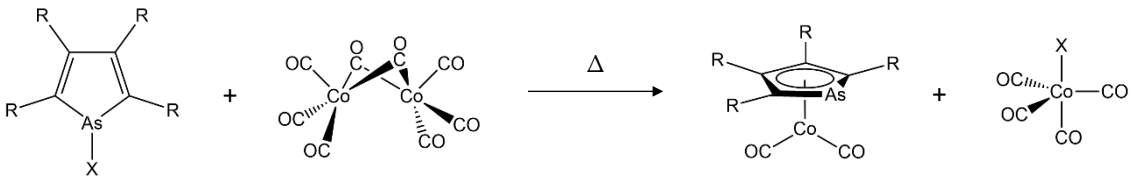
1) Yields were generally modest (≤ ~30%), though the reaction was highly reproducible. It transpired that virtually *any* arsole would afford the target *pentahapto* complex(es), and those which possessed a more reactive *As*-substituent bond (*e.g.*, As-Cl) gave *on average* slightly higher yields of $[Co(CO)_2(\eta^5\text{-}AsC_4R_4)]$ than did a phenyl residue (typically an increase of *ca* 5—10%).

2) The reaction was unaffected by the chemical identity of the solvent (*e.g.*, THF, *n*-hexane, benzene, toluene); whilst an exhaustive investigation of this variable was not carried out, temperatures exceeding *ca* 80 °C (*e.g.*, refluxing benzene) gave *on average* lower isolated yields of product, as did reactions carried out at lower temperatures (*e.g.*, refluxing $CH_2Cl_2$). For this reason, THF and *n*-hexane were the solvents of choice for their milder boiling points (65 °C).

* In this complex, it is the ring atoms themselves which are diametrically opposed to either the CO or $P(OMe)_3$ ligands. Indeed, the affected atoms are slightly displaced from the mean plane of the arsolyl ring by *ca* 0.040 (*trans* to CO) or 0.030 (*trans* to $(POMe)_3$) Å, which supports the assertion of competitive π-bonding effects about the $d^8$-cobalt(I) centre.

3) Despite being a more atom-economical process *in charta*, thermolysis of $[Co_2(CO)_8]$ with a biarsolyl $(AsC_4R_4)_2$ (two will be encountered in later chapters) was not attempted. MATHEY has obtained a pair of 2,5-disubstituted phospholyl complexes $[Co(CO)_2(\eta^5\text{-}PC_4R_2H_2)]$[36, 37] R = Ph or *t*-Bu) by this strategy (notably in high yields), though at the time this work was being carried out such reagents were not available since the reduction of $XAsC_4R_4$ to $[AsC_4R_4]^-$ (necessary for biarsolyl synthesis; X = Cl or Ph) was proving troublesome.

4) The fate of the *As*-substituent in these experiments is not known. It became apparent that increasing the Co(0)/$XAsC_4R_4$ ratio beyond 2:1 (that is, equimolar proportions $[Co_2(CO)_8]$ and arsole; X = Ph or Cl) to 2:2 (two equivalents of arsole per $[Co_2(CO)_8]$) did, on average, *not* increase isolated yields of $[Co(CO)_2(\eta^5\text{-}AsC_4R_4)]$. Where stable toward chromatography, varying quantities of unreacted arsole were recovered when equal stoichiometries were employed. A mechanism requiring at least one equivalent of Co(0) to serve as a reducing agent is suspected, which presumably captures the arsolyl ring as the other cobalt atom acquires the *As*-substituent (**Scheme 3.9**). The occurrence of $[CoX(CO)_4]$, for example, alongside $[Co(CO)_2(\eta^5\text{-}AsC_4R_4)]$ could substantiate this proposal however such species are acutely thermolabile (**Section 3.5**) and would inevitably decompose under the reaction conditions.




**Scheme 3.9**: Idealised route to $\eta^5$-arsolyl complex formation *via* thermolysis of an arsole $XAsC_4R_4$ with $[Co_2(CO)_8]$.

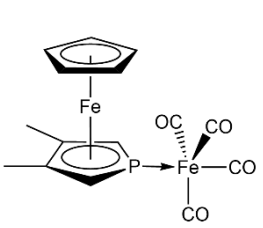
In an attempt to generate a thermally stable by-product, the heretofore unknown $(C_5Me_5)AsC_4Ph_4$ and $H_2C{=}CHCH_2AsC_4Ph_4$ were synthesised (a crystal structure of the former is shown in **Section 8.7** of the **Appendix**) and brought to reflux in *n*-hexane with one equivalent of $[Co_2(CO)_8]$: as expected, $[Co(CO)_2(\eta^5\text{-}AsC_4Ph_4)]$ *was* isolated but the known $[Co(CO)_2(\eta^5\text{-}C_5Me_5)]$[46] and $[Co(CO)_3(\eta^3\text{-}C_3H_5)]$[47] were *not*, nor were they spectroscopically detected in the corresponding reaction mixtures. Moreover, when $PhAsC_4Ph_4$ was employed in the synthesis of $[Co(CO)_2(\eta^5\text{-}AsC_4Ph_4)]$, no obvious aromatic species such as

biphenyl, benzophenone, benzaldehyde, naphthalene, anthraquinone *etc.* arising from radical-chain, hydrogen abstraction or carbonylation pathways were detected by GC-MS. The precise mechanism of $[Co(CO)_2(\eta^5\text{-}AsC_4R_4)]$ formation remains truly obscure at the present time.

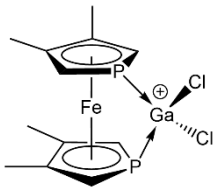
## 3.4 Coordination Complexes of $[Co(CO)_2(\eta^5\text{-}AsC_4Me_4)]$

An illustrative demonstration of the comparative maturity of phosphole chemistry to that of arsoles, stiboles *etc.*, is found in the abundance of examples exploiting the *P*-centred nucleophilicity of transition metal $\eta^5$-phospholyl complexes $[ML_n(\eta^5\text{-}PC_4R_4)]$ to generate $\eta^1{:}\eta^5$-bimetallic assemblies. Interest in these types of *metallo*-ligands is founded upon the oft-advocated synergistic effects of holding two (or more) metal centres within proximity on subsequent catalytic activity, notwithstanding the preceding fundamental relevance to potential intermetallic bonding between (dis)similar *d*-block elements.

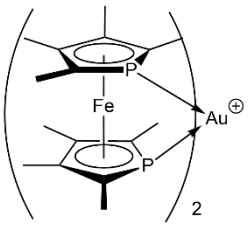
Such $\eta^1{:}\eta^5$-phospholyl complexes can be roughly divided into two categories: those which utilise the phospholyl *P*-donor atom as the sole donor function,[48-52] or those which act in tandem with a second, potentially hemilabile, donor function pendant to the ring system.[53-57] This distinction is warranted since – upon complexation of an extraneous metal fragment – the presence of a LEWIS base supplementing the *P*-phospholyl atom will dictate the relative spatial dispositions of the two metal centres to one another, thereby determining whether recourse to intermetallic bonding is even geometrically viable (ignoring any electronic demands of the metal centres). A representative albeit non-exhaustive selection of bimetallic bridge-assisted phospholyl complexes is shown in **Chart 3.1**.



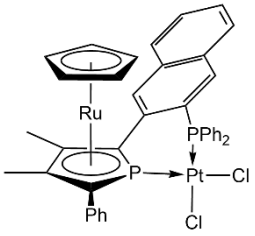

MATHEY, 1980



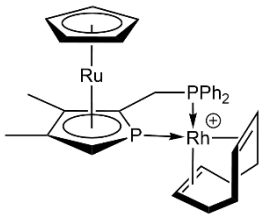

MATHEY, 2002



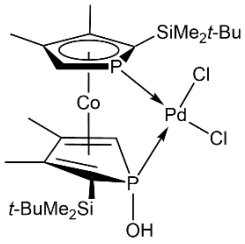

MATHEY, 2003




CARMICHAEL, 2007



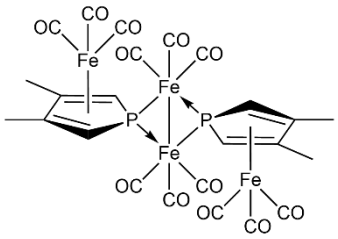

RICARD, 2009



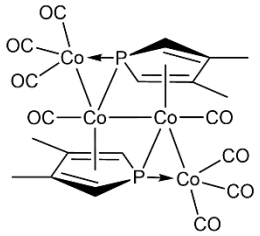

CARMICHAEL, 2019

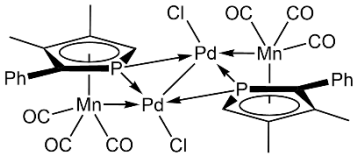
**Chart 3.1**: A selection of previously reported bimetallic $\eta^1$:$\eta^5$-phospholyl complexes.

Most examples are encountered *sans* intermetallic interactions since the π-binding metal is simply a chassis for the phospholyl *P*-donor function. This is invariably a consequence of the phospholyl ligand having been installed onto a metal centre which is already saturated (*e.g.*, Fe($\eta^5$-$C_5H_5$), Ru($\eta^5$-$C_5Me_5$)), though one should be mindful that this phenomenon is possibly self-selecting since replete metal complexes will invariably lend themselves to being synthetically accessible and thermally/chemically stable. Instances of $\eta^1$:$\eta^5$-phospholyl ligands which support an authentic intermetallic bond are few in number, being limited to the Pd-Pd and Mn→Pd bonded dimer $[Mn_2(CO)_6\{\mu\text{-}\eta^1\text{:}\eta^5\text{-}PC_4(H)PhMe_2\}_2\cdot\{PdCl\}_2]$ (**Chart 3.2**) obtained by MATHEY *via* addition of *cis*-$[PdCl_2(NCPh)_2]$ to $[Mn(CO)_3(\eta^5\text{-}PC_4(H)PhMe_2)]$.[58] Though not strictly containing $\eta^5$-phospholyl systems, the ligand can remain π-bound and still serve as a platform for intermetallic bonding, as observed in the tetranuclear complexes $[Fe_4(CO)_{12}(\mu_3\text{-}\eta^1\text{:}\eta^1\text{:}\eta^4\text{-}PC_4H_2Me_2)_2]$ and $[Co_4(CO)_8(\mu_3\text{-}\eta^1\text{:}\eta^1\text{:}\eta^4\text{-}PC_4H_2Me_2)_2]$[59] (also prepared by MATHEY; **Chart 3.2**), and the Pd-Pd bonded di(phospholyl)xanthene dimer $[Pd_2\{\mu\text{-}\eta^1\text{:}\eta^1\text{:}\eta^2\text{-}(PC_4H_2Me_2)_2\text{-xanthene}\}_2]$ characterised by LE FLOCH.[60]



MATHEY, 1983





MATHEY, 1994

**Chart 3.2**: Metal-metal bonded complexes featuring μ-σ:π-phospholyl ligands previously prepared by MATHEY.

No examples of metal-metal bonded complexes featuring μ-$\eta^5$-arsolyl ligands have been prepared to date. With this in mind, the following sections detail the synthesis of three such species utilising the previously described $[Co(CO)_2(\eta^5\text{-}AsC_4Me_4)]$ (**Section 3.3.4**) as a ditopic LEWIS base.

### 3.4.1 Computational Aspects of $[Co(CO)_2(\eta^5\text{-}EC_4H_4)]$ (E = CH, N, P, As, Sb)

Given the prototypical cyclopentadienyl cobalt(I) dicarbonyl has established LEWIS basic character,[61, 62] it was of interest to computationally probe the isoelectronic Group 15 heterocyclopentadienyl complexes to ascertain what effect – if any – the inclusion of a free donor within the ring might have on the electronic properties of the molecule(s). Calculations were carried out using DFT (gas phase: ωB97X-D/6-31G*/LANL2DZ) for both $[Co(CO)_2(\eta^5\text{-}C_5H_5)]$ and the series of model complexes $[Co(CO)_2(\eta^5\text{-}EC_4H_4)]$ (E = N, P, As, Sb); the calculated frontier orbital energies (LUMO, HOMO and HOMO-1) of $[Co(CO)_2(\eta^5\text{-}C_5H_5)]$ and $[Co(CO)_2(\eta^5\text{-}EC_4H_4)]$ are shown together in **Figure 3.14**. The frontier orbitals of $[Co(CO)_2(\eta^5\text{-}C_5H_5)]$ and $[Co(CO)_2(\eta^5\text{-}AsC_4H_4)]$ are shown in **Figure 3.15**.

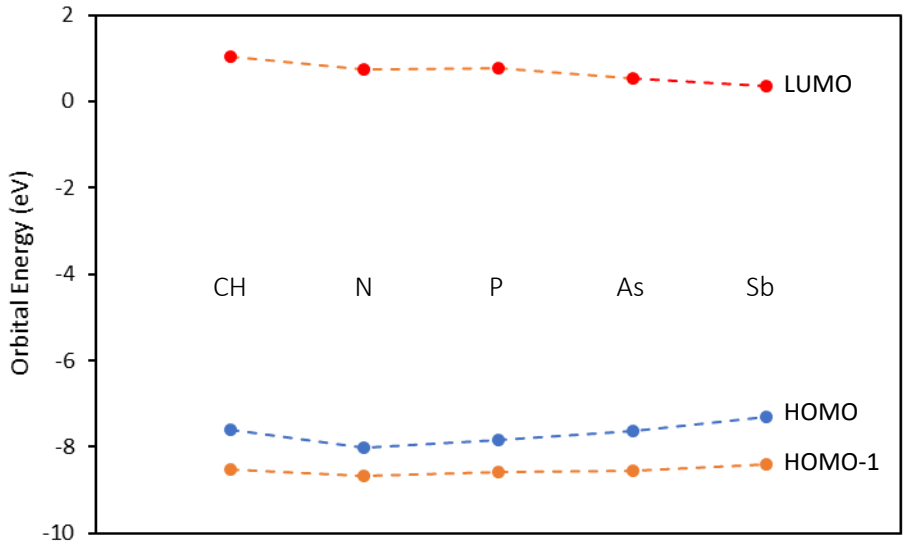



**Figure 3.14**: Calculated frontier orbital energies for $[Co(CO)_2(\eta^5\text{-}EC_4H_4)]$ (E = CH, N, P, As, Sb) using DFT at the ωB97X-D/6-31G*/LANL2DZ level of theory.

The LUMO of $[Co(CO)_2(\eta^5\text{-}C_5H_5)]$ is unsurprisingly constructed of metal- and cyclopentadienyl-centred orbitals. For the model $[Co(CO)_2(\eta^5\text{-}EC_4H_4)]$ complexes the LUMO is apportioned between the Co(I) atom and an out-of-plane E($p_x$) orbital lying perpendicular to the *pentahapto* ring. This lobe is topologically isolated from the remainder of the orbital and is purely localised on the heteroatom. In line with other $\lambda^3$-arsoles, nucleophilic attack is intuitively expected to occur at the arsenic atom for reasons of kinetic accessibility, though this was not examined during this work.

In all examples the HOMO-1 is constructed wholly or in large part from the Co($d_{z^2}$) orbital, which readily corroborates the metallocentric nucleophilicity of $[Co(CO)_2(\eta^5\text{-}C_5H_5)]$; for the prototypical complex, however, this is effectively the only frontier orbital which may practically function as a LEWIS base since the HOMO is predominantly involved in bonding to the cyclopentadienyl ligand. This is also the case for the Group 15 complexes $[Co(CO)_2(\eta^5\text{-}E_4H_4)]$, however in these examples the orbital emanates from the ring into the region of space beyond the heteroatom and the Co(I) centre – this lobe becomes increasingly voluminous and diffuse upon descending the Group 15 elements examined (**Figure 3.16**). The HOMO-1 of $[Co(CO)_2(\eta^5\text{-}EC_4H_4)]$ also receives an increasing contribution from the heteroatom with ascending atomic number; in this case it is the in-plane E($p_z$) orbital which protrudes prominently from the molecule, co-directional with the mutually antibonding Co($d_{z^2}$) orbital. This, taken together with the disposition and

energy of the Co($d_z^2$) orbital, suggests that *either the Co(I) or E(III) atoms (or both) may serve as nucleophilic functions* within [Co(CO)$_2$($\eta^5$-EC$_4$H$_4$)].

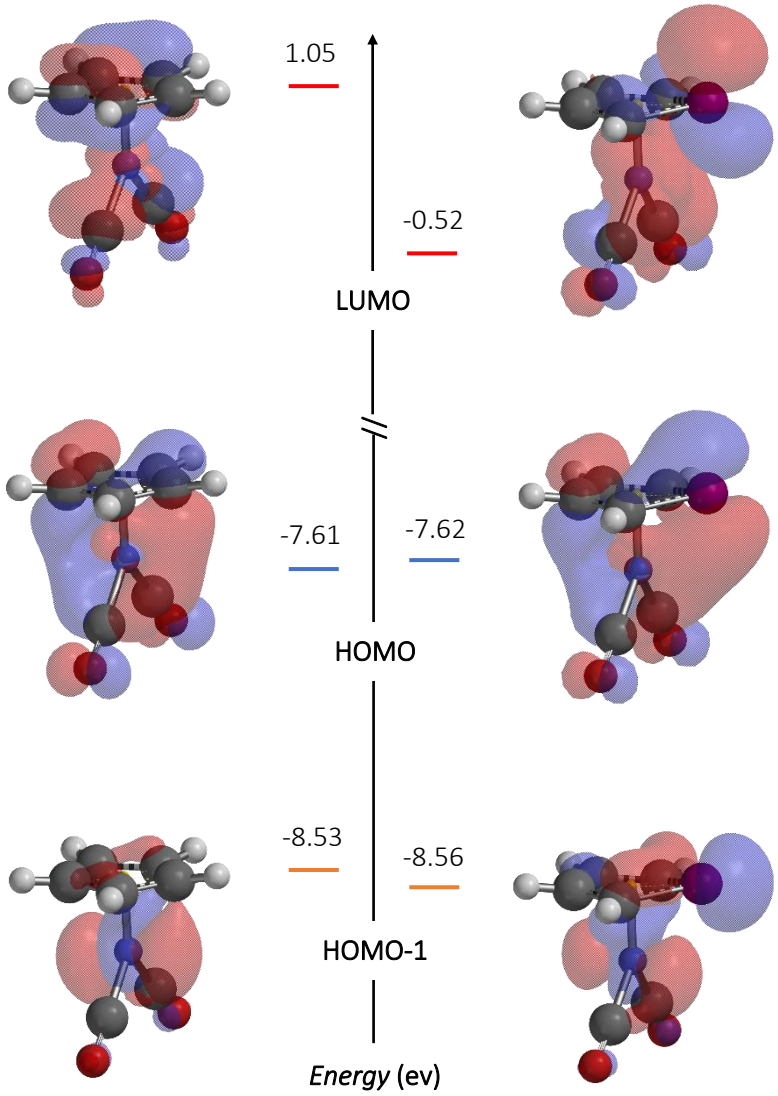



**Figure 3.15**: Frontier molecular orbitals of [Co(CO)$_2$($\eta^5$-C$_5$H$_5$)] (**left**) and [Co(CO)$_2$($\eta^5$-AsC$_4$H$_4$)] (**right**), calculated using DFT at the ωB97X-D/6-31G* level of theory.

Finally, it is worth mentioning in brief the calculated energies of the frontier orbitals (**Figure 3.14**): the LUMO steadily decreases in energy from [Co(CO)$_2$($\eta^5$-NC$_4$H$_4$)] to [Co(CO)$_2$($\eta^5$-SbC$_4$H$_4$)] with an increasing topological contribution from the heteroatom. Conversely, the HOMO and HOMO-1 monotonously *increase* in orbital energy on traversing N through Sb, curiously suggesting that [Co(CO)$_2$($\eta^5$-SbC$_4$H$_4$)] should in fact be the strongest nucleophile of the series; this outcome is counterintuitive in the

regard that the LEWIS basicities of tertiary pnictogines ($ER_3$) are universally recognised to *decrease* with increasing atomic number (all other factors being equal).

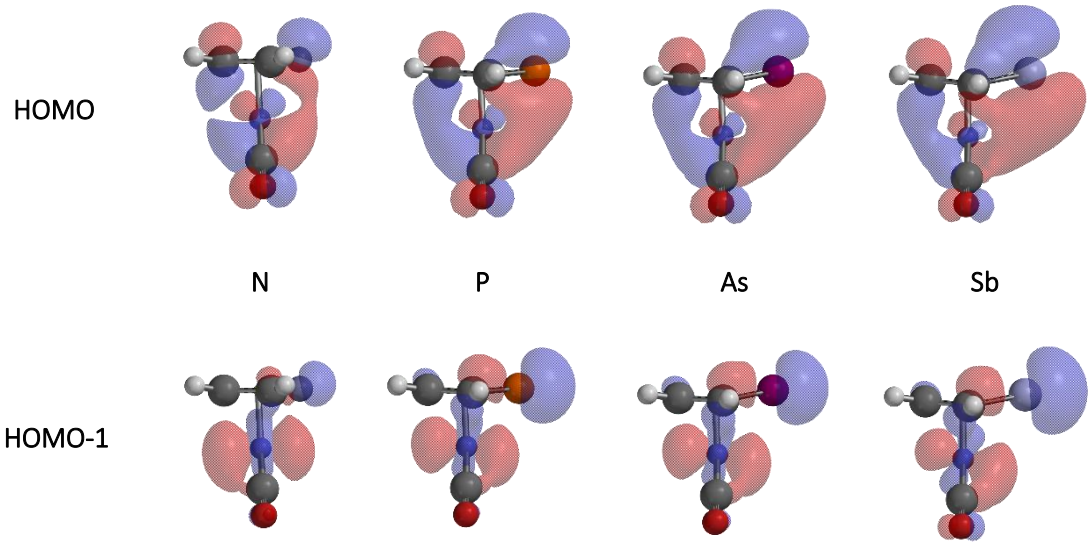
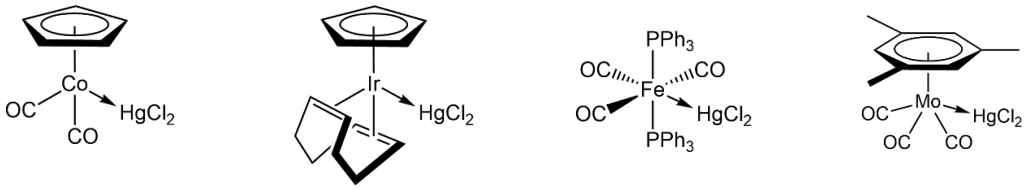



**Figure 3.16**: Comparisons of the HOMO and HOMO-1 topographies for $[Co(CO)_2(\eta^5\text{-}EC_4H_4)]$ (DFT, gas phase: ωB97X-D/6-31G*/LANL2Dζ).

### 3.4.2 Synthesis of $[Co(CO)_2(\mu\text{-}\eta^1\text{:}\eta^5\text{-}AsC_4Me_4)\cdot\{Hg(\mu\text{-}Cl)Cl\}]_2$

A classic demonstration of the LEWIS basicity of $[Co(CO)_2(\eta^5\text{-}C_5H_5)]$ (*inter alia*) is the formation of adducts with mercury(II) halides: $[Co(CO)_2(\eta^5\text{-}C_5H_5)\cdot\{HgCl_2\}]$ was in fact the first recognised example of a metal-only LEWIS acid-base pair, and its crystal structure (featuring an unsupported Co→Hg bond) was determined in 1972 by NOWELL and RUSSELL[61] several years after being first prepared by KEMMITT.[63] A variety of other transition metal-$HgX_2$ adducts have been prepared in the interim since, some of which preserve the Hg-X bond(s),[64-67] and some of which affect ionisation of the same.[65, 68-71] BRAUNSCHWEIG and colleagues discuss the phenomenon of metal-only LEWIS acid-base pairs in a recent and rather comprehensive review,[72] and the unifying feature of all of these LEWIS bases is that the metal centre is reasonably electron rich and coordinatively saturated *i.e.*, $[Mo(CO)_3(\eta^6\text{-}C_6H_3Me_3)]$ is 18-electron yet molybdenum (and tungsten) may frequently accommodate seven-coordinate geometries *e.g.*, $[Mo(CO)_3(\eta^6\text{-}C_6H_3Me_3)\cdot\{HgCl_2\}]$.




KEMMITT, 1966 KEMMITT, 1967 KEMMITT, 1968 WILD, 1968

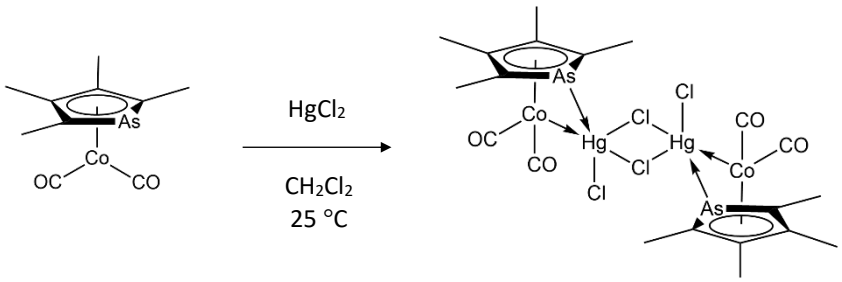
**Chart 3.3**: A selection of previously reported transition metal-$HgCl_2$ adducts.

Given that the model complex $[Co(CO)_2(\eta^5\text{-}AsC_4H_4)]$ was predicted to contain both nucleophilic Co(I) and As(III) centres (**Section 3.4.1**), it was of interest to experimentally determine whether both donor sites could act simultaneously or if one was privileged over the other in this role. The tetramethyl complex $[Co(CO)_2(\eta^5\text{-}AsC_4Me_4)]$ was selected for these experiments given its excellent solubility, simple NMR profile and electron-releasing arsolyl substituent pattern.

Thus, the addition of one equivalent of $HgCl_2$ to a $CH_2Cl_2$ solution of $[Co(CO)_2(\eta^5\text{-}AsC_4Me_4)]$ results in the precipitation of a light yellow solid in high yield. The material obtained proved to be *exceedingly* insoluble in almost all common solvents which precluded the collection of satisfactory NMR spectra, though a solution IR spectrum in acetonitrile* (the only solvent tested in which the product was even slightly soluble) found only two $\nu_{CO}$ absorptions at 2072(vs) and 2036(vs) $cm^{-1}$ (*cf.* $[Co(CO)_2(\eta^5\text{-}C_5H_5)\cdot\{HgCl_2\}]$ $\nu_{CO}$ 2074(vs) and 2040(vs) $cm^{-1}$ in benzonitrile[63]). Notably, the solution IR spectrum was completely devoid of dissociated $[Co(CO)_2(\eta^5\text{-}AsC_4Me_4)]$ whereas the prototypical example $[Co(CO)_2(\eta^5\text{-}C_5H_5)\cdot\{HgCl_2\}]$ reportedly exists in a solvent and temperature dependant equilibrium with its separated constituents.[63] A high-resolution mass spectrum confirms adduct formation between $[Co(CO)_2(\eta^5\text{-}AsC_4Me_4)]$ and $HgCl_2$, although the manifolds of the relevant ion fragments suggest the complex to be dimeric – notably, no fragments arising from mercury dissociation were observed (only successive losses of $Cl^-$) suggesting the coordination of $HgCl_2$ to $[Co(CO)_2(\eta^5\text{-}AsC_4Me_4)]$ to be abnormally strong.

* Attempts to collect NMR spectra in $CD_3CN$, acetone-$d_6$ and $CD_3NO_2$ were difficult since although some material could be induced to dissolve with prolonged trituration and some warming, in the time between partial dissolution and spectrum acquisition (as brief as a few minutes) almost all the product re-precipitated from solution. Even a $^1H$ NMR spectrum – with the high sensitivity of the hydrogen nucleus – consisted solely of the *protio*-solvent signal.

Single crystals were initially difficult to obtain given the very poor solubility of the complex, and traditional re-crystallisation methods from hot solvent mixtures did not afford samples suitable for X-ray diffraction. Therefore, a solution of $HgCl_2$ dissolved in acetone was layered upon a solution of $[Co(CO)_2(\eta^5\text{-}AsC_4Me_4)]$ in the same solvent and the bilayer allowed to slowly diffuse at -30 °C. Inspection of the sample after several days revealed two sets of well-formed crystals had formed: yellow needles (most abundant specimens) and orange prisms (least abundant). Interrogation of both sets of crystals by X-ray diffraction revealed these to be the dimeric complex $[Co(CO)_2(\mu\text{-}\eta^1\text{:}\eta^5\text{-}AsC_4Me_4)\cdot\{Hg(\mu\text{-}Cl)Cl\}]_2$ (**Scheme 3.10**) in agreement with the mass spectrum, which had crystallised in two different forms depending on the relative orientations of the $[Co(CO)_2(\eta^5\text{-}AsC_4Me_4)]$ "ligands" about the $Hg_2(\mu\text{-}Cl)_2$ core, namely *anti* (yellow needles) or *syn* (orange prisms). Both structures are shown in **Figure 3.17**.




**Scheme 3.10**: Synthesis of $[Co(CO)_2(\mu\text{-}\eta^1\text{:}\eta^5\text{-}AsC_4Me_4)\cdot\{Hg(\mu\text{-}Cl)Cl\}]_2$.

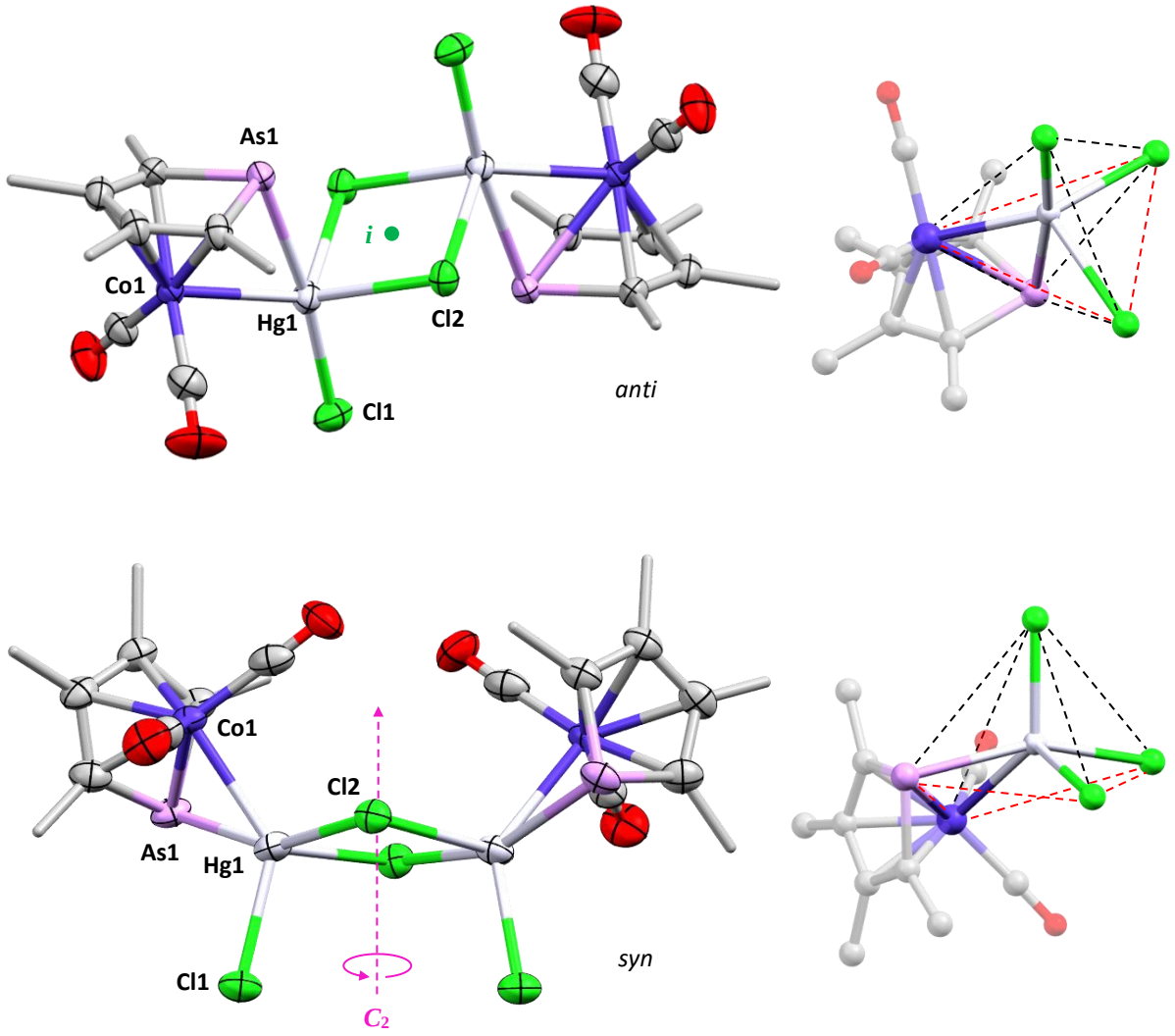



**Figure 3.17**: The molecular structures of the *anti* (**top**) and *syn* (**bottom**) isomers of $[Co(CO)_2(\mu\text{-}\eta^1\text{:}\eta^5\text{-}AsC_4Me_4)\cdot\{Hg(\mu\text{-}Cl)Cl\}]_2$ in a crystal. Methyl groups simplified and hydrogen atoms omitted for clarity. Ellipsoids shown at 50% displacement. **Inset**: Abbreviated perspectives of the molecules highlighting the *pseudo*-trigonal bipyramidal (**top**) and *pseudo*-square planar (**bottom**) geometries of the Hg(II) centres; the *quasi*-equatorial and -basal planes, respectively, are shown in red. *i* = crystallographic inversion centre; $C_2$ = crystallographic two-fold rotation axis.

The structure of each isomer will be discussed in turn. *Anti*-$[Co(CO)_2(\mu\text{-}\eta^1\text{:}\eta^5\text{-}AsC_4Me_4)\cdot\{Hg(\mu\text{-}Cl)Cl\}]_2$ crystallises in monoclinic $P2_1/n$ with a crystallographic centre of inversion located at the midpoint of the $Hg_2(\mu\text{-}Cl)_2$ rhomboid (**Figure 3.17**, **Top**). Only one half of the molecule is therefore crystallographically unique, and the *anti*-configuration is distinguished by the arsolyl moieties lying on diametrically opposed faces of the $Hg_2(\mu\text{-}Cl)_2$ plane. Perhaps the most salient feature concerns the nature of $[Co(CO)_2(\eta^5\text{-}AsC_4Me_4)]$ complexation to each $HgCl_2$ centre, bonding *via both* LEWIS basic Co(I) and As(III) functions in pleasing substantiation of computational predictions. From a valence bond perspective, the $[Co(CO)_2(\eta^5\text{-}AsC_4Me_4)]$ "ligand" formally serves as a four-electron donor with a rather narrow "bite"

angle of *ca* 55°. The coordination polyhedra of the Hg(II) atoms are strikingly different in each isomer: in the *anti*-example this resembles a deformed trigonal bipyramid ($\tau_5 = 0.88$) with the arsenic and cobalt donors occupying *pseudo* axial and equatorial sites, respectively (**Figure 3.17**, **Top Inset**). The As→Hg and Co→Hg dative bonds measure 2.6334(6) and 2.6702(9) Å, respectively, which are slightly longer than the sum of covalent radii for the elements (2.51 and 2.58 Å), and the latter compares to the somewhat shorter Co→Hg bond of 2.578(4) Å in $[Co(CO)_2(\eta^5\text{-}C_5H_5)\cdot\{HgCl_2\}]$.[61] The slight elongation of the Co→Hg interaction here is almost certainly a geometric compromise to accommodate the more highly coordinated Hg(II) centre within the disparate coordination spheres of the $sp^2$-As and Co(I) donor atoms, and is not indicative of any noteworthy electronic phenomenon beyond non-directional spodium* bonding.[73] Coordination of the $HgCl_2$ fragment elongates the Co-As distance by about 0.1 Å to 2.501(1) Å (*cf.* 2.4081(5) Å in $[Co\{P(OMe)_3\}(CO)(\eta^5\text{-}AsC_4Me_4)]$) beyond the calculated sum of covalent radii (2.45 Å), moreover displacing the arsenic atom from the mean plane of the ring by *ca* 13°. This also has the effect of increasing the Co-centroid and Co-carbonyl carbon distances to 1.701 and 1.774(6) Å, respectively (*cf.* 1.676 and 1.719(3) Å in $[Co\{P(OMe)_3\}(CO)(\eta^5\text{-}AsC_4Me_4)]$) and decreasing the C≡O length to 1.136(6) Å (*cf.* 1.158(3) Å in the phosphite complex), all of which are in agreement with a less basic Co(I) centre. The intermetallic (non-bonded) separation of the mercury atoms is 3.7303(4) Å and the terminal Hg-Cl bond measures 2.390(1) Å; the four bridging Hg-Cl bonds are crystallographically identical at 2.777(1) Å suggesting that each Hg-{μ-Cl}-Hg linkage might be described by a three-centre bonding model.

The structure of *syn*-$[Co(CO)_2(\mu\text{-}\eta^1\text{:}\eta^5\text{-}AsC_4Me_4)\cdot\{Hg(\mu\text{-}Cl)Cl\}]_2$ is similar in a few regards to the *anti*-isomer though markedly different in others: the quadrilateral formed by the $Hg_2(\mu\text{-}Cl)_2$ unit is non-planar with an approximate fold angle of *ca* 10° at the pivots defined by the bridging chloride ligands (that is, the crease is in the direction of the (μ-Cl)···(μ-Cl) vector) and *ca* 12° at the pivots defined by the mercury atoms (that is, along the Hg-Hg vector), visually resembling a "butterfly" type arrangement. Moreover, this isomer crystallises in monoclinic space group *C*2/*c* with a crystallographic two-fold axis of rotation located at the midpoint of the $Hg_2(\mu\text{-}Cl)_2$ unit, perpendicular to the mean plane of these atoms (**Figure 3.17**,

* The term "spodium bonding" refers to net attractive interactions between a Group 12 element (Zn, Cd, Hg) and an electron rich LEWIS base; the distinction is made to differentiate these non-covalent interactions from classical coordination bonds found in metal-ligand complexes. See A. FRONTERA *et al. Angew. Chem. Int. Ed.*, **2020**, *59*, 17482—17487 for an overview.

**Bottom**) – only one half of the molecule is therefore crystallographically unique. The coordination polyhedra of the Hg(II) atoms are best described as distorted square-based pyramids ($\tau_5$ = 0.37) with the arsenic and cobalt donors lying in the *pseudo*-basal plane(s) and the non-bridging chlorides occupying the eclipsing apices (**Figure 3.17**, **Bottom Inset**). The As→Hg and Co→Hg dative distances measure 2.7268(9) and 2.6200(4) Å which are crystallographically distinct from those in the *anti*-isomer above, the former being *ca* 0.1 Å longer, and the latter *ca* 0.05 Å shorter than its centrosymmetric counterpart. Whereas three-centre bonding could be invoked for the Hg-(μ-Cl)-Hg linkage in the *anti*-isomer, here the *syn*-configuration contains a $Hg_2(\mu\text{-}Cl)_2$ parallelogram which displays fixed Hg-Cl covalent and Cl→Hg dative bonds of 2.598(2) and 2.708(2) Å in length, respectively. The Co-centroid distance of 1.698 Å is crystallographically indistinguishable to that of the *anti*-isomer, as is the envelope fold of the arsolyl ring (*ca* 12°) and the "bite" angle of the $[Co(CO)_2(\eta^5\text{-}AsC_4Me_4)]$ "ligand" to the Hg(II) centre (*ca* 56°).

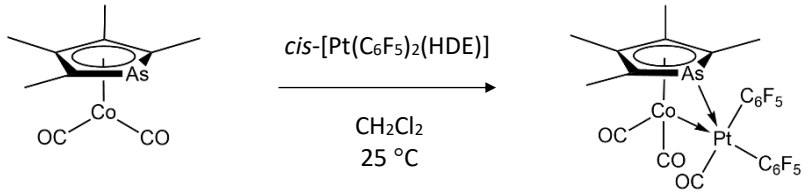
### 3.4.3 Synthesis of $[Co(CO)_2(\mu\text{-}\eta^1\text{:}\eta^5\text{-}AsC_4Me_4)\cdot\{Pt(C_6F_5)_2(CO)\}]$

In addition to Hg(II), coordination to Pt(II) could also be demonstrated: although no reaction was observed (by IR) between $[Co(CO)_2(\eta^5\text{-}AsC_4Me_4)]$ and $[PtR_2(COD)]$ (R = Cl, Me, $C_6F_5$; COD = $\eta^2\text{:}\eta^2$-1,5-cyclooctadiene) in $CH_2Cl_2$ solution and the cobalt arsolyl could be recovered unchanged, the labile diolefin is rapidly displaced from $[Pt(C_6F_5)_2(HDE)]$ (HDE = $\eta^2\text{:}\eta^2$-1,5-hexadiene) to provide after anaerobic chromatography* a bright orange complex in modest yield which displays $\nu_{CO}$ absorptions at 2084(vs), 2053(vs) and 2014(vs) $cm^{-1}$. The occurrence of three carbonyl stretching modes renders a simple $[Co(CO)_2(\mu\text{-}\eta^1\text{:}\eta^5\text{-}AsC_4Me_4)\cdot\{Pt(C_6F_5)_2\}]$ adduct untenable, a conclusion supported by high-resolution mass spectrometry. Analysis by $^1H$ NMR spectroscopy revealed a symmetric arsolyl ligand though the $^{19}F\{^1H\}$ NMR spectrum found *six* separate signals suggesting the two $C_6F_5$ residues affixed to the platinum centre are chemically inequivalent.

Single crystals were obtained by evaporation of $Et_2O$ solution at -30 °C and the molecule was revealed by X-ray diffraction to be $[Co(CO)_2(\mu\text{-}\eta^1\text{:}\eta^5\text{-}AsC_4Me_4)\cdot\{Pt(C_6F_5)_2(CO)\}]$ (**Scheme 3.11**). The Pt(II) centre has evidently scavenged a carbonyl ligand during the reaction and with this arrangement attains

* The complex suffered extensive decomposition on silica gel and neutral alumina, and like other complexes containing perfluoronated residues (discussed in a forthcoming chapter) Florisil® (magnesium silicate) proved to be the chromatography material of choice.

a formally 18-electron configuration. Repeating the reaction with an excess of $[Co(CO)_2(\eta^5\text{-}AsC_4Me_4)]$ provides the same complex in high yield (confirming that some cobalt arsolyl is sacrificed during complex formation, and explaining the modest yield initially obtained), though no attempt was made to perform the reaction in the presence of additional CO, since it was envisioned that *cis*-$[Pt(C_6F_5)_2(CO)_2]$[74] might form competitively.*




**Scheme 3.11**: Synthesis of $[Co(CO)_2(\mu\text{-}\eta^1\text{:}\eta^5\text{-}AsC_4Me_4)\cdot\{Pt(C_6F_5)_2(CO)\}]$; HDE = $\eta^2\text{:}\eta^2$-1,5-hexadiene.

The $^{13}C\{^1H\}$ NMR spectrum ($CD_2Cl_2$) of $[Co(CO)_2(\mu\text{-}\eta^1\text{:}\eta^5\text{-}AsC_4Me_4)\cdot\{Pt(C_6F_5)_2(CO)\}]$ finds the lone platinum-bound carbonyl ligand (177.1 ppm) to high frequency of the pair held by the cobalt atom (198.0 ppm), and the arsolyl ring-carbon nuclei (126.1 and 124.2 ppm) are shifted slightly to higher frequency of the free "ligand" (118.9 and 113.1 ppm, in $C_6D_6$). The pair of chemically inequivalent $C_6F_5$ groups manifest as a complicated pattern of signals in two distinct regions, 137.0—139.6 and 145.9—147.6 ppm (extraction of $J_{FC}$ couplings were not a straightforward task due to extensive overlap), and those signals to high field are tentatively assigned to the $C_6F_5$ group *trans* to the π-acidic carbonyl ligand. The platinum nucleus is found in the $^{195}Pt\{^1H\}$ spectrum† at -4079.7 ppm as an apparent quintet of quintets (approximating an $A_4B_4X$ spin-system) with $^3J_{FPt}$ = 344 Hz and $^4J_{FPt}$ = 83 Hz; the $^5J_{FPt}$ coupling could not be resolved. The signal is of aesthetic interest and a vignette is shown in **Figure 3.18**.

* *Cis*-$[Pt(C_6F_5)_2(CO)_2]$ readily forms upon placing *cis*-$[Pt(C_6F_5)_2L_2]$ (L = solvent, olefin, *etc.*) under an atmosphere of CO.
† $^{195}Pt$ is 33.8% naturally abundant with $I$ = ½.

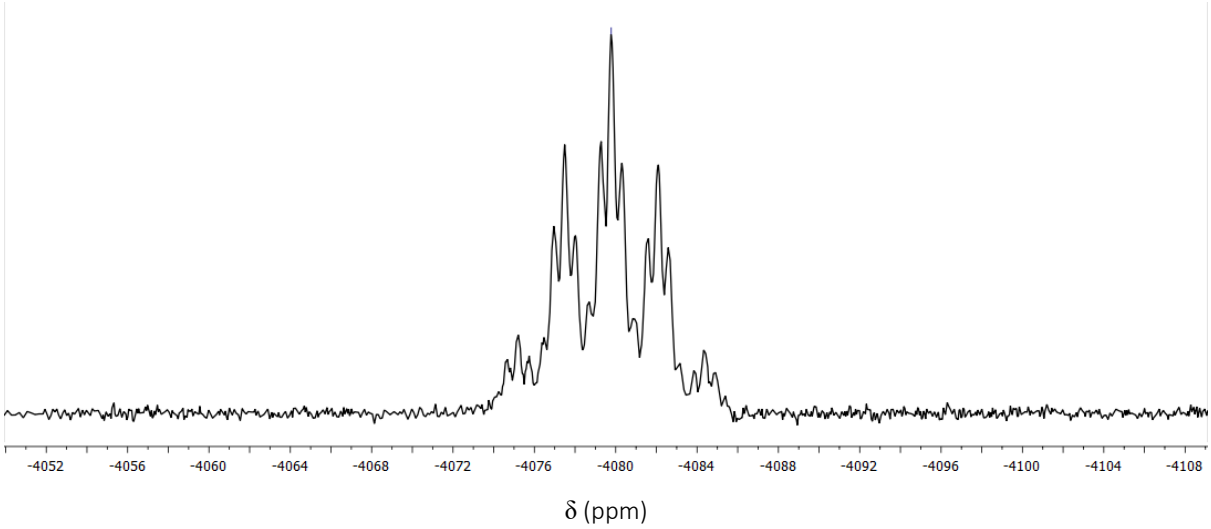



**Figure 3.18**: The $^{195}Pt\{^{1}H\}$ NMR signal for $[Co(CO)_2(\mu\text{-}\eta^1{:}\eta^5\text{-}AsC_4Me_4)\cdot\{Pt(C_6F_5)_2(CO)\}]$ ($CD_2Cl_2$, 150 MHz, 25 °C). See text for an explanation on the origin of fine structure.

In this example, given 3-bond coupling to two pairs of chemically inequivalent *ortho* $^{19}F$ nuclei (A & B), and 4-bond coupling to two pairs of chemically inequivalent *meta* $^{19}F$ nuclei (C & D), one may expect an $A_2B_2C_2D_2X$ spin-system (*i.e.*, a triplet of triplet of triplet of triplets) to arise (disregarding 5-bond coupling to the pair of chemically inequivalent *para* $^{19}F$ nuclei). The occurrence of a quintet of quintets implies that $^3J_{AX} \approx {}^3J_{BX}$ and $^4J_{CX} \approx {}^4J_{DX}$ *i.e.*, each $C_6F_5$ ring is not strictly magnetically equivalent, though they *appear* to be chemically equivalent within the resolution of the spectrometer employed.

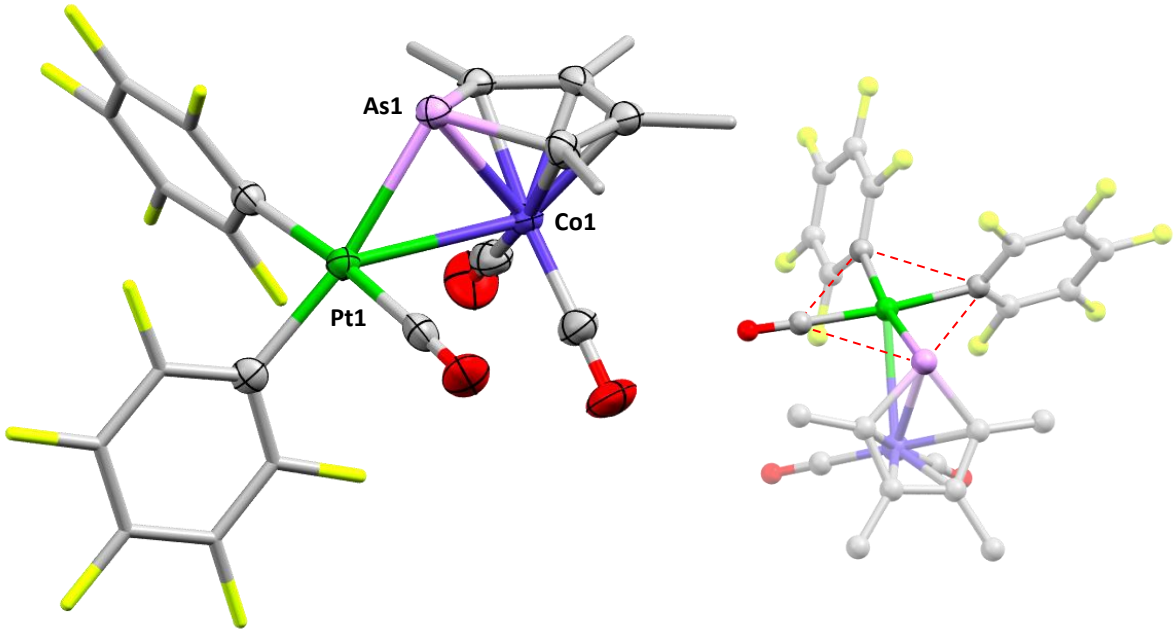



**Figure 3.19**: The molecular structure of $[Co(CO)_2(\mu\text{-}\eta^1{:}\eta^5\text{-}AsC_4Me_4)\cdot\{Pt(C_6F_5)_2(CO)\}]$ in a crystal. Methyl and pentafluorophenyl groups simplified and hydrogen atoms omitted for clarity. Ellipsoids shown at 50% displacement. **Inset**: Abbreviated perspective of the molecule highlighting the square planar geometry of the platinum centre (red).

The crystal structure of $[Co(CO)_2(\eta^5\text{-}AsC_4Me_4)\cdot\{Pt(C_6F_5)_2(CO)\}]$ shows that the $[Co(CO)_2(\eta^5\text{-}AsC_4Me_4)]$ "ligand" is coordinated *via* both Co(I) and As(III) donors to a *cis*-$Pt(C_6F_5)_2(CO)$ centre, with the arsenic donor lying in the coordination plane of the Pt(II) centre *cis* to the surplus carbonyl ligand. The Co→Pt interaction is appended to the mean square plane (**Figure 3.19**, **Inset**) at an angle of about 50°, and the Pt(II) centre is displaced by almost 0.1 Å from the mean plane formed by the carbonyl, arsenic, and bis(pentafluorophenyl) *ipso*-carbon atoms in the direction of the cobalt donor. The gross arrangement of the five donor atoms about the Pt(II) superficially resembles the "upright" coordination of the π-phenanthrene ligand in $[Pt(C_6F_5)_2(CO)(\eta^2\text{-}C_{14}H_{10})]$.[75] The complex crystallises in orthorhombic $P2_12_12_1$ and the examined specimen was therefore enantiomerically pure due to the absence of lateral symmetry within the molecule. Given that the $^1H$ NMR spectrum yielded a symmetric arsolyl ligand with sharp lines, an inversion process inevitably occurs in solution to render the product racemic (on the NMR timescale), though the $^{19}F\{^1H\}$ spectrum suggests whatever mechanism is traversed must preserve the *cis* arrangement of the pentafluorophenyl groups: one may envision a route involving temporarily disengagement of the rather long Co→Pt interaction (*vide infra*) followed by 180° rotation of the Pt(II) square plane about the As→Pt bond. The As→Pt distance of 2.5185(8) Å is shorter than the calculated sum of covalent radii (2.55

Å) albeit elongated compared to other tertiary arsine complexes of the $Pt(C_6F_5)_2$ centre (*ca* 2.39—2.42 Å),[76] however the Co-Pt distance is remarkably long at 2.9960(1) Å (*cf.* sum of covalent radii 2.62 Å).

At present, there are no examples of structurally characterised formal Co→Pt dative bonds to be found in the literature for comparison, though since square-planar Pt(II) possesses a vacant, high-lying *d*-orbital and is therefore not dissatisfied by a 16-electron configuration, the presence of the LEWIS basic Co(I) function is ostensibly superfluous from the perspective of the Pt(II) LEWIS acid. Whether the Co→Pt interaction is comparatively weak due to the "completeness" of the Pt(II) coordination plane, or the platinum centre garnishes itself an additional carbonyl ligand to compensate for weak electronic satisfaction from the Co(I) donor, is indeterminable at the present time. Regardless, whilst the Co→Pt interaction is supposedly rather weak indeed (allowing for symmetrisation of the complex on the NMR timescale; *vide supra*) it does appear to be genuine: DFT calculations (gas phase: ωB97X-D/6-31G*/LANL2DZ) carried out on $[Co(CO)_2(\eta^5\text{-}AsC_4Me_4)\cdot\{Pt(C_6F_5)_2(CO)\}]$* reveal the HOMO-10 to contain such a $Co(d_z^2)\rightarrow Pt(d_z^2)$ bond (**Figure 3.20**) and a LÖWDIN bond order of 0.41 is calculated between these atoms (*cf.* a bond order of 0.75 is found for As→Pt). Incidentally, the HOMO partially consists of *quasi* π-type bonding between As(*p*) and Pt(*d*) orbitals. The LUMO is partitioned between the mutually antibonding Pt, As, and Co atoms though in practise nucleophilic attack would invariably take place at the platinum centre, displacing the weakly-held $[Co(CO)_2(\eta^5\text{-}AsC_4Me_4)]$ "ligand". The As→Pt σ-interaction is found in the HOMO-22 with some mixing to the *trans* Pt-C bond and various networks within that $C_6F_5$ group.

* The DFT-optimised geometry returned from the initial model was in broad agreement with the crystal structure however the Co-Pt distance was appreciably underestimated by *ca* 0.4 Å, and the As-Pt distance overestimated by *ca* 0.2 Å, with significant deformation of the arsolyl ring. The extreme envelope angle produced (*ca* 35°) alongside the short Co-Pt and long As-Pt bonds would seem to suggest an alternate bonding description, namely one involving $\eta^4$-arsole coordination to the Co(I) centre and formally covalent Co-Pt and As-Pt bonds. Such an interpretation is not chemically implausible since complexes of the form $[CoR(CO)_2(\eta^4\text{-diene})]$ are known (*e.g.*, $[Co(SnPh_3)(CO)_2(\eta^4\text{-}Me_2SiC_4Ph_2H_2)]$. See R.J.P. CORRIU *et al. Organometallics* **1986**, *5*, 910—917). However, the gross configuration of the crystal structure supports a model involving an $\eta^5$-arsolyl ligand with As→Pt and Co→Pt interactions. Therefore, energy calculations were carried out using static atom coordinates obtained directly from the crystal structure.

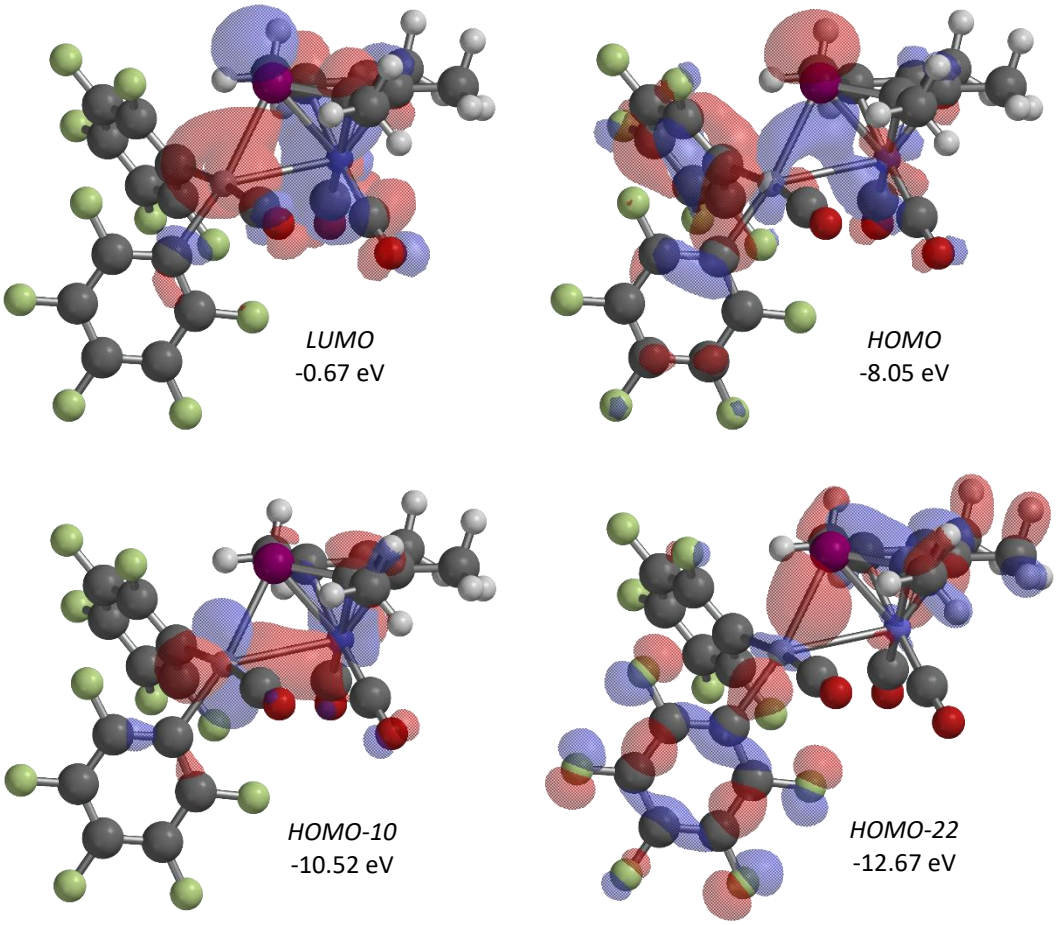



**Figure 3.20**: Selected molecular orbitals of interest for $[Co(CO)_2(\mu\text{-}\eta^1\text{:}\eta^5\text{-}AsC_4Me_4)\cdot\{Pt(C_6F_5)_2(CO)\}]$, calculated using DFT at the ωB97X-D/6-31G*/LANL2Dζ level of theory (gas phase).

### 3.4.4 Synthesis of $[\{Co(CO)_2(\mu\text{-}\eta^1\text{:}\eta^5\text{-}AsC_4Me_4)\}_2\cdot Au][Au(C_6F_5)_2]$

The treatment of $[Co(CO)_2(\eta^5\text{-}AsC_4Me_4)]$ with the non-oxidising LEWIS acidic gold(I) complex $[Au(C_6F_5)(THT)]$ (THT = tetrahydrothiophene, $SC_4H_8$) in $CH_2Cl_2$ provides a dark yellow mixture from which a complex of the same colour is isolated in good yield after workup. The $^{19}F\{^1H\}$ NMR spectrum ($CD_2Cl_2$) finds a trio of resonances at -115.6 (doublet, $^3J_{FF}$ = 30 Hz), -163.0 (triplet, $^3J_{FF}$ = 21 Hz) and -164.1 (doublet of doublets, $^3J_{FF}$ = 23 Hz) for the fluorine nuclei *ortho*, *para* and *meta* to the bound Au(I) atom, respectively, and the arsolyl ring is symmetric by $^1H$ NMR. The solution IR spectrum in $CH_2Cl_2$ finds three $\nu_{CO}$ peaks at 2062(sh), 2051(vs) and 2009(vs) $cm^{-1}$ and like the $HgCl_2$ adduct, a dimeric species is thus formulated. High-resolution mass spectrometry (positive ion) further confirms this assertion yielding an intense ion signal at $m/z \approx 792.8439$ corresponding to a fragment of the composition $[\{Co(CO)_2(\mu\text{-}\eta^1\text{:}\eta^5\text{-}AsC_4Me_4)\}_2\cdot Au]^+$. Single crystals were grown *via* vapour diffusion of $Et_2O$ into $CH_2Cl_2$ solution at -30 °C

and X-ray diffraction revealed the complex to indeed be the salt $[\{Co(CO)_2(\mu\text{-}\eta^1\text{:}\eta^5\text{-}AsC_4Me_4)\}_2\cdot Au][Au(C_6F_5)_2]$ arising from rearrangement of the $AuC_6F_5$ fragment(s), the structure of which is shown in **Figure 3.21**. The $^{13}C\{^1H\}$ NMR spectrum ($CD_2Cl_2$) of the salt is typically simple, with the carbonyl ligands observed at 200.1 ppm and the arsolyl ring-carbon nuclei resonating at 122.7 and 118.0 ppm; the $C_6F_5$ signals within the $[Au(C_6F_5)_2]^-$ anion appear as six well-separated multiplets in the region 150.0—136.8 ppm.

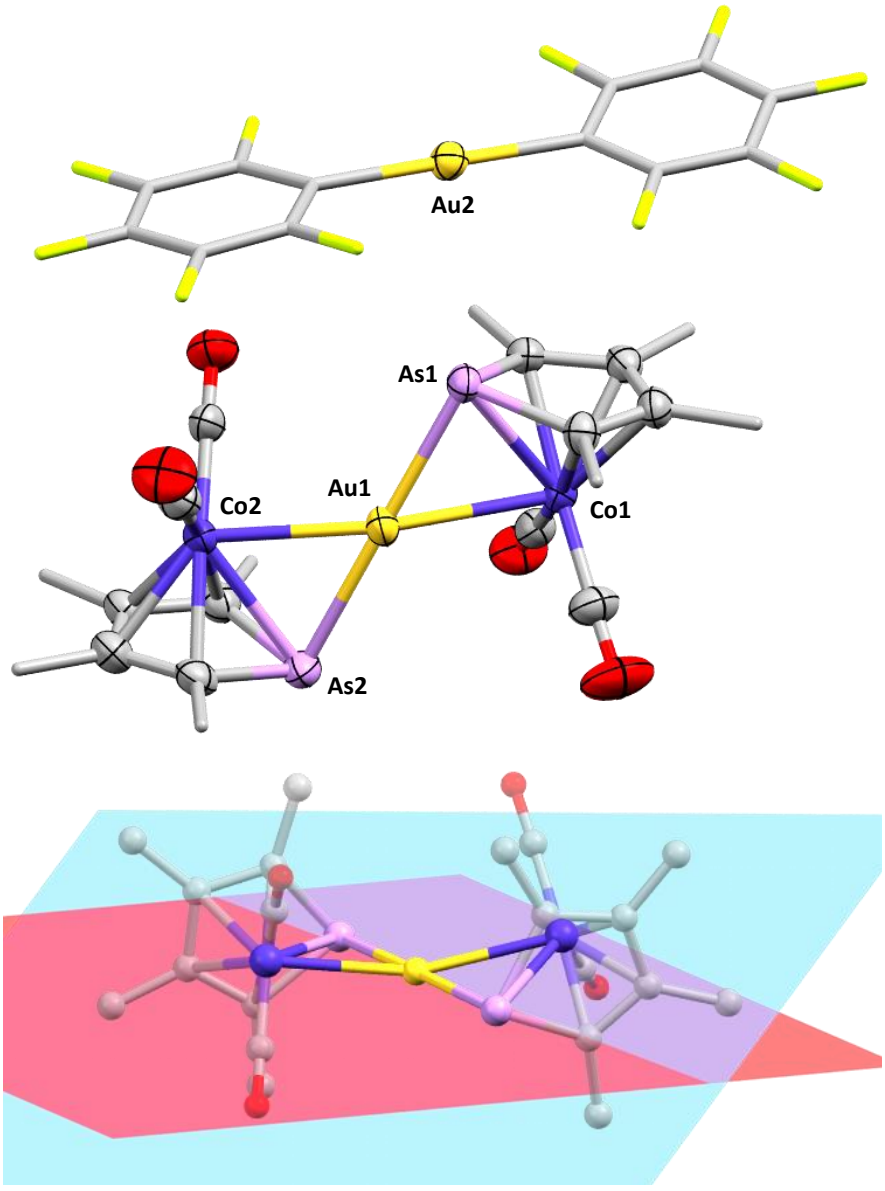



**Figure 3.21**: The molecular structure of $[\{Co(CO)_2(\mu\text{-}\eta^1\text{:}\eta^5\text{-}AsC_4Me_4)\}_2\cdot Au][Au(C_6F_5)_2]$ in a crystal. Methyl and pentafluorophenyl groups simplified and hydrogen atoms omitted for clarity. The asymmetric unit (*P*-1) contains four crystallographically unique molecules and only one is shown. Ellipsoids shown at 50% displacement. **Inset**: Abbreviated perspective of the molecule highlighting the non-planar geometry of the four coordinate $Au^+$ centre.

The unit cell (space group triclinic *P*-1) consists of eight cation-anion pairs of which four are crystallographically unique, though gross configurations and molecular dimensions do not vary appreciably from molecule to molecule. The bidentate nature of the $[Co(CO)_2(\eta^5\text{-}AsC_4Me_4)]$ "ligand" is further exemplified in the cation $[\{Co(CO)_2(\mu\text{-}\eta^1\text{:}\eta^5\text{-}AsC_4Me_4)\}_2\cdot Au]^+$ which contains a four coordinate $Au^+$ centre existing in a highly deformed "bowtie" conformation, somewhere intermediate between square planar and disphenoidal geometries ($\tau_4 = 0.15$, $\tau'_4 = 0.10$).* This coordination environment is nearly planar (As1-Au1-As2 *ca* 177°, Co1-Au1-Co2 *ca* 161°) with the $Au^+$ centre sitting *ca* 0.2 Å outside the plane defined by the quartet of Co(I) and As(III) donor atoms. The pair of $[Co(CO)_2(\eta^5\text{-}AsC_4Me_4)]$ "ligands" are asymmetrically disposed about the $Au^+$ centre, being transposed and offset by *ca* 22° when viewed along the As1-Au1-As2 vector (**Figure 3.21**, **Inset**). The As→Au distances are crystallographically equivalent at *ca* 2.52 Å (mean; sum of covalent radii 2.55 Å) as are the Co→Au bonds at 2.65 Å (mean; sum of covalent radii 2.62 Å). The arsenic atom is protruded from the mean plane of the arsolyl ring upon coordination of the $Au^+$ ion by *ca* 13° (Co-As 2.516 Å), and the Co-centroid distance measures *ca* 1.70 Å. The extended crystalline lattice consists of loosely parallel columns of alternating $[\{Co(CO)_2(\mu\text{-}\eta^1\text{:}\eta^5\text{-}AsC_4Me_4)\}_2\cdot Au]^+$ cations and $[Au(C_6F_5)_2]^-$ anions (**Figure 3.22**). The precise nature of their arrangement differs from pair to pair, with notably short As···$Au(C_6F_5)_2$ interactions (*i.e.*, between the arsolyl arsenic and $[Au(C_6F_5)_2]^-$ gold atoms). These intermolecular distances are not equal, however, varying capriciously between 3.07 Å (shortest) to 3.21 Å (longest) in an irregular fashion throughout the chain.

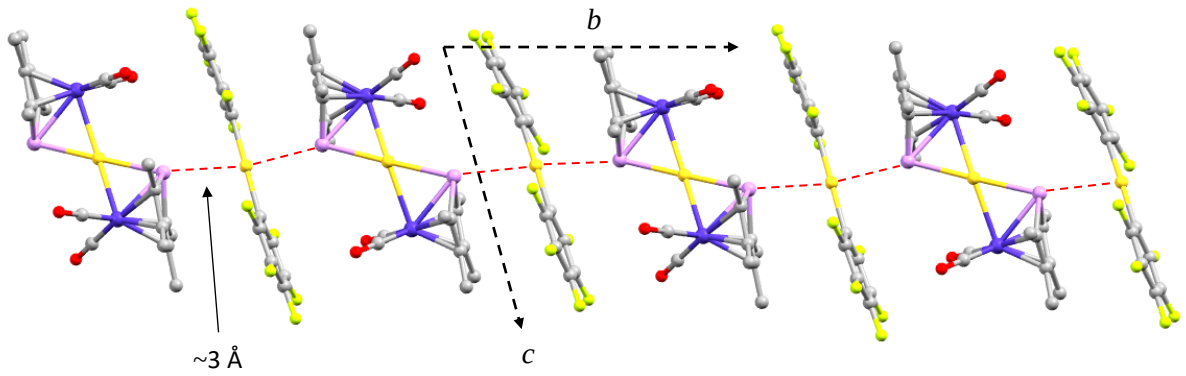



**Figure 3.22**: A section of the extended crystal lattice highlighting the column-like arrangement of the cation-anion pairs, viewed along the crystallographic *a* axis.

* The $\tau_4$ and $\tau'_4$ parameters distinguish between square planar, disphenoidal and tetrahedral geometries: for square planar $\tau_4 = \tau'_4 = 0$, for disphenoidal $\tau_4 \approx 0.43$ and $\tau'_4 \approx 0.24$, for tetrahedral $\tau_4 = \tau'_4 = 1$. See L. Yang, D.R. Powell and R.P. Houser *Dalton Trans.*, **2007**, 955—964 and D. Rosiak, A. Okuniewski and J. Chojnacki *Polyhedron*, **2018**, *146*, 35—41 for derivations of these parameters.

A computational investigation of the $[\{Co(CO)_2(\mu\text{-}\eta^1\text{:}\eta^5\text{-}AsC_4Me_4)\}_2\cdot Au]^+$ cation using DFT (gas phase: ωB97X-D/6-31G*/LANL2DZ) returns a core geometry in good agreement with the crystal structure, and produces LÖWDIN bond orders of 0.78 and 0.56 for the As→Au and Co→Au interactions, respectively. Selected molecular orbitals of interest are shown in **Figure 3.23**. Curiously, the HOMO of this model complex is totally non-bonding with respect to the Co(I) and As(III) donor atoms and the Au(I) cation, and superficially resembles in topology the HOMO of free $[Co(CO)_2(\eta^5\text{-}AsC_4H_4)]$ (**Figure 3.15** and **Figure 3.16**). Similarly, the HOMO-1 is antibonding between the donor atoms and the Au(I) cation, and in essence is a direct summation of the HOMO-1 of $[Co(CO)_2(\eta^5\text{-}AsC_4Me_4)]$ and an in-plane Au(*d*) orbital. The electronic infrastructure governing metal-ligand complexation are found in lower-energy domains, with the Co→Au bond comprising the HOMO-16 and the As→Au bond manifesting in the HOMO-22. Interestingly, the low energy HOMO-20 consists of a mutually bonding interaction between the arsenic and gold atoms which has partial π-symmetry and may be evidence for operative Au→As retrodonation. The LUMO of $[\{Co(CO)_2(\mu\text{-}\eta^1\text{:}\eta^5\text{-}AsC_4Me_4)\}_2\cdot Au]^+$ predominantly consist of the unoccupied Au(*s*) orbital with only very small antibonding contributions from the arsenic and cobalt centres; like the Pt(II) adduct described previously, nucleophilic attack is expected to displace the $[Co(CO)_2(\eta^5\text{-}AsC_4Me_4)]$ "ligand" from the $Au^+$ cation.

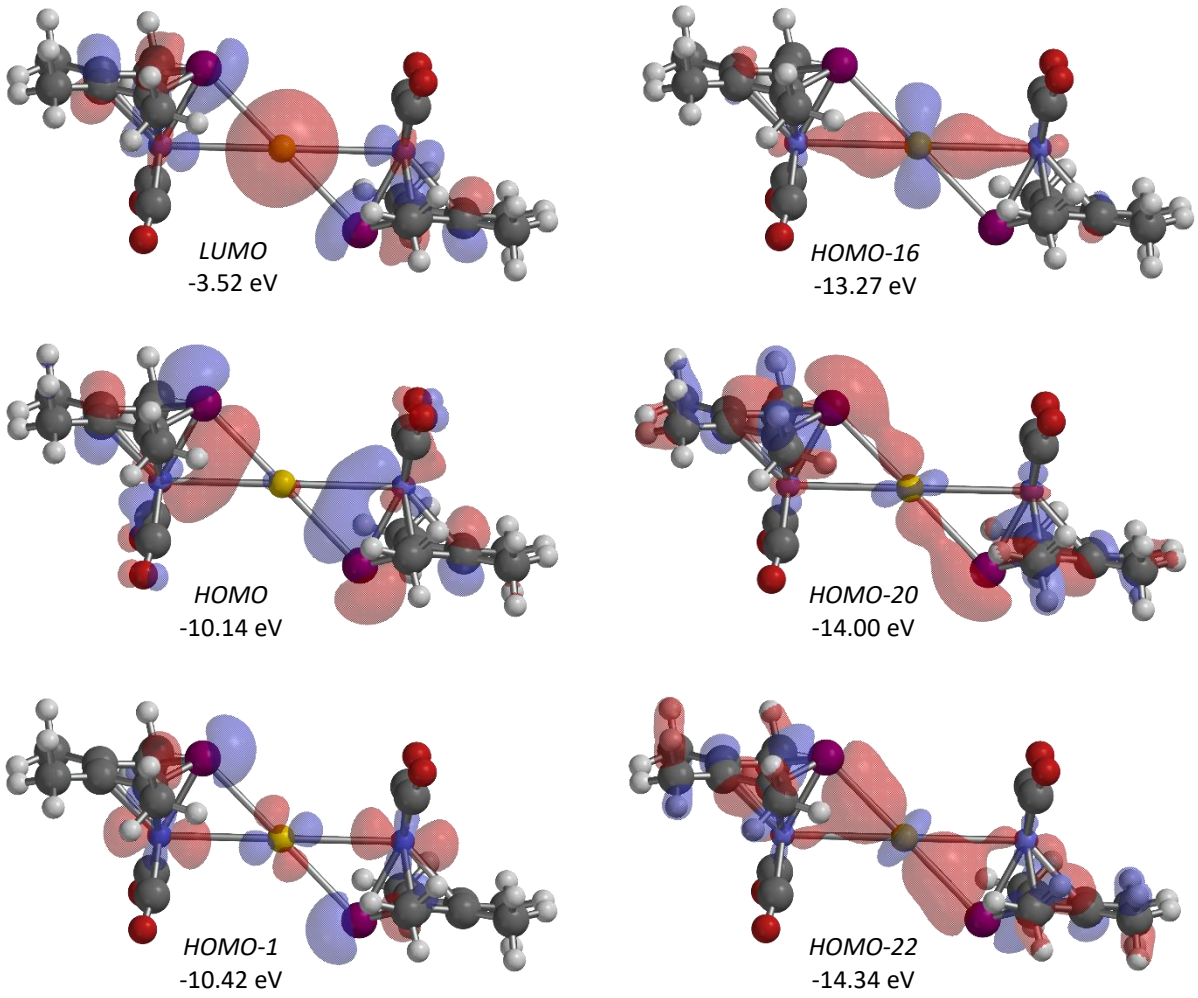



**Figure 3.23**: Selected molecular orbitals of the $[\{Co(CO)_2(\mu\text{-}\eta^1\text{:}\eta^5\text{-}AsC_4Me_4)\}_2\cdot Au]^+$ cation, calculated using DFT at the ωB97X-D/6-31G*/LANL2Dζ level of theory (gas phase).

It is apparent upon examination of the topologies of these frontier orbitals that the As···$Au(C_6F_5)_2$ interactions observed in the solid state (**Figure 3.22**) cannot be convincingly reconciled by the trivalent arsenic atom acting as an electron-acceptor, since the contribution of the heteroatom to the LUMO of the $[\{Co(CO)_2(\mu\text{-}\eta^1\text{:}\eta^5\text{-}AsC_4Me_4)\}_2\cdot Au]^+$ cation is 1) minimal, and 2) not of appropriate geometric disposition. The HOMO, however, *is* suitably directed for such an interaction and it has already been noted that this orbital is non-bonding within the electronic schema of $Au^+$ complexation – that is to say, the arsenic atom would appear to retain some LEWIS basic character upon coordination. DFT calculations were carried out on the $[Au(C_6F_5)_2]^-$ anion (at the same level of theory as $[\{Co(CO)_2(\mu\text{-}\eta^1\text{:}\eta^5\text{-}AsC_4Me_4)\}_2\cdot Au]^+$ for direct comparison) and the frontier orbitals are shown in **Figure 3.24**. Whereas the HOMO of this anion is constructed from mutually antibonding Au(*d*) and $C_6F_5(\pi)$ orbitals, attention is drawn to the LUMO which

consists of a prominent toroidal region encircling the Au(I) centre; the topological compatibility between the *arsenocentric* HOMO of the $[\{Co(CO)_2(\eta^5\text{-}AsC_4Me_4)\}_2{\cdot}Au]^+$ cation and the *aurocentric* LUMO of the $[Au(C_6F_5)_2]^-$ anion is readily obvious. The intermolecular As···$Au(C_6F_5)_2$ contacts observed in the crystal structure of $[\{Co(CO)_2(\mu\text{-}\eta^1{:}\eta^5\text{-}AsC_4Me_4)\}_2{\cdot}Au][Au(C_6F_5)_2]$ might therefore be described as having As→$Au(C_6F_5)_2$ directionality, a counterintuitive outcome when considering that a *cationic* species acting as a LEWIS base and an *anionic* species acting as a LEWIS acid would be, to say the least, non-classical behaviour.

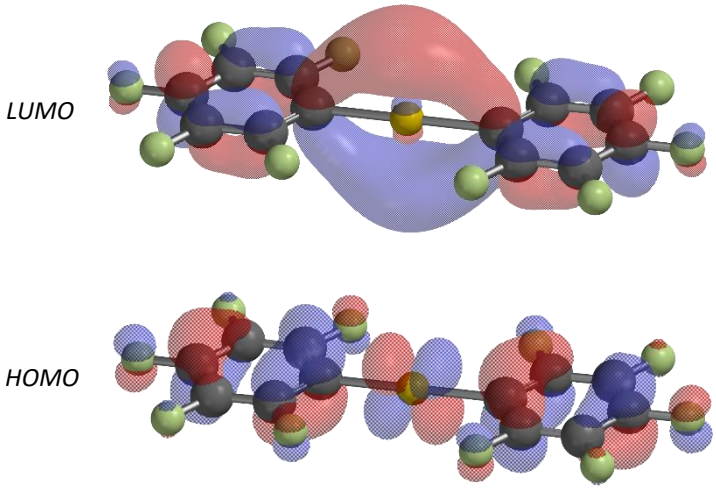
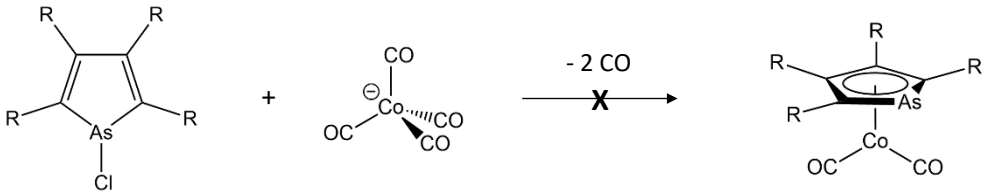



**Figure 3.24**: Frontier molecular orbitals of the $[Au(C_6F_5)_2]^-$ anion, calculated using DFT at the ωB97X-D/6-31G*/LANL2Dζ level of theory (gas phase).

## 3.5 σ-Covalent Arsolyl Complexes of Cobalt(I)

### 3.5.1 Attempted Synthesis of $[Co(CO)_2(\eta^5\text{-}AsC_4Ph_4)]$ from $[Co(CO)_4]^-$ and $ClAsC_4Ph_4$

Given the sub-optimal yields of $[Co(CO)_2(\eta^5\text{-}AsC_4R_4)]$ obtained *via* thermolysis of $[Co_2(CO)_8]$ with $\lambda^3$-arsoles, an alternative synthesis was sought. A strategy involving direct installation of the cobalt centre on an arsolyl ring was envisioned, and the idea born from this conceptualisation would be combination of the $[Co(CO)_4]^-$ nucleophile with an *As*-chloro arsole (**Scheme 3.12**). A similar strategy was successful for preparing complexes of the type $[Co(CO)_2(\eta^5\text{-}C_5R_5)]$ from $[Co(CO)_4]^-$ and $C_5R_5X$ (X = halide)[77] and it was optimistically hoped that thermal decarbonylation – being driven by the chelate effect of *pentahapto* coordination – would ensue upon mixing, as both ABEL and MATHEY have demonstrated during the synthesis of $[M(CO)_3(\eta^5\text{-}AsC_4Ph_4)]$ (M = Mn, Re) and $[Fe(\eta^5\text{-}C_5H_5)(\eta^5\text{-}AsC_4Me_2H_2)]$.[39, 78]



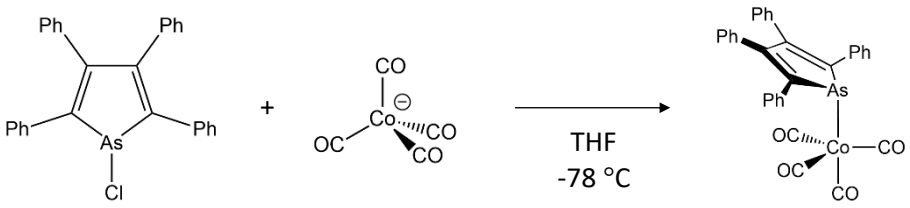

**Scheme 3.12**: Proposed alternate salt elimination synthesis of *pentahapto* arsolyl complexes $[Co(CO)_2(\eta^5\text{-}AsC_4R_4)]$.

The exceedingly air-sensitive $Na[Co(CO)_4]$* was isolated as a white crystalline solid in high yield *via* reduction of $[Co_2(CO)_8]$ with NaH† in $Et_2O$.[79] Combination of the anion with one equivalent of $ClAsC_4Ph_4$ in THF at -78 °C *immediately* affords a deep red solution which proved to be quite thermally sensitive, converting upon warming with gas evolution to a turbid brown suspension and deposition of insoluble reddish-brown residues. The target complex, namely $[Co(CO)_2(\eta^5\text{-}AsC_4Ph_4)]$, was neither observed in nor isolated from the soluble portion of the reaction mixture and the same outcome occurred in both $Et_2O$ and toluene media, even upon heating the latter to reflux (110 °C). Since the target $\eta^5$-arsolyl complex is itself stable in solution at ambient temperature, it became apparent at an early stage that this approach was profoundly futile.

An IR spectrum of a dilute, dark red mixture of $Na[Co(CO)_4]$ and $ClAsC_4Ph_4$ in THF (maintained at -78 °C and measured promptly) displayed four prominent $\nu_{CO}$ absorptions at 2095(m), 2032(sh), 2021(vs) and 2007(vs) $cm^{-1}$ (**Figure 3.25**); the initial product of the reaction is formulated as the trigonal bipyramidal complex $[Co(AsC_4Ph_4)(CO)_4]$ with the non-cylindrical σ-*As*-covalent arsolyl ligand positioned on the three-fold axis (**Scheme 3.13**). Aside from being the most-intuitive molecular geometry, the above IR data compare favourably with other five-coordinate $[CoR(CO)_4]$ complexes previously reported[80-83] and a simulated spectrum of the model complex $[Co(AsC_4H_4)(CO)_4]$ (**Figure 3.26**). In particular, the high energy $\nu_{CO}$ band near *ca* 2100 $cm^{-1}$ (irrespective of solvent) appears indicative of *very labile* carbonyl ligand.

* IR (THF, 25 °C) $\nu_{CO}$ 1889(vs), 1855(s) $cm^{-1}$.

† Alternative published methods involving the use of Na/Hg or NaOH as the reducing agents were avoided since $Hg[Co(CO)_4]_2$ and $H_2O$, respectively, may contaminate the $Na[Co(CO)_4]$ product. See R.B. King *J. Inorg. Nucl. Chem.*, **1963**, *25*, 1296—1298 and W.F. Edgell and J. Lyford *Inorg. Chem.*, **1970**, *9*, 1932—1933.




**Scheme 3.13**: Synthesis of thermally-sensitive $[Co(AsC_4Ph_4)(CO)_4]$

Attempts to isolate $[Co(AsC_4Ph_4)(CO)_4]$ or collect other spectroscopic information were frustrated by its extreme thermolability, a not-uncommon feature of mononuclear cobalt(I) arsenide complexes.[84-86] The complex appears to decompose to a second species, however: allowing a THF solution of $[Co(AsC_4Ph_4)(CO)_4]$ to warm to ambient temperature sees a gradual replacement of the above $\nu_{CO}$ absorptions with four new signals at 2035(vs), 2005(s), 1999(vs) and 1973(s) $cm^{-1}$ in addition to free carbon monoxide* at 2128 $cm^{-1}$ (a time-dependent IR spectrum is shown in **Figure 3.25**). A plot of $\ln[I_{2095}]$† *vs.* time shows the conversion to be first-order with respect to $[Co(AsC_4Ph_4)(CO)_4]$ with $k \approx 0.320$ $min^{-1}$ and a $t_{1/2}$ of ~2.5 min *for this particular decomposition process*.‡ The product of decomposition is formulated as the centrosymmetric binuclear dimer $[Co_2(\mu\text{-}AsC_4Ph_4)_2(CO)_6]$ by comparison with data reported for other bridging pnictogenido complexes $[Co_2(\mu\text{-}ER_2)_2(CO)_6]$,[84, 87-89] and with a simulated spectrum of the model complex $[Co_2(\mu\text{-}AsC_4H_4)_2(CO)_6]$ (**Figure 3.26**). The dimer itself was also of limited stability and gradually decomposed over time, or upon removal of the solvent, to dark red materials which are likely $[Co(AsC_4Ph_4)(CO)_3]_x$ oligomers.

* Confirmed by comparison with a CO-saturated THF solution.
† The intensity of the highest energy *A*' mode (2095 $cm^{-1}$) was chosen as a measure of $[Co(AsC_4Ph_4)(CO)_4]$ concentration since this peak does not overlap with any others observed in the spectrum.
‡ Caution is exercised in placing too much significance on these kinetic parameters since the decomposition process does not take place at a constant temperature, the data being measured over a *ca* 100 °C gradient.

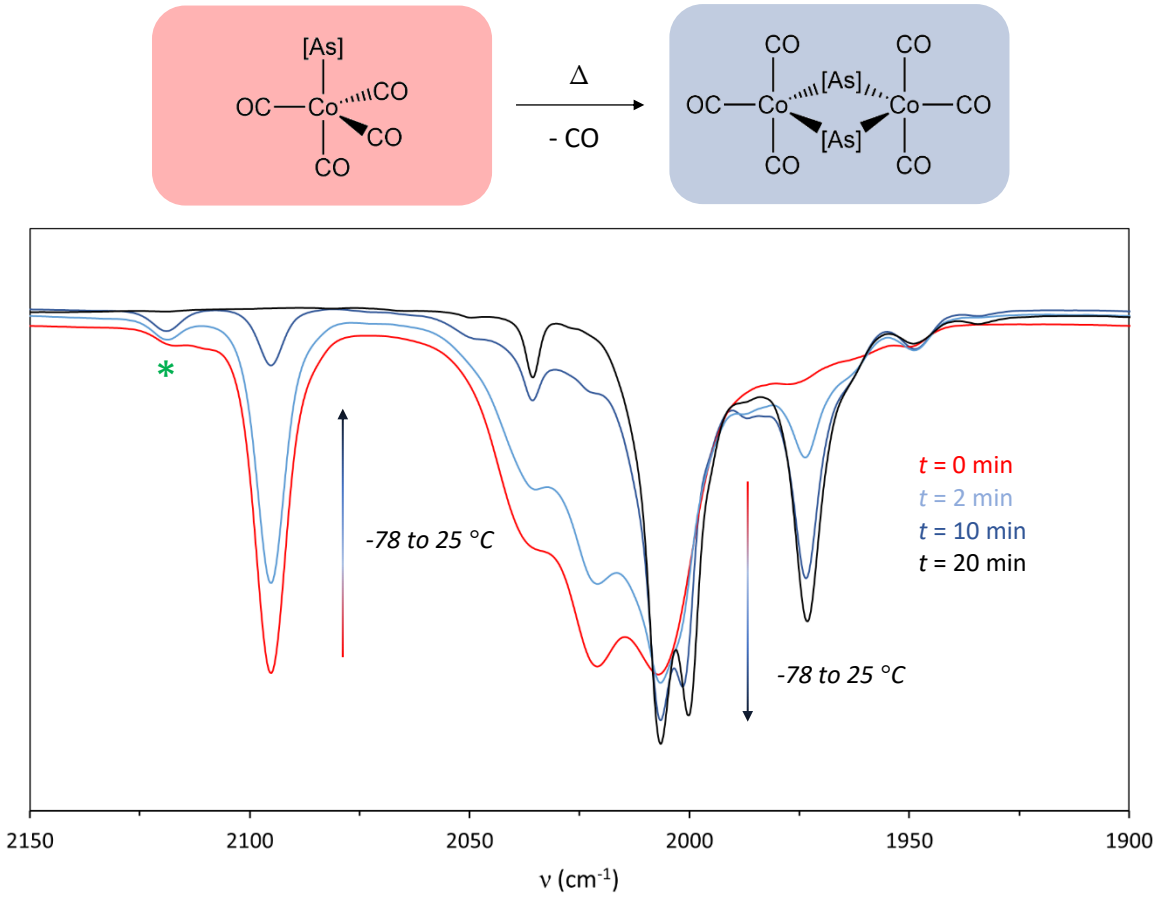



**Figure 3.25**: Time-dependent solution IR spectra following the decarbonylation of $[Co(AsC_4Ph_4)(CO)_4]$ at -78 °C (red trace) to $[Co_2(\mu\text{-}AsC_4Ph_4)_2(CO)_6]$ at ambient temperature (dark blue trace) in THF. See text for peak wavenumbers. Spectra were collected over the course of 20 minutes with unaided warming. The peak at *ca* 1950 $cm^{-1}$ arises from an unknown species whose concentration did not change over time; no $\nu_{CO}$ absorptions were observed below 1900 $cm^{-1}$. * = free CO. [As] = $AsC_4Ph_4$.

The molecular geometries of the model complexes $[Co(AsC_4H_4)(CO)_4]$ and $[Co_2(\mu\text{-}AsC_4H_4)_2(CO)_6]$ were optimised using DFT (gas phase: ωB97X-D/6-31G*) and the computed structures are shown in **Figure 3.26**, alongside their predicted IR spectra in the carbonyl region.

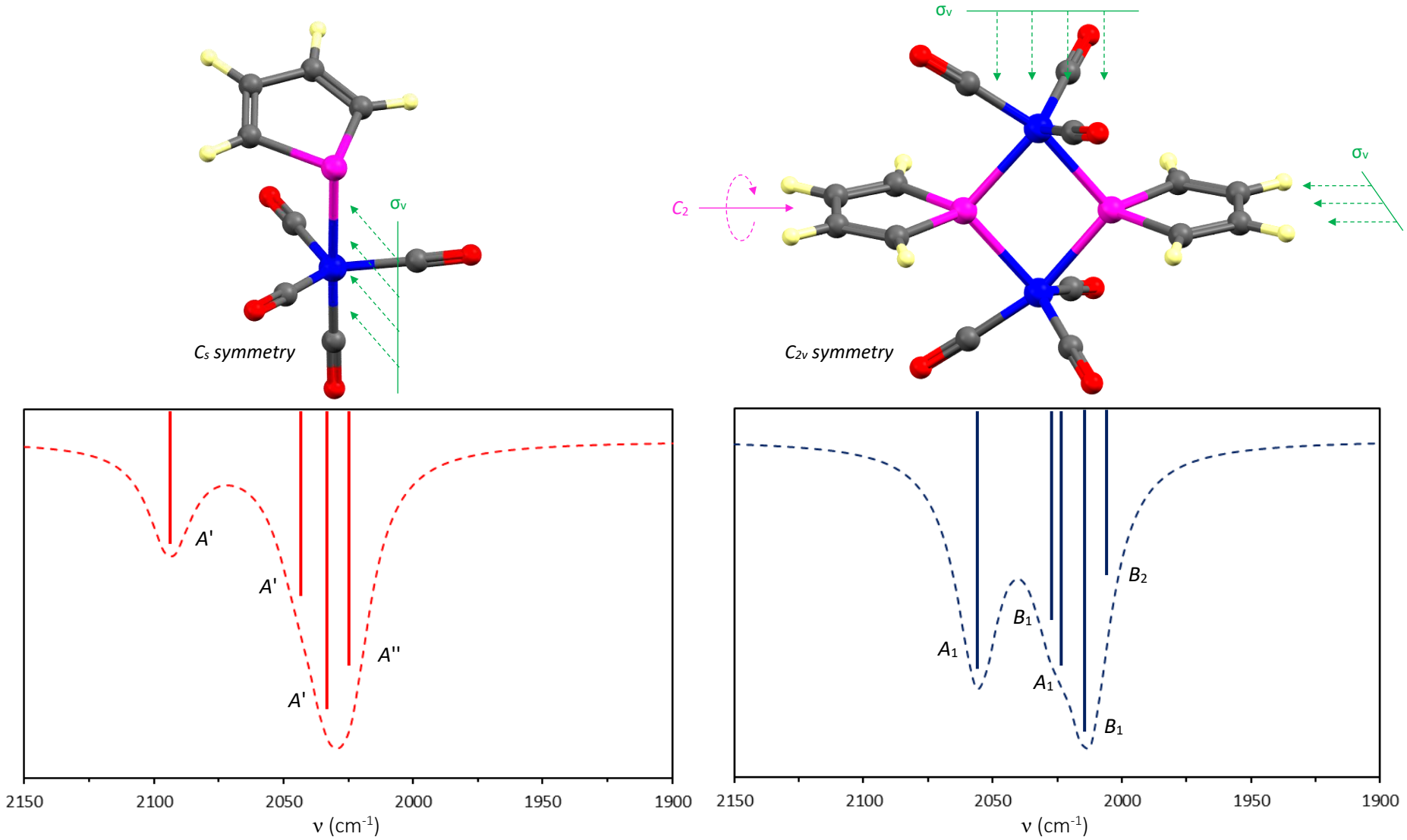



**Figure 3.26**: Optimised molecular geometries (**top**) and simulated IR spectra (**bottom**. DFT, gas phase: ωB97X-D/6-31G*) for $[Co(AsC_4H_4)(CO)_4]$ (**left**) and $[Co_2(\mu\text{-}AsC_4H_4)_2(CO)_6]$ (**right**). The resolutions of the simulated spectra are 5 $cm^{-1}$ and therefore the fundamental $\nu_{CO}$ modes are inset with corresponding peak positions, as a guide for the eye. Predicted peak positions are uncorrected.

The model of $[Co(AsC_4H_4)(CO)_4]$ is in agreement with the expected trigonal bipyramidal coordination geometry ($\tau_5$ = 0.93): the parent arsolyl ligand lies in an axial site with a predicted Co-As covalent bond of 2.47 Å, which is in good accord with the $[Co(AsC_4Ph_4)L_n(CO)_{4-n}]$ complexes to be discussed in the following sections. The mean Co-C and C≡O distances of *ca* 1.80 and *ca* 1.14 Å, respectively, agree with crystallographic data as does the arsolyl ring dimensions and the respective mean planes of the arsolyl and equatorial atoms intersect at an angle of *ca* 23°. Additionally, the cobalt centre is subtly displaced *ca* 0.25 Å from the equatorial plane in the direction opposite the arsenic atom,* a recurring feature in the crystal structures of many such related complexes to follow. The general profile of the simulated IR spectrum for the hypothetical $[Co(AsC_4H_4)(CO)_4]$ is in good agreement with the experimentally measured spectrum of $[Co(AsC_4Ph_4)(CO)_4]$, predicting four IR-active $\nu_{CO}$ vibrations ($3A'$ + $A''$ modes) for the formally $C_s$-symmetric complex(es).

The optimised geometry for the hypothetical $[Co_2(\mu\text{-}AsC_4H_4)_2(CO)_6]$ dimer – arising from *in silico* thermal decarbonylation of $[Co(AsC_4H_4)(CO)_4]$ – consists of a pair of distorted trigonal bipyramidal Co(I) centres ($\tau_5$ = 0.71) unsymmetrically-bridged by two parent arsolyl ligands. The quadrilateral formed by the planar $Co_2As_2$ unit is an irregular rhomboid with two pairs of similar, but distinct, computed Co-As bond distances of 2.34 and 2.37 Å and internal angles of *ca* 90° (at Co) and 100° (at As). The six terminal carbonyl ligands are eclipsed when viewed along the Co-Co vector and the orientations of the two $Co(CO)_3$ moieties are mutually *syn* with the axial carbonyls lying in the $Co_2As_2$ plane; one arsolyl ligand occupies the remaining axial sites on *both* metal centres (shorter Co-As bond) whilst the other arsolyl ligand assumes an equatorial position on each (longer Co-As bond), this being the origin of lateral asymmetry within the molecule. If such distortions are assumed to be absent (or at least, time-averaged) when placed in a solvent field then centrosymmetry may be imposed upon the "pruned" hypothetical molecule and only four fundamental $\nu_{CO}$ modes would arise† instead of the five shown in **Figure 3.26**, in agreement with the experimental IR spectrum of what is reasonably presumed to be $[Co_2(\mu\text{-}AsC_4Ph_4)_2(CO)_6]$ (**Figure 3.25**).

* This is equivalent to the three carbonyl ligands displaying an "umbrella" style concave in the direction of the anionic ligand.

† The presence of an inversion centre at the midpoint of the $Co_2As_2$ quadrilateral would elevate $[Co_2(\mu\text{-}AsC_4R_4)_2(CO)_6]$ from point group $C_{2v}$ to the higher-symmetry $D_{2h}$, for which four fundamental $\nu_{CO}$ modes are predicted ($2A_1 + B_1 + B_2$). In essence, the higher imposed molecular symmetry renders one of the $B_1$ vibrations shown in **Figure 3.26** IR-inactive.

GEOFFROY and co-workers have determined the crystal structure of the related $[Co_2(\mu\text{-}PPh_2)_2(CO)_6]$ and revealed the presence of two isomers within the unit cell, which differ in the arrangement of the $Co_2P_2$ atoms in either a bent or planar configuration;[90] both isomers, however, contain a pair of square-based pyramidal Co(I) centres ($\tau_5$ = 0.01 (bent) and 0.15 (planar)) which are either mutually *syn* or *anti*, respectively, and the phosphine donors both occupy purely basal coordination sites. The isoelectronic $[Fe_2(\mu\text{-}PPh_2)_2(CO)_6]^{2-}$ reported by DAHL *et al.*[91] also exists in a planar configuration in the solid state with trigonal bipyramidal Fe(0) centres ($\tau_5$ = 0.87), whereas the neutral $[Fe_2(\mu\text{-}PPh_2)_2(CO)_6]$ counterpart is bent with an intermetallic bond adhering the square-based pyramidal Fe(I) centres ($\tau_5$ = 0.11). These conformations of $[Co_2(\mu\text{-}PPh_2)_2(CO)_6]$ (reproduced in **Figure 3.27**) represent the two possible extremes for such phosphido-bridged complexes, and it is interesting that the optimised geometry of $[Co(\mu\text{-}AsC_4H_4)_2(CO)_6]$ contains structural elements of both. The energy barrier separating the planar and bent forms of these systems is apparently quite modest[90, 92-95] and this intrinsic non-rigidity probably allows the stochastic process of As→Co bond rupture to occur with higher frequency, explaining why these and other pnictogenido-bridged dicobalt hexacarbonyls are so acutely prone to oligomerisation and ostensibly difficult to isolate.

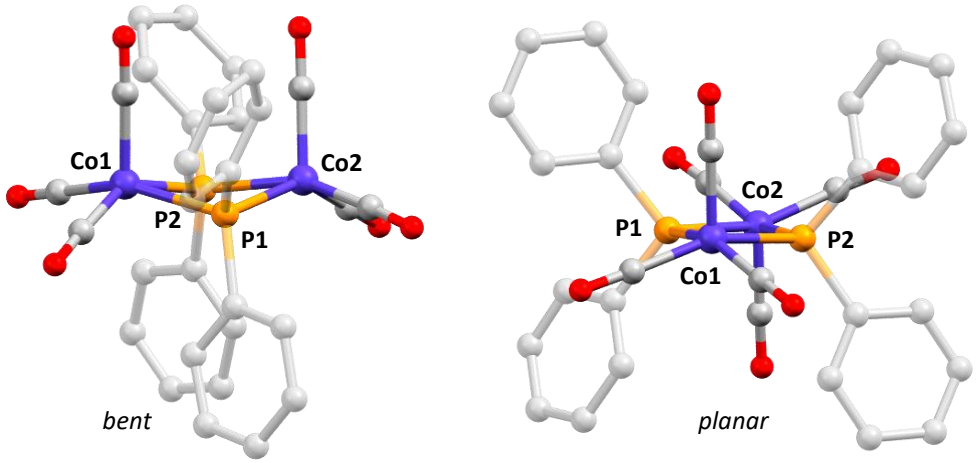
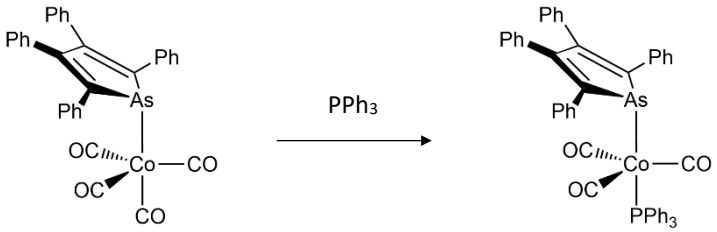



**Figure 3.27**: The abbreviated molecular structures of $[Co_2(\mu\text{-}PPh_2)_2(CO)_6]$ in bent (**left**) and planar (**right**) forms, with relevance to the structure of $[Co_2(\mu\text{-}AsC_4H_4)_2(CO)_6]$. Reproduced from *Ref.* 91.

### 3.5.2 Synthesis of *trans*-[Co(AsC$_4$Ph$_4$)(PPh$_3$)(CO)$_3$]

By analogy with other thermolabile* [CoR(CO)$_4$] complexes,[96-98] [Co(AsC$_4$Ph$_4$)(CO)$_4$] could be intercepted and stabilised by the presence of a neutral two-electron ligand; the addition of triphenylphosphine (PPh$_3$) to the reaction mixture at -78 °C provides the bright orange, moderately air-sensitive (but thermally stable) complex *trans*-[Co(AsC$_4$Ph$_4$)(PPh$_3$)(CO)$_3$] after re-crystallisation (**Scheme 3.14**).




**Scheme 3.14**: Synthesis of [Co(AsC$_4$Ph$_4$)(PPh$_3$)(CO)$_3$].

The equatorial disposition of all three carbonyl ligands is established by IR spectroscopy ($CH_2Cl_2$) revealing $\nu_{CO}$ vibrations at 2035(m), 1972(vs), 1961(vs) cm$^{-1}$. The formal $C_s$ symmetry of the complex in solution (and the non-cylindrical arsolyl ligand field) is established by the occurrence of three ($2A' + A''$) rather than two carbonyl stretching modes ($A_1 + E$) which an idealised $C_{3v}$ species would otherwise display (*cf.* [Co(SnPh$_3$)(PPh$_3$)(CO)$_3$][99] $\nu_{CO}$ 2024(m), 1956(vs) cm$^{-1}$). The phosphine ligand is evident at 62.3 ppm in the $^{31}P\{^1H\}$ NMR spectrum ($CD_2Cl_2$) and the $^1H$ NMR spectrum is populated only by aromatic signals of little diagnostic value. The $^{13}C\{^1H\}$ spectrum reveals a doublet for the three carbonyl ligands at 198.6 ppm with two-bond coupling to the phosphorus nucleus of the axial PPh$_3$ ligand ($^2J_{PC}$ = 20.2 Hz). Interestingly, the arsolyl ring-carbons in the 2,5-positions also appear as a doublet albeit with modest coupling ($^3J_{PC}$ = 2.2 Hz), possibly indicating that the Co(I) centre does not act as an electronic barricade separating the two *trans*-axial substituents (there is presumably some mixing through the Co($d_z^2$) and Co($p_z$) orbitals); four-bond $J_{PC}$ coupling to the ring-atoms in the 3,4-positions was, however, unresolved. High-resolution mass

* The thermal stability of [CoR(CO)$_4$] is primarily determined by the identity of the anionic ligand in the axial coordination site: specifically, those groups which have low-lying, unoccupied orbitals of π-symmetry which can engage in more efficient retrodonation with the Co(I) centre. As a generalisation this often refers to electron-withdrawing residues *e.g.*, $CF_3$, $C_2F_5$, $C_6F_5$ and the like, but more broadly includes heavier *p*- and *d*-block elements *e.g.*, SnR$_3$, HgR, AuL *etc.* Acyl groups are an exception since they may undergo thermal decarbonylation to provide the corresponding σ-organyl ligand. See R.D.W. Kemmitt and D.R. Russell in *Comprehensive Organometallic Chemistry*, **1982**, *7*, 1—276 and V. Galamb and G. Pályi *Coord. Chem. Rev.*, **1984**, *59*, 203—238 for an overview of organocobalt(I) chemistry.

spectrometry finds both the hydrogen and sodium adducts of the molecular ion, and large single crystals were grown by layering a benzene solution with *n*-hexane at ambient temperature; the molecular structure is shown in **Figure 3.28**.

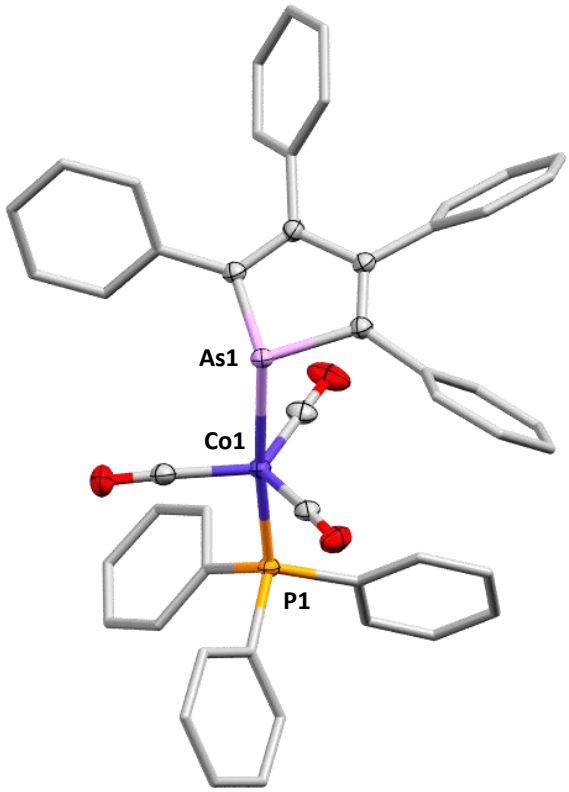


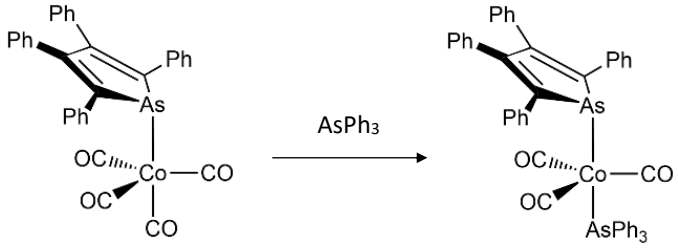

**Figure 3.28**: The molecular structure of *trans*-[Co(AsC$_4$Ph$_4$)(PPh$_3$)(CO)$_3$] in a crystal. Phenyl rings simplified and hydrogen atoms omitted for clarity. Ellipsoids shown at 50% displacement.

The expected five-coordinate complex – with molecular geometry in agreement with that surmised from spectroscopic data – is established: the coordination polyhedron of the cobalt centre is a distorted trigonal bipyramid with the three carbonyl ligands lying in the equatorial plane and the mutually *trans* arsolyl and phosphine ligands occupying the pair of apical sites. The arsolyl ligand lies above one of the equatorial carbonyl ligands though is not symmetrically aligned with the vertical axis of the trigonal bipyramidal Co(I) centre, finding a P-Co-As angle of *ca* 174° and an angle of intersection between the mean arsolyl and Co(CO)$_3$ planes of *ca* 23°. The Co-As covalent and P→Co dative bonds measure 2.4566(5) and 2.2106(6) Å, respectively, and the cobalt atom is displaced from the equatorial plane by *ca* 0.11 Å in the direction of the phosphorus donor. The three carbonyl ligands lie at the vertices of an approximately equilateral triangle with interligand angles of 114—124°. Mean distances within the arsolyl ring (As-C$_\alpha$ 1.949(3), C$_\alpha$=C$_\beta$

1.360(4) and $C_\beta$-$C_\beta$ 1.473(3) Å) are not particularly different from those found in previously encountered $XAsC_4Ph_4$ residues. Heating $[Co(AsC_4Ph_4)(PPh_3)(CO)_3]$ to reflux in toluene did not affect $\eta^1 \rightarrow \eta^5$ slippage of the arsolyl ligand and instead led to partial decomposition to insoluble residues (and free $PPh_3$).

### 3.5.3 Synthesis of *trans*-$[Co(AsC_4Ph_4)(AsPh_3)(CO)_3]$

The maroon-red triphenylarsine ($AsPh_3$) coordinated complex $[Co(AsC_4Ph_4)(AsPh_3)(CO)_3]$ was prepared similarly (**Scheme 3.15**). Reflecting the weaker donor strength of the tertiary arsine, isolated yields were lower than that of the $PPh_3$ complex above and the complex itself was observed to slowly degrade in solution to insoluble dark red materials upon standing overnight; likewise, neither a triphenylantimony ($SbPh_3$) nor a 1-phenyl-2,3,4,5-tetramethylarsole ($PhAsC_4Me_4$) ligated complex could be isolated.




**Scheme 3.15**: Synthesis of *trans*-$[Co(AsC_4Ph_4)(AsPh_3)(CO)_3]$.

The mixed arsenido/arsine species $[Co(AsC_4Ph_4)(AsPh_3)(CO)_3]$ displays a solution IR spectrum ($CH_2Cl_2$) analogous in profile to the $PPh_3$ example with three $\nu_{CO}$ at 2034(m), 1973(vs) and 1961(vs) $cm^{-1}$. The $^{13}C\{^1H\}$ NMR spectrum finds the carbonyl resonance at 198.5 ppm alongside the arsolyl ring-carbon signals at 165.4 (2,5-positions) and 147.6 (3,4) ppm. Single crystals were grown from benzene/*n*-hexane and the molecular structure is shown in **Figure 3.29**.

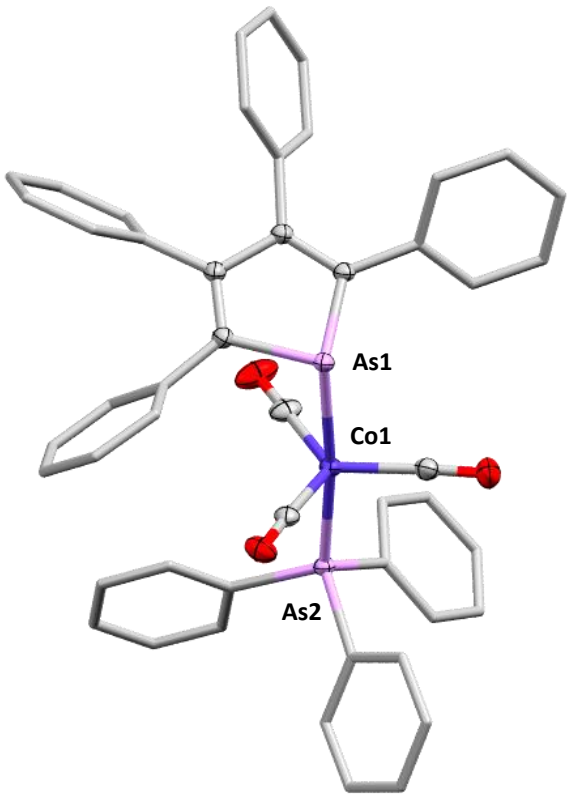
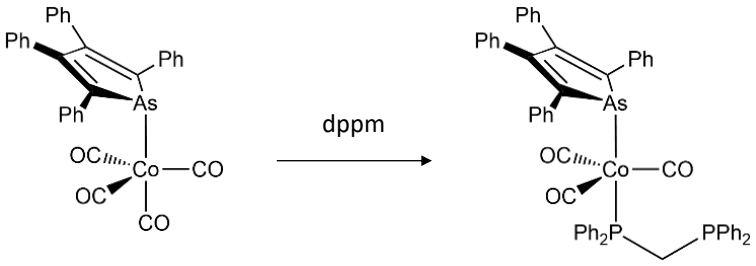



**Figure 3.29**: The molecular structure of *trans*-[Co(AsC$_4$Ph$_4$)(AsPh$_3$)(CO)$_3$] in a crystal. Phenyl groups simplified and hydrogen atoms omitted for clarity. Ellipsoids shown at 50% displacement.

The gross molecular configuration of [Co(AsC$_4$Ph$_4$)(AsPh$_3$)(CO)$_3$] as found in the crystal structure is analogous to that of [Co(AsC$_4$Ph$_4$)(PPh$_3$)(CO)$_3$], and only salient details will be mentioned. The trigonal bipyramidal geometry of the Co(I) centre is deformed from the idealised polyhedron along the vertical axis with an As-Co-As angle of *ca* 174° and the mean planes formed by the arsolyl ring and equatorial group intersect at a declination of *ca* 25°. The arsolyl As-Co covalent bond measures 2.4426(5) Å and is only *marginally* shorter than the same in the PPh$_3$ complex (**Figure 3.28**), presumably for the weaker σ-base in the present example to which the arsenido shares Co($d_z^2$) and Co($p_z$) orbitals. The As→Co dative bond distance of 2.3067(5) Å is unremarkable, and all other interatomic dimensions of interest are not crystallographically dissimilar to [Co(AsC$_4$Ph$_4$)(PPh$_3$)(CO)$_3$] warranting no further comment.

### 3.5.4 Synthesis of *trans*-[Co(AsC$_4$Ph$_4$)(κ$^1$-dppm)(CO)$_3$]

The bidentate ligand 1,2-bis(diphenylphosphino)methane (dppm, $Ph_2PCH_2PPh_2$) was added to [Co(AsC$_4$Ph$_4$)(CO)$_4$] at low temperature, and workup provides a bright yellow-orange crystalline solid in high yield. Spectroscopic features indicate tht the dppm ligand to be in a monodentate mode (common for this ligand in five-coordinate transition metal geometries[100]), since three $\nu_{CO}$ absorptions ($CH_2Cl_2$ solution; 2033(s), 1971(vs), 1960(vs) cm$^{-1}$) are observed in addition to a well-separated pair of doublets in the $^{31}P\{^1H\}$ NMR spectrum ($CD_2Cl_2$) at 58.3 and -25.5 ppm($^2J_{PP}$ = 84.5 Hz). The disparity in chemical shifts in addition to their relatively sharp line widths suggesting that, at ambient temperature, the uncomplexed $PPh_2$ pendant (low-field resonance; *cf.* free dppm $\delta_P$ = -22.1 ppm) and the complexed $PPh_2$ donor (high-field resonance) do not exchange positions on the NMR timescale. The bis(phosphino) methylene group is observed at 3.25 ppm as a doublet of doublets ($^2J_{PH}$ = 9.8 and 1.9 Hz) due to coupling with the pair of chemically inequivalent phosphorus nuclei, and the corresponding methylene carbon atom resonance is found at 34.1 ppm in the $^{13}C\{^1H\}$ NMR spectrum, also as a doublet of doublets ($^1J_{PC}$ = 32.4 and 24.6 Hz). The arsolyl ring-carbon nuclei are found at 165.2 and 147.3 ppm of which the former manifests as a doublet ($^3J_{PC}$ = 1.5 Hz), as does the carbonyl carbon signal at 198.7 ppm ($^2J_{PC}$ = 20.6 Hz). Single crystals were grown from benzene/*n*-hexane and the molecular structure is shown in **Figure 3.30**.




**Scheme 3.16**: Synthesis of *trans*-[Co(AsC$_4$Ph$_4$)(κ$^1$-dppm)(CO)$_3$]; dppm = $Ph_2PCH_2PPh_2$.

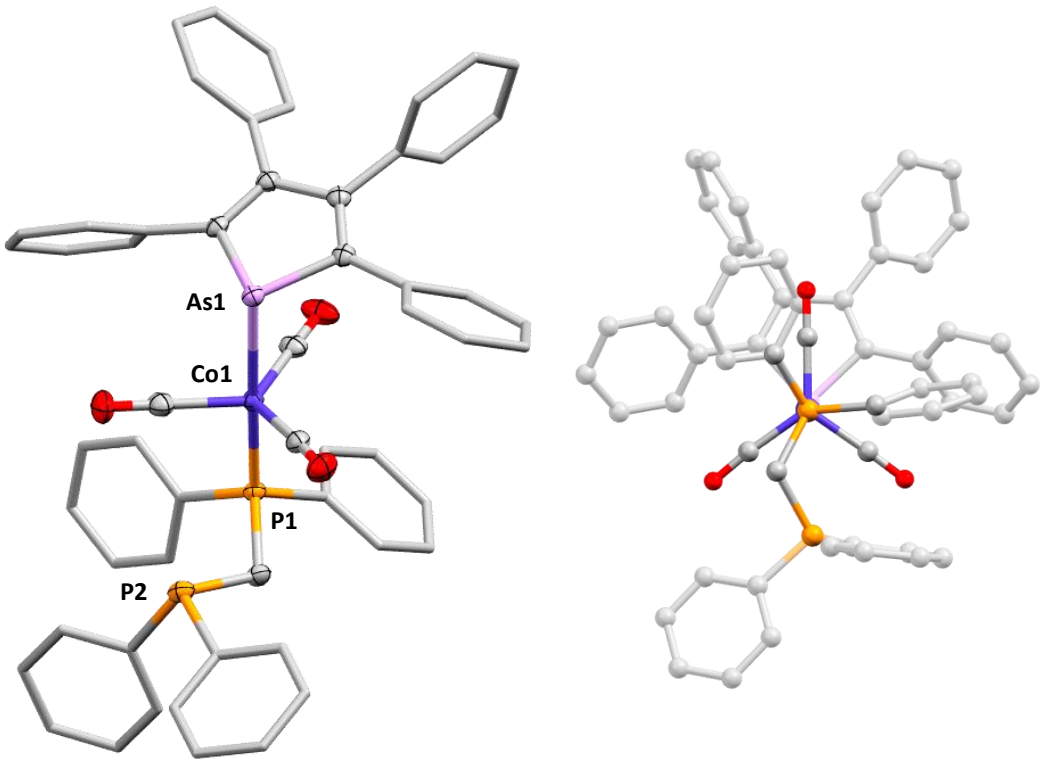



**Figure 3.30**: The molecular structure of *trans*-[Co(AsC$_4$Ph$_4$)(κ$^1$-dppm)(CO)$_3$] in a crystal. Phenyl groups simplified and hydrogen atoms omitted for clarity. Ellipsoids shown at 50% displacement. **Inset**: Abbreviated perspective of the molecule viewed along the P-Co-As vector highlighting the disposition of the diphosphino ligand.

An X-ray diffraction study confirms the monodentate nature of the dppm ligand with one phosphorus function attached in an axial position to the trigonal bipyramidal cobalt centre. The three carbonyl ligands and the three (coordinated) phosphorus substituents are approximately *gauche* (mean dihedral angle *ca* 32°) such that the pendant (non-coordinated) PPh$_2$ group projects into the region of space below the equatorial plane between two carbonyl ligands (**Figure 3.30**, **Inset**). The Co-As covalent bond is regular amongst this work at 2.4367(6) Å as is the P→Co dative bond (2.2106(6) Å), and the cobalt atom lies *ca* 0.02 Å below the mean tricarbonyl plane in the direct of the phosphine donor. The arsolyl group makes an angle of *ca* 20° with the equatorial plane and the P-Co-As axis deviates only slightly from linearity (transaxial angle *ca* 176°).

The diphosphino ligand in [Co(AsC$_4$Ph$_4$)(κ$^1$-dppm)(CO)$_3$] could not be induced to chelate the metal centre upon heating to 110 °C in toluene-d$_8$ whereupon partial decomposition to free dppm ($\delta_P$ = -23.8 ppm) and insoluble red materials (presumed to be oligomeric [Co(AsC$_4$Ph$_4$)(CO)$_3$]$_x$) was encountered.

It should be noted that the dppm ligand *is* capable of bidentate coordination ($[RuCl_2(\kappa^2\text{-dppm})_2]$ is a well-known example) though the difficulty encountered in accommodating a *ca* 90° angle in (hypothetical) $[Co(AsC_4Ph_4)(\kappa^2\text{-dppm})(CO)_2]$ (or 120° if the bis(phosphine) occupies two equatorial sites without the four phenyl groups impinging upon the steric cone of the $AsC_4Ph_4$ ligand) is probably due to the small covalent radius of the cobalt centre (1.26 Å; *cf.* 1.46 Å for Ru), for which some strain of the P-C-P linkage is required to displace an equatorial carbonyl ligand. That aside, the dppm ligand is better known for its proclivity to bridge a pair of metal centres and encourage intermetallic bonding (*e.g.*, so called "A-frame" complexes[101-104] and $[Co_2(CO)_6(\mu\text{-dppm})]$). To this end, $[Co(AsC_4Ph_4)(\kappa^1\text{-dppm})(CO)_3]$ was combined with the labile metal reagents $[Fe(BDA)(CO)_3]$ (BDA = $\eta^4$-benzylideneaceteone), $[Ir_2(\mu\text{-Cl})_2Cl_2(\eta^5\text{-}C_5Me_5)_2]$ and $[AuCl(SMe_2)]$ in an effort to induce bimetallic complex formation, though in both cases the only products recovered were those arising from sequestration of the dppm ligand* alongside disintegration of the cobalt arsolyl. The diphosphino ligand is evidently more prone to dissociation than expected.

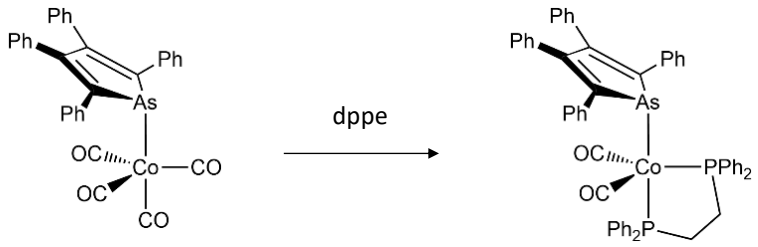
### 3.5.5 Synthesis of $[Co(AsC_4Ph_4)(\kappa^2\text{-dppe})(CO)_2]$

A di-coordinated cobalt complex could be obtained with the more-flexible 1,2-bis(diphenylphosphino)ethane (dppe, $Ph_2PCH_2CH_2PPh_2$) which – upon addition to $[Co(AsC_4Ph_4)(CO)_4]$ at -78 °C – afforded the bright orange $[Co(AsC_4Ph_4)(\kappa^2\text{-dppe})(CO)_2]$ in good yield. The axial-equatorial disposition of the bis(phosphine) ligand is established by solution IR spectroscopy ($CH_2Cl_2$) finding a pair of $\nu_{CO}$ absorptions 1979(s) and 1927(vs) $cm^{-1}$: the relative intensities of the symmetric (*A*' mode, higher energy) and antisymmetric (*A*", lower energy) vibrations suggest an intercarbonyl angle of *ca* 123° in solution, a condition naturally satisfied by their placement in the equatorial plane.† On the NMR timescale, however, both phosphorus atoms are evidently equivalent since only one signal is found in the $^{31}P\{^1H\}$

* Those being $[Fe(\kappa^1\text{-dppm})(CO)_4]$ ($^{31}P\{^1H\}$ ($CDCl_3$, 162 MHz, 25 °C) δ 66.2, -25.9 ($^2J_{PP}$ = 75.8 Hz) ppm; IR ($CH_2Cl_2$, 25 °C) $\nu_{CO}$ 2046(s), 1980(s), 1948(vs), 1936(vs) $cm^{-1}$. Data in agreement with those reported by R.L. Keiter *et al. Organometallics*, **1983**, *2*, 1635—1639), $[IrCl_2(\kappa^1\text{-dppm})(\eta^5\text{-}C_5Me_5)]$ ($^{31}P\{^1H\}$ ($CDCl_3$, 162 MHz, 25 °C) -2.2, -27.8 ($^2J_{PP}$ = 64.8 Hz) ppm. Data in agreement with those reported by M. Valderrama and R. Contreras *J. Organomet. Chem.*, **1996**, *513*, 7—15), and $[Au_2Cl_2(\mu\text{-}\kappa^1\text{:}\kappa^1\text{-dppm})]$ ($^{31}P\{^1H\}$ ($CDCl_3$, 162 MHz, 25 °C) δ 23.7 ppm. Confirmed by comparison with an authentic sample).

† The angle between a pair of carbonyl ligands is given by the relationship $\frac{I_A}{I_S} = \tan^2(\frac{\theta}{2})$ where $I_A$ and $I_S$ are the relative intensities of the antisymmetric and symmetric $\nu_{CO}$ vibrations, respectively. It follows that for $\frac{I_A}{I_S} = 3$, $\theta = \frac{2\pi}{3}$ (120°) and for $\frac{I_A}{I_S} = 1$, $\theta = \frac{\pi}{2}$ (90°). The relationship arises from the cross product of the two vectors describing the dipole moments of each vibrational mode and is derived from a simple trigonometric argument. The relationship holds provided $\theta \neq 180°$ and the vibrational modes describe the motions of two carbonyl ligands *only*. See W. Beck, A. Melnikoff and R. Stahl *Angew. Chem. Int. Ed. Eng.*, **1965**, *4*, 692—693 and *Id. Chem. Ber.*, **1966**, *99*, 3721—3727.

NMR spectrum ($CD_2Cl_2$) at 78.4 ppm, and the ethylene bridge manifests as one *pseudo*-triplet in both the $^1H$ (4.22 ppm, $^2J_{PH}$ = 1.9 Hz) and $^{13}C\{^1H\}$ (31.0 ppm, $^1J_{PC}$ = 22.8 Hz) NMR spectra. The complex presumably undergoes rapid BERRY *pseudo*-rotation[105] in a process which must involve motion of the phosphorus nuclei only since no higher energy $\nu_{CO}$ bands (*ca* 2100 $cm^{-1}$) were observed which could be attributed to a nascent intermediate complex with an axial carbonyl ligand. This exchange process all but conceals any three-bond coupling between the $^{31}P$ nuclei and the arsolyl ring-carbons in the 2,5-positions, since these appear as a sharp singlet at 167.0 ppm alongside those in the 3,4-positions at 146.5 ppm. Single crystals were grown from benzene/*n*-hexane and the structure is shown in **Figure 3.31**.




**Scheme 3.17**: Synthesis of $[Co(AsC_4Ph_4)(\kappa^2\text{-dppe})(CO)_2]$; dppe = $Ph_2PCH_2CH_2PPh_2$.

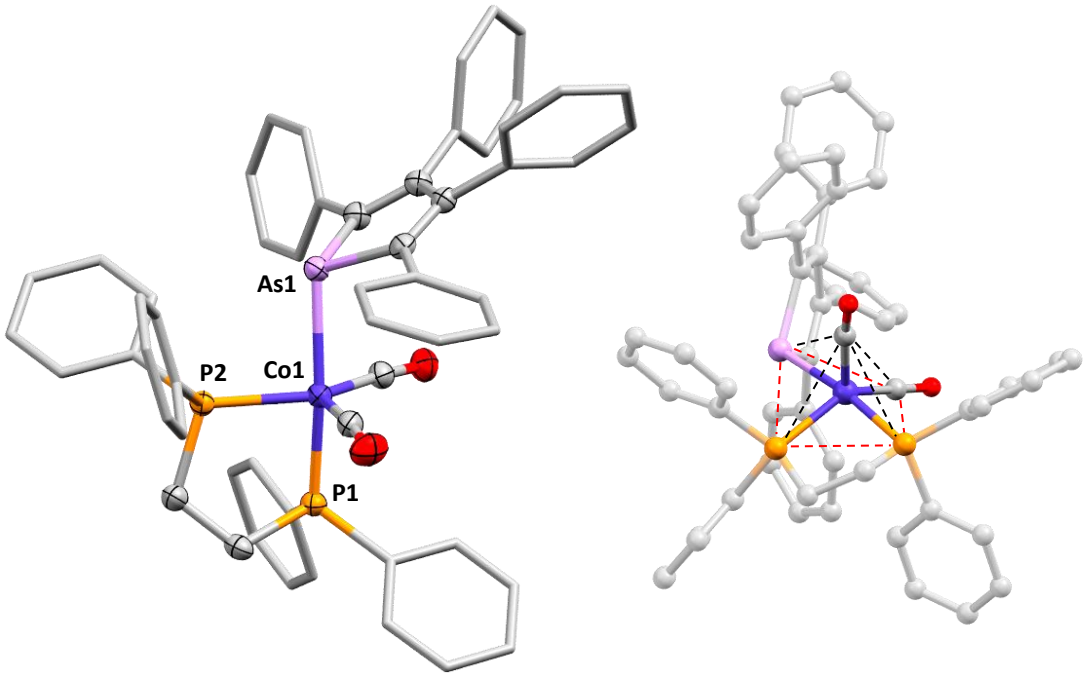



**Figure 3.31**: The molecular structure of [Co(AsC$_4$Ph$_4$)(κ$^2$-dppe)(CO)$_2$] in a crystal. Phenyl groups simplified and hydrogen atoms omitted for clarity. Ellipsoids shown at 50% displacement. dppe = 1,2-bis(diphenylphosphino)ethane. **Inset**: Abbreviated perspective of the molecule highlighting the deformed tetragonal pyramidal geometry of the Co(I) centre; the *quasi*-basal plane is shown in red.

The expected cobalt arsolyl complex crystallises in the tetragonal space group $P4_3$ which – given the absence of lateral symmetry and the acentric space group – means the crystalline sample was evidently enantiomerically pure. This is unlikely to persist in solution, however, as evidenced by the ambient temperature $^{31}P\{^1H\}$ NMR spectrum (*vide supra*). In agreement with the solution IR spectrum, the angle formed between the pair of carbonyl ligands is *ca* 119° (*cf.* 123° in solution by relative intensities of the *A*' and *A*" absorptions). Incidentally – and in contrast to the three previous cobalt complexes – the coordination polyhedron of the cobalt centre more closely resembles a square-based pyramid than a trigonal bipyramid ($\tau_5$ = 0.46; **Figure 3.31**, **Inset**). The superficial resemblance of the metal centre to a superposition of square pyramidal and trigonal bipyramidal geometries is not entirely surprising given the apparent rapid fluxionality of the complex in solution; there must evidently be little energetic impedance between the two forms if the crystal structure is taken to be representative of the ground state. Further evidence for a *quasi*-square pyramidal Co(I) centre is found in a comparison of the pair of Co-C and C≡O bond lengths, for which one ligand is apical and the other lying in the π-basic basal plane (**Figure 3.31**, **Inset**). Indeed, the latter carbonyl displays a shorter Co-C (1.748(6) Å) and longer C-O (1.152(3) Å) distance than the former

(1.795(6) and 1.137(3) Å), as expected from being in a coordination site of privileged π-retrodonation. The donor atoms of the dppe ligand occupy a pair of *cis* coordination sites (in the *quasi*-basal plane) with crystallographically distinct P→Co dative bond distances of 2.161(1) (P1-Co1) and 2.227(1) Å (P2-Co1), and the five-membered ring formed by the chelate is appreciably δ/λ-puckered with a P-C-C-P torsion angle of *ca* 41° and an envelope fold of (coincidentally) about the same magnitude. The Co-As covalent bond measures 2.4049(8) Å and is the shortest of the four complexes here by *ca* 0.02—0.04 Å; given the arsolyl ligand also lies in the *quasi*-basal plane, being diametrically opposed to the phosphine σ-donor implies that any π-acceptor faculty is compensatory for the repulsive electrostatic effect between the two Group 15 elements.

## 3.6 Summary

In this chapter, the first examples of $\lambda^3$-arsole coordination to cobalt were demonstrated by simple ligand replacement of $[Co_2(CO)_8]$, providing the mono- and disubstituted $[Co_2(PhAsC_4Ph_4)(CO)_7]$ and $[Co_2(PhAsC_4R_4)_2(CO)_6]$ (R = Me, Et) complexes in good yields. Their non-rigidity in solution was readily and qualitatively observed *via* IR spectroscopy (**Figure 3.4** and **Figure 3.7**), and further enunciated by the differing solid-state structures of $[Co_2(PhAsC_4Me_4)_2(CO)_6]$ and $[Co_2(PhAsC_4Et_4)_2(CO)_6]$. The former crystallised in a $C_{2v}$ configuration with a bent, carbonyl-bridged dicobalt core (**Figure 3.2**) whereas the latter crystallised in a cylindrical $D_{3h}$ conformation with an unsupported intermetallic covalent bond (**Figure 3.6**). The Co-Co bonded complex $[Co_2(\mu\text{-}CO)_2(CO)_2(\eta^4\text{-}PhAsC_4Et_4)_2]$ was serendipitously encountered and featured the first confirmed example of a *tetrahapto* arsole ligand (**Figure 3.8**).

Attempts to deliberately prepare $[Co_2(\mu\text{-}CO)_2(CO)_2(\eta^4\text{-}PhAsC_4Et_4)_2]$ (*inter alia*) under thermal conditions unexpectedly afforded another type of cobalt complex, namely the *pentahapto* species $[Co(CO)_2(\eta^5\text{-}AsC_4Et_4)]$ arising from elimination of the *As*-phenyl (or chloro) substituent and the first example of a late transition metal $\eta^5$-arsolyl complex. The reaction proved reproducible and generalisable, leading to a modest range of $[CoL(CO)(\eta^5\text{-}AsC_4R_4)]$ compounds which were spectroscopically and structurally characterised as the parent dicarbonyl ($[Co(CO)_2(\eta^5\text{-}AsC_4Ph_4)]$, **Figure 3.10** and $[Co(CO)_2(\eta^5\text{-}AsC_4Ph_2H_2)]$, **Figure 3.11**) or trimethylphosphite-substituted complexes ($[Co\{P(OMe)_3\}(CO)(\eta^5\text{-}AsC_4Me_4)]$, **Figure 3.12** and $[Co\{P(OMe)_3\}(CO)\{\eta^5\text{-}AsC_4(SiMe_3)_2Me_2\}]$, **Figure 3.13**). The precise

mechanism of their formation remains ambiguous though probably involves electron-transfer from one or more Co(0) centres with simultaneous reduction of the arsole ring and scission of the exocyclic As-R bond; the fate of the arsenic substituent could not be determined amongst the reaction detritus.

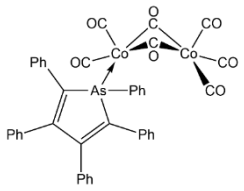
A computational analysis of the electronic structure of the model complex $[Co(CO)_2(\eta^5\text{-}AsC_4H_4)]$ revealed some superficial similarities to the prototypical $[Co(CO)_2(\eta^5\text{-}C_5H_5)]$ (**Figure 3.15**), however the Group 15 heteroatom also manifested as a LEWIS basic function alongside the Co(I) centre. Specifically, the HOMO and HOMO-1 were topologically pre-disposed to permit the *pentahapto* arsolyl (also phospholyl and stibolyl) complexes to function as a ditopic ligand. In pleasing confirmation of this assessment, $[Co(CO)_2(\eta^5\text{-}AsC_4Me_4)]$ readily complexed the LEWIS acidic $HgCl_2$, *cis*-$Pt(C_6F_5)_2$ and $Au^+$ centres *via* both the Co(I) and As(III) donor atoms. In each case the product obtained was subtly or saliently different from that expected from *a priori* assumptions: the dimeric $[Co(CO)_2(\mu\text{-}\eta^1\text{:}\eta^5\text{-}AsC_4Me_4)\cdot\{Hg(\mu\text{-}Cl)Cl\}]_2$ (**Figure 3.17**), the five-coordinate $[Co(CO)_2(\mu\text{-}\eta^1\text{:}\eta^5\text{-}AsC_4Me_4)\cdot\{Pt(C_6F_5)_2(CO)\}]$ (**Figure 3.19**), and the ionic $[\{Co(CO)_2(\mu\text{-}\eta^1\text{:}\eta^5\text{-}AsC_4Me_4)\}_2\cdot Au][Au(C_6F_5)_2]$ (**Figure 3.21**) were all characterised by X-ray crystallography and featured authentic Co→M and As→M bonds. These represent the first examples of the $\mu\text{-}\eta^1\text{:}\eta^5$-arsolyl ligand and compliment the equally small number of preceding $\mu\text{-}\eta^1\text{:}\eta^5$-phospholyls, all examples of which are devoid of metal-metal (M→M) polar covalent bonding.

Attempts to prepare $[Co(CO)_2(\eta^5\text{-}AsC_4Ph_4)]$ *via* combination of $ClAsC_4Ph_4$ with $Na[Co(CO)_4]$ – which *is* an established route to cyclopentadienyl metal carbonyls – instead produced the thermally-sensitive trigonal bipyramidal $[Co(AsC_4Ph_4)(CO)_4]$. This ephemeral species did not spontaneously decarbonylate to the target *pentahapto* compound, instead proceeding to a dimeric species of the form $[Co_2(\mu\text{-}AsC_4Ph_4)_2(CO)_6]$ in a process which could be observed by *in situ* spectroscopic monitoring (**Figure 3.25**). The labile tetracarbonyl could be intercepted by the addition of neutral monodentate or bidentate ligands, affording four relatively stable $[Co(AsC_4Ph_4)L(CO)_n]$ complexes (L = $PPh_3$, **Figure 3.28**; L = $AsPh_3$, **Figure 3.29**; L = $\kappa^1$-dppm, **Figure 3.30**; $n$ = 3) and $[Co(AsC_4Ph_4)(\kappa^2\text{-dppe})(CO)_2]$ (**Figure 3.31**; $n$ = 2) which contain an $\eta^1$-arsolyl ligand. These join the modest family of $\eta^1$-arsolyl complexes previously prepared (but in no case structurally characterised) and is the subject of the following chapter.

## 3.7 Experimental

### 3.7.1 Arsole complexes of Co(0)

#### 3.7.1.1 $[Co_2(PhAsC_4Ph_4)(CO)_7]$

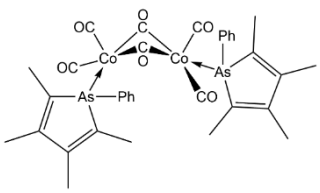



A 25 mL Schlenk tube was charged with 0.2 g $PhAsC_4Ph_4$ (0.4 mmol) and 0.135 g $[Co_2(CO)_8]$ (0.4 mmol) in an argon filled glovebox and then 15 mL $CH_2Cl_2$ admitted, resulting in gas evolution and a red-brown solution. After stirring for 30 minutes the solution was concentrated to a few mL and then 10 mL *n*-hexane was added resulting in precipitation of a red-brown solid. The mixture was stored at -20 °C overnight and the supernatant decanted from the red-brown solids, which were washed with 3 x 5 mL *n*-pentane and dried under reduced pressure. Isolated yield: 0.25 g (0.3 mmol, 76%). The product is readily soluble in polar organic and aromatic solvents, somewhat soluble in $Et_2O$ and less-so in aliphatic hydrocarbons. The product is moderately air-sensitive in solution however solids may be handled for some time without visible degradation.

Acquisition of satisfactory NMR spectra was difficult due to significant line broadening, presumed to arise from a soluble paramagnetic compound(s). IR ($CH_2Cl_2$, 25 °C) 2082(sh), 2071(s), 2039(vs), 2020(s), 1845(m, br), 1823 (m, br) $cm^{-1}$. HR-MS (ESI, MeCN, +ve ion) found $m/z$ 807.9698 (calc. for ION $[M-CO]^+$: 807.9688). Analysis found 59.48% C, 3.00% H (calc. for $C_{41}H_{25}O_7As_1Co_2$: 59.88% C, 3.06% H).

Single crystals were obtained from $CH_2Cl_2$/*n*-hexane at -30 °C. One and one-half molecules of $CH_2Cl_2$ were found in the asymmetric unit; the fractional molecule was severely disordered and could not be modelled satisfactorily. A solvent mask was calculated which found 48 electrons in a solvent accessible volume of 220 $Å^3$ per unit cell, which is consistent with one $CH_2Cl_2$ molecule (42 electrons) per unit cell (equivalently, $0.5{\cdot}CH_2Cl_2$ per asymmetric unit). $C_{42}H_{27}O_7As_1Co_2{\cdot}CH_2Cl_2$ ($M$ = 907.31 g/mol): red prism, 0.045 × 0.195 × 0.245 mm, triclinic, space group *P*-1 (no. 2), $a$ = 12.0082(3) Å, $b$ = 12.9414(4) Å, $c$ = 13.7654(4) Å, $\alpha$ = 91.596(2)°, $\beta$ = 104.453(3)°, $\gamma$ = 92.591(2)°, $V$ = 2067.67(11) $Å^3$, $Z$ = 2, multi-scan correction $T_{min}/T_{max}$ = 0.446/0.493, $\mu$(Cu-K$\alpha$) = 8.753 $mm^{-1}$, $\varrho_{calc}$ = 1.457 g/$cm^3$, 23481 reflections measured (6.842° ≤ 2Θ ≤ 133.196°), 7315 unique ($R_{int}$ = 0.0514, $R_{sigma}$ = 0.0587) which were used in all calculations, $GOF$ = 1.054, $D_{min}/D_{max}$ = -1.05/1.11 e/$Å^3$. The final $R_1$ was 0.0543 (I > 2σ(I)) and $wR_2$ was 0.1512 (all data).

#### 3.7.1.2 $[Co_2(PhAsC_4Me_4)_2(CO)_6]$

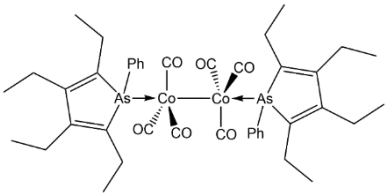


A 25 mL Schlenk tube was charged with 0.2 g $[Co_2(CO)_8]$ (0.58 mmol) and 10 mL *n*-hexane admitted. To this was added a solution of 0.31 g $PhAsC_4Me_4$ (1.2 mmol) in 10 mL *n*-hexane. Gas evolution takes place and a red-brown solution formed. After 30 minutes the volume of the solution is slowly reduced under reduced pressure until precipitation begins (a few mL), and the mixture then stored at -20 °C overnight. After this time the supernatant was decanted, and the red-brown solids washed with 2 x 5 mL cold *n*-pentane and dried under vacuum. Isolated yield: 0.26 g (0.32 mmol, 58%). The product is readily soluble in polar organic, $Et_2O$ and aromatic solvents, and moderately soluble in aliphatic hydrocarbons. The product is air-sensitive in solution however solids may be handled for some time without visible degradation.

Acquisition of satisfactory NMR spectra was difficult due to significant line broadening, presumed to arise from a soluble paramagnetic compound(s). IR (MeCN, 25 °C) $\nu_{CO}$ 2042(w), 20139(w), 1956(m), 1893(vs) $cm^{-1}$; ($CH_2Cl_2$, 25 °C) $\nu_{CO}$ 2077(m), 2069(m), 2033(s), 2006(vs), 1975(s), 1956(s), 1820(w, br), 1794(w, br) $cm^{-1}$; (*n*-hexane, 25 °C) $\nu_{CO}$ 2079(s), 2072(s), 2034(s), 2029(s), 2018(sh), 2015(vs), 2004(vs), 1997(s), 1981(s), 1972(s), 1967(s), 1963(s), 1849(w), 1832(m), 1820(w), 1812(w), 1797(m) $cm^{-1}$. HR-MS (ESI, MeCN, +ve ion) found $m/z$ 749.9550 (calc. for $C_{32}H_{34}O_4{}^{75}As_2{}^{59}Co_2$ $[M - 2CO]^+$: 749.9553). Analysis found 51.01% C, 4.66% H (calc. for $C_{34}H_{34}O_6As_2Co_2$: 50.64% C, 4.25% H).

Single crystals were obtained by slow evaporation of *n*-hexane solution at -30 °C. $C_{34}H_{34}O_6As_2Co_2$ ($M$ = 806.31 g/mol): red plate, 0.089 × 0.339 × 0.498 mm, monoclinic, space group $I2/a$ (no. 15), $a$ = 14.2548(7) Å, $b$ = 9.8169(4) Å, $c$ = 24.4535(11) Å, $\beta$ = 106.703(5)°, $V$ = 3277.6(3) Å$^3$, $Z$ = 4, multi-scan correction $T_{min}/T_{max}$ = 0.497/1.000, $\mu$(Mo-Kα) = 3.059 $mm^{-1}$, $\varrho_{calc}$ = 1.634 g/cm$^3$, 11096 reflections measured (6.668° ≤ 2Θ ≤ 63.376°), 4815 unique ($R_{int}$ = 0.0276, $R_{sigma}$ = 0.0423) which were used in all calculations, $GOF$ = 1.032, $D_{min}/D_{max}$ = -0.51/0.52 e/Å$^3$. The final $R_1$ was 0.0331 (I > 2σ(I)) and $wR_2$ was 0.0780 (all data).

### 3.7.1.3 $[Co_2(PhAsC_4Et_4)_2(CO)_6]$

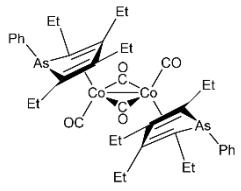



Prepared similarly to that above. Quantities: 0.25 g $[Co_2(CO)_8]$ (0.73 mmol) and 0.465 g $PhAsC_4Et_4$ (1.47 mmol). Isolated yield: 0.26 g (0.28 mmol, 39%). Properties are similar to that above except the solubility in aliphatic hydrocarbons is much improved, possibly accounting for the lower isolated yield.

Acquisition of satisfactory NMR spectra was difficult due to significant line broadening, presumed to arise from a soluble paramagnetic compound(s).. IR (MeCN, 25 °C) $\nu_{CO}$ 2000(w), 1953(w), 1893(vs) $cm^{-1}$; ($CH_2Cl_2$, 25 °C) $\nu_{CO}$ 2078(m), 2070(m), 2029(s), 2017(sh), 2004(vs), 1954(vs), 1918(w, br), 1787(w, br) $cm^{-1}$; (*n*-hexane, 25 °C) 2079(m), 2071(vs), 2030(sh), 2027(vs), 2012(vs), 2006(vs), 1997(m), 1972(w), 1849(m), 1829(s), 1794(m) $cm^{-1}$. HR-MS (ESI, MeCN, +ve ion) found $m/z$ 862.0806 (calc. for $C_{40}H_{50}{}^{75}As_2{}^{59}Co_2$ $[M - 2CO]^+$: 862.0805). Analysis found 54.55% C, 5.60% H (calc. for $C_{42}H_{50}O_6As_2Co_2$: 54.92% C, 5.49% H).

Single crystals were obtained by slow evaporation of *n*-hexane solution at -30 °C. One ethyl group (α to arsenic) was disordered over two positions and modelled accordingly $C_{42}H_{50}O_6As_2Co_2$ ($M$ = 918.52 g/mol): red needle, 0.043 × 0.056 × 0.115 mm, monoclinic, space group $P2_1/n$ (no. 14), $a$ = 10.7380(2) Å, $b$ = 19.2873(3) Å, $c$ = 10.7773(2) Å, $\beta$ = 108.088(2)°, $V$ = 2121.75(7) Å$^3$, $Z$ = 2, multi-scan correction $T_{min}/T_{max}$ = 0.021/0.103, $\mu$(Cu-Kα) = 8.202 mm$^{-1}$, $\varrho_{calc}$ = 1.438 g/cm$^3$, 7265 reflections measured (9.17° ≤ 2Θ ≤ 147.35°), 3959 unique ($R_{int}$ = 0.0153, $R_{sigma}$ = 0.0234) which were used in all calculations, $GOF$ = 1.115, $D_{min}/D_{max}$ = -0.23/1.00 e/Å$^3$. The final $R_1$ was 0.0481 (I > 2σ(I)) and $wR_2$ was 0.1207 (all data).

#### 3.7.1.4 $[Co_2(\mu\text{-}CO)_2(CO)_2(\eta^4\text{-}PhAsC_4Et_4)_2]$

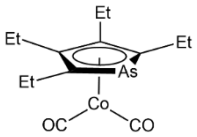



This compound was initially observed in trace quantities from attempts to re-crystallise $[Co_2(PhAsC_4Et_4)_2(CO)_6]$ from boiling $Et_2O$, and later by heating two equivalents of $PhAsC_4Et_4$ with one equivalent of $[Co_2(CO)_8]$ to reflux in *n*-pentane for 30 minutes followed by anaerobic chromatography on neutral alumina with 19:1 *n*-pentane/$Et_2O$ eluent (small quantities of $[Co(CO)_2(\eta^5\text{-}AsC_4Et_4)]$ elute prior with *n*-pentane eluent). Very low isolated yields in addition to gradual decomposition in solution meant that the complex was only characterised by IR spectroscopy and X-ray crystallography. IR (*n*-hexane, 25 °C) $\nu_{CO}$ 2001(vs), 1817(s) cm$^{-1}$.

Single crystals were obtained from $Et_2O$ solution at -20 °C. $C_{40}H_{50}As_2Co_2O_4$ ($M$ = 862.50 g/mol): yellow plate, 0.051 × 0.181 × 0.35 mm, triclinic, space group $P$-1 (no. 2), $a$ = 8.5575(4) Å, $b$ = 9.5814(4) Å, $c$ = 11.9189(5) Å, α = 89.796(4)°, $\beta$ = 82.427(4)°, $\gamma$ = 76.408(4)°, $V$ = 941.23(7) Å$^3$, Gaussian correction $T_{min}/T_{max}$ = 0.167/1.000, $\mu$(Cu-Kα) = 9.161 mm$^{-1}$, $\varrho_{calc}$ = 1.522 g/cm$^3$, 9042 reflections measured (7.486° ≤ 2Θ ≤ 147.42°), 3777 unique ($R_{int}$ = 0.0499, $R_{sigma}$ = 0.0541) which were used in all calculations, $GOF$ = 1.024, $D_{min}/D_{max}$ = -0.51/0.66 e/Å$^3$. The final $R_1$ was 0.0387 (I > 2σ(I)) and $wR_2$ was 0.0965 (all data).

### 3.7.2 $\eta^5$-Arsolyl Complexes of Co(I)

#### 3.7.2.1 $[Co(CO)_2(\eta^5\text{-}AsC_4Et_4)]$



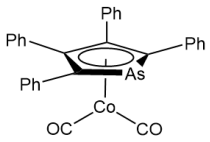

This compound was initially obtained as a side-product during attempts to prepare $[Co_2(\mu\text{-}CO)_2(CO)_2(\eta^4\text{-}PhAsC_4Et_4)_2]$. It could be deliberately prepared by heating 0.48 g [Co2(CO)8] (1.4 mmol) and 0.35 g PhAsC4Et4 (1.25 mmol) to reflux in n-hexane for 6 hours.

Chromatography on neutral alumina (25 x 2.5 cm) under nitrogen with *n*-pentane provides an orange-red band, which is collected under nitrogen and taken to dryness giving 105—130 mg of the product as a dark orange-red liquid in an

average isolated yield of 25 % (based on arsenic from 2 separate preparations; a 16 % yield was obtained with $PhAsC_4Et_4$ from one preparation). The product is readily soluble in most common organic solvents.

NMR: $^1H$ ($CDCl_3$, 400 MHz, 25 °C) δ 2.54 (dt, $J_{HH}$ = 15.2, 7.1 & 7.1 Hz, 2H, α-C$H_2$CH$_3$), 2.41 (dt, $J_{HH}$ = 15.2, 7.1 & 7.1 Hz, 2H, α-C$H_2$CH$_3$), 2.26 (dt, $J_{HH}$ = 15.2, 7.1 & 7.1 Hz, 2H, β-CH$_2$C$H_3$), 2.07 (dt, $J_{HH}$ = 15.2, 7.1, 7.1 Hz, 2H, β-CH$_2$C$H_3$), 1.19 (td, $J_{HH}$ = 7.1, 7.1, 3.5 Hz, 12H, α- & β-CH$_2$C$H_3$); $^{13}C\{^1H\}$ ($CDCl_3$, 176 MHz, 25 °C) δ 205.3 (*C*O), 128.4 (arsole {2,5}-*C*), 118.8 (arsole {3,4}-*C*), 24.4 (α-*C*H$_2$CH$_3$), 21.2 (β-*C*H$_2$CH$_3$), 16.9 (α-CH$_2$*C*H$_3$), 16.6 (β-CH$_2$*C*H$_3$); IR (*n*-hexane, 25 °C) $\nu_{CO}$ 2017(vs), 1965(vs) cm$^{-1}$. HR-MS (EI, MeCN, +ve ion) found *m*/*z* 354.0011 (calc. for $C_{14}H_{20}O_2{}^{59}Co_1{}^{75}As_1$ [*M*]$^+$: 354.0010). Satisfactory elemental microanalysis could not be obtained.

### 3.7.2.2 [Co(CO)$_2$($\eta^5$-AsC$_4$Ph$_4$)]

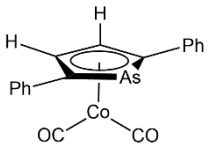



A 250 mL three-necked round bottom flask fitted with a water-cooled reflux condenser was charged 0.6 g [$Co_2(CO)_8$] (1.75 mmol) and 0.7 g $ClAsC_4Ph_4$ (1.5 mmol); 100 mL THF was admitted, and the mixture was brought to reflux under argon for 6 hours. After this time, volatiles were removed under reduced pressure and the residue was take up in $CH_2Cl_2$, filtered through a short celite plug and adsorbed onto a small quantity of oven-dried, degassed silica gel by evaporation of the solvent. This was transferred to a water-jacketed column of oven dried silica gel (30 x 2.5 cm) made up in *n*-pentane under nitrogen. Eluting with 4:1 *n*-pentane/benzene provides a bright orange band which is collected under nitrogen and taken to dryness. The residue is re-crystallised from the minimum amount of hot benzene/*n*-hexane cooled to -20 °C overnight. Isolated yield: 0.23 g (0.42 mmol, 28%). The product is encountered as a dark orange solid which is readily soluble in polar organic and aromatic solvents, somewhat soluble in $Et_2O$ and less-so in aliphatic hydrocarbons. The compound is air-sensitive in solution however solids may be handled for a short while without precaution.

NMR: $^1H$ (CDCl=, 400 MHz 25 °C) δ 7.78—7.15 (m, 8H, C$_6H_5$), 6.85—6.77 (m, 12H, C$_6H_5$). $^{13}C\{^1H\}$ ($CDCl_3$, 176 MHz, 25 °C) δ 203.2 (*C*O), 136.9 (arsole {2,5}-*C*), 134.6 (arsole {3,4}-*C*), 133.1 (*C*$_6$H$_5$), 132.5 (*C*$_6$H$_5$), 130.5 (*C*$_6$H$_5$), 128.2 (*C*$_6$H$_5$), 127.9 (*C*$_6$H$_5$), 127.7 (*C*$_6$H$_5$), 127.6 (*C*$_6$H$_5$), 119.5 (*C*$_6$H$_5$). IR (*n*-hexane, 25 °C) $\nu_{CO}$ 2022(vs), 1963(vs) cm$^{-1}$. HR-MS (EI, MeCN, +ve ion) found *m*/*z* 546.0014 (calc. for $C_{30}H_{20}O_2{}^{75}As_1{}^{59}Co_1$ [*M*]$^+$: 546.0011). Analysis found 65.91% C, 3.61% H (calc. for $C_{30}H_{20}O_2As_1Co_1$: 65.95% C, 3.69% H).

Single crystals were obtained from benzene/*n*-hexane at -20 °C. $C_{30}H_{20}As_1Co_1O_2$ (*M* = 546.31 g/mol): orange plate 0.083 × 0.110 × 0.298 mm, triclinic, space group *P*-1 (no. 2), *a* = 9.0514(4) Å, *b* = 10.5907(5) Å, *c* = 12.8357(6) Å, α = 76.116(4)°, *β* = 84.418(4)°, *γ* = 78.076(4)°, *V* = 1167.24(10) Å$^3$, *Z* = 2, Gaussian correction $T_{min}/T_{max}$ = 0.219/1.000, *μ*(Cu-K$_\alpha$) = 7.541 mm$^{-1}$, $\rho_{calc}$ = 1.554 g/cm$^3$, 11946 reflections measured (7.104° ≤ 2Θ ≤ 147.544°), 4691 unique ($R_{int}$ = 0.0239, $R_{sigma}$ = 0.0282) which were used in all calculations, *GOF* = 1.037, $D_{min}/D_{max}$ = -0.64/0.44 e/Å$^3$. The final $R_1$ was 0.0336 (I > 2σ(I)) and *w*$R_2$ was 0.0887 (all data).

### 3.7.2.3 $[Co(CO)_2(\eta^5\text{-}AsC_4Ph_2H_2)]$

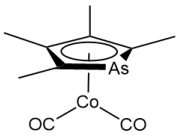



Prepared as above. Quantities: 0.5 g $[Co_2(CO)_8]$ (1.5 mmol), 0.45 g $PhAsC_4Ph_2H_2$ (1.25 mmol). Chromatography on silica gel (30 x 2.5 cm) under nitrogen with 9:1 *n*-pentane/benzene provided a bright orange band which was re-crystallised from the minimum amount of hot benzene/*n*-hexane cooled to -20 °C overnight. Isolated yield: 0.105 g (0.26 mmol, 21 %). Properties are similar to that above.

NMR: $^1H$ ($CDCl_3$, 400 MHz, 25 °C) δ 7.27 (m, 4H, $C_6H_5$), 6.99 (m, 6H, $C_6H_5$) 5.93 (s, 2H, C*H*). $^{13}C\{^1H\}$ ($CDCl_3$, 176 MHz, 25 °C) δ 202.7 (*C*O), 137.9 (arsole {2,5}-*C*), 128.9 ($C_6H_5$), 128.8 ($C_6H_5$) 128.3 ($C_6H_5$), 127.2 ($C_6H_5$), 94.7 (arsole {3,4}-C). IR (*n*-hexane, 25 °C) $\nu_{CO}$ 2027(vs), 1974(vs) $cm^{-1}$. HR-MS (EI, MeCN, +ve ion) found *m*/*z* 393.9383 (calc. for $C_{18}H_{12}O_2{}^{75}As_1{}^{59}Co_1$ $[M]^+$: 393.9385). Analysis found 54.86 C, 2.93 H (calc. for $C_{18}H_{12}O_2As_1Co_1$: 54.85 C, 3.07 H).

Single crystals were obtained from benzene/*n*-hexane at -20 °C. $C_{18}H_{12}As_1Co_1O_2$ ($M$ = 394.13 g/mol): orange needle, 0.029 × 0.061 × 0.109 mm, orthorhombic, space group $Pna2_1$ (no. 33), $a$ = 11.23470(10) Å, $b$ = 17.27710(10) Å, $c$ = 7.83560(10) Å, $V$ = 1520.91(3) Å$^3$, $Z$ = 4, multi-scan correction $T_{min}/T_{max}$ = 0.56452/1.00000, $\mu$(Cu-K$_\alpha$) = 11.289 $mm^{-1}$, $\varrho_{calc}$ = 1.721 g/cm$^3$, 27398 reflections measured (9.39° ≤ 2Θ ≤ 147.908°), 3057 unique ($R_{int}$ = 0.0453, $R_{sigma}$ = 0.0224) which were used in all calculations, $GOF$ = 1.085, $D_{min}/D_{max}$ = -0.65/0.97 e/Å$^3$. The final $R_1$ was 0.0368 (I > 2σ(I)) and $wR_2$ was 0.0890 (all data).

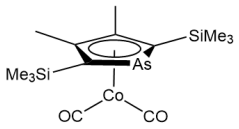
### 3.7.2.4 $[Co(CO)_2(\eta^5\text{-}AsC_4Me_4)]$




Prepared as above with the modification of heating to reflux in 50 mL *n*-hexane for 6 hours. Typical quantities: 0.72 g $[Co_2(CO)_8]$ (2.1 mmol) and 0.43 g freshly prepared $ClAsC_4Me_4$ (2 mmol). Chromatography on neutral alumina (25 x 2.5 cm) under nitrogen with *n*-pentane provides an orange-red band, which is collected under nitrogen and taken to dryness providing the product as a dark orange-red liquid in an average isolated yield of ~19% (*ca* 0.115 g, across 8 separate preparations). The product is readily soluble most common organic solvents, though was difficult to completely free from solvents with which it had previously been dissolved despite being held under reduced pressure for extended periods of time, as evidenced by NMR spectroscopy. The product is rather air-sensitive either neat or in solution.

NMR: $^1H$ ($CDCl_3$, 400 MHz, 25 °C) δ 2.12 (s, 6H, α-C$H_3$), 1.85 (s, 6H, β-C$H_3$). $^{13}C\{^1H\}$ ($CDCl_3$, 176 MHz, 25 °C) δ 205.8 (*C*O), 118.9 (arsole {2,5}-*C*), 113.1 (arsole {3,4}-*C*), 17.1 (α-*C*H$_3$), 14.5 (β-*C*H$_3$). IR (*n*-hexane, 25 °C) $\nu_{CO}$ 2019(vs), 1967(vs) $cm^{-1}$. HR-MS (EI, MeCN, +ve ion) found *m*/*z* 297.9389 (calc. for $C_{10}H_{12}O_2{}^{75}As_1{}^{59}Co_1$ $[M]^+$: 297.9385). Satisfactory elemental microanalysis could not be obtained.

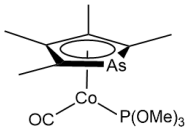
### 3.7.2.5 $[Co(CO)_2\{\eta^5\text{-}AsC_4(SiMe_3)_2Me_2\}]$




Prepared similarly to that above. Quantities: 0.45 g $[Co_2(CO)_8]$ (1.3 mmol) and 0.4 g $ClAsC_4(SiMe_3)_2Me_2$ (1.2 mmol). Isolated yield: 0.13 g (0.31 mmol, 26%). The product is encountered as a dark orange liquid and is rather air-sensitive in solution or neat and is readily soluble in common organic solvents.

NMR: $^1H$ ($CDCl_3$, 400 MHz, 25 °C) δ 2.21 (s, 6H, β-C$H_3$), 0.23 (s, 18H, α-Si(C$H_3$)$_3$). $^{13}C\{^1H\}$ ($CDCl_3$, 176 MHz, 25 °C) δ 204.5 (*C*O), 122.2 (arsole {2,5}-*C*), 119.8 (arsole {3,4}-*C*), 18.4 (β-*C*$H_3$), 1.3 (α-Si(*C*$H_3$)$_3$); IR (*n*-hexane, 25 °C) $\nu_{CO}$ 2015(vs), 1963(vs) $cm^{-1}$; HR-MS (EI, MeCN, +ve ion) found *m*/*z* 413.9851 (calc. for $C_{14}H_{24}O_2{}^{28}Si_2{}^{59}Co_1{}^{75}As_1$ $[M]^+$: 413.9863). Satisfactory elemental microanalysis could not be obtained.

### 3.7.2.6 $[Co\{P(OMe)_3\}(CO)(\eta^5\text{-}AsC_4Me_4)]$

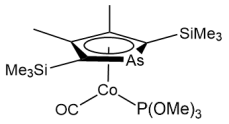



To a solution of 0.12 g $[Co(CO)_2(\eta^5\text{-}AsC_4Me_4)]$ (0.4 mmol) in 10 mL toluene was added ~0.1 mL neat $P(OMe)_3$ (large excess) and the mixture warmed to 100 °C. During this time the dark orange colour lightens and heating is continued for 2 hours. The mixture was transferred *via* syringe to a column of oven-dried neutral alumina (20 x 2.5 cm) made up in *n*-pentane under nitrogen. Eluting with *n*-pentane, followed by 4:1 *n*-pentane/$Et_2O$ provides a bright orange band which is collected under nitrogen and taken to dryness, and re-crystallised from the minimum amount of $SiMe_4$ at -30 °C. Isolated yield: 0.11 g (0.28 mmol, 70%). The product is encountered as a bright orange solid which is air-sensitive in solution, but solids may be handled for a short while without precaution. The product is readily soluble in common organic solvents however appeared to react with $CDCl_3$.

NMR: $^1H$ ($C_6D_6$, 400 MHz, 25 °C) δ 3.36 (d, $^3J_{PH}$ = 12.1 Hz, 9H, P(OC$H_3$)$_3$), 1.94 (s, 6H, α-C$H_3$), 1.83 (s, 6H, β-C$H_3$). $^{13}C\{^1H\}$ ($C_6D_6$, 176 MHz, 25 °C) δ 206.8 (*C*O), 114.3 (arsole {2,5}-*C*), 109.8 (arsole {3,4}-*C*), 51.0 (P(O*C*$H_3$)$_3$), 16.9 (α-*C*$H_3$), 14.4 (β-*C*$H_3$); $^{31}P\{^1H\}$ ($C_6D_6$, 161 MHz, 25 °C) δ 3.3 (s, broad). IR (*n*-hexane, 25 °C) $\nu_{CO}$ 1947(vs) $cm^{-1}$; HR-MS (EI, MeCN, +ve ion) found *m*/*z* 393.9725 (calc. for $C_{12}H_{21}O_4{}^{75}As_1{}^{59}Co_1{}^{31}P_1$ $[M]^+$: 393.9725). Analysis found 36.60 C, 5.16 H (calc. for $C_{12}H_{21}O_4As_1Co_1P_1$: 36.57 C, 5.37 H).

Single crystals obtained by slow evaporation of *n*-pentane solution at -30 °C. Two independent molecules were found in the asymmetric unit. $C_{12}H_{21}As_1Co_1O_4P_1$ (*M* = 394.11 g/mol): orange plate, 0.075 × 0.176 × 0.235 mm, monoclinic, space group $P2_1/n$ (no. 14), *a* = 8.19800(10) Å, *b* = 14.8986(2) Å, *c* = 26.2475(3) Å, β = 97.0710(10)°, *V* = 3181.45(7) Å$^3$, *Z* = 8, Gaussian correction $T_{min}/T_{max}$ = 0.29678/0.37651, $\mu$(Cu-K$_\alpha$) = 11.788 $mm^{-1}$, $\varrho_{calc}$ = 1.646 g/cm$^3$, 42721 reflections measured (6.786° ≤ 2Θ ≤ 148.738°), 6425 unique ($R_{int}$ = 0.0382, $R_{sigma}$ = 0.0223) which were used in all calculations, *GOF* = 1.065, $D_{min}/D_{max}$ = -0.89/1.46 e/Å$^3$. The final $R_1$ was 0.0360 (I > 2σ(I)) and $wR_2$ was 0.0875 (all data).

### 3.7.2.7 [Co{P(OMe)$_3$}(CO){$\eta^5$-AsC$_4$(SiMe$_3$)$_2$Me$_2$}]



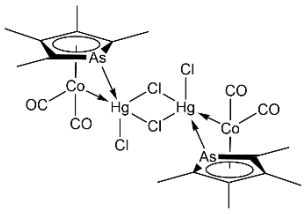

Prepared similarly to that above. Quantities: 0.11 g [Co(CO)$_2${$\eta^5$-AsC$_4$(SiMe$_3$)$_2$Me$_2$}] (0.27 mmol), ~0.1 mL P(OMe)$_3$. Isolated yield: 0.115 g (0.22 mmol, 81%). Properties are similar to the tetramethylarsolyl complex.

NMR: $^1$H (C$_6$D$_6$, 400 MHz, 25 °C) δ 3.40 (d, $^3J_{PH}$ = 12.2 Hz, 9H, P(OC*H*$_3$)$_3$), 2.15 (s, 6H, β-C*H*$_3$), 0.32 (s, 18H, α-Si(C*H*$_3$)$_3$). $^{13}$C{$^1$H} (C$_6$D$_6$, 176 MHz, 25 °C) δ 205.6 (*C*O), 118.7 (arsole {2,5}-*C*), 116.0 (arsole {3,4}-*C*), 51.5 (P(O*C*H$_3$)$_3$), 18.7 (β-*C*H$_3$), 1.6 (Si(*C*H$_3$)$_3$). $^{31}$P{$^1$H} (C$_6$D$_6$, 161 MHz, 25 °C) δ 3.8 (s, broad); IR (*n*-hexane, 25 °C) $\nu_{CO}$ 1941(vs) cm$^{-1}$; HR-MS (EI, MeCN, +ve ion) found *m*/*z* 510.0199 (calc. for C$_{16}$H$_{33}$O$_4$$^{75}$As$_1$$^{59}$Co$_1$$^{31}$P$_1$$^{29}$Si$_2$ [*M*]$^+$: 510.0203). Analysis found 37.55 C, 6.32 H (calc. for C$_{16}$H$_{33}$O$_4$As$_1$Co$_1$P$_1$Si$_2$: 37.65 C, 6.52 H).

Single crystals were obtained by slow evaporation of SiMe$_4$ solution at -30 °C. C$_{16}$H$_{33}$As$_1$Co$_1$O$_4$P$_1$Si$_2$ (*M* = 510.42 g/mol): orange needle, 0.042 × 0.091 × 0.554 mm, monoclinic, space group *Cc* (no. 9), *a* = 7.93850(10) Å, *b* = 19.9045(2) Å, *c* = 15.36370(10) Å, *β* = 90.3000(10)°, *V* = 2427.61(4) Å$^3$, *Z* = 4, Gaussian correction (*T*$_{min}$/*T*$_{max}$ = 0.178/0.672, *μ*(Cu-K$_α$) = 8.764 mm$^{-1}$, *ρ*$_{calc}$ = 1.397 g/cm$^3$, 23360 reflections measured (8.886° ≤ 2Θ ≤ 147.518°), 4232 unique (*R*$_{int}$ = 0.0252, *R*$_{sigma}$ = 0.0181) which were used in all calculations, *GOF* = 1.030, *D*$_{min}$/*D*$_{max}$ = -0.32/0.31 e/Å$^3$. The final *R*$_1$ was 0.0219 (I > 2σ(I)) and *w*R$_2$ was 0.0564 (all data).

## 3.7.3 Bimetallic μ-$\eta^1$:$\eta^5$-Arsolyl Complexes

### 3.7.3.1 [Co(CO)$_2$(μ-$\eta^1$:$\eta^5$-AsC$_4$Me$_4$)·{Hg(μ-Cl)Cl}]$_2$

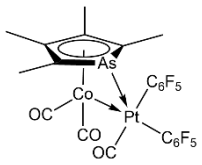



To a stirred solution of 0.15 g [Co(CO)$_2$($\eta^5$-AsC$_4$Me$_4$)] (0.5 mmol) in 5 mL CH$_2$Cl$_2$ is added 0.125 g solid HgCl$_2$ (0.46 mmol). After a brief while a bright yellow precipitate begins to form, and the mixture is stirred for a further 60 minutes before the almost colourless supernatant is decanted, and the solids washed further with acetone (3 x 3 mL portions) and Et$_2$O (3 x 3 mL portions) and dried under vacuum. Isolated yield: 230 mg (0.4 mmol, 91%). The product may be handled in air for some time as a solid however gains a brown cast overnight. The product was poorly soluble in virtually all available solvents and only partially dissolved in acetonitrile with prolonged trituration. Satisfactory NMR spectra could not be obtained due to precipitation before or during acquisition. As indicated by IR, the bulk sample obtained from this preparation is exclusively the *anti*-isomer. IR (MeCN, 25 °C) $\nu_{CO}$ 2072(vs), 2036(vs) cm$^{-1}$. HR-MS (ESI, MeCN, +ve ion) found *m*/*z* 1104.7222 (calc. for C$_{20}$H$_{24}$O$_4$$^{75}$As$_2$$^{35}$Cl$_3$$^{59}$Co$_2$$^{202}$Hg$_2$ [*M* – Cl]$^+$: 1104.7216). Analysis found 21.11 C, 1.98 H (calc. for C$_{20}$H$_{24}$O$_4$As$_2$Cl$_4$Co$_2$Hg$_2$: 21.09 C, 2.12 H).

Single crystals were obtained by layering an acetone solution of $[Co(CO)_2(\eta^5\text{-}AsC_4Me_4)]$ with an acetone solution of $HgCl_2$ at -30 °C. Two sets of crystalline specimens formed, which proved to be *anti*- and *syn*-isomers of the same compound. *anti*-$C_{20}H_{24}As_2Cl_4Co_2Hg_2O_4$ ($M$ = 1139.07 g/mol): yellow needle, 0.046 × 0.074 × 0.51 mm, monoclinic, space group $P2_1/n$ (no. 14), $a$ = 8.83040(10) Å, $b$ = 14.2969(2) Å, $c$ = 11.8460(2) Å, $\beta$ = 94.2220(10)°, $V$ = 1491.47(4) Å$^3$, $Z$ = 2, spherical correction $T_{min}/T_{max}$ = 0.07271/0.17197, $\mu$(Cu-K$_\alpha$) = 32.581 mm$^{-1}$, $\varrho_{calc}$ = 2.536 g/cm$^3$, 8025 reflections measured (9.712° ≤ 2Θ ≤ 147.534°), 3000 unique ($R_{int}$ = 0.0307, $R_{sigma}$ = 0.0342) which were used in all calculations, $GOF$ = 1.074, $D_{min}/D_{max}$ = -1.34/1.32 e/Å$^3$. The final $R_1$ was 0.0415 (I > 2σ(I)) and $wR_2$ was 0.1021 (all data).

*syn*-$C_{20}H_{24}As_2Cl_4Co_2Hg_2O_4$ ($M$ = 1139.07 g/mol): orange prism, 0.118 × 0.151 × 0.426 mm, monoclinic, space group $C2/c$ (no. 15), $a$ = 14.1928(3) Å, $b$ = 14.4745(3) Å, $c$ = 14.7169(3) Å, $\beta$ = 99.340(2)°, $V$ = 2983.26(11) Å$^3$, $Z$ = 4, spherical correction $T_{min}/T_{max}$ = 0.02226/0.10591, $\mu$(Cu-K$_\alpha$) = 32.578 mm$^{-1}$, $\varrho_{calc}$ = 2.536 g/cm$^3$, 8233 reflections measured (8.786° ≤ 2Θ ≤ 147.722°), 3020 unique ($R_{int}$ = 0.0468, $R_{sigma}$ = 0.0454) which were used in all calculations, $GOF$ = 1.109, $D_{min}/D_{max}$ = -2.61/4.25 e/Å$^3$. The final $R_1$ was 0.0660 (I > 2σ(I)) and $wR_2$ was 0.1782 (all data).

### 3.7.3.2 $[Co(CO)_2(\mu\text{-}\eta^1\text{:}\eta^5\text{-}AsC_4Me_4)\cdot\{Pt(C_6F_5)_2(CO)\}]$



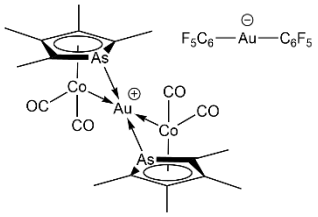

To a solution of 0.11 g $[Co(CO)_2(\eta^5\text{-}AsC_4Me_4)]$ (0.37 mmol) in 5 mL $CH_2Cl_2$ was added 0.145 g solid *cis*-$[Pt(C_6F_5)_2(\eta^2\text{:}\eta^2\text{-}C_6H_{10})$ (0.27 mmol). Over the course of about 60 minutes the orange colour discharges to a dark yellow-brown; the reaction is monitored by IR and is deemed complete after a further 60 minutes when the starting arsolyl is no longer observed. Volatiles are removed under reduced pressure and the residue extracted with the minimum amount of $Et_2O$ and transferred *via* syringe to a water-jacketed column of oven-dried Florisil® (15 x 1 cm) made up in *n*-pentane under nitrogen. Eluting with *n*-pentane, followed by 3:1 *n*-pentane/$Et_2O$ provides an orange band which is collected under nitrogen and taken to dryness. The orange solids are re-crystallised from the minimum amount of benzene overnight. Isolated yield: 0.095 g (0.12 mmol, 45%). The product is readily soluble in polar organic solvents, somewhat soluble in aromatic solvents and $Et_2O$, and less-so in *n*-hexane or *n*-pentane.

NMR: $^1$H ($CD_2Cl_2$, 400 MHz, 25 °C) δ 2.30 (s, 6H, α-C$H_3$), 1.48 (s, 6H, β-C$H_3$). $^{13}$C{$^1$H} ($CD_2Cl_2$, 176 MHz, 25 °C) δ 198.0 (Co-*C*O), 177.17 (Pt-*C*O), 146.7 (m, *C*$_6$F$_5$), 147.1 (m, *C*$_6$F$_6$), 146.3 (m, *C*$_6$F$_5$), 145.9 (m, *C*$_6$F$_5$), 139.6 (m, *C*$_6$F$_5$), 138.7 (m, *C*$_6$F$_5$), 138.2 (m, *C*$_6$F$_5$), 137.0 (m, *C*$_6$F$_5$), 126.2 (arsole {2,5}-*C*), 124.3 (arsole {3,4}-*C*), 17.3 (α-*C*H$_3$), 15.1 (β-*C*H$_3$). $^{19}$F{$^1$H} ($CD_2Cl_2$, 376 MHz, 25 °C) δ -112.44 (m, 2F), -119.74 (m, 2F), -159.87 (m, 1F), -160.44 (m, 1F), -163.58 (m, 2F), -163.96 (m, 2F). $^{195}$Pt{$^1$H} ($CD_2Cl_2$, 150 MHz, 25 °C) δ -4079.8 (apparent qq $^3J_{FPt}$ = 344, $^4J_{FPt}$ = 83 Hz) ppm. IR ($CH_2Cl_2$, 25 °C) $\nu_{CO}$ 2084(vs), 2053(vs), 2014(vs) cm$^{-1}$. HR-MS (ESI, MeCN, +ve ion) found $m/z$ 798.8942 (calc. for $C_{21}H_{12}O_1{}^{75}As_1{}^{59}Co_1{}^{19}F_{10}{}^{195}Pt_1$ [$M$ – 2CO]$^+$: 798.8936). Analysis found 32.41 C, 1.35 H (calc. for $C_{23}H_{12}O_3As_1Co_1F_{10}Pt_1$: 32.30 C, 1.41 H).

Single crystals were obtained by slow evaporation of $Et_2O$ solution at -30 °C. $C_{23}H_{12}As_1Co_1F_{10}O_3Pt_1$ ($M$ = 855.27 g/mol): orange prism, 0.067 × 0.12 × 0.264 mm, orthorhombic, space group $P2_12_12_1$ (no. 19), $a$ = 9.18910(10) Å, $b$ = 12.75590(10) Å, $c$ = 21.0227(2) Å, $V$ = 2464.18(4) Å$^3$, $Z$ = 4, spherical correction $T_{min}/T_{max}$ = 0.14128/0.23775, $\mu$(Cu-

Kα) = 18.190 mm$^{-1}$, $\varrho_{calc}$ = 2.305 g/cm$^3$, 8725 reflections measured (8.108° ≤ 2Θ ≤ 147.49°), 4597 unique ($R_{int}$ = 0.0233, $R_{sigma}$ = 0.0328) which were used in all calculations, *GOF* = 1.056, $D_{min}/D_{max}$ = -1.50/1.21 e/Å$^3$. The final $R_1$ was 0.0292 (I > 2σ(I)) and $wR_2$ was 0.0714 (all data).

### 3.7.3.3 [{Co(CO)$_2$(μ-η$^1$:η$^5$-AsC$_4$Me$_4$)}$_2$·Au][Au(C$_6$F$_5$)$_2$]



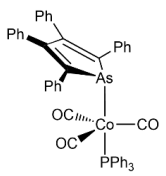

To a stirred solution of 0.11 g [Co(CO)$_2$(η$^5$-AsC$_4$Me$_4$)] (0.37 mmol) in 5 mL $CH_2Cl_2$ is added 0.15 g solid [Au(C$_6$F$_5$)(THT)] (0.33 mmol). After stirring overnight, the mixture is filtered through a short (2 x 2 cm) celite plug and the filtrate dried under reduced pressure. The yellow solids obtained were then washed with $Et_2O$ (3 x 3 mL portions) and re-crystallised from the minimum amount of $CH_2Cl_2$/$Et_2O$ at -20 °C overnight. Isolated yield: 0.18 g (0.14 mmol, 84%). The product is readily soluble in polar organic solvents and may be handled in air as a solid or solution for a short while however turns brown overnight.

NMR: $^1$H ($CD_2Cl_2$, 400 MHz, 25 °C) δ 2.33 (s, 6H, α-C*H*$_3$), 1.70 (s, 6H, β-C*H*$_3$). $^{13}$C{$^1$H} ($CD_2Cl_2$, 176 MHz, 25 °C) δ 200.2 (*C*O), 149.5 (m, *C*$_6$F$_5$), 138.7 (m, *C*$_6$F$_5$), 138.3 (m, *C*$_6$F$_5$), 137.35 (m, *C*$_6$F$_5$), 122.7 (arsole {2,5}-*C*), 118.0 (arsole {3,4}-*C*), 18.2 (α-*C*H$_3$), 14.4 (β-*C*H$_3$). $^{19}$F{$^1$H} δ -115.6 (d, $J_{FF}$ = 30 Hz, 2F, {2,6}-F), -163.0 (t, $J_{FF}$ = 21 Hz, 1F, {4}-F), -164.1 (dd, $J_{FF}$ = 23 Hz, 2F, {3,5}-F). IR ($CH_2Cl_2$, 25 °C) $\nu_{CO}$ 2062(sh), 2051(vs), 2009(vs) cm$^{-1}$; HR-MS (ESI, MeCN, +ve ion) found *m*/*z* 792.8439 (calc. for C$_{20}$H$_{24}$O$_4$$^{75}$As$_2$$^{197}$Au$_1$$^{59}$Co$_2$ [*M*]$^+$: 792.8436). Analysis found 29.03 C, 1.87 H (calc. for C$_{32}$H$_{24}$O$_4$As$_2$Au$_2$Co$_2$F$_{10}$: 29.03 C, 1.83 H).

Single crystals were obtained from the vapour diffusion of $Et_2O$ into $CH_2Cl_2$ solution at -30 °C. Four independent molecules were found within the asymmetric unit. C$_{32}$H$_{24}$O$_4$As$_2$Au$_2$Co$_2$F$_{10}$O$_4$ (*M* = 1324.14 g/mol): yellow needle, 0.08 × 0.085 × 0.346 mm, triclinic, space group *P*-1 (no. 2), *a* = 15.12080(10) Å, *b* = 21.7675(2) Å, *c* = 23.8537(2) Å, α = 100.2830(10)°, *β* = 104.7800(10)°, *γ* = 91.0780(10)°, *V* = 7452.43(11) Å$^3$, *Z* = 8, spherical correction $T_{min}/T_{max}$ = 0.10891/0.20750), *μ*(Cu-K$_α$) = 24.075 mm$^{-1}$, $\varrho_{calc}$ = 2.360 g/cm$^3$, 149532 reflections measured (7.102° ≤ 2Θ ≤ 146.294°), 29642 unique ($R_{int}$ = 0.0391, $R_{sigma}$ = 0.0298) which were used in all calculations, *GOF* = 1.041, $D_{min}/D_{max}$ = -1.82/1.22 e/Å$^3$. The final $R_1$ was 0.0265 (I > 2σ(I)) and $wR_2$ was 0.0631 (all data).

## 3.7.4 η$^1$-Arsolyl Complexes of Co(I)

### 3.7.4.1 [Co(AsC$_4$Ph$_4$)(PPh$_3$)(CO)$_3$]



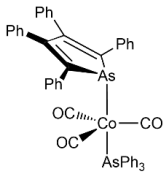

To a stirred solution of 0.25 g ClAsC$_4$Ph$_4$ (0.54 mmol) in 25 mL THF cooled to -78 °C was added a solution of 0.105 g Na[Co(CO)$_4$] (0.54 mmol) dissolved in 10 mL THF dropwise *via* syringe. The yellow colour rapidly changes to a

deep red and the mixture is stirred at low temperature for 5 minutes before a solution of 0.155 g $PPh_3$ dissolved in 10 mL THF was added. The mixture was allowed to warm to ambient temperature during which time the colour changes to a vibrant orange with gas evolution. After 2 hours all volatiles were removed under reduced pressure and the residue extracted with small portions of $CH_2Cl_2$ and filtered through a short plug of neutral alumina (5 x 2.5 cm) under nitrogen with the same solvent. The orange filtrate was collected under nitrogen and taken to dryness, and the residue washed with 3 x 20 mL *n*-hexane leaving the product as a bright yellow-orange solid. Isolated yield: 0.35 g (0.42 mmol, 77%). The product is readily soluble in polar organic and aromatic solvents and is air-sensitive in solution however solids may be handled for some time without precaution.

NMR: $^{1}H$ ($CD_2Cl_2$, 400 MHz, 25 °C) δ 7.46—7.27 (m, 15H, $C_6H_5$), 7.18—6.95 (m, 20H, $C_6H_5$) ppm. $^{13}C\{^{1}H\}$ ($CD_2Cl_2$, 176 MHz, 25 °C) δ 198.6 (d, $J_{PC}$ = 20.2 Hz, *C*O), 165.5 (d, $J_{PC}$ = 2.2 Hz, arsole {2,5}-*C*), 147.3 (arsole {3,4}-*C*), 140.4 ($C_6H_5$), 140.2 ($C_6H_5$), 133.7 ($C_6H_5$), 133.6 ($C_6H_5$), 131.5 ($C_6H_5$), 131.0 ($C_6H_5$), 129.5 ($C_6H_5$), 129.2 ($C_6H_5$), 127.9 ($C_6H_5$), 127.5 ($C_6H_5$), 126.4 ($C_6H_5$), 126.2 ($C_6H_5$) ppm. $^{31}P\{^{1}H\}$ ($CD_2Cl_2$, 162 MHz, 25 °C) δ 62.3 (s, *P*$Ph_3$) ppm. IR ($CH_2Cl_2$, 25 °C) $\nu_{CO}$ 2035(s), 1972(vs), 1961(vs) $cm^{-1}$. HR-MS (ESI, MeCN, +ve ion) found *m*/*z* 859.0773 (calc. for $C_{49}H_{35}O_3{}^{75}As_1{}^{59}Co_1{}^{23}Na_1{}^{31}P_1$ [*M* + Na]$^+$: 859.0769). Analysis found 70.40% C, 4.25% H (calc. for $C_{49}H_{35}O_3As_1Co_1P_1$: 70.35% C, 4.22% H).

Single crystals were obtained from benzene/*n*-hexane. $C_{49}H_{35}O_3As_1Co_1P_1$ (*M* = 836.59 g/mol): orange prism 0.052 × 0.119 × 0.136 mm, monoclinic, space group $P2_1/n$ (no. 14), $a$ = 13.78430(10) Å, $b$ = 11.86620(10) Å, $c$ = 23.9248(2) Å, $\beta$ = 96.1470(10)°, $V$ = 3890.81(5) Å$^3$, $Z$ = 4, spherical correction $T_{min}/T_{max}$ = 0.680/0.700, $\mu$(Cu-Kα) = 5.131 $mm^{-1}$, $\varrho_{calc}$ = 1.428 g/cm$^3$, 40315 reflections measured (7.09° ≤ 2Θ ≤ 147.618°), 7854 unique ($R_{int}$ = 0.0333, $R_{sigma}$ = 0.0270) which were used in all calculations, *GOF* = 1.035, $D_{min}/D_{max}$ = -0.46/0.44 e/Å$^3$. The final $R_1$ was 0.0310 (I > 2σ(I)) and $wR_2$ was 0.0806 (all data).

### 3.7.4.2 [Co(AsC$_4$Ph$_4$)(AsPh$_3$)(CO)$_3$]

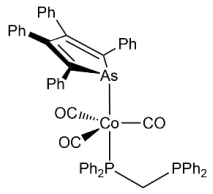



Prepared similarly to that above. Quantities: 0.25 g $ClAsC_4Ph_4$ (0.54 mmol), 0.105 g $Na[Co(CO)_4]$ (0.54 mmol) and 0.165 g $AsPh_3$ (0.54 mmol). Isolated yield: 0.17 g (0.19 mmol, 35%). Encountered as a dark red solid which is readily soluble in polar organic and aromatic solvents and is air-sensitive in solution. Solid samples acquired a brown cast after being exposed to the ambient atmosphere overnight, and solutions were also observed partially degrade upon standing overnight. For this reason, it was difficult to obtain analytically pure samples and NMR spectra contained more signals than predicted.

NMR: $^{1}H$ ($CD_2Cl_2$, 400 MHz, 25 °C) δ 7.50—7.20 (m, 15H, $C_6H_5$), 7.11—6.88 (m, 20H, $C_6H_5$) ppm (an adequate spectrum could be collected provided it was measured in a timely manner upon dissolution of the product). $^{13}C\{^{1}H\}$ ($CD_2Cl_2$, 176 MHz, 25 °C) 198.5 (*C*O), 165.4 (arsole {2,5}-*C*), 147.6 (arsole {3,4}-*C*) ppm (unambiguously assigning the twelve phenyl carbon signals was difficult due to partial decomposition in solution during acquisition). IR ($CH_2Cl_2$, 25 °C) $\nu_{CO}$ 2034(s), 1973(vs), 1961(vs) $cm^{-1}$. HR-MS (ESI, MeCN, +ve ion) found *m*/*z* 903.0245 (calc. for $C_{49}H_{35}O_3{}^{75}As_2{}^{59}Co_1{}^{23}Na_1$ [*M* + Na]$^+$: 903.0248). Satisfactory elemental microanalysis could not be obtained.

Single crystals were obtained from benzene/*n*-hexane. $C_{49}H_{35}O_2As_2Co_1$ ($M$ = 880.54 g/mol): red prism 0.168 × 0.177 × 0.337 mm, monoclinic, space group $P2_1/n$ (no. 14), $a$ = 13.7918(4) Å, $b$ = 11.9000(3) Å, $c$ = 23.9181(7) Å, $\beta$ = 95.615(3)°, $V$ = 3906.66(19) Å$^3$, $Z$ = 4, multi-scan correction $T_{min}/T_{max}$ = 0.953/1.000, $\mu$(Mo-Kα) = 2.164 mm$^{-1}$, $\varrho_{calc}$ = 1.497 g/cm$^3$, 47454 reflections measured (6.848° ≤ 2Θ ≤ 65.116°), 12727 unique ($R_{int}$ = 0.0312, $R_{sigma}$ = 0.0345) which were used in all calculations, $GOF$ = 1.041, $D_{min}/D_{max}$ = -0.50/0.45 e/Å$^3$. The final $R_1$ was 0.0321 (I > 2σ(I)) and $wR_2$ was 0.0682 (all data).

### 3.7.4.3 [Co(AsC$_4$Ph$_4$)(κ$^1$-dppm)(CO)$_3$]

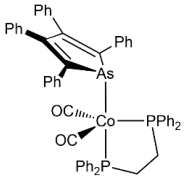



Prepared in a similar manner to that described above. Quantities: 0.25 g ClAsC$_4$Ph$_4$ (0.54 mmol), 0.105 g Na[Co(CO)$_4$] (0.53 mmol) and 0.205 g dppm (0.53 mmol). Isolated yield: 0.32 g (0.34 mmol, 63%). Encountered as a bright yellow-orange solid which is readily soluble in polar organic and aromatic solvents and is air-sensitive in solution, although solid samples could be handled for some time without precaution.

NMR: $^1$H ($CD_2Cl_2$, 400 MHz, 25 °C) δ 7.49—7.37 (m, 10H, C$_6$*H*$_5$), 7.34—7.22 (m, 10H, C$_6$*H*$_5$), 7.11—6.80 (m, 20H, C$_6$*H*$_5$), 3.25 (dd, $J_{PH}$ = 9.8 & 1.7 Hz, 2H, C*H*$_2$) ppm. $^{13}$C{$^1$H} ($CD_2Cl_2$, 176 MHz, 400 MHz) δ 198.6 (d, $J_{PC}$ = 20.6 Hz, *C*O), 165.2 (d, $J_{PC}$ = 1.5 Hz, arsole {2,5}-*C*), 147.3 (arsole {3,4}-*C*), the aromatic region was too congested for unambiguous assignment, 34.1 (dd, $J_{PC}$ = 34.2 & 24.6 Hz, *C*H$_2$) ppm. $^{31}$P{$^1$H} ($CD_2Cl_2$, 162 MHz, 25 °C) δ 58.3 (d, $J_{PP}$ = 84.5 Hz, 1P, Co-*P*Ph$_2$), -25.6 (d, $J_{PP}$ = 84.5 Hz, 1P, free *P*Ph$_2$). IR ($CH_2Cl_2$, 25 °C) $\nu_{CO}$ = 2033(s), 1971(vs), 1960(vs) cm$^{-1}$. HR-MS (ESI, MeCN, +ve ion) found $m/z$ 981.1050 (calc. for $C_{56}H_{42}O_3{}^{75}As_1{}^{59}Co_1{}^{23}Na_1{}^{31}P_2$ [$M$ + Na]$^+$: 981.1055). Analysis found 69.79% C, 4.40% H (calc. for $C_{56}H_{42}O_3As_1Co_1P_2$: 70.16% C, 4.42% H).

Single crystals were obtained from benzene/*n*-hexane. $C_{56}H_{42}O_3As_1Co_1P_2$ ($M$ = 958.68 g/mol): orange prism 0.05 × 0.064 × 0.10 mm, monoclinic, space group $P2_1/n$ (no. 14), $a$ = 11.3409(2) Å, $b$ = 18.7167(3) Å, $c$ = 21.4144(3) Å, $\beta$ = 95.3280(10)°, $V$ = 4525.87(13) Å$^3$, $Z$ = 4, multi-scan correction $T_{min}/T_{max}$ = 0.922/1.000, $\mu$(Cu-Kα) = 4.810 mm$^{-1}$, $\varrho_{calc}$ = 1.407 g/cm$^3$, 13736 reflections measured (8.294° ≤ 2Θ ≤ 141.884°), 8308 unique ($R_{int}$ = 0.0212, $R_{sigma}$ = 0.0353) which were used in all calculations, $GOF$ = 1.011, $D_{min}/D_{max}$ = -0.36/0.26 e/Å$^3$. The final $R_1$ was 0.0304 (I > 2σ(I)) and $wR_2$ was 0.0709 (all data).

### 3.7.4.4 [Co(AsC$_4$Ph$_4$)(κ$^2$-dppe)(CO)$_2$]




To a stirred solution of 0.2 g ClAsC$_4$Ph$_4$ (0.43 mmol) in 25 mL THF cooled to -78 °C was added a solution of 0.085 g Na[Co(CO)$_4$] (0.43 mmol) dissolved in 10 mL THF dropwise *via* syringe. The yellow colour rapidly changes to a deep red and the mixture is vigorously stirred at low temperature for 5 minutes before a solution of 0.175 g dppe (0.43

mmol) dissolved in 10 mL THF was added. The entire mixture was allowed to warm to ambient temperature during which time the colour changed to a deep orange with gas evolution. After 2 hours all volatiles were removed under reduced pressure and the residue extracted with small portions of $CH_2Cl_2$ and transferred to a short column of silica gel (15 x 2.5 cm) made up in *n*-hexane under nitrogen. Eluting with 9:1 *n*-hexane/$CH_2Cl_2$ provides a bright orange band which is collected under nitrogen and taken to dryness leaving the product as a bright orange microcrystalline solid. Isolated yield: 0.24 g (0.25 mmol, 58%). The product is readily soluble in polar organic and aromatic solvents and is air-sensitive in solution though solids may be handled for some time without precaution.

NMR: $^{1}$H ($CD_2Cl_2$, 400 MHz, 25 °C) δ 7.41—7.18 (m, 20H, $C_6H_5$), 7.10—6.85 (m, 20H, $C_6H_5$), 4.22 (t, $J_{PH}$ = 1.9 Hz, 4H, $C_2H_4$) ppm. $^{13}$C{$^{1}$H} ($CD_2Cl_2$, 176 MHz, 25 °C) δ 203.8 (*C*O), 167.0 (arsole {2,5}-*C*), 146.5 (arsole {3,4}-*C*), 141.6 ($C_6H_5$), 141.4 ($C_6H_5$), 135.9 ($C_6H_5$), 135.6 ($C_6H_5$), 132.9 ($C_6H_5$), 131.3 ($C_6H_5$), 130.5 ($C_6H_5$), 129.9 ($C_6H_5$), 128.8 ($C_6H_5$), 127.7 ($C_6H_5$), 127.3 ($C_6H_5$)125.8 ($C_6H_5$), 125.3 ($C_6H_5$), 31.0 (t, $J_{PC}$ = 22.8 Hz, $C_2H_4$). $^{31}$P{$^{1}$H} ($CD_2Cl_2$, 162 MHz, 25 °C) 78.4 (br s) ppm. IR ($CH_2Cl_2$, 25 °C) $\nu_{CO}$ 1979(s), 1927(vs) cm$^{-1}$. HR-MS (ESI, MeCN, +ve ion) found *m*/*z* 967.1253 (calc. for $C_{56}H_{44}O_2{}^{75}As_1{}^{59}Co_1{}^{23}Na_1{}^{31}P_2$ [*M* + Na]$^+$: 967.1262). Analysis found 71.20% C, 4.80% H (calc. for $C_{56}H_{44}O_2As_1Co_1P_2$ 71.19% C, 4.69% H).

Single crystals were obtained from benzene/*n*-hexane. $C_{56}H_{44}O_2As_1Co_1P_2$ (*M* = 944.70 g/mol): orange needle 0.05 × 0.057 × 0.111 mm, tetragonal, space group $P4_3$ (no. 78), $a$ = 13.77190(10) Å, $c$ = 24.5946(3) Å, $V$ = 4664.74(9) Å$^3$, $Z$ = 4, multi-scan correction $T_{min}/T_{max}$ = 0.758/1.000, $\mu$(Cu-Kα) = 4.641 mm$^{-1}$, $\rho_{calc}$ = 1.345 g/cm$^3$, 16538 reflections measured (7.356° ≤ 2Θ ≤ 147.802°), 9189 unique ($R_{int}$ = 0.0304, $R_{sigma}$ = 0.0485) which were used in all calculations, *GOF* = 1.041, $D_{min}/D_{max}$ = -0.25/0.48 e/Å$^3$. The final $R_1$ was 0.0358 (I > 2σ(I)) and $wR_2$ was 0.0852 (all data).

## 3.8 References


1. R. M. Kirk and A. F. Hill, *Chem. Sci.*, **2022**, *13*, 6830-6835.
2. P. C. Leung and P. Coppens, *Acta Cryst. B*, **1983**, *39*, 535-542.
3. H. B. Abrahamson, C. C. Frazier, D. S. Ginley, H. B. Gray, J. Lilienthal, D. R. Tyler and M. S. Wrighton, *Inorg. Chem.*, **1977**, *16*, 1554-1556.
4. J. W. Rathke, R. J. Klingler and T. R. Krause, *Organometallics*, **1992**, *11*, 585-588.
5. R. J. Klingler and J. W. Rathke, *J. Am. Chem Soc.,* **1994**, *116*, 4772-4785.
6. G. Bor, U. K. Dietler and K. Noack, *J. Chem. Soc. Chem. Comm.,* **1976**, 914-916.
7. G. Bor and K. Noack, *J. Organomet. Chem.*, **1974**, *64*, 367-372.
8. G. Bor and L. Markó, *Spectrochim. Acta*, **1959**, *15*, 747-748.
9. J. W. Cable, R. S. Nyholm and R. K. Sheline, *J. Am. Chem. Soc.,* **1954**, *76*, 3373-3376.
10. G. Bor, *Spectrochim. Acta*, **1963**, *19*, 2065-2073.
11. K. Noack, *Helv. Chim. Acta*, **1964**, *47*, 1064-1067.
12. A. R. Manning, *J. Chem. Soc. A,* **1968**, 1665-1667.
13. A. R. Manning and J. R. Miller, *J. Chem. Soc. A,* **1970**, 3352-3356.
14. D. J. Thornhill and A. R. Manning, *J. Organomet. Chem.,* **1972**, *37*, C41-C42.
15. D. J. Thornhill and A. R. Manning, *J. Chem. Soc. Dalton Trans.,* **1973**, 2086-2090.
16. D. J. Thornhill and A. R. Manning, *J. Chem. Soc. Dalton Trans.,* **1974**, 6-9.
17. R. L. Sweany and T. L. Brown, *Inorg. Chem.*, **1977**, *16*, 415-421.
18. G. G. Sumner, H. P. Klug and L. E. Alexander, *Acta Cryst.*, **1964**, *17*, 732-742.
19. T. Y. Garcia, J. C. Fettinger, M. M. Olmstead and A. L. Balch, *Chem. Comm.*, **2009**, 7143-7145.
20. A. E. Carpenter, I. Wen, C. E. Moore, A. L. Rheingold and J. S. Figueroa, *Chem. Eur. J.*, **2013**, *19*, 10452-10457.
21. J. M. Anna, M. R. Ross and K. J. Kubarych, *J. Phys. Chem. A,* **2009**, *113*, 6544-6547.
22. D. Karakaş and S. E. Kariper, *J. Mol. Struct.,* **2014**, *1062*, 77-81.

23. C. A. TOLMAN, *Chem. Rev.*, **1977**, *77*, 313-348.
24. J. P. KENNY, R. B. KING and H. F. SCHAEFER, *Inorg. Chem.*, **2001**, *40*, 900-911.
25. G. AULLÓN and S. ALVAREZ, *Eur. J. Inorg. Chem.*, **2001**, 3031-3038.
26. A. R. MANNING, *J. Chem. Soc. A,* **1968**, 1135-1137.
27. G. WINKHAUS and G. WILKINSON, *J. Chem. Soc.,* **1961**, 602-605.
28. F. CARRE, E. COLOMER, J. Y. COREY, R. J. P. CORRIU, C. GUERIN, B. J. L. HENNER, B. KOLANI and W. W. C. WONG CHI MAN, *Organometallics*, **1986**, *5*, 910-917.
29. P. A. MCARDLE and A. R. MANNING, *Chem. Comm.*, **1968**, 1020-1021.
30. D. J. IVERSON, G. HUNTER, J. F. BLOUNT, J. R. DAMEWOOD and K. MISLOW, *J. Am. Chem. Soc.*, **1981**, *103*, 6073-6083.
31. G. HUNTER, T. J. R. WEAKLEY, K. MISLOW and M. G. WONG, *J. Chem. Soc. Dalton Trans.,* **1986**, 577-587.
32. S. C. SENDLINGER, B. S. HAGGERTY, A. L. RBEINGOLD and K. H. THEOPOLD, *Chem. Ber.*, **1991**, *124*, 2453-2456.
33. G. MÄRKL and H. HAUPTMANN, *Angew. Chem. Int. Ed. Eng.*, **1972**, *11*, 439-440.
34. G. MÄRKL, H. HAUPTMANN and A. MERZ, *J. Organomet. Chem.,* **1983**, *249*, 335-363.
35. G. THIOLLET, R. POILBLANC, D. VOIGT and F. MATHEY, *Inorg. Chim. Acta*, **1978**, *30*, L294.
36. C. CHARRIER, H. BONNARD, F. MATHEY and D. NEIBECKER, *J. Organomet. Chem.*, **1982**, *231*, 361-367.
37. A. J. M. CAFFYN, D. CARMICHAEL, F. MATHEY and L. RICARD, *Organometallics*, **1997**, *16*, 2049-2054.
38. E. W. ABEL, I. W. NOWELL, A. G. J. MODINOS and C. TOWERS, *J. Chem. Soc. Chem. Comm.,* **1973**, 258-259.
39. E. W. ABEL, N. CLARK and C. TOWERS, *J. Chem. Soc. Dalton Trans.,* **1979**, 1552-1556.
40. I. R. LYATIFOV, G. M. JAFAROV, V. N. BABIN, P. V. PETROVSKII and V. D. ZAGOREVSKII, *J. Organomet. Chem.*, **1989**, *368*, 223-230.
41. M. ISHIDOSHIRO, Y. MATSUMURA, H. IMOTO, Y. IRIE, T. KATO, S. WATASE, K. MATSUKAWA, S. INAGI, I. TOMITA and K. NAKA, *Org. Lett.*, **2015**, *17*, 4854-4857.
42. J. L. ATWOOD, R. SHAKIR, J. T. MALITO, M. HERBERHOLD, W. KREMNITZ, W. P. E. BERNHAGEN and H. G. ALT, *J. Organomet. Chem.*, **1979**, *165*, 65-78.
43. L. R. BYERS and L. F. DAHL, *Inorg. Chem.*, **1980**, *19*, 277-284.
44. J. W. CHAMBERS, A. J. BASKAR, S. G. BOTT, J. L. ATWOOD and M. D. RAUSCH, *Organometallics*, **1986**, *5*, 1635-1641.
45. D. L. LICHTENBERGER, D. C. CALABRO and G. E. KELLOGG, *Organometallics*, **1984**, *3*, 1623-1630.
46. R. B. KING and M. B. BISNETTE, *J. Organomet. Chem.,* **1967**, *8*, 287-297.
47. R. F. HECK and D. S. BRESLOW, *J. Am. Chem. Soc.*, **1961**, *83*, 1097-1102.
48. Y. CABON, D. CARMICHAEL and X. F. LE GOFF, *Organometallics*, **2009**, *28*, 370-373.
49. D. CARMICHAEL, L. RICARD, N. SEEBOTH, J. M. BROWN, T. D. W. CLARIDGE and B. ODELL, *Dalton Trans.,* **2005**, 2173-2181.
50. X. SAVA, M. MELAIMI, L. RICARD, F. MATHEY and P. LE FLOCH, *New J. Chem.,* **2003**, *27*, 1233-1239.
51. M. OGASAWARA, T. NAGANO, K. YOSHIDA and T. HAYASHI, *Organometallics*, **2002**, *21*, 3062-3065.
52. Y. CABON, L. RICARD, G. FRISON and D. CARMICHAEL, *Eur. J. Inorg. Chem.,* **2019**, 1544-1551.
53. D. CARMICHAEL, J. KLANKERMAYER, E. MULLER, K. M. PIETRUSIEWICZ, L. RICARD, N. SEEBOTH, S. SOWA and M. STANKEVIČ, *Organometallics*, **2011**, *30*, 1804-1811.
54. D. CARMICHAEL, G. GOLDET, J. KLANKERMAYER, L. RICARD, N. SEEBOTH and M. STANKEVIČ, *Chem. Eur. J.*, **2007**, *13*, 5492-5502.
55. C. GANTER, L. BRASSAT and B. GANTER, *Chem. Ber.,* **1997**, *130*, 1771-1776.
56. C. GANTER, C. GLINSBÖCKEL and B. GANTER, *Eur. J. Inorg. Chem.*, **1998**, 1163-1168.
57. D. CARMICHAEL, L. RICARD and N. SEEBOTH, *Organometallics*, **2007**, *26*, 2964-2970.
58. L. BRUNET, F. MERCIER, L. RICARD and F. MATHEY, *Angew. Chem. Int. Ed. Eng.*, **1994**, *33*, 742-745.
59. S. HOLAND, F. MATHEY, J. FISCHER and A. MITSCHLER, *Organometallics*, **1983**, *2*, 1234-1238.
60. G. MORA, B. DESCHAMPS, S. VAN ZUTPHEN, X. F. LE GOFF, L. RICARD and P. LE FLOCH, *Organometallics*, **2007**, *26*, 1846-1855.
61. I. W. NOWELL and D. R. RUSSELL, *J. Chem. Soc. Dalton Trans.*, **1972**, 2393-2395.
62. I. W. NOWELL and D. R. RUSSELL, *J. Chem. Soc. Dalton Trans.*, **1972**, 2396-2399.
63. D. J. COOK, J. L. DAWES and R. D. W. KEMMITT, *J. Chem. Soc. A*, **1967**, 1547-1551.
64. J. L. DAWES and R. D. W. KEMMITT, *J. Chem. Soc. A*, **1968**, 1072-1073.
65. K. EDGAR, B. F. G. JOHNSON, J. LEWIS and S. B. WILD, *J. Chem. Soc. A*, **1968**, 2851-2855.

66. J. L. DAWES and R. D. W. KEMMITT, *J. Chem. Soc. A*, **1968**, 2093-2095.
67. D. M. ADAMS, D. J. COOK and R. D. W. KEMMITT, *J. Chem. Soc. A*, **1968**, 1067-1072.
68. B. DEMERSEMAN, G. BOUQUET and M. BIGORGNE, *J. Organomet. Chem.,* **1972**, *35*, 341-350.
69. R. S. NYHOLM and K. VRIEZE, *J. Chem. Soc.*, **1965**, 5337-5342.
70. M. C. JANZEN, M. C. JENNINGS and R. J. PUDDEPHATT, *Inorg. Chim. Acta*, **2005**, *358*, 1614-1622.
71. M. M. TAQUI KHAN, S. S. AHAMED, S. VANCHEESON and R. A. LEVENSON, *J. Inorg. Nucl. Chem.*, **1976**, *38*, 1279-1281.
72. J. BAUER, H. BRAUNSCHWEIG and R. D. DEWHURST, *Chem. Rev.,* **2012**, *112*, 4329-4346.
73. A. BAUZÁ, I. ALKORTA, J. ELGUERO, T. J. MOOIBROEK and A. FRONTERA, *Angew. Chem. Int. Ed.*, **2020**, *59*, 17482-17487.
74. R. USON, J. FORNIES, M. TOMAS and B. MENJON, *Organometallics*, **1986**, *5*, 1581-1584.
75. J. R. BERENGUER, J. FORNIÉS, L. F. MARTÍN, A. MARTÍN and B. MENJÓN, *Inorg. Chem.,* **2005**, *44*, 7265-7267.
76. A. BABAI, G. B. DEACON, A. P. ERVEN and G. MEYER, *Z. Anorg. Allg. Chem.*, **2006**, *632*, 639-644.
77. W. KLÄUI and L. RAMACHER, *Angew. Chem. Int. Ed. Eng.*, **1986**, *25*, 97-98.
78. G. THIOLLET, F. MATHEY and R. POILBLANC, *Inorg. Chim. Acta*, **1979**, *32*, L67-L68.
79. J. J. BRUNET, C. SIDOT and P. CAUBERE, *J. Organomet. Chem.*, **1981**, *204*, 229-241.
80. J. B. WILFORD, A. FORSTER and F. G. A. STONE, *J. Chem. Soc.,* **1965**, 6519-6523.
81. V. GALAMB, G. PALYI, F. CSER, M. G. FURMANOVA and Y. T. STRUCHKOV, *J. Organomet. Chem.*, **1981**, **209**, 183-195.
82. C. ZUCCHI, A. CORNIA, R. BOESE, E. KLEINPETER, H. ALPER and G. PÁLYI, *J. Organomet. Chem.*, **1999**, *586*, 61-69.
83. V. GALAMB, G. PALYI, R. BOESE and G. SCHMID, *Organometallics*, **1987**, *6*, 861-867.
84. R. MÜLLER and H. VAHRENKAMP, *Chem. Ber.,* **1980**, *113*, 3517-3538.
85. E. W. ABEL and G. V. HUTSON, *J. Inorg. Nucl. Chem.*, **1968**, *30*, 2339-2344.
86. Y. L. BAAY and A. G. MACDIARMID, *Inorg. Chem.*, **1969**, *8*, 986-994.
87. R. G. HAYTER, *J. Am. Chem. Soc.*, **1964**, *86*, 823-828.
88. G. BALÁZS, H. J. BREUNIG and E. LORK, *Z. Anorg. Allg. Chem.*, **2003**, *629*, 1937-1942.
89. F. CALDERAZZO, R. POLI and G. PELIZZI, *J. Chem. Soc. Dalton Trans.,* **1984**, 2535-2540.
90. A. D. HARLEY, R. R. WHITTLE and G. L. GEOFFROY, *Organometallics*, **1983**, *2*, 383-387.
91. R. E. GINSBURG, R. K. ROTHROCK, R. G. FINKE, J. P. COLLMAN and L. F. DAHL, *J. Am. Chem. Soc.*, **1979**, *101*, 6550-6562.
92. J. K. BURDETT, *J. Chem. Soc. Dalton Trans.*, **1977**, 423-428.
93. J. M. COLEMAN and L. F. DAHL, *J. Am. Chem. Soc.*, **1967**, *89*, 542-552.
94. R. D. ADAMS and F. A. COTTON, *J. Am. Chem. Soc.*, **1970**, *92*, 5003-5004.
95. T. C. FLOOD, F. J. DISANTI and K. D. CAMPBELL, *Inorg. Chem.*, **1978**, *17*, 1643-1646.
96. R. F. HECK and D. S. BRESLOW, *J. Am. Chem. Soc.*, **1962**, *84*, 2499-2502.
97. R. F. HECK, *J. Am. Chem. Soc.*, **1963**, *85*, 1220-1223.
98. R. F. HECK, *Adv. Organomet. Chem.*, **1966**, *4*, 243-266.
99. L. M. BOWER and M. H. B. STIDDARD, *J. Chem. Soc. A,* **1968**, 706-710.
100. C. LOUBSER, H. M. ROOS and S. LOTZ, *J. Organomet. Chem.*, **1991**, *402*, 393-412.
101. S. SABO, B. CHAUDRET and D. GERVAIS, *J. Organomet. Chem.*, **1985**, *292*, 411-418.
102. S. SABO, B. CHAUDRET and D. GERVAIS, *J. Organomet. Chem.*, **1983**, *258*, C19-C22.
103. G. B. JACOBSEN, B. L. SHAW and M. THORNTON-PETT, *J. Chem. Soc. Dalton Trans.*, **1987**, 1509-1513.
104. G. B. JACOBSEN, B. L. SHAW and M. THORNTON-PETT, *J. Chem. Soc. Chem. Comm.*, **1986**, 13-15.
105. C. C. TSO, A. R. CUTLER and R. K. KULLNIG, *J. Am. Chem. Soc.*, **1987**, *109*, 5844-5846.

# Chapter 4

# Arsolyl Complexes of Molybdenum, Tungsten, and Iron

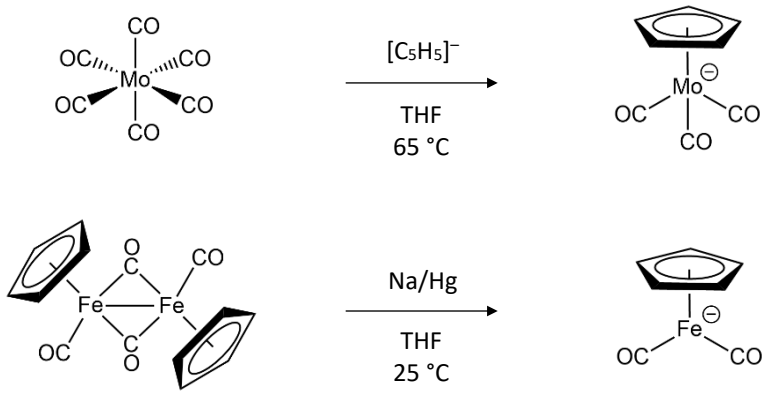
## 4.1 Preamble

Following the isolation of arsolyls with trigonal bipyramidal $CoL_n(CO)_{4-n}$ substituents at the arsenic atom, it was noted that a handful of similar σ-covalent arsolyl ($AsC_4R_4$) ligands have been described some time ago by ABEL[1] and MATHEY[2] and were first mentioned in **Chapter 1**, **Section 1.4.2**. It had been observed that apart from halogenation and hydrohalogenation of the metal-arsenic bond, and thermal decarbonylation leading to a $\eta^1 \rightarrow \eta^5$ hapticity shift, no further chemistry had been performed on any of them. In almost all cases the extent of spectroscopic characterisation reflected the standards of the era, and none were structurally characterised. Any subtle interplay between the metal centre, the arsenic lone pair and the dienic system could not have been observed or inferred with the limited data available, since these arsolyl complexes might be ostensibly viewed as an intermediate between poorly aromatic $\lambda^3$-arsoles and highly aromatic $\lambda^2$-arsolides depending on the balance of covalent and ionic bonding.

With this in mind, some of the complexes reported by ABEL were revisited with a view of obtaining more thorough spectroscopic characterisation and structural parameters *via* single crystal X-ray diffraction studies. Moreover, prior to this current work, their chemistry remained effectively unexplored – this pursuit in particular will be the subject of the latter half of this and two subsequent chapters. It is instructive that a substantial body of work exists regarding the syntheses and further reactions of cacodyl (dimethylarsenide, $AsMe_2$) transition metal complexes – almost all of it originating from the respective laboratories of VAHRENKAMP and MALISCH – which serve as useful points of comparison/inspiration throughout. This chapter describes the synthesis of arsolyl complexes of the $Mo(CO)_3(\eta^5\text{-}C_5H_5)$, $W(CO)_3(\eta^5\text{-}C_5H_5)$ and $Fe(CO)_2(\eta^5\text{-}C_5H_5)$ centres and some reactions of the lead compounds $[Mo(AsC_4R_4)(CO)_3(\eta^5\text{-}C_5H_5)]$ (R = Me or Ph).

## 4.2 From *As*-Chloroarsoles and Metal-Centred Anions

One of ABEL'S synthetic routes was employed in the initial stages of this study, namely the addition of a cyclopentadienyl metal carbonyl anion $[M(CO)_n(\eta^5\text{-}C_5H_5)]^-$ to an electrophilic arsole fragment. Molybdenum and iron systems were pursed first since their respective anions are among the most-accessible of the class: $[Mo(CO)_3(\eta^5\text{-}C_5H_5)]^-$ is obtained directly from $[Mo(CO)_6]$ and $[LiC_5H_5]$ or $[NaC_5H_5{\cdot}DME]$ (DME = 1,2-dimethoxyethane) in refluent THF (65 °C), and $[Fe(CO)_2(\eta^5\text{-}C_5H_5)]^-$ *via* ambient temperature reduction of the commercially available $[Fe_2(CO)_4(\eta^5\text{-}C_5H_5)_2]$ dimer with a dilute sodium/mercury amalgam* in THF (**Scheme 4.1**).



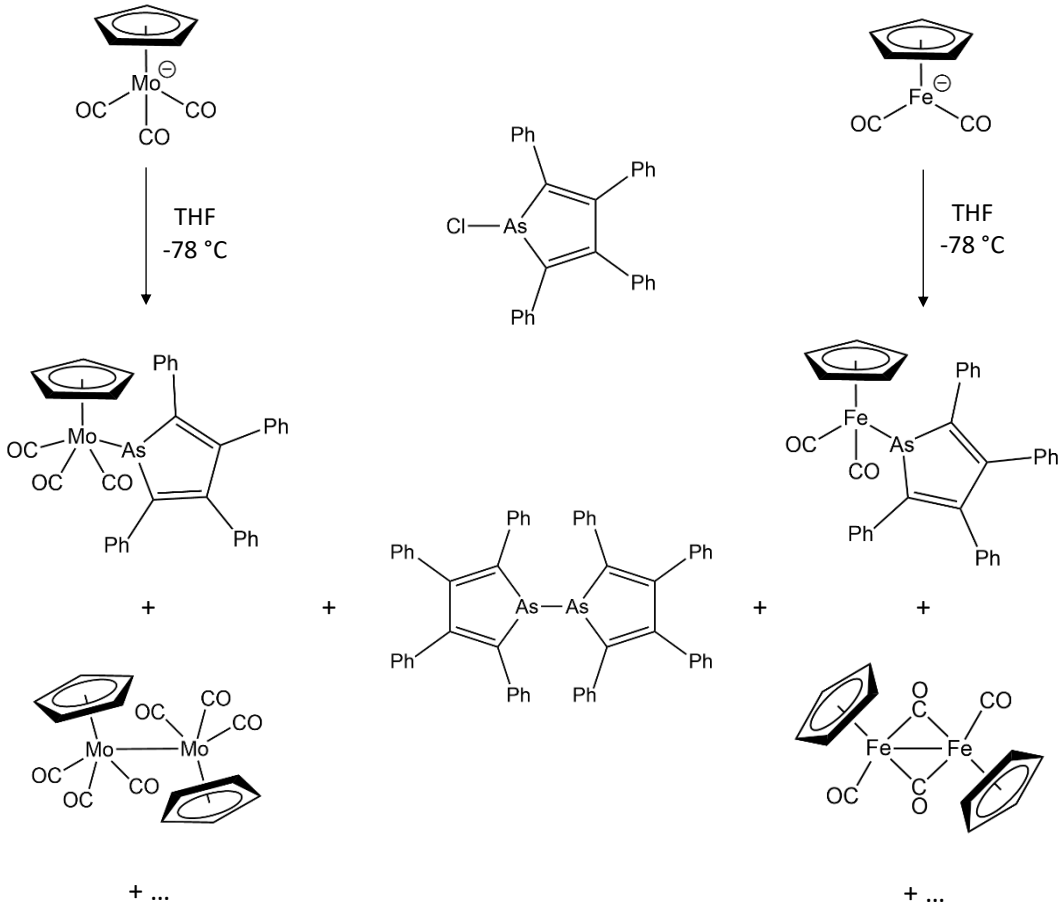

**Scheme 4.1**: Synthesis of $[Mo(CO)_3(\eta^5\text{-}C_5H_5)]^-$ and $[Fe(CO)_2(\eta^5\text{-}C_5H_5)]^-$. Cations are omitted for simplicity.

For reasons of pragmatism, *in situ* characterisation of these exceedingly air-sensitive anions is accomplished *via* IR spectroscopy. The former (as the sodium salt) displays three $\nu_{CO}$ absorptions of approximately equal intensity at 1898(s), 1788(s) and 1746(s) $cm^{-1}$, whereas the latter (sodium salt) displays four $\nu_{CO}$ of unequal intensity at 1880(s), 1865(m), 1812(s) and 1770(m) $cm^{-1}$. These IR data are in excellent agreement with that previously reported by ELLIS and FLOM.[3] The occurrence of more carbonyl vibrations than predicted for a pure $C_{3v}$ ($[Mo(CO)_3(\eta^5\text{-}C_5H_5)]^-$: $A_1 + E$ modes) or $C_{2v}$ ($[Fe(CO)_2(\eta^5\text{-}C_5H_5)]^-$: $A_1 + B_1$ modes) anion is generally attributed to ion pairing† with the sodium cation in solution.

* Other reducing agents, such as sodium or potassium mirrors, or K[(*s*-Bu)$_3$BH], were found to be less efficient.

† Three types of ion pairs have been proposed: tight ion pairing within the coordination sphere of the metal ($M\cdots Na^+$), contact ion pairing with a carbonyl oxygen atom ($M\text{-}C{\equiv}O\cdots Na^+$), and solvent-separated ion pairing ($M\cdots(solvent)\cdots Na^+$). The exact nature of the interaction depends on a variety of conditions not limited to the metal centre, the alkali metal cation, solvent, and temperature. If innocent cations are employed *e.g.*, $[NR_4]^+$, $[PR_4]^+$ or $[PPN]^+$, the effect is totally absent and the expected number of $\nu_{CO}$ are observed. See: M.Y. DARENSBOURG *Prog. Inorg. Chem.*, **1985**, *33*, 222—267.

The interaction between these $[M(CO)_n(\eta^5\text{-}C_5H_5)]^-$ nucleophiles (M = Mo, $n$ = 3; M = Fe, $n$ = 2) and THF solutions of $ClAsC_4Ph_4$ at low temperature produces dark orange-brown (Mo) or dark red-brown (Fe) mixtures containing $[M_2(CO)_{2n}(\eta^5\text{-}C_5H_5)_2]$, $(AsC_4Ph_4)_2$ and – in variable but generally modest proportions (by NMR) – $[M(AsC_4Ph_4)(CO)_n(\eta^5\text{-}C_5H_5)]$ among other unidentified materials (**Scheme 4.2**). The presence of the cyclopentadienyl metal carbonyl dimers *as the major product(s) of the reaction(s)* is established by $^1$H NMR and IR spectroscopies.* The biarsolyl $(AsC_4Ph_4)_2$ possesses no particularly informative spectroscopic signatures; however, the molecular ion is observed in a high-resolution mass spectrum ($m/z$ ≈ 862.1662) and a crystal structure determination (obtained from a different reaction) is shown in **Figure 4.4**. Isolation of the target complexes from these reaction mixtures proved more difficult than outlined by ABEL due to the very similar solubilities of all three above-named products; after several unsuccessful attempts this approach was ultimately abandoned.




**Scheme 4.2**: Attempted synthesis of tetraphenylarsolyl complexes *via* the method reported by ABEL.

* $[Mo_2(CO)_6(\eta^5\text{-}C_5H_5)_2]$: NMR: $^1$H ($C_6D_6$, 400 MHz, 25 °C) δ 4.68 ppm; IR ($CH_2Cl_2$, 25 °C) $\nu_{CO}$ 2014(m), 1958(vs) and 1912(s) cm$^{-1}$; $[Fe_2(CO)_4(\eta^5\text{-}C_5H_5)_2]$: NMR: $^1$H ($C_6D_6$, 400 MHz, 25 °C) δ 4.23 ppm; IR ($CH_2Cl_2$, 25 °C) $\nu_{CO}$ 1992(vs), 1953(vs) and 1782(s) cm$^{-1}$. Identities confirmed by comparisons with authentic samples.

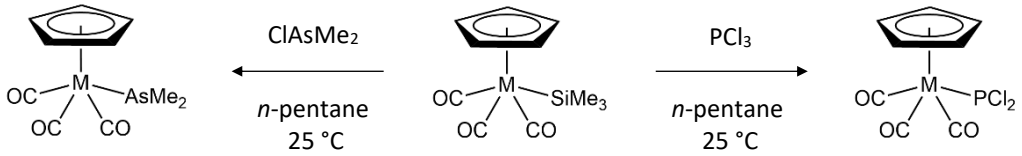
The occurrence of these competitive outer-sphere redox processes leading to the dimeric forms of the starting reagents was, in hindsight, understandable given the redox potentials of these metal carbonyl anions[4-6] coupled with the steric bulk surrounding the electrophilic arsenic, kinetically hindering metal-arsenic bond formation. The ability of $[Mo(CO)_3(\eta^5\text{-}C_5H_5)]^-$ and $[Fe(CO)_2(\eta^5\text{-}C_5H_5)]^-$ (among others) to act as both inner- and outer-sphere reducing agents ($[Fe(CO)_2(\eta^5\text{-}C_5H_5)]^-$ $E$ = -1.303 V *vs.* $Fc/Fe^+$ in MeCN; $[Mo(CO)_3(\eta^5\text{-}C_5H_5)]^-$ $E$ = -0.734 V *vs.* $Fc/Fe^+$ in MeCN[5]) towards electrophiles with which they are treated is a documented feature of their chemistry.[7-10] Moreover, MÄRKL has shown arsoles themselves to be reducible species (*e.g.*, $PhAsC_4Ph_2H_2$ $E$ = -1.77 V *vs.* SCE in MeCN).[11] This reactivity pattern (of metal carbonyl anions) is probably exacerbated by the presence of alkali metal counterions,* as MALISCH has found in reactions between $[C][Fe(CO)_2(\eta^5\text{-}C_5H_5)]$ and $ClAsMe_2$ which give differing products depending on the presence or absence of alkali cations ([C] = $Na^+$ or $[PMeBu_3]^+$).[12] ABEL does note in his report[1] that the action of these metal carbonyl anions upon the analogous 1-chloro-2,3,4,5-tetraphenylphosphole ($ClPC_4Ph_4$) leads to the corresponding redox products exclusively (including $(PC_4Ph_4)_2$), though no mention is made of the arsole and stibole ($ClEC_4Ph_4$; E = As or Sb) electrophiles which appear in the same text. It is worth mentioning that metal carbonyl anions can also engage in halogenophilic attack upon mixing with particularly electrophilic organic halides,[13] which if operative here would lead to the formation of both $[MCl(CO)_n(\eta^5\text{-}C_5H_5)]$ and $[AsC_4Ph_4]^-$, the latter then able to react with another equivalent of $ClAsC_4Ph_4$ encountered in the reaction medium. It need not be stated that both of these competing side-reactions (electron-transfer or halogen abstraction) may well be simultaneously operative in these scenarios.

## 4.3 From *As*-Chloroarsoles and Metal Stannyl Reagents

An alternative approach to circumvent the occurrence of redox products was required. By chance, MALISCH has provided such a strategy: the cyclopentadienyl carbonyl cacodyl complexes $[M(AsMe_2)(CO)_3(\eta^5\text{-}C_5H_5)]$ (M = Cr, Mo, W) may be obtained by treatment of the corresponding metal silyl reagent $[M(SiMe_3)(CO)_3(\eta^5\text{-}C_5H_5)]$ with $ClAsMe_2$, wherein the affinity of silicon for halide sources

* Excellent reviews by KING and ELLIS on transition metal carbonyl anion chemistry discuss this point with specific examples given. See R. B. KING *Adv. Organomet. Chem.*, **1965**, *2*, 157—256, *Id.*, *Acc. Chem Res.*, **1970**, *3*, 417—427, and J. E. ELLIS *J. Organomet. Chem.*, **1975**, *86*, 1—56, *Id. Organometallics*, **2003**, *22*, 3322—3338.

(*especially* chloride) is exploited to unite the chromium and arsenic centres.[14] Likewise, the very reactive complexes $[M(PCl_2)(CO)_3(\eta^5\text{-}C_5H_5)]$ (M = Cr, Mo, W) were prepared by stoichiometric addition of $PCl_3$ to the corresponding $[M(SiMe_3)(CO)_3(\eta^5\text{-}C_5H_5)]$ reagent,[15] avoiding the indiscriminate formation of higher-nuclearity compounds $[PCl_{3-x}\{M(CO)_3(\eta^5\text{-}C_5H_5)\}_x]$ ($x$ = 1—3) which might arise from direct combination of $PCl_3$ with $[M(CO)_3(\eta^5\text{-}C_5H_5)]^-$ (**Scheme 4.3**). The metal silyl complex, in essence, serves as a synthetic equivalent for the metal-centred anion when treated with a main-group electrophile of superior electronegativity, this difference being the primary thermodynamic driving force for transmetalation.




**Scheme 4.3**: Synthesis of Group 6 dimethylarsenido (**left**) and dichlorophosphido (**right**) complexes by MALISCH.

It was envisioned that a similar strategy could be used here to obtain metal derivatives of arsolyl ligands, though metal silyl reagents *specifically* would not be used; a combination of modest thermal stability, extreme air- and moisture-sensitivity and proclivity for solvolysis[16-18] would negate any convenience gained by expedition of purification steps. Instead, more-robust transition metal stannyl complexes $[M(SnBu_3)(CO)_n(\eta^5\text{-}C_5H_5)]$ were explored as a substitute on the basis of their superior thermal stability and reasonable tolerance to air and moisture, the toxicity of organotin residues notwithstanding.* Though less electropositive than silicon, transmetalation from tin to arsenic is still enthalpically feasible† as ASHE has shown by utilising 1-stannacyclohexa-2,5-dienes to prepare the corresponding 1-arsacyclohexa-2,5-dienes, *en route* to arsabenzene (also arsaanthracene and arsanaphthalene) derivatives.[19-21]

In some regards it is surprising that such reagents have not been more-widely utilised in other settings with reducible electrophilic substrates, by-passing any propensity for competing electron-transfer pathways which might otherwise occur with $[M\{L_n\}]^-$ nucleophiles. The high solubility of the (tri-*n*-butyl)stannyl residue also means such transmetalation reactions can be carried out in hydrocarbon medium

* The preferred use of $SnBu_3$ rather than $SnMe_3$ based reagents herein takes into account the extreme toxicity of permethylstannyl derivatives, notwithstanding the sacrifice in atom-efficiency, spectroscopic clarity and crystallinity.
† PAULING electronegativities: $\chi_{Si}$ = 1.90, $\chi_{Sn}$ = 1.96, $\chi_{As}$ = 2.18.

if particularly LEWIS acidic electrophiles (*e.g.*, boranes[22-24]) are being used, where direct installation onto $[M\{L_n\}]^-$ generally demands complete removal of the donor solvents (*e.g.*, THF, dioxane, DME and the like), the presence of which is typically a consequence of their preparation.

### 4.1.1 Synthesis of $[M(SnBu_3)(CO)_n(\eta^5\text{-}C_5H_5)]$

The requisite metal stannyl reagents, namely $[M(SnBu_3)(CO)_3(\eta^5\text{-}C_5H_5)]$ (M = Cr, Mo, W) and $[Fe(SnBu_3)(CO)_2(\eta^5\text{-}C_5H_5)]$ were obtained from the corresponding cyclopentadienyl metal carbonyl anion and $SnBu_3Cl$ in THF solution, analogous to the preparation of other metal stannyls.[25, 26] All were isolated in excellent yields (the $SnBu_3$ centre is apparently impervious to reduction in these situations, with no indication of $Sn_2Bu_6$ or $[M_2(CO)_{2n}(\eta^5\text{-}C_5H_5)_2]$ formation) as viscous yellow (Cr, Mo, W) or orange (Fe) liquids in acceptable purity,* and the syntheses are readily scalable: multi-gram quantities (> 10 g) were regularly prepared without difficulty. All except the chromium species are reasonably air-stable and workup may be carried out without the need for rigorous exclusion of ambient atmosphere. The chromium derivative $[Cr(SnBu_3)(CO)_3(\eta^5\text{-}C_5H_5)]$ is exceptionally air-sensitive, however standard SCHLENK techniques are adequate for handling this compound. From a practical standpoint, $[Mo(SnBu_3)(CO)_3(\eta^5\text{-}C_5H_5)]$ is the most accessible of the four here and for this reason the chemistry of molybdenum complexes in this and two subsequent chapters will feature prominently.

The complexes $[Cr(SnBu_3)(CO)_3(\eta^5\text{-}C_5H_5)]$, $[Mo(SnBu_3)(CO)_3(\eta^5\text{-}C_5H_5)]$ and $[W(SnBu_3)(CO)_3(\eta^5\text{-}C_5H_5)]$ all display three $\nu_{CO}$ bands ($C_s$ symmetry: $2A' + A''$) and $[Fe(SnBu_3)(CO)_2(\eta^5\text{-}C_5H_5)]$ two $\nu_{CO}$ ($C_s$ symmetry: $A' + A''$) in their $CH_2Cl_2$ solution IR spectra; $^1H$ NMR spectra are predictably simple finding a sharp cyclopentadienyl resonance and four distinct signals for the *n*-butyl chains, though all appear as unresolvable multiplets ($^{119}Sn$ NMR spectroscopy was not carried out, however).

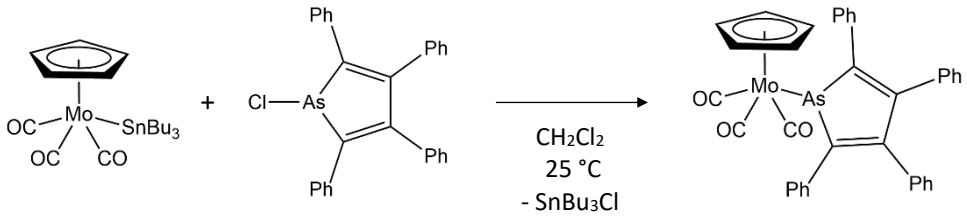
### 4.1.2 Complexes of the Tetraphenylarsolyl Ligand

#### 4.3.1.1 Synthesis of $[Mo(AsC_4Ph_4)(CO)_3(\eta^5\text{-}C_5H_5)]$

With the requisite metal stannyl reagents in hand, their transmetalation to *As*-chloroarsoles was duly investigated, and molybdenum was examined first. Thus, addition of a slight excess of

* The Group 6 stannyl complexes are decomposed upon contact with silica gel or neutral alumina and cannot be purified by chromatography, though $[Fe(SnBu_3)(CO)_3(\eta^5\text{-}C_5H_5)]$ was surprisingly stable toward the latter.

$[Mo(SnBu_3)(CO)_3(\eta^5\text{-}C_5H_5)]$ to a $CH_2Cl_2$ solution of $ClAsC_4Ph_4$ at ambient temperature affords a colour change to a deep orange over the course of ~30 minutes to several hours, depending on the scale of the reaction. Removal of the solvent and copious washing of the solids with *n*-pentane to remove expendable $SnBu_3Cl$ and unreacted metal stannyl provides the target complex $[Mo(AsC_4Ph_4)(CO)_3(\eta^5\text{-}C_5H_5)]$ as a moderately air-sensitive orange solid in high yield (**Scheme 4.4**). Bulk-material purity is sufficient for synthetic purposes however an analytically pure sample (alongside a specimen for X-ray diffractometry; **Figure 4.1**) was obtained after re-crystallisation by cooling a warm benzene/*n*-hexane mixture to -20 °C.




**Scheme 4.4**: Synthesis of $[Mo(AsC_4Ph_4)(CO)_3(\eta^5\text{-}C_5H_5)]$ by transmetalation.

Spectroscopic features are in good agreement with the limited data collected by ABEL.[1] The solution IR spectrum ($CH_2Cl_2$) finds two $\nu_{CO}$ absorptions at 2012(vs) and 1936(vs) $cm^{-1}$ (the unresolved lower energy *A*' and *A*'' vibrational modes appear to overlap) and a high-resolution mass spectrum includes the molecular ion ($m/z \approx 679.0161$). NMR spectroscopy ($C_6D_6$) finds the cyclopentadienyl ligand at 4.54 ppm in the $^1H$ spectrum with the corresponding $^{13}C\{^1H\}$ signal at 92.0 ppm; arsolyl ring resonances appear at 164.0 and 148.9 ppm with a pair of signals at 235.5 and 223.7 ppm (in an integrated 1:2 area ratio) assigned to the carbonyl ligands *transoid* and *cisoid* to the arsenic atom, respectively. The molecular structure of $[Mo(AsC_4Ph_4)(CO)_3(\eta^5\text{-}C_5H_5)]$ (as a benzene solvate) is shown in **Figure 4.1**.

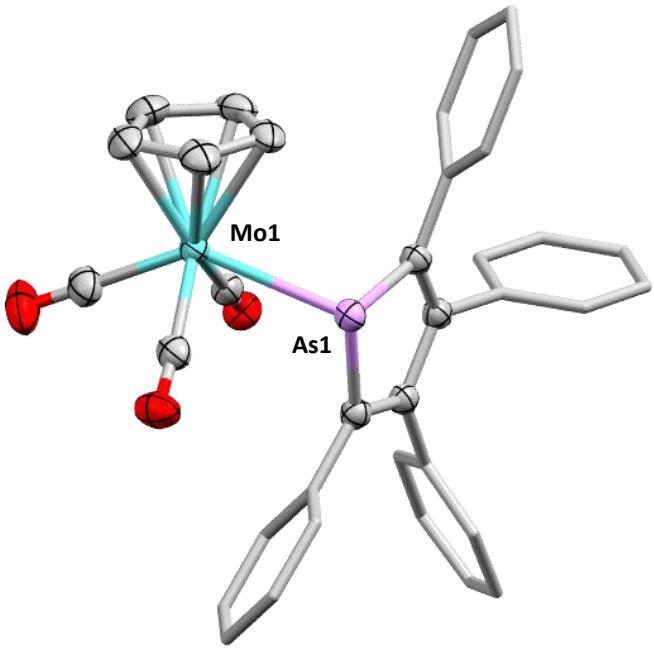



**Figure 4.1**: The molecular structure of $[Mo(AsC_4Ph_4)(CO)_3(\eta^5\text{-}C_5H_5)]\cdot C_6H_6$ in a crystal. Phenyl groups simplified and hydrogen atoms and benzene solvate omitted for clarity. Ellipsoids shown at 50% displacement.

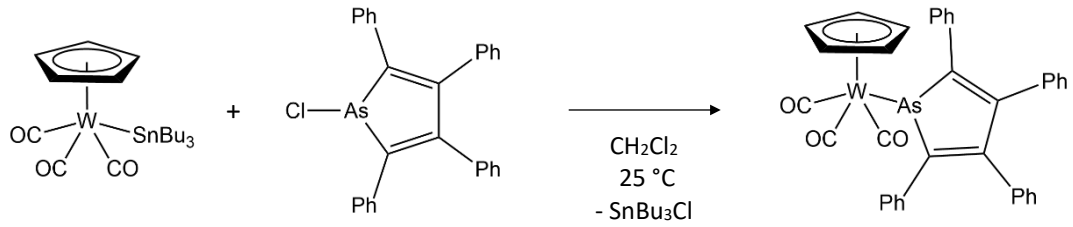
X-ray diffractometry finds the expected seven-coordinate* molybdenum complex: the three carbonyl ligands and the arsenic atom form the pedestal of a square-based pyramid with the centroid of the cyclopentadienyl ligand occupying the apex. The $AsC_4Ph_4$ ligand is unsymmetrically disposed about the molecule, being swivelled about the Mo-As bond by *ca* 60° from the (imaginary) vertical plane which bifurcates the $Mo(CO)_3(\eta^5\text{-}C_5H_5)$ group, presumably to avoid repulsive electrostatic interactions in the solid state between the *cisoid* carbonyl ligands and the phenyl residues in the 2,5-ring positions. The Mo-As covalent bond distance of 2.7190(6) Å will recur rather regularly in this work despite being slightly longer than comparable arsenides of Mo(II).[27, 28] Interatomic distances within the arsolyl ring are not significantly affected by the presence of the (cyclopentadienyl)molybdenum tricarbonyl substituent, being comparable to most other tetraphenylarsoles (mean As-$C_\alpha$ 1.934(5), mean $C_\alpha$=$C_\beta$ 1.361(4), $C_\beta$-$C_\beta$ 1.474(4) Å) though the envelope fold is measurably narrower with the arsenic atom being extruded from the mean plane of the butadiene atoms by only *ca* 3°. Several intermolecular π···H-C contacts between arsolyl phenyl hydrogens and benzene solvate molecules are measured (distance *ca* 2.6—3.0 Å) which likely assist with crystal packing,

* Based on the common perspective that a cyclopentadienyl ligand occupies three *pseudo*-facial coordination sites.

and perhaps explains why crystallisation did not occur as readily from other solvent mixtures ($CH_2Cl_2$/$Et_2O$, $CH_2Cl_2$/*n*-hexane, THF/*n*-hexane).

### 4.3.1.2 Synthesis of $[W(AsC_4Ph_4)(CO)_3(\eta^5\text{-}C_5H_5)]$

The transmetalation is readily extended to tungsten: addition of $[W(SnBu_3)(CO)_3(\eta^5\text{-}C_5H_5)]$ to a $CH_2Cl_2$ solution of $ClAsC_4Ph_4$ affords a colour change over a short while from yellow to orange and workup is carried out analogously to that described above, giving $[W(AsC_4Ph_4)(CO)_3(\eta^5\text{-}C_5H_5)]$ in good yield as a reasonably air-stable yellow solid (**Scheme 4.5**).




**Scheme 4.5**: Synthesis of $[W(AsC_4Ph_4)(CO)_3(\eta^5\text{-}C_5H_5)]$ by transmetalation.

The solution IR spectrum of the product finds two $\nu_{CO}$ bands at 2008(s) and 1937(vs) $cm^{-1}$ of which the symmetric *A*' vibrational mode is red-shifted by *ca* 5 wavenumbers in accordance with the increased π-basicity of W *vs*. Mo. This is also reflected in the $^{13}C\{^1H\}$ NMR spectrum ($C_6D_6$) with a shifting of the carbonyl (223.0 and 212.5 ppm; $^1J_{WC}$ = 140—160 Hz) and cyclopentadienyl (90.1 ppm) signals to higher frequency of the same nuclei in the molybdenum complex, though the arsolyl ring-carbon resonances only vary slightly for those directly α to the arsenic atom (163.3 and 148.9 ppm; *cf*. 164.0 and 148.9 ppm for Mo); the cyclopentadienyl hydrogens appear as a sharp peak at 4.32 ppm in the $^1H$ spectrum. Single crystals were obtained from a benzene/*n*-hexane mixture and the molecular structure (as the benzene solvate) is shown in **Figure 4.2**.

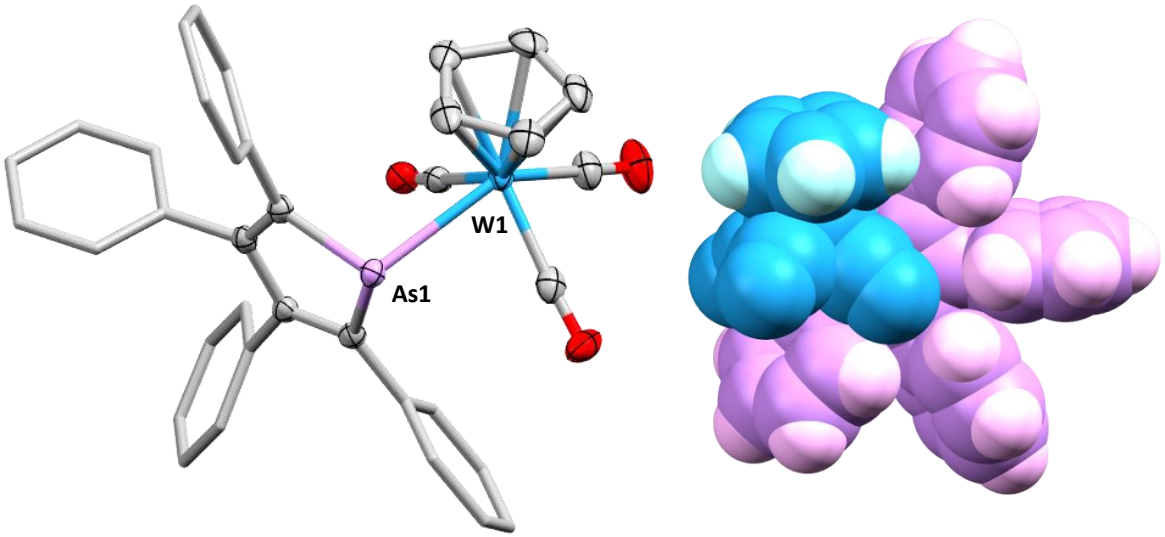
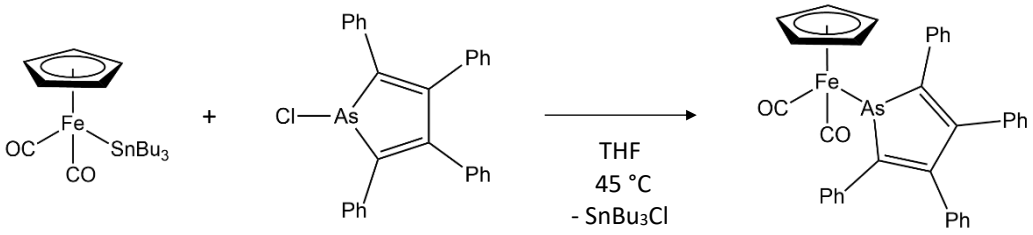



**Figure 4.2**: The molecular structure of $[W(AsC_4Ph_4)(CO)_3(\eta^5\text{-}C_5H_5)]\cdot C_6H_6$ in a crystal. Phenyl groups simplified and hydrogen atoms and benzene solvate molecule omitted for clarity. Ellipsoids shown at 50% displacement. **Inset**: Space-filling representation of the complex; blue = $W(CO)_3(\eta^5\text{-}C_5H_5)$, lilac = $AsC_4Ph_4$.

X-ray diffractometry reveals the expected complex to be isomorphous with its molybdenum analogue (identical unit cell dimensions in orthorhombic *Pbca*). Gross molecular dimensions are also in agreement with those for $[Mo(AsC_4Ph_4)(CO)_3(\eta^5\text{-}C_5H_5)]$: the $AsC_4Ph_4$ group is rotated about the W-As bond such that its "centre of mass" lies *ca* 60° offset from the vertical (non-crystallographic) symmetry plane of the $W(CO)_3(\eta^5\text{-}C_5H_5)$ unit, placing a phenyl ring in the region of space below the pair of *cisoid* carbonyl ligands. The W-As bond length of 2.7199(6) Å is crystallographically identical to the Mo-As bond in $[Mo(AsC_4Ph_4)(CO)_3(\eta^5\text{-}C_5H_5)]$ (*cf.* 2.7190(6) Å; **Figure 4.1**) which is to be expected given the similar covalent radii of these Group 6 metals. The same conclusions emerge for the mean arsolyl ring dimensions including the envelope fold (*ca* 4°) which are identical to the those of $[Mo(AsC_4Ph_4)(CO)_3(\eta^5\text{-}C_5H_5]$. A space-filling representation in the inset of **Figure 4.2** illustrates the formidable steric volume of the arsolyl ligand afforded by the four exocyclic phenyl groups and serves as a point of visual comparison with that of the more-discreet tetramethylarsolyl ligand (**Section 4.1.3**).

### 4.3.1.3 Synthesis of [Fe(AsC$_4$Ph$_4$)(CO)$_2$($\eta^5$-C$_5$H$_5$)]

In contrast to the preceding Mo and W complexes, [Fe(SnBu$_3$)(CO)$_2$($\eta^5$-C$_5$H$_5$)] is sluggish to react with ClAsC$_4$Ph$_4$ in CH$_2$Cl$_2$ at ambient temperature and the reaction is only complete after several days (*cf.* < 6 hours for [M(SnBu$_3$)(CO)$_3$($\eta^5$-C$_5$H$_5$)]; M = Mo, W) from which the orange-red [Fe(AsC$_4$Ph$_4$)(CO)$_3$($\eta^5$-C$_5$H$_5$)] is isolated in moderate yield. The complex is, however, superior in its stability toward aerobic oxidation and solutions displayed no evidence for decomposition overnight when not protected by inert atmosphere. The formation of the iron complex can be accelerated by mild warming in THF (*ca* 45 °C; **Scheme 4.6**).




**Scheme 4.6**: Synthesis of [Fe(AsC$_4$Ph$_4$)(CO)$_2$($\eta$5-C$_5$H$_5$)] by transmetalation.

The IR spectrum of [Fe(AsC$_4$Ph$_4$)(CO)$_2$($\eta^5$-C$_5$H$_5$)] finds only two $\nu_{CO}$ vibrations at 2021(vs) and 1966(vs) (to be expected from a simple $C_s$-symmetry dicarbonyl species) and resonances for the cyclopentadienyl ligand are found at 3.88 and 83.9 ppm in the $^1$H and $^{13}$C{$^1$H} NMR spectra, respectively. The $^{13}$C{$^1$H} NMR spectrum exhibits a single resonance at 213.6 ppm for the equivalent carbonyl carbon nuclei and the arsolyl ring manifests at 166.9 and 147.7 ppm for the carbon atoms α and β to the heteroatom, respectively. The gross composition is confirmed by high-resolution mass spectrometry which affords sequential products of decarbonylation. Single crystals of [Fe(AsC$_4$Ph$_4$)(CO)$_3$($\eta^5$-C$_5$H$_5$)] were obtained from a benzene/*n*-hexane mixture and the molecular structure is shown in **Figure 4.3**.

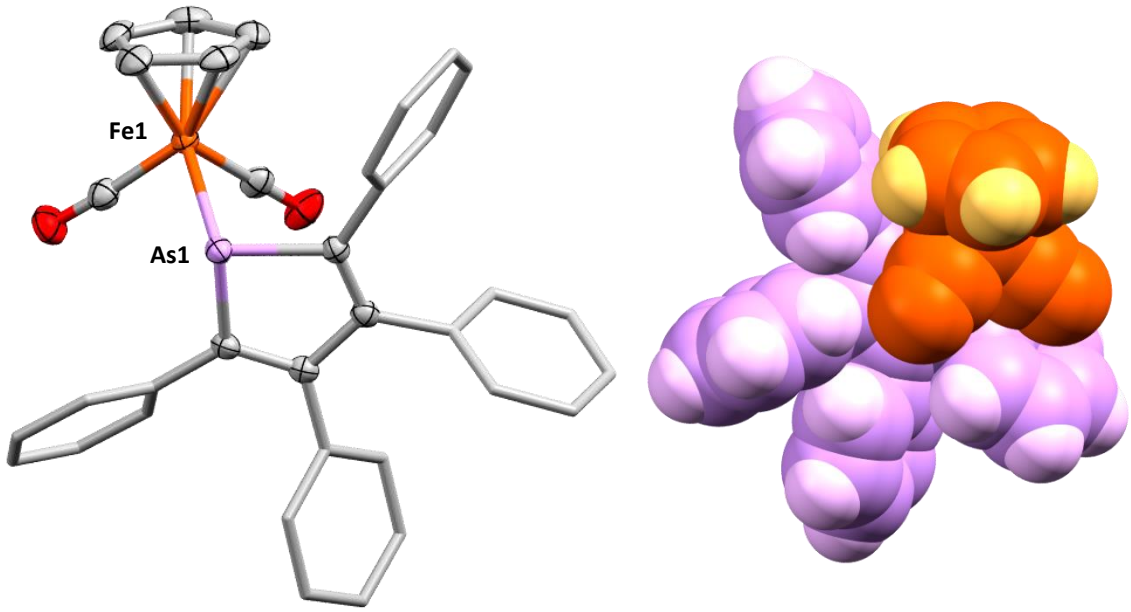


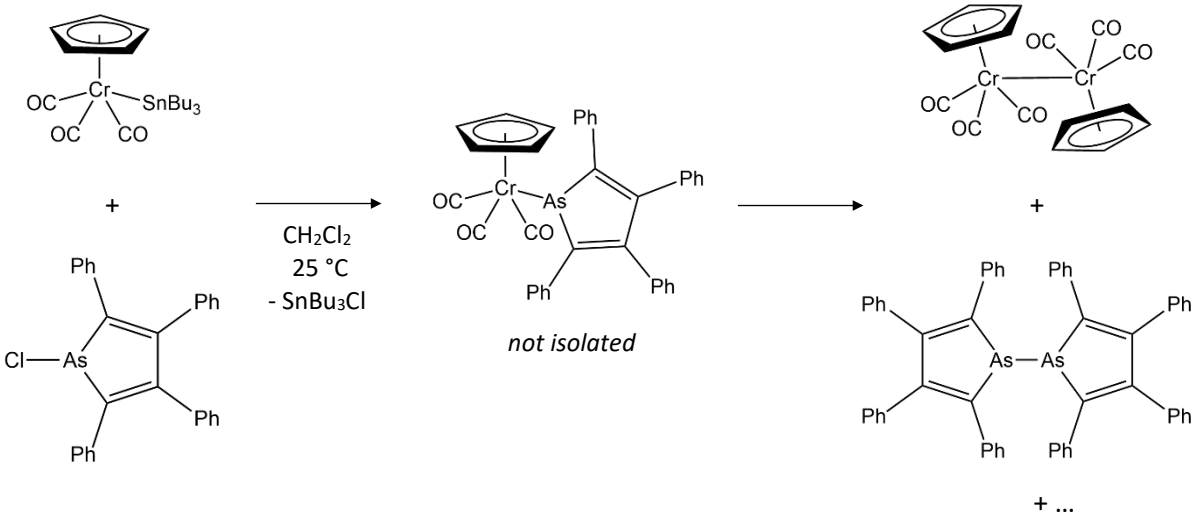

**Figure 4.3**: The molecular structure of $[Fe(AsC_4Ph_4)(CO)_3(\eta^5\text{-}C_5H_5)]$ in a crystal. Phenyl groups simplified and hydrogen atoms omitted for clarity. Ellipsoids shown at 50% displacement. The cyclopentadienyl ring exhibits five-fold rotational disorder about the Fe-centroid axis and only one contributor is depicted (occupancy ratio *ca* 66:34). **Inset**: Space-filling diagram of the complex; orange = $Fe(CO)_2(\eta^5\text{-}C_5H_5)$, lilac = $AsC_4Ph_4$.

X-ray diffractometry confirms the product identity finding the expected iron arsolyl complex, with the pair of carbonyl ligands and the arsenic atom forming the pedestal of a triangular pyramid (so-called "piano-stool" geometry) and the centroid of the cyclopentadienyl ring occupying the apex. Angles between the tripodal ligand-set reflect the *pseudo*-octahedral environment of the Fe(II) centre (88—94°) and like its molybdenum and tungsten counterparts (**Sections 4.3.1.1** and **4.3.1.2**), the tetraphenylarsolyl ligand is rotated about the Fe-As bond to position a phenyl ring within the region of space between the pair of iron-bound carbonyl ligands (**Figure 4.3**, **Inset**). The Fe-As covalent bond length of 2.4319(5) Å is slightly longer than in other comparable complexes (*cf.* $[Fe\{As(SiMe_3)C(OSiMe_3)=CPh_2\}(CO)_2(\eta^5\text{-}C_5Me_5)]$[29] 2.448(1) Å; $[Fe_2(\mu\text{-}PhAs=AsPh)(CO)_4(\eta^5\text{-}C_5H_5)_2]$[30] 2.450(2) Å) though reflecting the smaller covalent radius of iron (1.32 Å), is appreciably shorter than those found in $[M(AsC_4Ph_4)(CO)_3(\eta^5\text{-}C_5H_5)]$ (M = Mo, W; *ca* 2.7 Å). Dimensions of the arsolyl ring are not remarkably dissimilar to the latter and call for no comment.

### 4.3.1.4 Attempted Synthesis of $[Cr(AsC_4Ph_4)(CO)_3(\eta^5\text{-}C_5H_5)]$

The chromium stannyl reagent $[Cr(SnBu_3)(CO)_3(\eta^5\text{-}C_5H_5)]$ reacts rapidly with $ClAsC_4Ph_4$ in $CH_2Cl_2$ solution to afford – initially – a bright orange solution that spontaneously reverts to a dark brown

suspension within minutes. Analysis of the soluble portion of the reaction mixture by IR spectroscopy finds prominent $\nu_{CO}$ absorptions at 1950(vs), 1924(s) and 1912(sh) $cm^{-1}$ which are in good agreement with the known (*anti*-isomer* of) $[Cr_2(CO)_6(\eta^5\text{-}C_5H_5)_2]$ dimer.[31] Several other carbonyl vibrations of weaker intensity were observed throughout the region 2100—1700 $cm^{-1}$, though assignment to any one species was not a straightforward task in the absence of additional information and therefore not attempted; the reaction evidently affords a quagmire of carbonyl-containing products. A $^1H$ NMR spectrum of the residue (measured in $C_6D_6$) was not particularly informative given the presence of one or more paramagnetic entities ($[Cr(CO)_3(\eta^5\text{-}C_5H_5)]\cdot$ presumed to be among them) resulting in significant line-broadening of all signals. It is suspected – given the occurrence of $[Cr_2(CO)_6(\eta^5\text{-}C_5H_5)_2]$ – that the initial transmetalation reaction probably provides the anticipated $[Cr(AsC_4Ph_4)(CO)_3(\eta^5\text{-}C_5H_5)]$ which undergoes irreversible Cr-As bond homolysis in solution shortly after formation (**Scheme 4.7**). This is itself noteworthy in that the $SnBu_3$ group has a long history of use in organic syntheses as a radical initiator (*i.e.*, $Bu_3SnH$), however the Cr-Sn bond in $[Cr(SnBu_3)(CO)_3(\eta^5\text{-}C_5H_5)]$ appears *more* stable towards homolysis† than the Cr-As bond in $[Cr(AsC_4Ph_4)(CO)_3(\eta^5\text{-}C_5H_5)]$.




**Scheme 4.7**: Reaction between $[Cr(SnBu_3)(CO)_3(\eta^5\text{-}C_5H_5)]$ and $ClAsC_4Ph_4$ leading to disproportionation products.

* $[Cr_2(CO)_6(\eta^5\text{-}C_5H_5)_2]$ is known to exist as a concentration-dependant equilibrium between *anti* and *gauche* forms which apparently interconvert *via* Cr-Cr bond homolysis. It has been estimated that as much as 10% of a 0.01mM solution of $[Cr_2(CO)_6(\eta^5\text{-}C_5H_5)_2]$ is dissociated into the 17-electron radical. Here, only the *anti*-isomer was observed and it was not possible amongst the signals to definitively identify the monomeric $[Cr(CO)_3(\eta^5\text{-}C_5H_5)]\cdot$ radical. See R.D. Adams, D.E. Collins and F.A. Cotton *J. Am. Chem. Soc.*, **1974**, *96*, 749—754, S.J. McLain *J. Am. Chem. Soc.*, **1988**, *110*, 643—644, and T.J. Jaeger and M.C. Baird *Organometallics*, **1988**, *7*, 2074—2076.

† The $^1H$ NMR spectrum of $[Cr(SnBu_3)(CO)_3(\eta^5\text{-}C_5H_5)]$ in $C_6D_6$ was quite satisfactory and no line-broadening was observed, suggesting that the Cr-Sn bond has at least reasonable short-term stability in solution.

An alternative process involving prior homolysis of the Cr-Sn bond, giving $[Cr(CO)_3(\eta^5\text{-}C_5H_5)]\cdot$ which then serves as a reducing agent upon $ClAsC_4Ph_4$, is less-likely on the basis of 1) $[Cr(SnBu_3)(CO)_3(\eta^5\text{-}C_5H_5)]$ did not undergo spontaneous homolysis in either $C_6D_6$ or $CD_2Cl_2$ solution as evidenced by NMR monitoring, 2) $[CrCl(CO)_3(\eta^5\text{-}C_5H_5)]$[32] was not observed in the IR spectrum of the reaction mixture ($\nu_{CO}$ 2043(s), 1989(vs), 1690(m) $cm^{-1}$), and 3) the physical colour changes upon mixing the reagents are in line with those observed for the corresponding molybdenum and tungsten systems. The tendency of the $Cr(CO)_3(\eta^5\text{-}C_5R_5)$ fragment (and the first row transition metals in general) to engage in one-electron processes is well-documented and not entirely surprising in the present context (**Section 4.2**), and MALISCH does note $[Cr(AsMe_2)(CO)_3(\eta^5\text{-}C_5H_5)]$ to be the most thermolabile of the Group 6 dimethylarsenido complexes, producing $[Cr_2(CO)_6(\eta^5\text{-}C_5H_5)_2]$ and $As_2Me_4$ as decomposition products.[14]

The formation of $(AsC_4Ph_4)_2$ (presumably arising from the coupling of two $[AsC_4Ph_4]\cdot$ radicals) is confirmed by a high-resolution mass spectrum of an aliquot taken from the reaction mixture. The outcome was reproducible and eventuated to be a reliable (albeit inefficient and modest yielding) method for synthesising the heretofore unknown 2,2',3,3',4,4',5,5'-octaphenylbisarsole, the molecular structure of which was determined by X-ray diffraction and is shown in **Figure 4.4**.

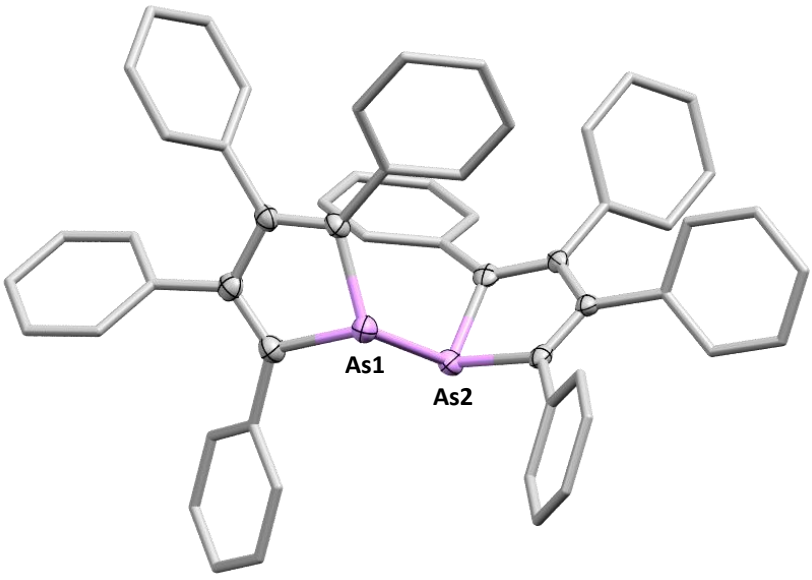



**Figure 4.4**: The molecular structure of $(AsC_4Ph_4)_2$ in a crystal. Phenyl groups simplified and hydrogen atoms omitted for clarity. Ellipsoids shown at 50% displacement.

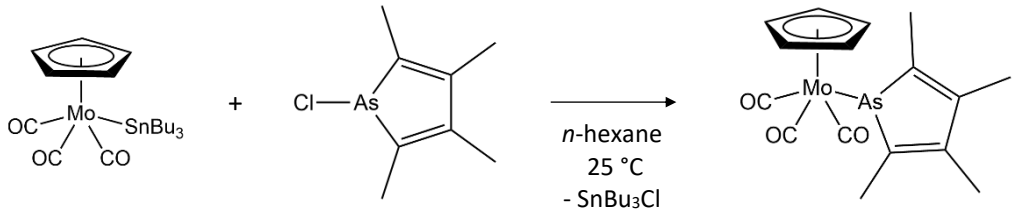
The crystal structure of $(AsC_4Ph_4)_2$ finds two tetraphenylarsolyl units adjoined at the arsenic atoms. The overall conformation of the two arsolyl groups is *gauche* (dihedral angle *ca* 104°) and in the solid state this $C_2$-arrangement is chiral – two enantiomeric molecules are found in the unit cell (triclinic *P*-1) related by the crystallographic inversion centre. The As(II) atoms are highly pyramidal with external bonding angles of 105—110° and accordingly the mean arsolyl ring planes are not parallel, forming an angle of intersection of *ca* 50°. The diarsine bond measures 2.478(1) Å which is slightly longer than the same bond in the only other structurally characterised biarsolyl (*cf.* 2.438(1) Å in $(AsC_4Me_2H_2)_2$[33]) though not unusually-so as to raise suspicion and is probably a consequence of the increased steric bulk afforded by the eight phenyl residues. Interatomic distances and angles within the separate arsolyl rings are unremarkable, being practically identical to those in $ClAsC_4Ph_4$ (**Chapter 2**, **Section 2.2.1**).

The compound $(AsC_4Ph_4)_2$ is the first of two biarsolyls that will be encountered in this work, and previously only one other biarsolyl has been structurally characterised, namely the 2,2',5,5'-tetramethylbiarsolyl obtained by ASHE.[33] It is interesting to note that regardless of substituent pattern or steric profile, all three biarsolyls exist in *gauche* conformations in the solid state, when a simple VSEPR analysis predicts the centrosymmetric *anti* configuration.

### 4.1.3 Complexes of the Tetramethylarsolyl Ligand

#### 4.3.1.5 Synthesis of $[Mo(AsC_4Me_4)(CO)_3(\eta^5\text{-}C_5H_5)]$

Mixing one equivalent each of freshly-prepared $ClAsC_4Me_4$ with $[Mo(SnBu_3)(CO)_3(\eta^5\text{-}C_5H_5)]$ in *n*-hexane solution results in the *immediate* formation of a deep orange solution and provides the expected $[Mo(AsC_4Me_4)(CO)_3(\eta^5\text{-}C_5H_5)]$ in acceptable yields after anaerobic chromatography (**Scheme 4.8**). Initial experiments required two iterations of this time-consuming process to separate the target arsolyl complex from oily tin-containing residues. Once it was discovered that the Mo-As bond was stable toward sources of fluoride (*vide infra*), the addition of excess $[Bu_4N]F$ to crude reaction mixtures (in $CH_2Cl_2$ solution) resulted in precipitation of insoluble tin-fluoride polymers, greatly expediting the anaerobic chromatography process. Small quantities of dark red $[Mo_2(CO)_6(\eta^5\text{-}C_5H_5)_2]$ were invariably isolated alongside during this process, which arises either from Mo-As bond homolysis in solution or decomposition of unreacted $[Mo(SnBu_3)(CO)_3(\eta^5\text{-}C_5H_5)]$ upon contact with the alumina column (or both).




**Scheme 4.8**: Synthesis of $[Mo(AsC_4Me_4)(CO)_3(\eta^5\text{-}C_5H_5)]$ by transmetalation.

The complex is notably more air-sensitive than the previously encountered tetraphenylarsolyl complex in solution, degrading over the course of several minutes upon exposure to the ambient atmosphere; despite this, $[Mo(AsC_4Me_4)(CO)_3(\eta^5\text{-}C_5H_5)]$ exhibited several favourable physiochemical properties which contributed to it being a lead compound in this and the following chapter. Principal among these were an excellent solubility in non-polar solvents, simple spectroscopic features and superior arsolyl pendant nucleophilicity (at both the heteroatom and diene; **Section 4.5**).

Spectroscopic features of $[Mo(AsC_4Me_4)(CO)_3(\eta^5\text{-}C_5H_5)]$ reflect the increased basicity of the tetramethyl substitution pattern: the solution IR spectrum ($CH_2Cl_2$) finds three resolved $\nu_{CO}$ absorptions at 2006(s), 1937(vs) and 1918(vs) $cm^{-1}$ (*cf.* $[Mo(AsC_4Ph_4)(CO)_3(\eta^5\text{-}C_5H_5)]$ $\nu_{CO}$ 2012(s), 1936(vs) $cm^{-1}$), and the $^1H$ NMR spectrum ($C_6D_6$) finds the cyclopentadienyl hydrogen nuclei as a sharp signal at 4.32 ppm with a pair of singlets at 2.10 and 1.93 ppm for the arsolyl methyl groups in the 2,5- and 3,4-ring positions. The $^{13}C\{^1H\}$ NMR spectrum reveals the usual pair of carbonyl resonances at 235.5 and 224.5 ppm (*transoid* and *cisoid* to the arsenic atom, respectively) and the arsolyl ring-carbon nuclei (148.7 and 141.9 ppm) are appreciably upfield of the same in the tetraphenyl complex (164.0 and 148.9 ppm). The basicity of not only the arsolyl ring atoms but also the Mo(II) centre is subtly influenced by the ring substituents, since the cyclopentadienyl carbon signal is found to marginally higher frequency (92.5 ppm) of that in $[Mo(AsC_4Ph_4)(CO)_3(\eta^5\text{-}C_5H_5)]$ (92.0 ppm); rather than the As(III) donating electron density toward the metal centre, it is inferred to be less electron-accepting. High-resolution mass spectrometry finds sequential decarbonylation products of the molecular ion and large single crystals of $[Mo(AsC_4Me_4)(CO)_3(\eta^5\text{-}C_5H_5)]$ were obtained by slow evaporation of an *n*-pentane solution at -30 °C. The molecular structure is shown in **Figure 4.5**.

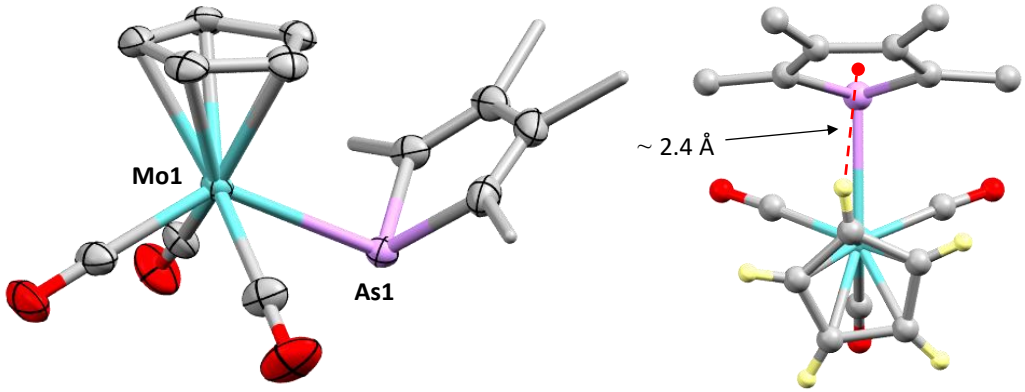
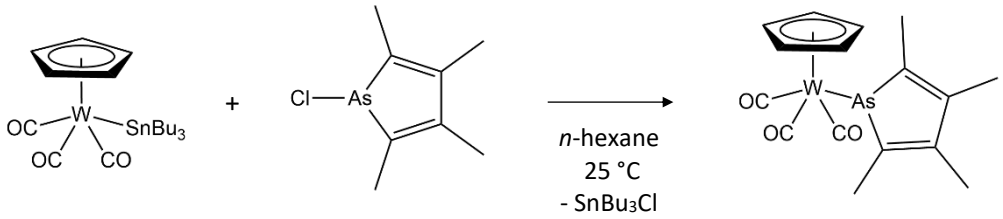



**Figure 4.5**: The molecular structure of [Mo(AsC$_4$Me$_4$)(CO)$_3$($\eta^5$-C$_5$H$_5$)] in a crystal. Methyl groups simplified and hydrogen atoms omitted for clarity. Ellipsoids shown at 50% displacement. **Inset**: Abbreviated perspective of the molecule highlighting an intramolecular π···H-C contact.

X-ray diffraction reveals the expected arsolyl complex; two enantiomeric molecules are found in the unit cell (triclinic *P*-1) related by the crystallographic inversion centre. The origin of chirality in the solid state arises from a slight rotation of the cyclopentadienyl ring from the mean vertical plane of the Mo(AsC$_4$Me$_4$)(CO)$_3$ moiety by *ca* 8°. One cyclopentadienyl hydrogen is nevertheless facing the butadiene portion of the arsolyl substituent affording a π···H-C contact of *ca* 2.4 Å (**Figure 4.5**, **Inset**), which likely accounts for the supine disposition of the AsC$_4$Me$_4$ group. The Mo-As covalent bond length of 2.7267(4) Å compares well with the same bond in [Mo(AsC$_4$Ph$_4$)(CO)$_3$($\eta^5$-C$_5$H$_5$)], and interatomic distances around the arsolyl backbone are typical finding mean As-C$_\alpha$, C$_\alpha$=C$_\beta$ and C$_\beta$-C$_\beta$ bonds of 1.934(5), 1.351(8) and 1.469(7) Å, respectively. The envelope fold of the arsolyl ring (*ca* 7°) is slightly wider than the tetraphenylarsolyl complexes (perhaps speaking to a diminished π-acceptor faculty) and measurably narrower than the *As*-organyl arsoles studied throughout this work.

### 4.3.1.6 Synthesis of [W(AsC$_4$Me$_4$)(CO)$_3$($\eta^5$-C$_5$H$_5$)]

The tungsten congener was prepared similarly: combination of [W(SnBu$_3$)(CO)$_3$($\eta^5$-C$_5$H$_5$)] with freshly-prepared ClAsC$_4$Me$_4$ in CH$_2$Cl$_2$ solution gives an intense orange solution from which [W(AsC$_4$Me$_4$)(CO)$_3$($\eta^5$-C$_5$H$_5$)] is isolated in modest yield as a moderately air-sensitive orange solid (**Scheme 4.9**). Purification is identical to that outlined above for [Mo(AsC$_4$Me$_4$)(CO)$_3$($\eta^5$-C$_5$H$_5$)].




**Scheme 4.9**: Synthesis of $[W(AsC_4Me_4)(CO)_3(\eta^5\text{-}C_5H_5)]$ by transmetalation.

The identitiy follows from the usual spectroscopic methods and high-resolution mass spectrometry: three $\nu_{CO}$ vibrations are measured in the solution IR spectrum ($CH_2Cl_2$) at 2005(s), 1928(vs) and 1909(vs) $cm^{-1}$ with the cyclopentadienyl and arsolyl-methyl signals appearing at 4.50, 2.10 and 1.90 ppm in the $^1H$ NMR spectrum ($C_6D_6$), respectively. In the $^{13}C\{^1H\}$ NMR spectrum, the pair of inequivalent carbonyl ligands *transoid* (223.4 ppm) and *cisoid* (213.6 ppm) to the arsolyl group appear with $^{183}W$ satellites ($^1J_{WC}$ = 140 and 160 ppm, respectively), whereas all other resonances including the arsolyl (148.9 and 141.0 ppm), cyclopentadienyl (91.5 ppm) and methyl (16.0 and 15.0 ppm) signals have unresolved couplings. Single crystals of $[W(AsC_4Me_4)(CO)_3(\eta^5\text{-}C_5H_5)]$ were grown from *n*-pentane solution at -30 °C and the molecular structure is shown in **Figure 4.6**.

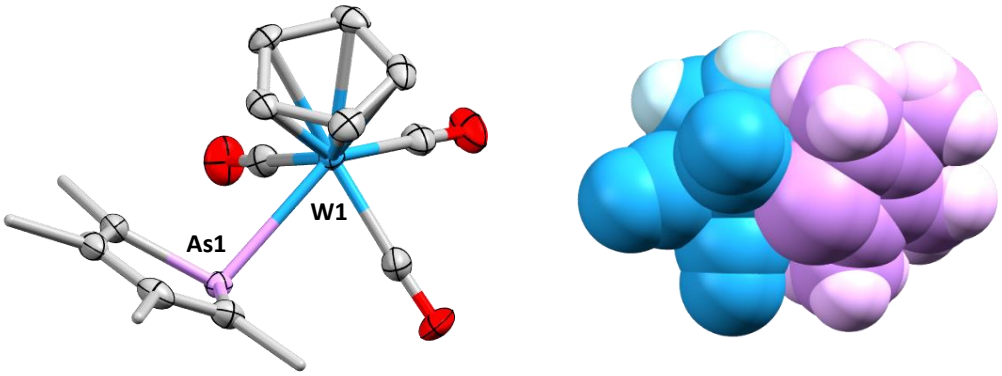



**Figure 4.6**: The molecular structure of $[W(AsC_4Me_4)(CO)_3(\eta^5\text{-}C_5H_5)]$ in a crystal. Methyl groups simplified and hydrogen atoms omitted for clarity. Ellipsoids shown at 50% displacement. **Inset**: Space-filling representation of the complex; blue = $W(CO)_3(\eta^5\text{-}C_5H_5)$, lilac = $AsC_4Me_4$.

Despite crystallising in a completely different space group (monoclinic $P2_1/c$) the complex is superficially isostructural with its molybdenum counterpart, including the slight rotation of the cyclopentadienyl ring from the mean vertical plane of the $W(AsC_4Me_4)(CO)_3$ unit and a π···H-C contact of

*ca* 2.4 Å between the arsolyl butadiene and a $C_5H_5$ hydrogen. Gross molecular features are essentially identical to those of $[Mo(AsC_4Me_4)(CO)_3(\eta^5\text{-}C_5H_5)]$ previously discussed (to be expected, given the similar covalent radii of Mo and W) with a slightly shorter W-As covalent bond distance of 2.7183(5) Å (*cf.* 2.7267(4) Å; **Figure 4.5**), though interatomic distances within the arsolyl group are crystallographically indistinguishable between the two Group 6 complexes. The inset space-filling representation highlights the comparatively unobtrusive steric profile of the $AsC_4Me_4$ residue compared to the $AsC_4Ph_4$ complex in **Figure 4.2**.

### 4.3.1.7 Attempted Synthesis of $[Fe(AsC_4Me_4)(CO)_2(\eta^5\text{-}C_5H_5)]$

It had been established in several previous experiments that the Group 6 stannyl reagents $[M(SnBu_3)(CO)_3(\eta^5\text{-}C_5H_5)]$ (M = Mo and W) readily eliminate $SnBu_3Cl$ upon treatment with *As*-chloroarsoles, whereas $[Fe(SnBu_3)(CO)_2(\eta^5\text{-}C_5H_5)]$ reacts with some reluctance under the same conditions; this is broadly attributed to a less-reactive metal-tin bond (**Section 4.4**). Hence, the addition of $[Fe(SnBu_3)(CO)_3(\eta^5\text{-}C_5H_5)]$ to an *n*-hexane solution of freshly-prepared $ClAsC_4Me_4$ gave only trace quantities of $[Fe(AsC_4Me_4)(CO)_3(\eta^5\text{-}C_5H_5)]$ after column chromatography, and the majority of the iron stannyl was recovered unchanged during this process.

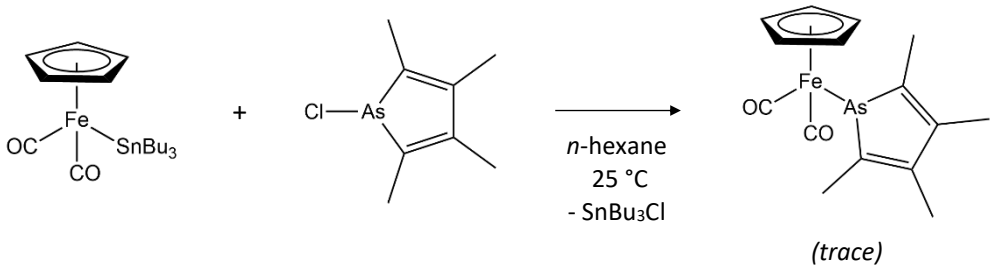



**Figure 4.7**: Synthesis of $[Fe(AsC_4Me_4)(CO)_2(\eta^5\text{-}C_5H_5)]$ in low yields by transmetalation.

The arsolyl compound was isolated as a dark orange residue which could not be obtained in a pure state, but the formulation follows unambiguously from a consideration of spectroscopic data. The $^1H$ NMR spectrum ($C_6D_6$) comprises a trio of resonances at 4.05, 2.19 and 1.92 ppm for the cyclopentadienyl and arsolyl methyl hydrogen atoms. A pair of $\nu_{CO}$ vibrations in the solution IR spectrum ($CH_2Cl_2$) 2005(vs) and 1955(vs) $cm^{-1}$; a high-resolution mass spectrum revealed the molecular ion ($m/z \approx 359.9991$). The milligram quantities obtained, in addition to sub-optimal purities, have precluded definitive analysis by $^{13}C\{^1H\}$ NMR

spectroscopy and the compound as received from the reaction could not be considered as fully characterised – crystals suitable for X-ray diffraction have not been forthcoming at the time of writing, either. The transmetalation reaction between the iron stannyl and $ClAsC_4Me_4$ is in fact *so slow* that colourless crystals of the arsole [4+2]-dimer* *endo*-$Cl_2As_2C_8Me_8$ form in the *n*-hexane mixture at ambient temperature overnight (the mixture was never heated), an outcome which was not encountered with molybdenum and tungsten stannyls; the crystal structure is shown in **Figure 4.8**.

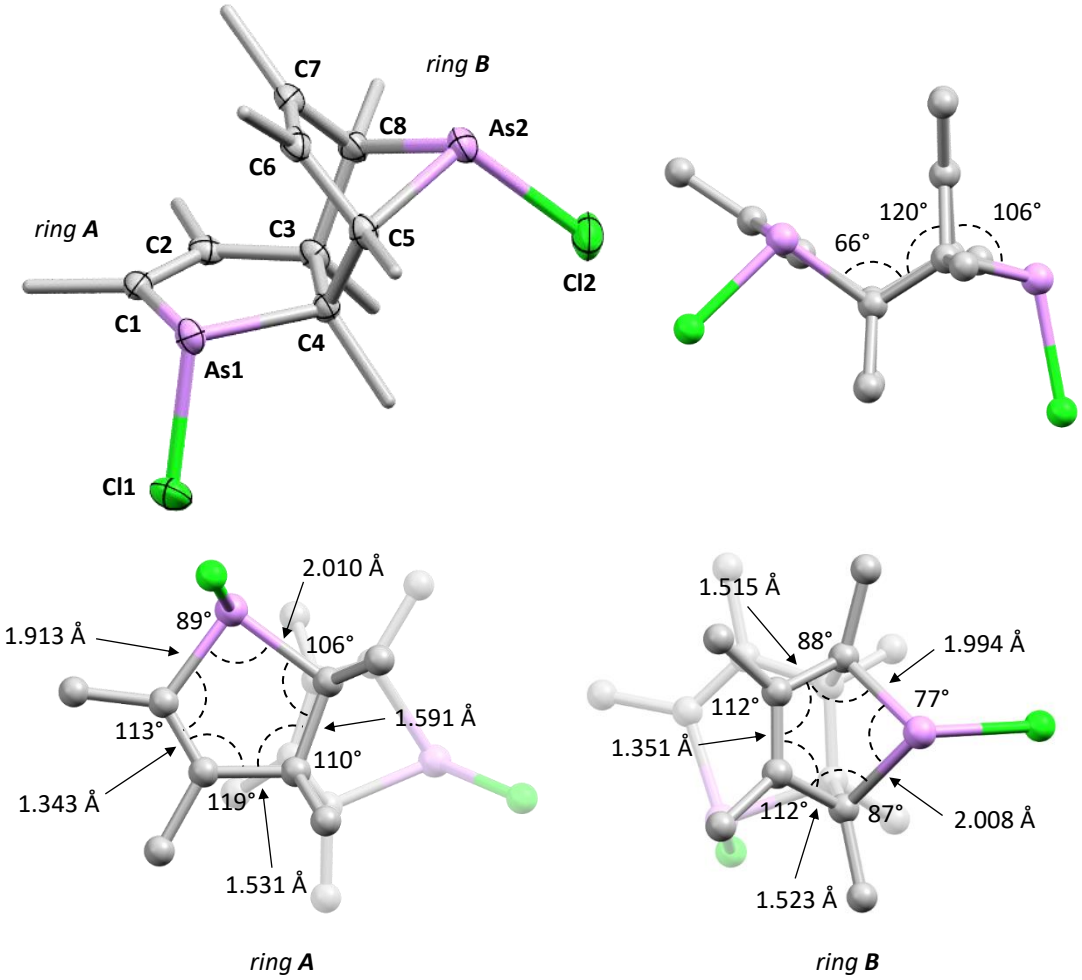
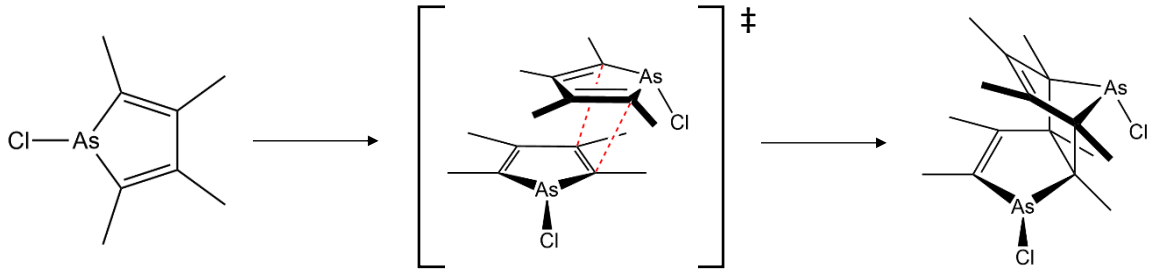



**Figure 4.8** The molecular structure of *endo*-$Cl_2As_2C_8Me_8$ in a crystal. Methyl groups simplified and hydrogen atoms omitted for clarity. Ellipsoids shown at 50% displacement. **Inset**: Abbreviated perspective of the molecule with angles between ring components (**top**) and internal ring dimensions (**bottom**).

* Biarsolyl is reserved for As-As bonded complexes such as that isolated in **Section 4.3.1.4**. The terms "diarsole" and "diarsacyclopentadiene" or the like are disfavoured to avoid possible confusion.

As a necessary consequence of [4+2] cycloaddition, the crystal structure of *endo*-$Cl_2As_2C_8Me_8$ features both 2-arsolene (ring **A**) and 3-arsolene (ring **B**) components. The former is essentially planar (envelope angle *ca* 3°) albeit irregularly deformed by the unsymmetric hybridisation pattern of the ring atoms, whereas the latter is conversely folded by *ca* 106° at the $sp^3$-carbon pivot atoms α to the arsenic yet is approximately even either side of its meridian. Interatomic distances reflect the alternating single and double bonds which impart a high degree of irregularity to the pair of arsolene rings (**Figure 4.8**, **Inset**). The occurrence of the *endo* isomer suggests secondary orbital interactions prevail over the decreased steric interactions encountered in the transition state junction leading to the *exo* counterpart. A probable mechanistic sequence leading to the *endo*-isomer observed is shown in **Scheme 4.10**.




**Scheme 4.10**: Formation of *endo*-$Cl_2As_2C_8Me_8$.

*Endo*-$Cl_2As_2C_8Me_8$ itself appeared to further decompose in solution over time: repeated dissolutions, heating, or re-crystallisations (in attempts to obtain spectroscopically pure samples) led to the accumulation of insoluble brown materials however composition was corroborated by high resolution mass spectrometry. It is noteworthy that crude samples of *endo*-$Cl_2As_2C_8Me_8$ (prepared by allowing *n*-hexane solutions of $ClAsC_4Me_4$ to decompose at ambient temperature) were apparently impervious to transmetalation upon treatment with excess $[Mo(SnBu_3)(CO)_3(\eta^5\text{-}C_5H_5)]$ in either $C_6D_6$ or $CH_2Cl_2$ solution. Presumably the increased steric encumbrance of the arsenic centres dissuades the formation of the cyclic transition state(s) required for tin-arsenic exchange (**Section 4.4**). THEOPOLD[34] has previously noted that $ClAsC_4Me_4$ has a rather brief shelf-life (in the order of 2—3 days, hence the use of freshly prepared samples throughout this work) and decomposes to unmentioned materials – there is little doubt that these materials include the cycloaddition compound obtained above. Indeed, this appears to be the first recorded

observation of a [4+2] self-cycloaddition of an arsole, a process well-documented[35-37] for the related 4π-antiaromatic borole ring (1*H*-boracyclopentadiene, $RBC_4R_4$) and of course analogous to the dimerisation of cyclopentadiene, perhaps *the* archetypal DIELS-ALDER reaction.

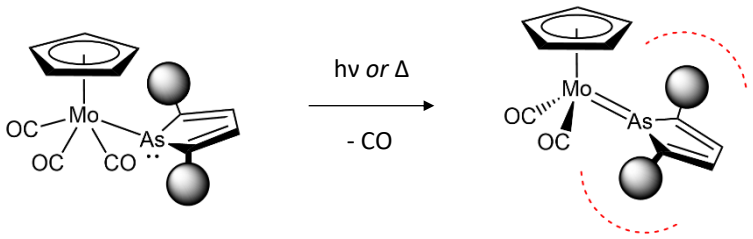
As a final comment, there are several reports of phospholes undergoing self-cycloadditions, both outside and inside the coordination sphere of a transition metal centre. The course of dimerisation depends foremost on the valency of the phosphorus atom, since *P*-oxides or -sulfides (tetrahedral P(V)) display "normal" head-to-tail [4+2] behaviour[38] whereas $\lambda^3$-phospholes (pyramidal P(III)) afford products arising from 1,5-substituent shifts and head-to-head dimerisation of the resultant 2*H*-systems.[39-42] Those within the coordination environment of a transition metal (tetrahedral P(III), $\lambda^4$) are consequently uniquely disposed and can follow intramolecular photochemical [2+2],[43, 44] or thermal [4+2] and H-transfer pathways[45-47] depending on the identity and position of the ring and *P*-substituents, and the geometry of the metal centre.* There do not appear to be any definitive examples of ambient temperature dimerisation of $\lambda^3$-phospholes as observed here for $ClAsC_4Me_4$.

### 4.1.4 Complexes of Bulky Arsolyl Ligands

MALISCH has previously obtained the first examples of a transition metal arsenium to contain a formal M=As multiple bond in the form of $[M\{As(t\text{-}Bu)_2\}(CO)_2(\eta^5\text{-}C_5H_5)]$ (M = Mo, W)[48] – the complexes are obtained by thermal decarbonylation of the corresponding tricarbonyl complex and the unsaturated metal centre is afforded kinetic stabilisation by the two proximal and sterically obtrusive *tert*-butyl substituents. Unfortunately, here, photolysis of $[Mo(AsC_4Ph_4)(CO)_3(\eta^5\text{-}C_5H_5)]$ in $C_6D_6$ did not proceed cleanly and a plethora of cyclopentadienyl-containing products were formed. Similarly, the same compound was decomposed by $Me_3NO$ in toluene at reflux. Preliminary computational studies, however, still suggested that an arsenium complex was feasible (at least *in silico*) using an arsolyl ligand. Therefore, attempts were made to synthesise an arsole ligand which was 1) formidably bulky in the 2,5-ring positions to provide more steric protection to an unsaturated metal centre than afforded by a pair of phenyl residues, 2) electron-releasing so as to increase the donor capacity of the arsenic "lone" pair, and 3) relatively non-polar so

* Coordinated phospholes may also undergo cycloaddition reactions with other dienophilic co-ligands *e.g.*, pendant vinyl groups. See J. H. NELSON *et al. Inorg. Chem.*, **2000**, *39*, 3392—3402 and references therein for specific examples. The general topic of metal-assisted cycloadditions has received thorough commentary. See H.W. FRÜHAUF *Chem. Rev.*, **1997**, *97*, 523—599 for a superbly-written review.

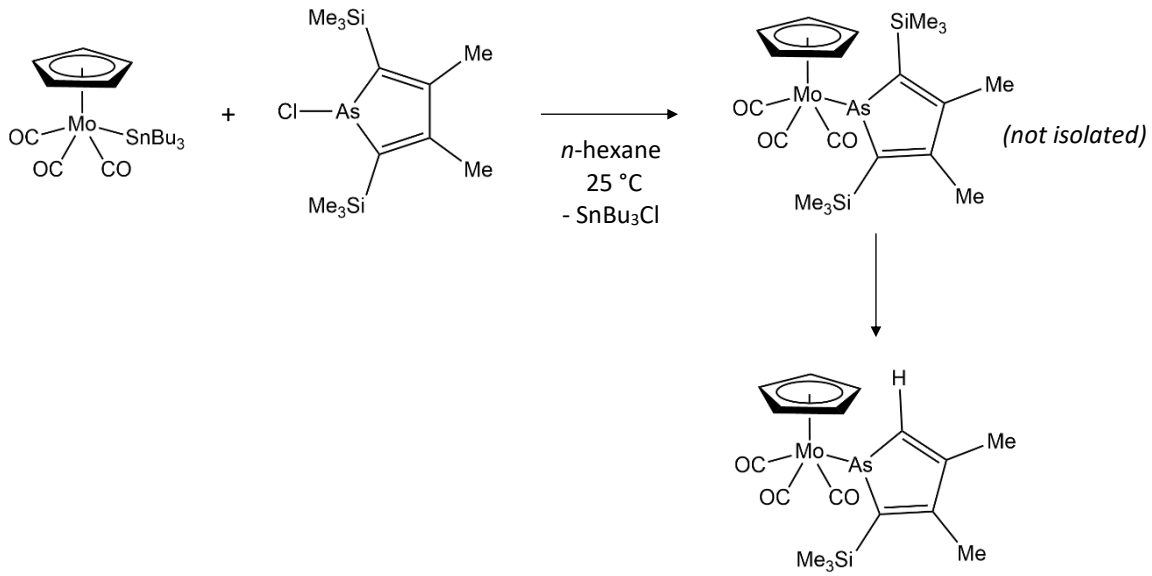
reactions could be carried out in hydrocarbon (*i.e.*, non-coordinating) media. The following section details the synthesis of these bulky arsolyl complexes.




**Scheme 4.11**: Envisioned decarbonylation of [Mo(arsole)(CO)$_3$($\eta^5$-C$_5$H$_5$)] to an arsenium, [Mo(=arsole)(CO)$_2$($\eta^5$-C$_5$H$_5$)].

### 4.3.1.8 Synthesis of [Mo{AsC$_4$H(SiMe$_3$)Me$_2$}(CO)$_3$($\eta^5$-C$_5$H$_5$)]

The bulky 1-chloro-2,5-di(trimethylsilyl)-3,4-dimethylarsole ligand (ClAsC$_4$(SiMe$_3$)$_2$Me$_2$) was obtained in good yield from the corresponding zirconacyclopentadiene and AsCl$_3$ in *n*-pentane; the compound is known, and spectroscopic data have been previously reported.[49] Treatment of this electrophile with one equivalent of [Mo(SnBu$_3$)(CO)$_3$($\eta^5$-C$_5$H$_5$)] in *n*-hexane solution gives an immediate colour change from yellow to a deep orange; column chromatography provides a single orange compound in modest yield which – unexpectedly – proved to be an *un*symmetrical complex featuring the heretofore unknown 2-(trimethylsilyl)-3,4-dimethylarsolyl ring system (**Scheme 4.12**).




**Scheme 4.12**: Synthesis of unsymmetrical [Mo{AsC$_4$H(SiMe$_3$)Me$_2$}(CO)$_3$($\eta^5$-C$_5$H$_5$)] by transmetalation and spontaneous desilylation.

The compound was readily identified from the $^{1}$H NMR spectrum ($C_6D_6$) which comprised a pair of resonances for inequivalent 3,4-methyl groups found at 2.21 and 2.04 ppm (the latter displaying $^{4}J_{HH}$ = 1.2 Hz) alongside the $SiMe_3$ signal at 0.38 ppm with a relative area integration of 3:3:9 – the lone olefinic hydrogen in the 5-ring position is found at rather high-field, 7.50 ppm and the cyclopentadienyl resonance at 4.29 ppm. The low molecular symmetry is evident in the solution IR spectrum ($CH_2Cl_2$) finding three $\nu_{CO}$ at 2007, 1938 and 1922 cm$^{-1}$, and best reflected in the $^{13}$C{$^{1}$H} NMR data ($C_6D_6$) for which all three carbonyl nuclei manifest in distinct environments at 235.7 (*transoid*), 225.6 and 223.6 (diastereotopic *cisoid*) ppm. Four arsolyl ring carbon signals are observed at 158.4, 157.2, 149.7 and 146.7 ppm though the cyclopentadienyl group falls in an unremarkable position, 90.9 ppm. High-resolution mass spectrometry finds the oxygen adduct of the molecular ion ($m/z \approx 490.9551$) and the product formulation is unequivocally established by X-ray crystallography; single crystals were obtained by slow evaporation of an *n*-pentane solution at -30 °C and the molecular structure is shown in **Figure 4.9**.

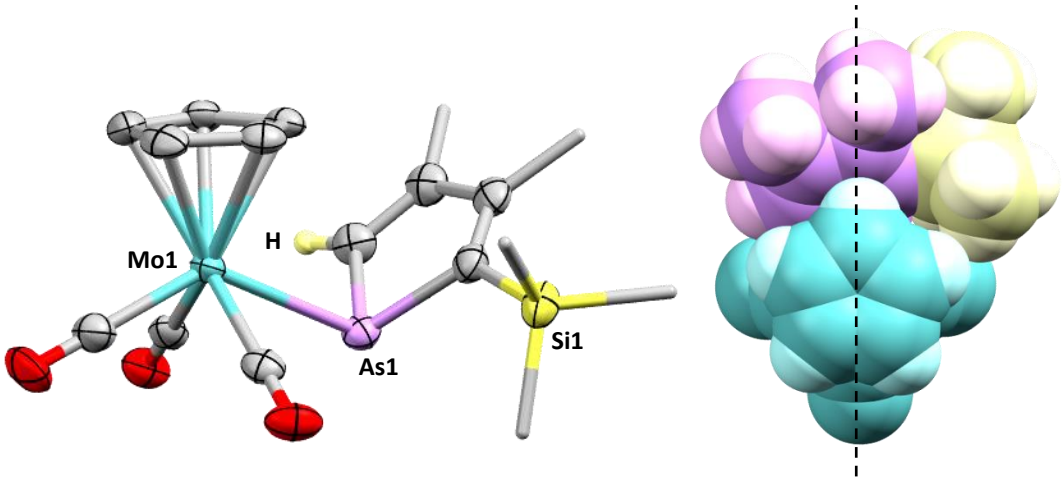



**Figure 4.9**: The molecular structure of $R_{As}$-[Mo{$AsC_4H(SiMe_3)Me_2$}$(CO)_3(\eta^5$-$C_5H_5)$] in a crystal. Methyl groups simplified and most hydrogen atoms omitted for clarity; the arsolyl ring-hydrogen is shown in light yellow for emphasis. Ellipsoids shown at 50% displacement. **Inset**: Space-filling representation highlighting the offset disposition of the arsolyl ring from the imaginary vertical plane of the molybdenum centre; blue = $Mo(CO)_3(\eta^5$-$C_5H_5)$, lilac = $AsC_4HMe_2$, lemon = $SiMe_3$.

The results of X-ray diffractometry reveal the anticipated unsymmetrical arsolyl complex; incidentally, the product crystallises in orthorhombic $P2_12_12_1$ which – given the compound belongs to point group $C_1$ and the acentric space group – means the solid-state sample obtained was evidently enantiomerically pure (FLACK parameter: 0.008). Free rotation about the Mo-As bond would not racemise the arsenic centre and inversion would be expected to be a high energy process.[50, 51] During the synthetic

process there would be no preference whatsoever toward an *R* or *S* arrangement during the original monodesilylation event and it might therefore be concluded that the bulk sample was a racemate of individually enantiopure crystals, one of which was selected for the present experiment.

Like $[Mo(AsC_4Me_4)(CO)_3(\eta^5\text{-}C_5H_5)]$, the arsolyl group is aligned *syn* with respect to the cyclopentadienyl ring – a short π···H-C contact (*ca* 2.5 Å) is measured between a hydrogen thereto and the arsolyl diene. The 2-(trimethylsilyl)-3,4-dimethylarsolyl ligand is approximately though not wholly aligned with the symmetry plane of the $Mo(CO)_3(\eta^5\text{-}C_5H_5)$ centre (**Figure 4.9**, **Inset**), and the irregular steric profile of the ring is reflected in a measurable deformation of the pyramidal geometry of the arsenic atom (exocyclic *As*-angles: 96.28(2)° and 108.28(1)°) to permit the bulky $SiMe_3$ group to recede slightly from a nearby *cisoid* carbonyl. The ring dimensions are also affected by this asymmetry: the As-$C_\alpha$ distances differ by nearly 0.04 Å to the carbon bearing the $SiMe_3$ group (1.948(5) Å) compared to the carbon bearing the hydrogen (1.911(5) Å). This difference is statistically significant (0.037 Å ≈ 7 e.s.d.) within the respective measurement errors while the C=C distances do not differ significantly (1.363(8) *vs.* 1.341(7) Å, ~3 e.s.d.). The arsenic atom protrudes from the mean plane formed by the remaining four carbon atoms by *ca* 6° with a Mo-As covalent bond distance of 2.7475(6) Å, which is comparable to those found in the two previous molybdenum-arsolyl complexes described above.

The reaction outcome proved highly reproducible, though the exact mechanistic sequence by which one (and *only* one) $SiMe_3$ group is deleted from the ring is not completely understood; it does appear to take place (at least to some extent) in the reaction mixture itself since *ca* 30 minutes after mixing the two components in $C_6D_6$ solution the title compound is present, albeit accompanied by no fewer than four unidentified cyclopentadienyl-containing species. It is suspected that the extreme steric congestion brought about by the $SiMe_3$ groups in the 2,5-ring positions induces a kinetic lability most-easily relieved by desilylation; whether this event is spontaneous or requires another actor (adventitious moisture and/or a non-innocent role for the $SnBu_3Cl$ by-product*) was not determined. Interestingly, $[Mo\{AsC_4H(SiMe_3)Me_2\}(CO)_3(\eta^5\text{-}C_5H_5)]$ itself proved resistant toward further desilylation and no reaction was observed with an excess of hydrated $[Bu_4N]F$ upon warming to 50 °C in THF. This contrasts with

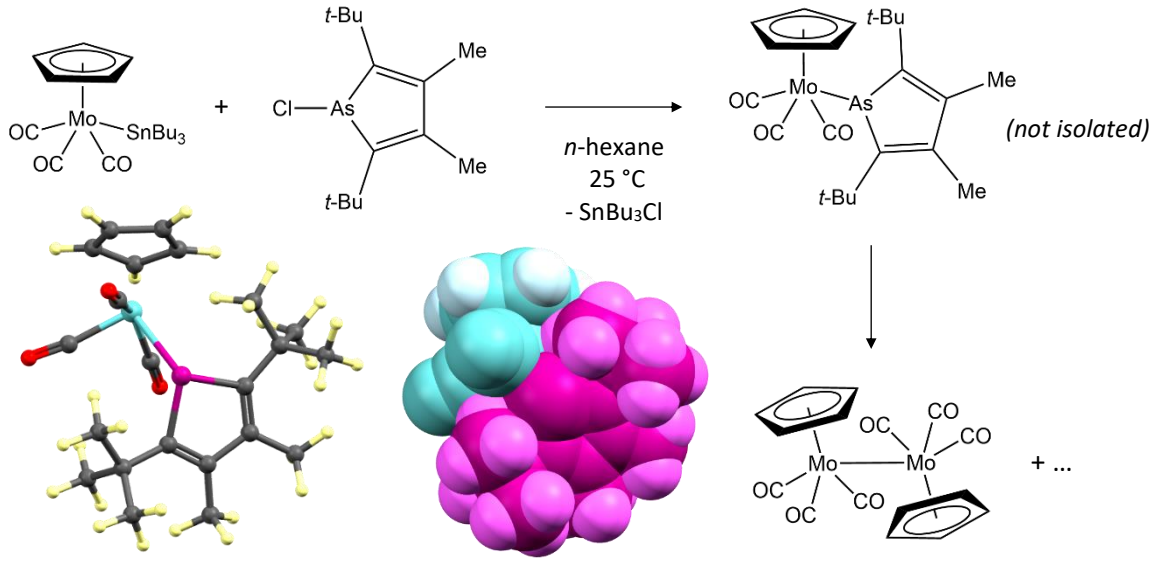
* Sn-Cl bond enthalpies are *ca* 90% those of Si-Cl bonds.

other arsenic heterocycles possessing silyl groups α to the heteroatom which are easily removed by the same reagent under very mild conditions,[49, 52] and indeed with [Co(CO)L($\eta^5$-$AsC_4(SiMe_3)_2Me_2$)] (L = CO, $P(OMe)_3$; **Chapter 3**, **Section 3.3.5**) which does not spontaneously desilylate in solution or during chromatography. Unfortunately, UV-photolysis of [Mo($AsC_4H(SiMe_3)(CO)_3(\eta^5$-$C_5H_5)$)] in *n*-hexane solution did not afford any recognisable arsenium complex and a complicated mixture of products alongside insoluble decomposition residues was observed.

#### 4.3.1.9 Attempted Synthesis of [Mo{$AsC_4$(*t*-Bu)$_2Me_2$}$(CO)_3(\eta^5$-$C_5H_5)$]

Given the apparently lability of a silyl group in the previous complex, the bulky 1-chloro-2,5-di(*tert*-butyl)-3,4-dimethylarsole ($ClAsC_4$(*t*-Bu)$_2Me_2$) was prepared in good yield from the corresponding zirconacyclopentadiene and $AsCl_3$ in *n*-pentane; the compound is known and spectroscopic data have been previously reported.[49] The crystal structure was collected during this work and is shown in **Appendix**, **Section 8.9**. The *As*-chloroarsole was combined with one equivalent of [Mo($SnBu_3$)$(CO)_3(\eta^5$-$C_5H_5)$] in *n*-hexane solution giving a gradual colour change from yellow to a deep red; $^1$H NMR analysis finds both reagents to be totally consumed after stirring overnight, though the only readily identifiable cyclopentadienyl species (and the major product) disappointingly proved to be [$Mo_2(CO)_6(\eta^5$-$C_5H_5)_2$] (**Scheme 4.13**). A multitude of alkyl signals were also observed in the $^1$H NMR spectrum though were not easily assigned to any one compound – column chromatography of the reaction mixture afforded the molybdenum dimer as the sole isolable product of the reaction and the fate of the arsolyl group remains unknown amongst the considerable quantity of immobile materials.

In line with the spontaneous mono-desilylation of the $AsC_4(SiMe_3)_2Me_2$ ring above, it is suspected that excessive steric congestion in and around the vicinity of the Mo-As bond is a destabilising influence seeking kinetic alleviation; unlike the above, however, homolysis of the Mo-As bond seems to be the preferred disintegration pathway (more-so than decarbonylation, apparently). This would account for the occurrence of $[Mo_2(CO)_6(\eta^5\text{-}C_5H_5)_2]$ in the reaction mixture, though it is not known whether a crowded $(AsC_4(t\text{-}Bu)_2Me_2)_2$ biarsolyl is even viable, in which case the arsolyl radical may degrade *via* alternative means *e.g.*, hydrogen atom abstraction.




**Scheme 4.13**: Attempted synthesis of $[Mo\{AsC_4(t\text{-}Bu)_2Me_2\}(CO)_3(\eta^5\text{-}C_5H_5)]$ by transmetalation. **Inset**: DFT-optimised geometry of the putative $[Mo\{AsC_4(t\text{-}Bu)_2Me_2\}(CO)_3(\eta^5\text{-}C_5H_5)]$ (gas phase, ωB97X-D/6-31G*/LANL2Dζ; **left**) and a space-filling representation of the same (**right**).

The difficulties encountered in even preparing a suitably bulky arsolyl complex before decarbonylation could be affected meant that the pursuit outlined in the preamble to this section was regrettably abandoned. The fact that such complexes with bulky silyl or hydrocarbon groups in the vicinity of the Mo-As bond do strive to alleviate this crowding is, however, counterintuitively promising because it outwardly suggests the arsolyl ligand is capable of fulfilling the role it was precisely designed for (*viz.* **Scheme 4.11**). With this in mind, it is possible that a certain substituent(s) in the 2,5-ring positions which are sterically imposing *but not excessively so* (the "Goldilocks" effect *e.g.*, *i*-Pr) might yet achieve the dual purpose of affording a stable arsolyl complex and stabilising an unsaturated arsenium therefrom.

## 4.4 Mechanistic Aspects of Sn→As Transmetalation

A plausible mechanism of Sn→As exchange operating during the synthesis of transition metal arsolyl complexes is shown in **Scheme 4.14**, with a range of possible transition states indicated. The sequence is derived in part from observations made by CHIPPERFIELD *et al.*[53, 54] regarding the nature of transmetalation between $[M(SnR_3)(CO)_n(\eta^5\text{-}C_5H_5)]$ and mercuric halides to give $[M(HgX)(CO)_n(\eta^5\text{-}C_5H_5)]$ and $SnR_3X$ (R = alkyl*), and from CLARK *et al.*[55, 56] regarding reactions of transition metal stannyls with a wider variety of electrophiles. In the absence of mechanistic studies regarding Sn/As exchange at transition metal centres, these serve as the closest available points of comparison at the present time. Though no kinetic experiments were carried out in this work, three simple qualitative observations arose (which have been alluded to in previous sections) and are summarised here:

1) The Group 6 stannyls $[Mo(SnBu_3)(CO)_3(\eta^5\text{-}C_5H_5)]$ and $[W(SnBu_3)(CO)_3(\eta^5\text{-}C_5H_5)]$ visibly react much faster with *As*-chloroarsoles than the iron analogue $[Fe(SnBu_3)(CO)_2(\eta^5\text{-}C_5H_5)]$,
2) 1-chloro-2,3,4,5-tetramethylarsole visibly reacts much faster than 1-chloro-2,3,4,5-tetraphenylarsole,
3) The good yields obtained would appear to argue against mechanisms involving coordinatively unsaturated intermediates $[M(SnBu_3)(CO)_{n-1}(\eta^5\text{-}C_5H_5)]$ followed by CO recapture (though cyclopentadienyl ring-slippage should perhaps not be discounted).

These observations are limited only to the above experiments since $[Cr(SnBu_3)(CO)_3(\eta^5\text{-}C_5H_5)]$ was never treated with $ClAsC_4Me_4$ and was also observed to undergo some manner of electron-transfer when exposed to $ClAsC_4Ph_4$. Likewise, $ClAsC_4R_2Me_2$ (R = $SiMe_3$ or *t*-Bu) were only ever combined with $[Mo(SnBu_3)(CO)_3(\eta^5\text{-}C_5H_5)]$. The main outcome of interest is the observation that $[Fe(SnBu_3)(CO)_2(\eta^5\text{-}C_5H_5)]$ was the slowest species to participate in Sn→As exchange, requiring days for complete consumption (notwithstanding $ClAsC_4Me_4$) whereas Mo and W only required hours or minutes. Both points signal

* When R = aryl, the products of the reaction are $[M(SnR_2X)(CO)_n(\eta^5\text{-}C_5H_5)]$ and HgRX, or $[M(SnRX_2)(CO)_n(\eta^5\text{-}C_5H_5)]$ and $HgR_2$, depending on reagent stoichiometry. The occurrence of Sn-C($sp^2$) rather than M-Sn bond rupture is attributed to the aryl carbon being a harder electrophile than the metal centre; softer electrophiles such as $I_2$ cleave both the M-Sn and Sn-C($sp^2$) bonds, whereas haloacids and $Cl_2$ attack the Sn-C($sp^2$) bond exclusively. The products formed by $HgBr_2$ are dependent on the identity of the $SnR_3$ group, whereas $HgI_2$ attacks the metal centre regardless. See U. KUNZE and S.B. SASTRAWAN, *Inorg. Nucl. Chem. Lett.*, **1978**, *14*, 485—490 and references therein for an overview. The addition of $ClAsC_4R_4$ to $[M(SnPh_3)(CO)_n(\eta^5\text{-}C_5H_5)]$ might very well lead to formation of $PhAsC_4R_4$ and $[M(SnPh_2X)(CO)_n(\eta^5\text{-}C_5H_5)]$, though this was not tested.

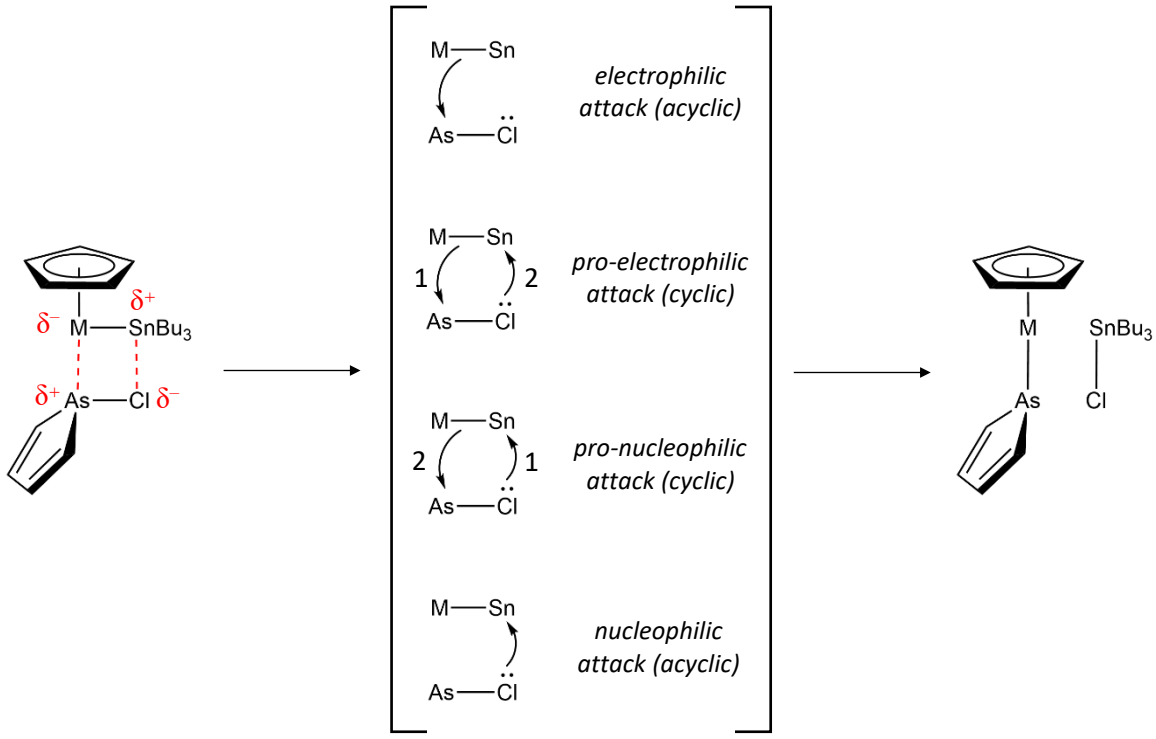
electronic effects being the dominant factor governing the efficiency of transmetalation, with steric effects of secondary but non-negligible importance.

Firstly, Sn→As transmetalation is faster at metal centres which affect a greater polarisation of the metal-tin bond, understood to a first approximation by considering the relative PAULING electronegativities of the elements (χ(Sn) = 1.90; χ(Fe) = 1.86; χ(Mo) = 2.16; χ(W) = 2.36), and the calculated natural charges of the elements in the model complexes $[M(SnMe_3)(CO)_n(\eta^5\text{-}C_5H_5)]$ (M = Mo, $n$ = 3; M = Fe, $n$ = 2. DFT, gas phase, ωB97X-D/6-31G*/LANL2Dζ): Mo (+0.017), Sn (+1.747) (Δ = 1.73) and Fe (+0.701), Sn (+1.541) (Δ = 0.84). Another perspective correlates the stability of the metal-tin bond with the nucleophilicity of the corresponding metal carbonyl anion.[4, 56, 57] Thus, iron being the most electropositive of the series here *and* the $[Fe(CO)_2(\eta^5\text{-}C_5H_5)]^-$ anion being the most potent nucleophile, the Fe-Sn bond is the least susceptible to exchange with the incoming *As*-chloroarsole.* One may also presume that a more π-basic metal fragment (such as that found in $Fe(CO)_2(\eta^5\text{-}C_5H_5)$[58]) engages in more efficient π-retrodonation, thereby deactivating the metal-tin bond (and simultaneously perhaps activating any tin-carbon bonds toward electrophilic attack; *vide supra*). That $[Fe(SnBu_3)(CO)_2(\eta^5\text{-}C_5H_5)]$ is both air-stable and amenable to column chromatography whereas $[Mo(SnBu_3)(CO)_3(\eta^5\text{-}C_5H_5)]$ and $[W(SnBu_3)(CO)_3(\eta^5\text{-}C_5H_5)]$ are decomposed gradually and rapidly by both, respectively, perhaps speaks to the lability of the metal-tin bond within these reagents and serves as a crude metric of reactivity if nuanced electronic arguments are overlooked.

Secondly, the visible reaction rate also depended on the incoming *As*-chloroarsole. Steric effects are apparent when comparing $ClAsC_4Me_4$ and $ClAsC_4Ph_4$ in isolation *viz.* $[M(AsC_4Me_4)(CO)_3(\eta^5\text{-}C_5H_5)]$ is formed within minutes whereas $[M(AsC_4Ph_4)(CO)_3(\eta^5\text{-}C_5H_5)]$ (M = Mo, W) emerge over the course of several hours (at ambient temperature). This is easily rationalised by considering that the four-centre quadrupolar transition state shown in **Scheme 4.14** is more congested for the tetraphenyl derivative and therefore possessing a greater kinetic barrier to surmount. However, the electronic properties of the *As*-chloroarsole also appear to be important – perhaps as much as steric factors – since the bulky $ClAsC_4R_2Me_2$ (R = $SiMe_3$ or *t*-Bu) also react *rapidly* with $[Mo(SnBu_3)(CO)_3(\eta^5\text{-}C_5H_5)]$, downstream reactions

* Incidentally, this reactivity pattern would in hindsight predict $[Co(SnBu_3)L_n(CO)_{4-n}]$ (L = CO, neutral ligand) to be a superb transmetalation agent toward *As*-chloroarsoles, though it was not examined in this work.

notwithstanding (it must be stressed that this is only of limited significance since these arsoles have yet to be combined with [Fe(SnBu$_3$)(CO)$_2$($\eta^5$-C$_5$H$_5$)]). The unifying feature of these faster reactions is that the arsenic centre is slightly more electron-rich than in the tetraphenyl ring-system (arsenic natural charges: +0.978 *vs.* +1.018, respectively), which is a counterintuitive outcome since the metal centre is considered nucleophilic in this context and a more *electro*philic arsenic should therefore encourage product formation. Rather, this could be evidence that the mechanism of transmetalation does not proceed *via* electrophilic attack of the arsenic atom on the metal-tin bond but instead begins with nucleophilic attack of the chloride upon the electrophilic and positively charged tin atom (**Scheme 4.14**). This interaction preceding development of the metal-arsenic bond is also sensible when considering that the stannyl reagents here are electronically and coordinatively saturated – association of the arsenic atom would demand further expansion of the metal's valence environment and if nothing else would be disfavoured on subtle steric grounds.




**Scheme 4.14**: Potential mechanisms of Sn→As transmetalation during the synthesis of transition metal arsolyl complexes.

Direct electrophilic attack by the arsenic at the metal of the metal-tin bond and direct nucleophilic attack of the chloride upon the tin atom both represent the two extremes for the system under examination. It is more likely that a four-centred transition state emerges and is governed primarily by electronic factors where Sn···Cl and M···As bond developments probably occur somewhat asynchronously, the former ahead of all other ruptures and formations. This would be in line with the results of other kinetic experiments in related metal-main group systems.[55, 59]

The slow exchange kinetics of $[Fe(SnBu_3)(CO)_2(\eta^5\text{-}C_5H_5)]$ towards $ClAsC_4Ph_4$ and $ClAsC_4Me_4$ have been mentioned above: $[Fe(AsC_4Ph_4)(CO)_2(\eta^5\text{-}C_5H_5)]$ is obtained after several days in modest yields (or overnight with additional warming), whereas $[Fe(AsC_4Me_4)(CO)_2(\eta^5\text{-}C_5H_5)]$ was only isolated in very poor yield. Although the above argument suggests that $ClAsC_4Me_4$ should react more rapidly than $ClAsC_4Ph_4$ (and one therefore might expect to isolate more than the few milligrams of $[Fe(AsC_4Me_4)(CO)_2(\eta^5\text{-}C_5H_5)]$ obtained from a *gram*-scale reaction), this assumes that $d^6$-iron stannyl complexes react *via* the same mechanism as $d^4$-$[M(SnBu_3)(CO)_3(\eta^5\text{-}C_5H_5)]$ (M = Mo, W). Indeed, a pathway involving initial electrophilic attack of $I_2$ upon $[Fe(SnMe_3)(CO)_2(\eta^5\text{-}C_5H_5)]$ rather than nucleophilic attack of the halide at the tin atom has been established and is itself attributed to the high basicity of the metal centre.[60] This could explain why $[Fe(AsC_4Ph_4)(CO)_2(\eta^5\text{-}C_5H_5)]$ is obtained in percentage yields roughly fifteen-fold that of $[Fe(AsC_4Me_4)(CO)_2(\eta^5\text{-}C_5H_5)]$, though the cyclo-dimerisation of $ClAsC_4Me_4$ in solution is a competitive process and cannot be excluded from any explanation ($ClAsC_4Ph_4$ was never observed to undergo cycloaddition with itself, so its presence in solution is guaranteed regardless of reaction rate with $[Fe(SnBu_3)(CO)_2(\eta^5\text{-}C_5H_5)]$). As the present discussion has elaborated, the transmetalation between metal stannyls and *As*-chloroarsoles is probably more complex than anticipated and in the absence of kinetic studies,* the conclusions drawn above should be taken as prospective rather than definitive.

## 4.5 Computational Aspects of Metal Arsenido Complexes

Of interest are the electronic properties of transition metal arsolyl complexes, particularly with regards to the potential communication between metal(*d*) orbitals and the unsaturated arsolyl ring system. Geometry optimisations were carried out for $[Mo(AsC_4Me_4)(CO)_3(\eta^5\text{-}C_5H_5)]$ and $[Mo(AsC_4Ph_4)(CO)_3(\eta^5\text{-}$

* Traversing the highly ordered quadrupolar transition state might be expected to contribute to a significantly positive entropy of activation.

$C_5H_5$)] using Density Functional Theory (gas phase: ωB97X-D/6-31G*/LANL2Dζ). For points of comparison, the known [Mo($AsMe_2$)$(CO)_3(\eta^5$-$C_5H_5)$] (which has not yet been the subject of a crystallographic study) and the unknown* [Mo{$As(CH{=}CH_2)_2$}$(CO)_3(\eta^5$-$C_5H_5)$] (to explore any effects of $sp^2$-carbon residues while obviating considerations of aromaticity) were similarly considered. **Figure 4.10** illustrates these geometries.

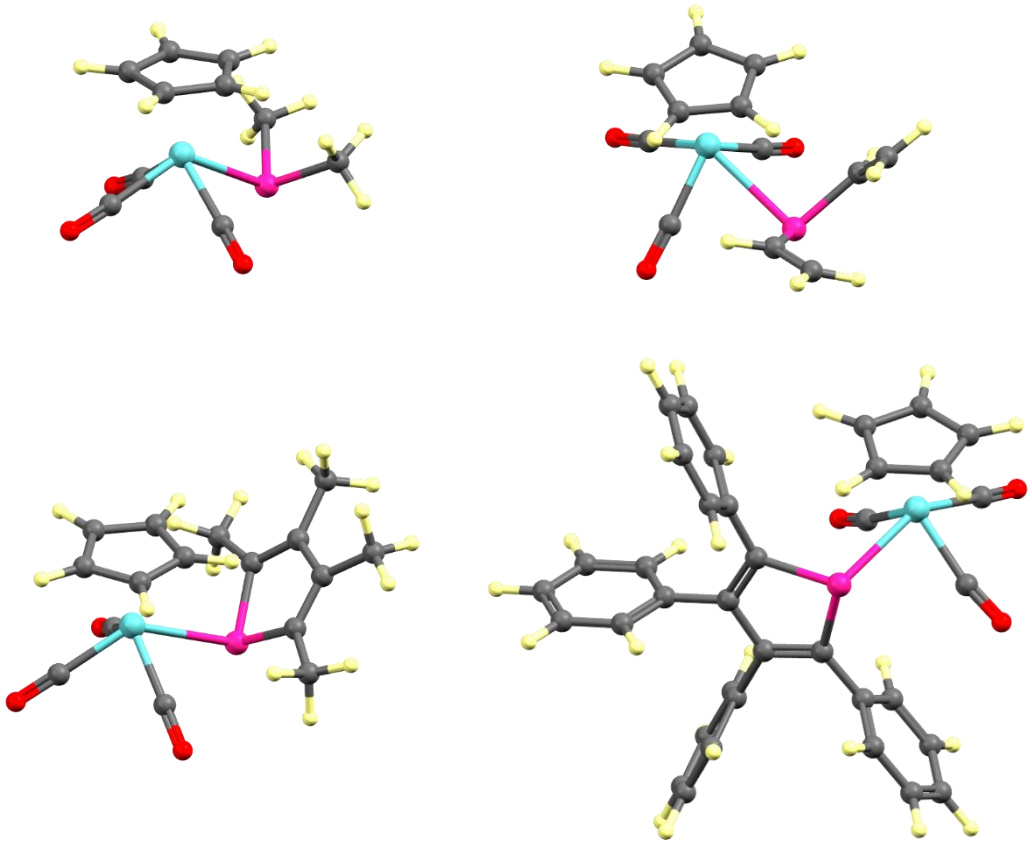


**Figure 4.10**: Optimised geometries of four [MoR$(CO)_3(\eta^5$-$C_5H_5)$] complexes (DFT: gas phase, ωB97X-D/6-31G*/LANL2Dζ). Shown clockwise from top left: R = $AsMe_2$, $As(CH{=}CH_2)_2$, $AsC_4Ph_4$, $AsC_4Me_4$.

For the arsolyl complexes, the returned core geometries were in excellent accord with the structures determined by X-ray diffraction, including the dispositions of the $AsC_4R_4$ substituent with respect to the cyclopentadienyl ring. The predicted Mo-As bond lengths (R = Me 2.769 Å; R = Ph 2.739 Å) are slightly overestimated (from crystallography: R = Me 2.7267(4) Å; R = Ph 2.7190(6) Å) though the margin of error is deemed acceptable. Predicted ring-atom bond distances are much closer to reality, generally agreeing with the crystal structures to the second decimal place; only the $C_\beta$-$C_\beta$ single bonds are overestimated by 0.01—

* Incidentally, there do not appear to be any transition metal complexes of the divinylarsenido ligand in the literature.

0.02 Å. The computed Mo-As covalent bond lengths in $[Mo(AsMe_2)(CO)_3(\eta^5\text{-}C_5H_5)]$ and $[Mo\{As(CH{=}CH_2)_2\}(CO)_3(\eta^5\text{-}C_5H_5)]$ are 2.621 and 2.760 Å, respectively, and the mean predicted As-C($sp^3$) and As-C($sp^2$) bond distances of 2.000 and 1.957 Å compare well with other bonds of the same type measured throughout this work.

Orbital energies were also calculated and those of interest – namely the LUMO, HOMO and HOMO-1 – are shown together for the four arsenido complexes in **Figure 4.11**; the frontier orbital topologies of $[Mo(AsMe_2)(CO)_3(\eta^5\text{-}C_5H_5)]$ and $[Mo(AsC_4Me_4)(CO)_3(\eta^5\text{-}C_5H_5)]$ are shown in **Figure 4.12**.

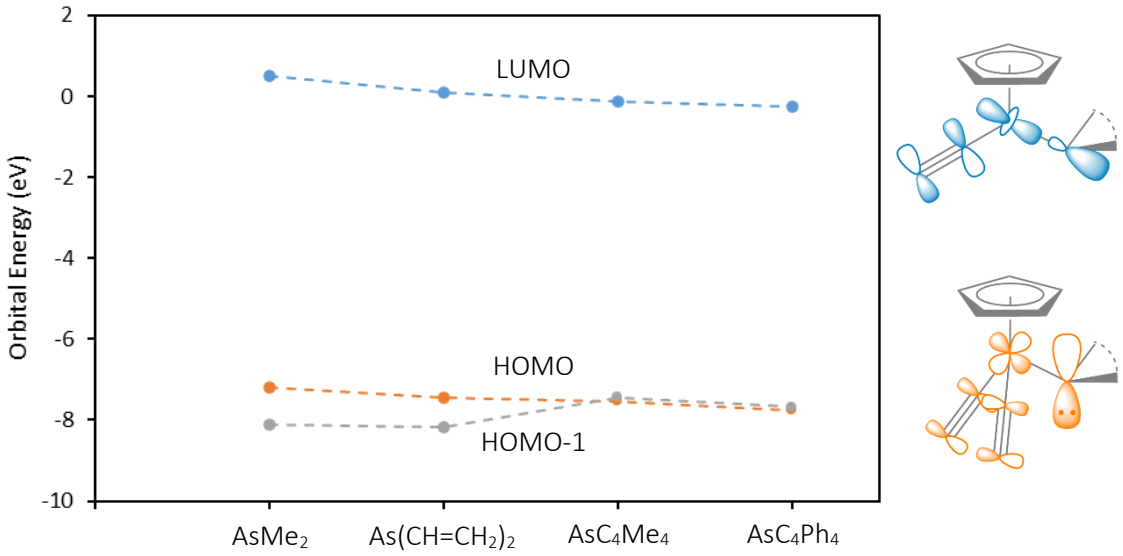



**Figure 4.11**: Calculated energies for the frontier orbitals of four $[MoR(CO)_3(\eta^5\text{-}C_5H_5)]$ complexes (DFT: gas phase, ωB97X-D/6-31G*/LANL2DZ). Blue trace = Mo-As(σ*), orange trace = As(*p*), grey trace = other.

Some general trends emerge from these calculations:

1) The LUMO's for all four complexes under examination are composed predominantly of the Mo-As(σ*) antibond and the Mo-CO(π*) antibond to the *transoid* carbonyl. It is interesting to note that for the arsolyl complexes (only) the former extends onto the ring-carbon atoms α to the arsenic centre, which is not observed in the divinylarsinido complex. Some mixing with the butadiene(π*) lobes appears to account for this topological feature. For all complexes, nucleophilic attack is expected to take place either at the arsenic centre or the *transoid* carbonyl carbon – in practise, only the former was observed, perhaps pointing to a degree of charge *vs.*

frontier orbital control. The LUMO energies (blue trace) decrease monotonously across the series from $[Mo(AsMe_2)(CO)_3(\eta^5\text{-}C_5H_5)]$ to $[Mo(AsC_4Ph_4)(CO)_3(\eta^5\text{-}C_5H_5)]$.

2) The HOMO's for all complexes also descend in energy across the arsenido series; as expected, $[Mo(AsMe_2)(CO)_3(\eta^5\text{-}C_5H_5)]$ is predicted to be the most nucleophilic and $[Mo(AsC_4Ph_4)(CO)_3(\eta^5\text{-}C_5H_5)]$ the least. Interestingly, for R = $AsMe_2$ and $As(CH{=}CH_2)_2$ the HOMO is prominently composed of the *p* orbital housing the arsenic lone pair whereas for the cyclic arsenido complexes it is the localised diene(π) bonds which comprise the HOMO although the energy difference between the HOMO and HOMO-1 is for all intents and purposes negligible. This perhaps speaks to the modest basicity of the As(III) centre rather than any remarkable feature of the diene. The nucleophilicity of the arsenic atom (that is, the lone pair electrons, **Figure 4.11** orange trace) decrease steadily along the series $AsMe_2$ > $As(CH{=}CH_2)_2$ > $AsC_4Me_4$ > $AsC_4Ph_4$, as expected from a first principles understanding of the inductive influences of the substituents.

3) The variations in HOMO-1 energies do not follow the same pattern as the LUMO and HOMO: for $[Mo(AsMe_2)(CO)_3(\eta^5\text{-}C_5H_5)]$ and $[Mo\{As(CH{=}CH_2)_2\}(CO)_3(\eta^5\text{-}C_5H_5)]$ this orbital is predominantly metal-centred with some minor bonding interactions amongst the arsenido and carbonyl ligands. For $[Mo(AsC_4Me_4)(CO)_3(\eta^5\text{-}C_5H_5)]$ and $[Mo(AsC_4Ph_4)(CO)_3(\eta^5\text{-}C_5H_5)]$ the HOMO-1 finds the *p* orbital containing the arsenic lone pair encountering appreciable overlap with a Mo(*d*) orbital; the latter extends somewhat onto the *cisoid* CO(π*) system and the Mo(*d*)-As(*p*) mixing observed has itself partial π-symmetry. It should be noted that although the diene systems and lone pairs of the arsolyl complexes are not degenerate, the magnitude of the difference in energies is modest (*ca* 0.1 eV) and in practical terms either may serve as the centre for electrophilic attack. In fact, later chapters will describe situations where both are utilised simultaneously.

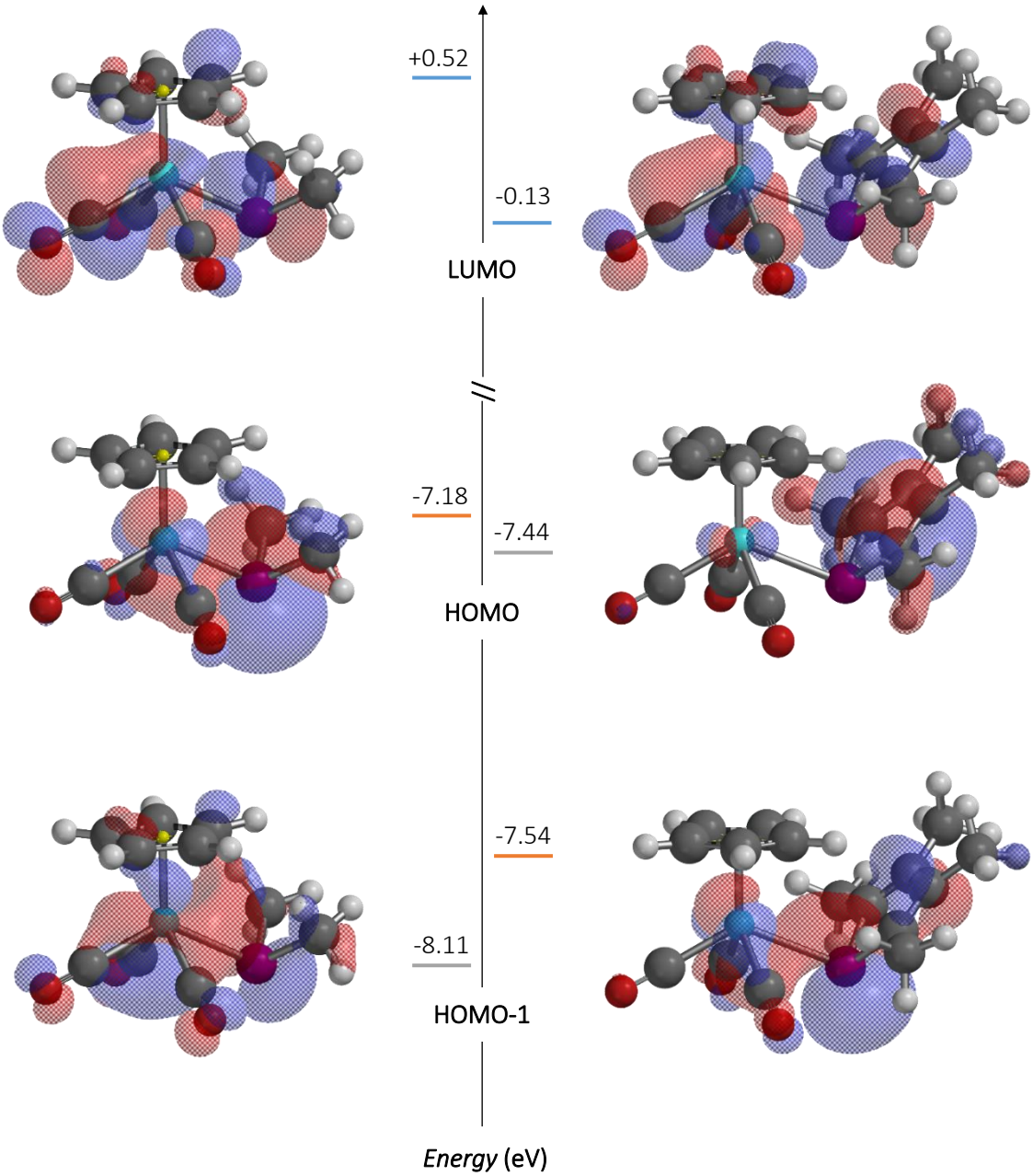



**Figure 4.12**: Frontier orbitals for [Mo(AsMe$_2$)(CO)$_3$($\eta^5$-C$_5$H$_5$)] (**left**) and [Mo(AsC$_4$Me$_4$)(CO)$_3$($\eta^5$-C$_5$H$_5$)] (**right**).

## 4.6 Reactions of Arsolyl Complexes with Electrophiles

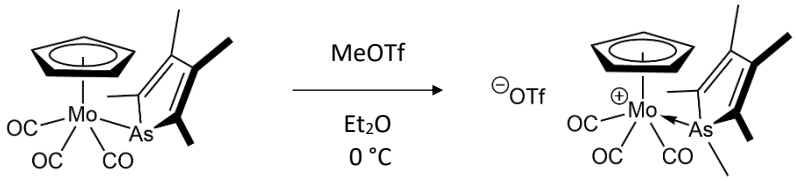
Transition metal arsenidos show pronounced nucleophilicity at the heteroatom; accordingly, many examples of their reactions with organic and inorganic electrophiles have been described. The arsenic atom in [Mo(AsC$_4$Me$_4$)(CO)$_3$($\eta^5$-C$_5$H$_5$)] is no different though the diminished basicity (**Section 4.5**) and/or fragility of the Mo-As bond became readily apparent in early experiments: some electrophiles (S$_8$, propylene sulfide, red selenium, ethyl diazoacetate) failed to react, whereas others (allyl acetate, HOSO$_2$CF$_3$,

$Me_3SiOSO_2CF_3$, $[Fe(\eta^5\text{-}C_5H_5)_2]PF_6$, $[NO]PF_6$) gave complex mixtures, unidentifiable paramagnetic products, or materials of destruction. The following section describes the results of reactions between $[Mo(AsC_4Me_4)(CO)_3(\eta^5\text{-}C_5H_5)]$ and simple electrophiles which yielded to chemical analysis.

### 4.1.5 Electrophilic Methylating Agents

#### 4.6.1.1 Synthesis of $[Mo(MeAsC_4Me_4)(CO)_3(\eta^5\text{-}C_5H_5)]OTf$

The complex $[Mo(AsC_4Me_4)(CO)_3(\eta^5\text{-}C_5H_5)]$ is readily alkylated at the heteroatom by methyl trifluoromethanesulfonate (MeOTf, OTf = $[SO_3CF_3]^-$) in $Et_2O$ solution at 0 °C. Bright yellow, X-ray quality crystals of the salt $[Mo(MeAsC_4Me_4)(CO)_3(\eta^5\text{-}C_5H_5)]OTf$ rapidly precipitate from solution and the product is isolated in near-quantitative yield (**Scheme 4.15**). Care must be taken to avoid too great an excess of MeOTf which results in decomposition to oily black residues.




**Scheme 4.15**: *As*-methylation of $[Mo(AsC_4Me_4)(CO)_3(\eta^5\text{-}C_5H_5)]$.

Spectroscopic data reflect the formal localisation of positive charge at the molybdenum centre with a shift of $\nu_{CO}$ absorptions to higher wavenumbers ($CH_2Cl_2$ solution, 2057(vs), 1998(sh), 1965(vs) $cm^{-1}$), and a shift of the $^1H$ cyclopentadienyl resonance from 5.16 ppm in $[Mo(AsC_4Me_4)(CO)_3(\eta^5\text{-}C_5H_5)]$ ($CD_2Cl_2$) downfield to 5.54 ppm in the cationic $[Mo(MeAsC_4Me_4)(CO)_3(\eta^5\text{-}C_5H_5)]^+$. The As-$CH_3$ group resonance is found at 1.66 ppm in the $^1H$ NMR spectrum ($CD_2Cl_2$), slightly upfield of the ring methyl groups at 1.95 and 1.82 ppm which are essentially identical in chemical shift to those of the precursor and seemingly unaffected by alkylation of the heteroatom. A shift to higher frequency is observed in the $^{13}C\{^1H\}$ NMR spectrum for the carbonyl ligands *transoid* (225.8 ppm) and *cisoid* (223.2 ppm) to the pentamethylarsole ligand (*cf.* 235.5 and 224.7 ppm for $[Mo(AsC_4Me_4)(CO)_3(\eta^5\text{-}C_5H_5)]$ in $CD_2Cl_2$) as the efficacy of Mo(*d*)→CO($\pi^*$) retrodonation is reduced; the same argument applies to the cyclopentadienyl signal (93.5 *vs.* 94.3 ppm). The arsolyl ring-carbon nuclei are similarly displaced to slightly higher frequency by *As*-methylation (145.8 and

134.5 ppm *vs.* 149.1 and 141.8 ppm), a feature which also manifests in binuclear complexes of the μ-$AsC_4Me_4$ ligand (**Chapter 5**) as the modest ring-current within the cyclic system is further diminished by appropriation of the arsenic lone pair. High-resolution mass spectrometry (ESI) reveals extensive fragmentation of the molecular ion, the primary mode of disintegration being loss of the arsenic-bound $CH_3$ group in addition to sequential products of decarbonylation; single crystals suitable for X-ray diffractometry were collected from the reaction mixture and the molecular structure is shown in **Figure 4.13**.

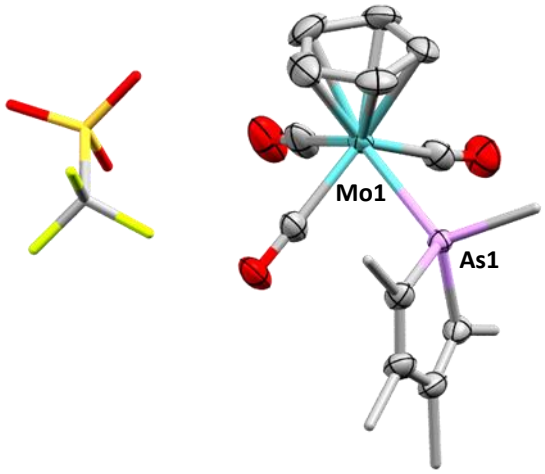



**Figure 4.13**: The molecular structure of $[Mo(MeAsC_4Me_4)(CO)_3(\eta^5\text{-}C_5H_5)]OTf$ in a crystal. Methyl groups and trifluoromethanesulfonate anion simplified and hydrogen atoms omitted for clarity. Ellipsoids shown at 50% displacement.

Crystallographic interrogation of the reaction product confirms *As*-methylation. Reflecting the formal positive charge residing on the Mo(II) atom and the change in bonding description between the metal and pnictogen, a contraction of the Mo-As distance by almost 0.15 Å to 2.5844(4) Å is measured (*cf.* $[Mo(AsC_4Me_4)(CO)_3(\eta^5\text{-}C_5H_5)]$ 2.7267(7) Å). A similar contraction (though of lesser magnitude) is observed upon coordination of LEWIS acidic metal centres to $[Mo(AsC_4Me_4)(CO)_3(\eta^5\text{-}C_5H_5)]$ (**Chapter 5**) and it is proposed that sequestration of the arsenic lone pair alleviates a repulsive interaction between the electronically saturated molybdenum centre, permitting closer approach of the two centres. The arsenic atom adopts a deformed tetrahedral geometry with external bonding angles of 105—117° and an internal C-As-C ring-angle of *ca* 89°. The pentamethylarsole ligand is swivelled about the Mo-As bond to lie in an unsymmetrical disposition about the molecule, similar to that found in $[Mo(AsC_4Ph_4)(CO)_3(\eta^5\text{-}C_5H_5)]$ (**Figure 4.1**), which all but obliviates the π···H-C contact found in the solid state structure of the neutral

precursor (**Figure 4.5**). Interatomic distances within the arsole ring are reflective of decreased aromatic character with a slight compression of the $C_\alpha$=$C_\beta$ bonds (mean 1.327(5) Å) and elongation of the $C_\beta$-$C_\beta$ bond (1.496(5) Å) compared to the neutral arsolyl complex (1.351(7) and 1.469(8) Å, respectively).

### 4.6.1.2 Synthesis of [Mo{MeAs$C_4$H(Si$Me_3$)$Me_2$}(CO)$_3$($\eta^5$-$C_5H_5$)]OTf

Alkylation of [Mo(As$C_4$H(Si$Me_3$)(CO)$_3$($\eta^5$-$C_5H_5$)] was carried out similarly: treatment with MeOTf in $Et_2O$ solution causes the product to rapidly precipitate from solution in excellent yield as bright yellow crystals suitable for X-ray diffraction. Spectroscopic features are comparable to those of the pentamethylarsole complex described in the previous section and for brevity only salient features will be mentioned. The solution IR spectrum ($CH_2Cl_2$) finds the usual trio of carbonyl vibrations at 2065(vs), 1992(sh) and 1971(vs) $cm^{-1}$ (shifted to higher wavenumbers from the neutral precursor, *cf.* 2007(vs), 1938(sh), 1922(vs) $cm^{-1}$), and the resonance for the olefinic hydrogen α to the arsenic atom appears at 6.97 ppm in $CD_2Cl_2$ solution. The $^1$H and $^{13}$C{$^1$H} NMR spectra for the neutral complex [Mo(As$C_4$H(Si$Me_3$)(CO)$_3$($\eta^5$-$C_5H_5$)] were not re-collected in $CD_2Cl_2$ (like [Mo(As$C_4Me_4$)(CO)$_3$($\eta^5$-$C_5H_5$)] was) therefore precluding direct comparisons with its *As*-methylated complex, though it is reasonable to assume that a similar shielding effect on the arsolyl ring nuclei would be observed if solvent effects were disregarded. The cyclopentadienyl ligand resonances appear at 5.82 and 92.4 ppm in the $^1$H and $^{13}$C{$^1$H} NMR spectra, respectively, and the carbonyl ligands at 235.7 (*transoid*), 225.6 and 223.6 ppm (*cisoid*) in the latter. The four chemically inequivalent arsole ring-carbon nuclei are found at 158.4, 157.1, 149.7 and 146.7 ppm of which the second-to-last signal listed bears the olefinic ring-hydrogen (by HSQC NMR experiment, and by noting the NOE enhancement). The molecular structure was determined by X-ray diffractometry and is shown in **Figure 4.14**.

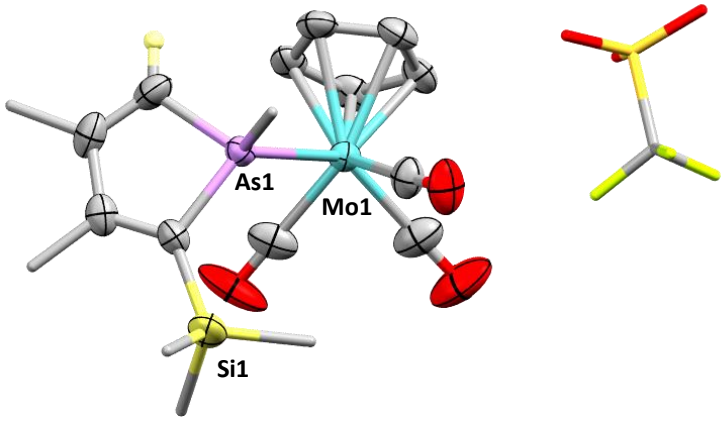



**Figure 4.14**: The molecular structure of [Mo(MeAsC$_4$H(SiMe$_3$)Me$_2$)(CO)$_3$($\eta^5$-C$_5$H$_5$)]OTf in a crystal. Methyl groups and trifluoromethanesulfonate anion simplified, and most hydrogen atoms omitted for clarity. The arsolyl hydrogen is shown in light yellow for emphasis. Ellipsoids shown at 50% displacement.

The crystal structure of [Mo(AsC$_4$H(SiMe$_3$)(CO)$_3$($\eta^5$-C$_5$H$_5$)] is largely similar to that of the previous pentamethylarsole complex (**Figure 4.13**) and only salient features will be noted. The 1-methyl-2-(trimethylsilyl)-3,4-dimethylarsole ligand lies "sideways" against the Mo(CO)$_3$($\eta^5$-C$_5$H$_5$) centre with the SiMe$_3$ group occupying the region of space between the *cisoid* carbonyl ligands. The As→Mo dative bond length of 2.6016(6) Å is slightly longer than that in [Mo(MeAsC$_4$Me$_4$)(CO)$_3$($\eta^5$-C$_5$H$_5$)]OTf (2.5844(4) Å), though it is noted that the Mo-As covalent bond in [Mo(AsC$_4$H(SiMe$_3$)(CO)$_3$($\eta^5$-C$_5$H$_5$)] is also *ca* 0.02 Å longer than in [Mo(AsC$_4$Me$_4$)(CO)$_3$($\eta^5$-C$_5$H$_5$)] which is similarly attributed to an intrinsic proximal steric influence of the SiMe$_3$ residue. Dimensions of the arsole ring follow the same pattern as the pentamethylarsole complex with a compression of the inequivalent $C_\alpha$=$C_\beta$ bonds (1.326(6) and 1.342(6) Å) and extension of the $C_\beta$-$C_\beta$ bond (1.489(6) Å) upon methylation of the arsenic atom, compared to neutral [Mo(AsC$_4$H(SiMe$_3$)(CO)$_3$($\eta^5$-C$_5$H$_5$)].

### 4.6.1.3 Attempted Synthesis of [Mo(MeAsC$_4$Ph$_4$)(CO)$_3$($\eta^5$-C$_5$H$_5$)]OTf

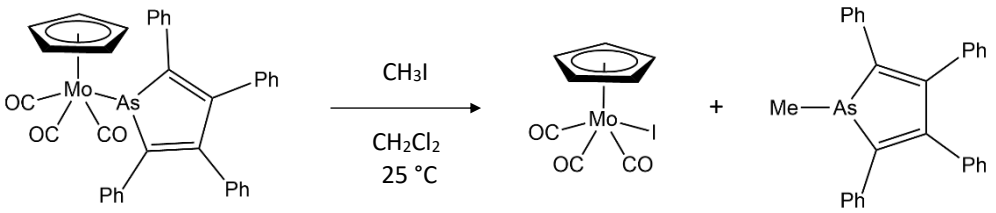
The tetraphenylarsolyl complex [Mo(AsC$_4$Ph$_4$)(CO)$_3$($\eta^5$-C$_5$H$_5$)] undergoes alkylation with reluctancy. Treatment with MeOTf in toluene solution gives no immediate precipitation of a salt, and only upon standing for several days at ambient temperature do a very small quantity of yellow crystals form which were regrettably unsuitable for X-ray diffractometry; accompanying these crystals were a larger quantity of oily brown residues. Dissolution of the isolated crystals precipitated more of these insipid residues and MeAsC$_4$Ph$_4$ was the only identifiable species in a $^1$H NMR spectrum (*vide infra*). The same

outcome was obtained in $CH_2Cl_2$ solution which resulted in the free arsole $MeAsC_4Ph_4$ being the only isolable product, and it was not practical to carry the reaction out in $Et_2O$ solution since $[Mo(AsC_4Ph_4)(CO)_3(\eta^5\text{-}C_5H_5)]$ is insufficiently soluble in this medium. The observation that tetraphenylarsoles are generally hesitant to quarternise on the grounds of a *very poorly basic* heteroatom is in line with other experiments involving methyl iodide as the alkylating agent, outlined in the following section.

#### 4.6.1.4 Reaction Between $[Mo(AsC_4Ph_4)(CO)_3(\eta^5\text{-}C_5H_5)]$ and Methyl Iodide

The tetraphenylarsole complex $[Mo(AsC_4Ph_4)(CO)_3(\eta^5\text{-}C_5H_5)]$ is cleaved by an excess of $CH_3I$ in $C_6D_6$ solution overnight to provide $[MoI(CO)_3(\eta^5\text{-}C_5H_5)]$* and 1-methyl-2,3,4,5-tetraphenylarsole as the only products by NMR spectroscopy. Repeating the reaction in $CH_2Cl_2$ on a preparative scale allows isolation of the dark red molybdenum iodide complex and the light yellow arsole as reasonably air-stable solids in high yields. Although it was unknown prior to this work, the arsole has appeared elsewhere in **Chapter 2**, **Section 2.4** as a product of nucleophilic substitution of $Me_3SiC{\equiv}CAsC_4Ph_4$ by MeLi·LiBr.

Here, the reaction almost certainly proceeds *via* initial methylation of the arsenic atom (which may or may not follow a radical pathway, *vide infra*) followed by rapid and irreversible nucleophilic substitution of the arsole ligand from $[Mo(MeAsC_4Ph_4)(CO)_3(\eta^5\text{-}C_5H_5)]^+$ by the iodide anion. This process is presumably dissociative in nature since the Mo(II) centre is both electronically-saturated and seven-coordinate, and the displacement of the arsole ligand from the cationic complex must be at least as rapid as its formation since at no point during the reaction were any other cyclopentadienyl signals observed in the $^1H$ NMR spectrum.

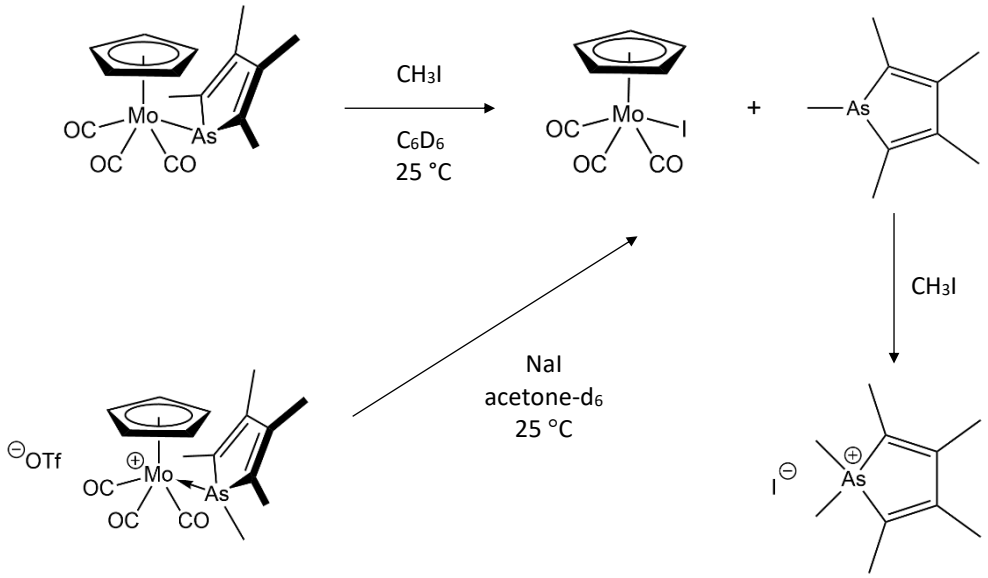



**Scheme 4.16**: Reaction between $[Mo(AsC_4Ph_4)(CO)_3(\eta^5\text{-}C_5H_5)]$ and methyl iodide.

* NMR: $^1H$ ($C_6D_6$, 400 MHz, 25 °C) δ 4.44 ppm. IR ($CH_2Cl_2$, 25 °C) $\nu_{CO}$ 2043(vs), 1961(vs) $cm^{-1}$. Identity confirmed by comparison with an authentic sample.

### 4.6.1.5 Reaction Between [Mo(AsC$_4$Me$_4$)(CO)$_3$($\eta^5$-C$_5$H$_5$)] and Methyl Iodide

The more-basic [Mo(AsC$_4$Me$_4$)(CO)$_3$($\eta^5$-C$_5$H$_5$)] also reacts with excess CH$_3$I in C$_6$D$_6$ solution, though the reaction was more-complicated than anticipated. Multiple products are generated, notwithstanding the large colourless crystals of [Me$_2$AsC$_4$Me$_4$]I which separate from solution. This – the first example of an authentic cationic arsole* (henceforth arsolylium) – was interrogated by X-ray diffraction and the crystal structure is shown in **Figure 4.15**. A simplified path showing the major products of the reaction are shown in **Scheme 4.17**.




**Scheme 4.17**: Reactions between [Mo(AsC$_4$Me$_4$)(CO)$_3$($\eta^5$-C$_5$H$_5$)] and methyl iodide, and between [Mo(MeAsC$_4$Me$_4$)(CO)$_3$($\eta^5$-C$_5$H$_5$)]OTf and sodium iodide.

* There are examples of annulated arsoles undergoing quaternisation which are excluded from the present discussion since the ring system does not technically contain a localised butadiene moiety, one of the major identifying features of arsoles. See G. WITTIG and D. HELLWINKEL *Angew. Chem.*, **1962**, *74*, 782—783 and *Id. Chem. Ber.*, **1964**, *93*, 769—783.

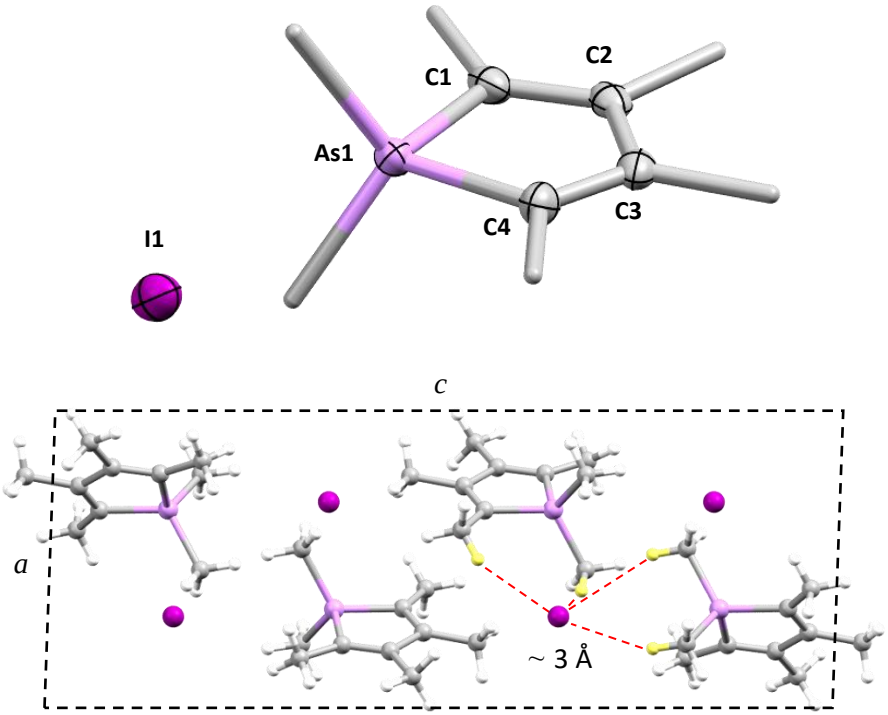



**Figure 4.15**: The molecular structure of $[Me_2AsC_4Me_4]I$ in a crystal. Methyl groups simplified and hydrogen atoms omitted for clarity. Ellipsoids shown at 50% displacement. **Inset**: The unit cell contents ($P2_1/c$) viewed along the crystallographic *b* axis highlighting extended H···I⁻ interactions.

1,1,2,3,4,5-hexamethylarsolylium iodide crystallises in monoclinic $P2_1/c$ with four separated cation-anion pairs contained in the unit cell. The inset diagram in **Figure 4.15** highlights a selection of intermolecular H···I⁻ interactions which are rather regular between 3.0—3.1 Å; incidentally, the iodide anions have distorted disphenoidal geometry ($\tau_4$ = 0.86, $\tau'_4$ = 0.57) in the solid-state since only four hydrogen bonds operate (per iodide) with approximate valence angles of *ca* 165° (*pseudo-trans* axial) and 82° (*pseudo*-equatorial). The $[Me_2AsC_4Me_4]^+$ cation is approximately though not crystallographically laterally-symmetric, and the quaternary arsenic atom exists in a distorted tetrahedral environment with external (local) bonding angles of 109—118°, though the internal $C_\alpha$-As-$C_\alpha$ vertex is regular within this work at 88°. Compared to other $RAsC_4Me_4$ arsoles which have been structurally characterised (R = organic, inorganic),[61, 62] interatomic distances within the $[Me_2AsC_4Me_4]^+$ cation reflect a true localisation of the π-electron density about the ring with a compression of the As-$C_\alpha$ (mean 1.903(3) Å) and $C_\alpha$=$C_\beta$ bonds (mean 1.327(4) Å), and an elongation of the C-C bond (1.500(3) Å).

The arsolylium salt $[Me_2AsC_4Me_4]I$ was isolated from the reaction mixture in good yield and was fully characterised. The internal symmetry of the cation is reflected in the $^1H$ NMR spectrum ($CDCl_3$) which finds only three equally integrating signals at 2.58, 2.32 and 2.00 ppm of which the latter is assigned to the arsenic-bound methyl groups by comparison with the *As*-methyl resonance in $[Mo(MeAsC_4Me_4)(CO)_3(\eta^5\text{-}C_5H_5)]OTf$. In the $^{13}C\{^1H\}$ NMR spectrum the arsolyl ring-carbon nuclei manifest at 150.3 and 123.5 ppm (α and β to the heteroatom, respectively) with three methyl environments at 15.0, 14.2 and 9.2. The latter is identified as the arsenic-bound methyl carbon atoms on the basis of HSQC and HMBC NMR experiments. High-resolution mass spectrometry reveals the molecular ion in high intensity ($m/z \approx$ 213.0628). The formation of $[Me_2AsC_4Me_4]I$ was confirmed in a separate experiment to arise from simple alkylation of $MeAsC_4Me_4$ by methyl iodide* (**Scheme 4.17**; $MeAsC_4Ph_4$ did not undergo such a reaction) – analogous to the $AsC_4Ph_4$ complex in **Section 4.6.1.4** a reasonable course of events involves initial alkylation of the heteroatom in $[Mo(AsC_4Me_4)(CO)_3(\eta^5\text{-}C_5H_5)]$ to form a cationic $[Mo(MeAsC_4Me_4)(CO)_3(\eta^5\text{-}C_5H_5)]^+$ complex which is then substituted at the metal centre by the iodide counterion thus-formed.

As an aside, $[Me_2AsC_4Me_4]^+$ did appear to react with $Li[N(i\text{-}Pr)_2]$ in $Et_2O$ solution at -78 °C to provide a very pleasant cherry-red mixture (the cation is colourless) which decomposed to poorly-soluble light brown materials upon warming. The addition of labile $[W(THF)(CO)_5]$ or $[Au(C_6F_5)(THT)]$ (THT = tetrahydrothiophene) to this red solution also did not afford an isolable ylide complex upon workup, and no trapping experiments with organic electrophiles (*e.g.*, ketones) were attempted due to limited quantities of the arsolylium on-hand. This may, however, be a fertile opportunity for future researchers.

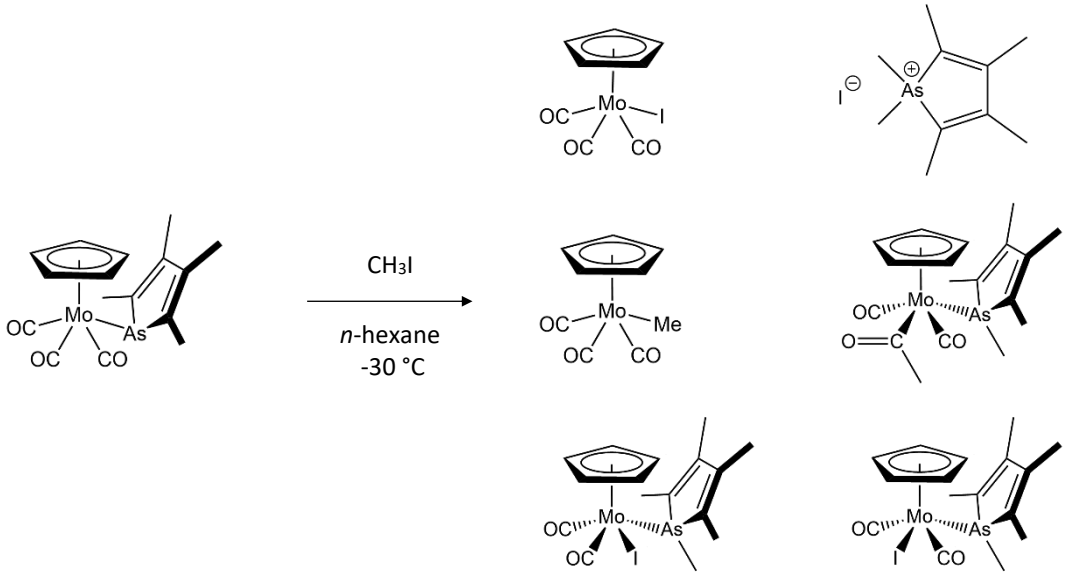
The remainder of the $C_6D_6$ reaction solution contained the expected $[MoI(CO)_3(\eta^5\text{-}C_5H_5)]$ as the major cyclopentadienyl-containing species. Interestingly, $[MoMe(CO)_3(\eta^5\text{-}C_5H_5)]$ is also observed† which speaks to the possible occurrence of radical reaction pathways, since the addition of NaI to $[Mo(MeAsC_4Me_4)(CO)_3(\eta^5\text{-}C_5H_5)]OTf$ (**Section 4.6.1.1**) in acetone-$d_6$ gave $[MoI(CO)_3(\eta^5\text{-}C_5H_5)]$‡ and

* Methyl triflate will also alkylate pentamethylarsole in $Et_2O$ at 0 °C, though the $[Me_2AsC_4Me_4]OTf$ salt formed degraded over several weeks in the solid state (under argon) to oily brown residues. Conversely, the iodide salt retained its integrity for > 2 years. Other methylating agents such as $[Me_3O]BF_4$ were not tested.
† NMR: $^1H$ ($C_6D_6$, 400 MHz, 25 °C) δ 4.41, 0.39 ppm. Confirmed by comparison with an authentic sample.
‡ NMR: $^1H$ (acetone-$d_6$, 400 MHz, 25 °C) δ 5.88 ppm. Confirmed by comparison with an authentic sample.

$MeAsC_4Me_4$ *exclusively* (**Scheme 4.17**); the presence of a fleeting pentavalent As(V) species *i.e.*, $[Mo\{Me(I)AsC_4Me_4\}(CO)_3(\eta^5\text{-}C_5H_5)]$ which then dismutates to $[MoI(CO)_3(\eta^5\text{-}C_5H_5)]$ and $[MoMe(CO)_3(\eta^5\text{-}C_5H_5)]$, is therefore discounted.* Repeating the reaction in *n*-hexane solution during storage at -30 °C provides an abundance of crystalline specimens comprising no fewer than five molybdenum-containing compounds which were interrogated by X-ray diffraction. In addition to $[Me_2AsC_4Me_4]I$ (**Figure 4.15**), they are:

1) $[MoI(CO)_3(\eta^5\text{-}C_5H_5)]$, which despite being a recognisable compound apparently had not been previously structurally characterised and was determined here for completeness (**Figure 4.16**),
2) $[MoMe(CO)_3(\eta^5\text{-}C_5H_5)]$, the crystal structure of which has been previously reported,[63]
3) *cis*-$[MoI(MeAsC_4Me_4)(CO)_2(\eta^5\text{-}C_5H_5)]$ (**Figure 4.17**), arising from carbonyl rather than arsole substitution,
4) A co-crystallite of *trans*-$[MoI(MeAsC_4Me_4)(CO)_2(\eta^5\text{-}C_5H_5)]$ and the novel acyl complex *trans*-$[Mo\{C(O)Me\}(MeAsC_4Me_4)(CO)_2(\eta^5\text{-}C_5H_5)]$ (**Figure 4.18**).

These are shown in **Scheme 4.18** and the structures of these products will be discussed in the order of their appearance above.




**Scheme 4.18**: Products of the reaction between $[Mo(AsC_4Me_4)(CO)_3(\eta^5\text{-}C_5H_5)]$ and methyl iodide as identified by X-ray crystallography.

* There is precedent for such a process, though not with a transition metal substituent: treatment of $PhCH_2AsC_4Ph_2H_2$ with MeCl results in formation of $MeAsC_4Ph_2H_2$ and $ClAsC_4Ph_2H_2$ alongside $PhCH_2Cl$ and $PhCH_2CH_3$. See G. MÄRKL and H. HAUPTMANN *J. Organomet. Chem.*, **1983**, *248*, 269—285.

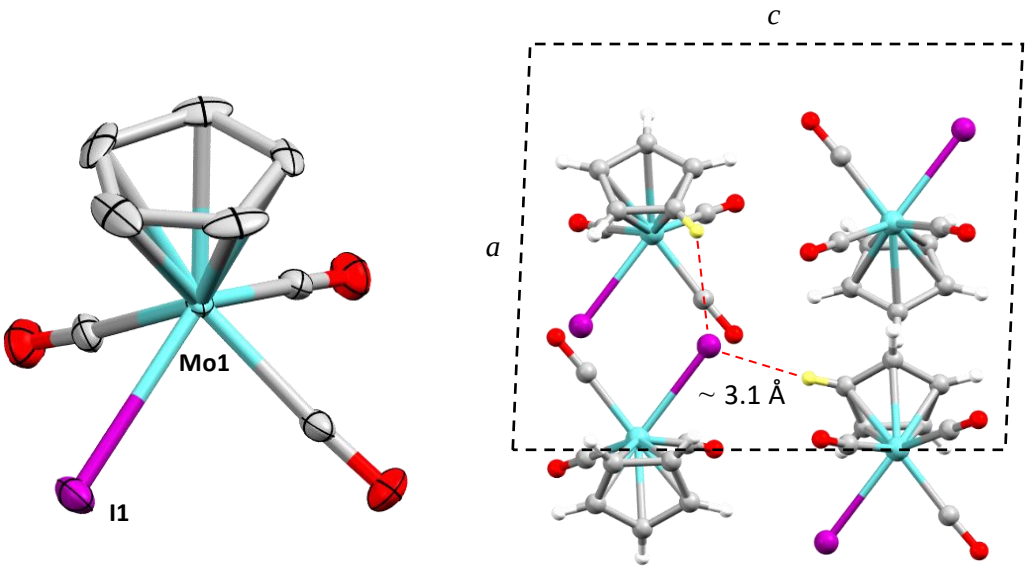



**Figure 4.16**: The molecular structure of $[MoI(CO)_3(\eta^5\text{-}C_5H_5)]$ in a crystal. Hydrogen atoms omitted for clarity. **Inset**: the unit cell contents ($P2_1/n$) viewed along the crystallographic *b* axis, highlighting a pair of H··I interactions.

1) Despite being first reported in 1956 by WILKINSON,[64] and having been utilised as a synthon in a variety of settings in the interregnum since,[65-70] the crystal structure of red $[MoI(CO)_3(\eta^5\text{-}C_5H_5)]$ had apparently been neglected. Understandably, molecular features are rather unexciting given the simplistic nature of the complex and only salient crystallographic aspects will be mentioned. A seven-coordinate molybdenum(II) centre is found which approximates a distorted square-based pyramid, where the three carbonyls and the iodide ligand comprise the basal plane and the centroid of the cyclopentadienyl ring occupies the apical site. The Mo-I bond length of 2.8419(6) Å is typical among similar complexes,[71-73] and the Mo-C bond *transoid* to the iodide (1.992(6) Å) is marginally shorter than the pair *cisoid* (mean 2.035(7) Å) due to the π-donor character of the halide. The unit cell (monoclinic $P2_1/n$) contains four symmetry-related molecules which display two intermolecular H···I interactions (per molecule) of *ca* 3.1 Å in length that likely assist with relative orientations during lattice formation.

2) The yellow organometallic complex $[MoMe(CO)_3(\eta^5\text{-}C_5H_5)]$ was structurally characterised in 2010 by VALENTE and co-workers[63] (first prepared in 1956 by WILKINSON[64]) who sought to utilise it for the catalytic epoxidation of cyclic alkenes in the presence of *tert*-butylperoxide. The dataset and structure solution reported by these authors was quite satisfactory and therefore not re-collected here. The Mo-C($sp^3$) distance was 2.326(3) Å and no unusual intermolecular interactions were found.

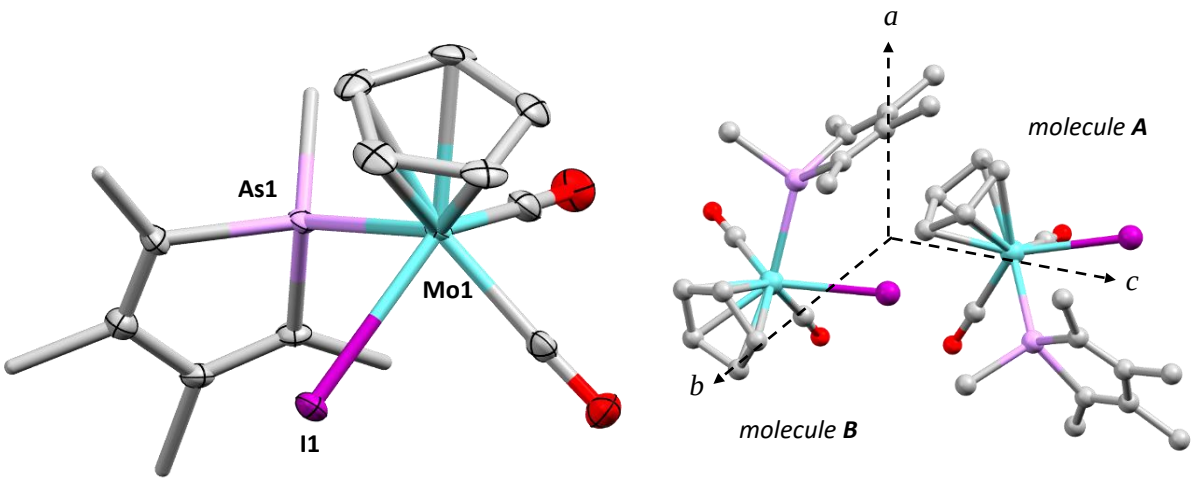



**Figure 4.17**: The molecular structure of *cis*-[MoI(MeAsC$_4$Me$_4$)(CO)$_2$($\eta^5$-C$_5$H$_5$)] in a crystal. Methyl groups simplified and hydrogen atoms omitted for clarity. Ellipsoids shown at 50% displacement. **Inset**: The asymmetric unit ($Z$ = 4, $P$-1) containing a pair of enantiomers **A** and **B** which differ in the relative positions of the iodide and arsenic donor atoms.

3) Dark red *cis*-[MoI(MeAsC$_4$Me$_4$)(CO)$_2$($\eta^5$-C$_5$H$_5$)] crystallises in triclinic $P$-1 and the unit cell contains four molecules comprising two pairs of enantiomers, which differ in the relative position of the pentamethylarsole ligand to the iodide (either to the "left" or "right") when viewed along the molybdenum-cyclopentadienyl centroid axis. The pair of molecules within the asymmetric unit are crystallographically unique though interatomic distances and angles are statistically indistinguishable between the two entities. The molybdenum atom exists in the usual seven-coordinate environment which approximates a square-based pyramid, and the As→Mo dative bond measures 2.5640(6) (molecule **A**) and 2.5717(6) (**B**) Å and the Mo-I covalent bonds are unremarkable at 2.8524(4) (**A**) and 2.8442(4) (**B**) Å in length. The pentamethylarsole ligand lies approximately orthogonal to the vertical plane bisecting the Mo(CO)$_3$($\eta^5$-C$_5$H$_5$) moiety. Distances between arsole ring atoms are typical of σ-dative coordination complexes for this ligand (which are measurably different from [Me$_2$AsC$_4$Me$_4$]I, however) with mean As-C$_\alpha$, C$_\alpha$=C$_\beta$ and C$_\beta$-C$_\beta$ bond lengths of *ca* 1.93, 1.35 and 1.50 Å, respectively.

4) The third set of red crystals contained two compounds in an unequal occupancy ratio which are apparently (or approximately) isosteric and superimposed within the lattice. They are *trans*-[MoI(MeAsC$_4$Me$_4$)(CO)$_2$($\eta^5$-C$_5$H$_5$)] (minor component, 11% occupancy) and *trans*-[Mo{C(O)Me}(MeAsC$_4$Me$_4$)(CO)$_2$($\eta^5$-C$_5$H$_5$)] (major component, 89% occupancy). Model refinement proceeding under these conditions led to a satisfactory structure solution ($R_1$ = 0.0398), albeit with some

eccentric thermal ellipsoids though no restraints/constraints to correct these were applied. The iodide complex is again presumed to arise from carbonyl rather arsole substitution, and the simplest explanation for the occurrence of the acyl complex is migratory insertion of [MoMe(CO)$_3$($\eta^5$-C$_5$H$_5$)] (*vide infra*) affected by free pentamethylarsole. The gross structures of *trans*-[MoI(MeAsC$_4$Me$_4$)(CO)$_2$($\eta^5$-C$_5$H$_5$)] and *trans*-[Mo{C(O)Me}(MeAsC$_4$Me$_4$)(CO)$_2$($\eta^5$-C$_5$H$_5$)] are shown separately in **Figure 4.18**.

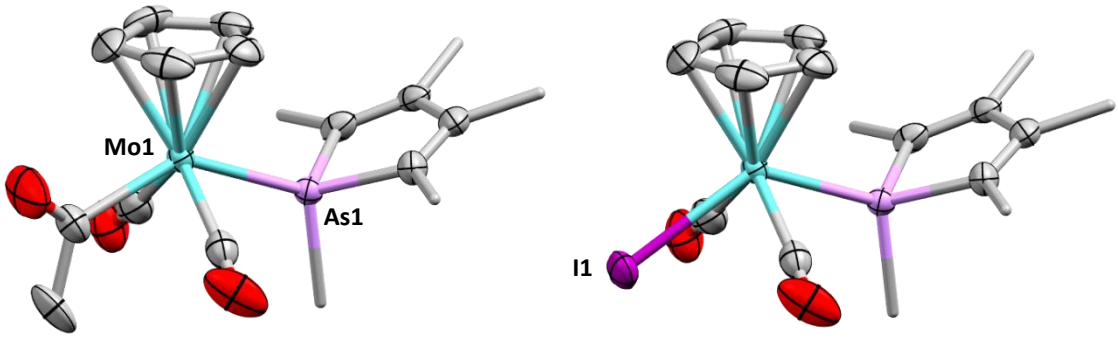



**Figure 4.18**: The molecular structures of *trans*-[Mo{C(O)Me}(MeAsC$_4$Me$_4$)(CO)$_2$($\eta^5$-C$_5$H$_5$)] (**left**) and *trans*-[MoI(MeAsC$_4$Me$_4$)(CO)$_2$($\eta^5$-C$_5$H$_5$)] (**right**) which co-crystallise in a 89:11 ratio, respectively. Methyl groups simplified and hydrogen atoms omitted for clarity. Ellipsoids shown at 50% displacement. The *trans*-Mo(MeAsC$_4$Me$_4$)(CO)$_2$($\eta^5$-C$_5$H$_5$) moieties are crystallographically identical between the two molecules.

The two compounds co-crystallise in monoclinic $P2_1/n$. In both species the pentamethylarsole ligand approximately straddles the (non-crystallographic) vertical symmetry plane of the Mo(CO)$_2$($\eta^5$-C$_5$H$_5$) centre with the *As*-methyl substituent projected between the pair of *cisoid* carbonyl ligands. Since the two complexes are superimposed within the crystal lattice, the positions of the Mo(MeAsC$_4$Me$_4$)(CO)$_2$($\eta^5$-C$_5$H$_5$) atoms are modelled as a weighted average of both and all interatomic dimensions therein are thus identical *viz.* the mean As→Mo dative bond for both complexes *in this particular crystal* is 2.5226(6) Å. All crystallographic uniqueness is observed in the region of the overlaid acyl and iodide substituents, with Mo-C($sp^2$), C=O and Mo-I distances of 2.230(9), 1.215(9) and 2.898(4) Å, respectively. The former two are typical[74-76] whereas the latter is elongated compared the other Mo-I bond lengths observed previously (*ca* 2.4—2.5 Å) since the presence of the arsenic atom in a *transoid* position is presumably a repulsive influence

given that the two σ-donors share a mutual Mo(*d*) orbital. It is noted that a *trans*- configuration* appears to be the preferred condition for Group 6 acyl complexes of the form $[M\{C(O)R\}L(CO)_2(\eta^5\text{-}C_5H_5)]$[77-80] with which $[Mo\{C(O)Me\}(MeAsC_4Me_4)(CO)_2(\eta^5\text{-}C_5H_5)]$ also complies. For $[MoIL(CO)_2(\eta^5\text{-}C_5H_5)]$ it is reasonable to predict that, on average, ligands of superior π-acidity would favour the coordination site *transoid* to the iodide though pentamethylarsole is not expected to be particularly superlative in this respect, possibly explaining why both *cis* and *trans* isomers have crystallised. No general trend emerges from a survey of the literature and any *regio* preferences appear to be highly contextual *e.g.*, steric demands.[81, 82] In many cases the *cis* and *trans* isomers interconvert depending on *inter alia* temperature and solvent polarity[70, 83-86] and in others it is not possible to distinguish from the spectroscopic data reported.

Acyl complexes of the mid-transition metals are well studied: their deliberate method of synthesis entails treatment of a metal carbonyl anion with an acyl halide or by migratory insertion of an alkyl complex,† often in the presence of a LEWIS base[77, 78, 87-90] although some LEWIS acids have also been reported to promote this process.[91, 92] Acyl complexes may be converted to cationic FISCHER-type carbenes by addition of strong alkylating agents[79, 93] and reversion to the metal alkyl can be achieved by thermal or photochemical decarbonylation.[94, 95] This discussion would be remiss if it were not mentioned that migratory insertion of a metal-bound alkyl facilitated by an incoming LEWIS base is foundational to the utility of $Na_2[Fe(CO)_4]$ (COLLMAN'S reagent), for the conversion of alkyl halides to aldehydes and unsymmetrical ketones.[96] For acyl complexes prepared *via* thermolysis of the corresponding alkyl in the presence of a neutral two-electron ligand, said ligand is usually of reasonable basicity (*e.g.*, isocyanides, $PR_3$ and $P(OR)_3$) and weaker nucleophiles (amines, nitriles, arsines, stibines *etc.*) either provide the product in low yield[97] or afford products of decarbonylation (especially for Group 6 centres, in contrast to those of Mn[98] and Fe[99]). Photochemical routes do, however, permit synthesis of such complexes with the aforementioned poor donor ligands.[100, 101]

* An alternative terminology for isomers of four-legged piano stool complexes such as $[MXL(CO)_2(\eta^5\text{-}C_5H_5)]$ is lateral ("*cis*") and diagonal ("*trans*") though such terms have not been adopted here for simplicity's sake. See R.B. KING, R.H. REIMANN and D.J. DARENSBOURG *J. Organomet. Chem.*, **1975**, *93*, C23—C25.

† These reactions are too broad in scope to discuss here, though some excellent reviews cover this topic with exquisite detail given to historical and mechanistic details: See A. WOJCICKI *Adv. Organomet. Chem.*, **1973**, *11*, 87—145, F. CALDERAZZO *Angew. Chem. Int. Ed. Engl.*, **1977**, *16*, 299—311 and K.J. CAVELL *Coord. Chem. Rev.*, **1996**, *155*, 209—243.

It is therefore intriguing that an acyl complex possessing an arsole ligand was observed, since 1) arsines appear less inclined to affect migratory insertion reactions upon exposure to [MoR(CO)$_3$($\eta^5$-C$_5$H$_5$)],[95] 2) the reaction was carried out at -30 °C whereas thermal impetus (*e.g.*, generally >> 25 °C) is often required, and 3) the reaction was carried out in *n*-hexane medium, which is supposed to disfavour the migration process since it cannot effectively stabilise the coordinatively unsaturated and dipolar transition state.[87] Attempts were made to deliberately synthesise [Mo{C(O)Me}(MeAsC$_4$Me$_4$)(CO)$_2$($\eta^5$-C$_5$H$_5$)] by heating [MoMe(CO)$_3$($\eta^5$-C$_5$H$_5$)] to 80 °C in CD$_3$CN with one equivalent of MeAsC$_4$Me$_4$, though the metal alkyl signals were unaffected and only gradual decomposition of the arsole was observed; a similar outcome was obtained with PhAsC$_4$Me$_4$, an arsole of superior thermal stability, wherein the spectrum was totally unchanged after heating. It is also noted that these arsoles did not proceed to carbonyl substitution products either (*i.e.*, *cis*- or *trans*-[MoMe(RAsC$_4$Me$_4$)(CO)$_2$($\eta^5$-C$_5$H$_5$)]), speaking to their poor nucleophilicity. The presence of [Mo{C(O)Me}(MeAsC$_4$Me$_4$)(CO)$_2$($\eta^5$-C$_5$H$_5$)] among the crystalline products is therefore inexplicable since the available prior knowledge would expect the reaction conditions to *disfavour* such a compound (*vide supra*); like the occurrence of [MoMe(CO)$_3$($\eta^5$-C$_5$H$_5$)] in the mixture, it is possible that radical processes may be operative though not *via* any photochemical route since this reaction was performed in the dark.

### 4.1.6 Activated Alkynes

Both metal-complexed phosphole and arsole ligands are known to undergo [4+2] cycloadditions upon treatment with dienophiles; for the former this activity led to the formation of stable 9-phosphanorbornene and -norbornadiene complexes *en route* to the first examples of saturated phosphirane (RPC$_2$R'$_4$) and unsaturated phosphirene (RPC$_2$R'$_2$) complexes.* As discussed in **Chapter 1**, **Section 1.3.3**, Voß and Schenk treated the Group 6 pentacarbonyl arsole complexes [M(RAsC$_4$Me$_4$)(CO)$_5$] (M = Cr, W; R = Me, *t*-Bu, Ph) with the electrophilic alkyne dimethylacetylene dicarboxylate (DMAD, MeO$_2$CC≡CCO$_2$Me) though only the corresponding tetramethyl-*ortho*-phthalate was isolated and no 9-arsanorbornadiene complex was obtained.[102] The following section describes the reaction between the

* See F. Mathey *Chem. Rev.*, **1990**, *90*, 997—1025 for an authoritative overview of these three-membered phosphorus-containing heterocycles.

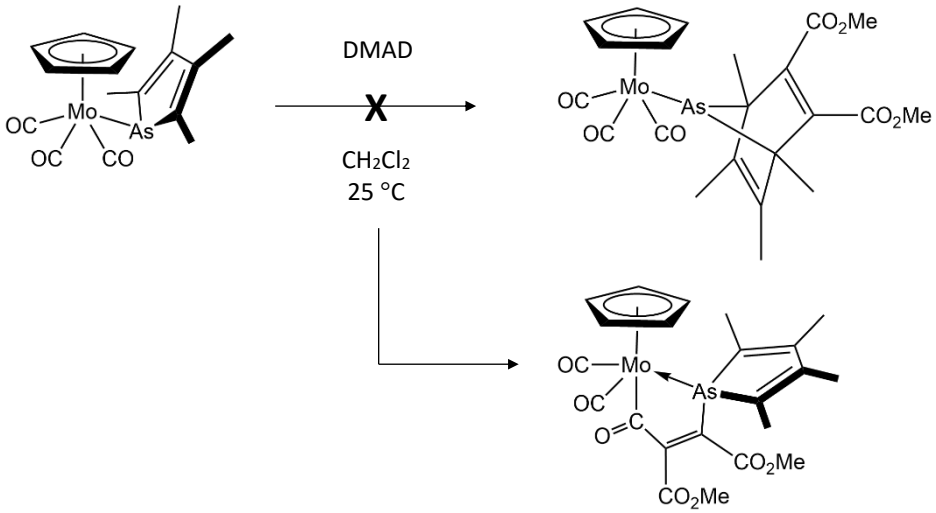
arsolyl complex $[Mo(AsC_4Me_4)(CO)_3(\eta^5\text{-}C_5H_5)]$ and electrophilic alkynes, which leads to stable arsole complexes.

#### 4.6.1.6 Reaction Between $[Mo(AsC_4Me_4)(CO)_3(\eta^5\text{-}C_5H_5)]$ and DMAD

The nucleophile $[Mo(AsC_4Me_4)(CO)_3(\eta^5\text{-}C_5H_5)]$ reacts swiftly with a slight excess of DMAD in $CH_2Cl_2$ solution at ambient temperature. Complete consumption of the starting complex within only a few minutes of mixing is evidenced by IR spectroscopy. Workup *via* column chromatography on Florisil® provides an air-stable, reddish-brown solid as the only isolable compound in good yield.* High-resolution mass spectrometry confirms the formation of a 1:1 $[Mo(AsC_4Me_4)(CO)_3(\eta^5\text{-}C_5H_5)]$/DMAD adduct ($m/z \approx$ 572.9797) though both the $^1$H NMR ($C_6D_6$) and IR spectra are *not* congruent with a [4+2] cycloaddition 9-arsanorbornadiene product of the form $[Mo\{AsC_6Me_4(CO_2Me)_2\}(CO)_3(\eta^5\text{-}C_5H_5)]$ (**Scheme 4.19**). For one, neither the arsolyl nor alkyne moieties exist in symmetrical environments since a pair of methyl ester (3.45 and 3.23 ppm, relative area integration 3:3) and trio of methyl (1.88, 1.59 and 1.54 ppm, relative area integration 3:3:6) signals clearly indicate the molecule to have chirality. Furthermore, the solution IR spectrum ($CH_2Cl_2$) exhibits a $\nu_{CO}$ profile *not* suggestive of a $C_s$-symmetric $Mo(CO)_3(\eta^5\text{-}C_5H_5)$ centre, instead revealing only two terminal carbonyl vibrations at 1962(vs) and 1889(s) cm$^{-1}$ in addition to a lower-energy band at 1732(s) cm$^{-1}$ indicative of a carbonyl group with strong ketonic character. A pair of medium-intensity methyl ester carbonyl absorptions are found at 1605 and 1580 cm$^{-1}$.

The compound was crystallised from $Et_2O$ at -20 °C and X-ray diffraction reveals its identity to be the novel arsolylpropenoyl chelate complex $[Mo\{C(O)C(CO_2Me)=C(CO_2Me)AsC_4Me_4\}(CO)_2(\eta^5\text{-}C_5H_5)]$. The *Z*-propenoyl linkage arises from insertion of a DMAD molecule into the region of space between the nucleophilic arsenic atom and an electrophilic *cisoid* carbonyl ligand, forming a new five-membered molybda-arsacyclopentenone (**Scheme 4.19**). The molecular structure is shown in **Figure 4.19**, and a proposed mechanism of formation is given in **Scheme 4.20**.

* Florisil is the trade name for magnesium silicate ($MgSiO_3$) chromatography aid; the use of silica gel or neutral alumina led to extensive decomposition of the product and very low isolated yields.




**Scheme 4.19**: The reaction between $[Mo(AsC_4Me_4)(CO)_3(\eta^5\text{-}C_5H_5)]$ and dimethylacetylene dicarboxylate.

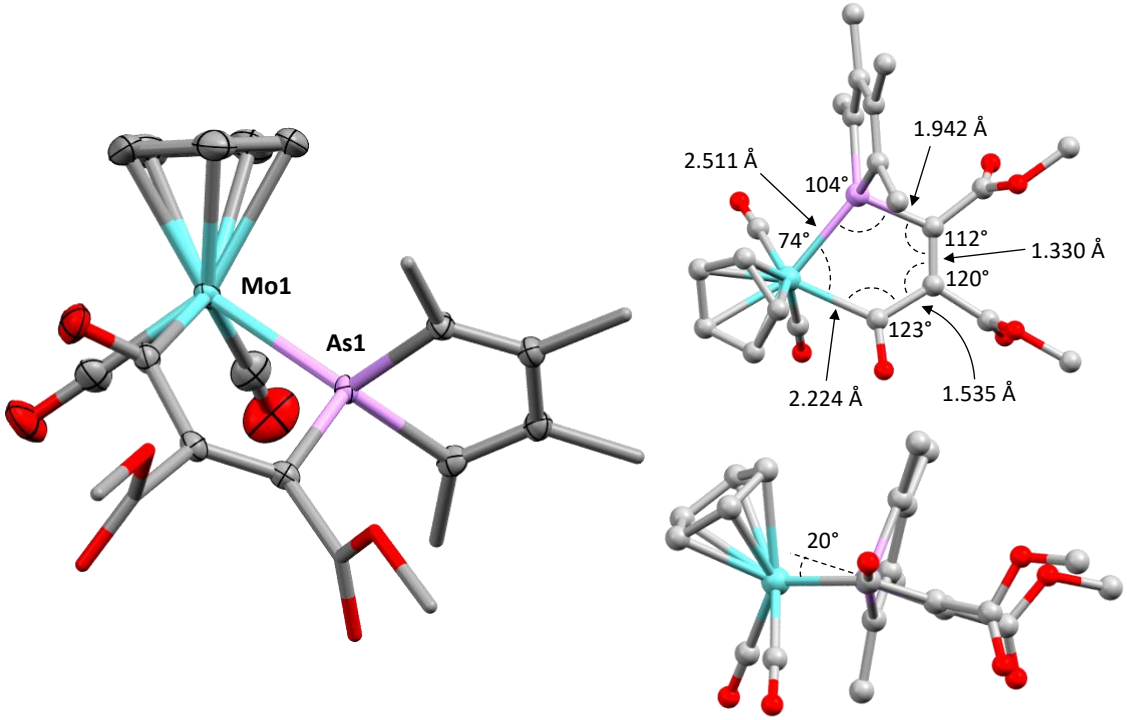
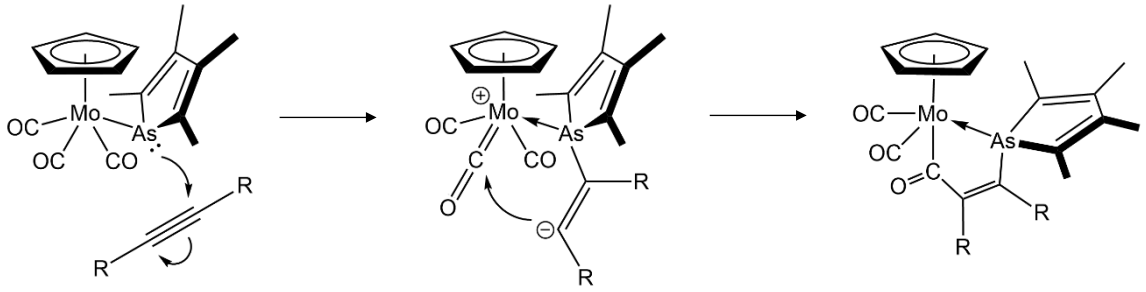



**Figure 4.19**: The molecular structure of $[Mo\{C(O)C(CO_2Me)=C(CO_2Me)AsC_4Me_4\}(CO)_2(\eta^5\text{-}C_5H_5)]$ in a crystal. Methyl and ester groups simplified and hydrogen atoms omitted for clarity. Ellipsoids shown at 50% displacement. **Inset**: Perspectives of the molecule showing geometric dimensions of interest (**top**) and the envelope fold of the molybda-arsacyclopentenone (**bottom**).

The adduct crystallises in triclinic *P*-1 and a pair of symmetry-related enantiomeric molecules are found in the unit cell. The net result of the reaction with DMAD is the formation of a new Mo-C covalent bond and conversion of the Mo-As bond to a As→Mo dative interaction. Thus, the molecular structure of

the spirocyclic product features a pair of vertex-sharing pentagons united at the deformed tetrahedral arsenic atom – their angle of intersection (defined by the separate mean planes of each five-membered ring) is nearly perpendicular at 87°. This geometric parameter does probably come with significant error, however, since only the arsole ring is approximately planar (envelope angle *ca* 7°) whereas the molybda-arsacyclopenteneone is puckered at the arsenic and acyl carbon atoms by *ca* 20° (**Figure 4.19**, **Inset**). Reflecting the fact that all interatomic bonds within the ring are unique, the dimensions of the metallocyclic system are severely distorted from that of the idealised polygon with the molybdenum atom skewed toward the acyl carbon by over 0.25 Å (Mo-C 2.244(2) *vs.* As→Mo 2.5110(2) Å). The latter compares to the marginally longer As→Mo dative interaction of 2.5844(4) Å found in [Mo(MeAsC$_4$Me$_4$)(CO)$_3$($\eta^5$-C$_5$H$_5$)]OTf (**Figure 4.13**). Ring-atom distances within the arsinopropenoyl are typical of the individual bonding partners and comprise regular C=O, C-C, C=C and C-As covalent bonds (**Figure 4.19**, **Inset**).

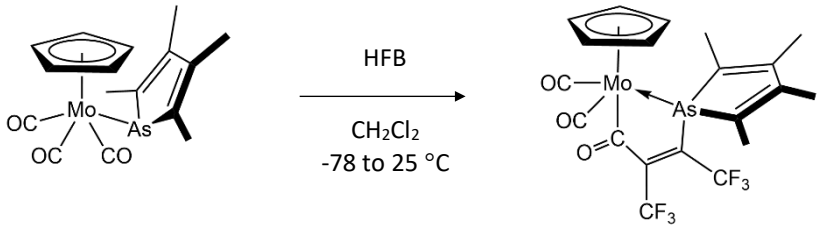



**Scheme 4.20**: Proposed mechanism of the reaction between [Mo(AsC$_4$Me$_4$)(CO)$_3$($\eta^5$-C$_5$H$_5$)] and electrophilic alkynes.

Reflecting the appreciable adjustment to bonding patterns surrounding the Mo(II) centre, the $^{13}$C{$^1$H} NMR spectrum ($C_6D_6$) of [Mo{C(O)C(CO$_2$Me)=C(CO$_2$Me)AsC$_4$Me$_4$}(CO)$_2$($\eta^5$-C$_5$H$_5$)] finds the pair of inequivalent terminal carbonyl ligands to low frequency of [Mo(AsC$_4$Me$_4$)(CO)$_3$($\eta^5$-C$_5$H$_5$)] at 263.2 and 245.5 ppm with the acyl carbonyl resonance at 234.7 ppm. The chemically unique methyl ester carbon signals appear at 167.1 and 159.9 ppm slightly downfield of the propenoyl olefin carbon atoms at 161.0 (acyl-bound) and 149.7 (arsenic-bound) ppm. The arsole ring atoms are all totally inequivalent, appearing as four distinct signals between 146.5—132.9 ppm though the cyclopentadienyl and six remaining methyl groups are found in their usual spectral positions, warranting no special mention.

### 4.6.1.7 Reaction Between [Mo(AsC$_4$Me$_4$)(CO)$_3$($\eta^5$-C$_5$H$_5$)] and HFB

With knowledge of the reaction outcome between [Mo(AsC$_4$Me$_4$)(CO)$_3$($\eta^5$-C$_5$H$_5$)] and DMAD, to the arsolyl complex was condensed an excess of hexafluoro-2-butyne (HFB, F$_3$CC≡CCF$_3$) in $CH_2Cl_2$ solution at -78 °C. Warming to ambient temperature is accompanied by a colour change from orange to a deep red, and purification by column chromatography on Florosil® provided the second example of an arsolylpropenoyl species, namely [Mo{C(O)C(CF$_3$)=C(CF$_3$)AsC$_4$Me$_4$}(CO)$_2$($\eta^5$-C$_5$H$_5$)] in high yield. Alkyne insertion is confirmed by inspection of the solution IR spectrum of the product ($CH_2Cl_2$) including a pair of terminal $\nu_{CO}$ vibrations at 1968(vs) and 1894(vs) cm$^{-1}$ and one acyl $\nu_{CO}$ absorption at 1599(m) cm$^{-1}$; the C=C stretch was not visible in the IR spectrum.




**Scheme 4.21**: The reaction between [Mo(AsC$_4$Me$_4$)(CO)$_3$($\eta^5$-C$_5$H$_5$)] and hexafluoro-2-butyne.

A high-resolution mass spectrum finds the molecular ion ($m/z \approx$ 592.9434) and NMR spectroscopy reveals the expected asymmetric adduct: the $^{19}F\{^1H\}$ spectrum ($C_6D_6$) comprises a pair of quartets (for the chemically unique $CF_3$ groups) at -56.7 and -59.1 ppm with $^5J_{FF}$ couplings of 10.2 Hz, toward the smaller end of the continuum (*ca* 10—15 Hz) for *cis*-C(CF$_3$)=C(CF$_3$) moieties in both organic[103, 104] and inorganic[105, 106] settings. The $^1H$ spectrum finds all four arsolyl $CH_3$ groups to be inequivalent. The $^{13}C\{^1H\}$ spectrum reveals the three carbonyl carbon nuclei in comparable locations to the DMAD adduct above (261.4 and 243.2 (terminal), 233.6 (acyl) ppm) with four distinct arsolyl ring-carbon signals between 147.5—133.0 ppm, and the propenyl carbon resonances appearing at 123.2 (acyl-bound) and 88.8 (arsenic-bound). All remaining signals are found in their usual regions and are largely similar to the previous example. Single crystals of [Mo{C(O)C(CF$_3$)=C(CF$_3$)AsC$_4$Me$_4$}(CO)$_2$($\eta^5$-C$_5$H$_5$)] were grown by evaporation of $Et_2O$ solution at 0 °C and the molecular structure, determined by X-ray diffraction, is shown in **Figure 4.20**.

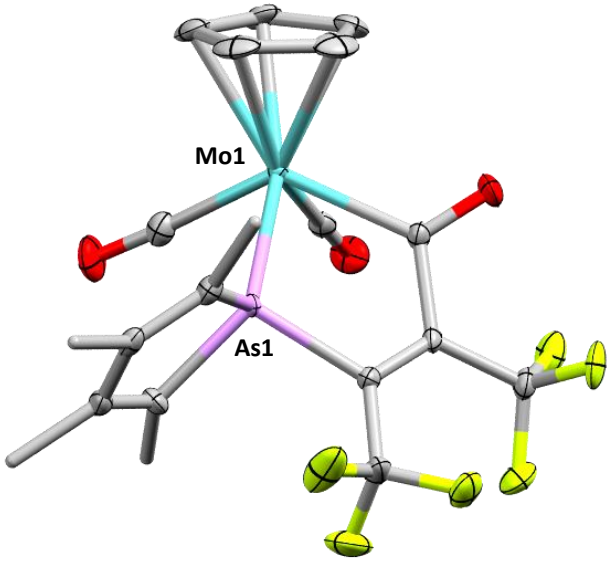



**Figure 4.20**: The molecular structure of [Mo{C(O)C($CF_3$)=C($CF_3$)As$C_4Me_4$}$(CO)_2(\eta^5$-$C_5H_5)$] in a crystal. Methyl groups simplified and hydrogen atoms omitted for clarity. Ellipsoids shown at 50% displacement.

The complex crystallises in centrosymmetric monoclinic $P2_1/n$ and the centric unit cell therefore contains both enantiomers, though only one is shown above. The gross molecular configuration of [Mo{C(O)C($CF_3$)=C($CF_3$)As$C_4Me_4$}$(CO)_2(\eta^5$-$C_5H_5)$] is analogous to that of the [Mo{C(O)C($CO_2$Me)=C($CO_2$Me)As$C_4Me_4$}$(CO)_2(\eta^5$-$C_5H_5)$] (**Figure 4.19**) and most salient features of the latter are applicable to the former. Thus, the formal [3+2] addition of one HFB molecule to the region between the arsenic atom and a *cisoid* carbonyl provides a new five-membered ring encompassing the arsolylpropenoyl chelate ligand. The respective As→Mo and Mo-C bonds measure 2.5161(5) and 2.216(3) Å and the mean planes of the vertex sharing five-membered rings intersect at an angle more acute than the previously discussed DMAD adduct, approximately 78°, though a similar puckering of the molybda-arsacyclopentenone ring (*ca* 17°) is measured. The remaining interatomic dimensions of interest are essentially identical between the DMAD and HFB adducts.

In contrast to the facile replacement of pentamethylarsole by iodide from [Mo(MeAs$C_4Me_4$)$(CO)_3(\eta^5$-$C_5H_5)]^+$, the arsolylpropenoyl complexes were surprisingly resistant toward displacement of the arsenic donor: no reaction whatsoever was observed upon treatment of [Mo{C(O)C($CO_2$Me)=C($CO_2$Me)As$C_4Me_4$}$(CO)_2(\eta^5$-$C_5H_5)$] with an excess of $PMe_3$, $P(OMe)_3$ or *t*-BuNC at elevated temperatures ($C_6D_6$, 80 °C). The NMR spectrum of

$[Mo\{C(O)C(CF_3)=C(CF_3)AsC_4Me_4\}(CO)_2(\eta^5\text{-}C_5H_5)]$ was unchanged after being sealed under an atmosphere of carbon monoxide for one week, and the addition of $[NO]PF_6$ to a $CD_3CN$ solution of the same led to complete decomposition with gas evolution. No reaction was observed between $[Mo(AsC_4Me_4)(CO)_3(\eta^5\text{-}C_5H_5)]$ and electron rich alkynes such as 2-butyne and diphenylacetylene, nor between $[Mo(RAsC_4Me_4)(CO)_3(\eta^5\text{-}C_5H_5)]^{x+}$ and DMAD (R = Me, $x$ = 1 (**Section 4.6.1.1**); R = $Au(C_6F_5)$, $x$ = 0 (**Chapter 5**, **Section 5.2.1**)).* The addition of other electrophilic substrates such as *ortho*-benzyne (*via* the KOBAYASHI protocol[107]), tetracyanoethylene and *N*-phenylmaleimide did not afford similar spirocyclic adducts (by mass spectrometry) and instead yielded chromatographically immobile compounds, except for the former which afford a very small quantity of $[Mo_2(CO)_6(\eta^5\text{-}C_5H_5)_2]$. The course of these latter reactions was not easily deduced from spectroscopic data.

In light of the above reactions between $[Mo(AsC_4Me_4)(CO)_3(\eta^5\text{-}C_5H_5)]$ and DMAD or HFB, it is unsurprising that other transition metal arsenidos undergo analogous ring forming process with electron-poor alkynes: DAVIDSON *et al.*[105] have treated the cacodyl complexes $[Fe(AsMe_2)(CO)_2(\eta^5\text{-}C_5H_5)]$ and $[W(AsMe_2)(CO)_3(\eta^5\text{-}C_5H_5)]$ with the same alkynes to produce the metallacycles $[Fe\{C(O)C(R)=C(R)AsMe_2\}(CO)(\eta^5\text{-}C_5H_5)]$ and $[W\{C(O)C(R)=C(R)AsMe_2\}(CO)_2(\eta^5\text{-}C_5H_5)]$ (R = $CO_2Me$ or $CF_3$) in good yields (**Chart 4.1**). In this regard the behaviour of the $AsC_4Me_4$ ligand resembles that of an ordinary arsenido despite the nucleophilic diene function (which in other contexts does participate in cycloaddition reactions, **Figure 4.8**), and the demonstrated dienophilic proclivities of DMAD and HFB. It is worth reiterating that in both of these reactions a large excess of the alkyne was employed yet the arsole butadiene remained intact, even when the lone pair electrons were already engaged in As→M bonding (*vide supra*); the kinetic preference to form the metallacycle must be reasonably strong to account for this. MATHEY has noted that the disubstituted phospholyl complexes $[W(PC_4R_2R'_2)(CO)_3(\eta^5\text{-}C_5H_5)]$ (R = H, R' = Me; R = Ph, R' = H) are also reluctant to undergo [4+2] cycloaddition reactions with dienophiles (despite the same phosphole rings entering into such reactions[108] when coordinated to $W(CO)_5$ – steric

* The alternative [4+2] *pseudo*-DIELS-ALDER reaction of coordinated arsole to provide 9-arsanorbornadiene derivatives would, in terms of the usual electron demand of DIELS-ALDER reactions, be expected to be retarded by inclusion of electron-releasing substituents on the dienophile and *vice-versa* for coordination of a LEWIS acid ($Me^+$, $Au(C_6F_5)$) to the diene.

effects are therefore discounted), instead yielding phospholylpropenoyl complexes[109] in a similar fashion to transition metal phosphido and phosphinidene reagents (**Chart 4.1**).[110-114]

MIHICHUK and colleagues[115] have reported a arsinopropenoyl complex of rhenium(I) tetracarbonyl (**Chart 4.1**), obtained by photolysis of $[Re_2(CO)_{10}]$ with the bis(arsine) *cis*-$Me_2AsC(CF_3)=C(CF_3)AsMe_2$. By analogy with certain dimanganese compounds obtained previously,[116, 117] this reaction probably traverses through a $[Re_2(\mu\text{-}AsMe_2)(\mu\text{-}C(CF_3)=C(CF_3)AsMe_2)(CO)_8]$ intermediate (or similar) followed by elimination-oligomerisation of a "$Re(AsMe_2)(CO)_3$" fragment; the low yields of product obtained would suggest a non-stoichiometric pathway of formation. Salient crystallographic[106] and spectroscopic features of $[Re\{C(O)C(CF_3)=C(CF_3)AsMe_2\}(CO)_4]$ are comparable to those of the α,β-unsaturated acyl pattern within $[Mo\{C(O)C(CF_3)=C(CF_3)AsC_4Me_4\}(CO)_2(\eta^5\text{-}C_5H_5)]$ (**Figure 4.20**). Finally, XI and co-workers have obtained Mo and W complexes of phosphinopropenoyl chelates (**Chart 4.1**) by transmetalation of vinylphosphino zirconocene complexes to $[MCl(CO)_3(\eta^5\text{-}C_5H_5)]$ in the presence of copper or palladium catalysts,[118] though a similar synthetic approach has not been extended to arsenic and the full potential of the novel $[ZrCl\{C(R)=C(R')E\}(\eta^5\text{-}C_5H_5)_2]$ reagents* (E = main group centre) seems yet to be realised.

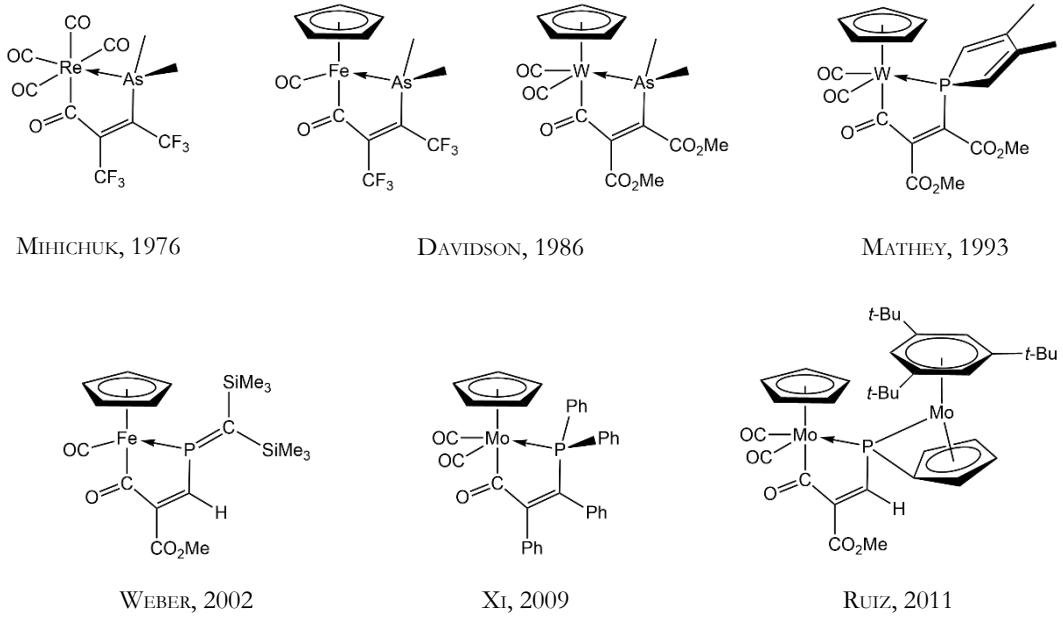



**Chart 4.1**: A representative selection of previously reported (main group)propenoyl transition metal complexes.

* The zirconium reagent is synthesised by a one-pot reaction between $[Zr(1\text{-butene})(p\text{-}NC_5H_4Me)(\eta^5\text{-}C_5H_5)_2]$, RC≡CR and $ClPPh_2$ in THF. See C. XI, X. YAN and C. LAI *Organometallics*, **2007**, *26*, 1084—1088.

## 4.7 Summary

In this chapter, σ-covalent arsolyl complexes of molybdenum, tungsten and iron were prepared *via* transmetalation from the appropriate metal stannyl complex and *As*-chloroarsole. This approach was chosen to circumvent the electron-transfer processes observed when metal carbonyl anions $[M(CO)_n(\eta^5\text{-}C_5H_5)]^-$ were utilised. The 2,3,4,5-tetraphenyl ligand was successfully installed onto $Mo(CO)_3(\eta^5\text{-}C_5H_5)$, $W(CO)_3(\eta^5\text{-}C_5H_5)$ and $Fe(CO)_2(\eta^5\text{-}C_5H_5)$ to give the corresponding $[M(AsC_4Ph_4)(CO)_n(\eta^5\text{-}C_5H_5)]$ complexes previously obtained by ABEL,[1] which were all structurally characterised by X-ray diffraction (**Figure 4.1**, **Figure 4.2** and **Figure 4.3**). The chromium complex could not be isolated and instead underwent electron-transfer processes to give octaphenylbiarsolyl, which was also structurally characterised (**Figure 4.4**).

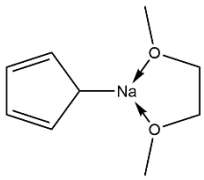
The more-basic 2,3,4,5-tetramethylarsole ligand was easily installed onto $Mo(CO)_3(\eta^5\text{-}C_5H_5)$ and $W(CO)_3(\eta^5\text{-}C_5H_5)$ platforms to provide the new $[M(AsC_4Me_4)(CO)_3(\eta^5\text{-}C_5H_5)]$ complexes in acceptable yields after anaerobic chromatography (**Figure 4.5** and **Figure 4.6**). The installation of bulkier arsolyl ligands onto molybdenum led to products arising from relief of steric congestion, namely spontaneous desilylation (**Figure 4.9**) or Mo-As bond homolysis. An iron complex of the $AsC_4Me_4$ ligand formed with difficulty and could only be obtained in very poor yield and purity. For the latter reaction, the transmetalation kinetics are apparently slower than [4+2] dimerisation of the *As*-chloroarsole electrophile in the reaction medium (**Figure 4.8**). The Sn→As exchange kinetics have been discussed, primarily from observations made by other researchers, in terms of the relative polarisations of the metal-tin bond within the stannyl reagents (**Section 4.4**).

Computational studies on the model arsenido complexes $[MoR(CO)_3(\eta^5\text{-}C_5H_5)]$ (R = $AsMe_2$, $As(CH{=}CH_2)_2$, $AsC_4Me_4$ and $AsC_4Ph_4$) revealed the electronic structures of the arsolyl complex to arise as a unique consequence of the unsaturated cyclic system, since the HOMO of the acyclic species was predominantly arsinocentric whereas the same orbital in the arsolyl systems was constructed from the localised butadiene function (**Section 4.5**). Nonetheless, $[Mo(AsC_4Me_4)(CO)_3(\eta^5\text{-}C_5H_5)]$ displayed nucleophilic reactivity only at the arsenic atom upon treatment with activated alkynes leading to arsolylpropenoyl chelate rings (**Figure 4.19** and **Figure 4.20**). Methylation also occurs at the arsenic atom

which subsequently afforded different products depending on the alkylating agent: methyl trifluoromethanesulfonate gave stable cationic molybdenum complexes (**Figure 4.13**and **Figure 4.14**), whereas methyl iodide gave mixtures of products including the first example of an authentic arsolylium salt (**Figure 4.15**), alongside other novel molybdenum iodide (**Figure 4.16** and **Figure 4.17**) or acyl (**Figure 4.18**) species arising from complicated alkylation, substitution or migratory insertion processes.

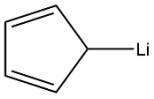
## 4.8 Experimental

### 4.1.7 [$NaC_5H_5$·DME]




To a suspension of 5 g NaH (0.2 mmol) in 250 mL *n*-hexane containing a slight excess of 1,2-dimethoxyethane (DME; 22 mL, 0.21 mmol) was added 25 mL freshly cracked cyclopentadiene (0.3 mol). The mixture was heated to reflux for 48 h (**Caution**: hydrogen gas evolution) during which time the light grey NaH dissolves and a voluminous pink precipitate of [$NaC_5H_5$·DME] forms. The product was collected on a glass frit under argon and washed copiously with *n*-hexane and further dried under reduced pressure. A qualitative test for residual NaH was made by treating a toluene suspension of the isolated material with a few drops of *i*-PrOH, and no bubbles of hydrogen gas were observed. The pyrophoric product was stored in an argon-filled glovebox. Isolated yield: *ca* 32 g (*ca* 90%).

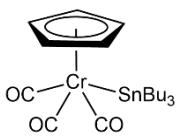
### 4.1.8 [$LiC_5H_5$]




To a solution of 9 mL freshly cracked cyclopentadiene (0.13 mol) in 100 mL *n*-hexane was added 40 mL *n*-BuLi solution (0.1 mol; 2.5 M in hexanes) at 0 °C. The mixture was vigorously stirred overnight during which time a flocculent white precipitate of [$LiC_5H_5$] forms, which is collected on a glass frit under argon and washed with portions of *n*-hexane and further dried under reduced pressure. The pyrophoric product was stored in an argon-filled glovebox. Isolated yield: *ca* 6 g (*ca* 80%).

### 4.1.9 Synthesis of [$M(SnBu_3)(CO)_n(\eta^5\text{-}C_5H_5)$]

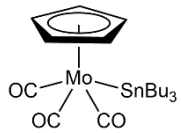
#### 4.8.1.1 [$Cr(SnBu_3)(CO)_3(\eta^5\text{-}C_5H_5)$]



A suspension of 1.5 g $[Cr(CO)_6]$ (7 mmol) was heated to reflux under argon atmosphere overnight in 100 mL degassed acetonitrile. After this time the yellow solution was dried under reduced pressure with the aid of a warm water bath – a small quantity of unreacted $[Cr(CO)_6]$ sublimed into the cold trap. The flask containing crude $[Cr(NCMe)_3(CO)_3]$ was taken into an argon-filled glovebox and weighed (crude yield: *ca* 1.5 g, *ca* 85%) and a stoichiometric quantity of $[NaC_5H_5{\cdot}DME]$ added (1.03 g, 5.7 mmol). A water condenser was fitted to the flask and 100 mL THF admitted, and the mixture heated to reflux for 3 hours. After this time the formation of yellow-brown $Na[Cr(CO)_3(\eta^5\text{-}C_5H_5)]$ was checked by IR ($\nu_{CO}$ 1900(s), 1803(vs), 1749(vs) $cm^{-1}$). 1.5 mL $SnBu_3Cl$ (5.5 mmol. **Caution**: toxic) was added and the mixture stirred overnight before all volatiles were removed under reduced pressure. The residue was extracted with *n*-pentane and filtered through a celite plug (5 x 2.5 cm) under argon, rinsing with small portions of the same solvent until washings were colourless. The solvent was removed under reduced pressure leaving the product as a very air-sensitive viscous yellow liquid, used without further purification. Isolated yield: *ca* 2.1 g (4 mmol, *ca* 57% with respect to $[Cr(CO)_6]$).

NMR: $^1H$ ($C_6D_6$, 400 MHz, 25 °C) δ 4.75 (s, 5H, $\eta^5\text{-}C_5H_5$), 1.60 (m, 6H), 1.38 (m 6H), 1.25 (m, 6H), 0.93 (m, 9H) ppm. IR ($CH_2Cl_2$, 25 °C) $\nu_{CO}$ 1974(vs), 1904(s), 1877(vs) $cm^{-1}$.

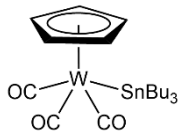
### 4.8.1.2 $[Mo(SnBu_3)(CO)_3(\eta^5\text{-}C_5H_5)]$




In a typical preparation, a two-necked round-bottomed flask was charged with 5 g $[Mo(CO)_6]$ (18.9 mmol) and an equimolar quantity of $[NaC_5H_5{\cdot}DME]$ (3.4 g) or $[LiC_5H_5]$ (1.4 g). A water condenser was fitted and 150 ml THF was admitted, and the mixture heated to reflux overnight under argon. The formation of yellow-brown $[Mo(CO)_3(\eta^5\text{-}C_5H_5)]^-$ was checked by IR (sodium salt, $\nu_{CO}$ 1901(s), 1797(vs), 1744(vs) $cm^{-1}$; lithium salt, $\nu_{CO}$ 1907(s), 1807(s), 1781(m), 1712(s) $cm^{-1}$) and 5.1 mL $SnBu_3Cl$ was added (18.8 mmol) and the mixture stirred for a further 2 hours. Operations are now carried out without exclusion of air or moisture. Volatiles are removed by rotary evaporation and the residue extracted with petroleum ether and filtered through a celite plug (5 x 2.5 cm), rinsing with portions of the same solvent until washings ran clear. The filtrate was dried by rotary evaporation leaving the product as a moderately air-stable viscous yellow-orange liquid. The product was stored in an argon-filled glovebox to prolong shelf-life. Isolated yield: *ca* 7.4 g (13.8 mmol, *ca* 73% with respect to $[Mo(CO)_6]$). The reaction was performed a total of 6 times during this work on different scales and isolated yields of $[Mo(SnBu_3)(CO)_3(\eta^5\text{-}C_5H_5)]$ were generally >70%.

NMR: $^1H$ ($C_6D_6$, 400 MHz, 25 °C) δ 5.27 (s, 5H, $\eta^5\text{-}C_5H_5$), 1.53 (m, 6H), 1.38 (m, 6H), 1.18 (m, 6H), 0.92 (m, 9H) ppm. IR ($CH_2Cl_2$, 25 °C) $\nu_{CO}$ 1987(vs), 1910(sh), 1884(vs) $cm^{-1}$.

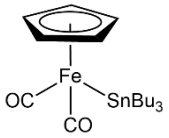
### 4.8.1.3 [W(SnBu$_3$)(CO)$_3$($\eta^5$-C$_5$H$_5$)]




A suspension of 3.5 g [W(CO)$_6$] (1 mmol) was heated to reflux under argon atmosphere in 100 mL degassed propionitrile for 48 h. After this time the yellow solution was dried under reduced pressure with the aid of a warm water bath – no unreacted [W(CO)$_6$] was observed to sublime. The flask containing crude [W(NCEt)$_3$(CO)$_3$] was taken in an argon-filled glovebox and weighed (crude yield: *ca* 3.8 g, *ca* 90%) and a stoichiometric quantity of [NaC$_5$H$_5$·DME] was added (1.6 g). A water condenser was fitted and 150 mL THF admitted, and the mixture heated to reflux for 3 hours. The formation of yellow-brown Na[W(CO)$_3$($\eta^5$-C$_5$H$_5$)] was checked by IR ($\nu_{CO}$ 1895(s), 1793(vs), 1742(vs) cm$^{-1}$). 2.4 mL SnBu$_3$Cl (8.8 mmol) was added, and the mixture stirred for a further 2 hours. Operations are now carried out without exclusion of air or moisture, and workup is identical to the molybdenum analogue above. The product is encountered as a moderately air-stable, viscous yellow-orange liquid which was stored in an argon-filled glovebox to prolong shelf-life. Isolated yield: *ca* 4 g (6.4 mmol, *ca* 64% with respect to [W(CO)$_6$]). The reaction was performed a total of 3 times during this work on different scales and isolated yields of [W(SnBu$_3$)(CO)$_3$($\eta^5$-C$_5$H$_5$)] were generally >60%.

NMR: $^1$H (C$_6$D$_6$, 400 MHz, 25 °C) 4.60 (s, 5H, $\eta^5$-C$_5$H$_5$), 1.67 (m, 6H), 1.44 (m, 6H), 1.31 (m, 6H), 0.98 (m, 9H) ppm. IR (CH$_2$Cl$_2$, 25 °C) $\nu_{CO}$ 1983(vs), 1902(sh), 1878(vs) cm$^{-1}$.

### 4.8.1.4 [Fe(SnBu$_3$)(CO)$_2$($\eta^5$-C$_5$H$_5$)]

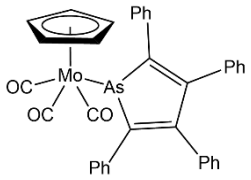



A dilute sodium amalgam was prepared by **slow** addition of **small** pieces of sodium (0.35 g, 15.2 mmol) to a stirred pool of elemental mercury (*ca* 5 mL. **Caution**: toxic) under argon. **Dissolution is exothermic and generates mercury vapour**, and the amalgam thickens to a dull grey paste as more sodium is incorporated. When complete, the amalgam is covered with 100 mL THF and 2.5 g solid [Fe$_2$(CO)$_4$($\eta^5$-C$_5$H$_5$)$_2$] (7 mmol) was added. The mixture is rapidly stirred for 6 hours during which time the amalgam reverts to the appearance of elemental mercury and the red colour of the dimer changes to the yellow-brown Na[Fe(CO)$_2$($\eta^5$-C$_5$H$_5$)] ($\nu_{CO}$ 1880(vs), 1869(s), 1809(vs), 1775(s) cm$^{-1}$). The THF solution is decanted into a second flask and the amalgam rinsed with small portions of THF until clear. 3.8 mL SnBu$_3$Cl (14 mmol) was added, and the reaction stirred overnight. Operations are now carried out without exclusion of air or moisture, and workup is identical to that of the molybdenum and tungsten analogues above. The compound may be further purified by flash chromatography on neutral alumina with petroleum ether eluent, if desired. The product is encountered as a moderately air-stable viscous orange liquid which was stored in an argon-filled glovebox to prolong shelf-life. Isolated yield: *ca* 5.8 g (12.4 mmol, *ca* 80% with respect to [Fe$_2$(CO)$_4$($\eta^5$-C$_5$H$_5$)$_2$]).

NMR: $^1$H (C$_6$D$_6$, 400 MHz, 25 °C) δ 4.73 (s, 5H, $\eta^5$-C$_5$H$_5$), 1.52 (m, 6H), 1.35 (m, 6H), 1.05 (m, 6H), 0.91 (m, 9H) ppm. IR (CH$_2$Cl$_2$, 25 °C) $\nu_{CO}$ 1980(vs), 1926(vs) cm$^{-1}$.

## 4.1.10 Synthesis of $[M(AsC_4Ph_4)(CO)_n(\eta^5\text{-}C_5H_5)]$

### 4.8.1.5 $[Mo(AsC_4Ph_4)(CO)_3(\eta^5\text{-}C_5H_5)]$

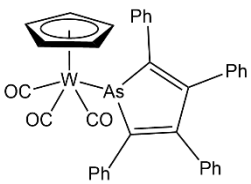



To a stirred solution of 2 g $ClAsC_4Ph_4$ (4.3 mmol) in 50 mL $CH_2Cl_2$ was added 2.4 g $[Mo(SnBu_3)(CO)_3(\eta^5\text{-}C_5H_5)]$ (4.4 mmol) at ambient temperature. A fairly rapid colour change from yellow to orange takes place and stirring is continued for *ca* 4 hours. The solvent is removed under reduced pressure and the solids copiously washed with *n*-pentane (with trituration) to remove $SnBu_3Cl$ and residual metal-stannyl precursor. The material as obtained is sufficiently pure for synthetic purposes however analytically pure samples are obtained by re-crystallisation from the minimum amount of $CH_2Cl_2$/*n*-hexane or hot benzene/*n*-hexane cooled to -20 °C overnight. Alternative, chromatography on neutral alumina with 19:1 *n*-pentane/$Et_2O$ followed by 9:1 *n*-pentane/$CH_2Cl_2$ gives an orange band containing the product which is collected under nitrogen and dried. The product is readily soluble in polar organic and aromatic solvents, somewhat soluble in $Et_2O$ and less-so in aliphatic hydrocarbons. The product is moderately air-sensitive in solution however solids may be handled for some time without inert atmosphere. Isolated yield: 2.1 g (3.1 mmol, 72%). The reaction was performed a total of 6 times during this work on different scales and isolated yields of $[Mo(AsC_4Ph_4)(CO)_3(\eta^5\text{-}C_5H_5)]$ were generally *ca* 50—70%.

NMR: $^1H$ ($C_6D_6$, 400 MHz, 25 °C) δ 7.32—7.29 (m, 8H, $C_6H_5$), 7.02—6.98 (m, 4H, $C_6H_5$), 6.91—6.88 (m , 6H, $C_6H_5$), 6.80—6.77 (m, 2H, $C_6H_5$), 4.54 (s, 5H, $\eta^5\text{-}C_5H_5$) ppm. $^{13}C\{^1H\}$ ($C_6D_6$, 176 MHz, 25 °C) δ 235.5 (*transoid CO*), 223.7 (*cisoid CO*), 164.0 (arsole {2,5}-*C*), 148.9 (arsole {3,4}-*C*), 140.7 ($C_6H_5$), 139.9 ($C_6H_5$), 131.1 ($C_6H_5$), 129.6 ($C_6H_5$), 128.4 ($C_6H_5$), 127.5 ($C_6H_5$), 126.4 ($C_6H_5$), 126.4 ($C_6H_5$), 129.3 ($C_6H_5$), 92.0 ($\eta^5\text{-}C_5H_5$) ppm. IR ($CH_2Cl_2$, 25 °C) $\nu_{CO}$ 2012(s), 1935(vs, br) $cm^{-1}$. HR-MS (ESI, MeCN, +ve ion) found *m/z* 679.0161 (calc. for $C_{36}H_{25}O_3{}^{75}As_1{}^{98}Mo_1$ $[M]^+$: 679.0161). Analysis found 64.00% C, 3.90% H (calc. for $C_{36}H_{25}O_3As_1Mo_1$ 63.92% C, 3.73% H).

Crystals grown from benzene/*n*-hexane solution at -20 °C; one molecule of $C_6H_6$ was found in the asymmetric unit. $C_{36}H_{25}As_1Mo_1O_3{\cdot}C_6H_6$ ($M$ = 754.53 g/mol): yellow prism 0.197 × 0.093 × 0.062 mm, orthorhombic, space group *Pbca* (no. 61), $a$ = 18.87950(10) Å, $b$ = 15.39100(10) Å, $c$ = 23.5717(2) Å, $V$ = 6849.33(8) Å$^3$, $Z$ = 8, spherical correction $T_{min}/T_{max}$ = 0.64271/0.66605, $\mu$(Cu-Kα) = 4.508 $mm^{-1}$, $\varrho_{calc}$ = 1.463 g/cm$^3$, 45669 reflections measured (7.5° ≤ 2Θ ≤ 147.786°), 6909 unique ($R_{int}$ = 0.0241, $R_{sigma}$ = 0.0159) which were used in all calculations, $GOF$ = 1.032, $D_{min}/D_{max}$ = -0.65/0.60 e/Å$^3$. The final $R_1$ was 0.0272 (I > 2σ(I)) and $wR_2$ was 0.0746 (all data).

### 4.8.1.6 $[W(AsC_4Ph_4)(CO)_3(\eta^5\text{-}C_5H_5)]$

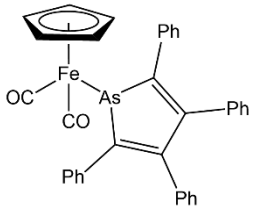


Prepared similar to that above. Quantities: 2 g $ClAsC_4Ph_4$ (4.3 mmol), 2.8 g $[W(SnBu_3)(CO)_3(\eta^5\text{-}C_5H_5)]$ (4.4 mmol). Properties are identical to that of the molybdenum analogue. Isolated 2.5 g (3.2 mmol, 74%) as a yellow-orange solid.

NMR: $^1H$ ($C_6D_6$, 400 MHz, 25 °C) δ 7.33—7.30 (m, 8H, $C_6H_5$), 7.02—6.99 (m, 4H, $C_6H_5$), 6.91—6.89 (m, 6H, $C_6H_5$), 6.80—6.77 (m, 2H, $C_6H_5$), 4.32 (s, 5H, $\eta^5$-$C_5H_5$) ppm. $^{13}C\{^1H\}$ ($C_6D_6$, 176 MHz, 25 °C) δ 223.0 ($^1J_{CW}$ = 155 Hz, *transoid CO*), 212.5 ($^1J_{CW}$ = 160 Hz, *cisoid CO*), 163.3 (arsole {2,5}-*C*), 148.9 (arsole {3,4}-*C*), 140.7 ($C_6H_5$), 140.0 ($C_6H_5$), 131.6 ($C_6H_5$), 130.7 ($C_6H_5$), 130.1 ($C_6H_5$), 129.2 ($C_6H_5$), 127.4 ($C_6H_5$), 127.1 ($C_6H_5$), 126.7 ($C_6H_5$), 125.9 ($C_6H_5$), 90.5 ($\eta^5$-$C_5H_5$) ppm. IR ($CH_2Cl_2$, 25 °C) $\nu_{CO}$ 2008(s), 1926(vs, br) $cm^{-1}$. HR-MS (ESI, MeCN, +ve ion) found *m/z* 781.0565 (calc. for $C_{36}H_{25}O_4{}^{75}As_1{}^{184}W_1$ [*M* + O]$^+$: 781.0563). Analysis found 55.59% C, 3.30% H (calc. for $C_{36}H_{25}O_3As_1W_1$ 55.57% C, 3.30% H).

Crystals grown from benzene/*n*-hexane solution at -20 °C; one molecule of $C_6H_6$ was found in the asymmetric unit. $C_{36}H_{25}As_1O_3W_1 \cdot C_6H_6$ (*M* = 842.44 g/mol): yellow prism 0.283 × 0.119 × 0.043 mm, orthorhombic, space group *Pbca* (no. 61), *a* = 18.88750(10) Å, *b* = 15.38100(10) Å, *c* = 23.5386(2) Å, *V* = 6838.17(8) Å$^3$, *Z* = 8, spherical correction $T_{min}/T_{max}$ = 0.51606/0.55396, $\mu$(Cu-Kα) = 7.639 $mm^{-1}$, $\varrho_{calc}$ = 1.637 g/cm$^3$, 27682 reflections measured (7.512° ≤ 2Θ ≤ 147.452°), 6869 unique ($R_{int}$ = 0.0286, $R_{sigma}$ = 0.0269) which were used in all calculations, *GOF* = 1.037, $D_{min}/D_{max}$ = -0.68/0.69 e/Å$^3$. The final $R_1$ was 0.0247 (I > 2σ(I)) and $wR_2$ was 0.0636 (all data).

### 4.8.1.7 $[Fe(AsC_4Ph_4)(CO)_2(\eta^5\text{-}C_5H_5)]$



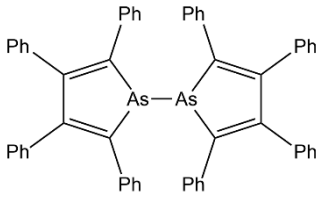

To a solution of 2 g $ClAsC_4Ph_4$ (4.3 mmol) in 50 mL $CH_2Cl_2$ was added 2.1 g $[Fe(SnBu_3)(CO)_2(\eta^5\text{-}C_5H_5)]$ (4.4 mmol), and the mixture allowed to stir at ambient temperature for 72 h. Workup is identical to that of the molybdenum and tungsten complexes above. Alternatively, the same quantities of reagents were warmed to *ca* 45 °C overnight in THF solution and the product is isolated as an orange-red solid. Properties are identical to that of the molybdenum and tungsten complexes above, though the air-stability is markedly improved here and may be handled as a solution or solid without inert atmosphere for some time. Isolated yield: 1.5 g (2.4 mmol, 55%). The reaction was performed a total of 4 times during this work and yields of $[Fe(AsC_4Ph_4)(CO)_2(\eta^5\text{-}C_5H_5)]$ were generally *ca* 50% irrespective of scale.

NMR: $^1H$ ($C_6D_6$, 400 MHz, 25 °C) δ 7.41—7.32 (m, 6H, $C_6H_5$), 7.10—7.02 (m, 4H, $C_6H_5$), 6.93—6.79 (m, 10H, $C_6H_5$), 3.88 (s, 5H, $\eta^5$-$C_5H_5$) ppm. $^{13}C\{^1H\}$ ($C_6D_6$, 176 MHz, 25 °C) δ 213.6 (*CO*), 166.9 (arsole {2,5}-*C*), 147.7 (arsole {3,4}-*C*), 141.2 ($C_6H_5$), 141.2 ($C_6H_5$), 140.5 ($C_6H_5$), 131.3 ($C_6H_5$), 130.2 ($C_6H_5$), 129.3 ($C_6H_5$), 128.5 ($C_6H_5$), 128.3 ($C_6H_5$), 127.6 ($C_6H_5$), 126.3 ($C_6H_5$), 126.1 ($C_6H_5$), 83.9 ($\eta^5$-$C_5H_5$) ppm. IR ($CH_2Cl_2$, 25 °C) $\nu_{CO}$ 2021(vs), 1966(vs) $cm^{-1}$. HR-MS (ESI, MeCN, +ve ion) found *m/z* 552.0533 (calc. for $C_{33}H_{25}{}^{75}As_1{}^{56}Fe_1$ [*M* – 2CO]$^+$: 552.0533). Analysis found 69.25% C, 4.20% H (calc. for $C_{35}H_{25}O_2As_1Fe_1$ 69.10% C, 4.14% H).

Crystals grown from benzene/*n*-hexane solution at -20 °C; the cyclopentadienyl ring exhibited five-fold rotational disorder (*ca.* 65:35 occupancy ratio) which was modelled accordingly. $C_{35}H_{25}As_1Fe_1O_2$ (*M* = 608.32 g/mol): orange

prism 0.222 × 0.159 × 0.105 mm, monoclinic, space group *C*2/*c* (no. 15), *a* = 20.34180(10) Å, *b* = 15.50870(10) Å, *c* = 17.76510(10) Å, *β* = 91.4300(10)°, *V* = 5602.70(6) Å$^3$, *Z* = 8, spherical correction $T_{min}/T_{max}$ = 0.51181/0.55013, *μ*(Cu-Kα) = 5.863 mm$^{-1}$, $\varrho_{calc}$ = 1.442 g/cm$^3$, 34915 reflections measured (7.168° ≤ 2Θ ≤ 147.542°), 5650 unique ($R_{int}$ = 0.0178, $R_{sigma}$ = 0.0117) which were used in all calculations, *GOF* = 1.033, $D_{min}/D_{max}$ = -0.21/0.26 e/Å$^3$. The final $R_1$ was 0.0195 (I > 2σ(I)) and *w*$R_2$ was 0.0525 (all data).

### 4.8.1.8 Reaction between [Cr(SnBu$_3$)(CO)$_3$(η$^5$-C$_5$H$_5$)] and ClAsC$_4$Ph$_4$

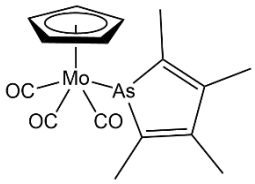



To a solution of 0.2 g ClAsC$_4$Ph$_4$ (0.43 mmol) in 10 mL $CH_2Cl_2$ was added a solution of 0.22 g [Cr(SnBu$_3$)(CO)$_3$(η$^5$-C$_5$H$_5$)] (0.45 mmol) also dissolved in 5 mL of $CH_2Cl_2$. The colour immediately changes from yellow to a bright orange and then over the course of a few minutes a dark orange-brown suspension forms. An IR spectrum finds [Cr$_2$(CO)$_6$(η$^5$-C$_5$H$_5$)$_2$] as the only readily identifiable carbonyl-containing species (1950(vs), 1924(s) and 1912(sh) cm$^{-1}$). The mixture is dried by rotary evaporation leaving a dark green-brown residue which is subjected to column chromatography on silica gel with 1:1 petroleum ether/$CH_2Cl_2$ providing an orange band – a significant quantity of immobile olive-green residues remained atop the column. Slow evaporation of the eluent provides [AsC$_4$Ph$_4$]$_2$ as large orange crystals. Isolated yield: *ca* 0.025 g (0.03 mmol, *ca* 6% by arsenic). The product was characterised only by X-ray crystallography due to poor yields.

Crystals grown by evaporation of $CH_2Cl_2$/petroleum ether solution. C$_{56}$H$_{40}$As$_2$ (*M* = 862.72 g/mol): triclinic, space group *P*-1 (no. 2), *a* = 10.03710(10) Å, *b* = 12.67500(10) Å, *c* = 17.32020(10) Å, α = 89.7530(10)°, β = 88.1950(10)°, γ = 71.8550(10)°, *V* = 2092.83(3) Å$^3$, *Z* = 2, spherical correction $T_{min}/T_{max}$ = 0.819/1.000 , *μ*(Cu Kα) = 2.259 mm$^{-1}$, $\varrho_{calc}$ = 1.369 g/cm$^3$, 80145 reflections measured (7.34° ≤ 2Θ ≤ 156.164°), 8843 unique ($R_{int}$ = 0.0356, $R_{sigma}$ = 0.0178) which were used in all calculations, *GOF* = 1.043, $D_{min}/D_{max}$ = -0.5/1.2 e/Å$^3$. The final $R_1$ was 0.0316 (I > 2σ(I)) and *w*$R_2$ was 0.0831 (all data).

## 4.1.11 Synthesis of [M(AsC$_4$Me$_4$)(CO)$_n$(η$^5$-C$_5$H$_5$)]

### 4.8.1.9 [Mo(AsC$_4$Me$_4$)(CO)$_3$(η$^5$-C$_5$H$_5$)]



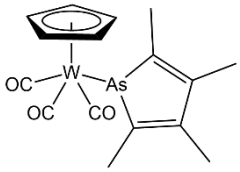

To a stirred solution of 1.1 g freshly prepared ClAsC$_4$Me$_4$ (5 mmol) in 25 mL *n*-hexane is added 2.7 g [Mo(SnBu$_3$)(CO)$_3$(η$^5$-C$_5$H$_5$)] (5.2 mmol) whereupon an immediate colour change from yellow to a deep orange takes place. The mixture is stirred for a further 2 hours before being transferred to a water-jacketed (*ca* 10 °C) column of neutral alumina (35 x 2.5 cm) made up in *n*-pentane under nitrogen. Eluting with 19:1 *n*-pentane/Et$_2$O provides a

pale-yellow band of tin-containing residues which are discarded (**caution**: toxic). Eluting with 4:1 *n*-pentane/$Et_2O$ provides an orange band which is collected under nitrogen and taken to dryness. Alternatively, the reaction may be carried out in $CH_2Cl_2$ solution and prior to chromatography (as above) treated with a slight excess of $[Bu_4N]F$ which helps to remove the majority of the tin-containing residues. The material as obtained is sufficiently pure for synthetic purposes however an analytically pure sample was prepared by re-crystallisation from *n*-pentane at -30 °C. The product is readily soluble in common organic solvents and is air-sensitive in solution, however solids may be handled for a short while. Isolated yield: 1.1 g (2.5 mmol, 50%). The reaction was performed a total of 5 times during this work and isolated yields of $[Mo(AsC_4Me_4)(CO)_3(\eta^5\text{-}C_5H_5)]$ were generally *ca* 50%, irrespective of scale.

NMR: $^1H$ ($C_6D_6$, 400 MHz, 25 °C) $^1H$ δ 4.54 (s, 5H, $\eta^5\text{-}C_5H_5$), 2.10 (s, 6H, α-$CH_3$), 1.93 (s, 6H, β-$CH_3$) ppm. $^{13}C\{^1H\}$ δ 235.5 (*transoid CO*), 224.5 (*cisoid CO*), 148.7 (arsole {2,5}-*C*), 141.9 (arsole {3,4}-*C*), 92.5 ($\eta^5\text{-}C_5H_5$), 16.0 (α-$CH_3$), 15.1 (β-$CH_3$) ppm. IR ($CH_2Cl_2$, 25 °C) $\nu_{CO}$ 2006(s), 1937(sh), 1918(vs) $cm^{-1}$. HR-MS (ESI, MeCN, +ve ion) found *m*/*z* 344.9542 (calc. for $C_{13}H_{16}{}^{75}As_1{}^{98}Mo_1$ [*M* – 3CO]$^+$: 344.9525). Analysis found 45.00% C, 4.40% H (calc. for $C_{16}H_{17}O_3As_1Mo_1$ 44.88% C, 4.00% H).

Crystals grown from evaporation of *n*-pentane solution at -30 °C; the selected crystal was twinned, and a suitable twin-law was applied. $C_{16}H_{17}As_1Mo_1O_3$ (*M* = 428.15 g/mol): orange prism 0.193 × 0.165 × 0.095 mm triclinic, space group *P*-1 (no. 2), *a* = 7.6134(2) Å, *b* = 7.7893(2) Å, *c* = 14.8554(6) Å, *a* = 78.829(3)°, *β* = 88.971(3)°, *γ* = 72.297(2)°, *V* = 822.56(5) Å$^3$, *Z* = 2, empirical correction $T_{min}/T_{max}$ = 0.87862/1.00000, $\mu$(Cu-Kα) = 8.814 $mm^{-1}$, $\varrho_{calc}$ = 1.729 g/$cm^3$, 9139 reflections measured (12.158° ≤ 2Θ ≤ 146.304°), 9139 unique ($R_{int}$ = 0.0441, $R_{sigma}$ = 0.0183) which were used in all calculations, *GOF* = 1.114, $D_{min}/D_{max}$ = -0.95/0.59 e/Å$^3$. The final $R_1$ was 0.0391 (I > 2σ(I)) and $wR_2$ was 0.1121 (all data).

### 4.8.1.10 $[W(AsC_4Me_4)(CO)_3(\eta^5\text{-}C_5H_5)]$



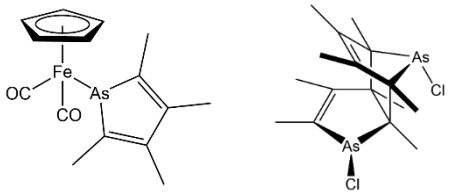

Prepared similarly to that above. Quantities: 0.45 g $ClAsC_4Me_4$ (2 mmol) and 1.3 g $[W(SnBu_3)(CO)_3(\eta^5\text{-}C_5H_5)]$ (2.1 mmol). Isolated yield: 0.4 g (0.77 mmol, 38%).

NMR: $^1H$ ($C_6D_6$, 400 MHz, 25 °C) δ 4.50 (s, 5H, $\eta^5\text{-}C_5H_5$), 2.10 (s, 6H, α-$CH_3$), 1.90 (s, 6H, β-$CH_3$) ppm. $^{13}C\{^1H\}$ ($C_6D_6$, 176 MHz, 25 °C) δ 223.4 ($^1J_{CW}$ = 140 Hz, *transoid CO*), 213.6 ($^1J_{CW}$ = 155 Hz, *cisoid CO*), 148.9 (arsole {2,5}-*C*), 141.0 (arsole {23,4}-*C*), 91.5 ($\eta^5\text{-}C_5H_5$), 16.0 (α-$CH_3$), 15.0 (β-$CH_3$) ppm. IR ($CH_2Cl_2$, 25 °C) $\nu_{CO}$ 2005(s), 1928(vs), 1909(vs) $cm^{-1}$. HR-MS (ESI, MeCN, +ve ion) found *m*/*z* 532.9933 (calc. for $C_{16}H_{17}O_4{}^{75}As_1{}^{184}W_1$ [*M* + O]$^+$: 532.9933). Analysis found 37.12% C, 3.42% H (calc. for $C_{16}H_{17}O_3As_1W_1$ 37.24% C, 3.32% H).

Crystals grown from evaporation of *n*-pentane solution at -30 °C. $C_{16}H_{17}As_1O_3W_1$ (*M* = 516.06 g/mol): orange plate 0.179 × 0.126 × 0.056 mm, monoclinic, space group $P2_1/c$ (no. 14), *a* = 7.66960(10) Å, *b* = 28.8296(3) Å, *c* = 7.74520(10) Å, *β* = 106.6740(10)°, *V* = 1640.54(4) Å$^3$, *Z* = 4, empirical correction $T_{min}/T_{max}$ = 0.46203/1.00000, $\mu$(Cu-Kα) = 15.349 $mm^{-1}$, $\varrho_{calc}$ = 2.089 g/$cm^3$, 28908 reflections measured (12.046° ≤ 2Θ ≤ 146.162°), 3293 unique ($R_{int}$ =

0.0231, $R_{sigma}$ = 0.0110) which were used in all calculations, *GOF* = 1.224, $D_{min}/D_{max}$ = -0.77/0.81 e/Å$^3$. The final $R_1$ was 0.0203 (I > 2σ(I)) and $wR_2$ was 0.0488 (all data).

### 4.8.1.11 [Fe(AsC$_4$Me$_4$)(CO)$_3$(η$^5$-C$_5$H$_5$)]



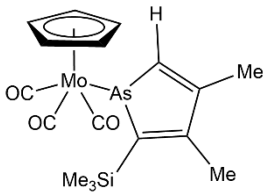

To a stirred solution of 0.6 g freshly prepared ClAsC$_4$Me$_4$ (2.7 mmol) in 25 mL *n*-hexane was added 1.3 g [Fe(SnBu$_3$)(CO)$_2$(η$^5$-C$_5$H$_5$)]. No obvious colour change takes place and the mixture is stirred at ambient temperature for 48 h. The mixture is transferred to a water-jacketed column of neutral alumina (35 x 2.5 cm) made up in *n*-pentane under nitrogen. Eluting with 19:1 *n*-pentane/Et$_2$O provides an orange band containing the majority of unreacted [Fe(SnBu$_3$)(CO)$_2$(η$^5$-C$_5$H$_5$)]. Eluting with 4:1 *n*-pentane/Et$_2$O provides a yellow-orange band which is collected under nitrogen and taken to dryness giving a dark orange residue which was not yielding to re-crystallisation attempts. Isolated yield: *ca* 0.05 g (0.14 mmol, < 5%, impure).

This compound was only partially characterised due to poor yield and purity. NMR: $^1$H (C$_6$D$_6$, 400 MHz, 25 °C) δ 4.05 (s, 5H, η$^5$-C$_5$*H*$_5$), 2.19 (s, 6H, α-C*H*$_3$), 1.92 (s, 6H, β-C*H*$_3$) ppm. IR (CH$_2$Cl$_2$, 25 °C) $\nu_{CO}$ 2005(vs), 1955(vs) cm$^{-1}$. HR-MS (ESI, MeCN, +ve ion) found *m*/*z* 359.9991 (calc. for C$_{14}$H$_{17}$O$_2$$^{75}$As$_1$$^{56}$Fe$_1$ [*M*]$^+$: 359.9995).

On one occasion, colourless crystals of *endo*-Cl$_2$As$_2$C$_8$Me$_8$ separated from the reaction mixture. This compound could be deliberately prepared by heating ClAsC$_4$Me$_4$ to reflux in *n*-hexane, though could not be obtained in a pure state.

Crystals grown from *n*-hexane solution at ambient temperature. C$_{16}$H$_{24}$As$_2$Cl$_2$ (*M* = 437.09 g/mol): colourless prism 0.37 × 0.261 × 0.222 mm, monoclinic, space group *P*2$_1$/*n* (no. 14), *a* = 14.355(4) Å, *b* = 9.7741(6) Å, *c* = 20.102(5) Å, *β* = 141.48(5)°, *V* = 1756.7(14) Å$^3$, *Z* = 4, empirical correction $T_{min}/T_{max}$ = 0.89692/1.00000, *μ*(Mo-Kα) = 4.098 mm$^{-1}$, $\varrho_{calc}$ = 1.653 g/cm$^3$, 12271 reflections measured (6.508° ≤ 2Θ ≤ 64.802°), 5547 unique ($R_{int}$ = 0.0320, $R_{sigma}$ = 0.0535) which were used in all calculations, *GOF* = 1.036. $D_{min}/D_{max}$ = -0.70/0.89 e/Å$^3$. The final $R_1$ was 0.0377 (I > 2σ(I)) and $wR_2$ was 0.0811 (all data).

### 4.1.12 [Mo{AsC$_4$(H)(SiMe$_3$)Me$_2$}(CO)$_3$(η$^5$-C$_5$H$_5$)]




To a solution of 1 g ClAsC$_4$(SiMe$_3$)$_2$Me$_2$ (3 mmol) in 25 mL *n*-hexane was added and 1.7 g [Mo(SnBu$_3$)(CO)$_3$(η$^5$-C$_5$H$_5$)] (3.1 mmol). An immediate colour change from yellow to a deep orange occurs, and after stirring for 2 hours the mixture is transferred to a water-jacketed column of neutral alumina (35 x 2.5 cm) made up in *n*-pentane under nitrogen. Eluting with 19:1 *n*-pentane/Et$_2$O, followed by 4:1 *n*-pentane/Et$_2$O provides an orange band which is

collected under nitrogen and taken to dryness. The material is re-crystallised from *n*-pentane at -30 °C. Isolated yield 0.45 g (0.95 mmol, 31%). The product is readily soluble in most common organic solvents and is air sensitive in solution however the solid product may be handled for a brief while.

NMR: $^{1}$H ($C_6D_6$, 400 MHz, 25 °C) δ 7.50 (s, 1H, α-C*H*), 4.62 (s, 5H, η$^5$-$C_5H_5$), 2.21 (s, 3H, β-C$H_3$), 2.04 (s, 3H, β-C$H_3$), 0.38 (s, 9H, Si(C$H_3$)$_3$) ppm; $^{13}$C{$^{1}$H} ($C_6D_6$, 176 MHz, 25 °C) δ 235.7 (*transoid* *C*O), 225.6 (*cisoid* *C*O), 223.6 (*cisoid* *C*O), 158.4 (arsole {3,4}-*C*), 157.2 (arsole {3,4}-*C*), 149.7 (arsole *C*H), 146.7 (arsole *C*-Si), 92.9 (η$^5$-$C_5H_5$), 20.5 (β-*C*H$_3$), 19.5 (β-*C*H$_3$), 2.0 (Si(*C*H$_3$)$_3$) ppm. IR ($CH_2Cl_2$, 25 °C) $\nu_{CO}$ 2007(vs), 1938(sh), 1922(vs) cm$^{-1}$. HR-MS (ESI, MeCN, +ve ion) found *m*/*z* 490.9551 (calc. for $C_{17}H_{21}O_4{}^{75}As_1{}^{98}Mo_1{}^{28}Si_1$ [*M* + O]$^+$: 490.9554). Analysis found 43.33% C, 4.74% H (calc. for $C_{17}H_{21}O_3As_1Mo_1Si_1$ 43.23% C, 4.48% H).

Crystals grown from evaporation of *n*-pentane solution at -30 °C. $C_{17}H_{21}As_1Mo_1O_3Si_1$ (*M* = 472.29 g/mol): orange needle 0.414 × 0.077 × 0.066 mm, orthorhombic, space group $P2_12_12_1$ (no. 19), *a* = 6.65790(10) Å, *b* = 13.0043(2) Å, *c* = 22.3782(5) Å, *V* = 1937.53(6) Å$^3$, *Z* = 4, Gaussian correction $T_{min}/T_{max}$ = 0.321/1.000, $\mu$(Cu-Kα) = 8.116 mm$^{-1}$, $\varrho_{calc}$ = 1.619 g/cm$^3$, 7373 reflections measured (7.864° ≤ 2Θ ≤ 147.634°), 3665 unique ($R_{int}$ = 0.0269, $R_{sigma}$ = 0.0383) which were used in all calculations, *GOF* = 1.036, $D_{min}/D_{max}$ = -0.45/0.4 e/Å$^3$. The final $R_1$ was 0.0264 (I > 2σ(I)) and $wR_2$ was 0.0617 (all data).

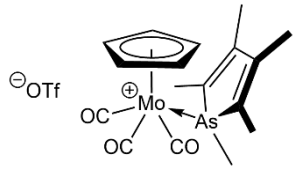
### 4.1.13 Reaction between [Mo(SnBu$_3$)(CO)$_3$(η$^5$-C$_5$H$_5$)] and ClAsC$_4$(*t*-Bu)$_2$Me$_2$

To a stirred solution of 1 g ClAsC$_4$(*t*-Bu)$_2$Me$_2$ (3.3 mmol) in 25 mL *n*-hexane was added 1.8 g [Mo(SnBu$_3$)(CO)$_3$(η$^5$-C$_5$H$_5$)] (3.4 mmol). A rapid colour change from yellow to a deep red takes place, and after 3 h the mixture was transferred to a column of neutral alumina (30 x 2.5 cm) made up in *n*-pentane under nitrogen. Eluting with 19:1 *n*-pentane/Et$_2$O, followed by 4:1 *n*-pentane/Et$_2$O gives a red band containing [Mo$_2$(CO)$_6$(η$^5$-C$_5$H$_5$)$_2$] as the only molybdenum-containing product. Isolated yield: 0.55 g (1.1 mmol, 66%).

NMR: $^{1}$H ($C_6D_6$, 400 MHz, 25 °C) δ 4.68 ppm. IR ($CH_2Cl_2$, 25 °C) $\nu_{CO}$ 2014(m), 1958(vs) and 1912(s) cm$^{-1}$. Identity confirmed by comparison with an authentic sample.

### 4.1.14 Alkylation of Molybdenum Arsolyl Complexes

#### 4.8.1.12 [Mo(MeAsC$_4$Me$_4$)(CO)$_3$(η$^5$-C$_5$H$_5$)]OTf



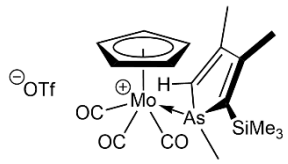

To a solution of 0.1 g [Mo(AsC$_4$Me$_4$)(CO)$_3$(η$^5$-C$_5$H$_5$)] (0.23 mmol) in 5 mL Et$_2$O cooled to 0 °C is added two-to-three drops neat MeOTf (excess. **Caution**: carcinogen) with swirling. Allowing the mixture to stand at ambient temperature for a few minutes gives a colour change from orange to yellow with the precipitation of bright yellow crystals. Cooling to -20 °C overnight affects complete crystallisation and the product is collected by decanting the pale-yellow supernatant (**caution**: residual MeOTf) and washing with Et$_2$O (3 x 3 mL portions) and *n*-pentane (2 x 3 mL portions) and dried under vacuum. Isolated yield 0.12 g (0.2 mmol, 86%). The salt is readily soluble in polar organic solvents

and may be handled in air as a solid or solution for a short while. Too great an excess of MeOTf is to be avoided and invites decomposition to oily brown residues.

NMR: $^{1}$H ($CD_2Cl_2$, 400 MHz, 25 °C) δ 5.54 (s, 5H, η$^5$-$C_5H_5$), 1.95 (s, 6H, α-$CH_3$), 1.82 (s, 6H, β-$CH_3$), 1.66 (s, 3H, As-$CH_3$) ppm. $^{13}$C{$^{1}$H} ($CD_2Cl_2$, 176 MHz, 25 °C) δ 225.8 (*transoid CO*), 223.2 (*cisoid CO*), 145.8 (arsole {2,5}-*C*), 134.5 (arsole {3,4}-*C*), 121.6 (q, $^{1}J_{FC}$ = 321.2 Hz, [$SO_3CF_3$]$^-$), 94.3 (η$^5$-$C_5H_5$), 14.8 (α-$CH_3$), 13.8 (β-$CH_3$), 11.7 (As-$CH_3$) ppm. IR ($CH_2Cl_2$, 25 °C) $\nu_{CO}$ 2057(vs), 1998(sh), 1965(vs) cm$^{-1}$. HR-MS (ESI, MeCN, +ve ion) found *m*/*z* 444.9686 (calc. for $C_{17}H_{20}O_3{}^{75}As_1{}^{98}Mo_1$ [*M*]$^+$: 444.9685). Analysis found 36.60% C, 3.41% H, 5.48% S (calc. for $C_{18}H_{20}O_6As_1F_3Mo_1S_1$ 36.50% C, 3.40% H, 5.41% S).

Crystals grown from $Et_2O$ solution at -20 °C. $C_{18}H_{20}As_1F_3Mo_1O_6S_1$ (*M* = 592.26 g/mol): yellow plate 0.183 × 0.145 × 0.046 mm, triclinic, space group *P*-1 (no. 2), *a* = 8.2247(2) Å, *b* = 8.7800(3) Å, *c* = 15.8527(5) Å, *α* = 98.816(2)°, *β* = 95.151(2)°, *γ* = 93.888(2)°, *V* = 1122.80(6) Å$^3$, *Z* = 2, analytical correction $T_{min}/T_{max}$ = 0.55803/0.59151, *μ*(Cu-Kα) = 7.804 mm$^{-1}$, $\varrho_{calc}$ = 1.752 g/cm$^3$, 8310 reflections measured (10.23° ≤ 2Θ ≤ 147.27°), 4447 unique ($R_{int}$ = 0.0298, $R_{sigma}$ = 0.0440) which were used in all calculations, *GOF* = 1.044, $D_{min}/D_{max}$ = -0.59/1.21 e/Å$^3$. The final $R_1$ was 0.0331 (I > 2σ(I)) and *w*$R_2$ was 0.0866 (all data).

### 4.8.1.13 [Mo{$MeAsC_4(H)(SiMe_3)Me_2$}$(CO)_3$(η$^5$-$C_5H_5$)]OTf

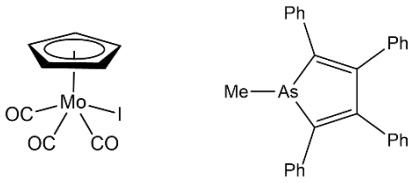



Prepared in an identical fashion to that above. Quantities: 0.1 g [Mo{$AsC_4(H)(SiMe_3)Me_2$}$(CO)_3$(η$^5$-$C_5H_5$)] (0.21 mmol), two-to-three drops neat MeOTf. Obtained as large bright yellow crystals which precipitate from the reaction mixture. Isolated yield: 0.11 g (0.17 mmol, 81%).

NMR: $^{1}$H ($CD_2Cl_2$, 400 MHz, 25 °C) δ 6.97 (s, 1H, α-*CH*), 5.81 (s, 5H, η$^5$-$C_5H_5$), 2.23 (s, 3H, β-$CH_3$), 2.16 (s, 3H, β-$CH_3$), 1.93 (s, 3H, As-$CH_3$), 0.31 (s, 9H, Si($CH_3$)$_3$) ppm. $^{13}$C{$^{1}$H} δ 227.5 (*transoid CO*), 225.0 (*cisoid CO*), 224.1 (*cisoid CO*), 161.3 (arsole {3,4}-*C*), 153.1 (arsole {3,4}-*C*), 142.1 (arsole *C*-Si), 133.5 (arsole *C*H), 121.6 (q, $^{1}J_{FC}$ = 321.2 Hz, [$SO_3CF_3$]$^-$), 94.4 (η$^5$-$C_5H_5$), 19.4 (β-$CH_3$), 18.7 (β-$CH_3$), 13.0 (As-$CH_3$), 0.8 (Si($CH_3$)$_3$) ppm. IR ($CH_2Cl_2$, 25 °C) $\nu_{CO}$ 2056(vs), 1994(sh), 1971(vs) cm$^{-1}$. HR-MS (ESI, MeCN, +ve ion) found *m*/*z* 488.9767 (calc. for $C_{18}H_{24}O_3{}^{75}As_1{}^{98}Mo_1{}^{28}Si_1$ [*M*]$^+$: 488.9770). Analysis found 35.90% C, 3.59% H, 5.11% S (calc. for $C_{19}H_{24}O_6As_1F_3Mo_1S_1Si_1$ 35.86% C, 3.80% H, 5.04% S).

Crystals grown from $Et_2O$ solution at -20 °C. $C_{19}H_{24}As_1F_3Mo_1O_6S_1Si_1$ (*M* = 636.39 g/mol): yellow prism 0.223 × 0.107 × 0.087 mm, monoclinic, space group $P2_1/n$ (no. 14), *a* = 16.9991(3) Å, *b* = 23.3532(3) Å, *c* = 7.29480(10) Å, *β* = 119.920(3)°, *V* = 2509.95(9) Å$^3$, *Z* = 4, spherical correction $T_{min}/T_{max}$ = 0.51041/0.54879, *μ*(Cu-Kα) = 7.470 mm$^{-1}$, $\varrho_{calc}$ = 1.684 g/cm$^3$, 9888 reflections measured (9.664° ≤ 2Θ ≤ 147.312°), 4964 unique ($R_{int}$ = 0.0207, $R_{sigma}$ = 0.0294) which were used in all calculations, *GOF* = 1.027, $D_{min}/D_{max}$ = -0.79/1.50 e/Å$^3$. The final $R_1$ was 0.0411 (I > 2σ(I)) and *w*$R_2$ was 0.1108 (all data).

### 4.8.1.14 Reaction between $[Mo(AsC_4Ph_4)(CO)_3(\eta^5\text{-}C_5H_5)]$ and $CH_3I$




To a solution of 0.2 g $[Mo(AsC_4Ph_4)(CO)_3(\eta^5\text{-}C_5H_5)]$ (0.3 mmol) in 5 mL $CH_2Cl_2$ is added two-to-three drops neat $CH_3I$ (excess. **Caution**: carcinogen) and allowed to stir overnight. A colour change from orange to a deep red takes place. The mixture is absorbed onto a small quantity of neutral alumina by evaporation of the solvent and transferred to a column of neutral alumina (25 x 1 cm) made up in petroleum ether. Eluting with 9:1 petroleum ether/$Et_2O$ provides a red band of $[MoI(CO)_3(\eta^5\text{-}C_5H_5)]$. Isolated yield 0.092 g (0.25 mmol, 83%).

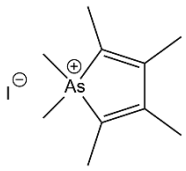
NMR: $^1H$ ($C_6D_6$, 400 MHz, 25 °C) δ 4.44 (s, 5H, $\eta^5\text{-}C_5H_5$) ppm. IR ($CH_2Cl_2$, 25 °C) $\nu_{CO}$ 2043(vs), 1966(vs) $cm^{-1}$. Identity confirmed by comparison with an authentic sample.

Eluting with 2:1 petroleum ether/$CH_2Cl_2$ provides a yellow band of $MeAsC_4Ph_4$ which is dried by rotary evaporation and re-crystallised from $CH_2Cl_2$/*n*-hexane at -20 °C. Isolated yield 0.095 g (0.21 mmol, 70%).

NMR: $^1H$ ($CDCl_3$, 400 MHz, 25 °C) δ 7.17—7.10 (m, 10H, $C_6H_5$), 7.08—7.40 (m, 6H, $C_6H_5$), 6.92—6.89 (m, 4H, $C_6H_5$), 1.48 (s, 3H, $CH_3$) ppm. $^{13}C\{^1H\}$ ($CDCl_3$, 176 MHz, 25 °C) δ 153.8 (arsole {2,5}-*C*), 149.1 (arsole {3,4}-*C*), 139.0 ($C_6H_5$), 138.5 ($C_6H_5$), 130.0 ($C_6H_5$), 129.2 ($C_6H_5$), 128.1 ($C_6H_5$), 127.6 ($C_6H_5$), 126.4 ($C_6H_5$), 10.0 ($CH_3$) ppm. HR-MS (EI, MeCN, +ve ion) found *m*/*z* 466.1006 (calc. for $C_{29}H_{23}{}^{75}As_1$ $[M]^+$: 446.1010). Analysis found 78.07% C, 5.28% H (calc. for $C_{29}H_{23}As_1$ 78.02% C, 5.19% H).

Crystals grown from $CH_2Cl_2$/*n*-hexane at -20 °C; the As-$CH_3$ moity was disordered over two positions by inflection about the mean arsole ring plane (occupancy ratio *ca.* 89:11) and was modelled accordingly. $C_{29}H_{23}As_1$ ($M$ = 446.39 g/mol): yellow prism 0.204 × 0.143 × 0.083 mm, tetragonal, space group $I4_1/a$ (no. 88), $a$ = 26.5014(2) Å, $c$ = 12.16700(10) Å, $V$ = 8545.18(15) Å$^3$, $Z$ = 16, empirical correction $T_{min}/T_{max}$ = 0.96719/1.00000, $\mu$(Cu-Kα) = 2.230 $mm^{-1}$, $\varrho_{calc}$ = 1.388 g/cm$^3$, 11604 reflections measured (7.996° ≤ 2Θ ≤ 147.138°), 4256 unique ($R_{int}$ = 0.0137, $R_{sigma}$ = 0.0168) which were used in all calculations, $GOF$ = 1.173, $D_{min}/D_{max}$ = -0.30/0.69 e/Å$^3$. The final $R_1$ was 0.0399 (I > 2σ(I)) and $wR_2$ was 0.1001 (all data).

### 4.8.1.15 Reaction between $[Mo(AsC_4Me_4)(CO)_3(\eta^5\text{-}C_5H_5)]$ and $CH_3I$




To a solution of 0.15 g $[Mo(AsC_4Me_4)(CO)_3(\eta^5\text{-}C_5H_5)]$ (0.35 mmol) in *ca* 1 mL $C_6D_6$ is added one-to-two drops neat $CH_3I$ (excess). Over the course of *ca* 5 minutes the colour begins to change from orange to a deep red, and after standing overnight large colourless crystals separate. The supernatant is decanted, and the crystals washed with $Et_2O$ (3 x 2 mL) and *n*-pentane (2 x 2 mL) and dried under vacuum. Yield: 0.076 g (0.22 mmol, 62%). $[Me_2AsC_4Me_4]I$ may be handled for a short while in air as a solution however decomposes to oily brown residues overnight; the solid

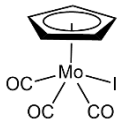
crystals are unchanged in air overnight however gain a brown cast over several days. The same compound (as the triflate salt) is also obtained by treatment of $Et_2O$ solutions of $MeAsC_4Me_4$ with neat MeOTf at 0 °C.

NMR: $^1$H ($CDCl_3$, 400 MHz, 25 °C) δ 2.58 (s, 6H, As-($CH_3$)$_2$), 2.32 (s, 6H, α-$CH_3$), 2.00 (s, 6H, β-$CH_3$) ppm. $^{13}$C{$^1$H} ($CDCl_3$, 176 MHz, 25 °C) δ 150.3 (arsole {2,5}-*C*), 123.5 (arsole {3,4}-*C*), 15.0 (α-$CH_3$), 14.2 (β-$CH_3$), 9.28 (As-($CH_3$)$_2$) ppm. HR-MS (ESI, MeCN, +ve ion) found $m/z$ 213.0628 (calc. for $C_{10}H_{18}{}^{75}As_1$ $[M]^+$: 213.0625). Analysis found 35.39% C, 5.36% H (calc. for $C_{10}H_{18}As_1I_1$ 35.32% C, 5.34% H).

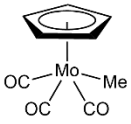
Crystals grown from $C_6D_6$ solution at ambient temperature. $C_{10}H_{18}As_1I_1$ ($M$ = 340.06 g/mol): colourless prism 0.298 × 0.085 × 0.056 mm, monoclinic, space group $P2_1/c$ (no. 14), $a$ = 7.9883(4) Å, $b$ = 7.6338(3) Å, $c$ = 21.1208(8) Å, $\beta$ = 91.549(4)°, $V$ = 1287.50(10) Å$^3$, $Z$ = 4, spherical correction $T_{min}/T_{max}$ = 0.48902/0.50085, $\mu$(Mo-Kα) = 4.995 mm$^{-1}$, $\varrho_{calc}$ = 1.754 g/cm$^3$, 24274 reflections measured (6.48° ≤ 2Θ ≤ 64.82°), 4258 unique ($R_{int}$ = 0.0406, $R_{sigma}$ = 0.0344) which were used in all calculations, $GOF$ = 1.046, $D_{min}/D_{max}$ = -0.56/0.74 e/Å$^3$. The final $R_1$ was 0.0322 (I > 2σ(I)) and $wR_2$ was 0.0583 (all data).

The remainder of the red $C_6D_6$ solution contains [MoI(CO)$_3$(η$^5$-$C_5H_5$)] as the major product (δ 4.44 ppm), [MoMe(CO)$_3$(η$^5$-$C_5H_5$)] (δ 4.41, 0.39 ppm) and tentatively [MoI($MeAsC_4Me_4$)(CO)$_2$(η$^5$-$C_5H_5$)] as the minor species (δ 4.74 ppm; the specific isomer (*cis* or *trans*) is not known) in an approximate ratio of 1 : 0.14 : 0.06, respectively, by integration of the η$^5$-$C_5H_5$ signals. No convincing evidence for an acyl complex was found (*cf.* *trans*-[Mo{C(O)Me}(PMe$_3$)(CO)$_2$(η$^5$-$C_5H_5$)] $^1$H ($C_6D_6$) δ 4.93 (η$^5$-$C_5H_5$), 2.90 (C(O)$CH_3$) ppm. See W. Malisch, H. Blau and F.J. Haaf *Chem. Ber.*, **1981**, *114*, 2956—2970).

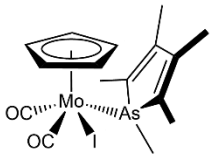
Repeating the reaction in *n*-hexane solution at -30 °C provides a mixture of colourless, yellow, and red crystals, all of which were analysed by X-ray diffraction.



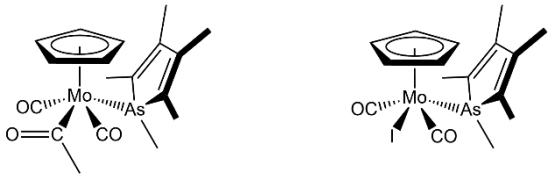

[MoI(CO)$_3$(η$^5$-$C_5H_5$)]: crystals grown from *n*-hexane solution at -30 °C. $C_8H_5I_1Mo_1O_3$ ($M$ = 371.96 g/mol): red prism 0.2 × 0.138 × 0.074 mm, monoclinic, space group $P2_1/n$ (no. 14), $a$ = 10.4658(3) Å, $b$ = 7.8509(2) Å, $c$ = 12.0747(3) Å, $\beta$ = 90.736(2)°, $V$ = 992.05(5) Å$^3$, $Z$ = 4, spherical correction $T_{min}/T_{max}$ = 0.57918/0.61017, $\mu$(Cu-Kα) = 35.053 mm$^{-1}$, $\varrho_{calc}$ = 2.490 g/cm$^3$, 3425 reflections measured (11.118° ≤ 2Θ ≤ 146.448°), 1924 unique ($R_{int}$ = 0.0343, $R_{sigma}$ = 0.0457) which were used in all calculations, $GOF$ = 1.054, $D_{min}/D_{max}$ = -2.02/2.29 e/Å$^3$. The final $R_1$ was 0.0464 (I > 2σ(I)) and $wR_2$ was 0.1216 (all data).



[MoMe(CO)$_3$($\eta^5$-C$_5$H$_5$)]: This complex was identified by agreement with the unit cell dimensions reported by VALENTE.[63] Monoclinic *P*2$_1$ (no. 4), *a* = 7.5663(4) Å, *b* = 7.7019(4) Å, *c* = 8.2091(4) Å, β = 96.837(3), *V* = 474.98(4) Å$^3$.

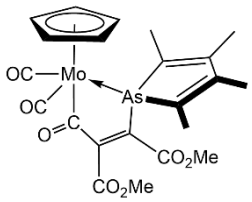



*Cis*-[MoI(MeAsC$_4$Me$_4$)(CO)$_3$($\eta^5$-C$_5$H$_5$)]: crystals grown from *n*-hexane solution at -30 °C; two independent molecules were found in the asymmetric unit. C$_{16}$H$_{20}$AsI$_1$Mo$_1$O$_2$ (*M* = 542.08 g/mol): red prism 0.285 × 0.217 × 0.142 mm, triclinic, space group *P*-1 (no. 2), *a* = 8.8572(3) Å, *b* = 13.9206(4) Å, *c* = 16.0715(5) Å, *a* = 104.867(3)°, *β* = 104.316(3)°, *γ* = 91.742(2)°, *V* = 1846.43(11) Å$^3$, *Z* = 4, spherical correction $T_{min}/T_{max}$ = 0.46185/0.50578, $\mu$(Cu-Kα) = 20.938 mm$^{-1}$, $\varrho_{calc}$ = 1.950 g/cm$^3$, 11500 reflections measured (7.562° ≤ 2Θ ≤ 146.734°), 7149 unique ($R_{int}$ = 0.0306, $R_{sigma}$ = 0.0444) which were used in all calculations, *GOF* = 1.067, $D_{min}/D_{max}$ = -1.64/1.13 e/Å$^3$ . The final $R_1$ was 0.0355 (I > 2σ(I)) and $wR_2$ was 0.0927 (all data).




Co-crystallite of *trans*-[Mo{C(O)Me}(MeAsC$_4$Me$_4$)(CO)$_2$($\eta^5$-C$_5$H$_5$)] and *trans*-[MoI(MeAsC$_4$Me$_4$)(CO)$_2$($\eta^5$-C$_5$H$_5$)]: crystals grown from *n*-hexane solution at -30 °C; the complexes are superimposed in a occupancy ratio of *ca* 89:11, respectively. C$_{17.7825}$H$_{22.675}$As$_1$I$_{0.1075}$Mo$_1$O$_{2.8925}$ (*M* = 467.20 g/mol): monoclinic, space group *P*2$_1$/*c* (no. 14), *a* = 8.23480(10) Å, *b* = 9.7875(2) Å, *c* = 23.5300(4) Å, *β* = 97.499(2)°, *V* = 1880.25(6) Å$^3$, *Z* = 4, spherical correction $T_{min}/T_{max}$ = 0.470/0.512, $\mu$(Cu-Kα) = 9.128 mm$^{-1}$, $\varrho_{calc}$ = 1.650 g/cm$^3$, 6393 reflections measured (7.58° ≤ 2Θ ≤ 145.896°), 3644 unique ($R_{int}$ = 0.0231, $R_{sigma}$ = 0.0345) which were used in all calculations, *GOF* = 1.119, $D_{min}/D_{max}$ = -0.86/0.60 e/Å$^3$. The final $R_1$ was 0.0339 (I > 2σ(I)) and $wR_2$ was 0.498 (all data).

### 4.1.15 [Mo{C(O)C(CO$_2$Me)=C(CO$_2$Me)AsC$_4$Me$_4$}(CO)$_2$($\eta^5$-C$_5$H$_5$)]



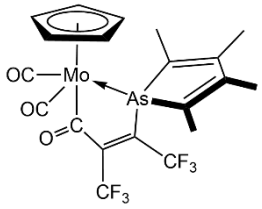

To a stirred solution of 0.2 g [Mo(AsC$_4$Me$_4$)(CO)$_3$($\eta^5$-C$_5$H$_5$)] (0.47 mmol) in 10 mL $CH_2Cl_2$ is added *ca* 100 mg neat dimethylacetylene dicarboxylate (DMAD, 0.75 mmol). The orange colour rapidly darkens over the course of a few minutes. Workup is now carried out without exclusion of air or moisture. After 15 minutes, the mixture is transferred to a short column of Florisil® (10 x 1 cm) made up in $Et_2O$. Eluting with 3:1 $Et_2O/CH_2Cl_2$, followed by neat $CH_2Cl_2$

provides an orange-red band which is collected and dried by rotary evaporation. Isolated yield: 0.23 g (0.40 mmol, 85%). The product is readily soluble in polar organic and aromatic solvents and is reasonably air stable as a solid or in solution. The use of silica gel or alumina appeared to decompose the product.

NMR: $^{1}$H ($C_6D_6$, 400 MHz, 25 °C) δ 4.82 (s, 5H, η$^5$-$C_5H_5$), 3.45 (s, 3H, $CO_2CH_3$), 3.23 (s, 3H, $CO_2CH_3$), 1.88 (s, 3H, α-$CH_3$), 1.59 (s, 3H, α-$CH_3$), 1.54 (s, 6H, β-$CH_3$) ppm. $^{13}$C{$^{1}$H} ($C_6D_6$, 176 MHz, 25 °C) δ 263.2 (terminal *C*O), 245.5 (terminal *C*O), 234.7 (acyl *C*O), 167.1 ($CO_2CH_3$), 165.9 ($CO_2CH_3$), 161.0 (C(O)-*C*=C), 149.7 (C=*C*-As), 146.5 (arsole {2,5}-*C*), 146.2 (arsole {2,5}-*C*), 133.5 (arsole {3,4}-*C*), 132.9 (arsole {3,4}-*C*), 91.8 (η$^5$-$C_5H_5$), 52.1 ($CO_2CH_3$), 51.9 ($CO_2CH_3$) 14.5 (α-$CH_3$), 14.4 (α-$CH_3$) 13.4 (β-$CH_3$), 13.2 (β-$CH_3$) ppm. IR ($CH_2Cl_2$, 25 °C) $\nu_{CO}$ 1962(vs), 1889(s), 1732(s), 1605(m), 1580(sh) cm$^{-1}$. HR-MS (ESI, MeCN, +ve mode) found *m*/*z* 572.9797 (calc. for $C_{22}H_{23}O_7{}^{75}As_1{}^{98}Mo_1$ [*M*]$^+$: 572.9800). Analysis found 46.31% C, 4.16% H (calc. for $C_{22}H_{23}O_7As_1Mo_1$ 46.33% C, 4.07% H).

Crystals grown from evaporation of $Et_2O$ solution at -20 °C. $C_{22}H_{23}As_1Mo_1O_7$ (*M* = 570.26 g/mol): orange prism 0.416 × 0.156 × 0.07 mm, triclinic, space group *P*-1 (no. 2), *a* = 8.3557(3) Å, *b* = 8.5540(2) Å, *c* = 15.9822(6) Å, *α* = 80.769(3)°, *β* = 87.205(3)°, *γ* = 81.552(2)°, *V* = 1114.92(6) Å$^3$, *Z* = 2, empirical correction 0.80946/1.00000, *μ*(Mo-Kα) = 2.101 mm$^{-1}$, $\rho_{calc}$ = 1.699 g/cm$^3$, 23753 reflections measured (6.53° ≤ 2Θ ≤ 65.278°), 7225 unique ($R_{int}$ = 0.0354, $R_{sigma}$ = 0.0442) which were used in all calculations, *GOF* = 1.059, $D_{min}/D_{max}$ = -0.63/0.58 e/Å$^3$. The final $R_1$ was 0.0308 (I > 2σ(I)) and $wR_2$ was 0.0678 (all data).

### 4.1.16 [Mo{C(O)C(CF$_3$)=C(CF$_3$)AsC$_4$Me$_4$}(CO)$_2$(η$^5$-C$_5$H$_5$)]




To a stirred solution of 0.2 g [Mo(AsC$_4$Me$_4$)(CO)$_3$(η$^5$-C$_5$H$_5$)] (0.47 mmol) in 10 mL $CH_2Cl_2$ cooled to -78 °C is condensed an excess of hexafluoro-2-butyne (B.P. = -25 °C. **Caution**: **asphyxiant**) by passing a gentle stream of the gas over the cooled surface for *ca* 20 seconds. The mixture is allowed to slowly warm to ambient temperature (with venting of excess gas) over the course of *ca* 30 minutes, and the orange colour becomes a more intense orange-red during this time. The mixture is transferred to a short column of Florisil® (10 x 1 cm) and eluted with $Et_2O$ giving a bright orange band which is collected and dried by rotary evaporation. Isolated yield 0.25 g (0.42 mmol, 90%). The product is readily soluble in polar organic and aromatic solvents and is reasonably air stable as a solid or in solution.

NMR: $^{1}$H ($C_6D_6$, 400 MHz, 25 °C) δ 4.77 (s, 5H, η$^5$-$C_5H_5$), 1.89 (s, 3H, α-$CH_3$), 1.45 (s, 3H, α-$CH_3$), 1.41 (s, 3H, β-$CH_3$), 1.39 (s, 3H, β-$CH_3$) ppm. $^{13}$C{$^{1}$H} ($C_6D_6$, 176 MHz, 25 °C) δ 261.4 (terminal *C*O), 243.2 (terminal *C*O), 233.6 (acyl *C*O), 147.5 (arsole {2,5}-*C*), 146.5 (arsole {2,5}-*C*), 133.2 (arsole {3,4}-*C*), 133.0 (arsole {3,4}-*C*), 123.2 (C(O)-*C*=C), 93.3 (η$^5$-$C_5H_5$), 88.8 (C=*C*-As), 30.5 (*C*F$_3$), 27.8 (*C*F$_3$), 14.4 (α-$CH_3$), 14.3 (α-$CH_3$), 13.7 (β-$CH_3$), 12.9 (β-$CH_3$) ppm. $^{19}$F{$^{1}$H} ($C_6D_6$, 376 MHz, 25 °C) δ -56.7 (q, $J_{FF}$ = 10.2 Hz, 3F), -59.1 (q, $J_{FF}$ = 10.2 Hz, 3F) ppm. IR ($CH_2Cl_2$, 25 °C) $\nu_{CO}$ 1968(vs), 1894(s), 1599(m) cm$^{-1}$. HR-MS (ESI, MeCN, +ve ion) found *m*/*z* 592.9434 (calc. for $C_{20}H_{17}O_3{}^{75}As_1{}^{19}F_6{}^{98}Mo_1$ [*M*]$^+$: 592.9432). Analysis found 40.54% C, 3.07% H (calc. for $C_{20}H_{17}O_3As_1F_6Mo_1$: 40.70% C, 2.90% H).

Crystals grown from evaporation of $Et_2O$ solution at -20 °C. $C_{20}H_{17}As_1F_6Mo_1O_3$ ($M$ = 590.20 g/mol): orange plate 0.261 × 0.109 × 0.052 mm, monoclinic, space group $P2_1/n$ (no. 14), $a$ = 8.62420(10) Å, $b$ = 17.9549(2) Å, $c$ = 14.1123(2) Å, $\beta$ = 103.3860(10)°, $V$ = 2125.87(5) Å$^3$, $Z$ = 4, Gaussian correction $T_{min}/T_{max}$ = 0.333/1.000, $\mu$(Cu-Kα) = 7.451 mm$^{-1}$, $\rho_{calc}$ = 1.844 g/cm$^3$, 13901 reflections measured (8.106° ≤ 2Θ ≤ 147.496°), 4288 unique ($R_{int}$ = 0.0247, $R_{sigma}$ = 0.0260) which were used in all calculations, $GOF$ = 1.049, $D_{min}/D_{max}$ = -1.16/1.06 e/Å$^3$. The final $R_1$ was 0.0420 (I > 2σ(I)) and $wR_2$ was 0.1066 (all data).

## 4.9 References


1. E. W. Abel and C. Towers, *J. Chem. Soc. Dalton Trans.*, **1979**, 814-819.
2. G. Thiollet, F. Mathey and R. Poilblanc, *Inorg. Chim. Acta*, **1979**, *32*, L67-L68.
3. J. E. Ellis and E. A. Flom, *J. Organomet. Chem.*, **1975**, *99*, 263-268.
4. R. E. Dessy, R. L. Pohl and R. B. King, *J. Am. Chem. Soc.*, **1966**, *88*, 5121-5124.
5. C. K. Lai, W. G. Feighery, Y. Zhen and J. D. Atwood, *Inorg. Chem.*, **1989**, *28*, 3929-3930.
6. R. G. Pearson and P. E. Figdore, *J. Am. Chem. Soc.*, **1980**, *102*, 1541-1547.
7. P. J. Krusic, P. J. Fagan and J. San Filippo, Jr., *J. Am. Chem. Soc.*, **1977**, *99*, 250-252.
8. Y. Zhen, W. G. Feighery, C. K. Lai and J. D. Atwood, *J. Am. Chem. Soc.*, **1989**, *111*, 7832-7837.
9. N. G. Connelly and W. E. Geiger, *Chem. Rev.*, **1996**, *96*, 877-910.
10. T. Michael Bockman and J. K. Kochi, *J. Phys. Org. Chem.*, **1997**, *10*, 542-562.
11. G. Märkl, H. Hauptmann and A. Merz, *J. Organomet. Chem.*, **1983**, *249*, 335-363.
12. W. Malisch, H. Blau, H. Rößner and G. Jäth, *Chem. Ber.*, **1980**, *113*, 1180-1183.
13. P. K. Sazonov and I. P. Beletskaya, *Chem. Eur. J.*, **2016**, *22*, 3644-3653.
14. W. Malisch and M. Kuhn, *Angew. Chem.*, **1974**, *86*, 51-52.
15. W. Malisch and R. Alsmann, *Angew. Chem. Int. Ed. Eng.*, **1976**, *15*, 769-770.
16. W. Malisch, H. Schmidbaur and M. Kuhn, *Angew. Chem. Int. Ed. Eng.*, **1972**, *11*, 516-517.
17. W. Malisch, *J. Organomet. Chem.*, **1973**, *61*, C15-C19.
18. W. Malisch and M. Kuhn, *Chem. Ber.*, **1974**, *107*, 979-995.
19. P. Jutzi and K. Deuchert, *Angew. Chem. Int. Ed. Eng.*, **1969**, *8*, 991-992.
20. A. J. Ashe, *J. Am. Chem. Soc.*, **1971**, *93*, 3293-3295.
21. A. J. Ashe, X. Fang and J. W. Kampf, *Organometallics*, **2001**, *20*, 2109-2113.
22. S. Aldridge, R. J. Calder, R. E. Baghurst, M. E. Light and M. B. Hursthouse, *J. Organomet. Che.*, **2002**, *649*, 9-14.
23. H. Braunschweig, K. Radacki, F. Seeler and G. R. Whittell, *Organometallics*, **2006**, *25*, 4605-4610.
24. J. F. Hartwig and S. Huber, *J. Am. Chem. Soc.*, **1993**, *115*, 4908-4909.
25. H. R. H. Patil and W. A. G. Graham, *Inorg. Chem.*, **1966**, *5*, 1401-1405.
26. J. A. Gladysz, G. M. Williams, W. Tam, D. L. Johnson, D. W. Parker and J. C. Selover, *Inorg. Chem.*, **1979**, *18*, 553-558.
27. M. H. Chisholm, J. C. Huffman and J. W. Pasterczyk, *Inorg. Chem.*, **1987**, *26*, 3781-3785.
28. E. Lindner, M. Heckmann, R. Fawzi and W. Hiller, *Chem. Ber.*, **1991**, *124*, 2171-2179.
29. L. Weber, S. Uthmann, S. Kleinebekel, H. G. Stammler, A. Stammler and B. Neumann, *Z. Anorg. Allg. Chem.*, **2000**, *626*, 1831-1836.
30. A. L. Rheingold, M. J. Foley and P. J. Sullivan, *Organometallics*, **1982**, *1*, 1429-1432.
31. A. R. Manning, P. Hacket, R. Birdwhistell, P. Soye, D. C. Miller and R. J. Angelici, *Inorg. Synth.*, **1990**, 148-150.
32. T. A. Huber, D. H. Macartney and M. C. Baird, *Organometallics*, **1995**, *14*, 592-602.
33. A. J. Ashe, W. M. Butler and T. R. Diephouse, *Organometallics*, **1983**, *2*, 1005-1008.
34. S. C. Sendlinger, B. S. Haggerty, A. L. Rbeingold and K. H. Theopold, *Chem. Ber.*, **1991**, *124*, 2453-2456.
35. J. J. Eisch, J. E. Galle and S. Kozima, *J. Am. Chem. Soc.*, **1986**, *108*, 379-385.
36. G. E. Herberich and H. Ohst, *Chem. Ber.*, **1985**, *118*, 4303-4313.
37. G. E. Herberich, M. Negele and H. Ohst, *Chem. Ber.*, **1991**, *124*, 25-29.
38. F. Mathey, *Chem. Rev.*, **1988**, *88*, 429-453.
39. F. Mercier and F. Mathey, *J. Organomet. Chem.*, **1984**, *263*, 55-66.

40. F. Mathey, F. Mercier, C. Charrier, J. Fischer and A. Mitschler, *J. Am. Chem. Soc.,* **1981**, *103*, 4595-4597.
41. G. de Lauzon, C. Charrier, H. Bonnard, F. Mathey, J. Fischer and A. Mitschler, *J. Chem. Soc. Chem. Comm.*, **1982**, 1272-1273.
42. C. Charrier, H. Bonnard, G. de Lauzon and F. Mathey, *J. Am. Chem. Soc.,* **1983**, *105*, 6871-6877.
43. H. L. Ji, J. H. Nelson, A. DeCian, J. Fischer, B. Li, C. Wang, B. McCarty, Y. Aoki, J. W. Kenney, L. Solujic and E. B. Milosavljevic, *J. Organomet. Chem.,* **1997**, *529*, 395-408.
44. C. C. Santini, J. Fischer, F. Mathey and A. Mitschler, *J. Am. Chem. Soc.,* **1980**, *102*, 5809-5815.
45. W. L. Wilson, J. Fischer, R. E. Wasylishen, K. Eichele, V. J. Catalano, J. H. Frederick and J. H. Nelson, *Inorg. Chem.*, **1996**, *35*, 1486-1496.
46. W. L. Wilson, J. A. Rahn, N. W. Alcock, J. Fischer, J. H. Frederick and J. H. Nelson, *Inorg. Chem.*, **1994**, *33*, 109-117.
47. K. D. Redwine and J. H. Nelson, *Organometallics*, **2000**, *19*, 3054-3061.
48. M. Luksza, S. Himmel and W. Malisch, *Angew. Chem. Int. Ed. Eng.,* **1983**, *22*, 416-417.
49. F. Nief and L. Ricard, *Organometallics*, **2001**, *20*, 3884-3890.
50. J. D. Andose, A. Rauk and K. Mislow, *J. Am. Chem. Soc.,* **1974**, *96*, 6904-6907.
51. S. Pelzer, K. Wichmann, R. Wesendrup and P. Schwerdtfeger, *J. Phys. Chem. A*, **2002**, *106*, 6387-6394.
52. J. Kurita, M. Ishii, S. Yasuike and T. Tsuchiya, *J. Chem. Soc. Chem. Comm.,* **1993**, 1309-1310.
53. J. R. Chipperfield, A. C. Hayter and D. E. Webster, *J. Chem. Soc. Dalton Trans.,* **1977**, 485-490.
54. J. R. Chipperfield, A. C. Hayter and D. E. Webster, *J. Chem. Soc. Dalton Trans.,* **1977**, 921-924.
55. R. E. J. Bichler, M. R. Booth and H. C. Clark, *J. Organomet. Chem.,* **1970**, *24*, 145-158.
56. R. E. J. Bichler, H. C. Clark, B. K. Hunter and A. T. Rake, *J. Organomet. Chemn.,* **1974**, *69*, 367-376.
57. J. M. Burlitch, *J. Am. Chem. Soc.,* **1969**, *91*, 4562-4563.
58. D. F. Shriver, *Acc. Chem. Res.,* **1970**, *3*, 231-238.
59. D. F. Marten and S. M. Wilburn, *J. Organomet. Chem.,* **1983**, *251*, 71-78.
60. J. R. Chipperfield, J. Ford and D. E. Webster, *J. Chem. Soc. Dalton Trans.,* **1975**, 2042-2047.
61. M. Ishidoshiro, Y. Matsumura, H. Imoto, Y. Irie, T. Kato, S. Watase, K. Matsukawa, S. Inagi, I. Tomita and K. Naka, *Org. Lett.,* **2015**, *17*, 4854-4857.
62. H. Imoto, A. Urushizaki, I. Kawashima and K. Naka, *Chem. Eur. J.,* **2018**, *24*, 8797-8803.
63. M. Abrantes, P. Neves, M. M. Antunes, S. Gago, F. A. Almeida Paz, A. E. Rodrigues, M. Pillinger, I. S. Gonçalves, C. M. Silva and A. A. Valente, *J. Mol. Cat. A.*, **2010**, *320*, 19-26.
64. T. S. Piper and G. Wilkinson, *J. Inorg. Nucl. Chem.*, **1956**, *3*, 104-124.
65. M. Mickiewicz, K. P. Wainwright and S. B. Wild, *J. Chem. Soc. Dalton Trans.,* **1976**, 262-269.
66. J. L. Davidson and D. W. A. Sharp, *J. Chem. Soc. Dalton Trans.,* **1975**, 2531-2534.
67. G. B. McVicker, *Inorg. Chem.*, **1975**, *14*, 2087-2092.
68. J. L. Davidson, *J. Chem. Soc. Chem. Comm.,* **1980**, 113-114.
69. E. Viola, C. Lo Sterzo and F. Trezzi, *Organometallics*, **1996**, *15*, 4352-4354.
70. A. R. Manning, *J. Chem. Soc. A.* **1967**, 1984-1987.
71. A. Mawby and G. E. Pringle, *J. Inorg. Nucl. Chem.*, **1972**, *34*, 525-530.
72. J. H. Brownie, M. C. Baird and H. Schmider, *Organometallics*, **2007**, *26*, 1433-1443.
73. A. Ricci, F. Angelucci, M. Chiarini, C. Lo Sterzo, D. Masi, G. Giambastiani and C. Bianchini, *Organometallics*, **2008**, *27*, 1617-1625.
74. M. R. Anstey, J. L. Bost, A. S. Grumman, N. D. Kennedy and M. T. Whited, *Acta Cryst. E*, **2020**, *76*, 547-551.
75. M. T. Whited, M. A. Ball, A. Block, B. A. Brewster, L. Ferrer, H. J. Jin-Lee, C. J. King, J. D. North, I. L. Shelton and D. G. Wilson, *Acta Cryst. E*, **2021**, *77*, 912-918.
76. M. T. Whited, G. E. Hofmeister, C. J. Hodges, L. T. Jensen, S. H. Keyes, A. Ngamnithiporn and D. E. Janzen, *Acta Cryst. E,* **2014**, *70*, 216-220.
77. K. W. Barnett, D. L. Beach, S. P. Gaydos and T. G. Pollmann, *J. Organomet. Chem.,* **1974**, *69*, 121-130.
78. R. B. King and M. Saran, *Inorg. Chem.*, **1974**, *13*, 364-367.
79. G. Grötsch and W. Malisch, *J. Organomet. Chem.,* **1983**, *258*, 297-305.
80. P. J. Craig and J. Edwards, *J. Organomet. Chem.,* **1972**, *46*, 335-337.

81. J. M. Smith, D. P. White and N. J. Coville, *Polyhedron*, **1996**, *15*, 4541-4554.
82. W. E. Stanclift and D. G. Hendricker, *J. Organomet. Chem.,* **1973**, *50*, 175-184.
83. P. Kalck, R. Pince, R. Poilblanc and J. Roussel, *J. Organomet. Chem.,* **1970**, *24*, 445-452.
84. R. J. Mawby and G. Wright, *J. Organomet. Chem.,* **1970**, *21*, 169-170.
85. G. Wright and R. J. Mawby, *J. Organomet. Chem.,* **1973**, *51*, 281-287.
86. M. D. Bala, D. C. Levendis and N. J. Coville, *J. Organomet. Chem.*, **2006**, *691*, 1919-1926.
87. J. P. Bibler and A. Wojcicki, *Inorg. Chem.*, **1966**, *5*, 889-892.
88. K. W. Barnett and P. M. Treichel, *Inorg. Chem.*, **1967**, *6*, 294-299.
89. O. G. Adeyemi and N. J. Coville, *Organometallics*, **2003**, *22*, 2284-2290.
90. M. Kumar, A. J. Metta-Magana, H. K. Sharma and K. H. Pannell, *Dalton Trans.,* **2010**, *39*, 7125-7131.
91. S. A. Llewellyn, M. L. H. Green and A. R. Cowley, *Dalton Trans.*, **2006**, 1776-1783.
92. S. B. Butts, S. H. Strauss, E. M. Holt, R. E. Stimson, N. W. Alcock and D. F. Shriver, *J. Am. Chem. Soc.,* **1980**, *102*, 5093-5100.
93. P. M. Treichel and K. P. Wagner, *J. Organomet. Chem.,* **1975**, *88*, 199-206.
94. K. W. Barnett and T. G. Pollmann, *J. Organomet. Chem.,* **1974**, *69*, 413-421.
95. A. C. Gingell, A. Harris, A. J. Rest and R. N. Turner, *J. Organomet. Chem.,* **1976**, *121*, 205-210.
96. J. P. Collman, *Acc. Chem. Res.,* **1975**, *8*, 342-347.
97. A. Harris and A. J. Rest, *J. Organomet. Chem.,* **1974**, *78*, C29-C30.
98. W. D. Bannister, M. Green and R. N. Haszeldine, *Chem. Comm.,* **1965**, 54-56.
99. K. H. Pannell and H. K. Sharma, *Organometallics*, **2010**, *29*, 4741-4745.
100. A. C. Gingell and A. J. Rest, *J. Organomet. Chem.,* **1975**, *99*, C27-C28.
101. H. G. Alt, *J. Organomet. Chem.,* **1977**, *124*, 167-174.
102. W. A. Schenk and E. Voß, *J. Organomet. Chem.,* **1994**, *467*, 67-73.
103. M. Bruce, M. Papke, A. W. Ehlers, M. Weber, D. Lentz, N. Mézailles, J. C. Slootweg and C. Müller, *Chem. Eur. J.*, **2019**, *25*, 14332-14340.
104. F. Y. Pétillon, J. L. L. Quéré, F. L. Floch, J. E. Guerchais, M. B. Gomes de Lima, L. Manojlović-Muir, K. W. Muir and D. W. A. Sharp, *J. Organomet. Chem.,* **1983**, *255*, 231-244.
105. L. Carlton, J. L. Davidson and M. Shiralian, *J. Chem. Soc. Dalton Trans.,* **1986**, 1577-1586.
106. R. J. Barton, S. Hu, L. M. Mihichuk and B. E. Robertson, *Inorg. Chem.*, **1982**, *21*, 3731-3734.
107. H. Yoshio, S. Takaaki and K. Hiroshi, *Chem. Lett.,* **1983**, *12*, 1211-1214.
108. A. Marinetti, F. Mathey, J. Fischer and A. Mitschler, *J. Chem. Soc. Chem. Comm.,* **1982**, 667-668.
109. F. Mercier, L. Ricard and F. Mathey, *Organometallics*, **1993**, *12*, 98-103.
110. W. F. McNamara, E. N. Duesler and R. T. Paine, *Organometallics*, **1986**, *5*, 1747-1749.
111. M. T. Ashby and J. H. Enemark, *Organometallics*, **1987**, *6*, 1323-1327.
112. H. Adams, N. A. Bailey, A. N. Day, M. J. Morris and M. M. Harrison, *J. Organomet. Chem.,* **1991**, *407*, 247-258.
113. L. Weber, S. Kleinebekel and P. Lönnecke, *Z. Anorg. Allg. Chem.,* **2002**, *628*, 803-809.
114. M. A. Alvarez, M. E. García, M. A. Ruiz and J. Suárez, *Angew. Chem. Int. Ed.,* **2011**, *50*, 6383-6387.
115. W. R. Cullen, L. Mihichuk, F. W. B. Einstein and J. S. Field, *J. Organomet. Chem.,* **1974**, *73*, C53-C55.
116. J. P. Crow, W. R. Cullen and F. L. Hou, *Inorg. Chem.*, **1972**, *11*, 2125-2129.
117. F. W. B. Einstein and J. S. Field, *J. Chem. Soc. Dalton Trans.,* **1975**, 172-175.
118. X. Yan, B. Yu, L. Wang, N. Tang and C. Xi, *Organometallics*, **2009**, *28*, 6827-6830.

# Chapter 5

# Bridging Complexes of the Arsolyl Ligand

## 5.1 Preamble

Whereas numerous examples of bridging arsenide (μ-$AsR_2$) ligands are known – a great many of them originating in the laboratories of VAHRENKAMP and MALISCH – there are but precisely *three* such cases of bridging arsolyl (arsolido) complexes, two of which were reported by ABEL[1] and one by MATHEY.[2] All were obtained *via* thermal decarbonylation of their respective $\eta^1$-arsolyl complexes *en route* to the *pentahapto* coordination mode (**Chapter 1**, **Section 1.4.5**). Given the established arsenic-centred nucleophilicity of Group 6, 7 and 8 terminal cacodyl complexes $[M(AsMe_2)L_n]$[3-18] (selected examples are shown in **Chart 5.1**) it is surprising that the free donor function in discrete $\eta^1$-arsolyls has remained largely that: free.

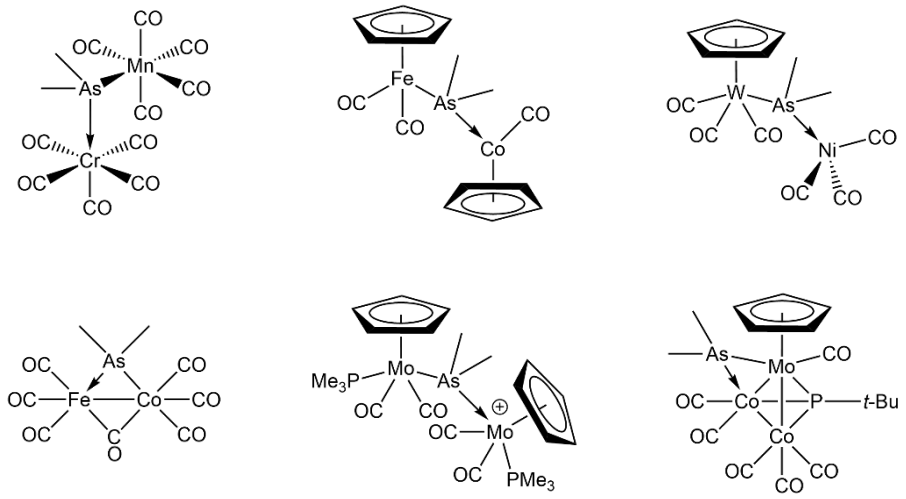


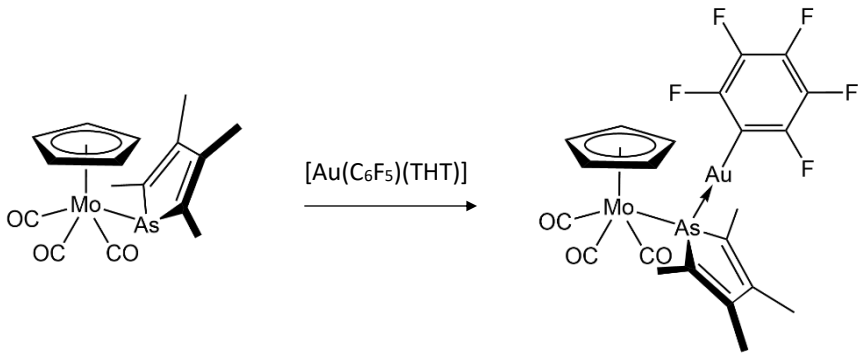

**Chart 5.1**: A representative selection of previously reported complexes bearing bridging cacodyl (dimethylarsenido) ligands.

With a small palette of arsolyl complexes now in hand from the previous chapter, the isolation of *As*-bridged binuclear complexes was naturally pursued; $[Mo(AsC_4Me_4)(CO)_3(\eta^5\text{-}C_5H_5)]$ was chosen for this role over other candidates due to superior envisioned heteroatom basicity, good reagent solubility in non-polar media, simple NMR profile (*cf.* $AsC_4Ph_4$), and ease of preparation of $[Mo(SnBu_3)(CO)_3(\eta^5\text{-}C_5H_5)]$. It was also anticipated that this choice would obviate any restrictions from inclusion of sterically intrusive 2,5-ring substituents. It is helpful now to establish the perception of $[Mo(AsC_4Me_4)(CO)_3(\eta^5\text{-}C_5H_5)]$ *as a ligand itself*, as it will be regularly referred to hereafter.

## 5.2 Coordination Complexes of the $[Mo(AsC_4Me_4)(CO)_3(\eta^5\text{-}C_5H_5)]$ *Metallo*-Ligand

### 5.2.1 Synthesis of $[MoAu(\mu\text{-}AsC_4Me_4)(CO)_3(C_6F_5)(\eta^5\text{-}C_5H_5)]$

Coordination experiments commenced with the highly-soluble, non-oxidising reagent $[Au(C_6F_5)(THT)]$ (THT = tetrahydrothiophene, $SC_4H_8$) which upon combining with $[Mo(AsC_4Me_4)(CO)_3(\eta^5\text{-}C_5H_5)]$ in $CH_2Cl_2$ solution gave the expected bridging complex $[MoAu(\mu\text{-}AsC_4Me_4)(CO)_3(C_6F_5)(\eta^5\text{-}C_5H_5)]$ as a bright yellow, air-stable solid in good yield (**Scheme 5.1**).




**Scheme 5.1**: Synthesis of $[MoAu(\mu\text{-}AsC_4Me_4)(CO)_3(C_6F_5)(\eta^5\text{-}C_5H_5)]$.

Complexation of the $Au(C_6F_5)$ fragment elicits an appreciable shift of $\nu_{CO}$ absorptions to higher wavenumbers ($CH_2Cl_2$ solution; 2034(vs), 1965(sh), 1949(vs) $cm^{-1}$) compared to the "free ligand" $[Mo(AsC_4Me_4)(CO)_3(\eta^5\text{-}C_5H_5)]$ (*cf.* 2006(s), 1937(vs), 1918(vs) $cm^{-1}$), suggesting a significant drift of electron density from the molybdenum centre toward the LEWIS acidic Au(I) atom, recalling that the arsenic lone pair of electrons in the precursor had π-donor character that is now curtailed. $^1H$ NMR spectroscopy ($C_6D_6$) of the adduct finds the cyclopentadienyl resonance at 4.36 ppm to slightly lower frequency of the "free ligand" (*cf.* 4.54 ppm), and similarly the exocyclic arsolyl methyl signals are marginally shifted to lower frequency of the starting material (2.07 and 1.73 *vs.* 2.10 and 1.93 ppm, respectively). The $^{13}C$ NMR shift for the cyclopentadienyl resonance (93.2 ppm) is only slightly downfield of the starting material (92.5 ppm), and a similarly minor shift downfield is observed for the arsolyl methyl carbon nuclei (14.8 and 14.5 *vs.* 16.0 and 15.1 ppm). The carbonyl carbon nuclei resonances appear at 233.0 and 223.7 ppm which are only marginally displaced from the those in $[Mo(AsC_4Me_4)(CO)_3(\eta^5\text{-}C_5H_5)]$ (*cf.* 235.5 and 224.5 ppm); the lower

frequency carbonyl *transoid* to the arsenic atom experiences a greater relative shift upfield than the *cisoid* pair. High-resolution mass spectrometry could not locate the molecular ion nor products of decarbonylation, instead yielding a myriad of signals with correct isotopic envelopes for the presence of Mo nuclei,* though no chemically sensible formulae was recognised. Single crystals of $[MoAu(\mu\text{-}AsC_4Me_4)(CO)_3(C_6F_5)(\eta^5\text{-}C_5H_5)]$ were obtained by vapour diffusion of $Et_2O$ into $CH_2Cl_2$ solution and the molecular structure is shown in **Figure 5.1**.

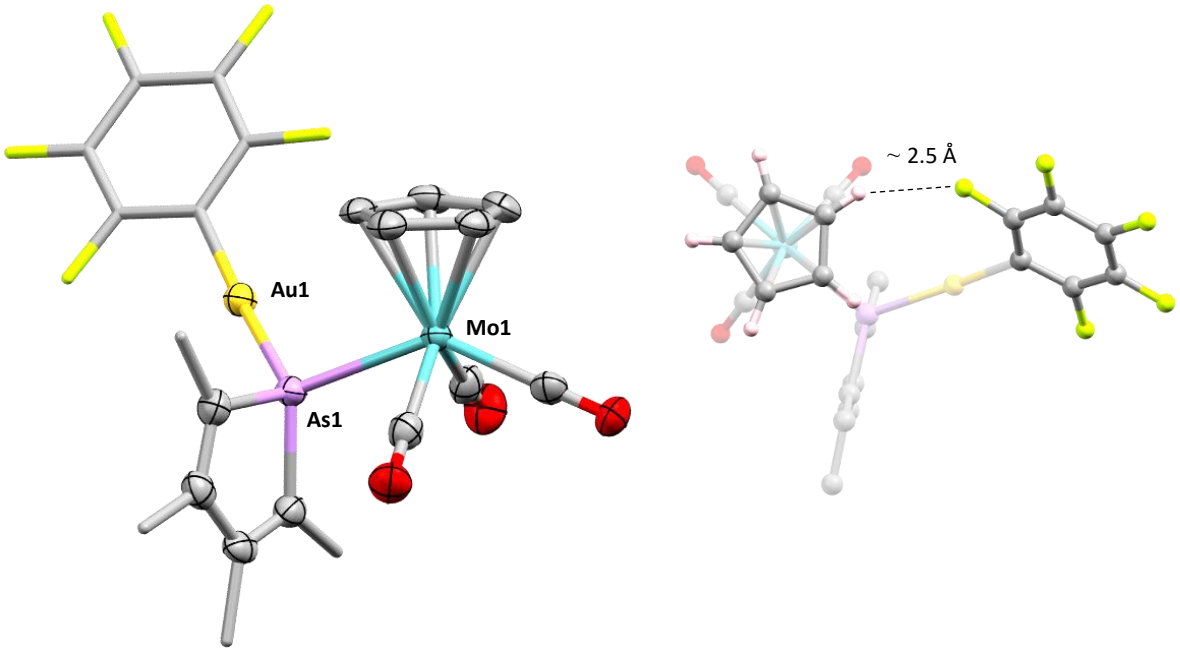



**Figure 5.1**: The molecular structure of $[MoAu(\mu\text{-}AsC_4Me_4)(CO)_3(C_6F_5)(\eta^5\text{-}C_5H_5)]$ in a crystal. Methyl and pentafluorophenyl groups simplified and hydrogen atoms omitted for clarity. Ellipsoids shown at 50% displacement. Four crystallographically independent molecules are found in the asymmetric unit (unit cell $P2_1/n$) with little structural variation and only one is shown. **Inset**: Abbreviated perspective of one molecule highlighting a F···H-C solid-state contact that does not, however, persist in solution.

The molecular structure confirms the expected bridging arsolyl complex; the asymmetric unit contains four crystallographically independent molecules ($Z = 16$, monoclinic $P2_1/n$) which are practically identical in gross molecular configuration and dimensions. The arsolyl group is swivelled about the Mo-As bond *ca* 60° from the vertical plane of the $Mo(CO)_3(\eta^5\text{-}C_5H_5)$ , such that the Au-$C_6F_5$ linkage projects toward the cyclopentadienyl ring affording an intramolecular F···H-C contact (mean distance *ca* 2.5 Å; **Figure 5.1, Inset**) imposing very slight bending of the As-Au-C spine (mean angle *ca* 172°) in the direction of the $\eta^5\text{-}C_5H_5$ ring (which does not persist in solution, however, on the $^{19}F$ NMR timescale). Complexation

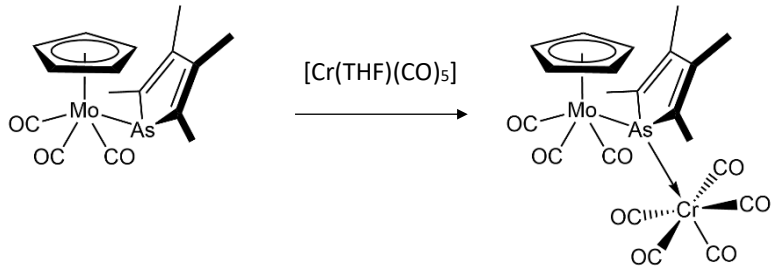
* Molybdenum contains seven naturally occurring isotopes rendering visual identification of relevant ion signals straightforward: $^{92}Mo$ (14.65% abundant), $^{94}Mo$ (9.19%), $^{95}Mo$ (15.87%), $^{96}Mo$ (16.67%), $^{97}Mo$ (9.58%), $^{98}Mo$ (24.29%), $^{100}Mo$ (9.74%).

of the $Au(C_6F_5)$ LEWIS acid invites a contraction in the Mo-As covalent bond distance from 2.7267(7) Å in the "free *metallo*-ligand" to 2.655(1) Å with a decrease in the arsole envelope angle to 1.80° (*cf.* $[Mo(AsC_4Me_4)(CO)_3(\eta^5\text{-}C_5H_5)]$: 7.92°). The mean As→Au distance of 2.399(8) Å is typical of conventional gold(I)-arsine interactions (*e.g.*, 2.3847 Å for $[Au(C_6F_5)(AsPh_3)]$[19]) and the Mo-As-Au angle (mean *ca* 110°) is nearly tetrahedral, and the shallowest of those encountered in this work (*vide infra*). Dimensions within the arsolyl ring are essentially identical to those of the free *metallo*-ligand $[Mo(AsC_4Me_4)(CO)_3(\eta^5\text{-}C_5H_5)]$ within crystallographic precision limits. A holistic discussion of NMR and crystallographic parameters for this and other bridging arsolyl complexes in this work is given in **Section 5.2.6**.

As an aside, the addition of metal halide reagents to $[Mo(AsC_4Me_4)(CO)_3(\eta^5\text{-}C_5H_5)]$ generally led to halogenation of the Mo-As bond with formation of $ClAsC_4Me_4$ (by NMR) – notably, $[MoCl(CO)_3(\eta^5\text{-}C_5H_5)]$ was *never* observed in these reaction mixtures potentially signalling the operation of a radical pathway. For $[AuCl(SMe_2)]$, purple nanoparticulate gold and $[Mo_2(CO)_6(\eta^5\text{-}C_5H_5)_2]$ were identified (alongside the *As*-chloro arsole) as products of the disintegration process. The halide bridged dimers $[Ir_2(\mu\text{-}Cl)_2Cl_2(\eta^5\text{-}C_5Me_5)_2]$ and $[Pd_2(\mu\text{-}Cl)_2(\eta^3\text{-}C_3H_5)_2]$ gave $ClAsC_4Me_4$ (by NMR) though the fate of the molybdenum and iridium/palladium centres in these reactions was not obvious; further evidence for homolysis of the Mo-As bond upon addition of potentially redox-active metal reagents (Au(I)→Au(0), Ir(III)→Ir(I), Pd(II)→Pd(0)) is presented in **Sections 5.2.3, 5.2.5** and **5.2.7**.

### 5.2.2 Synthesis of $[CrMo(\mu\text{-}AsC_4Me_4)(CO)_8(\eta^5\text{-}C_5H_5)]$

Ultra violet photolysis of $[Cr(CO)_6]$ in coordinating solvents produces labile *solvento* chromium(0) complexes of the form $[Cr(S)(CO)_5]$[20] (S = THF, MeCN, acetone *etc.*) which are invariably more selective precursors to monosubstituted chromium(0) pentacarbonyl derivatives than $[Cr(CO)_6]$ itself under thermal activation.[21] The $Cr(CO)_5$ fragment is popular adornment for donor functions of even modest basicity and has been employed as a means to attenuate the reactivity of unusual Group 15 species.[22-26] Here, $[Cr(THF)(CO)_5]$ was generated in THF solution which – upon treatment with $[Mo(AsC_4Me_4)(CO)_3(\eta^5\text{-}C_5H_5)]$ – produced the adduct $[CrMo(\mu\text{-}AsC_4Me_4)(CO)_8(\eta^5\text{-}C_5H_5)]$ in high yield as a reasonably air-stable, yellow-orange solid after column chromatography (**Scheme 5.2**).




**Scheme 5.2**: Synthesis of $[CrMo(\mu\text{-}AsC_4Me_4)(CO)_8(\eta^5\text{-}C_5H_5)]$.

The complex displays an IR spectrum with five $\nu_{CO}$ vibrations in $CH_2Cl_2$ solution which resolve into six in *n*-hexane. The NMR spectra ($C_6D_6$) that the $^1H$ signal for the cyclopentadienyl group shifts *up*field from the free *metallo*-ligand to 4.36 ppm (*cf.* $[Mo(AsC_4Me_4)(CO)_3(\eta^5\text{-}C_5H_5)]$ 4.54 ppm) whereas the $^{13}C\{^1H\}$ signal shifts *down*field to 93.2 ppm (*cf.* 92.5 ppm); the arsolyl methyl groups display the usual upfield shift to 2.07 and 1.73 ($^1H$) and 15.0 and 13.7 ($^{13}C$) ppm. Arsolyl ring-carbon nuclei are found at 149.4 (2,5-positions) and 137.5 (3,4) ppm and four carbonyl signals appear at 233.0 (*transoid* Mo), 224.7 (*cisoid* Mo), 223.8 (*trans* Cr) and 218.3 (*cis* Cr) ppm. Single crystals were obtained by cooling a hot $CHCl_3$/*n*-heptane mixture and the molecular structure is shown in **Figure 5.2**.

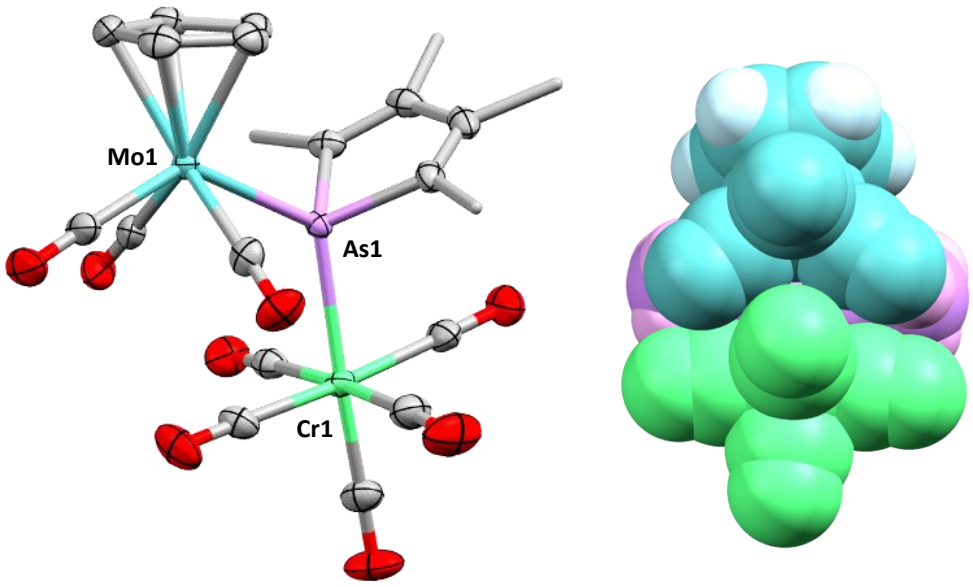
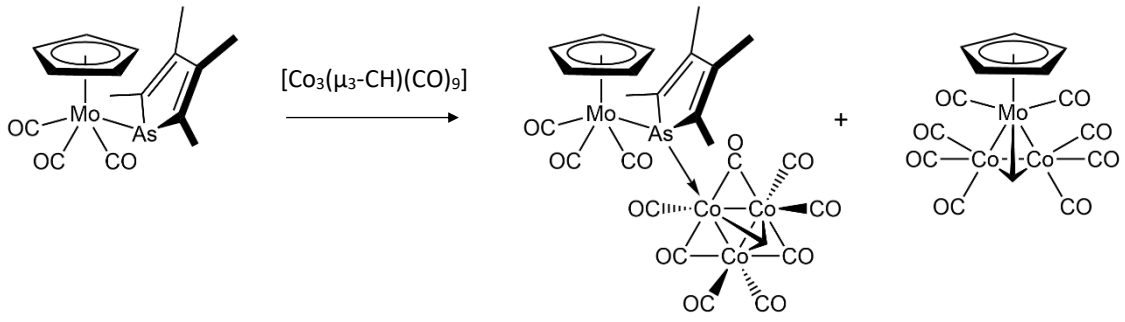



**Figure 5.2**: The molecular structure of $[CrMo(\mu\text{-}AsC_4Me_4)(CO)_8(\eta^5\text{-}C_5H_5)]$ in a crystal. Methyl groups simplified and hydrogen atoms omitted for clarity. Ellipsoids shown at 50% displacement. **Inset**: Space-filling representation viewed along the Mo1-As1-Cr1 plane from the face opposite the arsolyl group; blue = $Mo(CO)_3(\eta^5\text{-}C_5H_5)$, green = $Cr(CO)_5$, lilac = $AsC_4Me_4$.

The molecular structure of $[CrMo(\mu\text{-}AsC_4Me_4)(CO)_8(\eta^5\text{-}C_5H_5)]$ finds a nearly octahedral Cr(0) centre coordinated by the arsolyl donor function of $[Mo(AsC_4Me_4)(CO)_3(\eta^5\text{-}C_5H_5)]$. The local symmetry planes of the $Mo(CO)_3(\eta^5\text{-}C_5H_5)$, $AsC_4Me_4$ and $Cr(CO)_5$ groups are approximately (though not crystallographically) aligned such that one chromium carbonyl ligand in the equatorial plane lies in the cleft formed by the pair of molybdenum *cisoid* carbonyls (**Figure 5.2**, **Inset**). The As→Cr dative bond of 2.5144(5) Å is slightly longer than other similar arsine complexes of Cr(0) centres[27-31] but not remarkably-so to warrant special comment;* the Cr-C distance *trans* to the arsine donor (1.855(3) Å) is somewhat shorter than the four Cr-C bonds in the equatorial plane (mean 1.896(6) Å). The *trans* axial As-Cr-C angle deviates only slightly from linearity (*ca* 174°) and the intercarbonyl angles are nearly orthogonal (82—93°). Like the preceding $Au(C_6F_5)$ adduct (**Figure 5.1**), the Mo-As covalent bond length decreases upon coordination of the $Cr(CO)_5$ fragment to 2.6703(3) Å.

### 5.2.3 Synthesis of $[MoCo_3(\mu\text{-}AsC_4Me_4)(\mu_3\text{-}CH)(CO)_{11}(\eta^5\text{-}C_5H_5)]$

Whereas other arsole donors in this work were indifferent toward the quintessential methylidyne tricobalt cluster $[Co_3(\mu_3\text{-}CH)(CO)_9]$ even in the presence of trimethylamine-*N*-oxide,† the basicity of $[Mo(AsC_4Me_4)(CO)_3(\eta^5\text{-}C_5H_5)]$ appears anomalous that carbonyl displacement occurs rapidly in $CH_2Cl_2$ solution without moderators. The $[MoCo_3(\mu\text{-}AsC_4Me_4)(\mu_3\text{-}CH)(CO)_{11}(\eta^5\text{-}C_5H_5)]$ adduct is obtained after column chromatography as an air-stable red-brown solid (dark yellow in solution) in acceptable yield (**Scheme 5.3**).

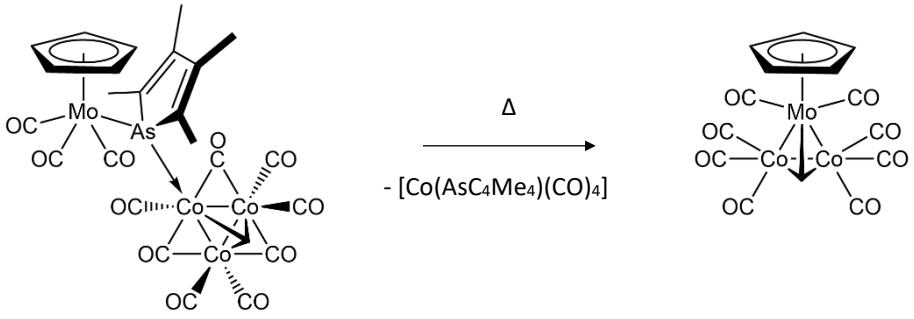



**Scheme 5.3**: Synthesis of $[MoCo_3(\mu\text{-}AsC_4Me_4)(\mu_3\text{-}CH)(CO)_{11}(\eta^5\text{-}C_5H_5)]$.

* Of the 11 crystal structures indexed within the CSD with $As^{III} \rightarrow Cr^0$ dative bonds, the mean As-Cr distance is 2.475 Å with a range of 2.368—2.638 Å.

† The 1,1-bis(arsolyl)ferrocene $[Fe\{\eta^5\text{-}C_5H_4(AsC_4Me_4)\}_2]$, to be introduced in **Chapter 7**, failed to react with the tricobalt cluster in the absence of $Me_3NO$; in the presence of the amine oxide decomposition was noted, and the ligand could be recovered unchanged.

Also isolated during chromatography was a small quantity of the known heterotrimetallic cluster $[MoCo_2(\mu_3\text{-}CH)(CO)_8(\eta^5\text{-}C_5H_5)]$* which elutes prior to the bridging arsolyl complex as a blue-green solid. The compound almost certainly arises *via* egress of a cobalt arsenide fragment *i.e.*, $[Co(AsC_4Me_4)(CO)_4]$,† with simultaneous insertion of the molybdenum centre into the $\mu_3$-methylidyne tetrahedron in a manner which is mechanistically ill-defined but has been exploited to good effect by VAHRENKAMP to obtain polymetallic clusters.[11, 14, 32, 33] The occurrence of a competing cobalt arsenide elimination pathway is evidence for the susceptibility of $[Mo(AsC_4Me_4)(CO)_3(\eta^5\text{-}C_5H_5)]$ to participate in Mo-As homolytic processes (see **Sections 5.2.4** and **5.2.5**), since most substitution reactions of $[Co_3(\mu_3\text{-}CR)(CO)_9]$ (and other closed-shell clusters) are thought to proceed *via* antecedent electron-transfer.[34-38] Indeed, heating a $C_6D_6$ solution of $[MoCo_3(\mu\text{-}AsC_4Me_4)(\mu_3\text{-}CH)(CO)_{11}(\eta^5\text{-}C_5H_5)]$ to 60° gave $[MoCo_2(\mu_3\text{-}CH)(CO)_8(\eta^5\text{-}C_5H_5)]$ as the only TLC-mobile product (**Scheme 5.4**).




**Scheme 5.4**: Thermolysis of $[MoCo_3(\mu\text{-}AsC_4Me_4)(\mu_3\text{-}CH)(CO)_{11}(\eta^5\text{-}C_5H_5)]$ with elimination of a cobalt arsenide.

The IR spectrum of $[MoCo_3(\mu\text{-}AsC_4Me_4)(\mu_3\text{-}CH)(CO)_{11}(\eta^5\text{-}C_5H_5)]$ displays six $\nu_{CO}$ absorptions in $CH_2Cl_2$ solution which resolve into nine in *n*-hexane; the presence of lower-intensity vibrations in the region *ca* 1880—1850 $cm^{-1}$ is suggestive of bridging carbonyl ligands which are indeed found in the crystal structure (**Figure 5.3**) and remain-so in an amorphous solid state as evidenced by an ATR-IR spectrum. A solution IR spectrum in acetonitrile also finds bands indicative of bridging carbonyl ligands suggesting an appreciable degree of structural rigidity within the methylidyne tricobalt cluster, in contrast not only to substituted

* $[MoCo_2(\mu_3\text{-}CH)(CO)_8(\eta^5\text{-}C_5H_5)]$: NMR $^1H$ ($C_6D_6$) δ 10.78, 4.48 ppm; $^{13}C\{^1H\}$ ($C_6D_6$) δ 251.3, 208.5, 90.7 ppm. IR ($CH_2Cl_2$) $\nu_{CO}$ 2083(s), 2071(s), 2040(sh), 2028(vs), 2015(vs), 2001(vs) $cm^{-1}$.

† This formulation as a discrete entity is not wholly accurate since $[CoR(CO)_4]$ readily decarbonylates when R is even mildly electron-releasing; when R contains a donor function, oligomeric materials of approximate compositions $[Co(\mu\text{-}R)(CO)_3]_x$ are probably the true product(s).

derivatives of the related $[Co_2(CO)_{8-n}(L)_n]$ platform which display skeletal fluxionality in different polarity media,[39] but also to the unsubstituted $[Co_3(\mu_3\text{-}CH)(CO)_9]$ itself which displays only terminal carbonyls.*

The $^1H$ NMR spectrum ($C_6D_6$) of $[MoCo_3(\mu\text{-}AsC_4Me_4)(\mu_3\text{-}CH)(CO)_{11}(\eta^5\text{-}C_5H_5)]$ finds the methylidyne hydrogen shifted upfield of the parent cluster* as a singlet at 9.75 ppm and the cyclopentadienyl at 4.63 ppm; two signals at 1.99 and 1.67 ppm correspond to the arsolyl methyl groups – all resonances are somewhat broadened, probably for the presence of three quadrupolar $^{59}Co$ nuclei. The $\mu_3$-methylidyne carbon atom is located at 235.5 ppm by means of an HSQC NMR experiment, and two sharp signals are measured at 232.8 and 224.8 ppm for the molybdenum-held carbonyl ligands *transoid* and *cisoid*, respectively, to the arsenic atom. The entire collective of eight carbonyl ligands attached to the tricobalt cluster are found at 206.8 ppm, typically broadened (FWHM = ~90 Hz) due to positional averaging (terminal ↔ bridging) on the NMR timescale, and invariably exacerbated by the quadrupolar $^{59}Co$ atoms. High-resolution mass spectrometry did not yield a molecular ion nor products of decarbonylation and no chemically sensible formulae could be devised from those which obviously contained a molybdenum atom. The identity was unambiguously confirmed by X-ray crystallography; single crystals of $[MoCo_3(\mu\text{-}AsC_4Me_4)(\mu_3\text{-}CH)(CO)_{11}(\eta^5\text{-}C_5H_5)]$ were obtained by slow evaporation of a benzene solution and the molecular structure is shown in **Figure 5.3**.

* NMR $^1H$ ($C_6D_6$, 400 MHz, 25 °C) δ 11.44 ppm. IR ($CH_2Cl_2$, 25 °C) $\nu_{CO}$ 2105(w), 2055(vs), 2038(s) $cm^{-1}$.

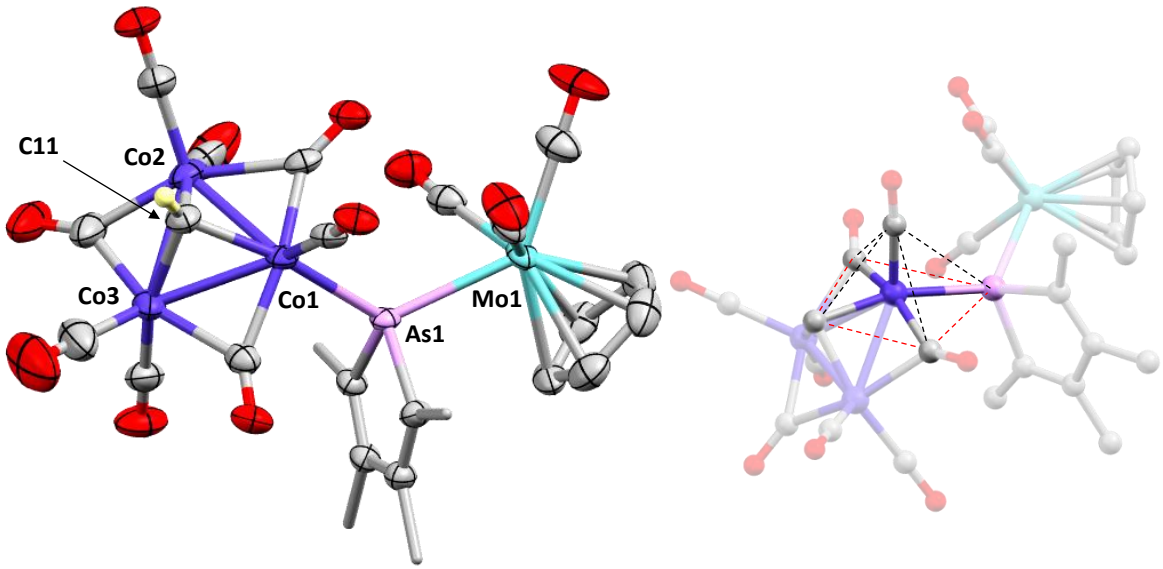
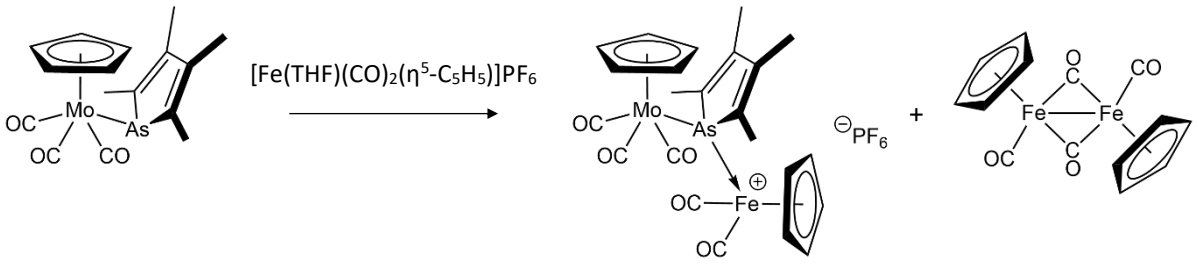



**Figure 5.3**: The molecular structure of $[MoCo_3(\mu\text{-}AsC_4Me_4)(\mu_3\text{-}CH)(CO)_{11}(\eta^5\text{-}C_5H_5)]$ in a crystal. Methyl groups simplified and most hydrogen atoms omitted except for the methylidyne hydrogen in light yellow. Ellipsoids shown at 50% displacement. **Inset**: Abbreviated perspective of the molecule highlighting the square-based pyramidal geometry of the Co(I) centre(s) and the equatorial disposition of the arsolyl donor. The *quasi*-basal plane is shown in red.

The crystal structure confirms mono-substitution of the tricobalt framework by the As(III) donor function of the $[Mo(AsC_4Me_4)(CO)_3(\eta^5\text{-}C_5H_5)]$ *metallo*-ligand. The triangular, approximately isosceles arrangement features three bridging carbonyl ligands adjoining each cobalt(I) atom, the local coordination polyhedra of which are deformed square-based pyramids (**Figure 5.3**, **Inset**). A terminal carbonyl ligand occupies the apical site of each metal with all other appendages – including the methylidyne carbon and the arsenic donor – populating the basal plane(s). The As→Co dative bond of 2.4086(7) Å compares with the 2.403 Å distance measured in the vinylidene cluster $[FeCo_2(\mu_3\text{-}\eta^1\text{:}\eta^1\text{:}\eta^2\text{-}CCPh)(CO)_8(AsPh_3)]$,[40] and the slightly shorter range of *ca* 2.3—2.4 Å for other Co(I) arsine complexes[7, 41, 42] whilst the Mo-As covalent bond distance of 2.6671(5) Å is notably shorter than the same bond in the free *metallo*-ligand $[Mo(AsC_4Me_4)(CO)_3(\eta^5\text{-}C_5H_5)]$. Intermetallic bonds emanating from the monosubstituted cobalt atom (mean 2.4788(10) Å) are slightly longer than the unique (opposite) edge (2.4414(8) Å) though all vertices are essentially 60° and distances to the $\mu_3$-methylidyne carbon are regular at *ca* 1.90 Å. Interatomic distances and angles within the arsolyl ring are not dissimilar to those of $[Mo(AsC_4Me_4)(CO)_3(\eta^5\text{-}C_5H_5)]$ although the envelope angle of the five-membered ring decreases to near-perfect planarity (0.04°).

### 5.2.4 Synthesis of $[MoFe(\mu\text{-}AsC_4Me_4)(CO)_5(\eta^5\text{-}C_5H_5)_2]PF_6$

The solvent molecule is also displaced from $[Fe(THF)(CO)_2(\eta^5\text{-}C_5H_5)]PF_6$ by $[Mo(AsC_4Me_4)(CO)_2(\eta^5\text{-}C_5H_5)]$ in $CH_2Cl_2$ solution to give the cationic binuclear adduct $[MoFe(\mu\text{-}AsC_4Me_4)(CO)_5(\eta^5\text{-}C_5H_5)_2]PF_6$ in acceptable yield as a dark yellow solid (**Scheme 5.5**). Some difficulties were encountered during workup and although product identity was established by the usual methods (*vide infra*), analytically pure specimens have evaded isolation. One by-product formed during the reaction in isolable quantities was $[Fe_2(CO)_4(\eta^5\text{-}C_5H_5)_2]$ which once again raises the possibility of competing outer-sphere redox processes involving $[Mo(AsC_4Me_4)(CO)_3(\eta^5\text{-}C_5H_5)]$; the identity of the reciprocal redox product(s) was not easily ascertained from the spectroscopic data on hand, though given the observations made in **Sections 5.2.5** and **5.2.7** it is not unreasonable to presume a biarsolyl of some form is among them. As an aside, THF solutions of $[Fe(THF)(CO)_2(\eta^5\text{-}C_5H_5)]PF_6$ prepared *in situ* by addition of $AgPF_6$ to $[FeBr(CO)_2(\eta^5\text{-}C_5H_5)]$ yielded $[Fe_2(CO)_4(\eta^5\text{-}C_5H_5)_2]$ in much greater quantities upon addition of $[Mo(AsC_4Me_4)(CO)_3(\eta^5\text{-}C_5H_5)]$ than did re-crystallised samples of $[Fe(THF)(CO)_2(\eta^5\text{-}C_5H_5)]PF_6$.




**Scheme 5.5**: Synthesis of $[MoFe(\mu\text{-}AsC_4Me_4)(CO)_5(\eta^5\text{-}C_5H_5)_2]PF_6$.

The $^1H$ NMR spectrum in $CD_2Cl_2$ reveals the respective molybdenum- and iron-bound cyclopentadienyl rings at 5.20 and 4.85 ppm with the arsolyl methyl substituents at 2.02 (2,5-positions) and 1.87 (3,4) ppm. The $^{13}C\{^1H\}$ NMR spectrum reveals the molybdenum carbonyl *transoid* to the arsolyl group at 229.2 ppm, with a pair of signals at 226.0 (*cisoid* Mo) and 211.2 (Fe) ppm of equal area integration. Resonances for the arsolyl ring-carbon nuclei are found at 148.2 and 139.3 ppm with the Mo- and Fe-cyclopentadienyl ligands at 95.1 and 86.4 ppm, respectively, by HSQC NMR; arsolyl methyl group resonances appear at 15.1 and 14.2 ppm. The fundamental carbonyl-stretching modes of the $C_s$-symmetric

$Mo(CO)_3(\eta^5\text{-}C_5H_5)$ ($2A'$ + $A''$) and $Fe(CO)_2(\eta^5\text{-}C_5H_5)$ ($A'$ + $A''$) centres are not independent but instead modestly coupled (by comparison with a simulated spectrum of the gas-phase complex at the ωB97X-D/6-31G*/LANL2Dζ level of theory) and the solution IR spectrum ($CH_2Cl_2$) comprises five $\nu_{CO}$ vibrations at 2052(vs), 2036(vs), 2004(s), 1980(m), 1947(s) $cm^{-1}$. Crystals of $[MoFe(\mu\text{-}AsC_4Me_4)(CO)_5(\eta^5\text{-}C_5H_5)_2]PF_6$ suitable for X-ray diffraction were obtained by vapour diffusion of $Et_2O$ into a $CH_2Cl_2$ solution and the molecular structure is shown in **Figure 5.4**.

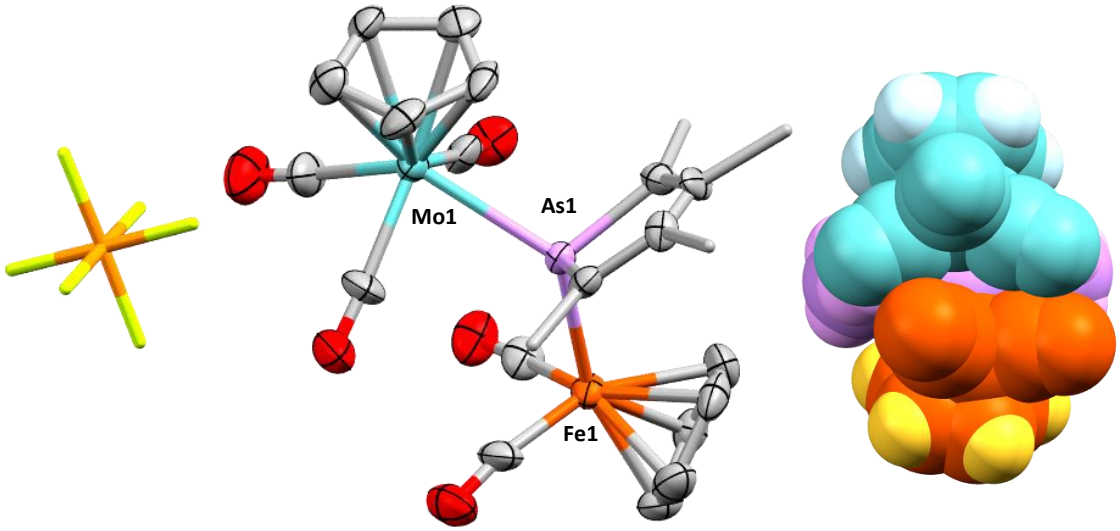


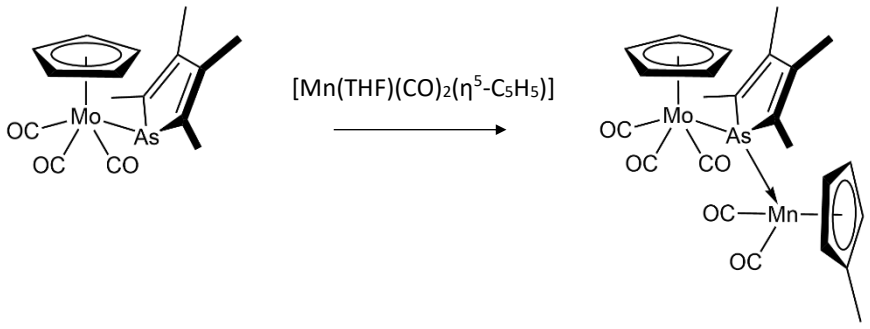

**Figure 5.4**: The molecular structure of $[MoFe(\mu\text{-}AsC_4Me_4)(CO)_5(\eta^5\text{-}C_5H_5)_2]PF_6$ in a crystal. Methyl and hexafluorophosphate groups simplified and hydrogen atoms omitted for clarity. Ellipsoids shown at 50% displacement. **Inset**: Space-filling representation viewed along the Mo1-As1-Fe1 plane from the face opposite the arsolyl group; blue = $Mo(CO)_3(\eta^5\text{-}C_5H_5)$, orange = $Fe(CO)_2(\eta^5\text{-}C_5H_5)$, lilac = $AsC_4Me_4$.

The crystalline sample(s) obtained proved to be twinned and although a suitable twin-law was found, data quality proved to be comparatively poor which is reflected in the eccentric profiles of the thermal ellipsoids; only superficial analysis can be extracted from the data although gross molecular composition and configuration of the expected adduct is established. The $Fe(CO)_2(\eta^5\text{-}C_5H_5)$ group is offset from the vertical plane which bifurcates the $Mo(CO)_3(\eta^5\text{-}C_5H_5)$ centre, permitting an iron-bound carbonyl to occupy the pocket formed by the pair of molybdenum *cisoid* carbonyls (**Figure 5.4**, **Inset**). The arsolyl bridge remains *syn* with respect each cyclopentadienyl ring and although a hydrogen atom on each appears to face the diene system, a precise measurement of the π···H-C distances is inappropriate given the grossly

aspherical thermal displacement of the carbon atoms to which they are attached.* The Mo-As covalent bond distance is *ca* 2.6 Å with a (formally) dative As→Fe bond distance of *ca* 2.4 Å; notably, whilst the general trend is one involving a decrease in the Mo-As covalent bond length upon complexation of the As(III) lone pair, here the (formal) As→Fe distance is also appreciably shorter than an authentic Fe-As covalent bond (*cf.* $[Fe(AsC_4Ph_4)(CO)_2(\eta^5\text{-}C_5H_5)]$ 2.4319(5) Å]) *and* longer than a genuine As→Fe bond measured in other areas of this work (**Chapter 4**, **Section 4.2.1.3**). A true bonding description of the $[MoFe(\mu\text{-}AsC_4Me_4)(CO)_5(\eta^5\text{-}C_5H_5)]$ cation probably involves partial distribution of the positive charge across the Mo-As-Fe linkage, though at the ωB97X-D/6-31G*/LANL2Dζ level of theory, the natural charges on molybdenum (+0.117), arsenic (+0.664) and iron (+0.884) suggest that the majority of positive charge remains on the Fe(II) centre with LÖWDEN bond orders for the Mo–As (0.85) and Fe–As (0.87) bonds being essentially identical.

### 5.2.5 Synthesis of $[MoMn(\mu\text{-}AsC_4Me_4)(CO)_5(\eta^5\text{-}C_5H_5)(\eta^5\text{-}C_5H_4Me)]$

Another labile *solvento* complex is the dark purple $[Mn(THF)(CO)_2(\eta^5\text{-}C_5H_4Me)]$, generated by UV-photolysis of $[Mn(CO)_3(\eta^5\text{-}C_5H_4Me)]$ in THF at ambient temperature. Addition of this reagent to $[Mo(AsC_4Me_4)(CO)_3(\eta^5\text{-}C_5H_5)]$ in THF gives a red-brown mixture from which column chromatography affords the moderately air-stable, purple-red adduct $[MoMn(\mu\text{-}AsC_4Me_4)(CO)_5(\eta^5\text{-}C_5H_5)(\eta^5\text{-}C_5H_4Me)]$ in good yield; a second orange arsolyl-containing species was also isolated during this process in very low yield (**Section 5.2.7**).




**Scheme 5.6**: Synthesis of $[MoMn(\mu\text{-}AsC_4Me_4)(CO)_5(\eta^5\text{-}C_5H_5)(\eta^5\text{-}C_5H_4Me)]$.

* Hydrogen atom positions are approximated using a "riding" model whereby the thermal displacement parameter *U*(H) is fixed to 1.2·*U*(C) (for aromatic hydrogens); therefore, a greater uncertainty in the carbon atom position will incur an additional 20% uncertainty in the hydrogen atom position to which it is bonded.

The IR spectrum of [MoMn(μ-$AsC_4Me_4$)$(CO)_5$($\eta^5$-$C_5H_5$)($\eta^5$-$C_5H_4Me$)] finds four $\nu_{CO}$ vibrations in both $CH_2Cl_2$ and *n*-hexane solution, and high-resolution mass spectrometry yields the molecular ion (*m*/*z* ≈ 619.9280). The NMR spectra are predictably simple: the $^1H$ spectrum in $C_6D_6$ includes the Mo-$\eta^5$-$C_5H_5$ resonance at 4.90 ppm and those for the arsolyl methyl groups at 2.07 (2,5-positions) and 1.79 (3,4) – the latter is accidentally isochronous with the $\eta^5$-$C_5H_4Me$ methyl group such that the combined signal has a relative area integration of 9 hydrogen nuclei. The $^{13}C\{^1H\}$ NMR spectrum mirrors the nearly identical chemical environments of the arsolyl- and $\eta^5$-$C_5H_5Me$ methyl groups with the two resonances separated by < 0.2 ppm. Arsolyl ring-carbon nuclei are found at 150.2 (2,5-positions) and 135.9 (3,4) ppm, and three signals at 235.8, 235.7 and 225.0 ppm assigned to the manganese, *transoid*-molybdenum, and *cisoid*-molybdenum carbonyl ligands respectively, by their 2:1:2 area integration. Single crystals were obtained by cooling a hot *n*-heptane solution and the molecular structure is shown in **Figure 5.5**.

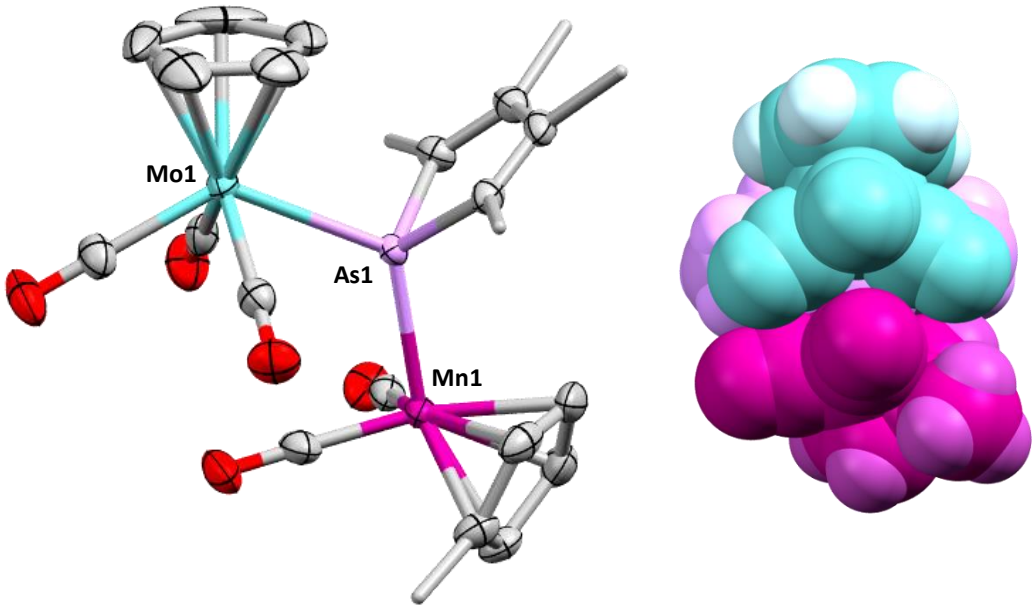



**Figure 5.5**: The molecular structure of [MoMn(μ-$AsC_4Me_4$)$(CO)_5$($\eta^5$-$C_5H_5$)($\eta^5$-$C_5H_4Me$)]. Methyl groups simplified and hydrogen atoms omitted for clarity. Ellipsoids shown at 50% displacement. **Inset**: Space-filling representation viewed along the Mo1-As1-Mn1 plane from the face opposite the arsolyl group; blue = Mo$(CO)_3$($\eta^5$-$C_5H_5$), magenta = Mn$(CO)_2$($\eta^5$-$C_5H_4Me$), lilac = $AsC_4Me_4$.

The molecular structure reveals the anticipated arsolyl-bridged adduct. The bridging $AsC_4Me_4$ group remains *syn* with respect to the molybdenum cyclopentadienyl with a C-H···π contact of *ca* 2.5 Å between the aforementioned ligand and the arsolyl diene system. The Mn$(CO)_2$($\eta^5$-$C_5H_5Me$) moiety is not bisected by the vertical symmetry plane of the Mo$(CO)_3$($\eta^5$-$C_5H_5$) group, instead being rotated about the

As→Mn bond by about 45° to avoid an eclipsing conformation between carbonyl ligands, presumably to minimise repulsive electrostatic interactions; one manganese carbonyl is nestled in the cleft formed by the pair of *cisoid* molybdenum carbonyl ligands to become approximately coplanar with the remaining *transoid* carbonyl (**Figure 5.5**, **Inset**). Coordination of the manganese(I) centre elicits a decrease in the Mo-As covalent bond distance to 2.6927(4) Å with an As→Mn dative bond of 2.3741(4) Å in measure; a Mo-As-Mn angle of *ca* 123° is found. A *very slight* decrease in the diene C=C bond (mean 1.346(4) Å) and an equally slight increase in the C-C bond (1.481(4) Å) is measured compared to the same bonds in the free *metallo*-ligand; all other key angles and distances are unremarkable.

### 5.2.6 General Comments Regarding Features of Bridging-Arsolyl Complexes

Key NMR and crystallographic data for [Mo(AsC$_4$Me$_4$)(CO)$_3$($\eta^5$-C$_5$H$_5$)] "{L}" and the bridging-arsolyl complexes described herein have been collated below in **Table 5.1** (NMR) and **Table 5.2** (XRD).

**Table 5.1**: Selected $^1$H and $^{13}$C{$^1$H} NMR data for [Mo(AsC$_4$Me$_4$)(CO)$_3$($\eta^5$-C$_5$H$_5$)] "{L}" and bridging arsolyl complexes prepared therefrom. Chemical shifts downfield from SiMe$_4$ measured in C$_6$D$_6$ solution (25 °C) unless otherwise stated.

| Complex | Mo-CO | Arsolyl-Ring | Mo-$\eta^5$-C$_5$H$_5$ | | Arsolyl-Me | |
|---|---|---|---|---|---|---|
| | $^{13}$C | $^{13}$C | $^1$H | $^{13}$C | $^1$H | $^{13}$C |
| {L} | 235.5 | 148.7 | 4.54 | 92.5 | 2.10 | 16.0 |
| | 224.5 | 141.9 | | | 1.93 | 15.1 |
| {L}Au(C$_6$F$_5$) | 232.7 | 142.7 | 4.70 | 92.7 | 1.84 | 14.8 |
| | 223.7 | 140.4 | | | 1.62 | 14.5 |
| {L}Cr(CO)$_5$ | 233.0 | 146.4 | 4.36 | 93.2 | 2.07 | 15.0 |
| | 224.7 | 137.5 | | | 1.73 | 13.7 |
| {L}Co$_3$($\mu_3$-CH)(CO)$_8$ | 232.8 | 147.5 | 4.63 | 93.0 | 1.99 | 14.7 |
| | 224.8 | 137.7 | | | 1.67 | 13.3 |
| {L}Mn(CO)$_2$($\eta^5$-C$_5$H$_4$Me) | 235.8 | 150.2 | 4.90 | 92.7 | 2.07 | 14.8 |
| | 225.0 | 135.9 | | | 1.79 | 13.6 |
| {L}* | 235.5 | 149.1 | 5.16 | 93.5 | 1.95 | 16.0 |
| | 224.7 | 141.8 | | | 1.85 | 15.1 |
| [{L}Fe(CO)$_2$($\eta^5$-C$_5$H$_5$)]$^+$* | 229.2 | 148.2 | 5.2 | 95.1 | 2.02 | 15.1 |
| | 226.0 | 139.3 | | | 1.87 | 14.2 |

*Measured in CD$_2$Cl$_2$ solution, 25 °C.

**Table 5.2**: Selected crystallographic data for [CpMo(AsC$_4$Me$_4$)(CO)$_3$] "{L}" and bridging arsolyl complexes prepared therefrom.

| Complex | Mo-As | As→M | As-C | C=C | C-C | Envelope |
|---|---|---|---|---|---|---|
| {L} | 2.7267(7) | - | 1.934(7) | 1.354(5) | 1.466(7) | 7.92 |
| {L}Au(C$_6$F$_5$) | 2.6551(3) | 2.399(3) | 1.925(6) | 1.340(7) | 1.485(4) | 1.8 |
| {L}Cr(CO)$_5$ | 2.6703(3) | 2.5144(5) | 1.935(4) | 1.342(6) | 1.487(4) | 4.01 |
| {L}Co$_3$($\mu_3$-CH)(CO)$_8$ | 2.6771(5) | 2.4086(7) | 1.935(4) | 1.338(5) | 1.483(5) | 0.04 |
| [{L}Fe(CO)$_2$($\eta^5$-C$_5$H$_5$)]$^{+}$* | ~2.62 | ~2.39 | ~1.93 | ~1.34 | ~1.49 | < 1 |
| {L}Mn(CO)$_2$($\eta^5$-C$_5$H$_4$Me) | 2.6927(4) | 2.3741(4) | 1.940(3) | 1.346(3) | 1.2481(2) | 5.26 |

*Poor data quality arising from crystal twinning; values have been rounded to two decimal places.

Some overarching trends can be extracted from these data. Coordination of an extraneous metal centre elicits (in all cases) an *up*field shift of the arsolyl methyl signals in both the $^{1}$H and $^{13}$C{$^{1}$H} NMR spectra compared to [Mo(AsC$_4$Me$_4$)(CO)$_3$($\eta^5$-C$_5$H$_5$)], and a similar trend is seen for the arsolyl ring-carbon nuclei which also experience a slight *up*field $^{13}$C shift from the free arsolyl complex (aside from one outlier). Presumably, the depletion of electron-density at the As(III) atom further diminishes whatever modest ring current may be present in the cyclic system,[43] thereby exerting a small but measurable shielding effect on the remainder of the nuclei comprising the ring. That the magnitudes of such differences in arsolyl chemical shifts between [Mo(AsC$_4$Me$_4$)(CO)$_3$($\eta^5$-C$_5$H$_5$)] and [Mo($\mu$-AsC$_4$Me$_4$)M(CO)$_3$L$_n$($\eta^5$-C$_5$H$_5$)]$^{x+}$ are relatively minor perhaps speaks to the low aromatic character of heavy-atom heteroles in general. Crystallographic data agree with a "more localised" diene system arising from a weakened ring current: on average, C$_\alpha$=C$_\beta$ distances compress and C$_\beta$-C$_\beta$ distances elongate upon confiscation of the arsenic lone pair though the absolute changes are reticent within the precision limits of the data. Nonetheless, the magnitudes of such adulterations to the butadiene system (0.01—0.02 Å) are in accord with the equally modest variations in NMR shifts.

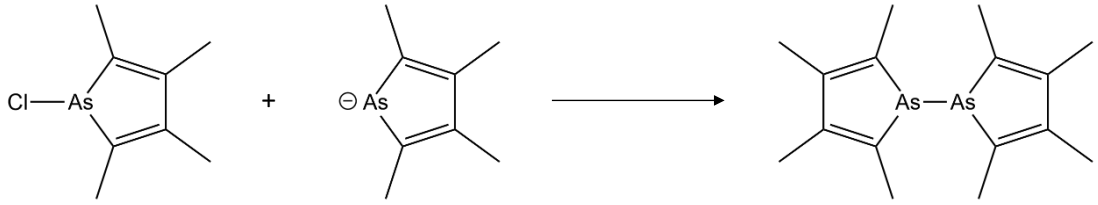
Aside from one outlier, $^{1}$H and $^{13}$C resonances for the molybdenum-bound cyclopentadienyl ligand shift *down*field upon complexation of the arsolyl which indicates depletion of electron-density at the trivalent arsenic atom affecting the basicity of the Mo(II) centre; once again, that the cyclopentadienyl and arsolyl nuclei observe opposing chemical shift directions compared to free [Mo(AsC$_4$Me$_4$)(CO)$_3$($\eta^5$-C$_5$H$_5$)] speaks

to the considerable electronic insulation of the heteroatom within the arsole ring. One also observes a small *up*field shift of the molybdenum-bound carbonyl carbon nuclei (*sans* the same outlier) upon bridging-arsolyl formation, with the lone *transoid* carbonyl generally experiencing a greater effect than the *cisoid* pair. This could be interpreted on the basis of the $AsC_4Me_4$ ring being a weak π-acceptor ligand (as tertiary arsines are known to be[44]) and directly competing with the *transoid* carbonyl for a mutually shared Mo(*d*) orbital, especially if rendered more-electropositive by attending two metal centres. Crystallographic data show a considerable decrease in the Mo-As covalent bond length (undoubtedly complementing any retrodonation with improved orbital overlap) with no discernible change to the As-$C_\alpha$ bond length whatsoever, curiously suggesting that drift of Mo(*d*) electrons to the As-$C_\alpha$(σ*) orbitals is probably *not* the operative mode of π-acidity. Regardless, formation of the bridging-arsolyl ligand serves to reduce the π-basicity of the Mo(II) centre, also seen in the shift of the cyclopentadienyl ligand resonances.

### 5.2.7 Synthesis of $(AsC_4Me_4)_2$ and $[Mn_2\{\mu\text{-}(AsC_4Me_4)_2\}(CO)_4(\eta^5\text{-}C_5H_4Me)_2]$

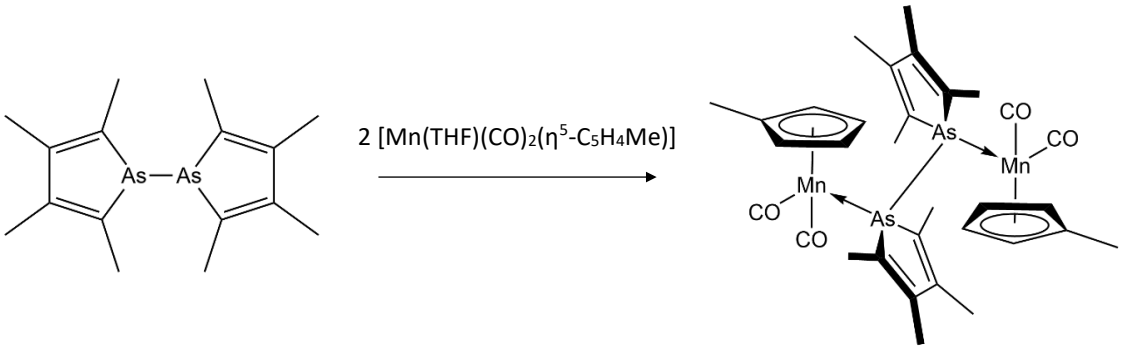
It was mentioned in **Section 5.2.5** that the synthesis of $[MoMn(\mu\text{-}AsC_4Me_4)(CO)_5(\eta^5\text{-}C_5H_5)(\eta^5\text{-}C_5H_4Me)]$ afforded a second product during chromatographic workup. This species – an orange solid – was isolated in very low yield (milligram quantities) for which the IR spectrum displayed only two $\nu_{CO}$ absorptions in $CH_2Cl_2$ solution (1921(vs) and 1864(vs) $cm^{-1}$) that resolved into three vibrations in *n*-hexane (1941(s), 1930(vs) and 1877(vs) $cm^{-1}$). The $^1H$ NMR spectrum ($C_6D_6$) was surprisingly simple and evidently devoid of a cyclopentadienyl ligand (and therefore a $Mo(CO)_x(\eta^5\text{-}C_5H_5)$ group) with peaks observed at 4.10, 3.95 and 1.70 ppm characteristic of a methylcyclopentadienyl ring, and the usual pair of signals for a tetramethylarsolyl ligand at 2.09 and 1.75 ppm. The relative area integration of the individual constituents suggested an empirical composition "$Mn(AsC_4Me_4)(CO)_2(\eta^5\text{-}C_5H_4Me)$" which – to satisfy the diamagnetic nature of the complex, IR spectra and electron-counting rules – was surmised to be a centrosymmetric *As*-*As* bonded dimer *i.e.*, $[Mn_2\{\mu\text{-}(AsC_4Me_4)_2\}(CO)_4(\eta^5\text{-}C_5H_4Me)_2]$, featuring the known 2,2',3,3',4,4',5,5'-octamethylbiarsolyl.[45] Low isolated yields precluded further spectroscopic analysis and in the absence of single-crystals, high-resolution mass spectrometry was regrettably inconclusive.

A deliberate synthesis of this species was undertaken to confirm its formulation as $[Mn_2\{\mu\text{-}(AsC_4Me_4)_2\}(CO)_4(\eta^5\text{-}C_5H_4Me)_2]$ and (astonishingly) the first example of a transition metal biarsolyl complex; the obvious approach would be addition of two equivalents of $[Mn(THF)(CO)_2(\eta^5\text{-}C_5H_4Me)]$ to the free octamethylbiarsolyl and this was indeed the route taken. Previously reported biarsolyls (including octamethylbiarsolyl) and their synthetic stratagem are discussed in **Section 1.3.4** of **Chapter 1**. Here, the necessary biarsolyl first reported by THEOPOLD[45] was obtained *via* a different strategy to that described therein (**Scheme 5.7**): the tetramethylarsolide anion $[AsC_4Me_4]^-$ was obtained by reduction of freshly-prepared $ClAsC_4Me_4$ with dilute sodium-mercury amalgam in THF to which was combined a second equivalent of freshly-prepared $ClAsC_4Me_4$ at -78 °C. Anaerobic chromatography on neutral alumina with *n*-hexane eluent provided the expected biarsolyl $(AsC_4Me_4)_2$ in moderate yield as a yellow crystalline solid for which spectroscopic data are in agreement with those reported by THEOPOLD *et al.*,[45] and confirmed by X-ray diffraction analysis; the crystal structure is shown in **Section 8.8** of the **Appendix**. As an aside, one may envision a method whereby $Na_2[Fe(CO)_4]$ is employed as a reducing agent to unite the two arsenic centres, as demonstrated by COLLMAN *et al.* in coupling $ClAsPh_2$ with $ClPPh_2$.[46]




**Scheme 5.7**: Synthesis of 2,2',3,3',4,4',5,5'-octamethylbiarsolyl.

The addition of excess $[Mn(THF)(CO)_2(\eta^5\text{-}C_5H_4Me)]$ to a THF solution of $(AsC_4Me_4)_2$ provided a bright orange mixture from which a single, moderately air-stable orange product was isolated during column chromatography; IR and $^1H$ NMR spectra are in perfect agreement with those of the side-product mentioned above and the proposed dimeric composition is confirmed by high-resolution mass spectrometry (molecular ion $m/z \approx 745.9956$; **Scheme 5.8**).




**Scheme 5.8**: Deliberate synthesis of $[Mn_2\{\mu\text{-}(AsC_4Me_4)_2\}(CO)_4(\eta^5\text{-}C_5H_4Me)_2]$.

Despite its novelty, the $^{13}C\{^1H\}$ NMR spectrum ($C_6D_6$) is fairly unremarkable alongside other arsole/arsolyl complexes in this work: the four equivalent carbonyl nuclei are found at 232.4 ppm and the biarsolyl ring-carbons at 143.5 (2,5-positions) and 139.7 (3,4) ppm. The remaining carbon environments are *so* similar to those of $[MoMn(\mu\text{-}AsC_4Me_4)(CO)_5(\eta^5\text{-}C_5H_5)(\eta^5\text{-}C_5H_4Me)]$ that no comment is warranted. Single crystals were obtained by slow evaporation of a benzene solution and the structure is shown in **Figure 5.6**.

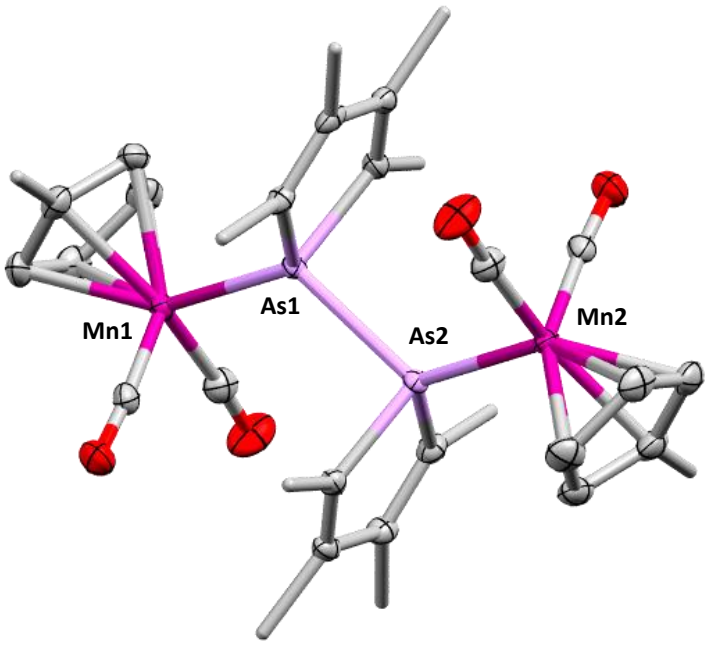


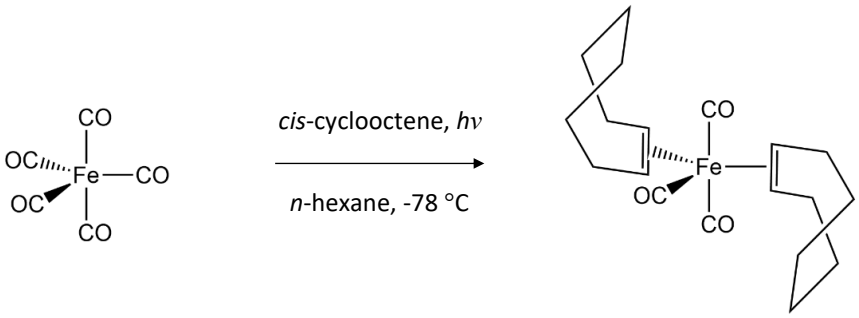

**Figure 5.6**: The molecular structure of $[Mn_2\{\mu\text{-}(AsC_4Me_4)_2\}(CO)_4(\eta^5\text{-}C_5H_4Me)_2]$ in a crystal. Methyl groups simplified and hydrogen atoms omitted for clarity. Ellipsoids shown at 50% displacement.

The molecular structure determination confirmed the expected dimanganese biarsolyl complex formation. It should be noted that although the solid-state structure ostensibly *appears* to contain an inversion centre (at the midpoint of the diarsine bond), no such symmetry element is crystallographically imposed upon the structural model and a satisfactory solution was obtained in a non-centrosymmetric space group (monoclinic *Cc*; $R_1$ = 0.024). Attempts to account for missing symmetry by model refinement in centric monoclinic space groups (*e.g.*, $P2_1/c$, $C2/c$) did not yield sensible structure solutions. The superficial centricity of the *anti*-conformation appears to be coincidental since the two *pseudo* halves of the molecule do indeed exhibit subtle differences from one another *viz.* Mn1-As1 2.3234(5) Å and Mn2-As2 2.3147(5) Å. The diarsine bond measures 2.4610(5) Å (*cf.* $[Mn_2(\mu\text{-PhHAsAsHPh})(CO)_4(\eta^5\text{-}C_5H_5)_2]$[47] As-As = 2.462(1) Å) which is slightly elongated compared to the free *metallo*-ligand (2.4462(4) Å; **Section 8.8**, **Appendix**), and the mean As→Mn dative bond of 2.3190(7) Å is somewhat shorter than the same in $[MoMn(\mu\text{-}AsC_4Me_4)(CO)_5(\eta^5\text{-}C_5H_5)(\eta^5\text{-}C_5H_4Me)]$ (2.3741(4) Å; **Figure 5.5**), though in accord with other complexes of similar constitution ($[Mn_2(\mu\text{-PhHAsAsHPh})(CO)_4(\eta^5\text{-}C_5H_5)_2]$[47] Mn-As = 2.319(2) Å). The As-As-Mn angle of *ca* 123° is highly typical of the bridging complexes in this work and the arsenic(II) atom(s) are essentially contained within the mean plane of the butadiene, extruded by only 0.6°; distances and angles about the arsole ring are crystallographically indistinguishable from other σ-bound $AsC_4Me_4$ ligands in this work.

The occurrence of the $[Mn_2\{\mu\text{-}(AsC_4Me_4)_2\}(CO)_4(\eta^5\text{-}C_5H_4Me)_2]$ dimer in reaction mixtures of $[MoMn(\mu\text{-}AsC_4Me_4)(CO)_5(\eta^5\text{-}C_5H_5)(\eta^5\text{-}C_5H_4Me)]$ – albeit in small quantities – signals a competing redox process in line with the addition of $[Fe(THF)(CO)_2(\eta^5\text{-}C_5H_5)]^+$ to $[Mo(AsC_4Me_4)(CO)_3(\eta^5\text{-}C_5H_5)]$ which yielded small quantities of $[Fe_2(CO)_4(\eta^5\text{-}C_5H_5)_2]$ (**Section 5.2.4**). In the present context, $[Mo_2(CO)_6(\eta^5\text{-}C_5H_5)_2]$ is the presumed reciprocal of $[Mn_2\{\mu\text{-}(AsC_4Me_4)_2\}(CO)_4(\eta^5\text{-}C_5H_4Me)_2]$ formation however no compounds (other than those listed) were isolated from the reaction mixture of $[Mo(AsC_4Me_4)(CO)_3(\eta^5\text{-}C_5H_5)]$ and $[Mn(THF)(CO)_2(\eta^5\text{-}C_5H_4Me)]$ (some chromatographically-immobile materials were formed, however).

### 5.2.8 Synthesis of $[MoFe_2(\mu_3\text{-}\eta^1\text{:}\eta^1\text{:}\eta^4\text{-}AsC_4Me_4)(CO)_9(\eta^5\text{-}C_5H_5)]$

Low temperature UV-photolysis of $[Fe(CO)_5]$ containing a large excess of *cis*-cyclooctene (COE) in *n*-hexane produces the exceedingly thermolabile $[Fe(COE)_2(CO)_3]$ (**Scheme 5.9**), which has been utilised by its discoverer GREVELS[48] and other workers as a source of the iron(0) tricarbonyl fragment in both organic[49-51] and organometallic applications.[52-54] The reagent is in some settings more convenient than $[Fe(CO)_5]$ itself, or $[Fe_2(CO)_9]$ and $[Fe_3(CO)_{12}]$, which invariably require forcing thermolysis to obtain higher products of decarbonylation* and – depending on the substrate – may be prone to side-reactions involving reactive element-carbon bonds, cyclisation, or cluster formation.[55] Whereas $[Fe(\eta^4\text{-L})(CO)_3]$ (L = benzylideneacetone, 1-azabutadienes) and the like have the benefit of being crystalline sources of "$Fe(CO)_3$" stable at ambient temperature, displacement of the α,β-unsaturated ketone/imine must proceed *via* a dissociative mechanism since the metal centre is electronically saturated. Notwithstanding the chelate effect, incoming donors of weaker nucleophilic constitution or modest thermal stability may struggle to abstract the iron(0) centre from the π-ligand (*vide infra*) for which it displays a well-known affinity;† $[Fe(COE)_2(CO)_3]$ obviates both of these concerns since the reagent is kinetically mobile at temperatures well below 0 °C.[48]



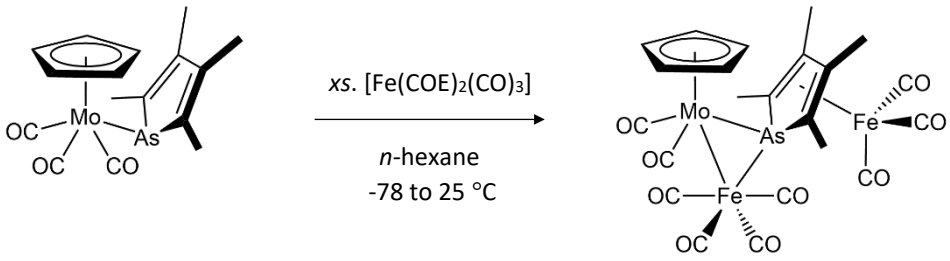

**Scheme 5.9**: Synthesis of labile $[Fe(COE)_2(CO)_3]$.

Here, an excess of $[Fe(COE)_2(CO)_3]$ was combined with $[Mo(AsC_4Me_4)(CO)_3(\eta^5\text{-}C_5H_5)]$ in *n*-hexane medium at -78 °C and allowed to slowly warm to ambient temperature overnight; a dark red-brown suspension forms from which chromatographic purification affords an air-stable, bright red solid in good yield. Large single crystals of the compound were obtained by evaporation of $Et_2O$ solution at 0 °C and X-

* $[Fe(CO)_5]$, $[Fe_2(CO)_9]$ and $[Fe_3(CO)_{12}]$ are all sources of "$Fe(CO)_4$" at or slightly above ambient temperature, though further decarbonylation to "$Fe(CO)_3$" generally demands forcing activation. These conditions necessarily require the organic substrate to be thermally stable.

† This affinity renders the $Fe(CO)_3$ centre a useful protecting group for reactive unsaturated substrates.

ray diffractometry revealed its identity to be the novel *tri*metallic complex [$MoFe_2(\mu_3\text{-}\eta^1\text{:}\eta^1\text{:}\eta^4\text{-}AsC_4Me_4)(CO)_9(\eta^5\text{-}C_5H_5)$], the structure of which is shown in **Figure 5.7**. Notably, the compound represents the first known example of a 7-electron arsolyl ligand where all conceivable donor functions are utilised.




**Scheme 5.10**: Synthesis of $[MoFe_2(\mu_3\text{-}\eta^1\text{:}\eta^1\text{:}\eta^4\text{-}AsC_4Me_4)(CO)_9(\eta^5\text{-}C_5H_5)]$; COE = $\eta^2$-*cis*-cyclooctene.

The product features not only a diene-bound $Fe(CO)_3$ group but also an extraneous $Fe(CO)_4$ centre bridging the arsenic and molybdenum atoms; $[Mo(AsC_4Me_4)(CO)_3(\eta^5\text{-}C_5H_5)]$ has evidently reacted with $[Fe(COE)_2(CO)_3]$ in the desired manner (at the arsolyl diene) whilst encountering a second envoy of iron(0) carbonyl within the reaction medium. Whether this involves another equivalent of $[Fe(COE)_2(CO)_3]$ before transfer of a carbonyl ligand, or directly with adventitious $[Fe(COE)(CO)_4]$ upon warming to ambient temperature (since $[Fe(COE)_2(CO)_3]$ is known to thermally decompose to such a species[48]) followed by decarbonylation, or by some other process involving an ephemeral iron source was not established with certainty. $[Mo(AsC_4Me_4)(CO)_3(\eta^5\text{-}C_5H_5)]$ did not react with $[Fe(BDA)(CO)_3]$ in $C_6D_6$ at 60 °C and binuclear complexes of the type $[MoFe(\mu\text{-}\eta^1\text{:}\eta^4\text{-}AsC_4Me_4)(CO)_n(\eta^5\text{-}C_5H_5)]$ ($n$ = 6 or 7) have not been forthcoming by other means.

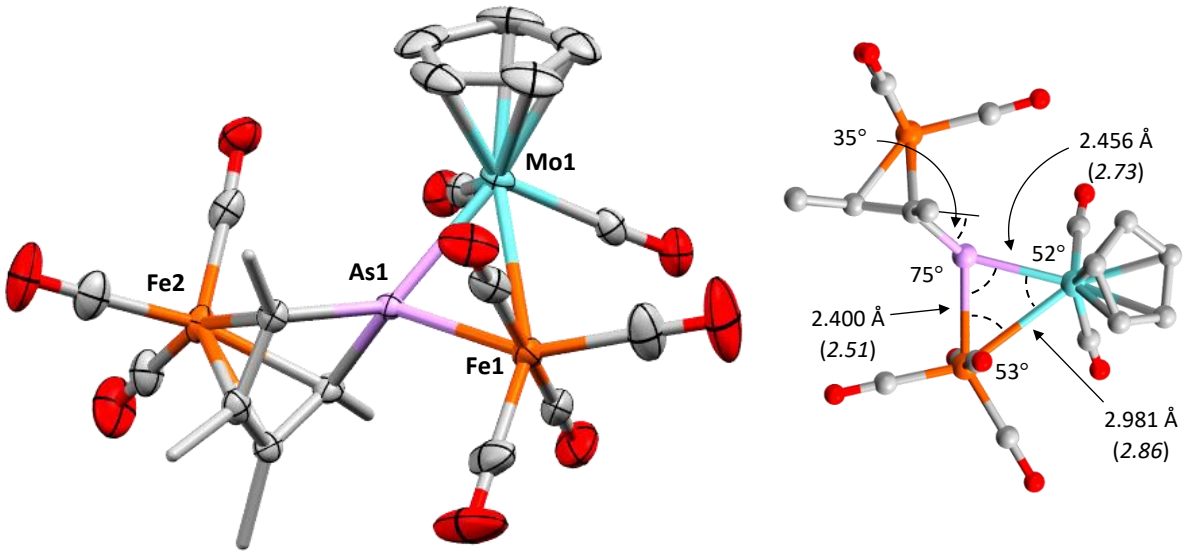



**Figure 5.7**: The molecular structure of [$MoFe_2(\mu_3\text{-}\eta^1\text{:}\eta^1\text{:}\eta^4\text{-}AsC_4Me_4)(CO)_9(\eta^5\text{-}C_5H_5)$] in a crystal. Methyl groups simplified and hydrogen atoms omitted for clarity. Ellipsoids shown at 50% displacement. **Inset**: abbreviated perspective of the molecule viewed perpendicular to the Mo1-As1-Fe1 triangle, with distances and angles of interest denoted; calculated sums of covalent radii are given in italics.

The molecular structure finds the molybdenum-arsolyl complex [$Mo(AsC_4Me_4)(CO)_3(\eta^5\text{-}C_5H_5)$] serving as a four-electron donor to a $Fe(CO)_3$ centre *via* the arsolyl diene system, and separately serving as a two-electron donor *via* the arsenic lone pair to an extraneous $Fe(CO)_4$ group. This iron centre also forms an interaction to the molybdenum atom with an intermetallic separation of 2.9806(5) Å, thus generating an exotic dimetalla-arsacyclopropane ring which incidentally approximates an isosceles triangle (**Figure 5.7**, **Inset**). This bonding distance is comparable though somewhat longer than the Mo-As interactions found in the elegantly simple bridging phosphidos [$MoFe(\mu\text{-}PPh_2)_2(CO)_7$] from MAK (Mo-Fe 2.854(1) Å) and [$MoFe(\mu\text{-}PCy_2)(CO)_6(\eta^5\text{-}C_5H_5)$] from RUIZ (Mo-Fe 2.929(1) Å).[56] The coordination polyhedron of the $Fe(CO)_4$ group best resembles a *pseudo* trigonal bipyramid (*trans* axial CO angle *ca* 170°, equatorial CO angle *ca* 111°; $\tau_5$ = 0.98) with the Mo-As unit occupying the equatorial plane. The respective Fe-As and Mo-As bonding distances of 2.3397(5) and 2.4570(5) Å are both appreciably shorter than the authentic Fe-As and Mo-As covalent bonds in comparable "free" arsolyl complexes (*cf.* [$Fe(AsC_4Ph_4)(CO)_2(\eta^5\text{-}C_5H_5)$] **Chapter 4**, **Section 4.2.1.3**, 2.4319(5) Å; [$Mo(AsC_4Me_4)(CO)_3(\eta^5\text{-}C_5H_5)$] **Section 4.1.3.2**, 2.7267(7) Å), and also

shorter than the same pair in $[MoFe(\mu\text{-}AsC_4Me_4)(CO)_5(\eta^5\text{-}C_5H_5)_2]PF_6$ (Fe-As *ca* 2.39 Å, Mo-As *ca* 2.62 Å; **Section 5.2.4**), and the Mo-As bond in other bridging arsolyl complexes here (*ca* 2.65—2.69 Å).

The title complex is the second such example of an $\eta^4$-arsacyclopentadiene ligand prepared in this work; the butadiene centroid-Fe(0) distance of *ca* 1.70 Å is unremarkable and angles about the tripodal ligand set of 95—100° are as expected for a classical square-based pyramidal metal centre, where the $\eta^4$-diolefin inhabits and is orthogonal-to the basal plane. Complexation of the $Fe(CO)_3$ group to the arsolyl pendant affects significant ring-folding at the carbon atoms α to the arsenic, the latter atom being extruded from the mean plane of the butadiene (with extensive diminution in $sp^2$-character) by *ca* 35° (**Figure 5.7**, **Inset**) which compares to an extrusion angle of *ca* 8° for the same atom in the free *metallo*-ligand $[Mo(AsC_4Me_4)(CO)_3(\eta^5\text{-}C_5H_5)]$. Comparable dihedrals have been measured in other structurally characterised heterole ligands acting in four-electron donor roles (*e.g.*, $[Ni(\eta^4\text{-}Me_2SiC_4Ph_2H_2)_2]$[57] 22°; $[Fe_2(\mu\text{-}\eta^1\text{:}\eta^4\text{-}PhPC_4H_2Me_2)_2(CO)_4]$[58] 29°; *cis*-$[Mo(\eta^4\text{-}Me_2SiC_4H_2Me_2)_2(CO)_2]$[59] 36°; $[Co(\eta^4\text{-}Me_2GeC_4H_2Me_2)(PMe_3)_3]BPh_4$[60] 44°) though the present example appears to fall within the middle of the broad continuum of such complexes. The depletion of olefinic character by the $Fe(CO)_3$ unit also invites significant structural changes to the arsolyl ring, with appreciable elongation of the $C_\alpha$=$C_\beta$ distance on the order of nearly 0.1 Å and a contraction in the $C_\beta$-$C_\beta$ bond of *ca* 0.05 Å – both distortions are statistically significant within the precision limits of the data, though the As-$C_\alpha$ bonds (mean 1.940(4) Å) are crystallographically identical to those in the free *metallo*-ligand.

The nature of interatomic bonding within the Mo-As-Fe triangle is intriguing. In the simplest valence bond interpretation (as was given above), the As-Fe bond is purely dative and the Mo-As bond purely covalent – electron-counting therefore demands that the intermetallic bond also be dative in the direction Fe→Mo (**Figure 5.8**, model **A**), and there is precedent for the LEWIS basicity of $d^8$ Fe(0) centres.[61] A purely covalent Mo-Fe bond is not inconceivable though in this model would impose abnormal oxidation states *i.e.*, Mo(III) and Fe(I); another equally valid perspective involves an As→Mo dative bond alongside Fe-As and Mo-Fe covalent bonds which preserve the elements in common formal oxidation states (**Figure 5.8**, model **B**). The possibility of incipient multiple bonding (**Figure 5.8**, model **C**) was mooted on the basis of a rather short Mo-As bonding distance, and it is worth pointing out that the uncomplexed unit "$[Mo(AsC_4Me_4)(CO)_2(\eta^5\text{-}C_5H_5)]$" would itself recall in both unsaturated geometric and electronic structure

the arsenium complexes [M{As(*t*-Bu)$_2$}(CO)$_2$($\eta^5$-C$_5$H$_5$)] (M = Mo, W) described by MALISCH.[62, 63] The absence of directly comparable arsolyl-bridging arsindiene complexes renders direct conclusions difficult,* though the Fe(CO)$_4$ group does have established proclivity for π-phosphinidene coordination[64-66] for which superficial similarities can be drawn.

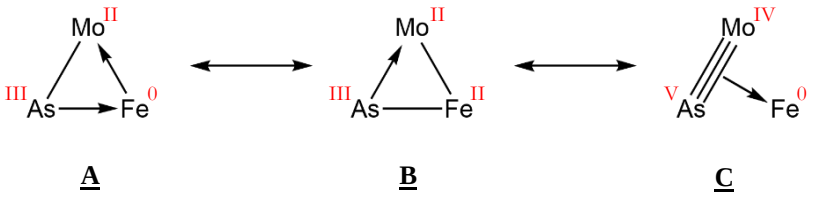



**Figure 5.8**: Canonical bonding descriptions for the dimetalla-arsacyclopropane unit within [MoFe$_2$($\mu_3$-$\eta^1$:$\eta^1$:$\eta^4$-AsC$_4$Me$_4$)(CO)$_9$($\eta^5$-C$_5$H$_5$)], with formal oxidation states denoted in red Roman numerals.

The resemblance of [MoFe$_2$($\mu_3$-$\eta^1$:$\eta^1$:$\eta^4$-AsC$_4$Me$_4$)(CO)$_9$($\eta^5$-C$_5$H$_5$)] to such an arrangement is a curious prospect, especially when considering that the Mo-As distance here (2.4570(5) Å) is intermediate of typical Mo-As single (*ca* 2.7 Å in this work) and structurally characterised Mo≡As triple bonds† (*viz.* 2.252(3) Å in [Mo(≡As){κ$^4$-N(CH$_2$CH$_2$NSiMe$_3$)$_3$}][67], 2.2248(5) Å in [Mo(≡As){N(*t*-Bu)(3,5-C$_6$H$_4$Me$_2$)}$_3$][68]). However, a computational assessment of the hypothetical [MoFe(μ-AsC$_4$Me$_4$)(CO)$_6$($\eta^5$-C$_5$H$_5$)] (DFT: ωB97X-D/6-31G*/LANL2DZ) whilst affording a core geometry in good agreement with the crystal structure found no convincing evidence for π-bonding within-and-around the Mo-As-Fe triangle; LÖWDIN bond orders of 1.09 (Mo-As), 0.79 (As-Fe) and 0.56 (Fe-Mo) are returned for which models **A** and **B** shown in **Figure 5.8** are the best representation of these parameters. The rather short Mo-As bonding distance is almost certainly then a geometric consequence of two 16-electron metal centres striving for structural and electronic saturation.

The IR spectrum of [MoFe$_2$($\mu_3$-$\eta^1$:$\eta^1$:$\eta^4$-AsC$_4$Me$_4$)(CO)$_9$($\eta^5$-C$_5$H$_5$)] finds five $\nu_{CO}$ vibrations in CH$_2$Cl$_2$ solution which resolve into eight in *n*-hexane, and high-resolution mass spectrometry finds the

* Metal bonded Mo-(μ-AsR$_2$)-Fe units are found in a variety of mixed-metal clusters, although these entities appear in contexts unyielding to localised 2-cente 2-electron bonding models and are excluded here to avoid semantic scrutiny.

† There are no examples of structurally characterised Mo=As bonds indexed in the CSD; there are two complexes bearing W=As bonds, however, which serve as the best available benchmark given the roughly similar covalent radii of Mo and W: 2.256(4) Å in [W(=As=S)(κ$^4$-N{CH$_2$CH$_2$NSiMe$_3$}$_3$)]·THF (M. SCHEER *et al. Chem. Eur. J.*, **2006**, *12*, 8603—8608), and 2.2494(14) Å in [W(=AsMe)(κ$^4$-N{CH$_2$CH$_2$NSiMe$_3$}$_3$)][SO$_3$CF$_3$] (R.R. SCHROCK *et al. J. Am. Chem. Soc.*, **1997**, *119*, 11037—11048).

sodium adduct of the molecular ion ($m/z \approx 732.7741$). In defiance of the formal $C_1$ (*i.e.*, chiral) symmetry of the trimetallic complex in the crystal structure (**Figure 5.7**), the ambient temperature $^1$H NMR spectrum ($C_6D_6$) finds a simple trio of signals for the cyclopentadienyl ring (4.96 ppm) and the (apparently equivalent) arsolyl methyl groups in the 2,5- (1.71 ppm) and 3,4-ring positions (1.41 ppm). The ambient temperature $^{13}$C{$^1$H} NMR spectrum also suggests some symmetry-equivalence from site-exchange within the molecule, finding a pair of arsolyl ring-carbon nuclei at 108.1 (α to arsenic) and 71.9 (β) and the exocyclic methyl groups at 16.7 and 12.5 ppm. Noted is the impressive upfield shift of the arsolyl diene function upon complexation of the $Fe(CO)_3$ group (*cf.* free $[Mo(AsC_4Me_4)(CO)_3(\eta^5\text{-}C_5H_5)]$: 148.7 and 141.9 ppm in $C_6D_6$), in accord with the depletion in $sp^2$ character determined crystallographically. Two sharp carbonyl resonances are found at 211.8 and 209.8 which – on the basis of their 4:3 area integration – are assigned to the $Fe(CO)_4$ and $Fe(CO)_3$ groups, respectively; a very weak, very broad signal at 239.3 ppm is assigned to the $Mo(CO)_2(\eta^5\text{-}C_5H_5)$ centre.

Despite being deficient of any formal point symmetry, these ambient temperature NMR data clearly indicate the molecule to be non-rigid; indeed, three independent modes of internal fluxionality are present in solution which confer time-averaged extant $C_s$ symmetry to $[MoFe_2(\mu_3\text{-}\eta^1\text{:}\eta^1\text{:}\eta^4\text{-}AsC_4Me_4)(CO)_9(\eta^5\text{-}C_5H_5)]$ (**Figure 5.9**):

1) Three-fold rotation of the $Fe(CO)_3$ group (red),

2) *Pseudo*-rotation of the $Fe(CO)_4$ group (blue),

3) Two-fold rotation of the $Mo(CO)_2(\eta^5\text{-}C_5H_5)$ group (orange).

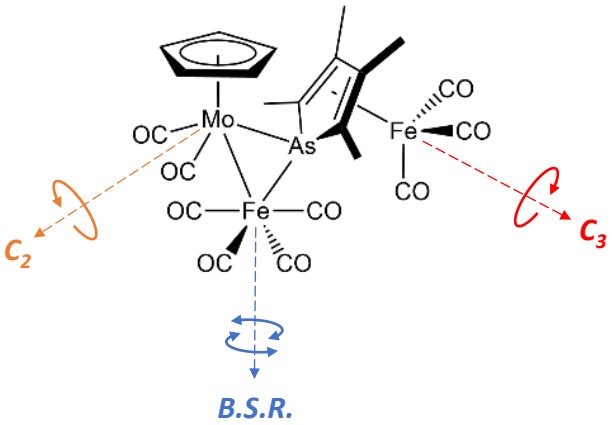



**Figure 5.9**: Modes of internal fluxionality within $[MoFe_2(\mu_3\text{-}\eta^1\text{:}\eta^1\text{:}\eta^4\text{-}AsC_4Me_4)(CO)_9(\eta^5\text{-}C_5H_5)]$.

Variable temperature $^{13}C\{^1H\}$ NMR spectra were collected in $CD_2Cl_2$ solution in the range 298—238 K (25 to -35 °C) and vignettes of these spectra are shown in **Figure 5.10**. Note that chemical shifts reported in the following section were collected in a different solvent to those above, though differences are subtle. Nevertheless, to assist with commutation their $^{13}C\{^1H\}$ assignments in both $C_6D_6$ and $CD_2Cl_2$ are collated below in **Table 5.3**.

**Table 5.3**: $^{13}C\{^1H\}$ NMR chemical shifts (ppm) for $[MoFe_2(\mu_3\text{-}\eta^1\text{:}\eta^1\text{:}\eta^4\text{-}AsC_4Me_4)(CO)_9(\eta^5\text{-}C_5H_5)]$ in $C_6D_6$ and $CD_2Cl_2$.

| | $Mo(CO)_2$ | $Fe(CO)_4$ | $Fe(CO)_3$ | 2,5-C | $C_5H_5$ | 3,4-C | 2,5-$CH_3$ | 3,4-$CH_3$ |
|---|---|---|---|---|---|---|---|---|
| Solvent | 298 K / 25 °C | | | | | | | |
| $C_6D_6$ | 239.3 | 211.8 | 209.8 | 108.1 | 90.3 | 71.9 | 16.8 | 12.6 |
| $CD_2Cl_2$ | 240.3 | 211.8 | 210.2 | 108.7 | 90.2 | 72.2 | 17.0 | 13.4 |
| | 238 K / -35 °C | | | | | | | |
| $CD_2Cl_2$ | 242.8<br>237.8 | 211.5 | 210.0 | 108.3<br>108.0 | 90.2 | 72.2<br>70.7 | 17.2<br>16.8 | 13.1 |

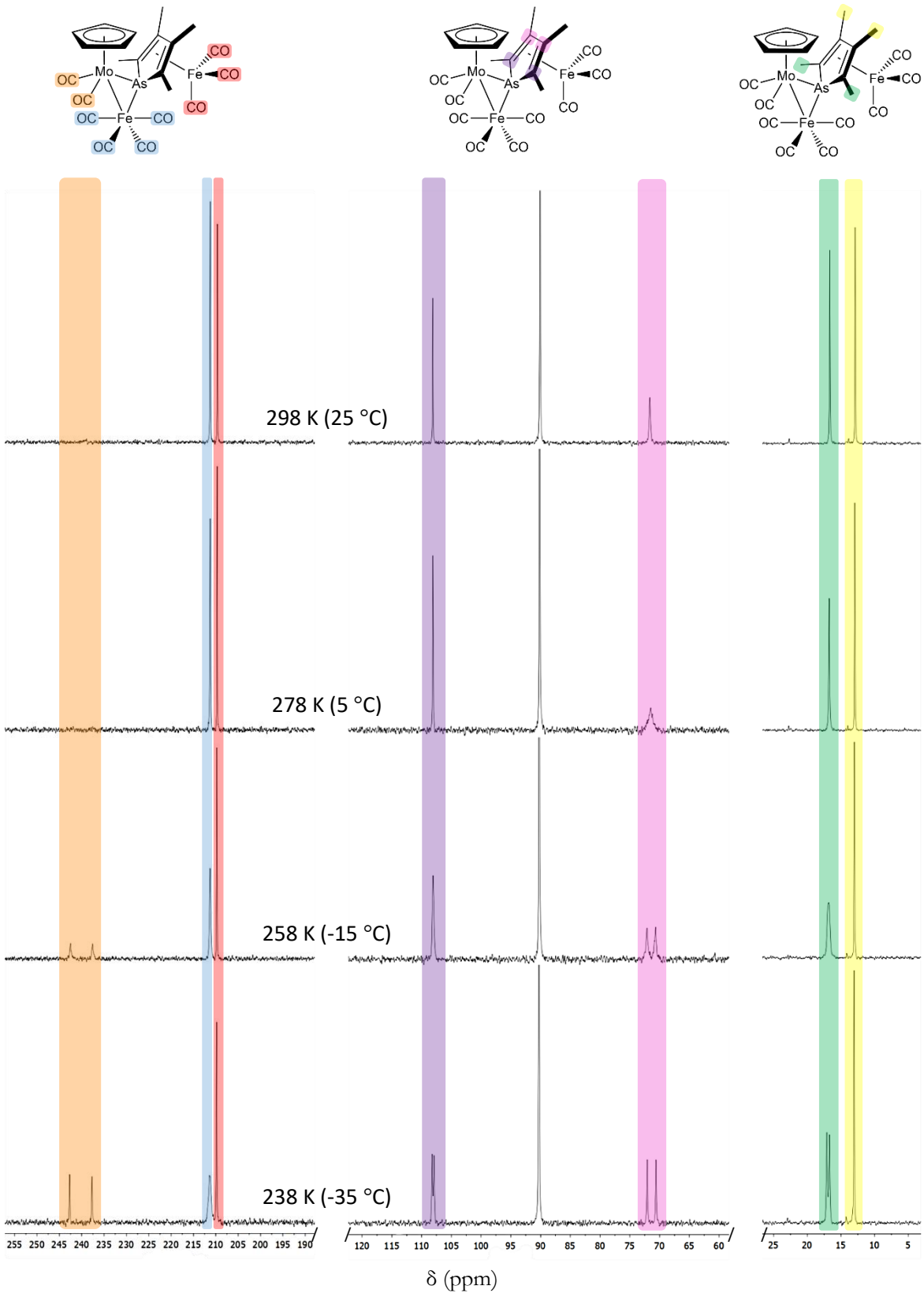



**Figure 5.10**: Vignettes of variable temperature $^{13}C\{^{1}H\}$ NMR spectra, collected over the range 298—238 K, of $[MoFe_2(\mu_3\text{-}\eta^1\text{:}\eta^1\text{:}\eta^4\text{-}AsC_4Me_4)(CO)_9(\eta^5\text{-}C_5H_5)]$ in $CD_2Cl_2$ solution. See **Table 5.3** for precise chemical shifts.

Of interest is the carbonyl region which sees the previously broad signal at 240.3 ppm (298 K) resolve into a pair of comparatively sharp resonances at 242.8 and 237.8 ppm as rotation of the $Mo(CO)_2(\eta^5\text{-}C_5H_5)$ group is arrested upon cooling (first discernible at 278 K; the coalescence point appears to be near this temperature though it was not determined precisely). Motion of the $Mo(CO)_2(\eta^5\text{-}C_5H_5)$ centre is unsurprisingly coupled to equivalency of the arsolyl constituents, since the same temperature gradient also results in resolution of the ring-carbon environments into pairs of diastereotopic nuclei as symmetric transition-state/intermediate geometry accessed at ambient temperature is no longer traversed at reduced temperatures. The methyl groups in the 2,5-ring positions also separate into a diastereotopic pair between 258 and 238 K, whilst those in the 3,4-ring positions remain rather sharp presumably for their distality to the epicentre of motion, lending their chemical environments a greater degree of apparent equivalence.

*Pseudo*-rotation of the $Fe(CO)_4$ is slowed at 238 K (-35 °C) but not totally halted, as evidenced by the gradual broadening of the signal at 211.8 ppm albeit without discernible resolution into axial and equatorial carbonyl environments; the single diene-bound $Fe(CO)_3$ resonance at 210.0 ppm remains well-defined at this temperature. Regrettably, internal motions in complexes of the type $[Fe(L)(CO)_4]$ (L = phosphine, alkene, alkyne) appear to remain in operation on the $^{13}C$ NMR time-scale at temperatures inaccessible to the spectrometer available* (*cf.* the coalescence point of $[Fe(Me_3SiC{\equiv}CSiMe_3)(CO)_4]$ is *ca* -70 °C at 101 MHz[69]).

## 5.3 Summary

In this work, a selection of labile LEWIS acidic metal centres – all of which have established proclivity for tertiary arsine coordination – were combined with the *metallo*-ligand $[Mo(AsC_4Me_4)(CO)_3(\eta^5\text{-}C_5H_5)]$ to provide five μ-arsolyl complexes in generally good yields. The nucleophilic As(III) function promptly displaces the weakly held solvent ligands from $[Au(C_6F_5)(THT)]$ (**Figure 5.1**), $[Cr(THF)(CO)_5]$ (**Figure 5.2**), $[Fe(THF)(CO)_2(\eta^5\text{-}C_5H_5)]PF_6$ (**Figure 5.4**) and $[Mn(THF)(CO)_2(\eta^5\text{-}C_5H_4Me)]$ (**Figure 5.5**), and a single carbonyl ligand from the methylidyne cluster $[Co_3(\mu_3\text{-}CH)(CO)_9]$ (**Figure 5.3**); crystal structures for all were determined, providing the first structural data for μ-arsolyl ligands. For the latter three reactions,

* The practical operating limit of the 700 MHz NMR spectrometer employed (176 MHz for $^{13}C$) was *ca* -40 °C.

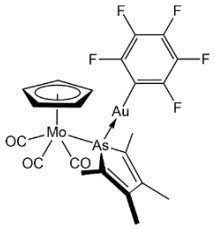
competing redox processes appear to operate since products of single electron transfer and/or Mo-As bond homolysis were also isolated: one of these included the first example of a biarsolyl complex in $[Mn_2\{\mu\text{-}(AsC_4Me_4)_2\}(CO)_4(\eta^5\text{-}C_5H_4Me)_2]$ arising from As(III)→As(II) reduction, which was identified by unequivocal synthesis and X-ray diffractometry (**Figure 5.6**). The addition of labile metal halide reagents invariably led to Mo-As bond cleavage with arsenic but *not* metal halogenation among other unknown decomposition routes.

Emergent spectroscopic and structural trends within $[MoM(\mu\text{-}AsC_4Me_4)(CO)_3L_n(\eta^5\text{-}C_5H_5)]^{n+}$ (**Section 5.2.6**) reveal coordination of the arsenic lone pair to have a very slight shielding effect on the hydrogen and carbon nuclei comprising the arsolyl ring, which is interpreted as compromising the at-best modest ring-current and associated magnetic anisotropy in $\lambda^3$-arsoles; conversely, a small deshielding effect is placed upon the Mo(II) centre as electron-density is reduced at the arsenic atom bonded thereto. These reciprocal phenomena highlight – above all else – the appreciable electronic insulation of the As(III) within the arsolyl group. It also emerged that crystallographic data were insufficiently precise to serve reliably as indicators (bond length alternation) of the gain or loss of aromatic character.

In contrast to the previous examples in which the π-system of the arsolyl ring assumed an essentially spectatorial role, addition of very labile $[Fe(COE)_2(CO)_3]$ to $[Mo(AsC_4Me_4)(CO)_3(\eta^5\text{-}C_5H_5)]$ produced the trimetallic complex $[MoFe_2(\mu_3\text{-}\eta^1\text{:}\eta^1\text{:}\eta^4\text{-}AsC_4Me_4)(CO)_9(\eta^5\text{-}C_5H_5)]$ in good yield; the adduct is noteworthy for featuring not only a diene-bound $Fe(CO)_3$ group but a *pseudo* trigonal bipyramidal $Fe(CO)_4$ centre attending an unsaturated $[Mo(AsC_4Me_4)(CO)_2(\eta^5\text{-}C_5H_5)]$ entity, forming a novel dimetalla-arsacyclopropane triangle. Notwithstanding the first example of a 7-electron donor arsolyl ligand, the complex exhibits several independent modes of internal fluxionality in solution and the molecular structure was determined by X-ray crystallography (**Figure 5.7**). The most relevant canonical description of bonding within the complex would appear to be that of localised Mo-As, As→Fe and Fe→Mo interactions with little supporting computational evidence for π-type mixing between the constituents.

## 5.4 Experimental

### 5.4.1 [MoAu(μ-AsC$_4$Me$_4$)(C$_6$F$_5$)(η$^5$-C$_5$H$_5$)]

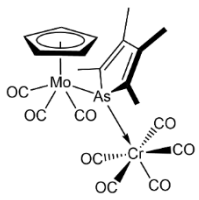



To a stirred solution of 0.12 g [Mo(AsC$_4$Me$_4$)(CO)$_3$(η$^5$-C$_5$H$_5$)] (0.28 mmol) in 5 mL $CH_2Cl_2$ was added 0.12 g solid [Au(C$_6$F$_5$)(THT)] (0.26 mmol) and the mixture stirred overnight; no obvious colour change takes place during this time. The mixture is dried by rotary evaporation and the yellow residue washed with $Et_2O$ and *n*-pentane (with trituration) and dried under vacuum. Isolated yield: 0.15 g (0.19 mmol, 67%). The product is readily soluble in polar organic and aromatic solvents, poorly soluble in $Et_2O$ and aliphatic hydrocarbons, and is air stable as a solid.

NMR $^1$H (C$_6$D$_6$, 400 MHz, 25 °C): $\delta_H$ 4.70 (s, 5H, η$^5$-C$_5$*H*$_5$), 1.84 (s, 6H, α-C*H*$_3$), 1.62 (s, 6H, β-C*H*$_3$). $^{13}$C{$^1$H} (C$_6$D$_6$, 176 MHz, 25 °C): $\delta_C$ = 232.7 (*transoid CO*), 223.7 (*cisoid CO*), 149.9 (m, *C*$_6$F$_5$), 148.8 (m, *C*$_6$F$_5$), 142.7 (arsole {2,5}-*C*), 140.4 (arsole {3,4}-*C*), 138.6 (m, *C*$_6$F$_5$), 137.0 (m, *C*$_6$F$_5$), 92.7 (η$^5$-*C*$_5$H$_5$), 14.8 (α-*C*H$_3$), 14.5 (β-*C*H$_3$). $^{19}$F{$^1$H} (C$_6$D$_6$, 376 MHz, 25 °C) $\delta_F$ = -115.9 (m, 2F, {2,6}-C$_6$*F*$_5$), -158.7 (t, $^3J_{FF}$ = 20 Hz, 1F, {4}-C$_6$*F*$_5$), -162.0 [m, 2F, {3,5}-C$_6$*F*$_5$)]. IR ($CH_2Cl_2$) $\nu_{CO}$ 2034(vs), 1965(sh), 1949(vs) cm$^{-1}$; HR-MS (ESI, MeCN, +ve ion) found many ion fragments with correct isotopic envelopes (for the presence of Mo nuclei) however no chemically-sensible formulae could be devised. Analysis Found C, 33.19; H, 2.14%. Calc. for $C_{22}H_{17}O_3AsAuF_5Mo$: C, 33.36; H, 2.16%.

Single crystals were obtained by vapour diffusion of $Et_2O$ into $CH_2Cl_2$ solution at -20 °C. Four discreet molecules were found within the asymmetric unit. Some excess residual electron density remained in the vicinity of the gold atoms which was not treated with any restraints or constraints. $C_{22}H_{17}O_3As_1Au_1F_5Mo_1$ ($M$ = 792.18 g/mol): yellow plate 0.058 × 0.058 × 0.077 mm, monoclinic, space group $P2_1/n$ (no. 14), $a$ = 23.8893(5) Å, $b$ = 38.4002(3) Å, $c$ = 14.8049(3) Å, $\beta$ = 136.531(4)°, $V$ = 9343.4(6) Å$^3$, $Z$ = 16, spherical correction $T_{min}/T_{max}$ = 0.367/0.426, $\mu$(Cu-Kα) = 18.183 mm$^{-1}$, $\varrho_{calc}$ = 2.253 g/cm$^3$, 37213 reflections measured (7.596° ≤ 2Θ ≤ 147.508°), 18440 unique ($R_{int}$ = 0.0266, $R_{sigma}$ = 0.0393) which were used in all calculations, $GOF$ = 1.028, $D_{min}/D_{max}$ = -2.0/3.9 e/Å$^3$. The final $R_1$ was 0.0369 (I > 2σ(I)) and $wR_2$ was 0.0840 (all data).

### 5.4.2 [CrMo(μ-AsC$_4$Me$_4$)(CO)$_8$(η$^5$-C$_5$H$_5$)]



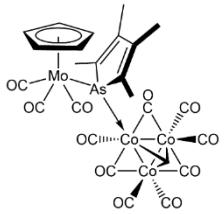

A dilute solution of [Cr(THF)(CO)$_5$] was prepared by UV-photolysis of [Cr(CO)$_6$] (0.1 g, excess. **Caution**: **toxic**) in 20 mL THF at ambient temperature: progress was monitored by IR spectroscopy ($\nu_{CO}$ 2072(w), 1935(vs), 1896(s) cm-

1). When complete, the orange solution was transferred to a solution of 0.11 g $[Mo(AsC_4Me_4)(CO)_3(\eta^5\text{-}C_5H_5)]$ (0.25 mmol) in 5 mL THF and the reaction stirred overnight. The mixture was dried by rotary evaporation and the yellow-brown residue extracted with small portions of petroleum ether and transferred to a column of neutral alumina (20 x 2.5 cm) made up in petroleum ether. Eluting with 9:1 petroleum ether/$Et_2O$ removed traces of unreacted/reformed $[Cr(CO)_6]$. Eluting with 4:1 petroleum ether/$CH_2Cl_2$ provided a yellow band which was collected under a stream of nitrogen and dried. The residue was re-crystallised from the minimum amount of hot $CHCl_3$/*n*-heptane cooled to -20 °C overnight under nitrogen. Isolated yield: 0.13 g (0.21 mmol, 84%). The product is readily soluble in polar organic and aromatic solvents, and somewhat soluble in aliphatic hydrocarbons. The solid product is reasonably air stable, however solutions decompose to insoluble green materials overnight.

NMR $^1H$ ($C_6D_6$, 400 MHz, 25 °C): $\delta_H$ 4.36 (s, 5H, $\eta^5\text{-}C_5H_5$), 2.07 (s, 6H, α-$CH_3$), 1.73 (s, 6H, β-$CH_3$). $^{13}C\{^1H\}$ ($C_6D_6$, 176 MHz, 25 °C): $\delta_C$ 223.1 (*transoid* Mo-*C*O), 224.7 (*cisoid* Mo-*C*O), 223.8 (axial Cr-*C*O), 218.3 (equatorial Cr-*C*O), 149.4 (arsole {2,5}-*C*), 137.5 (arsole {3,4}-*C*), 93.2 ($\eta^5\text{-}C_5H_5$), 15.0 (α-$CH_3$), 13.7 (β-$CH_3$). IR ($CH_2Cl_2$) $\nu_{CO}$ 2056(m), 2024(s), 1947(vs), 1934(sh), 1917(sh) $cm^{-1}$; IR (*n*-hexane) $\nu_{CO}$ 2058(s), 2025(vs), 1978(w), 1956(vs), 1939(vs), 1924(vs) $cm^{-1}$. HR-MS (ESI, MeCN, +ve ion) Found *m*/*z* 565.8706 (calc. for $C_{19}H_{17}O_6{}^{75}As_1{}^{52}Cr_1{}^{98}Mo_1$ $[M-2CO]^+$: 565.8704). Analysis Found: C, 40.68; H, 2.70%. Calc. for $C_{21}H_{17}O_8As_1Cr_1Mo_1$: C, 40.69; H, 2.76%.

Single crystals were obtained from cooling a hot $CHCl_3$/*n*-heptane solution to -20 °C. $C_{21}H_{17}O_8As_1Cr_1Mo_1$ ($M$ = 620.21 g/mol): yellow prism 0.044 × 0.107 × 0.139 mm, triclinic, space group *P*-1 (no. 2), $a$ = 10.0861(3) Å, $b$ = 10.5319(4) Å, $c$ = 13.2660(5) Å, α = 77.541(3)°, $\beta$ = 70.581(3)°, $\gamma$ = 61.676(3)°, $V$ = 1167.06(8) Å$^3$, $Z$ = 2, spherical correction $T_{min}/T_{max}$ = 0.480/0.521, $\mu$(Cu-Kα) = 10.200 $mm^{-1}$, $\varrho_{calc}$ = 1.765 g/cm$^3$, 11692 reflections measured (7.082° ≤ 2Θ ≤ 146.586°), 4647 unique ($R_{int}$ = 0.0293, $R_{sigma}$ = 0.0348) which were used in all calculations, *GOF* = 1.043, $D_{min}/D_{max}$ = -0.67/0.96 e/Å$^3$. The final $R_1$ was 0.0273 (I > 2σ(I)) and $wR_2$ was 0.0698 (all data).

### 5.4.3 $[MoCo_3(\mu\text{-}AsC_4Me_4)(\mu_3\text{-}CH)(CO)_{11}(\eta^5\text{-}C_5H_5)]$




A 20 mL Schlenk tube was charged with 0.14 g $[Mo(AsC_4Me_4)(CO)_3(\eta^5\text{-}C_5H_5)]$ (0.33 mmol) and 0.16 g $[Co_3(\mu_3\text{-}CH)(CO)_9]$ (0.36 mmol) under nitrogen. To this was added 10mL $CH_2Cl_2$ and the mixture stirred overnight. The brown solution is absorbed onto a small quantity of celite by evaporation of the solvent. Once dry, this was transferred to column of silica gel (20 x 2.5 cm) made up in petroleum ether. Eluting with the same solvent provided a purple band of unchanged $[Co_3(\mu_3\text{-}CH)(CO)_9]$ (recovered *ca* 15 mg). Subsequent elution with 9:1 petroleum ether/$Et_2O$ provided a blue-green band of the known cluster $[MoCo_2(\mu_3\text{-}CH)(CO)_8(\eta^5\text{-}C_5H_5)]$ which was collected and dried by rotary evaporation. Isolated yield: *ca* 20 mg (12 %).

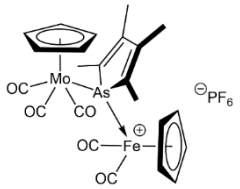
The following data for $[MoCo_2(\mu_3\text{-}CH)(CO)_8(\eta^5\text{-}C_5H_5)]$ may be compared with those reported by VAHRENKAMP.[33] NMR: $^1H$ ($C_6D_6$, 400 MHz, 25 °C) $\delta_H$ 10.78 (s, 1H, $\mu_3$-*CH*), 4.48 (s, 5H, $\eta^5\text{-}C_5H_5$). $^{13}C\{^1H\}$ ($C_6D_6$, 176 MHz, 25 °C) $\delta_C$ 251.3 ($\mu_3$-*C*H), 208.5 (br, Mo- & Co-CO, FWHM *ca* 100 Hz), 90.7 ($\eta^5\text{-}C_5H_5$) ppm; IR ($CH_2Cl_2$) $\nu_{CO}$ 2083(s), 2071(s), 2040(sh), 2028(vs), 2015(vs), 2001(vs) $cm^{-1}$.

Eluting with 9:1 petroleum ether/$CH_2Cl_2$ provides a dark yellow band containing the title compound which is collected and dried by rotary evaporation providing a brown residue. Solutions are dark yellow in colour, however repeated drying and prolonged trituration in *n*-pentane gives the product as a red-brown solid which is collected and dried under air. Isolated yield: 95 mg (0.11 mmol, 33%). The product is readily soluble in polar organic and aromatic solvents, and somewhat soluble in $Et_2O$ and aliphatic hydrocarbons. The product is reasonably air stable as a solid or solution however decomposes to insoluble grey residues over several days.

NMR: $^1$H ($C_6D_6$, 400 MHz, 25 °C) $\delta_H$ 9.75 (s, 1H, $\mu_3$-C*H*), 4.33 (s, 5H, $\eta^5$-$C_5H_5$), 1.99 (s, 6H, α-C$H_3$), 1.67 (s, 6H, β-C$H_3$); $^{13}$C{$^1$H} ($C_6D_6$, 176 MHz, 25 °C) $\delta_C$ 235.5 ($\mu_3$-*C*H), 232.8 (*transoid* Mo-*C*O), 224.8 (*cisoid* Mo-*C*O), 206.8 (br, Co-*C*O), 147.5 (arsole {2,5}-*C*), 137.7 (arsole {3,4}-*C*) , 93.0 ($\eta^5$-$C_5H_5$), 14.7 (α-*C*H$_3$), 13.3 (β-*C*H$_3$) ppm; IR ($CH_2Cl_2$) $\nu_{CO}$ 2072(s), 2032(vs), 2011(vs), 1961(s), 1936(s), 1862(m, br) cm$^{-1}$; HR-MS (ESI, MeCN, +ve ion) found many ion fragments corresponding to the presence of Mo nuclei, however no chemically sensible formulae could be devised; Analysis Found 35.51% C, 2.47% H; calc. for $C_{25}H_{18}O_{11}As_1Co_3Mo_1$: 35.66% C, 2.15% H.

Single crystals were obtained by slow evaporation of an NMR solution in $C_6D_6$. $C_{25}H_{18}O_{11}As_1Co_3Mo_1$ ($M$ = 842.04 g/mol): red prism 0.115 × 0.255 × 0.289 mm, monoclinic, space group $C2/c$ (no. 15), $a$ = 30.0109(4) Å, $b$ = 11.14800(10) Å, $c$ = 17.8024(2) Å, $\beta$ = 100.5150(10)°, $V$ = 5855.98(12) Å$^3$, $Z$ = 8, spherical correction $T_{min}/T_{max}$ = 0.479/0.520, μ(Cu Kα) = 18.264 mm$^{-1}$, $\rho_{calc}$ = 1.910 g/cm$^3$, 17415 reflections measured (8.478° ≤ 2Θ ≤ 147.656°), 5839 unique ($R_{int}$ = 0.0308, $R_{sigma}$ = 0.0285) which were used in all calculations, $GOF$ = 1.063/ $D_{min}/D_{max}$ = -1.29/0.50 e/Å$^3$. The final $R_1$ was 0.0340 (I > 2σ(I)) and $wR_2$ was 0.0877 (all data).

### 5.4.4 [MoFe(μ-AsC$_4$Me$_4$)(CO)$_5$($\eta^5$-C$_5$H$_5$)$_2$]PF$_6$



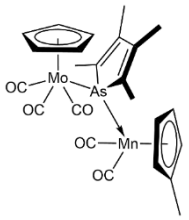

A solution of 0.12 g [Mo(AsC$_4$Me$_4$)(CO)$_3$($\eta^5$-C$_5$H$_5$)] (0.28 mmol) in 5mL $CH_2Cl_2$ was added to a stirred solution of 0.095 g [Fe(THF)(CO)$_2$($\eta^5$-C$_5$H$_5$)]PF$_6$ (0.25 mmol) also dissolved in 5 mL of the same solvent. A colour change from orange to a dark yellow-brown takes place over several minutes and the reaction stirred overnight. After this time, the mixture is filtered through a short plug of celite (2 x 1 cm) and the dark yellow filtrate dried under reduced pressure. The solids are washed with toluene (3 x 3 mL) and $Et_2O$ (3 x 3 mL) to remove any neutral species (including [Fe$_2$(CO)$_4$($\eta^5$-C$_5$H$_5$)$_2$]) and dried. The crude residue was then crystallised from $CH_2Cl_2$/$Et_2O$ at -20 °C overnight under nitrogen. Isolated yield 0.092 g (0.12 mmol, 42%). The product is readily soluble in polar organic solvents and may be handled in air as a solid, though solutions darken overnight with formation of brown residues. The compound could, however, not be isolated in an analytically pure state.

*Note*: the use of [Fe(THF)(CO)$_2$($\eta^5$-C$_5$H$_5$)]PF$_6$ prepared *in situ* from [FeBr(CO)$_2$($\eta^5$-C$_5$H$_5$)] and AgPF$_6$ in THF gave very low yields of impure product and the formation of [Fe$_2$(CO)$_4$($\eta^5$-C$_5$H$_5$)$_2$] as the major species (by IR and NMR spectroscopy) for reasons which remain presently unclear; it was thus preferable to first isolate [Fe(THF)(CO)$_2$($\eta^5$-C$_5$H$_5$)]PF$_6$ where this eventuality was not encountered to such an extent.

NMR: $^{1}$H ($CD_2Cl_2$, 400 MHz, 25 °C): $\delta_H$ 5.20 (s, br, 5H, Mo-$\eta^5$-$C_5H_5$), 4.85 (s, br, 5H, Fe-$\eta^5$-$C_5H_5$), 2.02 (s, br, 6H, α-$CH_3$), 1.87 (s, br, 6H, β-$CH_3$). $^{13}$C{$^{1}$H} ($CD_2Cl_2$, 176 MHz, 25 °C): $\delta_C$ 229.2 (*transoid* Mo-*C*O), 226.0 (*cisoid* Mo-*C*O), 211.2 (Fe-*C*O), 148.2 (arsole {2,5}-*C*), 139.3 (arsole {3,4}-*C*), 95.1 (Mo-$\eta^5$-$C_5H_5$), 86.4 (Fe-$\eta^5$-$C_5H_5$), 15.1 (α-$CH_3$), 14.2 (β-$CH_3$) ppm; IR ($CH_2Cl_2$) $\nu_{CO}$ 2052(vs), 2036(vs), 2004(s), 1980(m), 1947(s) cm$^{-1}$; HR-MS (ESI, MeCN) found many ion fragments with correct isotopic envelopes (for the presence of Mo nuclei) however no chemically-sensible formulae could be devised; Analysis Found C, 36.56; H, 3.05%. Calc. for $C_{23}H_{22}O_5As_1F_6Fe_1Mo_1P_1$: C, 36.93; H, 2.06%.

Crystals were obtained by vapour diffusion of $Et_2O$ into $CH_2Cl_2$ solution at -30 °C. The selected crystal proved to be twinned and a suitable twin-law was found an applied. Data quality was still comparatively poor, however. $C_{23}H_{22}O_5As_1F_6Fe_1Mo_1P_1$ ($M$ = 750.08 g/mol): orange needle 0.118 × 0.151 × 0.305 mm, monoclinic, space group $P2_1/n$ (no. 14), $a$ = 13.6104(11) Å, $b$ = 14.7837(7) Å, $c$ = 13.7151(12) Å, $\beta$ = 100.707(8)°, $V$ = 2711.6(4) Å$^3$, $Z$ = 4, multi-scan correction $T_{min}/T_{max}$ = 0.753/1.000, $\mu$(Cu-Kα) = 10.674 mm$^{-1}$, $\varrho_{calc}$ = 1.837 g/cm$^3$, 5784 reflections measured (8.404° ≤ 2Θ ≤ 147.16°), 5784 unique ($R_{int}$ = 0.0301, $R_{sigma}$ = 0.0363) which were used in all calculations, $GOF$ = 1.034, $D_{min}/D_{max}$ = -0.58/2.54 e/Å$^3$. The final $R_1$ was 0.0743 (I > 2σ(I)) and $wR_2$ was 0.2143 (all data).

### 5.4.5 [MoMn(μ-$AsC_4Me_4$)(CO)$_5$($\eta^5$-$C_5H_5$)($\eta^5$-$C_5H_4Me$)]



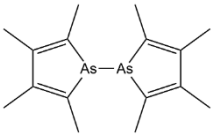

A dilute solution of [Mn(THF)(CO)$_2$($\eta^5$-$C_5H_4Me$)] was prepared by UV-photolysis of 0.1 mL [Mn(CO)$_3$($\eta^5$-$C_5H_4Me$)] (excess. **Caution: toxic**) in 20 mL THF at ambient temperature: progress was monitored by IR spectroscopy ($\nu_{CO}$ 1939(vs), 1841(vs) cm$^{-1}$). When complete, the purple solution was transferred to a solution of 0.11 g [Mo($AsC_4Me_4$)(CO)$_3$($\eta^5$-$C_5H_5$)] (0.25 mmol) in 5 mL THF and allowed to stir overnight. After this time, the mixture was dried by rotary evaporation and the dark brown residue extracted with small portions of petroleum ether and transferred to a column of neutral alumina (20 x 2.5 cm) made up in petroleum ether. Eluting with the same solvent provided a pale yellow band containing unreacted/reformed [Mn(CO)$_3$($\eta^5$-$C_5H_4Me$)] which was discarded. Eluting with 9:1 petroleum ether/$Et_2O$ provided a thin orange band of the biarsolyl complex [MoMn{(μ-$AsC_4Me_4$)$_2$}(CO)$_5$($\eta^5$-$C_5H_5$)($\eta^5$-$C_5H_4Me$)]. Eluting with 1:1 petroleum ether/$Et_2O$ provides a purple-red band which is collected under a stream of nitrogen and dried by rotary evaporation, and re-crystallised from the minimum amount of hot *n*-heptane cooled to -20 °C overnight under nitrogen. Isolated yield 0.105 g (0.17 mmol, 68%). The product is readily soluble in common organic solvents. The product is sufficiently air stable to permit workup without the need for inert atmosphere, however solutions decompose to insoluble brown materials overnight.

NMR: $^{1}$H ($C_6D_6$, 400 MHz, 25 °C): $\delta_H$ 4.90 (s, 5H, $\eta^5$-$C_5H_5$), 4.10 (br s, 2H, {2,5}-$\eta^5$-$C_5H_4(CH_3)$), 3.94 (br s, 2H, {3,4}-$\eta^5$-$C_5H_4(CH_3)$), 2.07 (s, 6H, α-$CH_3$), 1.79 (s, 9H, isochronous $\eta^5$-$C_5H_4(CH_3)$ & β-$CH_3$). $^{13}$C{$^{1}$H} ($C_6D_6$, 176 MHz, 25 °C): $\delta_C$ 235.8 (*transoid* Mo-*C*O), 235.7 (Mn-*C*O), 225.0 (*cisoid* Mo-*C*O), 150.2 (arsole {2,5}-*C*), 135.9 (arsole {3,4}-*C*), 96.4 ({1}-$\eta^5$-$C_5H_4(CH_3)$), 92.7 ($\eta^5$-$C_5H_5$), 82.0 ({2,5}-$\eta^5$-$C_5H_4(CH_3)$), 80.1 ({3,4}-$\eta^5$-$C_5H_4(CH_3)$), 14.8 (α-$CH_3$), 13.8 ($\eta^5$-$C_5H_4(CH_3)$), 13.6 (β-$CH_3$). IR ($CH_2Cl_2$) $\nu_{CO}$ 2021(vs), 1944(vs), 1903(s), 1839(s) cm$^{-1}$. IR (*n*-hexane) $\nu_{CO}$ 2022(s), 1952(vs), 1913(s), 1853(s) cm$^{-1}$. HR-MS (ESI, MeCN, +ve ion) found $m/z$ 619.9280 (calc. for

$C_{24}H_{24}O_5{}^{75}As_1{}^{55}Mn_1{}^{98}Mo_1$ $[M]^+$: 619.9285); Analysis Found: C, 46.57; H, 4.10%. Calc. for $C_{24}H_{24}O_5As_1Mn_1Mo_1$: 46.62% C, 3.91% H.

Single crystals were obtained by cooling a hot *n*-heptane solution to -20 °C. $C_{24}H_{24}O_5As_1Mn_1Mo_1$ ($M$ = 618.23 g/mol): red prism 0.047 × 0.078 × 0.133 mm, monoclinic, space group $P2_1/c$ (no. 14), $a$ = 14.9876(2) Å, $b$ = 9.27920(10) Å, $c$ = 17.3004(2) Å, $\beta$ = 96.5650(10)°, $V$ = 2390.24(5) Å$^3$, $Z$ = 4, spherical correction $T_{min}/T_{max}$ = 0.504/0.543, $\mu$(Cu-Kα) = 10.406 mm$^{-1}$, $\varrho_{calc}$ = 1.718 g/cm$^3$, 14799 reflections measured (10.294° ≤ 2Θ ≤ 147.604°), 4827 unique ($R_{int}$ = 0.0282, $R_{sigma}$ = 0.0322) which were used in all calculations, $GOF$ = 1.036, $D_{min}/D_{max}$ = -0.64/0.56 e/Å$^3$. The final $R_1$ was 0.0253 (I > 2σ(I)) and $wR_2$ was 0.0611 (all data).

### 5.4.6 $(AsC_4Me_4)_2$

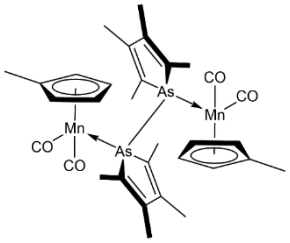



To a stirred solution of 2 g $[ZrCl_2(\eta^5\text{-}C_5H_5)_2]$ (6.8 mmol) in 50 mL THF cooled to -78 °C was added 5.5 mL *n*-BuLi solution (13.7 mmol; 2.5 M in hexanes). After 30 minutes at low temperature, 1.1 mL 2-butyne (13.8 mmol) was added and the mixture allowed to warm to ambient temperature. A colour change from yellow to deep red is observed. After 3 hours, volatiles are removed under reduced pressure and the crude $[ZrC_4Me_4(\eta^5\text{-}C_5H_5)_2]$ re-dissolved in 50 mL *n*-pentane and cooled to -40 °C. To this was added 0.55 mL $AsCl_3$ (6.6 mmol. **Caution: toxic**) dropwise causing the red colour to discharge to a pale-yellow suspension. After 15 minutes the suspension is filtered through a short celite plug (5 x 2.5 cm) into a flask cooled to -40 °C under nitrogen, rinsing with small portions of cold *n*-pentane until washings ran clear. The yellow filtrate is dried under reduced pressure at -40 °C leaving $ClAsC_4Me_4$ as a waxy yellow solid, used in the next step without further purification. Crude isolated yield: 1.3 g (5.9 mmol, 89%).

A dilute sodium amalgam is prepared by slow addition of 150 mg freshly cut sodium (6.6 mmol, in *ca* 30 mg pieces. **Caution: flammable**) to *ca* 1 mL of stirred elemental mercury (**caution: toxic, exothermic dissolution**) under argon. The amalgam was then covered with 5 mL THF. The crude $ClAsC_4Me_4$ from the previous step is dissolved in 20 mL THF, of which 10 mL was withdrawn by syringe and transferred to the amalgam. The remaining THF solution of $ClAsC_4Me_4$ is cooled to -78 °C to prolong shelf-life while $[AsC_4Me_4]^-$ is being prepared. The amalgam is rapidly stirred for 90 minutes over which time the colour of the mixture changes to green, and then eventually to an orange-brown with deposition of a fine grey precipitate. The solution of $[AsC_4Me_4]^-$ is then decanted back into the flask containing the remaining $ClAsC_4Me_4$ at -78 °C and allowed to warm to ambient temperature overnight with stirring. After this time, volatiles are removed under reduced pressure and the residue extracted with *n*-hexane and eluted through a short plug of oven-dried neutral alumina (10 x 2.5 cm) under nitrogen with the same solvent. A yellow band was collected under nitrogen and taken to dryness leaving the product as a lemon-yellow solid, which was deemed sufficiently pure by NMR and used as-is. Isolated yield: 0.64 g (1.7 mmol, 59%). The product is readily soluble in common organic solvents and is air sensitive both as a solid and solution, reverting to unidentified oily brown residues upon exposure to air.

The following data may be compared with those reported by THEOPOLD.[45] NMR: $^1$H ($C_6D_6$, 400 MHz, 25 °C) $\delta_H$ 1.91 (s, 6H, α-C$H_3$), 1.72 (s, 6H, β-C$H_3$) ppm. $^{13}$C{$^1$H} ($C_6D_6$, 400 MHz, 25 °C) $\delta_C$ 142.9 (arsole {2,5}-*C*), 139.5 (arsole {3,4}-*C*), 15.5 (α-*C*H$_3$), 14.6 (β-*C*H$_3$) ppm. HR-MS (EI, MeCN, +ve ion) found m/z 366.0303 (calc. for $C_{16}H_{24}As_2$ $[M]^+$: 366.0304). Crystal data and refinement parameters are given in **Section 8.8** of the **Appendix**.

### 5.4.7 $[Mn_2(AsC_4Me_4)_2(CO)_4(\eta^5\text{-}C_5H_5)_2]$

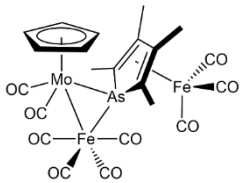



A dilute solution of $[Mn(THF)(CO)_2(\eta^5\text{-}C_5H_4Me)]$ was prepared by UV-photolysis of 0.2 mL $[Mn(CO)_3(\eta^5\text{-}C_5H_4Me)]$ (1.2 mmol. **Caution: toxic**) in 30 mL THF at ambient temperature. Progress is monitored by IR spectroscopy (see **Section 5.2.5**) and when deemed complete is transferred to a solution of 150 mg $[AsC_4Me_4]_2$ (0.4 mmol) in 5 mL THF and allowed to stir overnight. The orange solution is dried by rotary evaporation, extracted with portions of petroleum ether and transferred to a silica gel column (20 x 2.5 cm) made up in petroleum ether. Eluting with the same solvent provides a pale yellow band of unchanged/reformed $[Mn(CO)_3(\eta^5\text{-}C_5H_4Me)]$ which is discarded. Eluting with 9:1 petroleum ether/$Et_2O$ provides a bright orange band which is collected under a stream of nitrogen and dried by rotary evaporation giving an orange-red solid. Isolated yield: 185 mg (0.24 mmol, 61 %). No other products were obtained. The product is readily soluble in common organic solvents and is reasonably air stable in the solid state, however solutions exposed to air degrade to insoluble brown residues over several hours.

NMR: $^1$H ($C_6D_6$, 400 MHz, 25 °C) $\delta_H$ 4.10 (s, 4H, {2,5}-$\eta^5$-$C_5H_4(CH_3)$), 3.95 (s, 4H, {3,4}-$\eta^5$-$C_5H_4(CH_3)$), 2.09 (s, 12H, α-$CH_3$), 1.75 (s, 12H, β-$CH_3$), 1.70 (s, 6H, $\eta^5$-$C_5H_4(CH_3)$) ppm. $^{13}$C{$^1$H} ($C_6D_6$, 176 MHz, 25 °C) $\delta_C$ 232.4 (*C*O), 143.5 (arsole {2,5}-*C*), 139.7 (arsole {3,4}-*C*), 97.3 ({1}-$\eta^5$-$C_5H_4(CH_3)$), 80.1 ({2,5}-$\eta^5$-$C_5H_4(CH_3)$), 79.4 ({3,4}-$\eta^5$-$C_5H_4(CH_3)$), 15.4 (α-$CH_3$), 14.5 (β-$CH_3$), 13.7 ($\eta^5$-$C_5H_4(CH_3)$) ppm. IR ($CH_2Cl_2$) $\nu_{CO}$ 1921(vs), 1864(vs) cm$^{-1}$. IR (*n*-hexane) $\nu_{CO}$ 1941(s), 1930(vs), 1877(vs) cm$^{-1}$. HR-MS (ESI, MeCN, +ve ion) found *m*/*z* 745.9956 (calc. for $C_{32}H_{38}O_4{}^{55}Mn_2{}^{75}As_2$ $[M]^+$: 745.9963). Analysis found 51.61% C, 5.16% H; calc. for $C_{32}H_{38}O_4Mn_2As_2$: 51.50% C, 5.13% H.

Single crystals were obtained from slow evaporation of an NMR solution in $C_6D_6$. $C_{32}H_{38}O_4As_2Mn_2$ ($M$ = 746.34 g/mol): orange prism 0.111 × 0.239 × 0.289 mm, monoclinic, space group *Cc* (no. 9), $a$ = 15.1023(3) Å, $b$ = 10.6207(2) Å, $c$ = 19.3216(5) Å, $\beta$ = 99.683(2)°, $V$ = 3054.97(12) Å$^3$, $Z$ = 4, multi-scan correction $T_{min}/T_{max}$ = 0.830/1.000, $\mu$(Mo-Kα) = 3.012 mm$^{-1}$, $\varrho_{calc}$ = 1.623 g/cm$^3$, 32377 reflections measured (6.668° ≤ 2Θ ≤ 65.13°), 9848 unique ($R_{int}$ = 0.0247, $R_{sigma}$ = 0.0281) which were used in all calculations, *GOF* = 1.045, $D_{min}/D_{max}$ = -0.39/0.69 e/Å$^3$. The final $R_1$ was 0.0240 (I > 2σ(I)) and $wR_2$ was 0.0562 (all data).

### 5.4.8 $[MoFe_2(\mu_3\text{-}\eta^1\text{:}\eta^1\text{:}\eta^4\text{-}AsC_4Me_4)(CO)_9(\eta^5\text{-}C_5H_5)]$




A dilute solution of $[Fe(COE)_2(CO)_3]$ was prepared by UV-photolysis of 0.1 g $[Fe(CO)_5]$ (0.7 mmol, excess. **Caution: toxic**) at -78 °C in a solution of 10 mL *n*-hexane containing 0.5 mL *cis*-cyclooctene (4 mmol, large excess); over the course of 90 minutes a light yellow precipitate of thermolabile $[Fe(COE)_2(CO)_3]$ forms which was not isolated nor characterised. To this was added 0.14 g $[Mo(AsC_4Me_4)(CO)_3(\eta^5\text{-}C_5H_5)]$ (0.33 mmol) and the mixture allowed to warm

slowly with stirring overnight during which time a red-brown suspension forms. Operations are now carried out without exclusion of air. The reaction mixture was transferred to a column of neutral alumina (15 x 2.5 cm) made up in petroleum ether. Eluting with 9:1 petroleum ether/$Et_2O$ provides a pale yellow band containing unreacted [$Fe(CO)_5$] and *cis*-cyclooctene which is discarded. Eluting with 2:1 petroleum ether/$Et_2O$ provides an orange-red band which is collected and dried by rotary evaporation and further re-crystallised from the minimum amount of $Et_2O$ at 0 °C overnight. Isolated yield: 0.15 g (0.21 mmol, 64 %). The product is readily soluble in common organic solvents and is reasonably air stable both as a solid and in solution.

NMR: $^1$H ($C_6D_6$, 400 MHz, 25 °C) $\delta_H$ 4.96 (s, 5H, $\eta^5$-$C_5H_5$), 1.71 (s, 6H, α-$CH_3$), 1.41 (s, 6H, β-$CH_3$). $^{13}$C{$^1$H} ($C_6D_6$, 176 MHz, 25 °C) $\delta_C$ 239.3 (br, Mo-*C*O), 211.8 (Fe-(*C*O)$_4$), 209.8 (Fe-(*C*O)$_3$), 108.1 (arsole {2,5}-*C*), 90.2 ($\eta^5$-$C_5H_5$), 71.9 (arsole {3,4}-*C*), 16.8 (α-*C*H3), 12.6 (β-$CH_3$). ($CD_2Cl_2$, 400 MHz, 25 °C) $\delta_H$ 5.45 (s, 5H, $\eta^5$-$C_5H_5$), 2.31 (s, 6H, α-$CH_3$), 1.64 (s, 6H, β-$CH_3$) ppm. $^{13}$C{$^1$H} ($CD_2Cl_2$, 176 MHz, 25 °C) $\delta_C$ 240.3 (br, Mo-*C*O) 211.8 (Fe-(*C*O)$_4$), 209.8 (Fe-(*C*O)$_3$), 108.7 (arsole {2,5}-*C*), 90.2 ($\eta^5$-$C_5H_5$), 72.2 (arsole {3,4}-*C*), 17.2 (α-$CH_3$), 13.4 (β-$CH_3$) ppm. $^{13}$C{$^1$H} ($CD_2Cl_2$, 176 MHz, -35 °C) $\delta_C$ 242.8 (Mo-*C*O), 237.8 (Mo-*C*O), 211.5 (Fe-(*C*O)$_4$), 209.9 (Fe-(CO)$_3$), 108.3 (arsole {2,5}-*C*), 108.0 (arsole {2,5}-*C*), 90.3 ($\eta^5$-$C_5H_5$), 72.2 (arsole {3,4}-*C*), 70.7 (arsole {3,4}-*C*), 17.2 (α-$CH_3$), 16.8 (α-$CH_3$), 13.1 (β-$CH_3$). IR ($CH_2Cl_2$) $\nu_{CO}$ 2054(sh), 2041(vs), 1977(vs, br), 1923(s), 1854(s) cm$^{-1}$; IR (*n*-hexane) $\nu_{CO}$ 2055(s), 2042(vs), 1999(s), 1987(vs), 1979(vs), 1965(s), 1938(vs), 1878(vs) cm$^{-1}$; HR-MS (ESI, MeOH, +ve ion) found *m*/*z* 732.7741 (calc. for $C_{22}H_{17}O_9{}^{23}Na_1{}^{56}Fe_2{}^{75}As_1{}^{98}Mo_1$ [*M* + Na]$^+$: 732.7739); Analysis found 37.30% C, 2.42% H; calc. for $C_{22}H_{17}O_9As_1Fe_2Mo_1$: 37.33% C, 2.42% H.

Single crystals were obtained by slow evaporation of $Et_2O$ solution at 0 °C. $C_{22}H_{17}O_9As_1Fe_2Mo_1$ ($M$ = 707.91 g/mol): orange prism 0.156 × 0.186 × 0.313 mm, monoclinic, space group $P2_1/n$ (no. 14), $a$ = 10.5108(4) Å, $b$ = 17.0332(6) Å, $c$ = 14.9828(6) Å, $\beta$ = 110.271(5)°, $V$ = 2516.27(18) Å$^3$, $Z$ = 4, multi-scan correction $T_{min}/T_{max}$ = 0.827/1.000, $\mu$(Mo-Kα) = 2.982 mm$^{-1}$, $\varrho_{calc}$ = 1.869 g/cm$^3$, 16588 reflections measured (7.518° ≤ 2Θ ≤ 64.822°), 7810 unique ($R_{int}$ = 0.0335, $R_{sigma}$ = 0.0580) which were used in all calculations, *GOF* = 1.038, $D_{min}/D_{max}$ = -0.75/0.7 e/Å$^3$. The final $R_1$ was 0.0394 (I > 2σ(I)) and $wR_2$ was 0.0812 (all data).

## 5.5 References


1. E. W. Abel and C. Towers, *J. Chem. Soc. Dalton Trans.*, **1979**, 814-819.
2. G. Thiollet, F. Mathey and R. Poilblanc, *Inorg. Chim. Acta*, **1979**, *32*, L67-L68.
3. H. Vahrenkamp, *Chem. Ber.*, **1972**, *105*, 1486-1496.
4. R. Janta, W. Albert, H. Rößner, W. Malisch, H. J. Langenbach, E. Röttinger and H. Vahrenkamp, *Chem. Ber.*, **1980**, *113*, 2729-2738.
5. H. J. Langenbach, E. Keller and H. Vahrenkamp, *J. Organomet. Chem.*, **1979**, *171*, 259-271.
6. R. Müller and H. Vahrenkamp, *Chem. Ber.*, **1980**, *113*, 3517-3538.
7. E. Keller and H. Vahrenkamp, *Chem. Ber.*, **1976**, *109*, 229-236.
8. R. Müller and H. Vahrenkamp, *Chem. Ber.*, **1977**, *110*, 3910-3919.
9. J. Hirt, M. Börner and H. Vahrenkamp, *Chem. Ber.*, **1977**, *110*, 1187-1194.
10. H. J. Langenbach, E. Röttinger and H. Vahrenkamp, *Chem. Ber.*, **1980**, *113*, 42-54.
11. M. Müller and H. Vahrenkamp, *Chemische Berichte*, **1983**, *116*, 2748-2764.
12. E. Röttinger, A. Trenkle, R. Müller and H. Vahrenkamp, *Chem. Ber.*, **1980**, *113*, 1280-1289.
13. F. Richter and H. Vahrenkamp, *Angew. Chem. Int. Ed. Eng.*, **1979**, *18*, 531-531.
14. F. Richter and H. Vahrenkamp, *Chem. Ber.*, **1982**, *115*, 3224-3242.
15. H. Vahrenkamp, *Chem. Ber.*, **1973**, *106*, 2570-2579.
16. E. Groß, C. Burschka and W. Malisch, *Chem. Ber.*, **1986**, *119*, 378-382.
17. M. Börner and H. Vahrenkamp, *Chem. Ber.*, **1981**, *114*, 1382-1391.

18. E. Roland and H. Vahrenkamp, *Chem. Ber.*, **1980**, *113*, 1799-1805.
19. M. N. Peñas-Defrutos, C. Bartolomé, M. García-melchor and P. Espinet, *Angew. Chem. Int. Ed.*, **2019**, *58*, 3501-3505.
20. W. Strohmeier, *Angew. Chem. Int. Ed. Eng.*, **1964**, *3*, 730-737.
21. B. J. Frogley, A. F. Hill, H. Onagi and L. J. Watson, *Dalton Trans.*, **2022**, *51*, 17354-17360.
22. R. Rund, G. Balázs, M. Bodensteiner and M. Scheer, *Angew. Chem. Int. Ed.,* **2019**, *58*, 16092-16096.
23. J. Borm, L. Zsolnai and G. Huttner, *Angew. Chem. Int. Ed. Eng.*, **1983**, *22*, 977-978.
24. A. H. Cowley, J. G. Lasch, N. C. Norman and M. Pakulski, *Angew. Chem. Int. Ed. Eng.*, **1983**, *22*, 978-979.
25. J. J. Cherng, G. H. Lee, S. M. Peng, C. H. Ueng and M. Shieh, *Organometallics*, **2000**, *19*, 213-215.
26. G. Huttner and I. Jibril, *Angew. Chem. Int. Ed. Eng.*, **1984**, *23*, 740-741.
27. A. J. Carty, N. J. Taylor, A. W. Coleman and M. F. Lappert, *J. Chem. Soc. Chem. Comm.*, **1979**, 639-640.
28. L. H. Doerrer, J. C. Green, M. L. H. Green, I. Haiduc, C. N. Jardine, S. I. Pascu, L. Silaghi-dumitrescu and D. J. Watkin, *J. Chem. Soc. Dalton Trans.*, **2000**, 3347-3355.
29. L. R. Frank, I. Jibril, L. Zsolnai and G. Huttner, *J. Organomet. Chem.*, **1987**, *336*, 337-342.
30. F. A. Cotton and T. R. Webb, *Inorg. Chim. Acta*, **1974**, *10*, 127-131.
31. I. W. Nowell, S. Rettig and J. Trotter, *J. Chem. Soc. Dalton Trans.*, **1972**, 2381-2388.
32. H. Beurich and H. Vahrenkamp, *Angew. Chem. Int. Ed. Eng.*, **1978**, *17*, 863-864.
33. H. Beurich and H. Vahrenkamp, *Chem. Ber.*, **1982**, *115*, 2385-2408.
34. S. Jensen, B. H. Robinson and J. Simpson, *J. Chem. Soc. Chem. Comm.*, **1983**, 1081-1082.
35. D. N. Duffy, M. M. Kassis and A. D. Rae, *J. Organomet. Chem.*, **1993**, *460*, 97-104.
36. M. Arewgoda, P. H. Rieger, B. H. Robinson, J. Simpson and S. J. Visco, *J. Am. Chem. Soc.*, **1982**, *104*, 5633-5640.
37. M. Arewgoda, B. H. Robinson and J. Simpson, *J. Am. Chem. Soc.*, **1983**, *105*, 1893-1903.
38. M. L. Bruce, D. C. Kehoe, J. G. Matisons, B. K. Nicholson, P. H. Rieger and M. L. Williams, *J. Chem. Soc. Chem. Comm.*, **1982**, 442-444.
39. D. J. Thornhill and A. R. Manning, *J. Chem. Soc. Dalton Trans.*, **1974**, 6-9.
40. Q. L. Suo, H. Zhang, Y. Wang, L. Wang, L. Wen and X. Leng, *J. Organomet. Chem.*, **2001**, *631*, 87-93.
41. P. Macchi, D. M. Proserpio and A. Sironi, *J. Am. Chem. Soc.*, **1998**, *120*, 13429-13435.
42. C. Loubser, J. L. M. Dillen and S. Lotz, *Polyhedron*, **1991**, *10*, 2535-2539.
43. M. P. Johansson and J. Juselius, *Lett. Org. Chem.*, **2005**, *2*, 469-474.
44. G. Henrici-olivé and S. Olivé, *Angew. Chem. Int. Ed. Eng.*, **1971**, *10*, 105-115.
45. S. C. Sendlinger, B. S. Haggerty, A. L. Rbeingold and K. H. Theopold, *Chem. Ber.*, **1991**, *124*, 2453-2456.
46. J. P. Collman, R. G. Komoto and W. O. Siegl, *J. Am. Chem. Soc.*, **1973**, *95*, 2389-2390.
47. G. Huttner, H. G. Schmid and H. Lorenz, *Chem. Ber.*, **1976**, *109*, 3741-3748.
48. H. Fleckner, F. W. Grevels and D. Hess, *J. Am. Chem. Soc.*, **1984**, *106*, 2027-2032.
49. K. C. Shih and R. J. Angelici, *J. Org. Chem.*, **1996**, *61*, 7784-7792.
50. K. R. Sawyer, E. A. Glascoe, J. F. Cahoon, J. P. Schlegel and C. B. Harris, *Organometallics*, **2008**, *27*, 4370-4379.
51. G. Tewes, A. Hirschfelder and P. Eilbracht, *Tetrahedron*, **1996**, *52*, 5449-5460.
52. H. Schulz, H. Pritzkow and W. Siebert, *Chem. Ber.*, **1991**, *124*, 2203-2207.
53. Z. Nagy-magos, A. Feßenbecker, H. Pritzkow, W. Siebert, I. Hyla-kryspin and R. Gleiter, *Chem. Ber.*, **1991**, *124*, 2685-2689.
54. B. Deobald, J. Hauss, H. Pritzkow, D. Steiner, A. Berndt and W. Siebert, *J. Organomet. Chem.*, **1994**, *481*, 205-210.
55. H. J. Knölker, *Chem. Rev.*, **2000**, *100*, 2941-2962.
56. C. M. Alvarez, M. A. Alvarez, M. E. García, A. Ramos, M. A. Ruiz, C. Graiff and A. Tiripicchio, *Organometallics*, **2007**, *26*, 321-331.
57. F. Carre, E. Colomer, J. Y. Corey, R. J. P. Corriu, C. Guerin, B. J. L. Henner, B. Kolani and W. W. C. Wong chi man, *Organometallics*, **1986**, *5*, 910-917.
58. C. C. Santini, J. Fischer, F. Mathey and A. Mitschler, *Inorg. Chem.*, **1981**, *20*, 2848-2852.

59. F. Carré, E. Colomer, R. J. P. Corriu, M. Lheureux and A. Cavé, *J. Organomet. Chem.*, **1987**, *331*, 29-43.
60. L. C. Ananias de Carvalho, M. Dartiguenave, F. Dahan, Y. Dartiguenave, J. Dubac, A. Laporterie, G. Manuel and H. Iloughmane, *Organometallics*, **1986**, *5*, 2205-2211.
61. H. Braunschweig, R. D. Dewhurst, F. Hupp, C. Kaufmann, A. K. Phukan, C. Schneider and Q. Ye, *Chem. Sci.*, **2014**, *5*, 4099-4104.
62. M. Luksza, S. Himmel and W. Malisch, *Angew. Chem. Int. Ed. Eng.*, **1983**, *22*, 416-417.
63. M. Luksza, K. Jörg and W. Malisch, *Inorg. Chim. Acta*, **1984**, *85*, L49-L50.
64. E. Gross, K. Jörg, K. Fiederling, A. Göttlein, W. Malisch and R. Boese, *Angew. Chem. Int. Ed. Eng.*, **1984**, *23*, 738-739.
65. S. L. Li, Z. Z. Zhang, J. C. C. Chan, S. C. F. Au-Yeung and T. C. W. Mak, *J. Organomet. Chem.*, **1996**, *522*, 155-160.
66. M. A. Alvarez, I. Amor, M. E. García, D. García-Vivó, M. A. Ruiz and J. Suárez, *Organometallics*, **2010**, *29*, 4384-4395.
67. N. C. Mösch-Zanetti, R. R. Schrock, W. M. Davis, K. Wanninger, S. W. Seidel and M. B. O'Donoghue, *J. Am. Chem. Soc.*, **1997**, *119*, 11037-11048.
68. J. J. Curley, N. A. Piro and C. C. Cummins, *Inorg. Chem.*, **2009**, *48*, 9599-9601.
69. R. G. Ball, M. R. Burke and J. Takats, *Organometallics*, **1987**, *6*, 1918-1924.

# Chapter 6

# Arsolyl-Cyclopentadienyl Complexes of Molybdenum and Tungsten

## 6.1 Preamble

An interesting feature of complexes of the type $[M(ER_3)(CO)_n(\eta^5\text{-}C_5H_5)]$ (M = Mo, W, $n$ = 3; M = Fe, $n$ = 2; E = Si, Ge, Sn, Pb; R = alkyl, aryl) is their reaction with strong bases *e.g.*, organolithium (R'Li) or lithium amide ($R'_2NLi$) reagents. The interaction may proceed *via* one of three pathways (in some cases, concurrently and competitively) depending on the identity of:

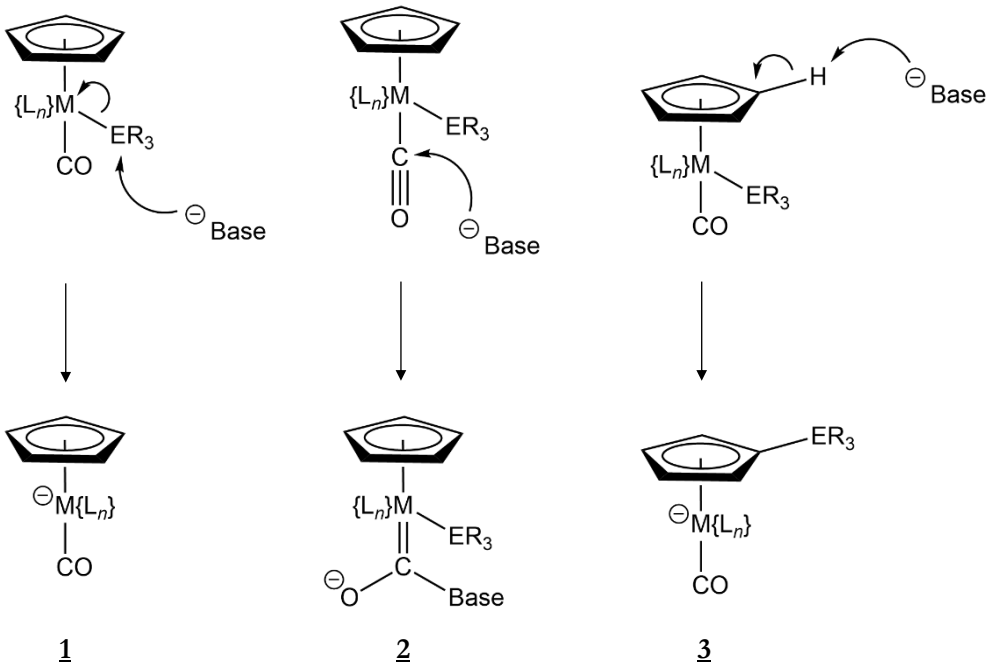
1) The metal centre M,
2) The heteroatom E,
3) The heteroatom substituents R,
4) The base R'Li or $R'_2NLi$.

These variables – an intimate combination of electronic and steric factors – usually act in concert to promote or retard one reaction course over the other, those courses* being:

1) Nucleophilic substitution by the base upon the $ER_3$ group, ejecting a metal carbonyl anion,
2) Nucleophilic addition of the base to a carbonyl ligand, giving a metal enolate,
3) Deprotonation of a cyclopentadienyl hydrogen, forming a ring-substituted metal carbonyl anion.

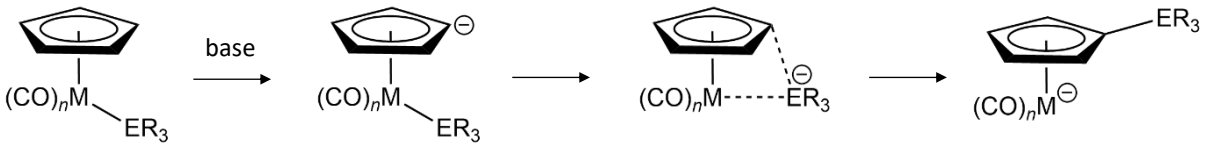
These pathways are illustrated for a generalised case in **Scheme 6.1**.

* Hydride bases *e.g.*, NaH or $[R_3BH]^-$ also react with cyclopentadienyl metal complexes, however their action involves nucleophilic addition to the $\eta^5\text{-}C_5H_5$ ring followed by migration of an *endo*-hydrogen onto a metal bound group (often a π-alkene or -alkyne); in essence, the direction of migration is in reverse and is here considered separate from other base-induced migrations. For an overview, see D.L. REGER, *Acc. Chem. Res.*, **1988**, *21*, 229—235.




**Scheme 6.1**: Three potential courses of reaction observed for a generic $[M(ER_3)(CO)_3(\eta^5\text{-}C_5H_5)]$ complex (M = Mo, W; E = Si, Ge, Sn, Pb; R = alkyl, aryl; Base = organolithium or lithium amide).

Of particular interest in the present work is outcome **3** above, where an *intra*molecular migration of the $ER_3$ group to the metalated cyclopentadienyl takes place, providing access to metal-centred nucleophiles of the form $[M(CO)_n\{\eta^5\text{-}C_5H_4(ER_3)\}]^-$ which are trapped with a suitable electrophile. One may presume a driving force for migration is relocation of the negative charge from the ring to the metal centre where it can be distributed amongst the π-acidic carbonyl ligands. The accepted mechanism is outlined in **Scheme 6.2** though is probably an oversimplification since the role and position of the *gegen*-cation in this sequence is neglected.




**Scheme 6.2**: Mechanism for base-induced intramolecular migration of Group 14 ligands to a cyclopentadienyl ring.

## 6.2 Base-Induced Ligand Migration

The base-induced migration of a metal-bound group to a cyclopentadienyl ring was first reported in 1977 by GRAHAM and DEAN during the attempted synthesis of FISCHER-type carbene complexes from $[M(ER_3)(CO)_3(\eta^5\text{-}C_5H_5)]$ (M = Mo, W; E = Ge, Sn; R = Me, Ph) and organolithium bases.[1] For certain combinations of reagents, ring substituted complexes $[MR'(CO)_3\{\eta^5\text{-}C_5H_4(ER_3)\}]$ were isolated alongside *or in lieu of* the expected carbene (or cleavage product) after alkylation. Migration of the $ER_3$ group was observed more-commonly for W over Mo complexes, only for germanium ligands (with strong preference for $GePh_3$ over $GeMe_3$), and with sterically encumbered bases *e.g.*, *t*-BuLi over PhLi and MeLi. The scope of this initial work was expanded upon by PANNELL in a comprehensive report involving the first examples of stannyl and plumbyl migrations by the agency of LDA (lithium diisopropylamide $Li[N(i\text{-}Pr)_2]$), who also provided some intriguing mechanistic observations.[8]

Shortly thereafter, BERRYHILL described the base-induced migration of silyl ligands during treatment of $[Fe(SiR_3)(CO)_2(\eta^5\text{-}C_5H_5)]$ with either *n*-BuLi or LDA at low temperatures.[9] Though it was not obvious at the time, the luxury of hindsight reveals a remarkable preponderance for iron silyl systems to yield ring substituted products. This is underscored in one aspect by the ability to use *n*-BuLi for cyclopentadienyl ring deprotonation where such a reagent upon the Group 6 metals invariably leads to nucleophilic substitution. As BERRYHILL perceptively noted: "*It is perhaps surprising that n-BuLi does not directly displace the* $[Fe(CO)_2(\eta^5\text{-}C_5H_5)]^-$ *anion from silicon, since the migration appears to involve the displacement of an analogous anion [from silicon]. The kinetic acidity of the cyclopentadienyl ring must be reasonably high to account for the observed course of the reaction*". It is intuitive to also consider that the $[Fe(CO)_2(\eta^5\text{-}C_5H_5)]^-$ core is a much superior nucleophile to $[M(CO)_3(\eta^5\text{-}C_5H_5)]^-$ (M = Cr, Mo, W) and therefore the poorest nucleofuge.[10, 11] Thus, silyl complexes of iron rapidly gained interest for the reliability of the migration process which BERRYHILL confirmed* to be strictly intramolecular in nature.[12, 13] MALISCH[14] and PANNELL[7, 15-20] recognised the utility of this reaction to prepare cyclopentadienyl iron complexes featuring oligosilyl residues which occasionally underwent

* Crossover experiments where a known mixture of iron silyl complexes was treated with base followed by an electrophile found no scrambling of substituents took place between the labelled and unlabelled reagents.

novel rearrangements, whilst others have extended the base-induced migration to cyclopentadienyl cobalt,[3] rhenium[21, 22] and osmium[4, 23] systems.

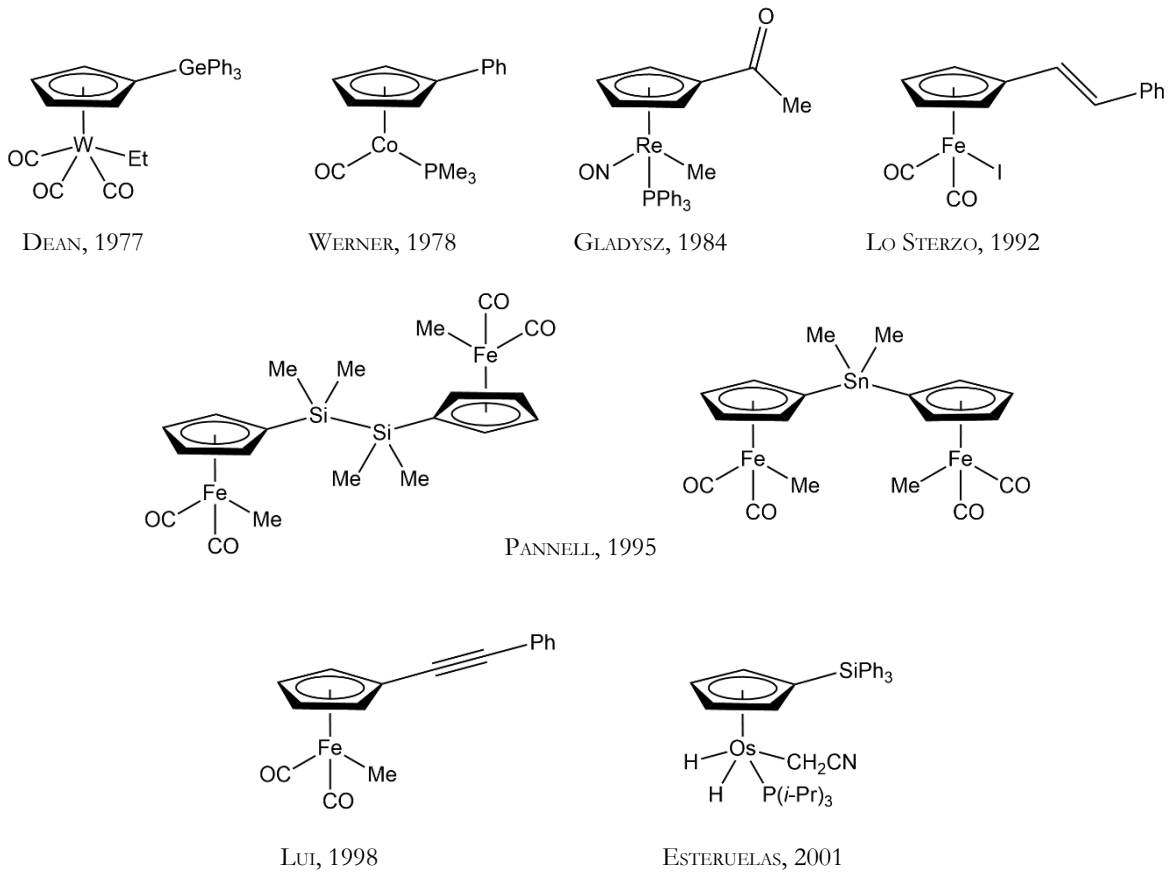
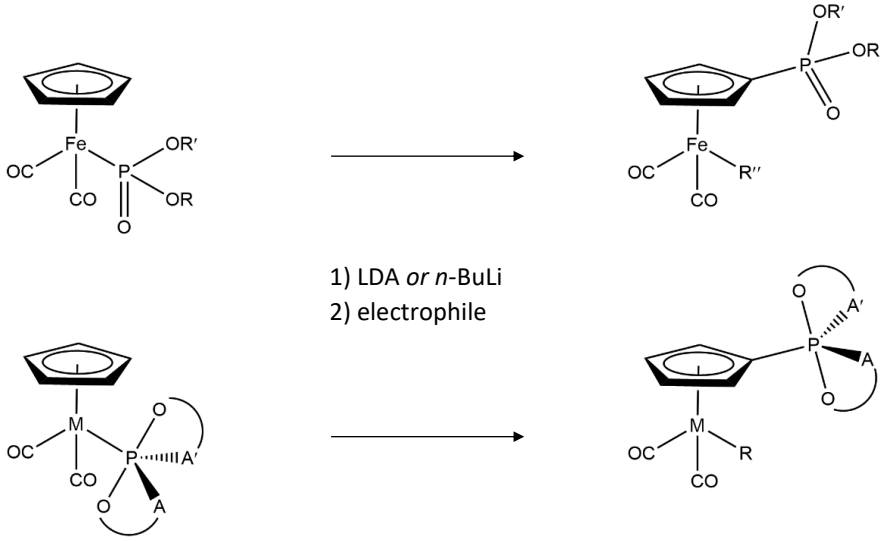



**Chart 6.1**: A selection of complexes previously obtained by base-induced metal → cyclopentadienyl migration.

It is readily apparent that the foremost requisite is the ability of the migrating atom to temporarily attain increased coordination during the transition state so as to bridge both the metal and the ring: thus, C($sp^3$) groups do not undergo migration whereas C($sp^2$) and C($sp$) groups (*e.g.*, acyl, alkenyl, ethynyl) – by virtue of vacant π* orbitals – can.[2, 5, 6, 24, 25] An important exception worth noting is the ability of hydride ligands to also undergo migration (though with less facility), as found by GLADYSZ.[26, 27] This restriction is less important for the heavier group 14 elements which can readily expand their valence environments during intramolecular nucleophilic attack by the deprotonated cyclopentadienyl ring carbon – the presence of an empty *d* orbital is often invoked.*

* It may be of interest to investigate if complexes with *metallo*-ligands *e.g.*, $[MR(CO)_n(\eta^5\text{-}C_5H_5)]$ where R = AuL, HgX *etc.* could undergo base-induced migration, which does not appear to have been reported nor considered in the literature.

With respect to migration of Group 15 ligands, examples are few, and all involve *penta*valent phosphorus centres: MIYOSHI has treated phosphonate and phosphorane complexes of the form $[Fe\{P(O)(OR)(OR')\}(CO)_2(\eta^5\text{-}C_5H_5)]$ and $[M\{\kappa^2\text{-}O,A\text{-}P(OC_6H_4A)(OC_6H_4A')\}(CO)_2(\eta^5\text{-}C_5H_5)]$ (M = Fe, Ru; R and R' = alkyl or aryl; A and A' = NH or O), respectively, with either LDA or *n*-BuLi to provide the corresponding substituted cyclopentadienyl complexes in high yield after alkylation of the resultant anion (**Scheme 6.3**).[28-30] Such migrations proceed with retention of configuration at the heteroatom, again consistent with an intramolecular process.




**Scheme 6.3:** Base-induced P(V) ligand migrations previously reported by MIYOSHI. M = Fe, Ru; R, R', R'' = alkyl or aryl; A, A' = O or NH.

It was envisioned that a similar reaction might ensue with $[M(AsC_4R_4)(CO)_n(\eta^5\text{-}C_5H_5)]$ to provide *As*-cyclopentadienyl arsole metal complexes. Though examples of arsenide migration are conspicuously absent from the chemical literature, a trivalent arsenic atom still fulfils the only apparent requirement (that is, the ability to form a hypervalent transition state) to be prone to intramolecular migration. With a selection of transition metal arsolyl complexes in hand, and with the view of observing the first example of a base-induced migration of an arsenido group, the following section details the reactivity of $[M(AsC_4R_4)(CO)_n(\eta^5\text{-}C_5H_5)]$ complexes toward strong bases.

## 6.3 Base-Induced Migration of the Arsolyl Ligand

### 6.3.1 Synthesis of [MoMe(CO)$_3${$\eta^5$-C$_5$H$_4$(AsC$_4$Ph$_4$)}]

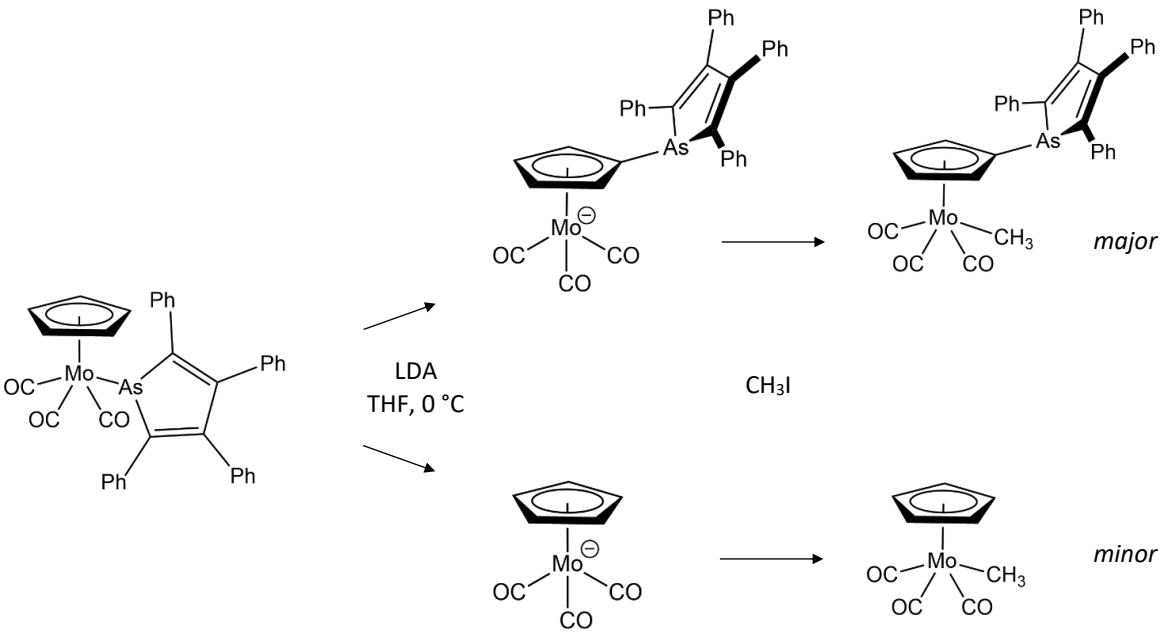
In emulation of literature procedures, the dropwise addition of LDA to a THF solution of [Mo(AsC$_4$Ph$_4$)(CO)$_3$($\eta^5$-C$_5$H$_5$)] at 0 °C results in evolution of the orange solution to a dark red colour. Analysis of the reaction mixture by IR spectroscopy after *ca* 30 minutes revealed complete consumption of the starting material with the emergence of four* new, prominent $\nu_{CO}$ bands at 1906(vs), 1809(vs), 1787(s) and 1718(vs) cm$^{-1}$ in excellent accord with those PANNELL[8] has reported for Li[Mo(CO)$_3$($\eta^5$-C$_5$H$_4$SnPh$_3$)] ($\nu_{CO}$ 1905, 1806, 1782 and 1716 cm$^{-1}$), and those reported by CASEY[31] for Li[Mo(CO)$_3$($\eta^5$-C$_5$H$_4$PPh$_2$)] ($\nu_{CO}$ 1905, 1807, 1780, 1714 cm$^{-1}$), supporting the formation of Li[Mo(CO)$_3$($\eta^5$-C$_5$H$_4$(AsC$_4$Ph$_4$)}]. A weaker set of vibrations at *ca* 1900, 1800, 1770 and 1710 cm$^{-1}$ were identified as corresponding to Li[Mo(CO)$_3$($\eta^5$-C$_5$H$_5$)],† suggesting some Mo-As bond scission in the reaction medium. Assuming these species to have comparable molar extinction coefficients, it may be estimated that the approximate ratio (by eye) of [Mo(CO)$_3${$\eta^5$-C$_5$H$_4$(AsC$_4$Ph$_4$)}]$^-$ to [Mo(CO)$_3$($\eta^5$-C$_5$H$_5$)]$^-$ is ~7:1.

Quenching the reaction with an excess of methyl iodide (CH$_3$I) promptly returned a yellow colour to the solution. Spectroscopic analysis of the crude material confirmed formation of the target [MoMe(CO)$_3${$\eta^5$-C$_5$H$_4$(AsC$_4$Ph$_4$)}]: in the $^1$H NMR spectrum (C$_6$D$_6$), a pair of virtual triplets (AA'BB' spin system) manifest at 4.79 and 4.43 ppm with typically small couplings for *syn*-coplanar hydrogens in five-membered rings ($J_{HH}$ = 2.2 Hz), alongside a corresponding sharp singlet at 0.38 ppm for the metal-bound methyl group, with relative intensities of 2:2:3. The side-product [MoMe(CO)$_3$($\eta^5$-C$_5$H$_5$)] is also found which arises from the presence of Li[Mo(CO)$_3$($\eta^5$-C$_5$H$_5$)] in the reaction medium. By integration of both cyclopentadienyl and methyl hydrogen signals, an approximate arsolyl migration/scission ratio of *ca* 9:1 is found in the crude reaction mixture, in agreement with the integrated IR absorption intensities.

* Four peaks are observed due to ion-pairing between the lithium cation and a carbonyl oxygen atom *viz.* [($\eta^5$-C$_5$H$_4$R)Mo(CO)$_2$(C≡O···Li(THF)$_x$)] is the most likely solution-bound structure.

† These peaks appear as shoulders to those of the major product, and therefore their position is given in terms of approximate wavenumbers though they are in good agreement with data previously reported: $\nu_{CO}$ 1905(s), 1807(s), 1780(m), 1714(s) cm$^{-1}$. See J.A. GLADYSZ *et al. Inorg. Chem.*, **1979**, *18*, 553—558.

This ratio proved somewhat variable (though not so far as to label erratic) during two further syntheses of $[MoMe(CO)_3\{\eta^5\text{-}C_5H_4(AsC_4Ph_4)\}]$ under identical conditions, although the fate of the cleaved arsole group (presumably as $(i\text{-}Pr_2N)AsC_4Ph_4$) could not be determined with certainty and appears to not endure in the reaction medium or upon workup.* The migration product, $[MoMe(CO)_3\{\eta^5\text{-}C_5H_4(AsC_4Ph_4)\}]$, is isolated by chromatography in acceptable yield as a reasonably air-stable dark yellow solid (**Scheme 6.4**); the yellow $[MoMe(CO)_3(\eta^5\text{-}C_5H_5)]$ side-product was also isolated during this process.†




**Scheme 6.4**: Competitive arsolyl migration and scission upon treatment of $[Mo(AsC_4Ph_4)(CO)_3(\eta^5\text{-}C_5H_5)]$ with LDA, and subsequent alkylation with methyl iodide. LDA = $Li[N(i\text{-}Pr)_2]$.

Spectroscopic features of $[MoMe(CO)_3\{\eta^5\text{-}C_5H_4(AsC_4Ph_4)\}]$ are – disregarding the most salient differences – remarkably similar to those of unsubstituted $[MoMe(CO)_3(\eta^5\text{-}C_5H_5)]$: infra-red spectroscopy ($CH_2Cl_2$) finds two $\nu_{CO}$ bands‡ for the former at 2017(vs) and 1926(vs) $cm^{-1}$ which compare to 2018(vs) and 1926(vs) $cm^{-1}$ for the latter. In the $^{13}C\{^1H\}$ NMR spectrum ($C_6D_6$), the metal-bound methyl group in $[MoMe(CO)_3\{\eta^5\text{-}C_5H_4(AsC_4Ph_4)\}]$ occurs at -20.1 ppm which compares to -21.9 ppm for the unsubstituted

* *As*-amino arsoles are presently unknown. Attempts to establish the presence of this species by mass spectrometry were inconclusive.

† NMR: $^1H$ ($C_6D_6$, 400 MHz, 25 °C) δ 4.41, 0.39 ppm; $^{13}C\{^1H\}$ ($C_6D_6$, 176 MHz, 25 °C) δ 240.5, 227.3, 92.4, -21.9 ppm; IR ($CH_2Cl_2$, 25 °C) $\nu_{CO}$ 2018(vs), 1926(vs) $cm^{-1}$. Both this species and $[MoMe(CO)_3\{\eta^5\text{-}C_5H_4(AsC_4Ph_4)\}]$ appeared to react gradually with $CDCl_3$ to afford paramagnetic green solutions.

‡ Despite the formal $C_s$ symmetry of these species, the lower energy *A*' (symmetric) and *A*" (antisymmetric) modes are often accidentally isochronous in complexes with high(er) symmetry in the $M(CO)_3$ locale, hence the recording of two rather than three resolved $\nu_{CO}$ vibrations. See E.W. Abel, A. Singh, G. Wilkinson *J. Chem. Soc.*, **1960**, 1321—1324.

cyclopentadienyl complex; carbonyl carbon signals mirror this similarity (239.7 and 226.5 ppm *vs.* 240.5 and 227.3 ppm, respectively). The $^{13}C\{^1H\}$ resonance for the cyclopentadienyl carbon bearing the $AsC_4Ph_4$ group is found at 102.8 ppm, to higher frequency of the remaining cyclopentadienyl ring-carbon atoms at 96.4 and 94.0 ppm (*cf.* 92.4 ppm for $[MoMe(CO)_3(\eta^5\text{-}C_5H_5)]$). On the basis of these data, the presence of the tetraphenylarsolyl substituent on the cyclopentadienyl ring appears to have little noticeable influence on the gross electronic properties of the majority of the molecule. Single crystals of $[MoMe(CO)_3\{\eta^5\text{-}C_5H_4(AsC_4Ph_4)\}]$ were grown from $CH_2Cl_2$/*n*-hexane and the molecular structure (as the *n*-hexane hemisolvate) is shown in **Figure 6.1**.

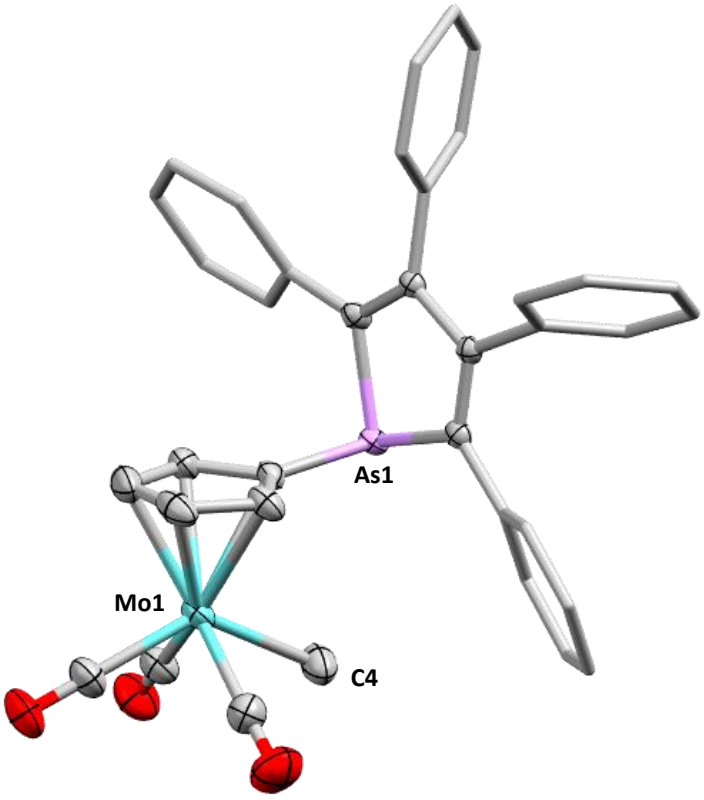



**Figure 6.1**: The molecular structure of $[MoMe(CO)_3\{\eta^5\text{-}C_5H_4(AsC_4Ph_4)\}]\cdot 0.5C_6H_{14}$. Phenyl rings simplified, *n*-hexane solvate molecule and hydrogen atoms omitted for clarity. Ellipsoids shown at 50% displacement.

The molecular structure of $[MoMe(CO)_3\{\eta^5\text{-}C_5H_4(AsC_4Ph_4)\}]$ confirms the course of the deprotonation/migration reaction; an otherwise ordinary cyclopentadienyl molybdenum tricarbonyl centre is decorated by the $AsC_4Ph_4$ group which almost perfectly eclipses the metal-bound alkyl. The arsolyl group itself is not aligned with the approximate (*i.e.*, non-crystallographic) vertical symmetry plane of the

$C_5H_4MoMe(CO)_3$ moiety, and is instead tilted about the cyclopentadienyl C-As bond by *ca* 45° with respect to the mean plane of the $\eta^5$-$C_5H_4$ ring atoms. A typical exocyclic As-C($sp^2$) bond distance and bond angles at arsenic of 1.951(4) Å and *ca* 96°, respectively, are measured, and the Mo-$CH_3$ distance of 2.303(5) Å is unremarkable for molybdenum(II)-carbon single bonds.* Noteworthy is that the Mo-$C_{Cp}$ distances are not all crystallographically equivalent finding one (2.399(3) Å) which is somewhat longer than the remaining four (mean 2.338(9) Å); unsurprisingly, this carbon bears the arsolyl pendant and the difference is statistically significant (~ 6 e.s.d) when also considering that the cyclopentadienyl ring deviates by no more than 0.007 Å from planarity. A slight tilting of cyclopentadienyl rings has been well-documented in a variety of transition metal complexes, though here one might suspect that the rather large steric profile of the $AsC_4Ph_4$ residue acts as a fulcrum upon the cyclopentadienyl ligand and deforming the molecule slightly within the close packing of the crystalline lattice. **Figure 6.2** shows a section of the crystalline lattice highlighting the proximity of the arsolyl residues to their neighbours.

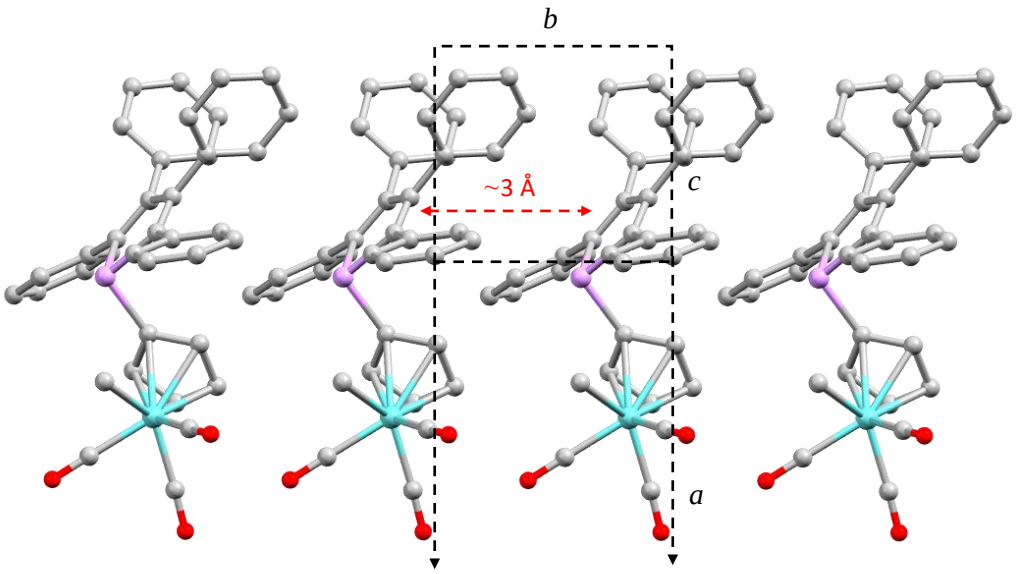



**Figure 6.2**: Packing diagram of [$MoMe(CO)_3\{\eta^5$-$C_5H_4(AsC_4Ph_4)\}$] viewed parallel to the *c* glide plane (monoclinic $P2_1/c$) with hydrogen atoms and solvate molecules omitted. Unit cell boundaries are shown in dashed black.

* Of the 15 crystal structures archived in the CSD with $Mo^{II}$-$CH_3$ fragments, the mean Mo-C distance is 2.300 Å with a range of 2.25—2.48 Å.

### 6.3.2 Synthesis of [WMe(CO)$_3${$\eta^5$-C$_5$H$_4$(AsC$_4$Ph$_4$)}]

An identical course of events was observed commencing with [W(AsC$_4$Ph$_4$)(CO)$_3$($\eta^5$-C$_5$H$_5$)]: treatment with LDA in THF at 0 °C provides a solution with $\nu_{CO}$ absorptions at 1901(vs), 1805(vs), 1780(s), 1716(vs) cm$^{-1}$ (*cf.*, Li[W(CO)$_3$($\eta^5$-C$_5$H$_4$SbPh$_3$)][8] $\nu_{CO}$ 1905, 1809, 1787, 1722 cm$^{-1}$), and after quenching with methyl iodide the expected complex [WMe(CO)$_3${$\eta^5$-C$_5$H$_4$(AsC$_4$Ph$_4$)}] is isolated as a yellow solid in modest yield. Like its molybdenum counterpart, [WMe(CO)$_3$($\eta^5$-C$_5$H$_5$)] was also isolated as a minor product during chromatography.

Spectroscopic features of the tungsten complex are similar to the molybdenum analogue finding in the $^1$H NMR spectrum (C$_6$D$_6$) the cyclopentadienyl ring protons as a pair of virtual triplets at 4.77 and 4.41 ppm ($J_{HH}$ = 2.2 Hz) and the tungsten-bound methyl group at 0.46 ppm ($^2J_{WH}$ = 1.9 Hz). The $^{13}$C{$^1$H} spectrum includes resonances for the *transoid* and *cisoid* carbonyl ligands at 229.3 ($^1J_{WC}$ = 65 Hz) and 216.0 ($^1J_{WC}$ = 77 Hz) ppm respectively, and the methyl group at -32.8 ($^1J_{WC}$ = 17 Hz) ppm. Cyclopentadienyl ring-carbon nuclei occur at 101.4 (*As*-bonded), 94.9 (α) and 92.8 (β) ppm without resolvable $^{185}$W satellites. The IR spectrum (CH$_2$Cl$_2$) comprises a pair of $\nu_{CO}$ bands at 2013(vs) and 1917(vs) cm$^{-1}$. Again, these compare favourably against the unsubstituted congener [WMe(CO)$_3$($\eta^5$-C$_5$H$_5$)].* Suitable X-ray quality crystals of [WMe(CO)$_3${$\eta^5$-C$_5$H$_4$(AsC$_4$Ph$_4$)}] have not been forthcoming at the time of writing, however the structure is assumed to not deviate significantly from that of its molybdenum counterpart given the comparable covalent radii of W (1.62 Å) and Mo (1.54 Å).

### 6.3.3 Comments Regarding the Base-Induced Migration of Arsolyl Ligands

The base-induced migration of the arsolyl ligand proved highly reproducible, although some key observations were made across numerous iterations of this experiment which are summarised below:

1) [W(AsC$_4$Ph$_4$)(CO)$_3$($\eta^5$-C$_5$H$_5$)] showed a practically similar propensity for metal-arsenic bond cleavage as [Mo(AsC$_4$Ph$_4$)(CO)$_3$($\eta^5$-C$_5$H$_5$)]. This contrasts to the observations by DEAN[1] and PANNELL[8] (separately) who found preference for Mo-E scission over W-E. Those authors

* NMR $^1$H (C$_6$D$_6$, 400 MHz, 25 °C) δ 4.41, 0.47 ppm; $^{13}$C{$^1$H} (C$_6$D$_6$, 176 MHz, 25 °C) δ 229.9, 216.8, 91.0, -34.6 ppm; IR (CH$_2$Cl$_2$, 25 °C) $\nu_{CO}$ 2015(vs), 1918(vs) cm$^{-1}$.

suggest that the increased electronegativity of W increases the kinetic acidity of the cyclopentadienyl ring relative to that for Mo, favouring deprotonation over nucleophilic attack.

2) The rate of addition of LDA had a considerable effect on the reaction: *very slow* dropwise addition gave visibly cleaner dark red reaction mixtures which were substantially easier to purify upon quenching with an electrophile, whereas more-rapid addition gave dark orange-brown mixtures that afforded a multitude of unidentified by-products during chromatography. Since LDA is commercially supplied as 2 M solutions it often proved advantageous to further dilute the reagent prior to use, or prepare a fresh, dilute sample from HN(*i*-Pr)$_2$ and *n*-BuLi. Large excesses of base are also to be avoided as these led to an increased occurrence of M-As scission products.

3) The reaction did not appear to scale efficiently, for reasons which are not obvious. Whilst tedious, it ultimately proved advantageous to perform several small-scale reactions (*ca* 0.2 mmol in 25 mL THF – for [Mo(AsC$_4$Ph$_4$)(CO)$_3$($\eta^5$-C$_5$H$_5$)], this equates to 135 mg of reagent at a concentration of *ca* 8 mmol L$^{-1}$) in parallel rather than one larger preparation – the separate reaction mixtures were then combined before being subjected to chromatography. Larger preparations often produced multiple by-products during chromatography and lower overall isolated yields of target compound(s).

4) The use of the bulkier potassium hexamethyldisilylazide (KHMDS, K[N(SiMe$_3$)$_2$]), in an attempt to circumvent metal-arsenic bond scission, counter-intuitively led *only* to metal-arsenic bond scission (although the reaction was comparatively slow): KHMDS is known to be appreciably less-basic than LDA (free amine p$K_a$ ≈ 24 *vs.* 36) and it seems the former is insufficient to deprotonate the cyclopentadienyl ring with sufficient rapidity to compete with nucleophilic addition at arsenic. The persistent interaction between reagents in solution leads to the eventual and irreversible accumulation of Li[M(CO)$_3$($\eta^5$-C$_5$H$_5$)] as the only product (by IR spectroscopy). The use of bulky but more-basic lithium 2,2,6,6-tetramethylpiperidide (LTMP, Li[NC$_5$Me$_4$H$_6$]; free amine p$K_a$ ≈ 37) also disappointingly gave quantitative formation of Li[M(CO)$_3$($\eta^5$-C$_5$H$_5$)].

5) Treating $[M(AsC_4Ph_4)(CO)_3(\eta^5\text{-}C_5H_5)]$ with *n*-BuLi or MeLi in THF results in the immediate formation of $Li[M(CO)_3(\eta^5\text{-}C_5H_5)]$ (by IR spectroscopy) in an outcome that was to be expected *a priori*. Quenching with $CH_3I$ permits isolation of $[MMe(CO)_3(\eta^5\text{-}C_5H_5)]$ and $MeAsC_4Ph_4$ in high yields after chromatography (*n*-$BuAsC_4Ph_4$ appeared to decompose during workup however could be identified by mass spectrometry). A similar outcome eventuated with *t*-BuLi giving *t*-$BuAsC_4Ph_4$ in high yield. This contrasts with the observations made by DEAN who found *t*-BuLi to be the base *de rigueur* for mediating Group 14 migration.

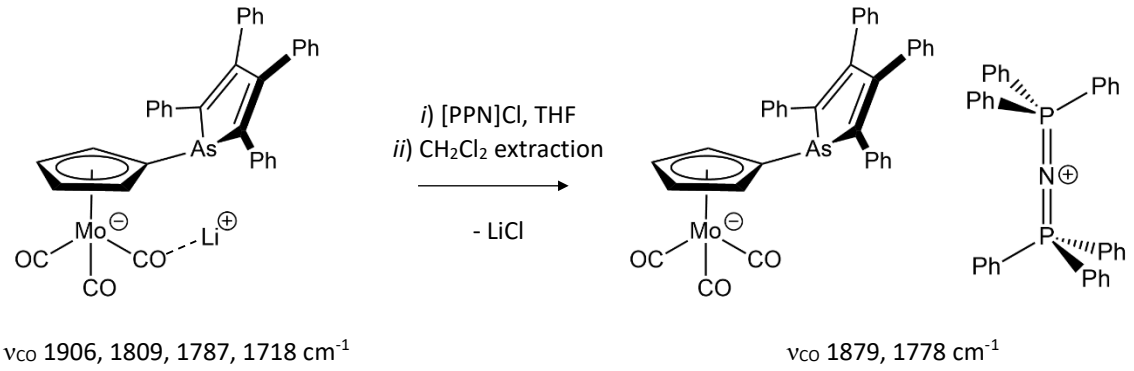
6) Despite possessing what must be a less-electrophilic As(III) centre, the $AsC_4Me_4$ ligand was totally detached no matter the reaction conditions giving $[M(CO)_3(\eta^5\text{-}C_5H_5)]^-$ as the only product (by IR spectroscopy): presumably the arsenic atom is more exposed in the per-alkylated complex allowing unobstructed nucleophilic attack by the base.

A precise diagnosis of all issues was not possible; however, it must be reiterated that the migration reaction was nonetheless habitually reproducible once the most-visible caveats were addressed (*vide supra*). As there was no synthetic advantage *viz.* Mo *vs.* W, the former was selected for the majority of subsequent reactions since the necessary precursor $[Mo(AsC_4Ph_4)(CO)_3(\eta^5\text{-}C_5H_5)]$ was available in greatest quantity.

### 6.3.4 Isolation of $[PPN][Mo(CO)_3\{\eta^5\text{-}C_5H_4(AsC_4Ph_4)\}]$

Whereas the lithium salt of $[(\eta^5\text{-}C_5H_4\{AsC_4Ph_4\})Mo(CO)_3]^-$ could only be characterised by IR spectroscopy *in situ* and could not be satisfactorily isolated from solution (a feature not uncommon to transition metal anions with alkali metal counterions), combination with innocent, bulky cations has a remarkable attenuating effect on the sensitivity of the otherwise highly reactive carbonyl metallates, especially in the case of crystalline $[PPN]^+$ (bis(triphenylphosphine)iminium, $[N(PPh_3)_2]^+$).[10, 32-34] An illustrative example is the $[Co(CO)_4]^-$ anion which is exceedingly air sensitive as the $M^+$ salt (M = H, Li, Na, K), however $[PPN][Co(CO)_4]$ is moderately air stable and dissolves without decomposition in solvents entirely incompatible with the former (*e.g.*, $CH_2Cl_2$ and $CHCl_3$).[35] The cyclopentadienyl metal carbonyl anions of the Group 6 metals are no different and a range of $[M(CO)_3(\eta^5\text{-}C_5H_5)]^-$ anions have been isolated and characterised both spectroscopically and crystallographically as the $[PPN]^+$ salts.[36-39]

Here, a slight excess of anhydrous [PPN]Cl was added to a THF solution of Li[Mo(CO)$_3${$\eta^5$-$C_5H_4(AsC_4Ph_4)$}]. Evaporation of the mixture leaves a bright orange-red residue which may be extracted into $CH_2Cl_2$ without visible degradation and washed copiously with $Et_2O$ to remove amine residues and other neutral species present (**Scheme 6.5**). The solution IR spectrum ($CH_2Cl_2$) reveals prominent $\nu_{CO}$ absorptions at 1899(vs) and 1778(vs) cm$^{-1}$ for a purely (locally) $C_{3v}$ tricarbonyl complex ($A_1$ + $E$ modes; *cf.* [PPN][Mo(CO)$_3$($\eta^5$-$C_5H_5$)] $\nu_{CO}$ (THF) 1896(vs), 1790(vs) cm$^{-1}$), whereas [Mo($AsC_4Ph_4$)(CO)$_3$($\eta^5$-$C_5H_5$)] and Li[Mo(CO)$_3$($\eta^5$-$C_5H_5$)] display three and four $\nu_{CO}$ bands due to formal $C_s$ symmetry or ion-pairing, respectively. The very modest bathochromic shift of the $E$ vibrational mode (12 cm$^{-1}$) upon arsolyl installation on the cyclopentadienyl ring indicates the group does not impact significantly on the π-basicity of the metal centre.




$\nu_{CO}$ 1906, 1809, 1787, 1718 cm$^{-1}$ $\nu_{CO}$ 1879, 1778 cm$^{-1}$

**Scheme 6.5**: Cation metathesis of Li[Mo(CO)$_3${$\eta^5$-$C_5H_4(AsC_4Ph_4)$}] with [PPN]Cl.

The $^1$H and $^{13}$C{$^1$H} NMR spectra of the crude reaction material are most insightful, with features of interest being surprisingly far-removed from the plethoric mixture of signals anticipated (aromatic regions notwithstanding): three anionic complexes of $C_{3v}$ (or *pseudo*-$C_{3v}$) symmetry are evidently present within the sample, and salient features of each will be briefly discussed in turn below. Annotated vignettes of the $^1$H and $^{13}$C{$^1$H} spectra may be found in **Figure 6.4** and **Figure 6.5**, respectively.

1) The major product of the migration reaction, namely [Mo(CO)$_3${$\eta^5$-$C_5H_4(AsC_4Ph_4)$}]$^-$, is observed in the $^1$H spectrum as a pair of virtual "roofed" triplets at 4.99 and 4.98 ppm ($J_{HH}$ = 2.2 Hz) which are readily assignable to the cyclopentadienyl hydrogens in the 2,5- and 3,4-ring positions, respectively (**Figure 6.4**, red highlights). The $^{13}$C{$^1$H} spectrum finds a single

resonance for the three equivalent carbonyl nuclei at 235.0 ppm and the arsolyl ring carbons at 153.0 and 149.0 ppm (α and β to arsenic, respectively); a pair of sharp cyclopentadienyl resonances at 91.5 and 87.8 ppm are assigned to the 2,5- and 3,4-ring carbons by an HSQC NMR experiment, finding one-bond correlation to the abovementioned pair of virtual triplet resonances. The higher-field quaternary cyclopentadienyl carbon atom bound to the arsenic was subsequently identified at 93.6 ppm by an HMBC NMR experiment (**Figure 6.5**, red highlights).

2) The second anion in solution is identified as $[Mo(CO)_3(\eta^5\text{-}C_5H_5)]^-$. The carbonyl signature is found at 235.9 ppm (**Figure 6.5**, blue highlight) – of notably diminutive intensity to the migration product above – by comparison with data previously reported by DARENSBOURG[34] for $[PPN][Mo(CO)_3(\eta^5\text{-}C_5H_5)]$ (*cf.* 236.2 ppm in THF-$d_8$), and also by considering the very subtle deshielding effect of the $AsC_4Ph_4$ pendant *vs.* H on $^{13}C$ shifts for other $[MoR(CO)_n(\eta^5\text{-}C_5H_4X)]$ complexes prepared in this work (**Sections 6.3.1**, **6.3.5** and **6.3.6**). The corresponding $^{13}C\{^1H\}$ cyclopentadienyl resonance is found at 86.7 ppm (*cf.* 86.4 ppm in THF-$d_8$) which – by HSQC NMR spectroscopy – reveals the affiliated $^1H$ signal as a singlet at 5.10 ppm (**Figure 6.4**, blue highlight). The presence of this anion (in ~¼ the proportion of $[Mo(CO)_3\{\eta^5\text{-}C_5H_4(AsC_4Ph_4)\}]^-$) is in line with the ring-*un*substituted complexes observed upon quenching these reaction mixtures with electrophiles.

3) By process of elimination, one carbonyl (234.0 ppm), four arsolyl (155.0, 151.3, 150.3 and 147.9 ppm) and three cyclopentadienyl signals (95.2, 94.2 and 92.8 ppm) remain unaccounted-for in the $^{13}C\{^1H\}$ spectrum (**Figure 6.5**, orange highlights); the presence of the *As*-amino arsole $(i\text{-}Pr)_2NAsC_4Ph_4$ is ruled out by comparison with an authentically prepared sample* and for the reasons outlined hereto these carbon nuclei probably arise from a single anionic compound. Indeed, the above-listed signals are *all* of equal proportion (~⅕) relative to the peaks of the major migration product when examining the discrete carbon environments

* NMR: $^{13}C\{^1H\}$ ($CD_2Cl_2$, 176 MHz, 25 °C) δ 152.1 (arsole $C_\alpha$), 149.1 (arsole $C_\beta$) ppm. Separately prepared by addition of $Li[N(i\text{-}Pr)_2]$ to a suspension of $ClAsC_4Ph_4$ in $Et_2O$; this compound is soluble in $Et_2O$ and is likely removed during washing of the crude reaction material with the same.

(where NOE enhancements are considered equivalent and area integrations are directly comparable). It is interesting to note this compound evidently features a slightly less-basic molybdenum centre (*viz.* $\delta_{CO}$ is upfield of $[Mo(CO)_3\{\eta^5\text{-}C_5H_4(AsC_4Ph_4)\}]^-$, itself upfield of $[Mo(CO)_3(\eta^5\text{-}C_5H_5)]^-$). This is also reflected in the location of the cyclopentadienyl resonances slightly downfield of the other two species. That three chemically-unique carbon nuclei are found – in addition to four arsolyl ring-carbon nuclei – invites the intriguing prospect of a doubly-substituted cyclopentadienyl complex *i.e.*, $[Mo(CO)_3\{\eta^5\text{-}C_5H_3(AsC_4Ph_4)_2\}]^-$. Strong evidence for a disubstituted cyclopentadienyl ring is provided by the $^1H$ spectrum which also includes a triplet at 5.09 and doublet at 4.82 ppm (both $^4J_{HH}$ = 1.7 Hz; **Figure 6.4**, orange highlights) in a 1:2 area ratio. The magnitude of their coupling constant* is suggestive of a 1,3-disposition of the arsolyl groups,[40-44] and their relative proportion to the major anionic product is also ~⅕. A 1,3-isomer also appears more likely than the alternative (1,2-isomer) given the encumbering profile of the $AsC_4Ph_4$ group(s), and it is doubtful the modest basicity of the As(III) donor is sufficient to favour site-directed metalation of an adjacent carbon atom (*vide infra*) and overcome the arduous steric interactions of a 1,2-arrangement. Nevertheless, the presence of four arsolyl ring-carbon resonances suggests a diastereotopic environment wherein both groups do not enjoy unrestricted rotation about the cyclopentadienyl periphery, presumably due to frustrating intramolecular interactions between nearby phenyl residues.

Optimised geometries for both the 1,2- and 1,3-isomers of $[Mo(CO)_3\{\eta^5\text{-}C_5H_3(AsC_4Ph_4)_2\}]^-$ were calculated using Density Functional Theory (gas phase: ωB97X-D/6-31G*/LANL2DZ) and are shown in **Figure 6.3**; the formidable steric congestion brought about by a 1,2-arrangment is readily apparent.

* Coupling constants for the AA'B spin-system found in $\eta^5\text{-}C_5H_3R_2$ cyclopentadienyl rings tends toward $J_{AB} \approx J_{A'B} \geq 2.0$—3.0 Hz for a 1,2-isomer, and $J_{AB} \approx J_{A'B} \leq 2.0$ Hz for a 1,3-isomer.

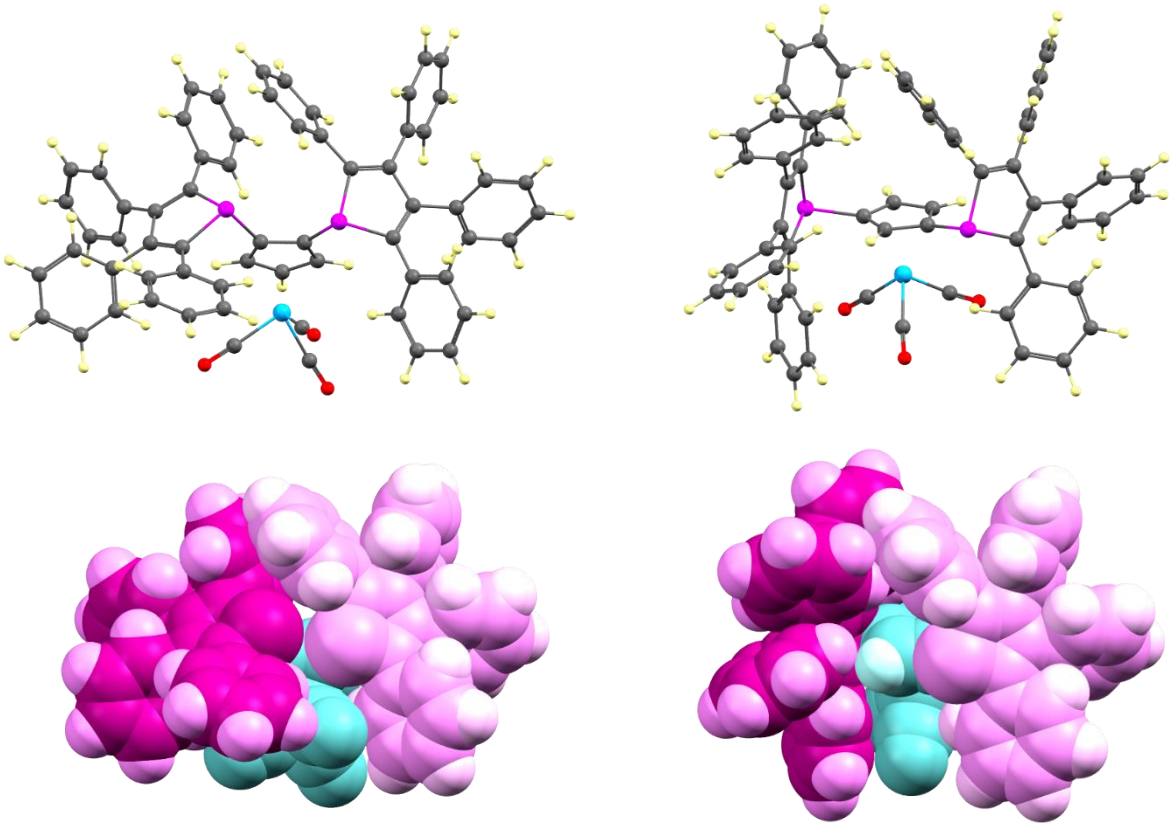


**Figure 6.3, top**: Calculated geometries of the 1,2- (**left**) and 1,3-isomers (**right**) of the $[Mo(CO)_3\{\eta^5\text{-}C_5H_3(AsC_4Ph_4)_2\}]^-$ anion in the gas phase using DFT at the ωB97X-D/6-31G*/LANL2Dζ level of theory. **Bottom**: Space-filling representations of the 1,2- (**left**) and 1,3-isomers (**right**) highlighting the steric congestion about the disubstituted cyclopentadienyl molybdenum tricarbonyl centre; blue = $Mo(CO)_3(\eta^5\text{-}C_5H_3)$, magenta & lilac = $AsC_4Ph_4$.

Mechanistically, a bis(tetraphenylarsolyl)cyclopentadienyl ring could plausibly arise from further deprotonation of $[Mo(CO)_3\{\eta^5\text{-}C_5H_4(AsC_4Ph_4)\}]^-$ (a sight excess of LDA was employed) to give $[Mo(CO)_3(\eta^5\text{-}C_5H_3Li(AsC_4Ph_4)\}]^-$ which then abstracts an arsolyl residue from unreacted $[Mo(AsC_4Ph_4)(CO)_3(\eta^5\text{-}C_5H_5)]$ *via* nucleophilic substitution. The susceptibility of the latter to attack by strong nucleophiles had already been established at multiple stages during this work and it is noteworthy that an equivalent of $[Mo(CO)_3(\eta^5\text{-}C_5H_5)]^-$ would also be generated by this process. Indeed, the NMR spectroscopic data in **Figure 6.4** and **Figure 6.5** find the proportion of $[Mo(CO)_3(\eta^5\text{-}C_5H_5)]^-$ to be only *slightly* greater than the proportion of $[Mo(CO)_3\{\eta^5\text{-}C_5H_3(AsC_4Ph_4)_2\}]^-$ within the isolated reaction product mixture. Such a sequence could be an alternative explanation for the formation of $[Mo(CO)_3(\eta^5\text{-}C_5H_5)]^-$ within this and other mixtures, rather than direct nucleophilic attack by the nitrogen base upon the arsolyl. This would also account for decreased isolated yields of $[MoR(CO)_n\{\eta^5\text{-}C_5H_4(AsC_4Ph_4)\}]$ in situations involving too great an excess of LDA and/or cavalier rates of LDA addition, and also the observation that

the arsolyl ligand appears more prone to nucleophilic attack by carbocentric nucleophiles (MeLi, *n*-BuLi, *t*-BuLi) than amides.

At present, no bis(arsolyl)cyclopentadienyl molybdenum complexes have ever been isolated during the experiments detailed throughout this chapter, though it should be disclosed that the preparation of [PPN][Mo(CO)$_3${$\eta^5$-$C_5H_4$($AsC_4Ph_4$)}] for NMR characterisation above was carried out (chronologically) after the ring-substituted products in **Sections 6.3.1**, **6.3.5** and **6.3.6** were obtained. Had the possible existence of such a species been recognised at the time, a deliberate synthesis would have been targeted.

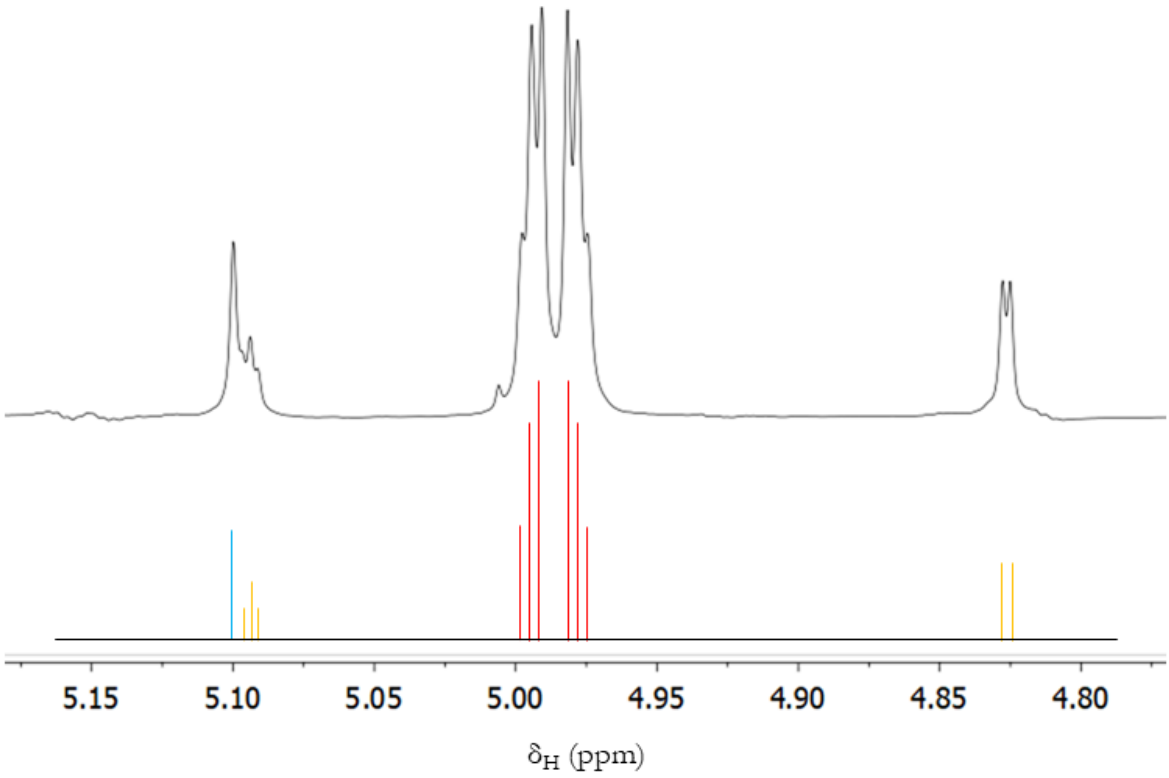



**Figure 6.4**: The $^1$H NMR spectrum ($CD_2Cl_2$, 700 MHz, 25 °C) of the isolated reaction material in the cyclopentadienyl region showing three anionic molybdenum complexes; see text for precise chemical shifts values and coupling constants. The simplified inset spectrum is given as a qualitative guide for the eye only to more easily distinguish the molecular origin of the signals observed. A colour-coded legend is provided in **Figure 6.3**.

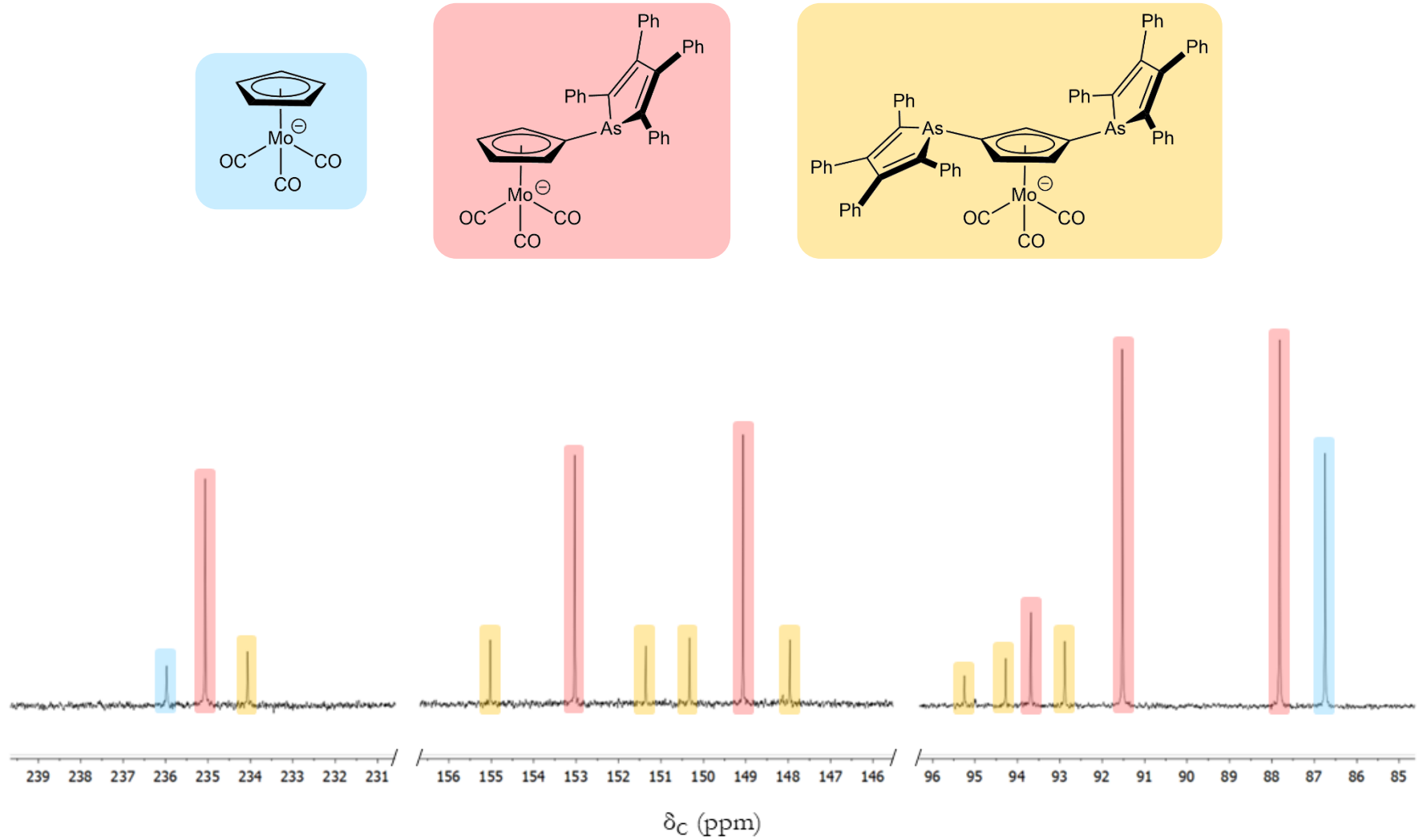
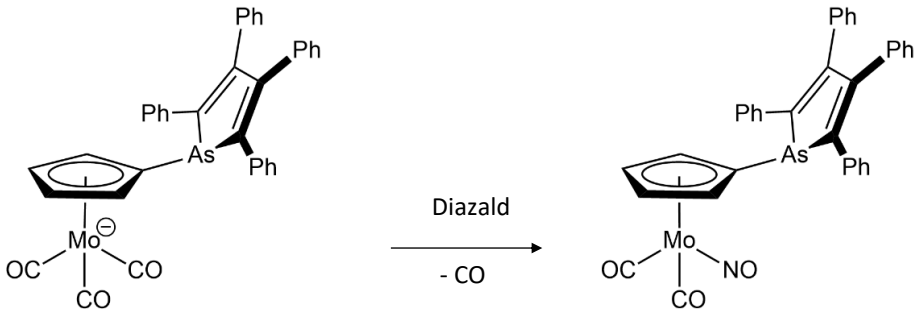



**Figure 6.5**: Selected vignettes of the $^{13}C\{^{1}H\}$ NMR spectrum ($CD_2Cl_2$, 176 MHz, 25 °C) of the isolated reaction material in (from left to right) the carbonyl, arsolyl ring, and cyclopentadienyl regions highlighting the presence of three distinct anionic molybdenum complexes. The aromatic region is of limited diagnostic value and is omitted due to severe congestion. Signals of interest have been colour coded and a legend is given above. See text for precise chemical shift values.

At the time of writing, X-ray quality crystals of [PPN][Mo(CO)$_3${$\eta^5$-C$_5$H$_4$(AsC$_4$Ph$_4$)}] have, much to this author's regret, not been forthcoming.

### 6.3.5 Synthesis of [Mo(NO)(CO)$_2${$\eta^5$-C$_5$H$_4$(AsC$_4$Ph$_4$)}]

Electrophiles other than CH$_3$I were deployed to neutralise [Mo(CO)$_3${$\eta^5$-C$_5$H$_4$(AsC$_4$Ph$_4$)}]$^-$: treating an *in situ* prepared THF solution with the stoichiometric quantity of Diazald® (*N*-methyl-*N*-nitroso-*p*-toluenesulfonamide, MeC$_6$H$_4$SO$_2$N(Me)NO; a mild source of NO$^+$) gives rapid gas evolution accompanied by a colour change to a vibrant orange-red. Chromatography provides the expected nitrosyl complex [Mo(NO)(CO)$_2${$\eta^5$-C$_5$H$_4$(AsC$_4$Ph$_4$)}] as a bright orange, air-stable solid in good yield, alongside a small quantity of [Mo(NO)(CO)$_2$($\eta^5$-C$_5$H$_5$)] which elutes prior (**Scheme 6.6**)*.




**Scheme 6.6**: Synthesis of [Mo(NO)(CO)$_2${$\eta^5$-C$_5$H$_4$(AsC$_4$Ph$_4$)}].

Like the preceding methylated derivative, the IR spectrum (CH$_2$Cl$_2$) of [Mo(NO)(CO)$_2${$\eta^5$-C$_5$H$_4$(AsC$_4$Ph$_4$)}] is almost identical to that of its non-substituted cyclopentadienyl counterpart, yielding a pair of $\nu_{CO}$ absorptions at 2017(vs) and 1940(vs) cm$^{-1}$ ($C_s$ symmetry: $A'$ + $A''$) with the single $\nu_{NO}$ absorption at 1667(vs) cm$^{-1}$. Interestingly, the $^1$H NMR spectrum of [Mo(NO)(CO)$_2${$\eta^5$-C$_5$H$_4$(AsC$_4$Ph$_4$)}] (CDCl$_3$) finds the pair of cyclopentadienyl α and β hydrogen signals partially overlapping such that a combined six-line pattern is observed, though improved resolution is obtained with a stronger-field instrument revealing a pair of "roofed" virtual triplets at 5.46 and 5.44 ppm ($J_{HH}$ = 2.0 Hz). The $^{13}$C{$^1$H} NMR spectrum (CDCl$_3$) is predictably simple with a lone carbonyl resonance occurring at 226.3 ppm – other spectroscopic features compare consistently with those for [MoMe(CO)$_3${$\eta^5$-C$_5$H$_4$(AsC$_4$Ph$_4$)}]. High-resolution mass

* NMR: $^1$H (CDCl$_3$, 400 MHz, 25 °C) δ 5.60 ppm; $^{13}$C{$^1$H} (CDCl$_3$, 176 MHz, 25 °C) δ 227.0, 93.6 ppm; IR (CH$_2$Cl$_2$, 25 °C) $\nu_{CO}$ 2018(vs), 1940(vs) cm$^{-1}$; $\nu_{NO}$ 1666(vs) cm$^{-1}$.

spectrometry (both ESI and EI modes) did not yield a molecular ion nor products of decarbonylation, however, and although a multitude of signals were found with the typical isotopic manifold for the presence of molybdenum no chemically sensible formulae could be devised.*

Single crystals of $[Mo(NO)(CO)_2\{\eta^5\text{-}C_5H_4(AsC_4Ph_4)\}]$ were obtained by slow evaporation of the chromatography eluate (9:1 *v*/*v* petroleum ether/$Et_2O$) providing large regular prisms, and the molecular structure is shown in **Figure 6.6**.

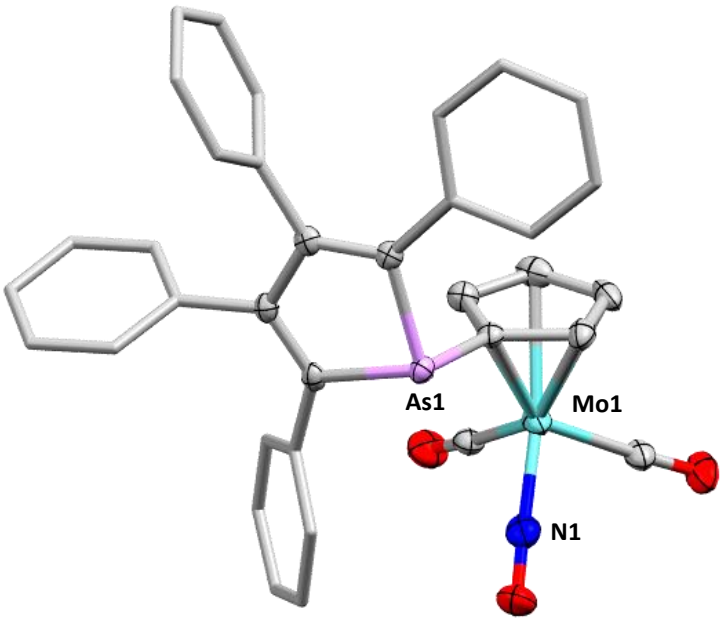



**Figure 6.6**: The molecular structure of $[Mo(NO)(CO)_2\{\eta^5\text{-}C_5H_4(AsC_4Ph_4)\}]$. Phenyl groups simplified and hydrogen atoms omitted for clarity. Ellipsoids shown at 50% displacement. The nitrosyl ligand is disordered amongst all three basal sites and only one contributor is depicted.

X-ray diffraction confirms product identity: a *pseudo*-octahedral Mo(0) centre is found which is best described as a three-legged piano-stool wherein the cyclopentadienyl ring occupies the apex of a triangular pyramid, with the nitrosyl and carbonyl ligands occupying the triangular basal plane. Given the one-electron difference between N and C (resulting in almost identical atomic scattering factors), the nitrosyl ligand is crystallographically indistinguishable amidst the tripodal ligand set and is disordered in such a way as to occupy each of the three equivalent sites one-third of the time; this positional disorder is an oft-encountered

* Molybdenum contains six naturally occurring isotopes which renders visual identification of relevant ion fragments in the mass spectrum straightforward: $^{92}Mo$ (14.65% natural abundance), $^{94}Mo$ (9.19%), $^{95}Mo$ (15.87%), $^{96}Mo$ (16.67%), $^{97}Mo$ (9.58%), $^{98}Mo$ (24.29%).

feature of complexes containing isosteric $NO^+$ and CO ligands.[45-47] Gross molecular features of interest are largely identical to those of $[MoMe(CO)_3\{\eta^5\text{-}C_5H_4(AsC_4Ph_4)\}]$ (**Figure 6.1**) with the arsolyl group unsymmetrically disposed about the cyclopentadienyl to which it is affixed; an As-$C_{Cp}$ distance of 1.943(3) Å – highly typical for As-C($sp^2$) bonds in this work – is observed. Most other interatomic relationships within the structure call for no specific mention, save for the individual Mo-$C_{Cp}$ distances.

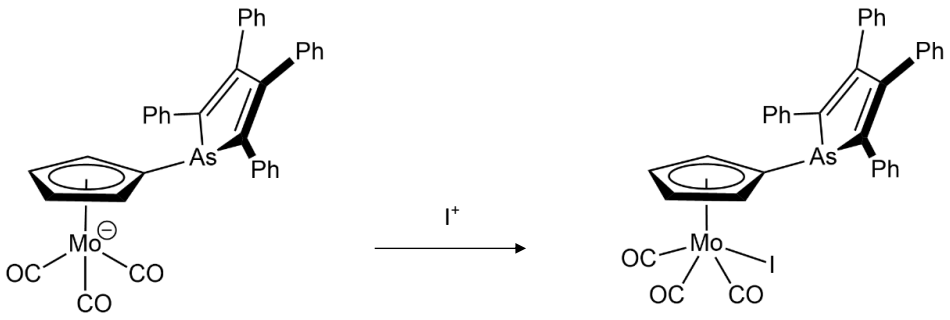
ATWOOD has previously noted that the homologous pentamethylcyclopentadienyl $[M(NO)(CO)_2(\eta^5\text{-}C_5Me_5)]$ complexes (M = Cr, Mo, W) display subtle but measurable tilting of the cyclopentadienyl ring(s), such that one Mo-$C_{Cp}$ distance (2.365(5) Å) is (somewhat) crystallographically distinct from the remaining four (mean 2.345(3) Å).[48] This was ascribed to the presence of an electron-accepting NO group *trans* to one of the M-$C_{Cp}$ bonds (although ATWOOD *et al.* also find the NO group disordered amongst the two CO ligands similar to that encountered here – it was not possible from their X-ray diffraction data to unambiguously locate the former), and was a feature also present in the (non-disordered) solid-state structure of the analogous $[Cr(NO)(CO)_2(\eta^5\text{-}C_{13}H_9)]$ complex[45] which *does* contain the NO group *trans* to the longest Cr-$C_{Cp}$ bond. Here, a comparable tilting of the cyclopentadienyl ring in $[Mo(NO)(CO)_2(\eta^5\text{-}C_5H_4(AsC_4Ph_4)\}]$ is measured (maximum deviation of the ring from planarity 0.004 Å), with four equivalent Mo-$C_{Cp}$ bonds (mean 2.340(6) Å) and one slightly longer (2.369(2) Å) – this difference is probably statistically significant however the chemical significance is less certain. It is noted that the longest Mo-$C_{Cp}$ bond is to the one carrying the arsolyl substituent, as was the case for $[MoMe(CO)_3(\eta^5\text{-}C_5H_4(AsC_4Ph_4)\}]$: the measured tilting of the cyclopentadienyl ring is thus more-convincingly attributed to packing effects within the crystal lattice which affect a slight deformation of the molecule.

### 6.3.6 Synthesis of $[MoI(CO)_3\{\eta^5\text{-}C_5H_4(AsC_4Ph_4)\}]$

Finally, a THF solution of $[Mo(CO)_3\{\eta^5\text{-}C_5H_4(AsC_4Ph_4)\}]^-$ was treated with one equivalent of *N*-iodosuccinimide or 1,2-diiodoethane (both mild sources of $I^+$) which immediately afford deep red-brown solutions. Purification by column chromatography gives a small quantity of $[MoI(CO)_3(\eta^5\text{-}C_5H_5)]$* followed by the expected $[MoI(CO)_3\{\eta^5\text{-}C_5H_4(AsC_4Ph_4)\}]$ as a red-brown solid after evaporation of the solvent

* NMR: $^1H$ ($C_6D_6$, 400 MHz, 25 °C) δ 4.48 ppm; $^{13}C\{^1H\}$ ($C_6D_6$, 176 MHz, 25 °C) δ 237.3, 221.2, 93.4 ppm; IR ($CH_2Cl_2$, 25 °C) $\nu_{CO}$ 2043(vs), 1966(vs) $cm^{-1}$.

(**Scheme 6.7**). The compound is sufficiently air-stable to permit workup and handling without exclusion of ambient atmosphere however – like $[MoI(CO)_3(\eta^5\text{-}C_5H_5)]$ – it gradually decomposes to insoluble green materials over the course of several weeks in the solid state, and several hours in solution when not stored under inert atmosphere. LO STERZO has noted that the related *P*-cyclopentadienyl phosphino complex $[MoI(CO)_3(\eta^5\text{-}C_5H_4PPh_2)]$ could not be isolated from the action of NIS or 1,2-diiodoethane upon the $[Mo(CO)_3(\eta^5\text{-}C_5H_4PPh_2)]^-$ anion, instead requiring an unusual strategy whereby the bimetallic $[MoMn(CO)_8(\eta^5\text{-}C_5H_4PPh_2)]$ intermediary affords the desired iodide complex quantitatively after treatment with $I_2$.[49] Here, no such difficulty was encountered the target molybdenum iodide complex could be isolated in acceptable yields with the iodinium sources indicated.




**Scheme 6.7**: Synthesis of $[MoI(CO)_3\{\eta^5\text{-}C_5H_4(AsC_4Ph_4)\}]$. $I^+$ = *N*-iodosuccinimide or 1,2-diiodoethane.

Spectroscopic features are comparable to the other ring-substituted complexes discussed above: the $^1H$ NMR spectrum ($C_6D_6$ – the product appears to slowly decompose in $CDCl_3$) yields the usual pair of virtual triplets (4.96 and 4.46 ppm; $J_{HH}$ = 2.1 Hz); the $^{13}C\{^1H\}$ spectrum reveals a pair of carbonyl nuclei at 236.9 (*transoid*) and 220.5 (*cisoid*) ppm, and the three cyclopentadienyl signals at 106.2 (*As*-bonded), 97.6 and 95.1 ppm. The high-resolution mass spectrum (ESI) finds a sharp ion signal corresponding to ionisation of the iodide bond ($[M - I]^+$: $m/z \approx 677.0008$) in addition to fragments of sequential decarbonylation, and the IR spectrum ($CH_2Cl_2$) reveals only two $\nu_{CO}$ absorptions at 2041(vs) and 1965(vs) $cm^{-1}$. Single crystals were obtained from $Et_2O$ solution at – 30 °C, and the molecular structure is shown in **Figure 6.7**.

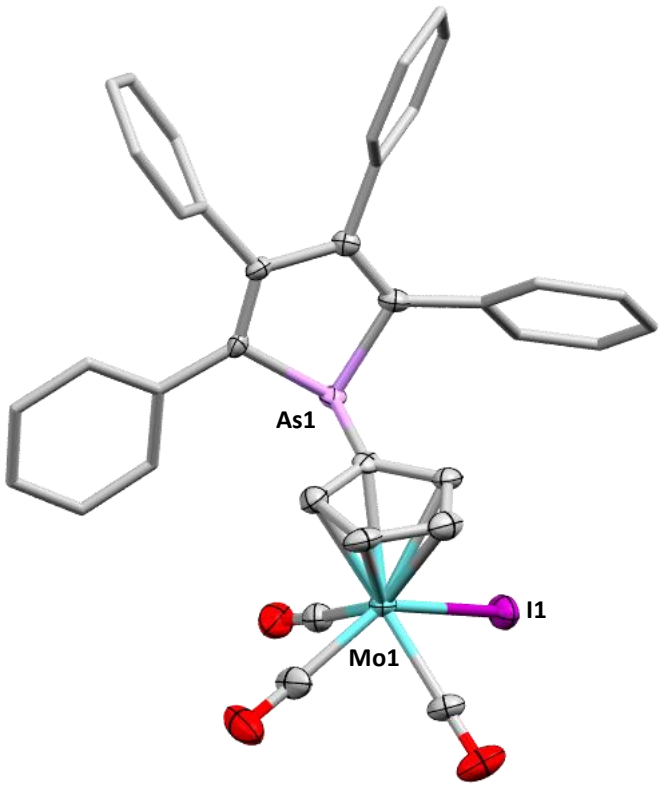



**Figure 6.7**: The molecular structure of [MoI(CO)$_3${$\eta^5$-$C_5H_4$($AsC_4Ph_4$)}]. Phenyl groups simplified and hydrogen atoms omitted for clarity. Ellipsoids shown at 50% displacement.

Two enantiomeric molecules are contained within the unit cell (triclinic *P*-1) which are related by means of the crystallographic inversion centre. The molecular structure of [MoI(CO)$_3${$\eta^5$-$C_5H_4$($AsC_4Ph_4$)}] comprises the expected four-legged piano stool complex with the iodide and carbonyl ligands occupying the basal plane of a square-based pyramid. The centroid of the monosubstituted cyclopentadienyl ring serves as the apex of this polyhedron, and the iodide and arsolyl groups form a dihedral of *ca* 65° when viewed along the molybdenum-centroid vector. The arsolyl substituent likewise lies above the plane of the cyclopentadienyl ligand opposite the metal centre, offset slightly about the As-$C_{Cp}$ bond. Interatomic dimensions do not vary greatly from the methyl (**Figure 6.1**) and nitrosyl (**Figure 6.6**) analogues previously encountered and the Mo-I bond length of 2.8314(7) Å is otherwise typical.* The mean cyclopentadienyl ring-plane deviates by no more than 0.005 Å from planarity though in contrast to the aforementioned methyl and nitrosyl complexes, the longest Mo-$C_{Cp}$ bond is not to that bearing the arsolyl substituent but

* Of the 18 crystal structures archived in the CSD with $Mo^{II}$-I fragments, the mean Mo-I distance is 2.839 Å with a range of 2.80—2.86 Å

to the cyclopentadienyl-carbon lying directly above the iodide (longest Mo-$C_{Cp}$ 2.360(7) Å *vs.* mean remainder Mo-$C_{Cp}$ 2.300(13) Å): this is interpreted on the basis of the iodide exhibiting a weaker *trans* influence on the cyclopentadienyl ring than does the corresponding *transoid* carbonyl ligand, thereby causing the ring to lift slightly above the iodide. Distances from the molybdenum to the carbonyl carbons and C≡O bond lengths do not vary greatly suggesting any π-donor ability of the iodide is largely negligible in the present complex.

### 6.3.7 Attempted Synthesis of $[MoRh(CO)_3(NBD)\{\mu\text{-}\eta^1\text{:}\eta^5\text{-}C_5H_4(AsC_4Ph_4)\}]$

With a view of preparing a bimetallic species, to a THF solution of *in situ* prepared $[Mo(CO)_3\{\eta^5\text{-}C_5H_4\{AsC_4Ph_4)\}]^-$ was added one-half the theoretical equivalent of the halide-bridged dimer $[Rh_2(\mu\text{-}Cl)_2(NBD)_2]$ (NBD = $\eta^2$:$\eta^2$-norbornadiene); the reaction mixture turns a dark yellow-brown and chromatography of the reaction mixture provides a golden yellow solid in moderate yield as the only isolable compound.

The identity of this compound was initially perplexing – no signals corresponding to a ring-substituted cyclopentadienyl were evident in the $^1$H NMR spectrum, and the solution IR spectrum showed a complete absence of any carbonyl-associated absorptions. Mass spectrometry concurred the absence of molybdenum nuclei and the material was therefore deemed insipid reaction detritus and earmarked for disposal. By chance, the product crystallised during slow evaporation of the chromatography eluate and X-ray diffraction revealed the compound to be the novel *pentahapto* complex $[Rh(NBD)(\eta^5\text{-}AsC_4Ph_4)]$, arising from an unknown mechanism but evidently one involving intermetallic transfer of the tetraphenylarsolyl ligand. The molecular structure (as the *n*-hexane solvate) is shown in **Figure 6.8**. The compound naturally recalls that of the *pentahapto* cobalt complexes previously synthesised in **Chapter 3**.

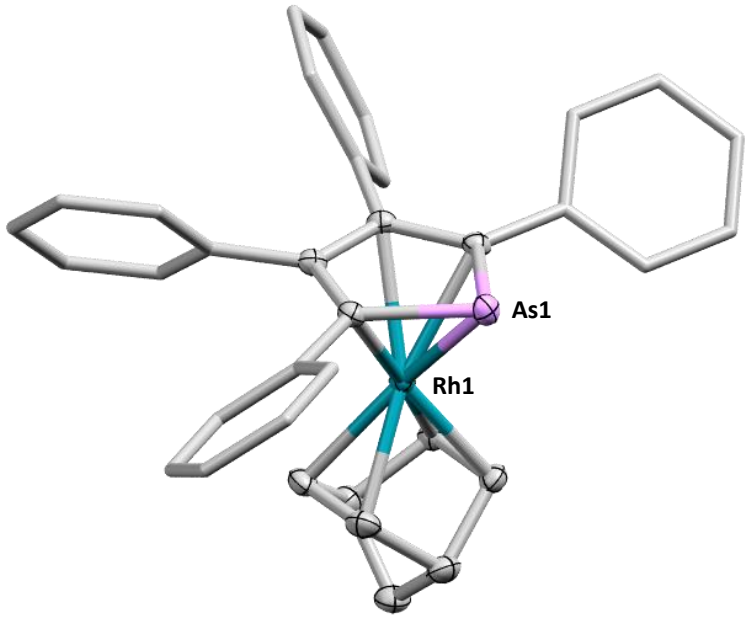



**Figure 6.8**: The molecular structure of [Rh(NBD)($\eta^5$-$AsC_4Ph_4$)]·$C_6H_{14}$ (NBD = norbornadiene). Phenyl groups simplified and hydrogen atoms and *n*-hexane solvate molecule omitted for clarity. Ellipsoids shown at 50% displacement.

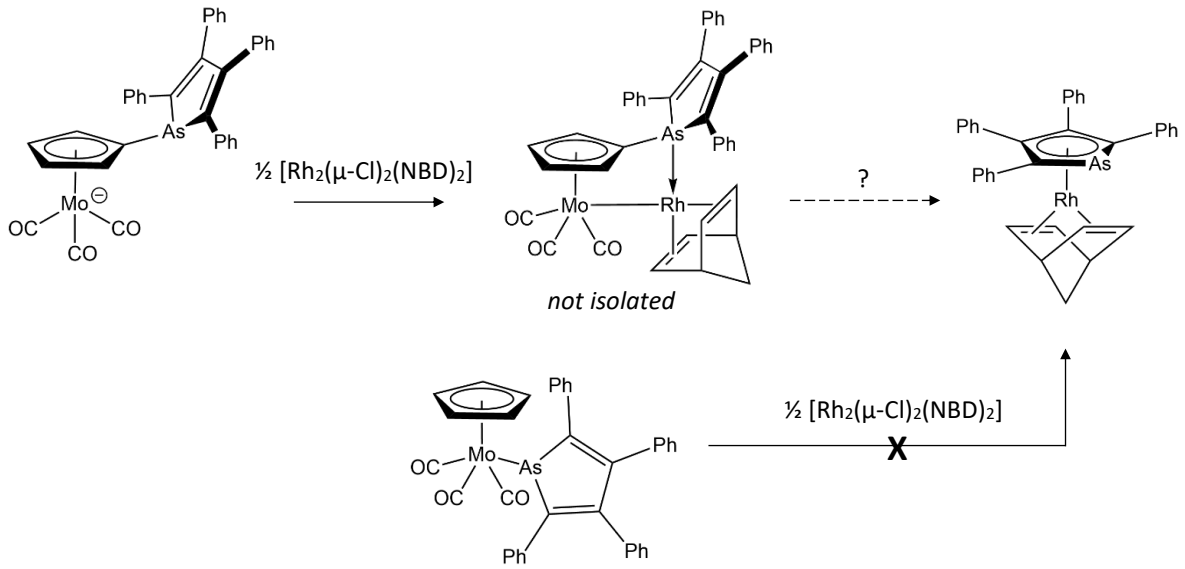
The unit cell (triclinic *P*-1) contains a pair of enantiomeric molecules related by the crystallographic inversion centre and the *n*-hexane solvent molecule conveniently exhibited no disorder. The Rh(I) centre exists in a two-legged piano stool conformation; the mean planes formed by the arsolyl ring and the four olefinic carbon atoms are approximately mutually parallel though the former is rotated by *ca* 10° from the vertical symmetry plane which bifurcates the Rh(NBD) moity, and underpins the molecular chirality in the solid state. The Rh-As distance of 2.2580(2) Å is significantly shorter than the Co-As distance of 2.4277(4) Å in [($\eta^5$-$AsC_4Ph_4$)$Co(CO)_2$] possibly for more-efficient orbital overlap between the soft As(III) and softer Rh(I) centres than for a harder Co(I).* Mean distances from the arsolyl ring carbons to the rhodium centre are regular at *ca* 2.25 Å which is slightly longer than the same mean distances in [($\eta^5$-$AsC_4Ph_4$)$Co(CO)_2$] (*ca* 2.11 Å), however internal ring-atom distances and angles are practically identical between the two Group 9 metals. Distances between the Rh(I) and olefinic carbon atoms of *ca* 2.12 Å are unremarkable,[50] as are other interatomic dimensions in and around the norbornadiene ligand.

Spectroscopic features are comparable to those of the cobalt species [$Co(CO)_2$($\eta^5$-$AsC_4Ph_4$)] encountered previously (**Chapter 3**, **Section 3.3.2**): the arsolyl ring-carbons signals are found at 139.4 and

* Within the HSAB concept. Covalent radii: Rh = 1.42 Å, Co = 1.26 Å.

137.0 ppm in the $^{13}C\{^{1}H\}$ NMR spectrum ($C_6D_6$) for the nuclei α and β to the arsenic atom, respectively (*cf.* 137.2 and 135.1 ppm for the cobalt analogue) with unresolved $^{103}Rh$-$^{13}C$ coupling. The norbornadiene carbon atoms π-bound to the rhodium centre are found as a doublet at 40.4 ppm ($^{1}J_{RhC}$ = 9.1 Hz) with the bridgehead carbon nuclei resonating at 57.8 ppm ($^{2}J_{RhC}$ = 6.7 Hz). A single equivalent of free *n*-hexane was also found in the NMR spectra and elemental microanalysis composition was correct for the presence of the same, suggesting that the solvate molecule is appreciably entrapped within the crystalline lattice. The complex is appreciably resistant toward aerobic oxidation and ligand substitution: placing a $C_6D_6$ solution of [($\eta^5$-$AsC_4Ph_4$)Rh(NBD)] under carbon monoxide atmosphere did not lead to displacement of the norbornadiene ligand even over one week, and no reaction was observed with 1,2-bis(diphenylphosphino)ethane in $C_6D_6$ at 60 °C. The high-resolution mass spectrum is bereft of disintegration products, comprising only the molecular ion ($m/z \approx$ 626.0455).

It was initially suspected that [Rh(NBD)($\eta^5$-$AsC_4Ph_4$)] could be formed by a transmetalation reaction between unreacted [Mo($AsC_4Ph_4$)$(CO)_3$($\eta^5$-$C_5H_5$)] and [$Rh_2$(μ-Cl)$_2$(NBD)$_2$]; however, combining these reagents in $C_6D_6$ gave *no detectable reaction whatsoever* and the spectrum was unchanged over two weeks at ambient temperature. The formation of [Rh(NBD)($\eta^5$-$AsC_4Ph_4$)] under the reaction conditions outlined above was reproducible (**Scheme 6.8**), though the means by which the arsolyl group is transferred from the [Mo$(CO)_3${$\eta^5$-$C_5H_4$($AsC_4Ph_4$)}]$^-$ anion (the existence of which was first confirmed by IR spectroscopy) is not obvious in the absence of evidence for the fate of the molybdenum centre ([$Mo_2(CO)_6$($\eta^5$-$C_5H_5$)$_2$], for example, was not isolated). No tractable products were obtained after addition of [RhCl(COD)($NH_2C_6H_4$Me-4)], [$Ir_2$(μ-Cl)$_2$(COD)$_2$] (COD = $\eta^2$:$\eta^2$-1,5-cyclooctadiene; $NH_2C_6H_4$Me-4 = *para*-toluidine) or [$Pd_2$(μ-Cl)$_2$($\eta^3$-$C_3H_5$)$_2$] to Li[Mo$(CO)_3${$\eta^5$-$C_5H_4$($AsC_4Ph_4$)}], *i.e.*, coordinatively unsaturated reagents that might reasonably have been expected to lead to bridge-assisted metal-metal bond formation.



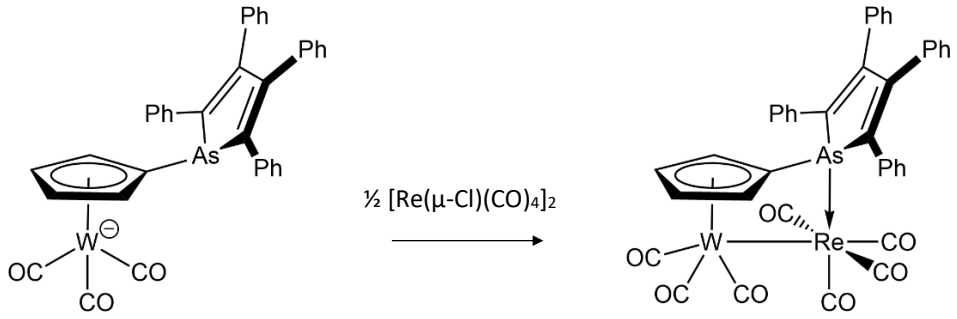

**Scheme 6.8**: Isolation of [Rh(NBD)($\eta^5$-$AsC_4Ph_4$)] from the reaction between [$Mo(CO)_3\{\eta^5$-$C_5H_4(AsC_4Ph_4)\}]^-$ and [$Rh_2(\mu$-$Cl)_2(NBD)_2$]. The mechanism of formation is unknown, however does *not* arise from a transmetalation between [$Mo(AsC_4Ph_4)(CO)_3(\eta^5$-$C_5H_5)$] and the rhodium(I) dimer.

### 6.3.8 Synthesis of [$WRe(CO)_7\{\mu$-$\eta^1$:$\eta^5$-$C_5H_4(AsC_4Ph_4)\}$]

To explore how arsolyl transfer might proceed in the above section, attention turned to metal reagents with characteristically slow reaction kinetics for which intermediates might be isolable. Amongst the potential candidates, the reagent [$Re_2(\mu$-$Cl)_2(CO)_8$] was considered since ABEL has previously reported the *pentahapto* arsolyl complex [$Re(CO)_3(\eta^5$-$AsC_4Ph_4)$].[51] In donor solvents, this dimeric complex serves as a source of the 16-electron "$ReCl(CO)_4$" *via* halide bridge cleavage (*cf.* [$Rh_2(\mu$-$Cl)_2(NBD)_2$]); CASEY successfully employed such a reagent (and its manganese counterpart) to obtain the phosphino-cyclopentadienyl bridged complexes [$MoM(CO)_7(\mu$-$\eta^1$:$\eta^5$-$C_5H_4PR_2$)] (M = Mn, Re; R = Ph or *p*-tolyl),[31] which seemed plausible analogues of $\mu$-$\eta^1$:$\eta^5$-$C_5H_4(AsC_4Ph_4)$-bridged species, which in turn might arise *en route* to arsolyl transmetalation. Disappointingly, no such Mo-Re complex was isolated from the reaction of the complex with $Li[Mo(CO)_3\{\eta^5$-$C_5H_4(AsC_4Ph_4)\}]$. Instead a small quantity of pale yellow [$ReCl(CO)_5$] was recovered as the only chromatographically-mobile material and identified by its characteristic IR profile* and quiescent $^1$H NMR spectrum.

* IR ($CH_2Cl_2$, 25 °C): $\nu_{CO}$ 2046(vs), 1985(s) $cm^{-1}$. Confirmed by comparison with an authentic sample.

It was, however, possible to isolate the analogous tungsten-rhenium complex: $[WRe(CO)_7\{\mu\text{-}\eta^1\text{:}\eta^5\text{-}C_5H_4(AsC_4Ph_4)\}]$ was obtained as an air stable yellow-orange solid albeit in very low yield after column chromatography, by addition of $[Re(\mu\text{-}Cl)(CO)_4]_2$ to a THF solution of $Li[W(CO)_3\{\eta^5\text{-}C_5H_4(AsC_4Ph_4)\}]$ (**Scheme 6.9**).




**Scheme 6.9**: Synthesis of an arsolyl-bridged bimetallic complex featuring an *As*-supported tungsten-rhenium covalent bond.

The solution IR spectrum ($CH_2Cl_2$) of $[WRe(CO)_7\{\mu\text{-}\eta^1\text{:}\eta^5\text{-}C_5H_4(AsC_4Ph_4)\}]$ is predictably congested exhibiting $\nu_{CO}$ absorptions at 2112(w), 2082(s), 2018(s), 1991(s), 1958(vs), 1886(w) and 1857(w) $cm^{-1}$. In the $^1H$ NMR spectrum ($C_6D_6$), the usual pair of apparent triplets corresponding to the monosubstituted cyclopentadienyl ring at 5.33 and 4.51 ppm ($J_{HH}$ = 2.2 Hz) were observed; high-resolution mass spectrometry confirmed gross composition (as did a crystal structure determination). The milligram-quantities obtained, however, unfortunately precluded $^{13}C\{^1H\}$ NMR spectroscopic analysis; it remains one of the few compounds in this work which could not be completely characterised. Single crystals were obtained from $CH_2Cl_2$/*n*-hexane and the molecular structure of $[WRe(CO)_7\{\mu\text{-}\eta^1\text{:}\eta^5\text{-}C_5H_4(AsC_4Ph_4)\}]$ (as the $CH_2Cl_2$ disolvate) is shown in **Figure 6.9**.

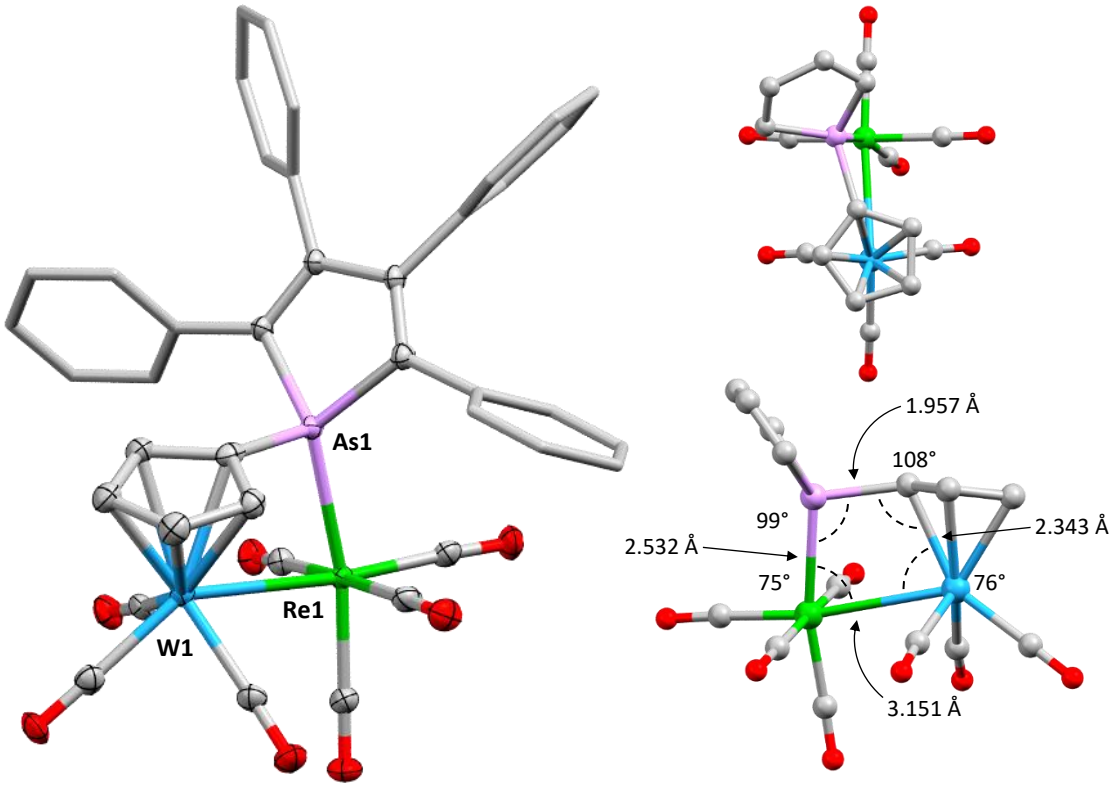



**Figure 6.9**: The molecular structure of $[WRe(CO)_7\{\mu\text{-}\eta^1\text{:}\eta^5\text{-}C_5H_4(AsC_4Ph_4)\}]\cdot 2CH_2Cl_2$. Phenyl groups simplified, dichloromethane solvate molecules and hydrogen atoms omitted for clarity. Ellipsoids shown at 50% displacement. **Inset**: abbreviated perspectives of the complex highlighting the asymmetric disposition of the monometallic components.

The expected bimetallic nature of the complex was established and features a covalent W-Re bond supported by a dative As→Re interaction. The rhenium(I) centre adopts a distorted octahedral environment wherein the coordination polyhedron is not perfectly aligned with the vertical symmetry plane of the $W(CO)_3(\eta^5\text{-}C_5H_5)$ moiety, instead being twisted *ca* 15° about the metal-metal axis which allows the W-Re and As-$C_{Cp}$ bonds to avoid a perfectly parallel conformation (**Figure 6.9**, **Inset**) – this feature also allows the rhenium-bound equatorial carbonyl ligands *cis* to the W-Re bond to minimise electrostatic repulsions with the *cisoid* carbonyls on the tungsten centre. The arrangement confers chirality to the molecule in the solid state – the unit cell (triclinic *P*-1) contains a pair of such enantiomers related by the crystallographic centre of inversion.

The intermetallic W-Re separation of 3.0510(4) Å falls comfortably within the *ca* 2.90—3.20 Å range previously measured for other authentic tungsten-rhenium covalent single bonds:[52, 53] those at the shorter end of the continuum exclusively feature one or more anionic ligands which abridge the two metal

centres.[54-57] The arsenic to rhenium dative bond of 2.5320(5) Å is not remarkably different to other As→M dative bonds measured during this work – or those from the literature[58, 59] – and the otherwise congested environment of the molecule has little effect on the arsenic to cyclopentadienyl carbon distance of 1.957(5) Å (*c.f* 1.951(4) Å in $[MoMe(CO)_3\{\eta^5\text{-}C_5H_4(AsC_4Ph_4)\}]$; **Figure 6.1**). The regular disposition of the cyclopentadienyl ring above the W centre (W-$C_{Cp}$ 2.32—2.35 Å) is noted, though in contrast to the solid state structure of $[MoMe(CO)_3\{\eta^5\text{-}C_5H_4(AsC_4Ph_4)\}]$ the arsenic atom is bent 0.44 Å *below* the mean plane of the cyclopentadienyl ring in the direction of the rhenium centre. Accordingly, the W-Re-As angle is contracted to 74.51(1)°. Given these contrasting dimensions, the imaginary quadrilateral formed by the arsenic, rhenium, tungsten, and *ipso*-cyclopentadienyl carbon atoms represents a slightly strained albeit nearly planar ring system (**Figure 6.9**, **Inset**).

CASEY *et al.*[31, 60] have prepared similar bimetallic complexes wherein an intermetallic covalent bond is supplemented by the presence of a pendant di(aryl)phosphino donor on the cyclopentadienyl ring. Their method of synthesis, however, differs from that herein: labile *P*-cyclopentadienyl diarylphosphines are prepared at low temperature and deprotonated *in situ* to provide isolable $Li[P(C_5H_4)R_2]$ salts (R = Ph, *p*-tolyl). Thermolysis with $[Mo(NCMe)_3(CO)_3]$ (similar to the preparation of $[Mo(CO)_3(\eta^5\text{-}C_5H_5)]^-$) provides* the requisite nucleophile $[Mo(CO)_3(\eta^5\text{-}C_5H_4PR_2)]^-$ (**Scheme 6.10**) which reacts with a selection of unsaturated group 7 and 9 metal halides; these products are shown in **Chart 6.2**.

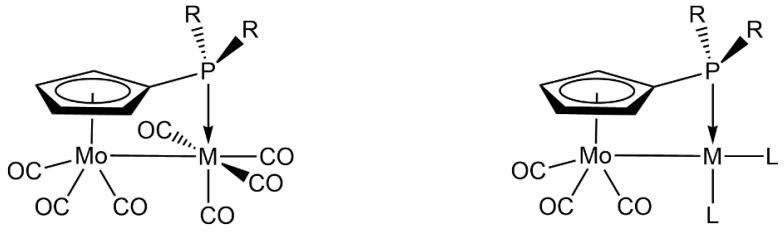



**Chart 6.2**: Bimetallic $[MoM(\mu\text{-}\sigma^1\text{:}\eta^5\text{-}C_5H_4PR_2)(CO)_3L_n]$ complexes previously prepared by CASEY, featuring phosphino-supported intermetallic covalent bonds (R = Ph or *p*-tolyl).

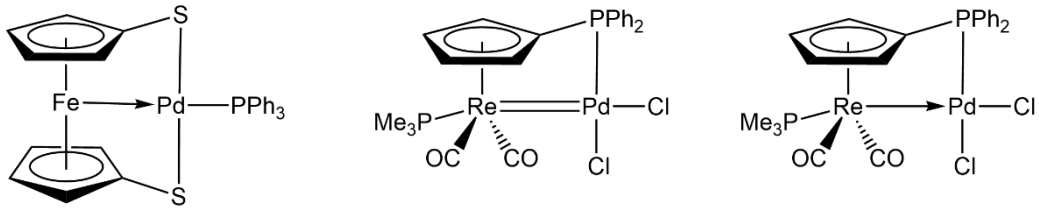
* CASEY notes that direct combination of $[C_5H_4PR_2]^-$ with $[Mo(CO)_6]$ leads to a mixture of $[Mo(CO)_3(\eta^5\text{-}C_5H_4PR_2)]^-$ (major) and $[(Mo\{\eta^1\text{-}PR_2(C_5H_4)\}(CO)_5]^-$ (minor) which defy separation. The use of a pre-formed labile molybdenum tricarbonyl centre *e.g.*, $[Mo(NCMe)_3(CO)_3]$ circumvents this issue.

An X-ray diffraction study[31]was previously performed on the complex $[MoMn(CO)_7\{\mu\text{-}\sigma^1{:}\eta^5\text{-}C_5H_4P(p\text{-tolyl})_2\}]$ for which the bulk molecular configuration is in general accord with that of $[WRe(CO)_7\{\mu\text{-}\eta^1{:}\eta^5\text{-}C_5H_4(AsC_4Ph_4)\}]$ (**Figure 6.9**), with respective Mo-Mn and P-Mn distances of 3.054(1) and 2.278(1) Å. CASEY'S intention was to explore these bimetallic complexes as catalysts for small-molecule hydrogenation although their ability to cooperatively activate $H_2$ was disappointingly unrealised, often leading to partial decomposition. The Mo-Mn and Mo-Re complexes do, however, react with strong acids to give cationic bridging hydrido complexes for which the proton is easily abstracted by even the weakest of bases, including donor solvents such as acetone.[61] The Mo-Mn species above was later shown to activate P-H bonds under thermal impetus to form the doubly-bridged $[MoMn(CO)_5(\mu\text{-}H)(\mu\text{-}PRPh)(\mu\text{-}\sigma^1{:}\eta^5\text{-}C_5H_4PPh_2)]$ (R = Ph, H) complexes.[62]

The $\mu\text{-}\eta^1{:}\eta^5\text{-}C_5H_4\{PR_2\}$ ligand has since proven to be a popular synthon for construction of metal-metal bonded complexes,* although the variety in donor function (arsenic, antimony *etc.*) is conspicuously limited save for minor adjustments to the phosphine-cyclopentadienyl linkage (*e.g.*, $C_5H_4(X)PPh_2$; X = $CH_2$, $SiMe_2$).[63, 64] Phosphinocyclopentadienyl ligands have been employed by ERKER[65, 66] and CASEY[67] to create highly polarised intermetallic covalent bonds between disparate early (Ti and Zr) and late (Fe, Co, Rh, Ir and Pd) transition metal elements. Especially simple examples include the Group 6 bimetallic $[Mo_2(CO)_4(\mu\text{-}\sigma^1{:}\eta^5\text{-}C_5H_4PPh_2)]$ and $[MoM(CO)_5(\mu\text{-}\sigma^1{:}\eta^5\text{-}C_5H_4PPh_2)(\eta^5\text{-}C_5H_5)]$ (M = Mo, W) complexes prepared by MAYS *et al.*,[68] and the heterobimetallic $[RePd(PMe_3)(CO)_2Cl_2(\mu\text{-}\sigma^1{:}\eta^5\text{-}C_5H_4PPh_2)]$ for which a dubious Re=Pd double bond is invoked on the basis of crystallographic (Re-Pd 2.763(1) Å) and computational interrogation (**Chart 6.3**, model **A**).[69] The LEWIS basicity of the Re(I) centre is likely encouraged by the phosphine donor in a *transoid* site to the Pd(II) LEWIS acid; the nature of the bond between Re(I) and Pd(II) is most-likely better perceived as polar covalent (that is, dative Re→Pd) in nature.[70] The claim of a formal Re=Pd double bond is, however, not entirely convincing. Chemical reactivity studies which might provide further support for this assertion are conspicuously absent from this and any subsequent papers. It may however be remarked that SEYFERTH has reported the complex $[FePd(PPh_3)(\mu\text{-}\sigma^1{:}\eta^5\text{-}C_5H_4S)_2]$ in which the two thiolatocyclopentadienyl ligands – by bridging the two metals – bring the iron centre within proximity

* Many non-bonded bimetallic complexes have also been obtained with this ligand. See: F. MATHEY *et al. J. Organomet. Chem.*, **1982**, *231*, C43—C48, M. RAUSCH *et al. J. Am. Chem. Soc.*, **1983**, *105*, 3882—3886 and W.A. SCHENK and C. LABUDE *Chem. Ber.*, **1989**, *122*, 1489—1490 for representative examples.

of the LEWIS acidic Pd(II) centre to invoke a dative interaction (**Chart 6.3**; Fe-Pd 2.878(1) Å).[71] The same description seems more apt in the case of [RePd(PMe$_3$)(CO)$_2$Cl$_2$(μ-σ$^1$:η$^5$-C$_5$H$_4$PPh$_2$)] (**Chart 6.3**, model **B**).*




**A** **B**

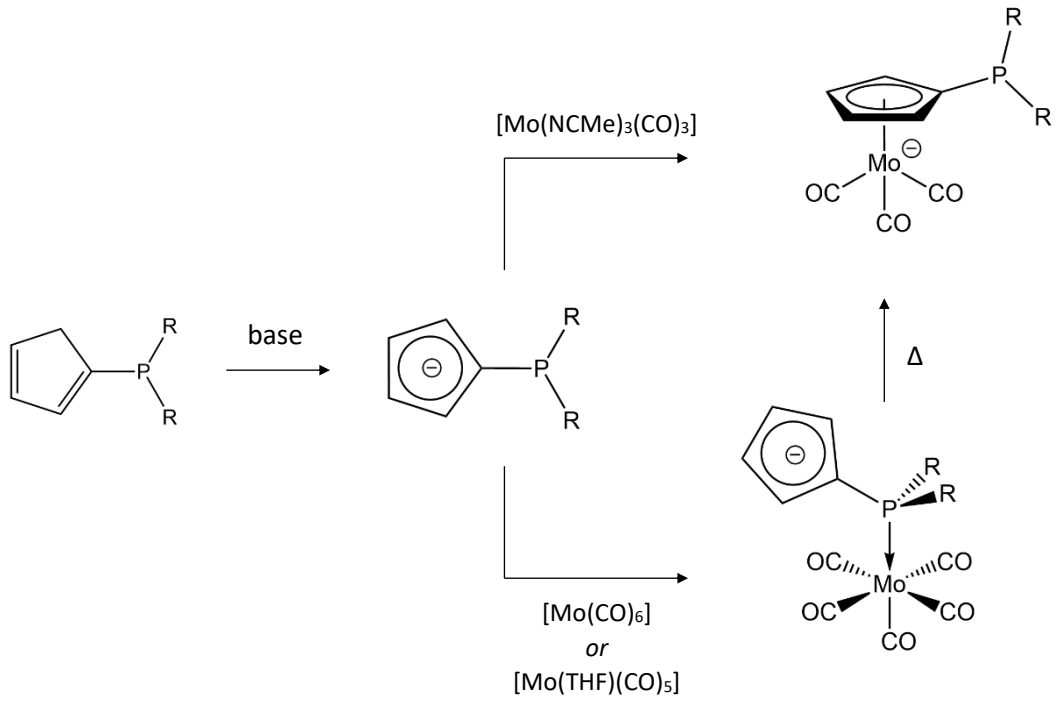
SEYFERTH, 1983 KLAHN, 2010

**Chart 6.3**: Examples of intermetallic dative bonds supported by bridging cyclopentadienyl ligands.

## 6.4 Attempted Syntheses of Free *As*-cyclopentadienyl Arsoles

It was mentioned that previous workers have utilised phosphinocyclopentadienyl anions ([C$_5$H$_4$PR$_2$]$^-$) to obtain nucleophiles of the form [M(CO)$_3$(η$^5$-C$_5$H$_4$PR$_2$)]$^-$ (M = Mo or W; R = aryl. **Scheme 6.10**). Prior to carrying out the work on base-induced arsolyl migration, an analogous preparation of an *As*-cyclopentadienyl arsole (*i.e.*, (C$_5$H$_5$)AsC$_4$Ph$_4$) was attempted with the intention of realising entry into group 6 complexes of the aforementioned arsolyl-functionalised cyclopentadienyl.

* Geometrical optimisation of the model complex [RePd(PMe$_3$)(CO)$_2$Cl$_2$(μ-σ$^1$:η$^5$-C$_5$H$_4$PMe$_2$)] at the DFT; ωB97X-D/6-31G*/LANL2Dζ (Re,Pd) level of theory returns a LÖWDEN bond order of 0.57 and a Re-Pd separation of *ca* 2.72 Å, which is comparable to the 2.763(1) Å distance found experimentally for [RePd(PMe$_3$)(CO)$_2$Cl$_2$(μ-η$^1$:η$^5$-C$_5$H$_4$PPh$_2$)].

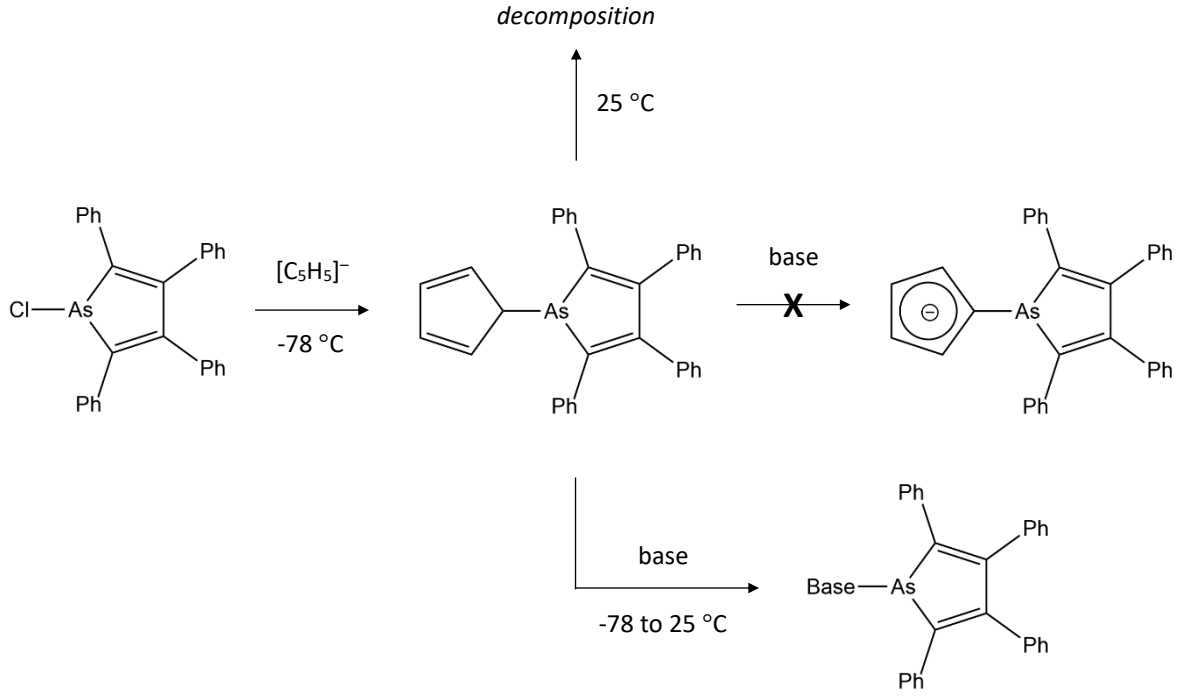



**Scheme 6.10**: Typical syntheses of $\eta^5$ (top) and $\eta^1$ (bottom) *P*-cyclopentadienyl phosphine molybdenum nucleophiles. R = aryl.

Attempts began by simple combination of $[LiC_5H_5]$ or $[Na(C_5H_5)\cdot DME]$ with $ClAsC_4Ph_4$ in THF at -78 °C, which initially gave an encouraging lemon-yellow mixture ($ClAsC_4Ph_4$ is orange in solution) however warming to ambient temperature was met with the formation of dark brown suspensions which defied purification, and no putative molecule corresponding to $C_5H_5AsC_4Ph_4$ could be observed spectroscopically. The target compound is suspected to initially form in the reaction medium before undergoing indiscriminate oligomerisation upon warming, likely [4+2] cycloaddition(s) (**Scheme 6.11**); a similar kinetic lability is known for certain cyclopentadienyl phosphines which also display limited shelf-lives at ambient temperature.[72] Evidence for kinetic instability of the $C_5H_5AsC_4Ph_4$ molecule is found by the contrasting ability to prepare and isolate the bulkier 1-(pentamethylcyclopentadienyl)-2,3,4,5-tetraphenylarsole ($C_5Me_5AsC_4Ph_4$) in high yield (so-prepared for the purpose mentioned in **Section 3.3.6** of **Chapter 3**) which remains monomeric after re-crystallisation from boiling *n*-hexane.

Efforts to circumvent product decomposition by *in situ* low temperature deprotonation of mixtures presumed to contain $C_5H_5AsC_4Ph_4$ with LDA, KHMDS or *t*-BuLi produced yellow-brown mixtures which did not form $[Mo(CO)_3\{\eta^5\text{-}C_5H_4(AsC_4Ph_4)\}]^-$ upon addition of $[Mo(NCMe)_3(CO)_3]$ and instead *only*

$[Mo(CO)_3(\eta^5\text{-}C_5H_5)]^-$ was identified (by IR spectroscopy). In these experiments, substitution of the nucleofugic cyclopentadienyl anion by the incoming base/nucleophile is almost certainly responsible for the failure of these experiments – for *t*-BuLi, the air-stable *t*-$BuAsC_4Ph_4$ could be isolated in good yield from the mixture after quenching all reactive species with an excess of methyl iodide ($[MoMe(CO)_3(\eta^5\text{-}C_5H_5)]$ was also isolated).



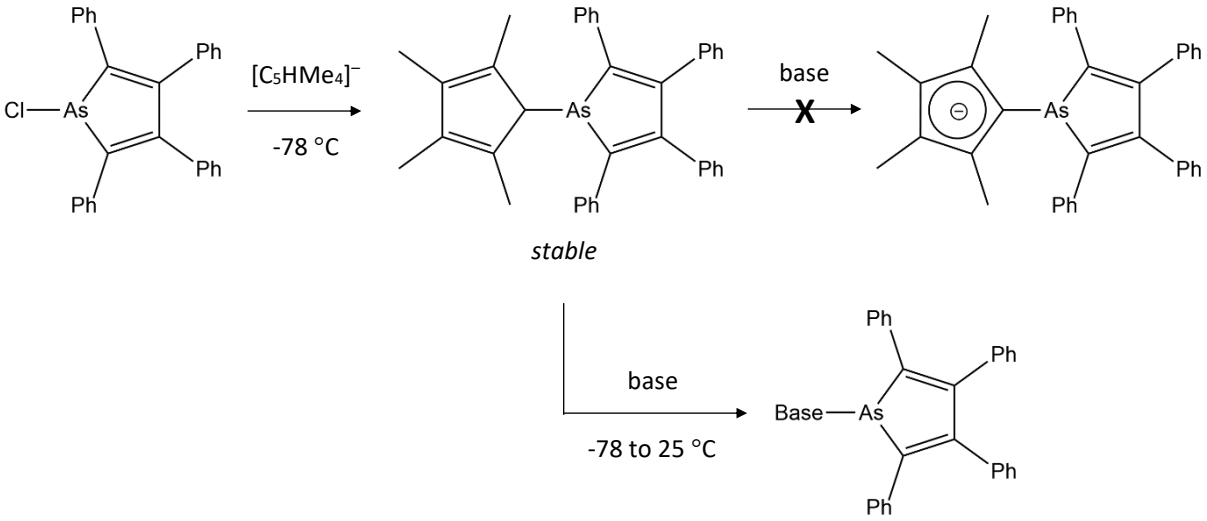

**Scheme 6.11**: Attempted synthesis of 1-(cyclopentadienyl)-tetraphenylarsole and its anion.

The viability of $C_5Me_5AsC_4Ph_4$ (which regrettably lacks an acidic hydrogen) suggested that it may still be possible to obtain a free arsolyl-cyclopentadienyl for direct preparation of Group 6 anions. One reagent on-hand in the laboratory was the (costly) 1-(trimethylsilyl)-2,3,4,5-tetramethylcyclopentadiene ($C_5H(SiMe_3)Me_4$, as a mixture of isomers by [1,5]-H shift) which is readily desilylated to tetramethylcyclopentadiene ($C_5H_2Me_4$) in almost quantitative yield.* Deprotonation with *n*-BuLi in THF solution provides an off-white suspension of $[LiC_5HMe_4]$ which upon addition of $ClAsC_4Ph_4$ results in the formation of $C_5HMe_4AsC_4Ph_4$ as an air-sensitive light yellow solid after extraction of the residue with warm *n*-hexane. The compound was obtained in a reasonably (but not analytically) pure form and identity was

* Tetramethylcyclopentadiene can alternatively be synthesised beginning with the base-catalysed condensation of 3-pentanone with acetaldehyde, followed by dehydration, reduction, and further dehydration; the procedure is straightforward and comparatively cost-effective though is by no means operationally trivial. See T.J. MARKS *et al. Organometallics*, **1988**, *7*, 1828—1838.

confirmed by high-resolution mass spectrometry and NMR spectroscopy; only one isomer is observed at ambient temperature (**Scheme 6.12**), that being the symmetric arrangement in contrast to $C_5H_5PPh_2$ for which the *P*-substituent is preferentially located in a vinylic rather than allylic position.[72]

Unfortunately, treatment of $C_5HMe_4AsC_4Ph_4$ with either LDA or KHMDS also resulted in displacement of the tetramethylcyclopentadienyl group (which, it must be inferred, is a relatively good leaving group compared to the incoming $[NR_2]^-$ nucleophile; **Scheme 6.12**) since $[MoMe(CO)_3(\eta^5\text{-}C_5HMe_4)]$ was obtained after sequential addition of $[Mo(NCMe)_3(CO)_3]$ and methyl iodide. The pursuit of obtaining a suitably acidic arsolylcyclopentadienyl synthon was – with regret – abandoned.




**Scheme 6.12**: Synthesis of 1-(tetramethylcyclopentadienyl)-tetraphenylarsole and attempts to prepare its anion.

## 6.5 Summary

The base-induced migration of σ-arsolyl ligands to a metal-bound cyclopentadienyl ring was investigated; the course of the reaction was sensitive to many variables *inter alia* the specific choice of base for which lithium diisopropylamide was the only effective option identified. Other amide or organolithium bases led to nucleophilic substitution at the arsenic atom with ejection of a metal carbonyl anion. One migration product, namely $[Mo(CO)_3\{\eta^5\text{-}C_5H_4(AsC_4Ph_4)\}]^-$, was intercepted and isolated in crude form as the $[PPN]^+$ salt for which NMR analysis was performed (**Figure 6.4** and **Figure 6.5**). This migration of the σ-arsolyl substituent is significant in recognition that no examples of arsenide migration, nor migration

of any residue possessing a lone pair on the migrating atom, have heretofore been reported; the latter is attributed to the contextual susceptibility of the As(III) centre to nucleophilic addition. NMR analysis also revealed compelling evidence for small quantities of a 1,3-disubstituted cyclopentadienyl anion, $[Mo(CO)_3\{\eta^5\text{-}C_5H_3(AsC_4Ph_4)_2\}]^-$.

The $[Mo(CO)_3\{\eta^5\text{-}C_5H_4(AsC_4Ph_4)\}]^-$ anion was quenched with a small selection of simple electrophiles providing $[MoMe(CO)_3\{\eta^5\text{-}C_5H_4(AsC_4Ph_4)\}]$ (**Figure 6.1**), $[Mo(NO)(CO)_2\{\eta^5\text{-}C_5H_4(AsC_4Ph_4)\}]$ (**Figure 6.6**) and $[MoI(CO)_3\{\eta^5\text{-}C_5H_4(AsC_4Ph_4)\}]$ (**Figure 6.7**) in acceptable yields; the corresponding parent-ring molybdenum complexes $[MoMe(CO)_3(\eta^5\text{-}C_5H_5)]$, $[Mo(NO)(CO)_2(\eta^5\text{-}C_5H_5)]$ and $[MoI(CO)_3(\eta^5\text{-}C_5H_5)]$ were also isolated as minor products of competitive Mo-As bond scission. Spectroscopic features of $[MoR(CO)_n\{\eta^5\text{-}C_5H_4(AsC_4Ph_4)\}]$ are notably very similar to those of $[MoR(CO)_n(\eta^5\text{-}C_5H_5)]$ suggesting the arsolyl residue has little effect on the electronic properties of the metal centre. All three *As*-cyclopentadienyl complexes listed above were characterised by X-ray diffraction.

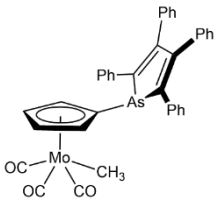
The addition of unsaturated transition metal reagents to $Li[M(CO)_3\{\eta^5\text{-}C_5H_4(AsC_4Ph_4)\}]$ successfully produced a bimetallic complex in one case only, leading to the isolation of $[WRe(CO)_7\{\mu\text{-}\eta^1\text{:}\eta^5\text{-}C_5H_4(AsC_4Ph_4)\}]$ featuring a covalent W-Re bond (3.0510(4) Å) supported by an As→Re dative interaction (2.5320(5) Å; calculated LÖWDIN bond orders: W-Re 0.901, As-Re 0.81). Low yields precluded complete characterisation though a crystal structure was determined which confirmed the formulation and other structural features of interest (**Figure 6.9**). The addition of $[Rh_2(\mu\text{-}Cl)_2(NBD)_2]$ to $Li[Mo(CO)_3\{\eta^5\text{-}C_5H_4(AsC_4Ph_4)\}]$ unexpectedly produced the monometallic complex $[Rh(NBD)(\eta^5\text{-}AsC_4Ph_4)]$ arising *via* an unknown mechanism involving inexplicable intermetallic transfer of the arsolyl residue from the cyclopentadienyl system. A crystal structure of this *pentahapto* arsolyl complex was determined (**Figure 6.8**).

Efforts to obtain a free *As*-cyclopentadienyl arsole were confounded by the thermal instability of $C_5H_5AsC_4Ph_4$, and the tendency for preferential nucleophilic substitution at the heteroatom upon attempts to deprotonate the cyclopentadienyl arsole with supposedly "non-nucleophilic" amide bases. However, $C_5HMe_4AsC_4Ph_4$ could be isolated at ambient temperature and may yet prove to be a useful pro-ligand in the future, especially if a method for successful deprotonation to $[C_5Me_4AsC_4Ph_4]^-$ is found, *e.g.*, RAUSCH

has shown that direct thalliation of $C_5H_5PPh_2$ with TlOEt affords the tractable reagent $Tl(C_5H_4PPh_2)$, the synthetic utility of which has been amply demonstrated.[73]

## 6.6 Experimental

### 6.6.1 $[MoMe(CO)_3\{\eta^5\text{-}C_5H_4(AsC_4Ph_4)\}]$




To a stirred solution of 0.135 g $[CpMo(AsC_4Ph_4)(CO)_3]$ (0.2 mmol) in 20 mL THF at 0 °C was added, dropwise over the course of several minutes, 0.11 mL LDA solution (0.22 mmol; 2 M in THF). The colour gradually changes from bright orange to a deep red during addition of the base. After stirring for 30 minutes at 0 °C, an IR spectrum finds $\nu_{CO}$ absorptions corresponding to $Li[Mo(CO)_3\{\eta^5\text{-}C_5H_4(AsC_4Ph_4)\}]$ at 1906(vs), 1809(vs), 1787(s), 1718(vs) $cm^{-1}$. The reaction mixture was quenched with three-to-four drops of neat methyl iodide (excess) which returns a deep yellow colour to the solution. After 60 minutes, volatiles are removed by rotary evaporation and the residue subjected to column chromatography on silica gel (25 x 2.5 cm). Eluting with petroleum ether, followed by 19:1 petroleum ether/$Et_2O$ provides a yellow band of $[MoMe(CO)_3(\eta^5\text{-}C_5H_5)]$. Eluting with 9:1 petroleum ether/$CH_2Cl_2$ provides a larger yellow band containing the product which is collected and dried by rotary evaporation. The product is encountered as a dark-yellow solid which is readily soluble in polar organic and aromatic solvents, somewhat soluble in $Et_2O$ and less-so in aliphatic hydrocarbons. The product is sufficiently air stable to permit workup without the need for inert atmosphere, however solutions exposed to air turn green and deposit insoluble materials over the course of several days. It appears to slowly react with $CDCl_3$. Average isolated yield across three preparations of the same scale: 0.065 g (0.09 mmol, 45%).

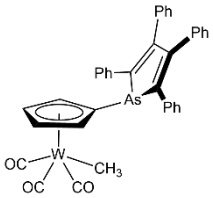
NMR: $^1H$ ($C_6D_6$, 700 MHz, 25 °C) $\delta_H$ 7.36—7.33 (m, 4H, $C_6H_5$), 7.05—7.00 (m, 8H, $C_6H_5$), 6.93—6.91 (m, 2H, $C_6H_5$), 6.87—6.85 (m, 4H, $C_6H_5$), 6.82—6.80 (m, 2H, $C_6H_5$), 4.79 (t, $^3J_{HH} \approx {}^4J_{HH}$ = 2.1 Hz, 2H, {2,5}-$\eta^5$-$C_5H_4$), 4.43 (t, $^3J_{HH} \approx {}^4J_{HH}$ = 2.1 Hz, 2H, {3,4}-$\eta^5$-$C_5H_4$), 0.38 (s, 3H, Mo-$CH_3$) ppm. $^{13}C\{^1H\}$ ($C_6D_6$, 176 MHz, 25 °C) $\delta_C$ 239.7 (*transoid* CO), 226.5 (*cisoid* CO), 150.9 (arsole {2,5}-*C*), 150.8 (arsole {3,4}-*C*), 138.6 ($C_6H_5$), 138.3 ($C_6H_5$), 130.6 ($C_6H_5$), 130.0 ($C_6H_5$), 128.7 ($C_6H_5$), 128.3 ($C_6H_5$), 127.3 ($C_6H_5$), 127.1 ($C_6H_5$), 102.8 ({1}-$\eta^5$-$C_5H_4$), 96.4 ({2,5}-$\eta^5$-$C_5H_4$), 94.0 ({3,4}-$\eta^5$-$C_5H_4$), -20.1 (Mo-$CH_3$) ppm. IR ($CH_2Cl_2$, 25 °C) $\nu_{CO}$ 2017(vs), 1926(vs, br) $cm^{-1}$. HR-MS (ESI, MeCN, +ve ion) found $m/z$ 608.0383 (calc. for $C_{34}H_{27}{}^{75}As_1{}^{98}Mo_1$ $[M - 3CO]^+$: 608.0380); Analysis found 64.40% C, 4.08% H (calc. for $C_{37}H_{27}O_3As_1Mo_1$: 64.36% C, 3.94% H).

$[MoMe(CO)_3(\eta^5\text{-}C_5H_5)]$: NMR: $^1H$ ($C_6D_6$, 700 MHz, 25 °C) $\delta_H$ 4.41 (s, 5H, $\eta^5$-$C_5H_5$), 0.39 (s, 3H, Mo-$CH_3$) ppm. $^{13}C\{^1H\}$ ($C_6D_6$, 176 MHz, 25 °C) $\delta_C$ 240.5 (*transoid* CO), 227.3 (*cisoid* CO), 92.4 ($\eta^5$-$C_5H_5$), -21.9 (Mo-$CH_3$). IR ($CH_2Cl_2$, 25 °C) $\nu_{CO}$ 2018(vs), 1926(vs) $cm^{-1}$.

Single crystals were obtained by layering a $CH_2Cl_2$ solution with *n*-hexane at -20 C. One-half an *n*-hexane molecule was found within the asymmetric unit. $C_{37}H_{27}O_3As_1Mo_1{\cdot}0.5C_6H_{14}$ ($M$ = 733.53 g/mol): yellow needle 0.062 × 0.077

× 0.44 mm, monoclinic, space group $P2_1/c$ (no. 14), $a$ = 22.5954(3) Å, $b$ = 6.24290(10) Å, $c$ = 23.8391(3) Å, $\beta$ = 98.2190(10)°, $V$ = 3328.22(8) Å$^3$, $Z$ = 4, multi-scan correction $T_{min}/T_{max}$ = 0.758/1.000, $\mu$(Cu-Kα) = 4.618 mm$^{-1}$, $\varrho_{calc}$ = 1.464 g/cm$^3$, 21717 reflections measured (7.494° ≤ 2Θ ≤ 147.404°), 6701 unique ($R_{int}$ = 0.0295, $R_{sigma}$ = 0.0333) which were used in all calculations, $GOF$ = 1.097, $D_{min}/D_{max}$ = -0.96/1.00 e/Å$^3$. The final $R_1$ was 0.0460 (I > 2σ(I)) and $wR_2$ was 0.1176 (all data).

### 6.6.2 [WMe(CO)$_3${η$^5$-C$_5$H$_4$(AsC$_4$Ph$_4$)}]

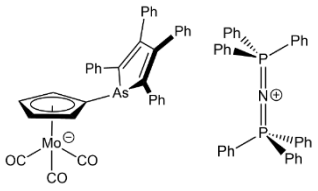



Prepared similarly to that above. Quantities: 0.15 g [W(AsC$_4$Ph$_4$)(CO)$_3$(η$^5$-C$_5$H$_5$)] (0.2 mmol), 0.11 mL LDA solution (0.22 mmol), two-to-three drops methyl iodide (excess). The Li[W(CO)$_3${η$^5$-C$_5$H$_4$(AsC$_4$Ph$_4$)}] migration product displays $\nu_{CO}$ at 1901(vs), 1805(vs), 1780(s), 1716(vs) cm$^{-1}$. Subjected to column chromatography on silica gel with 9:1 petroleum ether/Et$_2$O, followed by 9:1 petroleum ether/CH$_2$Cl$_2$ giving the product as a dark yellow solid. Average isolated yield across two preparations of the same scale: 0.060 g (0.07 mmol, 40%).

NMR: $^1$H (C$_6$D$_6$, 700 MHz, 25 °C) $\delta_H$ 7.36—7.33 (m, 4H, C$_6$*H*$_5$), 7.06—7.01 (m, 10H, C$_6$*H*$_5$), 6.93—6.81 (m, 6H, C$_6$*H*$_5$), 4.77 (t, $^3J_{HH} \approx {}^4J_{HH}$ = 2.2 Hz, 2H, {2,5}-η$^5$-C$_5$*H*$_4$), 4.41 (t, $^3J_{HH} \approx {}^4J_{HH}$ = 2.2 Hz, 2H, {3,4}-η$^5$-C$_5$*H*$_4$), 0.46 (s, $^3J_{WH}$ = 1.9 Hz, 3H, W-C*H*$_3$)ppm. $^{13}$C{$^1$H} (C$_6$D$_6$, 176 MHz, 25 °C) $\delta_C$ 229.3 ($^1J_{WC}$ = 65 Hz, *transoid CO*), 216.0 ($^1J_{WC}$ = 77 Hz, *cisoid CO*), 151.0 (arsole {2,5}-*C*), 150.7 (arsole {3,4}-*C*), 138.6 (*C*$_6$H$_5$), 138.1 (*C*$_6$H$_5$), 130.5 (*C*$_6$H$_5$), 130.0 (*C*$_6$H$_5$), 128.7 (*C*$_6$H$_5$), 128.3 (*C*$_6$H$_5$), 127.4 (*C*$_6$H$_5$), 127.1 (*C*$_6$H$_5$), 101.4 ({1}-η$^5$-*C*$_5$H$_4$), 94.9 ({2,5}-η$^5$-*C*$_5$H$_4$), 92.8 ({3,4}-η$^5$-*C*$_5$H$_4$), -32.8 ($^1J_{WC}$ = 17 Hz, W-*C*H$_3$) ppm. IR (CH$_2$Cl$_2$, 25 °C) $\nu_{CO}$ 2013(vs), 1917(vs, br) cm$^{-1}$. HR-MS (ESI, MeCN, +ve ion) found $m/z$ 795.0732 (calc. for C$_{37}$H$_{28}$O$_4$$^{75}$As$_1$$^{184}$W$_1$ [*M* + O]$^+$: 795.0713). Analysis found 57.17% C, 3.59% H (calc. for C$_{37}$H$_{27}$O$_3$As$_1$W$_1$: 57.09% C, 3.50% H).

[WMe(CO)$_3$(η$^5$-C$_5$H$_5$)]: NMR: $^1$H (C$_6$D$_6$, 700 MHz, 25 °C) $\delta_H$ 4.41 (s, 5H, η$^5$-C$_5$*H*$_5$), 0.47 (s, $^3J_{WH}$ = 1.9 Hz, 3H, W-C*H*$_3$) ppm; $^{13}$C{$^1$H} (C$_6$D$_6$, 176 MHz, 25 °C) $\delta_C$ 229.9 ($^1J_{WC}$ = 66 Hz, *transoid CO*), 216.8 ($^1J_{WC}$ = 80 Hz, *cisoid CO*), 91.0 (η$^5$-*C*$_5$H$_5$), -34.6 ($^1J_{WC}$ = 14 Hz, W-*C*H$_3$). IR (CH$_2$Cl$_2$, 25 °C) $\nu_{CO}$ 2015(vs), 1918(vs) cm$^{-1}$.

### 6.6.3 [PPN][Mo(CO)$_3${η$^5$-C$_5$H$_4$(AsC$_4$Ph$_4$)}]




A THF solution of [Mo(CO)$_3${η$^5$-C$_5$H$_4$(AsC$_4$Ph$_4$)}]$^-$ was prepared as described above from 0.075 g (0.11 mmol) and 0.07 mL LDA solution (0.14 mmol). To this was added 0.065 g [PPN]Cl (0.11 mmol) and the mixture stirred for 60 minutes. Volatiles are removed *in vacuo* and the orange-red residue washed with Et$_2$O (3 x 5 mL, with trituration) and

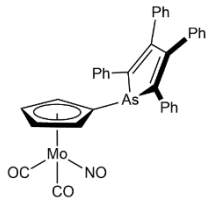
dried under vacuum. The material was used without further purification for NMR analysis; principal signals of diagnostic value are listed below with aromatic $^{1}H$ and $^{13}C$ resonances omitted.

[PPN][Mo(CO)$_3$($\eta^5$-$C_5H_5$)]: NMR: $^{1}H$ ($CD_2Cl_2$, 700 MHz, 25 °C) $\delta_H$ 5.10 (s, 5H, $\eta^5$-$C_5H_5$). $^{13}C\{^{1}H\}$ ($CD_2Cl_2$, 176 MHz, 25 °C) $\delta_C$ 235.9 (*C*O), 86.7 ($\eta^5$-*C*$_5H_5$) ppm. Relative proportion by NMR: 0.25.

[PPN][Mo(CO)$_3${$\eta^5$-$C_5H_4$(As$C_4Ph_4$)}]: NMR: $^{1}H$ ($CD_2Cl_2$, 700 MHz, 25 °C) $\delta_H$ 4.99 (t, $^{3}J_{HH} \approx {}^{4}J_{HH}$ = 2.2 Hz, 2H, {2,5}-$\eta^5$-$C_5H_4$), 4.98 (t, $^{3}J_{HH} \approx {}^{4}J_{HH}$ = 2.2 Hz, 2H, {3,4}-$\eta^5$-$C_5H_4$). $^{13}C\{^{1}H\}$ ($CD_2Cl_2$, 176 MHz, 25 °C) $\delta_C$ 235.0 (*C*O), 153.0 (arsole {2,5}-*C*), 149.0 (arsole {3,4}-*C*), 91.5 ({1}-$\eta^5$-*C*$_5H_4$), 87.8 ({2,5}-$\eta^5$-*C*$_5H_4$), 93.6 ({3,4}-$\eta^5$-*C*$_5H_4$) ppm. Relative proportion by NMR: 1.00.

[PPN][Mo(CO)$_3${1,3-$\eta^5$-$C_5H_3$(As$C_4Ph_4$)$_2$}] (*tentative assignment*): NMR: $^{1}H$ ($CD_2Cl_2$, 700 MHz, 25 °C) $\delta_H$ 5.09 (t, $^{4}J_{HH}$ = 1.7 Hz, 1H, {2}-$\eta^5$-$C_5H_3$), 4.82 (t, $^{4}J_{HH}$ = 1.7 Hz, 2H, {4,5}-$\eta^5$-$C_5H_3$). $^{13}C\{^{1}H\}$ ($CD_2Cl_2$, 176 MHz, 25 °C) $\delta_C$ 234.0 (*C*O), 155.0 (arsole *C*), 151.3 (arsole *C*), 150.3 (arsole *C*), 147.9 (arsole *C*), 95.2 ({1,3}-$\eta^5$-*C*$_5H_4$), 94.2 ({2}-$\eta^5$-*C*$_5H_4$), 92.8 ({4,5}-$\eta^5$-*C*$_5H_4$) ppm. Relative proportion by NMR: 0.20.

### 6.6.4 [Mo(NO)(CO)$_2${$\eta^5$-$C_5H_4$(As$C_4Ph_4$)}]



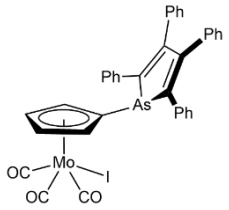

A THF solution of [Mo(CO)$_3${$\eta^5$-$C_5H_4$(As$C_4Ph_4$)}]$^-$ was prepared as described above from 0.135 g (0.2 mmol) and 0.11 mL LDA solution. To this was added 0.05 g solid Diazald (*N*-methyl-*N*-nitroso-*p*-toluenesulfonamide; 0.23 mmol) with rapid stirring, resulting in gas evolution and a colour change to a vibrant orange-red. After 60 minutes, the mixture was dried by rotary evaporation and the residue subjected to column chromatography on silica gel (25 x 2.5 cm) eluting with petroleum ether, followed by 9:1 petroleum ether/$Et_2O$ gives an orange band containing [Mo(NO)(CO)$_2$($\eta^5$-$C_5H_5$)]. Eluting with 4:1 petroleum ether/$Et_2O$ gives a larger orange band containing the product which is collected and dried by rotary evaporation. The product is encountered as an air stable orange solid which is readily soluble in common organic solvents. Average isolated yield across two preparations of the same scale: 0.07 g (0.1 mmol, 53%).

NMR: $^{1}H$ ($CDCl_3$, 700 MHz, 25 °C) $\delta_H$ 7.17—7.12 (m, 10H, $C_6H_5$), 7.06—7.04 (m, 6H, $C_6H_5$), 6.97—6.94 (m, 4H, $C_6H_5$), 5.46 (t, $^{3}J_{HH} \approx {}^{4}J_{HH}$ = 2.1 Hz, 2H, {2,5}-$\eta^5$-$C_5H_4$), 5.44 (t, $^{3}J_{HH} \approx {}^{4}J_{HH}$ = 2.1 Hz, 2H, {3,4}-$\eta^5$-$C_5H_4$) ppm. $^{13}C\{^{1}H\}$ ($CDCl_3$, 176 MHz, 25 °C) $\delta_C$ 226.3 (*C*O), 150.6 (arsole {2,5}-*C*), 150.4 (arsole {3,4}-*C*), 138.3 ($C_6H_5$), 137.7 ($C_6H_5$), 130.3 ($C_6H_5$), 129.6 ($C_6H_5$), 128.3 ($C_6H_5$), 127.7 ($C_6H_5$), 126.9 ($C_6H_5$), 126.8 ($C_6H_5$), 103.6 ({1}-$\eta^5$-$C_5H_4$), 98.5 ({2,5}-$\eta^5$-$C_5H_4$), 94.1 ({3,4}-$\eta^5$-$C_5H_4$) ppm. IR ($CH_2Cl_2$, 25 °C) $\nu_{CO}$ 2017(vs), 1940(vs) cm$^{-1}$, $\nu_{NO}$ 1667 cm$^{-1}$. HR-MS (ESI and EI modes, MeCN, +ve ion) found many ion fragments with the correct isotopic envelope for the presence of molybdenum however no chemically-sensible formulae could be devised – neither the molecular ion nor products of decarbonylation were found. Analysis found 62.00% C, 3.75% H, 2.31% N (calc. for $C_{35}H_{24}N_1O_3As_1Mo_1$: 62.05% C, 3.57% H, 2.07% N.

[Mo(NO)(CO)$_2$($\eta^5$-$C_5H_5$)]: NMR: $^{1}H$ ($CDCl_3$, 700 MHz, 25 °C) $\delta_H$ 5.60 (s, 5H, $\eta^5$-$C_5H_5$) ppm. $^{13}C\{^{1}H\}$ ($CDCl_3$, 176 MHz, 25 °C) $\delta_C$ 227.0 (*C*O), 93.6 ($\eta^5$-*C*$_5H_5$) ppm. IR ($CH_2Cl_2$, 25 °C) $\nu_{CO}$ 2018(vs), 1940(vs) cm$^{-1}$, $\nu_{NO}$ 1666(vs) cm$^{-1}$.

Single crystals were obtained by slow evaporation of a petroleum ether/$Et_2O$ solution. The nitrosyl group was disordered amongst the two carbonyl ligands in a ⅓:⅓:⅓ ratio which was modelled accordingly. $C_{35}H_{24}O_3As_1Mo_1N_1$ ($M$ = 677.41 g/mol): orange prism 0.127 × 0.146 × 0.193 mm, triclinic, space group $P$-1 (no. 2), $a$ = 8.7921(3) Å, $b$ = 10.5339(4) Å, $c$ = 15.3512(5) Å, α = 99.595(3)°, $\beta$ = 90.471(3)°, $\gamma$ = 98.032(3)°, $V$ = 1387.39(9) Å$^3$, $Z$ = 2, multi-scan correction $T_{min}/T_{max}$ = 0.984/1.000, $\mu$(Mo-Kα) = 1.694 mm$^{-1}$, $\varrho_{calc}$ = 1.622 g/cm$^3$, 12992 reflections measured (7.022° ≤ 2Θ ≤ 60.206°), 6578 unique ($R_{int}$ = 0.0254, $R_{sigma}$ = 0.0453) which were used in all calculations, $GOF$ = 1.011, $D_{min}/D_{max}$ = -0.69/0.66 e/Å$^3$. The final $R_1$ was 0.0352 (I > 2σ(I)) and $wR_2$ was 0.0748 (all data).

### 6.6.5 [MoI(CO)$_3${η$^5$-C$_5$H$_4$(AsC$_4$Ph$_4$)}]




A THF solution of [(η$^5$-C$_5$H$_4${AsC$_4$Ph$_4$})Mo(CO)$_3$]$^-$ was prepared as previously described from 0.135 g (0.2 mmol) and 0.11 mL LDA solution. To this was added either 0.05 g solid *N*-iodosuccinimide (0.25 mmol) or 0.06 g solid 1,2-diiodoethane (0.25 mmol) with rapid stirring, resulting in a colour change to a dark red-brown. After 60 minutes, the mixture was dried by rotary evaporation and the residue subjected to column chromatography on silica gel (25 x 2.5 cm) eluting first with petroleum ether, followed by 9:1 petroleum ether/$Et_2O$ giving a red band containing [CpMoI(CO)$_3$]. Eluting with 4:1 petroleum ether/$Et_2O$ gives a second red band containing the product which is collected and dried. The product is encountered as a red-brown solid which is readily soluble in polar organic and aromatic solvents, somewhat soluble in $Et_2O$ and less-so in aliphatic hydrocarbons. The product is sufficiently air stable to permit workup without the need for inert atmosphere, however solutions exposed to air turn green and deposit insoluble materials over the course of several days with tarnishing of the glass container. It appears to slowly react with $CDCl_3$. Isolated yield across two preparations of the same scale: 0.062 g (0.07 mmol, 36%)

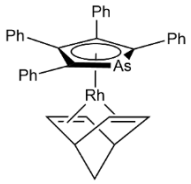
NMR: $^1$H ($C_6D_6$, 700 MHz, 25 °C) $\delta_H$ 7.34—7.33 (m, 4H, $C_6H_5$), 7.03—6.98 (m, 6H, $C_6H_5$), 6.91—6.81 (m, 10H, $C_6H_5$), 4.96 (t, $^3J_{HH} \approx {}^4J_{HH}$ = 2.1 Hz, 2H, {2,5}-η$^5$-$C_5H_4$), 4.51 (t, $^3J_{HH} \approx {}^4J_{HH}$ = 2.1 Hz, 2H, {3,4}-η$^5$-$C_5H_4$) ppm. $^{13}$C{$^1$H} ($C_6D_6$, 176 MHz, 25 °C) $\delta_C$ 236.9 (*transoid* *C*O), 220.5 (*cisoid* *C*O), 151.3 (arsole {2,5}-*C*), 150.5 (arsole {3,4}-*C*), 138.4 ($C_6H_5$), 137.8 ($C_6H_5$), 130.4 ($C_6H_5$), 130.0 ($C_6H_5$), 128.8 ($C_6H_5$), 127.6 ($C_6H_5$), 127.2 ($C_6H_5$), 106.2 ({1}-η$^5$-$C_5H_4$), 97.6 ({2,5}-η$^5$-$C_5H_4$), 95.1 ({3,4}-η$^5$-$C_5H_4$) ppm. IR ($CH_2Cl_2$, 25 °C) $\nu_{CO}$ 2041(vs), 1965(vs) cm$^{-1}$. HR-MS (ESI, MeCN, +ve ion) found $m/z$ 677.0008 (calc. for $C_{36}H_{24}O_3{}^{75}As_1{}^{98}Mo_1$ [$M$ – I]$^+$: 677.0004). Analysis found 53.67% C, 3.33% H (calc. for $C_{36}H_{24}O_3As_1I_1Mo_1$: 53.89% C, 3.02% H.

[CpMoI(CO)$_3$]: NMR: $^1$H ($C_6D_6$, 700 MHz, 25 °C) $\delta_H$ 4.48 (s, 5H, η$^5$-$C_5H_5$) ppm; $^{13}$C{$^1$H} ($C_6D_6$, 176 MHz, 25 °C) $\delta_C$ 237.3 (*transoid* *C*O), 221.2 (*cisoid* *C*O), 93.9 (η$^5$-$C_5H_5$) ppm; IR ($CH_2Cl_2$, 25 °C) $\nu_{CO}$ 2043(vs), 1966(vs) cm$^{-1}$.

Single crystals were obtained by slow evaporation of $Et_2O$ solution at -30 °C. $C_{36}H_{24}O_3As_1I_1Mo_1$ ($M$ = 802.31 g/mol): red needle 0.042 × 0.088 × 0.181 mm, triclinic, space group $P$-1 (no. 2), $a$ = 7.9945(5) Å, $b$ = 11.4680(6) Å, $c$ = 17.5970(10) Å, α = 100.183(5)°, $\beta$ = 100.875(5)°, $\gamma$ = 103.948(5)°, $V$ = 1495.22(16) Å$^3$, $Z$ = 2, multi-scan correction $T_{min}/T_{max}$ = 0.974/1.000, $\mu$(Mo-Kα) = 2.605 mm$^{-1}$, $\varrho_{calc}$ = 1.782 g/cm$^3$, 13754 reflections measured (6.798° ≤ 2Θ ≤

60.206°), 7096 unique ($R_{int}$ = 0.0471, $R_{sigma}$ = 0.0989) which were used in all calculations, *GOF* = 1.062, $D_{min}/D_{max}$ = -1.11/0.52 e/Å$^3$. The final $R_1$ was 0.0605 (I > 2σ(I)) and $wR_2$ was 0.1075 (all data).

### 6.6.6 [Rh(NBD)(η$^5$-AsC$_4$Ph$_4$)]

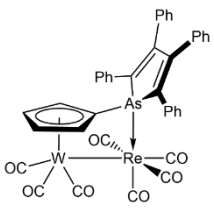



A THF solution of [Mo(CO)$_3${η$^5$-C$_5$H$_4$(AsC$_4$Ph$_4$)}]$^-$ was prepared as previously described from 0.135 g (0.2 mmol) and 0.11 mL LDA solution. To this was added 0.045 g [Rh$_2$(μ-Cl)$_2$(NBD)$_2$] (0.1 mmol) with rapid stirring, resulting in a colour change to yellow-brown. After stirring overnight, the mixture was dried by rotary evaporation and the residue subjected to column chromatography on silica gel (25 x 2.5 cm) eluting first with petroleum ether, followed by 1:1 petroleum ether/Et$_2$O giving a bright yellow band containing the product which is dried by rotary evaporation. No other mobile bands were obtained upon eluting with more-polar eluent mixtures. The product is encountered as a bright yellow crystalline solid which is air stable and is readily soluble in polar organic and aromatic solvents, moderately soluble in Et$_2$O and poorly soluble in aliphatic hydrocarbons. Average isolated yield across two preparations of the same scale: 0.065 g (0.07 mmol, 33%).

NMR: $^1$H (C$_6$D$_6$, 700 MHz, 25 °C) δ$_H$ 7.37 (m, 4H, C$_6$*H*$_5$), 6.92—6.87 (m, 16H, C$_6$*H*$_5$), 3.28 (m, 2H, bridgehead C*H*), 3.24 (m, 4H, olefin C*H*), 0.94 (t, $^3J_{HH}$ = 1.4 Hz, 2H, bridge C*H*$_2$) ppm. $^{13}$C{$^1$H} (C$_6$D$_6$, 176 MHz, 25 °C) δ$_C$ 139.4 (arsole {2,5}-*C*), 137.0 (arsole {3,4}-*C*), 133.2 (*C*$_6$H$_5$), 129.4 (*C*$_6$H$_5$), 127.6 (*C*$_6$H$_5$), 126.8 (*C*$_6$H$_5$), 126.4 (*C*$_6$H$_5$), 124.9 (*C*$_6$H$_5$), 124.8 (*C*$_6$H$_5$), 119.7 (*C*$_6$H$_5$), 119.7 (*C*$_6$H$_5$), 57.8 (d, $^2J_{RhC}$ = 6.7 Hz, bridgehead *C*), 46.9 (bridge *C*), 40.4 ($^1J_{RhC}$ = 9.1 Hz, olefin *C*) ppm. One equivalent of *n*-hexane was also observed in these spectra. HR-MS (ESI, MeCN, +ve ion) found *m*/*z* 626.0455 (calc. for C$_{35}$H$_{28}^{75}$As$_1^{103}$Rh$_1$ [*M*]$^+$: 626.0462. Analysis found 69.36% C, 5.35% H (calc. for C$_{35}$H$_{28}$As$_1$Rh$_1$·C$_6$H$_{14}$: 69.10% C, 5.94% H).

Single crystals were obtained by slow evaporation of a 1:1 petroleum ether/Et$_2$O chromatography eluate. One-half an n-hexane molecule was found in the asymmetric unit. C$_{35}$H$_{28}$As$_1$Rh$_1$·0.5C$_6$H$_{14}$ (*M* = 669.49 g/mol): yellow prism 0.103 × 0.251 × 0.298 mm, triclinic, space group *P*-1 (no. 2), *a* = 10.0502(4) Å, *b* = 12.9550(5) Å, *c* = 12.9608(4) Å, α = 111.429(3)°, *β* = 99.834(3)°, *γ* = 104.357(3)°, *V* = 1456.46(10) Å$^3$, *Z* = 2, multi-scan correction $T_{min}/T_{max}$ = 0.914/1.000, *μ*(Mo-Kα) = 1.740 mm$^{-1}$, ϱ$_{calc}$ = 1.527 g/cm$^3$, 16960 reflections measured (6.51° ≤ 2Θ ≤ 65.078°), 9071 unique ($R_{int}$ = 0.0281, $R_{sigma}$ = 0.0516) which were used in all calculations, *GOF* = 1.027, $D_{min}/D_{max}$ = -0.77/0.59 e/Å$^3$. The final $R_1$ was 0.0351 (I > 2σ(I)) and $wR_2$ was 0.0741 (all data).

### 6.6.7 [WRe(CO)$_7${μ-η$^1$:η$^5$-C$_5$H$_4$(AsC$_4$Ph$_4$)}]




A THF solution of [(η$^5$-C$_5$H$_4${AsC$_4$Ph$_4$})W(CO)$_3$]$^-$ was prepared as previously described from 0.15 g (0.2 mmol) and 0.11 mL LDA solution (0.22 mmol). Quenching with 0.065 g solid [Re(μ-Cl)(CO)$_4$]$_2$ (0.1 mmol) gives a yellow-brown

mixture after stirring overnight. Volatiles are moved by rotary evaporation and the residue subjected to column chromatography on silica gel (30 x 2.5 cm) with 9:1 petroleum ether/$Et_2O$ providing a pale yellow band of [$ReCl(CO)_5$]. Eluting with 4:1 petroleum ether/$CH_2Cl_2$ provides a yellow-orange band containing the product which is collected and dried by rotary evaporation. The product is air stable and readily soluble in polar organic and aromatic solvents, somewhat soluble in $Et_2O$ and less-so in aliphatic hydrocarbons. Isolated yield: *ca* 0.02 g (*ca* 9%). A great deal of chromatographically immobile brown residues were produced which probably accounts for the majority of molecular mass in the reaction. Low isolated yields precluded complete spectroscopic characterisation.

NMR: $^1H$ ($C_6D_6$, 700 MHz, 25 °C) $\delta_H$ 7.21—7.18 (m, 6H, $C_6H_5$), 7.07—7.01 (m, 10H, $C_6H_5$), 6.87—6.85 (m, 4H, $C_6H_5$), 5.33 (t, $^3J_{HH} \approx {}^4J_{HH}$ = 2.2 Hz, 2H, {2,5}-$\eta^5$-$C_5H_4$), 4.51 (t, $^3J_{HH} \approx {}^4J_{HH}$ = 2.2 Hz, 2H, {3,4}-$\eta^5$-$C_5H_4$) ppm. IR ($CH_2Cl_2$, 25 °C) $\nu_{CO}$ 2112(w), 2082(s), 2018(s), 1991(s), 1958(vs), 1886(w), 1857(w) $cm^{-1}$. HR-MS (ESI, MeCN, +ve ion) found $m/z$ 977.9950 (calc. for $C_{37}H_{24}O_4{}^{75}As_1{}^{184}W_1{}^{187}Re_1$ [$M$ – 3CO]$^+$: 977.9958).

Single crystals were obtained by layering a $CH_2Cl_2$ solution with *n*-hexane at -20 °C. Two molecules of dichloromethane were found in the asymmetric unit. $C_{40}H_{24}O_7As_1Re_1W_12{\cdot}CH_2Cl_2$ ($M$ = 1231.41 g/mol): yellow needle 0.048 × 0.066 × 0.117 mm, triclinic, space group $P$-1 (no. 2), $a$ = 11.9328(2) Å, $b$ = 12.9005(3) Å, $c$ = 14.4745(3) Å, $\alpha$ = 69.645(2)°, $\beta$ = 85.770(2)°, $\gamma$ = 77.480(2)°, $V$ = 2039.37(8) Å$^3$, $Z$ = 2, Gaussian correction $T_{min}/T_{max}$ = 0.336/0.667, $\mu$(Cu-K$\alpha$) = 14.580 $mm^{-1}$, $\varrho_{calc}$ = 2.005 g/$cm^3$, 22590 reflections measured (7.466° ≤ 2$\Theta$ ≤ 146.084°), 8108 unique ($R_{int}$ = 0.0304, $R_{sigma}$ = 0.0381) which were used in all calculations, $GOF$ = 1.049, $D_{min}/D_{max}$ = -1.01/1.34 e/Å$^3$. The final $R_1$ was 0.0298 (I > 2$\sigma$(I)) and $wR_2$ was 0.0755 (all data).

## 6.7 References


1. W. K. Dean and W. A. G. Graham, *Inorg. Chem.*, **1977**, *16*, 1061-1067.
2. C. Lo Sterzo, *J. Chem. Soc. Dalton Trans.*, **1992**, 1989-1990.
3. H. Werner and W. Hofmann, *Angew. Chem. Int. Ed. Eng.*, **1978**, *17*, 464-465.
4. M. Baya, P. Crochet, M. A. Esteruelas and E. Oñate, *Organometallics*, **2001**, *20*, 240-253.
5. P. C. Heah and J. A. Gladysz, *J. Am. Chem. Soc.*, **1984**, *106*, 7636-7637.
6. L. K. Liu, K. Y. Chang and Y. S. Wen, *J. Chem. Soc. Dalton Trans.*, **1998**, 741-744.
7. S. Sharma, J. Cervantes, J. L. Mata-Mata, M. C. Brun, F. Cervantes-Lee and K. H. Pannell, *Organometallics*, **1995**, *14*, 4269-4274.
8. J. Cervantes, S. P. Vincenti, R. N. Kapoor and K. H. Pannell, *Organometallics*, **1989**, *8*, 744-748.
9. S. R. Berryhill and B. Sharenow, *J. Organomet. Chem.*, **1981**, *221*, 143-146.
10. C. K. Lai, W. G. Feighery, Y. Zhen and J. D. Atwood, *Inorg. Chem.*, **1989**, *28*, 3929-3930.
11. J. M. Burlitch, *J. Am. Chem. Soc.*, **1969**, *91*, 4563-4564.
12. S. R. Berryhill, G. L. Clevenger and F. Y. Burdurlu, *Organometallics*, **1985**, *4*, 1509-1515.
13. S. R. Berryhill and R. J. P. Corriu, *J. Organomet Chem.*, **1989**, *370*, C1-C4.
14. G. Thum, W. Ries, D. Greissinger and W. Malisch, *J. Organomet. Chem.*, **1983**, *252*, C67-C72.
15. K. H. Pannell, J. Cervantes, C. Hernandez, J. Cassias and S. Vincenti, *Organometallics*, **1986**, *5*, 1056-1057.
16. K. H. Pannell, S. P. Vincenti and R. C. Scott, *Organometallics*, **1987**, *6*, 1593-1594.
17. S. Sharma, N. Caballero, H. Li and K. H. Pannell, *Organometallics*, **1999**, *18*, 2855-2860.
18. H. K. Sharma and K. H. Pannell, *Chem. Comm.*, **2004**, 2556-2557.
19. H. K. Sharma, F. Cervantes-Lee and K. H. Pannell, *J. Am. Chem. Soc.*, **2004**, *126*, 1326-1327.
20. K. Pannell, J. Castillo-Ramirez and F. Cervantes-Lee, *Organometallics*, **1992**, *11*, 3139-3143.
21. P. Pasman and J. J. M. Snel, *J. Organomet. Chem.*, **1986**, *301*, 329-335.
22. G. L. Crocco, C. S. Young, K. E. Lee and J. A. Gladysz, *Organometallics*, **1988**, *7*, 2158-2162.
23. M. Baya, M. A. Esteruelas and E. Oñate, *Organometallics*, **2001**, *20*, 4875-4886.
24. M. C. Milletti and R. F. Fenske, *Organometallics*, **1989**, *8*, 420-430.

25. P. C. Heah, A. T. Patton and J. A. Gladysz, *J. Am. Chem. Soc.,* **1986**, *108*, 1185-1195.
26. G. L. Crocco and J. A. Gladysz, *J. Chem. Soc. Chem. Comm.,* **1985**, 283-284.
27. G. L. Crocco and J. A. Gladysz, *J. Am. Chem. Soc.,* **1988**, *110*, 6110-6118.
28. H. Nakazawa, M. Sone and K. Miyoshi, *Organometallics*, **1989**, *8*, 1564-1566.
29. K. Kubo, H. Nakazawa, K. Kawamura, T. Mizuta and K. Miyoshi, *J. Am. Chem. Soc.,* **1998**, *120*, 6715-6721.
30. H. Nakazawa, K. Kawamura, K. Kubo and K. Miyoshi, *Organometallics*, **1999**, *18*, 4518-4523.
31. C. P. Casey, R. M. Bullock, W. C. Fultz and A. L. Rheingold, *Organometallics*, **1982**, *1*, 1591-1596.
32. J. K. Ruff, *Inorg. Chem.*, **1968**, *7*, 1818-1821.
33. W. Siegl and J. Collman, *J. Am. Chem. Soc.,* **1972**, *94*, 2516-2518.
34. M. Darensbourg, H. Barros and C. Borman, *J. Am. Chem. Soc.,* **1977**, *99*, 1647-1648.
35. K. Inkrott, R. Goetze and S. G. Shore, *J. Organomet. Chem.,* **1978**, *154*, 337-342.
36. D. V. Konarev, A. V. Kuzmin, S. I. Troyanov, Y. Nakano, S. S. Khasanov, A. Otsuka, H. Yamochi, G. Saito and R. N. Lyubovskaya, *Dalton Trans.*, **2015**, *44*, 9672-9681.
37. P. J. Fischer, K. M. Krohn, E. T. Mwenda and V. G. Young, *Organometallics*, **2005**, *24*, 1776-1779.
38. M. Tilset, A. A. Zlota, K. Folting and K. G. Caulton, *J. Am. Chem. Soc.,* **1993**, *115*, 4113-4119.
39. C. Evans, B. K. Nicholson and A. G. Oliver, *Acta Cryst. E*, **2001**, *57*, 504-505.
40. C. H. Winter, X. X. Zhou, D. A. Dobbs and M. J. Heeg, *Organometallics*, **1991**, *10*, 210-214.
41. A. Appel, H. Nöth and M. Schmidt, *Chem. Ber.,* **1995**, *128*, 621-626.
42. C. E. Petrisor, G. Chahboun, M. A. El Amrani, E. Royo and T. Cuenca, *Eur. J. Inorg. Chem.*, **2010**, 3666-3674.
43. M. Sudupe, J. Cano P. Royo and E. Herdtweck, *Eur. J. Inorg. Chem.*, **2004**, 3074-3083.
44. T. Gröer and M. Scheer, *Organometallics*, **2000**, *19*, 3683-3691.
45. J. L. Atwood, R. Shakir, J. T. Malito, M. Herberhold, W. Kremnitz, W. P. E. Bernhagen and H. G. Alt, *J. Organomet. Chem.* **1979**, *165*, 65-78.
46. R. J. Abernethy, M. R. S. J. Foreman, A. F. Hill, N. Tshabang, A. C. Willis and R. D. Young, *Organometallics*, **2008**, *27*, 4455-4463.
47. F. Hering, J. H. J. Berthel, K. Lubitz, U. S. D. Paul, H. Schneider, M. Härterich and U. Radius, *Organometallics*, **2016**, *35*, 2806-2821.
48. J. T. Malito, R. Shakir and J. L. Atwood, *J. Chem. Soc. Dalton Trans.* **1980**, 1253-1258.
49. L. Spadoni, C. Lo Sterzo, R. Crescenzi and G. Frachey, *Organometallics*, **1995**, *14*, 3149-3151.
50. J. J. Robertson, A. Kadziola, R. A. Krause and S. Larsen, *Inorg. Chem.*, **1989**, *28*, 2097-2102.
51. E. W. Abel, N. Clark and C. Towers, *J. Chem. Soc. Dalton Trans.,* **1979**, 1552-1556.
52. W. L. Ingham, S. D. Travlos, J. C. A. Boeyens, M. Berry and N. J. Coville, *Acta Cryst. C*, **1992**, *48*, 465-468.
53. J. C. Jeffery, D. B. Lewis, G. E. Lewis and F. G. A. Stone, *J. Chem. Soc. Dalton Trans.,* **1985**, 2001-2007.
54. W. C. Mercer, R. R. Whittle, E. W. Burkhardt and G. L. Geoffroy, *Organometallics*, **1985**, *4*, 68-74.
55. W. C. Mercer and G. L. Geoffroy, *Organometallics*, **1985**, *4*, 1418-1425.
56. C. W. Pin, J. J. Peng, C. W. Shiu, Y. Chi, S. M. Peng and G. H. Lee, *Organometallics*, **1998**, *17*, 438-445.
57. Y. Tang, J. Sun and J. Chen, *J. Chem. Soc. Dalton Trans.,* **1998**, 4003-4008.
58. R. D. Simpson and R. G. Bergman, *Organometallics*, **1993**, *12*, 781-796.
59. C. Commons and B. Hoskins, *Aust. J. Chem.*, **1975**, *28*, 1201-1209.
60. C. P. Casey, R. M. Bullock and F. Nief, *J. Am. Chem. Soc.,* **1983**, *105*, 7574-7580.
61. C. P. Casey and R. M. Bullock, *J. Organomet. Chem.*, **1983**, *251*, 245-248.
62. M. J. Doyle, T. J. Duckworth, L. Manojlović-Muir, M. J. Mays, P. R. Raithby and F. J. Robertson, *J. Chem. Soc. Dalton Trans.*, **1992**, 2703-2714.
63. N. E. Schore, *J. Am. Chem. Soc.*, **1979**, *101*, 7410-7412.
64. N. E. Schore, L. S. Benner and B. E. LaBelle, *Inorg. Chem.*, **1981**, *20*, 3200-3208.
65. C. Cornelißen, G. Erker, G. Kehr and R. Fröhlich, *Dalton Trans.,* **2004**, 4059-4063.
66. B. E. Bosch, I. Brümmer, K. Kunz, G. Erker, R. Fröhlich and S. Kotila, *Organometallics*, **2000**, *19*, 1255-1261.

67. C. P. CASEY and F. NIEF,*Organometallics*, **1985**, *4*, 1218-1220.
68. T. J. DUCKWORTH, M. J. MAYS, G. CONOLE and M. MCPARTLIN, *J. Organomet. Chem.*, **1992**, *439*, 327-339.
69. D. SIERRA, A. H. KLAHN, R. RAMIREZ-TAGLE, R. ARRATIA-PEREZ, F. GODOY, M. TERESA GARLAND and M. FUENTEALBA, *Dalton Trans.*, **2010**, 6295-6301.
70. J. BAUER, H. BRAUNSCHWEIG and R. D. DEWHURST, *Chem. Rev.*, **2012**, *112*, 4329-4346.
71. D. SEYFERTH, B. W. HAMES, T. G. RUCKER, M. COWIE and R. S. DICKSON, *Organometallics*, **1983**, *2*, 472-474.
72. F. MATHEY and J. P. LAMPIN, *Tetrahedron*, **1975**, *31*, 2685-2690.
73. M. D. RAUSCH, B. H. EDWARDS, R. D. ROGERS and J. L. ATWOOD, *J. Am. Chem. Soc.*, **1983**, *105*, 3882-3886.

# Chapter 7

# Coordination Complexes of 1,1'-Bis(Arsolyl)Ferrocenes

## 7.1 Preamble

Ferrocene-derived chelating phosphine ligands have enjoyed a central role in coordination chemistry since the introduction of the archetypical 1,1'-bis(diphenylphosphino)ferrocene (dppf, $[Fe(C_5H_4PPh_2)_2]$) by DAVISON *et al.* in 1971.[1] The ligand has since proven to be a valuable appliance in homogeneous catalytic reactions by virtue of the *cis*-enforcing bidentate mode of the molecule, and the appreciable degree of conformational flexibility arising from the mobility of the cyclopentadienyl rings (notwithstanding the good donor faculty of phosphinocentric LEWIS bases in general). The primary modes of internal motion are coarse torsional rotation about the iron-centroid axes (**A**) and subtle tilting toward or away from the iron centre (**B**) – both without compromise of Fe(*d*)-$C_5H_5(\pi)$ bonding orbital overlap – and swivelling of the donor pendants about the mean cyclopentadienyl planes (**C**).

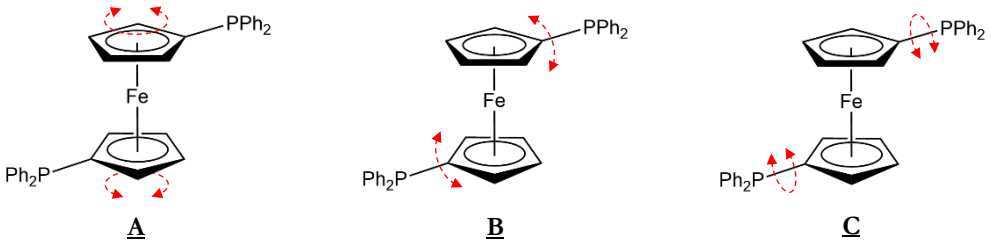
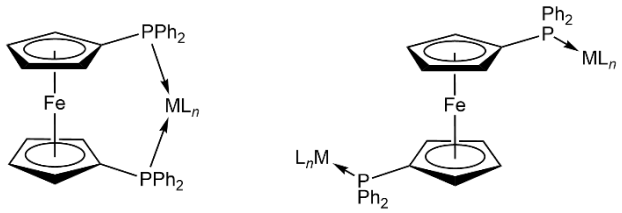



**Figure 7.1**: Geometric flexibility inherent to the 1,1'- bis(diphenylphosphino)ferrocene (dppf) molecule.

This flexibility, compared to other bidentate ligands, permits stabilisation of a range of metal centres. For the specific context of catalytic cycles where changes in oxidation state occur with dramatic variation in both atomic radius and coordination demand (*e.g.*, Ni(0)↔Ni(II) or Pd(0)↔Pd(II)), the ability of dppf (and analogues) to relieve geometric strain *via* expansion or contraction of the ligand bite angle with minimal energetic penalty is visibly advantageous. For the same reason, dppf (and analogues) are versatile ligands which can accommodate a spectrum of open (*i.e.*, trigonal planar, tetrahedral) and compressed (square planar, trigonal bipyramidal, octahedral) coordination complexes in the usual bidentate fashion, alongside other spatial orientations. The two most-common modes are the classical $\kappa^2$-chelate (**A**) and the $\mu$-$\kappa^1$:$\kappa^1$-open-bridge (**B**), shown in **Chart 7.1**.




**A** **B**

**Chart 7.1**: Two common bidentate (**left**) and monodentate (**right**) coordination modes for the dppf ligand.

Analogues of dppf are diverse; alongside this were described by DAVISON and co-workers the bis(dimethylphosphino)- (dmpf, [Fe($C_5H_4PMe_2$)$_2$]), bis(diphenylarsino)- ([Fe($C_5H_4AsPh_2$)$_2$], dpaf) and bis(dimethylarsino)- ([Fe($C_5H_4AsMe_2$)$_2$], dmaf) ferrocenes.[1] More-bespoke (or in some cases, Byzantine) chemical furniture has since been incorporated onto the ferrocene backbone – the topic has very recently been reviewed with a view toward sterically-demanding phosphino substituents.[2] Ferrocenes displaying phosphinocyclic pendants *e.g.*, phospholes,[3-5] phospholanes[6-8] or phosphetanes[9] abound in the chemical literature, and a representative (though by no means exhaustive) selection is shown in **Chart 7.2** overleaf.

A cursory interrogation of the CSD finds (up to early 2023) >130 analogues of dppf which have been structurally characterised and an impressive >1000 coordination complexes (all coordination modes) of the dppf ligand *alone*. When compared against the diminutive number of structurally characterised dpaf-like ligands and dpaf-like coordination complexes,[10, 11] the preferred popularity of bis(phosphino)ferrocene ligands becomes patently clear.* Notwithstanding the utility of the overall molecular assembly (*vide supra*), the imposing variety of bidentate ferrocenyl-derived ligands is in large part attributed to the ease of which functionalisation strategies can be applied. By far the most direct method involves the addition of a suitable electrophile to the TMEDA-stabilised complex of 1,1'-dilithioferrocene, precisely the strategy used in the work to follow.

* Naturally, the true number of reported compounds is far greater than this, since many will not have been subjected to X-ray diffraction studies. Nevertheless, these numbers are generally illustrative of the point being made.

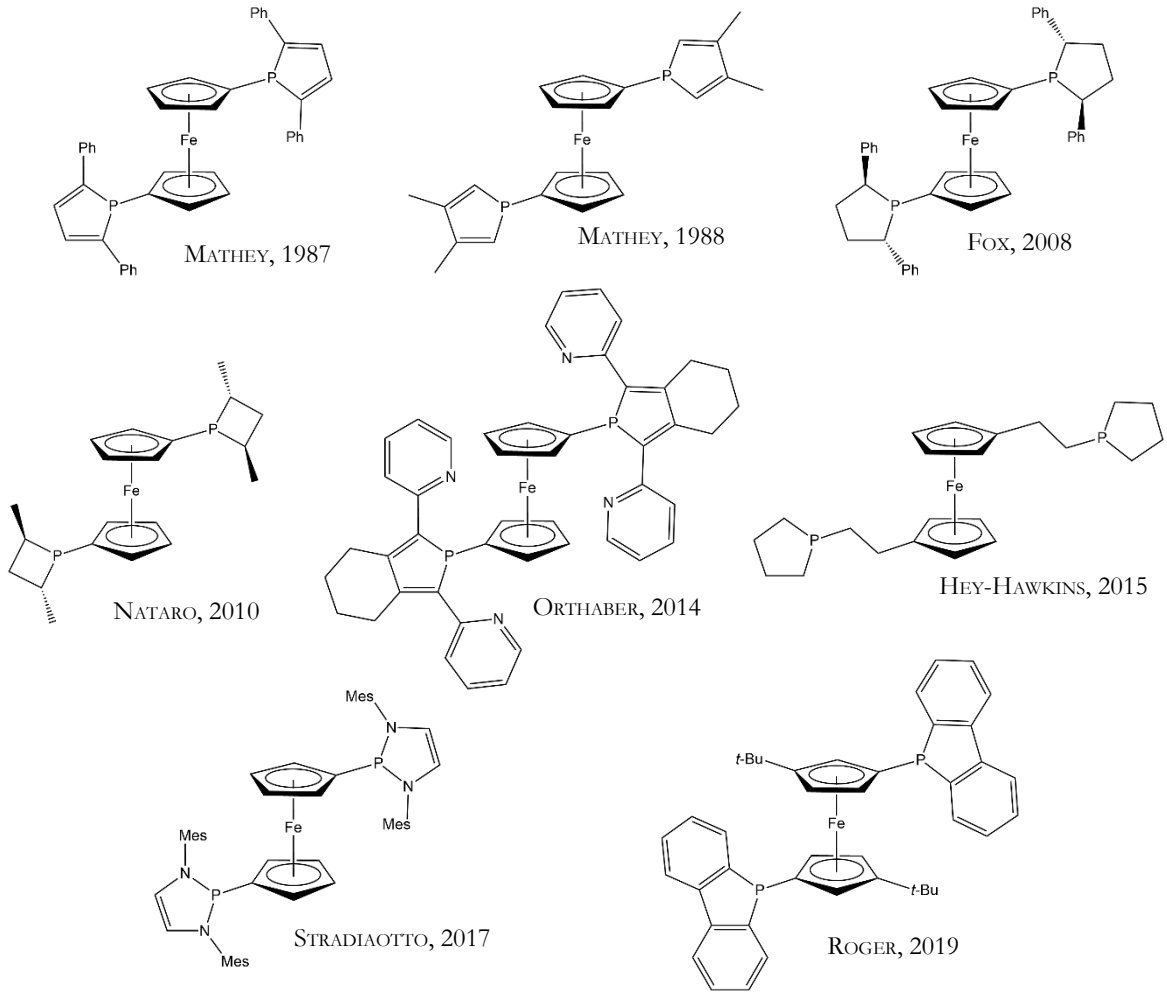


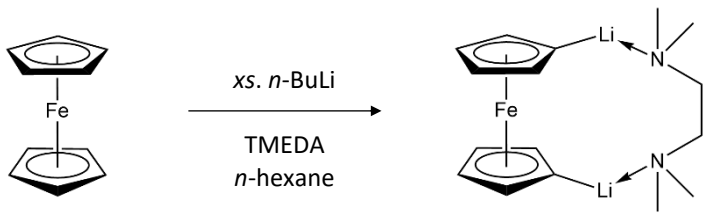

**Chart 7.2**: A selection of previously reported phosphacycle-functionalised ferrocenes.

Given the first examples of *As*-cyclopentadienyl arsoles were described in the previous chapter *via* a strategic base-induced migration of an anionic arsolyl ligand, it was natural to follow this with an analogous range of ferrocenes to which the arsolyl residue could be directly installed onto the cyclopentadienyl ring(s). This pursuit was in acknowledgement of 1) the total absence of any previously reported ferrocenes which possess arsinocyclic furnishings, and 2) the general paucity of bis(arsino)ferrocene ligands which have been neglected as their phosphorus counterparts have matured with accelerating pace. Accordingly, the first examples of 1,1'-bis(arsolyl)ferrocenes were synthesised and some classical $\kappa^2$–chelate and $\mu$-$\kappa^1$:$\kappa^1$–open-bridge coordination complexes of varying geometries were prepared. In most cases the arsines were the preferred donor functions, though with judicious selection of transition metal reagent the diene platform could also be accessed.

## 7.2 Synthesis of 1,1'-Bis(Arsolyl)Ferrocenes

### 7.2.1 1,1'-Bis(Tetraphenylarsolyl)Ferrocene (tpaf)

The synthesis of 1,1'-bis(arsolyl)ferrocenes was a procedurally straightforward task, beginning from the TMEDA (*N*,*N*,*N*,*N*-tetramethylethylenediamine) adduct of 1,1'-dilithioferrocene. This reagent was prepared from a stoichiometric mixture of ferrocene and TMEDA in *n*-hexane to which an excess of *n*-BuLi was added,[1, 12] resulting in the precipitation of [Fe($\eta^5$-$C_5H_4Li)_2$·TMEDA] as a pale-orange microcrystalline solid in good yield. The use of *n*-BuLi/TMEDA is *de rigueur* for obtaining the doubly-metalated ferrocene, whereas *t*-BuLi or *n*-BuLi in the absence of the diamine leads only to the single-deprotonated compound [Fe($\eta^5$-$C_5H_4Li$)($\eta^5$-$C_5H_5$)], or a mixture of both.[13, 14] Caution should be exercised when handling dry samples of [Fe($\eta^5$-$C_5H_4Li)_2$·TMEDA] since the solid compound is rather pyrophoric.

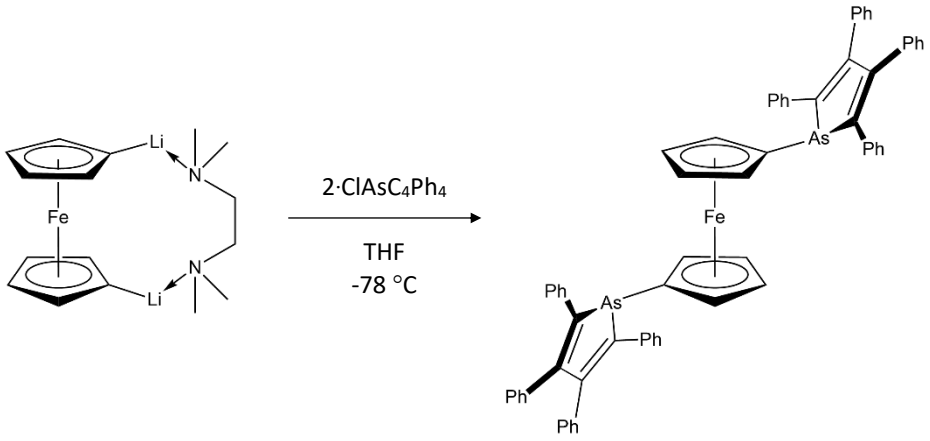



**Scheme 7.1**: Synthesis of [Fe($\eta^5$-$C_5H_4Li)_2$·TMEDA].

The addition of two equivalents of $ClAsC_4Ph_4$ to a solution of [Fe($\eta^5$-$C_5H_4Li)_2$·TMEDA] in THF at low temperature affords the expected 1,1'-bis(tetraphenylarsolyl)ferrocene [Fe{$\eta^5$-$C_5H_4(AsC_4Ph_4)$}$_2$] in acceptable yield as an air-stable, yellow solid of modest solubility (**Scheme 7.2**). The compound is the first example of an arsole ligand bearing a ferrocenyl substituent at the heteroatom. In line with the colloquial naming scheme for 1,1'-bis(**di**phenyl**p**hosphino)**f**errocene (dppf) and the like, the compound is henceforth abbreviated "tpaf" (1,1'-bis(**t**etra**p**henyl**a**rsolyl)**f**errocene;* likewise for similar ferrocenes which will follow). The disubstituted ferrocene exhibits a pair of apparent *pseudo*-triplets in the $^1$H NMR spectrum ($CDCl_3$) at 3.78 and 3.64 ppm ($J_{HH}$ = 1.8 Hz) for the AA'BB' cyclopentadienyl hydrogens α and β to the arsolyl residue, respectively. The $^{13}C\{^1H\}$ NMR spectrum finds the arsolyl ring-carbon nuclei in their usual location (151.7 and 149.6 ppm) and a set of three signals at 79.0, 71.8 and 70.8 ppm for the cyclopentadienyl carbon atoms.

* Care is taken to avoid the term "1,1'-diarsaferrocene" or similar since these refer to complexes of the type [Fe($\eta^5$-$AsC_4R_4)_2$]. The acronym tpaf was deliberately chosen to evoke memory of the ubiquitous dppf ligand of which the structure readily visualised.

The former was identified (by process of elimination) as the *As*-bonded atom *via* an HSQC NMR experiment. The modest solubility of this ferrocene derivative in common organic solvents has thus-far precluded the growth of X-ray quality crystals since the compound had a marked tendency to form amorphous precipitates, although a high-resolution mass spectrum yields the sodium adduct of the molecular ion ($m/z \approx 1069.1436$) and identity was unequivocally confirmed by a structure determination of the corresponding molybdenum(0) tetracarbonyl complex (**Figure 7.4**).

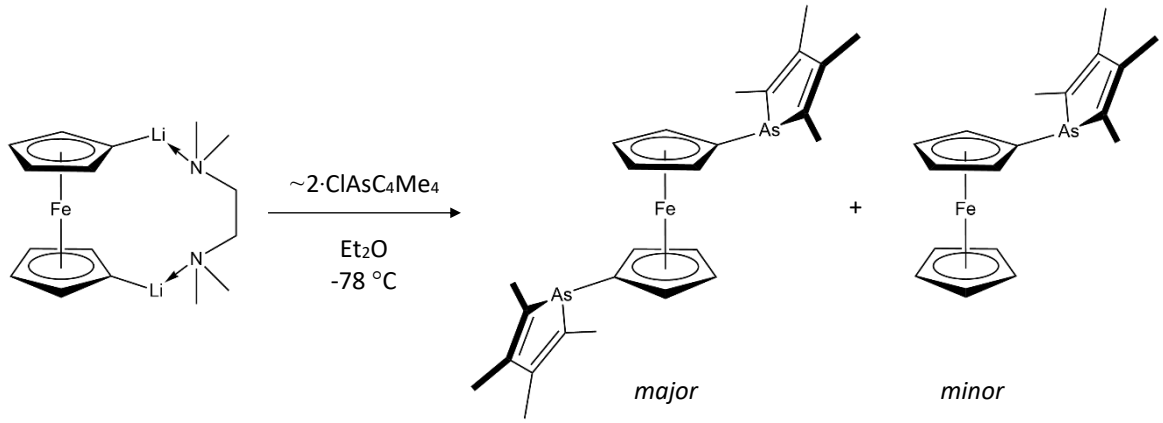



**Scheme 7.2**: Synthesis of [Fe{$\eta^5$-$C_5H_4$($AsC_4Ph_4$)}$_2$] (tpaf).

### 7.2.2 1,1'-Bis(Tetramethylarsolyl)Ferrocene (tmaf)

Similarly, the more-soluble (and more-basic) 1,1'-bis(tetramethylarsolyl)ferrocene [Fe{$\eta^5$-$C_5H_4$($AsC_4Me_4$)}$_2$] ("tmaf") was prepared by the combination of [Fe($\eta^5$-$C_5H_4Li$)$_2$·TMEDA] with two equivalents of freshly prepared $ClAsC_4Me_4$ in $Et_2O$ at -78 °C; the use of $Et_2O$ as the reaction medium consistently afforded superior yields compared to THF for reasons which are not presently obvious.* Purification of the reaction mixture *via* column chromatography provides two yellow-orange compounds which were identified as the target disubstituted [Fe{$\eta^5$-$C_5H_4$($AsC_4Me_4$)}$_2$] and the monosubstituted [Fe{$\eta^5$-$C_5H_4$($AsC_4Me_4$)}($\eta^5$-$C_5H_5$)], the former as the major product in acceptable yield (**Scheme 7.3**). Trace quantities of ferrocene were also isolated during these syntheses, presumed to arise from adventitious hydrolysis or as a trace contaminant in the [Fe($\eta^5$-$C_5H_4Li$)$_2$·TMEDA], or both.

* Interestingly, no deleterious solvent effect was observed during syntheses of tpaf (**Section 7.2.1**) where yields were, on average, identical in either THF or $Et_2O$ medium.




**Scheme 7.3**: Synthesis of [Fe{$\eta^5$-$C_5H_4$($AsC_4Me_4$)}$_2$] (tmaf) and [Fe{$\eta^5$-$C_5H_4$($AsC_4Me_4$)}($\eta^5$-$C_5H_5$)] ($FcAsC_4Me_4$).

Both *As*-ferrocenyl arsoles were encountered as bright orange, air-stable solids, the identities of which readily followed from spectroscopic data. For [Fe{$\eta^5$-$C_5H_4$($AsC_4Me_4$)}$_2$] (tmaf) the $^1$H NMR spectrum in $CDCl_3$ is predictably simple, revealing a pair of *pseudo*-triplets at 4.28 and 4.11 ppm ($J_{HH}$ = 1.7 Hz) for the monosubstituted cyclopentadienyl rings (α and β to the arsolyl group, respectively) and a pair of sharp singlets at 2.12 and 1.84 ppm for the arsolyl methyl groups. The $^{13}$C{$^1$H} NMR spectrum finds the arsole-pendant carbon nuclei in the normal region (143.6 and 139.9 ppm) and the monosubstituted cyclopentadienyl ring manifests as a set of three signals at 78.7 (*As*-bound), 71.4 and 71.0 ppm. The ferrocene is totally symmetric on the NMR timescale due to rotation about the Fe-centroid axes with very low energy barriers;[15, 16] spectra of tmaf in $CDCl_3$ measured down to -30 °C exhibited no "freezing" of internal molecular motion.

The monosubstituted ferrocene [Fe{$\eta^5$-$C_5H_4$($AsC_4Me_4$)}($\eta^5$-$C_5H_5$)] (or, equivalently, $FcAsC_4Me_4$) displays a similar $^1$H NMR profile in $CDCl_3$ solution with the $\eta^5$-$C_5H_5$ hydrogens and the $\eta^5$-$C_5H_4$ hydrogens α to the arsolyl manifesting as an isochronous resonance at 4.22 ppm (of relative area integration 7) and a broad signal at 4.07 for the $\eta^5$-$C_5H_4$ hydrogens in the β position ($J_{HH}$ unresolved). The chemical shifts of the arsolyl methyl signals are virtually identical to that of tmaf. In the $^{13}$C{$^1$H} NMR spectrum, the arsole ring-carbon signals are found at 143.5 and 139.9 ppm with the monosubstituted cyclopentadienyl ligand at 78.1 (*As*-bound), 70.8 and 69.7 ppm and the unadulterated cyclopentadienyl at 68.9 ppm. High-resolution mass spectrometry yields the molecular ions for both *As*-ferrocenyl arsoles and single crystals confirming their identities were obtained from slow evaporations of *n*-pentane solutions (**Figure 7.2** and

**Figure 7.3**). The disubstituted tmaf ligand in particular was a highly crystalline compound which on multiple occasions formed *centimetre*-sized crystals.

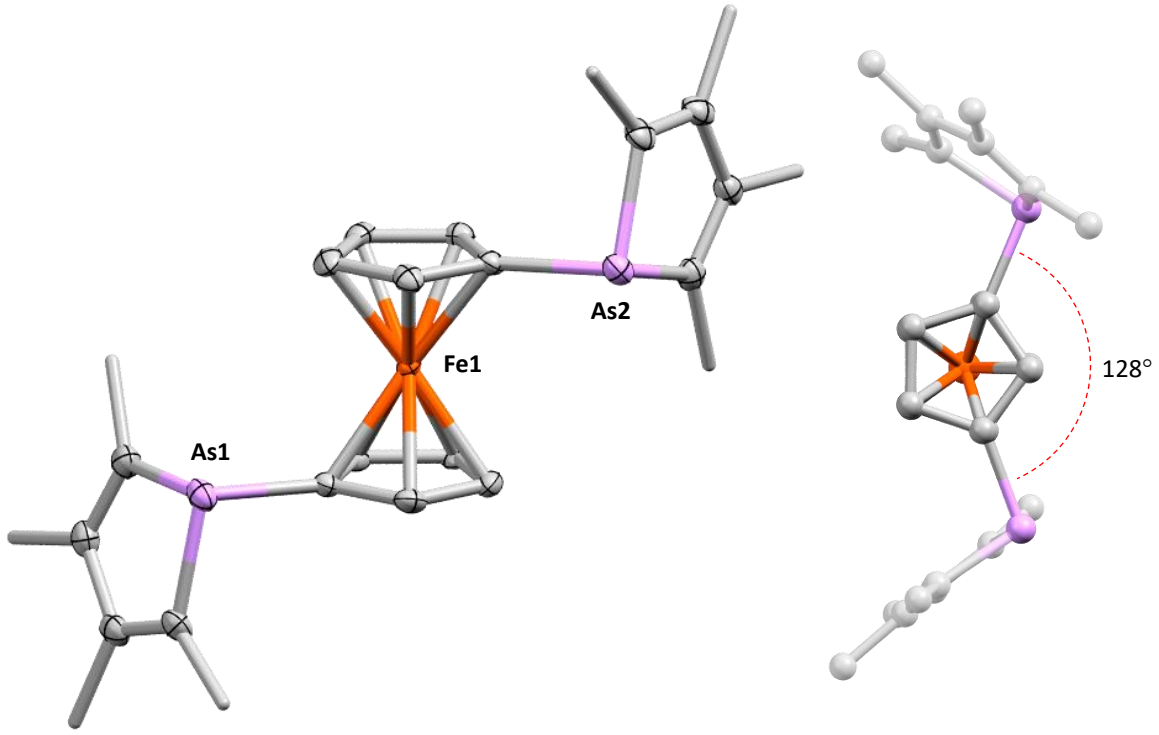



**Figure 7.2**: The molecular structure of [Fe{$C_5H_4(AsC_4Me_4)$}$_2$] ("tmaf") in a crystal. Methyl groups simplified and hydrogen atoms omitted for clarity. Ellipsoids shown at 50% displacement. **Inset**: Abbreviated perspective of the molecule highlighting the eclipsed-anticlinal conformation of the disubstituted ferrocene in the solid state.

The molecular structure of tmaf finds an otherwise typical ferrocene unit with each of the cyclopentadienyl rings bearing a tetramethylarsolyl pendant. The cyclopentadienyl carbon atoms are eclipsed when viewed along the centroid-Fe-centroid vector and the pair of arsolyl groups are mutually anticlinal (**Figure 7.2**, **Inset**). No crystallographic symmetry is imposed upon the acentric, approximately $C_2$-symmetric molecule in the solid state; however, the unit cell (triclinic *P*-1) contains both enantiomers related by means of the crystallographic inversion centre. The arsolyl groups are themselves swivelled about the exocyclic As-C($sp^2$) bond such that the majority of their "bodies" lie toward the exterior faces of the cyclopentadienyl rings. Distances within and around the arsolyl and ferrocenyl moieties are typical with mean exocyclic As-C($sp^2$) and Fe-centroid distances of *ca* 1.93 and 1.64 Å, respectively, and the mean planes of the monosubstituted cyclopentadienyl ligands are virtually parallel (angle of intersection < 1°). Mean As-$C_\alpha$, $C_\alpha$=$C_\beta$ and $C_\beta$-$C_\beta$ bond lengths within the arsolyl rings of *ca* 1.94, 1.33 and 1.49 Å are normal and

compare favourably with the various [MoR(CO)$_n${$\eta^5$-$C_5H_4$($AsC_4Ph_4$)}] complexes characterised in the previous chapter. The ten individual cyclopentadienyl carbon-Fe distances are crystallographically equivalent and the presence of the arsolyl appendages have no statistically significant impact on the bonding mode of the *pentahapto* rings.

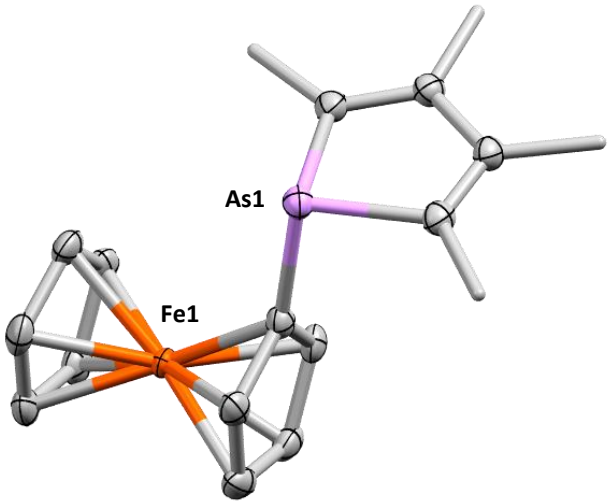
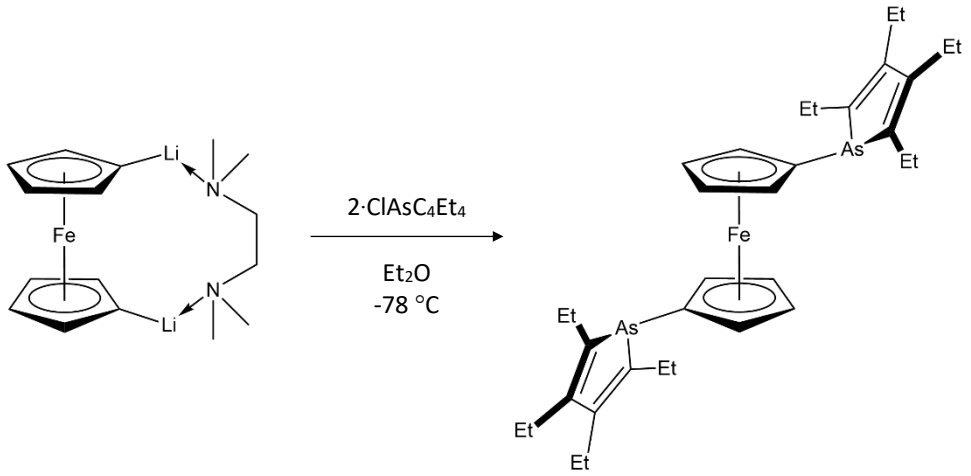



**Figure 7.3**: The molecular structure of [Fe{$\eta^5$-$C_5H_4$($AsC_4Me_4$)}($\eta^5$-$C_5H_5$)] in a crystal. Methyl groups simplified and hydrogen atoms omitted for clarity. Ellipsoids shown at 50% displacement.

The molecular structure of $FcAsC_4Me_4$ (a.k.a. [Fe{$\eta^5$-$C_5H_4$($AsC_4Me_4$)}($\eta^5$-$C_5H_5$)]) finds the expected monosubstituted ferrocene geometry. Like the tmaf ligand, the cyclopentadienyl rings are eclipsed and essentially co-planar with one another, and the disposition of the $AsC_4Me_4$ pendant with respect to the ferrocene chassis is also comparable to those of the disubstituted counterpart. Indeed, interatomic distances and angles are crystallographically identical with the tmaf ligand previously discussed and for brevity call for no further comment. The occurrence of [Fe{$\eta^5$-$C_5H_4$($AsC_4Me_4$)}($\eta^5$-$C_5H_5$)] as a minor product alongside [Fe{$\eta^5$-$C_5H_4$($AsC_4Me_4$)}$_2$] is presumed to arise from either 1) adventitious hydrolysis during synthetic manipulations, or more probably 2) an imprecise reagent stoichiometry since the $ClAsC_4Me_4$ precursor must be prepared fresh and used in crude form. The presence of [Fe($\eta^5$-$C_5H_4Li$)($\eta^5$-$C_5H_5$)] as a contaminant in the bulk sample of [Fe($\eta^5$-$C_5H_4Li$)$_2$·TMEDA] is less likely since this was the only context where both di- and monosubstituted ferrocene derivatives were isolated.

### 7.2.3 1,1'-Bis(Tetraethylarsolyl)Ferrocene (teaf)

The 1,1'-bis(tetraethylarsolyl)ferrocene (teaf) ligand was prepared in an identical fashion from two equivalents of $ClAsC_4Et_4$ and $[Fe(\eta^5\text{-}C_5H_4Li)_2{\cdot}TMEDA]$ in $Et_2O$ at -78 °C. Since this *As*-chloro arsole has a reasonable shelf-life at ambient temperature (*cf.* $ClAsC_4Me_4$ which gradually dimerises) a precise stoichiometry could be employed and a monosubstituted ferrocene of the form $[Fe\{\eta^5\text{-}C_5H_4(AsC_4Et_4)\}(\eta^5\text{-}C_5H_5)]$ was neither isolated nor sought. Purification of the reaction mixture *via* column chromatography gives the target compound $[Fe\{\eta^5\text{-}C_5H_4(AsC_4Et_4)\}_2]$ as a resinous orange oil in acceptable yield, which eventually solidified upon standing.




**Scheme 7.4**: Synthesis of $[Fe\{\eta^5\text{-}C_5H_4(AsC_4Et_4)\}_2]$ (teaf).

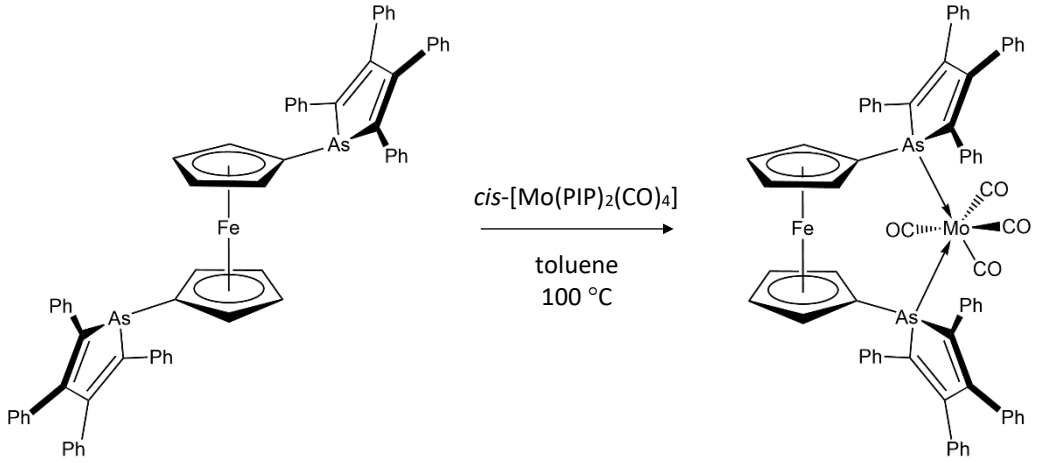
Spectroscopic features of the teaf ligand are superficially similar to those of tmaf, though this is not unexpected given the similar electronic properties of methyl *vs.* ethyl substituents. The $^1H$ NMR spectrum ($CDCl_3$) finds the cyclopentadienyl hydrogen atoms at 4.25 and 4.07 ppm ($J_{HH}$ unresolved) and – like $[Co(CO)_2(\eta^5\text{-}AsC_4Et_4)]$ (**Chapter 3**, **Section 3.3.1**) – the methylene units of the $AsC_4Et_4$ groups have diastereotopic proton environments in solution on the NMR timescale, with three resonances observed at 2.59, 2.45 and 2.26 ppm with relative area integrations of 4:4:8. A pair of triplets at 1.18 and 1.02 ppm ($J_{HH} \approx 7.5$ Hz) corresponding to the $CH_3$ hydrogens complete the spectrum. In the $^{13}C\{^1H\}$ spectrum a pair of arsolyl ring-carbon signals are found at 149.7 and 148.5 ppm downfield of the three cyclopentadienyl carbon environments at 79.8 (*As*-bound), 71.5 and 70.6 ppm. The ethyl carbon nuclei appear as a simple pattern of four signals at 23.4 and 21.2 (methylene), and 17.3 and 15.3 (methyl) ppm. High-resolution mass spectrometry yields the molecular ion, though at the time of writing single crystals suitable for X-ray

diffraction have proven elusive since the compound has a strong solventophilic tendency and solvent evaporations yielded waxy solids of low crystallinity. The identity was, however, unequivocally confirmed by a crystal structure determination of its molybdenum(0) tetracarbonyl complex (**Figure 7.6**).

## 7.3 Classical Bidentate Coordination Complexes

### 7.3.1 Synthesis of *cis*-[Mo(κ²-tpaf)(CO)₄]

As a means to unambiguously confirm ligand formulation one equivalent each [Fe{η⁵-$C_5H_4(AsC_4Ph_4)$}₂] (tpaf) and the labile *cis*-[Mo(PIP)₂(CO)₄] (PIP = piperidine, $C_5H_{11}N$), which serves as a synthetic source of "Mo(CO)₄", were combined in toluene solution and briefly heated to 100 °C; the reaction does proceed at ambient temperature in $CH_2Cl_2$ however required several days for the bis(piperidine) reagent to be fully consumed (by IR spectroscopy). Column chromatography provided the expected *cis*-[Mo(κ²-tpaf)(CO)₄] as a reasonably air-stable bright yellow solid in acceptable yield, which displays four $\nu_{CO}$ absorptions at 2025(s), 1948(vs), 1927(vs) and 1882(s) $cm^{-1}$ in *n*-hexane solution. In contrast to the free state, coordination of the molybdenum(0) tetracarbonyl centre greatly improves the solubility properties of the ligand and single crystals were readily obtained by slow evaporation of benzene solution; the molecular structure is shown in **Figure 7.4**.




**Scheme 7.5**: Synthesis of *cis*-[Mo(κ²-tpaf)(CO)₄].

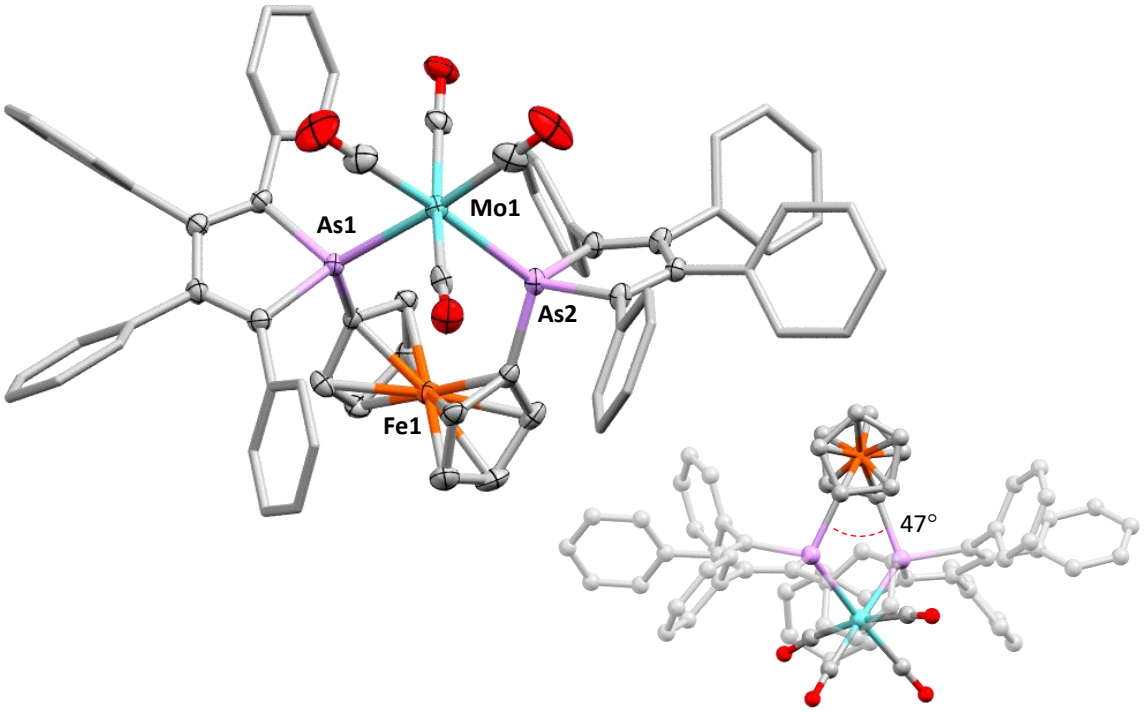
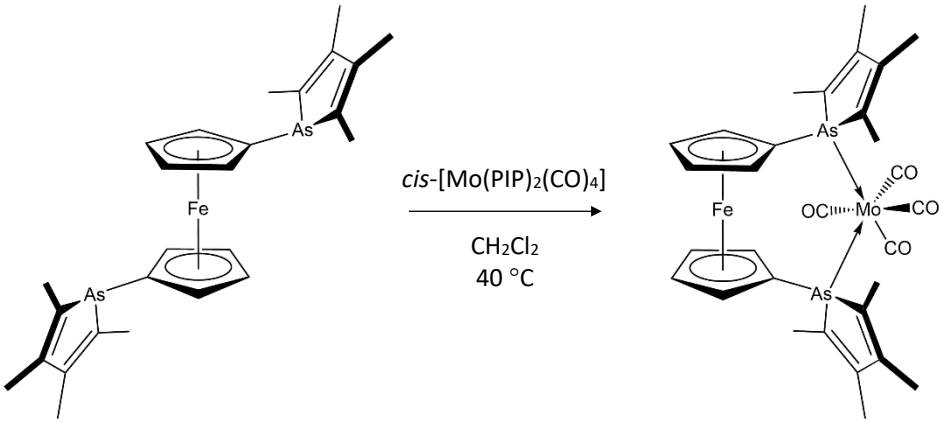



**Figure 7.4**: The molecular structure of *cis*-[Mo(κ²-tpaf)(CO)$_4$]·C$_6$H$_6$ in a crystal. Phenyl groups simplified and benzene solvate molecule and hydrogen atoms omitted for clarity. Ellipsoids shown at 50% displacement. **Inset**: Abbreviated perspective of the molecule highlighting the staggered-*gauche* conformation of the tpaf ligand.

The crystal structure determination finds the expected bis(arsolyl)ferrocene ligand complexing a Mo(CO)$_4$ fragment *via* the pair of *cis*-disposed arsenic donors. The Mo(0) centre exists in a slightly distorted octahedral environment with the arsenic donor atoms lying in the equatorial plane and angles of *ca* 169° and *ca* 175° for the respective OC-Mo-CO and As-Mo-CO *trans*-axes, both reclining away from the tpaf ligand. Moreover, whereas the carbonyl ligands in the equatorial plane (*trans* to the As(III) atoms) are linear at the carbon atoms, the mutually *trans* carbonyl ligands are bowed at the carbon atom by *ca* 10° away from the pairs of phenyl rings in the arsole 2,5-ring positions, suggesting some antagonistic steric interactions may be operative. The tpaf ligand exists in a *gauche* conformation with the arsolyl pendants separated by *ca* 47° and the cyclopentadienyl rings are staggered when viewed along the centroid-Fe-centroid vector (**Figure 7.4**, **Inset**), their mean planes being slightly tilted in the direction of the molybdenum centre by *ca* 3°. The mean As→Mo dative bonds measure 2.6301(7) Å (*cf.* 2.64 Å in *cis*-[Mo(AsPh$_3$)$_2$(CO)$_4$][17]) and the Mo-C bonds *trans* to the arsenic donors (mean 1.981(7) Å) are slightly shorter than those *cis* (mean 2.057(7) Å) due to the disparate π-acceptor properties of the ligand set.

### 7.3.2 Synthesis of *cis*-[Mo(κ²-tmaf)(CO)₄]

A Mo(0) complex of [Fe{η⁵-C₅H₄(AsC₄Me₄)}₂] was prepared similarly though reflecting the improved nucleophilicity of this ligand (and/or its decreased steric profile) compared to the all-phenyl analogue, coordination to *cis*-[Mo(PIP)₂(CO)₄] takes place in $CH_2Cl_2$ solution at reflux within 90 minutes to provide the anticipated *cis*-[Mo(κ²-tmaf)(CO)₄].




**Scheme 7.6**: Synthesis of *cis*-[Mo(κ²-tmaf)(CO)₄].

The complex was isolated after column chromatography in high yield as a reasonably air-stable yellow solid which displays four $\nu_{CO}$ in the solution IR spectrum (*n*-hexane) at 2020(vs), 1944(s), 1902(vs) and 1881(vs) $cm^{-1}$ for the *pseudo*-$C_{2v}$ tetracarbonyl arrangement ($2A_1 + B_1 + B_2$ vibrational modes), notably to lower wavenumbers than the octaphenyl complex. The $^1H$ NMR spectrum in $CDCl_3$ finds a pair of *pseudo*-triplets at 4.32 and 4.25 ppm ($J_{HH}$ = 1.8 Hz) which are slightly downfield of the free ligand (*cf.* 4.28 and 4.11 ppm), as are the singlets corresponding to the arsolyl methyl groups (2.25 and 1.89 ppm *vs.* 2.12 and 1.84 ppm in the free state). The carbonyl carbon nuclei are found at 214.4 and 210.4 ppm in the $^{13}C\{^1H\}$ NMR spectrum of which the former is assigned to those *trans* to the As(III) donor atoms, and the arsolyl ring-carbon resonances at 142.7 and 137.2 ppm are very slightly upfield of those in the free ligand (*cf.* 143.6 and 139.9 ppm). The cyclopentadienyl carbon and the arsolyl methyl signals are not appreciably shifted from the free ligand. Single crystals were obtained by cooling a hot *n*-hexane solution and the molecular structure is shown in **Figure 7.5**.

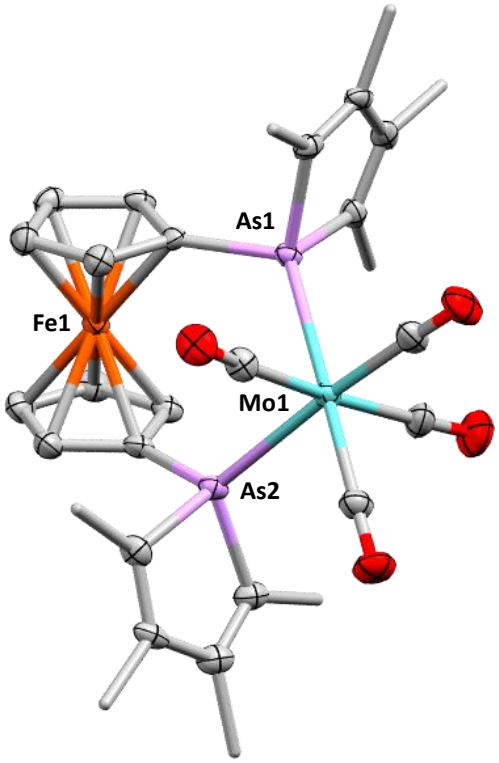
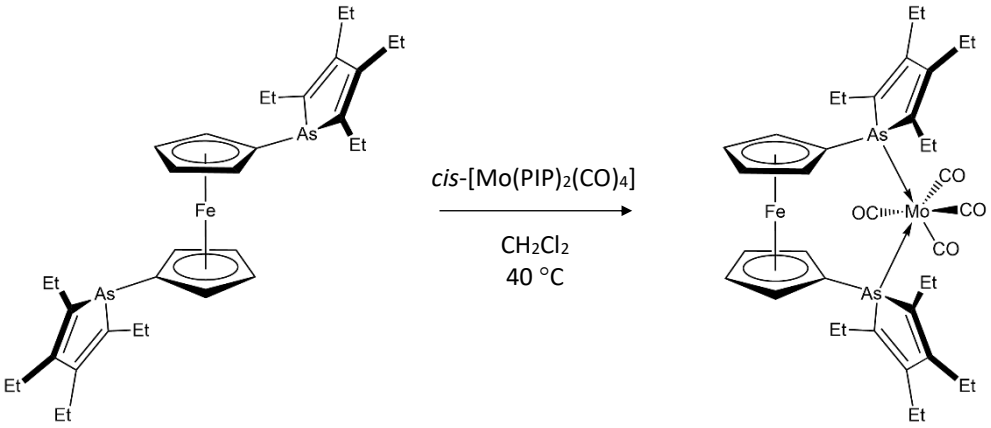



**Figure 7.5**: The molecular structure of *cis*-[Mo(κ²-tmaf)(CO)₄] in a crystal. Methyl groups simplified and hydrogen atoms omitted for clarity. Ellipsoids shown at 50% displacement.

The expected octahedral Mo(0) complex is found, with a gross configuration comparable to that of the tpaf analogue above (**Figure 7.4**). The tmaf ligand exists in a staggered-*gauche* conformation with a torsional angle between the arsolyl donors of *ca* 34° and mean As→Mo dative distances of 2.607(6) Å which are slightly shorter than those in *cis*-[Mo(κ²-tpaf)(CO)₄], being comparable to the same in other bis(dimethylarsino) chelates.[18-21] The coordination environment of the metal centre is less distorted than in the tpaf complex with rather regular transaxial angles of 174—178° and the carbonyl ligands do not display the same deflection since the tmaf is unquestionably of reduced steric and electrostatic profile. The increased basicity of the metal centre here is reflected in slightly shorter Mo-C distances of ~0.03 Å.

### 7.3.3 Synthesis of *cis*-[Mo(κ²-teaf)(CO)₄]

The corresponding [Fe{η⁵-C₅H₄(AsC₄Et₄)}₂] chelate of molybdenum(0) tetracarbonyl was prepared by combination of teaf and *cis*-[Mo(PIP)₂(CO)₄] in $CH_2Cl_2$ solution at 40 °C.




**Scheme 7.7**: Synthesis of *cis*-[Mo(κ²-teaf)(CO)₄].

The complex was isolated in high yield after column chromatography as a reasonably air-stable yellow solid with four $\nu_{CO}$ absorptions at 2017(vs), 1944(s), 1900(vs) and 1880(vs) $cm^{-1}$ in *n*-hexane. Contrasting these IR data suggest – as expected – the tpaf ligand to be the poorest donor ligand and the basicities of tmaf and teaf to be approximately identical. Coordination of $Mo(CO)_4$ elicits a slight downfield shift of the cyclopentadienyl $^1H$ signals ($CDCl_3$) from 4.25 and 4.07 ppm in the free ligand to 4.31 and 4.21 ppm. While the protons of the methylene group remain diastereotopic only two resonances of equal area integration are displayed due presumably to accidental isochronicity. In the $^{13}C\{^1H\}$ NMR spectrum the carbonyl ligands manifest at 214.3 (*trans* to arsenic) 210.8 (*cis* to arsenic) ppm which are essentially identical in position to those in the tmaf complex. Single crystals were obtained from *n*-pentane solution and the molecular structure is shown in **Figure 7.6**.

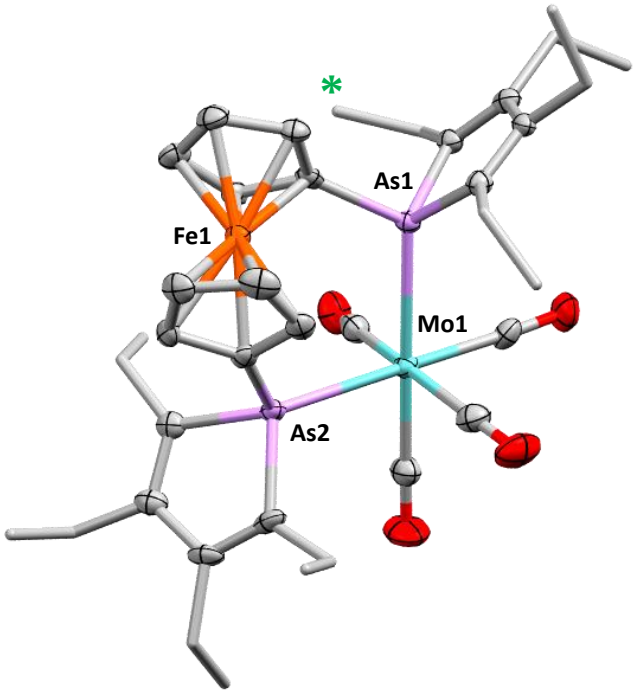
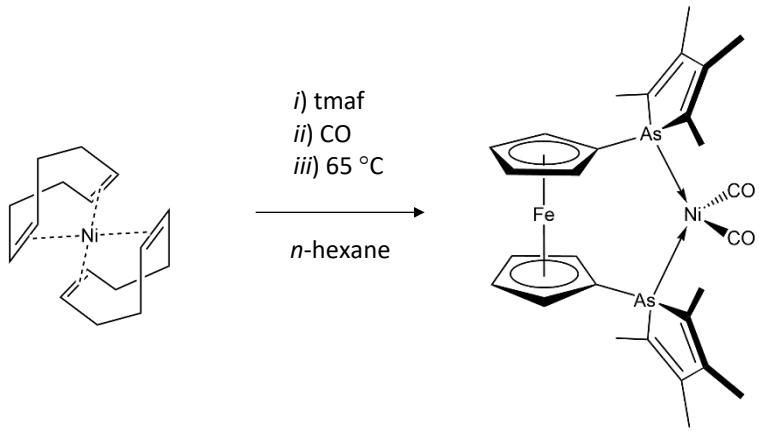



**Figure 7.6**: The molecular structure of *cis*-[Mo(κ²-teaf)(CO)₄] in a crystal. Ethyl groups simplified and hydrogen atoms omitted for clarity. Ellipsoids shown at 50% displacement. Only one of the two crystallographically unique molecules contained within the asymmetric unit is shown, which differ in the orientation of the ethyl group marked with *.

The expected complex is found which also serves to confirm the identity of the free ligand. The asymmetric unit contains a pair of crystallographically distinct molecules which are otherwise congruent in structure except for a single ethyl group (marked with a green asterisk in **Figure 7.6**) which is inflected about the mean plane of the arsole ring *i.e.*, either toward or away from the metal centre. It is also noteworthy that the complex crystalised in the non-centrosymmetric space group monoclinic *Ia* which means this particular solid-state specimen is enantiomerically pure, though a very low barrier to ferrocenyl rotation probably obliviate this feature in solution. In the molecule shown above, the orientations of the ethyl residues alternate (in an aesthetically pleasing manner) about the arsole peripheries and the teaf ligand exists in the usual staggered-*gauche* conformation (48° torsion) about the Mo(0) centre. The mean As→Mo distances are slightly longer (but not anomalously-so) than those found in the tmaf complex (**Figure 7.5**) at 2.653(5) Å though the Mo-C distances are crystallographically identical. Interestingly, the same deflection of the carbonyl ligands away from the chelating ligand measured in *cis*-[Mo(κ²-tpaf)(CO)₄] (**Figure 7.4**) are also observed here (OC-Mo-CO 166°) suggesting the inimical phenomenon is indeed steric in origin.

### 7.3.4 Synthesis of [Ni(κ²-tmaf)(CO)₂]

Another labile reagent in the Coordination Chemist's cache (albeit one which has receded from use in the modern era) is [Ni(CO)₄], which in the latter-half of the previous century served as a convenient model for establishing trends in ligand donor-acceptor abilities (the so-called "TOLMAN electronic parameter") due to the ease of substitution of the Ni(0) centre.[22] Given the malicious toxicity of this volatile metal carbonyl, coordination commenced not with [Ni(CO)₄] itself but with an excess of [Ni(COD)₂] (COD = $\eta^2$:$\eta^2$-1,5-cyclooctadiene) and tmaf in *n*-hexane solution yielding an orange-red suspension (itself not analysed). Placing the mixture under an atmosphere of carbon monoxide results in immediate dissolution of the solids with a spectacular colour change to a deep yellow. Briefly heating the mixture to reflux followed by chromatography provided the expected [Ni(κ²-tmaf)(CO)₂] complex in high yield as a reasonably air-stable golden yellow solid (**Scheme 7.8**).




**Scheme 7.8**: Synthesis of [Ni(κ²-tmaf)(CO)₂].

It is also worth noting that [NiL₂(CO)₂] complexes can alternatively be synthesised by reductive carbonylation of [NiL₂X₂] (X = halide or *pseudo*-halide) with [Fe(CO)₅],[23] or alkali metals under a CO atmosphere,[24] however the route here involving [Ni(COD)₂] proved more than satisfactory. The IR spectrum (*n*-hexane) of [Ni(κ²-tmaf)(CO)₂] includes the expected pair of carbonyl stretching modes ($A_1$ + $B_1$) at 2009(vs) and 1951(vs) cm$^{-1}$ which, on the basis of integrated intensities, indicate the ligands are at an angle of ~110° consistent with *pseudo*-tetrahedral geometry for the $d^{10}$ Ni(0) centre. It is fortunate that an extensive body of literature exists with a library of bis-coordinated nickel dicarbonyl complexes for comparison and – in general – slightly higher $\nu_{CO}$ frequencies (on the order of *ca* 10—20 cm$^{-1}$) are observed

for the tmaf complex here compared to the diverse family of bis(phosphino) compounds previously reported.[23-25] Naturally, the less-basic arsenic σ-donor (or slightly superior π-acceptor) compared to phosphorus elicits a poorer retrodative capacity from the Ni(0) centre toward the carbonyl ligands.

The $^{13}C\{^{1}H\}$ NMR spectrum ($C_6D_6$) of [Ni(κ²-tmaf)$(CO)_2$] finds a sharp signal at 200.6 ppm for the pair of carbonyl ligands; the arsolyl ring-carbon nuclei are observed at 142.9 (2,5-positions) and 137.0 (3,4) which are only slightly displaced from those of the free ligand (143.6 and 140.5 ppm in $C_6D_6$). The upfield shift probably signals a reduction in the (already very modest) ring current within the arsole group upon coordination of the lone pair, as was previously mooted in **Chapter 5** when the $AsC_4Me_4$ ligand bridged a pair of transition metal centres. A similar feature is noted for the relevant hydrogen signals in the $^{1}H$ NMR spectrum, the cyclopentadienyl proton resonances (4.20 and 4.02 ppm) appear marginally upfield of those for the free ligand (4.24 and 4.20 ppm) with the arsolyl-methyl protons shifting in opposing directions depending on their bonding proximity to the Ni(0) atom, from 2.12 (2,5-position) and 1.70 (3,4-position) ppm to 2.24 and 1.58 ppm. Large euhedral crystals were obtained by slow evaporation of benzene solution, and the molecular structure as determined by X-ray diffractometry is shown in **Figure 7.7**.

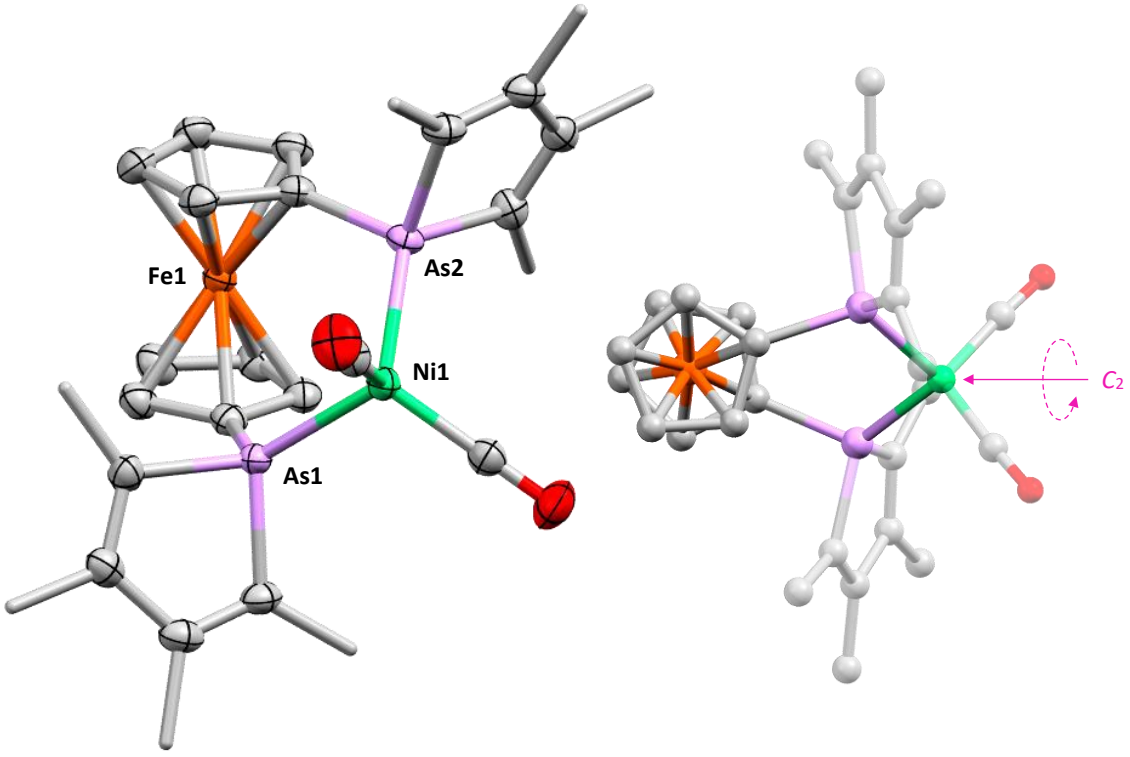



**Figure 7.7**: The molecular structure of [Ni(κ²-tmaf)$(CO)_2$] in a crystal. Methyl groups simplified and hydrogen atoms omitted for clarity. Only one half of the molecule is crystallographically unique. Ellipsoids shown at 50% displacement. **Inset**: Abbreviated perspective of the molecule highlighting the *gauche* conformation of the tmaf ligand. $C_2$ = two-fold crystallographic axis of rotation.

The molecular structure of [Ni(κ²-tmaf)(CO)$_2$] comprises a tetrahedral Ni(0) centre ($\tau_4$ = 0.96) holding the tmaf ligand *via* the arsenic donors. The tmaf ligand exists in a staggered conformation with the arsolyl pendants mutually *gauche* about the principle ferrocenyl axis (torsion angle *ca* 43°); only one half of the molecule is crystallographically unique due to the presence of two-fold rotational symmetry about the Fe-Ni vector, bisecting the pair of carbonyl ligands (intercarbonyl angle *ca* 114°). Interatomic dimensions within the molecule are typical of the individual constituents and the gross structure is virtually identical to that of the known [Ni(κ²-dppf)(CO)$_2$]:[26] the pair of cyclopentadienyl rings are effectively parallel (intersection of mean ring planes *ca* 3°, in the direction of the nickel captive) with the arsenic atoms lying in the same planes. The Ni-C and C≡O bond lengths of 1.772(3) and 1.145(3) Å compare favourably against other [Ni(L)$_2$(CO)$_2$] complexes[26, 27] with As→Ni dative bonds of 2.3257(3) Å (sum of covalent radii 2.43 Å). Incidentally, it seems that no prior examples of [Ni(arsine)$_2$(CO)$_2$] complexes have heretofore been structurally characterised and [Ni(κ²-tmaf)(CO)$_2$] appears to be the first. Only one other formally Ni(0) complex with an arsenic-based donor set has been crystallographically interrogated, namely the novel and rather exotic hexa-arsine species [Ni(As{*t*-Bu})$_6$] containing a circumcentric Ni(0) atom (**Figure 7.8**) prepared by HEY-HAWKINS *via* reduction of a mixture of $NiCl_2$ and As(*t*-Bu)$Cl_2$.[28] Longer As→Ni dative bonds of 2.4767(6) Å are measured for this species, though caution is exercised in placing too much significance in the *ca* 0.15 Å difference due to the atypical bonding situation within this geometrically-distinctive molecule. The As→Ni(0) dative bonds in [Ni(κ²-tmaf)(CO)$_2$] compare to the slightly shorter 2.30—2.32 Å range measured for several As→Ni(II) complexes.[29-31]

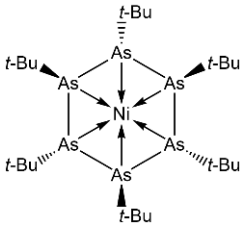


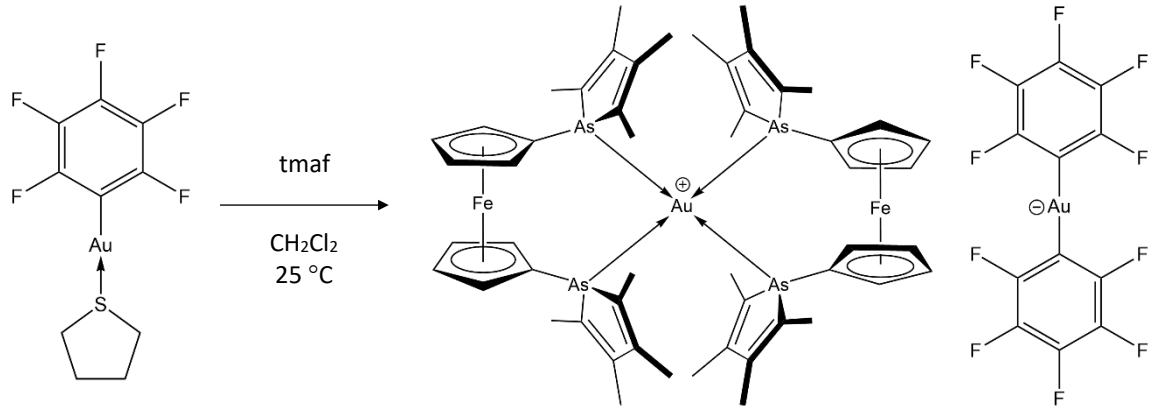

**Figure 7.8**: The hexa(*tert*-butylarsine)nickel(0) complex prepared by HEY-HAWKINS *et al.*

As an epilogue to this section and to provide Australian context for the significance of bidentate diarsines in nickel chemistry, it is of interest that Frances DWYER, a former faculty member of the Australian National University in the late 1950's, with Sir Ronal NYHOLM pioneered the chemistry of ortho-

bis(dimethylarsino)benzene which included the stabilisation of unusual (at the time) oxidation states *e.g.*, Ni(III).[32, 33] The (re)emergence of nickel diarsine complexes on the Canberra campus suggests *plus ça change, plus c'est la même chose*.

### 7.3.5 Synthesis of $[Au(\kappa^2\text{-tmaf})_2][Au(C_6F_5)_2]$

The tmaf ligand also reacts with $[Au(C_6F_5)(THT)]$ (THT = tetrahydrothiophene, $SC_4H_8$) in $CH_2Cl_2$ solution to provide a bright yellow solid which was shown by high-resolution mass spectrometry (positive and negative ion modes) and X-ray diffraction to be the salt $[Au(\kappa^2\text{-tmaf})_2][Au(C_6F_5)_2]$ (**Figure 7.9**), recalling the same dismutation of the $Au(C_6F_5)$ fragment upon complexation to $[Co(CO)_2(\eta^5\text{-}AsC_4Me_4)]$ (**Section 3.4.4** of **Chapter 3**). The alacrity with which the Au(I) centre is able to shed the $C_6F_5$ group (*inter alia*) has been noted in similar complexes *e.g.*, $[Au_2(\mu\text{-}\kappa^1\text{:}\kappa^1\text{-dppf})(C_6F_5)_2]$ which may interconvert between $[Au_2(\mu\text{-}\kappa^1\text{:}\kappa^1\text{-dppf})(C_6F_5)]^+$ and $[Au(\kappa^2\text{-dppf})_2]^+$ depending on experimental conditions.[34, 35] The outcome here was the same regardless of tmaf:$[Au(C_6F_5)(THT)]$ stoichiometry.




**Scheme 7.9**: Synthesis of $[Au(\kappa^2\text{-tmaf})_2][Au(C_6F_5)_2]$.

The $^1H$ and $^{19}F\{^1H\}$ NMR spectra are rather unassuming finding four and three signals, respectively, for the laterally-symmetric proton and fluorine environments of the $[Au(\kappa^2\text{-tmaf})_2]^+$ cation and $[Au(C_6F_5)_2]^-$ anion. The $^{13}C\{^1H\}$ spectrum in $CDCl_3$ is also largely unremarkable save for the unexpected occurrence of only one broad resonance each for the ferrocene cyclopentadienyl (72.0 ppm; FWHM = 67 Hz) and arsolyl methyl (14.9 ppm; FWHM = 58 Hz) carbon nuclei. The complex evidently displays internal fluxionality faster than the NMR timescale and remained in motion to -30 °C with no observable resolution

of signals, suggesting that positional exchange of the tmaf ligands about the tetrahedral $Au^+$ centre proceeds with very modest energy barrier. This inversion manoeuvre can be envisioned as a twisting motion, requiring partial rotation of the cyclopentadienyl rings about the Fe-centroid axis only with no breaking of As→Au bonds (similar to that shown in **Scheme 7.11**), hence the arsolyl ring-carbon atoms are observed as separate signals (145.2 and 136.0 ppm) but the cyclopentadienyl nuclei are not. One may then also expect the arsolyl methyl groups to be distinct, though given their modest separation of ≤ 1 ppm in other κ²-tmaf complexes described in this chapter, this radial motion may be sufficient for the signals to accidentally coalesce on the NMR timescale.

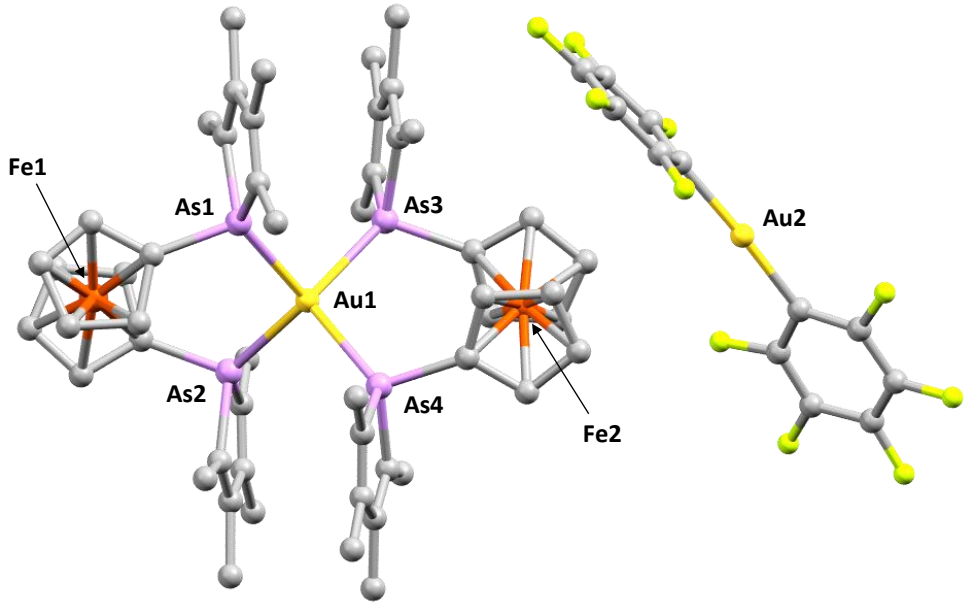


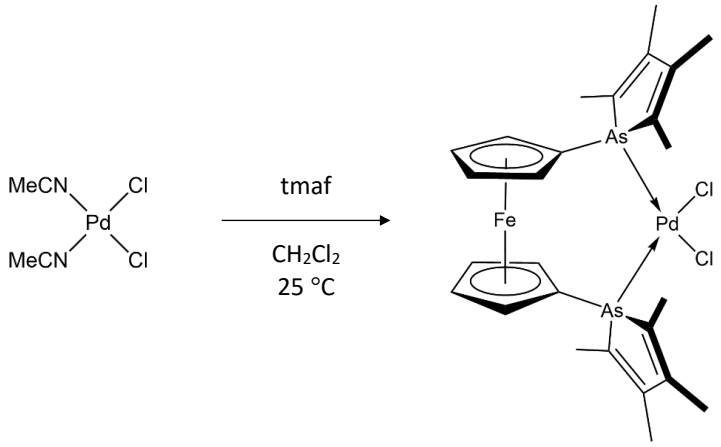

**Figure 7.9**: The molecular structure of $[Au(\kappa^2\text{-tmaf})_2][Au(C_6F_5)_2]$ in a crystal. All atoms shown as rigid spheres without thermal anisotropy due to poor data quality. Hydrogen atoms omitted for clarity. Only one of the two crystallographically independent cation-anion pairs contained within the asymmetric unit is shown.

X-ray diffraction reveals a slightly deformed tetrahedral Au(I) centre ($\tau_4 \approx 0.8$) hosted by a pair of tmaf ligands, which are offset from one-another by about 20° when viewed along the Fe1-Au1-Fe2 vector. For context, the only structural data for homoleptic four-coordinate gold-arsine complexes are those for the $[Au\{(AsMe_2)_2C_6H_4\}_2]^+$ (mean As→Au 2.471 Å[36]) and $[Au(AsPh_3)_4]^+$ (mean As→Au 2.584 Å[37]), the former with rather strict chelation-imposed geometric constraints while the latter involves considerable steric congestion. The tmaf ligand offers both geometric flexibility and As(III) donors which are intermediate between $AsPh_3$ and $AsMe_2R$ in terms of both steric and net donor properties. The tmaf ligands

exist in the usual staggered-*gauche* conformations (torsion angle *ca* 40°) with approximate As→Au dative bonds of 2.5 Å in length, and the perfluoroaryl groups within the $[Au(C_6F_5)_2]^-$ anion are rotated by *ca* 50° about the Au2 centre. It should be noted that data quality was rather poor and although atom connectivity is unambiguously established, extraction of precise crystallographic measurements is precluded by rather eccentric atomic displacement parameters (and positional disorder of the $[Au(C_6F_5)_2]^-$ anions). Other reasons for such poor model quality are not known since the selected crystals were of suitable size and appearance for X-ray diffractometry and yielded strong reflections to 0.8 Å resolution. Inspection of the EWALD construction of the reciprocal lattice showed no evidence of sample twinning or diffuse scattering, and the structure solution did not indicate the partial presence of solvate molecules which may have evaporated prior to or during data collection. It is regrettable that several crystals grown from separate solvent conditions all yielded sub-optimal structure solutions, and unfortunately nothing more should be said about the complex in the absence of high precision X-ray diffraction data.

### 7.3.6 Synthesis of *cis*-[Pd(κ²-tmaf)Cl₂]

Given the prevalence of the dppf ligand in homogeneous catalysis, coordination experiments with tmaf would be derelict if a divalent palladium complex was overlooked. To this end, one equivalent each of *cis*-$[Pd(NCMe)_2Cl_2]$ and tmaf were combined in $CH_2Cl_2$ solution giving a deep red mixture from which the air-stable *cis*-[Pd(κ²-tmaf)Cl₂] was isolated in high yield.




**Scheme 7.10**: Synthesis of *cis*-[Pd(κ²-tmaf)Cl₂].

The formulation of the Pd(II) complex follows from high-resolution mass spectrometry ($m/z \approx$ 733.9283 for $[M - Cl]^+$ ion) and a low-precision single crystal structure determination (**Figure 7.10**). The cyclopentadienyl hydrogen $^1$H resonances (4.42 and 4.36 ppm) are broadened in $CDCl_3$ solution such that $J_{HH}$ coupling is unresolved, possibly due to rotameric interconversion in solution (**Scheme 7.11**) though sub-ambient temperature NMR spectra were of unsatisfactory appearance due to precipitation of the compound (in $CDCl_3$) below ~0 °C. The arsolyl ring-carbon $^{13}C\{^1H\}$ signals at 144.6 and 132.1 ppm ($CDCl_3$) are slightly upfield of the free ligand (146.6 and 139.9 ppm) and all other nuclei are found in their usual regions of unremarkable spectroscopic position. Large crystals could be grown from a variety of solvents (it transpired that this complex was particularly easy to crystallise) and a simplified molecular structure is shown in **Figure 7.10**.

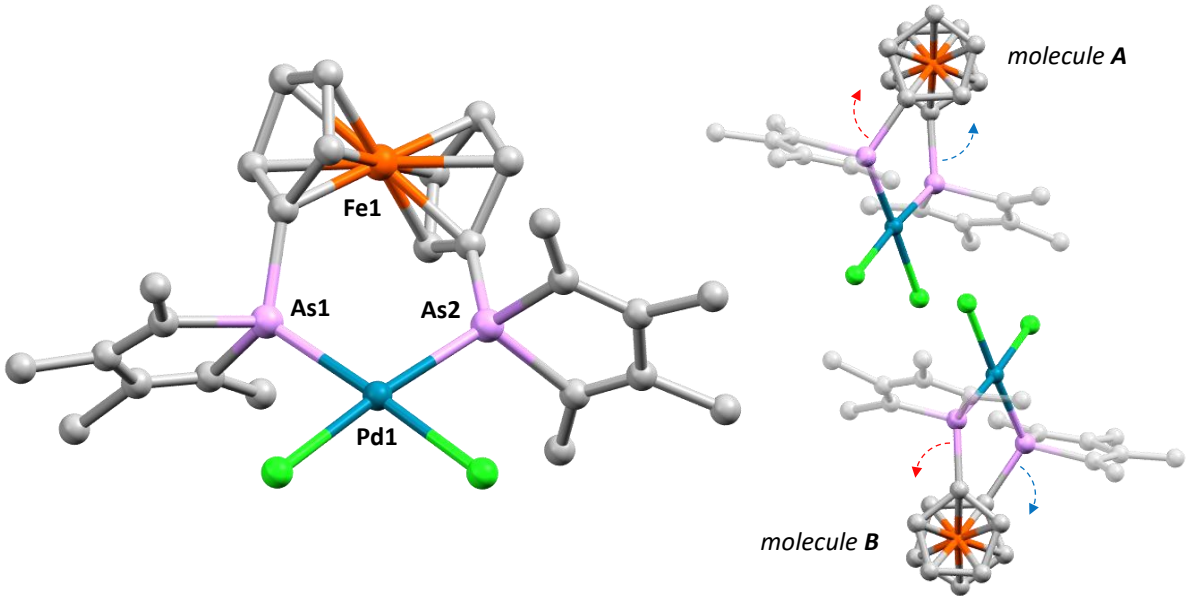
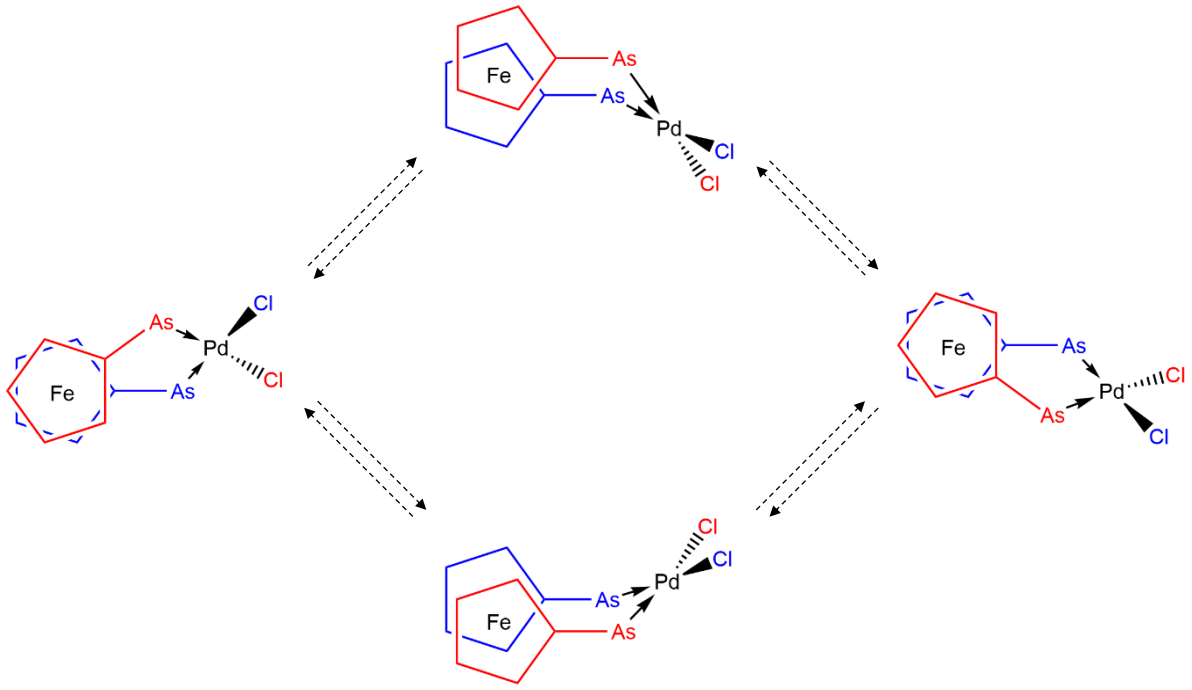



**Figure 7.10**: The molecular structure of *cis*-[Pd(κ²-tmaf)$Cl_2$] in a crystal. All features simplified due to poor data quality arising from high angle diffuse scattering (see text). **Inset**: The asymmetric unit containing two crystallographically unique rotamers **A** and **B** which differ in the relative "twist" of the tmaf ligand (denoted by blue and red arrows).

It should be remarked here that the molecular structure of *cis*-[Pd(κ²-tmaf)$Cl_2$] as depicted in **Figure 7.10** is without thermal displacement ellipsoids and all atoms were modelled as solid, isotropic spheres. Poor data quality arose from extensive diffuse scattering (**Figure 7.11**) particularly at high reflection angles, hence exceedingly low bond precision results and only atom connectivity alongside superficial structural features can be established (a short explanation is given below). The molecular structure of *cis*-

[Pd(κ²-tmaf)Cl₂] confirms product identity and is in accord with other chelating complexes of divalent palladium.[38-41] The tmaf moiety adopts a staggered-*gauche* conformation typical of those already seen for the chelating mode of this ligand, with As→Pd dative distances of *ca* 2.3 Å (sum covalent radii 2.58 Å). The asymmetric unit (orthorhombic $P2_12_12_1$,) finds a pair of discrete chiral (approximately $C_2$-symmetric) molecules which are distinguished by opposing directions of "twist" inherent to the ferrocene-diyl moiety.* Thus, when viewed along the same orientation (**Figure 7.10**, **Inset**) each molecule is perceived as rotameric about the square-planar Pd(II) centre; such a configuration is unlikely maintained in solution, since barriers to ferrocene rotation are typically small and "flipping" of the palladium square plane requires no breaking of As→Pd interactions (**Scheme 7.11**). A similar feature is noted for *cis*-[Pd(κ²-dmpf)Cl₂] (dmpf = 1,1'-bis(dimethylphosphino)ferrocene).[42]




**Scheme 7.11**: Rotational isomerism in *cis*-[Pd(κ²-tmaf)Cl₂] *via* a "flipping" manoeuvre of the Pd(II) centre.

A brief discussion on the phenomenon of diffuse scattering follows, which is a symptom of the crystal lattice deviating from short-range regularity. Whereas BRAGG diffraction arises from constructive

* Orthorhombic $P2_12_12_1$ is a non-centrosymmetric space group. Hence, the opposing configuration of one molecule cannot be generated by either an inversion or reflection operation performed on another, as would be the case in other commonly encountered and centrosymmetric space groups *e.g.*, triclinic *P*-1 or monoclinic $P2_1/n$. This means that the conformations of the molecules in the asymmetric unit (and by extension, the crystal lattice) are absolute.

(that is, additive) interference of scattering amplitudes, any internal defect, irregularity, or disorder will lead to suppression in the intensity of a BRAGG peak (at a given $hk\ell$) and the extraneous scattering intensity is instead reallocated into diffuse scattering. This manifests as weak lines which interconnect the BRAGG peaks and decreases the effective $I/\sigma$ (signal/noise) ratio in the vicinity of the bright diffraction spots, hence the poor bond precision measured here. It should be noted that whilst BRAGG peaks describe the unit cell of the crystalline lattice (and therefore the average *repetitive* arrangement of the entities within the crystal), diffuse scattering describes the average *deviation* from the repeating lattice and is always present to a non-zero (but ideally insignificant) extent in real crystalline samples. Strategies do exist for modelling diffuse scattering although none were attempted here since the physical origin of disorder was undetermined, and the computational expense is by no means trivial; an exceptionally-informative explanation of diffuse scattering in single crystals with focus given to a non-expert audience may be found in the review by WELBERRY and GOOSSENS.[43] **Figure 7.11** shows an EWALD projection of the reciprocal lattice (the FOURIER transform of the BRAVAIS lattice) along each of the reciprocal axes $a^*$, $b^*$ and $c^*$; the localised, short-range disorder is readily observable in the former whereas the latter pair have well-defined reciprocal crystal planes with clear BRAGG peaks. The *0KL*, *H0L* and *HK0* (reciprocal $0k\ell$, $h0\ell$ and $hk0$ MILLER planes) cross-sections are shown alongside; diffuse scattering connecting the BRAGG peaks is immediately visible in the former.

This phenomenon was (disappointingly) present in no fewer than four separate crystal specimens – all grown from varying solvent mixtures under different conditions – where it was hoped that subtle conditional influences on crystal packing may yield a more-regular material. As mentioned above, *cis*-[$PdCl_2(\kappa^2$-tmaf)] proved rather easy to crystallise and always yielded large, millimetre-sized needles, although given the trend here one might surmise that the occurrence of diffuse scattering in this compound could be simply inherent. It is still hoped that a suitable batch of crystals will be obtained eventually (perhaps by future researchers).

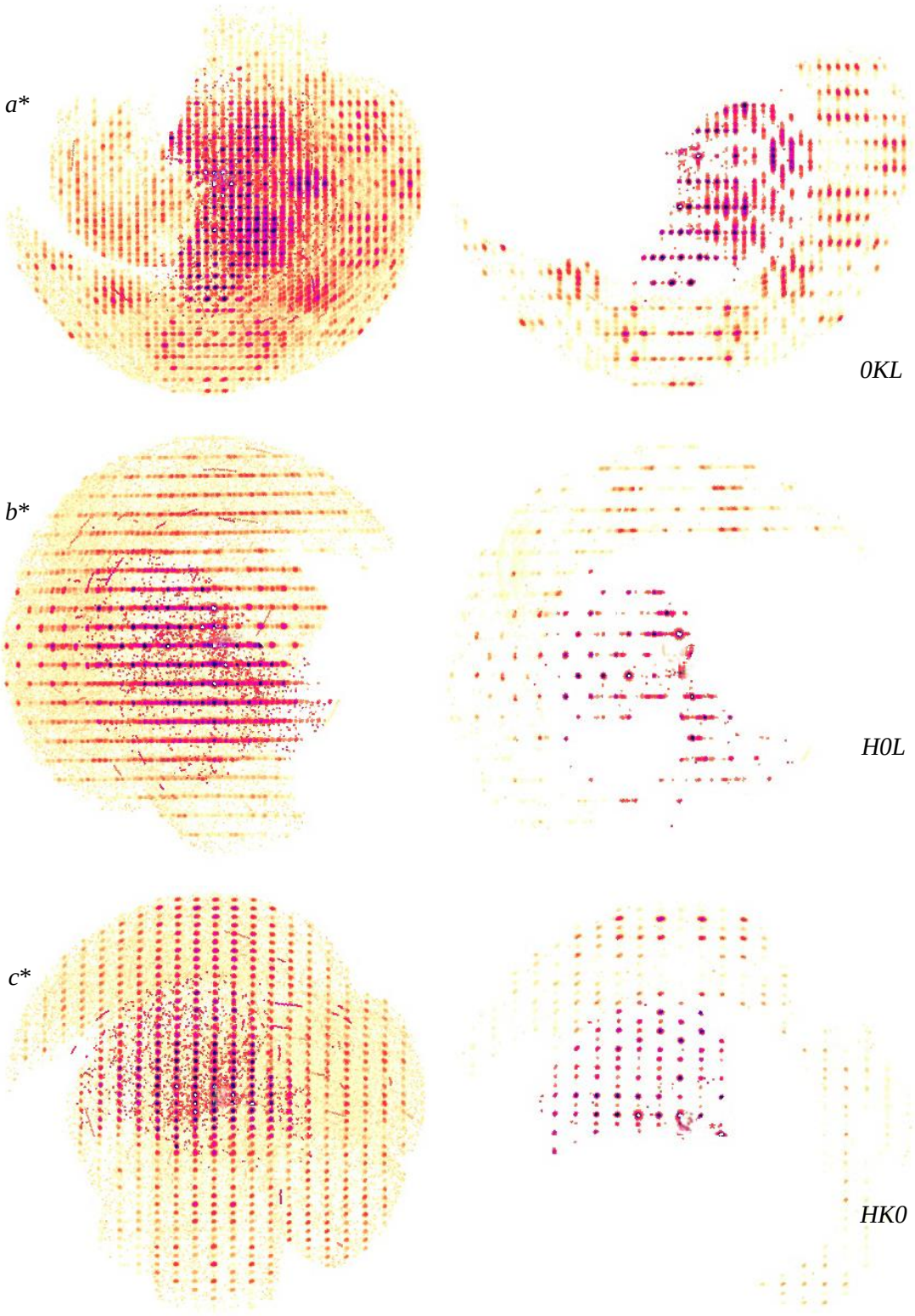



**Figure 7.11**, **left**: The reciprocal lattice of a crystal of [Pd(κ²-tmaf)$Cl_2$] viewed along the *a** (**top**), *b** (**middle**) and *c** (**bottom**) axes highlighting the short-range irregularity present in the *a** direction. **Right**: The *0KL* (**top**), *H0L* (**middle**) and *HK0* (**bottom**) reciprocal planes. See the accompanying text for an overview of diffuse scattering.

Insofar as the TOLMAN electronic parameter[22] (ν) is employed as a descriptor of the combined electronic properties (σ and π) of a ligand "L",* the $\%V_{bur}$ parameter was introduced by CLAVIER and NOLAN as a means to alternatively quantify the steric pressure imparted by a ligand "L" upon a metal centre.[44] The model imagines a sphere of arbitrary radius (typically 3.5 Å, sufficient to encompass the VAN DER WAALS radii of most *d*-block ions) with its origin at the centre of a transition metal complex; the volume of this sphere represents the potential coordination space around the metal centre and the proportion of this sphere occupied by the ligand of interest is defined as the percent buried volume, $\%V_{bur}$.[45] The concept has been widely embraced by the chemical community as a means to guide the design of artisanal/bespoke ligands for use in catalytic settings,[46] or simply as a tool to inspect and describe the fundamental nature of the metal-ligand interaction.[47] The $\%V_{bur}$ parameter is conveniently determined from X-ray crystallographic data, though since homogenous catalytic reactions almost universally take place in solution the value obtained therefrom is not totally independent of solid-state influences which may artificially inflate/deflate the measured steric bulk of the ligand. However, provided there are no extenuating inter- and/or intramolecular features which significantly distort the ligand within the crystal structure, and since almost all $\%V_{bur}$ values are obtained from atom coordinates measured in the solid-state making the library internally consistent, the caveat is of little consequence provided the limitation is recognised and judiciously applied.[48] The utility of $\%V_{bur}$ has all but surpassed that of the TOLMAN cone angle[22] since the former is an introspective model (from the perspective of the metal) whereas the latter is an extrospective model (from the perspective of the ligand). More generally, the $\%V_{bur}$ parameter better encapsulates the steric obtrusion of more irregularly shaped ligands than phosphines, for which free rotation about the Ni-P bond inscribes an *average* cone of influence.

Wherein such a ligand may find potential future application in homogenous catalysis (though not examined in this work), the percent buried volume ($\%V_{bur}$) of the tmaf ligand within the Pd(II) coordination sphere is calculated† to be 36.9%; a steric isocontour map is shown in **Figure 7.12**.‡

* Purely defined as the wavenumber of the $A_1$ symmetric $\nu_{CO}$ stretch displayed by the corresponding $[NiL(CO)_3]$ complex.
† The Samb*V*ca 2.1 web application was used for $\%V_{bur}$ calculations. Following the recommendations by NOLAN in *Ref.* 45, BONDI radii are scaled by a factor of 1.17 and a sphere radius of 3.5 Å was chosen.
‡ An explanation of the algorithm used to generate these steric maps is given by A.G. SUÁREZ, D.J. NELSON and S.P. NOLAN, *Chem. Comm.*, **2017**, *53*, 2650—2660.

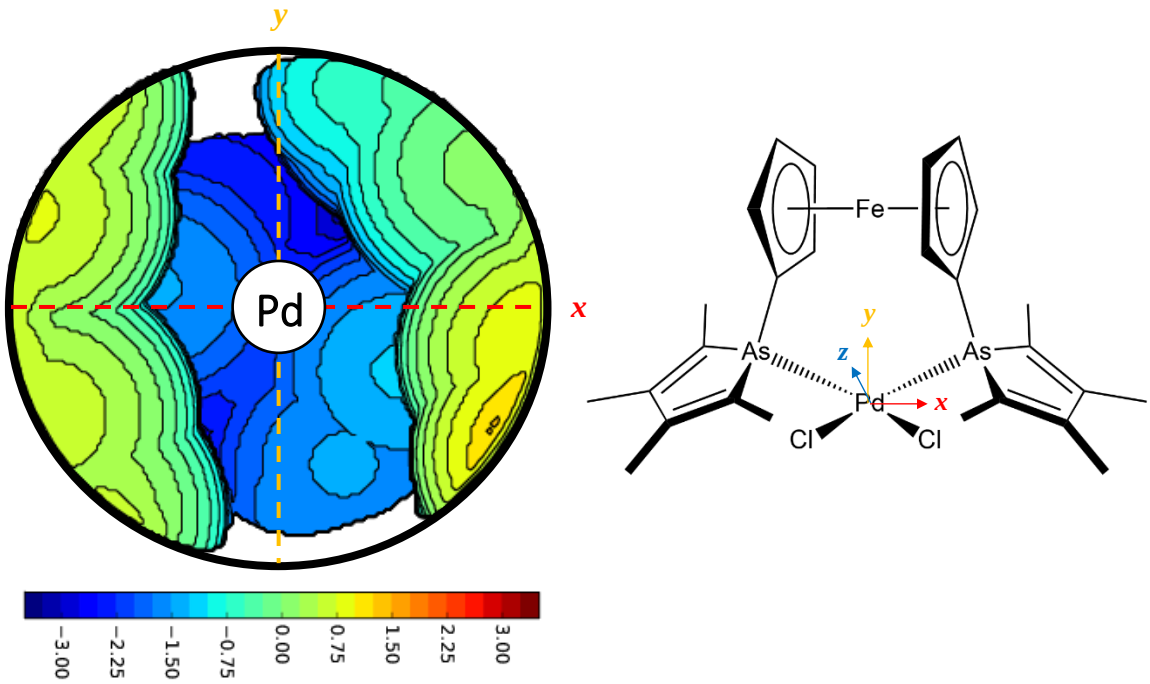



**Figure 7.12**: A topological steric map of [Pd(κ²-tmaf)Cl₂] viewed along the *xz*-coordination plane of the metal centre, with the chloride ligands (omitted for clarity) coming out of the page. Hydrogen atoms were included in calculations. Blue contours represent recessions of steric influence, and *vice-versa* for red contours.

The pocket formed by the tmaf ligand presents a valley which is approximately perpendicular to the square coordination plane of the of the palladium centre, running between the north and south poles of the steric map. As apparent from the crystal structure (**Figure 7.10**), the bis(arsolyl) substituents do not especially intrude into the coordination sphere of the metal centre and are splayed outward, their disposition resembling a "clam-shell" configuration where the Pd(II) atom is appreciably exposed. In this regard, the tmaf ligand is rather unobtrusive compared to other conventional bidentate ligands typically used in homogenous catalysis. A selection of these [Pd(κ²-ligand)Cl₂] complexes, their $\%V_{bur}$ values and selected crystallographic data are compiled in **Table 7.1** for the purposes of comparison. It is interesting that the average $\%V_{bur}$ value for these bidentate ligands is *ca* 50% and the tmaf ligand contrasts these with its rather diminutive presence of only *ca* 37%. In fact, the closest numerical approximation to the tmaf ligand would be a single tricyclohexylphosphine ($PCy_3$) entity, which consumes *ca* 35% of the buried volume within *trans*-$[Pd(PCy_3)_2Cl_2]$.[49]

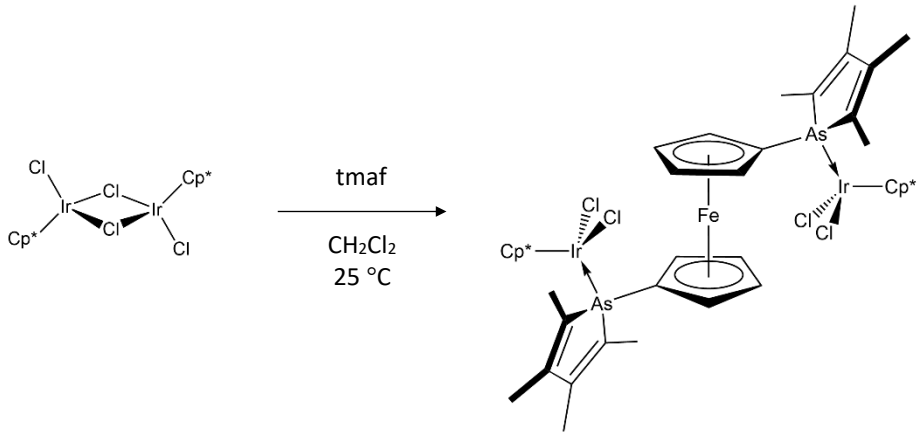
**Table 7.1**: Calculated percent buried volume (%$V_{bur}$) parameters and selected crystallographic data for some [Pd(κ²-ligand)$Cl_2$] complexes commonly used in homogenous catalysis.

| κ²-ligand | Abbreviation | %$V_{bur}$ | D→Pd (Å) | Bite angle (°) | *Ref.* |
|---|---|---|---|---|---|
| [Fe{η⁵-$C_5H_4$($AsC_4Me_4$)}₂] | tmaf | 36.9 | ~2.36 | ~99 | This work |
| **Ferrocenes** | | | | | |
| [Fe{η⁵-$C_5H_4PMe_2$}₂] | dmpf | 46.7 | 2.26 | 98 | 42 |
| [Fe{η⁵-$C_5H_4$($PC_4Me_2H_6$)}₂] | MeFL | 53.2 | 2.27 | 100 | 9 |
| [Fe{η⁵-$C_5H_4PPh_2$}₂] | dppf | 55.7 | 2.28 | 97 | 38 |
| [Fe{η⁵-$C_5H_4$P(*i*-Pr)₂}₂] | dippf | 56.5 | 2.30 | 104 | 50 |
| [Fe{η⁵-$C_5H_4$P(*t*-Bu)₂}₂] | dtbpf | 61.0 | 2.35 | 104 | 51 |
| **Alkanes** | | | | | |
| $Ph_2PCH_2CH_2PPh_2$ | dppe | 46.8 | 2.22 | 85 | 52 |
| $Ph_2PCH_2PPh_2$ | dppm | 48.3 | 2.24 | 73 | |
| $Ph_2PCH_2CH_2CH_2PPh_2$ | dppp | 53.4 | 2.25 | 90 | |
| $Cy_2PCH_2CH_2Cy_2$ | dcpe | 55.1 | 2.33 | 87 | 53 |
| (*t*-Bu)$_2$$PCH_2CH_2$P(*t*-Bu)$_2$ | dtbpe | 58.9 | 2.27 | 89 | 54 |
| **Other** | | | | | |
| (IMes)$CH_2CH_2$(IMes) | bis-NHC | 52.6 | 2.00 | 87 | 55 |
| $C_{44}H_{32}P_2$ | BINAP | 52.8 | 2.25 | 92 | 56 |
| $C_{39}H_{32}OP_2$ | xantphos | 54.4 | 2.28 | 101 | 57 |

## 7.4 Monodentate Open-Bridge Coordination Complexes

### 7.4.1 Synthesis of [$Ir_2$(μ-κ¹:κ¹-tmaf)$Cl_4$(η⁵-$C_5Me_5$)₂]

It was also possible to coordinate both donor atoms to separate metal centres to generate the open-bridge form of the tmaf ligand. Thus, combination of one equivalent each [$Ir_2$(μ-Cl)$_2$$Cl_2$(η⁵-$C_5Me_5$)₂] and the bis(arsolyl)ferrocene in $CH_2Cl_2$ solution gives the expected [$Ir_2$(μ-κ¹:κ¹-tmaf)$Cl_4$(η⁵-$C_5Me_5$)₂] (**Scheme 7.12**) as a bright yellow solid in high yield after re-crystallisation from $CH_2Cl_2$/*n*-hexane. Spectroscopic features are unremarkable with a slight downfield shift of the relevant hydrogen signals in the $^1$H NMR spectrum, and *vice-versa* for the tmaf ligand nuclei in the $^{13}$C{$^1$H} spectrum. Perhaps the most noteworthy feature of the product is its precedent as the first iridium complex of any arsole ligand. Large single crystals of this milestone compound were obtained from $CH_2Cl_2$/*n*-hexane and the molecular structure is shown in **Figure 7.13**.




**Scheme 7.12**: Synthesis of $[Ir_2(\mu\text{-}\kappa^1\text{:}\kappa^1\text{-tmaf})Cl_4(\eta^5\text{-}C_5Me_5)_2]$; Cp* = $\eta^5$-$C_5Me_5$.

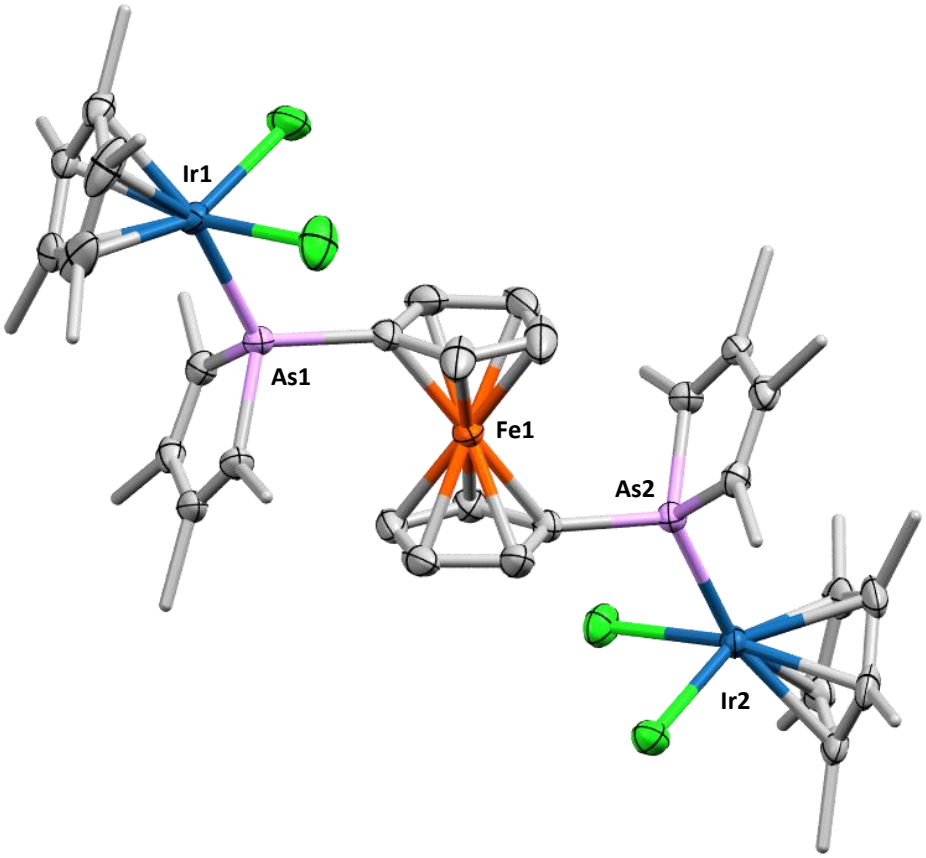


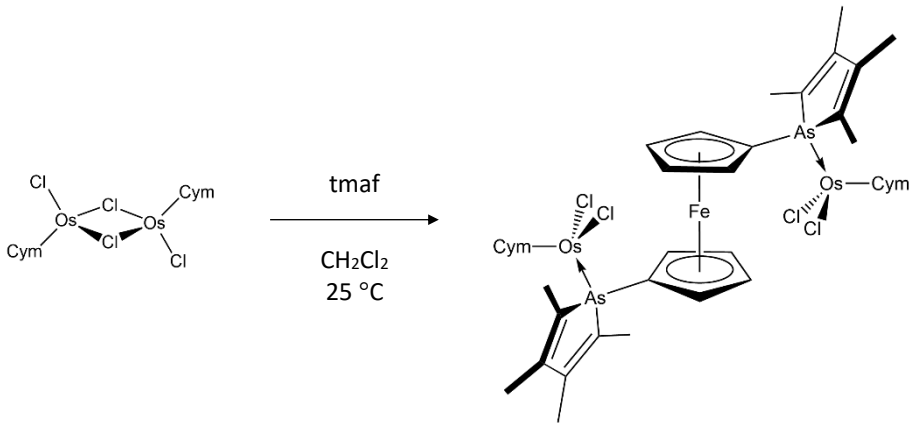

**Figure 7.13**: The molecular structure of $[Ir_2(\mu\text{-}\kappa^1\text{:}\kappa^1\text{-tmaf})Cl_4(\eta^5\text{-}C_5Me_5)_2]$. Methyl groups simplified and hydrogen atoms omitted for clarity. Ellipsoids shown at 50% displacement.

Though the solid-state configuration appears to be centrosymmetric (with an inversion centre located at Fe1) no formal crystallographic symmetry is imposed upon the molecule and each iridium-arsole locale is technically unique; differences in interatomic distances and angles are, however, statistically indistinguishable. The complex features the tmaf ligand acting as a monodentate bridge between a pair of

$IrCl_2(\eta^5\text{-}C_5Me_5)$ centres. The tmaf chassis exists in a staggered-*anti* conformation (torsion angle 172°) with the arsolyl pendants gathered at the interior of the ferrocene-diyl moiety. The *pseudo*-octahedral Ir(III) centre is best described as a three-legged piano stool with mean As→Ir dative distances of 2.401(5) Å (sum of covalent radii: 2.60 Å), intermediate between relevant distances in $[Ir(AsEt_3)Cl_2(\eta^5\text{-}C_5Me_5)]$ (2.382(4) Å) and $[Ir(AsPh_3)Cl_2(\eta^5\text{-}C_5Me_5)]$ (2.430(7) Å)[58] (probably speaking to the relative donor strength of the As(III) function) and comparable to other arsine complexes of the $IrCl_2(\eta^5\text{-}C_5Me_5)$ centre.[59, 60] Other dimensions of interest, such as the internal distances within the arsolyl rings, are indistinguishable from the free ligand and call for no comment.

### 7.4.2 Synthesis of $[Os_2(\mu\text{-}\kappa^1\text{:}\kappa^1\text{-tmaf})Cl_4\{\eta^6\text{-}MeC_6H_4(i\text{-}Pr)\text{-}4\}_2]$

The first osmium-arsole complex was prepared similarly: combining one equivalent tmaf and the halide bridged dimer $[Os_2(\mu\text{-}Cl)_2Cl_2\{\eta^6\text{-}MeC_6H_4(i\text{-}Pr)\text{-}4\}_2]$ in $CH_2Cl_2$ gives the expected $[Os_2(\mu\text{-}\kappa^1\text{:}\kappa^1\text{-tmaf})Cl_4\{\eta^6\text{-}MeC_6H_4(i\text{-}Pr)\text{-}4\}_2]$ (**Scheme 7.13**) as an air-stable, bright yellow solid in high yield. The composition is established by the usual spectroscopic methods and a single crystal structure determination (**Figure 7.14**).




**Scheme 7.13**: Synthesis of $[Os_2(\mu\text{-}\kappa^1\text{:}\kappa^1\text{-tmaf})Cl_4\{\eta^6\text{-}MeC_6H_4(i\text{-}Pr)\text{-}4\}_2]$; Cym = $\eta^6\text{-}C_6H_4Me(i\text{-}Pr)\text{-}4$, *para*-cymene.

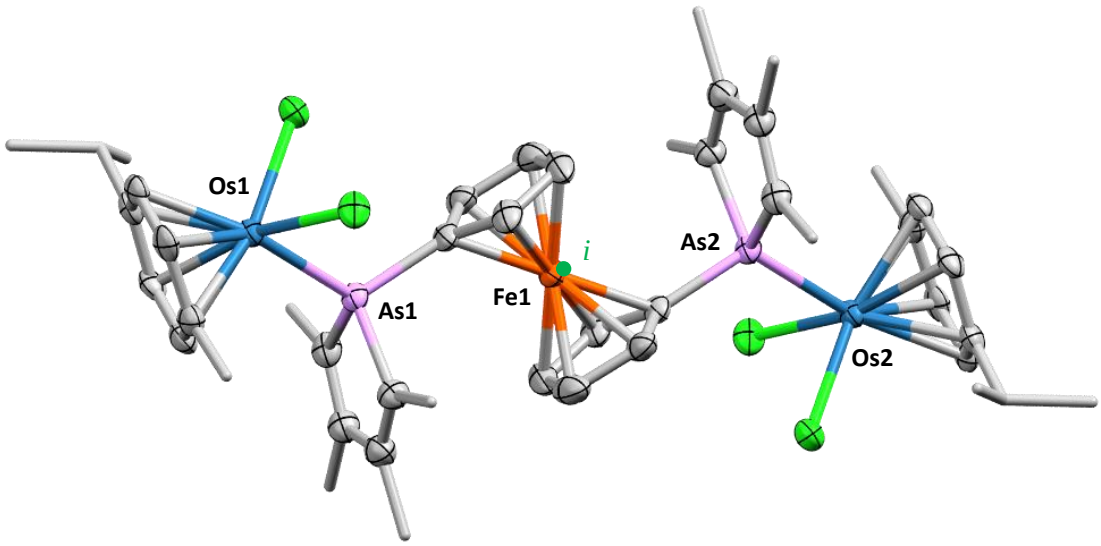



**Figure 7.14**: The molecular structure of $[Os_2(\mu\text{-}\kappa^1\text{:}\kappa^1\text{-tmaf})Cl_4\{\eta^6\text{-}MeC_6H_4(i\text{-}Pr)\text{-}4\}_2]\cdot 2CHCl_3$ in a crystal. Methyl and isopropyl groups simplified and chloroform solvate molecules and hydrogen atoms omitted for clarity. Ellipsoids shown at 50% displacement. Only one half of the molecule is crystallographically unique in $P2_1/n$. *i* = inversion centre.

The overall molecular configuration of $[Os_2(\mu\text{-}\kappa^1\text{:}\kappa^1\text{-tmaf})Cl_4\{\eta^6\text{-}MeC_6H_4(i\text{-}Pr)\text{-}4\}_2]$ in the solid-state is similar to the iridium complex described above and only brief details will be given here. The tmaf ligand exists in a perfect staggered-*anti* conformation (torsion angle 180°) since Fe1 coincides with a crystallographic centre of inversion and only one half of the molecule is structurally unique. The As→Os dative distance of 2.4369(6) Å is smaller than the sum of covalent radii (2.63 Å) but comparable to the same in $[WOs(\mu\text{-}CAsPh_2)Cl_2(CO)_2\{\eta^6\text{-}MeC_6H_4(i\text{-}Pr)\text{-}4\}\{\kappa^3\text{-}HB(C_3HN_2Me_2)_3\}]$ (2.4715(5) Å), the only other structurally characterised arsine complex of the $OsCl_2\{\eta^6\text{-}C_6H_4Me(i\text{-}Pr)\}$ fragment. Distances and angles within and around the arsolyl and ferrocene-diyl moieties are typical.

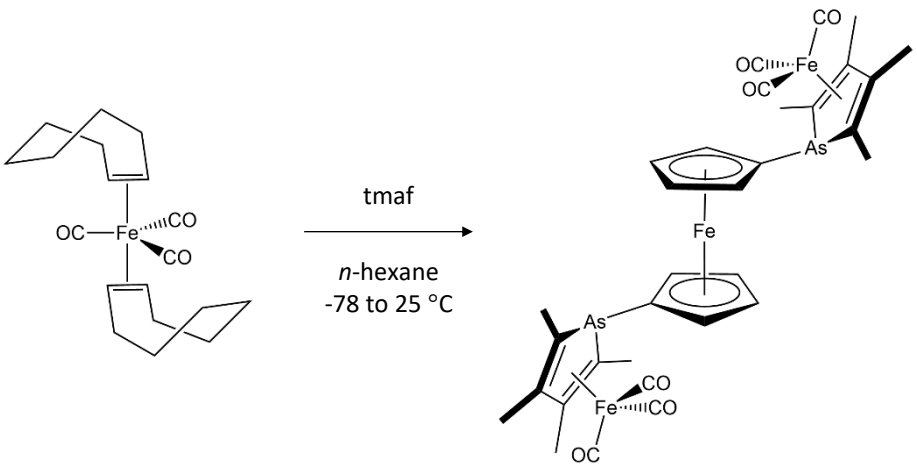
### 7.4.3 Synthesis of $[Fe_2(\mu\text{-}\eta^4\text{:}\eta^4\text{-tmaf})(CO)_6]$

Further displaying the utility of the tmaf ligand, the exceedingly labile $[Fe(COE)_2(CO)_3]$[61] (COE = $\eta^2$-*cis*-cyclooctene) reacts in *n*-hexane medium to provide three orange complexes in low-to-modest isolated yields following chromatography. None of these would prove to be the anticipated $[Fe(\kappa^2\text{-tmaf})(CO)_3]$,*

* Such a complex was pursued to demonstrate coordination of the tmaf ligand to a trigonal bipyramidal metal centre since octahedral, tetrahedral, and square-planar geometries had already been encountered.

which in hindsight would have been better prepared by reductive decarbonylation of $[Fe(CO)_5]$ with alcoholic $NaBH_4$ in the presence of the bidentate ligand.[62]

The first compound encountered during chromatography was obtained in the highest yield of the trio (*ca* 40%) and was symmetric by $^1H$ NMR ($C_6D_6$), displaying four signals at 4.04 and 3.76 (*pseudo*-triplets; $J_{HH}$ = 1.7 Hz) and 1.76 and 1.55 ppm (singlets) for the cyclopentadienyl and arsolyl units, respectively. The solution IR spectrum (*n*-hexane) exhibited three $\nu_{CO}$ absorptions at 2037(vs), 1976(s) and 1965(s) $cm^{-1}$; whereas a *pseudo-fac* tricarbonyl complex of the type $[Fe(\kappa^2\text{-tmaf})(CO)_3]$ would also be expected to display three carbonyl vibrational modes, such a formulation is explicitly ruled-out by high-resolution mass spectrometry which finds ion fragments corresponding to and deriving from a species of the composition $[Fe_2(tmaf)(CO)_6]$. Furthermore, the $^{13}C\{^1H\}$ NMR spectrum of this compound finds *no signals whatsoever* in the region 150—130 ppm where the arsolyl ring-carbon nuclei resonances would typically appear and are instead located appreciably upfield at 108.9 and 88.1 ppm. From these combined data, the complex does thus not appear to feature the tmaf ligand in a coordination mode which was initially anticipated – rather, an open-bridge doubly-coordinated $\eta^4$-complex (as is the *penchant* for the $Fe(CO)_3$ fragment) was thus proposed. Single crystals were grown by evaporation of $Et_2O$ solution at -20 °C and the molecular structure was confirmed to be – in agreement with spectroscopic data – $[Fe_2(\mu\text{-}\eta^4\text{:}\eta^4\text{-tmaf})(CO)_6]$ as shown in **Figure 7.15**. The complex is noteworthy for being the third definitive example of the $\eta^4$ coordination mode for an arsole ligand alongside $[Co_2(\mu\text{-CO})_2(CO)_2(\eta^4\text{-PhAsC}_4Et_4)_2]$ (**Chapter 3**, **Section 3.2.4**) and $[MoFe_2(\mu_3\text{-}\eta^1\text{:}\eta^1\text{:}\eta^4\text{-AsC}_4Me_4)(CO)_9(\eta^5\text{-C}_5H_5)]$ (**Chapter 5**, **Section 5.4.8**).




**Scheme 7.14**: Synthesis of $[Fe_2(\mu\text{-}\eta^4\text{:}\eta^4\text{-tmaf})(CO)_6]$.

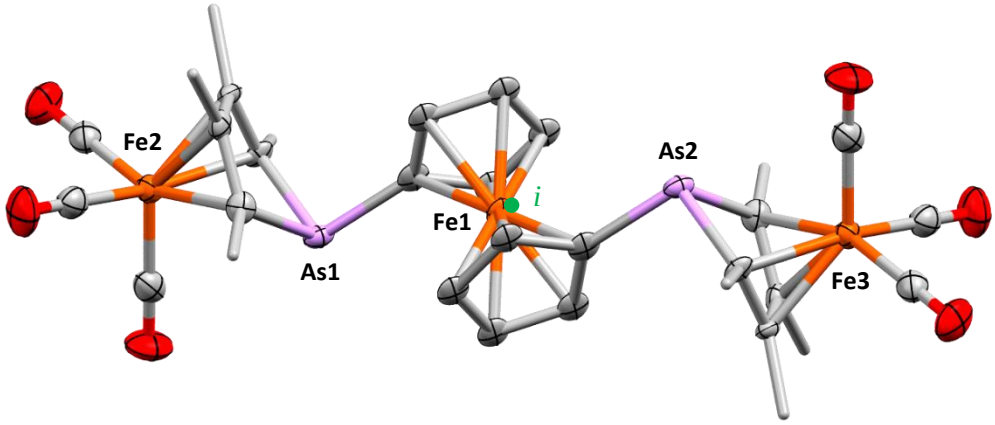


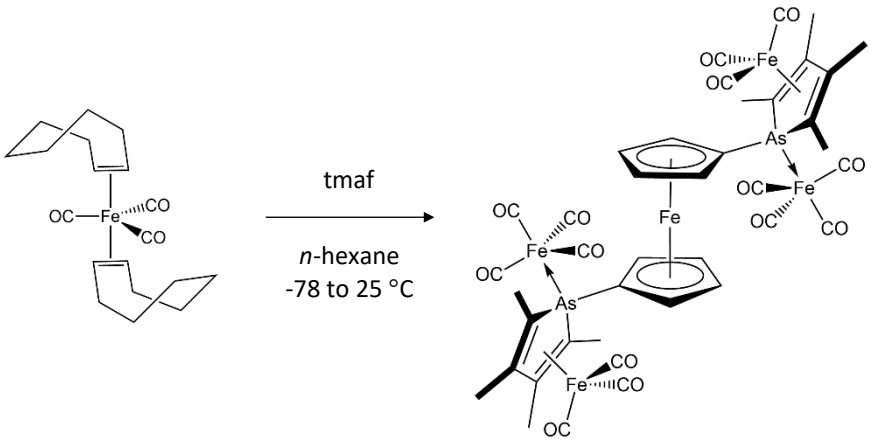

**Figure 7.15**: The molecular structure of $[Fe_2(\mu\text{-}\eta^4\text{:}\eta^4\text{-tmaf})(CO)_6]$ in a crystal. Methyl groups simplified and hydrogen atoms omitted for clarity. Ellipsoids shown at 50% displacement. Only one half of the molecule is crystallographically unique in *P*-1. *i* = inversion centre.

The crystal structure finds the tmaf ligand serving as four-electron donors *via* the dearomatised arsolyl butadiene moieties to a pair of $Fe(CO)_3$ groups, the coordination geometries of which are square-based pyramids ($\tau_5$ = 0.05) with the two butadiene C=C donors occupying a pair of mutually *cis* basal sites. The tmaf ligand exists in a staggered-*anti* confirmation and only one half of the centrosymmetric molecule is crystallographically unique (unit cell triclinic *P*-1) with Fe1 situated on an inversion centre. The arsolyl ring displays conspicuous envelope folding upon complexation of the $Fe(CO)_3$ fragment with the arsenic atom extruded by *ca* 32° from the mean plane of the butadiene atoms, compared to *ca* 8° for the free tmaf ligand (**Figure 7.2**) – similar extrusion angles are noted for other $\eta^4$-heterocyclopentadiene ligands serving transition metal centres (*e.g.*, $[Fe(\eta^4\text{-}Me(Me_3Si)SiC_4Ph_4)(CO)_3]$[63] 34.5°; $[Mo(\eta^4\text{-}Me_2SiC_4H_2Me_2)_2(CO)_2]$[64] 36.6°; $[Co(\eta^4\text{-}O_2SC_4H_4)(\eta^5\text{-}C_5H_5)]$[65] 34.8°). Reflecting the relocation of electron density from the diene to the Fe(0) atom and a formal $sp^2 \rightarrow sp^3$ re-hybridisation of the same, carbon-carbon distances around the arsolyl ring are also appreciably affected with the $C_\alpha$=$C_\beta$ bonds being elongated by some 0.1 Å (from the free ligand) to 1.435(5) Å (mean). These are crystallographically indistinguishable from the formal $C_\beta$-$C_\beta$ single bond (1.440(6) Å); the mean endocyclic As-$C_\alpha$ bond lengths of *ca* 1.94 Å are, however, otherwise invariant upon complexation of the $Fe(CO)_3$ centre. The Fe-diene centroid distance of *ca* 1.71 Å compares favourably against the substantial library of $[Fe(\eta^4\text{-diene})(CO)_3]$ complexes already structurally characterised[66-70] and the related $[MoFe_2(\mu_3\text{-}\eta^1\text{:}\eta^1\text{:}\eta^4\text{-}AsC_4Me_4)(\eta^5\text{-}C_5H_5)(CO)_9]$ complex described in **Section 5.4.8** of **Chapter 5**. The individual Fe-$C_{diene}$ distances (mean 2.10 Å) are crystallographically

equivalent within the precision limits of the data such that the iron centre is symmetrically disposed about the butadiene entity.

### 7.4.4 Synthesis of $[Fe_4(\mu\text{-}\kappa^1\text{:}\kappa^1\text{-}\eta^4\text{:}\eta^4\text{-tmaf})(CO)_{14}]$

The identity of second product isolated from the reaction (in *ca* 20% yield) was more difficult to deduce from spectroscopic data, since the solution IR spectrum (*n*-hexane) finds six $\nu_{CO}$ vibrations at 2058(s), 2044(vs), 1994(s), 1981(vs), 1966(s) and 1948(s) $cm^{-1}$. The $^{13}C\{^1H\}$ NMR spectrum is similar to $[Fe_2(\mu\text{-}\eta^4\text{:}\eta^4\text{-tmaf})(CO)_6]$ above – that is, no signals appear in the region 150—130 ppm which could be attributed to arsolyl ring-carbon nuclei in "ordinary" chemical environments, though a pair of resonances at 218.2 and 210.6 ppm are suggestive of two distinct time-averaged carbonyl environments. High resolution mass spectrometry was also regrettably less informative than had been hoped, although the general manifold of ion signals suggested the unknown compound possessed a reasonably greater molecular mass than the previous product. Single crystals were obtained from benzene/cyclohexane and revealed the product to be $[Fe_4(\mu\text{-}\kappa^1\text{:}\kappa^1\text{-}\eta^4\text{:}\eta^4\text{-tmaf})(CO)_{14}]$ featuring $Fe(CO)_4$ and $Fe(CO)_3$ fragments saturating the tmaf ligand *via* both the arsenic and diene donor functions, respectively. The molecular structure is shown in **Figure 7.16**




**Scheme 7.15**: Synthesis of $[Fe_4(\mu\text{-}\kappa^1\text{:}\kappa^1\text{-}\eta^4\text{:}\eta^4\text{-tmaf})(CO)_{14}]$.

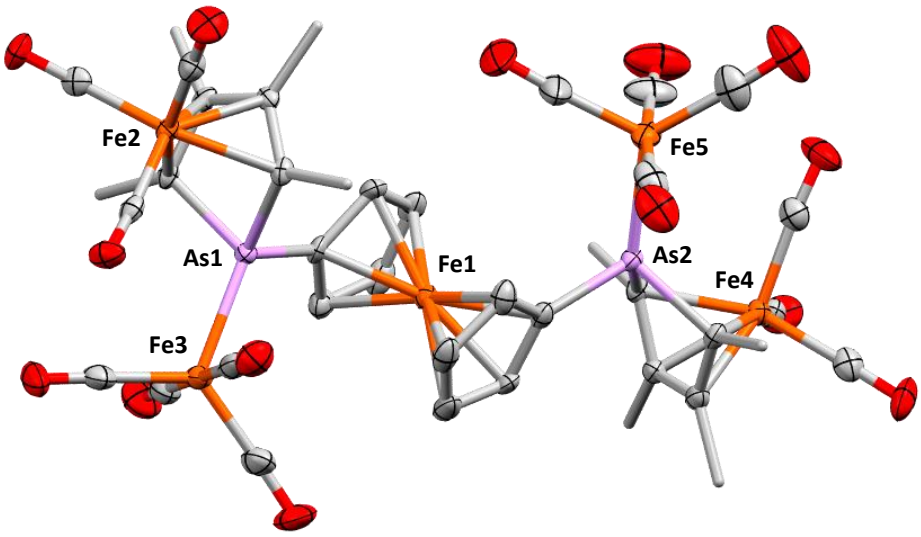



**Figure 7.16**: The molecular structure of $[Fe_4(\mu\text{-}\kappa^1\text{:}\kappa^1\text{-}\eta^4\text{:}\eta^4\text{-tmaf})(CO)_{14}]$ in a crystal. Methyl groups simplified and hydrogen atoms omitted for clarity. Ellipsoids shown at 50% displacement.

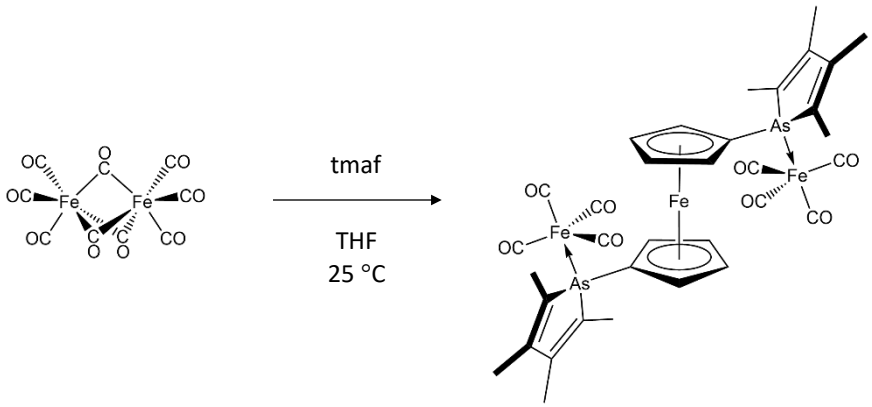
The molecular structure of $[Fe_4(\mu\text{-}\kappa^1\text{:}\kappa^1\text{-}\eta^4\text{:}\eta^4\text{-tmaf})(CO)_{14}]$ in the solid state comprises a non-centrosymmetric arrangement wherein the tmaf ligand exists in an eclipsed conformation with anticlinal arsolyl pendants (torsion angle 135°) and the *As*-bound $Fe(CO)_4$ and diene-bound $Fe(CO)_3$ fragments all outwardly facing from the exterior of the molecule. The butadiene-iron tricarbonyl portions of the molecule are essentially identical in arrangement to $[Fe_2(\mu\text{-}\eta^4\text{:}\eta^4\text{-tmaf})(CO)_6]$ previously discussed above and deserve no special mention. The pair of As→Fe dative bonds of 2.3372(7) and 2.3404(7) Å are crystallographically equivalent (sum of covalent radii 2.51 Å) and although the literature is largely devoid of structurally characterised $[Fe(AsR_3)(CO)_4]$ complexes for comparison (for R = Me, As→Fe 2.296 Å and R = $C_6H_4Me$, As→Fe 2.392 Å), these bond lengths are favourable against the same in $[MoFe_2(\mu_3\text{-}\eta^1\text{:}\eta^1\text{:}\eta^4\text{-}AsC_4Me_4)(\eta^5\text{-}C_5H_5)(CO)_9]$ (**Chapter 5**, **Section 5.4.8**) and $[Fe_2(\mu\text{-}\kappa^1\text{:}\kappa^1\text{-tmaf})(CO)_8]$ (*vide infra*). Noteworthy is the *equatorial* disposition of the arsenic donors within the trigonal bipyramidal coordination spheres of the Fe(0) atoms ($\tau_5$ = 0.81), finding a set of four crystallographically identical Fe-C and C≡O bonds (mean 1.785 and 1.445 Å, respectively). This in itself is relatively uncommon for monosubstituted $[Fe(L)(CO)_4]$ complexes which show strong tendencies toward axial substitution patterns[71-76] (extenuating steric or electronic features notwithstanding[77, 78]) for the same reason that the complex $[Co(AsC_4Ph_4)(CO)_4]$ was also substituted by incoming ligands in the axial position (**Chapter 3**, **Section 3.5**): that is, the privileged π-acceptor ligands typically populate the equatorial plane since 1) the π-basicity of the metal centre is enhanced

in these sites, and 2) no two ligands are directly *trans* to one-another, reducing competition for retrodonation.

Since there is no convincing evidence to suggest this As(III) ligand to be an objectively superior π-acid to CO *per se*, the equatorial disposition of the arsolyl donors about the $Fe(CO)_4$ centres in [$Fe_4$(μ-κ$^1$:κ$^1$-η$^4$:η$^4$-tmaf)$(CO)_{14}$] cannot be wholly explained by π-bonding arguments. Concessions could be made based on geometric demands within the molecule: some *exceptionally voluminous* phosphine ligands (*e.g.*, $PPh(PPh_2)_2$ or P{=C$(SiMe_3)_2$}{N$(SiMe_3)_2$}) adopt equatorial positions about the $Fe(CO)_4$ fragment in the solid-state,[79, 80] though it should be noted that even the bulkiest "mainstream" phosphine ligand P(*t*-Bu)$_3$ assumes axial substitution in [Fe{P(*t*-Bu)$_3$}$(CO)_4$].[81] Clearly, the steric profile of the 2,3,4,5-tetramethylarsolyl ring could not reasonably exceed that of P(*t*-Bu)$_3$. The presence of the diene-bound $Fe(CO)_3$ group may, however, increase the *effective* steric encumbrance of the arsine donor in the solid state; inspection of the crystal structure of [$Fe_4$(μ-κ$^1$:κ$^1$-η$^4$:η$^4$-tmaf)$(CO)_{14}$] finds the closest approach between carbonyl ligands on neighbouring $Fe(CO)_4$ and $Fe(CO)_3$ groups to be *ca* 3.2—3.6 Å, such that an *axially* substituted $Fe(CO)_4$ centre could invite greater steric and/or electrostatic interactions in this locale. Thus, the equatorial disposition of the arsine donor perhaps more-efficiently allows the tetracarbonyl ligand-set to recede from both the ferrocenyl centre and the cone of influence formed by the neighbouring $Fe(CO)_3$ group. Indeed, a DFT-optimised geometry of [$Fe_4$(μ-κ$^1$:κ$^1$-η$^4$:η$^4$-tmaf)$(CO)_{14}$] (gas phase: ωB97X-D/6-31G*) returned a core structure in excellent agreement with crystallographic data, correctly predicting the equatorial position of the arsenic donors. As a final comment on the matter, the $Fe(CO)_4$ group is undoubtedly undergoing BERRY *pseudo*-rotation (*viz.* one carbonyl signal for the entire group in the $^{13}C\{^1H\}$ NMR spectrum) in a process which has very modest energy penalty in $d^8$-Group 8 complexes.[82, 83] The equatorial disposition of the arsine donor in the solid state is not totally preserved in solution and the solid-state molecular structure should be viewed with some prudent discernment in light of the unexceptional electronic and steric properties of the tmaf ligand, and the crystal structure of [$Fe_2$(μ-κ$^1$:κ$^1$-tmaf)$(CO)_8$] which *does* contain axially-substituted $Fe(CO)_4$ centres (*vide infra*).

### 7.4.5 Synthesis of $[Fe_2(\mu\text{-}\kappa^1\text{:}\kappa^1\text{-tmaf})(CO)_8]$

The third and final compound isolated from the above reaction mixture, in very low yield (milligram quantities), was another symmetric complex tentatively identified as the open-bridged monodentate complex $[Fe_2(\mu\text{-}\kappa^1\text{:}\kappa^1\text{-tmaf})(CO)_8]$ on the basis of solution IR and NMR spectra. A high yielding synthesis (as a means to confirm product identity) involved treating the tmaf ligand with an excess of $[Fe_2(CO)_9]$ in THF medium (**Scheme 7.16**), which serves as a source of the $Fe(CO)_4$ fragment in donor solvents.[71] An orange crystalline solid with identical spectroscopic properties to those noted above was obtained.




**Scheme 7.16**: Synthesis of $[Fe_2(\mu\text{-}\kappa^1\text{:}\kappa^1\text{-tmaf})(CO)_8]$.

The solution IR spectrum (*n*-hexane) displays four $\nu_{CO}$ absorptions at 2048(vs), 1975(vs), 1945(vs) and 1935(vs) $cm^{-1}$ which compare favourably to other bis(iron(0) tetracarbonyl) complexes (*cf.* $[Fe_2(\mu\text{-}\kappa^1\text{:}\kappa^1\text{-dppf})(CO)_8]$ $\nu_{CO}$ 2052(vs), 1975(vs), 1944(vs), 1921(vs) $cm^{-1}$) and only one carbonyl resonance is observed in the $^{13}C\{^1H\}$ NMR spectrum (214.0 ppm; $C_6D_6$), with the arsolyl ring-carbon nuclei reprised to their usual region (142.6 and 136.5 ppm). Single crystals were obtained from n-hexane solution at -20 °C and the molecular structure is shown in **Figure 7.17**.

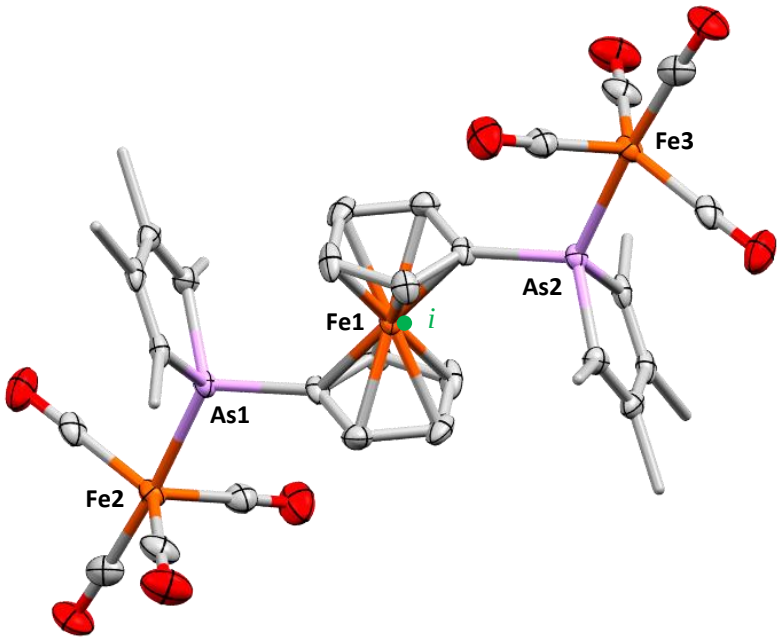



**Figure 7.17**: The molecular structure of [$Fe_2$(μ-κ$^1$:κ$^1$-tmaf)$(CO)_8$] in a crystal. Methyl groups simplified and hydrogen atoms omitted for clarity. Ellipsoids shown at 50% displacement. Only one half of the molecule is crystallographically unique in $P2_1/n$. *i* = inversion centre.

The molecular structure of [$Fe_2$(μ-κ$^1$:κ$^1$-tmaf)$(CO)_8$] reveals the expected complex *sans* diene-bound $Fe(CO)_3$ groups – it is noteworthy that many [Fe(η$^4$-diene)$(CO)_3$] complexes may be prepared by direct combination of [$Fe_2(CO)_9$] and the butadiene,[84] however without thermal impetus the diiron reagent instead serves more generally as a source of the $Fe(CO)_4$ group. Local molecular dimensions of the tmaf ligand are ordinary and call for little comment: the complex is centrosymmetric in the solid state with the ferrocenyl iron atom situated on a crystallographic inversion centre (unit cell monoclinic $P2_1/c$). The staggered-*anti* tetramethylarsolyl groups lie facing the interior of the ligand with the $Fe(CO)_4$ centres projecting toward the exterior, a common solid-state configuration for this ligand in the open-bridge coordination mode (*viz.* **Figure 7.13** and **Figure 7.14**). Of interest is the *axial* disposition of the arsenic donor(s) about the trigonal bipyramidal $Fe(CO)_4$ centres ($\tau_5$ = 0.82), lending credibility to the steric argument for the equatorial coordination in [$Fe_4$(μ-κ$^1$:κ$^1$-η$^4$:η$^4$-tmaf)$(CO)_{14}$] made above (**Figure 7.16**).

## 7.5 Summary

In this chapter, the first three examples of bis(arsolyl)-decorated ferrocenes were prepared from 1,1'-dilithioferrocene and the corresponding *As*-chloro arsole; in one case a monosubstituted ferrocene was

serendipitously obtained alongside (**Figure 7.3**). Three bidentate ligands, namely 1,1'-bis(tetraphenylarsolyl)ferrocene (tpaf), 1,1'-bis(tetramethylarsolyl)ferrocene (tmaf; **Figure 7.2**), and 1,1'-bis(tetraethylarsolyl)ferrocene (teaf) were all receptive toward a labile source of molybdenum(0) tetracarbonyl giving the anticipated octahedral *cis*-[Mo($\kappa^2$-tRaf)$(CO)_4$] complexes which were structurally characterised (R = Ph, **Figure 7.4**; R= Me, **Figure 7.5**; R = Et, **Figure 7.6**). The tmaf ligand was selected as a lead compound for further studies, providing a classical bidentate complex of $Ni(CO)_2$ (**Figure 7.7**), a tetrahedral complex of the $Au^+$ cation featuring a pair of tmaf entities (**Figure 7.9**), and a square-planar $PdCl_2$ species with relevance to potential catalytic applications (**Figure 7.10**). All were characterised *via* X-ray diffraction, although the latter exhibited the enigmatic phenomenon of diffuse scattering which precluded a high-precision structural model being developed at the present time.

Five open-bridge complexes were prepared which utilise the arsolyl donor pendants separately; these included the first examples of iridium and osmium centres bearing an arsole ligand (**Figure 7.13** and **Figure 7.14**, respectively), and two further cases of the $\eta^4$-coordination mode for an arsole ligand in [$Fe_2$($\mu$-$\eta^4$:$\eta^4$-tmaf)$(CO)_6$] (**Figure 7.15**) and [$Fe_4$($\mu$-$\kappa^1$:$\kappa^1$-$\eta^4$:$\eta^4$-tmaf)$(CO)_{14}$] (**Figure 7.16**) where the butadiene platforms serve as $\pi$-olefin donors to square-pyramidal iron(0) tricarbonyl fragments. A conventional iron(0) tetracarbonyl compound utilising the arsenic donors was also synthesised (**Figure 7.17**); all three of these novel species were obtained upon treating the tmaf ligand with labile Fe(0) reagents, once again showcasing the synthetic utility of [$Fe(COE)_2(CO)_3$] in coordination chemistry which has not yet been widely exploited.

## 7.6 Afterword to this Thesis

The foreward to this thesis (**Chapter 1**, **Section 1.5**) outlined the goal of preparing new transition metal arsole and arsolyl complexes, with a view toward novel coordination arrangements. A secondary goal was the collection of as much X-ray crystallographic data as possible to augment the sparse collection of species for which structural data was known, and perhaps unveil subtle evidence (if any) for aromatic delocalisation. **Figure 7.18** charts the contribution of this work (orange areas) to the field of arsole chemistry prior (blue).

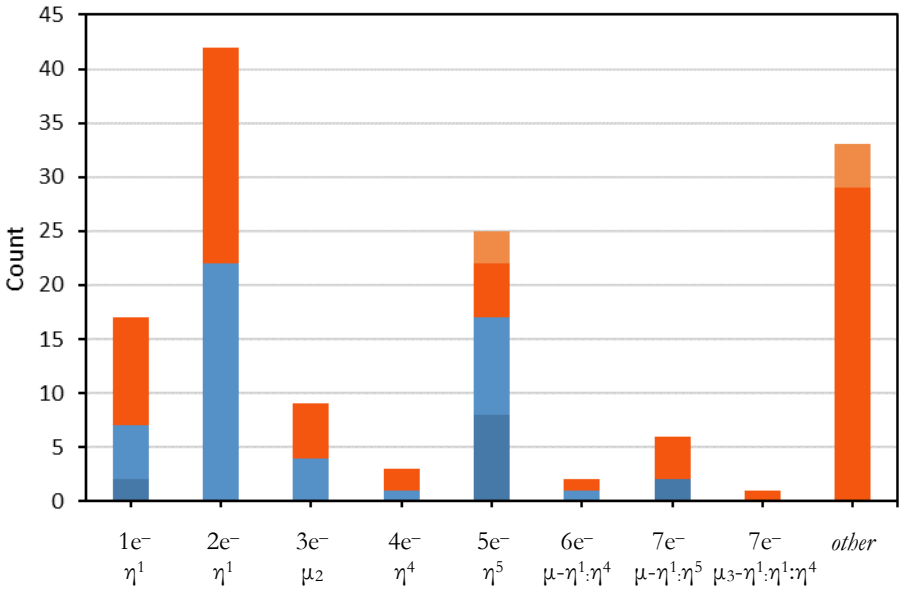
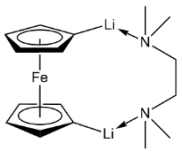



**Figure 7.18**: Number of transition metal arsole (neutral) and arsolyl (anionic) complexes by coordination mode prepared prior to (blue) and during (orange) this work. Darker shaded areas correspond to proportions which have had crystal structures determined. The "other" category comprises most of the complexes prepared in **Chapters 2** and **6** and any free λ³-arsole or similar.

## 7.7 Experimental

### 7.7.1 Synthesis of 1,1'-Bis(Arsolyl)Ferrocenes

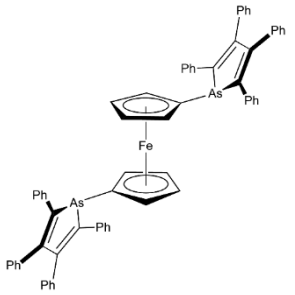
#### 7.7.1.1 [Fe(η⁵-C₅H₄Li)₂·TMEDA]




To a solution of 5 g ferrocene (26.8 mmol) in 100 mL *n*-hexane and 4 mL TMEDA (27 mmol) is added 30 mL *n*-BuLi solution (75 mmol; 2.5 M in hexanes) and the mixture vigorously stirred at ambient temperature under argon atmosphere for one week. During this time a light-orange precipitate forms and the colour of the supernatant darkens. The suspension is transferred *via* a wide-bore cannula under argon to a 100 mL Schlenk column fitted with a medium-porosity glass frit and leading to a 500 mL receiving flask. The collected solids are rinsed with portions of *n*-hexane until washings ran clear. After exchanging the receiving flask, the orange product is partially dried by flushing the column with argon (exiting *via* a one-way oil bubbler), and then fully dried by placing the apparatus under reduced pressure for several hours. The product was then permanently stored in an argon-filled glovebox and was used as-is without characterisation. Isolated yield: 5.1 g (16.2 mmol, 60%). The product is readily soluble in THF and partially soluble in $Et_2O$, and insoluble in hydrocarbons. **Caution**: the dry product is pyrophoric in the solid state and exposure to air results in formation of embers, occasionally igniting after a brief period of smouldering. Solutions did not appear to be pyrophoric however an occasion to confirm this did not eventuate, hence solutions should also be handled with

care. **Caution**: the reaction supernatant and product washings in the receiving flask contain residual *n*-BuLi and other reactive species which should be quenched appropriately.

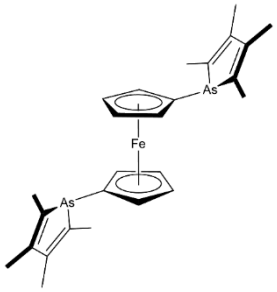
### 7.7.1.2 [Fe{η⁵-C₅H₄(AsC₄Ph₄)}₂]




To a stirred solution of 0.5 g [Fe(η⁵-$C_5H_4Li)_2$·TMEDA] (1.6 mmol) in 50 mL scrupulously anhydrous THF cooled to -78 °C was added 1.4 g solid $ClAsC_4Ph_4$ (3.0 mmol). The mixture was allowed to warm slowly to ambient temperature overnight giving a dark yellow suspension. A few drops of isopropanol were added as a precaution to quench any unreacted dilithioferrocene and the mixture dried by rotary evaporation. The residue was repeatedly extracted with portions of boiling chloroform and filtered whilst hot through a short plug of celite (2.5 x 2.5 cm) giving a yellow-orange filtrate, rinsing further with hot chloroform until washings ran clear. A quantity of insoluble light-yellow materials remained atop the plug. The filtrate was again dried by rotary evaporation and the residue washed with 3 x 20 mL $Et_2O$ (with trituration) to remove a small quantity of ferrocene and residual TMEDA. The yellow solids were re-dissolved in the minimum amount of boiling chloroform and hot ethanol was added until the mixture became cloudy, before being stored at -20 °C overnight. The yellow solids were collected by filtration and washed with 3 x 20 mL ethanol and 2 x 20 mL $Et_2O$ and dried under suction. Isolated yield: 0.52 g (0.49 mmol, 33%). The product is air stable and is moderately soluble in polar organic and aromatic solvents, and poorly soluble in $Et_2O$, aliphatic hydrocarbons and light alcohols.

NMR: $^1$H ($CDCl_3$, 400 MHz, 25 °C) δ 7.12—7.08 (m, 20H, $C_6H_5$), 7.00—6.98 (m, 12H, $C_6H_5$), 6.83—6.81 (m, 8H, $C_6H_5$), 3.78 (t, $J_{HH}$ = 1.8 Hz, 4H, α-η⁵-$C_5H_4$), 3.64 (t, $J_{HH}$ = 1.8 Hz, 4H, β-η⁵-$C_5H_4$) ppm. $^{13}$C{$^1$H} ($CDCl_3$, 176 MHz, 25 °C) δ 151.7 (arsole {2,5}-*C*), 149.6 (arsole {3,4}-*C*), 139.1 ($C_6H_5$), 138.6 ($C_6H_5$), 130.4 ($C_6H_5$), 129.6 ($C_6H_5$), 128.0 ($C_6H_5$), 127.5 ($C_6H_5$), 126.4 ($C_6H_5$), 79.0 (*As*-bonded η⁵-$C_5H_4$), 71.8 ({2,5}-η⁵-$C_5H_4$), 70.8 ({3,4}-η⁵-$C_5H_4$) ppm. HR-MS (ESI, MeCN, +ve ion) found *m*/*z* 1069.1436 (calc. for $C_{66}H_{48}{}^{75}As_2{}^{56}Fe_1{}^{23}Na_1$ [*M* + Na]⁺: 1069.1435). Analysis found 75.85% C, 4.81% H (calc. for $C_{66}H_{48}As_2Fe_1$: 75.73% C, 4.62% H).

### 7.7.1.3 [Fe{η⁵-C₅H₄(AsC₄Me₄)}₂]

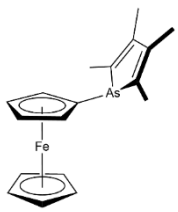


To a stirred suspension of 2 g [Fe($\eta^5$-$C_5H_4Li)_2$·TMEDA] (6.36 mmol) in 50 mL scrupulously anhydrous $Et_2O$ cooled to -78 °C was added a solution of *ca* 2.9 g freshly prepared $ClAsC_4Me_4$ (*ca* 13 mmol) also dissolved in 50 mL of the same solvent. The solids dissolve rapidly upon warming to ambient temperature giving a deep orange solution which is allowed to stir overnight. After this time a few drops of isopropanol are added and the mixture dried by rotary evaporation giving an oily orange residue which was extracted with portions of petroleum ether, filtered through celite, and transferred to a water-jacketed column of silica gel (35 x 2.5 cm; water temperature *ca* 10 °C) made up in the same solvent. Eluting with petroleum ether provides a yellow-orange band of ferrocene which is collected and discarded (isolated *ca* 0.06 g, < 10%). Eluting with 49:1 petroleum ether/$Et_2O$ provides a second yellow-orange band of [Fe{$\eta^5$-$C_5H_4(AsC_4Me_4)$}($\eta^5$-$C_5H_5$)] (*vide infra*). Eluting with 19:1 petroleum ether/$Et_2O$ gives a large yellow-orange band containing the product which is collected and dried by rotary evaporation giving the product as an orange solid. Isolated yield: 1.9 g (3.4 mmol, 53%). The product is encountered as a crystalline orange solid which is air-stable and is readily soluble in common organic solvents. The use of a cooled column gave superior resolution of the two *As*-ferrocenyl arsoles. As mentioned in the main text, the use of THF as the reaction solvent consistently gave lower isolated yields (< 10%) with the concurrent formation of a great deal of insoluble residues.

NMR: $^1$H ($CDCl_3$, 400 MHz, 25 °C) δ 4.28 (t, $J_{HH}$ = 1.7 Hz, 4H, α-$\eta^5$-$C_5H_4$), 4.11 (t, $J_{HH}$ = 1.7 Hz, 4H, β-$\eta^5$-$C_5H_4$), 2.12 (s, 12H, α-$CH_3$), 1.84 (s, 12H, β-$CH_3$ ppm. $^{13}$C{$^1$H} ($CDCl_3$, 176 MHz, 25 °C) δ 143.6 (arsole {2,5}-*C*), 139.9 (arsole {3,4}-*C*), 78.7 (*As*-bonded $\eta^5$-$C_5H_4$), 71.4 (α-$\eta^5$-$C_5H_4$), 71.0 (β-$\eta^5$-$C_5H_4$), 15.5 (α-$CH_3$), 14.6 (β-$CH_3$) ppm. $^1$H ($C_6D_6$, 400 MHz, 25 °C) δ 4.24 (t, $J_{HH}$ = 1.7 Hz, 4H, α-$\eta^5$-$C_5H_4$), 4.20 (t, $J_{HH}$ = 1.7 Hz, 4H, β-$\eta^5$-$C_5H_4$), 2.12 (s, 12H, α-$CH_3$), 1.70 (s, 12H, β-$CH_3$) ppm. $^{13}$C{$^1$H} ($C_6D_6$, 176 MHz, 25 °C) δ 143.6 (arsole {2,5}-*C*), 140.5 (arsole {3,4}-*C*), 79.2 (*As*-bonded $\eta^5$-$C_5H_4$), 71.9 (α-$\eta^5$-$C_5H_4$), 71.2 (β-$\eta^5$-$C_5H_4$), 15.6 (α-$CH_3$), 14.5 (β-$CH_3$) ppm. HR-MS (ESI, MeCN, +ve ion) found *m*/*z* 573.0180 (calc. for $C_{26}H_{32}{}^{75}As_2{}^{56}Fe_1{}^{23}Na_1$ [*M* + Na]$^+$: 573.0183). Analysis found 54.60% C, 5.78% H (calc. for $C_{26}H_{32}As_2Fe_1$: 54.48% C, 5.63% H).

Single crystals were obtained by slow evaporation of *n*-pentane solution at 0 °C. $C_{26}H_{32}As_2Fe_1$ (*M* = 550.20 g/mol): orange needle 0.053 × 0.134 × 0.404 mm, triclinic, space group *P*-1 (no. 2), *a* = 5.8077(3) Å, *b* = 13.3234(5) Å, *c* = 15.9112(7) Å, α = 108.166(4)°, *β* = 95.264(4)°, *γ* = 92.680(4)°, *V* = 1161.18(9) Å$^3$, *Z* = 2, multi-scan correction $T_{min}/T_{max}$ = 0.724/1.000, *μ*(Mo-Kα) = 3.488 mm$^{-1}$, $\varrho_{calc}$ = 1.574 g/cm$^3$, 10874 reflections measured (6.99° ≤ 2Θ ≤ 63.832°), 6994 unique ($R_{int}$ = 0.0277, $R_{sigma}$ = 0.0599) which were used in all calculations, *GOF* = 1.040, $D_{min}/D_{max}$ = -0.51/0.90 e/Å$^3$. The final $R_1$ was 0.0398 (I > 2σ(I)) and *w*$R_2$ was 0.0821 (all data).

### 7.7.1.4 [Fe{$\eta^5$-$C_5H_4(AsC_4Me_4)$}($\eta^5$-$C_5H_5$)]

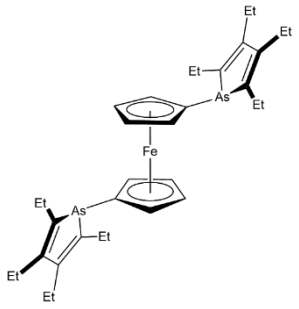



This compound was isolated from syntheses of [Fe{$\eta^5$-$C_5H_4(AsC_4Me_4)$}$_2$] above and elutes prior on silica gel with 49:1 petroleum ether/$Et_2O$ as a yellow-orange band. Isolated yield: 0.25 g (0.68 mmol, 11%). The product is encountered as a crystalline orange solid which readily soluble in common organic solvents and is air stable.

NMR: $^{1}$H ($CDCl_3$, 400 MHz, 25 °C) δ 4.22 (overlapping pair of s, 7H, η$^5$-$C_5H_5$ + α-η$^5$-$C_5H_4$), 4.07 (br s, 2H, β-η$^5$-$C_5H_4$), 2.11 (s, 6H, α-$CH_3$), 1.83 (s, 6H, β-$CH_3$) ppm. $^{13}$C{$^{1}$H} ($CDCl_3$, 176 MHz, 25 °C) δ 143.5 (arsole {2,5}-*C*), 139.9 (arsole {3,4}-*C*), 78.1 (*As*-bonded η$^5$-$C_5H_4$), 70.8 ({2,5}-η$^5$-$C_5H_4$), 69.7 ({3,4}-η$^5$-$C_5H_4$), 68.9 (η$^5$-$C_5H_5$), 15.4 (α-$CH_3$), 14.6 (β-$CH_3$) ppm. HR-MS (ESI, MeCN, +ve ion) found *m*/*z* 391.0108 (calc. for $C_{18}H_{21}{}^{75}As_2{}^{56}Fe_1{}^{23}Na_1$ [*M* + Na]$^+$: 391.0106). Analysis found 58.80% C, 5.88% H (calc. for $C_{18}H_{21}As_1Fe_1$: 58.71% C, 5.75% H).

Single crystals were obtained by slow evaporation of *n*-pentane solution at 0 °C. $C_{18}H_{21}As_1Fe_1$ (*M* = 368.12 g/mol): orange needle 0.057 × 0.085 × 0.233 mm, triclinic, space group *P*-1 (no. 2), *a* = 5.7845(2) Å, *b* = 11.6838(5) Å, *c* = 11.8075(5) Å, α = 78.979(4)°, *β* = 81.553(4)°, *γ* = 79.726(4)°, *V* = 765.46(6) Å$^3$, *Z* = 2, spherical correction $T_{min}/T_{max}$ = 0.436/0.484, *μ*(Cu-Kα) = 10.170 mm$^{-1}$, $\varrho_{calc}$ = 1.597 g/cm$^3$, 7120 reflections measured (7.68° ≤ 2Θ ≤ 147.842°), 3084 unique ($R_{int}$ = 0.0257, $R_{sigma}$ = 0.0352) which were used in all calculations, *GOF* = 1.048, $D_{min}/D_{max}$ = -0.76/0.77 e/Å$^3$. The final $R_1$ was 0.0294 (I > 2σ(I)) and *w*$R_2$ was 0.0707 (all data).

### 7.7.1.5 [Fe{η$^5$-$C_5H_4$($AsC_4Et_4$)}$_2$]

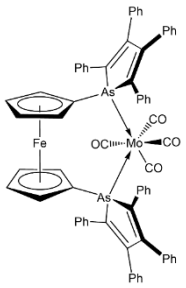



Prepared similarly as described above in $Et_2O$ medium. Quantities: 0.5 g [Fe(η$^5$-$C_5H_4Li)_2$·TMEDA] (1.6 mmol) and 1.0 g $ClAsC_4Et_4$ (3.6 mmol). Purified by column chromatography on silica gel (30 x 2.5 cm) with petroleum ether eluent giving a yellow-orange band of ferrocene (isolated *ca* 0.02 g, < 5%) followed by a second yellow-orange band containing the product. Isolated yield: 0.52 g (0.78 mmol, 48%). The product is air stable and is readily soluble in common organic solvents. The product is encountered as a waxy orange solid or an orange oil depending on ambient temperature or traces of residual solvent.

NMR: $^{1}$H ($CDCl_3$, 400 MHz, 25 °C) δ 4.25 (t, $J_{HH}$ = 1.7 Hz, 4H, α-η$^5$-$C_5H_4$), 4.07 (t, $J_{HH}$ = 1.7 Hz, 4H, β-η$^5$-$C_5H_4$), 2.59 (dq, $J_{HH}$ = 14.7 & 7.5 Hz, 4H, $CH_2CH_3$), 2.45 (dq, $J_{HH}$ = 14.7 & 7.5 Hz, 4H, $CH_2CH_3$), 2.26 (ddq, $J_{HH}$ = 28.6 & 14.7 & 7.5 Hz, 8H, $CH_2CH_3$), 1.18 (t, $J_{HH}$ = 7.4 Hz, 12H, α-$CH_2CH_3$), 1.02 (t, $J_{HH}$ = 7.6 Hz, 12H, β-$CH_2CH_3$) ppm. $^{13}$C{$^{1}$H} ($CDCl_3$, 176 MHz, 25 °C) δ 149.7 (arsole {2,5}-*C*), 148.5 (arsole {3,4}-*C*), 79.8 (*As*-bonded η$^5$-$C_5H_4$), 71.5 ({2,5}-η$^5$-$C_5H_4$), 70.6 ({3,4}-η$^5$-$C_5H_4$), 23.4 (α-$CH_2CH_3$), 21.2 (β-$CH_2CH_3$), 17.3 (α-$CH_2CH_3$), 15.3 (β-$CH_2CH_3$) ppm. HR-MS (ESI, MeCN, +ve ion) found *m*/*z* 685.1434 (calc. for $C_{34}H_{48}{}^{75}As_2{}^{56}Fe_1{}^{23}Na_1$ [*M* + Na]$^+$: 685.1435). Analysis found 61.80% C, 7.65% H (calc. for $C_{34}H_{48}As_2Fe_1$: 61.65% C, 7.30% H).

## 7.7.2 Synthesis of Bidentate Coordination Complexes

### 7.7.2.1 *cis*-[Mo(κ²-tpaf)(CO)₄]

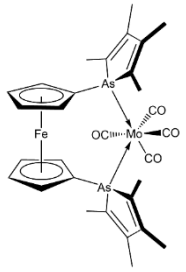



A 100 mL round-bottomed flask was charged with 0.1 g *cis*-[Mo(PIP)$_2$(CO)$_4$] (0.26 mmol) and 0.275 g tpaf (0.26 mmol). A reflux condenser was fitted and the apparatus flushed with nitrogen before 40 mL toluene was admitted and the mixture heated to 100 °C for two hours, monitored intermittently by IR. After this time the mixture was dried by rotary evaporation and the residue re-dissolved in $CH_2Cl_2$ and absorbed onto a small quantity of silica gel by evaporation of the solvent. This was transferred to a column of silica gel (25 x 2.5 cm) made up in the same solvent. Eluting with 9:1 petroleum ether/$Et_2O$ provides a thin yellow band of unchanged *cis*-[Mo(PIP)$_2$(CO)$_4$]. Eluting with 9:1 petroleum ether/$CH_2Cl_2$ gives a bright yellow band containing the product which is collected and dried by rotary evaporation giving a microcrystalline yellow solid. Only partial resolution of the target compound and unreacted tpaf could be achieved. Isolated yield: 0.125 g (0.10 mmol, 38%). The product is air stable in the solid state however solutions turn green overnight if unprotected. Partial decomposition was also observed in solutions allowed to stand over extended periods, even under inert atmosphere, and totally clean NMR spectra were difficult to obtain.

NMR: $^1$H ($CDCl_3$, 400 MHz, 25 °C) δ 7.20—7.13 (m, 26H, $C_6H_5$), 7.00-6.91 (m, 16H, $C_6H_5$), 6.75—6.74 (m, 8H, $C_6H_5$), 3.97 (br s, 4H, α-η$^5$-$C_5H_4$), 3.93 (br s, 4H, β-η$^5$-$C_5H_4$) ppm. $^{13}$C{$^1$H} ($CDCl_3$, 176 MHz, 25 °C) δ 214.2 (*C*O), 208.4 (*C*O), 149.3 (arsole {2,5}-*C*), 147.9 (arsole {3,4}-*C*), 137.4 ($C_6H_5$), 137.1 ($C_6H_5$), 130.3 ($C_6H_5$), 129.6 ($C_6H_5$), 128.1 ($C_6H_5$), 128.0 ($C_6H_5$), 127.5 ($C_6H_5$), 127.4 ($C_6H_5$), 76.1 (*As*-bonded η$^5$-$C_5H_4$), 74.4 ({2,5}-η$^5$-$C_5H_4$), 71.1 ({3,4}-η$^5$-$C_5H_4$) ppm. IR (*n*-hexane, 25 °C) $\nu_{CO}$ 2025(s), 1948(vs), 1927(vs), 1882(s) cm$^{-1}$. HR-MS (ESI, MeCN, +ve ion) found *m*/*z* 1256.0404 (calc. for $C_{70}H_{48}O_4{}^{56}Fe_1{}^{75}As_1{}^{98}Mo_1$ [*M*]$^+$: 1256.0388). Analysis found 67.15% C, 3.99% H (calc. for $C_{70}H_{48}O_4As_2Fe_1Mo_1$: 67.00% C, 3.86% H).

Single crystals were grown from benzene/*n*-hexane solution. One molecule of benzene was found in the asymmetric unit. $C_{70}H_{48}O_4As_2Fe_1Mo_1{\cdot}C_6H_6$ ($M$ = 1332.82 g/mol): yellow prism 0.067 × 0.098 × 0.181 mm, monoclinic, space group *Cc* (no. 9), $a$ = 10.9511(3) Å, $b$ = 22.4541(5) Å, $c$ = 25.4421(9) Å, $\beta$ = 95.737(3)°, $V$ = 6224.8(3) Å$^3$, $Z$ = 4, Gaussian correction $T_{min}/T_{max}$ = 0.850/1.000, $\mu$(Mo-Kα) = 1.540 mm$^{-1}$, $\varrho_{calc}$ = 1.422 g/cm$^3$, 17119 reflections measured (6.708° ≤ 2Θ ≤ 63.88°), 13040 unique ($R_{int}$ = 0.0272, $R_{sigma}$ = 0.0630) which were used in all calculations, *GOF* = 1.070, $D_{min}/D_{max}$ = -0.71/0.92 e/Å$^3$. The final $R_1$ was 0.0458 (I > 2σ(I)) and $wR_2$ was 0.1006 (all data).

### 7.7.2.2 *cis*-[Mo(κ²-tmaf)(CO)₄]

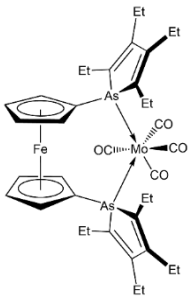



A 100 mL round-bottomed flask was charged with 0.1 g *cis*-[Mo(PIP)$_2$(CO)$_4$] (0.26 mmol) and 0.145 g tmaf (0.26 mmol). A reflux condenser was fitted, and the apparatus flushed with nitrogen before 40 mL $CH_2Cl_2$ was admitted and the mixture heated to reflux for 90 minutes. The colour did not visibly change, though an IR spectrum taken after this time finds complete consumption of the starting material. The mixture was dried by rotary evaporation and extracted with portions of petroleum spirit and transferred to a column of silica gel (20 x 2.5 cm) made up in the same solvent. Eluting with petroleum ether followed by 9:1 petroleum ether/$Et_2O$ provides a yellow band which is collected and dried by rotary evaporation giving the product as a microcrystalline yellow solid. Isolated yield: 0.14 g (0.18 mmol, 69%). The product is air stable in the solid state however solutions turn green over several days without protection. The product is readily soluble in common organic solvents.

NMR: $^1$H ($CDCl_3$, 400 MHz, 25 °C) δ 4.32 (t, $J_{HH}$ = 1.8 Hz, α-η$^5$-C$_5$*H*$_4$), 4.25 (t, $J_{HH}$ = 1.8 Hz, β-η$^5$-C$_5$*H*$_4$), 2.25 (s, 12H, α-C*H*$_3$), 1.89 (s, 12H, β-C*H*$_3$) ppm. $^{13}$C{$^1$H} ($CDCl_3$, 176 MHz, 25 °C) δ 214.4 (*C*O), 210.4 (*C*O), 142.7 (arsole {2,5}-*C*), 137.2 (arsole {3,4}-*C*), 78.7 (*As*-bonded η$^5$-*C*$_5$H$_4$), 72.0 ({2,5}-η$^5$-*C*$_5$H$_4$), 70.8 ({3,4}-η$^5$-*C*$_5$H$_4$), 14.9 (α-*C*H$_3$), 14.5 (β-*C*H$_3$) ppm. IR (*n*-hexane, 25 °C) $\nu_{CO}$ 2020(vs), 1944(s), 1902(vs), 1881(vs) cm$^{-1}$. HR-MS (ESI, MeCN, +ve ion) found *m*/*z* 759.9169 (calc. for $C_{29}H_{32}O_4{}^{75}As_2{}^{56}Fe_1{}^{98}Mo_1$ [*M*]$^+$: 759.9163). Analysis found 47.50% C, 4.25% H (calc. for $C_{30}H_{32}O_4As_2Fe_1Mo_1$: 47.52% C, 4.25% H).

Single crystals were obtained by cooling a hot *n*-hexane solution to -20 °C under nitrogen. One-half an *n*-hexane molecule was found within the asymmetric unit which was disordered along a symmetry element and could not be modelled satisfactorily. A solvent mask was calculated which found 28 electrons in a volume of 188 Å$^3$ in one void per asymmetric unit. This is consistent with the presence of 0.5 $C_6H_{14}$ which account for 25 electrons per asymmetric unit. $C_{30}H_{32}O_4As_2Fe_1Mo_1$ (*M* = 758.18 g/mol): yellow plate 0.06 × 0.386 × 0.529 mm, monoclinic, space group $P2_1/c$ (no. 14), $a$ = 9.2234(4) Å, $b$ = 19.7509(10) Å, $c$ = 19.1298(12) Å, $\beta$ = 94.351(5)°, $V$ = 3474.8(3) Å$^3$, $Z$ = 4, multi-scan correction $T_{min}/T_{max}$ = 0.516/1.000, $\mu$(Mo-Kα) = 2.697 mm$^{-1}$, $\varrho_{calc}$ = 1.449 g/cm$^3$, 27448 reflections measured (6.732° ≤ 2Θ ≤ 64.684°), 10912 unique ($R_{int}$ = 0.0508, $R_{sigma}$ = 0.0898) which were used in all calculations, *GOF* = 1.060, $D_{min}/D_{max}$ = -0.87/1.43 e/Å$^3$. The final $R_1$ was 0.0638 (I > 2σ(I)) and $wR_2$ was 0.1475 (all data).

### 7.7.2.3 *cis*-[Mo(κ²-teaf)(CO)₄]

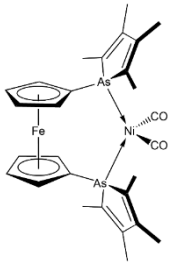



Prepared similarly to that above. Quantities: 0.1 g *cis*-[Mo(PIP)$_2$(CO)$_4$] (0.26 mmol) and 0.175 g teaf (0.26 mmol). Chromatography on silica gel (20 x 2.5 cm) with 9:1 petroleum ether/Et$_2$O provides a yellow band containing the product which is collected and dried giving a yellow microcrystalline solid. Isolated yield: 0.18 g (0.20 mmol, 76%). Properties are identical to that above.

NMR: $^1$H (CDCl$_3$, 400 MHz, 25 °C) δ 4.31 (br s, 4H, α-η$^5$-C$_5$*H*$_4$), 4.21 (br s, 4H, β-η$^5$-C$_5$*H*$_4$), 2.70 (dp, $J_{HH}$ = 28.9 & 7.3 Hz, 8H, α-C*H*$_2$CH$_3$), 2.33 (hept, $J_{HH}$ = 6.8 Hz, 8H, β-C*H*$_2$CH$_3$), 1.24 (t, $J_{HH}$ = 7.5 Hz, 12 H, α-C*H*$_3$), 1.07 (t, $J_{HH}$ = 7.5 Hz, 12H, β-C*H*$_3$) ppm. $^{13}$C{$^1$H} (CDCl$_3$, 176 MHz, 25 °C) δ 214.3 (*C*O), 210.8 (*C*O), 149.1 (arsole {2,5}-*C*), 144.0 (arsole {3,4}-*C*), 78.2 (*As*-bonded η$^5$-*C*$_5$H$_4$), 73.4 ({2,5}-η$^5$-*C*$_5$H$_4$), 71.0 ({3,4}-η$^5$-*C*$_5$H$_4$), 22.3 (α-*C*H$_2$CH$_3$), 21.4 (β-*C*H$_2$CH$_3$), 15.4 (α-CH$_2$*C*H$_3$), 15.1 (β-CH$_2$*C*H$_3$) ppm. IR (*n*-hexane, 25 °C) $\nu_{CO}$ 2017(vs), 1944(s), 1900(vs), 1880(vs) cm$^{-1}$. HR-MS (ESI, MeCN, +ve ion) found *m*/*z* 873.0475 (calc. for C$_{38}$H$_{49}$O$_4$$^{56}$Fe$_1$$^{75}$As$_2$$^{98}$Mo$_1$ [*M* + H]$^+$: 873.0466). Analysis found 52.51% C, 5.56% H (calc. for C$_{38}$H$_{48}$O$_4$As$_2$Fe$_1$Mo$_1$: 52.44% C, 5.56% H).

Single crystals were obtained from *n*-pentane solution at -20 °C. C$_{38}$H$_{48}$O$_4$As$_2$Fe$_1$Mo$_1$ (*M* = 870.39 g/mol): yellow prism 0.074 × 0.155 × 0.254 mm, monoclinic, space group *Ia* (no. 9), *a* = 19.4410(3) Å, *b* = 19.5555(3) Å, *c* = 19.7350(3) Å, *β* = 99.2440(10)°, *V* = 7405.4(2) Å$^3$, *Z* = 8, multi-scan correction $T_{min}/T_{max}$ = 0.686/1.000, *μ*(Mo-Kα) = 2.542 mm$^{-1}$, $\rho_{calc}$ = 1.561 g/cm$^3$, 20270 reflections measured (6.592° ≤ 2Θ ≤ 63.648°), 13918 unique ($R_{int}$ = 0.0259, $R_{sigma}$ = 0.0466) which were used in all calculations, *GOF* = 1.020, $D_{min}/D_{max}$ = -0.62/0.69 e/Å$^3$. The final $R_1$ was 0.0329 (I > 2σ(I)) and $wR_2$ was 0.0702 (all data).

### 7.7.2.4 [Ni(κ²-tmaf)(CO)₂]



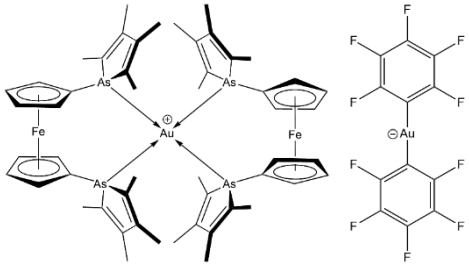

A 50 mL two-necked round-bottomed Schlenk flask was charged with 0.2 g [Ni(COD)$_2$] (0.72 mmol) and 0.3 g tmaf (0.55 mmol). To this was admitted 25 mL *n*-hexane giving a deep red suspension which was stirred at ambient temperature for 2 hours. After this time, a gentle stream of carbon monoxide was bubbled through the reaction mixture for *ca* 60 seconds giving a rapid colour change to a golden yellow with dissolution of the solids. A water condenser was fitted and the mixture heated to reflux for 60 minutes. From this point forward, operations are carried

out under air. The reaction mixture was transferred to a column of silica gel (20 x 2.5 cm) made up in petroleum ether and eluted with the same solvent, followed by 9:1 petroleum ether/$Et_2O$ giving a bright yellow band which was collected and dried by rotary evaporation giving the product as a golden yellow microcrystalline solid. Isolated yield: 0.25 g (mmol, 84%). The product is readily soluble in common organic solvents and is reasonably air-stable, though solutions precipitate insoluble green materials (probably nickel oxide) over several days without protective atmosphere. **Caution**: $[Ni(CO)_4]$ is generated in the reaction mixture and trace amounts may remain upon workup.

NMR: $^1H$ ($C_6D_6$, 400 MHz, 25 °C) δ 4.20 (t, $J_{HH}$ = 1.8 Hz, 4H, α-η$^5$-$C_5H_4$), 4.02 (t, $J_{HH}$ = 1.8 Hz, 4H, β-η$^5$-$C_5H_4$), 2.24 (s, 12H, α-$CH_3$), 1.58 (s, 12H, β-$CH_3$) ppm. $^{13}C\{^1H\}$ ($C_6D_6$, 176 MHz, 25 °C) δ 200.6 (*C*O), 142.9 (arsole {2,5}-*C*), 137.0 (arsole {3,4}-*C*), 80.7 (*As*-bonded η$^5$-$C_5H_4$), 71.9 ({2,5}-η$^5$-$C_5H_4$), 70.6 ({3,4}-η$^5$-$C_5H_4$), 14.4 (α-$CH_3$), 14.0 (β-$CH_3$) ppm. IR (*n*-hexane, 25 °C) $\nu_{CO}$ 2009(vs), 1951(vs) cm$^{-1}$. HR-MS (ESI, MeCN, +ve ion) found *m*/*z* 607.9645 (calc. for $C_{26}H_{32}{}^{56}Fe_1{}^{58}Ni_1{}^{75}As_1$ [*M* – 2CO]$^+$: 607.9639). Analysis found 50.64% C, 4.89% H (calc. for $C_{28}H_{32}O_2As_2Fe_1Ni_1$: 50.58% C, 4.85% H).

Single crystals were grown by slow evaporation of benzene solution. $C_{28}H_{32}O_2As_2Fe_1Ni_1$ (*M* = 664.93 g/mol): yellow prism 0.048 × 0.084 × 0.313 mm, monoclinic, space group *C*2/*c* (no. 15), *a* = 14.8743(2) Å, *b* = 9.91190(10) Å, *c* = 19.2806(3) Å, *β* = 106.502(2)°, *V* = 2725.50(7) Å$^3$, *Z* = 4, Gaussian correction $T_{min}/T_{max}$ = 0.272/1.000, *μ*(Cu-Kα) = 7.996 mm$^{-1}$, $\varrho_{calc}$ = 1.620 g/cm$^3$, 8485 reflections measured (9.568° ≤ 2Θ ≤ 147.654°), 2755 unique ($R_{int}$ = 0.0160, $R_{sigma}$ = 0.0154) which were used in all calculations, *GOF* = 1.030, $D_{min}/D_{max}$ = -0.43/0.39 e/Å$^3$. The final $R_1$ was 0.0228 (I > 2*σ*(I)) and *w*$R_2$ was 0.0607 (all data).

### 7.7.2.5 [Au(κ$^2$-tmaf)$_2$][Au($C_6F_5$)$_2$]

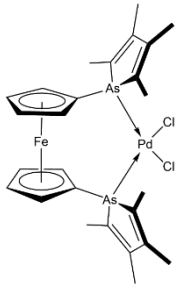



To a solution of 0.15 g tmaf (0.27 mmol) in 10 mL $CH_2Cl_2$ was added 0.125 g solid [Au($C_6F_5$)(THT)] (0.27 mmol) and stirred overnight giving a yellow solution. The mixture was dried by rotary evaporation and washed with 5 x 10 mL portions of $Et_2O$ (with trituration) to remove tetrahydrothiophene and any unreacted reagents. The yellow solids were dissolved in the minimum amount of $CH_2Cl_2$ and $Et_2O$ added until the solution became cloudy and stored at -20 °C overnight. The yellow microcrystalline solids were collected by filtration, washed with small portions of $Et_2O$ and dried under suction. Isolated yield: 0.16 g (0.09 mmol, 66%). The product is air-stable and is readily soluble in polar organic solvents.

NMR: $^1H$ ($CDCl_3$, 400 MHz, 25 °C) δ 4.49 (br s, 8H, α-η$^5$-$C_5H_4$), 4.30 (br s, 8H, β-η$^5$-$C_5H_4$), 2.13 (s, 24H, α-$CH_3$), 1.91 (s, 24H, β-$CH_3$) ppm. $^{13}C\{^1H\}$ ($CDCl_3$, 176 MHz, 25 °C) δ 149.1 ($C_6F_5$), 147.8 ($C_6F_5$), 145.2 (arsole {2,5}-*C*), 138.0 ($C_6F_5$), 136.4 ($C_6F_5$), 136.0 (arsole {3,4}-*C*), 72.0 (br s, FWHM = 67 Hz), 14.9 (br s, FWHM = 58 Hz) ppm. $^{19}F\{^1H\}$ ($CDCl_3$, 376 MHz, 25 °C) δ -115.5 (m, 4F, {2,6}-$C_6F_5$), -158.4 (t, $J_{FF}$ = 20.0 Hz, 2F, {4}-$C_6F_5$), -162.2 (m, 4F, {3,5}-$C_6F_5$) ppm. HR-MS (ESI, MeCN, +ve ion) found *m*/*z* 1297.0228 (calc. for $C_{52}H_{64}{}^{75}As_4{}^{197}Au_1{}^{56}Fe_2$ [*M*]$^+$: 1297.0236). Analysis found 43.12% C, 3.77% H (calc. for $C_{64}H_{64}As_4Au_2F_{10}Fe_2$: 42.04% C, 3.53% H).

Single crystals were obtained by vapour diffusion of $Et_2O$ into $CH_2Cl_2$ solution at -20 °C. Two crystallographically unique cation-anion pairs were found within the asymmetric unit, including one $[Au(C_6F_5)_2]^-$ anion which was disordered over two positions and modelled accordingly. Crystal quality was comparatively poor in this case resulting in rather swollen ADP's although no evidence for twinning was found upon inspection of the EWALD projection of the reciprocal lattice. These atoms were handled with suitable restraints. An appreciable amount of residual electron density remained nearest the heavy atoms after model refinement which was left untreated. Attempts to grow better-quality crystals were unsuccessful and a second interrogated specimen was also plagued by the same issues. $C_{64}H_{64}As_4Au_2F_{10}Fe_2$ ($M$ = 1828.46 g/mol): yellow plate 0.066 × 0.239 × 0.281 mm, monoclinic, space group $P2_1/c$ (no. 14), $a$ = 15.2403(2) Å, $b$ = 30.1728(4) Å, $c$ = 28.8569(4) Å, $\beta$ = 97.1570(10)°, $V$ = 13166.2(3) Å$^3$, $Z$ = 8, spherical correction $T_{min}/T_{max}$ = 0.00751/0.07046, $\mu$(Cu-Kα) = 14.445 mm$^{-1}$, $\varrho_{calc}$ = 1.845 g/cm$^3$, 51130 reflections measured (7.536° ≤ 2Θ ≤ 146.32°), 25745 unique ($R_{int}$ = 0.0281, $R_{sigma}$ = 0.0369) which were used in all calculations, $GOF$ = 1.106, $D_{min}/D_{max}$ = -1.10/4.41 e/Å$^3$. The final $R_1$ was 0.0822 (I > 2σ(I)) and $wR_2$ was 0.2230 (all data). This dataset was not deposited within the CSD for the reasons outlined above.

### 7.7.2.6 [Pd(κ²-tmaf)Cl₂]




A 25 mL Schlenk tube was charged with 0.1 g *cis*-$[Pd(NCMe)_2Cl_2]$ (0.38 mmol) and dissolved in 10 mL $CH_2Cl_2$. To the stirred yellow solution was added 0.22 g solid tmaf (0.4 mmol) which after a short induction period of *ca* 10—20 seconds a rapid colour change to a deep red occurs. The mixture is stirred overnight at ambient temperature before being filtered through a short plug of celite (2.5 x 2.5 cm) and the filtrate dried by rotary evaporation. The red-brown residue was suspended in 25 mL $Et_2O$ (with trituration), collected by filtration, and washed further with 3 x 10 mL $Et_2O$ and 2 x 10 mL *n*-pentane and dried under suction. Isolated yield: 0.24 g (0.34 mmol, 91%). The product is air stable in both the solid state and in solution and is readily soluble in polar organic and aromatic solvents, and poorly soluble in $Et_2O$ and aliphatic hydrocarbons.

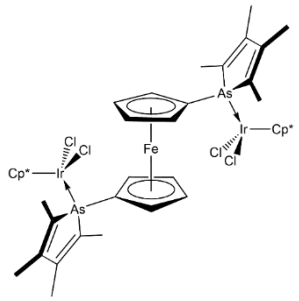
NMR: $^1$H ($CDCl_3$, 400 MHz, 25 °C) δ 4.42 (br s, 4H, α-η$^5$-$C_5H_4$), 4.36 (br s, 4H, β-η$^5$-$C_5H_4$), 2.29 (s, 12H, α-$CH_3$), 1.86 (s, 12H, β-$CH_3$) ppm. $^{13}$C{$^1$H} ($CDCl_3$, 176 MHz, 25 °C) δ 144.6 (arsole {2,5}-*C*), 132.1 (arsole {3,4}-*C*), 76.1 (*As*-bonded η$^5$-$C_5H_4$), 72.3 ({2,5}-η$^5$-$C_5H_4$), 72.1 ({3,4}-η$^5$-$C_5H_4$), 15.2 (α-$CH_3$), 14.4 (β-$CH_3$) ppm. HR-MS (ESI, MeCN, +ve ion) found $m/z$ 733.9283 (calc. for $C_{28}H_{32}{}^{35}Cl_1{}^{56}Fe_1{}^{75}As_2{}^{108}Pd_1$ [$M$ – Cl]$^+$: 733.9272. The particular batch of $PdCl_2$ used to synthesise *cis*-$[Pd(NCMe)_2Cl_2]$ was evidently enriched in $^{108}$Pd instead of $^{106}$Pd, the latter of which is typically quoted as being of higher natural abundance). Analysis found 40.99% C, 4.20% H (calc. for $C_{26}H_{32}As_2Cl_2Fe_1Pd_1$: 42.92% C, 4.43% H).

Crystals were obtained from $CH_2Cl_2$/*n*-hexane, $CH_2Cl_2/Et_2O$, $CH_2Cl_2$/ethanol, acetone/$Et_2O$, and benzene mixtures. For the reasons outlined in **Section 7.3.6** all of these proved to be unsuitable for X-ray diffraction due to high angle diffuse scattering, resulting in low-resolution datasets. Therefore, only unit cell information is reported here:

$C_{26}H_{32}As_2Cl_2Fe_1Pd_1$ ($M$ = 727.55 g/mol), orthorhombic, $P2_12_12_1$ (no. 19), $a$ = 8.9818(3) Å, $b$ = 29.5254(7) Å, $c$ = 19.9852(6) Å, $V$ = 5299.90(10) Å$^3$, $Z$ = 4.

## 7.7.3 Synthesis of Monodentate Open-Bridge Complexes

### 7.7.3.1 [$Ir_2$(μ-η$^1$:η$^1$-tmaf)$Cl_4$(η$^5$-$C_5Me_5$)$_2$]



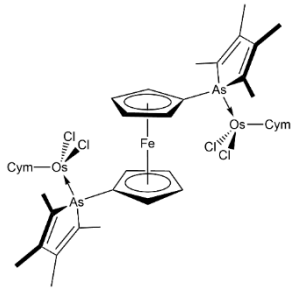

To a stirred solution of 0.1 g tmaf (0.18 mmol) in 20 mL $CH_2Cl_2$ is added 0.145 g [$Ir_2$(μ-Cl)$_2Cl_2$(η$^5$-$C_5Me_5$)$_2$] (0.18 mmol). No effort was made to exclude air or moisture from the reaction. After stirring overnight, the mixture is concentrated by rotary evaporation and *n*-hexane added until the mixture became cloudy. Cooling to -20 °C overnight provides the product as a bright yellow microcrystalline solid which is collected by filtration and washed with $Et_2O$ and dried under suction. The process was repeated with the supernatant giving an additional crop of product. Isolated yield: 0.22 g (0.16 mmol, 78%). The product is air-stable and is readily soluble in polar organic and aromatic solvents, and poorly soluble in $Et_2O$ and aliphatic hydrocarbons.

NMR: $^1$H ($CDCl_3$, 400 MHz, 25 °C) δ 4.38 (br s, 4H, α-η$^5$-$C_5H_4$), 4.19 (br s, 4H, β-η$^5$-$C_5H_4$), 2.13 (s, 12H, α-$CH_3$), 1.97 (s, 12H, β-$CH_3$), 1.54 (s, 30H, η$^5$-$C_5(CH_3)_5$) ppm. $^{13}$C{$^1$H} ($CDCl_3$, 176 MHz, 25 °C) δ 143.7 (arsole {2,5}-*C*), 133.1 (arsole {3,4}-*C*), 89.1 (η$^5$-$C_5(CH_3)_5$), 75.0 (*As*-bonded η$^5$-$C_5H_4$), 73.5 ({2,5}-η$^5$-$C_5H_4$), 70.9 ({3,4}-η$^5$-$C_5H_4$), 15.0 (α-$CH_3$), 13.8 (β-$CH_3$), 8.3 (η$^5$-$C_5(CH_3)_5$) ppm. HR-MS (ESI, MeCN, +ve ion) found m/z 1311.0947 (calc. for $C_{46}H_{62}{}^{35}Cl_3{}^{56}Fe_1{}^{75}As_2{}^{193}Ir_2$ [$M$ – Cl]$^+$: 1311.0957). Analysis found 41.10% C, 4.77% H (calc. for $C_{46}H_{62}As_2Cl_2Fe_1Ir_2$: 41.02% C, 4.64% H).

Single crystals were obtained by layering a $CH_2Cl_2$ solution with *n*-hexane at 0 °C. $C_{46}H_{62}As_2Cl_4FeIr_2$ ($M$ = 1346.84 g/mol): yellow plate 0.074 × 0.206 × 0.377 mm, orthorhombic, space group *Pbca* (no. 61), $a$ = 16.3877(6) Å, $b$ = 20.8037(10) Å, $c$ = 27.8856(12) Å, $V$ = 9506.9(7) Å$^3$, $Z$ = 8, spherical correction $T_{min}/T_{max}$ = 0.278/0.301, $\mu$(Mo-Kα) = 7.524 mm$^{-1}$, $\varrho_{calc}$ = 1.882 g/cm$^3$, 44422 reflections measured (6.912° ≤ 2Θ ≤ 66.536°), 15921 unique ($R_{int}$ = 0.0440, $R_{sigma}$ = 0.0651) which were used in all calculations, $GOF$ = 1.042, $D_{min}/D_{max}$ = -1.26/1.45 e/Å$^3$. The final $R_1$ was 0.0401 (I > 2σ(I)) and $wR_2$ was 0.0854 (all data).

### 7.7.3.2 [$Os_2$(μ-η$^1$:η$^1$-tmaf)$Cl_4${η$^6$-$C_6H_4Me$(*i*-Pr)}$_2$]

Prepared in an identical fashion to that above. Quantities: 0.1 g tmaf (0.18 mmol) and 0.14 g [$Os_2$(μ-Cl)$_2Cl_2${η$^6$-$C_6H_4Me$(*i*-Pr)}$_2$] (0.18 mmol). Re-crystallised from $CH_2Cl_2$/*n*-hexane at -20 °C giving the product as a bright yellow

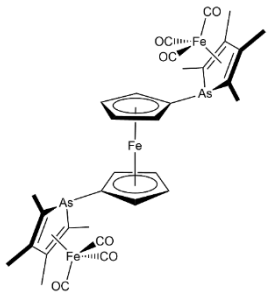



microcrystalline solid which was collected by filtration and washed with $Et_2O$ and dried under suction. Isolated yield: 0.19 g (0.14 mmol, 77%). Properties are identical to that above.

NMR: $^{1}H$ ($CDCl_3$, 400 MHz, 25 °C) δ 5.46 (s, 4H, η⁶-$C_6H_4(CH_3)(CH(CH_3)_2)$), 5.41 (s, 4H, η⁶-$C_6H_4(CH_3)(CH(CH_3)_2)$), 4.31 (br s, 4H, α-η⁵-$C_5H_4$), 4.21 (br s, 4H, β-η⁵-$C_5H_4$), 2.65 (m, 2H, η⁶-$C_6H_4(CH_3)(CH(CH_3)_2)$), 2.17 (s, 12H, α-$CH_3$), 2.07 (s, 6H, η⁶-$C_6H_4(CH_3)(CH(CH_3)_2)$), 1.97 (s, 12H, β-$CH_3$), 1.18 (d, $J_{HH}$ = 8.8 Hz, 12H, η⁶-$C_6H_4(CH_3)(CH(CH_3)_2)$) ppm. $^{13}C\{^{1}H\}$ ($CDCl_3$, 176 MHz, 25 °C) δ 143.9 (arsole {2,5}-*C*), 134.4 (arsole {3,4}-*C*), 98.1 (quart. η⁶-$C_6H_4(CH_3)(CH(CH_3)_2)$), 87.4 (quart. η⁶-$C_6H_4(CH_3)(CH(CH_3)_2)$), 77.6 (η⁶-$C_6H_4(CH_3)(CH(CH_3)_2)$), 75.6 (*As*-bonded η⁵-$C_5H_4$), 74.8 (η⁶-$C_6H_4(CH_3)(CH(CH_3)_2)$), 72.8 ({2,5}-η⁵-$C_5H_4$), 71.3 ({3,4}-η⁵-$C_5H_4$), 30.5 (η⁶-$C_6H_4(CH_3)(CH(CH_3)_2)$), 22.5 (η⁶-$C_6H_4(CH_3)(CH(CH_3)_2)$), 18.1 (α-$CH_3$), 16.0 (β-$CH_3$), 13.9 (η⁶-$C_6H_4(CH_3)(CH(CH_3)_2)$) ppm. HR-MS (ESI, MeCN, +ve ion) found *m*/*z* 1303.0590 (calc. for $C_{46}H_{58}{}^{75}As_2{}^{35}Cl_3{}^{56}Fe_1{}^{192}Os_2$ [*M* – Cl]⁺: 1303.0585). Analysis found 41.10% C, 4.55% H (calc. for $C_{46}H_{58}As_2Cl_4Fe_1Os_2$: 41.27% C, 4.37% H).

Single crystals were obtained by cooling a hot $CHCl_3$/*n*-heptane mixture to -20 °C. Two molecules of chloroform were found within the asymmetric unit, of which one was disordered by threefold rotation and modelled accordingly. $C_{50}H_{64}As_2Cl_{16}FeOs_2$ (*M* = 1818.30 g/mol): yellow prism 0.108 × 0.192 × 0.397 mm, monoclinic, space group $P2_1/n$ (no. 14), *a* = 9.7563(4) Å, *b* = 15.8203(7) Å, *c* = 20.5470(8) Å, *β* = 91.729(4)°, *V* = 3169.9(2) Å³, *Z* = 2, spherical correction $T_{min}/T_{max}$ = 0.213/0.235, *μ*(Mo-Kα) = 5.968 mm⁻¹, $\varrho_{calc}$ = 1.905 g/cm³, 16919 reflections measured (6.886° ≤ 2Θ ≤ 58.246°), 7062 unique ($R_{int}$ = 0.0331, $R_{sigma}$ = 0.0502) which were used in all calculations, *GOF* = 1.018, $D_{min}/D_{max}$ = -0.89/1.31 e/Å³. The final $R_1$ was 0.0373 (I > 2σ(I)) and *w*$R_2$ was 0.0724 (all data).

### 7.7.3.3 [$Fe_2$(μ-η⁴:η⁴-tmaf)$(CO)_6$]



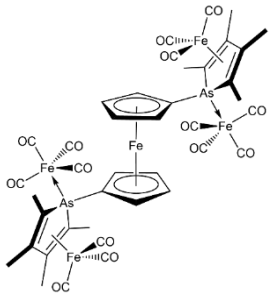

A suspension of [$Fe(COE)_2(CO)_3$] was prepared by UV-photolysis of 0.1 mL [$Fe(CO)_5$] (0.74 mmol) in 20 mL *n*-hexane containing 0.5 mL *cis*-cyclooctene (3.8 mmol, large excess) at -78 °C over 60 minutes. The complex is thermolabile and was not characterised. To this was added 0.2 g solid tmaf (0.36 mmol) and the mixture stirred at low temperature for 60 minutes giving a deep red solution. This was allowed to warm to ambient temperature overnight producing a green solution with red-brown solids. The mixture was dried by rotary evaporation and extracted with

portions of $Et_2O$ and eluted through a short column of neutral alumina (10 x 2.5 cm). An immobile green band (presumed to be $[Fe_3(CO)_{12}]$) remains atop the column and the orange filtrate is collected and dried by rotary evaporation. The residue was extracted with portions of petroleum ether and transferred to a water-jacketed column of silica gel (35 x 2.5 cm; water temperature *ca* 10 °C) made up in the same solvent. Eluting with petroleum ether provides a thin yellow band containing $[Fe(CO)_5]$ and *cis*-cyclooctene which is discarded. Eluting with 49:1 petroleum ether/$Et_2O$ gives an orange band containing the product which is collected and dried by rotary evaporation giving a yellow-orange solid. Isolated yield: 0.12 g (0.14 mmol, 38%). The product is air-stable and is readily soluble in common organic solvents. The use of a water-jacketed column was necessary for sufficient resolution of the two products however some overlap of bands was observed, and this mixed fraction was discarded.

NMR: $^1$H ($C_6D_6$, 400 MHz, 25 °C) δ 4.04 (t, $J_{HH}$ = 1.7 Hz, 4H, α-η$^5$-$C_5H_4$), 3.76 (t, $J_{HH}$ = 1.7 Hz, 4H, β-η$^5$-$C_5H_4$), 1.76 (s, 12H, α-$CH_3$), 1.55 (s, 12H, β-$CH_3$) ppm. $^{13}$C{$^1$H} ($C_6D_6$, 176 MHz, 25 °C) δ 211.9 (*C*O), 108.9 (arsole {2,5}-*C*), 88.1 (*As*-bonded η$^5$-$C_5H_4$), 70.7 ({2,5}-η$^5$-$C_5H_4$), 70.4 ({3,4}-η$^5$-$C_5H_4$), 67.7 (arsole {3,4}-*C*), 18.0 (α-$CH_3$), 13.2 (β-$CH_3$) ppm. IR (*n*-hexane, 25 °C) $\nu_{CO}$ 2037(vs), 1976(s), 1965(s) cm$^{-1}$. HR-MS (ESI, MeCN, +ve ion) found *m*/*z* 829.8674 (calc. for $C_{32}H_{32}O_6{}^{75}As_2{}^{56}Fe_3$ $[M]^+$: 829.8679). Analysis found 46.35% C, 3.99% H (calc. for $C_{32}H_{32}O_6As_2Fe_3$: 46.31% C, 3.89% H).

Crystals were obtained by slow evaporation of $Et_2O$ solution at -20 °C. The selected crystal proved to be twinned and suitable twin law was applied. $C_{32}H_{32}As_2Fe_3O_6$ (*M* = 829.96 g/mol): yellow plate 0.061 × 0.16 × 0.395 mm, triclinic, space group *P*-1 (no. 2), *a* = 7.7655(8) Å, *b* = 8.1370(6) Å, *c* = 13.1813(13) Å, α = 82.991(7)°, *β* = 85.868(9)°, *γ* = 81.688(8)°, *V* = 816.73(13) Å$^3$, *Z* = 1, multi-scan correction $T_{min}/T_{max}$ = 0.743/1.000, *μ*(Mo-Kα) = 3.366 mm$^{-1}$, $\varrho_{calc}$ = 1.687 g/cm$^3$, 4176 reflections measured (6.836° ≤ 2Θ ≤ 53.448°), 4176 unique ($R_{int}$ = 0.0511, $R_{sigma}$ = 0.0937) which were used in all calculations *GOF* = 0.961, $D_{min}/D_{max}$ = -0.52/0.87 e/Å$^3$. The final $R_1$ was 0.0439 (I > 2σ(I)) and *w*$R_2$ was 0.0788 (all data).

### 7.7.3.4 [$Fe_4$(μ-η$^1$:η$^1$:η$^4$:η$^4$-tmaf)(CO)$_{14}$]



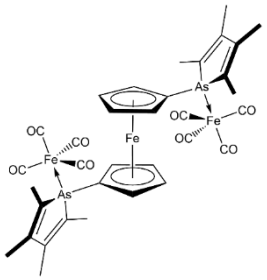

This complex was obtained during chromatography of $Fe_2$(μ-η$^4$:η$^4$-tmaf)(CO)$_6$] above. Eluting with 24:1 petroleum ether/$Et_2O$ gave a second orange band containing the product, which was collected and dried by rotary evaporation giving a yellow-orange solid. Isolated yield: 0.095 g (0.08 mmol, 22%). Properties are identical to that above.

NMR: $^1$H ($C_6D_6$, 400 MHz, 25 °C) δ 4.28 (br s, 4H, α-η$^5$-$C_5H_4$), 3.95 (br s, 4H, β-η$^5$-$C_5H_4$), 1.67 (s, 12H, α-$CH_3$), 1.36 (s, 12H, β-$CH_3$) ppm. $^{13}$C{$^1$H} ($C_6D_6$, 176 MHz, 25 °C) δ 218.2 (*C*O), 210.6 (*C*O), 105.9 (arsole {2,5}-*C*), 91.2 (As-bonded η$^5$-$C_5H_4$), 71.9 ({2,5}-η$^5$-$C_5H_4$), 71.1 ({3,4}-η$^5$-$C_5H_4$), 67.3 (arsole {3,4}-*C*), 15.7 (α-$CH_3$), 13.3 (β-$CH_3$) ppm. IR (*n*-hexane, 25 °C) $\nu_{CO}$ 2058(s), 2044(vs), 1994(s), 1981(vs), 1966(s), 1948(s) cm$^{-1}$. HR-MS (ESI, MeCN, +ve ion)

found $m/z$ 1109.7071 (calc. for $C_{38}H_{32}O_{12}{}^{75}As_2{}^{56}Fe_5$ $[M - 2CO]^+$: 1109.7073). Analysis found 41.45% C, 3.00% H (calc. for $C_{40}H_{32}O_{14}As_2Fe_5$: 41.21% C, 2.77% H).

Single crystals were obtained by slow evaporation of benzene/cyclohexane solution. $C_{40}H_{32}As_2Fe_5O_{14}$ ($M$ = 1165.74 g/mol): yellow prism 0.104 × 0.172 × 0.228 mm, monoclinic, space group $P2_1/n$ (no. 14), $a$ = 19.1736(9) Å, $b$ = 9.0836(4) Å, $c$ = 25.1005(14) Å, $\beta$ = 91.384(4)°, $V$ = 4370.4(4) Å$^3$, $Z$ = 4, multi-scan correction $T_{min}/T_{max}$ = 0.939/1.000, $\mu$(Mo-Kα) = 3.187 mm$^{-1}$, $\varrho_{calc}$ = 1.772 g/cm$^3$, 24714 reflections measured (6.618° ≤ 2Θ ≤ 60.206°), 10523 unique ($R_{int}$ = 0.0450, $R_{sigma}$ = 0.0682) which were used in all calculations, $GOF$ = 1.021, $D_{min}/D_{max}$ = -0.88/1.11 e/Å$^3$. The final $R_1$ was 0.0439 (I > 2σ(I)) and $wR_2$ was 0.0990 (all data).

### 7.7.3.5 [Fe$_2$(μ-η$^1$:η$^1$-tmaf)(CO)$_8$]




This compound was isolated in trace quantities from reactions between tmaf and [Fe(COE)$_2$(CO)$_3$] however could be directly prepared from iron carbonyl. A 25 mL Schlenk tube was charged with 0.1 tmaf (0.18 mmol) and 0.2 g [Fe$_2$(CO)$_9$] (0.55 mmol) and 10 mL THF admitted, and briefly triturated to provide a deep orange solution which is stirred overnight at ambient temperature. After this time the mixture is filtered through a short plug of celite (1 x 1 cm) and the orange filtrate dried by rotary evaporation. The residue was extracted with portions of petroleum ether and transferred to a column of silica gel (20 x 2.5 cm) made up in the same solvent. Eluting with petroleum ether provides a thin yellow band of [Fe(CO)$_5$] which is discarded. Eluting with 9:1 petroleum ether/Et$_2$O gives a bright orange band containing the product which is collected and dried by rotary evaporation giving a microcrystalline orange solid. Isolated yield: 0.1 g (0.11 mmol, 61%). The product is air stable and is readily soluble in common organic solvents. **Caution**: [Fe(CO)$_5$] is produced in the reaction and may be present during workup.

NMR: $^1$H ($C_6D_6$, 400 MHz, 25 °C) δ 4.33 (br s, 4H, α-η$^5$-C$_5$*H*$_4$), 4.23 (br s, 4H, β-η$^5$-C$_5$*H*$_4$), 1.96 (s, 12H, α-C*H*$_3$), 1.46 (br s, 12H, β-C*H*$_3$) ppm. $^{13}$C{$^1$H} ($C_6D_6$, 176 MHz, 25 °C) δ 214.0 (*C*O), 142.6 (arsole {2,5}-*C*), 136.5 (arsole {3,4}-*C*), 79.2 (*As*-bonded η$^5$-*C*$_5$H$_4$), 72.2 ({2,5}-η$^5$-*C*$_5$H$_4$), 71.6 ({3,4}-η$^5$-*C*$_5$H$_4$), 13.8 (α-*C*H$_3$), 13.5 (β-*C*H$_3$) ppm. IR (*n*-hexane, 25 °C) $\nu_{CO}$ 2048(vs), 1975(vs), 1945(vs), 1935(vs) cm$^{-1}$. HR-MS (ESI, MeCN, +ve ion) found $m/z$ 886.8551 (calc. for $C_{34}H_{32}O_8{}^{75}As_2{}^{56}Fe_3$ $[M + H]^+$: 886.8656). Analysis found 46.18% C, 3.66% H (calc. for $C_{34}H_{32}O_8As_2Fe_3$: 46.09% C, 3.64% H).

Single crystals were obtained by slow evaporation of *n*-hexane solution at -20 °C. $C_{34}H_{32}As_2Fe_3O_8$ ($M$ = 885.98 g/mol): yellow plate 0.072 × 0.14 × 0.222 mm, monoclinic, space group $P2_1/c$ (no. 14), $a$ = 8.2175(6) Å, $b$ = 24.4124(15) Å, $c$ = 8.7590(6) Å, $\beta$ = 97.107(7)°, $V$ = 1743.6(2) Å$^3$, $Z$ = 2, multi-scan correction $T_{min}/T_{max}$ = 0.895/1.000, $\mu$(Mo-Kα) = 3.164 mm$^{-1}$, $\varrho_{calc}$ = 1.688 g/cm$^3$, 6794 reflections measured (6.86° ≤ 2Θ ≤ 57.23°), 3600 unique ($R_{int}$ = 0.0364, $R_{sigma}$ = 0.0645) which were used in all calculations, $GOF$ = 1.069. $D_{min}/D_{max}$ = -0.52/0.56 e/Å$^3$. The final $R_1$ was 0.0435 (I > 2σ(I)) and $wR_2$ was 0.0881 (all data).

## 7.8 References


1. J. J. Bishop, A. Davison, M. L. Katcher, D. W. Lichtenberg, R. E. Merrill and J. C. Smart, *J, Organomet. Chem.,* **1971**, *27*, 241-249.
2. S. Dey and R. Pietschnig, *Coord. Chem. Rev.*, **2021**, *437*, 213850.
3. J. Roger, S. Royer, H. Cattey, A. Savateev, R. V. Smaliy, A. N. Kostyuk and J. C. Hierso, *Eur. J. Inorg. Chem.*, **2017**, 330-339.
4. A. Orthaber, S. Borucki, W. Shen, R. Réau, C. Lescop and R. Pietschnig, *Eur. J. Inorg. Chem.*, **2014**, 1751-1759.
5. E. Deschamps and F. Mathey, *J. Organomet. Chem.,* **1987**, *332*, 141-152.
6. R. T. McGuire, J. S. K. Clark, A. V. Gatien, M. Y. Shen, M. J. Ferguson and M. Stradiotto, *Eur. J. Inorg. Chem.*, **2019**, 4112-4116.
7. M. E. Fox, M. Jackson, I. C. Lennon, J. Klosin and K. A. Abboud, *J. Org. Chem.*, **2008**, *73*, 775-784.
8. A. Schmied, A. Straube, T. Grell, S. Jähnigen and E. Hey-Hawkins, *Dalton Trans.*, **2015**, *44*, 18760-18768.
9. C. L. Mandell, S. S. Kleinbach, W. G. Dougherty, W. S. Kassel and C. Nataro, *Inorg. Chem.*, **2010**, *49*, 9718-9727.
10. M. G. Fitzpatrick, L. R. Hanton and J. Simpson, *Inorg. Chim. Acta*, **1996**, *244*, 131-136.
11. L. C. Song, G. F. Wang, P. C. Liu and Q. M. Hu, *Organometallics*, **2003**, *22*, 4593-4598.
12. M. D. Rausch and D. J. Ciappenelli, *J. Organomet. Chem.*, **1967**, *10*, 127-136.
13. F. Rebiere, O. Samuel and H. B. Kagan, *Tet. Lett.*, **1990**, *31*, 3121-3124.
14. D. Guillaneux and H. B. Kagan, *J. Org. Chem.*, **1995**, *60*, 2502-2505.
15. E. W. Abel, N. J. Long, K. G. Orrell, A. G. Osborne and V. Šik, *J. Organomet. Chem.*, **1991**, *403*, 195-208.
16. D. Carmichael, L. Ricard, N. Seeboth, J. M. Brown, T. D. W. Claridge and B. Odell, *Dalton Trans.*, **2005**, 2173-2181.
17. C. L. Bergstrom and R. L. Luck, *Inorg. Chim. Acta*, **2001**, *318*, 77-83.
18. J. Grobe, S. Göbelbecker, B. Krebs and M. Läge, *Z. Anorg. Allg. Chem.*, **1992**, *611*, 11-22.
19. W. R. Cullen, A. W. Wu, A. R. Davis, F. W. B. Einstein and J. D. Hazlett, *Can. J. Chem.*, **1976**, *54*, 2871-2878.
20. A. R. Davis, F. W. B. Einstein and J. D. Hazlett, *Acta Cryst. B*, **1977**, *33*, 212-215.
21. P. J. Roberts and J. Trotter, *J. Chem. Soc. A*, **1971**, 1501-1505.
22. C. A. Tolman, *Chem. Rev.*, **1977**, *77*, 313-348.
23. F. Döttinger and M. R. Ringenberg, *Organometallics*, **2019**, *38*, 586-592.
24. C. F. Nobile, G. Vasapollo, P. Giannoccaro and A. Sacco, *Inorg. Chim. Acta*, **1981**, *48*, 261-263.
25. D. Schaarschmidt, J. Kühnert, S. Tripke, H. G. Alt, C. Görl, T. Rüffer, P. Ecorchard, B. Walfort and H. Lang, *J. Organomet. Chem.*, **2010**, *695*, 1541-1549.
26. M. R. Ringenberg and F. Döttinger, *Eur. J. Inorg. Chem.*, **2019**, 2430-2435.
27. N. A. LaBerge and J. A. Love, *Eur. J. Org. Chem.*, **2015**, 5546-5553.
28. E. Hey-Hawkins, M. Pink, H. Oesen and D. Fenske, *Z. Anorg. All. Chem.*, **1996**, *622*, 689-691.
29. C. G. Pierpont and R. Eisenberg, *Inorg. Chem.*, **1972**, *11*, 828-832.
30. N. Bricklebank, S. M. Godfrey, C. A. McAuliffe and R. G. Pritchard, *J. Chem. Soc., Dalton Trans.*, **1996**, 157-160.
31. J. A. Casares, P. Espinet, J. M. Martín-Alvarez, J. M. Martínez-Ilarduya and G. Salas, *E. J. Inorg. Chem.*, **2005**, 3825-3831.
32. R. S. Nyholm, *Nature*, **1950**, *165*, 154-154.
33. R. S. Nyholm, *J. Chem. Soc.,* **1951**, 2602-2607.

34. M. C. Gimeno, A. Laguna, C. Sarroca and P. G. Jones, *Inorg. Chem.*, **1993**, *32*, 5926-5932.
35. T. A. Nguyen, M. J. Penouilh, H. Cattey, N. Pirio, P. Fleurat-Lessard, J. C. Hierso and J. Roger, *Organometallics*, **2021**, *40*, 3571-3584.
36. R. Usón, A. Laguna, J. Vicente, J. Garcia, P. G. Jones and G. M. Sheldrick, *J. Chem. Soc. Dalton Trans.*, **1981**, 655-657.
37. U. M. Tripathi, A. Bauer and H. Schmidbaur, *J. Chem. Soc. Dalton Trans.*, **1997**, 2865-2868.
38. I. R. Butler, W. R. Cullen, T. J. Kim, S. J. Rettig and J. Trotter, *Organometallics*, **1985**, *4*, 972-980.
39. T. Hayashi, M. Konishi, Y. Kobori, M. Kumada, T. Higuchi and K. Hirotsu, *J. Am. Chem. Soc.,* **1984**, *106*, 158-163.
40. C. Herrera-Álvarez, V. Gómez-Benítez, R. O. Redón, J. J. Garcí´a, S. Hernández-Ortega, R. A. Toscano and D. Morales-Morales, *J. Organomet. Chem.,* **2004**, *689*, 2464-2472.
41. O. V. Gusev, A. M. Kalsin, M. G. Peterleitner, P. V. Petrovskii, K. A. Lyssenko, N. G. Akhmedov, C. Bianchini, A. Meli and W. Oberhauser, *Organometallics*, **2002**, *21*, 3637-3649.
42. C. Bianchini, A. Meli, W. Oberhauser, S. Parisel, E. Passaglia, F. Ciardelli, O. V. Gusev, A. M. Kal'si and N. V. Vologdin, *Organometallics*, **2005**, *24*, 1018-1030.
43. T. R. Welberry and D. J. Goossens, *I. U. Cryst. J.*, **2014**, *1*, 550-562.
44. A. C. Hillier, W. J. Sommer, B. S. Yong, J. L. Petersen, L. Cavallo and S. P. Nolan, *Organometallics*, **2003**, *22*, 4322-4326.
45. H. Clavier and S. P. Nolan, *Chem. Comm.*, **2010**, *46*, 841-861.
46. L. Falivene, Z. Cao, A. Petta, L. Serra, A. Poater, R. Oliva, V. Scarano and L. Cavallo, *Nat. Chem.*, **2019**, *11*, 872-879.
47. A. Poater, F. Ragone, R. Mariz, R. Dorta and L. Cavallo, *Chem. Eur. J.*, **2010**, *16*, 14348-14353.
48. A. Gómez-Suárez, D. J. Nelson and S. P. Nolan, *Chem. Comm.*, **2017**, *53*, 2650-2660.
49. V. V. Grushin, C. Bensimon and H. Alper, *Inorg. Chem.*, **1994**, *33*, 4804-4806.
50. A. R. Elsagir, F. Gaßner, H. Görls and E. Dinjus, *J. Organomet. Chem.*, **2000**, *597*, 139-145.
51. G. A. Grasa and T. J. Colacot, *Org. Lett.*, **2007**, *9*, 5489-5492.
52. W. L. Steffen and G. J. Palenik, *Inorg. Chem.*, **1976**, *15*, 2432-2439.
53. S. Ganguly, J. T. Mague and D. M. Roundhill, *Acta Cryst. C*, **1994**, *50*, 217-219.
54. C. Ortiz-Cervantes, M. Flores-Alamo and J. J. García, *ACS Cat.*, **2015**, *5*, 1424-1431.
55. T. S. Wierenga, C. R. Vanston, A. Ariafard, M. G. Gardiner and C. C. Ho, *Organometallics*, **2019**, *38*, 3032-3038.
56. F. Ozawa, A. Kubo, Y. Matsumoto, T. Hayashi, E. Nishioka, K. Yanagi and K. Moriguchi, *Organometallics*, **1993**, *12*, 4188-4196.
57. A. M. Johns, M. Utsunomiya, C. D. Incarvito and J. F. Hartwig, *J. Am. Chem. Soc.*, **2006**, *128*, 1828-1839.
58. B. A. Chalmers, M. Bühl, P. S. Nejman, A. M. Z. Slawin, J. D. Woollins and P. Kilian, *J. Organomet. Chem.*, **2015**, *800*, 70-74.
59. D. Morrogh, S. Schwarz, C. Maichle-Mössmer and J. Strähle, *Z. Anorg. Allg. Chem.*, **2006**, *632*, 801-806.
60. B. J. Frogley and A. F. Hill, *Dalton Trans.*, **2022**, 1907-1917.
61. H. Fleckner, F. W. Grevels and D. Hess, *J. Am. Chem. Soc.,* **1984**, *106*, 2027-2032.
62. R. L. Keiter, E. A. Keiter, K. H. Hecker and C. A. Boecker, *Organometallics*, **1988**, *7*, 2466-2469.

63. Z. ZHANG, J. GU, C. ZHANG and H. SUN, *Organometallics*, **2008**, *27*, 2149-2151.
64. F. CARRÉ, E. COLOMER, R. J. P. CORRIU, M. L' HEUREUX and A. CAVÉ, *J. Organomet. Chem.*, **1987**, *331*, 29-43.
65. R. ALBRECHT and E. WEISS, *J. Organomet. Chem.,* **1991**, *413*, 355-377.
66. K. HOFFMANN and E. WEISS, *J. Organomet. Chem.,* **1977**, *128*, 237-246.
67. F. EDELMANN, B. LUBKE and U. BEHRENS, *Chem. Ber.*, **1982**, *115*, 1325-1331.
68. I. EMME, T. LABAHN and A. DE MEIJERE, *Eur. J. Org. Chem.*, **2006**, 399-404.
69. L. A. PAQUETTE, G. A. O'DOHERTY, B. L. MILLER, R. D. ROGERS, A. L. RHEINGOLD and S. L. GEIB, *Organometallics*, **1989**, *8*, 2167-2172.
70. G. SCHRÖDER, H. BUTENSCHÖN, R. BOESE, T. LENDVAI and A. D. MEIJERE, *Chem. Ber.*, **1991**, *124*, 2423-2427.
71. F. A. COTTON and J. M. TROUP, *J. Am Chem. Soc.,* **1974**, *96*, 3438-3443.
72. P. E. RILEY and R. E. DAVIS, *Inorg. Chem.*, **1980**, *19*, 159-165.
73. A. H. COWLEY, R. E. DAVIS and K. REMADNA, *Inorg. Chem.*, **1981**, *20*, 2146-2152.
74. R. L. KEITER, A. L. RHEINGOLD, J. J. HAMERSKI and C. K. CASTLE, *Organometallics*, **1983**, *2*, 1635-1639.
75. W. M. DOUGLAS and J. K. RUFF, *J. Chem. Soc. A*, **1971**, 3558-3561.
76. R. G. MONTEMAYOR, D. T. SAUER, S. FLEMING, D. W. BENNETT, M. G. THOMAS and R. W. PARRY, *J. Am. Chem. Soc.,* **1978**, *100*, 2231-2233.
77. C. A. UDOVICH, R. J. CLARK and H. HAAS, *Inorg. Chem.*, **1969**, *8*, 1066-1072.
78. D. P. BAUER and J. K. RUFF, *Inorg. Chem.*, **1983**, *22*, 1686-1689.
79. W. S. SHELDRICK, S. MORTON and O. STELZER, *Z. Anorg. Allg. Chem.*, **1981**, *475*, 232-240.
80. R. H. NEILSON, R. J. THOMA, I. VICKOVIC and W. H. WATSON, *Organometallics*, **1984**, *3*, 1132-1133.
81. J. PICKARDT, L. RÖSCH and H. SCHUMANN, *J. Organomet. Chem.,* **1976**, *107*, 241-248.
82. L. R. MARTIN, F. W. B. EINSTEIN and R. K. POMEROY, *Inorg. Chem.*, **1985**, *24*, 2777-2785.
83. P. PORTIUS, M. BÜHL, M. W. GEORGE, F. W. GREVELS and J. J. TURNER, *Organometallics*, **2019**, *38*, 4288-4297.
84. A. J. PEARSON, *Acc. Chem. Res.*, **1980**, *13*, 463-469.

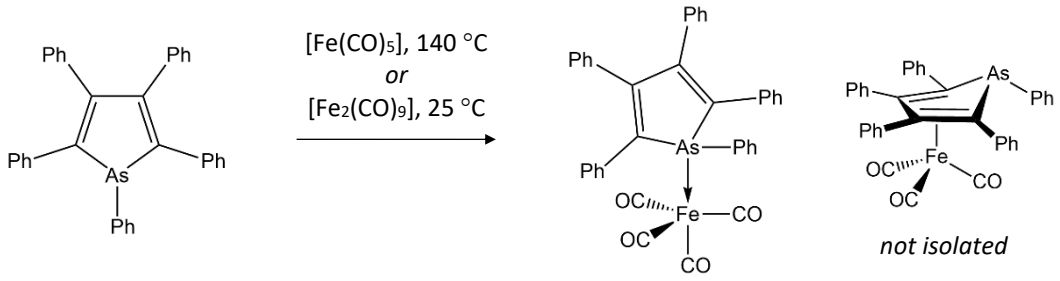
# Appendix

## 8.1 Preamble

Throughout the course of this work, several compounds were prepared or serendipitously obtained which are tangential (to varying degrees) to the results already described in **Chapters 1—7**, though were not included in the primary discussion since they diverted somewhat from the narrative. They are included here in this appendix so as not to be lost to time and, where relevant, to the efforts of future researchers.

## 8.2 The Crystal Structure of [Fe(PhAsC$_4$Ph$_4$)(CO)$_4$]

This complex was prepared during attempts to replicate the synthesis of [Fe($\eta^4$-PhAsC$_4$Ph$_4$)(CO)$_3$] reported by BRAYE ,[1] although the iron *tetra*carbonyl was the only species isolated. Salient features and some spectroscopic data have been discussed in **Chapter 1**, **Section 1.4.3**. Single crystals were obtained from $CH_2Cl_2$/*n*-hexane at -20 °C and the molecular structure is shown in **Figure 8.1**.




**Scheme 8.1**: Synthesis of [Fe(PhAsC$_4$Ph$_4$)(CO)$_4$].

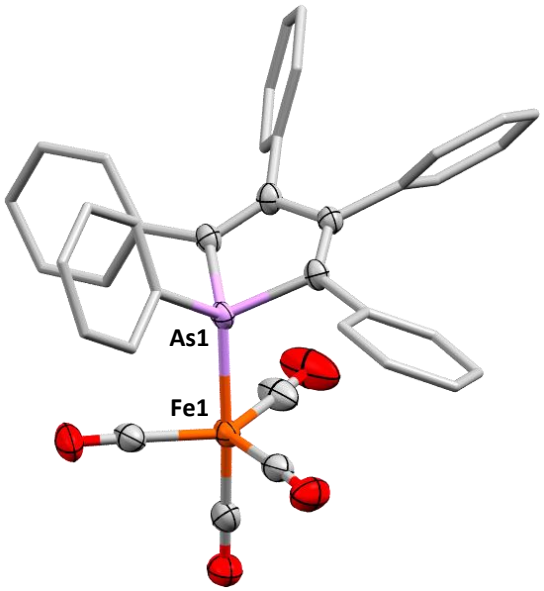


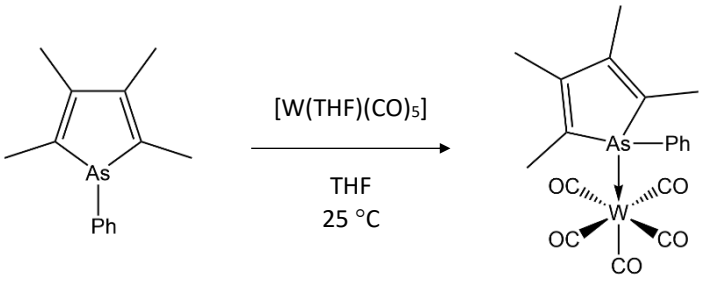

**Figure 8.1**: The molecular structure of [Fe(PhAsC$_4$Ph$_4$)(CO)$_4$]·1.5$CH_2Cl_2$ in a crystal. Phenyl groups simplified and dichloromethane solvent molecules and hydrogen atoms omitted for clarity. Ellipsoids shown at 50% displacement.

A distorted trigonal bipyramidal Fe(0) centre is found ($\tau_5$ = 0.71). The pentaphenylarsole ligand lies along the principal axis of the coordination polyhedron with a As→Fe distance of 2.3319(8) Å. The three equatorial carbonyl ligands are not evenly distributed about the trigonal plane with angles of *ca* 128°, 116° and 115° with the widest angle measured between the carbonyl ligands sitting directly below the *As*-phenyl substituent. The four Fe-C and C≡O bonds are crystallographically equivalent (mean 1.789 and 1.145 Å, respectively) despite being in chemically inequivalent coordination sites, and the arsole ring carbon dimensions are unremarkable.

Data for $C_{38}H_{25}O_4As_1Fe_1 \cdot 1.5CH_2Cl_2$ ($M$ = 808.73 g/mol): yellow plate 0.05 × 0.072 × 0.175 mm, triclinic, space group *P*-1 (no. 2), $a$ = 10.5122(2) Å, $b$ = 12.9134(6) Å, $c$ = 13.3258(4) Å, $\alpha$ = 89.855(3)°, $\beta$ = 88.366(2)°, $\gamma$ = 87.340(3)°, $V$ = 1806.27(11) Å$^3$, $Z$ = 2, Gaussian correction $T_{min}/T_{max}$ = 0.677/1.000, $\mu$(Cu-K$\alpha$) = 6.737 mm$^{-1}$, $\varrho_{calc}$ = 1.487 g/cm$^3$, 13087 reflections measured (8.424° ≤ 2$\Theta$ ≤ 148.448°), 7099 unique ($R_{int}$ = 0.0261, $R_{sigma}$ = 0.0445) which were used in all calculations, $GOF$ = 1.077, $D_{min}/D_{max}$ = -1.02/0.66 e/Å$^3$. The final $R_1$ was 0.0604 (I > 2$\sigma$(I)) and $wR_2$ was 0.1692 (all data).

## 8.3 The Crystal Structure of [W(PhAsC$_4$Me$_4$)(CO)$_5$]

This arsole complex was previously reported and spectroscopically characterised by Voß,[2] though the crystal structure was not determined. It was prepared in the exact same manner as described by the authors, by simple addition of excess UV-generated [W(THF)(CO)$_5$] to a THF solution of PhAsC$_4$Me$_4$.




**Scheme 8.2**: Synthesis of [W(PhAsC$_4$Me$_4$)(CO)$_5$].

The compound was prepared with a view of reinvestigating arsinidine formation upon treatment with dimethylacetylene dicarboxylate (DMAD), for which a corresponding phosphole complex afforded the first example of the triangular phosphirene ligand ($R'PC_2R_2$) attached to $W(CO)_5$.[3, 4] Whilst tetramethyl-*ortho*-phthalate *was* isolated from the reaction between $[W(PhAsC_4Me_4)(CO)_5]$ and DMAD at 50 °C, no analogous arsirene complex (*i.e.*, $[W(PhAsC_2R_2)(CO)_5]$) was observed when carried out in the presence of excess alkyne (DMAD, EtC≡CEt, or $Me_3SiC{\equiv}CSiMe_3$) and efforts were unfortunately abandoned. Single crystals of $[W(PhAsC_4Me_4)(CO)_5]$ were grown from *n*-hexane solution at 0 °C.

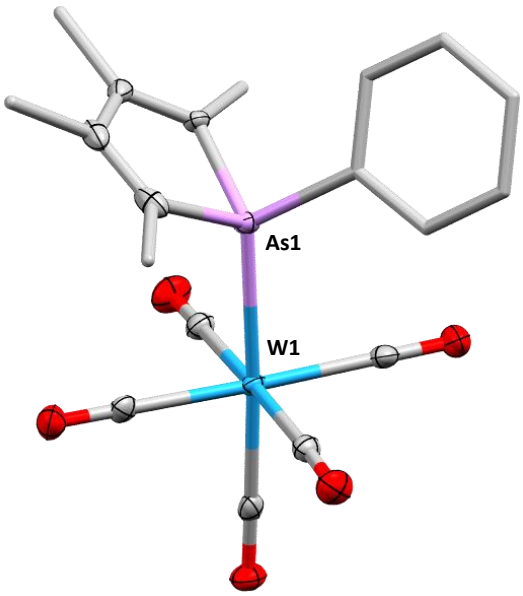



**Figure 8.2**: The molecular structure of $[W(PhAsC_4Me_4)(CO)_5]$ in a crystal. Phenyl and methyl groups simplified and hydrogen atoms omitted for clarity. Ellipsoids shown at 50% displacement.

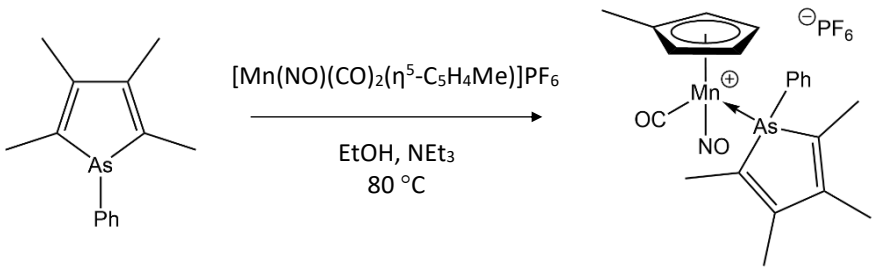
An approximately octahedral W(0) centre is found; the As→W dative bond length of 2.6011(6) Å is comparable to other tertiary arsine complexes* of W(0) and the W-C bond *trans* to the arsole (1.998(4) Å) is only marginally shorter than the four W-C bonds *cis* (mean 2.039(8) Å). The *trans* axial As-W-C angle is *ca* 176° with angles of 88—92° being made between mutually *cis* substituents, and angles about the As(III) atom exterior reflect the distorted tetrahedral valence environment (117—120°). Interatomic distances within the arsole ring are normal finding mean As-$C_\alpha$ bond lengths of 1.924(4) Å, and mean $C_\alpha$=$C_\beta$ and $C_\beta$-$C_\beta$ bond within the butadiene of 1.334(6) and 1.486(5) Å.

* Of the 7 crystal structures indexed in the CSD with As → W(0) dative bonds, the mean distance is 2.626 Å with a range of 2.589—2.646 Å.

Data for $C_{19}H_{17}O_5As_1W_1$ ($M$ = 584.09 g/mol): yellow needle 0.135 × 0.357 × 0.357 mm, monoclinic, space group $I2/a$ (no. 15), $a$ = 16.8307(6) Å, $b$ = 10.3126(4) Å, $c$ = 23.5516(7) Å, $\beta$ = 98.928(3)°, $V$ = 4038.3(2) Å$^3$, $Z$ = 8, spherical correction $T_{min}/T_{max}$ = 0.213/0.239, $\mu$(Mo-Kα) = 7.372 mm$^{-1}$, $\varrho_{calc}$ = 1.921 g/cm$^3$, 12817 reflections measured (6.45° ≤ 2Θ ≤ 64.782°), 6330 unique ($R_{int}$ = 0.0258, $R_{sigma}$ = 0.0411) which were used in all calculations, $GOF$ = 1.087, $D_{min}/D_{max}$ = -1.55/1.07 e/Å$^3$. The final $R_1$ was 0.0316 (I > 2σ(I)) and $wR_2$ was 0.0637 (all data).

## 8.4 The Crystal Structure of [Mn(PhAsC$_4$Me$_4$)(NO)(CO)(η$^5$-C$_5$H$_4$Me)]PF$_6$

This compound was also described by Voß[2] and reinvestigated here for the same purpose as the tungsten complex above, though was also unsuccessful at producing an arsirene complex. [Mn(PhAsC$_4$Me$_4$)(NO)(CO)(η$^5$-C$_5$H$_4$Me)]PF$_6$ was prepared by combining [Mn(NO)(CO)$_2$(η$^5$-C$_5$H$_4$Me)]PF$_6$ with PhAsC$_4$Me$_4$ and triethylamine in ethanol at reflux (following the protocol outlined by the above authors). Single crystals were obtained by diffusion of Et$_2$O into CH$_2$Cl$_2$ solution at -20 °C.




**Scheme 8.3**: Synthesis of [Mn(PhAsC$_4$Me$_4$)(NO)(CO)(η$^5$-C$_5$H$_4$Me)]PF$_6$.

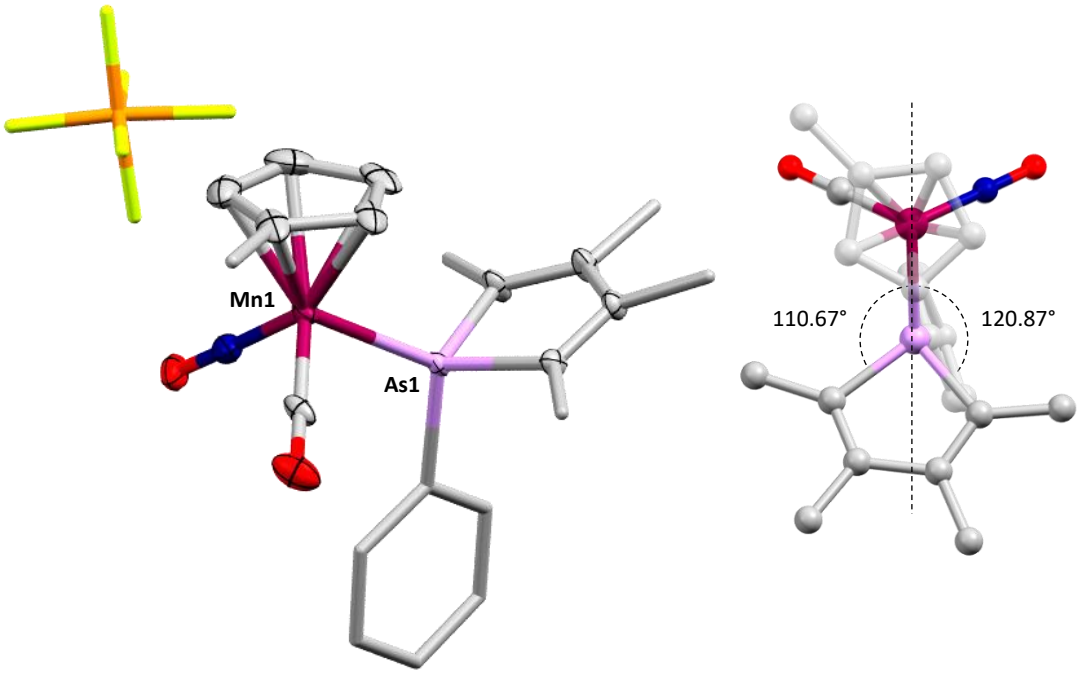



**Figure 8.3**: The molecular structure of $[Mn(PhAsC_4Me_4)(NO)(CO)(\eta^5\text{-}C_5H_4Me)]PF_6$ in a crystal. Phenyl, methyl and hexafluorophosphate groups simplified and hydrogen atoms omitted for clarity. Ellipsoids shown at 50% displacement. **Inset**: Abbreviated perspective of the molecule highlighting the asymmetric disposition of the arsole ligand.

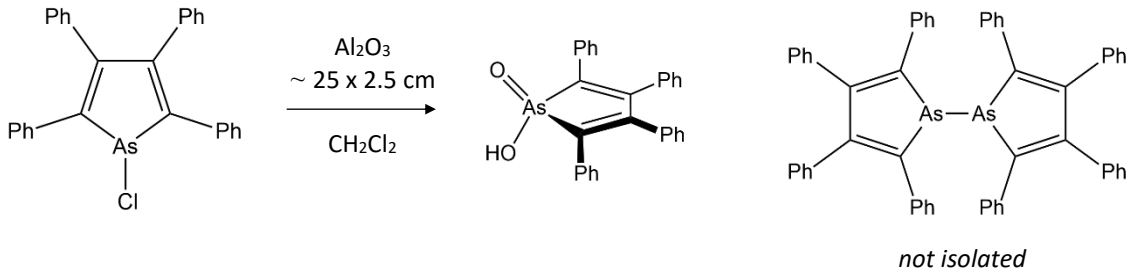
The crystal structure reveals the expected arsole complex. The acentric unit cell (orthorhombic *Pca*$2_1$) contains four molecules comprising two pairs of enantiomers – the nitrosyl group was not disordered amongst the isosteric carbonyl ligand and could be located in an electron-density difference map. A *pseudo*-octahedral Mn(I) centre is found with a *ca* 98° angle made between the nitrosyl and carbonyl ligands, a cleft in which the *As*-phenyl substituent resides. The As → Mn dative bond measures 2.3561(7) Å, and the arsole ligand is not aligned with median plane of the $Mn(NO)(CO)(\eta^5\text{-}C_5H_4Me)$ centre – one methyl group in a 2,5-ring position recedes slightly from the nitrosyl ligand affording a visible asymmetry to the complex when viewed perpendicular to the cyclopentadienyl ring plane (**Figure 8.3**, **Inset**). Thus, the spatial distribution of the tripodal ligand set find a smaller carbonyl-arsolyl angle (*ca* 110°) than the nitrosyl-arsolyl angle (*ca* 120°). This also introduces a slight irregularity to the arsole ring system, with one set of As-$C_\alpha$ and $C_\alpha$=$C_\beta$ bonds (1.921(3) and 1.350(5) Å, respectively) slightly longer than the other two (1.902(3) and 1.338(6) Å).

Data for $C_{21}H_{24}N_1O_2As_1F_6Mn_1P_1$ ($M$ = 597.24 g/mol): orange needle 0.109 × 0.138 × 0.515 mm, orthorhombic, space group *Pca*$2_1$ (no. 29), $a$ = 17.5496(9) Å, $b$ = 8.2642(3) Å, $c$ = 16.1495(7) Å, $V$ = 2342.22(18) Å$^3$, $Z$ = 4, multi-scan correction $T_{min}/T_{max}$ = 0.891/1.000, $\mu$(Mo-Kα) = 2.101 mm$^{-1}$, $\varrho_{calc}$ = 1.694 g/cm$^3$, 10896 reflections measured

(6.772° ≤ 2Θ ≤ 59.15°), 5067 unique ($R_{int}$ = 0.0254, $R_{sigma}$ = 0.0371) which were used in all calculations, *GOF* = 1.022, $D_{min}/D_{max}$ = -0.33/0.52 e/Å$^3$. The final $R_1$ was 0.0311 (I > 2σ(I)) and $wR_2$ was 0.0699 (all data).

## 8.5 The Crystal Structure of (HO)(O)AsC$_4$Ph$_4$

This yellow As(V) species was obtained from column chromatography of ClAsC$_4$Ph$_4$ on neutral alumina. The intent was to test the validity of biarsolyl formation as THEOPOLD has previously reported,[5] where (AsC$_4$Me$_4$)$_2$ was apparently isolated after contact of ClAsC$_4$Me$_4$ with neutral alumina. Instead, it appears that hydrolysis and oxidation of the arsenic centre has occurred here. In fact, (AsC$_4$Ph$_4$)$_2$ could be obtained (admittedly not efficiently) by a redox transmetalation reaction with [Cr(SnBu$_3$)(CO)$_3$($\eta^5$-C$_5$H$_5$)] and isolated as an *orange* crystalline solid (**Chapter 4**, **Section 4.1.2**). Single crystals were obtained from CH$_2$Cl$_2$/methanol at -20 °C and the molecular structure is shown in **Figure 8.4**.




**Scheme 8.4**: Isolation of (HO)(O)AsC$_4$Ph$_4$.

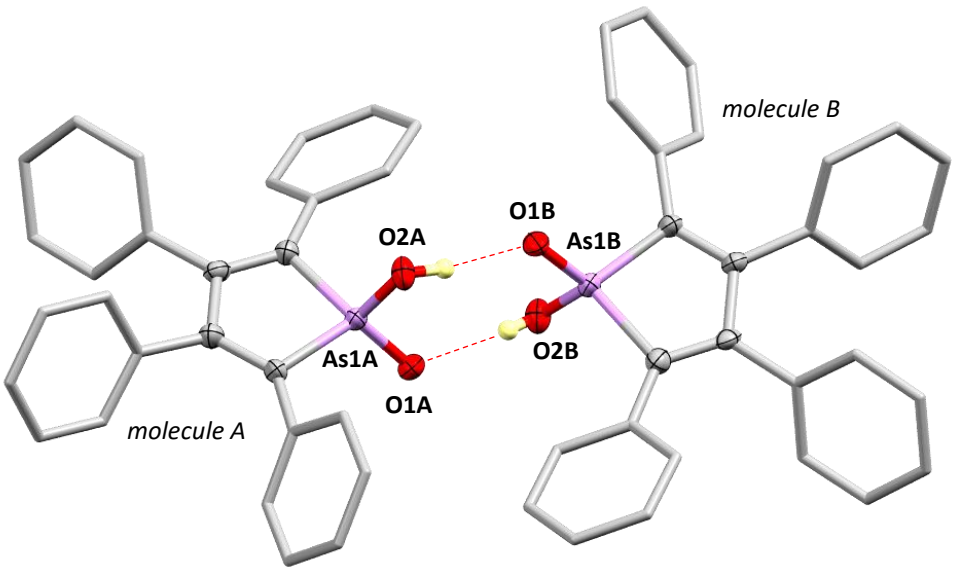



**Figure 8.4**: The molecular structure of (HO)(O)AsC$_4$Ph$_4$·0.5CH$_2$Cl$_2$ in a crystal. Phenyl groups simplified and dichloromethane solvate molecule and most hydrogen atoms omitted for clarity, except for the hydroxyl protons which are shown in light yellow. Ellipsoids shown at 50% displacement.

The asymmetric unit comprises a pair of crystallographically unique (HO)(O)$AsC_4Ph_4$ molecules linked *mann gegen mann via* a pair of O-H···O hydrogen bonds, which measure 2.509 and 2.589 Å (from O1 to O2). The arsenic atom(s) exist in a tetrahedral environment ($\tau_4 \approx 0.9$) and distances within the arsole rings are typical, though the five-membered rings are essentially planar (envelope angle < 1°). The As=O and As-OH bonds are crystallographically distinct at *ca* 1.64 and 1.72 Å, respectively. Despite being a highly novel compound and the first As(V) arsole to be structurally characterised, other interatomic dimensions are rather uninteresting and call for no further comment. The deprotonated form $[O_2AsC_4Ph_4]^-$ would superficially resemble a $\kappa^2$-carboxylate ligand of which the inventory of transition metal complexes is extensive, though a deliberate synthesis of (HO)(O)$AsC_4Ph_4$ would be required, perhaps involving the addition of $H_2O_2$ to $ClAsC_4Ph_4$.

Two crystallographically independent molecules were found in the asymmetric unit, in addition to one $CH_2Cl_2$ molecule. Data for $C_{57}H_{44}O_4As_2{\cdot}CH_2Cl_2$ ($M$ = 1013.66 g/mol): yellow plate 0.058 × 0.104 × 0.155 mm, triclinic, space group *P*-1 (no. 2), $a$ = 10.2783(7) Å, $b$ = 13.7546(7) Å, $c$ = 18.0191(14) Å, $\alpha$ = 109.589(6)°, $\beta$ = 100.457(6)°, $\gamma$ = 92.543(5)°, $V$ = 2344.9(3) Å$^3$, $Z$ = 2, multi-scan correction $T_{min}/T_{max}$ = 0.937/1.000, $\mu$(Cu-K$\alpha$) = 3.192 mm$^{-1}$, $\varrho_{calc}$ = 1.436 g/cm$^3$, 13580 reflections measured (7.066° ≤ 2Θ ≤ 141.796°), 8728 unique ($R_{int}$ = 0.0520, $R_{sigma}$ = 0.1006) which were used in all calculations, $GOF$ = 1.062, $D_{min}/D_{max}$ = -1.25/1.34 e/Å$^3$. The final $R_1$ was 0.0609 (I > 2σ(I)) and $wR_2$ was 0.1706 (all data).

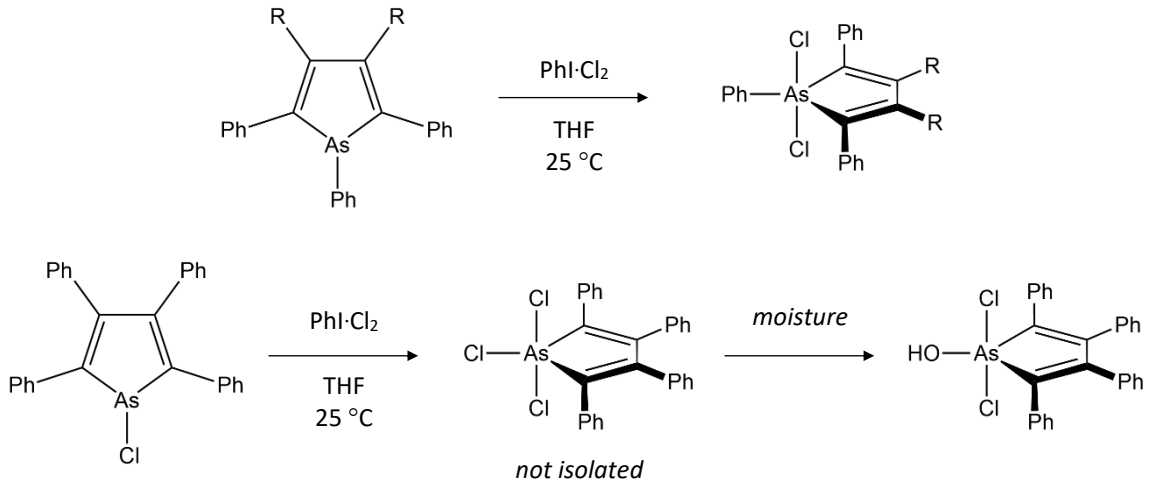
## 8.6 The Crystal Structures of $Ph(Cl)_2AsC_4Ph_4$, $Ph(Cl)_2AsC_4Ph_2H_2$ and $(HO)(Cl)_2AsC_4Ph_4$

The three title As(V) compounds were obtained by treatment of $PhAsC_4Ph_4$, $PhAsC_4Ph_2H_2$ and $ClAsC_4Ph_4$ with iodobenzene dichloride ($PhI{\cdot}Cl_2$) in THF solution,* as per the method outlined by MÄRKL.[6] $Ph(Cl)_2AsC_4Ph_2R_2$ (R = Ph or H) were isolated in good yields from the reaction mixtures as bright-yellow, air stable crystalline solids for which single crystals were obtained from THF/*n*-hexane mixtures. For $ClAsC_4Ph_4$, the reaction initially gives a deep red solution from which yellow-orange crystals were grown from THF/*n*-hexane; X-ray diffraction did not reveal the anticipated $(Cl)_3AsC_4Ph_4$ arsole, instead the hydrolysis product $(HO)(Cl)_2AsC_4Ph_4$. A consequence of the aqueous preparation of $PhI{\cdot}Cl_2$ the chlorinating agent presumably contained adventitious moisture,† which is otherwise difficult to remove

* MÄRKL performed the halogenation reaction in benzene, from which the product precipitated. The use of THF here added no additional difficulty during workup.

† The synthesis involves the addition of concentrated HCl to an aqueous mixture of iodobenzene and sodium hypochlorite (NaOCl) (producing $Cl_2$ *in situ*) from which $PhI{\cdot}Cl_2$ precipitates. Removing traces of moisture from the product is complicated by the fact that the compound cannot be placed under reduced pressure since this will liberate $Cl_2$ gas and washing with ethanol (to scavenge moisture) also destroys the compound. See *Ref.* 7.

since placing the compound under vacuum or warming leads to loss of diatomic chlorine.[7] The crystal structures of all three are so similar that they are shown *en echelon* in **Figure 8.5**.




**Scheme 8.5**: Halogenation of λ³-arsoles.

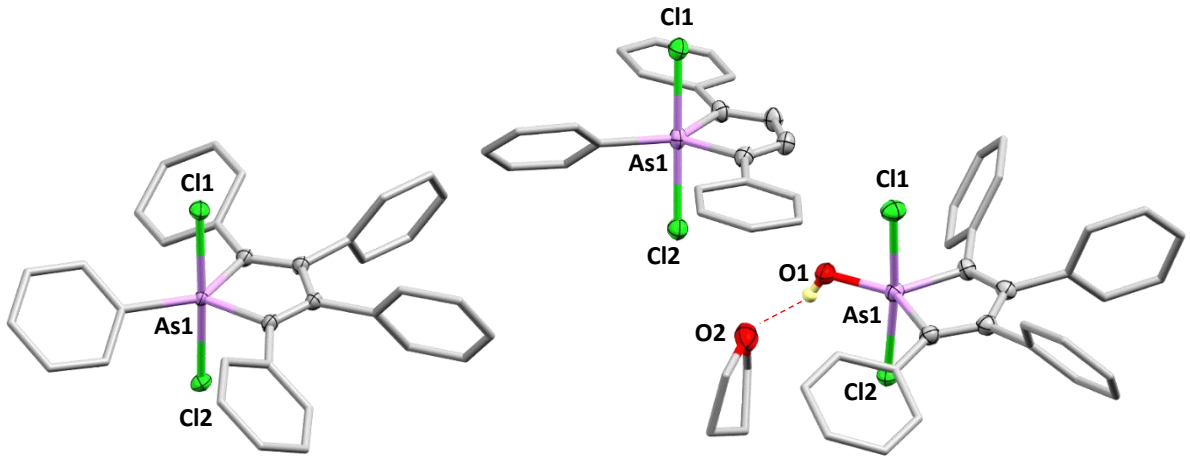



**Figure 8.5**: From left to right, the molecular structures of $Ph(Cl)_2AsC_4Ph_4{\cdot}C_4H_8O$, $Ph(Cl)_2AsC_4Ph_2H_2$, and $(HO)(Cl)_2AsC_4Ph_4{\cdot}C_4H_8O$ in three crystals. Phenyl groups simplified and most hydrogen atoms and solvate molecules omitted for clarity. Ellipsoids shown at 50% displacement.

Both $Ph(Cl)_2AsC_4Ph_4$ and $(HO)(Cl)_2AsC_4Ph_4$ are encountered as THF solvates, the latter exhibiting a O-H···O hydrogen bond (2.570 Å from O1 to O2). The pentavalent arsenic centres exist in trigonal bipyramidal environments with the pair of chloride residues occupying the axial valence sites, as correctly posited by MÄRKL.[6] The As-Cl covalent bond lengths of *ca* 2.32—2.35 Å are rather regular across all three compounds though notably longer than the same in $ClAsC_4Ph_4$ (*cf.* 2.196(2); **Chapter 2**, **Section 2.2.1**). For $Ph(Cl)_2AsC_4Ph_2R_2$ (R = Ph or H), the exocyclic As-C($sp^2$) bond distances of *ca* 1.94 Å is virtually unchanged

from $\lambda^3$-$PhAsC_4Ph_2R_2$.[8, 9] For $(HO)(Cl)_2AsC_4Ph_4$, the As-O single bond measures 1.717(2) Å which compares to the favourably against the same in $(HO)(O)AsC_4Ph_4$ (*vide supra*). Also like $(HO)(O)AsC_4Ph_4$, the arsole rings are essentially planar (< 1°) and internal distances and angles within the rings are unaffected by oxidation of the heteroatom.

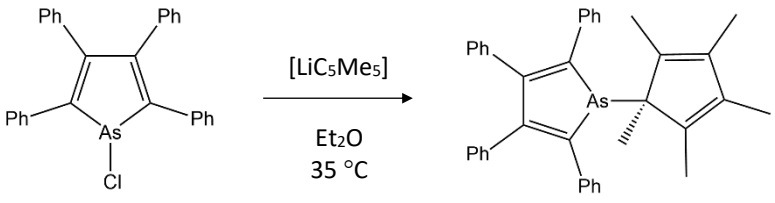
Crystal data for for $C_{34}H_{25}As_1Cl_2 \cdot C_4H_8O_1$ ($M$ = 651.46 g/mol): yellow prism 0.121 × 0.140 × 0.200 mm, monoclinic, space group $P2_1/n$ (no. 14), $a$ = 18.62350(10) Å, $b$ = 9.06920(10) Å, $c$ = 19.16650(10) Å, $\beta$ = 98.9400(10)°, $V$ = 3197.90(4) Å$^3$, $Z$ = 4, multi-scan correction $T_{min}/T_{max}$ = 0.585/1.000, $\mu$(Cu-Kα) = 3.191 mm$^{-1}$, $\varrho_{calc}$ = 1.353 g/cm$^3$, 44691 reflections measured (7.202° ≤ 2Θ ≤ 147.52°), 6469 unique ($R_{int}$ = 0.0311, $R_{sigma}$ = 0.0167) which were used in all calculations, $GOF$ = 1.035, $D_{min}/D_{max}$ = -0.74/086 e/Å$^3$. The final $R_1$ was 0.0371 (I > 2σ(I)) and $wR_2$ was 0.1005 (all data).

Crystal data for $C_{22}H_{17}As_1Cl_2$ ($M$ = 427.17 g/mol): yellow needle 0.044 × 0.055 × 0.133 mm, triclinic, space group $P$-1 (no. 2), $a$ = 7.4780(4) Å, $b$ = 10.6370(6) Å, $c$ = 12.4597(8) Å, α = 71.252(5)°, $\beta$ = 79.868(5)°, $\gamma$ = 80.818(5)°, $V$ = 918.21(10) Å$^3$, $Z$ = 2, multi-scan correction $T_{min}/T_{max}$ = 0.939/1.000, $\mu$(Cu-Kα) = 5.175 mm$^{-1}$, $\varrho_{calc}$ = 1.545 g/cm$^3$, 6139 reflections measured (8.834° ≤ 2Θ ≤ 147.44°), 3631 unique ($R_{int}$ = 0.0250, $R_{sigma}$ = 0.0442) which were used in all calculations, $GOF$ = 1.083, $D_{min}/D_{max}$ = -0.50/2.00 e/Å$^3$. The final $R_1$ was 0.0483 (I > 2σ(I)) and $wR_2$ was 0.1329 (all data).

Crystal data for $C_{28}H_{21}O_1As_1Cl_2 \cdot C_4H_8O_1$ ($M$ = 591.37 g/mol): yellow needle 0.068 × 0.185 × 0.567 mm, orthorhombic, space group $Pna2_1$ (no. 33), $a$ = 16.67540(10) Å, $b$ = 17.88840(10) Å, $c$ = 9.36480(10) Å, $V$ = 2793.48(4) Å$^3$, $Z$ = 4, spherical correction $T_{min}/T_{max}$ = 0.593/0.622, $\mu$(Cu-Kα) = 3.619 mm$^{-1}$, $\varrho_{calc}$ = 1.406 g/cm$^3$, 38852 reflections measured (7.248° ≤ 2Θ ≤ 147.738°), 5631 unique ($R_{int}$ = 0.0405, $R_{sigma}$ = 0.0259) which were used in all calculations, $GOF$ = 1.064, $D_{min}/D_{max}$ = -0.18/0.24 e/Å$^3$. The final $R_1$ was 0.0212 (I > 2σ(I)) and $wR_2$ was 0.0561 (all data).

## 8.7 The Crystal Structure of $(C_5Me_5)AsC_4Ph_4$

The compound 1-(pentamethylcyclopentadienyl)-2,3,4,5-tetraphenylarsole was prepared from $[LiC_5Me_5]$ and $ClAsC_4Ph_4$ in $Et_2O$ at reflux and isolated as an air-sensitive yellow solid in good yield.




**Scheme 8.6**: Synthesis of $C_5Me_5AsC_4Ph_4$.

This arsole was prepared during attempts to elucidate the mechanism of formation of $[Co(CO)_2(\eta^5\text{-}AsC_4Ph_4)]$ from $[Co_2(CO)_8]$ and $RAsC_4Ph_4$ (**Chapter 3**, **Section 3.3.6**): it was hypothesised that during As-X bond scission one cobalt atom received the arsolyl group and the other the *As*-substituent. When R = Ph or Cl, for example, $[CoX(CO)_4]$ was presumed to decompose under the reaction conditions since such complexes are acutely thermolabile. Hence, the synthesis of $(C_5Me_5)AsC_4Ph_4$, since $[Co(CO)_2(\eta^5\text{-}C_5Me_5)]$ is thermally stable[10, 11] and possesses readily identifiable NMR and IR spectroscopic signatures. Unfortunately, whilst thermolysis of $[Co_2(CO)_8]$ with $(C_5Me_5)AsC_4Ph_4$ *did* produce $[Co(CO)_2(\eta^5\text{-}AsC_4Ph_4)]$, strangely no $[Co(CO)_2(\eta^5\text{-}C_5Me_5)]$ was ever detected nor isolated from the reaction mixture. Single crystals of $C_5Me_5AsC_4Ph_4$ were obtained from *n*-hexane at -20 °C.

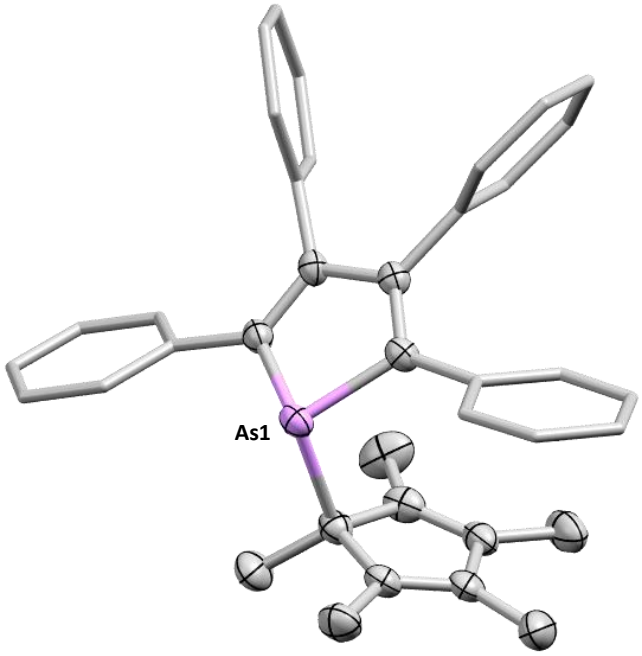



**Figure 8.6**: The molecular structure of $(C_5Me_5)AsC_4Ph_4$ in a crystal. Phenyl groups simplified and hydrogen atoms omitted for clarity. Ellipsoids shown at 50% displacement.

The arsole crystallises in triclinic *P*-1 and two enantiomeric molecules are found within the unit cell, related by means of the inversion centre. The origin of chirality in the solid state is the relative orientations of the arsole and cyclopentadienyl rings, which do not lie along a common symmetry plane. Dimensions within the arsole ring are typical of *As*-organyl arsoles and the $C_5Me_5$ group contains localised C=C (mean 1.346(4) Å) and C-C bonds, though the C($sp^2$)-C($sp^2$) single bond (1.468(3) Å) is somewhat

shorter than the C($sp^2$)-C($sp^3$) single bonds (mean 1.504(4) Å). The exocyclic distance between the arsenic atom and the cyclopentadienyl carbon atom measures 2.036(3) Å which appears typical of such a bond.

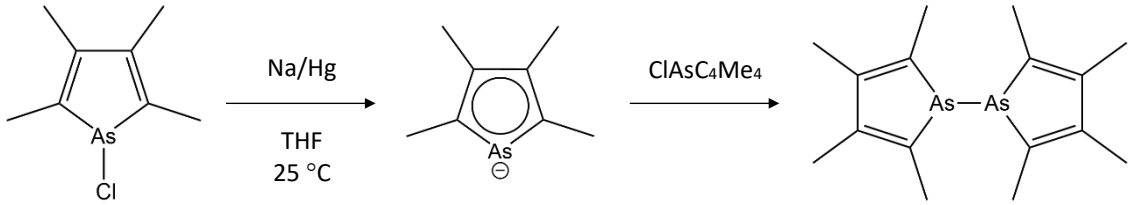
A 250 mL three-necked round-bottomed Schlenk flask was charged with 1 g $ClAsC_4Ph_4$ (2.1 mmol) and 0.35 g [$LiC_5Me_5$] (2.4 mmol) under argon. A water condenser was fitted and 100 mL $Et_2O$ admitted. The mixed was heated to reflux for 48 h (the organolithium dissolves slowly over this time) giving a lemon-yellow suspension. The solvent was removed under reduced pressure and the residue extracted with portions of boiling *n*-hexane and filtered through a short plug of celite (2.5 x 2.5 cm) under nitrogen whilst hot, rinsing with portions of hot *n*-hexane until washings were clear. The yellow filtrate was concentrated until precipitation began, and the solution was stored at -20 °C giving the product as a microcrystalline yellow solid which was decanted from the supernatant and washed with small portions of cold *n*-pentane and dried under reduced pressure. A further crop of product is obtained from the supernatant (alongside a specimen for X-ray diffraction). Isolated yield 0.73 g (1.3 mmol, 62 %). The product is air-sensitive and is readily soluble in polar organic and aromatic solvents, and moderately soluble in $Et_2O$ and aliphatic hydrocarbons.

NMR: $^1$H ($CDCl_3$, 400 MHz, 25 °C) δ 0.96 (s, 3H, 1-$C_5(CH_3)_5$), 1.27 (s, 6H, 2,5-$C_5(CH_3)_5$), 1.82 (s, 6H, 3,4-$C_5(CH_3)_5$), 6.96—7.10 (m, 20H, $C_6H_5$) ppm. $^{13}$C NMR ($CDCl_3$, 156 MHz, 25 °C) δ 150.5 (arsole {2,5}-*C*), 148.9 (arsole {3,4}-*C*), 139.5 ($C_6H_5$), 139.0 ($C_6H_5$), 133.5 ($C_6H_5$), 130.6 ($C_6H_5$), 129.9 ($C_6H_5$), 127.5 ($C_6H_5$), 127.4 ($C_6H_5$), 126.3 ($C_6H_5$), 125.1 ($C_6H_5$), 100.1 (*As*-bound $C_5(CH_3)_5$), 66.4 (2,5-$C_5(CH_3)_5$), 66.0 (3,4-$C_5(CH_3)_5$), 17.5 (1-$C_5(CH_3)_5$), 11.2 (2,5-$C_5(CH_3)_5$), 10.6 (3,4-$C_5(CH_3)_5$) ppm. HR-MS (EI, MeCN, +ve ion) found *m*/*z* 566.1948 (calc. for $C_{38}H_{35}{}^{75}As_1$ $[M]^+$: 566.1995).

Single crystals were obtained by cooling a hot *n*-hexane solution to -20 °C. Two crystallographically independent molecules were found within the asymmetric unit. Data for for $C_{76}H_{70}As_2$ ($M$ = 1133.16 g/mol): yellow plate 0.033 × 0.129 × 0.152 mm, triclinic, space group *P*-1 (no. 2), $a$ = 12.3243(3) Å, $b$ = 13.8269(6) Å, $c$ = 18.4889(6) Å, α = 76.352(3)°, $\beta$ = 81.660(2)°, $\gamma$ = 76.777(3)°, $V$ = 2966.66(18) Å$^3$, $Z$ = 2, multi-scan correction $T_{min}/T_{max}$ = 0.977/1.000, $\mu$(Cu-Kα) = 1.716 mm$^{-1}$, $\varrho_{calc}$ = 1.269 g/cm$^3$, 22186 reflections measured (7.402° ≤ 2Θ ≤ 147.364°), 11735 unique ($R_{int}$ = 0.0303, $R_{sigma}$ = 0.0498) which were used in all calculations, *GOF* = 1.012, $D_{min}/D_{max}$ = -0.50/0.56 e/Å$^3$. The final $R_1$ was 0.0376 (I > 2σ(I)) and $wR_2$ was 0.0950 (all data).

## 8.8 The Crystal Structure of $(AsC_4Me_4)_2$

The yellow 2,2',3,3',4,4',5,5'-octamethylbiarsolyl was obtained in an *As*-*As* bond forming reaction between $ClAsC_4Me_4$ and $[AsC_4Me_4]^-$ (**Chapter 5**, **Section 5.2.7**); the compound was previously reported by THEOPOLD who obtained it following chromatography of $ClAsC_4Me_4$ on neutral alumina and characterised *via* spectroscopic techniques.[5] The compound is moderately air sensitive and slowly degrades to oily brown residues of low solubility. Single crystals were grown by slow evaporation of $Et_2O$ solution at -30 °C.




**Scheme 8.7**: Synthesis of $(AsC_4Me_4)_2$.

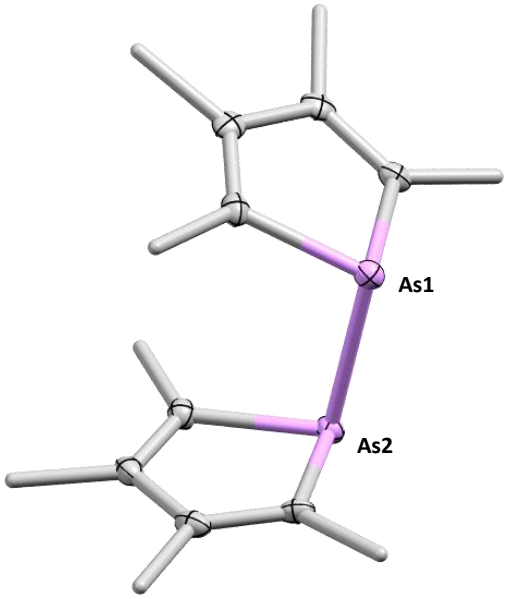



**Figure 8.7**: The molecular structure of $(AsC_4Me_4)_2$. Methyl groups simplified and hydrogen atoms omitted for clarity. Ellipsoids shown at 50% displacement.

The structure of $(AsC_4Me_4)_2$ reveals a non-centrosymmetric arrangement with the arsole rings mutually *gauche* about the diarsine bond; a similar conformation has been observed in the crystal structure of 2,2',5,5'-tetramethylbiarsole[12] and a low barrier to rotation is presumed in the absence of sterically imposing ring substituents. Each half of the molecule is crystallographically unique though local interatomic distances and angles amongst the two components are essentially identical within the precision limits of the data. The unit cell (triclinic *P*-1) contains two molecules related by means of an external inversion centre and no unusually short contacts are found. The diarsine bond measures 2.4462(4) Å which is unremarkable amongst other structurally characterised As-As single bonds (*cf.* 2.457(3) Å in $As_2Ph_4$,[13] 2.440(1) Å in $As_2(C_5Me_5)_4$[14]) and the abovementioned $(AsC_4Me_2H_2)_2$ reported by ASHE (As-As 2.438(1) Å). Interatomic distances and angles within the arsole rings are typical: the mean As-$C_\alpha$ distance is 1.929(5) Å, the mean

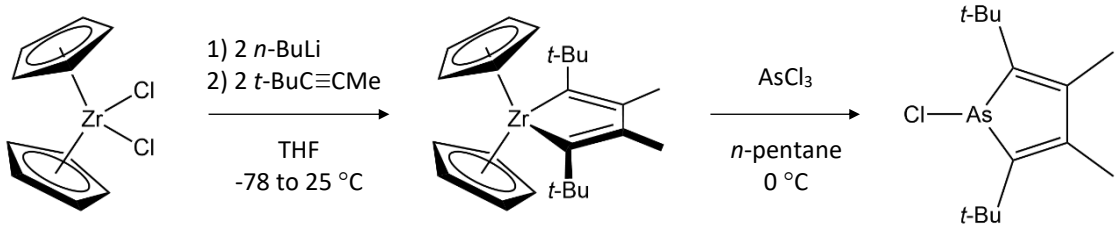
$C_\alpha$=$C_\beta$ double bond length is 1.341(9) Å and the mean $C_\beta$-$C_\beta$ bond length is 1.481(5) Å. The mean $C_\alpha$-As-$C_\alpha$ angle is *ca* 88° and the torsion angle between respective arsole midpoints is *ca* 42°; two As-$C_\alpha$ bonds are essentially eclipsing when viewed along the diarsine bond though a wholly overlapping *syn* configuration is perhaps disfavoured in the solid state by steric interactions between stacking methyl groups.

Synthetic details and spectroscopic data are given in **Chapter 5**, **Section 5.4.6**.

Data for $C_{16}H_{24}As_2$ ($M$ = 366.19 g/mol): yellow plate 0.079 × 0.161 × 0.311 mm, triclinic, space group $P$-1 (no. 2), $a$ = 7.9490(3) Å, $b$ = 9.1682(4) Å, $c$ = 11.5715(5) Å, α = 86.399(4)°, $\beta$ = 87.580(4)°, $\gamma$ = 77.707(4)°, $V$ = 821.99(6) Å$^3$, $Z$ = 2, multi-scan correction $T_{min}/T_{max}$ = 0.795/1.000, $\mu$(Mo-Kα) = 4.048 mm$^{-1}$, $\varrho_{calc}$ = 1.480 g/cm$^3$, 6873 reflections measured (6.914° ≤ 2Θ ≤ 52.736°), 3349 unique ($R_{int}$ = 0.0276, $R_{sigma}$ = 0.0482) which were used in all calculations, $GOF$ = 1.055, $D_{min}/D_{max}$ = -0.40/0.56 e/Å$^3$. The final $R_1$ was 0.0309 (I > 2σ(I)) and $wR_2$ was 0.0662 (all data).

## 8.9 The Crystal Structure of $ClAsC_4(t\text{-}Bu)_2Me_2$

1-chloro-2,5-di(*tert*-butyl)-3,4-dimethylarsole was prepared from $AsCl_3$ and the corresponding zirconacycle in *n*-pentane solution and isolated as an air-sensitive waxy yellow solid in good yield. Spectroscopic data have been given by MATHEY.[15]




**Scheme 8.8**: Synthesis of $ClAsC_4(t\text{-}Bu)_2Me_2$.

The ligand was prepared with a view of synthesising $[Mo\{AsC_4(t\text{-}Bu)_2Me_2\}(CO)_3(\eta^5\text{-}C_5H_5)]$ for which the bulky *tert*-butyl groups in the 2,5-ring positions might provide sufficient kinetic stabilisation to a 16-electron $Mo(CO)_2(\eta^5\text{-}C_5H_5)$ centre upon photolytic decarbonylation (*cf.* $[Mo(=As\{t\text{-}Bu\}_2)(CO)_2(\eta^5\text{-}C_5H_5)]$ prepared by MALSICH[16]). The ultimate intention was to prepare an arsenium with a Mo=As double bond, though interestingly the $AsC_4(t\text{-}Bu)_2Me_2$ ligand could not be indefinitely installed onto the metal centre by the usual transmetalation method, and only $[Mo(CO)_3(\eta^5\text{-}C_5H_5)]_2$ was obtained upon combining $ClAsC_4(t\text{-}Bu)_2Me_2$ and $[Mo(SnBu_3)(CO)_3(\eta^5\text{-}C_5H_5)]$ in *n*-hexane medium. The ligand is perhaps

counterintuitively *too* bulky which encourages homolysis of the Mo-As bond thus-formed upon transmetalation (and not decarbonylation, it seems). The fate of the arsole group was not easily determined, though *in situ* NMR monitoring did show all reagents to be consumed after mixing. Large single crystals were obtained by slow evaporation of $Et_2O$ solution at -30 °C and the structure is shown in **Figure 8.8**.

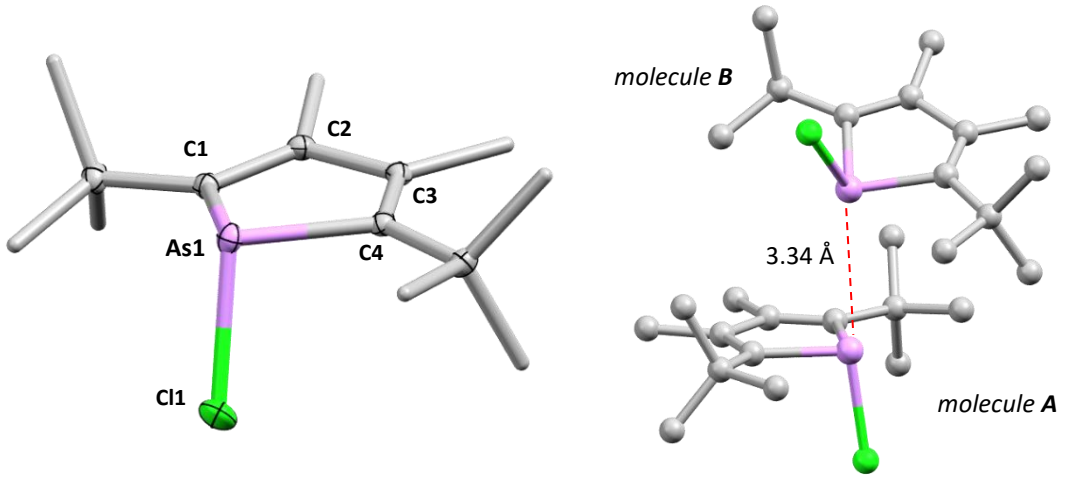



**Figure 8.8**: The molecular structure of $ClAsC_4(t\text{-}Bu)_2Me_2$. Methyl groups simplified and hydrogen atoms omitted for clarity. Ellipsoids shown at 50% displacement. **Inset, top right**: The asymmetric unit containing two crystallographically unique molecules **A** and **B**.

The asymmetric unit contains two crystallographically unique molecules which do subtly differ from one another (*vide infra*), and the contents of the unit cell (triclinic *P*-1; four molecules) are generated by means of a centre of inversion. An intermolecular contact is found between the arsenic atoms of adjacent molecules (**Figure 8.8**, **Inset**) with an interpnictogen distance of *ca* 3.34 Å (sum of Van der Waals radii: 3.70 Å). The arrangement recalls that of some open-chained bis(arsino)sulfur diimides *e.g.*, $Ph_2AsN{=}S{=}NAsPh_2$ (**Figure 8.9**), which are geometrically predisposed in the solid-state toward non-repulsive As···As interactions of 3.38 Å in length,[17] or in the crystal structures of the elegantly simple 2,3-bis(diphenylarsino)pyrazine (3.34 Å)[18] and 2,2'-bis(dibenzoarsolyl)biphenyl (3.24 Å).[19] The topic of non-covalent interpnictogen bonding has very recently been reviewed.[20]

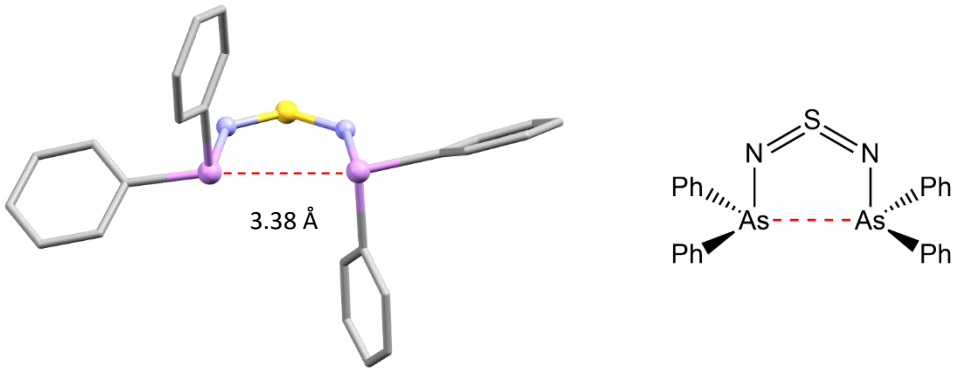



**Figure 8.9**: The molecular structure of bis(diphenylarsino)sulfur diimide in a crystal as determined by GIEREN *et al.* (*Ref.* 17), featuring an attractive non-covalent interpnictogen interaction.

This interaction appears to have directionality (As1B → As1A) since one molecule (**B**) is essentially planar (envelope *ca* 0.2°) whilst the other (**A**) displays the usual fold (envelope *ca* 9.5°) *i.e.*, As1B is "more tetrahedral" in the donor molecule (mean $C_{\alpha}$-As-$C_{\alpha}$ *ca* 102°) than in the acceptor (mean $C_{\alpha}$-As-$C_{\alpha}$ *ca* 95°), recalling the near-planarity of $\lambda^4$-arsole donor ligands in transition metal complexes. Additionally, the As-Cl bond in the acceptor molecule (**A**; 2.2474(6) Å) is longer than the same in the donor molecule (**B**; 2.2212(6) Å), ostensive evidence for an As(*s*)→As-Cl(σ*) interaction which is an intuitive outcome since the LUMO is invariably composed of the exocyclic arsenic-substituent antibond. Indeed, the As1B-As1A-Cl1A vector is *quasi*-linear (~170°) *i.e.*, from the posterior of the As-Cl bond in molecule **A**. That being said, interatomic distances within-and-about the arsole rings are statistically indistinguishable within the precision limits of the data.

Data for $C_{28}H_{42}As_2Cl_2$ ($M$ = 605.14 g/mol): yellow plate 0.071 × 0.169 × 0.321 mm, triclinic, space group $P$-1 (no. 2), $a$ = 9.0412(3) Å, $b$ = 11.8621(4) Å, $c$ = 14.5361(5) Å, $\alpha$ = 80.871(3)°, $\beta$ = 81.879(3)°, $\gamma$ = 77.842(3)°, $V$ = 1495.27(9) Å$^3$, $Z$ = 4, spherical correction $T_{min}/T_{max}$ = 0.590/0.620, $\mu$(Cu-Kα) = 4.495 mm$^{-1}$, $\varrho_{calc}$ = 1.345 g/cm$^3$, 15607 reflections measured (7.692° ≤ 2Θ ≤ 146.496°), 5973 unique ($R_{int}$ = 0.0312, $R_{sigma}$ = 0.0351) which were used in all calculations, $GOF$ = 1.028, $D_{min}/D_{max}$ = -0.50/0.36 e/Å$^3$. The final $R_1$ was 0.0285 (I > 2σ(I)) and $wR_2$ was 0.0753 (all data).

## 8.10 References


1. E. H. Braye, W. Hübel and I. Caplier, *J. Am. Chem. Soc.,* **1961**, *83*, 4406-4413.
2. W. A. Schenk and E. Voß, *J. Organomet. Chem.*, **1994**, *467*, 67-73.
3. A. Marinetti, F. Mathey, J. Fischer and A. Mitschler, *J. Chem. Soc., Chem. Comm.*, **1982**, 667-668.
4. A. Marinetti, F. Mathey, J. Fischer and A. Mitschler, *J. Am. Chem. Soc.*, **1982**, *104*, 4484-4485.
5. S. C. Sendlinger, B. S. Haggerty, A. L. Rbeingold and K. H. Theopold, *Chem. Ber.*, **1991**, *124*, 2453-2456.
6. G. Märkl and H. Hauptmann, *J. Organomet. Chem.*, **1983**, *248*, 269-285.
7. X. F. Zhao and C. Zhang, *Synthesis*, **2007**, 551-557.
8. M. Ishidoshiro, Y. Matsumura, H. Imoto, Y. Irie, T. Kato, S. Watase, K. Matsukawa, S. Inagi, I. Tomita and K. Naka, *Org. Lett.*, **2015**, *17*, 4854-4857.
9. H. Imoto, A. Urushizaki, I. Kawashima and K. Naka, *Chem. Eur. J.*, **2018**, *24*, 8797-8803.
10. R. B. King and M. B. Bisnette, *J. Organomet. Chem.*, **1967**, *8*, 287-297.
11. L. R. Byers and L. F. Dahl, *Inorg. Chem.*, **1980**, *19*, 277-284.
12. A. J. Ashe, W. M. Butler and T. R. Diephouse, *Organometallics*, **1983**, *2*, 1005-1008.
13. W. S. Tay, X. Y. Yang, Y. Li, S. A. Pullarkat and P. H. Leung, *Dalt. Trans.*, **2019**, *48*, 4602-4610.
14. X. W. Li, J. Lorberth and K. Harms, *J. Organomet. Chem.*, **1994**, *483*, 229-233.
15. F. Nief and L. Ricard, *Organometallics*, **2001**, *20*, 3884-3890.
16. M. Luksza, S. Himmel and W. Malisch, *Angew. Chem. Int. Ed. Eng.*, **1983**, *22*, 416-417.
17. A. Gieren, H. Betz, T. Hübner, V. Lamm, M. Herberhold and K. Guldner, *Z. Anorg. Allg. Chem.*, **1984**, *513*, 160-174.
18. R. Kobayashi, T. Fujii, H. Imoto and K. Naka, *Eur. J. Inorg. Chem.*, **2021**, 217-222.
19. A. K. Gupta, S. Akkarasamiyo and A. Orthaber, *Inorg. Chem.*, **2017**, *56*, 4504-4511.
20. A. Varadwaj, P. R. Varadwaj, H. M. Marques and K. Yamashita, *Molecules*, **2022**, *27*, 3421.